2015 NEHRP Recommended Seismic Provisions: Design Examples

FEMA P-1051 / July 2016

2015 NEHRP (National Earthquake Hazards Reduction Program)

Recommended Seismic Provisions: Design Examples

FEMA P-1051/ July 2016

FOREWORD

The Federal Emergency Management Agency (FEMA) has committed under the National Earthquake Hazard Reduction Program (NEHRP) to support implementation of new knowledge and research results for improving seismic design and building practices in the nation. One of the goals of FEMA and NEHRP is to encourage design and building practices that address the earthquake hazard and minimize the resulting risk of damage and injury. The 2015 edition of the *NEHRP Recommended Seismic Provisions for New Buildings and Other Structures* (FEMA P-1050) affirmed FEMA's ongoing support to improve the seismic safety of construction in this country. The *NEHRP Provisions* serves as a key resource for the seismic requirements in the ASCE/SEI 7 Standard *Minimum Design Loads for Buildings and Other Structures* as well as the national model building codes, the *International Building Code (IBC), International Residential Code (IRC) and NFPA 5000 Building Construction Safety Code.* FEMA welcomes the opportunity to provide this material and to work with these codes and standards organizations.

FEMA P-1051 provides a series of design examples that will assist the users of the 2015 *NEHRP Provisions* and the ASCE/SEI 7 standard the *Provisions* adopted by reference. This product has included several new chapters to provide examples for nonlinear response history analysis procedures, horizontal diaphragm analysis, soil structural interaction, and structures with energy dissipation devices. The eighteen chapters not only illustrate how to apply the new methods and requirements adopted in the *2015 NEHRP Provisions* for engineering design, but also cover code conforming updates for the design examples of different structural materials and non-structural components. This product serves as an educational and supporting resource for the 2015 *NEHRP Provisions.* The new changes in the *2015 NEHRP Provisions* have incorporated extensive results and findings from recent research projects, problem-focused studies, and post-earthquake investigation reports conducted by various professional organizations, research institutes, universities, material industries and the NEHRP agencies.

FEMA wishes to express its gratitude to the authors listed in the acknowledgements for their significant efforts in preparing this material and to the BSSC Board of Direction and staff who made this possible. Their hard work has resulted in a resource product that will provide important assistance to a significant number of users of the 2015 *NEHRP Provisions,* and the upcoming new edition of national design standards and model building codes with incorporated changes based-on the *Provisions*.

Federal Emergency Management Agency

Page intentionally left blank.

PREFACE and
ACKNOWLEDGEMENTS

Since its creation in 1979, the National Earthquake Hazard Reduction Program (NEHRP) has provided a framework for efforts to reduce the risk from earthquakes. The Building Seismic Safety Council (BSSC) is proud to have been selected by the Federal Emergency Management Agency (FEMA) to continue to play a role under NEHRP in improving the seismic resistance of the built environment. The BSSC is pleased to mark the delivery to FEMA of the 2015 Design Examples, the companion document to the 2015 *NEHRP Recommended Seismic Provisions for New Buildings and Other Structures.*

This volume of design examples is intended for those experienced structural designers, who are relatively new to the field of earthquake-resistant design and to the 2015 NEHRP *Provisions.* By extension, it also applies to use of the current model codes and standards because the *Provisions* is the key resource for updating seismic design requirements in most of those documents including ASCE 7 Standard, *Minimum Design Loads for Buildings and Other Structures;* and the *International Building Code* (IBC). Furthermore, the *2015 NEHRP Provisions* (FEMA P-1050) adopted ASCE7-10 by reference, and the 2012 *International Building Code* adopted ASCE7-10 by reference; therefore, seismic design requirements are essentially equivalent across the *Provisions,* ASCE7 and the national model code. The *Provisions* and the national model codes and standards attest to the success of FEMA and NEHRP and BSSC efforts to ensure that the nation's building codes and standards reflect the state-of-the art of earthquake-resistant design.

This edition of the design examples reflects the technical changes in the 2015 NEHRP *Provisions* just as the previous version, the FEMA P-751 Design Examples published in September 2012, reflected the 2009 NEHRP *Provisions.* Updated education/training materials to supplement this set of design examples will be published as a separate FEMA product, *2015 NEHRP Recommended Seismic Provisions: Training Material,* FEMA P-1052.

The BSSC is grateful to all those individuals whose assistance made the 2015 edition of the design examples a reality:

- Robert Pekelnicky, who served as project lead and managing technical editor, and James Malley, who served as project advisor for the 2015 Design Examples.

- The Design Examples chapter authors: Finley Charney, Kelly Cobeen, S.K. Ghosh, John Gillengerten, Steven Harris, Curt Haselton, John Hooper, Dominic Kelley, Charlie Kircher, Nico Luco, James Malley, Ian McFarlane, Robert Pekelnicky, Gregory Soules, and Andrew Taylor.

- Robert Hanson, who provided a review for each chapter.

And finally, the BSSC Board is grateful to FEMA Project Officer Mai Tong for his support and guidance and to Philip Schneider of the NIBS staff for his efforts in providing project management, assembling the 2015 volume for publication, and issuance as an e-document available for download and on CD-ROM.

Jimmy W. Sealy, FAIA
Chair, BSSC Board of Direction

TABLE OF CONTENTS

1. Introduction

2. Fundamentals

3. Earthquake Ground Motion

4. Linear Response History Provision

5. Nonlinear Response History Analysis

6. Horizontal Diaphragm Analysis

7. Foundation and Liquefaction Design

8. Soil-Structure Interaction

9. Structural Steel Design

10. Reinforced Concrete

11. Precast Concrete Design

12. Composite Steel and Concrete

13. Masonry

14. Wood Design

15. Seismically Isolated Structures

16. Structures with Supplemental Energy Dissipation Devices

17. Nonbuilding Structure Design

18. Design for Nonstructural Components

1

Introduction
Robert G. Pekelnicky, P.E., S.E.

Contents

The *NEHRP Recommended Provisions: Design Examples* are written to illustrate and explain the applications of the *2015 NEHRP Recommended Seismic Provisions for Buildings and Other Structures, ASCE 7-16 Minimum Design Loads for Buildings and Other Structures* and the material design standards referenced therein and to provide explanations to help understand them. Designing structures to be resistant to a major earthquake is complex and daunting to someone unfamiliar with the philosophy and history of earthquake engineering. The target audience for the *Design Examples* is broad. College students learning about earthquake engineering, engineers studying for their licensing exam, or those who find themselves presented with the challenge of designing in regions of moderate and high seismicity for the first time should all find this document's explanation of earthquake engineering and the *Provisions* helpful.

Fortunately, major earthquakes are a rare occurrence, significantly rarer than the other hazards, such as damaging wind and snow storms that one must typically consider in structural design. However, past experiences have shown that the destructive power of a major earthquake can be so great that its effect on the built environment cannot be underestimated. This presents a challenge since one cannot typically design a practical and economical structure to withstand a major earthquake elastically in the same manner traditionally done for other hazards.

Since elastic design is not an economically feasible option for most structures where major earthquakes can occur, there must be a way to design a structure to be damaged but still safe. Unlike designing for strong winds, where the structural elements that resist lateral forces can be proportioned to elastically resist the pressures generated by the wind, in an earthquake the lateral force resisting elements must be proportioned to deform beyond their elastic range in a controlled manner. In addition to deforming beyond their elastic range, the lateral force resisting

system must be robust enough to provide sufficient stability so the building is not at risk of collapse. Furthermore, major falling hazards form architectural, mechanical, electrical, and plumbing (henceforth referred to as nonstructural) components that could kill or cause serious injury should be prevented.

While typical structures are designed to be robust enough to have a minimal risk of collapse and no significant nonstructural falling hazards in major earthquakes, there are other structures whose function or type of occupants warrants higher performance designs. Structures, like hospitals, fire stations and emergency operation centers need to be designed to maintain their function immediately after or returned to function shortly after the earthquake. Structures like schools and places where large numbers of people assemble have been deemed important enough to require a greater margin of safety against collapse than typical buildings. Additionally, earthquake resistant requirements and ruggedness testing are needed for the design and anchorage of architectural elements and mechanical, electrical and plumbing systems to prevent loss of system function in essential facilities.

Current building standards, specifically the American Society of Civil Engineers (ASCE) 7 *Minimum Design Loads for Buildings and Other Structures* and the various material design standards published by the American Concrete Institute (ACI), the American Institute of Steel Construction (AISC), the American Iron and Steel Institute (AISI), the American Forest & Paper Association (AF&PA) and The Masonry Society (TMS) provide a means by which an engineer can achieve these design targets. These standards represent the most recent developments in earthquake resistant design. The majority of the information contained in ASCE 7 comes directly from the *NEHRP Recommended Seismic Provisions for New Buildings and Other Structures*. The stated intent of the *NEHRP Provisions* is to provide reasonable assurance of seismic performance that will:

1. Avoid serious injury and life loss due to
   a. Structural collapse
   b. Failure of nonstructural components or systems
   c. Release of hazardous materials
2. Preserve means of egress
3. Avoid loss of function in critical facilities, and
4. Reduce structural and nonstructural repair costs where practicable.

The *Provisions* have explicit requirements to provide life safety for buildings and other structures though the design forces and detailing requirements. The current provisions have adopted a target risk of collapse of 1% over a 50 year period for a structure designed to the *Provisions.* The *Provisions* provide prevention of loss of function in critical facilities and reducing repair costs in a more implicit manner though prescriptive requirements.

Having good building codes and design standards is only one action necessary to make a community's buildings resilient to a major earthquake. A community also needs engineers who can carry out designs in accordance with the requirements of the codes and standards and contractors who can construct the designs in accordance with properly prepared construction documents. The first item is what the *NEHRP Recommended Provisions: Design Examples*

seeks to foster. The second item is typically addressed through quality assurance provisions found in building codes or recommended by the design professional.

The purpose of this introduction is to offer general guidance for users of the design examples and to provide an overview. Before introducing the design examples, a brief history of earthquake engineering is presented. That is followed by a history of the *NEHRP Provisions* and its role in setting standards for earthquake resistant design. This is done to give the reader a perspective of the evolution of the *Provisions* and some background for understanding the design examples. Following that is a brief summary of each chapter in the *Design Examples*.

1.1 EVOLUTION OF EARTHQUAKE ENGINEERING

It is helpful to understand the evolution of the earthquake design standards and the evolution of the field of earthquake engineering in general. Much of what is contained within the *Provisions* and standards reference therein is based on lessons learned from earthquake damage and the ensuing research.

Prior to 1900 there was little consideration of earthquakes in the design of buildings. Major earthquakes were experienced in the United States, notably the 1755 Cap Ann Earthquake around Boston, the 1811 and 1812 New Madrid Earthquakes, the 1868 Hayward California Earthquake and the 1886 Charleston Earthquake. However, none of these earthquakes led to substantial changes in the way buildings were constructed.

Many things changed with the Great 1906 San Francisco Earthquake. The earthquake and ensuing fire destroyed much of San Francisco and was responsible for approximately 3,000 deaths. To date it is the most deadly earthquake the United States has ever experienced. While there was significant destruction to the built environment, there were some important lessons learned from those buildings that performed well and did not collapse. Most notable was the exemplary performance of steel framed buildings which consisted of riveted frames designed to resist wind forces and brick infill between frame columns, built in the Chicago style.

The recently formed San Francisco Section of the American Society of Civil Engineers (ASCE) studied the effects of the earthquake in great detail. An observation was that "a building designed with a proper system of bracing wind pressure at 30 lbs. per square foot will resist safely the stresses caused by a shock of the intensity of the recent earthquake." (ASCE, 1907) That one statement became the first U.S. guideline on how to provide an earthquake resistant design.

Earthquakes in Tokyo in 1923 and Santa Barbara in 1925 spurred major research efforts. Those efforts led to the development of the first seismic recording instruments, shake tables to investigate earthquake effects on buildings, and committees dedicated to creating code provisions for earthquake resistant design. Shortly after these earthquakes, the 1927 *Uniform Building Code* (UBC) was published (ICBO, 1927). It was the first model building code to contain provisions for earthquake resistant design, albeit in an appendix. In addition to that, a committee began working on what would become California's first state-wide seismic code in 1939.

Another earthquake struck Southern California in Long Beach in 1933. The most significant aspect of that earthquake was the damage done to school buildings. Fortunately the earthquake occurred after school hours, but it did cause concern over the vulnerabilities of these buildings. That concern led to the Field Act, which set forth standards and regulations for earthquake resistance of school buildings. This was the first instance of what has become a philosophy engrained in the earthquake design standards: Requiring higher levels of safety and performance for certain buildings society deems more important that a typical building. In addition to the Field Act, the Long Beach earthquake led to a ban on unreinforced masonry construction in California, which in subsequent years was extended to all areas of moderate and high seismic risk.

Following the 1933 Long Beach Earthquake there was significant activity both in Northern and Southern California, with the local Structural Engineers Associations of each region drafting seismic design provisions for Los Angeles in 1943 and San Francisco in 1948. Development of these codes was facilitated greatly by observations from the 1940 El Centro Earthquake. Additionally, that earthquake was the first major earthquake where the strong ground motion shaking was recorded with an accelerograph.

A joint committee of the San Francisco Section of ASCE and the Structural Engineers Association of Northern California (SEAONC) began work on seismic design provisions which were published in 1951 as ASCE *Proceedings-Separate No. 66*. *Separate 66,* as it is commonly referred to*,* was a landmark document which set forth earthquake design provisions which formed the basis of US building codes for the next 40 years. Many concepts and recommendations put forth in *Separate 66*, such as the a period dependent design spectrum, different design forces based on the ductility of a structure and design provisions for architectural components are still found in today's standards.

Following *Separate 66*, the Structural Engineers Association of California (SEAOC) formed a Seismology committee and in 1959 put forth the first edition of the *Recommended Lateral Force Requirements*, commonly referred to as the "The SEAOC Blue Book." The Blue Book became the base document for updating and expanding the seismic design provisions of the Uniform Building Code (UBC), the model code adopted by most western states including California. SEAOC regularly updated the Blue Book from 1959 until 1999. Updates and new recommendations in each new edition of the Blue Book were incorporated into each subsequent edition of the UBC.

The 1964 Anchorage Earthquake and the 1971 San Fernando Earthquake both were significant events. Both earthquakes exposed significant issues with the way reinforced concrete structures would behave if not detailed for ductility. There were failures of large concrete buildings which had been designed to recent standards and those buildings had to be torn down. To most engineers and the public this was unacceptable performance.

Following the 1971 San Fernando Earthquake, the National Science Foundation gave the Applied Technology Council (ATC) a grant to develop more advanced earthquake design provisions. That project engaged over 200 preeminent experts in the field of earthquake engineering. The landmark report they produced in 1978, ATC 3-06, *Tentative Provisions for*

the Development of Seismic Regulations for Buildings (1978)*,* has become the basis for the current earthquake design standards. The *NEHRP Provisions* trace back to ATC 3-06, as will be discussed in more detail in the following section.

There have been additional earthquakes since the 1971 San Fernando Earthquake which have had significant influence on seismic design. Table 1 provides a summary of major North American earthquakes and changes to the building codes that resulted from them through the 1997 UBC. Of specific note are the 1985 Mexico City, 1989 Loma Prieta and 1994 Northridge Earthquakes.

Table 1: Recent North American Earthquakes and Subsequent Code Changes (from SEOAC, 2009)

Earthquake	UBC Edition	Enhancement
1971 San Fernando	1973	Direct positive anchorage of masonry and concrete walls to diaphragms
	1976	Seismic Zone 4, with increased base shear requirements
		Occupancy Importance Factor *I* for certain buildings
		Interconnection of individual column foundations
		Special Inspection requirements
1979 Imperial Valley	1985	Diaphragm continuity ties
1985 Mexico City	1988	Requirements for column supporting discontinuous walls
		Separation of buildings to avoid pounding
		Design of steel columns for maximum axial forces
		Restrictions for irregular structures
		Ductile detailing of perimeter frames
1987 Whittier Narrows	1991	Revisions to site coefficients
		Revisions to spectral shape
		Increased wall anchorage forces for flexible diaphragm buildings
1989 Loma Prieta	1991	Increased restrictions on chevron-braced frames
		Limitations on b/t ratios for braced frames
	1994	Ductile detailing of piles
1994 Northridge	1997	Restrictions on use of battered piles
		Requirements to consider liquefaction
		Near-fault zones and corresponding base shear requirements
		Revised base shear equations using 1/T spectral shape
		Redundancy requirements
		Design of collectors for overstrength
		Increase in wall anchorage requirements
		More realistic evaluation of design drift
		Steel moment connection verification by test

The 1985 Mexico City Earthquake was extremely devastating. Over 10,000 people were killed and there was the equivalent of $3 to $4 billion of damage. The most significant aspect of this earthquake was ground shaking with a much longer period and larger amplitudes than would be expected from typical earthquakes. While the epicenter was located over 200 miles away from Mexico City, the unique geologic nature of Mexico City sited on an ancient lake bed of silt and clay caused long period ground shaking that lasted for an extended duration. This long period shaking was much more damaging to mid-rise and larger structures because these buildings were in resonance with the ground motions. In current design practice site factors based on the underlying soil are used to modify the seismic hazard parameters to account for this effect.

The 1989 Loma Prieta Earthquake caused an estimated $6 billion in damage, although it was far less deadly than other major earthquakes throughout history. Only 63 people lost their lives, a testament to the over 40 years of awareness and consideration of earthquakes in the design of structures. A majority of those deaths, 42, resulted from the collapse of the Cyprus Street Viaduct, a nonductile concrete elevated freeway. In this earthquake the greatest damage occurred in Oakland, parts of Santa Cruz and the Marina District in San Francisco where the subsurface material was soft soil or poorly compacted fill. As with the Mexico City experience, this illustrated the importance of subsurface conditions on the amplification of earthquake shaking. The earthquake also highlighted the vulnerability of soft and weak story buildings. A significant number of the collapsed buildings in the Marina District were wood framed apartment buildings with weak first stories because of the garages door openings. Those openings greatly reduced the wall area at the first story.

Five years later the 1994 Northridge earthquake struck California near Los Angeles. Fifty seven people lost their lives and the damage was estimated at around $20 billion. The high cost of damage repair emphasized the need for engineers to consider overall building performance, in addition to building collapse, and spurred the movement toward Performance-Based design. As with the 1989 Loma Prieta earthquake, there was a disproportionate number of collapses of soft/weak first story wood framed apartment buildings.

The most significant issue from the 1994 Northridge Earthquake was the unanticipated damage to steel moment frames that was discovered. Steel moment frames had generally been thought of as the best seismic force resisting system due to their good performance in the 1906 San Francisco Earthquake. However, many moment frames experienced fractures of the weld that connected the beam flange to the column flange. This led to a multi-year, FEMA funded problem-focused study to assess and improve the seismic performance of steel moment frames. It also led to requirements for the number of frames in a structure, and penalties for having a lateral force resisting system that does not have sufficient redundancy.

The profession is still learning from earthquakes. The 2010 Chile earthquake has led to updates in the design provisions for concrete wall structures, which have been incorporated into the latest edition of the ACI 318 standard referenced in the *Provisions*. The 2011 Christchurch Earthquake spurred significant changes to the design of egress stairs in the *Standard*.

1.2 HISTORY AND ROLE OF THE NEHRP PROVISIONS

Following the completion of the ATC 3 project in 1978, there was desire to make the ATC 3-06 approach the basis for new regulatory provisions and to update them periodically. FEMA, as the lead agency of the National Earthquake Hazard Reduction Program (NEHRP) at the time, contracted with the then newly formed Building Seismic Safety Council (BSSC) to perform trial designs based on ATC 3-06 to exercise the proposed new provisions. The BSSC put together a group of experts consisting of consulting engineers, academics, representatives from various building industries and building officials. The result of that effort was the first (1985) edition of the *NEHRP Recommended Provisions for the Development of Seismic Regulations for New Buildings*.

Since the publication of the first edition through the 2003 edition, the *NEHRP Provisions* were updated every three years. Each update incorporated recent advances in earthquake engineering research and lessons learned from previous earthquakes. The intended purpose of the *Provisions* was to serve as a code resource document. While the SEAOC Blue Book continued to serve as the basis for the earthquake design provisions in the *Uniform Building Code,* the *BOCA National Building Code* and the *Standard Building Code* both adopted the 1991 *NEHRP Provisions* in their 1993 and 1994 editions respectively. The 1993 version of the ASCE 7 standard *Minimum Design Loads for Buildings and Other Structures* (which had formerly been American National Standards Institute (ANSI) Standard A58.1) also utilized the 1991 *NEHRP Provisions*.

In the late 1990's the three major code organizations, ICBO (publisher of the UBC), BOCA, and SBC decided to merge their three codes into one national model code. When doing so they chose to incorporate the 1997 *NEHRP Provisions* as the seismic design requirements for the inaugural 2000 edition of the *International Building Code* (IBC). Thus, the SEAOC Blue Book was no longer the base document for the UBC/IBC. The 1997 *NEHRP Provisions* had a number of major changes. Most significant was the switch from the older seismic maps of ATC 3-06 to new, uniform hazard spectral value maps produced by USGS in accordance with BSSC Provisions Update Committee (PUC) Project 97. The 1998 edition of ASCE 7 was also based on the 1997 *NEHRP Provisions*.

ASCE 7 continued to incorporate the 2000 and 2003 editions of the *Provisions* for its 2002 and 2005 editions, respectively. However, the 2000 IBC adopted the 1997 *NEHRP Provisions* by directly transferring the text from the provisions into the code. In the 2003 IBC the provisions from the 2000 IBC were retained and there was also language, for the first time, which pointed the user to ASCE 7-02 for seismic provisions instead of adopting the 2000 *NEHRP Provisions* directly. The 2006 IBC explicitly referenced ASCE 7 for the earthquake design provisions, as did the 2009 and 2012 editions.

With the shift in the IBC from directly incorporating the *NEHRP Provision* for their earthquake design requirements to simply referencing the provisions in ASCE 7, the 2009 BSSC Provisions Update Committee decided to move the *2009 NEHRP Provisions* in a new direction. Instead of providing all the seismic design provisions within the *NEHRP Provisions*, which would essentially be repeating the provisions in ASCE 7, and then modifying them, the PUC chose to adopt ASCE 7-05 by reference and then provide recommendations to modify it as necessary. Therefore, Part 1 of the *2009 NEHRP Provisions* contained major technical modifications to

ASCE 7-05 which, along with other recommendations from the ASCE 7 Seismic Subcommittee, were the basis for proposed changes that were incorporated into ASCE 7-10 and included associated commentary on those changes. The PUC also developed a detailed commentary to the seismic provisions of ASCE 7-05, which became Part 2 of the *2009 NEHRP Provisions*.

In addition to Part 1 and Part 2 in the *2009 NEHRP Provisions*, a new section was introduced – Part 3. The intent of this new portion was to showcase new research and emerging methods, which the PUC did not feel was ready for adoption into national design standards but was important enough to be disseminated to the profession. This new three part format marked a change in the *Provisions* from a code-language resource document to the key knowledge-based resource for improving the national seismic design standards and codes.

The *2015 NEHRP Provisions* follows the same three part format as the *2009 NEHRP Provisions*. Part 1 provides recommended technical changes to ASCE 7-10 including Supplements 1 and 2. Those changed from Part 1 of the *2015 NEHRP Provisions* have been adopted, with some modifications, into ASCE 7-16. Part 2 contains an updated expanded commentary to ASCE 7-10, including commentary associated with the recommended technical changes from Part 1. In the 2015 Provisions several chapters in ASCE 7 were completely re-written, those dealing with nonlinear response history analysis, seismic isolation, supplemental energy dissipation, and soil-structure interaction. In addition to the new chapters, significant changes were made to the seismic design parameters through new site factors and new requirements for when site specific spectra are required, updated linear analysis procedures, a new diaphragm design methodology, and a new procedure for designing structures on liquefiable soils.

Part 3 of the 2015 NEHRP Provisions contains five new resource papers. The resource papers form the 2009 NEHRP Provisions were evaluated by the 2015 NEHRP Provisions Update Committee. In some cases the material from the 2009 resource papers formed the basis for or were Part 1 recommended technical changes in the 2015 NEHRP Provisions, such as ultimate strength design of foundations, nonlinear response history analysis, and the new diaphragm provisions. A number of papers were removed from Part 3 because the 2015 NEHRP Provisions Update Committee chose not to carry those papers forward. That decision does not necessarily mean that the information contained in the papers is not valid anymore, but that either new modifications to the *2015 NEHRP Provisions* eliminated the need for the paper or the material in the paper need only be correlated with Part 1 changes in the *2015 NEHRP Provisions* and material standards to be referred to as it is published in Part 3 of the *2009 NEHRP Provisions*. Today, someone needing to design a seismically resilient building in the U.S. would first go to the local building code which has generally adopted the IBC with or without modifications by the local jurisdiction. For seismic design requirements, the building code typically points to relevant Chapters of ASCE 7. Those chapters of ASCE 7 set forth the seismic hazard, design forces and system detailing requirements. The seismic forces in ASCE 7 are dependent upon the type of detailing and specific requirements of the lateral force resisting system elements. ASCE 7 then points to material specific requirements found in the material design standards published by ACI, AISC, AISI, AF&PA and TMS for those detailing requirements. Within this structure, the NEHRP Provisions serves as a consensus evaluation of the design standards and a vehicle to transfer new knowledge to ASCE 7 and the material design standards.

1.3 THE NEHRP DESIGN EXAMPLES

Design examples were first prepared for the 1985 *NEHRP Provisions* in a publication entitled *Guide to Application of the NEHRP Recommended Provisions*, FEMA 140. These design examples were based on real buildings. The intent was the same as it is now, to show people who are not familiar with seismic design of how to apply the *Provisions*, the standards referenced by the *Provisions* and the concepts behind the *Provisions*.

Because of the expanded role that the *Provisions* were having as the basis for the seismic design requirements for the model codes and standards, it was felt that there should be an update and expansion of the original design examples. Following the publication of the 2003 NEHRP Provisions, FEMA commissioned a project to update and expand the design examples. This resulted in *NEHRP Recommended Provisions: Design Examples,* FEMA 451. Many of the design problems drew heavily on the examples presented in FEMA 140, but were completely redesigned based on first the 2000 and then the 2003 *NEHRP Provisions* and the materials standards referenced therein. Additional examples were created to reflect the myriad of structures now covered under the *Provisions*.

With the 2009 update to the *NEHRP Provisions,* the Design Examples were revised and expanded upon and published as FEMA 751. This volume is an update of the design examples in FEMA 751 to reflect the *2015 NEHRP Provisions* and the updated standards referenced therein. Many of the design examples are the same as presented in FEMA 751, with only changes made due to changes in the provisions. There are also several new examples to illustrate new material or significant changes from Part 1 of the *2015 NEHRP Provisions.*

The *Design Examples* not only covers the application of ASCE 7, the material design standards and the *NEHRP Provisions*, it also illustrates the use of analysis methods and earthquake engineering knowledge and judgment in situations which would be encountered in real designs. The authors of the design examples are subject matter experts in the specific area covered by the chapter they authored. Furthermore, the companion *NEHRP Recommend Provisions: Training Materials* provides greater background information and knowledge, which augment the design examples.

It is hoped that with the Part 2 Expanded Commentary in the *2015 NEHRP Provisions*, the *Design Examples* and the *Training Materials*, an engineer will be able to understand not just how to use the Provisions, but also the philosophical and technical basis behind the provisions. Through this understanding of the intent of the seismic design requirements found in ASCE 7, the material design standards and the *2015 NEHRP Provisions*, it is hoped that more engineers will find the application of those standards less daunting and thereby utilize the standards more effectively in creating innovative and safe designs.

Chapter 2 – Fundamentals presents a brief but thorough introduction to the fundamentals of earthquake engineering. While this section does not present any specific applications of the *Provisions,* it provides the reader with the essential philosophical background to what is contained within the *Provisions*. The concepts of idealizing a seismic dynamic load as an equivalent static load and providing ductility instead of pure elastic strength are explained.

Chapter 3 - Earthquake Ground Motion explains the basis for determining seismic hazard parameters used for design in the *Provisions*. It discusses the updated Risk Targeted maps found in the *2015 NEHRP Provisions* and ASCE 7-16. The chapter also discusses probabilistic seismic hazard assessment, the maximum direction response parameters, the development of a site specific response spectrum and selection and scaling of ground motion histories for use in linear and nonlinear response history analysis.

Chapter 4 – Liner Structural Analysis presents the analysis of a building using the equivalent lateral force procedure, a modal response spectrum analysis and the new linear response history analysis procedure. The three analysis procedures are compared to illustrate the difference in results between them. This chapter is a complete re-write from the previous chapter, but uses a similar building as was used in the previous *Design Examples.* That is because significant changes were made to the modal response spectrum analysis provisions and the linear response history procedures were completely rewritten in the *2015 NEHRP Provisions*.

Chapter 5 – Nonlinear Response History Analysis presents the analysis of a building new nonlinear response history analysis procedure contained in the *Provisions* and the *Standard.* This chapter illustrates how the new procedures in Chapter 16 can be used to perform a performance-based design of a tall concrete core wall building with features that would not be permitted under Chapter 12 of the *Standard.* How the linear analysis of Chapter 12 is used in conjunction with the nonlinear analysis procedures is also illustrated.

Chapter 6 – Horizontal Diaphragm Analysis presents an example of the determination of diaphragm design forces using the tradition diaphragm design force method in the *Standard* and the new alternate diaphragm design method in the *Provisions* first in general then for several example buildings. The design forces levels between the traditional and the alternative methods are compared.

Chapter 7 – Foundation and Liquefaction Design presents design examples for both shallow and deep foundations using the ultimate strength design in Part 1 of the *Provisions* and illustrates the new liquefaction design provisions. First, a spread footing foundation for a 7-story steel framed building is presented. Second the design of a pile foundation for a 12-story concrete moment frame building is presented. Designs of the steel and concrete structures whose foundations are designed in this chapter are presented in Chapters 9 and 10 respectively. Lastly, the chapter presents examples on the design and detailing of foundation systems on liquefiable soils based on the new material in the *Provisions.*

Chapter 8 – Soil Structure Interaction presents the design of a four story reinforced concrete shear wall building with and without the use of the new soil-structure interaction chapter of the *Provisions.* The example first illustrates the effect that foundation damping soil-structure interaction has on reducing the design forces for stiff buildings with shallow foundations on soft subsurface material. The example also illustrates how kinematic soil-structure interaction can alter the foundation input response spectrum from the free-field spectrum and how that SSI modified spectrum affects the nonlinear response history analysis of a structure. This chapter also provides discussion and explanation of the restrictions on the use of soil structure interaction.

Chapter 9 – Structural Steel Design presents the design of three different types of steel buildings. The first building is a high-bay industrial warehouse which uses an ordinary concentric braced frame in one direction and an intermediate steel moment frame in the other direction. The second example is a 7-story office building which is designed using two alternate framing systems, special steel moment frames and special concentric braced frames. The majority of the changes in this chapter relates to changes made in the material design standards.

Chapter 10 – Reinforced Concrete presents the designs of a 12-story office building located in moderate and high seismicity. The same building configuration is used in both cases, but in the moderate seismicity region "Intermediate" moment frames are used while "Special" moment frames are used in the high seismicity region. Also in the high seismicity region, special concrete walls are needed in one direction and their design is presented. The majority of the changes in this chapter relates to changes made in the material design standards.

Chapter 11 – Precast Concrete Design presents examples of four common cases where precast concrete elements are a component of a seismic force resisting system. The first example presents the design of precast concrete panels being used as horizontal diaphragms both with and without a concrete topping slab based on the new diaphragm analysis procedure and updated requirements for precast concrete diaphragms. The second example presents the design of 3-story office building using intermediate precast concrete shear walls in a region of low or moderate seismicity The third example presents the design of a one-story tilt-up concrete industrial building in a region of high seismicity. The last example presents the design of a precast Special Moment Frame.

Chapter 12 – Composite Steel and Concrete presents the design of a 4-story medical office building in a region of moderate seismicity. The building uses composite partially restrained moment frames in both directions as the lateral force resisting system.

Chapter 13 – Masonry presents the design of two common types of buildings using reinforced masonry walls as their lateral force resisting system. The first example is a single-story masonry warehouse building with tall, slender walls. The second example is a five-story masonry hotel building with a bearing wall system designed in areas with different seismicity. The majority of the changes in this chapter relate to changes made in the material design standards.

Chapter 14 – Wood Design presents the design of a variety of wood elements in common seismic force resisting applications. The first example is a three-story, wood-frame apartment building. The second example illustrates the design of the roof diaphragm and wall-to-roof anchorage for the masonry building featured in the first example of Chapter 13 using both the traditional diaphragm analysis procedure in the *Standard* and the new alternate diaphragm analysis procedure from the *Provisions.*

Chapter 15 – Seismically Isolated Structures presents both the basic concepts of seismic isolation and then the design of an essential facility using a seismic isolation system. The example building has a special concentrically braced frame superstructure and uses lead rubber bearing. The example illustrates the significantly revised provisions, including the provision which now allows for the use of an ordinary braced frame above the isolation plane.

Chapter 16 – Structures with Supplemental Energy Dissipation Devices presents both the basic concepts of designing a structure with supplemental energy dissipation devices (dampers) and then the design of steel moment frame building with fluid viscous dampers. This example is new to the *Design Examples* and illustrates the major revisions that were made to the damping chapter in the *Provisions*.

Chapter 17 – Nonbuilding Structure Design presents the design of various types of structures other than buildings that are covered by the nonbuidling structure *Provisions*. First there is a brief discussion about the difference between a nonbuilding structure and a nonstructural component. The first example is the design of a pipe rack, which is a nonbuilding structure similar to a building. The second example is of an industrial storage rack. The third example is a power generating plant with significant mass irregularities. The third example is a pier. The fourth examples are flat-bottomed storage tanks, which also illustrates how the *Provisions* are used in conjunction with industry design standards. The last example is of a tall, slender vertical storage vessel containing hazardous materials, which replaces an example of an elevated transformer.

Chapter 18 – Design for Nonstructural Components presents a discussion on the design of nonstructural components and their anchorage plus several design examples. The examples are of an architectural concrete wall panel, an egress stair, the supports for a large rooftop fan unit, the analysis and bracing of a piping system and an elevated vessel. The egress stair example in particular illustrates significant changes to the *Provisions* recognizing the importance of these nonstructural components.

1.4 REFERENCES

American Society of Civil Engineers, 1907, *The Effects of the San Francisco Earthquake of April 18, 1906,* New York, NY.

American Society of Civil Engineers, 1951, *Proceedings-Separate No. 66.,* New York, NY.

American Society of Civil Engineers, 2016, ASCE 7-16: *Minimum Design Loads for Buildings and Other Structures,* Reston, VA.

Applied Technology Council, 1978, ATC 3-06: *Tentative Provisions for the Development of Seismic Regulations for Buildings,* Redwood City, California.

Federal Emergency Management Agency, 2015, FEMA P-1050, *NEHRP Recommended Seismic Provisions for New Buildings and Other Structures*, Washington, D.C.

International Conference of Building Officials, 1927, *Uniform Building Code.* Whittier, CA.

Structural Engineers Association of California, *SEAOC Blue Book: Seismic Design Recommendations*, Sacramento, CA.

2

Fundamentals

James Robert Harris, P.E., PhD

Contents

In introducing their classic text, *Fundamentals of Earthquake Engineering*, Newmark and Rosenblueth (1971) comment:

> In dealing with earthquakes, we must contend with appreciable probabilities that failure will occur in the near future. Otherwise, all the wealth of the world would prove insufficient to fill our needs: the most modest structures would be fortresses. We must also face uncertainty on a large scale, for it is our task to design engineering systems – about whose pertinent properties we know little – to resist future earthquakes and tidal waves – about whose characteristics we know even less. . . . In a way, earthquake engineering is a cartoon. . . . Earthquake effects on structures systematically bring out the mistakes made in design and construction, even the minutest mistakes.

Several points essential to an understanding of the theories and practices of earthquake-resistant design bear restating:

1. Ordinarily, a large earthquake produces the most severe loading that a building is expected to survive. The probability that *failure* will occur is very real and is greater than for other loading phenomena. Also, in the case of earthquakes, the definition of *failure* is altered to permit certain types of behavior and damage that are considered unacceptable in relation to the effects of other phenomena.

2. The levels of uncertainty are much greater than those encountered in the design of structures to resist other phenomena. This is in spite of the tremendous strides made since the Federal government began strongly supporting research in earthquake engineering and seismology following the 1964 Prince William Sound and 1971 San Fernando earthquakes. The high uncertainty applies both to knowledge of the loading function and to the resistance properties of the materials, members and systems.

3. The details of construction are very important because flaws of no apparent consequence often will cause systematic and unacceptable damage simply because the earthquake loading is so severe and an extended range of behavior is permitted.

The remainder of this chapter is devoted to a very abbreviated discussion of fundamentals that reflect the concepts on which earthquake-resistant design are based. When appropriate, important aspects of the *NEHRP Recommended Seismic Provisions for New Buildings and Other Structures* are mentioned and reference is made to particularly relevant portions of that document or the standards that are incorporated by reference. The *2015 Provisions* is composed of three parts: 1) "Provisions", 2) "Commentary on ASCE/SEI 7-2010" and 3) "Resource Papers on Special Topics in Seismic Design". Part 1 states the intent and then cites ASCE/SEI 7-2010 *Minimum Design Loads for Buildings and Other Structures* as the primary reference. The remainder of Part 1 contains recommended changes to update ASCE/SEI 7-2010; the recommended changes include commentary on each specific recommendation. All three parts are referred to herein as the *Provisions,* but where pertinent the specific part is referenced and ASCE/SEI 7-2010 is referred to as the *Standard*. ASCE/SEI 7-2010 itself refers to several other standards for the seismic design of structures composed of specific materials and those standards are essential elements to achieve the intent of the *Provisions*.

2.1 EARTHQUAKE PHENOMENA

According to the most widely held scientific belief, most earthquakes occur when two segments of the earth's crust suddenly move in relation to one another. The surface along which movement occurs is

known as a fault. The sudden movement releases strain energy and causes seismic waves to propagate through the crust surrounding the fault. These waves cause the surface of the ground to shake violently, and it is this ground shaking that is the principal concern of structural engineering to resist earthquakes.

Earthquakes have many effects in addition to ground shaking. For various reasons, the other effects generally are not major considerations in the design of buildings and similar structures. For example, seismic sea waves or tsunamis can cause very forceful flood waves in coastal regions, and seiches (long-period sloshing) in lakes and inland seas can have similar effects along shorelines. These are outside the scope of the *Provisions*. This is not to say, however, that they should not be considered during site exploration and analysis. Designing structures to resist such hydrodynamic forces is a very specialized topic, and it is common to avoid constructing buildings and similar structures where such phenomena are likely to occur. Long-period sloshing of the liquid contents of tanks is addressed by the *Provisions*.

Abrupt ground displacements occur where a fault intersects the ground surface. (This commonly occurs in California earthquakes but apparently did not occur in the historic Charleston, South Carolina, earthquake or the very large New Madrid, Missouri, earthquakes of the nineteenth century.) Mass soil failures such as landslides, liquefaction and gross settlement are the result of ground shaking on susceptible soil formations. Once again, design for such events is specialized, and it is common to locate structures so that mass soil failures and fault breakage are of no major consequence to their performance. Modification of soil properties to protect against liquefaction is one important exception; large portions of a few metropolitan areas with the potential for significant ground shaking are susceptible to liquefaction. Lifelines that cross faults require special design beyond the scope of the *Provisions*. The structural loads specified in the *Provisions* are based solely on ground shaking; they do not provide for ground failure. Resource Paper 12 ("Evaluation of Geologic Hazards and Determination of Seismic Lateral Earth Pressures") in Part 3 of the *Provisions* includes a description of current procedures for prediction of seismic-induced slope instability, liquefaction and surface fault rupture.

Nearly all large earthquakes are *tectonic* in origin – that is, they are associated with movements of and strains in large segments of the earth's crust, called *plates*, and virtually all such earthquakes occur at or near the boundaries of these plates. This is the case with earthquakes in the far western portion of the United States where two very large plates, the North American continent and the Pacific basin, come together. In the central and eastern United States, however, earthquakes are not associated with such a plate boundary, and their causes are not as completely understood. This factor, combined with the smaller amount of data about central and eastern earthquakes (because of their infrequency), means that the uncertainty associated with earthquake loadings is higher in the central and eastern portions of the nation than in the West. Even in the West, the uncertainty (when considered as a fraction of the predicted level) about the hazard level is probably greater in areas where the mapped hazard is low than in areas where the mapped hazard is high.

The amplitude of earthquake ground shaking diminishes with distance from the source, and the rate of attenuation is less for lower frequencies of motion than for higher frequencies. This effect is captured, to an extent, by the fact that the *Provisions* use three parameters to define the hazard of seismic ground shaking for structures. Two are based on statistical analysis of the database of seismological information: the S_S values are pertinent for higher frequency motion, and the S_1 values are pertinent for other middle frequencies. The third value, T_L, defines an important transition point for long period (low frequency) behavior; it is not based upon as robust an analysis as the other two parameters.

Two basic data sources are used in establishing the likelihood of earthquake ground shaking, or seismicity, at a given location. The first is the historical record of earthquake effects and the second is the geological record of earthquake effects. Given the infrequency of major earthquakes, there is no place in the United States where the historical record is long enough to be used as a reliable basis for earthquake

prediction – certainly not as reliable as with other phenomena such as wind and snow. Even on the eastern seaboard, the historical record is too short to justify sole reliance on the historical record. Thus, the geological record is essential. Such data require very careful interpretation, but they are used widely to improve knowledge of seismicity. Geological data have been developed for many locations as part of the nuclear power plant design process. On the whole, there is more geological data available for the far western United States than for other regions of the country. Both sets of data have been taken into account in the *Provisions* seismic ground shaking maps.

The *Commentary* provides a more thorough discussion of the development of the maps, their probabilistic basis, the necessarily crude lumping of parameters and other related issues. Prior to its 1997 edition, the basis of the *Provisions* was to "provide *life safety* at the design earthquake motion," which was defined as having a 10 percent probability of being exceeded in a 50-year reference period. As of the 1997 edition, the basis became to "avoid *structural collapse* at the maximum considered earthquake (MCE) ground motion," which is defined as having a 2 percent probability of being exceeded in a 50-year reference period. In the 2015 edition of the *Provisions* the design basis has been refined to target a 1% probability of structural collapse for ordinary buildings in a 50 year period. The MCE ground motion has been adjusted to deliver this level of risk combined with a 10% probability of collapse should the MCE ground motion occur. This new approach incorporates a fuller consideration of the nature of the seismic hazard at a location than was possible with the earlier definitions of ground shaking hazard, which were tied to a single level of probability of ground shaking occurrence.

2.2 STRUCTURAL RESPONSE TO GROUND SHAKING

The first important difference between structural response to an earthquake and response to most other loadings is that the earthquake response is *dynamic*, not *static*. For most structures, even the response to wind is essentially static. Forces within the structure are due almost entirely to the pressure loading rather than the acceleration of the mass of the structure. But with earthquake ground shaking, the aboveground portion of a structure is not subjected to any applied force. The stresses and strains within the superstructure are created entirely by its dynamic response to the movement of its base, the ground. Even though the most used design procedure resorts to the use of a concept called the equivalent static force for actual calculations, some knowledge of the theory of vibrations of structures is essential.

2.2.1 Response Spectra

Figure 2.2-1 shows accelerograms, records of the acceleration at one point along one axis, for several representative earthquakes. Note the erratic nature of the ground shaking and the different characteristics of the different accelerograms. Precise analysis of the elastic response of an ideal structure to such a pattern of ground motion is possible; however, it is not commonly done for ordinary structures. The increasing power and declining cost of computational aids are making such analyses more common but, at this time, only a small minority of structures designed across the country, are analyzed for specific response to a specific ground motion.
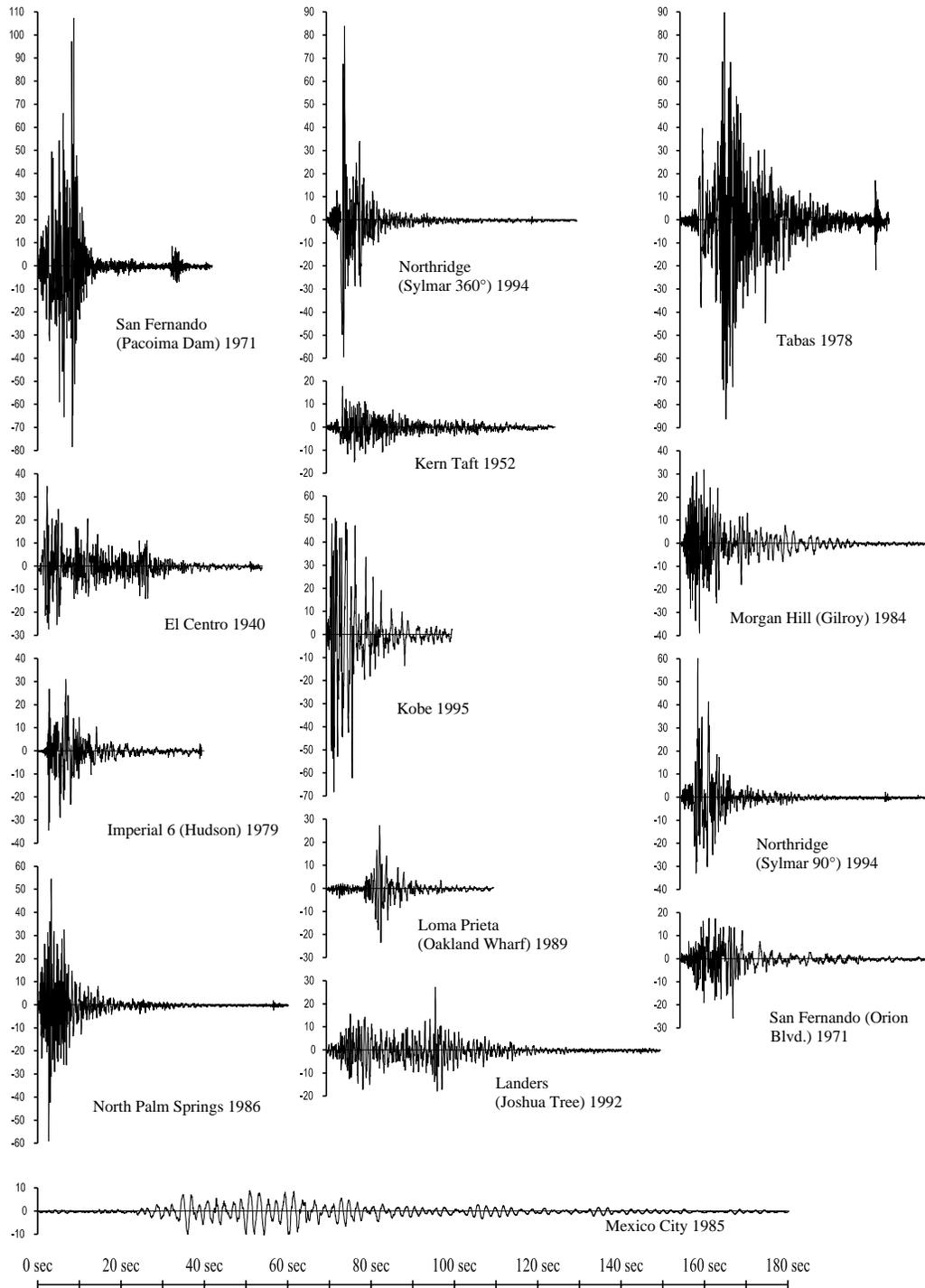
Figure 2.2-1 Earthquake Ground Acceleration in Epicentral Regions

Note: All accelerograms are plotted to the same scale for time and acceleration – the vertical axis is % gravity). Great earthquakes extend for much longer periods of time.)

Figure 2.2-2 shows further detail developed from an accelerogram. Part (a) shows the ground acceleration along with the ground velocity and ground displacement derived from it. Part (b) shows the acceleration, velocity and displacement for the same event at the roof of the building located where the ground motion was recorded. Note that the peak values are larger in the diagrams of Figure 2.2-2(b) (the vertical scales are essentially the same). This increase in response of the structure at the roof level over the motion of the ground itself is known as dynamic amplification. It depends very much on the vibrational characteristics of the structure and the characteristic frequencies of the ground shaking at the site.

(a) Motion at ground level   (b) Motion at roof
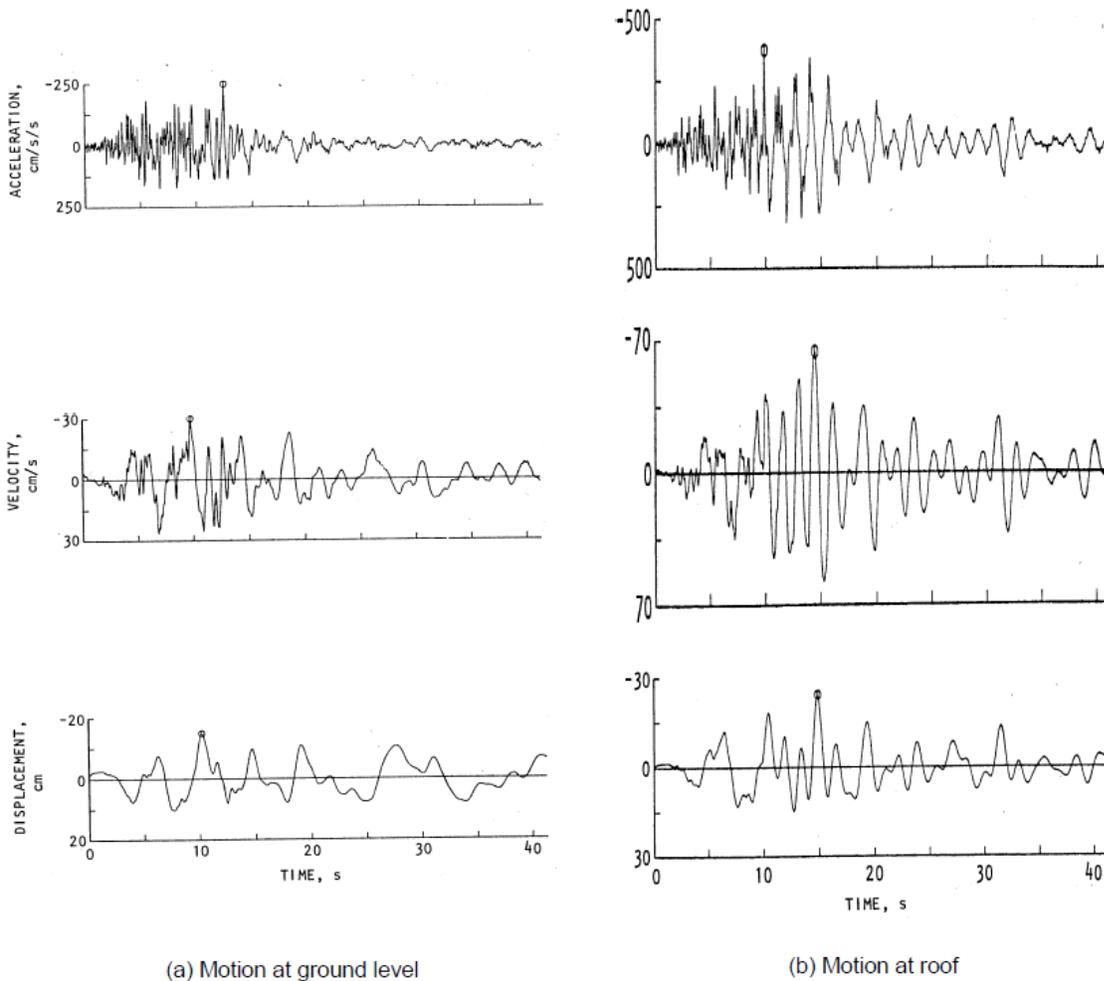
Figure 2.2-2 Holiday Inn Ground and Building Roof Motion During the M6.4 1971 San Fernando Earthquake: (a) north-south ground acceleration, velocity and displacement and (b) north-south roof acceleration, velocity and displacement (Housner and Jennings, 1982).

Note: The Holiday Inn, a 7-story, reinforced concrete frame building, was approximately 5 miles from the closest portion of the causative fault. The recorded building motions enabled an analysis to be made of the stresses and strains in the structure during the earthquake.

In design, the response of a specific structure to an earthquake is ordinarily estimated from a design response spectrum such as is specified in the *Provisions*. The first step in creating a design response spectrum is to determine the maximum response of a given structure to a specific ground motion (see Figure 2.2-2). The underlying theory is based entirely on the response of a single-degree-of-freedom oscillator such as a simple one-story frame with the mass concentrated at the roof. The vibrational characteristics of such a simple oscillator may be reduced to two: the natural period[1] and the amount of damping. By recalculating the record of response versus time to a specific ground motion for a wide range of natural periods and for each of a set of common amounts of damping, the family of response spectra for one ground motion may be determined. It is simply the plot of the maximum value of response for each combination of period and damping.

Figure 2.2-3 shows such a result for the ground motion of Figure 2.2-2(a) and illustrates that the erratic nature of ground shaking leads to a response that is very erratic in that a slight change in the natural period of vibration brings about a very large change in response. The figure also illustrates the significance of damping. Different earthquake ground motions lead to response spectra with peaks and valleys at different points with respect to the natural period. Thus, computing response spectra for several different ground motions and then averaging them, based on some normalization for different amplitudes of shaking, will lead to a smoother set of spectra. Such smoothed spectra are an important step in developing a design spectrum.

---

[1] Much of the literature on dynamic response is written in terms of frequency rather than period. The cyclic frequency (cycles per second, or Hz) is the inverse of period. Mathematically it is often convenient to use the angular frequency expressed as radians per second rather than Hz. The conventional symbols used in earthquake engineering for these quantities are T for period (seconds per cycle), f for cyclic frequency (Hz) and ω for angular frequency (radians per second). The word frequency is often used with no modifier; be careful with the units.
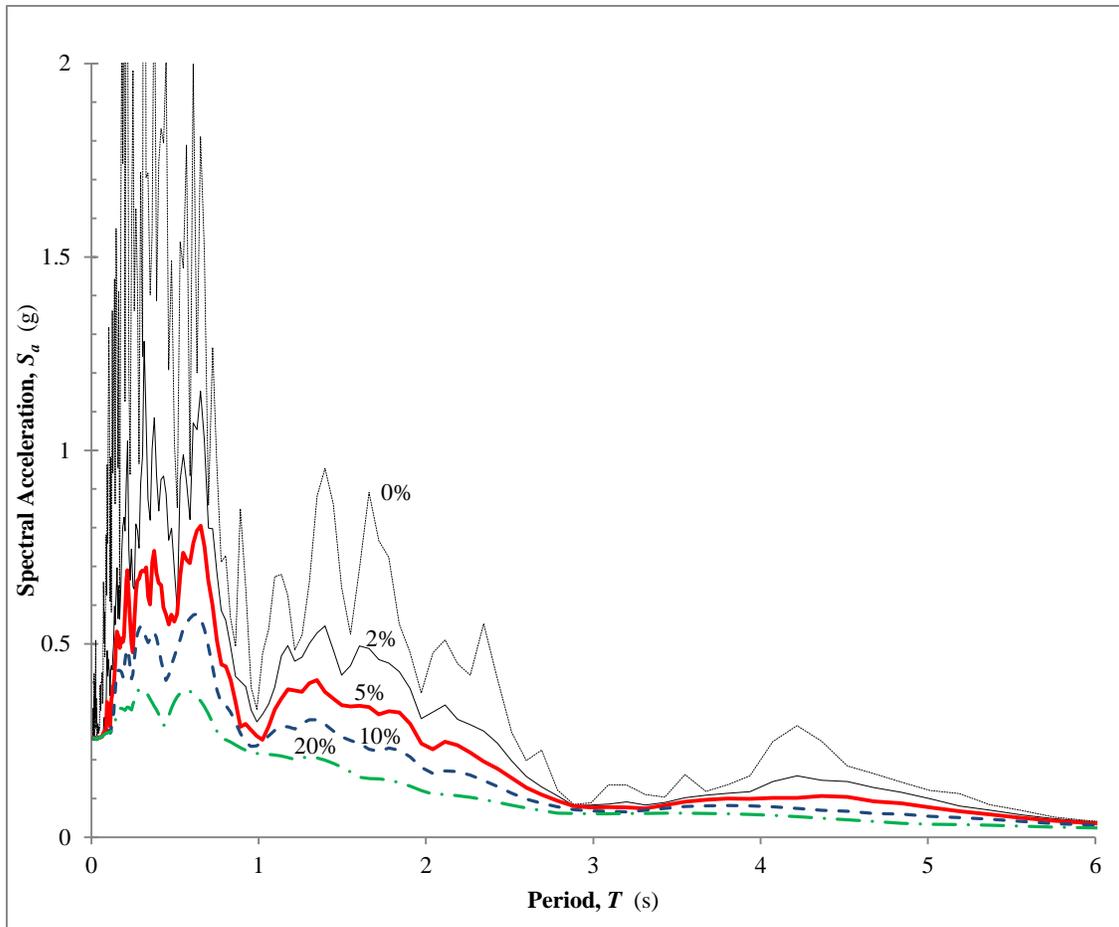
Figure 2.2-3 Response spectrum of north-south ground acceleration (0%, 2%, 5%, 10%, 20% of critical damping) recorded at the Holiday Inn, approximately 5 miles from the causative fault in the 1971 San Fernando earthquake.

Figure 2.2-4 is an example of an averaged spectrum. Note that acceleration, velocity, or displacement may be obtained from Figure 2.2-3 or 1.2-4 for a structure with known period and damping.
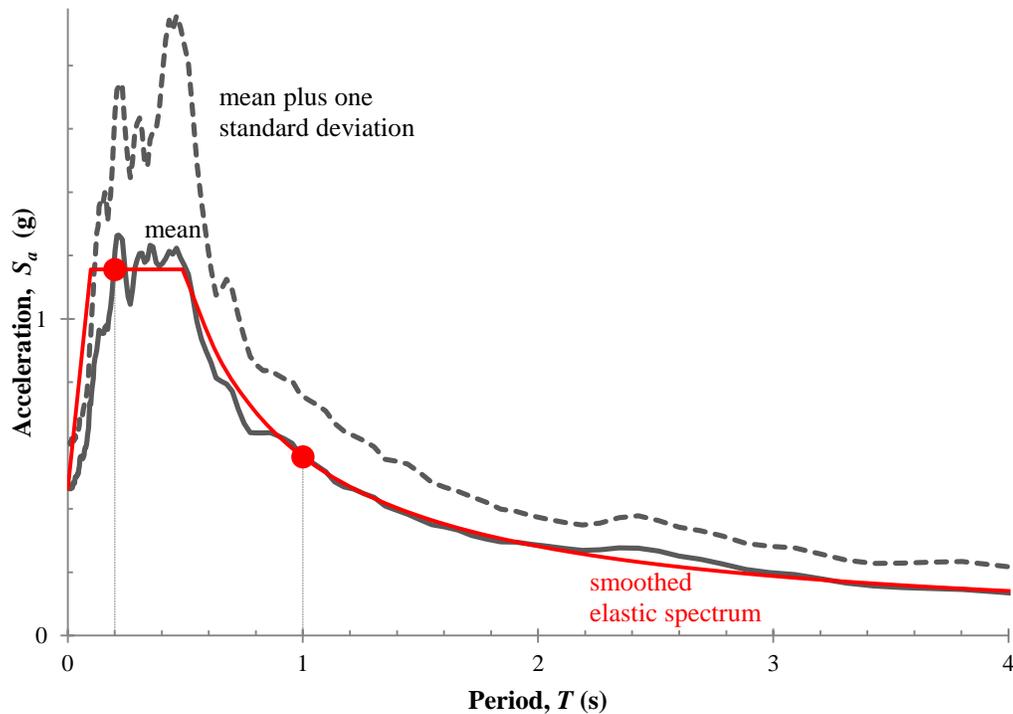
Figure 2.2-4 Averaged Spectrum

Note: In this case, the statistics are for seven ground motions representative of the de-aggregated hazard at a particular site.

Prior to the 1997 edition of the *Provisions*, the maps that characterized the ground shaking hazard were plotted in terms of peak ground acceleration (at period, T, = 0), and design response spectra were created using expressions that amplified (or de-amplified) the ground acceleration as a function of period and damping. With the introduction of the new maps in the 1997 edition, this procedure changed. Now the maps present spectral response accelerations at two periods of vibration, 0.2 and 1.0 second, and the design response spectrum is computed more directly, as implied by the smooth line in Figure 2.2-4. This has removed a portion of the uncertainty in predicting response accelerations.

Few structures are so simple as to actually vibrate as a single-degree-of-freedom system. The principles of dynamic modal analysis, however, allow a reasonable approximation of the maximum response of a multi-degree-of-freedom oscillator, such as a multistory building, if many specific conditions are met. The procedure involves dividing the total response into a number of natural modes, modeling each mode as an equivalent single-degree-of-freedom oscillator, determining the maximum response for each mode from a single-degree-of-freedom response spectrum and then estimating the maximum total response by statistically summing the responses of the individual modes. The *Provisions* does not require consideration of all possible modes of vibration for most buildings because the contribution of the higher modes (lower periods) to the total response is relatively minor.

The soil at a site has a significant effect on the characteristics of the ground motion and, therefore, on the structure's response. Especially at low amplitudes of motion and at longer periods of vibration, soft soils amplify the motion at the surface with respect to bedrock motions. This amplification is diminished somewhat, especially at shorter periods as the amplitude of basic ground motion increases, due to yielding in the soil. The *Provisions* accounts for this effect by providing amplifiers that are to be applied to the 0.2 and 1.0 second spectral accelerations for various classes of soils. (The ground motion maps in the *Provisions* are drawn for sites on rock.) Thus, very different design response spectra are specified

depending on the type of soil(s) beneath the structure. The *Commentary* (Part 2) contains a thorough explanation of this feature.

2.2.2 Inelastic Response

The preceding discussion assumes elastic behavior of the structure. The principal extension beyond ordinary behavior referenced at the beginning of this chapter is that structures are permitted to strain beyond the elastic limit in responding to earthquake ground shaking. This is dramatically different from the case of design for other types of loads in which stresses and therefore strains, are not permitted to approach the elastic limit. The reason is economic. Figure 2.2-3 shows a peak acceleration response of about 1.0 g (the acceleration due to gravity) for a structure with moderately low damping – for only a moderately large earthquake! Even structures that resist lateral forces well will have a static lateral strength of only 20 to 40 percent of gravity.

The dynamic nature of earthquake ground shaking means that a large portion of the shaking energy can be dissipated by inelastic deformations if the structure is ductile and some damage to the structure is accepted. Figure 2.2-5 will be used to illustrate the significant difference between wind and seismic effects. Figure 2.2-5(1) would represent a cantilever beam if the load W were small and a column if W were large. Wind pressures create a force on the structure, which in turn produces a displacement. The force is the independent variable and the displacement is the dependent result. Earthquake ground motion creates displacement between the base and the mass, which in turn produces an internal force. The displacement is the independent variable, and the force is the dependent result. Two graphs are plotted with the independent variables on the horizontal axis and the dependent response on the vertical axis. Thus, part (b) of the figure is characteristic of the response to forces such as wind pressure (or gravity weight), while part (c) is characteristic of induced displacements such as earthquake ground shaking (or foundation settlement).

Note that the ultimate resistance (H_u) in a force-controlled system is marginally larger than the yield resistance (H_y), while the ultimate displacement (Δ_u) in a displacement-controlled system is much larger than the yield displacement (Δ_y). The point being made with the figures is that ductile structures have the ability to resist displacements much larger than those that first cause yield.

The degree to which a member or structure may deform beyond the elastic limit is referred to as ductility. Different materials and different arrangements of structural members lead to different ductilities. Response spectra may be calculated for oscillators with different levels of ductility. At the risk of gross oversimplification, the following conclusions may be drawn:

1. For structures with very long natural periods, the acceleration response is reduced by a factor equivalent to the ductility ratio (the ratio of maximum usable displacement to effective yield displacement – note that this is displacement and not strain).

2. For structures with very short natural periods, the acceleration response of the ductile structure is essentially the same as that of the elastic structure, but the displacement is increased.

3. For intermediate periods (which applies to nearly all buildings), the acceleration response is reduced, but the displacement response is generally about the same for the ductile structure as for the elastic structure strong enough to respond without yielding.

<div align="center">

(a)   (b)   (c)

</div>
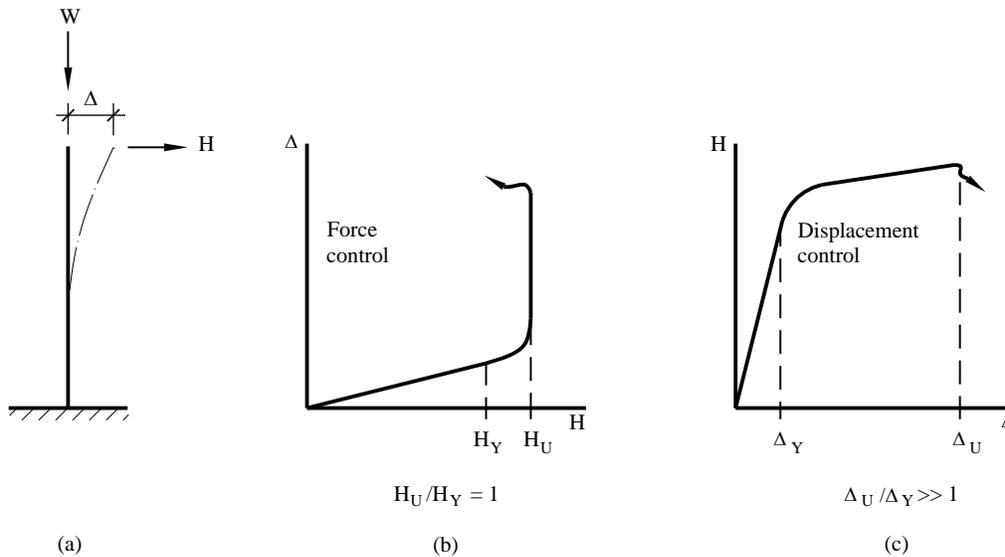
Figure 2.2-5 Force Controlled Resistance Versus Displacement Controlled Resistance (after Housner and Jennings 1982). In part (b) the force *H* is the independent variable. As *H* is increased, the displacement increases until the yield point stress is reached. If *H* is given an additional increment (about 15 percent) a plastic hinge forms, giving large displacements. For this kind of system, the force producing the yield point stress is close to the force producing collapse. The ductility does not produce a large increase in load capacity, although in highly redundant structures the increase is more than illustrated for this very simple structure. In part (c) the displacement is the independent variable.

Note: As the displacement is increased, the base moment increases until the yield point is reached. As the displacement increases still more, the resistance (*H*) increases only a small amount. For a highly ductile element, the displacement can be increased 10 to 20 times the yield point displacement before the system collapses under the weight *W*. (As *W* increases, this ductility is decreased dramatically.) During an earthquake, the oscillator is excited into vibrations by the ground motion and it behaves essentially as a displacement-controlled system and can survive displacements much beyond the yield point. This explains why ductile structures can survive ground shaking that produces displacements much greater than yield point displacement.

Inelastic response is quite complex. Earthquake ground motions involve a significant number of reversals and repetitions of the strains. Therefore, observation of the inelastic properties of a material, member, or system under a monotonically increasing load until failure can be very misleading. Cycling the deformation can cause degradation of strength, stiffness, or both. Systems that have a proven capacity to maintain a stable resistance to a large number of cycles of inelastic deformation are allowed to exercise a greater portion of their ultimate ductility in designing for earthquake resistance. This property is often referred to as toughness, but this is not the same as the classic definition used in mechanics of materials.

Most structures are designed for seismic response using a linear elastic analysis with the strength of the structure limited by the strength at its critical location. Most structures possess enough complexity so that the peak strength of a ductile structure is not accurately captured by such an analysis. Figure 2.2-6 shows the load versus displacement relation for a simple frame. Yield must develop at four locations before the peak resistance is achieved. The margin from the first yield to the peak strength is referred to as overstrength, and it plays a significant role in resisting strong ground motion. Note that a few key design standards (for example, American Concrete Institute (ACI) 318 for the design of concrete structures) do allow for some redistribution of internal forces from the critical locations based upon ductility; however,

the redistributions allowed therein are minor compared to what occurs in response to strong ground motion.

(a) Structures

(b) H - δ curve
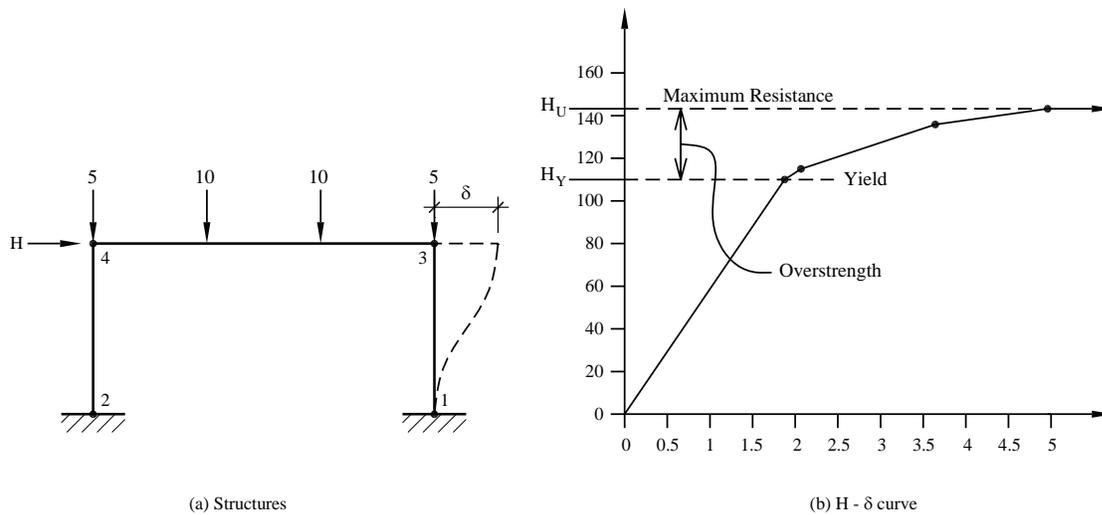
Figure 2.2-6 Initial Yield Load and Failure for a Ductile Portal Frame

Note: The margin from initial yield to failure (mechanism in this case) is known as overstrength.

To summarize, the characteristics important in determining a building's seismic response are natural period, damping, ductility, stability of resistance under repeated reversals of inelastic deformation and overstrength. The natural frequency is dependent on the mass and stiffness of the building. Using the *Provisions* the designer calculates, or at least approximates, the natural period of vibration (the inverse of natural frequency). Damping, ductility, toughness and overstrength depend primarily on the type of building system, but not the building's size or shape. Three coefficients – R, C_d and Ω_0 – are provided to encompass damping, ductility, stability of resistance and overstrength. R is intended to be a conservatively low estimate of the reduction of acceleration response in a ductile system from that for an elastic oscillator with a certain level of damping. It is used to compute a required strength. Computations of displacement based upon ground motion reduced by the factor R will underestimate the actual displacements. C_d is intended to be a reasonable mean for the amplification necessary to convert the elastic displacement response computed for the reduced ground motion to actual displacements. Ω_0 is intended to deliver a reasonably high estimate of the peak force that would develop in the structure. Sets of R, C_d and Ω_0 are specified in the *Provisions* for the most common structural materials and systems.

2.2.3 Building Materials

The following brief comments about building materials and systems are included as general guidelines only, not for specific application.

2.2.3.1 Wood. Timber structures nearly always resist earthquakes very well, even though wood is a brittle material as far as tension and flexure are concerned. It has some ductility in compression (generally monotonic), and its strength increases significantly for brief loadings, such as earthquake. Conventional timber structures (plywood, oriented strand board, or board sheathing on wood framing) possess much more ductility than the basic material primarily because the nails, and other steel connection devices yield, and the wood compresses against the connector. These structures also possess a much higher degree of damping than the damping that is assumed in developing the basic design spectrum. Much of this damping is caused by slip at the connections. The increased strength, connection ductility, and high damping combine to give timber structures a large reduction from elastic response to design level. This large reduction should not be used if the strength of the structure is actually controlled by bending or tension of the gross timber cross sections. The large reduction in acceleration combined with the light weight timber structures make them very efficient with regard to earthquake ground shaking when they are properly connected. This is confirmed by their generally good performance in earthquakes. Capacities and design and detailing rules for wood elements of seismic force-resisting systems are now found in the *Special Design Provisions for Wind and Seismic* supplement to the *National Design Specification for Wood Construction*.

2.2.3.1 Steel. Steel is the most ductile of the common building materials. The moderate-to-large reduction from elastic response to design response allowed for steel structures is primarily a reflection of this ductility and the stability of the resistance of steel. Members subject to buckling (such as bracing) and connections subject to brittle fracture (such as partial penetration welds under tension) are much less ductile and are addressed in the *Provisions* in various ways. Defects, such as stress concentrations and flaws in welds, also affect earthquake resistance as demonstrated in the Northridge earthquake. The basic and applied research program that grew out of that experience has greatly increased knowledge of how to avoid low ductility details in steel construction. Capacities and design and detailing rules for seismic design of hot-rolled structural steel are found in the *Seismic Provisions for Structural Steel Buildings* (American Institute of Steel Construction (AISC) Standard 341) and similar provisions for cold-formed steel are found in the "Lateral Design" supplement to the *North American Specification for the Design of Cold-Formed Steel Structures* published by AISI (American Iron and Steel Institute).

2.2.3.1 Reinforced Concrete. Reinforced concrete achieves ductility through careful limits on steel in tension and concrete in compression. Reinforced concrete beams with common proportions can possess ductility under monotonic loading even greater than common steel beams; in which local buckling is usually a limiting factor. Providing stability of the resistance to reversed inelastic strains, however, requires special detailing. Thus, there is a wide range of reduction factors from elastic response to design response depending on the detailing for stable and assured resistance. The *Commentary* and the commentary with the ACI 318 standard *Building Code Requirements for Structural Concrete* explain how to design to control premature shear failures in members and joints, buckling of compression bars, concrete compression failures (through confinement with transverse reinforcement), the sequence of plastification and other factors, which can lead to large reductions from the elastic response.

2.2.3.1 Masonry. Masonry is a more complex material than those mentioned above and less is known about its inelastic response characteristics. For certain types of members (such as pure cantilever shear walls), reinforced masonry behaves in a fashion similar to reinforced concrete. The nature of masonry construction, however, makes it difficult, if not impossible, to take some of the steps (e.g., confinement of compression members) used with reinforced concrete to increase ductility, and stability. Further, the

discrete differences between mortar, grout and the masonry unit create additional failure phenomena. Thus, the response reduction factors for design of reinforced masonry are not quite as large as those for reinforced concrete. Unreinforced masonry possesses little ductility or stability, except for rocking of masonry piers on a firm base and very little reduction from the elastic response is permitted. Capacities and design and detailing rules for seismic design of masonry elements are contained within The Masonry Society (TMS) 402 standard *Building Code Requirements for Masonry Structures*.

2.2.3.1 Precast Concrete. Precast concrete obviously can behave quite similarly to reinforced concrete but it also can behave quite differently. The connections between pieces of precast concrete commonly are not as strong as the members being connected. Clever arrangements of connections can create systems in which yielding under earthquake motions occurs away from the connections, in which case the similarity to reinforced concrete is very real. Some carefully detailed connections also can mimic the behavior of reinforced concrete. Many common connection schemes, however, will not do so. Successful performance of such systems requires that the connections perform in a ductile manner. This requires some extra effort in design but it can deliver successful performance. As a point of reference, the most common wood seismic resisting systems perform well yet have connections (nails) that are significantly weaker than the connected elements (structural wood panels). The *Provisions* includes guidance, some only for trial use and comment (Part 3), for seismic design of precast structures. ACI 318 also includes provisions for precast concrete elements resisting seismic forces, and there are also supplemental ACI standards for specialized seismic force-resisting systems of precast concrete.

2.2.3.1 Composite Steel and Concrete. Reinforced concrete is a composite material. In the context of the *Provisions*, *composite* is a term reserved for structures with elements consisting of structural steel and reinforced concrete acting in a composite manner. These structures generally are an attempt to combine the most beneficial aspects of each material. Capacities and design and detailing rules are found in the *Seismic Provisions for Structural Steel Buildings* (AISC Standard 341).

2.2.4   Building Systems

Three basic lateral-load-resisting elements – walls, braced frames and unbraced frames (moment resisting frames) – are used to build a classification of structural types in the *Provisions*. Unbraced frames generally are allowed greater reductions from elastic response than walls and braced frames. In part, this is because frames are more redundant, having several different locations with approximately the same stress levels and common beam-column joints frequently exhibit an ability to maintain a stable response through many cycles of reversed inelastic deformations. Systems using connection details that have not exhibited good ductility and toughness, such as unconfined concrete and the welded steel joint used before the Northridge earthquake, are penalized: the *R* factors permit less reduction from elastic response.

Connection details often make development of ductility difficult in braced frames, and buckling of compression members also limits their inelastic response. The actual failure of steel bracing often occurs because local buckling associated with overall member buckling frequently leads to locally high strains that then lead to brittle fracture when the member subsequently approaches yield in tension. Eccentrically braced steel frames and new proportioning and detailing rules for concentrically braced frames have been developed to overcome these shortcomings. But the newer and potentially more popular bracing system is the buckling-restrained braced frame. This new system has the advantages of a special steel concentrically braced frame, but with performance that is superior as brace buckling is controlled to preserve ductility. Design provisions appear in the *Seismic Provisions for Structural Steel Buildings* (AISC Standard 341).

Shear walls that do not bear gravity load are allowed a greater reduction than walls that are load bearing. Redundancy is one reason; another is that axial compression generally reduces the flexural ductility of concrete and masonry elements (although small amounts of axial compression usually improve the performance of materials weak in tension, such as masonry and concrete). The 2010 earthquake in Chile is expected to lead to improvements in understanding and design of reinforced concrete shear wall systems because of the large number of significant concrete shear wall buildings subjected to strong shaking in that earthquake. Systems that combine different types of elements are generally allowed greater reductions from elastic response because of redundancy.

Redundancy is frequently cited as a desirable attribute for seismic resistance. A quantitative measure of redundancy is included in the *Provisions* in an attempt to prevent use of large reductions from elastic response in structures that actually possess very little redundancy. Only two values of the redundancy factor, ρ, are defined: 1.0 and 1.3. The penalty factor of 1.3 is placed upon systems that do not possess some elementary measures of redundancy based on explicit consideration of the consequence of failure of a single element of the seismic force-resisting system. A simple, deemed-to-comply exception is provided for certain structures.

2.2.5 Supplementary Elements Added to Improve Structural Performance

The *Standard* includes provisions for the design of two systems to significantly alter the response of the structure to ground shaking. Both have specialized rules for response analysis and design detailing.

Seismic isolation involves placement of specialized bearings with low lateral stiffness and large lateral displacement capacity between the foundation and the superstructure. It is used to substantially increase the natural period of vibration and thereby decrease the acceleration response of the structures. (Recall the shape of the response spectrum in Figure 2.2-4; the acceleration response beyond a threshold period is roughly proportional to the inverse of the period). Seismic isolation is becoming increasingly common for structures in which superior performance is necessary, such as major hospitals and emergency response centers. Such structures are frequently designed with a stiff superstructure to control story drift, and isolation makes it feasible to design such structures for lower total lateral force. The design of such systems requires a conservative estimate of the likely deformation of the isolator. The early provisions for that factor were a precursor of the changes in ground motion mapping implemented in the 1997 *Provisions*.

Added damping involves placement of specialized energy dissipation devices within stories of the structure. The devices can be similar to a large shock absorber, but other technologies are also available. Added damping is used to reduce the structural response, and the effectiveness of increased damping can be seen in Figure 2.2-3. It is possible to reach effective damping levels of 20 to 30 percent of critical damping, which can reduce response by factors of 2 or 3. The damping does not have to be added in all stories; in fact, it is common to add damping at the isolator level of seismically isolated buildings.

Isolation and damping elements require extra procedures for analysis of seismic response. Both also require considerations beyond common building construction to assure quality and durability.

2.3   ENGINEERING PHILOSOPHY

The *Commentary*, under "Intent," states:

> "The primary intent of the *NEHRP Recommended Seismic Provisions* for normal buildings and structures is to prevent serious injury and life loss caused by damage from earthquake ground shaking. Most earthquake injuries and deaths are caused by structural collapse. Thus, the main thrust of the *Provisions* is to prevent collapse for

very rare and intense ground motion, termed the maximum considered earthquake (MCE) motion…Falling exterior walls and cladding, and falling ceilings, light fixtures, pipes, equipment and other nonstructural components also cause deaths and injuries."

The *Provisions* states:

"The degree to which these goals can be achieved depends on a number of factors including structural framing type, building configuration, materials, as-built details and overall quality of design. In addition, large uncertainties as to the intensity and duration of shaking and the possibility of unfavorable response of a small subset of buildings or other structures may prevent full realization of the intent."

At this point it is worth recalling the criteria mentioned earlier in describing the risk-targeted ground motions used for design. The probability of structural collapse due to ground shaking is not zero. One percent in 50 years is actually a higher failure rate than is currently considered acceptable for buildings subject to other natural loads, such as wind and snow. The reason is as stated in the quote at the beginning of this chapter "…all the wealth of the world would prove insufficient…" Damage is to be expected when an earthquake equivalent to the design earthquake occurs. (The "design earthquake" is currently taken as two-thirds of the MCE ground motion). Some collapse is to be expected when and where ground motion equivalent to the MCE ground motion occurs.

The basic structural criteria are strength, stability and distortion. The yield-level strength provided must be at least that required by the design spectrum (which is reduced from the elastic spectrum as described previously). Structural elements that cannot be expected to perform in a ductile manner are to have greater strength, which is achieved by applying the Ω_0 amplifier to the design spectral response. The stability criterion is imposed by amplifying the effects of lateral forces for the destabilizing effect of lateral translation of the gravity weight (the P-delta effect). The distortion criterion is a limit on story drift and is calculated by amplifying the linear response to the (reduced) design spectrum by the factor C_d to account for inelastic behavior.

Yield-level strengths for steel and concrete structures are easily obtained from common design standards. The most common design standards for timber and masonry are based on allowable stress concepts that are not consistent with the basis of the reduced design spectrum. Although strength-based standards for both materials have been introduced in recent years, the engineering profession has not yet embraced these new methods. In the past, the *Provisions* stipulated adjustments to common reference standards for timber and masonry to arrive at a strength level equivalent to yield, and compatible with the basis of the design spectrum. Most of these adjustments were simple factors to be applied to conventional allowable stresses. With the deletion of these methods from the *Provisions*, other methods have been introduced into model building codes, and the ASCE standard *Minimum Design Loads for Buildings and Other Structures* to factor downward the seismic load effects based on the *Provisions* for use with allowable stress design methods.

The *Provisions* recognizes that the risk presented by a particular building is a combination of the seismic hazard at the site and the consequence of failure, due to any cause, of the building. Thus, a classification system is established based on the use and size of the building. This classification is called the Occupancy Category (Risk Category in the *Standard*). A combined classification called the Seismic Design Category (SDC) incorporates both the seismic hazard and the Occupancy Category. The SDC is used throughout the *Provisions* for decisions regarding the application of various specific requirements. The flow charts in Chapter 2 illustrate how these classifications are used to control application of various portions of the *Provisions*.

2.4   STRUCTURAL ANALYSIS

The *Provisions* sets forth several procedures for determining the force effect of ground shaking. Analytical procedures are classified by two facets: linear versus nonlinear and dynamic versus equivalent static. The two most fully constrained and frequently used are both linear methods: an equivalent static force procedure and a dynamic modal response spectrum analysis procedure. A third linear method, a full history of dynamic response (previously referred to as a time-history analysis, now referred to as a response-history analysis), and a nonlinear method are also permitted, subject to certain limitations. These methods use real or synthetic ground motions as input but require them to be scaled to the basic response spectrum at the site for the range of periods of interest for the structure in question. Nonlinear analyses are very sensitive to assumptions about structural behavior made in the analysis and to the ground motions used as input, and a peer review is required. A nonlinear static method, also known as a pushover analysis, is described in Part 3 of the *Provisions*, but it is not included in the *Standard*. The *Provisions* also reference ASCE 41, *Seismic Rehabilitation of Existing Buildings*, for the pushover method. The method is instructive for understanding the development of mechanisms but there is professional disagreement over its utility for validating a structural design.

The two most common linear methods make use of the same design spectrum. The reduction from the elastic spectrum to design spectrum is accomplished by dividing the elastic spectrum by the coefficient *R*, which ranges from 1-1/4 to 8. Because the design computations are carried out with a design spectrum that is two-thirds the MCE spectrum that means the full reduction from elastic response ranges from 1.9 to 12. The specified elastic spectrum is based on a damping level at 5 percent of critical damping, and a part of the *R* factor accomplishes adjustments in the damping level. Ductility and overstrength make up the larger part of the reduction. The *Provisions* define the total effect of earthquake actions as a combination of the response to horizontal motions (or forces for the equivalent static force method) with response to vertical ground acceleration. The response to vertical ground motion is roughly estimated as a factor (positive or negative) on the dead load force effect. The resulting internal forces are combined with the effects of gravity loads and then compared to the full strength of the members, reduced by a resistance factor, but not by a factor of safety.

With the equivalent static force procedure, the level of the design spectrum is set by determining the appropriate values of basic seismic acceleration, the appropriate soil profile type and the value for *R*. The particular acceleration for the building is determined from this spectrum by selecting a value for the natural period of vibration. Equations that require only the height and type of structural system are given to approximate the natural period for various building types. (The area and length of shear walls come into play with an optional set of equations.) Calculation of a period based on an analytical model of the structure is encouraged, but limits are placed on the results of such calculations. These limits prevent the use of a very flexible model in order to obtain a large period and correspondingly low acceleration. Once the overall response acceleration is found, the base shear is obtained by multiplying it by the total effective mass of the building, which is generally the total permanent load.

Once the total lateral force is determined, the equivalent static force procedure specifies how this force is to be distributed along the height of the building. This distribution is based on the results of dynamic studies of relatively uniform buildings and is intended to give an envelope of shear force at each level that is consistent with these studies. This set of forces will produce, particularly in tall buildings, an envelope of gross overturning moment that is larger than many dynamic studies indicate is necessary. Dynamic analysis is encouraged, and the modal procedure is required for structures with large periods (essentially this means tall structures) in the higher seismic design categories.

With one exception, the remainder of the equivalent static force analysis is basically a standard structural analysis. That exception accounts for uncertainties in the location of the center of mass, uncertainties in

the strength and stiffness of the structural elements and rotational components in the basic ground shaking. This concept is referred to as horizontal torsion. The *Provisions* requires that the center of force be displaced from the calculated center of mass by an arbitrary amount in either direction (this torsion is referred to as accidental torsion). The twist produced by real and accidental torsion is then compared to a threshold and if the threshold is exceeded, the accidental torsion must be amplified.

In many respects, the modal analysis procedure is very similar to the equivalent static force procedure. The primary difference is that the natural period and corresponding deflected shape must be known for several of the natural modes of vibration. These are calculated from a mathematical model of the structure. The procedure requires inclusion of enough modes so that the dynamic response of the analytical model captures at least 90 percent of the mass in the structure that can vibrate. The base shear for each mode is determined from a design spectrum that is essentially the same as that for the static procedure. The distribution of displacements and accelerations (forces) and the resulting story shears, overturning moments and story drifts are determined for each mode directly from the procedure. Total values for subsequent analysis and design are determined by taking the square root of the sum of the squares for each mode. This summation gives a statistical estimate of maximum response when the participation of the various modes is random. If two or more of the modes have very similar periods, more advanced techniques for summing the values are required; these procedures must account for coupling in the response of close modes. The sum of the absolute values for each mode is always conservative.

A lower limit to the base shear determined from the modal analysis procedure is specified based on the static procedure, and the approximate periods specified in the static procedure. When this limit is violated, which is common, all results are scaled up in direct proportion. The consideration of horizontal torsion is the same as for the static procedure. Because the equivalent static forces applied at each floor, the story shears and the overturning moments are separately obtained from the summing procedure, the results are not statically compatible (that is, the moment calculated from the summed floor forces will not match the moment from the summation of moments). Early recognition of this will avoid considerable problems in later analysis and checking.

For structures that are very uniform in a vertical sense, the two procedures give very similar results. The modal analysis method is better for buildings having unequal story heights, stiffnesses, or masses. The modal procedure is required for such structures in higher seismic design categories. Both methods are based on purely elastic behavior, and, thus, neither will give a particularly accurate picture of behavior in an earthquake approaching the design event. Yielding of one component leads to redistribution of the forces within the structural system; while this may be very significant, none of the linear methods can account for it.

Both of the common methods require consideration of the stability of the building as a whole. The technique is based on elastic amplification of horizontal displacements created by the action of gravity on the displaced masses. A simple factor is calculated and the amplification is provided for in designing member strengths when the amplification exceeds about 10 percent. The technique is referred to as the P-delta analysis and is only an approximation of stability at inelastic response levels.

2.5 NONSTRUCTURAL ELEMENTS OF BUILDINGS

Severe ground shaking often results in considerable damage to the nonstructural elements of buildings. Damage to nonstructural elements can pose a hazard to life in and of itself, as in the case of heavy partitions or facades, or it can create a hazard if the nonstructural element ceases to function, as in the case of a fire suppression system. Some buildings, such as hospitals and fire stations, need to be

functional immediately following an earthquake; therefore, many of their nonstructural elements must remain undamaged.

The *Provisions* treats damage to and from nonstructural elements in three ways. First, indirect protection is provided by an overall limit on structural distortion; the limits specified, however, may not offer enough protection to brittle elements that are rigidly bound by the structure. More restrictive limits are placed upon those Occupancy Categories (Risk Categories in the *Standard*) for which better performance is desired given the occurrence of strong ground shaking. Second, many components must be anchored for an equivalent static force. Third, the explicit design of some elements (the elements themselves, not just their anchorage) to accommodate specific structural deformations or seismic forces is required.

The dynamic response of the structure provides the dynamic input to the nonstructural component. Some components are rigid with respect to the structure (light weights, and small dimensions often lead to fundamental periods of vibration that are very short). Application of the response spectrum concept would indicate that the response history of motion of a building roof to which mechanical equipment is attached looks like a ground motion to the equipment. The response of the component is often amplified above the response of the supporting structure. Response spectra developed from the history of motion of a point on a structure undergoing ground shaking are called floor spectra, and are useful in understanding the demands upon nonstructural components.

The *Provisions* simplifies the concept greatly. The force for which components are checked depends on:

1. The component mass;

2. An estimate of component acceleration that depends on the structural response acceleration for short period structures, the relative height of the component within the structure and a crude approximation of the flexibility of the component or its anchorage;

3. The available ductility of the component or its anchorage; and

4. The function or importance of the component or the building.

Also included in the *Provisions* is a quantitative measure for the deformation imposed upon nonstructural components. The inertial force demands tend to control the seismic design for isolated or heavy components whereas the imposed deformations are important for the seismic design for elements that are continuous through multiple levels of a structure or across expansion joints between adjacent structures, such as cladding or piping.

2.6   QUALITY ASSURANCE

Since strong ground shaking has tended to reveal hidden flaws or *weak links* in buildings, detailed requirements for assuring quality during construction are contained in the *Provisions* by reference to the *Standard*, where they are located in an appendix. The actively implemented provisions for quality control are actually contained in the model building codes, such as the *International Building Code*, and the material design standards, such as *Seismic Provisions for Structural Steel Buildings*. Loads experienced during construction provide a significant test of the likely performance of ordinary buildings under gravity loads. Tragically, mistakes occasionally will pass this test only to cause failure later, but it is fairly rare. No comparable proof test exists for horizontal loads, and experience has shown that flaws in construction show up in a disappointingly large number of buildings as distress and failure due to earthquakes. This is coupled with the seismic design approach based on excursions into inelastic straining, which is not the case for response to other loads.

The quality assurance provisions require a systematic approach with an emphasis on documentation and communication. The designer who conceives the systems to resist the effects of earthquake forces must identify the elements that are critical for successful performance as well as specify the testing and inspection necessary to confirm that those elements are actually built to perform as intended. Minimum levels of testing and inspection are specified in the *Provisions* for various types of systems and components.

The *Provisions* also requires that the contractor and building official be aware of the requirements specified by the designer. Furthermore, those individuals who carry out the necessary inspection and testing must be technically qualified, and must communicate the results of their work to all concerned parties. In the final analysis, there is no substitute for a sound design, soundly executed.

3

Earthquake Ground Motion

Nicolas Luco, Ph.D., P.E.,
Charlie Kircher, P.E., PhD,
C.B. Crouse, P.E., Ph.D.
Finley Charney, Ph.D.
Curt B. Haselton, P.E., Ph.D.
Jack W. Baker, Ph.D.
Reid Zimmerman, P.E.
John D. Hooper, S.E.
William McVitty, MS
Andy Taylor, S.E.

Contents

Most of the effort in seismic design of buildings and other structures is focused on structural design. This chapter addresses another key aspect of the design process—characterization of earthquake ground motion into parameters for use in design. Section 3.1 describes the basis of the earthquake ground motion maps in the *Provisions* and in ASCE 7 (the *Standard)*. Section 3.2 has examples for the determination of ground motion parameters and spectra for use in design. Section 3.3 describes site-specific ground motion requirements and provides example site-specific design and MCE$_R$ response spectra and example values of site-specific ground motion parameters. Section 3.4 discusses and provides an example for the selection and scaling of ground motion records for use in various types of response history analysis permitted in the *Standard.*

3.1 BASIS OF EARTHQUAKE GROUND MOTION MAPS

This section explains the basis of the maps of (i) Risk-Targeted Maximum Considered Earthquake (MCE$_R$) ground motion, (ii) Peak Ground Acceleration (PGA), and (iii) long-period transition period (T_L) in the 2015 *Provisions* and ASCE 7-16. The MCE$_R$ and PGA maps for the conterminous US have been updated with respect to those in ASCE 7-10, and the MCE$_R$ and PGA maps for Guam and the Northern Mariana Islands, and for American Samoa, are new. The T_L maps for all of the US territories are identical to those in ASCE 7-10. This section also explains the basis for the vertical ground motion equations the *Standard* requires be used in the design of certain non-building structures. For comparison purposes, we start with a review of the Maximum Considered Earthquake (MCE) ground motion maps in ASCE 7-05 and earlier editions, which were first introduced in the 1997 *Provisions*.

3.1.1 MCE Ground Motion Intensity Maps in ASCE 7-05 and Earlier Editions

The basis for the MCE ground motion intensity maps in ASCE 7-05 and earlier editions was established by the Building Seismic Safety Council (BSSC) Seismic Design Procedures Group, also referred to as Project '97. The maps can be described as applications of the site-specific ground motion hazard analysis procedure in Chapter 21, using ground motion values computed by the USGS National Seismic Hazard Modeling Project for a grid of locations and/or polygons that covers the US. In particular, the 1996 USGS update of the ground motion intensity values was used for ASCE 7-98 and ASCE 7-02, and the 2002 USGS update was used for ASCE 7-05. The site-specific procedure in all three editions calculates the MCE ground motion intensity as the lesser of a probabilistic and a deterministic ground motion intensities. Hence, the USGS computed both types of ground motion intensities, whereas otherwise it would have only computed probabilistic ground motion intensities. Brief reviews of how the USGS computed the probabilistic and deterministic ground motions are provided in the next few paragraphs. For additional information, see the commentary of the 1997 *Provisions* (FEMA 303) and Leyendecker et al. (2000).

The USGS computation of the probabilistic ground motion intensities that are part of the basis of the MCE ground motion intensity maps in ASCE 7-98/02 and ASCE 7-05 is explained in detail in Frankel et al. (1996) and (2002), respectively. In short, the USGS combines research on potential sources of earthquakes (e.g., faults and locations of past earthquakes), the potential magnitudes of earthquakes from these sources and their frequencies of occurrence, and the potential ground motions generated by these earthquakes. Uncertainty and randomness in each of these components is accounted for in the computation via contemporary Probabilistic Seismic Hazard Analysis (PSHA), which was originally conceived by Cornell (1968). The primary output of PSHA computations are hazard curves for locations on a grid covering the US in the case of the USGS computation. Each hazard curve provides mean annual frequencies of exceeding various user-specified ground motions intensity amplitudes. From these hazard curves, the ground motion amplitudes for a user-specified mean annual frequency can be interpolated and then mapped. The results are known as uniform-hazard ground motion maps, since the mean annual frequency (or corresponding probability) is uniform geographically.

For ASCE 7-05 and the earlier editions, a mean annual exceedance frequency of ½,475 per year, corresponding to 2% probability of exceedance in 50 years, was specified by the BSSC Project '97. That project also specified that the ground motion intensity parameters be spectral response accelerations at vibration periods of 0.2 seconds and 1 second, for 5% of critical damping for the average shear wave velocity at small shear strains in the upper 100 feet (30 m) of subsurface below each location ($v_{S,30}$)based on a reference value of 760 m/s. The BSSC subsequently decided to regard this reference value, which is at the boundary of Site Classes B and C, as corresponding to Site Class B. Justifications for the decisions summarized in this paragraph are provided in the FEMA 303 *Commentary*.

The USGS computation of the deterministic ground motion intensities for ASCE 7-05 and the earlier editions is detailed in the FEMA 303 *Commentary*. As defined by Project '97 and subsequently specified in the site-specific procedure of ASCE 7-98/02/05 (Section 21.2.2), each deterministic ground motion is calculated as 150% of the median spectral response acceleration for a characteristic earthquake on a known active fault within the region. The specific characteristic earthquake is that which generates the largest median spectral response acceleration at the given location. As for the probabilistic ground motions, the spectral response accelerations are at vibration periods of 0.2 seconds and 1 second, for 5% of critical damping. The same reference site class is used as well. Lower limits of 1.5g for the vibration period of 0.2 seconds and 0.6g for the vibration period of 1 second are applied to the deterministic ground motions.

As mentioned at the beginning of this section, the lesser of the probabilistic and deterministic ground motions described above yields the MCE ground motions mapped in ASCE 7-05 and the earlier editions. Thus, the MCE spectral response accelerations at 0.2 seconds and 1 second are equal to the corresponding probabilistic ground motions wherever they are less than the lower limits of the deterministic ground motions (1.5g and 0.6g, respectively). Where the probabilistic ground motions are greater than the lower limits, the deterministic ground motions sometimes govern, but only if they are less than their probabilistic counterparts. On the MCE ground motion maps in ASCE 7-05, the deterministic ground motions govern mainly near major faults in California (like the San Andreas), in Reno and in parts of the New Madrid Seismic Zone. The deterministic ground motions that govern are as small as 40% of their probabilistic counterparts.

3.1.2 MCE$_R$ Ground Motions Introduced in the 2009 *Provisions* and ASCE 7-10

Like the MCE ground motion maps in ASCE 7-05 and earlier editions, the Risk-Targeted Maximum Considered Earthquake (MCE$_R$) ground motions in the *Provisions* since 2009 and in ASCE 7 since 2010 can be described as applications of the site-specific ground motion hazard analysis procedure in Chapter 21 (Section 21.2). The ground motion values for a grid of locations and/or polygons covering the US that are used in the procedure are still from the USGS, and the site-specific procedure still calculates the MCE$_R$ ground motion as the lesser of a probabilistic and a deterministic ground motion. However, the definitions of the probabilistic and deterministic ground motions are different than in ASCE 7-05 and earlier editions. The definitions were revised for the 2009 *Provisions* and ASCE 7-10 by the BSSC Seismic Design Procedures Reassessment Group, also referred to as Project '07. Three revisions were made:

1) The probabilistic ground motions are redefined as risk-targeted ground motion intensities, in lieu of the uniform-hazard (2% in 50-year) ground motions that underlie the MCE ground motion maps in ASCE 7-05 and earlier editions,

2) the deterministic ground motions are redefined as 84$^{\text{th}}$-percentile ground motions, in lieu of median ground motions multiplied by 1.5; and

3) the probabilistic and deterministic ground motions are redefined as maximum-direction ground motions, in lieu of geometric mean ground motions.

Each of the above three differences between the basis of the MCE and MCE$_R$ ground motion maps is explained in the subsections below. In addition to these differences, the MCE$_R$ ground motions in the 2009 *Provisions* and ASCE 7-10 use USGS ground motion values from its 2008 update (Petersen et al., 2008), whereas earlier updates (2002 and 1996) were used for the MCE ground motion maps in ASCE 7-05 and earlier editions. The USGS ground motion values used for the 2015 Provisions and ASCE 7-16 are discussed below in Section 3.1.6.

3.1.2.1 Risk-Targeted Probabilistic Ground Motion Intensities. For the MCE ground motion maps in ASCE 7-05 and earlier editions the underlying probabilistic ground motions are specified to be uniform-hazard ground motions that have a 2% probability of being exceeded in 50 years. It has long been recognized, though, that "it really is the probability of structural failure with resultant casualties that is of concern; and the geographical distribution of that probability is not necessarily the same as the distribution of the probability of exceeding some ground motion" (p. 296 of ATC 3-06, 1978). The primary reason that the distributions of the two probabilities are not the same is that there are geographic differences in the shape of the hazard curves from which uniform-hazard ground motions are read. The *Commentary* of FEMA 303 (p. 289) reports that "because of these differences, questions were raised concerning whether definition of the ground motion based on a constant probability for the entire United States would result in similar levels of seismic safety for all structures".

The changeover to risk-targeted probabilistic ground motions introduced in the 2009 *Provisions* and ASCE 7-10 takes into account the differences in the shape of hazard curves across the US. Where used in design, the risk-targeted ground motions are expected to result in buildings with a geographically uniform mean annual frequency of collapse, or uniform risk. The BSSC Project '07 decided on a target risk level corresponding to 1% probability of collapse in 50 years. This target is based on the average of the mean annual frequencies of collapse across the Western US (WUS) expected to result from design for the probabilistic ground motion intensities in ASCE 7-05. Consequently, in the WUS the risk-targeted ground motions are generally within 15% of the corresponding uniform-hazard (2% in 50-year) ground motions. In the Central and Eastern US, where the shapes of hazard curves are known to differ from those in the WUS, the risk-targeted ground motions generally are smaller. For instance, in the New Madrid Seismic Zone and near Charleston, South Carolina ratios of risk-targeted to uniform-hazard ground motions are as small as 0.7.

The computation of risk-targeted probabilistic ground motions for the MCE$_R$ ground motion intensities is detailed in the 2009 *Provisions* Part 1 Sections 21.2.1.2 and C21.2.1 and in Luco et al. (2007). While the computation of the risk-targeted ground motion intensities is different than that of the uniform-hazard ground motion intensities specified for the MCE ground motion intensities in ASCE 7-05 and earlier editions, both begin with USGS computations of hazard curves. As explained in Section 3.1.1, the uniform-hazard ground motion intensities simply interpolate the hazard curves for a 2% probability of exceedance in 50 years. In contrast, the risk-targeted ground motion intensities make use of entire hazard curves resulting in MCE$_R$ values that have different return periods throughout the country. In either case, the end results are probabilistic spectral response accelerations at 0.2 seconds and 1 second, for 5% of critical damping and the reference site class.

3.1.2.2 84th-Percentile Deterministic Ground Motion Intensities. For the MCE ground motion intensity maps in ASCE 7-05 and earlier editions, recall (from Section 3.1.1) that the underlying deterministic ground motions are defined as 150% of median spectral response accelerations. As explained in the FEMA 303 *Commentary* (p. 296),

Increasing the median ground motion estimates by 50 percent [was] deemed to provide an appropriate margin and is similar to some deterministic estimates for a large magnitude characteristic earthquake using ground motion attenuation functions with one standard deviation.

Estimated standard deviations for some active fault sources have been determined to be higher than 50 percent, but this increase in the median ground motions was considered reasonable for defining the maximum considered earthquake ground motions for use in design.

For the MCE$_R$ ground motion intensities introduced in the 2009 *Provisions* and ASCE 7-10, however, the BSSC decided to directly define the underlying deterministic ground motion intensities as those at the level of one standard deviation. More specifically, they are defined as 84th-percentile ground motion intensities, since it has been widely observed that ground motion intensities follow lognormal probability distributions. The remainder of the definition of the deterministic ground motion intensities remains the same as that used for the MCE ground motion intensity maps in ASCE 7-05 and earlier editions. For example, the lower limits of 1.5g and 0.6g described in Section 3.1.1 are retained.

The USGS applies a simplification specified by the BSSC in computing the 84th-percentile deterministic ground motion intensities. The 84th-percentile spectral response accelerations are approximated as 180% of median values. This approximation corresponds to a logarithmic ground motion intensity standard deviation of approximately 0.6, as demonstrated in the 2009 *Provisions* Part 1 Section C21.2.2. The computation of deterministic ground motions is further described in the 2009 *Provisions* Part 2 Section C21.2.2.

3.1.2.3 Maximum-Direction Probabilistic and Deterministic Ground Motion Intensities. The ground motion intensity attenuation models used by the USGS in computing the MCE spectral response accelerations in ASCE 7-05 and earlier editions represent the geometric mean of two horizontal components of ground motion intensity. Most users were unaware of this fact, particularly since the discussion notes on the MCE ground motion maps incorrectly stated that they represent "the random horizontal component of ground motion." Starting with the 2009 *Provisions*, the BSSC decided that it would be an improvement if the MCE$_R$ ground motions represented the maximum direction of horizontal spectral response acceleration. Reasons for this decision are explained in the 2009 *Provisions* Part 1 Section C21.2.

Since the attenuation models used in computing the MCE$_R$ ground motions represent "geomean" spectral response accelerations, the BSSC provided factors to convert approximately to "maximum-direction" ground motions. Based on research by Huang et al. (2008) and others, the factors are 1.1 and 1.3 for the spectral response accelerations at 0.2 seconds and 1.0 second, respectively. The basis for these factors is elaborated upon in the 2009 *Provisions* Part 1 Section C21.2. They are applied to both the USGS probabilistic hazard curves from which the risk-targeted ground motions (described in Section 3.1.2.1) are derived and the deterministic ground motions computed by the USGS (described in Section 3.1.2.2). However, they are not applied to the deterministic ground motion intensity lower limit values of 1.5 and 0.6. The site-specific ground motion hazard analysis procedure of ASCE 7-10 and ASCE 7-16 (Section 21.2) allows for "other scale factors [that can be shown to] more closely represent the maximum response," such as those in Part 3 of the 2015 *Provisions*.

3.1.3   PGA Maps Introduced in the 2009 *Provisions* and ASCE 7-10

The basis of the Peak Ground Acceleration (PGA) maps in the *Provisions* since 2009 and in ASCE 7 since 2010 nearly parallels that of the MCE ground motion intensity maps in ASCE 7-05 and earlier editions (described in Section 3.1.1). More specifically, the mapped PGA values are calculated as the lesser of uniform-hazard (2% in 50-year) probabilistic and deterministic PGA values that represent the geometric mean of two horizontal components of ground motion, for Site Class B. Correspondingly, the PGA maps are labeled "Maximum Considered Earthquake Geometric Mean (MCE$_G$) PGA" maps, in contrast to the MCE$_R$ abbreviation. Unlike the MCE ground motion intensities in ASCE 7-05 and earlier editions, though, the deterministic values are defined as 84th-percentile ground motions rather than 150% of median ground motions. This definition of deterministic ground motion intensities parallels that which is described above for the MCE$_R$ ground motion intensities that were also first introduced in the 2009 *Provisions* and ASCE 7-10. The deterministic PGA values, though, are stipulated to be no lower than

0.5g, as opposed to 1.5g and 0.6g for the MCE$_R$ 0.2- and 1.0-second spectral response accelerations, respectively. All of these details of the basis of the PGA maps are provided in the site-specific procedure (Section 21.5) of ASCE 7-10, the 2015 *Provisions*, and ASCE 7-16. For mapping purposes, the 84th-percentile deterministic PGA values are approximated as median values multiplied by 1.8, like their MCE$_R$ ground motion counterparts are. Also like the MCE$_R$ ground motion maps, the PGA maps in the 2009 *Provisions* and ASCE 7-10 use USGS ground motion values from its 2008 update (Petersen et al., 2008).

3.1.4   Long-Period Transition Period (T_L) Maps Introduced in ASCE 7-05

The basis for the T_L maps in the *Provisions* and ASCE 7, which were first introduced in ASCE 7-05, was established by the Technical Subcommittee 1 (TS-1) of the 2003 Provisions Update Committee. The details of the procedure and rationale used in developing the T_L maps are found in Crouse et al. (2006). In short, the procedure consisted of two steps. First, a relationship between T_L and earthquake magnitude was established. Second, the modal magnitude from deaggregation of the USGS 2% in 50-year ground motion hazard at a 2-second period (1 second for Hawaii) was mapped. The long-period transition period (T_L) maps that combined these two steps delimit the transition of the design response spectrum from a constant velocity ($1/T$) to a constant displacement ($1/T^2$) shape.

3.1.5   Vertical Ground Motions Introduced in the 2009 *Provisions*

For the design of most structures vertical seismic load effects are determined via a single constant fraction of the horizontal short-period spectral response acceleration S_{DS}. The *Standard* requires that for certain types of nonbuilding structures, a vertical design response spectrum, S_{av}, be determined that is analogous to the horizontal design response spectrum, S_a and used in the structure's design. The S_{av} values are determined via functions (for four different ranges of vertical period of vibration) that each depend on S_{DS} and a coefficient C_v representing the ratio of vertical to horizontal spectral response acceleration. This is in contrast to determination of S_a via mapped horizontal spectral response accelerations. The coefficient C_v, in turn, depends on the amplitude of spectral response acceleration (by way of S_S) and site class. These dependencies, as well as the period dependence of the equations for S_{av}, are based on studies by Bozorgnia and Campbell (2004) and others. Those studies observed that the ratio of vertical to horizontal spectral response acceleration is sensitive to period of vibration, site class, earthquake magnitude (for relatively soft sites) and distance to the earthquake. The sensitivity to the latter two characteristics is captured by the dependence of C_v on S_S.

The basis of the equations for vertical response spectra in the *Standard* is explained in more detail in the commentary to Section 11.9. Note that for vertical periods of vibration greater than 2 seconds, Section 11.9 stipulates that the vertical spectral response accelerations be determined via a site-specific procedure. A site-specific study also may be performed for periods less than 2 seconds, in lieu of using the equations for vertical response spectra.

3.1.6   Updated MCE$_R$ Ground Motion and PGA Maps in the *2015 Provisions* and ASCE 7-16

The MCE$_R$ ground motion intensity and PGA maps in the 2015 *Provisions* and ASCE 7-16 have been prepared via the same procedures applied for ASCE 7-10 (as described above in Section 3.1.2). However, the ground motion intensity values used in the procedures are from the 2014 USGS update of its National Seismic Hazard Model. The 2014 USGS update is documented in Petersen et al. (2014) and supersedes the 1996, 2002, and 2008 USGS ground motion values. It involved interactions with hundreds of scientists and engineers at regional and topical workshops, including advice from working groups, expert panels, state geological surveys, other federal agencies and hazard experts from industry and academia. Based in large part on new published studies, the 2014 update incorporated changes in both earthquake source models (including magnitudes and occurrence frequencies) and models of ground motion propagation. Three examples, among many, are Version 3 of the Unified California Earthquake Rupture Forecast (Field et al., 2013), the Central and Eastern US Seismic Source Characterization for Nuclear Facilities (CEUS-SSCn, 2012), and Version 2 of the Next Generation Attenuation Relations for the

Western US (Bozorgnia et al., 2014). The end results are updated ground motions that represent the "best available science" as determined by the USGS from an extensive information-gathering and review process. It is important to note that the USGS hazard curves and uniform-hazard maps posted on its website represent the "geomean" ground motions discussed above in Section 3.1.2.3. Only the MCE_R ground motions represent the maximum direction of horizontal spectral response acceleration.

In addition to using the 2014 USGS update, the MCE_R ground motion maps in the 2015 *Provisions* and ASCE 7-16 use a so-called β, the collapse-fragility logarithmic standard deviation, value for calculating risk-targeted probabilistic ground motion intensities that is consistent with the Chapter 22 site-specific hazard analysis procedure, namely β=0.6. In contrast, the MCE_R ground motion intensity maps in ASCE 7-10 used a value of β from the 2009 Provisions, namely β=0.8. For more information on β see Part 1 Sections 21.2.1.2 and C21.2.1 of the 2009 *Provisions* and Luco et al. (2007).

3.1.7   Summary

The procedures for deriving the MCE_R ground motion and PGA maps in the 2015 *Provisions* and ASCE 7-16 from the computations of the USGS National Seismic Hazard Modeling Project are the same as those for the maps in ASCE 7-10. These procedures are established in the site-specific ground motion chapter, in Section 21.2 for the MCE_R ground motion maps and in Section 21.5 for the PGA maps. The ground motion values used in these procedures, however, are different for the two sets of conterminous US maps; those used for the 2015 *Provisions* and ASCE 7-16 are based on the 2014 USGS update of the National Seismic Hazard Model, whereas the maps in ASCE 7-10 used the 2008 USGS update. Furthermore, the β=0.6 value used for the MCE_R ground motion maps in the 2015 *Provisions* and ASCE 7-16 is consistent with the site-specific procedure (Section 21.2). The ground motion values used for Guam and the Northern Mariana Islands, and for American Samoa, are based on new USGS hazard models for those territories (Petersen et al., 2012 and Mueller et al., 2012). The β=0.6 value is used for the MCE_R ground motion maps of those territories. The MCE_R and PGA maps for the other US territories – Alaska, Hawaii, and Puerto Rico and the US Virgin Islands – are unchanged from ASCE 7-10 to the 2015 *Provisions* and ASCE 7-16. Also unchanged are the T_L maps and the vertical ground motion equations.

3.2   DETERMINATION OF GROUND MOTION VALUES AND SPECTRA

This example illustrates the determination of seismic design parameters for a site in Seattle, Washington. The site is located at 47.65ºN latitude, 122.3ºW longitude. Using the results of a site-specific geotechnical investigation and the procedure specified in Chapter 20, the site is classified as Site Class C.

In the sections that follow, design ground motion intensity parameters, horizontal response spectra, and peak ground accelerations are determined using ASCE 7-10, the 2015 *Provisions*, and ASCE 7-16. Using the *Standard*, vertical response spectra are computed for both design and maximum considered earthquake ground motions.

3.2.1   ASCE 7-10 MCE_R Ground Motion Values

ASCE 7-10 Section 11.4.1 requires that spectral response acceleration parameters S_S and S_1 be determined using the maps in Chapter 22. Those maps are too small to permit reading values to a sufficient degree of precision for most sites, so in practice the mapped parameters are determined using a software application available at http://earthquake.usgs.gov/hazards/designmaps/. That application requires that longitude be entered in degrees east of the prime meridian; negative values are used for degrees west. Given the site location, the following values may be determined using the online application (or read from Figures 22-1 and 22-2).

$S_S = 1.289$
$S_1 = 0.498$

Using these mapped spectral response acceleration values and the site class, site coefficients F_a and F_v are determined in accordance with Section 11.4.3 using Tables 11.4-1 and 11.4-2. Using Table 11.4-1, for S_S = 1.289 > 1.25, F_a = 1.0 for Site Class C. Using Table 11.4-2, read F_v = 1.4 for S_I = 0.4 and F_v = 1.3 for $S_I \geq 0.5$ for Site Class C. Using linear interpolation for S_I = 0.498,

$$F_v = 1.4 + \frac{0.498 - 0.4}{0.5 - 0.4}(1.3 - 1.4) = 1.302$$

Using Equations 11.4-1 and 11.4-2 to determine the adjusted maximum considered earthquake spectral response acceleration parameters,

$S_{MS} = F_a S_S = 1.0(1.289) = 1.289$
$S_{MI} = F_v S_I = 1.302(0.498) = 0.649$

Using Equations 11.4-3 and 11.4-4 to determine the design earthquake spectral response acceleration parameters,

$$S_{DS} = \frac{2}{3}S_{MS} = \frac{2}{3}(1.289) = 0.860$$
$$S_{DI} = \frac{2}{3}S_{MI} = \frac{2}{3}(0.649) = 0.433$$

Given the site location read Figure 22-12 for the long-period transition period, T_L = 6 seconds.

3.2.2   2015 *Provisions* and ASCE 7-16 MCE$_R$ Ground Motion Values

The 2015 *Provisions* and ASCE 7-16 modify Chapter 22 and Section 11.4.3 of ASCE 7-10 to update the seismic design ground motion parameters, as described in Section 3.1.6 above. Given the site location, the following values may be determined using the online application (or read from Figures 22-1 and 22-2 of the 2015 *Provisions* or ASCE 7-16).

S_S = 1.397
S_I = 0.487

Using these spectral response acceleration values and the site class, the updated site coefficients F_a and F_v are determined in accordance with Section 11.4.3 using Tables 11.4-1 and 11.4-2 (which are different than the Tables in ASCE 7-10 and the 2009 *Provisions*). Using Table 11.4-1, for S_S = 1.397, F_a = 1.2 for Site Class C. Using Table 11.4-2, for S_I = 0.487, F_v = 1.5 for Site Class C.

Using Equations 11.4-1 and 11.4-2 to determine the MCE$_R$ spectral response acceleration parameters,

$S_{MS} = F_a S_S = 1.2(1.397) = 1.676$
$S_{MI} = F_v S_I = 1.5(0.487) = 0.731$

Using Equations 11.4-3 and 11.4-4 to determine the design earthquake spectral response acceleration parameters,

$$S_{DS} = \frac{2}{3}S_{MS} = \frac{2}{3}(1.676) = 1.118$$
$$S_{DI} = \frac{2}{3}S_{MI} = \frac{2}{3}(0.731) = 0.487$$

Given the site location read ASCE 7-16 Figure 22-14 (which is identical to Figure 22-12 in ASCE 7-10) for the long-period transition period, $T_L = 6$ seconds.

3.2.3 2015 *Provisions* and ASCE 7-16 Horizontal Response Spectra

Using the S_{DS}, S_{D1}, and T_L parameters determined in the preceding section, the design spectrum is constructed in accordance with ASCE 7 Section 11.4.5 using Figure 11.4-1 and Equations 11.4-5, 11.4-6 and 11.4-7. The design spectral response acceleration ordinates, S_a, may be divided into four regions based on period, T, as described below.

From $T = 0$ to $T_0 = 0.2\left(\frac{S_{D1}}{S_{DS}}\right) = 0.2\left(\frac{0.487}{1.118}\right) = 0.087$ seconds, S_a varies linearly from $0.4S_{DS}$ to S_{DS}.

From T_0 to $T_S = \left(\frac{S_{D1}}{S_{DS}}\right) = \left(\frac{0.487}{1.118}\right) = 0.436$ seconds, S_a is constant at S_{DS}.

From T_S to T_L, S_a is inversely proportional to T, being anchored to S_{D1} at $T = 1$ second.

At periods greater than T_L, S_a is inversely proportional to the square of T, being anchored to $\dfrac{S_{D1}}{T_L}$ at T_L.

As prescribed in ASCE 7 Section 11.4.6, the MCE$_R$ response spectrum is determined by multiplying the design response spectrum ordinates by 1.5. Figure 3.2-1 shows the design and MCE$_R$ response spectra determined using the ground motion parameters computed in Section 3.2.3.
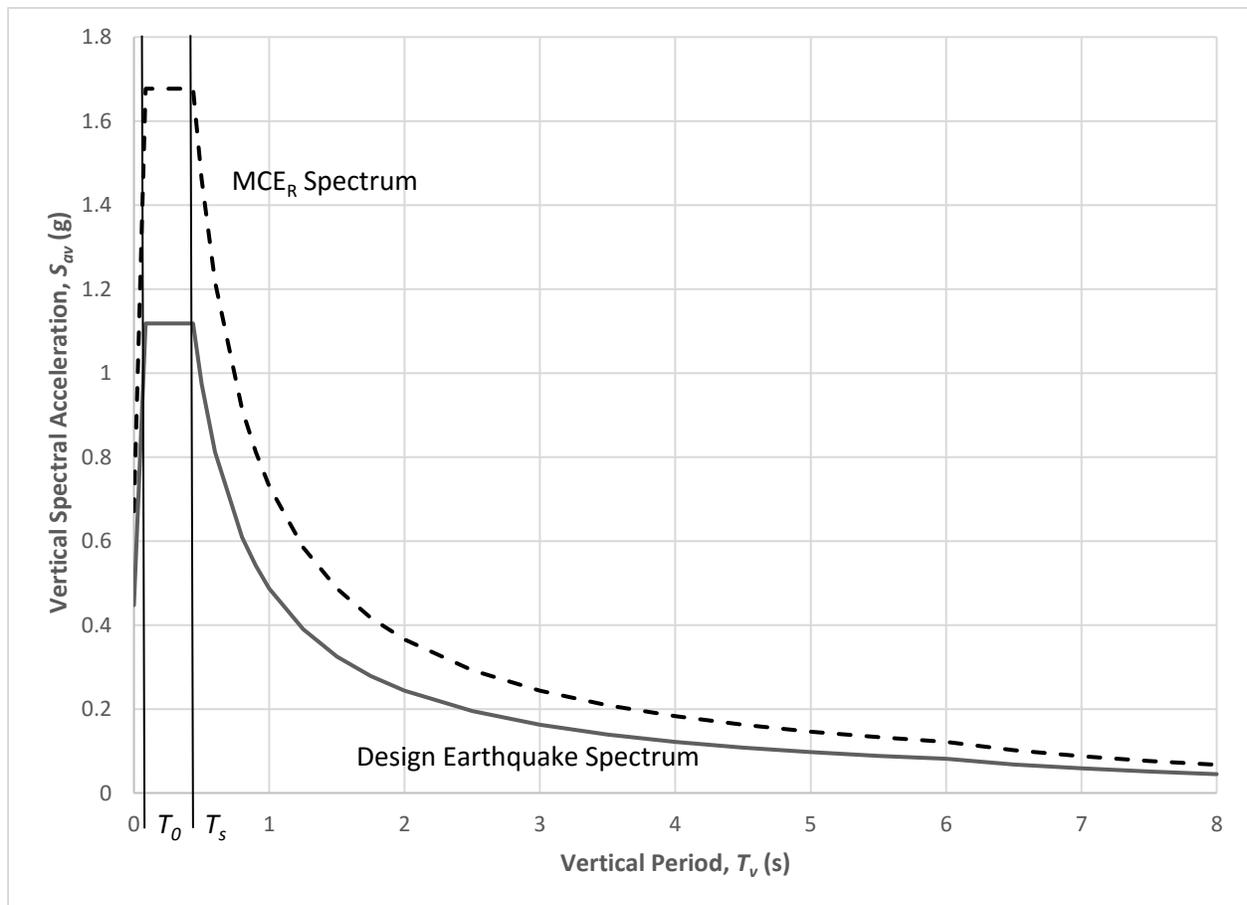
Figure 3.2-1 Horizontal Response Spectra for Design and MCE$_R$ Ground Motions

3.2.4 ASCE 7-16 Vertical Response Spectra

Chapter 23A of the 2015 (and 2009) *Provisions* defines vertical ground motions for seismic design. The design vertical response spectrum is constructed in accordance with Section 23.1 using Equations 23.1-1, 23.1-2, 23.1-3 and 23.1-4. Vertical ground motion values are related to horizontal ground motion values by a vertical coefficient, C_v, which is determined as a function of site class and the MCE_R spectral response parameter at short periods, S_S. The design vertical spectral response acceleration ordinates, S_{av}, may be divided into four regions based on vertical period, T_v, as described below.

Using *Provisions* Table 23.1-1 and $S_S = 1.397$ from Section 3.2.2 above, read $C_v = 1.3$ for $S_S \geq 2.0$ and $C_v = 1.1$ for $S_S = 1.0$ for Site Class C. Using linear interpolation,

$$C_v = 1.1 + \left(\frac{1.397-1}{2-1}\right)(1.3\text{-}1.1) = 1.179$$

From $T_v = 0$ to 0.025 seconds, S_{av} is constant at $0.3C_vS_{DS} = 0.3(1.179)(1.118) = 0.395$. Fro $T_v = 0.025$ to 0.05 seconds, S_{av} varies linearly from $0.3C_vS_{DS} = 0.395$ to $0.8C_vS_{DS} = 0.8(1.179)(1.118) = 1.054$. From $T_v = 0.05$ to 0.15 seconds, S_{av} is constant at $0.8C_vS_{DS} = 1.054$. From $T_v = 0.15$ to 2.0 seconds, S_{av} is inversely proportional to $T_v^{0.75}$, being anchored to $0.8C_vS_{DS} = 1.054$ at $T_v = 0.15$ seconds. For vertical periods greater than 2.0 seconds, the vertical response spectral acceleration must be determined using site-specific procedures.

As prescribed in *Provisions* Section 23.2, the MCE_R vertical response spectrum is determined by multiplying the design vertical response spectrum ordinates by 1.5. Figure 3.2-2 shows the design and MCE_R vertical response spectra.
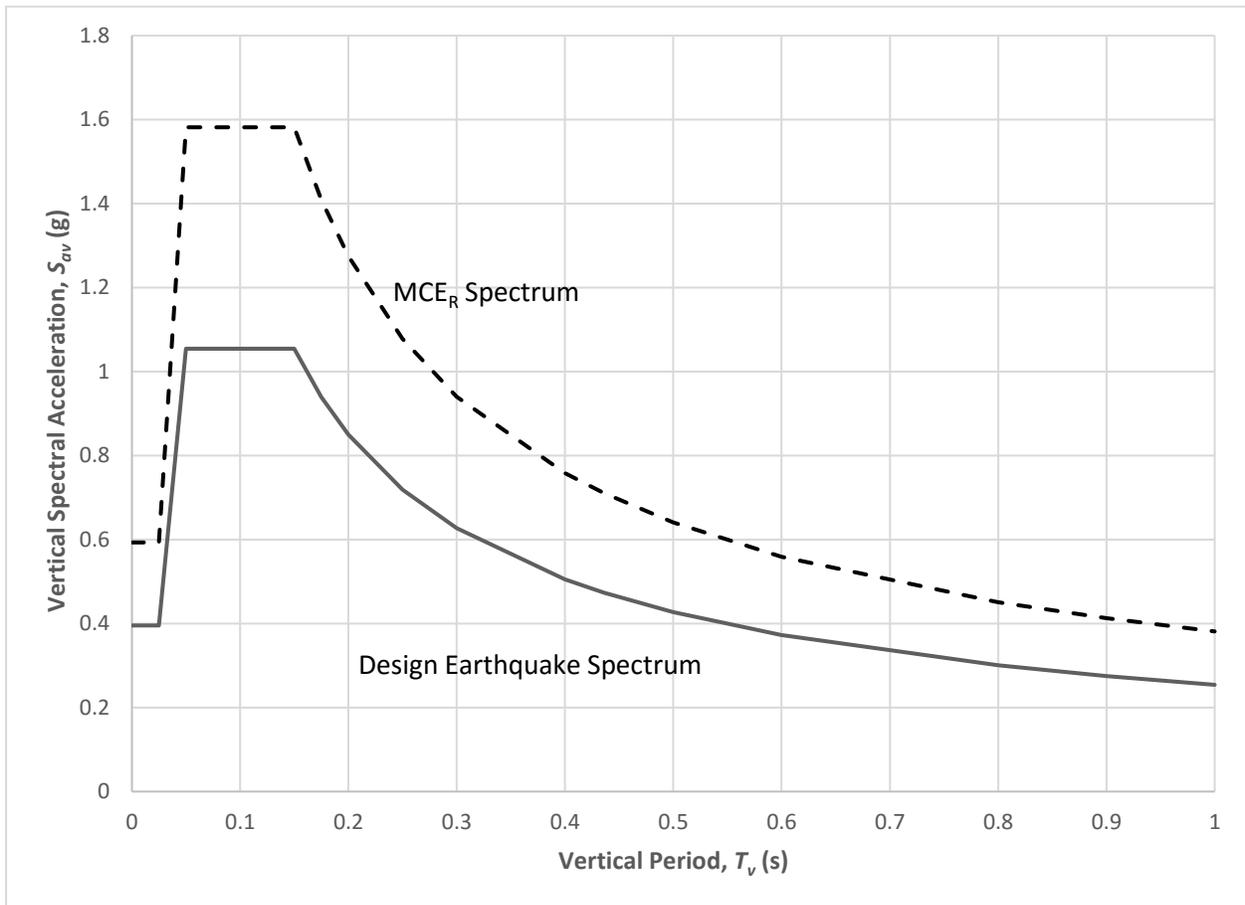
Figure 3.2-2 Vertical Response Spectra for Design and MCE$_R$ Ground Motions

3.2.5 ASCE 7-10 Peak Ground Accelerations

Section 11.8.3 of ASCE 7-10 calculates peak ground accelerations used for assessment of the potential for liquefaction and soil strength loss and for determination of lateral earth pressures for design of basement and retaining walls. Given the site location, the following value of maximum considered earthquake geometric mean peak ground acceleration may be determined using the online application (or read from ASCE 7-10 Figure 22-7).

$$PGA = 0.521 \text{ g}$$

Using this mapped peak ground acceleration value and the site class, site coefficient F_{PGA} is determined in accordance with Section 11.8.3 using Table 11.8-1. Using Table 11.8-1, for $PGA = 0.521 > 0.5$, $F_{PGA} = 1.0$ for Site Class C. Using ASCE 7-10 Equation 11.8-1 to determine the maximum considered earthquake geometric mean peak ground acceleration adjusted for site class effects,

$$PGA_M = F_{PGA} \, PGA = 1.0(0.521) = 0.521 \text{ g}$$

This value is used directly to assess the potential for liquefaction or for soil strength loss. The design peak ground acceleration used to determine dynamic seismic lateral earth pressures for design of basement and retaining walls is computed as $\frac{2}{3} PGA_M = \frac{2}{3}(0.521) = 0.347$ g.

3.2.6   2015 *Provisions* and ASCE 7-16 Peak Ground Accelerations

The 2015 *Provisions* and ASCE 7-16 modify Chapter 22 and Section 11.8.3 of ASCE 7-10 to update the peak ground accelerations, as described in Section 3.1.6 above. Given the site location, the following value of maximum considered earthquake geometric mean peak ground acceleration may be determined using the online application (or read from Figure 22-9 of the 2015 *Provisions* or ASCE 7-16).

$PGA = 0.596$ g

Using this mapped peak ground acceleration value and the site class, the updated site coefficient F_{PGA} is determined in accordance with Table 11.8-1 of the 2015 *Provisions* or ASCE 7-16. For $PGA = 0.596$, $F_{PGA} = 1.2$ for Site Class C. Using Equation 11.8-1 to determine the maximum considered earthquake geometric mean peak ground acceleration adjusted for site class effects,

$PGA_M = F_{PGA}\ PGA = 1.2(0.596) = 0.715$ g

The design peak ground acceleration is computed as $\frac{2}{3}PGA_M = \frac{2}{3}$ (0.715) = 0.477 g.

3.3   SITE-SPECIFIC GROUND MOTION SPECTRA

Site-specific design and MCE_R ground motion spectra characterize the intensity and frequency content of ground motions at the site of interest in terms of the peak response of a discrete set of 5%-damped single-degree-of freedom (SDOF) systems with periods distributed over the range of design interest, typically from 0.0 seconds to a period as long as 10 seconds. Site-specific ground motion spectra serve the same purpose as the design and MCE_R response spectra of Chapter 11 that are based on the mapped values of short-period (0.2s) and 1.0-second response (Chapter 22), but provide response spectral accelerations for multiple response periods that more accurately characterize the intensity and frequency content of the ground motions at the site of interest (when properly calculated). Typically, site-specific ground motion spectra have been used for design of structures of special importance or unique configuration such as a seismically-isolated hospital building for which peer review is required that necessarily includes review of the development of site-specific ground motion spectra.

The following steps illustrate the method of ASCE 7-16 Chapter 21 including consideration of deterministic and probabilistic hazard, adjustment for risk targeting, and treatment of maximum direction spectra. All the steps are explained in detail in the subsequent sections.

Step 1: Determine Probabilistic Spectra

   a. *Compute site-specific geometric mean uniform hazard spectrum (UHS)* - This is obtained from the USGS disggregation tool (USGS 2008) based on site location, V_{s30} for Site Class C, and a ground motion level with 2% probability of exceedance in 50 years.
   b. *Adjust geometric mean to maximum direction UHS* - The geometric mean spectrum of Step 1a is multiplied by the period-dependent maximum direction scale factors of ASCE 7 Section 21.2. Note that this step may be omitted if a maximum direction UHS is computed directly.
   c. *Adjust UHS to uniform risk spectrum (URS)* - The maximum direction uniform hazard spectrum of Step 1b is multiplied by the period-dependent risk coefficients of ASCE 7 Section 21.2.1.1. Note that one could also adjust from UHS to URS through iterative integration of the hazard curve with a collapse fragility curve per ASCE 7 Section 21.2.1.2.

Step 2: Determine Deterministic Spectra

   a. *Compute site-specific maximum direction deterministic spectrum* - This is constructed based on the 84th percentile spectral values for the controlling fault. If the ground motion prediction equations used to compute the 84th percentile values for the controlling fault predict geometric

mean, then the resulting spectrum must be adjusted by the maximum direction scale factors (e.g. see Step 1b above). Adjustment for risk-targeting (i.e. Step 1c above) does not apply to deterministic spectra.

b. *Compute transition spectrum* - This is constructed based on a code-shape spectrum having $S_s = 1.5g$, $S_1 = 0.6g$ and corresponding site amplification factors F_a and F_v. It is often referred to as the transition spectrum since it tends to geographically transition between deterministically-controlled and probabilistically-controlled sites.

c. *Define deterministic spectrum* - The deterministic spectrum is the larger of the spectrum from Steps 2a and 2b.

Step 3: Determine Lower Limit Spectrum

Compute lower limit spectrum - The MCE$_R$ spectrum constructed per ASCE 7 Section 11.4.5 and 11.4.6 for the site is multiplied by 80% to define a lower limit on the site-specific values.

Step 4: Determine Target Spectrum

Define MCE$_R$ target spectrum - The MCE$_R$ target spectrum used in design is taken as the period-by-period minimum of the probabilistic (Step 1c) and the deterministic (Step 2c) but not less than the lower limit (Step 3).

3.3.1 Site-Specific MCE$_R$ and Design Ground Motion Requirements

Chapter 21 provides procedures for performing a site response analysis (Section 21.1) and for performing a site-specific ground motion hazard analysis to determine risk-targeted maximum considered earthquake (MCE$_R$) ground motions (21.2). Site-specific ground motion hazard analysis accounts for regional tectonic setting, geology and seismicity, and the expected recurrence rates of maximum magnitude earthquakes, the characteristics of ground motion attenuation, near source effects and subsurface conditions. The characteristics of subsurface conditions are considered either by attenuation relations or by site response analysis (Section 21.1), the latter being required for Site Class F sites or when available attenuation relations do not adequately incorporate site effects. Results of a site-specific ground motion hazard analysis are used to determine the MCE$_R$ response spectrum (Section 21.2), the design response spectrum (Section 21.3) and site-specific values of short-period and 1-second design acceleration parameters, S_{DS} and S_{D1}, and S_{MS} and S_{M1} (Section 21.4). The underlying methods of a site-specific ground motion analysis are necessarily complex and highly technical, requiring a unique combination of earth science, geotechnical and probabilistic expertise.

Section 11.4.7 permits use of site-specific ground motion procedures to determine seismic ground motion values for design of any structure and requires their use for certain structures and site conditions in lieu of the mapped acceleration parameters of Chapter 22 and the seismic ground motion requirements of Sections 11.4.1 through 11.4.6. Structures and site conditions required by Section 11.4.7 to be designed for site-specific ground motions include seismically isolated structures (Chapter 17) and structures with an energy dissipation system (Chapter 18) at sites with mapped values of 1-second MCE$_R$ spectral response acceleration S_1 greater than or equal to 0.6. Chapters 17 and 18 also effectively require site-specific ground motions for nonlinear response history analysis of isolated or damped structures located near active faults, or with certain configurations or dynamic characteristics (i.e., most isolated and damped structures). Similarly, the nonlinear response history analysis procedures of Chapter 16 effectively require site-specific ground motions as the appropriate basis for selection and scaling of ground motions. Arguably, structures with an isolation or damping system or designed using the nonlinear response history analysis procedures of Chapter 16 represent a limited number of unique structures, often of special importance (e.g., Risk Category IV structures) warranting the additional effort required to develop site-specific ground motions.

Section 11.4.7 also requires site-specific ground motions for design of structures at Site Class E sites with mapped values of short-period MCE$_R$ spectral response acceleration S_S greater than or equal to 1.0, and structures at Site Class D or Site Class E sites with mapped values of 1-second MCE$_R$ spectral response

acceleration S_1 greater than or equal to 0.2. These requirements are new additions to the 2015 NEHRP Provisions and ASCE 7-16 and were adopted to address an identified short-coming in ELF and MSRA procedures for which the design ground motion requirements of Sections 11.4.1 through 11.4.6 were found to be deficient with respect to actual site hazard (Kircher & Associates 2015). Unlike the limited applications of site-specific ground motions required for isolated and damped structures, the new requirements for site-specific ground motions apply to all structures and therefore have a much more significant impact on design practice. Accordingly, Section 11.4.7 provides exceptions that effectively allow designers to use conservative values of ground motion parameters for design using ELF and MRSA procedures in lieu of developing site-specific ground motions.

3.3.2   Site-Specific Seismic Hazard Characterization

Site-specific ground motion hazard is characterized by "seismic hazard" curves for the site of interest that relate the annual frequency of occurrence to a ground motion intensity parameter, typically 5%-damped response spectra acceleration at a given period of response. A uniform hazard spectrum (UHS) is a plot of ground motion intensity parameter as a function of response period for a given annual frequency of occurrence (e.g., annual frequency of 1/1,000 corresponding to a mean annual return period of 1,000 years). Site-specific seismic hazard curves account for the potential sources of earthquakes (e.g., fault location), the potential magnitudes of earthquakes from these sources and their frequencies of occurrence, and the potential ground motions generated by these earthquakes, and necessarily incorporate the uncertainty and randomness in each of these components (also referred to as epistemic and aleatory sources of uncertainty, respectively).

Site-specific seismic hazard curves are calculated using Probabilistic Seismic Hazard Analysis (PSHA) methods, the probabilistic framework used by United States Geological Survey (USGS) to characterize the ground motions of the *United States National Seismic Hazard Maps* (Petersen et al. 2008, Petersen et al., 2014). PSHA, as originally conceived by Cornell (1968), has evolved greatly in terms of scope and complexity requiring considerable geotechnical and earth science expertise and sophisticated computer programs to properly implement. Interested readers may refer to the EERI monograph, *Seismic Hazard and Risk Analysis* (McGuire 2004) for a comprehensive description of PSHA methods. Public domain PSHA software packages include OpenSHA (Field 2003) and proprietary software packages include EZ FRISK, the program used by a number of geotechnical engineering firms to perform a site-specific ground motion hazard analysis.

This example relies on the underlying seismic hazard data, uniform hazard curves and UHS and related results of PSHA calculations developed by the USGS as part of their work *United States National Seismic Hazard Maps* available online at USGS web sites. At the time this example was prepared, most of this information was not yet available online for the 2014 update of seismic hazard maps (Petersen et al., 2014). In such cases, values of various parameters shown in the examples are taken from the 2008 update of the seismic hazard maps (Petersen 2008). While seismic design parameters have changed somewhat from 2014, the underlying methods remain largely the same, and do not affect the validity of the concepts illustrated in the examples of site-specific MCE$_R$ and design ground motion response spectra. Additionally, the examples incorporate current MCE$_R$ ground motions based on 2014 hazard functions obtained from on-going research of the Southern California Earthquake Consortium (SCEC) CyberShake project (Milner 2015).

3.3.3   Example Site-Specific MCE$_R$ and Design Ground Motion Spectra

3.3.3.1 Example Site – Riverside California.   This section develops an example of site-specific MCE$_R$ and design ground motion spectra for a site in Riverside California (33.935, -117.403). The example Riverside site is shown in Figure 3.3-1 (labeled as SCEC Site S684). An important first step in a site-specific analysis is the identification of the location and properties of seismic sources (active faults) close enough to contribute to seismic hazard at the site of interest. Figure 3.3-1 shows the surface projection of

active faults (or segments of a fault system) obtained from the USGS fault database (Petersen et al., 2014), including, in particular, fault segments of the San Jacinto, San Andreas and Whittier-Elsinore fault systems. The closest distances of the site to each of these fault systems is about 18 km to the San Jacinto (SB) fault, about 29 km to the San Andreas (SB) fault and about 21 km to the Elsinore (GI) fault.

Figure 3.3-1   Google earth map showing location of the example site (SCEC Site S684) in Riverside California and fault segments of active fault systems

Other important fault data available from USGS fault database include the magnitude potential and slip rate of individual fault segments and multi-segment ruptures of fault systems. Earthquake magnitude is related to the length of fault rupture (i.e., larger earthquake magnitudes are expected for longer lengths of fault rupture). The recurrence rate or likelihood of an earthquake occurring is related to the fault slip rate (i.e., earthquakes are expected to occur more frequently on faults which have larger values of the slip rate). Fault segments of the San Jacinto and San Andreas systems have the potential to generate large magnitude (i.e., $\geq$ M7.0) earthquakes as well as exceptionally high slip rates (i.e., $\geq$ 10 mm/year) and are, therefore, are expected to be the primary contributors to seismic ground motion hazard at the example Riverside site.

Site characteristics which include the site shear wave velocity (site class) and basin depth significantly influence seismic hazard. As discussed in Section 3.3.1, site characteristics may be determined by performing a site response analysis (Section 21.1 of ASCE 7-16), although such analysis is not typically performed for sites in the western United States. In general, a geotechnical study of the site is performed that includes determination of an appropriate value of the shear wave velocity in the upper 30 meters ($v_{s,30}$) and the corresponding site class. For this example, the value of site shear wave velocity at the Riverside site is taken as $v_{s,30}$ = 1,200 fps (Site Class CD boundary) consistent with estimates of shear wave velocity available from on-line databases of OpenSHA (http://www.opensha.org/apps-SiteData) and the USGS (http://earthquake.usgs.gov/hazards/). While generally accurate, these estimates of shear wave velocity which are based on the research of Wills and Clahan (2006) for California sites and on Wald and Allen (2007) for United States sites are inferred from topographical features and other characteristics, rather than based on actual site-specific measurements of shear wave velocity.

The USGS provides a number of useful site-specific ground motion hazard tools online, including interactive de-aggregation of hazard functions (USGS 2015). De-aggregations of 2% in 50-year ground motion response spectral acceleration (i.e., mean return period of 2,475 years) for the example Riverside site are shown in Figure 3.3-2 for three response periods 0.2s (top), 1s (middle) and 5s (bottom). Each of the three de-aggregation plots show the collective contribution of the various sources to site hazard binned in terms of the earthquake magnitude and closest distance of the site to fault rupture. The height of the vertical bars indicates the relative contribution of the magnitude-distance bin to site hazard.

The color scheme indicates the value of the de-aggregation parameter ε_0, a measure of the rareness of the ground motions of the mean return period of interest relative to median ground motions of the magnitude-distance pair of the bin of interest. In this example, light blue shading (which represents values of ε_0, $1.0 < \varepsilon_0 < 2.0$) indicates that 2,475-year ground motions are between 1 and 2 lognormal standard deviations above median ground motions, or about 1.8 ($e^{0.6 \times 1.0}$) to 3.3 ($e^{0.6 \times 2.0}$) times as strong as median ground motions (assuming a lognormal standard deviation value of 0.6).

Plots in Figure 3.3-2 show that large magnitude earthquakes on the San Jacinto fault system (i.e., vertical bars of bins at a closest distance of about 18 km) and the San Andreas fault system (i.e., vertical bars at a closest distance of about 29 km form the site) dominate site hazard at all periods, except at short-periods (0.2s) for which smaller-magnitude seismic sources at closer distances also contribute to site hazard. The relatively large values of ε_0 for the example Riverside site are due to the relatively high slip rates of these fault systems and the mean annual return period of 2,475 years which is effectively many time longer than the expected time between the occurrence of large-magnitude earthquakes on these highly active sources.

Modal values of distance (R), magnitude (M) and ε_0 refer to the magnitude-distance bin with tallest vertical bar (i.e., the magnitude-distance bin with the largest de-aggregation probability). Modal results for 1s response indicate that 2,475-year ground motions (0.8627 g) are about 2.5 ($e^{0.6 \times 1.53}$) times median ground motions (approx. 0.35 g) of a magnitude M7.61 earthquake on the San Jacinto fault at a closest distance of 17.8 km ($\varepsilon_0 = 1.53$). Modal results also indicate that an earthquake on the San Jacinto fault system (i.e., closest distance of about 18 km) with a magnitude as low as M7.0 (based on 0.2s response) or as large as M7.8 (based on 5s response) could be assumed for evaluation of deterministic MCE_R ground motions (Section 3.3.2.3).
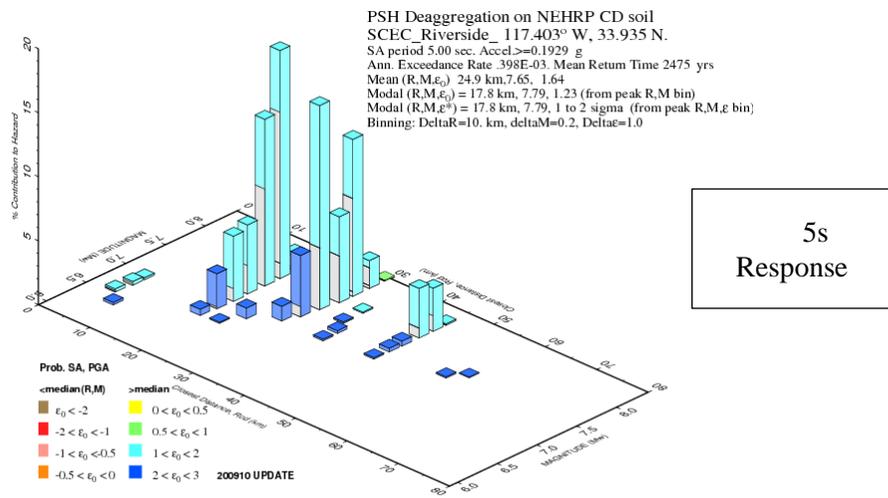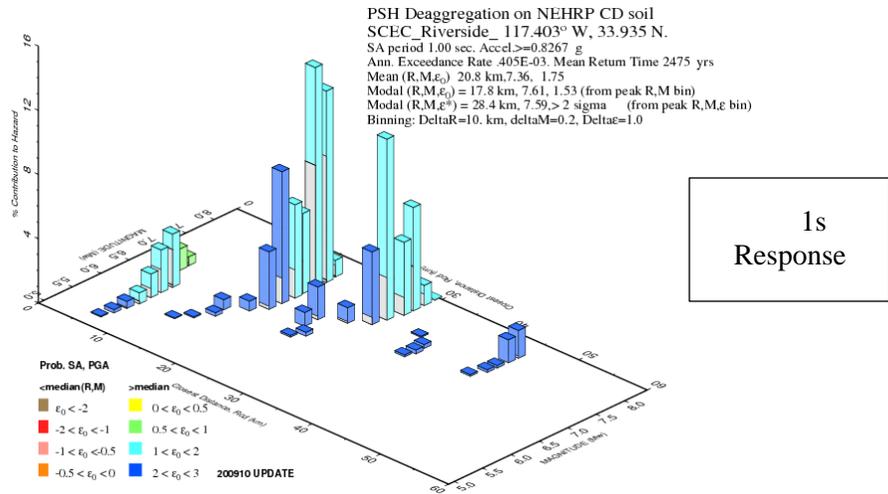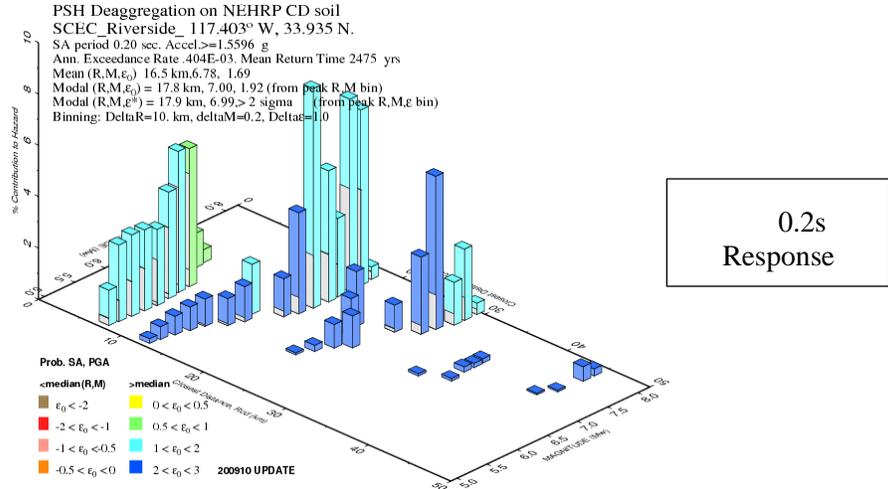
Figure 3.3-2 Example de-aggregation of 2,475-year mean annual return period seismic hazard for 0.2s response (top), 1s response (middle) and 5s response (bottom) (USGS 2015a)

Site-specific seismic design parameters of the 2009 NEHRP Provisions and ASCE 7-10 are available from the "U.S. Seismic Design Maps" web site (USGS 2015) and in the future will be available for the 2015 NEHRP Provisions and ASCE 7-16 from this web site (or equivalent). For this example, values of seismic design parameters of the 2014 NEHRP Provisions (and ASCE 7-16) were provided by the USGS for the example Riverside site (Luco 2015). These parameters provide important information for "sanity checking" of site-specific response spectra (at response periods of 0.2s and 1.0s) and are required by Section 21.3 to establish lower-bound limits on site-specific design spectra to avoid potential underestimation of site ground motion hazard. Table 3.3-1 provides a summary of seismic design parameters of the 2009 and 2014 NEHRP Provisions for the example Riverside site. It should be noted that the values of the seismic design parameters S_{MS}, S_{M1}, S_{DS} and S_{D1} are the same for the 2009 NEHRP Provisions and ASCE 7-10 (and, likewise, the same for the 2015 NEHRP Provisions and ASCE 7-16), although the NEHRP Provisions provides more in-sight into the basis for these parameters.

Table 3.3-1   Seismic design parameters of the 2009 NEHRP Provisions (ASCE 7-10) and the 2015 NEHRP Provisions (ASCE 7-16) for the example Riverside site (USGS 2013, Luco 2015)

Parameter Symbol	Parameter Definition	2009 Source or Equation	2009 Value	2015 Value
S_{SUH}	Uniform-hazard (2% in 50-year) ground motions of 0.2s response spectral acceleration, Site Class BC	Fig. 22-1	1.660 g	1.659
C_{RS}	Risk coefficient at 0.2s spectral response period	Fig. 22-3	1.106	0.945
C_{RS} x S_{SUH}	Uniform-risk (1% in 50-year) ground motions of 0.2s response spectral acceleration, Site Class BC	Eq. (11.4-1)	1.836 g	1.568
S_{SD}	Deterministic ground motions of 0.2s response spectral acceleration, Site Class BC	Fig. 22-5	1.50 g	1.50 g
S_S	MCE$_R$ 0.2s response spectral acceleration, Site Class BC (minimum of S_{SD} and C_{RS} x S_{SUH})		1.50 g	1.50 g
S_{1UH}	Uniform-hazard (2% in 50-year) ground motions of 0.2s response spectral acceleration, Site Class BC	Fig. 22-2	0.658 g	0.624
C_{R1}	Risk coefficient at 1.0s spectral response period	Fig. 22-4	1.072	0.919
S_{1D}	Deterministic ground motions of 0.2s response spectral acceleration, Site Class BC	Fig. 22-6	0.60 g	0.60 g
S_1	MCE$_R$ 1.0s response spectral acceleration, Site Class BC (minimum of S_{SD} and C_{RS} x S_{SUH})		0.60 g	0.573 g
F_a (C)	Short-period (0.2s) site coefficient, Site Class C	Table 11.4-1	1.0	1.2
F_a (D)	Short-period (0.2s) site coefficient, Site Class D	Table 11.4-1	1.0	1.0
F_a (CD)	Short-period (0.2s) site coefficient, Site Class CD	[F_a(C)+F_a(D)]/2	1.0	1.1
F_v (C)	Long-period (1.0s) site coefficient, Site Class C	Table 11.4-2	1.3	1.4
F_v (D)	Long-period (1.0s) site coefficient, Site Class D	Table 11.4-2	1.5	1.7
F_v (CD)	Long-period (1.0s) site coefficient, Site Class CD	[F_v(C)+F_v(D)]/2	1.4	1.55
S_{MS}	MCE$_R$ 0.2s response spectral acceleration, Site Class CD (F_a x S_S)	Eq. (11.4-5)	1.50 g	1.65 g
S_{M1}	MCE$_R$ 1.0s response spectral acceleration, Site Class CD (F_v x S_1)	Eq. (11.4-6)	0.84 g	0.89 g
S_{DS}	Design 0.2s response spectral acceleration, Site Class CD (2/3 x S_{MS})	Eq. (11.4-7)	1.00 g	1.10 g
S_{D1}	Design 1.0s response spectral acceleration, Site Class CD (2/3 x S_{M1})	Eq. (11.4-8)	0.56 g	0.62 g
T_s (CD)	Short-period transition period (S_{D1}/S_{DS})	Fig. 11.4-1	0.52 s	0.59 s
T_0 (CD)	ZPA transition period (0.2 x S_{D1}/S_{DS})	Fig. 11.4-1	0.104 s	0.108 s
T_L	Long-period transition period	Fig. 22-7	8 s	8 s

3.3.3.2 Probabilistic MCE$_R$ Ground Motions. Section 21.2.1 of ASCE 7-16 (and ASCE 7-10) defines the site-specific probabilistic MCE$_R$ ground motions in terms of 5-percent damped response spectral acceleration at each period in the direction of maximum horizontal response that is expected to achieve a 1 percent probability of collapse within a 50-year period, and specifies two methods for determining the probabilistic MCE$_R$ response spectrum.

The first method (Method 1) recognizes that PSHA methods define ground motion intensity in terms of a uniform hazard probability (e.g., 2% in 50-year) rather than a uniform collapse probability, and provides mapped values of the risk coefficient C$_R$ for converting 2% in 50-year uniform hazard spectra (UHS) to 1% in 50-year uniform collapse risk-target ground motion (RTGM) spectra. Values of the risk coefficient are period-dependent and vary as function of the slope and shape of the site hazard function, including site effects. Mapped values of the risk coefficient developed by the USGS at periods of 0.2s (C$_{RS}$) and 1.0s (C$_{R1}$) for Site Class BC site conditions are assumed applicable to other site conditions.

The second method (Method 2) directly calculates 1% in 50-year uniform collapse risk-targeted ground motions from site hazard functions by an iterative process of integrating a lognormal probability density function that is the derivative of a hypothetical collapse fragility curve defined as having a 10 percent conditional probability of collapse at MCE$_R$ ground motion intensity and an associated lognormal standard deviation value of 0.6. Method 2 was used by the USGS to calculate the mapped values of the risk coefficients of Method 1. Probabilistic MCE$_R$ response spectra determined by Method 2 are conceptually more accurate than those of Method 1 since they do not rely on risk coefficients that are defined at only two response periods for Site Class BC site conditions, although the differences in probabilistic MCE$_R$ response spectra of the two methods is typically very small.

Prior to about 2005, attenuation relations (now referred to as ground motion predictive equations) defined ground motion intensity in terms of the average or "geomean" horizontal response, where geomean response at the period of interest is calculated as the square root of the product of peak responses of two orthogonal horizontal components of recorded ground motions. Geomean response has no physical meaning since the peak response of one horizontal component seldom occurs at the same point in time during the earthquake as that of the other horizontal component, and is not uniquely defined since the values of peak response of the two horizontal components vary with the orientation of the two horizontal components (e.g., vary with orientation of the horizontal axes of the ground motion recording unit).

As part of the change in the basis of design ground motions from uniform hazard to uniform risk during the 2009/2010 Code cycle, *Project 07* defined ground motion intensity at the period of interest as the "maximum" response in the horizontal plane (i.e., peak response from the origin occurring in any direction in the horizontal plane during the earthquake). The maximum direction definition was deemed more appropriate (e.g., than the geomean definition) for seismic design of buildings that are considered equally likely to collapse in any direction and provided a non-ambiguous, physically realizable, definition of response (albeit of a linear-elastic single-degree-of-freedom system). Ratios of maximum direction response to geomean response were developed for conversion of geomean-based ground motions to the maximum direction ground motions, as described in the commentary of the 2009 NEHRP Provisions (BSSC 2009).

Short-comings with the use of the geomean definition of ground motion intensity prompted earthquake ground motion modelers to develop statistically-based, orientation-independent, definitions of median (i.e., RotD50) and maximum (i.e., RotD100) response in the horizontal plane (Boore et al., 2006, Boore 2010). Current ground motion predictive equations (e.g., PEER NGA-West2 relations) now use RotD50 as the ground intensity parameter. Recognizing the need to allow use of a consistent definition of S$_a$ throughout the design process, formulas relating RotD100 to RotD50 have been developed (Shahi & Baker 2013) that are somewhat different from the ratios of maximum direction response to geomean response used by the USGS to develop the ground motion maps of the 2009 NEHRP Provisions and ASCE 7-10 and to update the ground motion maps of the 2015 NEHRP Provisions and ASCE 7-16.

This section illustrates development of probabilistic MCE$_R$ response spectra for the example Riverside site using both Method 1 and Method 2 requirements. For Method 1, probabilistic MCE$_R$ response spectra are separately calculated with (1) the ratios of maximum to geomean response used by the USGS to develop the seismic design values maps of ASCE 7-10 and ASCE 7-16 (2009/2015 NEHRP Provisions) and (2) the ratios of RotD100 to RotD50 response of Shahi & Baker (2013). Method 1 illustrates how users could develop site-specific probabilistic MCE$_R$ response spectra from 2% in 50-year UHS. While not yet available (during development of this example), the USGS intends to update their web-based Seismic Hazard Curve application (USGS 2012) and provide 2% in 50 year UHS for sites in the U.S. based on the hazard functions of the 2014 update of seismic hazard maps (Petersen et al., 2014).

For the example Riverside site, the SCEC provided 2% in 50-year UHS and 1% in 50-year RTGM response spectra (Milner 2015). These spectra incorporate the same ground motion relations (e.g., PEER NGA West2 relations) and the same hazard functions as those of the 2014 update, except that PSHA calculations did not include the updated forecast of UCERF3 (Field et al., 2015). Incorporation of UCERF3 would not be expected to significantly change ground motions at the Riverside site. Table 3.3-2 summarizes the values of SCEC response spectra for two site conditions, hypothetical Site Class BC ($v_{s,30}$ = 762 mps) conditions (reference conditions) and actual Site Class CD ($v_{s,30}$ = 366 mps) conditions. SCEC spectra represent maximum (RotD100) ground motion intensity based on Shahi & Baker (2013).

Table 3.3-2 Summary of SCEC 2% in 50-year UHS and 1% in 50-year RTGM spectra for hypothetical ($v_{s,30}$ = 762 mps) and actual ($v_{s,30}$ = 366 mps) site conditions of the example Riverside site (Milner 2015) and derived values of site amplification and risk coefficients

Period T (s)	2%-50yr UHS RotD100 762 mps	2%-50yr UHS RotD100 366 mps	1%-50yr RTGM RotD100 762 mps	1%-50yr RTGM RotD100 366 mps	Derived Site Amplification	Derived Values of the Risk Coefficient
0.01	0.758	0.907	0.746	0.904	1.20	0.997
0.02	0.774	0.909	0.762	0.906	1.17	0.997
0.03	0.869	0.957	0.853	0.955	1.10	0.998
0.05	1.166	1.151	1.132	1.148	0.99	0.997
0.075	1.535	1.472	1.483	1.459	0.96	0.991
0.1	1.742	1.725	1.685	1.721	0.99	0.997
0.15	1.923	2.060	1.859	2.055	1.07	0.998
0.2	1.847	2.250	1.789	2.244	1.22	0.997
0.25	1.692	2.349	1.641	2.318	1.39	0.987
0.3	1.545	2.366	1.494	2.318	1.53	0.980
0.4	1.308	2.242	1.264	2.180	1.71	0.973
0.5	1.132	2.054	1.089	1.986	1.81	0.967
0.75	0.828	1.598	0.790	1.527	1.93	0.956
1.0	0.628	1.262	0.595	1.198	2.01	0.950
1.5	0.408	0.850	0.385	0.804	2.08	0.946
2.0	0.300	0.627	0.282	0.589	2.09	0.940
3.0	0.196	0.411	0.183	0.384	2.09	0.935
4.0	0.148	0.303	0.137	0.282	2.05	0.930
5.0	0.124	0.245	0.114	0.226	1.98	0.922
7.5	0.084	0.154	0.077	0.141	1.84	0.915
10	0.056	0.096	0.051	0.088	1.71	0.913

Table 3.3-2 also shows derived values of period-dependent site amplification and the risk coefficient. Period-dependent values of site amplification are the ratios of 2% in 50-year UHS of Site Class CD (366 mps) and 2% in 50-year UHS of Site Class BC (762 mps). Period-dependent values of the risk coefficient are the ratios of 1% in 50-year RTGM spectra and 2% in 50-year UHS for Site Class CD (366 mps). It may be noted that at longer periods, derived values of Site Class CD site amplification (e.g., 2.0 at 1.0s) tends to be about 30 percent greater than the long-period site coefficient, $F_v = 1.55$ (Table 3.3-1). It may also be noted that derived values of the risk coefficient are somewhat different in general from the values of C_{RS} and C_{R1} (Table 3.3-1), although these differences are generally small.

Table 3.3-3 summarizes 2% in 50-year UHS, factors converting geomean to maximum or RotD50 to RotD100 response and mapped values of risk coefficients and probabilistic MCE_R ground motions calculated from these parameters in accordance with Method 1 of Section 21.2.1, and probabilistic MCE_R ground motions calculated using Method 2 of Section 21.2.1 of ASCE 7-16 for the example Riverside site. The 2% in 50-year UHS for hypothetical Site Class BC (reference) site conditions are provided for comparison with actual site conditions to illustrate the importance of site affects and are not used in the calculation of site-specific ground motions. Values in Columns with headings (A), (B1) or (B2) and (C) are multiplied together for Method 1 calculation of probabilistic MCE_R response spectra. Table 3.3-3 is included primarily for documenting values; Figure 3.3-3 provides a more comprehensible comparison of UHS and probabilistic MCE_R response spectra for the example Riverside site.

Table 3.3-3   Summary of 2% in 50-year UHS, maximum/geomean and RotD100/RotD50 ratios, mapped values of risk coefficients and probabilistic MCE_R ground motions calculated from these parameters using Method 1 of Section 21.2.1, and probabilistic MCE_R ground motions calculated using Method 2 of Section 21.2.1 of ASCE 7-16 for the example Riverside site

Period T (s)	2%-50yr UHS RotD50 762 mps	2%-50yr UHS RotD100 762 mps	(A) 2%-50yr UHS RotD50 366 mps	(B1) Maximum/ Geomean (ASCE 7-10/16)	(B2) RotD100/ RotD50 (Shahi & Baker)	(C) Risk Coefficient (ASCE 7-16)	Prob MCE_R Method 1 366 mps (AxB1xC)	Prob MCE_R Method 1 366 mps (AxB2xC)	Prob MCE_R Method 2 366 mps (SCEC)
0.01	0.635	0.758	0.760	1.10	1.19	0.945	0.790	0.857	0.904
0.02	0.650	0.774	0.763	1.10	1.19	0.945	0.793	0.859	0.906
0.03	0.732	0.869	0.806	1.10	1.19	0.945	0.838	0.904	0.955
0.05	0.983	1.166	0.970	1.10	1.19	0.945	1.009	1.088	1.148
0.075	1.292	1.535	1.239	1.10	1.19	0.945	1.288	1.391	1.459
0.1	1.467	1.742	1.453	1.10	1.19	0.945	1.510	1.630	1.721
0.15	1.603	1.923	1.717	1.10	1.20	0.945	1.785	1.947	2.055
0.2	1.532	1.847	1.866	1.10	1.21	0.945	1.940	2.126	2.244
0.25	1.391	1.692	1.931	1.11	1.22	0.943	2.027	2.216	2.318
0.3	1.268	1.545	1.941	1.13	1.22	0.942	2.057	2.228	2.318
0.4	1.064	1.308	1.824	1.15	1.23	0.939	1.969	2.104	2.180
0.5	0.921	1.132	1.671	1.18	1.23	0.935	1.837	1.921	1.986
0.75	0.669	0.828	1.291	1.24	1.24	0.927	1.482	1.482	1.527
1.0	0.506	0.628	1.017	1.30	1.24	0.919	1.215	1.160	1.198
1.5	0.328	0.408	0.684	1.33	1.24	0.919	0.833	0.781	0.804
2.0	0.241	0.300	0.504	1.35	1.24	0.919	0.625	0.576	0.589
3.0	0.157	0.196	0.330	1.40	1.25	0.919	0.424	0.378	0.384
4.0	0.117	0.148	0.240	1.45	1.26	0.919	0.320	0.278	0.282
5.0	0.098	0.124	0.194	1.50	1.26	0.919	0.267	0.225	0.226
7.5	0.065	0.084	0.120	1.50	1.29	0.919	0.165	0.142	0.141
10	0.043	0.056	0.075	1.50	1.29	0.919	0.103	0.089	0.088
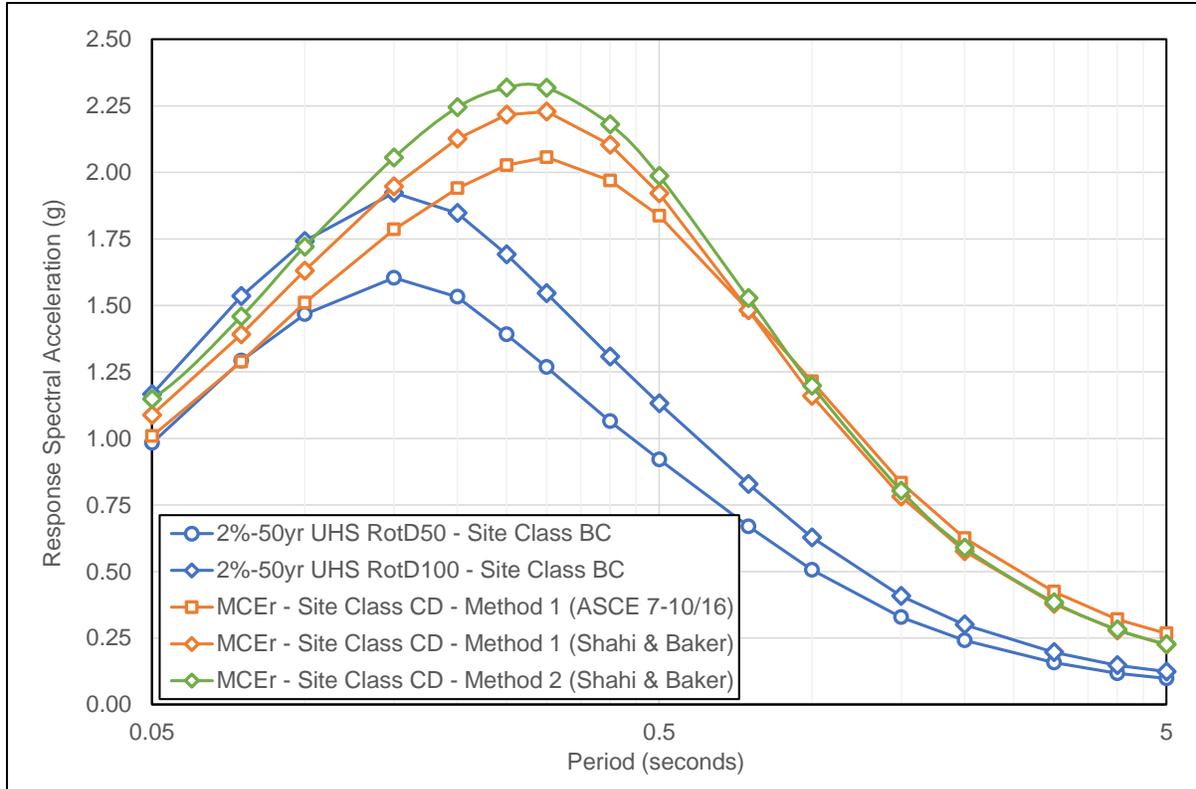
Figure 3.3-3   Plots of 2% in 50-year UHS for Site Class BC (hypothetical, reference site conditions) and probabilistic MCE$_R$ response spectra for Site Class CD (actual site conditions) calculated in accordance with either Method 1 or Method 2 of Section 21.2.1 of ASCE 7-16 for the example Riverside site

Review of the various plots of the response spectra shown in Figure 3.3-3 provide the following insights into the example calculation of probabilistic MCE$_R$ ground motions and the underlying seismic hazard at the Riverside site:

(1)   Although the example Riverside site is about 18 km from the San Jacinto fault system and about 29 km from the San Andreas fault system (i.e., the fault systems dominating seismic hazard at the Riverside site), site-specific probabilistic MCE$_R$ ground motions are quite strong reflecting the influence of the very high activity rates of these two fault systems on site hazard.

(2)   Comparison of 2% in 50-year UHS for hypothetical Site Class BC (reference) site conditions and probabilistic MCE$_R$ response spectra for actual Site Class CD site conditions illustrates the importance of site conditions and the associated value of $v_{s,30}$ on the intensity and frequency content of site-specific probabilistic ground motions.

(3)   Comparison of the probabilistic MCE$_R$ response spectrum calculated using Method 1 and ratios of maximum to geomean response of ASCE 7-10/ASCE 7-16 with the probabilistic MCE$_R$ response spectrum calculated using Method 1 and the ratios of RotD100 to RotD50 response of Shahi & Baker (2013) indicate a non-negligible difference in maximum response estimated by these two methods, although of much less significance than the effects of site conditions.

(4)   Comparison of probabilistic MCE$_R$ response spectra calculated using Method 1 and Method 2 show negligible difference when both methods are based on the same ratios of RotD100 to

RotD50 response indicating that differences, if any, between the mapped values of the risk coefficients (Method 1) and actual values implicit of Method 2 are not very important.

3.3.3.3 Deterministic MCE$_R$ Ground Motions. Section 21.2.2 of ASCE 7-16 (and ASCE 7-10) defines the site-specific deterministic MCE$_R$ ground motions in terms of 84th percentile 5-percent damped response spectral acceleration at each period in the direction of maximum horizontal response that is the largest such acceleration at the site of interest calculated for the characteristic earthquake on all known active faults in the region, subject to a deterministic "lower-limit." The deterministic lower-limit on the MCE$_R$ response spectrum is defined by the shape of the design response spectrum (Figure 11.4-1 of ASCE 7-16) with the domain of constant acceleration equal to $1.5F_a$ and the domain of constant velocity equal to $0.6F_v/T$, as illustrated in Figure 21.2-1 of ASCE 7-16. Values of F_a and F_v are obtained from Tables 11.4-1 and 11.4-2 at the mapped values of MCE$_R$ ground motions, $S_S = 1.5$ and $S_1 = 0.6$. For the example Riverside site, values of site coefficients are, $F_a = 1.1$ (at $S_s = 1.5$) and $F_v = 1.55$ (at $S_1 = 0.6$) for Site Class CD site conditions ($v_{s,30} = 366$ mps) based on linear interpolation of the site coefficients of Site Class C and Site Class D, as shown in Table 3.3-1.

In addition to site conditions ($v_{s,30}$), the two key parameters in the calculation of site-specific deterministic MCE$_R$ ground motions are the "characteristic earthquake" magnitude (M_w) and the closest distance to fault rupture (e.g., R_X) associated with each fault that governs site seismic hazard. For this example, a magnitude M7.8 earthquake on the San Jacinto fault (closest fault rupture distance, $R_X = 18$ km) is assumed to be an appropriate (perhaps conservative) value of characteristic earthquake magnitude for the San Jacinto fault system which governs deterministic hazard at the example Riverside site. The magnitude M7.8 at $R_X = 18$ km is based on the de-aggregation results shown in Figure 3.3-2 and the assumption that response periods of design interest are greater than 1-second (e.g., the site-specific MCE$_R$ response spectrum would be appropriate for design of taller buildings).

There are a number of other site-source and fault characteristics required for calculation of deterministic MCE$_R$ ground motions which include (for western U.S. sites governed by shallow crustal earthquakes), fault type (e.g., strike-slip, normal, reverse, thrust), site-source distances (R_{JB} and R_{RUP}, as well as R_X), depth to the top of the fault rupture plane (Z_{TOR}), fault width (W), fault dip angle, hanging wall or footwall site location (for dipping faults), and "basin depth" parameters ($Z_{1.0}$ and $Z_{2.5}$). Values of these terms may be found in the USGS fault database or can be derived based on fault geometry (e.g., R_{JB}, R_{RUP} and R_X), or taken as equal to "default" values (e.g., default values of $Z_{1.0}$ and $Z_{2.5}$ inferred from $v_{s,30}$). It may be noted that each of the site-source and fault terms required for calculation of deterministic MCE$_R$ ground motions is also required for calculation of probabilistic MCE$_R$ ground motions. Other than the deterministic values of M_w and R_X, the same values of these terms should be used for both calculations and, in general, be the same as the values of these terms used by the USGS for the 2014 update of the United States National Seismic Hazard Maps (Petersen et al. 2014).

For the example Riverside site, deterministic median and 84th percentile RotD50 (geomean) response spectra were conveniently calculated with the Excel spreadsheet program, "Weighted Average of 2014 NGA West-2 GMPEs" (Seyhan 2014) obtained from PEER NGA West-2 web site (http://peer.berkeley.edu/ngawest2/databases/). The Excel program calculates the weighted average of the five ground motion predictive equations (GMPEs) developed as part of the PEER NGA West-2 project (ASK 14, BSSA14, CB14, CY14 and I14) for user-specified values of M_w, R_X and $v_{s,30}$, other site-source and fault properties and the respective weights to be applied to each of the individual GMPEs. Consistent with the weights used by SCEC to develop 2% in 50-year UHS and probabilistic MCE$_R$ ground motions, equal weights of 25 percent each were used to combine median and 84th response spectra of the ASK14, BSSA14, CB14 and CY14 GMPEs. The I14 was excluded from these calculations since this GMPE does not apply to soil sites with values of $v_{s,30} \leq 450$ mps. Note. These are the same GMPEs used by the USGS for the 2014 update of the United States National Seismic Hazard Maps, except that the I14 GMPE (with a weight of 12 percent) was also included in the calculation of the mapped values of seismic parameters for reference Site Class BC ($v_{s,30} \leq 762$ mps) site conditions.

Table 3.3-4 summarizes M7.8 RotD50 (geomean) response spectra calculated for the example Riverside site using the PEER NGA West-2 spreadsheet (i.e., response spectra listed in columns labeled A0, A1 and A2), values of the maximum/geomean and RotD100/RotD50 ratios (i.e., ratios listed in columns labeled B1 and B2) and M7.8 84th percentile RotD100 (maximum) response spectra based on these data, and the deterministic lower-limit on MCE_R response spectrum which governs in this example. Although not required for calculation of site-specific ground motions, response spectra are provided for hypothetical Site Class BC (762 mps) reference site conditions for comparison with site-specific ground motions for actual Site Class CD (366 mps) site conditions. It may be noted that the maximum/geomean and RotD100/RotD50 ratios used to convert geomean (or RotD50) response to maximum (or RotD100) response are the same as those of the probabilistic MCE_R ground motions (Table 3.3-3). Table 3.3-4 is included primarily for documenting values; Figure 3.3-4 provides a more comprehensible comparison of various M7.8 response spectra and the deterministic lower-limit on MCE_R response for the example Riverside site.

Table 3.3-4   Summary of 1.8 x median and 84th percentile RotD50 (geomean) response spectra, maximum/geomean and RotD100/RotD50 ratios, and deterministic 84th percentile RotD100 (maximum) response spectra at the example Riverside site for a magnitude M7.8 earthquake on the San Jacinto fault at R_X = 18 km, and the deterministic MCE_R response spectrum based on the lower-limit of deterministic response (Figure 21.2-1 of ASCE 7-16)

Period T (s)	(A0) M7.8 RotD50 84th %ile 762 mps	(A1) M7.8 RotD50 1.8 x Median 366 mps	(A2) M7.8 RotD50 84th %ile 366 mps	(B1) Maximum/ Geomean (ASCE 7-10/16)	(B2) RotD100/ RotD50 (Shahi & Baker)	M7.8 Maximum 1.8 x Median 366 mps (A1xB1)	M7.8 RotD100 84th %ile 366 mps (A2xB2)	M7.8 RotD100 84th %ile 762 mps (A0xB2)	Deter-ministic Lower Limit (Fig. 21.2-1)
0.01	0.45	0.51	0.50	1.10	1.19	0.56	0.59	0.53	0.75
0.02	0.45	0.51	0.50	1.10	1.19	0.56	0.59	0.54	0.84
0.03	0.49	0.53	0.52	1.10	1.19	0.58	0.62	0.58	0.92
0.05	0.61	0.60	0.60	1.10	1.19	0.66	0.71	0.73	1.10
0.08	0.78	0.73	0.73	1.10	1.19	0.80	0.87	0.93	1.32
0.10	0.88	0.84	0.85	1.10	1.19	0.93	1.01	1.05	1.54
0.15	0.98	1.03	1.03	1.10	1.20	1.13	1.23	1.17	1.65
0.20	0.95	1.14	1.13	1.10	1.21	1.25	1.36	1.15	1.65
0.25	0.88	1.18	1.18	1.11	1.22	1.31	1.44	1.07	1.65
0.30	0.81	1.18	1.21	1.13	1.22	1.33	1.47	0.99	1.65
0.40	0.70	1.11	1.17	1.15	1.23	1.28	1.43	0.86	1.65
0.50	0.61	1.02	1.09	1.18	1.23	1.19	1.33	0.75	1.65
0.75	0.45	0.77	0.85	1.24	1.24	0.95	1.05	0.55	1.24
1.00	0.34	0.61	0.68	1.30	1.24	0.79	0.85	0.42	0.93
1.50	0.23	0.42	0.48	1.33	1.24	0.56	0.59	0.28	0.62
2.00	0.17	0.32	0.36	1.35	1.24	0.43	0.44	0.21	0.47
3.00	0.12	0.21	0.24	1.40	1.25	0.30	0.30	0.14	0.31
4.00	0.09	0.16	0.18	1.45	1.26	0.23	0.23	0.11	0.23
5.00	0.07	0.12	0.14	1.50	1.26	0.18	0.17	0.09	0.19
7.50	0.04	0.07	0.08	1.50	1.29	0.10	0.10	0.05	0.12
10.00	0.03	0.04	0.05	1.50	1.29	0.06	0.06	0.03	0.09
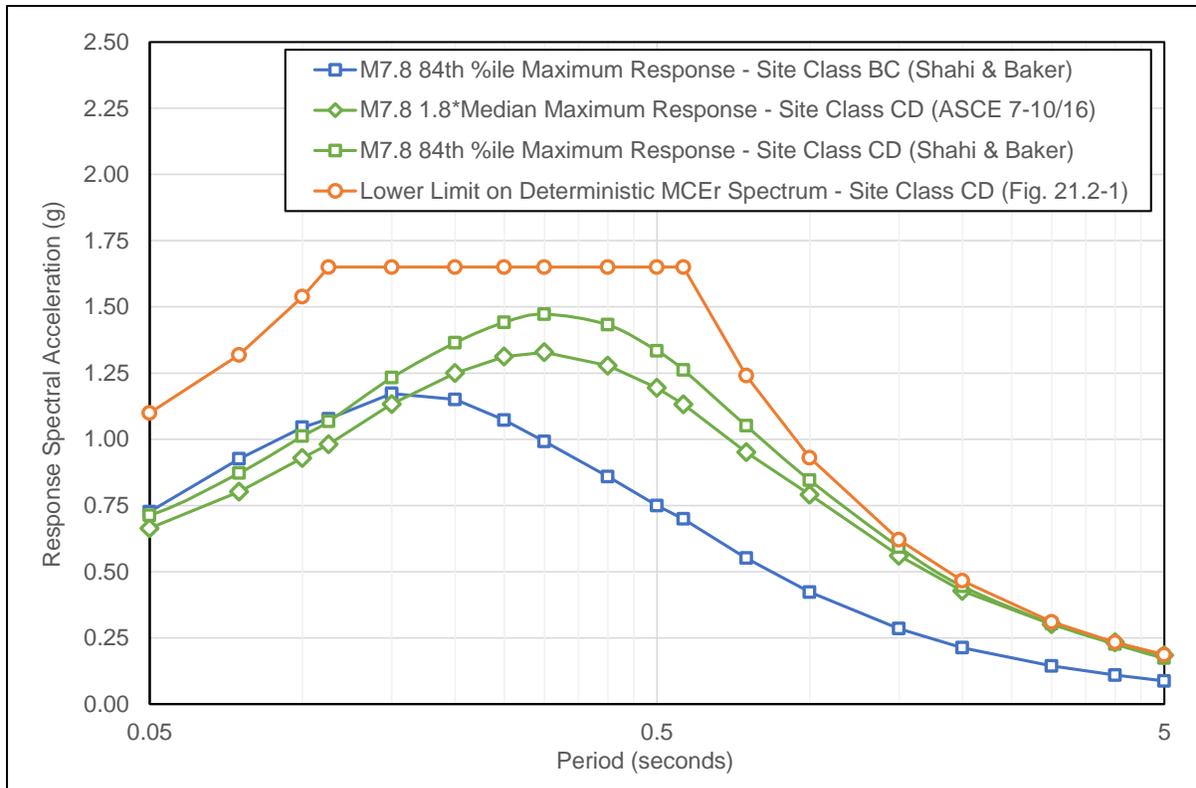
Figure 3.3-4   Plots of 1.8 times median and 84th percentile ground motion response spectra for a magnitude M7.8 earthquake on the San Jacinto fault system at a closest distance of R_X = 18 km, and the deterministic MCE$_R$ response spectrum based on the lower-limit of deterministic response based on Figure 21.2-1 of ASCE 7-16

Review of the various plots of the response spectra shown in Figure 3.3-4 provide the following insights into the example calculation of deterministic MCE$_R$ ground motions and the underlying seismic hazard at the Riverside site:

(1)   The deterministic lower-limit governs deterministic MCE$_R$ ground motions at all periods for the example Riverside site, although lower-limit and 84th percentile values are similar at long periods (e.g., at 3.0s). The deterministic lower-limit governs since at a closest distance of R_X = 18 km from fault rupture, the NGA West-2 GMPEs substantial attenuate M7.8 84th percentile ground motions and response spectral accelerations are below the lower-limit values of 1.65 g = 1.5F$_a$ at short-periods and 0.93/T g = 0.6F$_v$/T at periods in the domain of constant velocity.

(2)   Comparison of M7.8 response spectra for hypothetical Site Class BC (reference) site conditions and M7.8 response spectra for actual Site Class CD site conditions (in both cases for 84th percentile response and other common assumptions) illustrates the importance of site conditions and the associated site-specific value of $v_{s,30}$ on the intensity and frequency content of site-specific deterministic ground motions. Site amplification of Site Class CD is about a factor of 2 at mid and long periods (i.e., same site-specific probabilistic ground motions amplification).

(3)   Comparison of the M7.8 response spectrum calculated consistent with the methods used by the USGS to develop the design values maps of ASCE 7-10 and ASCE 7-16 (i.e., 1.8 x median and maximum/geomean ratios) with the M7.8 response spectrum calculated using actual 84th percentile response of the GMPEs (rather than 1.8 x median) and the more defendable RotD100/RotD50 ratios of Shahi & Baker indicate a non-negligible difference in maximum

response estimated by these two approaches (at short periods), although the difference is much less significant than that due to the effects of site conditions.

3.3.3.4 Site-Specific MCE$_R$ and Design Response Spectra. Section 21.2.3 of ASCE 7-16 (and ASCE 7-10) defines the site-specific MCE$_R$ ground motions as the lesser of (1) the probabilistic MCE$_R$ ground motions (Section 21.2.1) and (2) the deterministic MCE$_R$ ground motions (Section 21.2.2) at each response period. Section 21.3 of ASCE 7-16 (and ASCE 7-10) defines the site-specific design response spectrum as 2/3 of site-specific MCE$_R$ ground motions (Section 21.2.3) subject to not being taken less than 80 percent of design response spectrum of Section 11.4.5 at any period. Figure 3.3-5 illustrates these requirements and shows plots of the probabilistic MCE$_R$ response spectrum (Section 3.3.3.2), the deterministic MCE$_R$ response spectrum (Section 3.3.3.3), the site-specific MCE$_R$ response spectrum and the design response spectrum for example Riverside site.
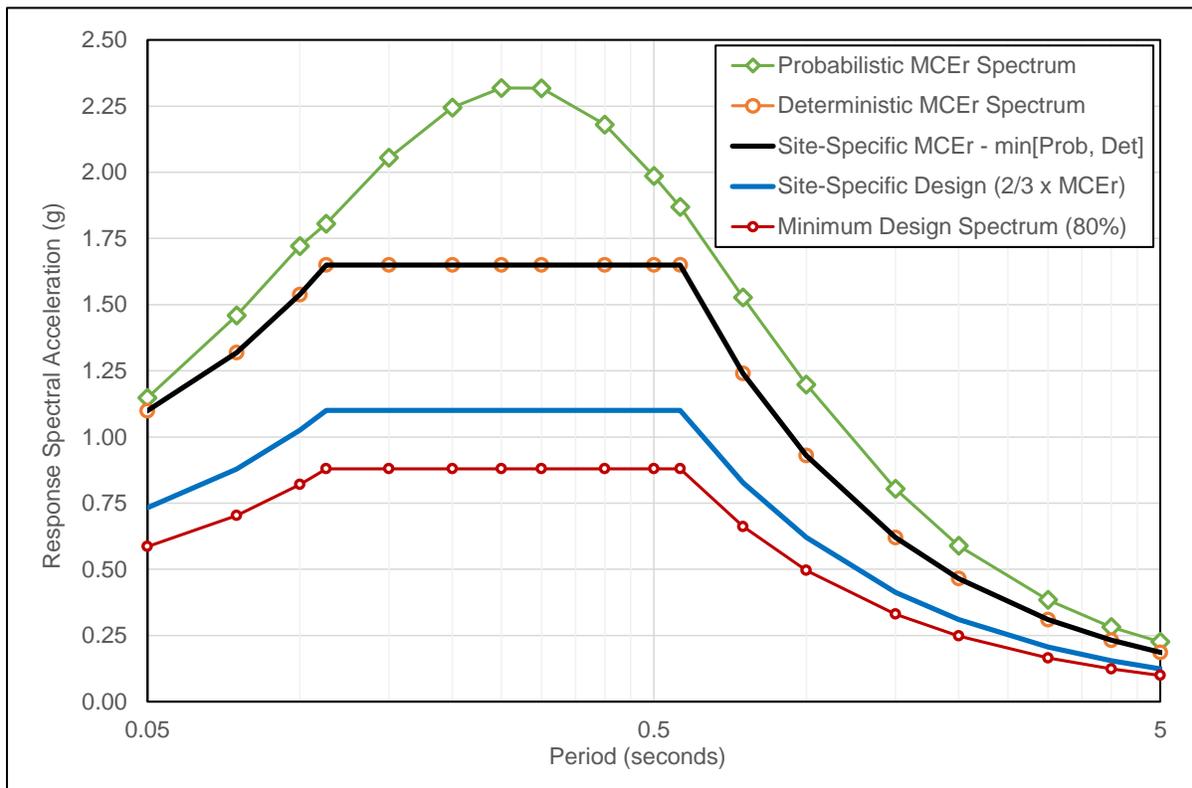
Figure 3.3-5   Plots of the probabilistic MCE$_R$ response spectrum and the deterministic MCE$_R$ response spectrum, the sites-specific MCE$_R$ response spectrum (minimum of probabilistic and deterministic MCE$_R$ response spectra) and the site-specific design response spectrum (2/3 of the MCE$_R$ response spectrum, but not less than 80% of the design response spectrum of Section 11.4.5) for the example Riverside site

As shown in Figure 3.3-5, the deterministic (lower-limit) MCE$_R$ ground motion are less than the probabilistic MCE$_R$ ground motions at all periods and, therefore, govern MCE$_R$ ground motions at the example Riverside site. In this example, deterministic MCE$_R$ ground motions govern since site hazard is dominated by the combined effects of the highly active San Jacinto and San Andreas fault systems which cause relatively strong, if rare, probabilistic MCE$_R$ ground motions for an effective return period (i.e., about 2,000 years) that is much longer than mean occurrence rate of large earthquakes on these systems (i.e., about 200 years). It is precisely for these types of sites that the 2015 NEHRP Provisions (and ASCE 7-16) consider deterministic MCE$_R$ ground motions to be more appropriate for design.

The example Riverside site illustrates the site-specific requirements of Sections 21.2 and 21.3 including the lower-limit on deterministic MCE_R ground motions which governs in this example, but not in general. MCE_R ground motions of all CEUS sites and most WUS sites are governed by probabilistic MCE_R ground motions. Deterministic MCE_R ground motions (not defined by the lower-limit) tend to govern site-specific MCE_R ground motions at sites in WUS regions that are very close to highly active fault systems (e.g., San Bernardino sites near the San Andreas fault system in Southern California and San Francisco sites near the San Andreas fault system in Northern California). Deterministic MCE_R ground motions defined by the lower-limit, such as the example Riverside site, govern site-specific MCE_R ground motions at sites in WUS regions whose hazard is dominated highly active fault systems, but which are not very close to these systems. It may be noted that the "plateau" regions of constant response spectral acceleration (i.e., $S_S = 1.5$ g or $S_1 = 0.6$ g) of the MCE_R design values maps of Chapter 22 of ASCE 7-16 are based on the deterministic lower-limit of MCE_R ground motions for hypothetical Site Class BC (vs,30 = 762 mps) site conditions.

3.3.3.5 Site-Specific Values of Design Acceleration Parameters. Section 21.4 of ASCE 7-16 defines site-specific values of design parameters S_{DS} and S_{D1} (and $S_{MS} = 1.5$ x S_{DS} and $S_{M1} = 1.5$ x S_{D1}) based on the site-specific design spectrum of Section 21.3. Site-specific values of design parameters S_{DS} and S_{D1} (and S_{MS} and S_{M1}) are used for design in lieu of the values of these parameters determined in accordance with Sections 11.4.3 and 11.4.4 subject to the site-specific values not being taken as less than 80 percent of the values determined in accordance with these sections.

Section 21.4 of ASCE 7-16 incorporates significant changes to the requirements of Section 21.4 of ASCE 7-10. Section 21.4 of ASCE 7-10 requires S_{DS} to taken as 100 percent of site-specific design spectrum at a period of 0.2 s, but not less than 90 percent of the peak value of the design spectrum at periods greater than 0.2s. Like ASCE 7-10, Section 21.4 of ASCE 7-16 requires S_{DS} to be taken as 90 percent of peak value of site-specific design spectrum at periods greater than or equal to 0.2 s, but no longer requires 100 percent of the value of the design spectrum at a period of 0.2s.

Section 21.4 of ASCE 7-10 requires S_{D1} to be taken as 100 percent of the larger of the site-specific design spectrum at a period of 1 s or 2 times the value of the site-specific design spectrum at a period of 2 s. Like ASCE 7-10, Section 21.4 of ASCE 7-16 requires S_{D1} to be taken as 100 percent of largest of the product the site-specific design spectrum and value of the period T for the period range, $1 \text{ s} \leq T \leq 2$ s, for stiffer sites ($v_{s,30}$ ft/s > 1,200 ft/s), but now extends this requirement to larger range of periods, $1 \text{ s} \leq T \leq 5$ s, for softer sites ($v_{s,30}$ ft/s $\leq$ 1,200 ft/s).

Table 3.3-5 summarizes site-specific values of the parameters S_{DS}, S_{D1}, S_{DS} and S_{M1} derived from the site-specific design spectrum of the example Riverside site (Figure 3.3-5) using the requirements of Section 21.4 of ASCE 7-10 and ASCE 7-16. It may be noted that the values of these parameters are similar to those of Table 3.3-1 that are based on Sections 11.4.3 and Section 11.4.4 of ASCE 7-10 and ASCE 7-16.

Table 3.3-5   Summary of site-specific values of the parameters S_{DS}, S_{D1}, S_{DS} and S_{M1} of ASCE 7-10 and ASCE 7-16 derived from the site-specific design spectrum of the example Riverside site

Design Parameter	Section 21.4 Requirement ASCE 7-10	Value (7-10)	Section 21.4 Requirement ASCE 7-16	Value (7-16)
S_{DS}	100% of S_{aD} [T = 0.2s]	1.1 g	90% of S_{aD} [T ≥ 0.2s]	0.99 g
S_{D1}	Max{S_{aD} [T = 1s], 2 x S_{aD} [T = 2s]}	0.62 g	Max{T x S_{aD} [1s ≤ T ≤ 5s]}	0.62 g
S_{MS}	1.5 x S_{DS}	1.65 g	1.5 x S_{DS}	1.49 g
S_{M1}	1.5 x S_{D1}	0.93 g	1.5 x S_{D1}	0.93 g

3.4   SELECTION AND SCALING OF GROUND MOTION RECORDS

Response history analysis (whether linear or nonlinear) consists of the step-wise application of time-varying ground accelerations to a mathematical model of the subject structure. The selection and scaling of appropriate horizontal ground motion acceleration time histories is essential to produce meaningful results. For three-dimensional structural analysis two-component records are used. The sections that follow discuss the approach to selection and scaling of ground motion records as prescribed in the *Provisions* (and ASCE 7), illustrate the selection and scaling of two-component ground motions.

There are three different places where response history analysis is permitted in the Provisions. The first is the linear response history analysis procedure in Chapter 12. The second is the nonlinear response history analysis procedure in Chapter 16. The last is in the design of structure with seismic isolation systems or supplemental energy dissipation in Chapter 17 and 18 respectively.

Where linear response history analysis of the *Standard* is used, it is necessary to select and modify a suite of ground motions to use as input in the form of ground acceleration histories. There are different requirements for the selection and scaling of ground motion acceleration history records in each of those sections. Each analysis procedure has a different number of ground motion acceleration records required and requirements to scale records to the target spectrum. For each earthquake event two orthogonal components must be provided, and prior to analysis, each component must be modified to represent the actual seismic hazard at the site.

There are generally two approaches to ground motion modification: amplitude scaling and spectral matching. In both cases the objective is to "fit" the pseudoacceleration spectrum computed from the modified record to some target design spectrum. In amplitude scaling, each acceleration value in the record is multiplied by the same scale factor such that the ordinates of the scaled pseudoacceleration spectrum and the target spectrum coincide at some pre-selected period of vibration, or such that the average of the scaled components from the suite of earthquakes closely matches (within some tolerance) the target spectrum. One of the advantages of amplitude scaling is that the frequency characteristics of the original record are preserved.

In spectral matching, the original ground motion record is nonuniformly scaled (essentially different scale factors are used for each recorded value of the original record) such that the pseudoacceleration response spectrum of the matched record closely matches the shape of the target spectrum. There are a variety of approaches to achieve this goal, and procedures utilizing Fourier transforms or wavelets are the most common. The main advantage of using spectrally matched ground motions is that a desired median response among multiple earthquakes can be obtained with fewer records than required when amplitude scaling is used. There is some concern, however, with spectral matching that the unique characteristics of each ground motion record is lost. That is why there is a penalty applied to its use in the nonlinear response history analysis procedure.

It is beyond the scope of this example to delve into the theoretical basis of ground motion selection and modification, and for this reason the reader is referred to NIST (2011) for additional details.

3.4.1   Nonlinear Response History Selection and Scaling
This section illustrates the Chapter 16 ground motion selection and scaling approach for the design example presented in Chapter 5.

3.4.1.1 Target Response Spectrum.

3.4.1.1.1 Example Site and Building. The example site location used in the Chapter 5 design example is located in San Francisco, California, just south of Market Street. The site is in the transition region of the seismic hazard maps (where the $S_S = 1.5$g and $S_1 = 0.6$g caps govern most of the design spectral values) and the site is considered by ASCE 7-16 to be a near-fault site (because it is within 15 km of a large fault, as discussed further in Section 3.4.2). The following provides a summary of some additional details for this site location.

Site Class: C
$S_S = 1.50$g, $S_1 = 0.60$g
$S_{DS} = 1.00$g, $S_{D1} = 0.52$g
Seismic Design Category: C

The Chapter 5 example building illustrates a design for a 40-story reinforced concrete shear wall building. The fundamental period of the building is 3.75 seconds and the second-mode period is 0.75 seconds. The period range of interest for this building is 0.15 seconds (controlled by the mass participation requirement) to 7.5 seconds (i.e. twice the fundamental period).

Figure 3.4-1 provides a regional fault map for the San Francisco California area. Table 3.4-1 and Figure 3.4-2 both provide disaggregation information for the 2% in 50 year level ground motions at this site. This disaggregation information is provided for both Sa(0.75s) and Sa(3.75s), since individual ground motion sets will later be selected and scaled with focus on these two periods important to the building dynamic response.
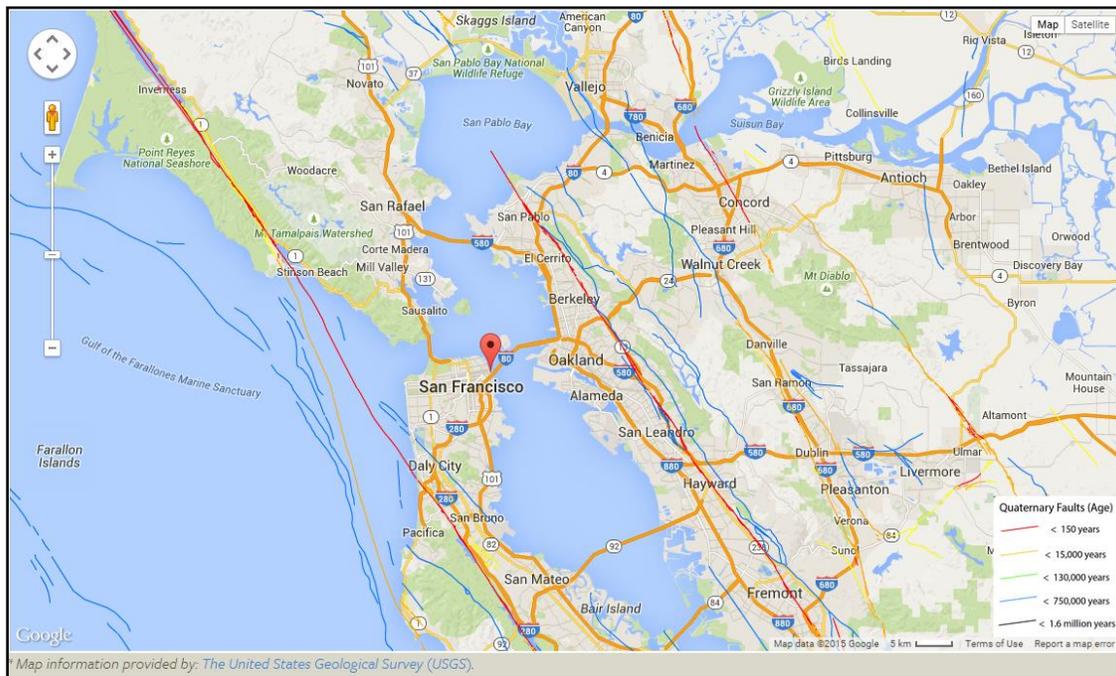
Figure 3.4-1. Regional Fault Map for San Francisco, California
(fault data from U.S. Geological Survey and map courtesy of Google)

Table 3.4-1. Seismic Source Disaggregation for Example Site for 2% in 50 year Hazard [Table (a) is for Sa(0.75s) and Table (b) is for Sa(3.75s)]

(a) Table for a period of 0.75 seconds (disaggregation run at 1.0s)

Fault Category	Percentage Contribution	Distance to Fault (km)	Magnitude	Epsilon
California A-faults	91%	14.5	7.7	1.5
CA Compr. crustal gridded	5%	6.5	6.3	1.5
California B-faults Char	4%	19.4	7.5	2.0

Fault Name	Percentage Contribution	Distance to Fault (km)	Magnitude	Epsilon
N. San Andreas;SAO+SAN MoBal	14%	16.0	7.8	1.6
N. San Andreas;SAP+SAS MoBal	12%	13.6	7.5	1.6
N. San Andreas Unsegmented A-flt	7%	13.7	7.7	1.5
N. San Andreas;SAO+SAN+SAP+SAS M	6%	13.6	8.0	1.3
N. S.Andr.;SAO+SAN APriori	5%	16	7.8	1.6
N. S.Andr.;SAP+SAS aPriori	5%	13.6	7.5	1.6
San Gregorio Connected Char	4%	19.4	7.5	2.0
Hayward-Rodgers Crk;HN+HS aPrior	3%	15.6	7.0	2.2
Hayward-Rodgers Creek;HN+HS MoBa	2%	15.6	6.9	2.2
	Average:	14.5	7.6	1.6

(b) Table for a period of 3.75 seconds (disaggregation run at 4.0s)

Fault Category	Percentage Contribution	Distance to Fault (km)	Magnitude	Epsilon
California A-faults	96%	14.3	7.8	1.3
California B-faults Char	3%	19.4	7.5	2.0

Fault Category	Percentage Contribution	Distance to Fault (km)	Magnitude	Epsilon
N. San Andreas;SAO+SAN MoBal	17%	16.0	7.8	1.4
N. San Andreas;SAP+SAS MoBal	10%	13.6	7.5	1.7
N. San Andreas;SAO+SAN+SAP+SAS M	7%	13.6	8.0	1.1
N. San Andreas Unsegmented A-flt	7%	13.8	7.8	1.4
N. S.Andr.;SAO+SAN APriori	7%	16.0	7.8	1.4
N. S.Andr.;SAP+SAS aPriori	4%	13.6	7.5	1.7
San Gregorio Connected Char	3%	19.4	7.5	2.0
	Average:	14.4	7.8	1.3
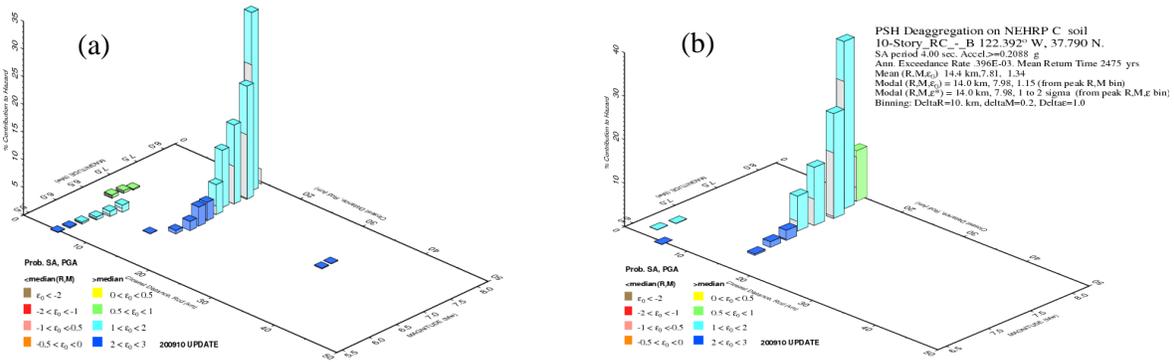
Figure 3.4-2. Seismic Source Disaggregations for Example Site for 2% in 50 year Hazard [Figure (a) is for Sa(0.75s) and Figure (b) is for Sa(3.75s)]

3.4.1.1.2 Method 1 for Single MCE$_R$ Target Spectrum. In this design example, the "Method 2" approach will be used for creating the target spectra (often called the "scenario" or "conditional mean" spectrum approach). Even so, this section demonstrates the process for computing the "Method 1" MCE$_R$ Target Spectrum, both for this completeness and because this is the first step to computing the Method 2 spectra.

First a site specific response spectrum must be derived using the procedures in Chapter 12 of the *Standard.* Table 3.4-2 shows the resulting spectrum coming from the site specific response spectrum procedure. For this example site, the deterministic lower limits control for most of the period ranges.

Table 3.4-2. MCE$_R$ Target Spectrum

Period (s)	MCE$_R$ (g)
0.01	0.61
0.1	1.50
0.2	1.50
0.3	1.50
0.4	1.50
0.5	1.50
0.6	1.30
0.75	1.04
1.0	0.78
1.5	0.53
2.0	0.40
3.0	0.28
4.0	0.21
5.0	0.16
6.0	0.14
7.0	0.13
8.0	0.11

3.4.1.1.3 Method 2 for Multiple Site-Specific Spectra. The Method 2 "scenario spectra" option is used for the Chapter 5 design example and is illustrated in this section. Scenario spectra recognize the fact that a uniform hazard spectrum is controlled by different earthquake "scenarios" at different periods (thereby reducing conservatism). The scenario spectra in this example are computed using the Conditional Mean Spectrum (CMS) approach (Baker 2011).

To begin this process, we start with to two periods representing the important structural modes with the most significant mass participation. In this example, these are the first mode period (3.75s) and second-model period (0.75s); see Section 5.3.1.3 for more information on the building dynamic properties. A CMS is then constructed such that the spectral ordinate at all other periods represents the expected value given that the value at the conditioning period matches the MCE_R.

To complete the calculation of the CMS target spectra, a publically available tool available from Stanford (http://web.stanford.edu/~bakerjw/research/epsilon.html), is used in this example. The U.S. Geological Survey also provides a tool to compute CMS target spectra (USGS 2008, Lin et al. 2013). If the USGS tool is used, one would find a CMS with spectral amplitude closest to the target MCE_R at the conditioning period, and then do some minor scaling of the resulting spectrum to provide an exact match to the MCE_R at the conditioning period. Additionally, for the case that the target spectrum is controlled by the transition-region "capped spectrum", the CMS must be modified accordingly to account for the difference between the uncapped and capped MCE_R spectra.

In accordance with Section 16.2.1.2 of the *Standard*, the envelope of the scenario spectra must exceed 75% of the target MCE_R spectrum for all periods within the period range of interest (which is 0.15s to 7.5s for this example). In this example, the 75% floor was reached near the extreme ends of the period range of interest and thus it was deemed preferable to increase the controlling scenario spectrum at those periods, rather than add scenario spectra, to satisfy this requirement. If the range of periods over which the 75% floor controlled became more significant, it may then become necessary to add an additional scenario spectrum.

Figure 3.4-3 provides an example of the two scenario spectra for this building example. One spectrum is anchored at 0.75s, the other is anchored at 3.75s, and they fulfill the Section 16.2.1.2 requirements for the period range of 0.15s to 7.5s.
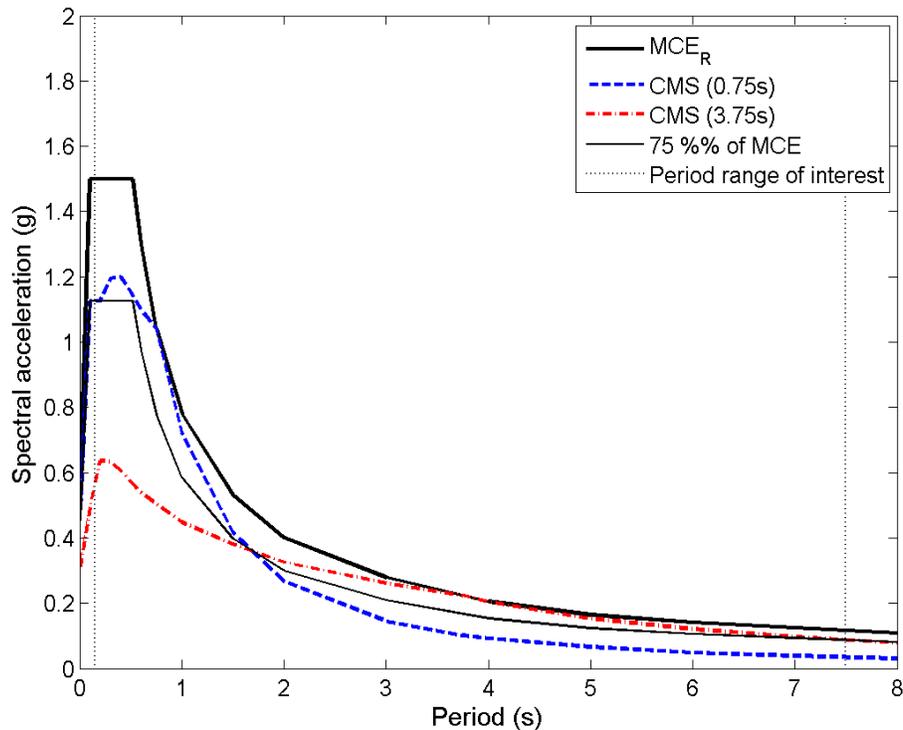
Figure 3.4-3. Target Method 2 Scenario Spectra for the Example Site and Building

3.4.1.2 Ground Motion Selection.

For each of the two scenario spectra, eleven ground motion time histories are selected and two separate ground motion sets are formed. The traditional approach has been to select ground motions having magnitudes, fault distances, source mechanisms, and site soil conditions that are roughly similar to those likely to cause the ground motion intensity level of interest, and not to explicitly consider spectral shape in ground motion selection. In many cases, however, response spectrum shape is the ground motion property most correlated with structural response (PEER 2009), so the updated Chapter 16 selection method includes spectral shape as an important consideration when selecting ground motions.

The selection of recorded motions occurs in two steps. Step 1 involves pre-selecting the ground motion records in the database having reasonable magnitude, fault distance, source mechanisms, site soil conditions, and range of useable frequencies; the PEER database is used in this example (Chiou et al. 2008). In completing this pre-selection, it is permissible to use relatively liberal ranges because Step 2 involves selecting motions that provide good matches to a target spectrum (which implicitly accounts for many of the above issues).

The following lists explain the Step 1 and Step 2 criteria and Table 3.4-3 summarizes the target values and chosen ranges for the selection of ground motions.

Step 1 Criteria for initial screening of ground motions are as follows:

- **Tectonic Regime:** Select recordings from the same tectonic regime as present at the site (typical choices are active crustal regions, stable continental regions, and subduction zones; details in Stewart et al. 2014). In this example, the seismic sources are shallow crustal events from strike-slip faults. In the selection, we constrain to shallow crustal events but do not constrain to only strike-slip.
- **Magnitude and Distance:** These parameters are obtained from disaggregation of the hazard at a period of interest and were shown previously in Section 3.4.2.1.1. We selected ground motions having reasonably similar magnitude and distance in order to provide generally compatible durations and spectral contents. Since spectral shape criteria are separately enforced in Step 2, the duration compatibility is the principal consideration. Duration is more related to magnitude than distance, so distance criteria were not made to be strict.
- **Site Soil Conditions:** Site soil conditions (Site Class) exert a large influence on ground motions, but are already reflected in the spectral shape used in Step 2. For Step 1, reasonable limits on site soil conditions are imposed but are not made to be overly restrictive as to unnecessarily limit the number of candidate motions.
- **Useable Frequency of the Ground Motion:** Only processed ground motion records should be considered for RHA. Processed motions have a usable frequency range and the most critical parameter is the lowest usable frequency. In the selection, the useable frequencies of the record (after filtering) are checked, to ensure that the useable period range accommodate the range of frequencies important to the building response.
- **Pulse Characteristics (for near-fault sites):** For near-fault sites, selection of pulse motions is an important consideration. Assuming the target ground motions come from a large Northern San Andreas rupture, we assume that there is 150 km of rupture between the epicenter and the closest point on the rupture to the site, the site is 14 km from the closest point to the rupture, and 'theta' angle associated with this geometry is then 5 degrees, the prediction equation of Shahi and Baker (2014, equation 23) gives a 67% probability of the ground motion containing a directivity pulse.

Step 2 Criteria for final selection of ground motions are as follows:

- **Spectral Shape:** The shape of the response spectrum should be the primary consideration when selecting ground motions.
- **Scale Factor:** A scale factor limit of approximately 0.25 to 4.0 is not uncommon.

▪ **Maximum Motions from a Single Event:** Although less important than spectral shape and scale factor, it is common to limit the number of motions from a single seismic event to three or four motions when possible.

Table 3.4-3. Ground motion selection criteria

Selection Parameter	Scenario Spectrum Set for 0.75s	Scenario Spectrum Set for 3.75s
Tectonic regime		
Target from deaggregation	Strike-slip	Strike-slip
Range allowed in selection	All shallow crustal	All shallow crustal
Earthquake magnitude (M_w)		
Target from deaggregation	7.6	7.8
Range allowed in selection	≥ 6.9	≥ 6.9
Site-source distance (km)		
Target from deaggregation	14.5	14.4
Range allowed in selection	0-20	0-20
Vs30 (m/s)		
Target (for Site Class C)	525	525
Range for selected motions	250-800	250-800
Period range for matching spectrum (sec)	0.15-1.75	1.75-7.5
Max. usable frequency of record (Hz)	0.5	0.1
Approximate percentage of pulse records	60%	80%
Scale factor range	0.5-3.5	0.5-3.5
Maximum motions from single event	3	3

During Step 2 of the ground motion selection process, each potential ground motion is scaled to match the target spectrum on average over the period range of interest and then sum of squared errors are computed between the ground motion spectrum and the target spectrum, in order to select motions that have appropriate spectral shape. The eleven motions which fulfill all of the selection criteria with the smallest sum of the squared errors are chosen as a ground motion suite.

The following two tables provide the properties of the ground motions used in the two ground motion sets. Table 3.4-4 provides the information for the set selected for a 0.75s period and Table 3.4-5 provides the information for the set selected for a 3.75s period.

Table 3.4-4. Properties of Selected Ground Motions for Set #1 (for 0.75s period)

No.	NGA #	Earthquake	Station	Mag.	Distance (km)	Vs30 (m/s)	Scale Factor	Pulse?	Pulse Period (s)
1	779	Loma Prieta	LGPC	6.9	3.9	595	0.89	No	--
2	1119	Kobe, Japan	Takarazuka	6.9	0.3	312	0.79	Yes	1.8
3	1158	Kocaeli, Turkey	Duzce	7.5	15.4	282	1.50	No	--
4	1161	Kocaeli, Turkey	Gebze	7.5	10.9	792	3.22	Yes	6.0
5	1495	Chi-Chi, Taiwan	TCU055	7.6	6.3	359	2.12	No	--
6	1513	Chi-Chi, Taiwan	TCU079	7.6	11.0	364	1.04	No	--
7	1528	Chi-Chi, Taiwan	TCU101	7.6	2.1	389	2.38	Yes	10.3
8	1602	Duzce, Turkey	Bolu	7.1	12.0	294	0.89	Yes	0.9
9	1605	Duzce, Turkey	Duzce	7.1	6.6	282	1.13	Yes	5.9
10	4457	Montenegro, Yugo.	Ulcinj - Hotel Albatros	7.1	4.4	410	2.53	No	--
11	6927	Darfield, NZ	LINC	7.0	7.1	263	1.71	Yes	7.4

Table 3.4-5. **Properties of Selected Ground Motions for Set #2 (for 3.75s period)**

No.	NGA #	Earthquake	Station	Mag.	Distance (km)	Vs30 (m/s)	Scale Factor	Pulse?	Pulse Period (s)
1	1158	Kocaeli, Turkey	Duzce	7.5	15.4	282	0.93	No	--
2	1176	Kocaeli, Turkey	Yarimca	7.5	4.8	297	0.77	Yes	5.0
3	1193	Chi-Chi, Taiwan	CHY024	7.6	9.6	428	1.07	Yes	6.7
4	1491	Chi-Chi, Taiwan	TCU051	7.6	7.6	350	1.44	Yes	10.4
5	1515	Chi-Chi, Taiwan	TCU082	7.6	5.2	473	1.18	Yes	8.1
6	3744	Cape Mendocino	Bunker Hill FAA	7.0	12.2	566	1.12	Yes	5.4
7	4806	Wenchuan, China	Bixianzoushishan	7.9	17.0	418	2.38	No	--
8	4816	Wenchuan, China	Mianzuqingping	7.9	6.6	551	0.81	Yes	9.4
9	6927	Darfield, NZ	LINC	7.0	7.1	263	0.80	Yes	7.4
10	6960	Darfield, NZ	Riccarton H.S.	7.0	13.6	293	1.23	Yes	9.4
11	6962	Darfield, NZ	ROLC	7.0	1.5	296	0.76	Yes	7.1

3.4.1.3 Ground Motion Modification. Because the building is located at a near-fault site, this design example utilizes the amplitude-scaling approach rather than the spectral matching approach. This is both to avoid the complication of demonstrating that the pulse characteristics are retained through the matching process (as required by Section 16.2.3) and to avoid the 10% higher target spectrum required when spectral matching is utilized (as required by Section 16.2.3.3).

The target spectrum is defined in ASCE 7-16 to be a maximum direction spectrum. Therefore, when the ground motions are scaled to the target spectrum, the maximum direction spectral acceleration spectrum is scaled to meet or exceed the target spectrum over the period range of interest. The scaling is not done for the spectra in each direction of the building (e.g. x-direction versus y-direction or fault-normal versus fault-parallel), but is rather done based on this maximum direction spectrum definition.

The following two figures show the spectra of the final two scaled ground motions sets. Figure 3.4-4 shows the set selected and scaled for a 0.75s period and Figure 3.4-5 shows the set selected and scaled for a 3.75s period.
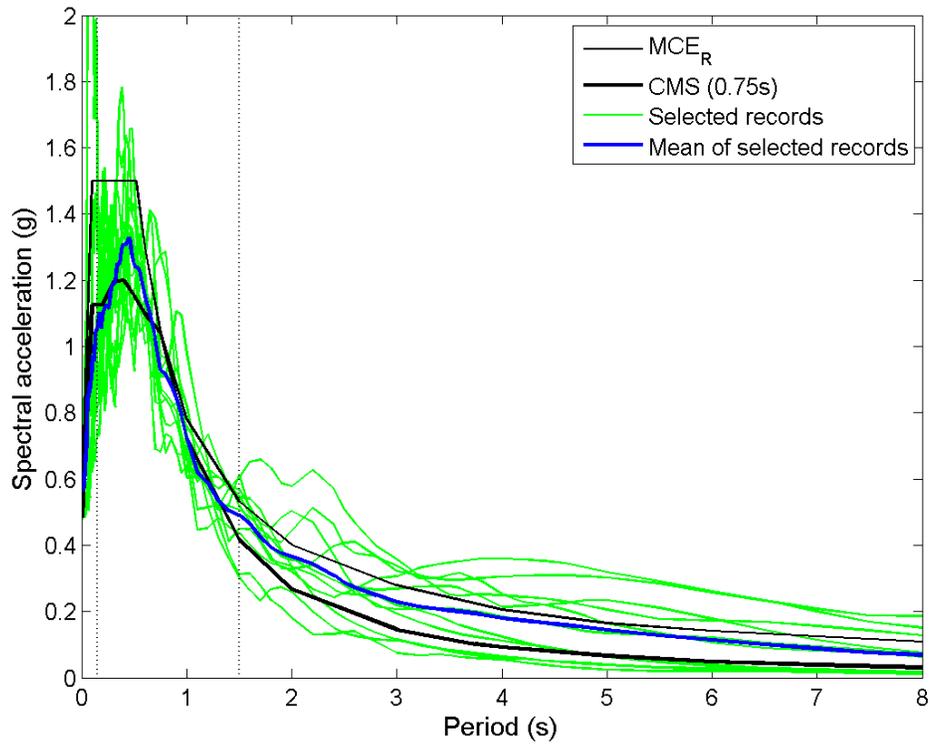
Figure 3.4-4. Spectra of Scaled Ground Motion Set #1 (for 0.75s period), with Comparison to Target Spectra
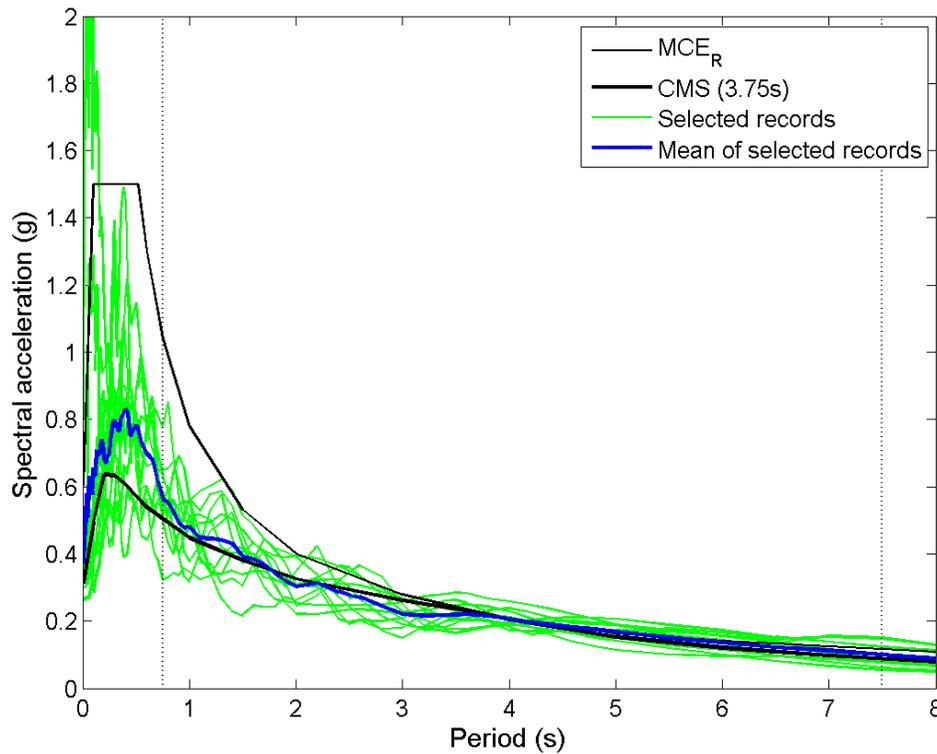
**Figure 3.4-5. Spectra of Scaled Ground Motion Set #2 (for 3.75s period),
with Comparison to Target Spectra**

3.4.1.4 Application of Ground Motions to the Structural Model. In accordance with Section 16.2.4 of ASCE 7-16, since this example site is characterized as a near-fault site, the two horizontal ground motion components are applied to the building in the fault-normal and fault-parallel orientations.

3.4.1.5 Closing. Section 3.4.2 demonstrated the ground motion selection and scaling process for an example design of a 40-story reinforced-concrete shear wall building in San Francisco, California. The balance of the design example is provided in Chapter 5.

3.4.2   Linear Response History Selection and Scaling

In Section 12.9.2 of the *Standard*, which covers linear response history analysis, it is required that a suite of not less than three earthquake events be used. Section 12.9.2.3 of the *Standard* requires spectral matching of ground motions in linear response history analysis. There are two reasons for this requirement. First, it is recognized that elastic response history analysis cannot be expected to "predict" the behavior of highly nonlinear systems, and as such it is merely a tool to be used for design. The same basic philosophy applies to the modal response spectrum method, so it seems logical to develop a response history procedure that, in essence, uses the same response spectrum as does the response spectrum method. Second, with amplitude scaling, it is likely that some frequencies will receive disproportionally high or low scaling, and this can non-uniformly affect the results. Consider, for example, Figure 3.4-6a which shows the response spectra for three earthquakes, amplitude scaled such that all three have the same spectral acceleration at a given period of vibration (in this case 2.22 seconds). The vertical dashed lines at the left and right of the plotted region represent the range of periods associated with the modes that will be represented in the analysis. As is evident in the short period region, the higher modes (with lower periods of vibration) for two of the earthquakes (G03090 and TCU045N) have spectral amplitudes much higher than that of the

target spectrum, and hence, the higher modes in the response will be overrepresented in the analysis. The third earthquake, MUL279, more closely matches the target spectrum in the low period region. It is certainly possible that a better fit could be obtained by use of different records (not using G03090 and TCU045N), and trying to find additional records that provide a match more like that shown for MUL279.

The same suite of earthquakes that were modified by spectral matching is shown in Figure 3.4-6b. Here, in the spectrum matching range, the variation in the spectral accelerations for the three matched records are virtually indistinguishable from the target spectrum over the expected period range, and the higher modes are not over-represented relative to the target spectrum. There are some variations outside the matching range, particularly at low periods, but this will not affect the computed response because modes associated with these periods are not included in the analysis.

The *Standard* requires that the period range used for spectral matching is 0.8 T_{min} to 1.2 T_{max}, where T_{min} is the period at which 90% of the effective modal mass is captured, and T_{max} is the largest period of vibration for the system. The average of the matched spectra in each direction of response should not fall outside the range of + or – 10% of the target spectrum.

It is noted that the requirements stated above are based in the implicit assumption that the analysis will be performed using modal response history, and not direct integration of the equations of motion. If direct integration is used in association with the matched ground motions represented in Figure 4.2-1b there will be some "over amplification" of the higher mode response and periods less than T_{min}, but this will not be as severe as if the amplitude scaled records were used. If there is a concern, the over amplification could be reduced by using a lower value of T_{min}.

There are a variety of programs available for performing spectral matching. In the example to be presented later, the program RSPMatch (Al Atik and Abrahamson 2010) was utilized via a special Matlab application developed by Jayamon and Charney (2015). See also Grant and Diaferia (2012) for additional information regarding spectrum matching.

(a) Ground motion scaled for same ordinate at $T=C_uT_a$

(b) Ground motion spectrally matched over period range $0.8T_{min}$ to $1.2T_{max}$

Figure 3.4-6. Amplitude Scaling vs Spectral Matching for Three Earthquakes

3.4.3 With Seismic Isolation and Damping Systems Selection and Scaling

3.4.3.1 Spectral Accelerations. Chapter 17 and Chapter 18 of the *Standard* address the design of buildings that incorporate a seismic isolation and damping systems, respectively. These types of structural systems have specific requirements for the seismic ground motions that are used for design which are different than the requirements for nonlinear analysis of Chapter 16.

The *Standard* has incorporated new USGS design value maps and site coefficients and new site-specific analysis requirements which, depending on the site location and site conditions, may have a significant effect on the parameters used for analysis and design.

A ground motion hazard analysis shall be performed in accordance with Section 21.2 where either:
- For Site Class A, B and C sites, S_1 is greater than or equal to 0.6
- For Site Class D and E sites, S_1 is greater than or equal to 0.2

For Site Class F, a site response analysis shall be performed in accordance with Section 21.1.

The reason for these changes is that the design response spectrum, which is defined by a constant acceleration domain (S_{MS}) and a constant velocity domain (S_{M1}/T), may not be conservative at softer sites (e.g. Site Classes D and E) and particularly at sites where the seismic hazard is dominated by large magnitude earthquakes. Since structures with seismic isolation and damping tend to have a high fundamental periods and are implemented on important structures in high seismic regions, it is typical practice that the spectral accelerations of MCE$_R$ ground motions are calculated using the site-specific procedures of Chapter 21 for a number of different periods of response (so-called multi-period MCE$_R$ response spectra).

3.4.3.2 Ground Motion Records Selection and Scaling.

3.4.3.2.1 Design Criteria. Ground motion records are only required when a response history analysis is undertaken. These records are scaled to match the maximum spectral response in the horizontal plane. In concept, at a given period of interest, maximum spectral response of scaled record pairs should, on average, be the same as that defined by the MCE_R spectrum (or other design spectrum, as required).

The ground motions are selected, scaled and applied in a similar way to Chapter 16 of *Standard*, with the exception that a minimum of seven rather than eleven ground motions are required. The use of seven motions is consistent with current practice and was considered an adequate number by the Code committee to estimate the mean response for a given hazard level. The ground motion acceleration records are scaled to the target spectrum differently in Chapter 17 and 18 than Chapter 16. Instead of scaling the average of the maximum direction response spectrum from each acceleration record to be within 90% of the target spectra at every period within a given range, the square root sum of squares of each ground motion acceleration record pair's response spectra ordinate is scaled to 100% of the target spectra at ever period within a given range.

The *Standard* requires that these seven pairs of horizontal ground motion acceleration components must be selected from actual earthquake records and scaled to match the MCE_R spectrum (or other design spectrum, as required), where the average value of the response parameter of interest is used for design. Where the required number of recorded pairs is not available, say for Eastern United States, then the *Standard* permits the use of simulated ground motion records.

The requirements for selection and scaling are similar for structures with seismic isolation and seismic damping systems (Chapters 17 and 18, respectively). Differences are in the number of suites of ground motions required and the period range of interest for scaling. This is because structures with damping systems consider both the design earthquake and MCE_R, whereas seismically isolated buildings are only analyzed at the MCE_R hazard level. Therefore, the structures with damping systems require two scaled suites (of seven orthogonal pairs of ground motions) for response history analysis, compared to only one suite required for seismically isolated structures.

Chapters 17 and 18 of the *Standard* recognize two types of scaling methods: amplitude scaling and spectral matching (described in Section 3.4), and the *Standard* defines specific requirements for each. Table 3.4-.6 lists the *Standards* requirements based on scaling method and proximity to an active fault, with Table 3.4-7 listing the respective period ranges of interest for scaling.

Checking compliance with the *Standard* involves using the scaled ground motion records, which typically consist of acceleration values (in units of g, cm/s^2, etc) at constant increments of time (say 0.01 seconds) to construct a 5 percent-damped response spectrum for each of the two horizontal components. For both amplitude scaling and spectral matching, the square root sum of the squares (SRSS) of the two components is calculated and compared to the spectrum used for design. The average SRSS spectrum (of the seven pairs of records) shall not fall below the corresponding ordinate of the MCE_R spectrum (or other design spectrum, as required), between the period range of interest shown in Table 3.4-7. For spectral matching and sites close to an active fault, the *Standard* has additional requirements where the 5% damped spectrum of a ground motion component is compared directly to the spectrum used for design.

Table 3.4-6 Ground Motion Records Scaling Procedures

Scaling Method	Site Proximity to Active Fault	Seismically Isolated Structures	Structures with Damping Systems
Amplitude Scaling	within 3 miles (5km)	Each pair of components shall be rotated to FN and FP directions of the causative fault and scaled so that the average spectrum (of the seven records) of the FN and FP components are not less than 100% and 50%, respectively, of the corresponding MCE$_R$ spectrum ordinate between the period range shown in Table 3.4-2.	Same as for seismically isolated structures but there are two suites of ground motions: one suite is scaled to the design earthquake spectrum and one suite is scaled to the MCE$_R$
	Other sites	For each pair of horizontal components a SRSS spectrum shall be constructed and the average SRSS spectrum (of the seven pairs of records) shall not fall below the corresponding MCE$_R$ ordinate between the period range shown in Table 3.4-2. An identical scale factor is applied to both components of a pair	
Spectral Matching	within 3 miles (5km)	Method should not be utilized, unless: 1) a site-specific response spectrum is utilized, and 2) the pulse characteristics are included in the spectra and retained in the individual ground motions.	Same as for seismically isolated structures but there are two suites of ground motions: one suite is scaled to the design earthquake spectrum and one suite is scaled to the MCE$_R$ spectrum
	Other sites	For each pair of horizontal components a SRSS spectrum shall be constructed and the average SRSS spectrum (of the seven pairs of records) shall not fall below the corresponding MCE$_R$ ordinate between the period range shown in Table 3.4-2. The pair of ground motions shall be scaled such that the response spectrum of one component of a pair is at least 90% of the corresponding MCE$_R$ spectrum ordinate between the period range per Table 3.4-2.	

1. Definitions: Fault-normal (FN), Fault-parallel (FP), Square root sum of the squares (SRSS)

Table 3.4-7 Ground Motion Records Period Range for Scaling

Scaling Method	Site Proximity to Active Fault	Seismically Isolated Structures	Structures with Damping Systems
Amplitude Scaling	within 3 miles (5km)	$0.2T_{M,UB}$ to $1.25T_{M,LB}$	$0.2T_{ID}$ to $1.25T_{IM}$
	Other sites	$0.75T_{M,UB}$ to $1.25T_{M,LB}$	
Spectral Matching	within 3 miles (5km)	$0.2T_{M,UB}$ to $1.25T_{M,LB}$	
	Other sites		

1. $T_{M,UB}$, $T_{M,LB}$ = effective period of the isolated structure at the maximum displacement D_M using upper-bound or lower-bound properties, respectively, in the direction under consideration
2. T_{ID} = effective period of the structure at the design displacement using upper bound properties, in the direction under consideration
3. T_{IM} = effective period of the structure at the MCE$_R$ displacement using lower bound properties, in the direction under consideration

3.4.3.2.2 Example of Application. Selection and scaling of appropriate ground motions should be performed by a ground motion expert experienced with earthquake hazards of the region. Scaling should be carried out with consideration of site conditions, earthquake magnitudes, fault distances and source mechanisms that influence ground motion hazards at the building site. Section 3.3 gives guidance and commentary on this process. This section makes use of the seismically isolated building design example

of Chapter 14 to illustrate compliance with the *Standards* ground motion scaling requirements. The method of scaling is similar for structures with damping systems.

The key design information for the seismically isolated building is:

Site Location, Hazard and Soil Conditions:

Site location: North Seattle

Nearest active fault: greater than 3 miles away

Site soil type: Site Class D

Short-Period Design Parameters:

Short-period MCE$_R$ spectral acceleration: $S_S = 1.4$

Site coefficient (*Standard* Table 11.4-1): $F_a = 1.0$

Short-period MCE$_R$ spectral acceleration adjusted for site class (F_aS_S): $S_{MS} = 1.4$

1-Second Design Parameters:

1-Second MCE$_R$ spectral acceleration: $S_1 = 0.50$

Site coefficient (*Standard* Table 11.4-2): $F_v = 1.8$

1-Second MCE$_R$ spectral acceleration adjusted for site class (F_vS_1): $S_{M1} = 0.9$

Upper Bound Effective Period, $T_M = 1.5$ seconds

Lower Bound Effective Period, $T_M = 2.1$ seconds

Ground Motion Scaling Method: Amplitude Scaling

Since the 1-second MCE$_R$ spectral acceleration, S_1, is greater than 0.2 and the soil type is a Site Class D, a site-specific hazard analysis is conducted in accordance *Standard* Section 11.4.7 requirements. For convenience, it is assumed that the resulting MCE$_R$ response spectrum (the target spectrum) is identical to the response spectrum developed in accordance with *Standard* Section 11.4.5 with spectral values as stated above. It is also assumed that the ground motion expert recommends the suite of ground motions and scaling factors listed in Table 3.4-8.

Table 3.4-8 Selected and Scaled Ground Motions for Seismically Isolated Building Site[1]

GM No.	Year	Earthquake name	M	Source type	Recording station	Distance (km)	Scale factor
1	2003	Tokachi-oki, Japan	8.3	Subduction zone	HKD 094	67	3.00
2	2003	Tokachi-oki, Japan	8.3	Subduction zone	HKD 092	46	1.20
3	1968	Tokachi-oki, Japan	8.2	Subduction zone	Hachinohe (S-252)	71	1.65
4	1949	Western Washington	7.1	Deep intraplate	Olympia	75	2.95
5	1989	Loma Prieta	6.9	Shallow crustal	Saratoga -- Aloha Ave	9	1.65
6	1999	Duzce, Turkey	7.1	Shallow crustal	Duzce	7	1.10
7	1995	Kobe, Japan	6.9	Shallow crustal	Nishi-Akashi	7	1.75

1. Motions obtained from K-NET (http://www.kyoshin.bosai.go.jp/kyoshin/quake/index_en.html), PEER Ground Motion Database (http://ngawest2.berkeley.edu/) and with assistance from Doug Lindquist, GE of Hart Crowser, Seattle.

For this example building, the site is more than 3 miles away from an active fault, and amplitude scaling is the chosen scaling method. In this case, the *Standard* requires that the earthquake records are scaled to match a target spectrum over the period range of interest, defined as $0.75T_M$ determined using upper-bound properties to $1.25T_M$ using lower-bound properties. This gives a period range of interest of 1.13 to 2.62 seconds for the example building of Chapter 14, which is isolated using elastomeric bearings.

Scaling factors were developed by a ground motion expert in such a way that the average of the seven scaled ground motions square-root-of-the-sum-of-the-squares (SRSS) combination (of each pair of response spectra of scaled horizontal components) equals or exceeds the target (MCE$_R$) spectrum at every period over the range of 1.13 to 2.62 seconds. These scaling factors are given in Table 3.4-8 and reflect the total amount that each as-recorded ground motion is scaled for response history analysis. The scale factors are applied identically to each of the two horizontal components of each ground motion. Each of the seven ground motions has different scale factors as a two-step scaling process is used. The first step involves scaling the SRSS spectrum of each ground motion individually so that it is a "good match" to the target spectrum. The second step involves re-scaling all seven ground motions identically by a factor such that the average SRSS spectra of the seven scaled ground motions does not fall below any ordinate of the target spectrum in the period range of interest. The final scale factor therefore consists of the product of the initial scale factor and the second scale factor.

Figure 3.4-7 gives the unscaled acceleration histories for ground motion (GM) number 3, in Table 3.4-8. The two components of horizontal acceleration are usually oriented orthogonally to one another. The peak acceleration in these records is 0.3g which, after scaling, would becomes a peak acceleration of 0.5g. The scaling can be applied to the acceleration histories themselves or, equally, the unscaled record can be input and then scaled in the analysis software (e.g. ETABS).
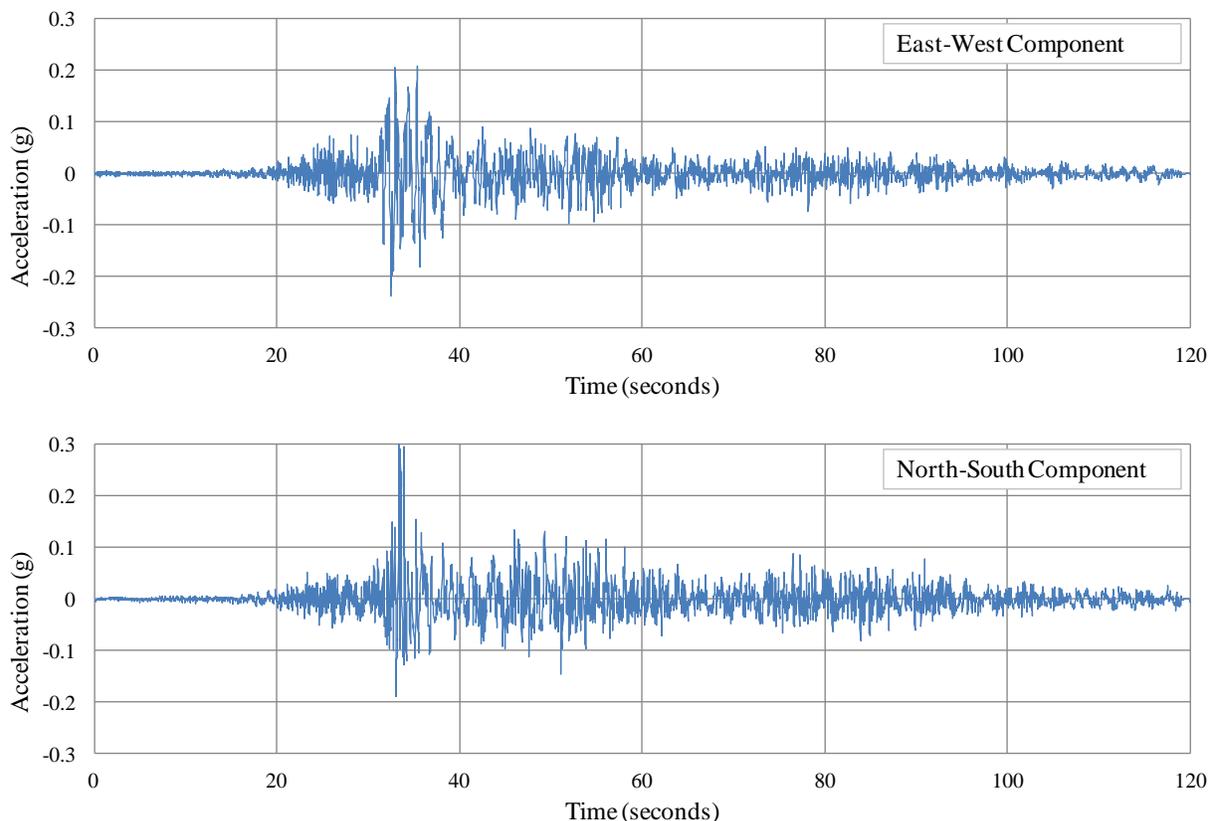
Figure 3.4-7 Unscaled horizontal acceleration histories for GM3 (1968 Tokachi-oki earthquake)

The 5-percent damped response spectrum for each ground motion component can be constructed using a range of software (e.g. Seismosignal). The scaled response spectrum for each of the acceleration histories

in Figure 3.4-8 are shown in Figure 3.4-9. The SRSS combination of these two components is also shown in comparison to the target MCE$_R$ spectrum for the North Seattle site. Over the period range of interest there is a reasonable fit of this ground motion to the target spectrum with a moderate scale factor of 1.65.
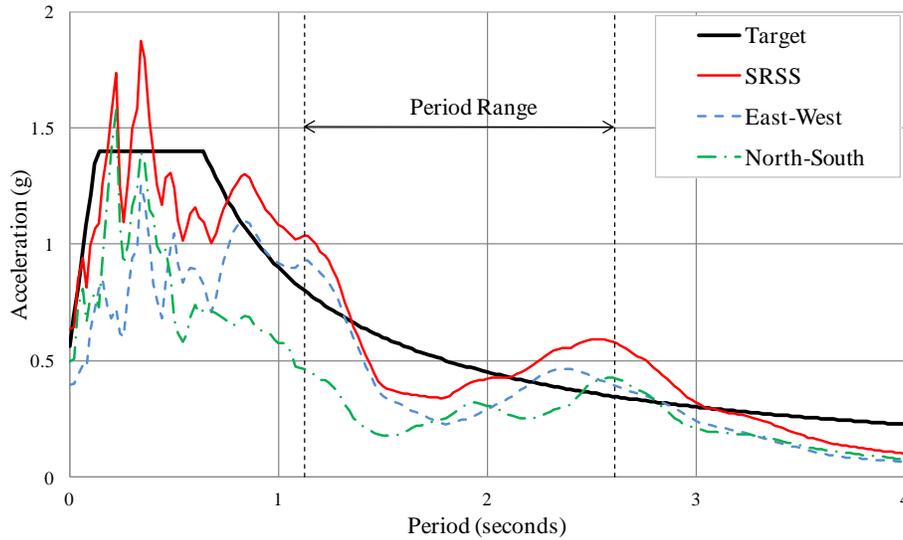
Figure 3.4-8 Scaled horizontal response sepctra for record 3 (1968 Tokachi-oki) earthquake

The SRSS combination of one ground motion's response spectra is permitted to be below the target spectrum over the period range of interest, as shown in Figure 3.4-8, provided that the average SRSS from all seven motions does not fall below the spectrum at any ordinate over the period range. Figure 3.4-9 compares the individual and average spectrum of the SRSS combination to the target spectrum. This figure shows:
- The scatter of the SRSS combination of each of the seven ground motions compared to the target spectrum.
- That the average of the seven SRSS combinations of scaled records envelop the MCE$_R$ spectrum from 1.13 seconds ($0.75T_{M,UB}$) to 2.62 seconds ($1.25T_{M,LB}$), as required by *Standard* Section 17.3.2.
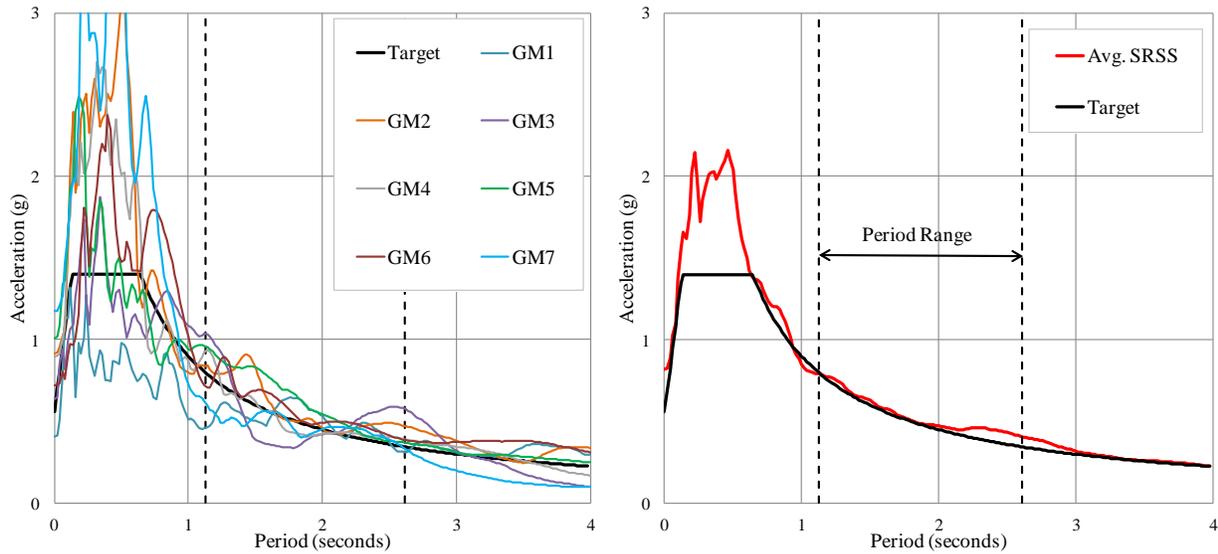
(a) SRSS combination of each ground motion spectra   (b) Average of seven SRSS spectra

Figure 3.4-9 Comparison of the MCE$_R$ target spectrum with the SRSS combination of individual ground motion components and average spectrum of the seven scaled records listed in Table 3.4-3

3.5   REFERENCES

American Society of Civil Engineers. 1998. *Minimum Design Loads for Buildings and Other Structures*, ASCE/SEI 7-98. ASCE, Reston, Virginia.

American Society of Civil Engineers. 2002. *Minimum Design Loads for Buildings and Other Structures*, ASCE/SEI 7-02. ASCE, Reston, Virginia.

American Society of Civil Engineers. 2006. *Minimum Design Loads for Buildings and Other Structures*, ASCE/SEI 7-05. ASCE, Reston, Virginia.

American Society of Civil Engineers. 2010. *Minimum Design Loads for Buildings and Other Structures*, ASCE/SEI 7-10. ASCE, Reston, Virginia.

Applied Technology Council. 1978. *Tentative Provisions for the Development of Seismic Regulations for Buildings*, ATC 3-06. ATC, Palo Alto, California.

ASK14 (Abrahamson, N. A., Silva, W. J., and Kamai, R.), 2013. Update of the AS08 Ground-Motion Prediction Equations Based on the NGA-West2 Data Set, PEER Report No. 2013/04, Pacific Earthquake Engineering Research Center, University of California, Berkeley, CA, 143 pp.

Boore, D. M., 2010. Orientation-independent, nongeometric-mean measures of seismic intensity from two horizontal components of motion, Bull. Seismol. Soc. Am. 100, 1830–1835.

Boore, D. M., Watson-Lamprey, J., and Abrahamson, N. A., 2006. Orientation-independent measures of ground motion, Bull. Seismol. Soc. Am. 96, 1502–1511.

Bozorgnia, Y. and K.W. Campbell. 2004. "The Vertical-to-Horizontal Response Spectral Ratio and Tentative Procedures for Developing Simplified V/H and Vertical Design Spectra," *Journal of Earthquake Engineering*, 8:175-207.

Bozorgnia, Y., N.A. Abrahamson, L. Al Atik, T.D. Ancheta, G.M. Atkinson, J.W. Baker, A. Baltay, D.M. Boore, K.W. Campbell, B.S.-J. Chiou, R. Darragh, S. Day, J. Donahue, R.W. Graves, N. Gregor, T. Hanks, I.M. Idriss, R. Kamai, T. Kishida, A. Kottke, S.A. Mahin, S. Rezaeian, B. Rowshandel, E. Seyhan, S. Shahi, T. Shantz, W. Silva, P. Spudich, J.P. Stewart, J. Watson-Lamprey, K. Wooddell and R. Youngs. 2014. "NGA-West2 Research Project," *Earthquake Spectra*, 30(3): 973-987.

BSSA14 (Boore, D. M., Stewart, J. P., Seyhan, E., and Atkinson, G. A.), 2013. NGA-West2 Equations for Predicting Response Spectral Accelerations for Shallow Crustal Earthquakes, PEER Report No. 2013/05, Pacific Earthquake Engineering Research Center, University of California, Berkeley, CA, 134 pp.

Federal Emergency Management Agency, 1997. *NEHRP Recommended Provisions for Seismic Regulations for New Buildings and Other Structures, Part 2: Commentary*, FEMA 303. FEMA, National Institute of Building Sciences Building Seismic Safety Council, Washington, D.C.

Federal Emergency Management Agency, 2000. *NEHRP Recommended Provisions for Seismic Regulations for New Buildings and Other Structures, Part 2: Commentary*, FEMA 369. FEMA, National Institute of Building Sciences Building Seismic Safety Council, Washington, D.C.

Federal Emergency Management Agency, 2003. *NEHRP Recommended Provisions and Commentary for Seismic Regulations for New Buildings and Other Structures*, FEMA 450. FEMA, National Institute of Building Sciences Building Seismic Safety Council, Washington, D.C.

Federal Emergency Management Agency, 2009. *NEHRP Recommended Seismic Provisions for New Buildings and Other Structures*, FEMA P-750. FEMA, National Institute of Building Sciences Building Seismic Safety Council, Washington, D.C.

CB14 (Campbell, K. W., and Bozorgnia, Y.), 2013. NGA-West2 Campbell-Bozorgnia Ground Motion Model for the Horizontal Components of PGA, PGV, and 5%-Damped Elastic Pseudo-Acceleration Response Spectra for Periods Ranging from 0.01 to 10 s, PEER Report No. 2013/06, Pacific Earthquake Engineering Research Center, University of California, Berkeley, CA, 238 pp.

CEUS-SSCn. 2012. *Central and Eastern United States seismic source characterization for nuclear facilities*, Electric Power Research Institute, US Department of Energy, and US Nuclear Regulatory Commission (http://www.ceus-ssc.com/).

Cornell, C.A. 1968. "Engineering Seismic Risk Analysis," *Bulletin of the Seismological Society of America*, 58(5):1583-1606.

Crouse, C.B., E.V. Leyendecker, P.G. Somerville, M. Power and W.J. Silva. 2006. "Development of Seismic Ground-Motion Criteria for the ASCE 7 Standard," in *Proceedings of the 8th US National Conference on Earthquake Engineering*. Earthquake Engineering Research Institute, Oakland, California.

CY14 (Chiou, B. S.-J., and Youngs, R. R.), 2013. Update of the Chiou and Youngs NGA Ground Motion Model for Average Horizontal Component of Peak Ground Motion and Response Spectra, PEER Report No. 2013/07, Pacific Earthquake Engineering Research Center, University of California, Berkeley, CA, 76 pp.

Field, E.H., T.E. Dawson, K.R. Felzer, A.D. Frankel, V. Gupta, T.H. Jordan, T. Parsons, M.D. Petersen, R.S. Stein, R.J. Weldon and C.J. Wills. 2008. *The Uniform California Earthquake Rupture Forecast, Version 2 (UCERF 2)*, USGS Open File Report 2007-1437 (http://pubs.usgs.gov/of/2007/1437/). USGS, Golden, Colorado.

Field, E.H., G.P. Biasi, P. Bird, T.E. Dawson, K.R. Felzer, D.D. Jackson, K.M. Johnson, T.H. Jordan, C. Madden, A.J. Michael, K.R. Milner, M.T. Page, T. Parsons, P.M. Powers, B.E. Shaw, W.R. Thatcher, R.J. Weldon and Y. Zeng. 2013. *Uniform California earthquake rupture forecast, version 3 (UCERF3) – The time-independent model*, USGS Open File Report 2013-1165, California Geological Survey Special Report 228, and Southern California Earthquake Center Publication 1792 (http://pubs.usgs.gov/of/2013/1165/). USGS, Golden, Colorado.

Field, E.H., and 2014 Working Group on California Earthquake Probabilities, 2015, UCERF3: A new earthquake forecast for California's complex fault system: U.S. Geological Survey 2015–3009, 6 p., http://dx.doi.org/10.3133/fs20153009.

Field, E.H., T.H. Jordan, and C.A. Cornell (2003), OpenSHA: A Developing Community-Modeling Environment for Seismic Hazard Analysis, *Seismological Research Letters*, 74, no. 4, p. 406-419. http://www.opensha.org/

Frankel, A., C. Mueller, T. Barnhard, D. Perkins, E.V. Leyendecker, N. Dickman, S. Hanson and M. Hopper. 1996. *National Seismic-Hazard Maps: Documentation June 1996*, USGS Open File Report 96-532 (http://pubs.usgs.gov/of/1996/532/). USGS, Golden, Colorado.

Frankel, A.D., M.D. Petersen, C.S. Mueller, K.M. Haller, R.L. Wheeler, E.V. Leyendecker, R.L. Wesson, S.C. Harmsen, C.H. Cramer, D.M. Perkins and K.S. Rukstales. 2002. *Documentation for the 2002 Update of the United States National Seismic Hazard Maps*, USGS Open File Report 02-420 (http://pubs.usgs.gov/of/2002/ofr-02-420/). USGS, Golden, Colorado.

Huang, Y.-N., A.S. Whittaker and N. Luco, 2008. "Maximum Spectral Demands in the Near-Fault Region," *Earthquake Spectra*, 24(1):319-341.

I14 (Idriss, I. M.), 2013. NGA-West2 Model for Estimating Average Horizontal Values of Pseudo-Absolute Spectral Accelerations Generated by Crustal Earthquakes, PEER Report No. 2013/08, Pacific Earthquake Engineering Research Center, University of California, Berkeley, CA, 31 pp.

Kircher & Associates (2015). "Investigation of an identified short-coming in the seismic design procedures of ASCE 7-10 and development of recommended improvements for ASCE 7-16," prepared for the Building Seismic Safety Council, National Institute of Building Sciences, Washington, D.C., prepared by Kircher & Associates, Consulting Engineers, Palo Alto, CA, March 15, 2015.

Leyendecker, E.V., R.J. Hunt, A.D. Frankel and K.S. Rukstales. 2000. "Development of Maximum Considered Earthquake Ground Motion Maps," *Earthquake Spectra*, 16(1):21-40.

Luco, N., 2015. "Site-Specific Values of Seismic Design Parameters of the 2015 NEHRP Provisions for a Site in Riverside, California (33.93515, -117.40266). Private communication.

Luco, N., B.R. Ellingwood, R.O. Hamburger, J.D. Hooper, J.K. Kimball and C.A. Kircher. 2007. "Risk-Targeted versus Current Seismic Design Maps for the Conterminous United States," in *Proceedings of the SEAOC 76th Annual Convention*. Structural Engineers Association of California, Sacramento, California.

McGuire, R.K., 2004, *Seismic Hazard and Risk Analysis*: Earthquake Engineering Research Institute, Monograph 10, 221 p.

Milner, K. (2015a). "gmpe_site_amp_all_classes_mean_no_determ" zip file. Private communication (6/11/2015).

Milner, K. (2015b). "gmpe_site_amp_all_classes_mean_no_determ_2pin50" zip file. Private communication (6/11/2015).

Petersen, M.D., A.D. Frankel, S.C. Harmsen, C.S. Mueller, K.M. Haller, R.L. Wheeler, R.L. Wesson, Y. Zeng, O.S. Boyd, D.M. Perkins, N. Luco, E.H. Field, C.J. Wills and K.S. Rukstales. 2008. *Documentation for the 2008 Update of the United States National Seismic Hazard Maps*, USGS Open File Report 2008-1128 (http://pubs.usgs.gov/of/2008/1128/). USGS, Golden, Colorado.

Petersen, M.D., Moschetti, M.P., Powers, P.M., Mueller, C.S., Haller, K.M., Frankel, A.D., Zeng, Yuehua, Rezaeian, Sanaz, Harmsen, S.C., Boyd, O.S., Field, Ned, Chen, Rui, Rukstales, K.S., Luco, Nico, Wheeler, R.L., Williams, R.A., and Olsen, A.H. (2014). *Documentation for the 2014 Update of the United States National Seismic Hazard Maps*, U.S. Geological Survey, Open-File Report 2014–1091, 243 p.

Seyhan, E. (2014). Weighted Average of 2014 NGA West-2 GMPEs, Excel file: NGAW2_GMPE_Spreadsheets_v5.6_070514, Pacific Earthquake Engineering Center, http://peer.berkeley.edu/ngawest2/databases/

Shahi, S. K., and Baker, J. W., 2013. NGA-West2 Models for Ground-Motion Directionality, PEER Report No. 2013/10, Pacific Earthquake Engineering Research Center, University of California, Berkeley, 45 pp.

USGS (2015). "2008 Interactive Deaggregations," http://geohazards.usgs.gov/deaggint/2008/

USGS (2013). U.S. Seismic Design Maps, web-based tool, version 3.1.0, 11 July 2013, http://earthquake.usgs.gov/hazards/designmaps.php

USGS (2012). Hazard Curve Application, web-based tool, version 1.0.1, 2012-07-16, http://geohazards.usgs.gov/hazardtool/

Wald, D. J., and T. I. Allen (2007). Topographic slope as a proxy for seismic site conditions and amplification, Bull. Seismol. Soc. Am. 97, 1379–1395.

Wills, C.J., and Clahan, K.B. (2006), Developing a map of geologically defined site-condition categories for California, Bull. Seism. Soc. Am., v. 96, no. 4A, p. 1483–1501.

<div style="text-align:right;">

4

</div>

Linear Response History Provision

Finley Charney, PhD and James Malley, SE

Contents

This chapter presents a detailed example that focuses on the seismic analysis of building structures using the linear procedures of Chapter 12 of ASCE 7-16. The system analyzed is a 12-story special moment resisting steel frame building in Stockton, California. The highly irregular structure is analyzed using three techniques: equivalent lateral force analysis, modal response spectrum analysis, and linear response history analysis. In each case, the structure is modeled in three dimensions. The results from each of the analyses are compared, and the relative merits of the different analytical approaches are discussed.

Prior to presenting the example, the chapter provides a summary of the relevant changes and additions in analysis requirements that are provided in ASCE 7-16 relative to ASCE 7-10. Many of these changes were addressed in a similar fashion in the 2015 NEHRP Provisions, and differences between the requirements in ASCE 7-16 and the 2015 NEHRP Provisions are briefly discussed.

Also provided in this chapter is a detailed theoretical background of the mathematical and modeling procedures used to perform seismic design related structural analysis. This is done to provide an appreciation for a host of assumptions that have been utilized to allow (in some cases) very simple 2-dimensional linear static analysis in lieu of more advanced procedures that explicitly account for nonlinear dynamic 3-dimensional response.

In the discussion that follows, ASCE 7-16 is referred to as the *Standard*, and the 2015 NEHRP Provisions are referred to as the *Provisions*. Several other documents are cited in the discussion, and these are listed as follows:

- Al Atik and Abrahamson (2010)   An Improved Method for Nonstationary Spectral Matching, *Earthquake Spectra*, 26(3), 601-617.

- Chopra (2012)   *Dynamics of Structures*, 4th Edition, Prentice Hall

- Grant and Diaferia (2012)   Assessing Adequacy of Spectrum Matched Ground Motions for Response History Analysis, *Earthquake Engineering and Structural Dynamics*, 42(9), 1265-1280.

- Howell (2007)   *Statistical Methods for Psychology,* Thompson Wadsworth.

- Jayamon and Charney (2015)   Multiple Ground Motions Response Spectrum Matching Tool for Use in Response History Analysis, *Proceedings of the 2015 Structures Congress*, Portland, OR.

- NBS (1978)   *Tentative Provisions for the Development of Seismic Regulations for New Buildings* (ATC 3-06)

- NIST (2010)   *Evaluation of the FEMA P-695 Methodology for Quantification of Building Seismic Performance Factors* (NIST GCR 10-917-8)

- NIST (2011)   *Selecting and Scaling Earthquake Ground Motions for Performing Response-History Analysis* (NIST GCR 11-917-15)

■ NIST (2012a) *Tentative Framework for Development of Advanced Seismic Design Criteria for New Buildings* (NIST GCR 12-917-20).

■ NIST (2012b) *Soil-Structure Interaction for Building Structures* (NIST GCR 12-917-21).

■ NUREG (2014) *Standard Review Plan for the Review of Safety Analysis Reports for Nuclear Power Plants* (NUREG-800)

■ Wilson and Habibullah (1987) Static and Dynamic Analysis of Multi-Story Buildings Including P-Delta Effects, *Earthquake Spectra*, 3(2*).*

The authors would like to acknowledge the assistance on this project of Virginia Tech graduate students Adrian Tola and Jeena Jayamon. Mr. Tola performed the analysis of the 12-story building on ETABS, and Ms. Jayamon performed the matching of ground motions utilized in the linear response history analysis. Dr. Francisco Flores, a former Virginia Tech student, worked on the preliminary analysis and design of the structure, and performed analysis using SAP 2000.

Also, it is noted that the example analysis presented in this chapter is based on the analysis of a similar structure in Chapter 4 of FEMA P-751.

Computers and Structures International provided the ETABS 2015 and SAP 2000 software used for the analysis at no cost to the authors.

4.1   NEW PROVISIONS FOR LINEAR DYNAMIC ANALYSIS IN FEMA P-1050 AND ASCE 7-16

All of the changes related to linear dynamic analysis were initially proposed for inclusion in the 2015 NEHRP Provisions, and were then addressed and adopted, with some modifications, by the ASCE 7-16 standard. The changes incorporated into ASCE 7 are described first, and then the differences relative to the *Provisions* are discussed. It is noted that items not specifically related to structural analysis but pertinent to this chapter (e.g. changes to the site modification factors) are not included in the following discussion, but were included in the example calculations.

4.1.1   Changes in the ASCE 7-16 Standard

The following changes were made in the ASCE 7-16 Standard:

1) Section 12.8.4.2 was modified to exempt accidental torsion requirements in certain situations, as follows:

> **EXCEPTION:** For structures assigned to Seismic Design Category B, the accidental torsional moments (M_{ta}) need not be included in the design of buildings that do not have a Type 1b horizontal structural irregularity. For structures assigned to Seismic Design Category C, D, E, or F, the accidental torsional moments (M_{ta}) need not be included in design of buildings that do not have a Type 1a or 1b horizontal structural irregularity.

2) Section 12.9 has been renamed "Linear Dynamic Analysis", and has been divided into two sub-sections, one for Modal Response Spectrum analysis (Section 12.9.1) and one for Response History analysis (Section 12.9.2).

3) The Modal Response Spectrum (MRS) procedure of Section 12.9 of ASCE 7-10 was moved to Section 12.9.1, and several significant changes were made. These changes are summarized as follows:

    a. Three-dimensional analysis is required for all systems analyzed using MRS procedures.

    b. In ASCE 7-10 it was required to include a sufficient number of modes to capture not less than 90% of the system mass in the direction of response. For some systems it takes a large number of modes to capture 90% of the mass, so a provision was added to enable the use of rigid-body modes. This procedure is not required, and the ability to capture the required mass using only the natural mode shapes was retained as an exception.

    c. In ASCE 7-10 is was required to scale the results of modal response spectrum analysis such that the dynamic base shear was not less than 85% of the Equivalent Lateral Force (ELF) base shear in the given direction. This requirement was changed to require that the dynamic base shear be not less than 100% of the ELF base shear in each direction of response.

    d. The commentary associated with combination of response parameters computed (using SRSS or CQC) was clarified.

4) The Linear Response History (LRH) analysis procedures that were in Section 16.1 of ASCE 7-10 have been deleted, and new provisions were developed and placed in Section 12.9.2 of ASCE 7-16. While the revised LRH procedures are similar to those in ASCE 7-10, several important changes were made as follows:

    a. Three-dimensional analysis is required for all systems analyzed using LRH procedures.

    b. Accidental torsion, where required, must be included by physically offsetting the center of mass.

    c. P-Delta effects must always be included directly in the analysis.

    d. Spectrally matched ground motions must be used.

    e. Requirements for the number of modes to use in analysis (where modal response history analysis is used) were made consistent with the updated provisions for MRS analysis.

    f. Requirements for scaling the results to 100% of the ELF seismic base shear were made consistent with the updated requirements provisions for MRS analysis.

    g. It is required to combine the effects of ground shaking in orthogonal directions.

    h. Procedures for scaling of the results were clarified.

5) The Nonlinear Response History (NRH) analysis provisions in Chapter 16.2 of ASCE 7-10 have been deleted, and new provisions were developed and placed in Chapter 16 of ASCE 7-16.

4.1.2 Differences between ASCE 7-16 and the 2015 NEHRP Provisions.

With the exception of several editorial changes, the modified modal response spectrum and linear response history analysis provisions that are incorporated into ASCE 7-16 are essentially the same as those that are included in the 2015 NEHRP provisions.

4.2   THEORETICAL BACKGROUND

In this section, the various analysis procedures available in Chapters 12 of the *Standard* are described from a theoretical perspective, starting with the most general approach, linear response history (LRH) analysis, and ending with the simplest approach, the equivalent lateral force (ELF) method. Also presented are issues related to system modeling, selection and modification of ground motions, and some statistics that provide insight on computational requirements for the various methods of analysis. Emphasis is placed on the linear procedures throughout.

4.2.1   Analysis Procedures

In the example presented in Section 4.3 of this chapter, three methods of structural analysis are utilized for determination of design forces and deformations; the Equivalent Lateral Force (ELF) procedure, Modal Response Spectrum (MRS) analysis, and Linear Response History (LRH) analysis. Each of these procedures and methodologies are described below, and advantages and disadvantages of each are presented and discussed.

4.2.1.1 Linear Response History Analysis by Direct Integration of the Equations of Motion.
The equations of motion (EOM) used in linear response history analysis are presented in Eq. 4.2-1, wherein it is assumed that the structure is modeled in an *X-Y-Z* Cartesian coordinate system with the *X* and *Y* axes being horizontal, and *Z* vertical.

$$M\ddot{U}(t) + C\dot{U}(t) + K_E U(t) + K_G(t)U(t) = F_G - M\left(\iota_X \ddot{u}_{g,X}(t) + \iota_Y \ddot{u}_{g,Y}(t)\right) \qquad [4.2\text{-}1]$$

The terms in the equation are defined as follows:

$\ddot{U}(t), \dot{U}(t), U(t)$	Relative accelerations, velocities, and displacement at the individual degrees of freedom
M	System mass matrix
C	System inherent damping matrix
K_E	System elastic stiffness matrix
$K_G(t)$	System geometric stiffness matrix
F_G	Gravity forces acting on the system
$\ddot{u}_{gX}(t)$	Ground acceleration history in the translational *X* direction
$\ddot{u}_{gX}(t)$	Ground acceleration history in the translational *Y* direction
ι_X	Ground motion influence vector in the translational *X* direction
ι_Y	Ground motion influence vector in the translational *Y* direction

Before proceeding, some important aspects of selected terms are provided as follows.
- The accelerations, velocities, and displacements are called "relative" because they are based on the deformation of the system relative to the base of the structure, and do not include the rigid body components of ground motion. The base of the structure is defined in Chapter 11 of the *Standard* as "the level at which the horizontal seismic ground motions are considered to be imparted to the structure".

- The inherent damping matrix, *C,* remains constant and accounts for natural sources of energy dissipation in the structural and nonstructural system, not including soil/foundation radiation damping, inelastic material behavior, or added mechanical devices. *C* cannot be developed from first principles, and when explicitly formed, is generally taken as a linear combination of mass and elastic stiffness such that $C = a_0 M + a_1 K_E$, where a_0 and a_1 are scalar parameters determined to produce specified damping ratios at two selected frequencies. Damping ratios at other frequencies are dependent on the proportionality constants and on the frequency, i.e. $X(W) = 0.5(a_0/W + a_1 W)$. It is noted, however, that *C* is not needed when the equations of motion are uncoupled, and instead, damping ratios can be assigned arbitrarily to each uncoupled equation.
- The elastic system properties represented by K_E are used even though it is expected that significant inelastic response will occur when the structure is subjected to design level ground motions. Inelastic effects are accounted for by analyzing the system for force levels that are $1/R$ times the elastic demands, and multiplying computed elastic displacements by C_d/R. See the ATC 84 report (NIST, 2012a) for a review of some of the consequences of this assumption, particularly as it relates to very short period or very long period structures.
- The geometric stiffness, $K_G(t)$ varies with time because it is dependent on the current axial forces in the elements of the structure. Hence, strictly speaking, equations 4.2-1 are nonlinear.
- The gravity forces, F_G, must be applied to the system prior to the application of ground motions, and then held constant during the analysis.
- The ground motions in the two orthogonal directions must be applied simultaneously due to the nonlinearity associated with the geometric stiffness.

A numerical procedure such as the Newmark method (see Chopra, 2012) is used to solve the equations, and iteration is required due to the nonlinearity associated with geometric stiffness. While the computed response is arguably the most accurate that can be obtained for elastic systems, the computer time required to obtain a solution can be high (relative to the other methods described in this section) and it is difficult to scale results (to the ELF base shear) because the *X* and *Y* directions responses must be obtained simultaneously.

A variation of Eq. 4.2-1 presented in Eqs. 4.2-2a and 4.2-2b, eliminates iteration by using a constant geometric stiffness, K_{G0}, which is determined from a separate gravity load analysis. Now, the equations are fully linear and elastic superposition of results is allowed. As a result the gravity loading need not be carried through the analysis. For the same reason, the two horizontal components of ground motion can be analyzed separately, the results in each direction can be independently computed, scaled if necessary, and then added to the results obtained from the separately executed gravity load analysis.

$$M\ddot{U}(t) + C\dot{U}(t) + K_E U(t) + K_{G0} U(t) = -M\iota_X \ddot{u}_{g,X}(t) \qquad \text{[4.2-2a]}$$

$$M\ddot{U}(t) + C\dot{U}(t) + K_E U(t) + K_{G0} U(t) = -M\iota_Y \ddot{u}_{g,Y}(t) \qquad \text{[4.2-2b]}$$

It is noted that the assumption of a constant geometric stiffness will introduce some error into the solution of three dimensional systems which display significant global torsional response. (Wilson and Habibullah, 1987).

While iteration is eliminated, the solution time required for analysis by direct integration is significantly greater than required for modal analysis, and storage requirements are also greater due to the need to store the system displacements at each degree of freedom for each time step analyzed. For these reasons, and due to difficulty in scaling results, performing response history analysis by direct integration is not recommended, even though it is specifically allowed by the *Standard*.

4.2.1.2 Linear Response History Analysis by Modal Superposition. Eqns. 4.2-3a and 4.2-3b are a somewhat simplified form of the EOM in which the elastic stiffness K_E and the initial geometric stiffness K_{G0} have been added to produce the linear system stiffness $K=K_E + K_{G0}$.

$$M\ddot{U}(t)+C\dot{U}(t)+KU(t)=-M\iota_X \ddot{u}_{g,X}(t)$$
[4.2-3a]

$$M\ddot{U}(t)+C\dot{U}(t)+KU(t)=-M\iota_Y \ddot{u}_{g,Y}(t)$$
[4.2-3b]

The equations may be uncoupled by representing the global displacement vector at any time as a linear combination of the individual modal responses

$$U(t)= \sum_{i=1}^{nmodes} \phi_i y_i(t) = \phi_1 y_1(t) + \phi_2 y_2(t) + \phi_3 y_3(t) + \cdots + \phi_{nmodes} y_{nmodes}(t)$$
[4.2-4a]

where ϕ is an individual mode shape and $y(t)$ is a scalar history of modal amplitude multipliers associated with the shape. The mode shapes and vibration frequencies ω are determined by solution of the eigenvalue problem, $K\phi=\omega^2 M\phi$. The maximum number of mode shapes that can be obtained, *nmodes*, is equal to the number of mass degrees of freedom in the structure. Alternate bases to represent system deformations, such as Ritz vectors, may offer some advantages. The reader is referred to Chopra (2012) for details.

Eq. 4.2-4a can be re-written in matrix form as

$$U(t)=\Phi Y(t) = \begin{bmatrix} \phi_1 & \phi_2 & \cdots & \phi_{nmodes} \end{bmatrix} \begin{bmatrix} y_1(t) \\ y_2(t) \\ \vdots \\ y_{nmodes}(t) \end{bmatrix}$$
[4.2-4b]

Substituting Eq. 4.2-4b and its time derivatives into Eq. 4.2-3a gives

$$M\Phi\ddot{Y}(t)+C\Phi\dot{Y}(t)+K\Phi Y(t)=-M\iota_X \ddot{u}_{g,X}(t)$$
[4.2-5]

Pre-multiplying each side of Eq. 4.2-5 by the transpose of the mode shape matrix results in

$$\Phi^T M\Phi\ddot{Y}(t)+\Phi^T C\Phi\dot{Y}(t)+\Phi^T K\Phi Y(t)=-\Phi^T M\iota_X \ddot{u}_{g,X}(t)$$
[4.2-6]

Due to the orthogonality property of the mode shapes the triple matrix products on the left hand side of Eq. 4.2-6 result in diagonal "generalized" matrices, with each diagonal term represented by the symbol m^*, c^*, or k^* for the given mode. Thus, for the *i*th mode, the following equation can be written

$$m_i^* \ddot{y}_i(t) + c_i^* \dot{y}_i(t) + k_i^* y_i(t) = -\phi_i^T M \iota_X \ddot{u}_{g,X}(t) \qquad\qquad [4.2\text{-}7]$$

where, for example, $m_i^* = f_i^T M f_i$.

Eq. 4.2-7 is a single degree of freedom equation of motion with the modal multiplier history, $y_i(t)$ as the principal unknown. This equation can be easily solved using a variety of procedures. Due to the presence of the generalized damping term c_i^* in Eq. 4.2-7, which is not obtainable from first principles, it is convenient to divide all terms in the equation by the generalized mass (which will never be zero) resulting in

$$\ddot{y}_i(t) + \frac{c_i^*}{m_i^*} \dot{y}_i(t) + \frac{k_i^*}{m_i^*} y_i(t) = -\frac{\phi_i^T M \iota_X}{m_i^*} \ddot{u}_{g,X}(t) \qquad\qquad [4.2\text{-}8]$$

which may be written as

$$\ddot{y}_i(t) + 2\xi_i \omega_i \dot{y}_i(t) + \omega_i^2 y_i(t) = -\Gamma_{iX} \ddot{u}_{g,X}(t) \qquad\qquad [4.2\text{-}9]$$

where $\xi_{\square}$ is the damping ratio, $\omega_{\square}$ is the circular frequency of vibration, and $\Gamma_{\square}$ is the modal participation factor in the given mode. Now, the modal damping ratios (usually 0.05) can simply be assigned to the mode. Note that the value of the modal participation factor is dependent on the method used to normalize the mode shapes because, as seen from Eq. 4.2-8, there is one mode shape in the numerator, and two in the denominator (in the m^* term) of the collection of terms that represent Γ. This is not an issue in the analysis because the normalization factors cancel out in the formation of the product $f_i y_i(t)$.

After each of the modal response histories $y_i(t)$ are obtained, the full system response, in the original coordinate system, is obtained using Eq. 4.2-4a.

In terms of solution efficiency, the vast majority of the time required to perform an analysis using modal superposition is associated with the computation of the mode shapes and frequencies. To minimize this time, some solution accuracy is sacrificed by solving only a subset of modal responses, starting with the mode with the lowest natural frequency (greatest period) and including all modes up to mode n where $n <$ *nmodes*.

The minimum number of modes to include in the analysis is specified by the *Standard* in Section 12.9.2.2.4, which refers to Section 12.9.1.1, and is as follows:

12.9.1.1 Number of Modes

An analysis shall be conducted to determine the modes of vibration for the structure. The analysis shall include a sufficient modes to capture participation of 100% of the structure's mass. For this purpose, it shall be permitted to represent all modes with periods less than 0.05 seconds in a single rigid body mode having a period of 0.05 seconds.

EXCEPTION: Alternatively, the analysis shall be permitted to include a sufficient number of modes to obtain a combined modal mass participating of at least 90 percent of the actual mass in each orthogonal horizontal direction of response considered in the model.

The language in the exception is the same as specified in ASCE 7-10, and this approach can be used for any structure. In some cases, however, a significant percentage of the mass is associated with very high frequency modes, and it takes a large number of modes to capture more than 90% of the mass. In this case, it is possible to capture 100 percent of mass by use of the "static correction method", which includes all modes with periods less than 0.05 seconds (20Hz) as "rigid body" modes.

The mass participation of a given mode, called the effective modal mass, is determined by considering the forces acting on the system at a given point in time. These can be represented as

$$F_i(t) = K f_i G_i s_i(t) \qquad [4.2\text{-}10]$$

where $s(t)$ represents the solution to 4.2-9 if $\Gamma = 1.0$. Given that for any mode $K f_i = W_i^2 M f_i$ Eq. 4.2-10 can be re-written as

$$F_i(t) = M f_i G_i W_i^2 s_i(t) \qquad [4.2\text{-}11]$$

The total base shear in the mode can be written as

$$V_i(t) = i_X^T M f_i G_{iX} W_i^2 s_i(t) \qquad [4.2\text{-}12]$$

Transposing the right hand side and multiplying numerator and denominator by the generalized mass in the mode results in

$$V_i(t) = \frac{f_i^T M i_X}{m_i^*} G_{iX} m_i^* W_i^2 s_i(t) = G_{iX}^2 m_i^* W_i^2 s_i(t) \qquad [4.2\text{-}13]$$

In Eq. 4.2-13 the term $W_i^2 s_i(t)$ is the modal acceleration, and the product $G_{iX}^2 m_i^*$ is the effective modal mass in the mode. This effective mass value is independent of the way the mode shapes are normalized, and the sum of the values for all the modes is equal to the total mass of the system. Most of the mass will be associated with the lower modes, so only a small fraction of the total modes in a MDOF system are required to obtain an acceptable solution.

4.2.1.3 Modal Response Spectrum Analysis. Modal response spectrum analysis is similar to modal response history analysis from the perspective that the uncoupled equations of motion are utilized, but instead of computing the complete history of response for each mode, the absolute value of the maximum modal response, $y_{i,max}$, is obtained from a response spectrum. The response spectrum used to provide $y_{i,max}$ may be based on a given ground motion, the average of several ground motion spectra, or may be empirical. Since, in the development of the response spectrum, the sign (positive or negative) and the time of occurrence of the maximum modal response are lost (or are never determined in the case of empirical spectra), the total system response must be obtained statistically instead of by direct addition of individual modal responses.

When the response spectrum approach is used, the individual modal maxima are obtained as shown in Eq. 4.2-14 for ground shaking in the X direction

$$y_{i,max} = G_{iX} S_{di} f_i \qquad [4.2\text{-}14]$$

where S_{di} is the spectral displacement amplitude for the period of vibration associated with mode *i*. A similar equation would be used to compute the *Y* direction response.

It is impossible to capture the exact response of the system, even if all the modes are included, because the true sign (positive or negative) of the modal response, and the time of maximum response is not available. Additionally, even if this information was available, the modes could not be directly combined because the maximum quantities would generally occur at different times in the response. For this reason, the combined response is determined approximately by using statistical combinations, such as the square root of the sum of the square (SRSS) of the modal responses, or by the complete quadratic combination (CQC) approach, or one of the several CQC descendants. The computation of the response by statistical means rather than by direct addition of the true modal responses introduces some error into the response relative to the modal response history approach. However, given that an empirical response spectrum is used, and that the true inelastic behavior of the response is not evaluated, the error is considered to be insignificant from a design perspective.

Where a 3-D analysis is used, it is generally preferred to use the CQC method to combine modal responses, as this method provides more accurate results when the modal frequencies are closely spaced (e.g the periods for two modes, one with dominant response in the *X* direction, and the other with a dominant response on the *Y* direction, are nearly identical).

It is important to note, however, that there are two distinct advantages of the modal response history approach relative to the response spectrum method. First, in the response history method, the true signs of the deformations and the member actions are known, and second, the true force interactions (e.g. bending moments in a column at the time of maximum axial force) are available.

4.2.1.4 Equivalent Lateral Force Analysis

The Equivalent Lateral Force (ELF) method is essentially a one-mode response spectrum approach which utilizes an empirical mode shape, and which assigns 100% of the mass to the single mode. The method was developed for analysis of 2-Dimensinal (planar) structural systems with regular mass and stiffness distribution along the height. For this reason, *Standard* Table 12.6-1 imposes restrictions on the use of the method (no torsional irregularities, no vertical stiffness or mass irregularities). For long period systems ($T > 3.5T_s$) it has been shown that the empirical mode shape is not capable of representing higher mode effects, thus an additional restriction is placed on the use of ELF for these systems even when the structure has none of the stated irregularities.

The equilibrium equations for 3-D structural systems as used in the ELF method are presented in Eq. 4.2-15:

$$KU = F + T \hspace{6cm} [4.2\text{-}15]$$

where *K* is the stiffness matrix, *U* are the computed nodal displacements, *F* are the equivalent lateral forces determined in accordance with *Standard* Equation 12.8-12, applied at the center of mass of the floor plates, and *T* are the amplified accidental story torques computed in accordance with *Standard* Sections 12.8.4.2 and 12.8.4.3. Where P-Delta effects are included directly in the analysis, $K=K_E+K_{G0}$, otherwise $K=K_E$.

It is recommended that P-Delta effects always be included directly in the analysis. For three-dimensional models, "accurate" evaluation of P-Delta effects requires that all gravity load-resisting elements be included in the analysis, and that design level gravity loads are applied to the model prior to the application of lateral loads. Performing analysis in this manner will include torsional P-delta effects (due to rotation about the vertical axis), which are neglected in the procedures provided in Section 12.8.7 of the *Standard*. The

evaluation of θ, used for assessing compliance with *Standard* Equation 12.8-17 ($\theta < \theta_{max}$), can be based on analysis with and without P-delta effects, wherein $\theta = 1 - (\Delta_0 / \Delta_F)$, and Δ_F and Δ_0 are story drifts computed with and without P-Delta effects, respectively.

4.2.2 Modeling Systems for 3-D Response

The current ASCE 7 analysis requirements evolved from the *Tentative Provisions for the Development of Seismic Regulations for New Buildings* (NBS, 1978), more commonly known as ATC 3-06. In the era of development of ATC 3-06 personal computers were not readily available, so analysis procedures were based on simplified two-dimensional mathematical models. The emphasis on 2-D models still existed in ASCE 7-10, but a movement was made towards the requirement for 3-D analysis in ASCE 7-16, where 3-D models are *required* for response spectrum analysis and for linear and nonlinear response history analysis. Prior editions of the standard required 3-D analysis only when horizontal irregularities 1a, 1b, 4, or 5 existed, or where the diaphragm could not be represented as rigid. ASCE 7-16 maintains these requirements for structures analyzed using the ELF method, and based on these requirements it is more likely than not that 3-Dimensional analysis will be required. Additionally, it is noted that modern computer software easily accommodates 3-D modeling. Given the above, this section focuses on the development of 3-D mathematical models, with emphasis on modeling where the modal response spectrum or the modal response history methods of analysis are used.

Modeling the full structural system
To the extent practicable, the "full structural system" should be represented in the mathematical model. This system includes all of the elements of the lateral load resisting systems, the gravity framing system, the floor and roof diaphragms, and foundation and soil characteristics where soil-foundation-structure interaction is included in the analysis. While this approach may not yet be common practice, the authors feel that the use of such an approach provides the most robust analysis possible (with the exception of the fact that inelastic effects are not considered), and that using modern software tools, the additional effort required to develop a full system model has marginal impact on the total analysis/design effort.

Before proceeding with modeling recommendations, it is noted that the purpose of including the gravity system is to (a) provide a realistic distribution of gravity forces throughout the structure as needed to represent P-delta effects, and (b) to provide vertical support for diaphragm elements. It is important to note however, that the gravity framing should be modeled such that it does not influence the lateral elastic stiffness of the structure. The modeling of the diaphragms is important for the purpose of (a) distributing floor and roof mass throughout the structure, and (b) producing a realistic force transfer between lateral load resisting systems. As with the gravity system, the modeling of the diaphragms should not influence the overall lateral stiffness of the structure.

Modeling the Gravity System
Only the major gravity elements of the gravity system need be included (beams and columns), and they should be modeled as pinned-pinned such that they do not develop any shear due to lateral loads. For structures of simple geometry a few strategically located "leaning columns" could be used in lieu of modeling the gravity system. This approach is not practical for the structure analyzed in this example because the complex geometry makes it difficult to determine the appropriate location of and axial forces in the leaning columns. It is important to note that for structures of simple geometry where leaning columns might be used, the use of a single leaning column located at the center of the structure should be avoided because it is difficult if not impossible to obtain the proper spatial distribution of gravity forces that are necessary to represent lateral softening (P-Delta effects) and rotational softening (P-Theta effects) that are associated with geometric nonlinearity.

Gravity Loads used in P-delta Analysis
The gravity loads to be used in analyses incorporating P-Delta effects should be taken as 1.0 times dead load plus 1.0 times design live load plus 0.2 times snow load, if applicable. A factor of 0.5 on the live load is allowed for all occupancies in which L_o in *Standard* Table 4-1 is less than 100 psf, with the exception of garages or places of public assembly.

Mass
There are a variety of ways to model mass in the system, and in some cases, mass is automatically included for the structural elements (beams, columns, diaphragm elements). The authors recommend a different approach, wherein the mass density of structural materials is set to zero, and all of the system mass (including vertical mass) is input directly using point, line, or area masses. Using the direct mass modeling approach makes it easier to obtain an accurate representation of the system mass, and it makes it easier to accommodate relocations of center of mass associated with accidental torsion.

Where only horizontal ground shaking is used in the analysis, and where vertical accelerations and associated vertical inertial forces resulting from horizontal shaking are expected to be small relative to horizontal accelerations and forces, the exclusion of vertical mass in the mathematical model may significantly reduce the number of modes required to obtain an accurate solution.

Floor and Roof Diaphragms
Section 12.3.1.2 of the *Standard* sets the conditions wherein rigid diaphragms may be used in the analysis, and one of the requirements is that *the structure have no horizontal irregularities*. Given that the lack of such irregularities is rare (the example building used in this chapter has Horizontal Irregularity Types 1a, 2, and possibly3), the diaphragm will very often need to be modeled as semi-rigid. Even where rigid diaphragms are allowed, the main incentives for using them are (1) to reduce storage requirements and solution times for analysis run on personal computers, and (2) to avoid additional labor required to model the diaphragm using finite elements. Current computer capabilities are such that analysis is virtually instantaneous even for systems modeled with semi-rigid diaphragms, and the modeling of the diaphragm is not difficult when graphical used interfaces are employed. Hence, the use of semi-rigid diaphragms is practical, and is recommended for most structures.

Typically, the semi-rigid diaphragm will be modeled using shell elements which are semi-rigid in plane, and which have significant out-of-plane bending stiffness. However, the out-of-plane stiffness should be modified to near-zero to prevent the development of bending moments in the diaphragm, which if present, will reduce the moments in the elements of the main lateral force reciting system. (While the diaphragms have the capability to resist bending, the ductility of the diaphragm elements that resist bending is unknown, and is certainly less than the ductility of the lateral load resisting system).

In most cases a very coarse mesh may be used for modeling the diaphragms, and only one finite element is needed for each (rectangular) bay of the system. If a finer mesh is used, nodes will need to be placed within the interior regions of the diaphragm, and this may lead to "instabilities" associated with a lack of vertical or rotational restraint (which is caused by to the zero out-of-place stiffness requirement). These issues may be resolved by restraining the interior diaphragm nodes in the vertical and rotational directions, or by modeling the diaphragms using shell elements and using a very small out of plane stiffness.

Damping
Methodologies for modeling damping depend on the analysis approach used. For linear analysis, the damping should not be taken as greater than 5% in any included mode of response.

The requirement for a ceiling of 5% damping can be difficult to obtain where analysis is performed using direct integration of the equations of motion and where the damping matrix C is represented as stiffness

mass and stiffness proportional (using Rayleigh damping). In such a case the damping ratio may be specified at only two frequencies, and the damping at other frequencies may be higher or lower than the specified amount. If the maximum damping ratio is limited to 5% for any frequency, the average damping ratio across all included frequencies will be less than 5%.

Where modal response history analysis is used, 5% damping should be specified in each included mode. In modal response spectrum analysis, the damping is incorporated into the development of the response spectrum and need not be specified on a modal basis. It is noted, however, that the damping ratios are required separately as a parameter in the CQC modal combination procedure, and this value should be set to 5% in each included mode.

Damping of 5% critical is inherently included in the seismic ground motion parameters S_{DS} and S_{D1} that are used in the ELF method, and need not be specified separately in the analysis.

Equivalent viscous damping should never be used to represent increased damping due to the use of added damping devices. Instead such devices (often with nonlinear characteristics) should be explicitly included in the mathematical model. Chapter 18 of ASCE-16 provides requirements for the analysis of structures that incorporate added damping devices.

Foundation and Soil Modeling
In many cases it is necessary or even advantageous to model the effects of soil-foundation-structure interaction. The reader is referred to the NIST document *Soil-Structure Interaction for Building Structures* (NIST, 2012b) for details.

Scaling of Results
Where modal response spectrum or modal response history analysis is used, the *Standard* requires that all component forces are scaled such that, in each direction of response, the base shear computed from the dynamic approach (MRS or MRH) is not less than the design base shear obtained using Eq. 12.8-1. Since the fundamental period of the structure used in the dynamic analysis is generally greater than ELF's upper limit period $C_u T_a$, the results coming from the dynamic analysis will generally be scaled up. If it happens that the base shears from the dynamic analysis are greater than the ELF shears, they should *not* be scaled down.

Orthogonal Load Combinations
Where response history analysis by direct integration of the equations of motion is used, and where P-delta effects are updated based on current element forces, the ground motions in the two orthogonal directions must be run simultaneously, making it difficult to scale the results in strict accordance with the standard. However, when any of the other dynamic analysis methods (MRS, MRH) are used, the ground motions may be applied independently in the orthogonal directions, and the responses in the individual directions can be appropriately scaled prior to combining the results in the two orthogonal directions.

4.2.3   Selection and Modification of Ground Motions

Where response history analysis is used, it is necessary to select and modify a suite of ground motions to use as input in the form of ground acceleration histories. In Section 12.9.2 of the *Standard*, which covers linear response history analysis, it is required that a suite of not less than three earthquake events be used. For each earthquake event two orthogonal components must provided, and prior to analysis, each component must be modified to represent the actual seismic hazard at the site.

There are generally two approaches to ground motion modification: amplitude scaling and spectral matching. In both cases the objective is to "fit" the pseudoacceleration spectrum computed from the

modified record to some target design spectrum. In amplitude scaling, each acceleration value in the record is multiplied by the same scale factor such that the ordinates of the scaled pseudoacceleration spectrum and the target spectrum coincide at some pre-selected period of vibration, or such that the average of the scaled components from the suite of earthquakes closely matches (within some tolerance) the target spectrum. One of the advantages of amplitude scaling is that the frequency characteristics of the original record are preserved.

In spectral matching, the original ground motion record is nonuniformly scaled (essentially different scale factors are used for each recorded value of the original record) such that the pseudoacceleration response spectrum of the matched record closely matches the shape of the target spectrum. There are a variety of approaches to achieve this goal, and procedures utilizing Fourier transforms or wavelets are the most common. The main advantage of using spectrally matched ground motions is that a reasonable variation in response among multiple earthquakes can be obtained with fewer records than required when amplitude scaling is used.

It is beyond the scope of this example to delve into the theoretical basis of ground motion selection and modification, and for this reason the reader is referred to NIST (2011) for additional details. See also Section 3.4 of this publication (FEMA P-1051). It is noted, however, that Section 12.9.2.3 of the *Standard* requires spectral matching of ground motions in linear response history analysis. There are two reasons for this requirement. First, it is recognized that elastic response history analysis cannot be expected to "predict" the behavior of highly nonlinear systems, and as such it is merely a tool to be used for design. The same basic philosophy applies to the modal response spectrum method, so it seems logical to develop a response history procedure that, in essence, uses the same response spectrum as does the response spectrum method. Second, with amplitude scaling, it is likely that some frequencies will receive disproportionally high (or low) scaling, and this can non-uniformly affect the results. Consider, for example, Figure 4.2-1a which shows the response spectra for three earthquakes, amplitude scaled such that all three have the same spectral acceleration at a given period of vibration (in this case 2.22 seconds). The vertical dashed lines at the left and right of the plotted region represent the range of periods associated with the modes that will be represented in the analysis. As is evident in the short period region, the higher modes (with lower periods of vibration) for two of the earthquakes (G03090 and TCU045N) have spectral amplitudes much higher than that of the target spectrum, and hence, the higher modes in the response will be overrepresented in the analysis. The third earthquake, MUL279, more closely matches the target spectrum in the low period region. It is certainly possible that a better fit could be obtained by use of different records (not using G03090 and TCU045N), and trying to find additional records that provide a match more like that shown for MUL279.

The same suite of earthquakes that were modified by spectral matching is shown in Figure 4.2-1b. Here, in the spectrum matching range, the variation in the spectral accelerations for the three matched records are virtually indistinguishable from the target spectrum over the expected period range, and the higher modes are not over-represented relative to the target spectrum. There are some variations outside the matching range, particularly at low periods, but this will not affect the computed response because modes associated with these periods are not included in the analysis.

The *Standard* requires that the period range used for spectral matching is 0.8 T_{min} to 1.2 T_{max}, where T_{min} is the period at which 90% of the effective modal mass is captured, and T_{max} is the largest period of vibration for the system. The average of the matched spectra in each direction of response should not fall outside the range of + or − 10% of the target spectrum.

It is noted that the requirements stated above are based in the implicit assumption that the analysis will be performed using modal response history, and not direct integration of the equations of motion. If direct integration is used in association with the matched ground motions represented in Figure 4.2-1b there will

be some "over amplification" of the higher mode response and periods less than T_{min}, but this will not be as severe as if the amplitude scaled records were used. If there is a concern, the over amplification could be reduced by using a lower value of T_{min}.

There are a variety of programs available for performing spectral matching. In the example to be presented later, the program RSPMatch (Al Atik and Abrahamson 2010) was utilized via a special Matlab application developed by Jayamon and Charney (2015). See also Grant and Diaferia (2012) for additional information regarding spectrum matching.

(a) Ground motion scaled for same ordinate at $T=C_uT_a$

(b) Ground motion spectrally matched over period range $0.8T_{min}$ to $1.2T_{max}$

Figure 4.2-1. Amplitude Scaling vs Spectral Matching for Three Earthquakes

4.2.4 Runtimes and Storage Requirements

In order to obtain some idea of the relative run times and storage requirements, a series of analyses were run for a hypothetical building which is 80 stories in height, has five bays in one direction and 3 bays on the orthogonal direction, and utilized perimeter moment resisting frames for lateral load resistance. All interior gravity columns were directly modeled, and a semi rigid diaphragm (modeled with shell elements) was used with each bay represented by a 4 by 4 mesh. Thus, the total number of degrees of freedom for the model was 80x13x21x6=131,040. Analysis was run using Version 17 of SAP 2000. Solution times for running one ground motion (or response spectrum) are as follows:

MRS with 60 modes (capturing 99% of mass)
Time to compute modal properties	2 minutes and 47 seconds
Time to compute modal responses	0 minutes and 5 seconds
Storage requirements	457 mb

LRH using modal superposition with 60 modes (capturing 99% of mass):
Time to compute modal properties	2 minutes and 58 seconds
Time to compute modal responses	0 minutes and 5 seconds
Storage requirements	467 mb

LRH using direct integration (P-delta not included)
Time to compute modal properties	2 minutes and 50 seconds*
Time to compute response history	26 minutes and 27 seconds
Storage requirements	9010 mb

LRH using direct integration (P-Delta included)
Time to compute modal properties	2 minutes and 50 seconds*
Time to compute response history	3 hours and 27 minutes
Storage requirements	48100 mb

* The modal properties are not used directly in the analysis but are required for determining the range of periods required for spectral matching.

As may be seen the computation times and storage requirements for the modal analyses are similar, and are insignificant for the very large model analyzed. Indeed, all analysis required to run 18 response histories as required by the *Standard* for LRH would be less than five minutes (3 minutes for modal properties, 18x5=90 seconds for response history calculations). Since P-Delta effects are included in the modal analysis, little if any time is added to include this feature in the analysis.

Time requirements for direct integration analysis are significantly greater, as are storage requirements. Using direct analysis without P-Delta would require approximately 9 hours for 18 analyses. If P-delta effects are included, the analysis is essentially nonlinear, and the run times increase drastically, requiring 3.5 hours per run, or 63 hours for all 18 analyses.

4.3 EXAMPLE APPLICATION FOR 12-STORY SPECIAL STEEL MOMENT FRAME STRUCTURE

The building utilized for this example was designed to house business offices, and using *Standard* Table 1.5-1 is classified as Risk Category II. According to *Standard* Table 1.5-2, the Seismic Importance Factor I_e is 1.0. The building is situated on site class C soils.

The 5% damped MCE$_R$ spectral response parameters for the site, located near downtown Stockton, California, are as follows:

$S_s = 1.041$
$S_1 = 0.373$

The site class coefficients, determined from *Standard* Tables 11.4-1 and 11.4-2 are:

$F_a = 1.2$
$F_v = 1.5$

Using *Standard* Equations 11.4-1 through 11.4-4, the design spectral response parameters are computed as

$S_{DS} = 1.2(1.041)(2/3) = 0.833$
$S_{D1} = 1.4(0.373)\ (2/3) = 0.373$

Using *Standard* Tables 11.6-1 and 11.6-2 it is determined that the structure is in Seismic Design Category D.

4.3.1 Description of Building and Lateral Load Resisting System

The building has 12 stories above grade and a one-story basement below grade and is laid out on a rectangular grid with a maximum of seven 30-foot-wide bays in the *X* direction and seven 25-foot bays in the *Y* direction. Both the plan and elevation of the structure are irregular with setbacks occurring at Levels 5 and 9. All stories have a height of 12.5 feet except for the first story, which is 15 feet high, and the basement that extends 18 feet below grade. Reinforced concrete walls, 1 foot in thickness, form the perimeter of the basement. The total height of the building above grade is 152.5 feet. A three-dimensional rendering of the building is shown in Figure 4.3-1, and typical floor plans are given in Figure 4.3-2. Two different elevations (section cuts) are shown in Figure 4.3-3.

Gravity loads are resisted by composite beams and girders that support a normal-weight concrete slab on metal deck. The slab has an average thickness of 4.0 inches at all levels except Levels G, 5, and 9. The slabs on Levels 5 and 9 have an average thickness of 6.0 inches for more effective shear transfer through the diaphragm. The slab at Level G is 6.0 inches thick to minimize pedestrian-induced vibrations and to support heavy floor loads. The low roofs at Levels 5 and 9 are used as outdoor patios and support heavier live loads than do the upper roofs or typical floors.

At the perimeter of the base of the building, the columns are embedded into pilasters cast integrally with the basement walls, with the walls supported on reinforced concrete tie beams over drilled piers. Reinforced concrete caps support interior columns over drilled piers. A grid of reinforced concrete grade beams connects all tie beams and pier caps.

The lateral load-resisting system consists of five special steel moment resisting frames with reduced beam sections. Each frame has three bays. For this type of system, *Standard* Table 12.2-1 specifies a response modification coefficient (*R*) of 8 and a deflection amplification coefficient (*C$_d$*) of 5.5. There is no height limit for special moment frames.

The special steel moment frame locations and designations are shown in Figure 4.3-4. Frames 1 and 2 are 12-stories tall and are supported on pilasters cast together with the basement walls. Frames 3 and 4 are 12-stories tall above grade, but extend 18 feet into the basement below and are supported by the pier caps.

Frame 5 is eight stories tall, and is supported on the basement wall pilasters. Columns that are supported on the basement walls are detailed to provide essentially fixed support conditions. The columns that are supported on the basement slab are assumed to be pinned-base. The gravity columns are also shown in Fig. 4.3-2, and these were explicitly included in the analysis as described later.

Columns in the moment-resisting frame range in size from W24x131 at the upper levels to W24x279 at the lower levels. Girders in the moment frames vary from W27x94 at the roof to W33x130 at Level G. Members of the moment-resisting frames have a nominal yield strength of 50 ksi, and floor members and interior columns that are sized strictly for gravity forces have a nominal yield strength of 50 ksi.
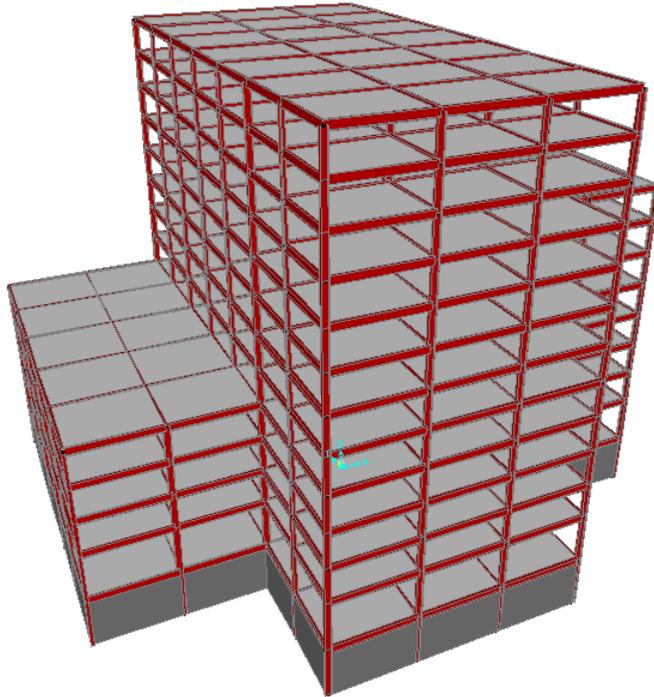
Figure 4.3-1. Three-Dimensional rendering of Stockton building

(a) Level 10

(b) Level 6

(c) Level 2
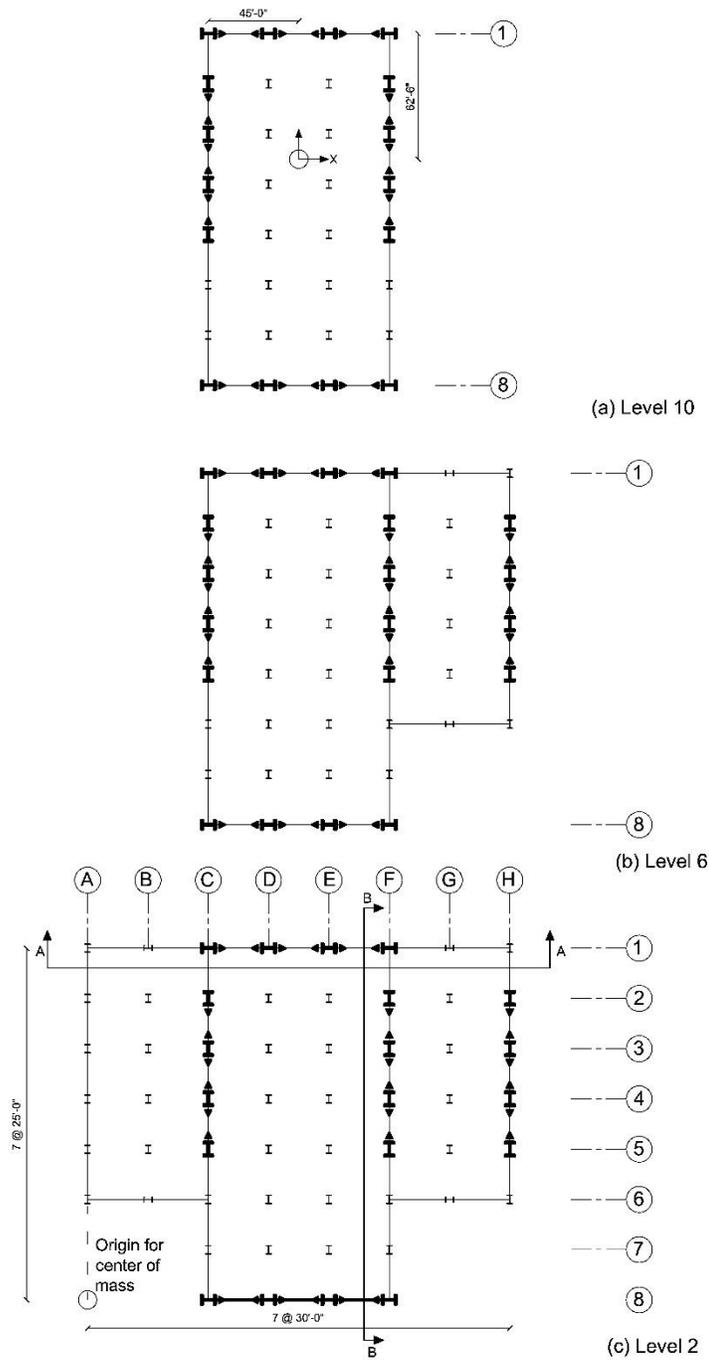
Figure 4.3-2. Various floor plans of 12-Story Stockton building
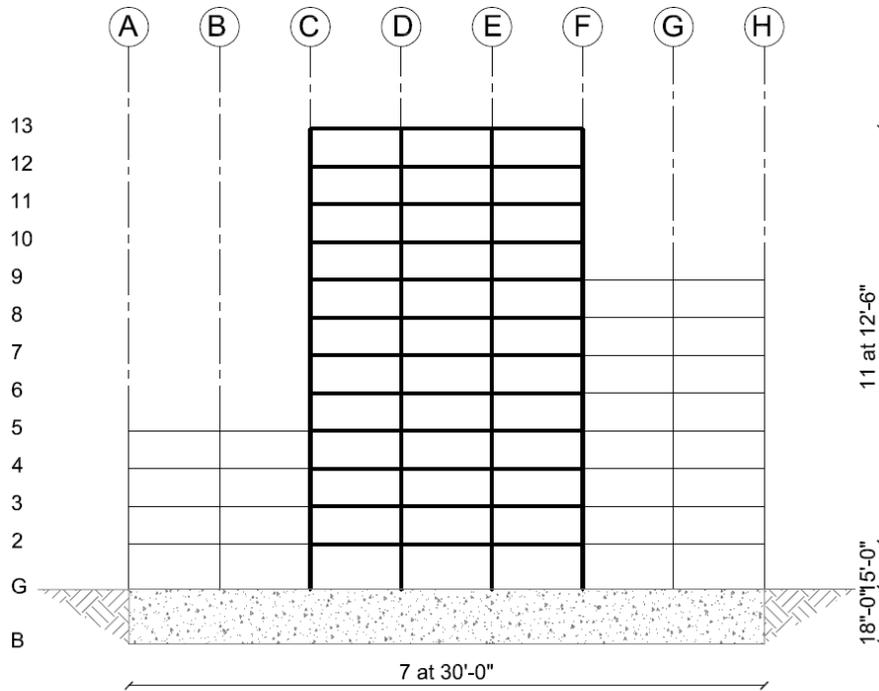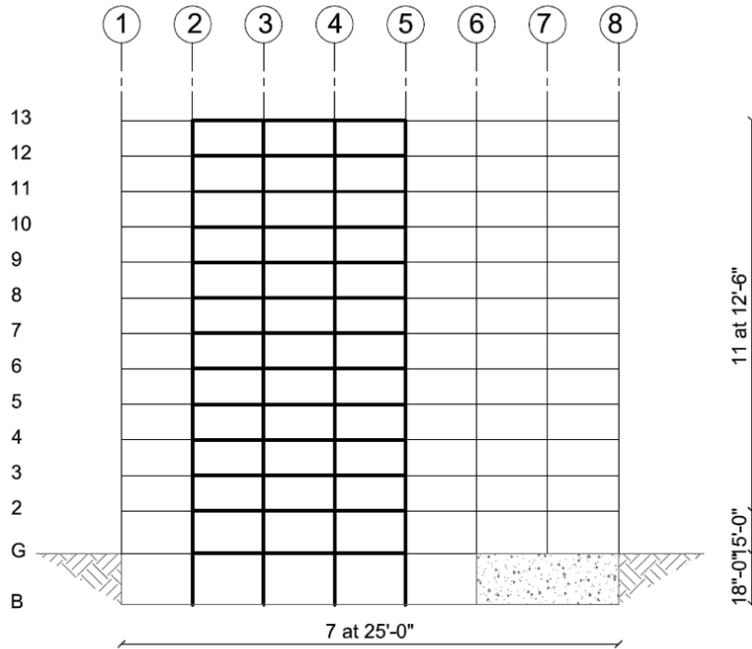
Figure 4.3-3. Section cut elevations
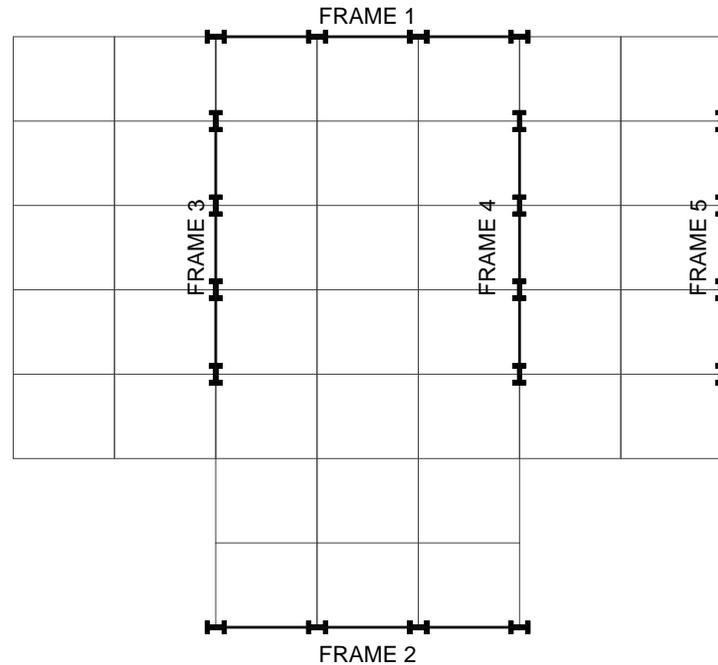
FRAME 1

FRAME 2

Figure 4.3-4. Plan showing location and designations of special moment frames

4.3.2 Analysis and Modeling Approach

Section 12.6 and Table 12.6-1 of the *Standard* provide the analysis requirements for buildings. It is clear for this Seismic Design Category D building that the Equivalent Lateral Force (ELF) method is not allowed due to the presence of a number of system irregularities (re-entrant corner, mass). Thus modal response spectrum analysis, linear response history analysis, or nonlinear response history analysis must be used to determine the design member forces and the displacements in the structure.

It is noted, however, that the ELF procedure is an essential part of the overall analysis and design process because it is often used for preliminary design and it must be used to determine if certain irregularities, such as a torsional irregularity, exist in the system. For this reason, the example presented herein will include ELF analysis. Also included in the example is Modal Response Spectrum (MRS) analysis, and Linear Response History (LRH) analysis. The LRH analysis is performed using modal superposition. The results from the three analysis procedures are then compared, and differences and similarities are discussed.

The analysis is carried out in three dimensions, as required by the *Standard* for both modal response spectrum analysis and linear response history analysis. Due to the presence of a torsional irregularity (see Section 4.3.6) a three dimensional analysis is also required where the ELF procedure is used (see *Standard* Section 12.7.3). Additionally, due to the presence of a re-entrant corner irregularity, the diaphragms cannot be considered as rigid (see *Standard* Section 12.3.1.2), and must be analyzed as semi-rigid. This is done using shell elements as described below.

Additional features of the mathematical model are described as follows:

- P-Delta effects are included directly in the analysis (as required by the *Standard* for LRH analysis and used for consistency in MRS analysis). Gravity loading for use in P-Delta analysis consists of 1.0 times dead load plus 0.5 times reduced live load. This loading follows from Section 12.8.7

of the *Standard* that states, in the definition of P_x, that individual load factors in gravity loads used for P-Delta effects need not exceed 1.0, and from Section 12.4.2.3 which allows for use of 0.5 times reduced live load. In ELF analysis P-Delta effects are included by use of geometric stiffness. In MRS and modal LRH analysis, the modal properties are computed from the same mathematical model, incorporating the same elastic and geometric stiffness, which was used for ELF analysis.

- All major gravity-framing elements are included in the mathematical model, but these elements are modeled (i.e. by releasing end moments) such that they do not contribute to the lateral stiffness of the system. The elements are included only for the purpose of providing an accurate spatial distribution of geometric stiffness as needed for representation of P-Delta effects.

- As shown in Section 4.3.6.1, the structure has a Type-1a torsional irregularity, and as stated in *Standard* Section 12.8.4.2, systems with such irregularities must be analyzed with the effects of accidental torsion included. For ELF analysis accidental torsion (amplified if necessary) is considered by creating an accidental torsion load case consisting of story torques acting along the height of the structure. For MRS and LRH analysis accidental torsion is implemented by use of mass offsets (as required by the *Standard* for LRH analysis and used in MRS analysis for consistency). Amplification of accidental torsion is not required when MRS or LRH analysis is used.

- Special moment frames were modeled using centerline analysis, with axial, flexural, and shear deformations included in all members. Centerline modeling means that no rigid offsets are provided at the overlap of the beam-column joint. The centerline analysis approximately accounts for deformations in the panel zones of the beam-column joints. Moments of inertia for beams with reduced beam sections were modeled with the full cross section moment of inertia. The full section stiffness was used because other compensating sources of stiffness in the system, such as composite behavior, were not included in the analysis. No reduction in beam stiffness was taken for the cutouts of the Reduced Beam Section.

- Roof and floor diaphragms are modeled using one shell element for each 30 ft. by 25 ft. bay, are assigned realistic in-plane stiffness, and near-zero out-of-plane stiffness. These elements were added manually to the model, and provide the minimum mesh resolution required to incorporate semi-rigid diaphragm characteristics for this structure. A finer mesh would be needed if were necessary to recover stresses in the diaphragm.

- Basement walls are modeled explicitly using shell elements.

All analysis was performed using ETABS 2015, developed by Computers and Structures International, Walnut Creek, California. For verification of results, certain aspects of the analysis were performed using SAP 2000 version 18, also developed by Computers and Structures.

Where an equivalent lateral force analysis or a modal response spectrum analysis is performed, the structure's damping ratio, assumed to be 0.05 (5% of critical), is included in the development of the spectral accelerations S_S and S_1. An equivalent viscous damping ratio of 0.05 is appropriate for linear analysis of lightly damaged steel structures. For linear modal response history analysis, ETABS allows an explicit damping ratio to be used in each mode. For this structure, a damping ratio of 0.05 was specified in each mode.

Where combining the individual modal responses in modal response spectrum analysis, the square root of the sum of the squares (SRSS) technique has generally been replaced in practice by the complete quadratic combination (CQC) approach. Indeed, *Standard* Section 12.9.3 requires that the CQC approach be used where the modes are closely spaced. When using the CQC approach, the analyst must correctly specify a damping factor. This factor, which is entered into the ETABS program, must match that used in developing the response spectrum. It should be noted that if zero damping is used in CQC, the results are the same as those for SRSS.

Requirements for combining results in orthogonal directions (Direction of Load Effects) are provided in Section 12.5 of the *Standard*. For the Seismic Design Category D building under consideration, combination of results from analyses in the orthogonal direction are not required for ELF or MRS analysis because there are no intersecting elements in the lateral load resisting system. Inclusion of orthogonal load effects is required to be included in LRH analysis (see *Standard* Sections 12.9.2.5.3 and 12.9.2.5.4).

For consistency in reporting results from the three methods of analysis, orthogonal load effects are considered in the results presented in this Chapter. This required individual analyses for each method of analysis as follows:

Equivalent Lateral Force:

Designation	Description
ELFX	*X* direction lateral load with no mass eccentricity
ELFY	*Y* direction lateral load with no mass eccentricity
ELFTeX	Accidental torsion (applied story torques) due to *X* direction mass eccentricity
ELFTeY	Accidental torsion (applied story torques) due to *Y* direction mass eccentricity

Modal Response Spectrum:

Designation	Description
MRSX	*X* response spectrum using model with no mass eccentricity
MRSY	*Y* response spectrum using model with no mass eccentricity
MRSXe+Y	*X* response spectrum using model with +*Y* mass eccentricity
MRSXe-Y	*X* response spectrum using model with –*Y* mass eccentricity
MRSYe+X	*Y* response spectrum using model with +*X* mass eccentricity
MRSYe-X	*Y* response spectrum using model with –*X* mass eccentricity

Linear Response History (for each ground motion):

Designation	Description
LRHX	*X* direction shaking using model with no mass eccentricity
LRHY	*Y* direction shaking using model with no mass eccentricity
LRHXe+Y	*X* direction shaking using model with +*Y* mass eccentricity
LRHXe-Y	*X* direction shaking using model with –*Y* mass eccentricity
LRHYe+X	*Y* direction shaking using model with +*X* mass eccentricity
LRHYe-X	*Y* direction shaking using model with –*X* mass eccentricity

For this example, it is of some interest to compare the results for the different methods of analyses with varying assumptions regarding direction of load, and with or without P-delta effects. It is important to note, however, that this type of variation of parameter analysis would not typically be done as part of a typical design-office project.

For the analyses completed only a limited number of results are presented, and these are summarized as follows:

> *X*-Direction Story Drifts in Frame 1 (measured on grid intersection C-1)
> Girder Shears in Middle Bay of Frame 1 (spanning D-1 and E-1)
>
> *Y*-Direction story Drifts in Frame 5 (measured on grid intersection H-1)
> Girder Shears in Middle Bay of Frame 5 (spanning H-3 and H-4)

Note that Section 12.8.6 of the *Standard* requires that for torsionally irregular buildings, drift must be checked at the edge of the building. This requirement is satisfied because Frames 1 and 5 are located at the perimeter of the building. For each method of analysis results are presented for individual load cases and for combinations described in the relevant analysis result sections of this chapter.

4.3.3 Seismic Weight and Masses

In the past it was advantageous to model floor plates as rigid diaphragms because this allowed for a reduction in the total number of degrees of freedom used in the analysis, and a significant reduction in analysis time. Given the speed and capacity of most personal computers, the use of rigid diaphragms is no longer necessary, and the floor plates may be modeled using finite elements. The use of such elements provides an added benefit of improved accuracy because the true "semi-rigid" behavior of the diaphragms is modeled directly. Where it is not necessary to recover diaphragm stresses, a very coarse element mesh may be used for modeling the diaphragm.

While it is possible to represent floor mass by assigning mass density to the diaphragm and frame elements, it is felt that more control over assigning mass is available through the use of area and line masses. Thus, for the analysis described herein, all element mass densities were set to zero, and mass was assigned using area and line designations.

The uniform area and line masses (in weight units) associated with the various floor plates of the structure are given in Tables 4.3-1 and 4.3-2. The line masses are based on a cladding weight of 15.0 psf, story heights of 12.5, 15.0, or 18.0 feet, and parapets 4.0 feet high bordering each roof region. Figure 4.3-5 shows where each mass type occurs. The total computed floor mass, mass moment of inertia, and locations of center of mass are shown in Table 4.3-3. The center of mass locations are required for determination of mass modification needed to accommodate accidental torsion. Note that the mass moments of inertia are not required for the analysis because of the use of direct mass modeling in the floor diaphragm elements. However, they would be needed where rigid diaphragms are used, and are provided in the table for completeness. The reference point for center of mass location is the intersection of Grids A and 8.

The given "Level" in the first column of Table 4.3-3 identifies items relevant to properties or results associated with that level. Items related to story drift (presented later in this chapter) are identified at the relevant "Story" of the building because these quantities represent the deformations between levels.

Table 4.3-3 includes a mass computed for Level G of the building. This mass is associated with an extremely stiff story (the basement level) and is dynamically excited by the earthquake in very high frequency modes of response. As shown later, this mass is not included in equivalent lateral force computations, and can complicate modal response spectrum and modal response history analysis.

Table 4.3-1. Area weights contributing to masses on diaphragms (See Fig. 4.3-5)

Mass Source	Area A	Area B	Area C	Area D	Area E
Slab and Deck (psf)	50	75	50	75	75
Structure (psf)	20	20	20	20	50
Ceiling and Mechanical (psf)	15	15	15	15	15
Partition (psf)	10	10	0	0	10
Roofing (psf)	0	0	15	15	0
Special (psf)	0	0	0	60	25
Total (psf)	95	120	100	185	175

Table 4.3-2. Line weights contributing to masses on diaphragms (See Fig. 4.3-5)

Mass Source	Line 1	Line 2	Line 3	Line 4	Line 5
From Story Above (plf)	60.0	93.8	93.8	93.8	135.0
From Story Below (plf)	93.8	93.8	0.0	135.0	1,350.0
Total (plf)	153.8	187.6	93.8	228.8	1,485.0
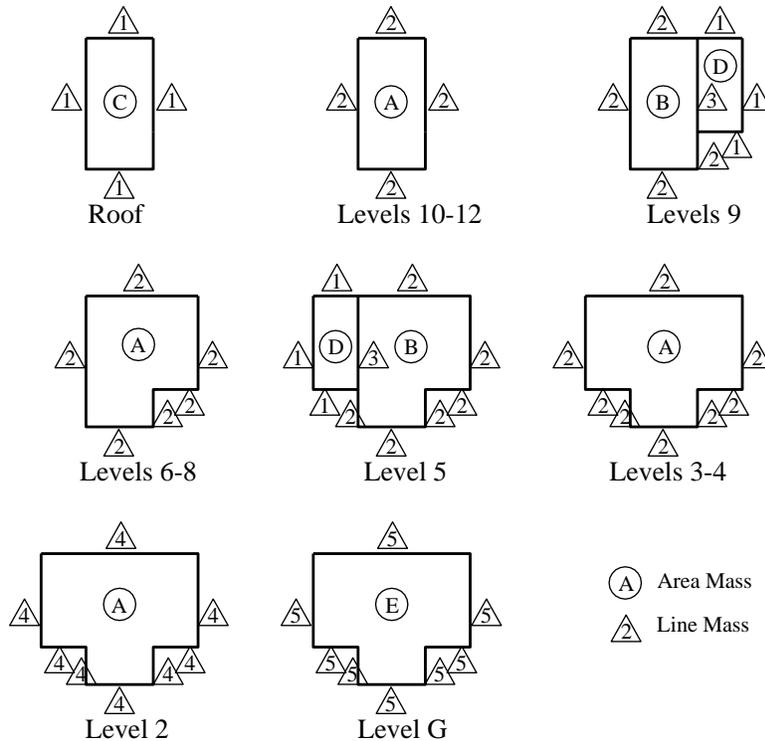
Figure 4.3-5. Key diagram for computation of floor weights

Table 4.3-3. Floor weight mass, mass moment of inertia, and center of mass locations

Level	Weight (kips)	Mass (kip-s²/in.)	Mass Moment of Inertia (in.-kip-s²/radian)	X Distance to C.M. (in.)	Y Distance to C.M. (in.)
R	1,657	4.287	2.072×10^6	1,260	1,050
12	1,596	4.130	2.016×10^6	1,260	1,050
11	1,596	4.130	2.016×10^6	1,260	1,050
10	1,596	4.130	2.016×10^6	1,260	1,050
9	3,403	8.807	5.308×10^6	1,637	1,175
8	2,331	6.032	3.703×10^6	1,551	1,145
7	2,331	6.032	3.703×10^6	1,551	1,145
6	2,331	6.032	3.703×10^6	1,551	1,145
5	4,325	11.19	9.089×10^6	1,159	1,212
4	3,066	7.935	6.354×10^6	1,260	1,194
3	3,066	7.935	6.354×10^6	1,260	1,194
2	3,097	8.015	6.474×10^6	1,260	1,193
G	6,525	16.89	1.503×10^7	1,260	1,187
□	36,920				

4.3.4 Preliminary Design using the ELF Procedure

For the ELF analysis the mass above the grade level is considered, hence the seismic weight W=36920-6525=30395 kips.

The ground motion parameters, determined in Section 4.3 of the this chapter, are

$S_{DS} = 0.833$
$S_{D1} = 0.373$

The translational period between the constant velocity and the constant velocity parts of the design spectrum is:

$T_s = S_{D1}/S_{DS} = 0.373/0.833 = 0.448$ s.

The height of the building above grade, h_n^x is 152.5 ft., thus the approximate period of vibration is computed, using *Standard* Eqn. 12.8- 7 and Table 12.8-2:

$$T_a = C_t h_n^x = 0.028(152.5)^{0.8} = 1.562 \text{ s.}$$

The upper limit period for computing base shear is determined from *Standard* Section 12.8.2 and Table 12.8-1:

$T = C_u T_a = 1.4(1.562) = 2.187$ s.

Since $T_s < T < 4.0$ seconds, *Standard* Eq. 12.8-3 will control the base shear, but this values must not be less than given by Eq. 12.8-5 (for $S_1 < 0.6g$). Using R=8 for special steel moment frames and $I_e = 1.0$,

$$C_S = \frac{S_{D1}}{T\left(\dfrac{R}{I_e}\right)} = \frac{0.373}{2.187\left(\dfrac{8}{1.0}\right)} = 0.0213$$

$$C_S = 0.044 S_{DS} I_e = 0.044(0.833)(1.0) = 0.0367 \text{ controls}$$

Thus, the minimum design base shear is

$$V = C_s W = 0.0367(30395) = 1114 \text{ kips.}$$

It is of some interest to plot the range of periods that are computed for this structure, and this is shown in Figure 4.3-6 where the ELF design spectrum is shown (solid blue line) together with C_s for minimum base shear (horizontal brown line), and vertical lines representing $C_u T_a$, the computed period of 3.558 s. (discussed later), and the period of 1.272 seconds at which the horizontal line representing the minimum base shear intersects with the design spectrum. Thus, from the perspective of determining lateral design forces, the "effective" period based on minimum base shear requirements is 1.272 seconds, and the period that will be used to determine displacements is 3.558 seconds. Implications of these differences are discussed later in the example when the computed drifts for the various methods of analysis are presented.
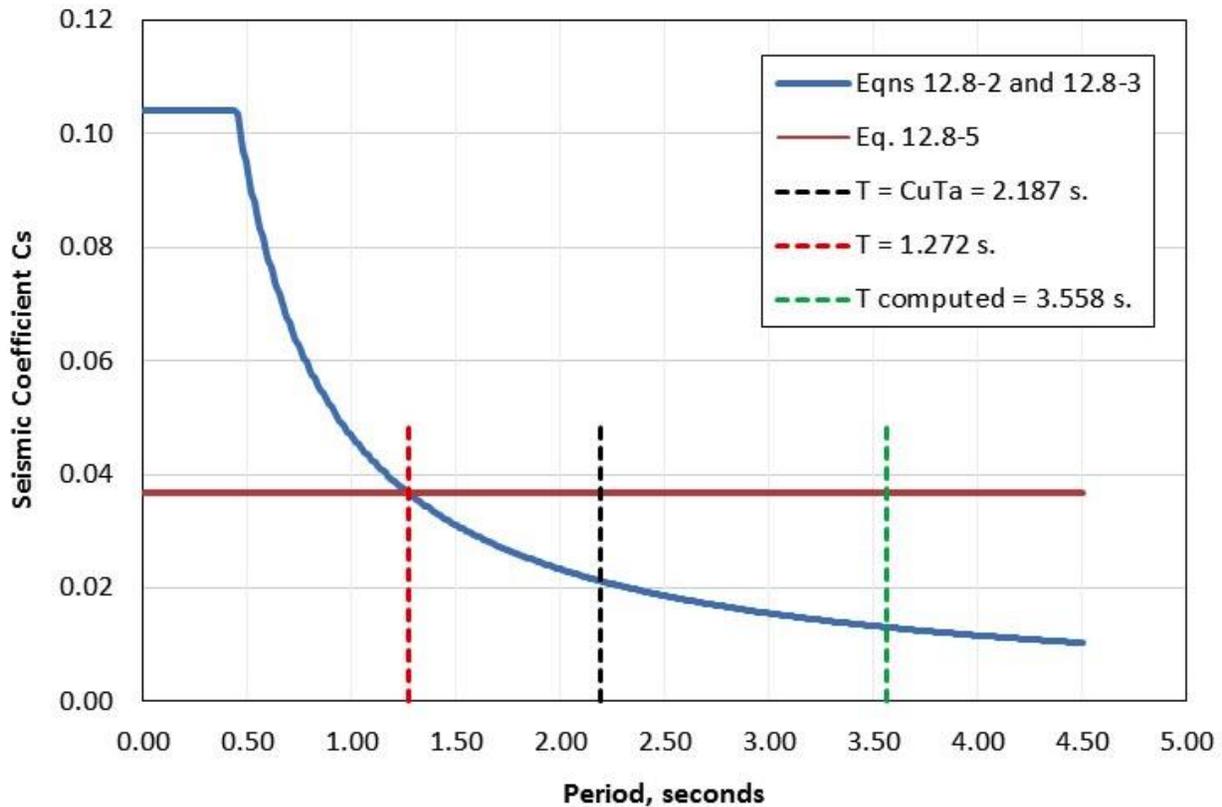
Figure 4.3-6. Design spectrum, minimum base shear, and related periods of vibration

The seismic base shear is distributed along the height of the structure using *Standard* Eqs. 12.8-11 and 12.8-12 with $k=1.84$ for $T=2.187$ s. The results, applicable for each direction of response because $C_u T_a$ is the applicable period in each direction, are provided in Table 4.3-1.

Based on the forces shown in Table 4.3-4, a preliminary design of the structure was performed, and the initial member sizes for all frames are shown in Figs. 4.3-7a and 4.3-7b. These members conform to strength requirements, but must be checked for compliance with drift limits. Additionally, compliance with stability requirements must be met. For checking drift Sections 12.8.6.1 and 12.6.8.2 of the *Standard* allows the use of a separate set of lateral forces for checking drift, with these forces based on the computed period of vibration. Compliance with stability requirements are also based on lateral forces obtained through use of the computed period. Period computations are discussed in some detail in the next section.

Table 4.3-4. Distribution of equivalent lateral forces along height of structure

Level	h_x	w_x	$h_x w_x^k$	C_{vx}	F_x	V_x	M_x
x	(ft)	(kips)			(kips)	(kips)	(kips-ft)
R	152.5	1,657	17,557,905	0.17	187.9	187.9	2,349
12	140.0	1,596	14,444,655	0.14	154.6	342.5	6,631
11	127.5	1,596	12,156,897	0.12	130.1	472.6	12,540
10	115.0	1,596	10,050,905	0.10	107.6	580.2	19,793
9	102.5	3,403	17,334,069	0.17	185.5	765.7	29,366
8	90.0	2,331	9,342,216	0.09	100.0	865.7	40,189
7	77.5	2,331	7,091,250	0.07	75.9	941.6	51,961
6	65.0	2,331	5,127,323	0.05	54.9	996.5	64,419
5	52.5	4,325	6,416,970	0.06	68.7	1,065.2	77,736
4	40.0	3,066	2,755,397	0.03	29.5	1,094.7	91,421
3	27.5	3,066	1,380,939	0.01	14.8	1,109.5	105,291
2	15.0	3,097	456,271	0.00	4.9	1,114.4	122,008
Σ	-	30,395	104,114,802	1.00	1,114	-	-
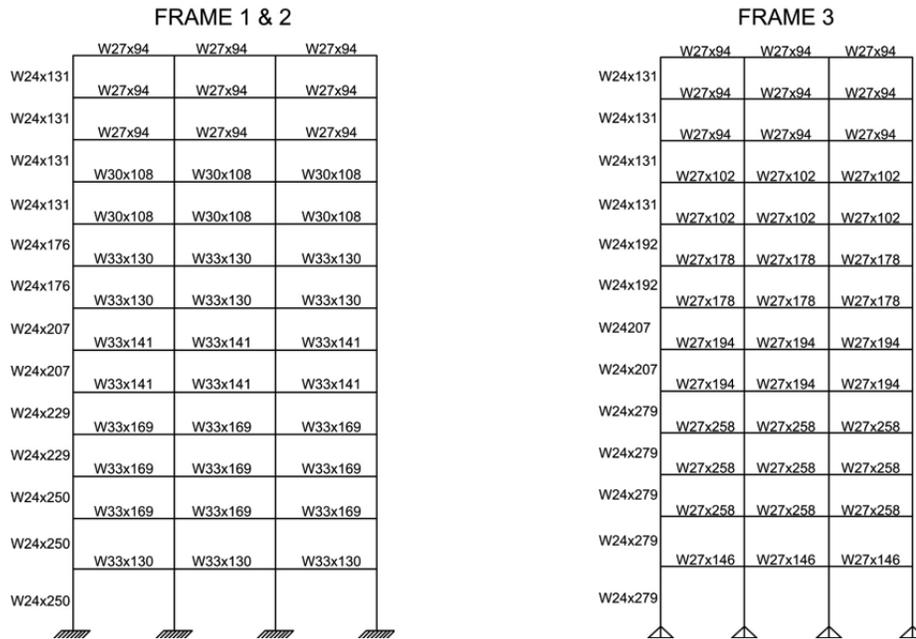
Figure 4.3-7a. Member Sizes for Frames 1, 2, and 3
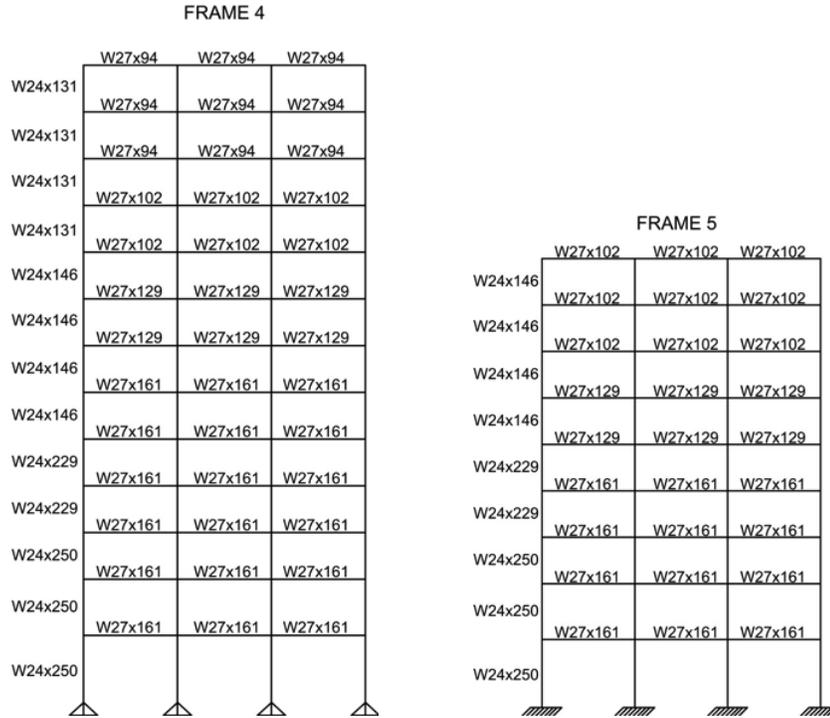
Figure 4.3-7b. Member sizes for Frames 4 and 5

4.3.5 Modal Properties

Eigenvalue analysis was carried out for a variety of mathematical models for the system designed using the ELF procedure (see Figures 4.3-7a and b). The following parameters were investigated in the modal analysis, with each parameter being either not included, or included

1) P-Delta effects
2) Mass offsets required to capture accidental torsion
3) Vertical mass
4) Mass at grade level

Before presetting the results, it is noted that such a detailed variation of parameter analysis is typically not required. This is done here to provide insight into the influence of the various parameters. It is suggested, however, that modal properties be computed for models with and without P-Delta effects, as the change in modal periods is a strong indicator of the importance of P-Delta effects in the analysis.

Table 4.3-5a presents the periods of vibration and the effective modal mass participation ratios (relative to total mass) for the system modeled without P-delta effects, without accidental torsion, with vertical mass, and without mass at the grade level. As may be seen, the first modem with T=3.349 s., is primarily *X*-direction translation and the second mode period, with T=2.983 s., is *Y*-direction translation. The third mode, with T= 1.936 s., is predominantly torsional (θZ). It takes seven modes to capture 90 percent of the system mass in the translational directions, but 90% of the torsional mass is not captured until mode 21.

Table 4.3-5a. Modal properties for system without P-Delta, without accidental torsion, without grade level mass, and with vertical mass included

Mode	Period (s.)	Mass Ratio X	Cumulative Mass Ratio X	Mass Ratio Y	Cumulative Mass Ratio Y	Mass Ratio θZ	Cumulative Mass Ratio θZ
1	3.349	0.762	0.762	0.001	0.001	0.000	0.000
2	2.983	0.001	0.763	0.726	0.727	0.013	0.013
3	1.936	0.000	0.763	0.017	0.744	0.735	0.748
4	1.320	0.133	0.896	0.002	0.747	0.000	0.748
5	1.234	0.002	0.898	0.152	0.898	0.010	0.758
6	0.864	0.002	0.899	0.001	0.899	0.110	0.868
7	0.795	0.040	**0.939**	0.001	**0.900**	0.004	0.872
8	0.690	0.000	0.940	0.045	0.945	0.018	0.890
9	0.641	0.000	0.940	0.000	0.945	0.000	0.890
10	0.636	0.000	0.940	0.000	0.945	0.000	0.890
11	0.634	0.000	0.940	0.000	0.945	0.000	0.890
12	0.629	0.000	0.940	0.000	0.945	0.000	0.890
21	0.518	0.007	0.947	0.000	0.945	0.031	**0.921**

☐P-Delta ☐Accidental Torsion ☐Grade Level Mass ☑ Vertical Mass

Table 4.3-5b presents the modal properties for the same system as Table 4.3-5a, but P-delta effects are now included. The mode shapes for the first 8 modes are shown in Figure 4.3-8. The dominant *X* and *Y* periods are 3.558 s. and 3.108 s., respectively, which represents a significant increase relative to the model without P-delta effects. The third mode period has increased slightly to 1.966 s., and is still predominantly torsional. This small increase in the torsional period indicates that torsional P-delta effects (referred to as P-Theta) effects) are not significant for this structure. Due to the inclusion of P-Delta effects the mass participation ratios for the first two modes have increased slightly, and as a result of this, the number of modes required to capture 90 percent of the mass in the horizontal directions reduced from seven to six. Twenty-one modes are still required to capture 90% of the torsional mass.

Table 4.3-5b. Modal properties for system with P-Delta, without accidental torsion, without grade level mass, and with vertical mass included.

Mode	Period (s.)	Mass Ratio X	Cumulative Mass Ratio X	Mass Ratio Y	Cumulative Mass Ratio Y	Mass Ratio θZ	Cumulative Mass Ratio θZ
1	3.558	0.767	0.767	0.001	0.001	0.000	0.000
2	3.108	0.001	0.768	0.732	0.733	0.013	0.013
3	1.966	0.000	0.768	0.016	0.748	0.739	0.751
4	1.378	0.130	0.897	0.002	0.751	0.001	0.752
5	1.279	0.002	0.899	0.149	0.899	0.009	0.761
6	0.881	0.003	**0.902**	0.001	**0.901**	0.102	0.863
7	0.823	0.037	0.939	0.001	0.902	0.008	0.871
8	0.707	0.000	0.940	0.045	0.946	0.021	0.892
9	0.640	0.000	0.940	0.000	0.946	0.000	0.892
10	0.638	0.000	0.940	0.000	0.946	0.000	0.892
11	0.635	0.000	0.940	0.000	0.946	0.000	0.892
12	0.631	0.000	0.940	0.000	0.946	0.000	0.892
21	0.533	0.020	0.959	0.000	0.946	0.011	**0.904**

☑ P-Delta ☐ Accidental Torsion ☐ Grade Level Mass ☑ Vertical Mass

Mode 1: *T*=3.558 sec   Mode 2: *T*=3.108 sec

Mode 3: *T*=1.965 sec   Mode 4: *T*=1.377 sec

Mode 5: *T*=1.278 sec   Mode 6: *T*= 0.881 sec

Mode 7: *T*=0.823 sec   Mode 8: *T*=0.707 sec
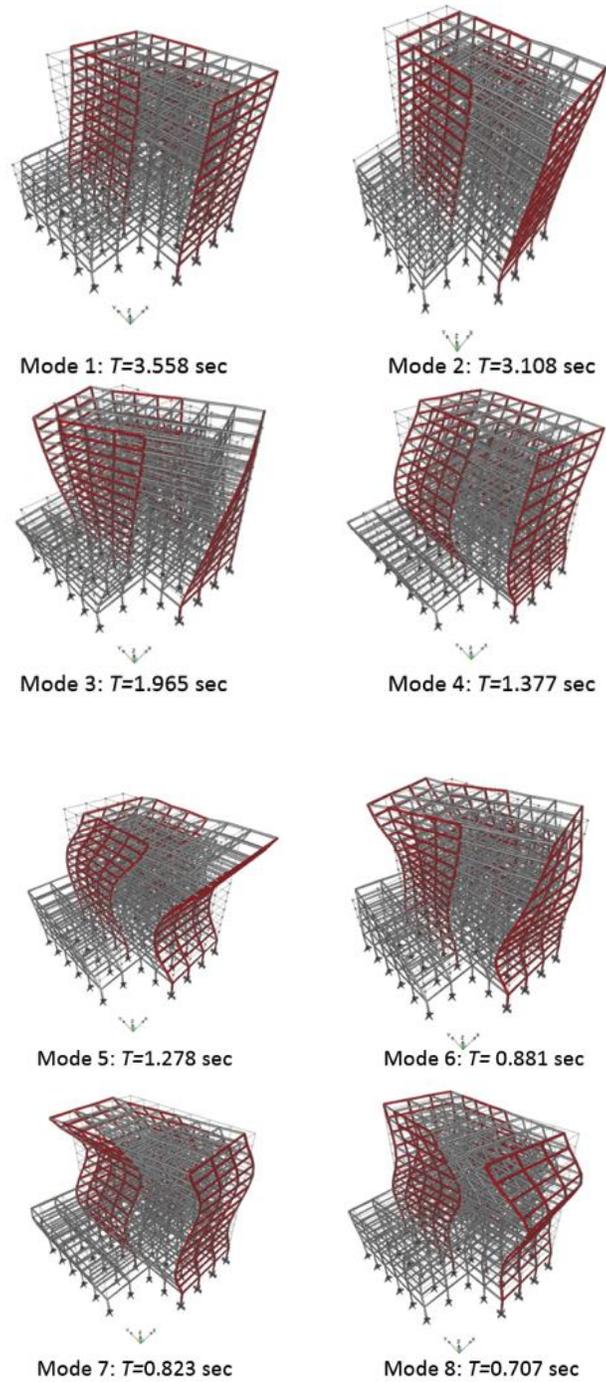
Figure 4.3-8. First eight mode shapes of system modeled including P-delta effects, without accidental torsion, and without mass at grade level

In Table 4.3-5c the modal properties are presented for the system with P-delta effects, with vertical mass, without grade level mass, but with masses at each level modified such that the center of mass shifts 5 percent of the building width in the positive *X* direction. Here, the first two periods T1=3.559 sec and T2= 3.072 sec are still principally translational, and the third mode with period T3=1.983 seconds is still torsional. The inclusion of accidental torsion has not affected the number of modes required to capture 90% of the mass. Clearly, the shift of the center of mass used to incorporate accidental torsion has little influence on the modal properties of this structure.

Table 4.3-5c. Modal properties for system with P-Delta, with accidental torsion, and without grade level mass. Vertical mass included

Mode	Period (s.)	Mass Ratio X	Cumulative Mass Ratio *X*	Mass Ratio Y	Cumulative Mass Ratio *Y*	Mass Ratio θ*Z*	Cumulative Mass Ratio θ*Z*
1	3.559	0.767	0.767	0.000	0.000	0.000	0.000
2	3.072	0.000	0.768	0.739	0.739	0.006	0.006
3	1.983	0.000	0.768	0.009	0.748	0.743	0.749
4	1.377	0.131	0.898	0.001	0.749	0.001	0.750
5	1.261	0.001	0.899	0.148	0.897	0.007	0.757
6	0.876	0.004	**0.903**	0.003	**0.900**	0.107	0.864
7	0.824	0.037	0.939	0.002	0.901	0.009	0.873
8	0.714	0.000	0.940	0.045	0.946	0.024	0.897
9	0.640	0.000	0.940	0.000	0.946	0.000	0.897
10	0.638	0.000	0.940	0.000	0.946	0.000	0.897
11	0.635	0.000	0.940	0.000	0.946	0.000	0.897
12	0.631	0.000	0.940	0.000	0.946	0.000	**0.897**
21	0.532	0.022	0.962	0.000	0.946	0.007	**0.904**

☑ P-Delta�   ☑ Accidental Torsion   ☐ Grade Level Mass   ☑ Vertical Mass

The next model analyzed, with results shown in Table 4.3-6, included P-delta effects, accidental torsion, and vertical mass, and now also includes the heavy mass at the laterally stiff and heavy grade level. As may be seen in the table, the periods of vibration for the first 12 modes are virtually identical to those presented in Table 4.3-5c, but the mass participation ratios are much lower. It now takes 222 modes to fully capture 90 percent of the horizontal mass, and the period of vibration associated with the 222nd mode is only 0.058 seconds. Recall from Table 4.3-5c that only six modes were required to capture 90 percent of the horizontal mass when the mass associated with the grade level was not included in the model.

To investigate the effect of vertical mass, the model was analyzed including P-Delta effects, excluding accidental torsion, including grade level mass, but not including vertical mass. Results are presented in Table 4.3-7, where it may be seen that only 50 modes are required to capture 90 percent of the effective mass in the two orthogonal directions. For this model, 92 modes are required to capture 90% of the torsional mass.

If the grade level mass is eliminated, the model includes P-Delta effects, no vertical mass, and no accidental torsion. These results, shown in Table 4.3-8, indicate virtually no change in periods in the first 12 modes relative to the analysis shown in Table 4.3-7. However, now only 6 modes are required to capture 90 percent of the lateral mass, and only 9 modes are needed to capture 90 percent of the torsional mass.

Table 4.3-6 Modal properties for system with P-Delta, with accidental torsion, and with grade level mass. Vertical mass included

Mode	Period (s.)	Mass Ratio X	Cumulative Mass Ratio *X*	Mass Ratio Y	Cumulative Mass Ratio *Y*	Mass Ratio θ*Z*	Cumulative Mass Ratio θ*Z*
1	3.559	0.632	0.632	0.000	0.000	0.000	0.000
2	3.072	0.000	0.632	0.609	0.609	0.003	0.003
3	1.983	0.000	0.632	0.007	0.616	0.587	0.591
4	1.377	0.108	0.740	0.001	0.617	0.001	0.592
5	1.261	0.001	0.741	0.123	0.740	0.005	0.597
6	0.876	0.003	0.744	0.002	0.742	0.084	0.681
7	0.824	0.030	0.774	0.001	0.744	0.007	0.688
8	0.714	0.000	0.774	0.037	0.781	0.019	0.708
9	0.642	0.000	0.774	0.000	0.781	0.000	0.708
10	0.640	0.000	0.774	0.000	0.781	0.000	0.708
11	0.636	0.000	0.774	0.000	0.781	0.000	0.708
12	0.633	0.000	0.774	0.000	0.781	0.000	0.708
189	0.066	0.000	0.826	0.139	**0.972**	0.000	0.792
222	0.058	0.139	**0.967**	0.000	0.973	0.000	0.792
384	0.038	0.002	0.977	0.001	0.975	0.020	**0.916**

☑ P-Delta   ☑ Accidental Torsion   ☑ Grade Level Mass   ☑ Vertical Mass

Table 4.3-7. Modal properties for system with P-Delta, without accidental torsion, and with grade level mass. Vertical mass NOT included

Mode	Period (s.)	Mass Ratio X	Cumulative Mass Ratio *X*	Mass Ratio Y	Cumulative Mass Ratio *Y*	Mass Ratio θ*Z*	Cumulative Mass Ratio θ*Z*
1	3.558	0.631	0.631	0.001	0.001	0.000	0.000
2	3.108	0.001	0.632	0.604	0.604	0.007	0.007
3	1.965	0.000	0.632	0.013	0.617	0.585	0.592
4	1.377	0.107	0.739	0.002	0.619	0.001	0.593
5	1.278	0.001	0.741	0.123	0.742	0.006	0.599
6	0.881	0.003	0.743	0.001	0.743	0.080	0.679
7	0.823	0.031	0.774	0.001	0.744	0.006	0.685
8	0.707	0.000	0.774	0.038	0.781	0.018	0.703
9	0.533	0.016	0.790	0.000	0.781	0.009	0.712
10	0.515	0.007	0.797	0.000	0.782	0.025	0.737
11	0.461	0.000	0.797	0.020	0.801	0.001	0.738
12	0.410	0.011	0.808	0.000	0.801	0.001	0.739
45	0.066	0.000	0.826	0.141	**0.974**	0.001	0.792
50	0.058	0.147	**0.974**	0.000	0.974	0.000	0.793
92	0.040	0.000	0.978	0.000	0.974	0.122	**0.915**

☑ P-Delta⬚⬚⬚⬚⬚   ☐ Accidental Torsion   ☑ Grade Level Mass   ☐ Vertical Mass

Table 4.3-8. Modal properties for system with P-Delta, without accidental torsion, and without grade level mass. Vertical mass NOT included

Mode	Period (s.)	Mode Mass Ratio X	Cumulative Mass Ratio X	Mode Mass Ratio Y	Cumulative Mass Ratio Y	Mode Mass Ratio θZ	Cumulative Mass Ratio θZ
1	3.558	0.767	0.767	0.001	0.001	0.000	0.000
2	3.108	0.001	0.768	0.732	0.733	0.013	0.013
3	1.965	0.000	0.768	0.016	0.749	0.739	0.752
4	1.377	0.130	0.898	0.002	0.751	0.001	0.753
5	1.278	0.002	0.899	0.149	0.899	0.009	0.761
6	0.881	0.003	**0.902**	0.001	**0.901**	0.102	0.863
7	0.823	0.037	0.939	0.001	0.902	0.008	0.871
8	0.707	0.000	0.940	0.045	0.946	0.021	0.892
9	0.533	0.019	0.959	0.000	0.946	0.012	**0.904**
10	0.515	0.008	0.967	0.000	0.947	0.032	0.935
11	0.461	0.000	0.967	0.023	0.969	0.001	0.936
12	0.410	0.013	0.980	0.000	0.969	0.001	0.937

☑ P-Delta ☐ Accidental Torsion ☐ Grade Level Mass ☐ Vertical Mass

A summary of all the modal analyses are provided in Table 4.3-9. Based on this summary, and on the more detailed results from the individual analyses the following conclusions can be drawn:

1. If only the capturing of 90 percent of the mass in the main directions of response is important, and the mass associated with the stiff and heavy grade level is not included, a minimum of six modes is required in the modal response spectrum and the modal response history analyses.
2. If only the capturing of 90 percent of the mass in the main directions of response is important, and the mass associated with the stiff and heavy grade level is included, a minimum of 50 modes is required in the modal response spectrum and the modal response history analyses. This is based on the model not incorporating vertical mass, and inclusion of P-delta effects. It is noted, however, that the member forces and deformations above the grade level of the structure would be virtually identical to those obtained if the grade level mass was not included. Hence, if the forces in the basement walls are not needed, the "spirit" of the code provisions (to capture 90 percent of the mass) would be obtained by using only 6 modes).
3. If it were necessary to capture in-plane diaphragm distortions in the analysis, a larger number of modes would be required than presented in points (1) and (2) above.

In both the modal response spectrum analysis and the modal response history analysis, the model did not include vertical mass, nor did it include the mass at grade level. All analysis included P-delta effects, and accidental torsion was included or not included as described later in this example. Twelve modes were used in the analysis, thereby capturing approximately 98 percent of the mass in the X-direction, 97% of the mass in the Y direction, and 94 percent of the torsional mass (see Table 4.3-8).

Before proceeding with the results of the ELF analysis, it is noted that the computed first mode period in Table 4.3-9, 3.558 seconds, is considerably larger than C_uT_a, which is 2.187 s. This represents a difference in lateral stiffness of $(3.558/2.187)^2 = 2.65$. Similar discrepancies have been shown by others. For example, in the ATC-76 report (NIST, 2010) a 12-story moment resisting frame (archetype 11RSA) had a computed period of 4.48 s. but C_uT_a was much lower at 2.41 s. Here the stiffness difference is a factor of 3.46. These

stiffness differences are very difficult to justify. As seen in the next section, the use of the computed period to check drift indicates that drift is not a controlling issue for this structure. However, use of forces based on $C_u T_a$ would indicate that drifts are slightly above the limit for near the limit for several stories.

Table 4.3-9. Summary of Modal Properties for All Analyses

P-Delta Inc. ?	Acc. Tor. Inc. ?	Vert. Mass Inc. ?	Grade Mass Inc. ?	T1 (s.)	T2 (s.)	T3 (s.)	*n* 90% *X* and *Y**	*n* 90% Tors.*	T12 (s.)
No	No	Yes	No	3.349	2.983	1.936	7	21	0.629
Yes	No	Yes	No	3.558	3.108	1.966	6	21	0.631
Yes	Yes	Yes	No	3.559	3.072	1.983	6	21	0.631
Yes	Yes	Yes	Yes	3.559	3.072	1.983	222	384	0.633
Yes	Yes	No	Yes	3.558	3.108	1.965	50	92	0.410
Yes	No	No	No	3.558	3.108	1.965	6	9	0.410

* *n* is the number of modes required to capture 90% of the mass in the indicated direction

4.3.6 Analysis Results

4.3.6.1 Equivalent Lateral Force Analysis. Preliminary drift results for loading in the *X*-direction, not including accidental torsion or P-Delta effects, are shown in Table 4.3-10. These drifts, as well as all other drifts reported in this example, include the deflection amplifier C_d, taken as 5.5 as required in *Standard* Table 12.2-1 for special steel moment frames. The reported drifts are for Frame 1. Drifts were computed for three different sets of lateral forces. "Design Loads" shown in Table 4.3-4 were used first, with results shown in the second column of Table 4.3-10. As can be seen, the limiting drift of 2% of the story height is exceeded at almost all of the stories. Recall that the lateral loads that produced these drifts are governed by the minimum base shear requirements (*Standard* Eq. 12.8-5). The third column of Table 4.3-10 lists the drifts computed using lateral loads that are based on the period of vibration $C_u T_a$, and the limiting drifts are exceeded in stories 3 through 8. Finally, in the fourth column of Table 4.3-10, drifts are based on lateral forces computed using the computed period of vibration, *T*=3.558 s. Now, none of the story drifts come even close to exceeding the limits. The *Standard*, in Section 12.8.6.2, specifically allows drifts to be computed on the basis of the computed period, so drift limits for the structure are not violated. Given the strong likelihood that the actual period of the structure is significantly less than the computed period, there is some comfort in knowing that the drifts determined using *T*=$C_u T_a$ are close to allowable 2% story drift limit.

Table 4.3-10. Comparison of story drifts in plane of Frame 1 computed using loads based on different periods

Story	Using Design Loads	Using Loads Based on $C_u T_a$	Using Computed Period	Limit
	(in.)	(in.)	(in.)	(in.)
12	2.43	1.41	0.87	3.00
11	**3.63**	2.11	1.30	3.00
10	**4.51**	2.62	1.61	3.00
9	**5.13**	2.99	1.84	3.00
8	**5.29**	**3.08**	1.89	3.00
7	**5.50**	**3.20**	1.97	3.00
6	**5.49**	**3.19**	1.96	3.00
5	**5.54**	**3.22**	1.98	3.00
4	**5.45**	**3.17**	1.95	3.00
3	**5.19**	**3.02**	1.86	3.00
2	**4.81**	2.80	1.72	3.00
1	**4.06**	2.36	1.45	3.60

As stated earlier, the building being analyzed has several irregularities that can be determined from inspection, including Type 2 (re-entrant corner) horizontal irregularity and a Type 2 (mass) vertical irregularity. Using the lateral forces shown in Table 4.3-4, applied statically at a 5% eccentricity relative to the computed center of mass, it was determined that the structure has a Type 1a horizontal (torsional) irregularity when loaded in the *Y* direction. The monitoring stations used to determine presence of the irregularity are shown in Figure 4.3-9 and tabulated results are presented in Table 4.3-11. In an "actual" building design where the torsional irregularity is marginally present it would be advisable to eliminate the irregularity by making appropriate modifications to the stiffness of the lateral load resisting systems. For the purposes of this example, however, the irregularity is convenient in the sense that it triggers the requirement for accidental torsion and thereby allows for a description of methodologies for implementing accidental torsion in the analysis.

Section 12.8-7 of the *Standard* provides requirements for inclusion of P-Delta effects in the analysis. In most cases, it is expected that the analysis will be performed without P-Delta effects included, and then the system is investigated to determine if such effects must be included ($\theta > 0.1$), determine if the system is too sensitive to such effects ($\theta > \theta_{max}$), and make modification to the results of the analysis if it is determined that P-Delta effects need be included in the analysis.

The results of the stability analysis for loading in the *X* direction are presented in Table 4.3-12. In the table, the term Δ is the story drift, including the drift magnifier C_d, determined at the center of mass of the building for the system loaded with the forces listed in Table 4.3-4 applied without accidental torsion. The term θ_x is determined in accordance with *Standard* Equation 12.8-16.

For the structure under consideration $\theta_{max} = 0.5/5.5 = 0.091$ *when the factor β in Standard equation 12.8-17 is set to 1.0.* (In is interesting to note that in this case θ_{max} is less than 0.1, the minimum value of θ for which P-delta effects need be included. Thus, for a given level of the building $\theta = 0.095$ (for example), the *Standard* is simultaneously saying that P-Delta effects need not be included, and that the building is too sensitive to P-Delta effects. (This potential contradiction is applicable to all systems with C_d greater than or equal to 5.0).
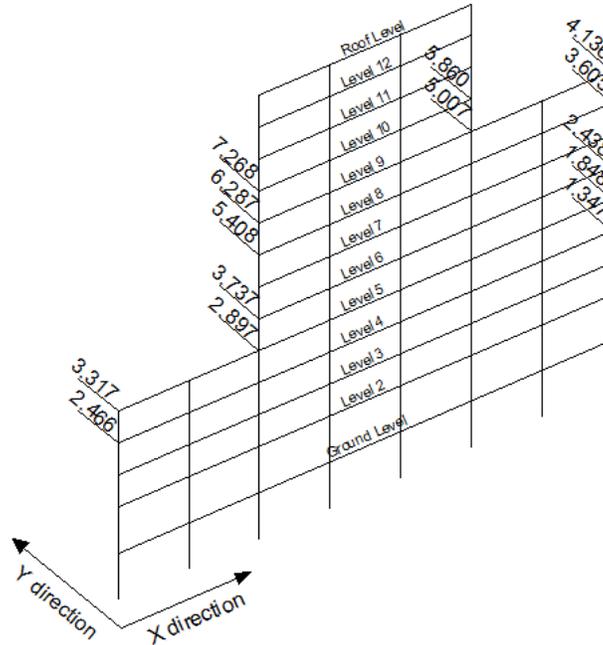
Figure 4.3-9. Drift monitoring stations for determining of torsional irregularity

As shown in Table 4.3-12, $\theta > \theta_{max}$ for the bottom seven stories of the building, indicating that the building "is potentially unstable and need be redesigned". The term β is essentially the inverse of the oversthrength of the story, and the last column of Table 4.3-12 is the value of β that is required to just satisfy the requirement that $\theta = \theta_{max} = 0.091$. For level 3, for example, $\beta_{req}=0.62$, and an overstrength of $1/0.62=1.61$ would be required to eliminate the stability issue. While not shown in this example, it is assumed that the required overstrength would be available for each story of the building, and hence, that the building need not be redesigned. However, it is required that P-Delta effects be included in the analysis. This can be done by running the ELF analysis without P-Delta effects and then modifying displacements and forces by multiplying by $1/(1-\theta)$, or, by directly including P-Delta effects in the analysis. In the example presented in this chapter P-Delta effects are included directly in the analysis. This provides consistency with the MRS and LRH analyses that also directly incorporate P-Delta effects.

Aside from the consistency issue, it is important to note that, strictly speaking, the P-Delta provisions as provided in Section 12.8-7 of the *Standard* are not correct when applied to three-dimensional systems because the reduction in the system's global torsional stiffness (twisting about the vertical axis) are not evaluated, and procedures required to amplify results to account for the torsional P-Delta effects are not provided.

As mentioned in Section 4.2 of this chapter, it is possible to determine the stability coefficients by performing analysis with and without P-Delta effects, and computing θ for each story as $1-(\Delta_o/\Delta_F)$ where Δ_0 is the story drift computed without P-Delta effects, and Δ_F is the drift computed with P-Delta effects. The results of such an analysis are shown in Table 4.3-13, where it is seen that the stability coefficients are similar to those computed using *Standar*d Equation 12.8-16.

Table 4.3-11. Accidental torsion check for Y-Direction load with counterclockwise accidental torsion

Story	δ1 (in.)	δ2 (in.)	Δ1 (in.)	Δ2 (in.)	Δ$_{avg}$ (in.)	Δ$_{max}$ (in.)	Δ$_{max}$/Δ$_{avg}$	Irregularity
R	9.271	7.656	0.455	0.407	0.431	0.455	1.06	None
12	8.816	7.249	0.678	0.608	0.643	0.678	1.05	None
11	8.138	6.641	0.870	0.781	0.825	0.870	1.05	None
10	7.268	5.860	0.981	0.853	0.917	0.981	1.07	None
9	6.287	5.007 / 4.136	0.878	0.531	0.705	0.878	1.25	Irregularity
8	5.408	3.605	0.836	0.577	0.707	0.836	1.18	None
7	4.572	3.028	0.835	0.589	0.712	0.835	1.17	None
6	3.737	2.438	0.840	0.590	0.715	0.840	1.17	None
5	2.897 / 3.317	1.848	0.851	0.501	0.676	0.851	1.26	Irregularity
4	2.466	1.347	0.816	0.473	0.645	0.816	1.27	Irregularity
3	1.650	0.874	0.800	0.452	0.626	0.800	1.28	Irregularity
2	0.850	0.422	0.847	0.418	0.632	0.847	1.34	Irregularity
1	0.003	0.003						

Table 4.3-12. P-Delta stability check for loads X-direction

Story	h$_{sx}$ (in.)	Drift (Δ) (in.)	P$_D$ (Kips)	P$_L$ (Kips)	P$_T$ (Kips)	P$_X$ (Kips)	V$_X$ (Kips)	Θ$_X$	B$_{Reqd}$	1/ β$_{Reqd}$
12	150	0.866	1656.5	157.5	1814.0	1814.0	67.2	0.028	-	-
11	150	1.299	1595.7	157.5	1753.2	3567.2	122.5	0.046	-	-
10	150	1.617	1595.7	157.5	1753.2	5320.4	169.0	0.062	-	-
9	150	1.797	1595.7	157.5	1753.2	7073.5	207.5	0.074	-	-
8	150	1.876	3402.9	232.5	3635.4	10708.9	273.8	0.089	-	-
7	150	1.933	2330.7	232.5	2563.2	13272.1	309.6	0.100	0.90	1.11
6	150	1.930	2330.7	232.5	2563.2	15835.3	336.7	0.110	0.83	1.20
5	150	1.919	2330.7	232.5	2563.2	18398.5	356.3	0.120	0.76	1.32
4	150	1.915	4325.4	307.5	4632.9	23031.4	380.9	0.140	0.65	1.54
3	150	1.808	3065.7	307.5	3373.2	26404.6	391.4	0.148	0.62	1.61
2	150	1.678	3065.7	307.5	3373.2	29777.8	396.7	0.153	0.60	1.67
1	180	1.420	3097.4	307.5	3404.9	33182.7	398.5	0.119	0.76	1.32

Table 4.3-13. Computing stability coefficient for *X*-direction loads based on analysis with and without P-Delta effects

Story	Drift Computed Without P-Delta Effects, Δ_0 (in.)	Drift Computed With P-Delta Effects, Δ_f (in.)	Stability Coefficient, 1-Δ_0/Δ_f	Stability Coefficient (ASCE 7)
12	0.825	0.866	0.047	0.028
11	1.229	1.299	0.054	0.046
10	1.513	1.617	0.064	0.062
9	1.664	1.797	0.074	0.074
8	1.708	1.876	0.089	0.089
7	1.741	1.933	0.099	0.100
6	1.714	1.930	0.112	0.110
5	1.709	1.919	0.109	0.120
4	1.637	1.915	0.145	0.140
3	1.572	1.808	0.131	0.148
2	1.471	1.678	0.124	0.153
1	1.259	1.420	0.114	0.119

Results obtained from the ELF analysis of the structure are presented next. As mentioned earlier, accidental torsion must be included in the analysis, but combination of forces from bi-directional loading is not required. However, since the system is being modeled in three dimensions, it is easy to accommodate bidirectional loading, and for this reason bi-directional effects are included in the results presented herein. Including such effects also provides consistency with the MRS and MRH analysis.

As discussed previously, the ELF analysis requires the following load cases:

ELFX	*X* direction with no accidental torsion
ELFY	*Y* direction with no accidental torsion
ELFTeX	Accidental torsion (story torque) due to *X* direction mass eccentricity
ELFTeY	Accidental torsion (story torque) due to *Y* direction mass eccentricity

From these load cases it is possible to generate sixteen permutations as shown in Figure 4.3-10. In this figure the longer black arrows represent 100% of the lateral load applied in a given direction, and the shorter gray arrow represents 30% of the orthogonal loading applied without any eccentricity. Accidental torsion, applied as story torques, is shown by the black curved arrows. Analyses in the following discussion are related to loading conditions 1 and 2 for principally *X*-direction loading, and conditions 9 and 10 for principally *Y*-direction loading. Story torques were applied by strategically located positive and negative horizontal forces distributed along the edge of the diaphragm.

Story drifts for the *X* direction loading are shown in Table 4.3-14a for analysis performed without P-Delta effects, and in Table 4.3-14b for analysis with P-Delta effects included directly in the analytical model. In each table *X direction drifts* are computed in the plane of Frame 1 for ELF forces in the *X* direction with (plan) clockwise accidental torsion, for ELF forces in the *X* direction with counterclockwise torsion, and for ELF forces acting in the *Y* direction without accidental torsion. The combined values represent the results for 100% of the *X*-direction loading plus 30% of the *Y*-direction loading. As may be seen, the combined drifts are well below the limit of 2% of the story height. This is due to the fact that the ELF forces used in the analysis are based on the computed period of vibration, and not the design base shear which is controlled by *Standard* Equation 12.8-5. As expected, the drifts computed with the model that includes P-Delta effects are slightly larger than those computed without P-Delta.
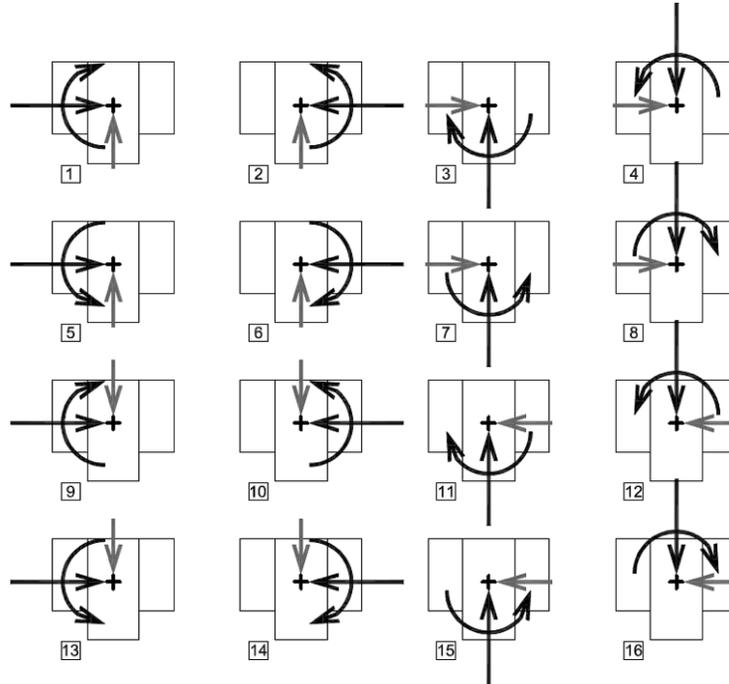
Figure 4.3-10. Loading conditions applicable for ELF analysis

Table 4.3-14a. *X*-Direction ELF story drifts in Frame 1 – Without P-Delta

Story	1	2	3	Combined	Combined	LIMIT
	X Load+eY Torsion	X-Load-eYTorsion	0.3 Times Y load	1 + 3	2 + 3	(in.)
	(in.)	(in.)	(in.)	(in.)	(in.)	
12	0.898	0.772	0.004	0.902	0.776	3.00
11	1.335	1.145	0.005	1.339	1.149	3.00
10	1.636	1.403	0.008	1.644	1.411	3.00
9	1.833	1.582	0.023	1.856	1.606	3.00
8	1.835	1.627	0.068	1.903	1.695	3.00
7	1.883	1.673	0.053	1.936	1.726	3.00
6	1.857	1.650	0.047	1.904	1.697	3.00
5	1.864	1.658	0.047	1.911	1.705	3.00
4	1.767	1.580	0.047	1.814	1.627	3.00
3	1.698	1.521	0.045	1.743	1.566	3.00
2	1.587	1.419	0.049	1.636	1.468	3.00
1	1.360	1.209	0.060	1.420	1.269	3.60

Table 4.3-14b. *X*-**Direction ELF story drifts in Frame 1 – With P-Delta**

Story	1	2	3	Combined	Combined	LIMIT
	X Load+eY Torsion	X-Load-eYTorsion	0.3 Times Y load	1 + 3	2 + 3	(in.)
	(in.)	(in.)	(in.)	(in.)	(in.)	
12	0.930	0.804	0.004	0.934	0.808	3.00
11	1.393	1.203	0.005	1.397	1.207	3.00
10	1.729	1.495	0.008	1.737	1.503	3.00
9	1.960	1.710	0.023	1.984	1.733	3.00
8	1.997	1.788	0.068	2.064	1.856	3.00
7	2.072	1.862	0.053	2.124	1.914	3.00
6	2.065	1.858	0.047	2.112	1.905	3.00
5	2.084	1.879	0.047	2.132	1.926	3.00
4	2.041	1.854	0.047	2.088	1.901	3.00
3	1.945	1.767	0.045	1.990	1.812	3.00
2	1.803	1.635	0.049	1.852	1.684	3.00
1	1.529	1.378	0.060	1.589	1.437	3.60

Story drifts for Frame 5 due to *Y* direction loading are shown in Tables 4.3-15a and 4.3-15b for analysis not including and including P-Delta effects, respectively. Recall that this frame is only eight stories tall above the basement wall. Trends are generally consistent with those determined for *X* direction loading.

Table 4.3-15a. *Y*-**Direction ELF story drifts in Frame 5 – Without P-Delta**

Story	1	2	3	Combined	Combined	LIMIT
	Y Load+eX Torsion	Y-Load-eX Torsion	0.3 Times X load	1 + 3	2 + 3	(in.)
	(in.)	(in.)	(in.)	(in.)	(in.)	
8	1.193	0.974	0.006	1.199	0.980	3.00
7	1.304	1.067	0.009	1.313	1.076	3.00
6	1.303	1.070	0.010	1.313	1.080	3.00
5	1.272	1.042	0.012	1.283	1.053	3.00
4	1.088	0.883	0.011	1.099	0.894	3.00
3	1.043	0.846	0.011	1.054	0.857	3.00
2	0.993	0.811	0.010	1.003	0.821	3.00
1	0.901	0.748	0.007	0.909	0.755	3.60

Table 4.3-15b. *Y*-Direction ELF story drifts in Frame 5 – With P-Delta

Story	1	2	3	Combined	Combined	LIMIT
	Y Load+eX Torsion	Y-Load-eX Torsion	0.3 Times X load	1 + 3	2 + 3	(in.)
	(in.)	(in.)	(in.)	(in.)	(in.)	
8	1.263	1.044	0.006	1.270	1.051	3.00
7	1.376	1.139	0.009	1.385	1.148	3.00
6	1.395	1.162	0.010	1.405	1.172	3.00
5	1.390	1.160	0.012	1.401	1.172	3.00
4	1.192	0.986	0.011	1.203	0.997	3.00
3	1.129	0.933	0.011	1.140	0.944	3.00
2	1.073	0.891	0.010	1.083	0.901	3.00
1	0.974	0.820	0.007	0.981	0.828	3.60

Beam shears for the middle bay of Frame 1 are provided in Tables 4.3-16a and 4.3-16b for analysis with P-Delta effects excluded and included, respectively. Tables 4.3-17a and 4.3-17b list similar results for Frame 5. Two basic conclusions are drawn from these tables. First, accidental torsion is having a significant effect on the results, (forces results with positive and negative story torques are significantly different), and P-Delta effects increase shears at the lower levels by about 10 percent, which is consistent with the increases in computed displacement.

Table 4.3-16a. *X*-Direction ELF beam shears in center bay of Frame 1 - Without P-Delta □

Story	1	2	3	Combined	Combined
	X Load+eY Torsion	X-Load-eYTorsion	0.3 Times Y load	1 + 3	2 + 3
	(k)	(k)	(k)	(k)	(k)
12	12.9	11.1	0.1	13.0	11.2
11	22.4	19.3	0.1	22.5	19.4
10	30.0	25.8	0.1	30.2	25.9
9	41.5	35.8	0.4	41.9	36.1
8	48.0	42.1	1.3	49.3	43.4
7	63.6	56.5	2.0	65.6	58.5
6	67.5	60.0	1.8	69.2	61.7
5	73.1	65.0	1.8	74.9	66.8
4	73.6	65.7	1.9	75.5	67.6
3	80.3	71.8	2.1	82.4	73.9
2	78.4	70.2	2.2	80.6	72.4
1	69.8	62.2	2.6	72.3	64.8

Table 4.3-16b. *X*-Direction ELF beam shears in center bay of Frame 1 – With P-Delta ☐

Story	1	2	3	Combined	Combined
	X Load+eY Torsion	X-Load-eYTorsion	0.3 Times Y load	1 + 3	2 + 3
	(k)	(k)	(k)	(k)	(k)
12	13.2	11.4	0.1	13.2	11.5
11	23.1	20.0	0.1	23.2	20.1
10	31.4	27.2	0.1	31.5	27.3
9	44.0	38.2	0.4	44.4	38.6
8	51.7	45.8	1.3	53.0	47.1
7	69.4	62.3	2.0	71.4	64.3
6	74.5	67.0	1.8	76.2	68.7
5	81.2	73.1	1.8	83.0	74.9
4	83.6	75.6	1.9	85.5	77.6
3	92.2	83.7	2.1	94.3	85.8
2	89.2	81.0	2.2	91.4	83.2
1	78.6	71.1	2.6	81.2	73.6

Table 4.3-17a. *Y*-Direction ELF beam shears in center bay of Frame 5 – Without P-Delta

Story	1	2	3	Combined	Combined
	Y Load+eX Torsion	Y-Load-eX Torsion	0.3 Times X load	1 + 3	2 + 3
	(k)	(k)	(k)	(k)	(k)
8	24.6	20.1	-0.1	24.5	20.0
7	37.8	30.9	-0.2	37.6	30.7
6	38.8	31.8	-0.3	38.5	31.6
5	44.0	36.2	-0.4	43.6	35.8
4	45.0	36.7	-0.4	44.5	36.2
3	51.7	41.9	-0.6	51.1	41.4
2	50.7	41.3	-0.5	50.1	40.7
1	47.2	38.9	-0.4	46.8	38.5

Table 4.3-17b. *Y*-Direction ELF beam shears in center bay of Frame 5 – With P-Delta

Story	1	2	3	Combined	Combined
	Y Load+eX Torsion	Y-Load-eX Torsion	0.3 Times X load	1 + 3	2 + 3
	(k)	(k)	(k)	(k)	(k)
8	26.0	21.5	-0.1	25.9	21.4
7	39.7	32.8	-0.2	39.4	32.6
6	41.2	34.2	-0.3	40.9	34.0
5	47.5	39.6	-0.4	47.1	39.3
4	49.1	40.8	-0.4	48.7	40.4
3	56.0	46.3	-0.6	55.5	45.7
2	54.5	45.1	-0.5	54.0	44.6
1	50.8	42.5	-0.4	50.3	42.0

4.3.6.2 Modal Response Spectrum Analysis. Modal response spectrum analysis was performed using the first 12 modes. As described in Section 4.3.5 of this example, this is a sufficient number of modes to capture more than 90% of the effective mass in the two orthogonal horizontal directions, and for twisting about the vertical axis. Analysis was run with and without P-Delta effects. Accidental torsion was provided by

modification of the system mass properties such that the computed center of mass was appropriately shifted relative to the original center of mass location.

The modal spectral acceleration values associated with the modal periods of vibration are shown in Figure 4.3-11.
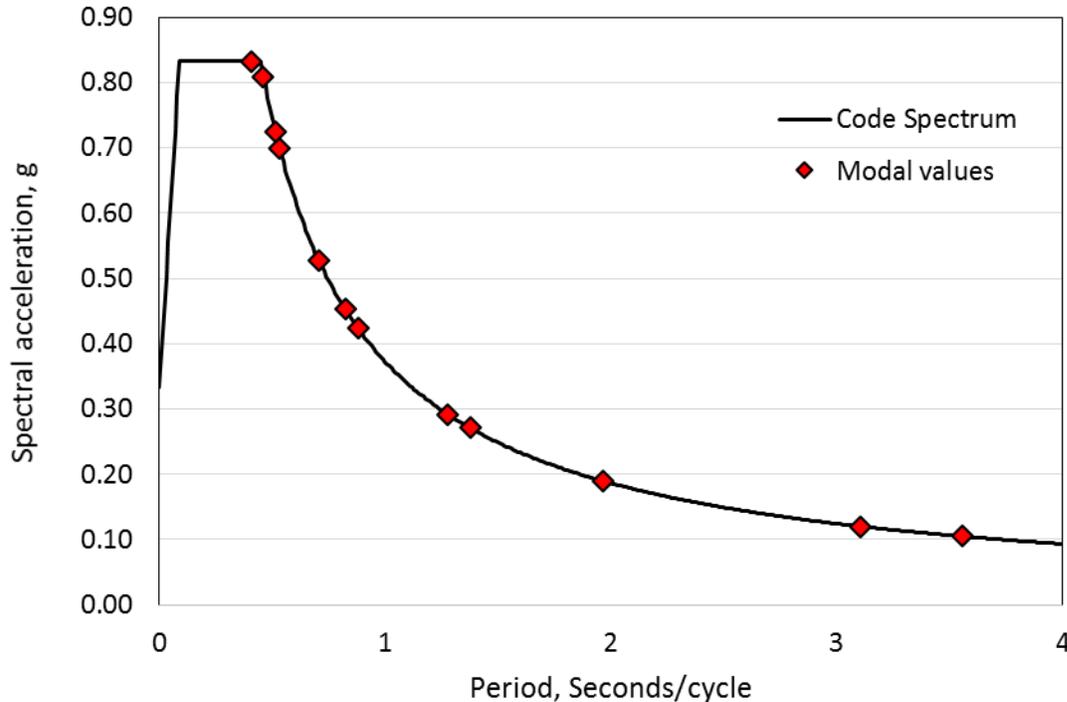
Figure 4.3-11. Response spectrum ordinates for modal response spectrum analysis

The analysis was performed as follows:

I.   Results were determined in each direction of response without accidental torsion (load cases A and B in Figure 4.3-12) and then with accidental torsion included by physically moving the center of mass 5% of the building width in the direction perpendicular to the direction of motion (load cases C, D, E, and F in Figure 4.3-11).   For the purpose of presenting results, these cases are labeled X, Y, XeY+, XeY-, YeX+, and YeX- (where, for example, XeY+ refers to an analysis run in the *X* direction with a positive *Y* mass eccentricity.

II. For the purpose of determining drift values scaling is not required. Thus, to determine design values, all modal deflections were multiplied by C_d/R, modal inter-story drifts were determined and combined using CQC, and then the appropriate orthogonal combinations were created by direct addition of 100 percent of the response in the direction including accidental torsion with 30% of the response in the orthogonal direction, not including accidental torsion. Note that drifts were checked at the edges of the building as required for torsionally irregular systems (see Standard Section 12.8.6). The resulting combined values are provided in Tables 4.3-18a and 4.3-18b for analyses performed without and with P-Delta effects, respectively.

III. The force scale factors in each direction were computed in accordance with *Standard* Section 12.9.1.4.1. (Details for computing scale factors are presented at the end of this list.)

IV. For the purpose of determining force values, all of the *X*-direction force results were multiplied by I_e/R_X and then scaled by the *X*-direction scale factor, and the *Y* direction results multiplied by I_e/R_X and scaled by the *Y*-direction scale factor.

V. For the purpose of determining force values, all of the *X*-direction results were scaled by the *X*-direction scale factor, and the *Y* direction results were scaled by the *Y*-direction scale factor. Then, to determine design values, the appropriate combinations (e.g. 100% of X with accidental torsion plus 30% of Y without accidental torsion). The resulting girder seismic shears for the four different load combinations are provided for Frames 1 and 5 as pictured in Figure 4.3-4.

A

X Shaking, No Mass Eccentricity
[X Only]

B

Y Shaking, No Mass Eccentricity
[Y Only]

C

X Shaking, +Y Mass Eccentricity
[X+eY]

D

X Shaking, -Y Mass Eccentricity
[X-eY]

E

Y Shaking, +X Mass Eccentricity
[Y+eX]

F

Y Shaking, -X Mass Eccentricity
[Y-eX]
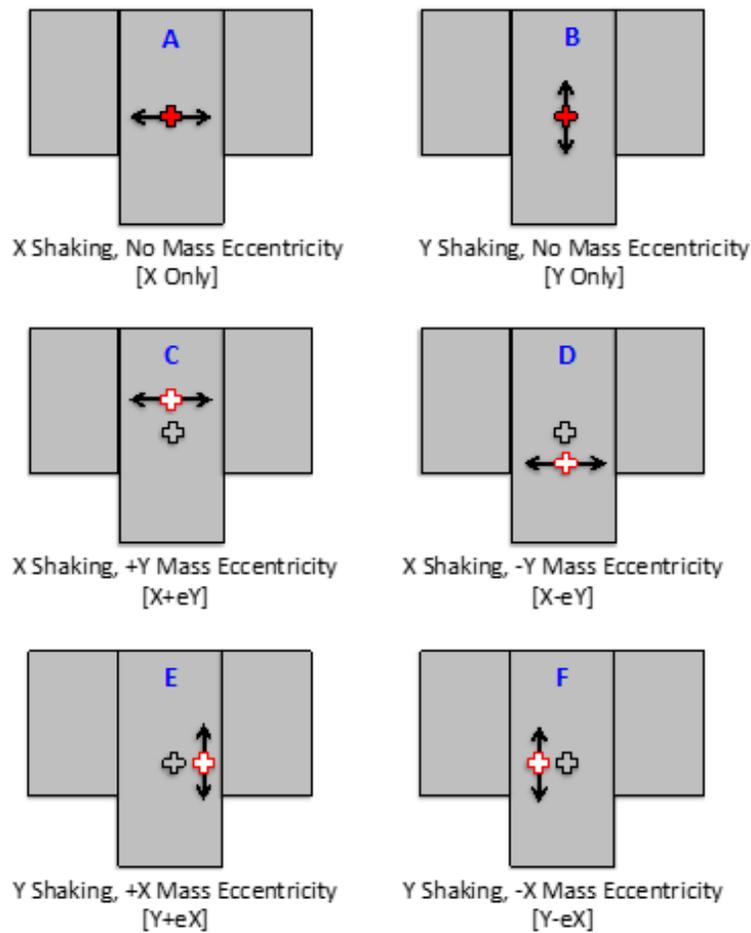
Figure 4.3-12. Dynamic loadings for linear response history analysis

It is noted that the use of the 100% / 30% combination was used instead of taking the SRSS of the *X* and *Y* direction results. This was done for consistency with the ELF method, and for consistency with the linear response history method (which combines 100% of *X* with 100% of *Y*). Separate analysis (not shown herein) used the SRSS combinations and the results were generally consistent with the values presented using the 100% / 30% approach.

Details for Computing Scale Factors
Standard Section 12.9.1.4 provides the requirements for scaling the results of MRS analysis. All member forces must be scaled such that the base shear computed from the MRS procedure is equal to the seismic base shear computed in accordance with *Standard* Section 12.8. For this example displacements need not

be scaled because *Standard* Eq. 12.8.6 was not applicable (S_1 for the building is less than 0.6). The computed seismic base shear for the building under consideration is 1114 kips in each direction. Note that the terminology used below for determination the scale factors used in *Standard* Section 12.9.2 for LRH, and is used below for consistency.

From the MRS analysis not including accidental torsion and *not including P-Delta* effects the elastic base shears in the *X* and *Y* directional are:

Loaded in the *X* direction $V_{EX} = 3033$ k

Loaded in the *Y* direction $V_{EY} = 3282$ k

The fact that the *X* direction shear is less than the *Y* direction shear is consistent with the fact that the fundamental period of vibration in the *X* direction of 3.5 seconds is greater than the Y direction period where the period is 3.1 seconds (see Table 4.3-9).

The elastic base shears are based on the elastic spectrum shown in Figure 4.3-11 and must be multiplied by I_e/R to obtain the inelastic base shears:

$V_{IX} = V_{EX}(Ie/R_X) = 3033(1.0/8.0) = 375.3$ k

$V_{IY} = V_{EY}(Ie/R_Y) = 3282(1.0/8.0) = 410.2$ k

Using the ELF base shear of 1114 kips in each direction, the required scale factors are

$\eta_X = 1114/375.3 = 2.97$

$\eta_Y = 1114/410.2 = 2.71$

From the MRS analysis not including accidental torsion and *including P-Delta* effects the elastic base shears in the *X* and *Y* directional are:

Loaded in the *X* direction $V_{EX} = 2841$ k

Loaded in the *Y* direction $V_{EY} = 3160$ k

$V_{IX} = V_{EX}(Ie/R_X) = 2841(1.0/8.0) = 355.1$ k

$V_{IY} = V_{EY}(Ie/R_Y) = 3160(1.0/8.0) = 395.0$ k

$\eta_X = 1114/355.1 = 3.14$

$\eta_Y = 1114/395.0 = 2.82$

In the following, two sets of results are presented, one not including P-Delta effects and the other including P-delta effects. The analysis that did not incorporate P-Delta effects used the scale factors $\eta_X = 2.97$ and $\eta_Y = 2.71$. The analysis that did include P-delta effects used scale factors $\eta_X = 3.14$ and $\eta_Y = 2.82$. P-Delta effects, where included, were incorporated into the analysis by using modal properties based on the mathematical model with geometric stiffness.

Tables 4.3-18a and 4.3-18b provide the story drift results for Frame 1 excluding and including P-Delta effects, respectively. Tables 4.3-19a and 4.3-19 show the results for Frame 5. Three basic conclusions can be drawn from the tables: (1) drifts are well within the allowable limit of 2% of the story height, (2) drifts for the analysis including P-Delta effects are generally larger than those determined without such effects, and (3) drifts are somewhat larger than those computed using ELF analysis (Tables 4.3-14 and 4.3-15).

Table 4.3-18a. *X*-Direction MRS story drifts in Frame 1 – Without P-Delta

Level	1	2	3	1 + 3	2 + 3	LIMIT
	X+eY	X-eY	0.3 Y	(in.)	(in.)	(in.)
	(in.)	(in.)	(in.)			
R-12	0.862	0.701	0.037	0.899	0.738	3.00
12-11	1.217	0.987	0.055	1.272	1.042	3.00
11-10	1.389	1.133	0.064	1.453	1.196	3.00
10-9	1.451	1.201	0.064	1.515	1.265	3.00
9-8	1.390	1.187	0.078	1.469	1.266	3.00
8-7	1.408	1.206	0.069	1.478	1.275	3.00
7-6	1.387	1.189	0.065	1.452	1.254	3.00
6-5	1.418	1.217	0.066	1.484	1.283	3.00
5-4	1.415	1.217	0.069	1.484	1.286	3.00
4-3	1.426	1.226	0.073	1.500	1.299	3.00
3-2	1.409	1.209	0.079	1.488	1.289	3.00
2-G	1.280	1.089	0.088	1.368	1.177	3.6

Table 4.3-18b. *X*-Direction MRS story drifts in Frame 1 – With P-Delta

Level	1	2	3	1 + 3	2 + 3	LIMIT
	X+eY	X-eY	0.3 Y	(in.)	(in.)	(in.)
	(in.)	(in.)	(in.)			
R-12	0.844	0.694	0.037	0.881	0.731	3.00
12-11	1.201	0.986	0.055	1.256	1.041	3.00
11-10	1.388	1.147	0.064	1.452	1.210	3.00
10-9	1.473	1.238	0.064	1.537	1.302	3.00
9-8	1.436	1.244	0.078	1.514	1.322	3.00
8-7	1.469	1.280	0.069	1.538	1.349	3.00
7-6	1.459	1.275	0.065	1.525	1.341	3.00
6-5	1.497	1.313	0.066	1.563	1.379	3.00
5-4	1.539	1.357	0.069	1.609	1.426	3.00
4-3	1.540	1.350	0.073	1.614	1.423	3.00
3-2	1.509	1.317	0.079	1.588	1.396	3.00
2-G	1.358	1.174	0.088	1.446	1.262	3.60

Table 4.3-19a. *Y*-Direction MRS story drifts in Frame 5 – Without P-Delta

Level	1	2	3	1 + 3	2 + 3	LIMIT
	Ye+X	Ye-X	0.3 X	(in.)	(in.)	(in.)
	(in.)	(in.)	(in.)			
9-8	0.920	0.720	0.025	0.945	0.745	3.00
8-7	0.996	0.785	0.029	1.025	0.813	3.00
7-6	0.996	0.794	0.027	1.023	0.822	3.00
6-5	0.983	0.785	0.025	1.007	0.810	3.00
5-4	0.864	0.683	0.020	0.884	0.703	3.00
4-3	0.874	0.692	0.020	0.893	0.712	3.00
3-2	1.069	0.856	0.024	1.093	0.880	3.00
2-G	1.024	0.833	0.021	1.045	0.854	3.60

Table 4.3-19b. *Y*-Direction MRS story drifts in Frame 5 – With P-Delta

Level	1	2	3	1 + 3	2 + 3	LIMIT
	Ye+X	Ye-X	0.3 X	(in.)	(in.)	(in.)
	(in.)	(in.)	(in.)			
9-8	0.935	0.740	0.025	0.959	0.765	3.00
8-7	1.010	0.804	0.029	1.039	0.832	3.00
7-6	1.026	0.829	0.027	1.054	0.856	3.00
6-5	1.035	0.843	0.025	1.060	0.868	3.00
5-4	0.911	0.735	0.020	0.931	0.755	3.00
4-3	0.912	0.734	0.020	0.931	0.754	3.00
3-2	1.115	0.908	0.024	1.139	0.932	3.00
2-G	1.069	0.885	0.021	1.091	0.906	3.60

Shears in the center bay beams for Frames 1 are listed in Tables 4.3-20a and 4.3-20b for analyses excluding and including P-Delta effects, respectively. Tables 4.3-21a and 4.3-21b provide the shears in the center bay of Frame 5. Results follow the trends for drift in that the shears for models including P-Delta are larger than shears computed with such effects not included, and the values are larger than those reported using ELF (Tables 4.3-16 and 4.3-17.

Table 4.3-20a. *X*-Direction MRS beam shears in center bay of Frame 1 – Without P-Delta

Level	1	2	3	1 + 3	2 + 3
	Xe+Y	Xe-Y	0.3 Y	(kip)	(kip)
	(kip)	(kip)	(kip)		
12	12.6	10.3	0.5	13.1	10.8
11	22.0	17.9	0.9	22.9	18.8
10	27.7	22.5	1.2	28.9	23.7
9	35.7	29.3	1.4	37.1	30.7
8	38.7	32.7	1.7	40.5	34.4
7	50.3	43.1	2.4	52.7	45.5
6	53.1	45.5	2.3	55.4	47.8
5	58.0	49.7	2.5	60.4	52.2
4	60.5	52.0	2.6	63.1	54.6
3	69.4	59.7	3.2	72.6	62.8
2	71.3	61.2	3.5	74.8	64.7
1	67.1	57.4	3.8	70.9	61.2

Table 4.3-20b. *X*-Direction MRS beam shears in center bay of Frame 1 – With P-Delta

Level	1	2	3	1 + 3	2 + 3
	Xe+Y	Xe-Y	0.3 Y	(kip)	(kip)
	(kip)	(kip)	(kip)		
12	13.1	10.8	0.5	13.6	11.3
11	22.9	18.8	0.9	23.8	19.7
10	29.1	23.9	1.2	30.2	25.1
9	38.0	31.7	1.4	39.4	33.1
8	42.0	36.0	1.7	43.7	37.7
7	55.2	48.0	2.4	57.6	50.4
6	58.8	51.3	2.3	61.1	53.6
5	64.5	56.4	2.5	66.9	58.9
4	68.6	60.4	2.6	71.2	62.9
3	79.6	69.9	3.2	82.7	73.1
2	80.9	70.7	3.5	84.4	74.2
1	75.6	65.7	3.8	79.4	69.5

Table 4.3-21a. *Y*-Direction MRS beam shears in center bay of Frame 5 – Without P-Delta

Level	1	2	3	1 + 3	2 + 3
	Ye+X	Ye-X	0.3 X	(kip)	(kip)
	(kip)	(kip)	(kip)		
9	17.5	14.3	0.5	18.0	14.9
8	26.7	21.9	0.8	27.6	22.7
7	27.4	22.6	0.9	28.3	23.5
6	31.3	26.0	0.9	32.2	27.0
5	32.4	26.9	0.9	33.3	27.8
4	38.8	32.0	1.0	39.8	33.0
3	40.7	33.7	1.0	41.7	34.8
2	40.5	33.9	1.0	41.5	34.9

Table 4.3-21b. *Y*-Direction MRS Beam Shears in Center Bay of Frame 5 – With P-Delta

Level	1	2	3	1 + 3	2 + 3
	Ye+X	Ye-X	0.3 X	(kip)	(kip)
	(kip)	(kip)	(kip)		
9	19.3	15.3	0.5	19.9	15.9
8	29.3	23.3	0.8	30.2	24.1
7	30.4	24.4	0.9	31.3	25.3
6	35.3	28.7	0.9	36.2	29.6
5	37.2	30.2	0.9	38.1	31.0
4	44.1	35.5	1.0	45.1	36.5
3	45.8	37.1	1.0	46.9	38.1
2	45.5	37.3	1.0	46.5	38.3

4.3.6.3 Modal Response History Analysis. Linear response history analysis is covered in Section 12.9.2 of the *Standard.* In this procedure it is required to use a suite of three pairs of spectrum-matched ground motions. Procedures for developing these records are described in Section 4.2.3 of this example.

The analysis is required to be run in three dimensions, with accidental torsion (where required) included by physically relocating the center of mass. P-Delta effects must be included in the analysis. Diaphragms shall be modeled as semi-rigid where required by *Standard* Section 12.7.3. The *Standard* does not specify a procedure for solving the equations of motion, but as described in Section 4.2 of this example, the modal superposition method is generally preferred over direct integration of the uncoupled equations due to reduced solution times and storage requirements. The analysis presented herein utilized modal response spectrum analysis, including the first twelve modes. This is the same as used for the modal response spectrum analysis.

Section 12.9.2 of the *Standard* provides basic information on how the procedure is managed. This procedure is described in more detail as follows:

To determine *Member Design Forces*, do the following:

I. For <u>each</u> of six ground motions, run the following analyses as illustrated in Figure 4.3-12 and summarized below:

        [A]   Shaking in X direction only, no torsional eccentricity
        [B]   Shaking in Y direction only, no torsional eccentricity
        [C]   Shaking in X direction only with mass offset in the +Y direction
        [D]   Shaking in X direction only with mass offset in the –Y direction
        [E]   Shaking in Y direction only with mass offset in the +X direction
        [F]   Shaking in Y direction only with mass offset in the –X direction

Note that these analyses are run with $R=1$ and $I_e=1$ because the ground motion were matched to the spectrum given in Section 11.4.5 of the *Standard*.

II. Find the maximum absolute value of the elastic seismic base shears, V_{EX} and V_{EY}, in the X and Y directions, respectively. This is done using analyses [X Only] in the X direction, and [Y Only] in the Y direction.

III. Convert the elastic base shear to the inelastic base shear by multiplying by I_e/R;

$$V_{IX}=V_{EX}(I_e/R_X)$$
$$V_{IY}=V_{EY}(I_e/R_Y)$$

In the example presented herein $R_X = R_Y=8.0$ for special steel moment frames, and $I_e=1.0$.

IV. Find the appropriate force scale factors

$$\eta_X = V_X/V_{IX} \geq =1.0$$
$$\eta_Y = V_Y/V_{IY} > =1.0$$

where V_X is the design base shear in the X direction and V_Y is the design base shear in the Y direction, computed using *Standard* equation 12.8-1.

V. Form the following load combinations:
      1: $(\eta_X \times C + \eta_Y \times B$ (I_e/R_X)
      2: $(\eta_X \times D + \eta_Y \times B)$ (I_e/R_X)
      3: $(\eta_Y \times E + \eta_X \times A)$ (I_e/R_Y)
      4: $(\eta_Y \times F + \eta_X \times A)$ (I_e/R_Y)

VI. Find and record the maximum positive and negative force of interest, the corresponding times of occurrence, and the load combination that produced the result. Note that the load combination and time of occurrence may be used to determine forces that act concurrently with the computed maximum. For example, one might want to know the moment that occurs at the time of maximum axial force.

Repeat the above six steps for each of three ground motion pairs, and use as the design value the maximum positive and negative value and the corresponding time of occurrence among all twelve load combinations (4 combinations for each of three earthquakes).

To determine Design Drifts, do the following:

For computing drifts, the procedure is similar, but scaling of drifts is not required. The following combinations are formed for each ground motion:

1) $(C + B) (C_{dX}/R_X)$
2) $(D + B) (C_{dX}/R_X)$
3) $(E + A) (C_{dY}/R_Y)$
4) $(F + A) (C_{dY}/R_Y)$

It is important to note that the quantities determined are the inter-story drifts, not the total drifts at each level. Note also, that for torsional irregular buildings the drift must be computed at the edge of the building.

The procedure described above is cumbersome because combinations are being made between different runs, with different models (due to the various mass eccentricities) in each run. Thus, if the software does not automatically allow the formation of such combinations it will be necessary to post-process the results. It is likely that commercial software will have the capability to perform the needed combinations by the time that ASCE 7-16 is adopted. (Similar combinations are required in the nonlinear analysis procedures of Chapter 16 of the *Standard*).

Of course, the method is simplified considerably if accidental torsion is not required, and this is a good incentive for avoiding torsionally irregular systems.

Selection and Modification of Ground Motion

Section 12.9.2.3 of the LRH provisions requires that not less than three pairs of spectrally matched orthogonal components, derived from artificial or recorded ground motions, be used in the analysis. For the example presented herein, the recorded events presented in Table 4.3-22 were used as "seeds" for the spectrum matching.

Table 4.3-22. Ground motions used in analysis

Earthquake	Northridge	Loma Prieta	Chi Chi
Year	1994	1989	1999
Station	Beverly Hills	Gilroy Array 3	TCU045
Magnitude	6.7	6.9	7.6
Source Mechanism	Thrust	Strike-Slip	Thrust
Site Class	D	D	C
Epicentral Distance	13.3 km	31.4 km	77.5 km
PGA	0.52 g	.56g	.51g
PEER NGA Rec. No.	953	767	1485
Original Duration	30.0 s.	39.9 s.	90 s.
Digitization Interval	0.01 s.	0.005 s.	0.005 s.
Component 1 name	MUL009	G03000	TCU045-E
Component 2 name	MUL279	G03090	TCU045-N

These records were selected based on a deaggregation of the site hazard, the results of which are shown in Figure 4.3-13 for a 1-second spectral acceleration and a 2% in 50 year probability of occurrence. As may be seen from the figure, earthquake magnitudes in the range of 6.5 of 8.0, and epicentral distances ranging from 0 to 120 km from the site are characteristic of the hazard.

The ground motions must be altered such their computed 5% damped pseudoacceleration response spectrum closely matches the target spectrum shown in Figure 4.3-11 of this example. Section 12.9.2.3 of the *Standard* provides the requirements for the matching, and these are that matching be performed over the period range 0.8 T_{min} to 1.2 T_{max}, and that the average of the matched spectra in each direction (average of three *X*-Direction and average of three *Y*-Direction) does not exceed the target by more than + or – 10%. Individual matched spectra may fall outside these bounds.

The matching was performed using RSP-Match (Al Atik and Abrahamson, 2010), as implemented into a special utility developed by Jayamon and Charney (2015). *X*-Direction spectra before and after matching are shown in Figure 4.3-14, *Y*-Direction spectra before and after matching are presented in Figure 4.3-15. In the matching the lower bound of the matching range is 0.25 seconds, and the upper bound is 4.2 seconds. Recall from Table 4.3-9 that T_{min}=0.41 seconds (where 12 modes are used), and T_{max}=3.558 seconds. The lower bound for matching, 0.25 seconds, is slightly less than 0.8x0.41=0.33 seconds, and the upper bound of 4.2 seconds is slightly less than 1.2x3.558=4.26. Hence, the period range for matching is appropriate. As shown in Figures 4.3-14 and 4.3-15 the average of the matched spectra easily fall within the + or – 10% envelope.

Matching Parameters are shown in Table 4.3-23a through 4.3-23c for the Northridge, Loma Prieta, and Chi Chi earthquakes, respectively. It is important to note that the information provided for the "Original" record is for the as-recorded ground motion (corrected for instrument response) without any additional scaling. As may be seen, the basic character of the original ground motion is preserved in the matched records. Of particular interest is the correlation coefficient (Howell, 2007), which is a measure of the statistical independence of the two orthogonal components. The Nuclear Regulatory Commission requirements (NUREG, 2014) states that time histories may be considered statistically independent when the correlation coefficient does not exceed 0.16. Given this criterion, it can be seen that the matched components of the modified acceleration histories are within acceptable bounds for all three earthquakes. For the original records, The Northridge and Loma Prieta records have a correlation coefficient less than 0.16, but the value for the original Chi Chi records is somewhat greater than 0.3.
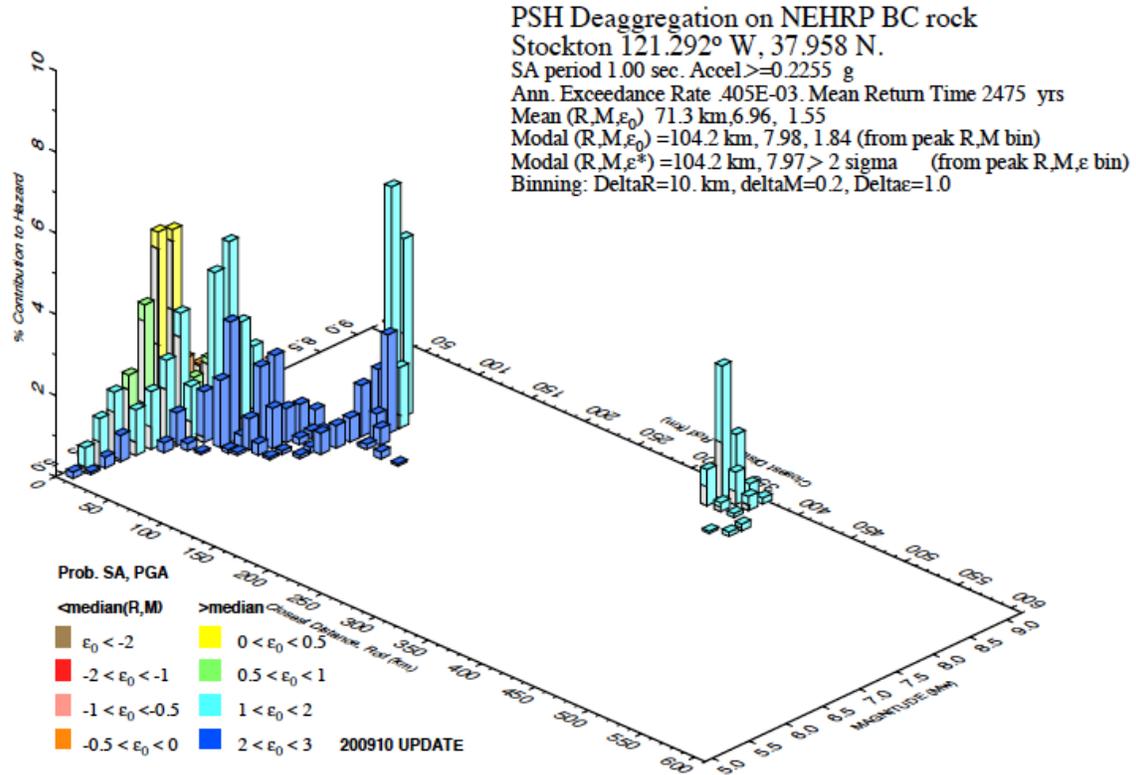
Figure 4.3-13. Disaggregation of site hazard

Table 4.3-23a. Matching parameters for Northridge earthquake

Parameter	Original MUL009	Modified MUL009	Original MUL279	Modified MUL279
PGA (g)	0.416	0.277	0.516	0.408
PGV (in./s.)	18.2	13.7	21.9	12.9
PGD (in.)	5.18	4.06	4.31	3.29
Dominant Frequency (Hz)	0.586	0.903	0.952	1.172
Correlation Coefficient	0.0247	0.0739	0.0247	0.0739
Duration of Corrective Acceleration (s.)	0.0	3.97	0.00	4.53
Duration of Blank Padding (s.)	4.53	0.56	4.53.	0.00

Table 4.3-23b. Matching parameters for Loma Prieta earthquake

Parameter	Original G03000	Modified G03000	Original G03090	Modified G03090
PGA (g)	0.555	0.433	0.367	0.402
PGV (in./s.)	14.1	17.1	17.6	17.4
PGD (in.)	2.91	4.68	7.59	5.06
Dominant Frequency (Hz)	0.873	0.403	0.256	0.958
Correlation Coefficient	0.0451	0.1126	0.0451	0.1126
Duration of Corrective Acceleration (s.)	0.00	5.975	0.00	7.205
Duration of Blank Padding (s.)	7.205	1.230	7.205	0.00

Table 4.3-23c. Matching parameters for Chi Chi earthquake

Parameter	Original TCU045-E	Modified TCU04-E	Original TU045-N	Modified TU045-N
PGA (g)	0.474	0.447	0.512	0.435
PGV (in./s.)	14.5	17.5	10.8	10.2
PGD (in.)	8.45	9.41	5.28	6.69
Dominant Frequency (Hz)	0.781	0.708	0.659	0.760
Correlation Coefficient	0.335	0.122	0.335	0.122
Duration of Corrective Acceleration (s.)	N.A.	0.00	N.A.	0.00
Duration of Blank Padding (s.)	N.A.	0.0	N.A.	0.00
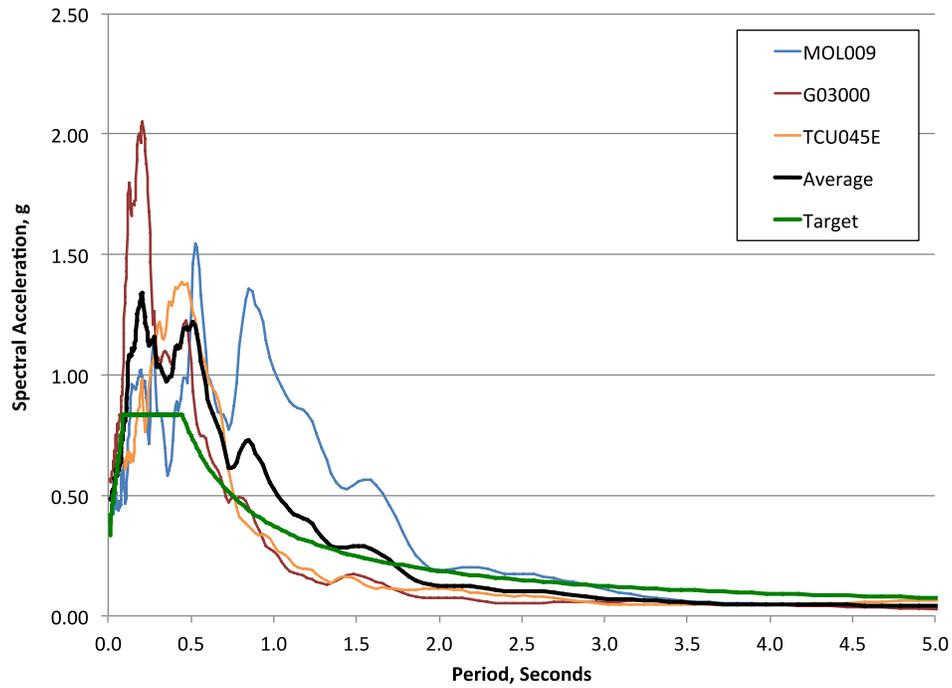
(a) *Unmatched*
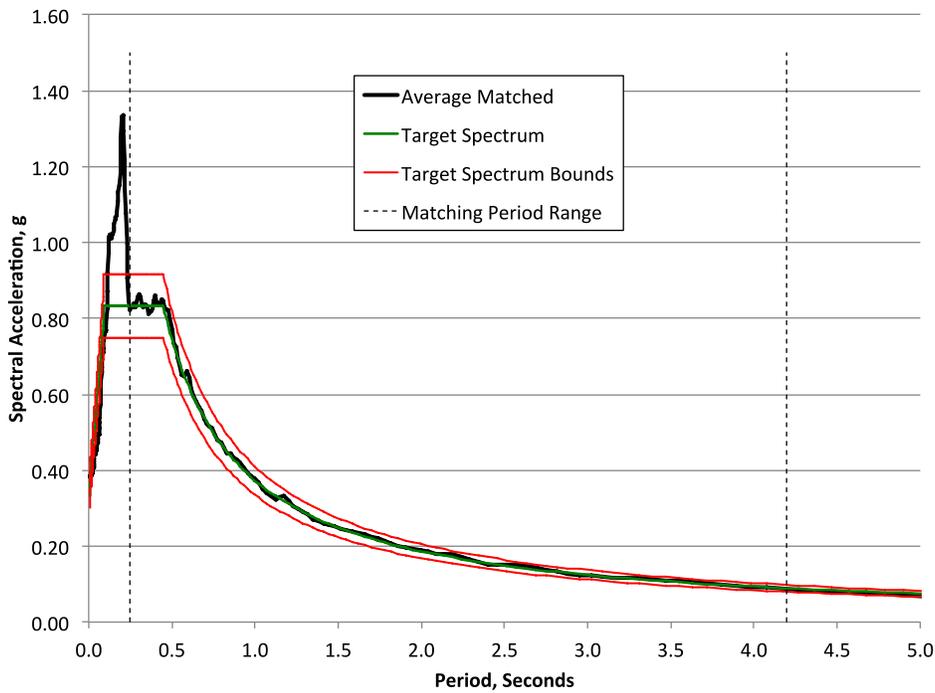
(a) *Matched*

Figure 4.3-14. Response spectra for unmatched and matched *X*-Direction records
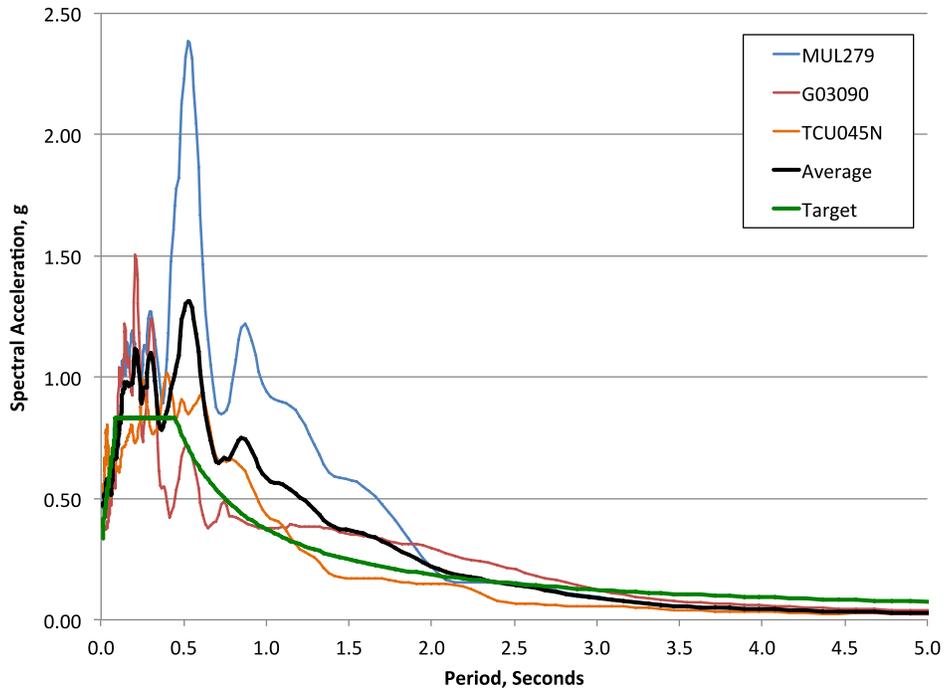
(a) *Unmatched*
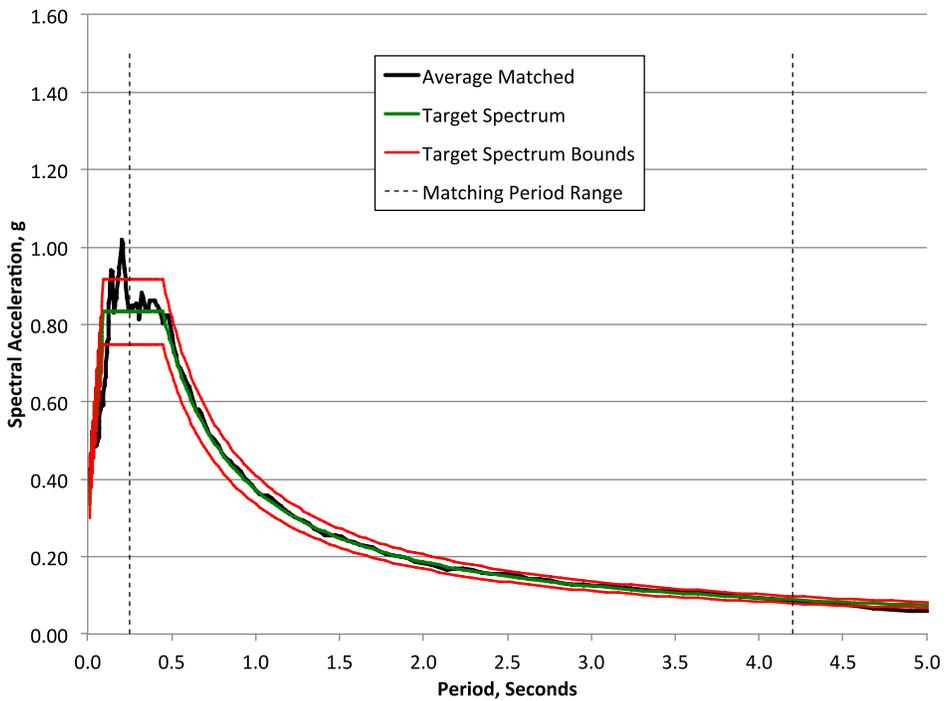
(a) *Matched*

Figure 4.3-15. Response spectra for unmatched and matched *Y*-Direction records

Histories of the ground acceleration, velocity, and displacement are shown for the original and matched records for the Northridge earthquake are shown in Figures 4.3-16 and for the MUL009 component, and Figure 4.3-17 for MUL279 component, where it is seen from visual inspection that the character of the original ground motion has been preserved after matching. It is very important to note, however, that RSPMatch (and possibly other programs) may add to the beginning of the matched acceleration record a period of very low amplitude shaking, the intent of which is to produce near zero ground velocity at the end of the earthquake. Where this is done it is likely that a *different* duration of low duration shaking will be added to the *X* and *Y* components. Where this happens, it is essential to blank pad (add zeros) to the beginning of the matched record with the shorter period of added near-zero shaking to ensure the fact that the motions are correlated from a time-perspective before and after shaking.   Table 4.3-23a shows, for example, that 3.97 seconds of "corrective acceleration" has been added to the beginning of the MUL009 record, and 4.53 second has been added to the MUL279 component. In order to synchronize the records, an additional 0.56 seconds of blank padding (zero acceleration) has been added to the matched MUL009 component. For the purpose of comparing the records before and after modification, the 4.53 seconds of blank padding is added to the original records. The ground history plots shown in Figure 4.3-16 include the necessary corrective acceleration and blank padding. Figure 4.3-18 shows details of the corrections for the MUL279 record that has both blank-padding and corrective acceleration.

Figure 4.3-19 shows the two orthogonal components of ground motion plotted together, where it is seen that there is not a dominant response in any particular direction for the Northridge earthquake. The other earthquakes (not shown) have similar characteristics.
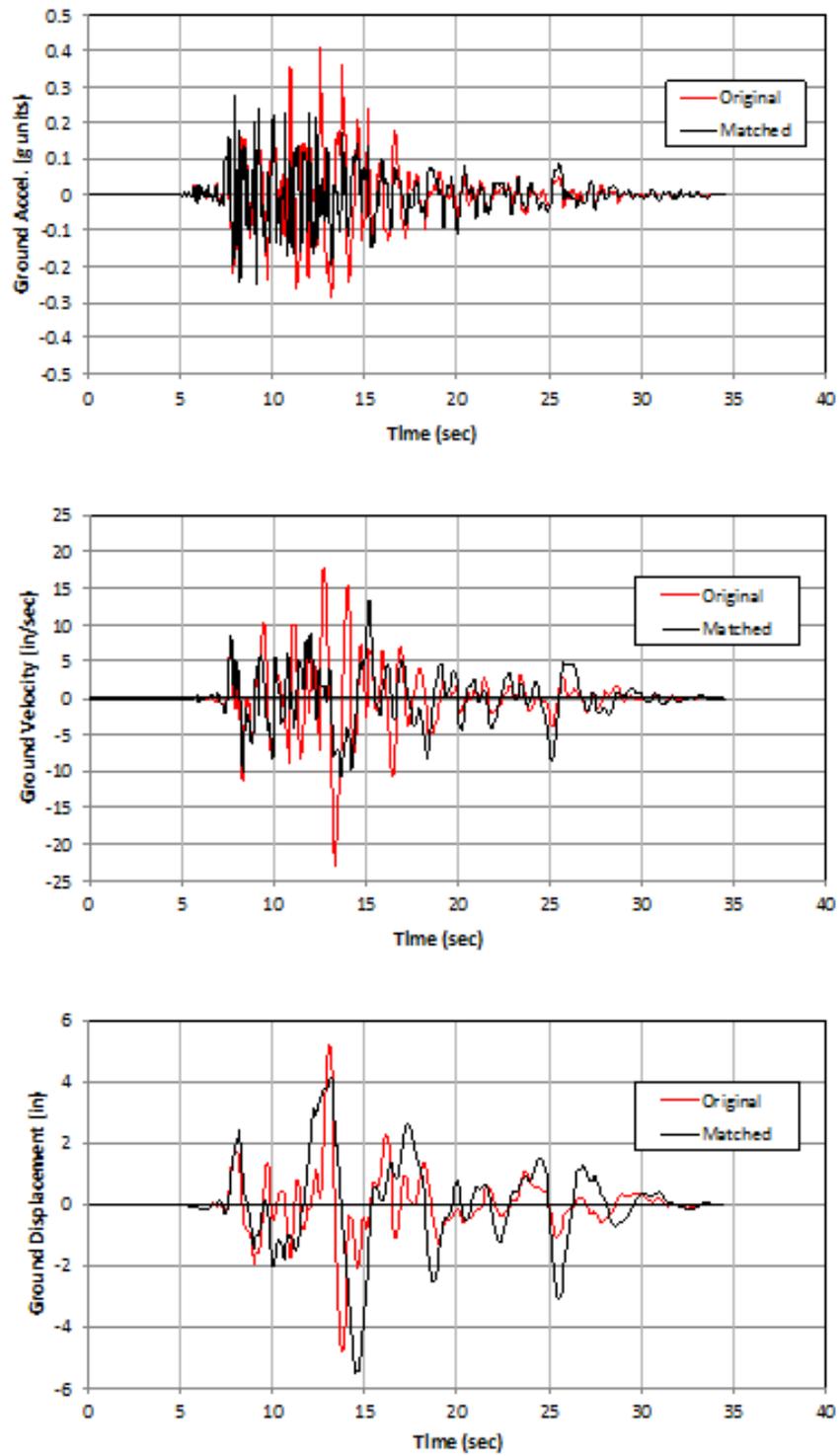
Figure 4.3-16. *X*-Direction ground motion histories for Northridge earthquake
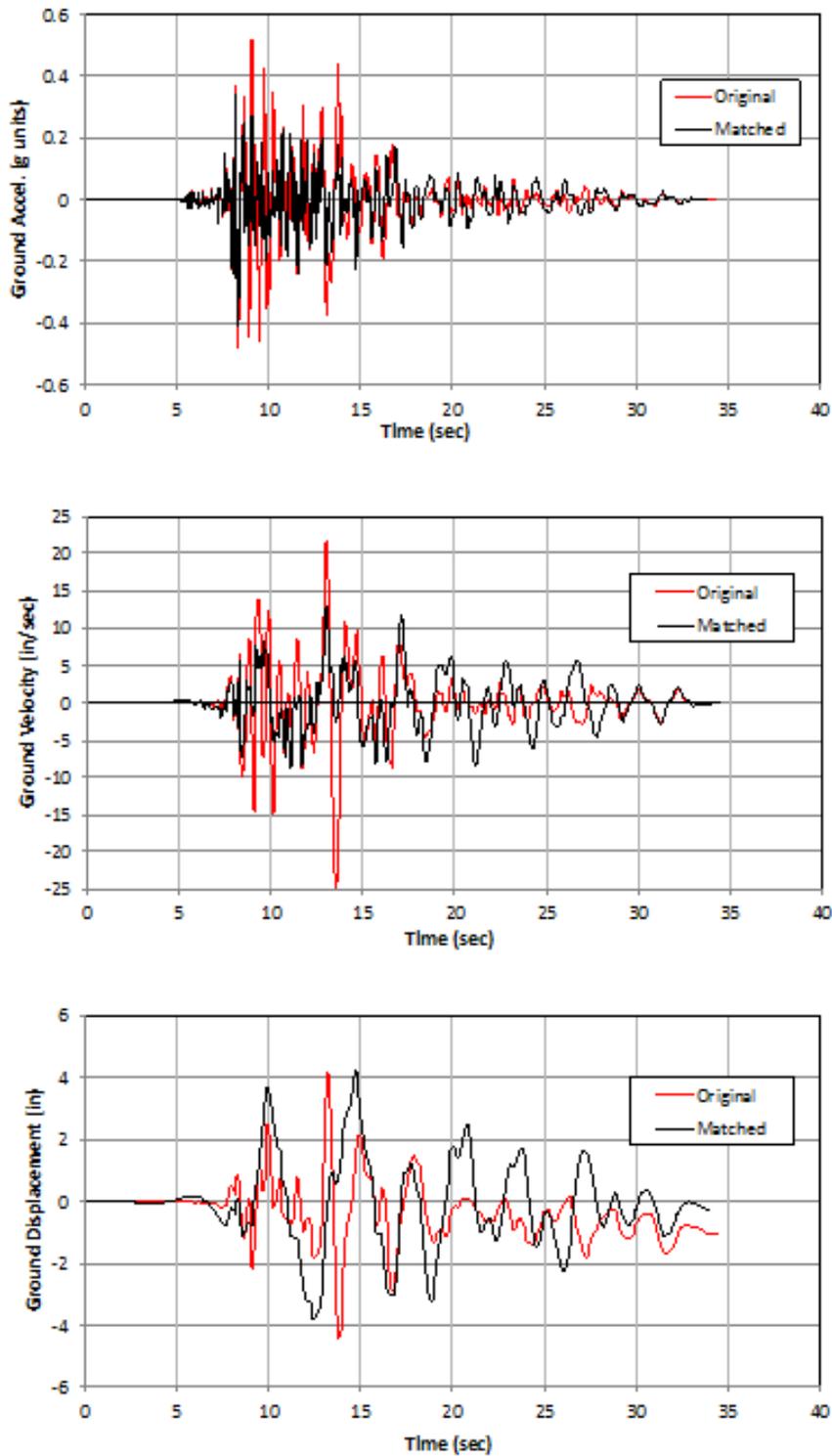
Figure 4.3-17. *Y*-**Direction ground motion histories for Northridge earthquake**
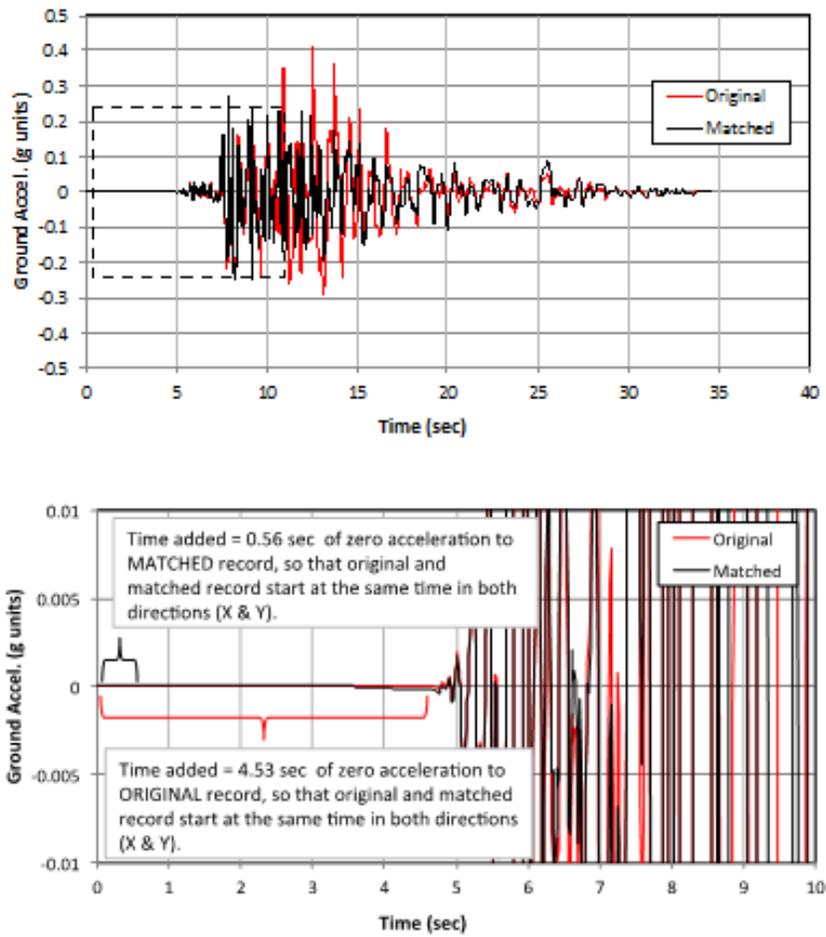
Figure 4.3-18. Procedure for synchronizing ground acceleration records
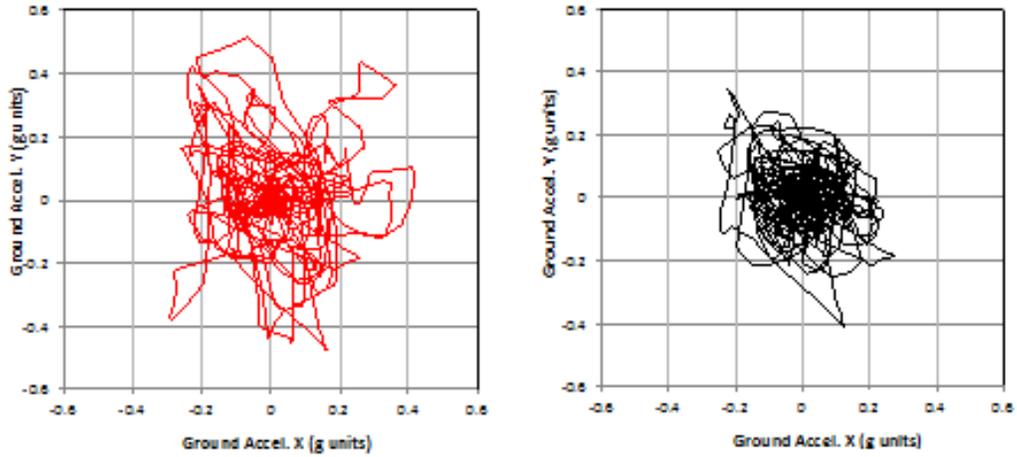
(a) Ground Displacement
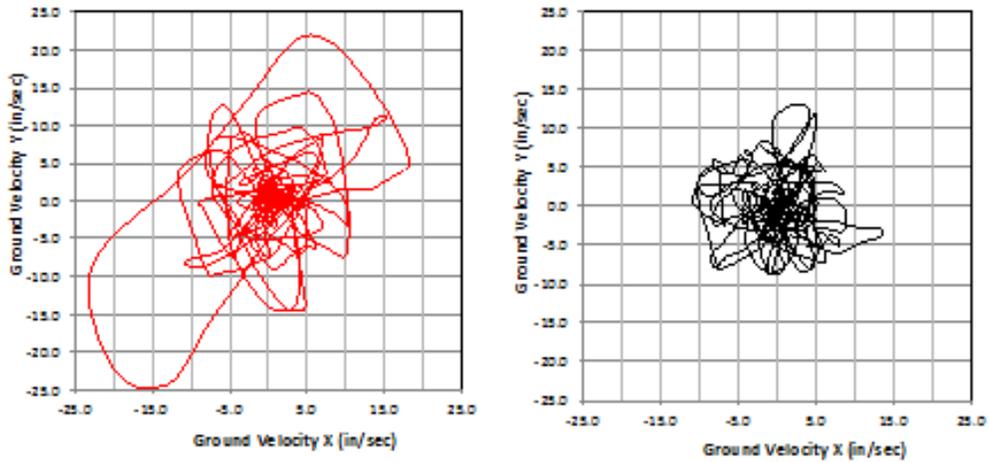
(b) Ground Velocity
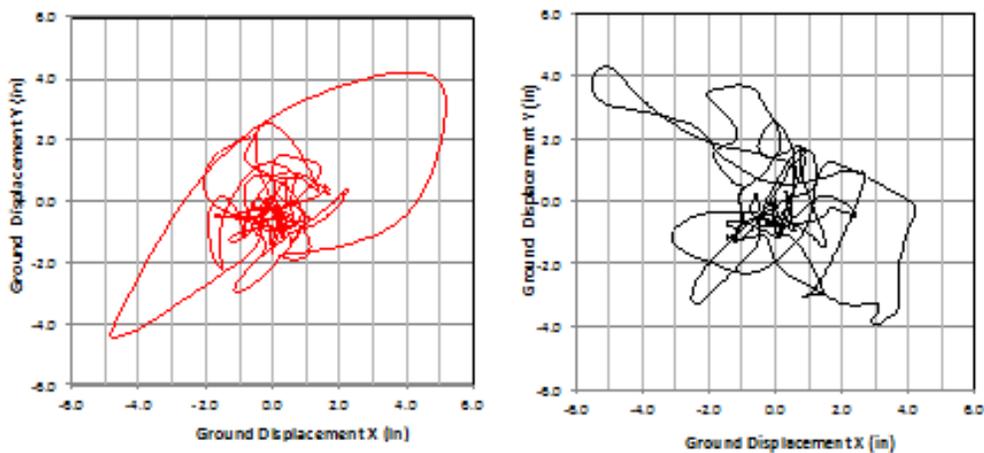
(c) Ground Displacement X-Y Component History Plots

Figure 4.3-19 *X-Y* **plots of component acceleration, velocity, and displacement histories**

Scale factors required for normalizing LRH base shears to the design seismic base shear are provided below for analysis without P-Delta effects included. The analyses used to determine the dynamic bases shears did not include accidental torsion, and are based on shaking only in the appropriate direction for the ground motion indicated. In all case the design base shear $V_X=V_Y$ is 1114 kips, and was based on minimum base shear requirements. $R_X = R_Y = 8$ in both directions of response. $I_e=1.0$.

Northridge: MUL009

V_{EX} min=-2484 k

V_{EX} max=2252 k

V_{EX} = 2484 k

$V_{IX} = V_{EX}(I_e/R) = 2484(1.0/8) = 311$

$\eta_X = V_X/V_{IX} = 1114/311 = 3.59$

Loma Prieta: GO3000

V_{EX} min=-3346

V_{EX} max=3468

$\eta_X = 1114/(3468/8)=2.57$

Chi Chi TCU045-E

V_{EX} min=-2314

V_{EX} max=2368

$\eta_X = 1114/(2368/8)=3.76$

Northridge: MUL2799

V_{EY} min=-3471

V_{EY} max=3816

$\eta_Y=1114/(3816/8)=2.34$

Loma Prieta: GO3090

V_{EY} min=-3701

V_{EY} max=3623

$\eta_Y=1114/(3701/8)=2.41$

Chi Chi TCU045-N

V_{EY} min=-2080

V_{EY} max=3140

$\eta_Y=1114/(3140/8)=2.84$

Calculation of Scale Factors for results including P-Delta

Northridge: MUL009

V_{EX} min=-2289

V_{EX} max=2213

η_X =1114/(2289/8)=3.89

Loma Prieta: GO3000

V_{EX} *min*=-3263

V_{EX} max=3088

η_X =1114/(3263/8)=2.73

Chi Chi TCU045-E

V_{EX} min=-2478

V_{EX} max=2519

η_X =1114/(2519/8)=3.54

Northridge: MUL2799

V_{EY} min=-3300

V_{EY} max=3403

η_Y =1114/(3403/8)=2.62

Loma Prieta: GO3090

V_{EY} min=-3651

V_{EY} max=3401

η_Y =1114/(3651/8)=2.44

Chi Chi TCU045-N

V_{EY} min=-2402

V_{EY} max=3047

η_Y =1114/(3047/8)=2.93

Results for all analyses are presented in Tables 4.3-24 through 4.3-39. These include story drifts in Frames 1 and 5 and shears in the middle bays beams of Frames 1 and 5. Analysis either did not or did include P-delta effects as indicated, and accidental torsion and orthogonal load effects were included as appropriate. Results are discussed in the context of the other methods of analysis in Section 4.3.6.4 of this example. Combinations shown in the Tables are relative to Figure 4.3-12 as follows:

C1 = C+ B

C2 = D + B

C3 = E + A

C4 = F + A

4.3-24a. Results for Drift in Frame 1 for Loma Prieta Earthquake Without P-Delta

Story	C1 Max (in.)	C1 Time (s.)	C2 Max (in.)	C2 Time (s.)	C3 Max (in.)	C3 Time (s.)	C4 Max (in.)	C4 Time (s.)
12	1.177	14.455	0.936	16.860	1.076	14.440	1.099	16.865
11	1.634	14.445	1.296	16.860	1.502	14.425	1.535	16.865
10	1.768	14.400	1.375	16.870	1.649	14.380	1.640	16.870
9	1.828	14.300	1.550	14.250	1.714	14.290	1.704	14.255
8	1.897	14.200	1.655	14.185	1.803	14.190	1.781	14.195
7	1.978	14.160	1.698	14.140	1.895	14.150	1.816	14.145
6	1.793	14.140	1.540	14.110	1.715	14.130	1.651	14.115
5	1.582	17.350	1.328	14.025	1.425	17.340	1.439	17.315
4	1.624	17.360	1.393	13.855	1.485	17.350	1.535	17.335
3	1.715	13.825	1.570	13.800	1.577	13.820	1.728	13.795
2	1.795	13.770	1.647	13.760	1.643	13.770	1.813	13.760
1	1.678	13.750	1.525	13.745	1.527	13.750	1.675	13.745

4.3-24b. Results for Drift in Frame 1 for Northridge Earthquake Without P-Delta

Story	C1 Max (in.)	C1 Time (s.)	C2 Max (in.)	C2 Time (s.)	C3 Max (in.)	C3 Time (s.)	C4 Max (in.)	C4 Time (s.)
12	0.889	10.980	0.757	9.090	0.855	10.960	0.879	9.100
11	1.139	9.090	0.977	9.080	1.112	10.960	1.149	9.090
10	1.248	26.400	1.008	10.530	1.096	26.370	1.157	10.540
9	1.295	26.380	1.089	15.170	1.144	15.180	1.167	15.190
8	1.334	15.130	1.231	15.100	1.292	15.110	1.287	15.110
7	1.352	15.130	1.252	15.110	1.320	15.120	1.305	15.110
6	1.314	16.950	1.125	16.920	1.271	16.940	1.219	16.940
5	1.385	15.390	1.246	15.370	1.339	15.360	1.283	15.390
4	1.445	15.390	1.366	15.390	1.425	15.380	1.400	15.400
3	1.362	15.400	1.349	15.400	1.378	15.400	1.377	15.410
2	1.177	15.450	1.218	15.420	1.227	15.430	1.240	15.440
1	1.058	13.730	1.029	15.460	1.037	15.480	1.059	15.500

4.3-24c. Results for Drift in Frame 1 for Chi Chi Earthquake Without P-Delta

Story	C1 Max (in.)	C1 Time (s.)	C2 Max (in.)	C2 Time (s.)	C3 Max (in.)	C3 Time (s.)	C4 Max (in.)	C4 Time (s.)
12	0.869	51.885	0.664	51.850	0.776	51.865	0.786	51.865
11	1.284	51.880	0.980	51.840	1.146	51.860	1.164	51.860
10	1.505	51.880	1.154	51.830	1.344	51.855	1.373	51.850
9	1.543	51.880	1.205	53.670	1.381	51.850	1.426	51.845
8	1.480	53.745	1.338	53.660	1.410	53.675	1.452	53.700
7	1.544	53.725	1.380	53.665	1.459	53.675	1.502	53.695
6	1.546	53.720	1.361	53.670	1.446	53.685	1.488	53.695
5	1.558	53.720	1.353	53.680	1.446	53.695	1.481	53.700
4	1.454	53.705	1.248	53.695	1.345	53.705	1.358	53.700
3	1.364	53.660	1.235	52.225	1.269	52.245	1.274	52.260
2	1.259	53.620	1.171	52.230	1.194	52.265	1.213	52.285
1	1.152	50.565	1.028	52.235	1.045	52.275	1.075	50.575

4.3-25. Results for Drift in Frame 1 Envelope Values from All EQS Without P-Delta

Story	Max (in.)	EQ	Comb	Time (s.)	Limit (in.)
12	1.18	Loma Prieta	C1	14.455	3
11	1.63	Loma Prieta	C1	14.445	3
10	1.77	Loma Prieta	C1	14.400	3
9	1.83	Loma Prieta	C1	14.300	3
8	1.90	Loma Prieta	C1	14.200	3
7	1.98	Loma Prieta	C1	14.160	3
6	1.79	Loma Prieta	C1	14.140	3
5	1.58	Loma Prieta	C1	17.350	3
4	1.62	Loma Prieta	C1	17.360	3
3	1.73	Loma Prieta	C4	13.795	3
2	1.81	Loma Prieta	C4	13.760	3
1	1.68	Loma Prieta	C1	13.750	3.6

4.3-26a. Results for Drift in Frame 1 for Loma Prieta Earthquake With P-Delta

Story	C1 Max (in.)	C1 Time (s.)	C2 Max (in.)	C2 Time (s.)	C3 Max (in.)	C3 Time (s.)	C4 Max (in.)	C4 Time (s.)
12	1.20	14.510	0.92	14.495	1.13	14.495	1.04	14.500
11	1.65	14.500	1.25	14.485	1.55	14.485	1.41	14.490
10	1.77	14.460	1.35	14.405	1.67	14.440	1.50	14.430
9	1.86	14.340	1.62	14.295	1.77	14.330	1.76	14.300
8	1.96	14.255	1.77	14.245	1.89	14.245	1.88	14.250
7	2.02	14.210	1.78	14.200	1.96	14.195	1.89	14.210
6	1.84	14.190	1.61	14.165	1.78	14.175	1.71	14.175
5	1.62	14.365	1.39	14.055	1.50	14.340	1.47	14.060
4	1.80	15.865	1.55	13.910	1.62	15.835	1.66	13.910
3	1.85	15.850	1.70	13.850	1.71	13.870	1.84	13.850
2	1.87	13.790	1.77	13.780	1.75	13.790	1.92	13.780
1	1.79	13.770	1.67	13.760	1.66	13.765	1.81	13.760

4.3-26b. Results for Drift in Frame 1 for Northridge Earthquake With P-Delta

Story	C1 Max (in.)	C1 Time (s.)	C2 Max (in.)	C2 Time (s.)	C3 Max (in.)	C3 Time (s.)	C4 Max (in.)	C4 Time (s.)
12	0.85	15.420	0.76	9.120	0.81	11.010	0.87	9.130
11	1.25	15.410	1.07	26.420	1.15	26.450	1.16	26.440
10	1.46	26.480	1.31	26.410	1.39	26.450	1.40	26.430
9	1.58	26.480	1.43	26.400	1.51	26.440	1.52	26.430
8	1.51	26.500	1.42	26.390	1.45	26.420	1.48	26.450
7	1.56	15.640	1.37	26.370	1.42	15.620	1.42	26.460
6	1.49	15.560	1.30	15.510	1.41	15.520	1.37	15.540
5	1.58	15.450	1.46	15.430	1.56	15.430	1.50	15.440
4	1.64	15.420	1.55	15.410	1.61	15.410	1.57	15.420
3	1.44	15.410	1.39	15.410	1.42	15.410	1.41	28.070
2	1.41	21.170	1.36	21.160	1.30	21.140	1.40	21.170
1	1.39	21.160	1.32	21.150	1.27	21.140	1.36	21.160

4.3-26c. Results for Drift in Frame 1 for Chi Chi Earthquake With P-Delta

Story	C1 Max (in.)	C1 Time (s.)	C2 Max (in.)	C2 Time (s.)	C3 Max (in.)	C3 Time (s.)	C4 Max (in.)	C4 Time (s.)
12	0.86	46.375	0.69	51.905	0.77	51.920	0.78	51.920
11	1.24	51.940	1.01	51.900	1.13	51.920	1.15	51.915
10	1.46	51.945	1.20	51.890	1.33	51.920	1.36	51.915
9	1.51	51.960	1.26	51.890	1.38	51.930	1.43	51.925
8	1.49	53.955	1.35	53.825	1.41	53.875	1.44	53.890
7	1.58	53.880	1.43	53.810	1.50	53.835	1.53	53.850
6	1.64	53.840	1.45	53.800	1.54	53.815	1.57	53.830
5	1.69	53.820	1.46	53.790	1.57	53.800	1.60	53.810
4	1.66	53.790	1.40	53.765	1.53	53.775	1.55	53.775
3	1.56	53.755	1.33	52.280	1.42	53.740	1.44	53.725
2	1.45	50.615	1.22	52.315	1.29	55.580	1.34	55.585
1	1.33	50.595	1.06	45.585	1.18	50.570	1.22	50.595

4.3-27. Results for Drift in Frame 1 Envelope Values from All EQS With P-Delta

Story	Max (in.)	EQ	Comb	Time (s.)	Limit (in.)
12	1.20	Loma Prieta	C1	14.510	3
11	1.65	Loma Prieta	C1	14.500	3
10	1.77	Loma Prieta	C1	14.460	3
9	1.86	Loma Prieta	C1	14.340	3
8	1.96	Loma Prieta	C1	14.255	3
7	2.02	Loma Prieta	C1	14.210	3
6	1.84	Loma Prieta	C1	14.190	3
5	1.69	Chichi	C1	53.820	3
4	1.80	Loma Prieta	C1	15.865	3
3	1.85	Loma Prieta	C1	15.850	3
2	1.92	Loma Prieta	C4	13.780	3
1	1.81	Loma Prieta	C4	13.760	3.6

4.3-28a. Results for Drift in Frame 5 for Loma Prieta Earthquake Without P-Delta

Story	C1 Max (in.)	C1 Time (s.)	C2 Max (in.)	C2 Time (s.)	C3 Max (in.)	C3 Time (s.)	C4 Max (in.)	C4 Time (s.)
8	1.01	16.430	1.03	16.490	1.05	16.465	0.89	16.460
7	1.11	16.430	1.13	16.480	1.17	16.470	0.97	16.455
6	1.05	16.425	1.06	16.470	1.11	16.460	0.92	16.445
5	0.95	22.225	0.89	18.020	0.96	19.250	0.79	16.420
4	0.84	22.200	0.84	17.970	0.85	17.945	0.69	17.980
3	0.83	22.180	0.87	17.925	0.89	17.900	0.72	17.925
2	0.85	17.820	0.90	17.865	0.97	13.455	0.76	17.860
1	0.83	17.810	0.88	13.465	0.97	13.455	0.74	17.845

4.3-28b. Results for Drift in Frame 5 for Northridge Earthquake Without P-Delta

Story	C1 Max (in.)	C1 Time (s.)	C2 Max (in.)	C2 Time (s.)	C3 Max (in.)	C3 Time (s.)	C4 Max (in.)	C4 Time (s.)
8	0.94	24.170	0.92	24.230	1.04	24.150	0.81	24.280
7	1.00	24.200	0.99	24.250	1.11	24.190	0.87	24.290
6	0.96	24.230	0.98	24.280	1.08	24.230	0.86	24.300
5	0.98	22.920	0.94	24.330	1.03	24.270	0.86	22.940
4	0.93	22.900	0.83	21.270	0.96	22.890	0.79	22.930
3	0.96	22.880	0.86	22.880	1.01	22.860	0.79	22.910
2	0.97	22.860	0.88	22.860	1.04	22.840	0.79	22.890
1	0.92	22.850	0.84	22.850	0.99	22.830	0.75	22.870

4.3-28c. Results for Drift in Frame 5 for Chi Chi Earthquake Without P-Delta

Story	C1 Max (in.)	C1 Time (s.)	C2 Max (in.)	C2 Time (s.)	C3 Max (in.)	C3 Time (s.)	C4 Max (in.)	C4 Time (s.)
8	0.79	43.960	0.79	43.955	0.91	43.965	0.66	43.945
7	0.87	43.935	0.85	43.930	0.99	43.950	0.70	43.910
6	0.85	43.900	0.82	43.895	0.97	43.915	0.75	42.705
5	0.88	42.690	0.87	42.680	0.96	42.680	0.79	42.685
4	0.81	42.655	0.80	42.650	0.89	42.655	0.72	42.650
3	0.82	42.620	0.82	42.615	0.90	42.630	0.72	42.610
2	0.82	42.580	0.82	42.585	0.89	42.595	0.74	42.575
1	0.78	42.560	0.78	42.570	0.84	42.570	0.71	42.560

4.3-29. Results for Drift in Frame 5 Envelope Values from All EQS Without P-Delta

Story	Max (in.)	EQ	Comb	Time (s.)	Limit
8	1.05	Loma Prieta	C3	16.465	3
7	1.17	Loma Prieta	C3	16.470	3
6	1.11	Loma Prieta	C3	16.460	3
5	1.03	Northridge	C3	24.270	3
4	0.96	Northridge	C3	22.890	3
3	1.01	Northridge	C3	22.860	3
2	1.04	Northridge	C3	22.840	3
1	0.99	Northridge	C3	22.830	3.6

4.3-30a. Results for Drift in Frame 5 for Loma Prieta Earthquake With P-Delta

Story	C1 Max (in.)	C1 Time (s.)	C2 Max (in.)	C2 Time (s.)	C3 Max (in.)	C3 Time (s.)	C4 Max (in.)	C4 Time (s.)
8	1.01	16.490	0.99	18.320	1.06	18.310	0.88	16.510
7	1.13	16.490	1.10	16.530	1.19	16.520	0.98	16.510
6	1.11	16.490	1.07	16.520	1.16	16.510	0.95	16.505
5	0.99	16.480	0.94	18.080	1.04	16.495	0.84	16.500
4	0.87	18.015	0.89	18.035	0.98	18.015	0.75	18.040
3	0.90	17.980	0.91	18.005	1.01	17.995	0.76	18.000
2	0.92	17.950	0.94	13.500	1.04	13.500	0.78	15.220
1	0.88	13.485	0.95	13.495	1.05	13.495	0.79	13.490

4.3-30b. Results for Drift in Frame 5 for Northridge Earthquake With P-Delta

Story	C1 Max (in.)	C1 Time (s.)	C2 Max (in.)	C2 Time (s.)	C3 Max (in.)	C3 Time (s.)	C4 Max (in.)	C4 Time (s.)
8	0.92	24.320	0.93	24.380	1.04	24.290	0.79	24.440
7	1.01	24.310	1.03	24.370	1.15	24.300	0.88	27.770
6	1.03	24.320	1.05	24.370	1.16	24.310	0.92	27.790
5	1.08	22.980	1.04	24.390	1.14	24.340	0.98	23.000
4	0.99	22.970	0.93	22.980	1.04	22.960	0.86	22.990
3	0.98	22.960	0.91	22.960	1.05	22.940	0.82	22.980
2	0.96	22.940	0.89	22.930	1.04	22.910	0.79	22.960
1	0.90	22.920	0.84	22.910	0.98	22.890	0.74	22.930

4.3-30c. Results for Drift in Frame 5 for Chi Chi Earthquake With P-Delta

Story	C1 Max (in.)	C1 Time (s.)	C2 Max (in.)	C2 Time (s.)	C3 Max (in.)	C3 Time (s.)	C4 Max (in.)	C4 Time (s.)
8	0.78	44.010	0.78	44.005	0.90	44.015	0.64	42.905
7	0.83	43.985	0.81	43.980	0.96	44.000	0.72	42.790
6	0.89	42.765	0.87	42.745	0.95	42.765	0.81	42.740
5	0.97	42.725	0.96	42.715	1.05	42.720	0.88	42.720
4	0.88	42.690	0.87	42.685	0.96	42.690	0.79	42.685
3	0.87	42.655	0.87	42.650	0.96	42.660	0.78	42.645
2	0.87	42.615	0.88	42.615	0.95	42.625	0.78	42.610
1	0.83	42.595	0.83	42.600	0.89	42.600	0.75	42.595

4.3-31. Results for Drift in Frame 1 Envelope Values from All EQS With P-Delta

Story	Max (in.)	EQ	Comb	Time (s.)	Limit
8	1.06	Loma Prieta	C3	18.310	3
7	1.19	Loma Prieta	C3	16.520	3
6	1.16	Northridge	C3	24.310	3
5	1.14	Northridge	C3	24.340	3
4	1.04	Northridge	C3	22.960	3
3	1.05	Northridge	C3	22.940	3
2	1.04	Northridge	C3	22.910	3
1	1.05	Loma Prieta	C3	13.495	3.6

4.3-32a. Results for beam shear in Frame 1 for Loma Prieta Earthquake Without P-Delta

Level	C1 Max + (k)	C1 Max- (k)	C2 Max + (k)	C2 Max- (k)	C3 Max + (k)	C3 Max- (k)	C4 Max + (k)	C4 Max- (k)
12	14.9	12.3	11.7	9.0	13.6	10.9	13.8	11.0
11	25.9	20.7	20.4	15.0	23.7	18.0	24.0	18.7
10	31.4	23.2	24.6	18.1	29.1	19.6	29.1	22.7
9	38.7	29.3	31.2	25.8	36.3	25.8	34.5	31.1
8	43.8	32.8	38.2	29.9	41.2	29.0	41.5	34.0
7	60.4	42.9	52.3	39.2	57.7	39.3	56.1	43.0
6	62.1	41.2	53.3	37.7	59.4	38.6	57.1	41.3
5	59.2	48.3	51.1	37.7	56.3	44.3	55.1	44.5
4	59.6	56.5	47.9	43.7	54.2	50.9	55.3	51.1
3	68.2	69.8	62.1	52.9	63.0	63.1	67.7	62.2
2	75.5	73.7	69.3	56.9	69.3	66.4	76.2	66.0
1	74.3	67.7	67.8	55.1	68.0	62.7	74.4	63.6

4.3-32b. Results for beam shear in Frame 1 for Northridge Earthquake Without P-Delta

Level	C1 Max + (k)	C1 Max- (k)	C2 Max + (k)	C2 Max- (k)	C3 Max + (k)	C3 Max- (k)	C4 Max + (k)	C4 Max- (k)
12	15.1	15.6	12.8	12.3	13.7	14.8	14.8	13.7
11	25.7	26.3	21.6	20.9	23.2	25.3	25.1	23.2
10	28.8	29.3	23.8	22.5	26.2	27.4	27.6	25.2
9	33.9	38.4	28.0	29.7	31.0	33.7	31.7	33.0
8	32.3	42.1	28.6	37.9	30.4	39.8	32.8	39.8
7	51.9	58.3	45.1	53.5	49.8	56.4	49.3	56.0
6	60.2	58.8	51.2	53.9	57.8	57.2	56.0	56.4
5	66.6	65.9	56.3	57.8	63.5	62.6	61.8	60.2
4	70.7	74.5	59.8	67.8	66.3	72.0	65.4	70.3
3	80.8	84.0	67.1	79.5	75.1	83.1	73.2	82.1
2	76.7	77.0	62.7	76.2	71.2	78.6	68.4	78.3
1	64.2	63.6	55.1	64.9	60.0	66.5	60.3	66.5

4.3-32c. Results for beam shear in Frame 1 for Chi Chi Earthquake Without P-Delta

Level	C1 Max + (k)	C1 Max- (k)	C2 Max + (k)	C2 Max- (k)	C3 Max + (k)	C3 Max- (k)	C4 Max + (k)	C4 Max- (k)
12	16.0	14.6	12.4	9.9	14.3	13.4	14.5	11.3
11	28.5	24.5	22.0	17.5	25.6	22.4	25.8	19.4
10	37.3	28.1	28.8	24.3	33.5	26.2	33.9	27.0
9	48.2	40.5	37.5	35.2	43.4	37.9	44.2	39.1
8	49.4	49.7	39.7	44.2	44.8	47.2	46.1	48.3
7	57.8	68.4	46.7	61.1	52.1	65.1	54.1	66.3
6	58.8	73.9	48.8	65.1	52.6	69.6	53.3	70.9
5	67.8	81.0	58.8	70.4	62.6	75.6	62.4	76.9
4	72.5	81.1	65.2	69.6	68.8	75.3	68.4	76.0
3	81.2	86.5	75.2	73.4	78.6	80.0	78.4	80.0
2	79.6	82.8	74.9	69.1	77.6	75.9	78.0	75.3
1	73.8	74.1	67.2	60.1	69.5	66.6	70.3	68.4

4.3-33a. Envelope positive value results for beam shear in Frame 1 Without P-Delta

Level	Max + (k)	EQ	Comb	Time (s.)
12	16.0	Chichi	C1	51.880
11	28.5	Chichi	C1	51.880
10	37.3	Chichi	C1	51.875
9	48.2	Chichi	C1	51.875
8	49.4	Chichi	C1	51.880
7	60.4	Loma Prieta	C1	14.175
6	62.1	Loma Prieta	C1	14.150
5	67.8	Chichi	C1	52.205
4	72.5	Chichi	C1	52.230
3	81.2	Chichi	C1	52.255
2	79.6	Chichi	C1	52.285
1	74.4	Loma Prieta	C4	13.755

4.3-33b. Envelope negative value results for beam shear in Frame 1 Without P-Delta

Level	Max – (k)	EQ	Comb	Time (s.)
12	15.6	Northridge	C1	10.980
11	26.3	Northridge	C1	10.980
10	29.3	Northridge	C1	26.410
9	40.5	Chichi	C1	53.800
8	49.7	Chichi	C1	53.755
7	68.4	Chichi	C1	53.730
6	73.9	Chichi	C1	53.720
5	81.0	Chichi	C1	53.720
4	81.1	Chichi	C1	53.715
3	86.5	Chichi	C1	53.690
2	82.8	Chichi	C1	53.650
1	74.1	Chichi	C1	50.575

4.3-34a. Results for beam shear in Frame 1 for Loma Prieta Earthquake with P-Delta

Level	C1 Max + (k)	C1 Max- (k)	C2 Max + (k)	C2 Max- (k)	C3 Max + (k)	C3 Max- (k)	C4 Max + (k)	C4 Max- (k)
12	16.3	13.2	12.7	9.7	15.3	11.7	14.2	11.7
11	28.1	22.1	21.6	16.3	26.3	19.6	24.3	19.8
10	33.7	24.9	25.7	19.5	31.7	21.5	28.8	23.9
9	41.2	31.5	34.3	28.0	39.3	27.2	37.2	33.2
8	48.1	35.9	43.2	32.9	46.0	32.2	46.3	37.1
7	65.8	46.7	58.7	43.0	63.6	43.2	62.4	46.6
6	67.5	47.2	59.3	42.1	65.4	43.9	62.9	45.6
5	64.5	54.1	56.6	42.8	62.1	50.3	60.2	49.7
4	61.3	66.2	55.8	52.2	57.5	60.2	59.2	59.3
3	78.3	82.5	72.2	64.6	73.9	74.6	77.3	74.9
2	83.4	83.3	78.1	64.7	78.1	75.6	84.5	76.4
1	82.6	73.6	77.5	57.6	77.1	67.1	83.8	68.3

4.3-34b. Results for beam shear in Frame 1 for Northridge Earthquake with P-Delta

Level	C1 Max + (k)	C1 Max- (k)	C2 Max + (k)	C2 Max- (k)	C3 Max + (k)	C3 Max- (k)	C4 Max + (k)	C4 Max- (k)
12	16.1	16.8	13.9	13.9	14.8	15.3	16.0	15.1
11	27.3	29.7	23.5	24.7	25.7	26.9	27.0	26.8
10	32.9	38.4	26.8	33.1	31.6	35.8	30.6	35.9
9	40.5	51.1	32.6	45.0	37.2	48.3	37.4	48.5
8	44.6	56.2	37.7	50.8	39.1	53.5	41.1	53.9
7	56.9	74.9	53.1	64.6	52.7	67.3	54.2	67.9
6	62.5	77.4	56.9	65.4	60.5	71.4	60.6	70.0
5	71.4	83.3	60.7	75.0	67.7	80.3	68.1	78.2
4	78.8	92.1	69.1	85.1	75.9	89.8	73.7	87.5
3	91.7	100.8	79.5	94.2	88.4	98.2	85.7	96.2
2	90.4	86.2	79.0	81.1	82.7	83.8	88.8	86.0
1	86.8	80.1	77.8	71.7	78.1	74.9	83.1	80.2

4.3-34c. Results for beam shear in Frame 1 for Chi Chi Earthquake with P-Delta

Level	C1 Max + (k)	C1 Max- (k)	C2 Max + (k)	C2 Max- (k)	C3 Max + (k)	C3 Max- (k)	C4 Max + (k)	C4 Max- (k)
12	14.8	14.6	12.0	9.4	13.5	13.0	13.6	11.2
11	26.2	24.9	21.4	16.6	24.0	22.1	24.2	18.7
10	34.3	28.7	28.0	22.6	31.4	25.5	31.8	25.5
9	44.6	40.3	36.7	33.0	40.8	36.4	41.8	36.7
8	47.2	47.7	39.6	41.9	43.2	44.6	45.0	45.4
7	61.0	65.5	49.0	59.2	54.3	62.3	56.8	63.3
6	68.6	72.8	55.1	64.9	61.2	68.8	62.6	69.8
5	77.9	81.7	64.6	71.5	70.8	76.5	71.6	77.5
4	81.4	85.1	70.2	72.8	75.6	79.0	75.9	79.8
3	88.3	93.1	78.9	77.6	83.6	85.7	83.4	86.3
2	84.7	88.4	75.5	72.2	79.3	80.8	79.3	81.5
1	80.7	81.8	66.3	65.1	72.7	72.9	75.2	74.8

4.3-35a. Envelope positive value results for beam shear in Frame 1 with P-Delta

Level	Max + (k)	EQ	Comb	Time (s.)
12	16.3	Loma Prieta	C1	14.510
11	28.1	Loma Prieta	C1	14.505
10	34.3	Chichi	C1	51.940
9	44.6	Chichi	C1	51.945
8	48.1	Loma Prieta	C1	14.290
7	65.8	Loma Prieta	C1	14.230
6	68.6	Chichi	C1	52.250
5	77.9	Chichi	C1	52.270
4	81.4	Chichi	C1	52.275
3	91.7	Northridge	C1	16.830
2	90.4	Northridge	C1	28.160
1	86.8	Northridge	C1	21.150

4.3-35b. Envelope negative value results for beam shear in Frame 1 with P-Delta

Level	Max – (k)	EQ	Comb	Time (s.)
12	16.8	Northridge	C1	15.430
11	29.7	Northridge	C1	15.420
10	38.4	Northridge	C1	15.410
9	51.1	Northridge	C1	26.480
8	56.2	Northridge	C1	26.490
7	74.9	Northridge	C1	15.650
6	77.4	Northridge	C1	15.610
5	83.3	Northridge	C1	15.500
4	92.1	Northridge	C1	15.430
3	100.8	Northridge	C1	15.410
2	88.4	Chichi	C1	53.735
1	81.8	Chichi	C1	50.600

4.3-36a. Results for beam shear in Frame 5 for Loma Prieta Earthquake without P-Delta

Level	C1 Max + (k)	C1 Max- (k)	C2 Max + (k)	C2 Max- (k)	C3 Max + (k)	C3 Max- (k)	C4 Max + (k)	C4 Max- (k)
8	17.7	14.6	18.0	16.1	18.5	16.0	15.7	12.3
7	27.4	21.9	27.9	23.6	28.8	23.7	24.2	18.3
6	27.5	21.4	27.9	22.0	29.1	22.4	24.2	18.3
5	28.6	23.6	28.7	25.4	30.3	26.4	25.1	21.8
4	29.5	25.6	24.3	28.6	29.5	28.7	22.2	23.9
3	35.0	31.4	29.9	35.5	34.8	36.2	28.3	29.2
2	35.7	34.9	35.5	37.7	39.0	38.7	31.1	31.3
1	35.2	35.7	37.8	38.0	41.5	38.7	31.2	32.0

4.3-36b. Results for beam shear in Frame 5 for Northridge Earthquake without P-Delta

Level	C1 Max + (k)	C1 Max- (k)	C2 Max + (k)	C2 Max- (k)	C3 Max + (k)	C3 Max- (k)	C4 Max + (k)	C4 Max- (k)
8	16.0	13.8	15.7	13.8	17.7	16.1	13.9	11.0
7	24.1	19.3	24.1	19.4	26.7	22.7	21.3	16.5
6	23.8	19.4	24.6	20.2	26.8	21.3	21.5	17.5
5	26.0	26.3	27.6	23.6	29.7	25.2	23.7	23.0
4	26.3	31.1	28.7	25.9	30.2	30.8	25.3	26.1
3	31.0	38.7	34.0	32.6	35.8	39.3	29.7	31.5
2	31.0	40.6	33.9	34.7	35.6	42.2	29.6	32.4
1	29.6	40.0	32.2	34.5	33.6	42.0	28.3	31.7

4.3-36c. Results for beam shear in Frame 5 for Chi Chi Earthquake without P-Delta

Level	C1 Max + (k)	C1 Max- (k)	C2 Max + (k)	C2 Max- (k)	C3 Max + (k)	C3 Max- (k)	C4 Max + (k)	C4 Max- (k)
8	16.3	15.5	16.5	14.5	18.8	16.9	13.6	12.8
7	25.1	23.6	25.0	22.0	28.9	25.8	20.7	19.4
6	25.7	24.2	25.1	23.3	29.5	26.1	20.8	21.4
5	28.3	29.7	27.3	29.3	32.6	32.2	22.5	26.8
4	26.8	33.0	25.8	32.7	31.5	36.1	20.6	29.4
3	28.6	39.8	27.8	39.9	34.2	43.9	22.2	35.4
2	27.6	41.1	27.1	41.5	32.2	45.2	23.0	36.9
1	27.1	40.3	26.0	40.6	29.9	43.7	24.7	36.6

4.3-37a. Envelope positive value results for beam shear in Frame 5 Without P-Delta

Level	Max + (k)	EQ	Com b	Time (s.)
8	18.8	Chichi	C3	43.970
7	28.9	Chichi	C3	43.960
6	29.5	Chichi	C3	43.935
5	32.6	Chichi	C3	43.900
4	31.5	Chichi	C3	43.865
3	35.8	Northridge	C3	21.260
2	39.0	Loma Prieta	C3	13.455
1	41.5	Loma Prieta	C3	13.455

4.3-37b. Envelope negative value results for beam shear in Frame 5 Without P-Delta

Level	Max + (k)	EQ	Com b	Time (s.)
8	16.9	Chichi	C3	42.900
7	25.8	Chichi	C3	42.890
6	26.1	Chichi	C3	42.820
5	32.2	Chichi	C3	42.690
4	36.1	Chichi	C3	42.665
3	43.9	Chichi	C3	42.645
2	45.2	Chichi	C3	42.610
1	43.7	Chichi	C3	42.580

4.3-38a. Results for beam shear in Frame 5 for Loma Prieta Earthquake With P-Delta

Level	C1 Max + (k)	C1 Max- (k)	C2 Max + (k)	C2 Max- (k)	C3 Max + (k)	C3 Max- (k)	C4 Max + (k)	C4 Max- (k)
8	18.0	16.0	17.7	17.8	18.8	18.8	15.7	14.2
7	28.1	23.9	27.5	26.3	29.4	28.0	24.4	21.0
6	29.2	22.6	28.4	24.6	30.6	26.3	25.1	20.4
5	31.4	26.5	30.1	26.6	32.8	29.0	26.7	23.8
4	27.9	29.3	26.7	30.8	30.2	33.1	23.3	26.0
3	33.8	37.2	32.9	38.0	36.4	41.8	27.8	31.7
2	37.7	39.3	38.6	39.6	42.3	43.5	30.9	33.2
1	37.9	38.5	41.3	38.8	45.3	41.9	33.7	33.3

4.3-38b. Results for beam shear in Frame 5 for Northridge Earthquake With P-Delta

Level	C1 Max + (k)	C1 Max- (k)	C2 Max + (k)	C2 Max- (k)	C3 Max + (k)	C3 Max- (k)	C4 Max + (k)	C4 Max- (k)
8	17.3	15.4	18.1	15.7	19.8	16.8	15.3	13.2
7	26.5	23.3	27.7	23.2	30.3	24.8	23.5	19.8
6	27.8	23.8	29.2	24.0	31.7	25.8	25.4	22.7
5	32.1	32.4	33.8	29.4	36.3	32.2	30.1	29.7
4	32.4	37.3	36.2	33.9	36.8	38.2	31.5	32.7
3	36.1	44.4	42.2	40.5	42.9	46.6	35.8	37.6
2	36.2	44.7	41.5	40.8	42.1	47.8	35.2	36.9
1	35.4	43.1	39.3	39.4	39.8	46.6	34.4	35.2

4.3-38c. Results for beam shear in Frame 5 for Chi Chi Earthquake With P-Delta

Level	C1 Max + (k)	C1 Max- (k)	C2 Max + (k)	C2 Max- (k)	C3 Max + (k)	C3 Max- (k)	C4 Max + (k)	C4 Max- (k)
8	16.7	16.3	16.7	15.4	19.3	17.9	13.6	13.7
7	25.2	25.0	25.0	23.5	29.2	27.3	20.4	21.1
6	25.5	26.6	24.9	25.7	29.5	28.5	20.4	23.9
5	28.2	33.3	27.2	32.8	32.6	35.8	22.3	30.3
4	26.8	37.1	25.7	36.9	31.4	40.4	22.1	33.4
3	28.0	44.3	26.9	44.3	33.1	48.7	27.5	39.5
2	30.4	45.3	27.5	45.5	30.2	49.7	31.8	40.5
1	33.2	44.2	30.0	44.4	30.1	48.1	34.0	39.9

4.3-39a. Envelope positive value results for beam shear in Frame 5 Without P-Delta

Level	Max + (k)	EQ	Comb	Time (s.)
8	19.8	Northridge	C3	24.300
7	30.3	Northridge	C3	24.300
6	31.7	Northridge	C3	24.310
5	36.3	Northridge	C3	24.330
4	36.8	Northridge	C3	21.310
3	42.9	Northridge	C3	21.310
2	42.3	Loma Prieta	C3	13.505
1	45.3	Loma Prieta	C3	13.495

4.3-39b. Envelope positive value results for beam shear in Frame 5 With P-Delta

Level	Max – (k)	EQ	Comb	Time (s.)
8	18.8	Loma Prieta	C3	18.305
7	28.0	Loma Prieta	C3	18.310
6	28.5	Chichi	C3	42.835
5	35.8	Chichi	C3	42.730
4	40.4	Chichi	C3	42.700
3	48.7	Chichi	C3	42.675
2	49.7	Chichi	C3	42.640
1	48.1	Chichi	C3	42.610

4.3.6.4 Overview and Discussion of Results. The 12-story structure pictured in Figure 4.3-1 was analyzed using three approaches: Equivalent Lateral Force (ELF) analysis, Modal Response Spectrum (MRS) analysis, and Linear Response History (LRH) analysis using modal superposition. All analyses were conducted with P-Delta effects excluded, and again with such effects included directly by use of geometric stiffness that was computed for the structure prior to the analysis, and maintained as constant during the analysis. In the ELF method accidental torsion was included by application of story torsions, and in the MRS and LRH method accidental torsion was included by physically relocating the center of mass to provide the desired eccentricity. In all cases orthogonal load effects were considered in the analysis.

Table 4.3-40 presents the computed story drifts for Frame 1 for the analysis without P-Delta effects included. Recall that for the ELF method the drifts are based on lateral forces based on the computed period of vibration, and for the MRS and LRH methods the drifts have been adjusted for C_d and R, but have not been scaled otherwise. As may be seen, the drifts are similar, and in no case do they exceed the limits of 2% of the story height. The general trend is for the drifts from the ELF and LRH methods to be larger than those obtained from MRS. Additionally, there is more similarity between the ELF and LRH results than there is between ELF and MRS or LRH and MRS.

Table 4.3-41 lists the drifts computed for the analysis that did include P-Delta effects, and it can be seen that these are generally larger than those computed without P-Delta effects included. However, for the LRH method the drifts at stories 2 and 3 were slightly larger when P-Delta effects were not included.

Comparisons in the shear in the middle bay beams of Frame 1 are presented in Tables 4.3-42 and 4.2-43 for analysis without and with P-Delta effects, respectively. Here, two observations are made. First, the shears computed at the lower stories for each method of analysis, for a given P-Delta approach, are very similar. This is due to requirement of normalizing the results to the design base shear, which for this structure was controlled by minimum base shear requirements (*Standard* Equation 12.8-5). Second, shears computed from analysis that included P-Delta effects are consistently larger than those computed without such effects.

4.3-40. Result comparisons for drift in Frame 1 analyzed without P-Delta effects

STORY	ELF (in.)	MRS (in.)	LRH (in.)	Limit (in.)
12	0.90	0.90	1.18	3.00
11	1.34	1.27	1.63	3.00
10	1.64	1.45	1.77	3.00
9	1.86	1.51	1.83	3.00
8	1.90	1.47	1.90	3.00
7	1.94	1.48	1.98	3.00
6	1.90	1.45	1.79	3.00
5	1.91	1.48	1.58	3.00
4	1.81	1.48	1.62	3.00
3	1.74	1.50	1.73	3.00
2	1.64	1.49	1.81	3.00
1	1.42	1.37	1.68	3.60

4.3-41 Result comparisons for drift in Frame 1 analyzed with P-Delta effects

STORY	ELF (in.)	MRS (in.)	LRH (in.)	Limit (in.)
12	0.93	0.88	1.20	3.00
11	1.40	1.26	1.65	3.00
10	1.74	1.45	1.77	3.00
9	1.98	1.54	1.86	3.00
8	2.06	1.51	1.96	3.00
7	2.12	1.54	2.02	3.00
6	2.11	1.52	1.84	3.00
5	2.13	1.56	1.69	3.00
4	2.09	1.61	1.80	3.00
3	1.99	1.61	1.85	3.00
2	1.85	1.59	1.92	3.00
1	1.59	1.45	1.81	3.60

4.3-42. Result comparisons beam shears in Frame 1 analyzed without P-Delta effects

LEVEL	ELF (k)	MRS (k)	LRH (k)
R	13.0	13.1	16.0
12	22.5	22.9	28.5
11	30.2	28.9	37.3
10	41.9	37.1	48.2
9	49.3	40.5	49.7
8	65.6	52.7	68.4
7	69.2	55.4	73.9
6	74.9	60.4	81.0
5	75.5	63.1	81.1
4	82.4	72.6	86.5
3	80.6	74.8	82.8
2	72.3	70.9	74.4

3.2-43 Result comparisons beam shears in Frame 1 analyzed with P-Delta effects

LEVEL	ELF (k)	MRS (k)	LRH (k)
R	13.2	13.6	16.8
12	23.2	23.8	29.7
11	31.5	30.2	38.4
10	44.4	39.4	51.1
9	53.0	43.7	56.2
8	71.4	57.6	74.9
7	76.2	61.1	77.4
6	83.0	66.9	83.3
5	85.5	71.2	92.1
4	94.3	82.7	100.8
3	91.4	84.4	90.4
2	81.2	79.4	86.8

5

Nonlinear Response History Analysis

Curt B. Haselton, P.E., Ph.D.
John D. Hooper, S.E.

Contents

This chapter illustrates how the 2015 *NEHRP Recommended Provisions* (the *Provisions*) are applied to the design of a reinforced concrete shear wall structure using the updated Chapter 16 nonlinear response-history design approach.

In addition to the *Standard* and the *Provisions* and *Commentary*, the following documents are referenced in this chapter:

- ASCE/SEI 41-13   *Seismic Evaluation and Retrofit of Existing Buildings*
- ACI 318-14   *Building Code Requirements for Structural Concrete and Commentary*
- PEER TBI   *Guidelines for Performance-Based Seismic Design of Tall Buildings*
- LATBSDC   *An Alternative Procedure for Seismic Analysis and Design of Tall Buildings Located in the Los Angeles Region.*
- SF AB-083   *Requirements and Guidelines for the Seismic Design of New Tall Buildings using Non-Prescriptive Seismic-Design Procedures*
- Eq. Spectra   *Response-History Analysis for the Design of New Buildings: Part I - Development of Recommendations for the NEHRP Provisions and the ASCE/SEI 7 Standard, Earthquake Spectra (in review).*
- Eq. Spectra   *Response-History Analysis for the Design of New Buildings in the NEHRP Provisions and ASCE/SEI 7 Standard: Part II – Structural Analysis Procedures and Acceptance Criteria, Earthquake Spectra (near submission).*
- Eq. Spectra   *Response History Analysis for the Design of New Buildings: Part III - Example Applications to Illustrate the Recommended Methodology, Earthquake Spectra (accepted for publication).*

The nonlinear response-history analysis from this chapter was carried out using Perform 3D and the linear structural analysis was carried out using the ETABS Building Analysis Program. Both programs were developed by Computers and Structures, Inc., Berkeley, California.

5.1 OVERVIEW OF EXAMPLE AND GENERAL REQUIREMENTS

5.1.1 Summary of the Chapter 16 Design Approach

In the 2015 revision of the *Provisions* and in the 2016 revision of ASCE 7, there was a multi-year effort to rewrite Chapter 16, *Seismic Response-History Procedure,* to include detailed, consensus-based, procedures for using nonlinear dynamic analysis in the performance assessment and design of new buildings. The new Chapter 16 replaces earlier versions that effectively date from 1997, when the response history analysis (RHA) approach was introduced to the National Earthquake Hazard Reduction Program (NEHRP) Provisions.

The updated Chapter 16 RHA procedure uses the following framework:

1. Ensure that the design conforms to all applicable requirements of the ASCE/SEI 7 Standard. Exceptions to these requirements, other than those explicitly incorporated in the procedures, as indicted below, must be handled under the criteria of ASCE 7 Section 1.3 for performance-based designs.
2. Perform a linear code-level (i.e., DE-level) evaluation using either the equivalent lateral force procedure of ASCE/SEI 7 Section 12.8 or response spectrum method of Section 12.9, including the minimum base shear requirement. The purpose of this step is to enforce the same minimum levels of strength required for all buildings and to provide a basic evaluation of torsional behavior. Bearing in mind that further requirements will be imposed in the MCE_R-level evaluation, the following modifications are incorporated to the procedures of Section 12.8 and 12.9:
   - For Risk Category I, II, and III structures, the drift limits of Section 12.12.1 do not apply.

- For Risk Category IV structures, the drift limits are 125 percent of those specified in Section 12.12.1.
- The overstrength factor, Ω_0, is permitted to equal 1.0 for the seismic load effects of Section 12.4.3.
- The redundancy factor, ρ, is permitted to equal 1.0.

3. A service-level evaluation (which is required by some current guideline documents such as PEER-TBI 2009 and LATBSDC 2014) is not required.
4. Perform a nonlinear MCE_R-level evaluation. The step is intended to (a) demonstrate that the building has predictable and stable response at MCE_R ground shaking levels and (b) determine the deformation demands on ductile elements and forces for the design of force-controlled (brittle) components. Fulfillment of the acceptance criteria implicitly demonstrates that the building has equivalent or better seismic resistance as compared with designs using the basic Chapter 12 requirements.
5. Complete an independent design review of the work performed for the above steps.

The code-level evaluation provides a clear basis for establishing minimum strength and stiffness and this step takes care of many of the detailed design safeguards that are then not required for the MCE_R-level evaluation. For example, the code-level evaluation includes provisions for accidental torsion, enforcement of multiple gravity load combinations, and wind loads, in addition to many other requirements. Accordingly, many of these design safeguards are not expressly required in the MCE_R-level RHA evaluation.

Following from Section 11.1.3 and Section 12.6, Chapter 16 applies to the analysis and design of building structures which comply with the requirements of Chapters 11 and 12. Some exceptions to the Chapter 11-12 ASCE/SEI 7-16 design requirements will be taken later in this design example. This design formally invokes Section 1.3.1.3 of ASCE/SEI 7-16 (i.e. "alternate means and methods") and then acceptable performance is demonstrated through the Chapter 16 nonlinear response-history analysis. The reason for inclusion of a design which takes exception to additional provisions of Chapter 12 beyond those explicitly allowed in Chapter 16 is because this is a common justification of the added engineering effort Chapter 16 requires. The additional exceptions taken would need to be agreed upon by the peer reviewers and the authority having jurisdiction over the design.

5.1.2 Description of Example Building and Site

The design example is located in San Francisco, California, just south of Market Street. The project is comprised of four residential structures resting on a common sub-structure and podium. The structural design for the two tall towers is performed using the requirements outlined in ASCE/SEI 7-16 Chapter 16.

The four structures consist of the following list of buildings; Tower B is the subject of this design example:

- Southeast High-Rise (Tower D): 37 stories and 350 feet tall
- Northeast Low-Rise (Plaza A): 8 stories and 85 feet tall
- Northwest High-Rise (Tower B): 42 stories and 400 feet tall
- Southwest Low-Rise (Plaza C): 8 stories and 85 feet tall

Figure 5.1-1 provides an overall rendering of the project and Figure 5.1-2 provides a plan view.

Figure 5.1-1. Three-Dimensional Rendering of the Example Project
[Editorial Note: Figure permissions – figure supplied directly by J.D. Hooper]
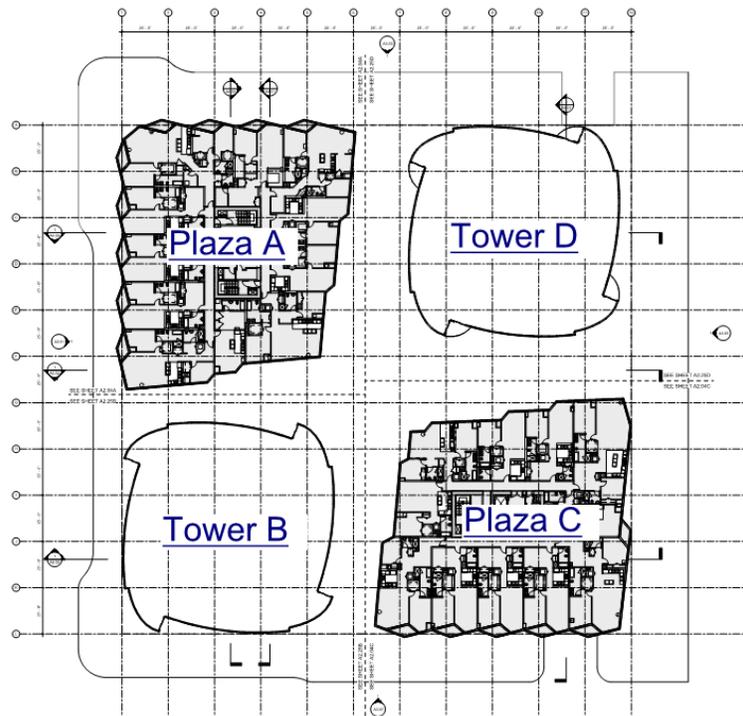
Figure 5.1-2. Example Project Plan Overview

The building site location is in the transition region of the seismic hazard maps (where the $S_S = 1.5g$ and $S_1 = 0.6g$ caps govern most of the design spectral values) and the site is considered by ASCE/SEI 7-16 to be a near-fault site (because it is within 15 km of a large fault, as discussed further in Section 3.4.2). The following provides a summary of some additional details for this site location.

Site Class: C
$S_S = 1.5g$, $S_1 = 0.6g$
$S_{DS} = 1.0g$, $S_{D1} = 0.52g$
Seismic Design Category: D

5.1.3 Linear Analysis for Initial Proportioning

In accordance with the Section 16.1.2 requirements, a modified linear analysis is used to do the initial proportioning of the building and to enforce some important design requirements that are not enforced as part of the nonlinear response-history analysis step (e.g. minimum base shear requirements, etc.). This design step is further explained in Section 5.1.3.4.3.

5.1.4 Project-Specific Design Criteria

In accordance with the Section 16.1.4 requirements, project-specific design criteria shall be created and approved by the independent structural design reviewer(s) and the Authority Having Jurisdiction. The design criteria shall be completed prior to performing the nonlinear analysis. This section provides a comprehensive example of the content that should typically be included in such a project-specific design criteria. Much of the information in the design example chapter is provided as part of this project-specific design criteria section (because this is what is provided to the design review team prior to performing the nonlinear analysis); this detail is then referenced in many of the later sections of this chapter (e.g. sections on modeling, etc.).

5.1.4.1 Building Overview

5.1.4.1.1 Geotechnical Characteristics and Foundation. The geotechnical report and seismic hazard analysis for the project indicate that the site is underlain with subsurface materials of fill, dense and silty sands, and bedrock. Beneath the upper sands including the fill, the site is underlain by dense to very dense sand, silty sand, and clayey sand of the Colma Formation. The Colma Formation was encountered at an average depth of about 30-feet across the majority of the site (except for the south boundary where the layer slopes up). Below the Colma Formation exists colluvium, residual bedrock, and bedrock layers of the Franciscan Complex Melange.

Tower B will be founded on concrete mat foundations of varied thicknesses and will rest directly on the bedrock. Recommended allowable bearing on the Colma formation and/or bedrock is anticipated to be in the 10,000 to 15,000 pounds per square foot (psf) range.

5.1.4.1.2 Superstructure. Lateral forces for Tower B are resisted by coupled concrete structural shear walls placed around the central elevator and stair cores. It was elected to exclude secondary framing, so as to reduce story heights and provide better views from the windows of the building. The combination of the building height and the lack of a dual system resulted in this building not meeting the traditional requirements of ASCE/SEI 7 Chapters 11-12 and, therefore, the design acceptability is being demonstrated though the new Chapter 16 Response-History Analysis procedure. Table 5.1-1 provides a more complete summary of structural components and expected sizes.

Table 5.1-1. Anticipated Structural System, Components, and Sizes

Element	Structural System and Sizes
Foundation	Concrete mat foundation of varied thicknesses
Shear Walls	Walls of varied thickness, 24 to 32 inches thick
Coupling Beams	Diagonally reinforced concrete or embedded composite steel coupling beams
Columns	Reinforced concrete columns ranging from approximately 24"×24" to 40"×40"
Basement Walls	Reinforced concrete basement walls around the perimeter of the below-grade parking levels, 18 inches thick on average
Below-Grade Slabs	10-inch-thick reinforced concrete flat slabs
Grade-Level Diaphragm Slab	12 to 15-inch-thick reinforced concrete flat slab
Podium-Level Slab	12-inch thick reinforced concrete flat slab
Residential Slabs	8-inch-thick post-tensioned concrete flat slabs
Amenity Deck Roof Slab	12-inch-thick reinforced concrete slab
Unoccupied Roof Slab	10-inch-thick reinforced concrete slab

5.1.4.2 Basic Seismic Design Criteria and Load Combinations

5.1.4.2.1 Seismic Design Criteria. The seismic loads pertaining to Tower B are in accordance with the building code requirements and are summarized in Table 5.1-2.

Table 5.1-2. Seismic Design Criteria

Parameter	Value
Building Location	San Francisco, California
Occupancy Category	II
Importance Factor (I_e)	1.0
Mapped Spectral Parameters	$S_S = 1.5g$ $S_1 = 0.6g$
Site Class	C
Site Coefficients	$F_a = 1.0$ $F_v = 1.3$
Spectral Response Coefficients	$S_{ds} = 1.0g$ $S_{d1} = 0.52g$
Seismic Design Category	D
Lateral System	Bearing Wall System – Special Reinforced Concrete Shear Walls
Response Modification Coefficient, R	6
Seismic Response Coefficient, C_s	0.050 (12.8-6 governs)
Design Base Shear, V	3909 kips
Analysis Procedure Used	Modal Analysis Procedure

5.1.4.2.2 Gravity Loads. The following loads in Table 5.1-3 are in addition to the self-weight of the structure. The minimum loading requirements have been taken from Table 4-1 of ASCE/SEI 7-16 (and Table 1607.1 of the SFBC). For more detailed gravity loading assumptions, refer to the load maps included in the structural drawings. Live loads are reduced where permitted in accordance Section 4.8 of ASCE/SEI 7-16. Loads are given in pounds per square foot (psf).

Table 5.1-3. Gravity Loads

Use	Live Loading (psf)	Superimposed Dead Loading (psf)
Amenity/Heath Club	100	30
Corridor/Stairs/Exit Facilities	100	15
Elevator Machine Room	as indicated on plans	10
Kitchen/Retail	100	35
Light Storage	125	10
Loading Dock	250 or AASHTO HS-20	70 (includes 60 psf built-up slabs, where exist)
Mechanical/Electrical	125	15
Meeting Room/Lobbies/Assembly	100	30
Parking (Garages)	40 (reducible)	5
Pool	100	320 (assumes 4 feet of water)
Residential	40 + 15 partition (reducible)	15
Residential Balconies (less than 100 square feet)	60	5
Roof	20	25

5.1.4.2.3 Load Combinations

Design Earthquake Load Combinations

The design basis event is analyzed with modal response spectrum analysis per the code requirements. The Design Earthquake (DE) load combinations are show in Table 5.1-4 and follow the strength design load combinations.

Table 5.1-4. Design Earthquake Load Combinations

Identifier	Load Combination	Code Reference
Load Combination 2	$(1.2+0.2S_{DS}) D + Q_E + (f_1 L + f_2 S)$	SFBC 1605.2.1 (16-5)
Load Combination 3	$(0.9–0.2S_{DS}) D + Q_E$	SFBC 1605.2.1 (16-7)

Where: D = dead load
L = reduced live load
f_1 and f_2 = factors per the SFBC, Section 1605.2
Q_E = horizontal earthquake load (DE response spectrum)
S = snow load

Seismic directional effects are considered as follows:

$E_{hX} = \pm 1.0 \ E_x \pm 0.3 \ E_y \pm T$

$E_{hY} = \pm 0.3 \ E_x \pm 1.0 \ E_y \pm T$

Where: E_x and E_y = earthquake forces in the primary structural directions
T = the actual and accidental torsion per the ASCE/SEI 7-16, Section 12.8.4.2

Maximum-Considered Earthquake Load Combinations

Table 5.1-5 shows that the nonlinear response history analysis (NLRHA) utilizes one load combination for the MCE event. This load combination is used for each of the eleven earthquake records. Per ASCE/SEI 7-16 Section 16.3.4, accidental torsion is not considered in this analysis because the linear analysis per Chapter 12 indicates that the building does not have a Type 1A torsional irregularity.

Table 5.1-5. MCE Load Combination for NLRHA

Identifier	Load Combination
Load Combination 1	1.0D + 0.5L +1.0E with L defined in Section 16.3.2

Where: D = dead load
L = unreduced live load
E = earthquake record (pairs of orthogonal ground motion components)

5.1.4.3 Response Spectra and Ground Motions. A description of the response spectra and approach to ground motion selection and scaling is an important component of the project-specific design criteria. To avoid duplicating materials in this design example, this information is contained in Section 5.2 and Section 3.4.2.

5.1.4.4 Design Approach. This section of the project-specific design requirements summarize the design approach. Figure 5.1-3 provides an overview of the ASCE/SEI 7-16 Chapter 16 design approach.

To demonstrate that the design is capable of providing appropriate seismic performance, a two-step analysis and design procedure is performed:

PRELIMINARY DESIGN PHASE (DE)

ELASTIC ANALYSIS AND DESIGN

Design structural components that are anticipated to yield based on the code-level demands, satisfying minimum strength requirements of the SFBC.

Perform initial design for structural components that are to remain essentially elastic (using amplification factors based on lessons learned on previous projects).

The design conforms to all Building Code provisions except those noted in the following section of this example.

VERIFICATION PHASE (MCE)

NON-LINEAR TIME HISTORY ANALYSIS VERIFICATION

Design verification using a three-dimensional non-linear response history analysis (NLRHA) considering the MCE. The initial design is adjusted as required to meet the acceptance criteria.

Figure 5.1-3. Overview of ASCE/SEI 7-16 Chapter 16 Design Approach

5.1.4.4.1 Code Reference and Exceptions. This example building is designed in accordance with ASCE/SEI 7-16 Chapter 16 requirements. In the linear analysis step of the procedure (Section 16.1.2), the following exceptions to the code requirements are taken in this example design, and acceptable performance is demonstrated through the nonlinear response-history analysis. As stated above, based on these exceptions being taken, this design is formally invoking Section 1.3.1.3 of ASCE/SEI 7-16 (i.e. "alternate means and methods"); then acceptable performance is being demonstrated through the Chapter 16 nonlinear response-history analysis.

Maximum Height Limit per ASCE/SEI 7-16, Table 12.2-1, Building Frame Systems, Special Reinforced Concrete Shear Walls. This table limits the height of special reinforced concrete wall systems to 160 feet. The proposed structural system is a ductile reinforced concrete shear wall system with a maximum height above this limit.

Embedded Steel Coupling Beam detailing as part of Composite Special Shear Walls (C-SSW) per AISC 341-10, Section H.5. Coupling between concrete wall piers will utilize embedded steel link beams following the guidelines as discussed in Section H.5 of AISC 341-10, as modified by the ongoing research at UCLA by Motter et al. (2013 and 2012).

Response Modification Coefficient, R per ASCE/SEI 7-16, Section 12.2. Given the nonlinear analysis that is being performed to validate the performance-based design approach for the PBD Towers, an R-Value of 6 is utilized for the response modification coefficient in the DE code

equivalency check. This value is associated with a "building frame system" rather than a "bearing wall system" seismic force-resisting system.

5.1.4.4.2 Hierarchy of Yielding in the Structural System. The Chapter 16 design method is based on component actions being separated into those that are expected to have ductility capacity and be designed to yield (deformation-controlled) and those that are brittle actions that are designed to remain essentially elastic (force-controlled).

The following structural elements are designed and modeled as deformation-controlled component actions, in anticipation of non-linear response during earthquake shaking:

- Shear wall coupling beams – primary lateral system fuse
- Shear wall flexural reinforcing – primary lateral system fuse
- Flexural yielding of "outrigger slab" – secondary effect due to displacement compatibility of gravity system

The following structural elements are designed and modeled as force-controlled component actions, such that they should remain essentially elastic during the non-linear response of the items listed above:

- Shear wall shear
- Diaphragms and collectors
- Basement walls
- Foundations
- Column axial behavior

5.1.4.4.3 Initial Design Based on Design Earthquake Linear Analysis. The linear analysis design step using the design earthquake ground motion level (per ASCE/SEI 7-16 Section 16.1.2) is used to proportion and design many aspects of the building. The following list summarizes the basic approach to this analysis step and the design approach for the various structural components.

Elastic Analysis at DE Level:

- Working in collaboration with the Architect, define the building's structural system and select the preliminary structural member sizes.
- Prepare the three-dimensional linear-elastic computer model including P-delta effects.
- Calculate the building's seismic mass.
- Determine the code base shear per the code requirements.
- Subject the model to the DE site-specific elastic response spectrum, scaled in accordance with ASCE/SEI 7-16, Section 12.9.
- Determine the torsional amplification factors per ASCE/SEI 7-16, Section 12.8.4.3.

Shear Wall Coupling Beam Design:

- Design the embedded steel coupling beams in accordance with Section H.5 of AISC 341-10.

Shear Wall Flexural Strength Design:

- Establish location and extent of the primary flexural yielding region based on the critical demand location determined in the DE analysis. Peak flexural demands are expected to occur immediately above the ground-floor diaphragm level since the above-grade slabs are all seismically isolated at the four individual buildings.
- Perform gravity framing analysis for vertical elements to determine dead and live loads.

- Design the core wall vertical reinforcement using forces calculated from the DE-level analysis.

Shear Wall Shear Design:

- Design the shear wall horizontal reinforcement per ACI 318-14, section 21.9.4.1 using specified material strengths and code-specified phi factors. Note that this step is only a preliminary design step and the strength will be designed in accordance with the ASCE/SEI 7-16 Section 16.4.2.1 criteria for force-controlled actions (and note that the force-controlled shear wall design criteria clearly controls the required shear strength of the wall).

Core Wall Confinement:

- Provide full confinement per ACI 318, Section 21.9.6.4(c) for the entire cross section of the shear walls from the foundations up to the level at which full confinement is no longer required. Full confinement will, at a minimum, be provided for at least a minimum of four levels above the grade-level diaphragm.
- Consistent with the code requirements, determine where boundary elements are required per ACI 318, Section 21.9.6.3. Where required, provide confinement ties.
- Where full confinement is not required, provide intermediate-level confinement at wall ends and corners up to 75 percent of the height of the tower. Intermediate-level confinement will consist of #4 hoops and cross-ties spaced at 6 inches on center vertically and 12 inches on center horizontally. Additionally, the intermediate-level confinement will be provided where the density of vertical reinforcement exceeds $f_y/400$ per ACI 318, Section 21.9.6.5(a).

5.1.4.4.4 Nonlinear Response-History Verification for MCE Ground Motion. The last step of the Chapter 16 design process is to create a nonlinear structural model and ensure compliance with all of the acceptance criteria of Section 16.4. For this design example, this step of the process is demonstrated in later sections of this chapter.

5.1.4.5 Structural Modeling

5.1.4.5.1 Material Properties. Tables 5.1-6 through 5.1-8 provide the nominal and expected material properties for the various materials used in the construction of this example building. The nominal values are used in the linear design earthquake step and the expected values are used when creating the nonlinear model for response-history analysis.

Table 5.1-6. Concrete Properties

Member	Nominal f'$_c$	Expected f'$_c$ **
Basement Walls	5.0 ksi	6.5 ksi
Foundation Mats	6.0 ksi	7.8 ksi
Non-post-tensioned Beams and Slabs	5.7 ksi	7.4 ksi
Post-tensioned Floor Slabs	5.7 ksi	7.4 ksi
Columns	6.0 ksi	7.8 ksi
	8.0 ksi	10.4 ksi
Shear Walls	6.0 ksi	7.8 ksi
	8.0 ksi	10.4 ksi

** Assumes 1.3 x f'$_c$ expected concrete strength.

Table 5.1-7. Reinforcement and Post-Tensioning Properties

Standard	Nominal f$_y$	Expected f$_y$	Expected f$_u$
ASTM A615 Grade 60	60 ksi (non-seismic)	N/A	N/A
ASTM A706 Grade 60	60 ksi (seismic)	70 ksi	105 ksi
ASTM A615 Grade 75	75 ksi (where noted on the drawings)**	85 ksi	130 ksi

** Excluded from carrying seismic and/or axial forces in the primary LFRS.
Expected to be considered for shear wall confinement reinforcing, column confinement reinforcing, and mat foundation reinforcing.

Table 5.1-8. Post-Tensioned Tendon Properties

Standard	Nominal f$_u$	Expected f$_u$
0.5-inch-diameter, 7-wire strand	f$_{pu}$ = 270 ksi	N/A

5.1.4.5.2 Linear Model. A complete, three-dimensional elastic computer model is created using ETABS. The model includes the shear walls, ground-level diaphragms, and basement walls. The diaphragms and walls are modeled using shell elements. The coupling beams are modeled using frame elements. Openings through the shear walls are modeled with separate wall elements coupled together with concrete and/or steel link beams.

The model includes all of the structural elements (core walls, diaphragms, and basement walls) down to the top of the mat foundation with all analytical nodes fixed at the top of the mat. Soil springs are not included in the elastic models.

The elastic model is used for both the DE-level design and the wind analysis. The stiffness parameters for the various elements are varied between the two analyses. The concrete strengths and member stiffnesses used in the two linear models are listed in Table 5.1-9.

Table 5.1-9. Linear Modeling Assumptions

Concrete Element	Stiffness Assumptions DE-Level Analysis (Design)	Stiffness Assumptions Wind Analysis
Specified versus Expected Concrete Strength	Specified concrete strength used to calculate member stiffness	Expected concrete strength used to calculate member stiffness
Shear Walls	Flexural – 0.5Ig Shear – 1.0A	Flexural – 0.75Ig Shear – 1.0A Axial – 1.0A
Basement Walls	Flexural – 0.5Ig Shear – 1.0A	Flexural – 0.75Ig Shear – 1.0A
Concrete Coupling Beams	Flexural – 0.2Ig Shear – 1.0A	Flexural – 0.5Ig Shear – 1.0A
Steel Coupling Beams	Flexural – 0.6Ig Shear – 1.0A	Flexural – (based on ACI transformed section) Shear – 1.0A
Ground Level Diaphragm	Flexural – 0.25Ig Shear – 0.5A	Flexural – 0.5Ig Shear – 1.0A
Concrete Columns	Not included in code design	Flexural – 0.5Ig Shear – 1.0A Axial – 1.0A
Outrigger Slabs	Not included in code design	Flexural – 0.35Ig Shear – 1.0A

5.1.4.5.3 Nonlinear Model. A nonlinear verification model is created using CSI Perform-3D. The model includes inelastic member properties for elements that are anticipated to be loaded beyond their elastic limits. These include the coupling beams, shear wall flexural behavior, and "slab-beams" to account for any outriggering effect of the flat slabs. Elements that are assumed to remain elastic are modeled with elastic member properties. These include shear wall shear behavior, diaphragm slabs, columns, and basement walls. Elements modeled elastically are verified to remain essentially elastic.

The boundary conditions at the base of the core walls in the non-linear model were developed to include the effects of foundation flexibility. Vertical and rotational stiffness of the mat foundation were approximated at the base of each tower using a SAFE model with non-linear soil springs. This was then incorporated into the Perform model through four vertical spring elements at each tower core, slaved to the core and located at a distance from the centerline of the core that would provide the correct rotational resistance. The nodes of all the basement walls are pinned (vertical and horizontal translation supports) at

the level of the mat foundation. The nodes of the columns are fixed at the level of the mat foundation. Horizontal resistance of the soil is ignored. The damping effects of the soil are neglected.

The Chapter 16 requirements do not explicitly require design sensitivity studies, but important modeling assumptions should be assessed to determine the extent to which the assumption affects the predicted structural responses and the implied performance. One such important modeling assumption is the stiffness of the major transfer diaphragms in the building (which connect the buildings together at grade and below grade). To assess the modeling assumptions for these important components, two non-linear models are developed which are identical other than the stiffness of the diaphragms which connect the shear walls together. These two models are intended to envelop the behavior related to the potential variation in diaphragm stiffness. One model (stiff) sets the diaphragms to 25 percent gross section properties in shear and 25 percent gross section properties in flexure. The other model (soft) will set the diaphragms to 10 percent gross section properties in shear and 10 percent gross section properties in flexure.

Demands are calculated from the NLRHA and are compared against the acceptance criteria, for verification of design. Where parameters of interest do not meet the acceptance criteria, elements are redesigned and reanalyzed until acceptable performance is achieved. The design parameter is deemed acceptable when it meets the acceptable criteria noted above for both sets of the 11 short period and 11 long period ground motion analysis results (see Section 5.2 and 3.4.2 for more detail on the ground motion sets).

5.1.4.6 Acceptance Criteria

Table 5.1-10 provides the specific acceptance criteria used for this design example, as based on ASCE/SEI 7-16 Section 16.4. These criteria are provided here as part of the project-specific design requirements and are then verified later in Section 5.4.

Table 5.1-10. MCE-Level Acceptance Criteria

Item	Value
Story Drift	A 4 percent story drift, taken as the average of each of the sets of 11 analyses, is required by Chapter 16. Even so, for this project, the design team chose to use a more stringent 3 percent drift limit (to be consistent with more stringent requirements for design of tall buildings; e.g. PEER TBI 2009).
Residual Story Drift	Not limited because there are no requirements regarding this in Chapter 16.
Coupling Beam Rotation (embedded composite steel)	0.06 radian rotation limit, taken as the average of each of the sets of 11 analyses (from Motter et. al. 2013 and 2012).
Shear Wall Reinforcement Axial Strain*	Rebar tensile strain is 0.05 in tension and 0.02 in compression, taken as the average of each of the sets of 11 analyses.
Shear Wall Concrete Axial Strain*	Fully confined concrete compression strain is 0.015, taken as the average of each of the sets of 11 analyses.
Shear Wall Shear	Taken as a critical force-controlled component action, so complies with ASCE/SEI 7-16 Equation 16-1 with $\gamma = 2.0$.
Grade Level Diaphragm	Taken as a critical force-controlled component action, so complies with ASCE/SEI 7-16 Equation 16-1 with $\gamma = 2.0$.
Basement Walls	Taken as a critical force-controlled component action, so complies with ASCE/SEI 7-16 Equation 16-1 with $\gamma = 2.0$.

* Strain gage lengths in wall elements are set to the effective hinge zone length (min. of width of adjacent wall pier and the story height).

5.2 GROUND MOTIONS

The ground motion selection and scaling for this design example can be found in Section 3.4.2.

5.3 STRUCTURAL MODELING

Much of the structural modeling information has already been presented as part of the comprehensive example project-specific design criteria documentation in Section 5.1.3. This modeling section provides some additional modeling detail but also refers back to the subsections of Section 5.1.3, so as to not repeat material.

5.3.1 Overview of Modeling

5.3.1.1 Linear Model

A complete, three-dimensional elastic computer model is analyzed using ETABS, as described previously in Section 5.1.3.5.2. This linear model is used for both the DE-level design and the wind analysis.

5.3.1.2 Nonlinear Model

5.3.1.2.1 Overview. A nonlinear verification model is created using CSI Perform-3D, as described previously in Section 5.1.3.5.3, and as depicted in Figures 5.3-1 and 5.3-2. The model includes inelastic member properties for elements that are anticipated to be loaded beyond their elastic limits. These include the coupling beams, core wall flexural behavior, and "slab-beams" to account for any outriggering effect of the flat slabs. Structural elements are modeled as accurately as possible using expected material properties. Core wall shear behavior, diaphragm slabs, columns, and basement walls are expected to remain elastic and are modeled with elastic properties. The modeling also includes two model variants, as described in Section 5.1.3.5.3, which capture the range of possible stiffness of the transfer diaphragms that connect the shear walls together.
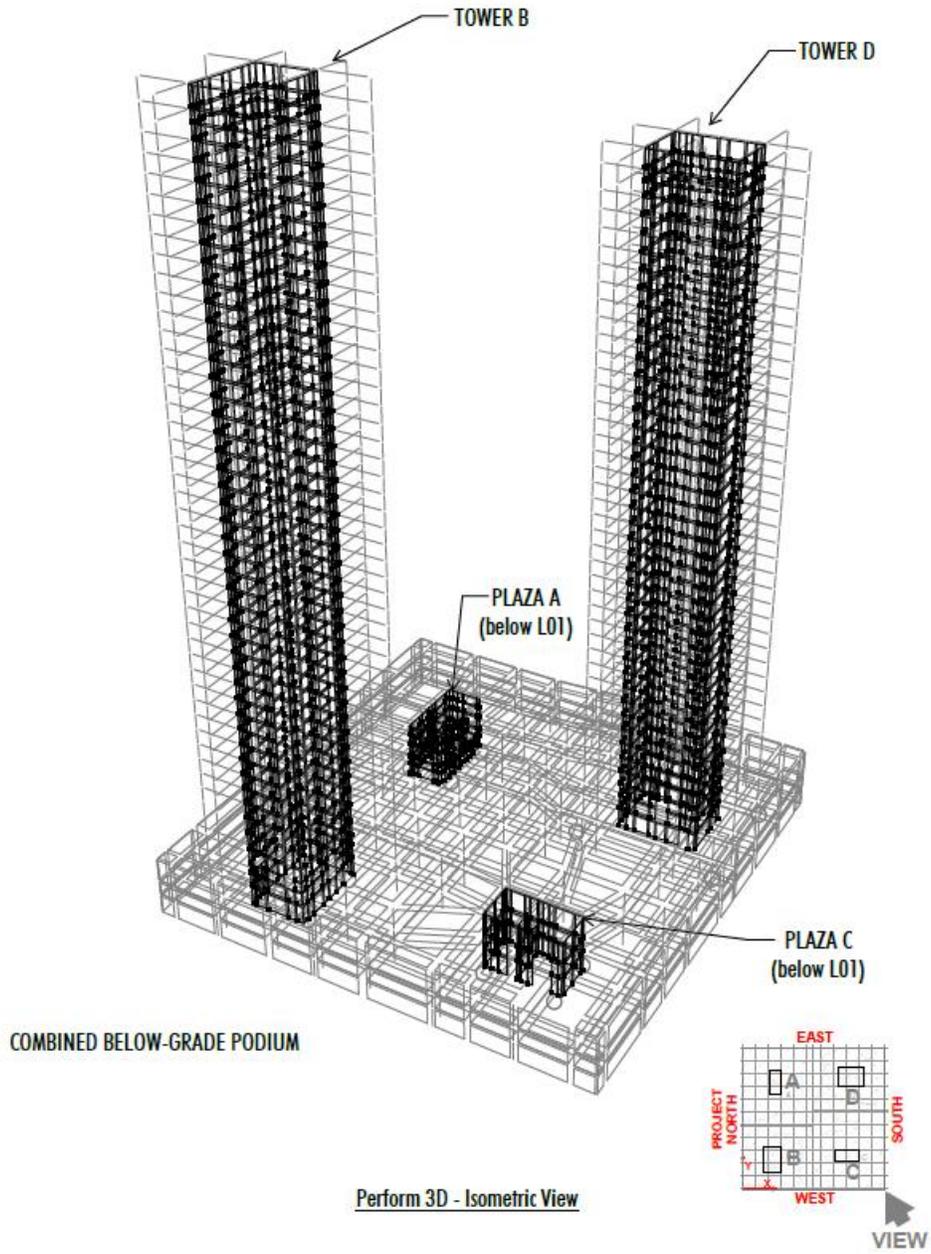
Figure 5.3-1. Isometric View of Nonlinear Model
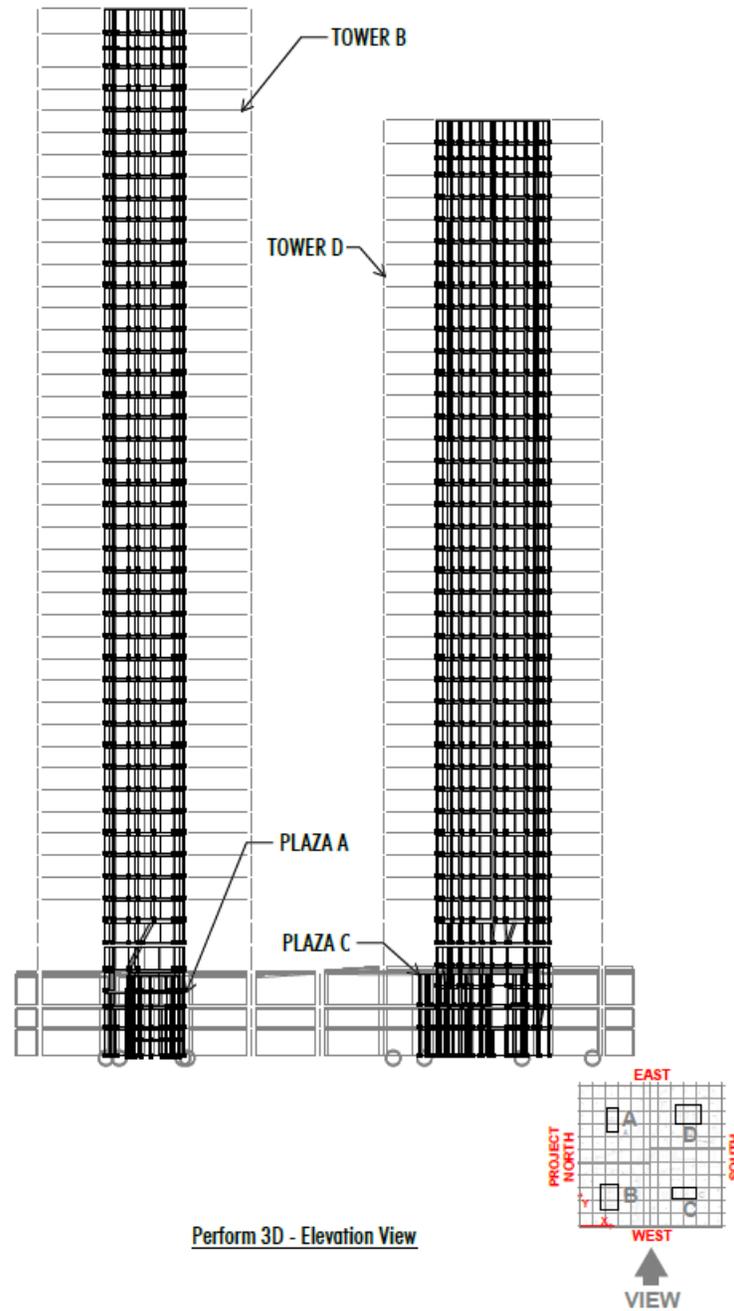
Figure 5.3-2. Elevation View of Nonlinear Model

5.3.1.2.2 Definition of Inelastic Properties of the Gravity Slab Outrigger System. The effect of slab micro-outriggering is included in the model through the inclusion of wide, shallow slab-beams connecting the core walls to concrete columns. The micro-outriggering effects of the slab increases axial demands on the perimeter columns and/or shear in the core walls. Figure 5.3-3 illustrates how gravity columns are "lumped" together and how slab-beams are connected to these columns from the core wall, in order to reflect this outrigger effect in the nonlinear structural model.

Conceptual Representation of a Slab Outrigger System
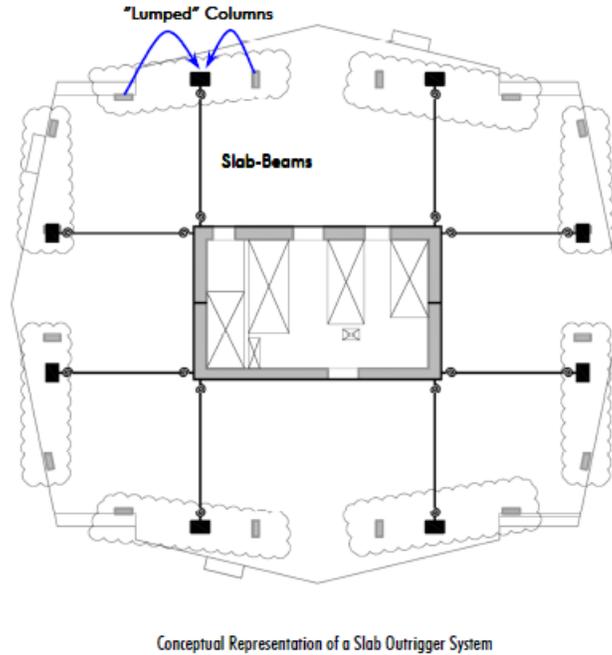
Figure 5.3-3. Conceptual Representation of the Slab Outrigger System

5.3.1.2.3 Treatment of Diaphragms at Transfer Levels. Transfer levels are those levels at which the (4) tower lateral systems are connected one to another and also connected to the perimeter basement wall by way of concrete slab diaphragms. The ground level (L01) and below grade levels (LB2, LB1) are transfer levels and these diaphragms are modeled with coarse finite element meshes of shell elements. Stiffness assumptions for the diaphragms were provided previously in Table 5.1-9.

Two non-linear models are developed which are identical except for the in-plane stiffness of the transfer diaphragms. These two models are intended to envelope the behavior related to the potential variation in diaphragm stiffness. The "stiff" model designates the in-plane shear and flexural stiffness as 25 percent of gross section properties. The "soft" model designates the in-plane shear and flexural stiffness as 10 percent of gross section properties.   These two models are then both used to envelope the demands that are affected by the diaphragm stiffness assumptions.

5.3.1.3 Summary of Model Periods and Mode Shapes

Table 5.3-1 presents the fundamental and second mode periods calculated from the non-linear model of Tower B. Based on these periods, the target anchor periods of 3.75s and 0.75s were selected for use in the ground motion selection and scaling step shown in Section 3.4.2 (to reflect the average first and second mode period ranges of the building).This results in an upper bound period of 7.5s for the ground motion selection and scaling. To achieve 90% modal mass in each direction for this building, a period of 0.15s is required, so 0.15s is the lower-bound period used for ground motion selection and scaling. Figure 5.3-4 also illustrates the mode shapes of the example building (Tower B).

Table 5.3-1. Modal Periods of Models

Mode	Translational X	Translational Y	Rotational Z
First	4.1 sec.	3.4 sec.	2.2 sec.
Second	0.8 sec.	0.7 sec.	0.7 sec.

(a)

(b)
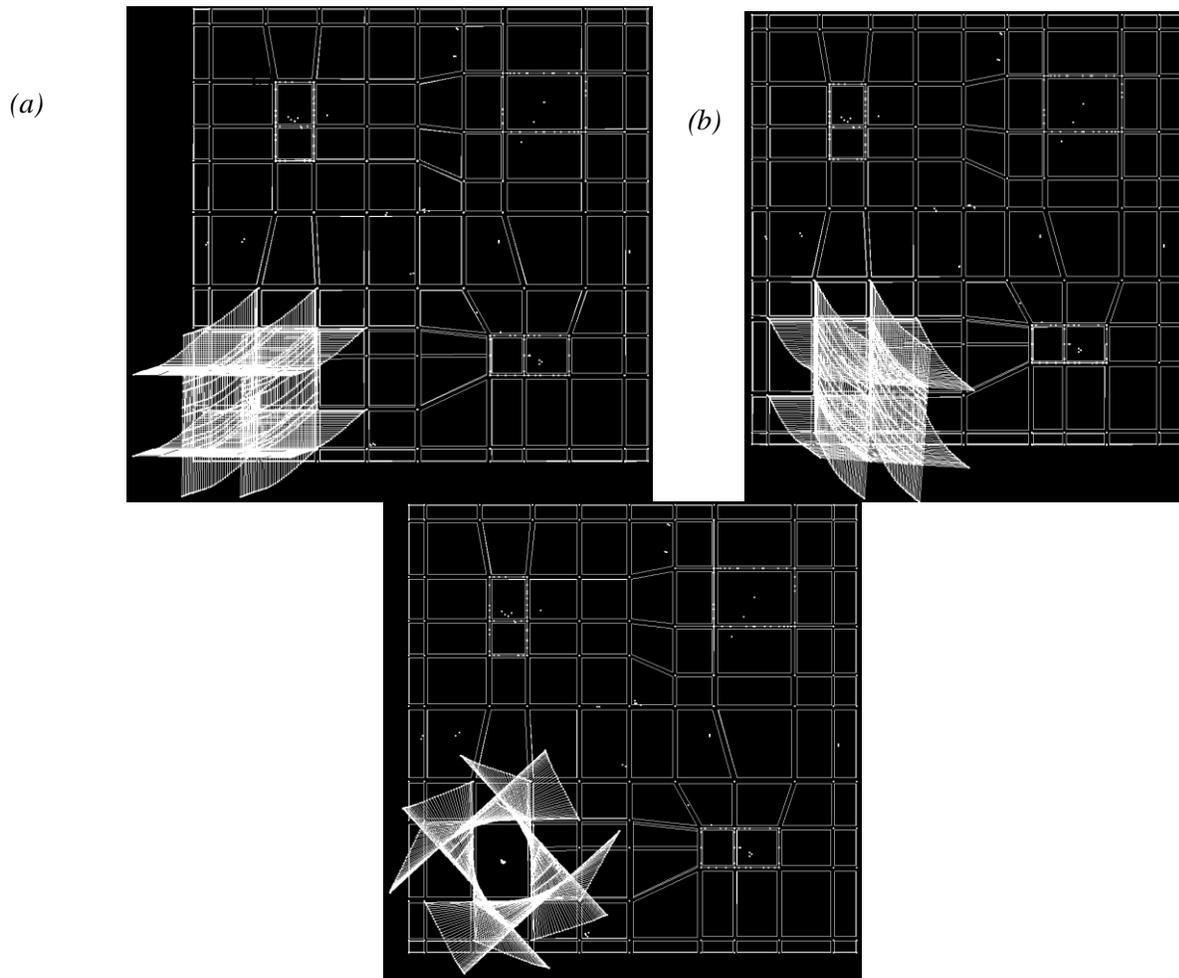
Figure 5.3-4. Mode Shapes of Tower B

5.3.2 Gravity Load

The expected gravity load is used in the nonlinear structural model, in accordance with ASCE/SEI 7-16 Section 16.3.2 and the basic gravity loads were presented previously in Table 5.1-3. The second load combination from Section 16.3.2 is not required because the live loads are small enough and the exception of ASCE/SEI 7-16 Section 16.3.2 was met in this example.

5.3.3 P-Delta Effects

The P-delta effects are captured directly in the nonlinear model by applying the full gravity load to the model, including all non-lateral-force-resisting vertical elements in the model as "leaning" columns, and using a geometric transformation in the numerical analysis which is capable of capturing the P-delta effects.

5.3.4 Torsion

Inherent torsion is accounted for directly in the nonlinear model, through accurate modeling of the mass location throughout the building. Accidental torsion is handled in the linear design step (per ASCE/SEI 7-16 Section 16.1.2) and is not considered in this analysis because this building does not have a Type 1A torsional irregularity (per ASCE/SEI 7-16 Section 16.3.4).

5.3.5 Damping

Elastic viscous damping is included in the model to account for the inherent elastic energy dissipation expected. CSI Perform uses the C=αM+βK model (Rayleigh damping), which assumes that the structure has a non-varying damping matrix, C, where M is the structure mass matrix, K is the initial elastic stiffness matrix, and α and β are multiplying factors. By combining αM and βK damping, it is possible to have essentially constant damping over a significant range of periods. The target damping is 2.5% over a significant range of interest. To achieve this reasonably well, anchor periods of 0.6 seconds (which captures 90% modal mass) and 6.0 seconds (which is slightly above $1.5T_1$) were used and the damping at these periods was set to be 3.0%. This resulted in the damping varying from 2.25% to 3.0% over the period range of interest.

5.3.6 Foundation Modeling and Soil-Structure Interaction

For this example building, the foundation is modeled in detail using SAFE (for the foundation design). Any beneficial effects of soil-structure interaction are neglected (the effect is expected to be small for this type of building).

5.4 ACCEPTANCE CRITERIA

ASCE/SEI 7-16 defines expected performance in the form of acceptable probabilities of collapse based on the occurrence of risk-target maximum considered earthquake (MCE$_R$) shaking. Table 5.4-1 indicates these goals.

Table 5.4-1. Collapse Performance Goals in ASCE/SEI 7-10 (Table C.1.3.1b)

Risk Category	Tolerable Probability of Total or Partial Structural Collapse	Tolerable Probability of Individual Life Endangerment	Ground Motion Level
I or II	10%	25%	MCE$_R$
III	6%	15%	MCE$_R$
IV	3%	10%	MCE$_R$

The Chapter 16 acceptance criteria are intended to provide confidence that the structure's response is stable and within a range predictable by analysis and substantiated by testing. In contrast to the option of requiring explicit demonstration that a building meets the safety goals of Table 5.4-1, the Chapter 16 acceptance criteria maintain a simpler approach of *implicitly* demonstrating adequate performance through a prescribed set of analysis rules and acceptance criteria. This approach requires demonstration that buildings have predictable and stable responses under maximum considered earthquake (MCE$_R$) ground motions, that deformation and strength demands on elements are in the range of modeling validity and acceptable behavior, and that story drifts are within specified limits (where drift limits are more historically based).

In this example, the Method 2 Conditional Mean Spectrum approach was utilized and two resulting ground motion sets were created (as documented in Section 3.4.2). The acceptance criteria are all checked individually for each ground motion set and each set must pass all of the criteria.

5.4.1   Global Acceptance Criteria

5.4.1.1 Unacceptable Response. The primary acceptance criteria are the story drift and element-level criteria. However, unacceptable responses are also checked in the acceptance criteria as a secondary safeguard.   This example building is for a Risk Category II structure and ground motion scaling (not spectral matching) is employed, so one unacceptable response in a suite of 11 motions is acceptable. While this criterion does not ensure that the collapse safety goal has been met, it is intended to screen out designs that are likely not to meet the collapse safety goals.

In this design example, the following four possible types of unacceptable responses were checked and it was found that none controlled:

- Dynamic instability collapse
- Non-convergence
- Response exceeding the valid range of modeling of a deformation-controlled component (where the valid range of modeling can extend a reasonable amount beyond the range of deformations that have been experimentally tested)
- Force demand that exceeding the average strength of a critical force-controlled component

5.4.1.2 Story Drift. Figures 5.4-1 and 5.4-2 show the story drift checks for the X- and Y-direction, respectively. The story drifts are much below the 3% limit and do not control the design for this type of shear wall building. The figures show the checks for both ground motion sets (CMS sets at 0.75s and 3.75s) and both the 10% and 25% bounding stiffness assumptions for the transfer diaphragms. All four of these combinations pass the drift acceptance criteria checks. For this type of building, the design is controlled by the flexural and shear strength designs and the minimum base shear requirements.
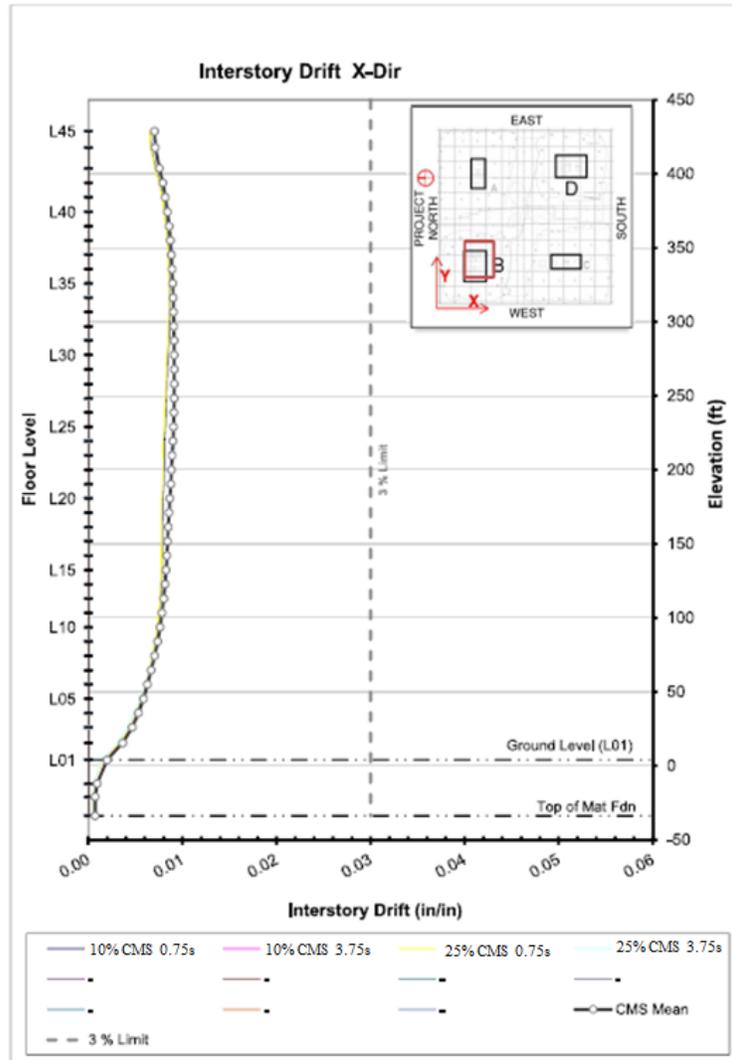
Figure 5.4-1. Acceptance Criteria Checks for Story Drift in the X-direction
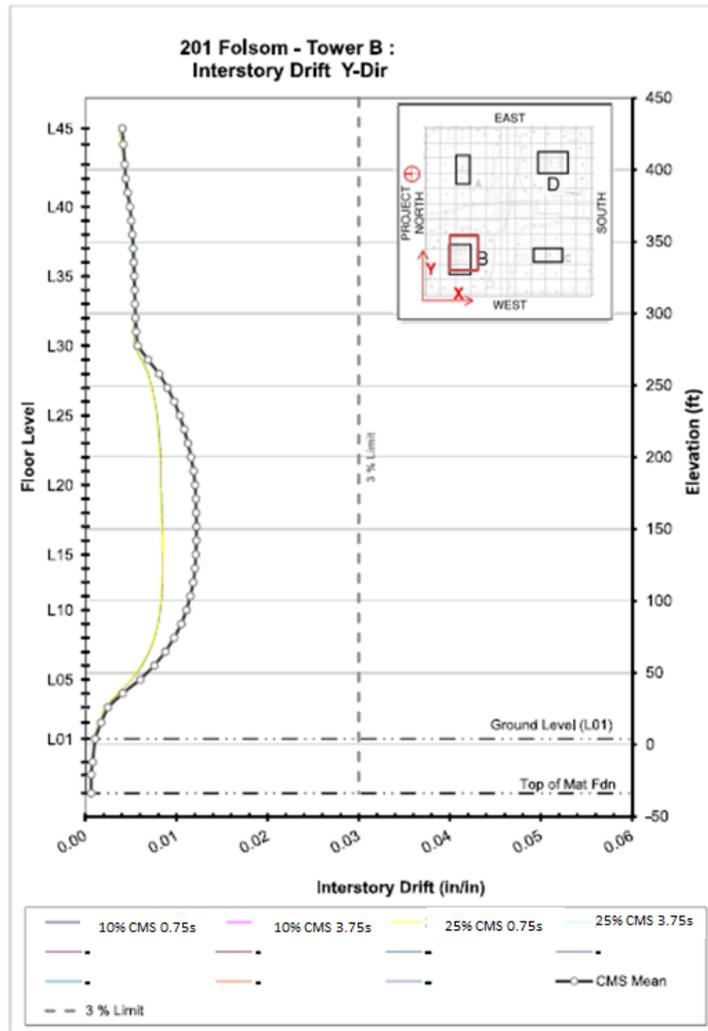
Figure 5.4-2. Acceptance Criteria Checks for Story Drift in the Y-direction

[Note Figures 5.4.1 and 5.4.2 captions use "Story Drift" which is correct, but the figures' internal text uses "interstory drift" which is incorrect.]

5.4.2 Element-Level Acceptance Criteria

Element-level acceptance criteria are dependent on a two-tier classification system. The first tier classifies each action as either force- or deformation-controlled. This classification is done for each element action, rather than each element.

Deformation-controlled actions are those that have reliable inelastic deformation capacity without substantial strength decay. Force-controlled actions are associated with brittle modes where inelastic deformation capacity cannot be assured. Based on the structure of the acceptance criteria, any element action that is modeled elastically must be classified as force-controlled.

The second tier of classification takes the force- and deformation-controlled actions separately and further distinguishes each action based on its consequence of failure (with failure defined as the action exceeding its strength or deformation limit). The consequence classifications are listed and defined as:

- *Critical element actions* - Those in which failure would result in the collapse of multiple bays of multiple stories of the building or would result in a significant reduction of the seismic resistance of the structure.

- *Ordinary element actions* - Those in which failure would result in only local collapse, comprising not more than one bay in a single story, and would not result in a significant reduction of the seismic resistance of the structure.

- *Non-critical element actions* - Those in which failure would not result in either collapse or substantive loss of the seismic resistance of the structure.

The remainder of this section illustrates the classification of component actions for this example and demonstrates the acceptance criteria checks for each important component action.

5.4.2.1 Force-Controlled Actions

5.4.2.1.1 Classification of Force-Controlled Actions. For this example building, the following are examples of the force-controlled actions:

- Shear wall shear (critical)

- Grade level transfer diaphragm (critical)

- Collectors (critical)

- Basement walls (critical)

- Gravity frame column axial behavior (critical)

5.4.2.1.2 Evaluation of Shear Demands in Structural Walls. Figures 5.4-3 and 5.4-4 show the mean shear demands over building height, in both the x- and y-directions. These figures show the mean demands from each of the ground motion sets and each of the transfer diaphragm stiffness assumptions, for a total of four analysis combinations. The core walls throughout the entire height of the building are designed for the worst case shear demand for each of these four analysis cases. For each case, the mean shear demand from the eleven earthquakes multiplied by an amplification factor in accordance with the requirements of Equation 16-1 in Section 16.4.2.1, with the amplification factor being 2.0 for critical components. The shear design meets the criteria of ACI 318, Section 21.9.4 where the shear capacity is defined as follows; note that the capacity is the expected capacity rather than the nominal capacity.

$V_e = Acv (2c f'c + \rho nfy)$

where:

V_e = expected shear strength (not nominal)

Acv = net area of concrete section

f'c = expected concrete strength

ρ_n = ratio of distributed shear reinforcement

fy = expected yield strength of reinforcement

ϕ = code specified strength reduction factor

The minimum shear reinforcement in the core is determined from ACI 318, Section 21.9.2.1:

As,min = 0.0025 Bwd

The shear design from the MCE analysis is found to govern over the shear demands from both the DE and Wind analyses.

Figure 5.4-5 shows the designations of the various shear wall segments in the building. Pier #3 in the East elevation is selected for demonstration a sample shear design for this pier. Table 5.4-2 illustrates the shear design for this pier, showing the results for each story of the building.
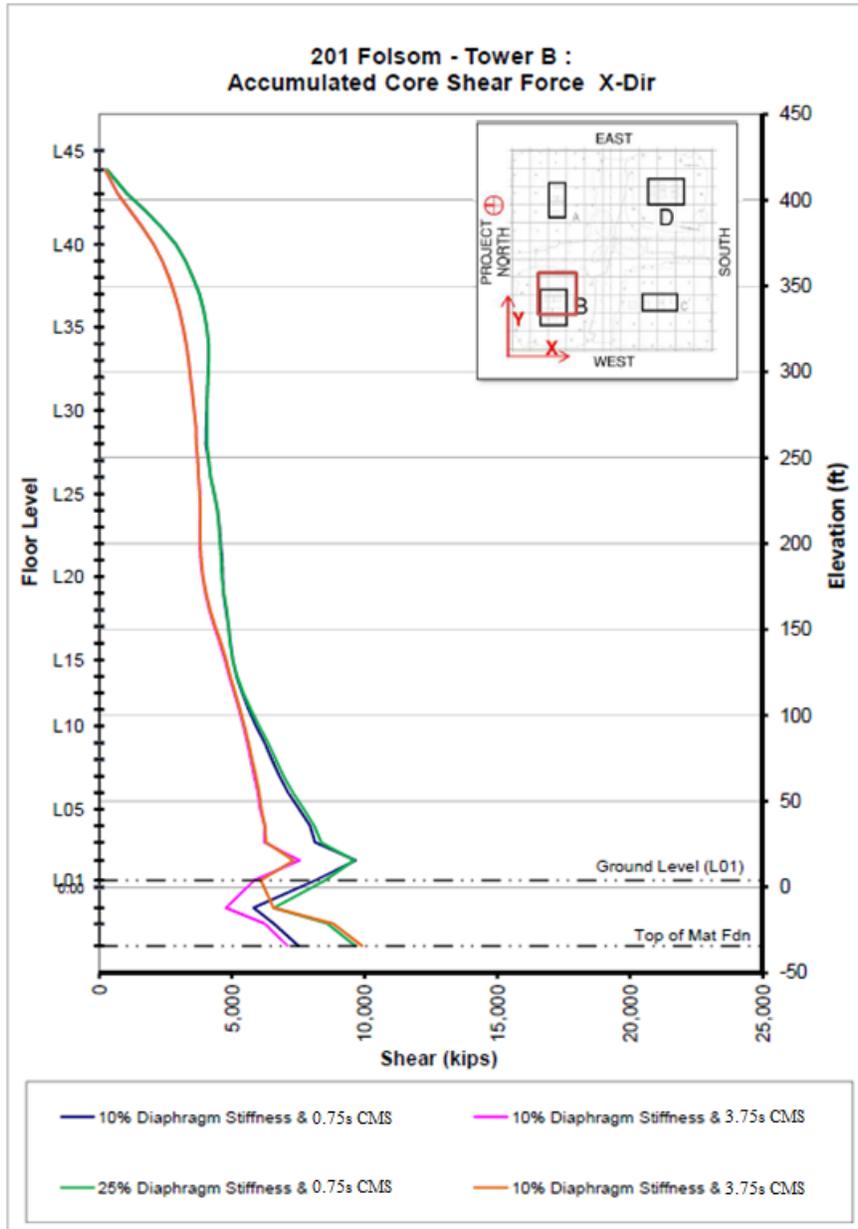
Figure 5.4-3. Acceptance Criteria Checks for Design of Wall Shear Capacity on the X-Direction
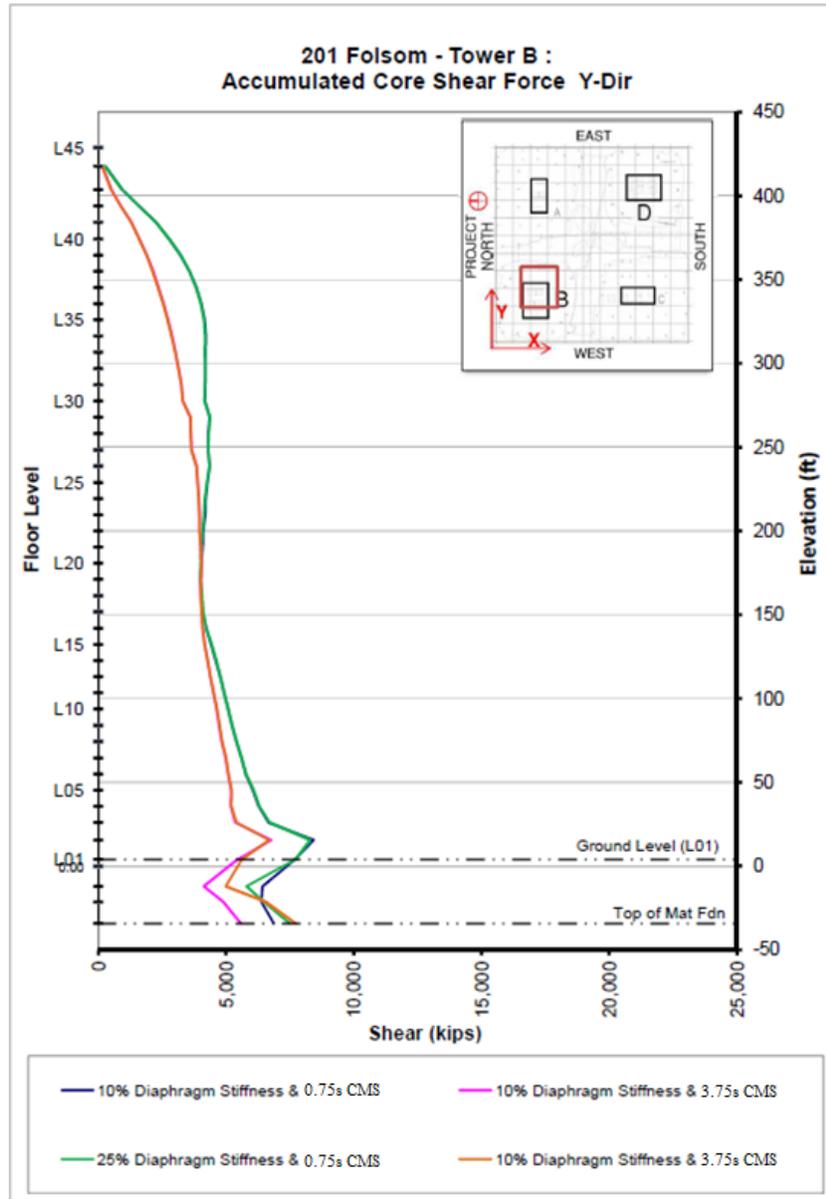
Figure 5.4-4. Acceptance Criteria Checks for Design of Wall Shear Capacity on the Y-Direction
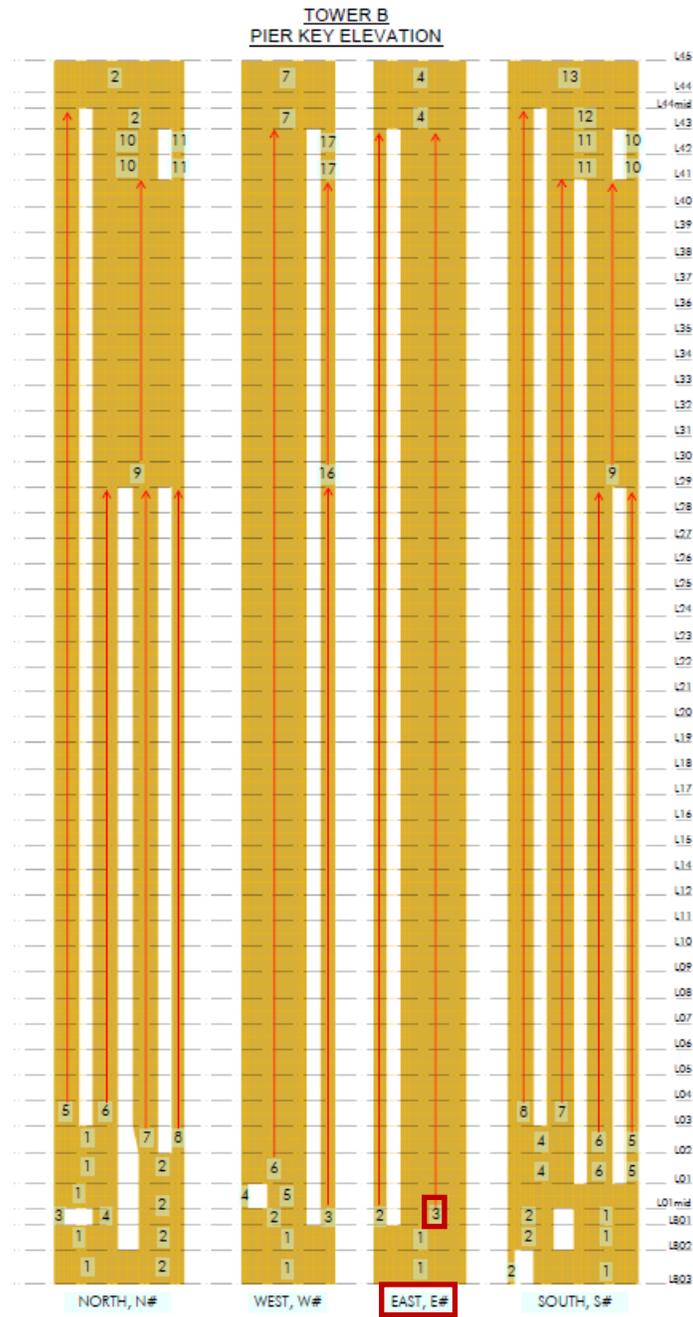
Figure 5.4-5. Shear Wall Elevations and Pier Designations

Table 5.4-2. Design Details for the Shear Design of Pier #3 of the East Elevation

		Pier Design Data			Demand			Calculate Reinforcement Required	
Story	Pier ID	Wall Length (ft)	Wall Thickness (in)	Concrete Strength (ksi)	Governing EQ Load Case	Vu, analysis (kips)	Vc (kips)	ΦVs req'd (kips)	Reinf Req'd (in²/ft)
L43	E3	24.8	24.0	7.8	MCE	1058	1263	0	0.72
L42	E3	24.8	24.0	7.8	MCE	1770	1263	507	0.72
L41	E3	24.8	24.0	7.8	MCE	1955	1263	692	0.72
L40	E3	24.8	24.0	7.8	MCE	2531	1263	1268	0.73
L39	E3	24.8	24.0	7.8	MCE	2859	1263	1595	0.92
L38	E3	24.8	24.0	7.8	MCE	3098	1263	1834	1.05
L37	E3	24.8	24.0	7.8	MCE	3232	1263	1969	1.13
L36	E3	24.8	24.0	7.8	MCE	3298	1263	2034	1.17
L35	E3	24.8	24.0	7.8	MCE	3287	1263	2024	1.16
L34	E3	24.8	24.0	7.8	MCE	3217	1263	1953	1.12
L33	E3	24.8	24.0	7.8	MCE	3232	1263	1969	1.13
L32	E3	24.8	24.0	7.8	MCE	3249	1263	1986	1.14
L31	E3	24.8	24.0	7.8	MCE	3293	1263	2030	1.16
L30	E3	24.8	24.0	7.8	MCE	3398	1263	2135	1.22
L29	E3	24.8	24.0	7.8	MCE	3124	1263	1861	1.07
L28	E3	24.8	24.0	10.4	MCE	3295	1458	1837	1.05
L27	E3	24.8	24.0	10.4	MCE	3290	1458	1831	1.05
L26	E3	24.8	24.0	10.4	MCE	3327	1458	1869	1.07
L25	E3	24.8	24.0	10.4	MCE	3379	1458	1920	1.10
L24	E3	24.8	24.0	10.4	MCE	3412	1458	1953	1.12
L23	E3	24.8	24.0	10.4	MCE	3450	1458	1991	1.14
L22	E3	24.8	24.0	10.4	MCE	3515	1458	2056	1.18
L21	E3	24.8	24.0	10.4	MCE	3567	1458	2108	1.21
L20	E3	24.8	28.0	10.4	MCE	3687	1701	1985	1.14
L19	E3	24.8	28.0	10.4	MCE	3665	1701	1963	1.13
L18	E3	24.8	28.0	10.4	MCE	3705	1701	2003	1.15
L17	E3	24.8	28.0	10.4	MCE	3722	1701	2020	1.16
L16	E3	24.8	28.0	10.4	MCE	3805	1701	2103	1.21
L15	E3	24.8	28.0	10.4	MCE	3962	1701	2260	1.30
L14	E3	24.8	28.0	10.4	MCE	4127	1701	2425	1.39
L12	E3	24.8	28.0	10.4	MCE	4303	1701	2601	1.49
L11	E3	24.8	28.0	10.4	MCE	4484	1701	2782	1.60
L10	E3	24.8	28.0	10.4	MCE	4754	1701	3052	1.75
L09	E3	24.8	28.0	10.4	MCE	5096	1701	3394	1.95
L08	E3	24.8	28.0	10.4	MCE	5396	1701	3694	2.12
L07	E3	24.8	28.0	10.4	MCE	5747	1701	4046	2.32
L06	E3	24.8	28.0	10.4	MCE	6141	1701	4439	2.55
L05	E3	24.8	28.0	10.4	MCE	6551	1701	4850	2.78
L04	E3	24.8	28.0	10.4	MCE	6430	1701	4729	2.71
L03	E3	24.8	28.0	10.4	MCE	7318	1701	5616	3.22
L02	E3	24.8	28.0	10.4	MCE	6730	1701	5028	2.88
L01	E3	24.8	28.0	10.4	MCE	5087	1701	3386	1.94

5.4.2.1.3 Evaluation of Axial Demands in Gravity Columns. The axial capacities of the gravity columns are designed as critical force controlled components, including the effects of gravity load demands and the additional earthquake-induced demands from the outriggering effect. Note that the approach to modeling the outriggering effect has been summarized in Section 5.3.1.2.2.

Figure 5.4-6 shows the floor plan of the building and Column C2 is selected for the demonstration of how the demands are computed for the gravity columns. Table 5.4-3 shows the calculation of demands for example column C2. Both the DE and MCE loading cases are checked for the design of the gravity columns (with different ϕ factors being used for each check) and the MCE case governs the column axial design in every case.
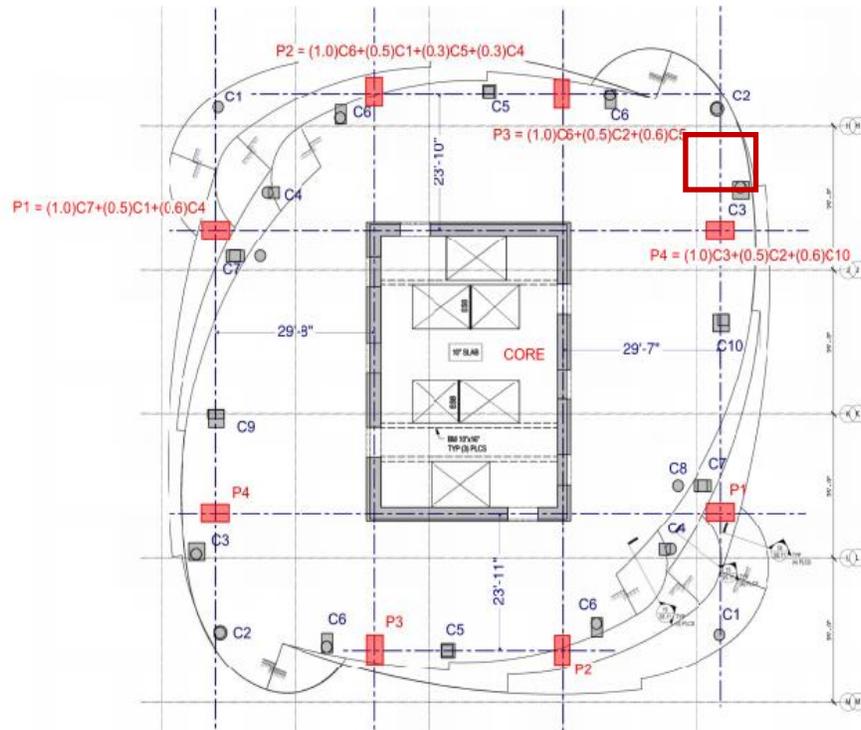
Figure 5.4-6. Floor Plan to Show the Gravity Column Locations and Labels

Table 5.4-3. Design Details for the Axial Load Demands on Column C2

Level Above Column	DL (k)	LL (k)	Outrigger Force Mean*2.0 (kips)	Pu 1.0D+0.2L+ 1.5E (kips)	Pu 0.9D-2.0E (kips)	Pu Gravity (kips)	Governing Load Combo
Roof	-46	-6	-153	-200	111	-64	MCE
L42	-81	-14	-164	-247	91	-113	MCE
L41	-117	-23	-175	-296	69	-164	MCE
L40	-153	-32	-186	-345	48	-214	MCE
L39	-188	-41	-197	-394	28	-263	MCE
L38	-224	-50	-209	-443	7	-314	MCE
L37	-260	-59	-221	-493	-13	-364	MCE
L36	-295	-68	-233	-541	-33	-413	MCE
L35	-331	-77	-245	-591	-53	-463	MCE
L34	-367	-85	-257	-641	-74	-514	MCE
L33	-402	-94	-269	-690	-93	-563	MCE
L32	-438	-103	-281	-740	-113	-613	MCE
L31	-474	-112	-293	-790	-133	-664	MCE
L30	-509	-121	-306	-839	-153	-713	MCE
L29	-544	-129	-320	-889	-170	-762	MCE
L28	-578	-138	-336	-941	-185	-809	MCE
L27	-613	-146	-349	-991	-202	-858	MCE
L26	-647	-155	-363	-1041	-219	-906	MCE
L25	-681	-163	-377	-1090	-236	-953	MCE
L24	-716	-172	-391	-1141	-253	-1002	MCE
L23	-750	-180	-405	-1191	-270	-1050	MCE
L22	-784	-189	-419	-1241	-286	-1098	MCE
L21	-819	-197	-433	-1292	-304	-1147	MCE
L20	-856	-206	-450	-1347	-320	-1198	MCE
L19	-892	-214	-465	-1400	-338	-1249	MCE
L18	-929	-222	-480	-1453	-357	-1301	MCE
L17	-966	-231	-494	-1506	-375	-1352	MCE
L16	-1002	-239	-509	-1558	-393	-1403	MCE
L15	-1039	-248	-523	-1612	-412	-1455	MCE
L14	-1076	-256	-537	-1664	-431	-1506	MCE
L12	-1113	-264	-551	-1717	-450	-1558	MCE
L11	-1149	-273	-565	-1769	-469	-1609	MCE
L10	-1186	-281	-579	-1821	-489	-1660	MCE
L09	-1223	-290	-592	-1873	-509	-1712	MCE
L08	-1260	-298	-605	-1924	-529	-1764	MCE
L07	-1296	-306	-617	-1974	-549	-1814	MCE
L06	-1333	-315	-629	-2025	-570	-1866	MCE
L05	-1370	-323	-641	-2076	-592	-1918	MCE
L04	-1406	-332	-652	-2125	-613	-1968	MCE
L03	-1508	-353	-653	-2231	-705	-2111	MCE
L02	-1556	-379	-653	-2285	-747	-2178	MCE
L01	-1623	-405	-646	-2350	-815	-2272	MCE
LB1	-1663	-425	-651	-2399	-845	-2328	MCE
LB2	-1707	-446	-650	-2446	-886	-2390	MCE

5.4.2.1.4 Evaluation of Shear Demands in Transfer Diaphragm. Figure 5.4-7 illustrates the demands used for the design of the transfer diaphragms at the grade level and at the two basement levels, showing the demands from both the MCE loading case (with the appropriate amplifications factor of 2.0 for this force-controlled component) and the DE loading case (using the typical DE design approach). This figure shows that the MCE loads are substantially larger than the DE loads and clearly control the design. This figure also shows that most of the transfer occurs at the grade level, but that some also occurs at reducing rates for the two subsequent levels below grade.
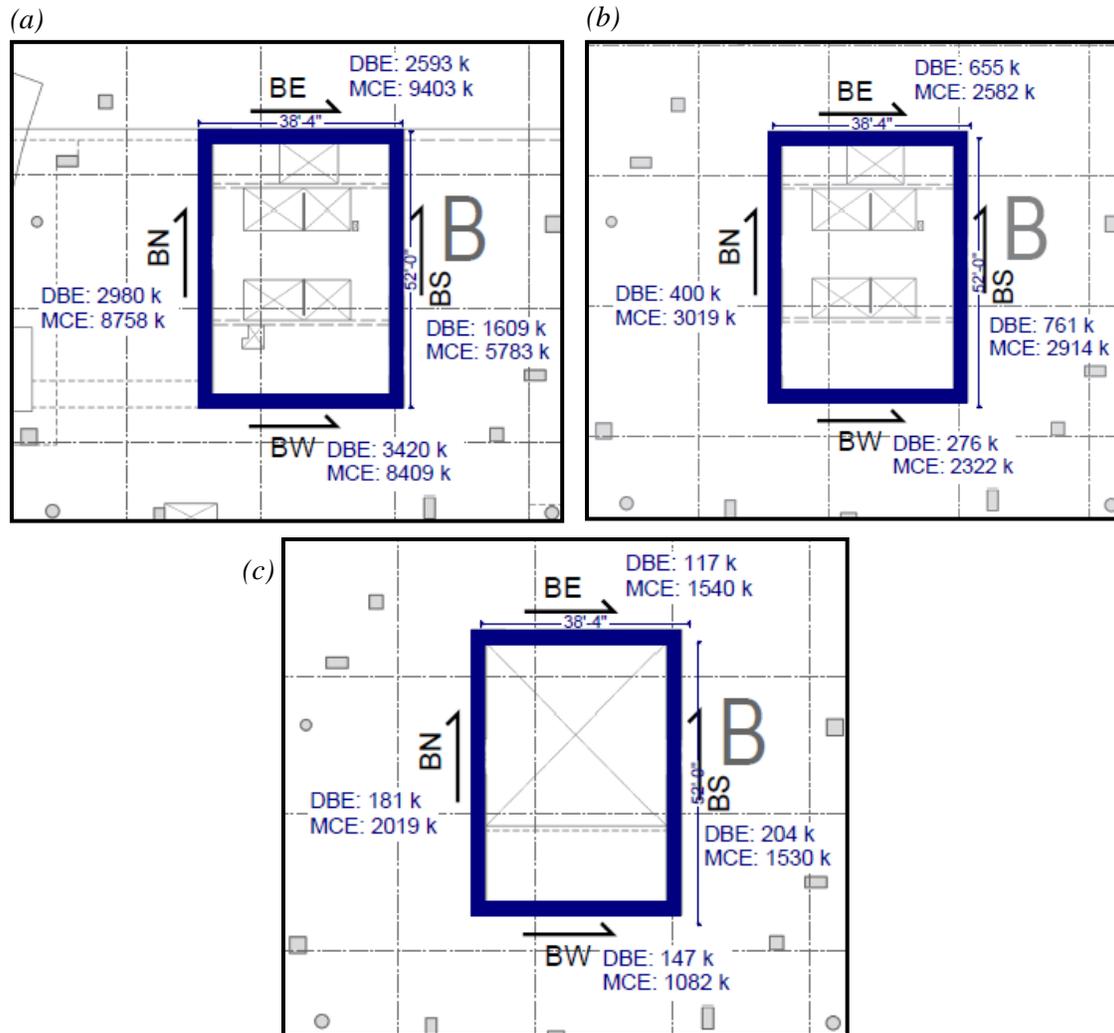
Figure 5.4-7. Illustration of Shear Demands in Transfer Diaphragms, for (a) Level 01, (b) Level B1, and (c) Level B2

5.4.2.2 Deformation-Controlled Actions. For this example building, the following are examples of the deformation-controlled actions:

- Shear wall flexural reinforcing – primary lateral system fuse

- Shear wall coupling beams – primary lateral system fuse

- Flexural yielding of "outrigger slab" – secondary effect due to displacement compatibility of gravity system

5.4.2.2.1 Evaluation of Flexural Demands in Structural Walls. Figures 5.4-8 and 5.4-9 show the overturning moment demands for the shear walls, primarily for illustration purposes. Consistent with previous figures, these show the demand from both ground motion sets (CMS sets at 0.75s and 3.75s) and both the 10% and 25% bounding stiffness assumptions for the transfer diaphragms, for a total of four analysis combinations.
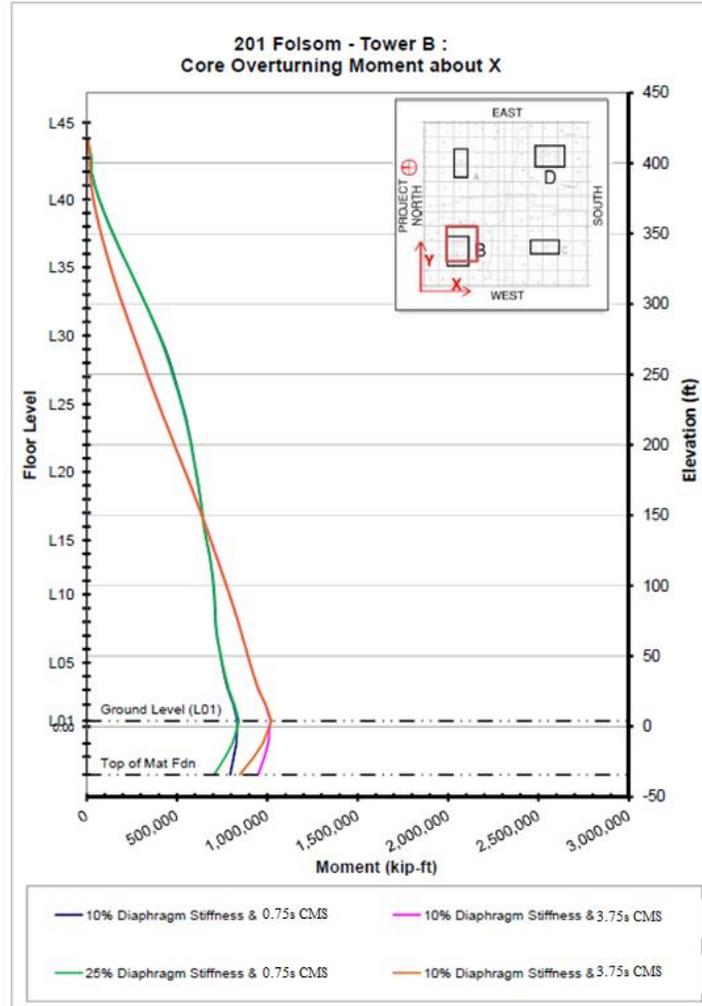
Figure 5.4-8. Demonstration of Code Wall Overturning Moment in the X-Direction
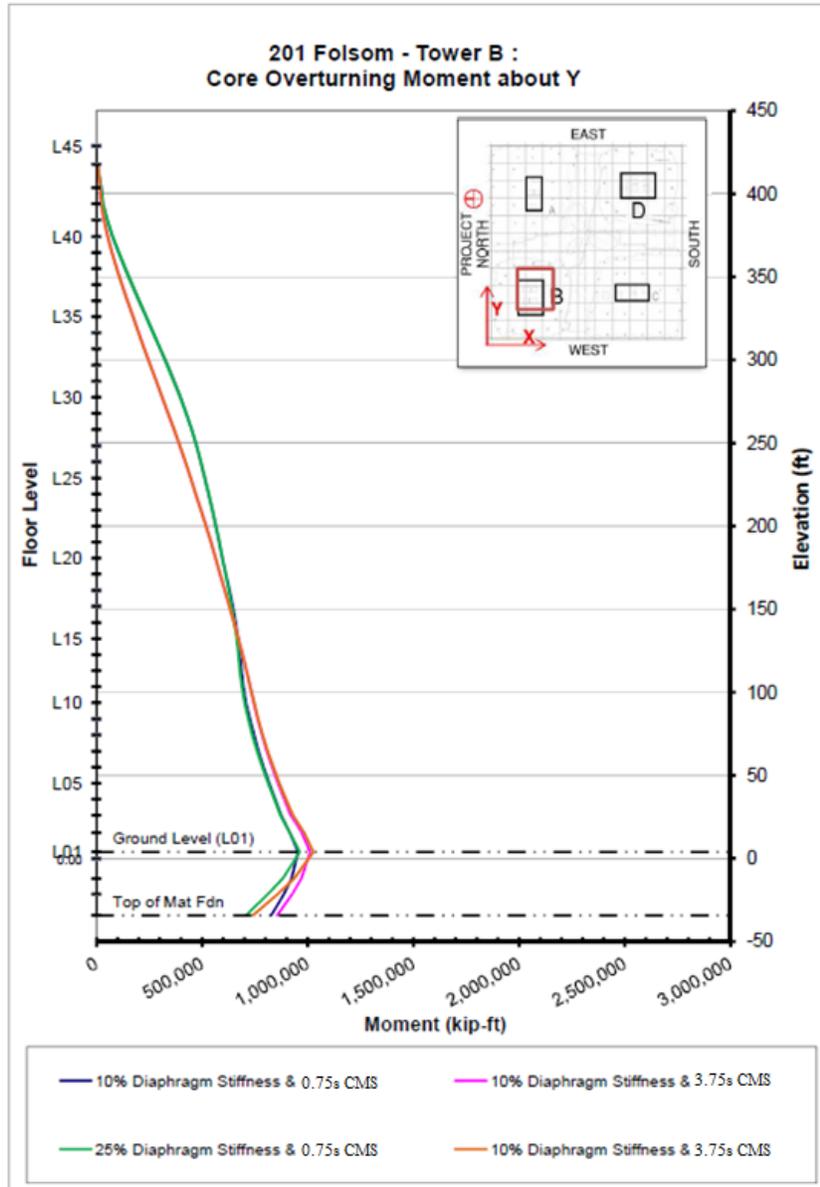
Figure 5.4-9. Demonstration of Code Wall Overturning Moment in the Y-Direction

Figures 5.4-10, 5.4-11, and 5.4-12 show the mean compression strain demands for MCE$_R$ motions for three selected locations in the core. This shows that the crushing strain is not reached in any of the locations and for any of the fours analysis cases.
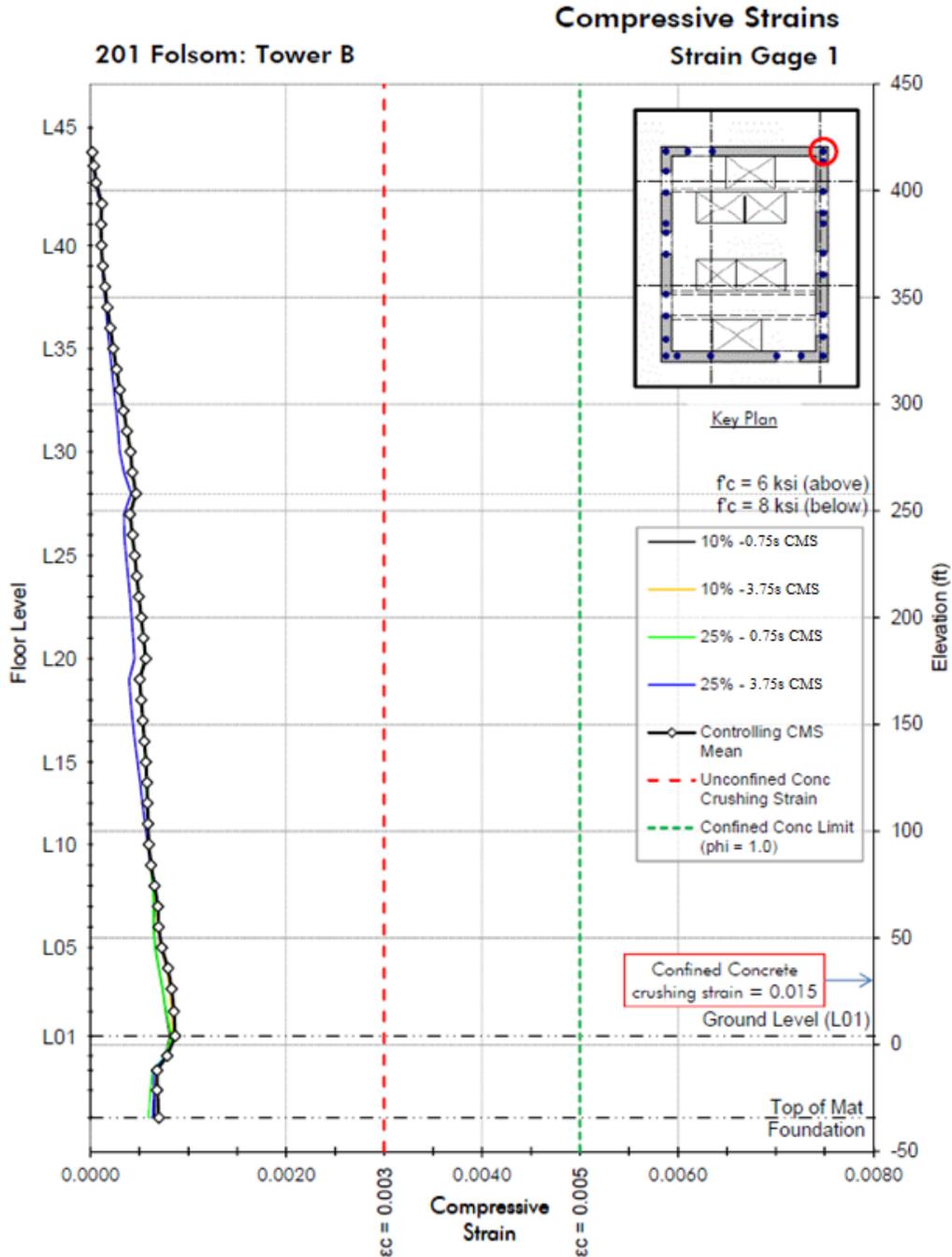
Figure 5.4-10. Acceptance Criteria Checks for Shear Wall Compressive Strain (example for Gauge Location 1)
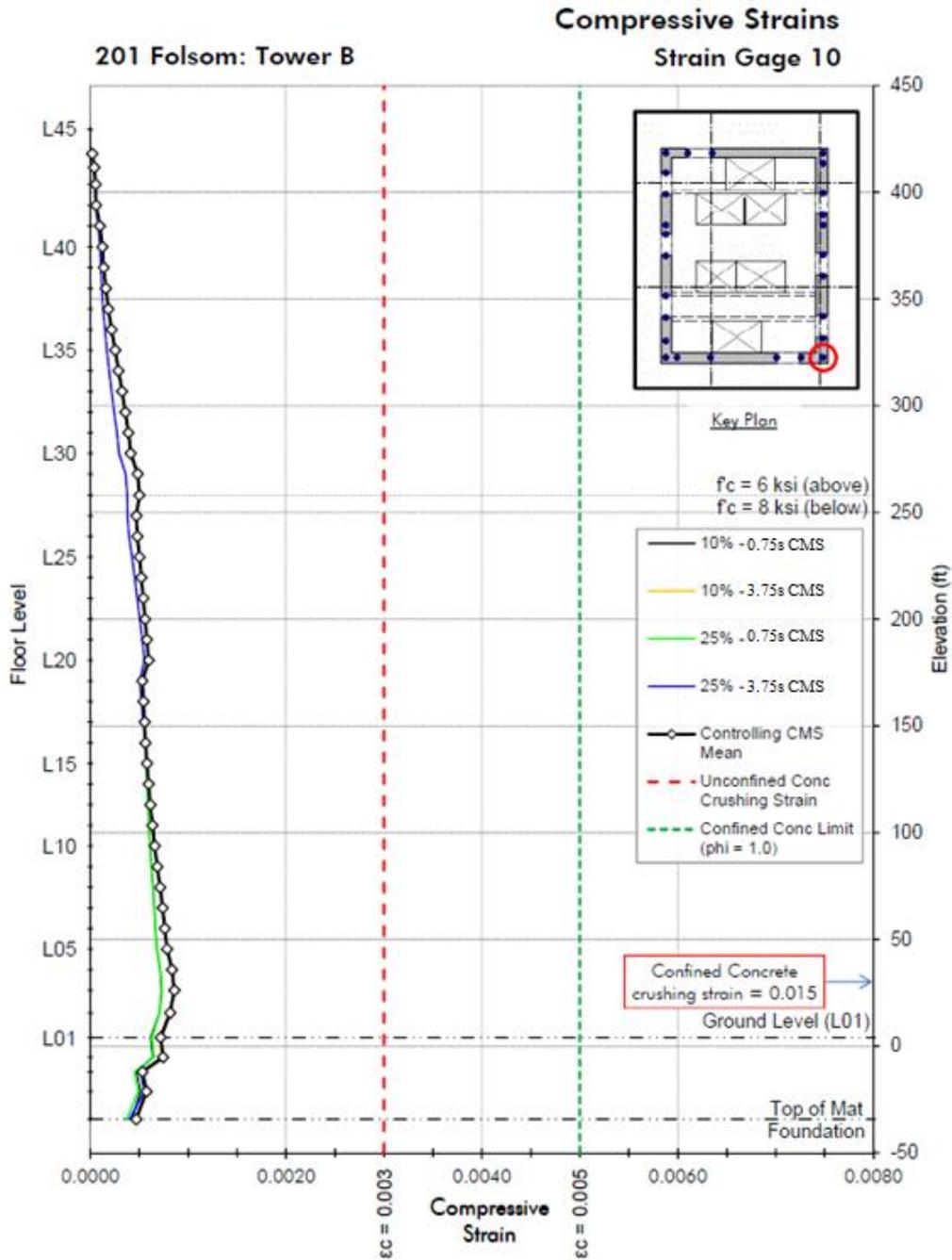
Figure 5.4-11. Acceptance Criteria Checks for Shear Wall Compressive Strain (example for Gauge Location 10)
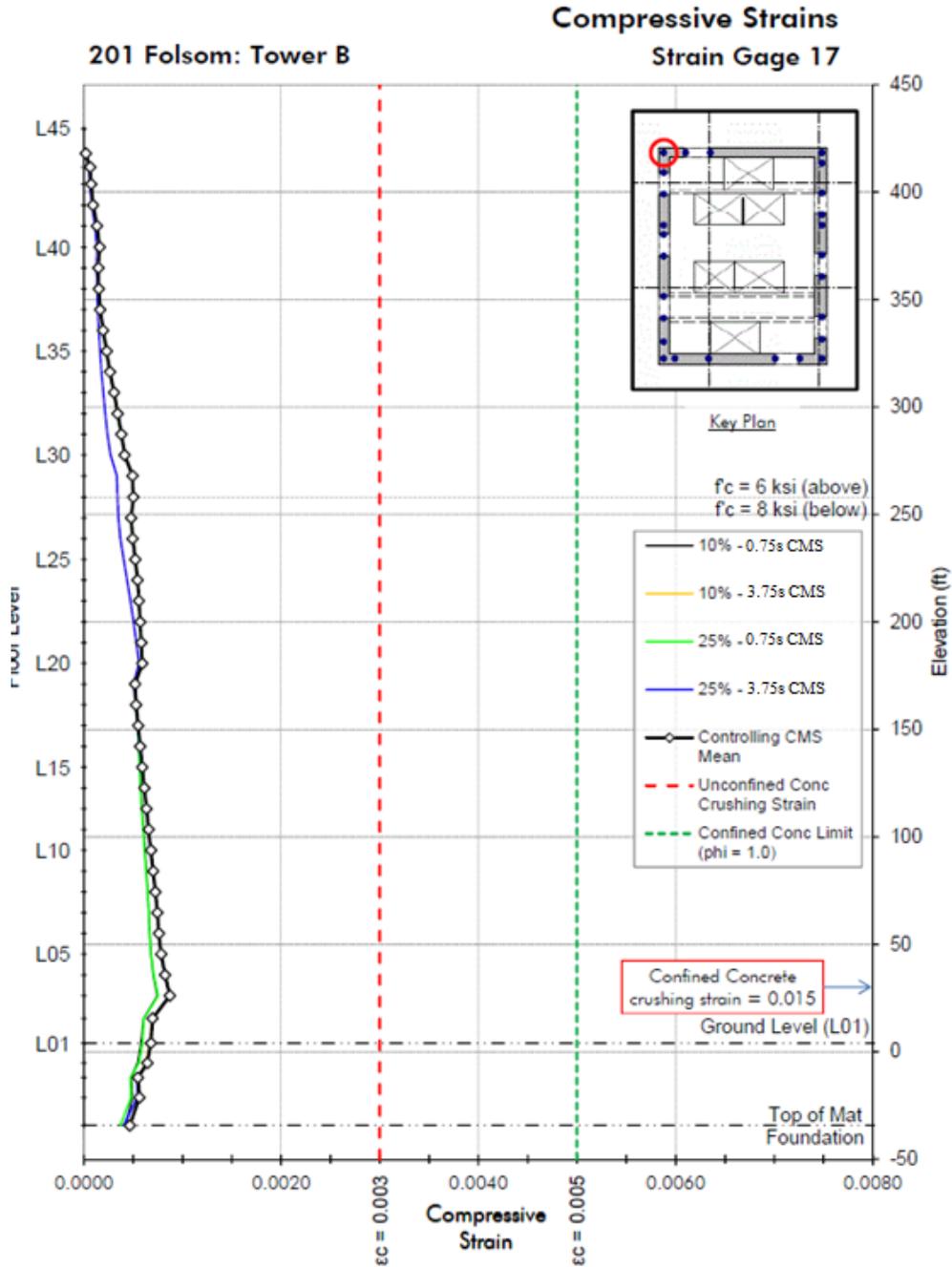
Figure 5.4-12. Acceptance Criteria Checks for Shear Wall Compressive Strain (example for Gauge Location 17)

Figures 5.4-13, 5.4-14, and 5.4-15 show the mean tensile strain demands for MCE$_R$ motions for the same three selected locations in the core. This shows that the yield tensile strain is not reached in any of the locations and for any of the fours analysis cases.
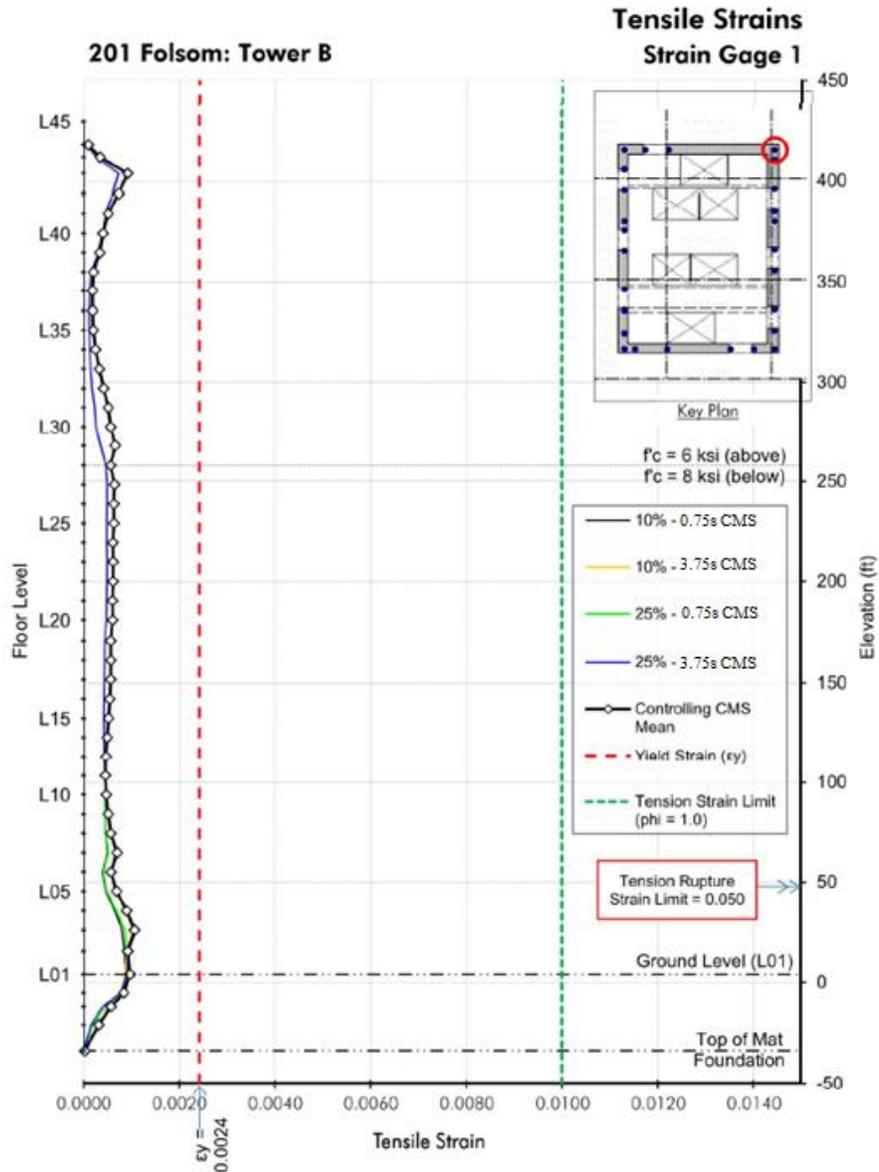
Figure 5.4-13. Acceptance Criteria Checks for Shear Wall Tensile Strain
(example for Gauge Location 1)
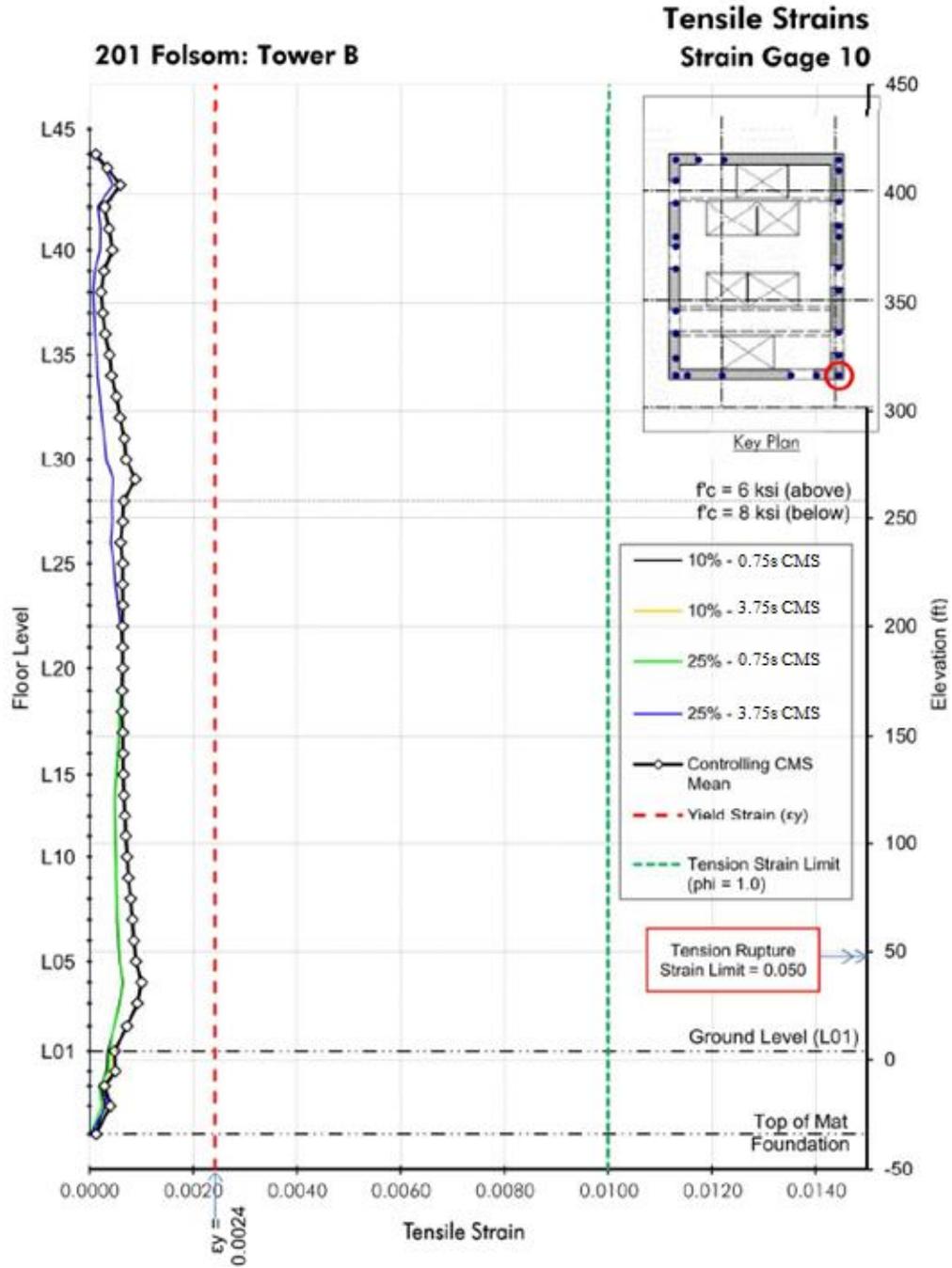
Figure 5.4-14. Acceptance Criteria Checks for Shear Wall Tensile Strain
(example for Gauge Location 10)
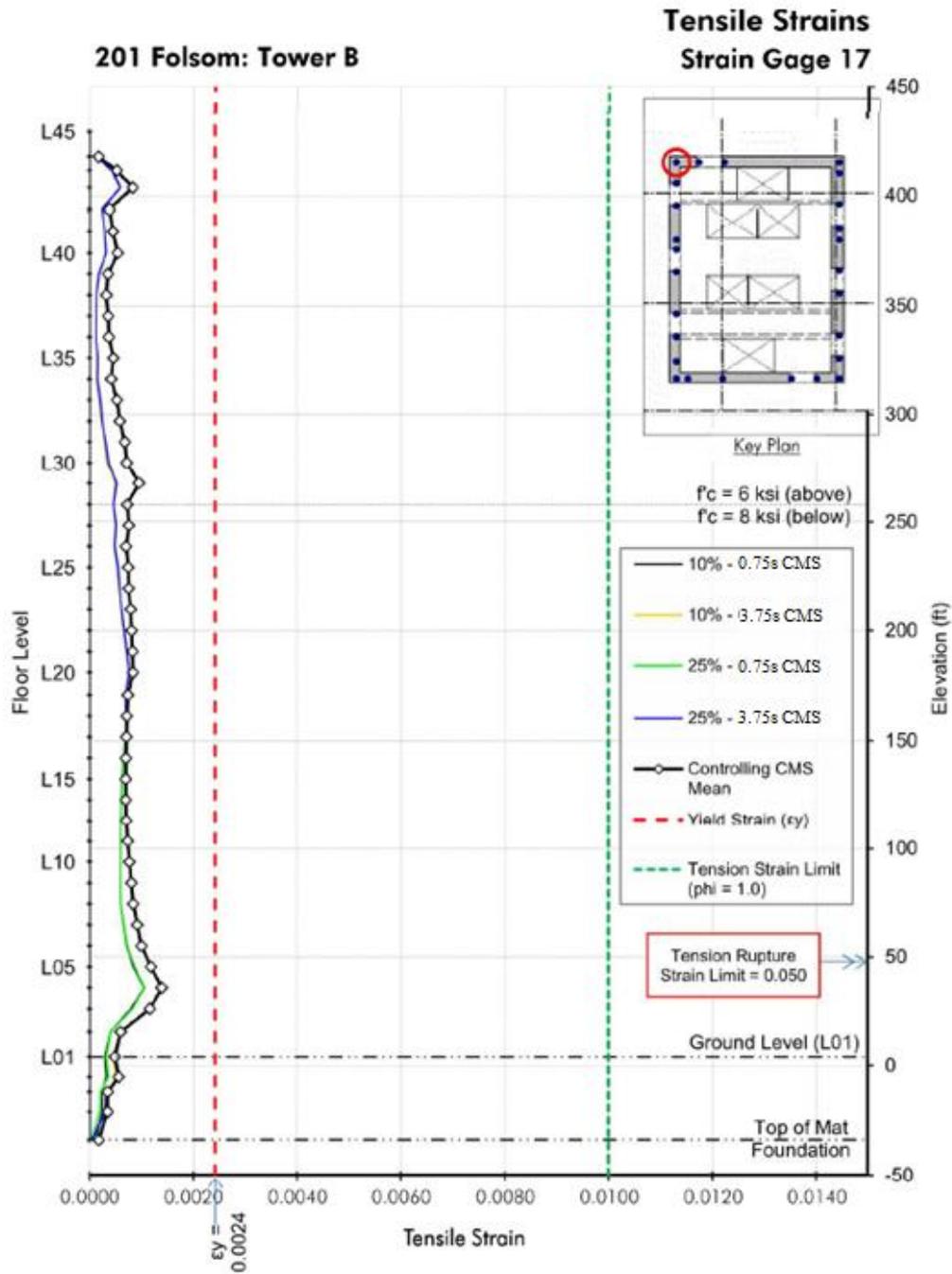
Figure 5.4-15. Acceptance Criteria Checks for Shear Wall Tensile Strain
(example for Gauge Location 17)

5.4.2.2.2 Evaluation of Rotational Demands in Coupling Beams. Figures 5.4-16 through 5.4-20 shows the mean coupling beam chord rotation demands for MCE_R motions for four selected coupling beams. This shows that the coupling beams are the primary component that is handling the inelastic deformations in the building system under the MCE_R motions. Even so, the mean chord rotations are still well below the acceptance criterion limit of 6% for all of the fours analysis cases.
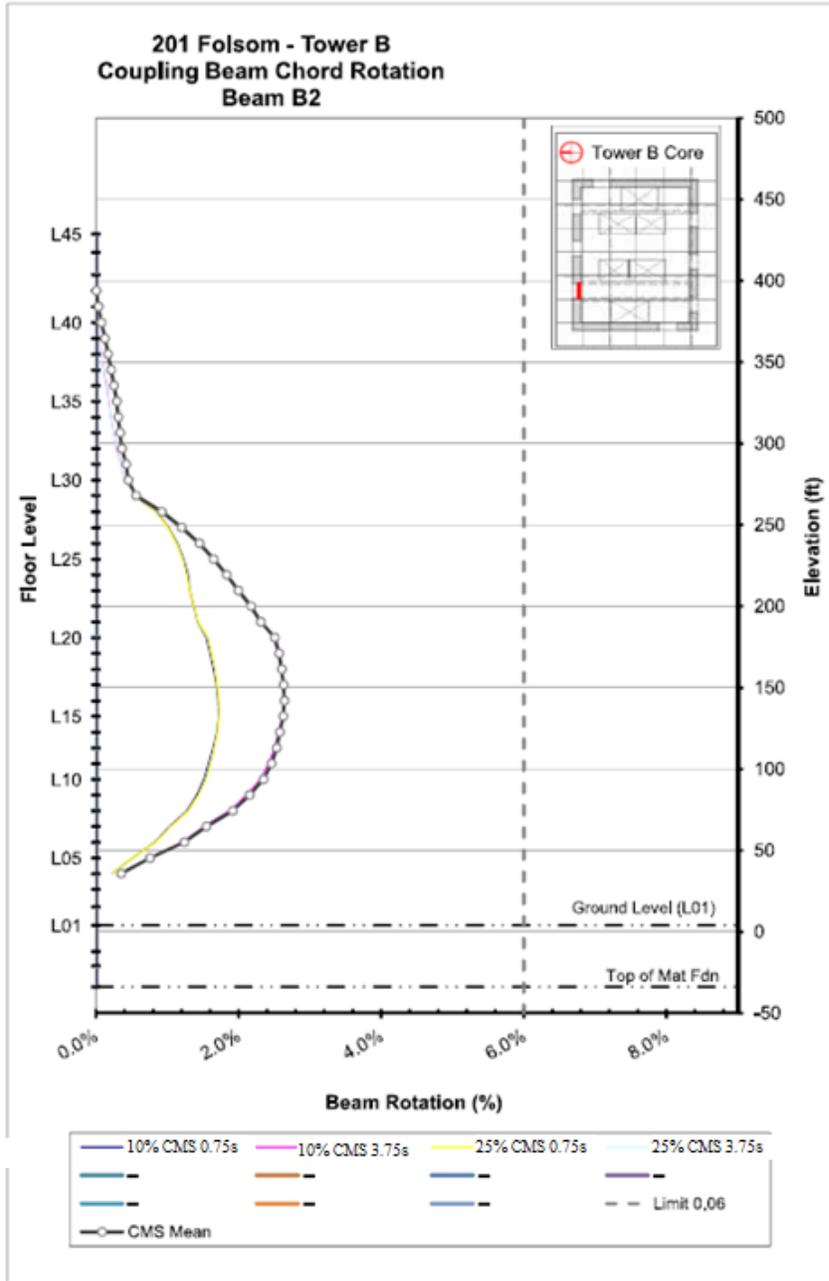
Figure 5.4-16. Acceptance Criteria Checks for Coupling Beam Rotations
(example for Beam B2)
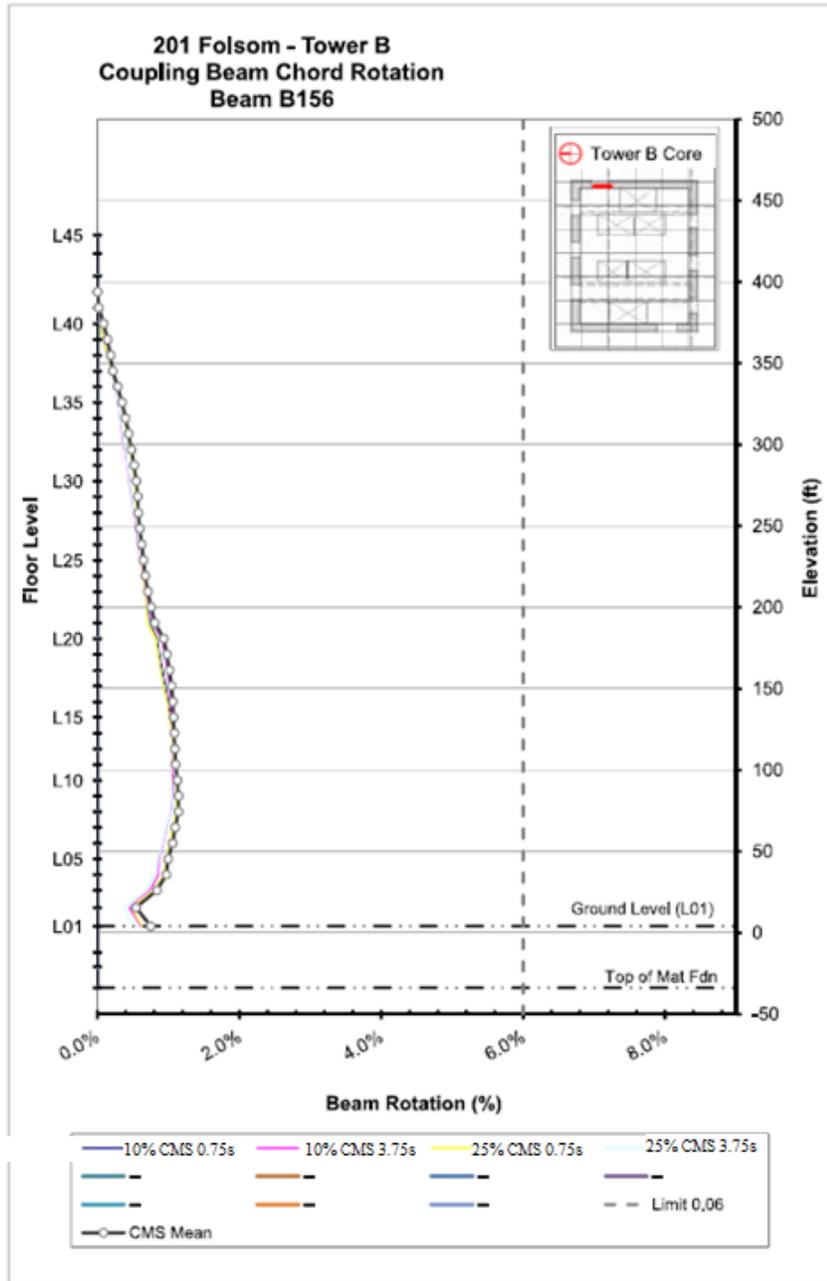
Figure 5.4-17. Acceptance Criteria Checks for Coupling Beam Rotations
(example for Beam B156)
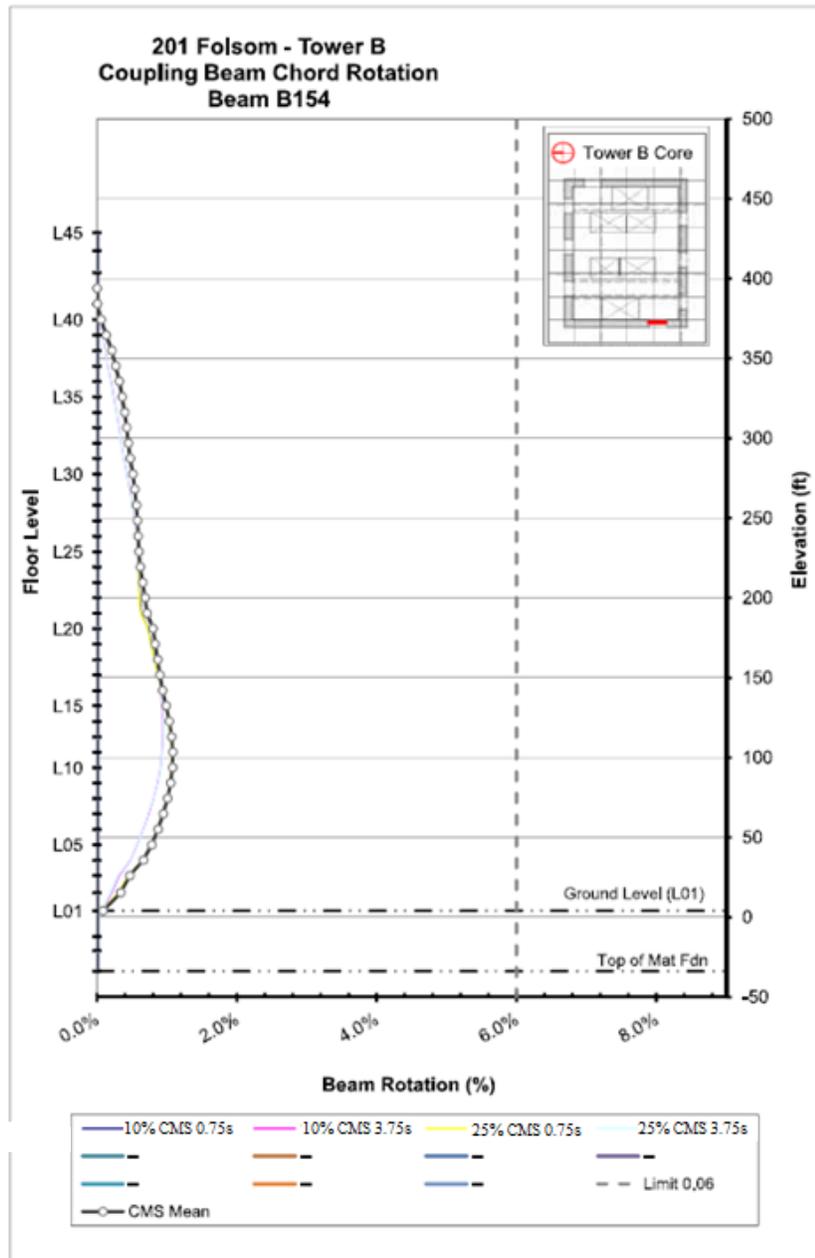
Figure 5.4-18. Acceptance Criteria Checks for Coupling Beam Rotations
(example for Beam B154)
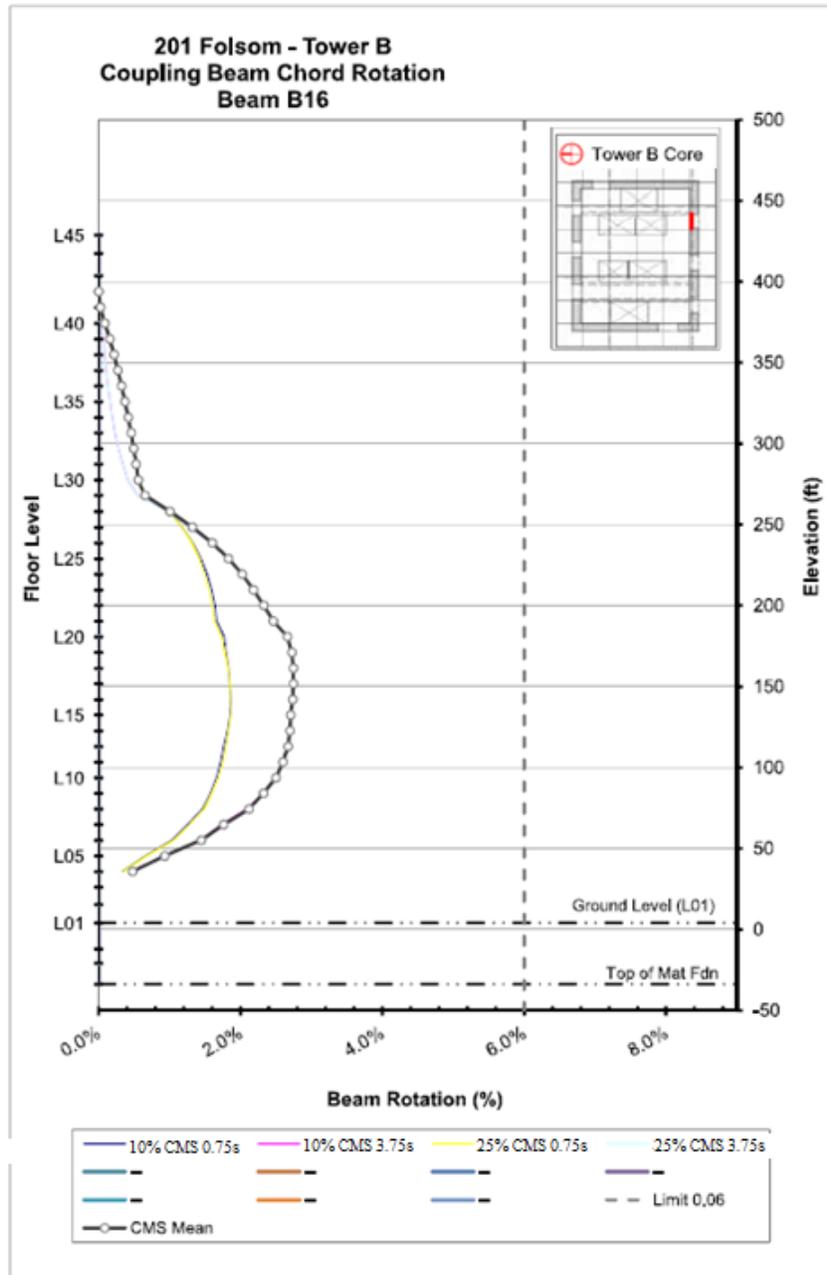
Figure 5.4-19. Acceptance Criteria Checks for Coupling Beam Rotations
(example for Beam B16)

5.5   SUMMARY AND CLOSING

THIS CHAPTER PROVIDED A DESIGN EXAMPLE FOR A 40-STORY REINFORCED CONCRETE
SHEAR WALL BUILDING LOCATED IN SAN FRANCISCO, CALIFORNIA. THIS BUILDING
WAS DESIGNED USING THE NONLINEAR RESPONSES HISTORY ANALYSIS DESIGN
APPROACH OF THE UPDATED CHAPTER 16 OF ASCE/SEI 7-16. AS PART OF THIS DESIGN

EXAMPLE, CODE REQUIREMENTS EXCEPTIONS WERE ALSO INVOKED, SO THIS DESIGN
WAS TECHNICALLY COMPLETED UNDER THE ALTERNATE MEANS AND METHODS
CLAUSE OF ASCE/SEI 7-16, WITH THE CHAPTER 16 REQUIREMENTS USED TO GUIDE THE
DESIGN AND ANALYSIS APPROACH.

5.6   REFERENCES

*San Francisco Department of Building Inspection (2013). AB-083: Requirements and Guidelines for the Seismic
Design of New Tall Buildings using Non-Prescriptive Seismic-Design Procedures, March* 25, 2008 (Updated
01/01/14 for code references)

Haselton, C.B., Andy Fry, Jack W. Baker, Ronald O. Hamburger, Andrew S. Whittaker, Jonathan P. Stewart,
Kenneth J. Elwood, Nicolas Luco, John D. Hooper, Finley A. Charney, and Robert G. Pekelnicky (2015).
"Response-History Analysis for the Design of New Buildings: Part I - Development of Recommendations for the
NEHRP Provisions and the ASCE/SEI 7 Standard," *Earthquake Spectra* (in review).

Haselton, C.B., Andy Fry, Ronald O. Hamburger, Jack W. Baker, Nicolas Luco, Kenneth J. Elwood, John D.
Hooper, Finley A. Charney, Reid Zimmerman, Robert G. Pekelnicky, and Andrew S. Whittaker (2015). Response-
History Analysis for the Design of New Buildings in the NEHRP Provisions and ASCE/SEI 7 Standard: Part II –
Structural Analysis Procedures and Acceptance Criteria, *Earthquake Spectra* (near submission).

LATBSDC (2014). *An Alternative Procedure for Seismic Analysis and Design of Tall Buildings Located in the Los
Angeles Region*. Los Angeles Tall Buildings Structural Design Council, available at http://www.tallbuildings.org/.

Motter, C.J., J.W. Wallace, D.C. Fields, J.D. Hooper, and R. Klemencic (2013). Design Recommendations for
Steel-Reinforced Concrete (SRC) Coupling Beams, *University of California, Los Angeles, Technical Report, UCLA-
SGEL Report 2013/06.*

Motter, C.J., J.W. Wallace, R. Klemencic, J.D. Hooper, and D.C. Fields (2012). Large-Scale Testing and Analysis
of Concrete Encased Steel Coupling Beams under High Ductility Demands, *15th World Conference on Earthquake
Engineering, Lisboa, Portugal.*

PEER (2009). *Guidelines for Performance-Based Seismic Design of Tall Buildings*, prepared by the Tall Buildings
Initiative Guidelines Working Group for the Pacific Earthquake Engineering Research Center, University of
California, Berkeley.

Reid B. Zimmerman, Jack Baker, C.B. Haselton, Stephen Bono, Albert Engel, John Hooper, Ron Hamburger, Ayse
Celikbas, and Afshar Jalalian (2015). "Response History Analysis for the Design of New Buildings: Part III -
Example Applications to Illustrate the Recommended Methodology," *Earthquake Spectra* (in review).

6

Horizontal Diaphragm Analysis

S. K. Ghosh, Ph.D.

Contents

The 2015 *NEHRP Recommended Provisions* (referred to herein as the *Provisions*) includes two significant items related to the design of diaphragms, which represent changes from the 2009 *Provisions*. First, ASCE 7-10 (referred to herein as the *Standard*) has been modified to include a new Section 12.10.3, Alternative Design Provisions for Diaphragms including Chords and Collectors, within Section 12.10, Diaphragm Chords and Collectors. This modification has been accepted for inclusion in ASCE 7-16. The new section provides for an alternative determination of diaphragm design force level, which is mandatory for precast concrete diaphragms in buildings assigned to SDC C, D, E, or F. The alternative is permitted to be used for other precast concrete diaphragms, cast-in-plane concrete diaphragms, and wood diaphragms supported on wood framing. *Standard* Section 12.10.3 does not apply to steel deck diaphragms. Second, ASCE 7-10 has also been modified to add a Section 14.2.4, containing detailed seismic design provisions for precast concrete diaphragms including a connector qualification protocol. This modification has also been accepted for inclusion in ASCE 7-16.

The seismic design of structures has long been based on an approximation of the inelastic response of the seismic force-resisting system. The approximation reduces the results of an elastic analysis in consideration of the reserve strength, ductility, and energy dissipation inherent in the vertical elements of the seismic force-resisting system. In 1978, ATC-3 (ATC, 1978) provided design force reduction factors based on consideration of inelastic behavior of the vertical elements of the seismic force-resisting system and the performance of structures in past earthquakes. The primary assumption leading to these factors is that yielding in the vertical elements of the seismic force-resisting system is the primary mechanism for inelastic behavior and energy dissipation.

In contrast, the design requirements for the horizontal elements of the lateral force-resisting system (the diaphragms) have been established by empirical considerations, rather than by reduction of the elastic diaphragm forces due to inelastic action. For established diaphragm construction types, this empirical approach has been generally satisfactory. Satisfactory system performance, however, requires that the diaphragms have sufficient strength and ductility to mobilize the inelastic behavior of the vertical elements.

In order to help achieve the intended seismic performance of structures, the designs of horizontal and vertical elements of the seismic force-resisting system need to be made more consistent. Analytical results as well as experimental results from shake-table tests in Japan, Mexico, and the United States have shown that diaphragm forces over much of the height of the structure actually experienced in the design-level earthquake may at times be significantly greater than code-level diaphragm design forces, particularly where diaphragm response is near-elastic. There are material-specific factors that are related to overstrength and deformation capacity that may account for satisfactory diaphragm performance, however. ASCE 7-16 Section 12.10.3 ties the design of diaphragms to levels of force and deformation that represent actual anticipated behavior.

ASCE 7-16 Section 12.10.3 presents an elastic diaphragm force as the statistical sum of first mode effect and higher mode effects (Rodriguez et al., 2002). The first mode effect is reduced by the R-factor of the seismic force-resisting system, but then amplified by the overstrength factor, Ω_0, because vertical element overstrength will generate higher first mode forces in the diaphragm. The effect caused by higher mode response is not reduced. In recognition of the deformation capacity and overstrength of the diaphragm, the elastic diaphragm force from the first and higher modes of response is then reduced by a diaphragm force reduction factor, R_s.

With the modification by R_s, the proposed design force level may not be significantly different from the diaphragm design force level of ASCE 7-16 Sections 12.10.1 and 12.10.2 for many practical cases. For some types of diaphragms and for some locations within structures, the proposed diaphragm design forces will change significantly, resulting in noticeable changes to resulting construction. Based on data from

testing and analysis and on building performance observations, it is believed that these changes are warranted.

Detailed explanation of added ASCE 7-10 Section 12.10.3 is provided in Part 2 (Commentary) to the 2015 NEHRP *Provisions*. These are not repeated here. The aim here is to provide a step-by-step guidance to implementing Section 12.10.3 and to point out how it is different from implementation of Sections 12.10.1 and 12.10.2.

The alternative design force level of Section 12.10.3 is based on work by Rodriguez, Restrepo, and Carr (Rodriguez et al., 2002), verified by more recent work by Fleischman et al. (Pankow, 2014), which was part of the major DSDM (Diaphragm Seismic Design Methodology) research effort funded by the National Science Foundation, the Precast/Prestressed Concrete Institute, and the Pankow Foundation. The research was carried out at the University of Arizona, Tucson, Lehigh University, and the University of California at San Diego.

In addition to the *Provisions* and the *Standard*, the following documents are either referred to directly or may serve as useful design aids:

ACI 318	American Concrete Institute. 2014. *Building Code Requirements for Structural Concrete*.
ATC 3-06	Applied Technology Council. 1978. *Tentative Provisions for the Development of Seismic Regulations for Buildings.*
Rodriguez, Restrepo	Rodriguez, M, Restrepo, J. I. and Carr, A. J. 2002. "Earthquake induced floor horizontal accelerations in buildings", *Earthquake Engineering - Structural Dynamics*, Vol. 31**,** pp.693-718.
Pankow Foundation	Pankow Foundation, 2014. *Seismic Design Methodology Document for Precast Concrete.*
ATLSS Report	Naito, C., Ren, R., Jones, C., Cullent, T., "Development of a Seismic Design Methodology for Precast Diaphragms - Connector Performance Phase 1B," ATLSS Report No. 07-04, ATLSS Center, Lehigh University, June, 2007, 169 pages.
ATLSS Report	Naito, C., Peter, W., Cao, L., "Development of a Seismic Design Methodology for Precast Diaphragms - PHASE 1 SUMMARY REPORT," ATLSS Report No. 06-03, ATLSS Center, Lehigh University, January, 2006, 118 pages.
Ren and Naito	Ren, R., and Naito, C. J., 2013. "Precast Concrete Diaphragm Connector Performance Database, *Journal of Structural Engineering*, ASCE, January.

6.1   STEP-BY-STEP DETERMINATION OF TRADITIONAL DIAPHRAGM DESIGN FORCE

The following describes in a step-by-step fashion the determination of diaphragm seismic design force by ASCE 7-16 Sections 12.10.1 and 12.10.2. The procedure in these sections has been in use since before the first edition of the IBC and has, in the past, been applicable to diaphragms of all materials. ASCE 7-16 Sections 12.10.1 and 12.10.2 cannot be used for design of precast concrete diaphragms in buildings assigned to C, D, E, or F.

Step 1: Determine w_{px}. ASCE 7-16 Section 12.7.2 defines effective seismic weight, W. w_x is the portion of W that is tributary to level x. w_{px} is different from w_x only in that the weights of the walls parallel to the earthquake forces may be excluded from w_{px}.

Step 2: Determine w_i for all levels from x to n, n being the roof level. Determine the sum of the above,

$$\sum_{i=x}^{n} w_i \, .$$
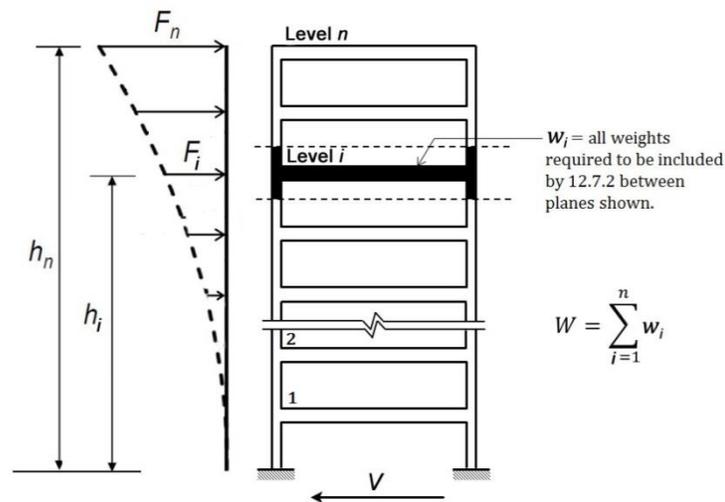
Figure 6.1-1 Seismic weights and lateral forces obtained from vertical distribution of design base shear at various floor levels

Step 3: Determine seismic design base shear, V, from ASCE 7-16 Section 12.8.1.

Step 4: Determine portion of V induced at level i, F_i, for all levels from x to n, from ASCE 7-16 Section 12.8.3. Determine the sum of the above, $\sum_{i=x}^{n} F_i$.

Step 5: Determine diaphragm design force at level x, F_{px}, from:

$$F_{px} = \frac{\sum_{i=x}^{n} F_i}{\sum_{i=x}^{n} w_i} \, w_{px}$$

Step 6: Check F_{px} against maximum and minimum values.
F_{px} shall not be less than F_x or $0.2S_{DS}I_ew_{px}$
F_{px} need not be greater than $0.4S_{DS}I_ew_{px}$

6.2   STEP-BY-STEP DETERMINATION OF ALTERNATIVE DIAPHRAGM DESIGN FORCE

The following describes in a step-by-step fashion the determination of diaphragm seismic design force by ASCE 7-16 Section 12.10.3.

The differences between the procedure in Sections 12.10.1 and 12.10.2 and the design force determination by Section 12.10.3 become apparent from a side-by-side review of Section 6.1 above and this section.

Step 1: Determine w_{px} (ASCE 7-16 Section 12.10.3.2)

ASCE 7-16 Section 12.7.2 defines effective seismic weight, W. w_x is the portion of W that is tributary to level x. w_{px} is different from w_x only in that the weights of the walls parallel to the earthquake forces may be excluded from w_{px}.

Step 2: Determine R_s, Diaphragm Design Force Reduction Factor (ASCE 7-16 Table 12.10.3.5-1)

ASCE 7-16 Table 12.10.3.5-1 Diaphragm Design Force Reduction factor, R_s

Diaphragm System		Shear-Controlled[a]	Flexure-Controlled[a]
Cast-in-place concrete designed in accordance with Section 14.2 and ACI 318	-	1.5	2
Precast concrete designed in accordance with Section 14.2.4 and ACI 318	EDO[1, b]	0.7	0.7
	BDO[2, b]	1.0	1.0
	RDO[3, b]	1.4	1.4
Wood sheathed designed in accordance with Section 14.5 and AF&PA (now AWC) Special Design Provisions for Wind and Seismic	-	3.0	NA
[1] EDO is precast concrete diaphragm Elastic Design Option. [2] BDO is precast concrete diaphragm Basic Design Option. [3] RDO is precast concrete diaphragm Reduced Design Option. [a] Flexure-controlled and Shear-controlled diaphragms are defined in ASCE 7-16 Section 11.2. [b] Elastic, basic, and reduced design options are defined in ASCE 7-16 Section 11.2.			

The Diaphragm Design Force Reduction Factor, R_s, accounts for diaphragm overstrength and/or the inelastic displacement capacity of a diaphragm. For diaphragm systems with inelastic deformation capacity sufficient to permit inelastic response under the design earthquake, R_s is typically greater than 1.0, so that F_{px} is reduced relative to the design force demand for a diaphragm that remains linear elastic under the design earthquake. For diaphragm systems that do not have sufficient inelastic deformation

capacity, R_s should be less than 1.0, or even 0.7, so that linear elastic force-deformation response can be expected under the MCE.

Step 3: Determine C_{px}, Diaphragm Design Acceleration (Force) Coefficient at Level x (ASCE 7-16 Section 12.10.3.2)

In order to determine C_{px}, C_{p0}, C_{pi}, and C_{pn} need to first be determined.

Step 3A: Determine C_{p0}, Diaphragm Design Acceleration (Force) Coefficient at the Structure Base (ASCE 7-16 Section 12.10.3.2.1)

$$C_{p0} = 0.4 S_{DS} I_e$$

Step 3B: Determine C_{pi}, Diaphragm Design Acceleration (Force) Coefficient at 80 percent of h_n (ASCE 7-16 Section 12.10.3.2.1)

C_{pi} is the greater of values given by:

$$C_{pi} = C_{p0}$$

$$C_{pi} = 0.9 \Gamma_{m1} \Omega_0 C_s$$

where:

Γ_{m1} is first mode contribution factor

$$\Gamma_{m1} = 1 + 0.5 z_s \left(1 - \frac{1}{N} \right)$$

z_s = modal contribution coefficient modifier dependent on seismic force-resisting system (see Table below).

Table 6.2-1 Modal Contribution Coefficient Modifier, z_s

Description	z_s - value
Buildings designed with Buckling Restrained Braced Frame systems defined in Table 12.2-1	0.30
Buildings designed with Moment-Resisting Frame systems defined in Table 12.2-1	0.70
Buildings designed with Dual Systems defined in Table 12.2-1 with Special or Intermediate Moment Frames capable of resisting at least 25% of the prescribed seismic forces	0.85
Buildings designed with all other seismic force-resisting systems	1.00

Step 3C: Determine C_{pn}, Diaphragm Design Acceleration (Force) Coefficient at h_n (ASCE 7-16 Section 12.10.3.2.1)

$$C_{pn} = \sqrt{\left(\Gamma_{m1} \Omega_0 C_s \right)^2 + \left(\Gamma_{m2} C_{s2} \right)^2}$$

where:

Γ_{m2} is higher mode contribution factor

$$\Gamma_{m2} = 0.9 z_s \left(1 - \frac{1}{N}\right)^2$$

C_{s2} is higher mode seismic response coefficient. C_{s2} is the smallest of values given by

$$C_{s2} = (0.15N + 0.25) I_e S_{DS}$$

$$C_{s2} = I_e S_{DS}$$

$$C_{s2} = \frac{I_e S_{D1}}{0.03(N-1)} \qquad \text{For } N \geq 2$$

$$C_{s2} = 0 \qquad \text{For } N = 1$$

Step 3D: Use Figure 12.10.3-1 to determine C_{px} (ASCE 7-16 Section 12.10.3.2)
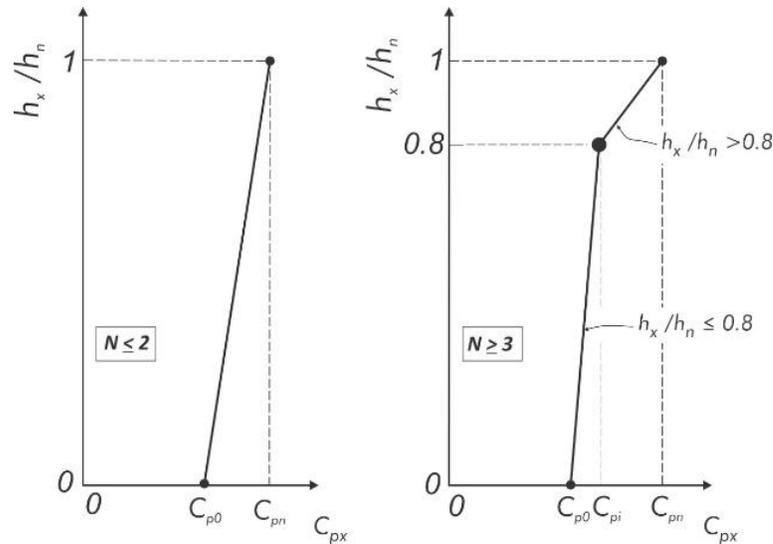
ASCE 7-16 Figure 12.10.3-1 Calculating the design acceleration coefficient C_{px} in buildings two stories or less in height and in buildings three stories or more in height

The distribution of diaphragm design forces along the height of a building is somewhat different in the *Provisions* from that given in ASCE 7-16 Figure 12.10.3-1. The NEHRP distribution is shown below in *Provisions* Figure 12.10-2. For buildings three stories or taller in height, the parameter C_{pi} is not used. The parameter C_{px} remains constant and equal to C_{p0} from the base to 80% of the structural height, h_n, above the base. Also, in ASCE 7-16, the parameter C_{pn} cannot be less than C_{pi}. However, no such lower limit is imposed on C_{pn} in the *Provisions*. As a result, it is possible to have lower diaphragm forces in the upper 20% of the height of a building compared to those in the lower 80% of the height of the building when following the requirements of the *Provisions*. This can be seen in Figures 6.4-13 and 6.4-14 later in this chapter.
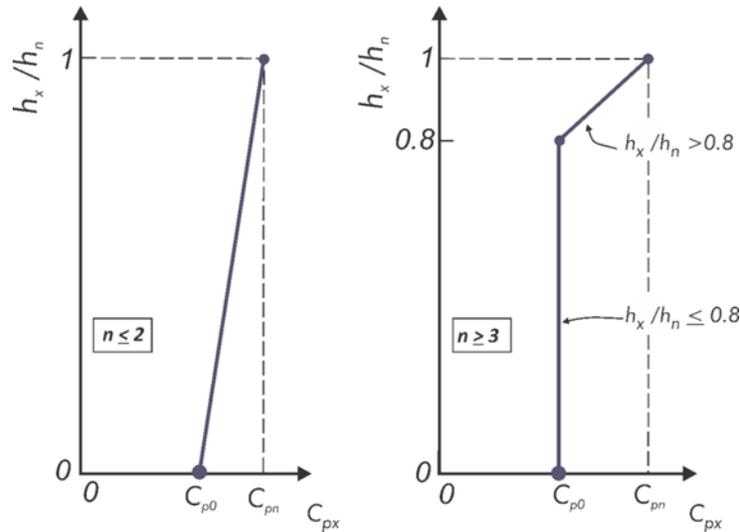
Provisions **Figure 12.10-2 Calculating the design acceleration coefficient C_{px} in buildings with $N \leq 2$ and in buildings with $N \geq 3$**

Step 4: Determine F_{px}, Diaphragm Design Force at Level x (Section 12.10.3.2)

$$F_{px} = \frac{\overbrace{C_{px}}^{\text{Step 3}}}{\underbrace{R_s}_{\text{Step 2}}} \overbrace{w_{px}}^{\text{Step 1}}$$

$$\geq 0.2 S_{DS} I_e w_{px}$$

6.3 DETAILED STEP-BY-STEP CALCULATION OF DIAPHRAGM DESIGN FORCES FOR EXAMPLE BUILDINGS

Detailed calculations of diaphragm seismic design forces along the height of a precast concrete building assigned to Seismic Design Category B, following the step-by-step procedures given above, are shown in Sections 11.1.1.1 through 11.1.1.3 of this publication. The procedure in *Standard* Sections 12.10.1 and 12.10.2 as well as the procedure in *Standard* Section 12.10.3 is illustrated, because a precast concrete diaphragm in a building assigned to SDC B is eligible to be designed by both. Sections 11.1.1.4 illustrates the detailed calculation of diaphragm design forces along the height of a building assigned to SDC C following the procedure in Section 6.2 above; this diaphragm is not eligible to be designed by the procedure in Section 6.1. An illustration of the detailed calculation of diaphragm design forces along the height of a precast concrete building assigned to SDC D, following the procedure in Section 6.2 above, is found in Section 11.1.2.

In addition to the above, design force level computations for two wood-frame buildings are illustrated below in Sections 6.3.1 and 6.3.2.

Example – One Story Wood Assembly Hall

Building Configuration

One Story
Assembly use, $I_e = 1.25$
Mean roof height = 25 feet
Length = 90 feet
Width = 40 feet
$S_{DS} = 1.0$, $S_{D1} = 0.60$
Wood structural panel diaphragm
Wood structural panel shear walls - $R=6.5$, $\Omega_0=3$
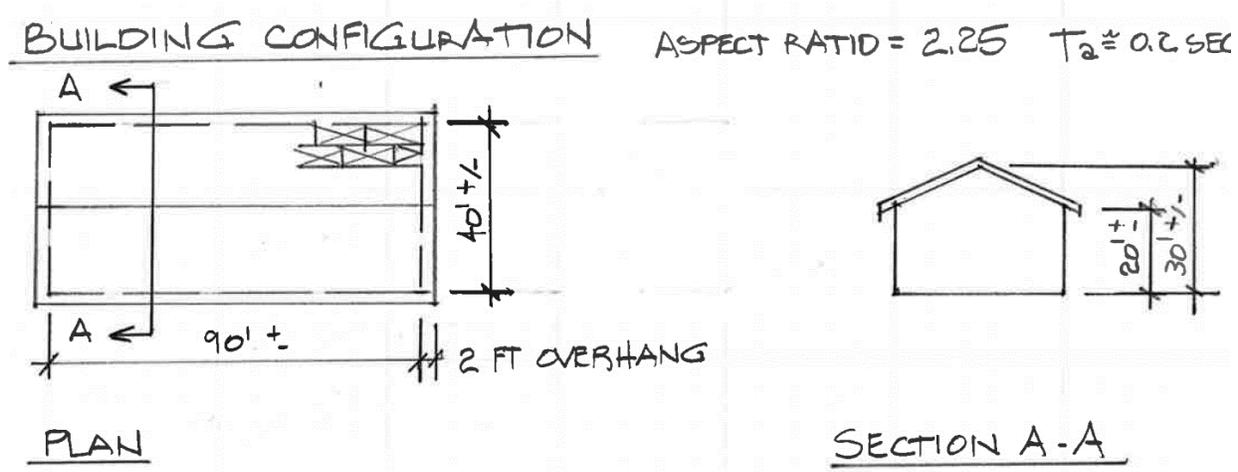
Weight for Seismic Analysis

Roof + ceiling	= 15 psf
Roof only	= 8 psf
Wall	= 10 psf

Seismic weight –	Roof:	(15 psf)(40 ft.)(90 ft.)	= 54,000 lbs
	Overhang:	(8 psf)(2 ft.)(41 ft.)(91 ft.)(2 sides)	= 4,200 lbs
	Side walls:	(10 psf)(10 ft.)(90 ft.)(2 sides)	= 18,000 lbs
	End walls:	(10 psf)(25 ft./2)(40 ft.)(2 sides)	= 10,000 lbs
	TOTAL		= 86,200 lbs acting at roof

ASCE 7-16 Base Shear

$$T_a = C_t h_n^x = 0.20(25)^{0.75} = 0.22 \text{ sec} \tag{12.8-7}$$

$$C_s = \frac{S_{DS}}{R/I_e} = \frac{1.00}{6.5/1.25} = 0.192 \tag{12.8-2}$$

C_s need not exceed:

$$C_s = \frac{S_{D1}}{T(R/I_e)} = \frac{0.60}{0.24(6.5/1.25)} = 0.481 \qquad \text{(12.8-3)}$$

$$V = C_s W = (0.192)(86,200) = 16,550 \text{ lbs} \qquad \text{(12.8-1)}$$

Diaphragm Weight, w_{px}, at the Roof

Diaphragm weight = Total seismic weight – weight of the walls resisting seismic forces

= 86,200 – 10,000 = 76,200 lbs (for seismic forces acting in transverse direction)

= 86,200 – 18,000 = 68,200 lbs (for seismic forces acting in longitudinal direction)

ASCE 7-16 Traditional Roof Diaphragm Design Force

Strength Level diaphragm design force:

$$F_{px} = \frac{\sum_{i=x}^{n} F_i}{\sum_{i=x}^{n} w_i} w_{px} \qquad \text{(Eq. 12.10-1)}$$

For a single story building, $F_{px} = V = 16,550$ lbs

The minimum value of $F_{px} = 0.2 S_{DS} I_e w_{px}$ (Eq. 12.10-2)

= 0.2(1.0)(1.25)(76,200 lbs) = 19,050 lbs (transverse direction)

= 0.2(1.0)(1.25)(68,200 lbs) = 17,050 lbs (longitudinal direction)

The maximum value of $F_{px} = 0.4 S_{DS} I_e w_{px}$ (Eq. 12.10-3)

= 0.4(1.0) (1.25)(76,200 lbs) = 38,100 lbs (transverse direction)

= 0.4(1.0) (1.25)(68,200 lbs) = 34,100 lbs (longitudinal direction)

Governing diaphragm design forces   = 19,050 lbs (transverse direction)

= 17,050 lbs (longitudinal direction)

ASD Level diaphragm design force:

$F_{pr} = 0.7(19,050) = 13,335$ lbs (transverse direction)

$F_{pr} = 0.7(17,050) = 11,935$ lbs (longitudinal direction)

ASCE 7-16 Alternative/2015 NEHRP *Provisions* Roof Diaphragm Design Force

For a building two stories or less, the determination of diaphragm forces is the same for ASCE 7-16 and the 2015 NEHRP *Provisions*, which is illustrated below. Equation and table numbers shown below are from ASCE 7-16.
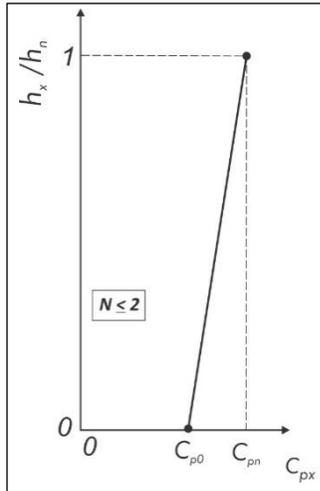
Calculating the design acceleration coefficient C_{px} in buildings with $N \le 2$

$N = 1$

$z_s = 1.0$ (for wood shear wall buildings)

$R_s = 3.0$ (from Table 12.10.3.5-1)

$$\Gamma_{m1} = 1 + 0.5 z_s \left(1 - \frac{1}{N}\right) = 1 + 0.5 \times 1.00 \times \left(1 - \frac{1}{1}\right) = 1.0 \quad \text{(Eq. 12.10.3-10)}$$

$$\Gamma_{m1} = 0.9 z_s \left(1 - \frac{1}{N}\right)^2 = 0.9 \times 1.00 \times \left(1 - \frac{1}{1}\right)^2 = 0 \quad \text{(Eq. 12.10.3-11)}$$

$$C_{p0} = 0.4 S_{DS} I_e = 0.4(1.0)(1.25) = 0.50 \quad \text{(Eq. 12.10.3-3)}$$

$$C_{pn} = \sqrt{\left(\Gamma_{m1}\Omega_0 C_s\right)^2 + \left(\Gamma_{m2}C_{s2}\right)^2} \quad \text{(Eq. 12.10.3-4)}$$

$$= \left(\Gamma_{m1}\Omega_0 C_s\right) = 1.0(3.0)(0.192) = 0.576$$

Strength Level diaphragm design force:

$$F_{pr} = \frac{C_{pr}}{R_s} w_{px} \quad \text{(Eq. 12.10.3-1)}$$

$$= \frac{0.576}{3.0} 76,200 = 14,630 \, \text{lbs} \quad \text{(transverse direction)}$$

$$= \frac{0.576}{3.0} 68,200 = 13,094 \, \text{lbs} \quad \text{(longitudinal direction)}$$

But not less than:

$$F_{pr} = 0.2 S_{DS} I_e w_{px} \quad \text{(Eq. 12.10.3-2)}$$

$$= 0.2(1.0)(1.25)(76,200) = 19,050 \, \text{lbs} \quad \text{(transverse direction)}$$

$$= 0.2(1.0)(1.25)(68,200) = 17,050 \, \text{lbs} \quad \text{(longitudinal direction)}$$

ASD Level diaphragm design force:

$F_{pr} = 0.7(19,050) = 13,335$ lbs (transverse direction)

$F_{pr} = 0.7(17,050) = 11,935$ lbs (longitudinal direction)

Transverse   Longitudinal

w_{ASD}= 13,335 lbs/90 ft.   = 148 plf w_{ASD} = 11,935 lbs/40 ft.   = 298 plf
$R = V$ = 148 plf (90 ft./2)   = 6660 lbs $R = V$ = 298 plf(40 ft./2)   = 5968 lbs
$v = V/b$ = 6660/40 ft.   = 167 plf $v = V/b$ = 5968/90 ft.   = 66 plf

Sheathing Design per SDPWS - Table 4.2C - Unblocked Diaphragms:

3/8-inch Sheathing with 8d common nails at 6-inch supported edge, 12-inch field
Transverse -   Load Case 1 - capacity = 430 plf/2 = 215 plf > 167 plf OK
Longitudinal - Load Case 3 - capacity = 320 plf/2 = 160 plf > 66 plf OK

Example – Three-Story Multi-Family Residential

Building Configuration

Three Story
Standard Occupancy, I_e = 1.0
Mean roof height = 31 feet
Length = 192 feet
Width = 54 feet
S_{DS} = 1.0, S_{D1} = 0.60
Wood structural panel diaphragm
Wood structural panel shear walls - R= 6.5, Ω_0= 3
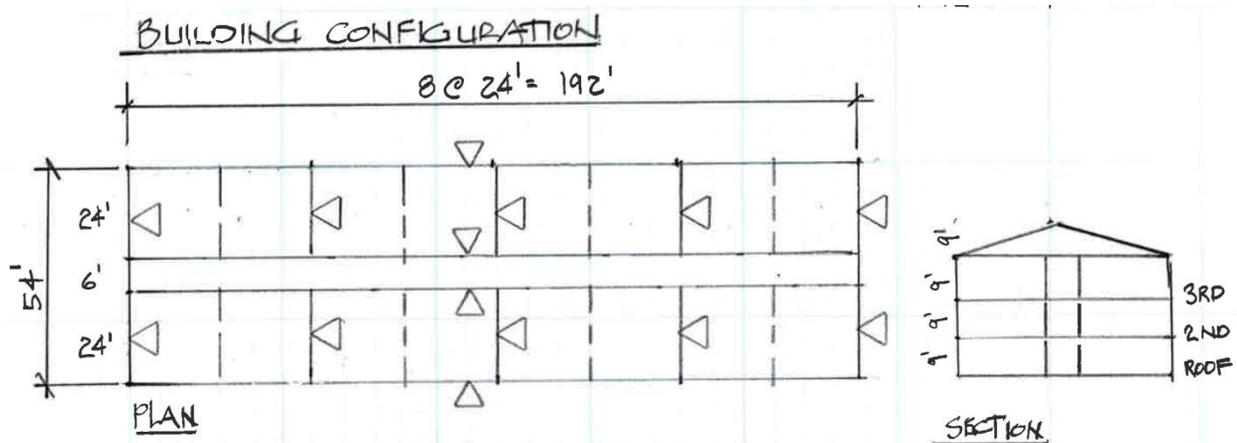
Weight for Seismic Analysis

Roof + ceiling   = 15 psf
Floor + ceiling   = 10
Exterior wall   = 15
Interior wall   = 10

Seismic weight at roof
   Roof: (15 psf)(54 ft.)(192 ft.) = 155.5 kips
   Longitudinal exterior wall: (15 psf)(192 ft.)(4 ft.)(2 sides) = 23.0 kips
   Transverse exterior wall: (15 psf)(54 ft.)(4 ft.)(2 sides) = 6.5 kips
   Longitudinal interior wall: (10 psf)(192 ft.)(4 ft.)(2 lines) = 15.4 kips

Transverse interior wall: (10 psf)(24 ft.)(4 ft.)(14 lines) = 13.4 kips

TOTAL = 214 kips acting at roof

Seismic weight at 2nd and 3rd floors

Floor: (10 psf)(54 ft.)(192 ft.) = 103.7 kips

Longitudinal exterior wall: (15 psf)(192 ft.)(8 ft.)(2 sides) = 46.0 kips

Transverse exterior wall: (15 psf)(54 ft.)(8 ft.)(2 sides) = 13.0 kips

Longitudinal interior wall: (10 psf)(192 ft.)(8 ft.)(2 lines) = 30.8 kips

Transverse interior wall: (10 psf)(24 ft.)(8 ft.)(14 lines) = 26.8 kips

TOTAL = 220 kips acting at floors

Seismic weight TOTAL = 214+220+220 = 654 kips

ASCE 7-16 Base Shear

$$T_a = C_t h_n^x = 0.20(31)^{0.75} = 0.26 \text{ sec} \qquad (12.8\text{-}7)$$

$$C_s = \frac{S_{DS}}{R/I_e} = \frac{1.00}{6.5/1.00} = 0.154 \qquad (12.8\text{-}2)$$

C_s need not exceed:

$$C_s = \frac{S_{D1}}{T(R/I_e)} = \frac{0.60}{0.26(6.5/1.00)} = 0.355 \qquad (12.8\text{-}3)$$

$$V = C_s W = (0.154)(654) = 101 \text{ kips} \qquad (12.8\text{-}1)$$

Diaphragm Weights

Diaphragm weight, w_{px}, at the roof:

Total seismic weight – weight of the walls resisting seismic forces

= 214 – 6.5 – 13.4 = 194.1 kips (for seismic forces acting in transverse direction)

= 214 – 23 – 15.4 = 175.6 kips (for seismic forces acting in longitudinal direction)

Diaphragm weight, w_{px}, at the 2nd and 3rd floors:

Total seismic weight – weight of the walls resisting seismic forces

= 220 – 13 – 26.8 = 180.2 kips (for seismic forces acting in transverse direction)

= 220 – 46 – 30.8 = 143.2 kips (for seismic forces acting in longitudinal direction)

ASCE 7-16 Traditional Roof Diaphragm Design Force

Vertical distribution of seismic base shear:

The lateral seismic force at any level is determined as

$$F_x = C_{vx}V \qquad\qquad \text{(Eq. 12.8-11)}$$

Where

$$C_{vx} = \frac{w_x h_x^k}{\sum\limits_{i=1}^{n} w_i h_i^k} \qquad\qquad \text{(Eq. 12.8-12)}$$

For $T \le 0.5$ sec., $k = 1.0$

Force distribution along the height of the building is shown in the table below

Level x	w_x (kips)	h_x (ft)	$w_x h_x^k$ (ft-kips)	C_{vx}	F_x (kips)
3	214	31	6634	0.53	53.4
2	220	18	3960	0.31	31.4
1	220	9	1980	0.16	16.2
$\sum$	654		12,574	1.00	101

1.0 kip = 4.45 kN, 1.0 ft = 0.3048 m, 1.0 ft-kip = 1.36 kN-m

Strength level diaphragm design force:

Diaphragm design force is given by the larger of F_x determined above and F_{px} determined below.

$$F_{px} = \frac{\sum\limits_{i=x}^{n} F_i}{\sum\limits_{i=x}^{n} w_i} w_{px} \qquad\qquad \text{(Eq. 12.10-1)}$$

Strength level diaphragm forces are determined in the table below.

Level	w_i (kips)	$\sum\limits_{i=x}^{n} w_i$ (kips)	F_i (kips)	$\sum\limits_{i=x}^{n} F_i = V_i$ (kips)	w_{px} (kips) Trans.	w_{px} (kips) Long.	F_{px} (kips) Trans.	F_{px} (kips) Long.
Roof	214	214	53.4	53.4	194.1	175.6	48.4	43.8
2	220	434	31.4	84.8	180.2	143.2	35.2	28.0
1	220	654	16.2	101	180.2	143.2	27.8	22.0

1.0 kip = 4.45 kN.

F_{px} at roof cannot be less than:

$F_{pr} = 0.2S_{DS}I_e w_{pr}$ (Eq. 12.10-2)

$= 0.2(1.0)(1.0)(194.1) = 38.8$ kips (transverse direction)

$= 0.2(1.0)(1.0)(175.6) = 35.1$ kips (longitudinal direction)

F_{px} at the floor levels cannot be less than:

$F_{px} = 0.2S_{DS}I_e w_{px}$ (Eq. 12.10-2)

$= 0.2(1.0)(1.0)(180.2) = 36$ kips (transverse direction)

$= 0.2(1.0)(1.0)(143.2) = 28.6$ kips (longitudinal direction)

F_{px} at roof need not exceed:

$F_{pr} = 0.4S_{DS}I_e w_{pr}$ (Eq. 12.10-3)

$= 0.4(1.0)(1.0)(194.1) = 77.6$ kips (transverse direction)

$= 0.4(1.0)(1.0)(175.6) = 70.2$ kips (longitudinal direction)

F_{px} at the floor levels need not exceed:

$F_{px} = 0.4S_{DS}I_e w_{px}$ (Eq. 12.10-3)

$= 0.4(1.0)(1.0)(180.2) = 72$ kips (transverse direction)

$= 0.4(1.0)(1.0)(143.2) = 57.3$ kips (longitudinal direction)

ASD Level diaphragm design force:

$F_{px,\text{ASD}} = 0.7(F_{px,\text{Strength}})$

Summary of diaphragm design force (kips):

	Transverse Direction		Longitudinal Direction	
	Strength Level	ASD Level	Strength Level	ASD Level
Roof	53.4	37.4	53.4	37.4
3rd Floor	36.0	25.2	31.4	22.0
2nd Floor	36.0	25.2	28.6	20.0

ASCE 7-16 Roof Diaphragm Design Force - ASD

Transverse - Roof

$w_{ASD} = 37,400$ lbs/192 ft.	$= 195$ plf
$R = V = 195$ plf (48 ft./2)	$= 4680$ lbs
$v = V/b = 4680/54$ ft.	$= 87$ plf

Longitudinal - Roof

$w_{ASD} = 37,400$ lbs/54 ft.	$= 693$ plf
$R = V = 693$ plf(24 ft./2)	$= 8316$ lbs
$v = V/b = 8316/192$ ft.	$= 43$ plf

Sheathing Design per SDPWS - Table 4.2C - Unblocked Diaphragms:

5/16-inch Sheathing with 6d common nails at 6-inch supported edge, 12-inch field

Transverse - Load Case 1 - capacity   = 300 plf/2   = 150 plf   > 87 plf OK
Longitudinal - Load Case 3 - capacity = 220 plf/2   = 110 plf   > 43 plf OK

Same sheathing OK for second and third floors by inspection, thicker than 5/16-inch sheathing will be used based on gravity load requirements.

ASCE 7-16 Alternative Diaphragm Design Force
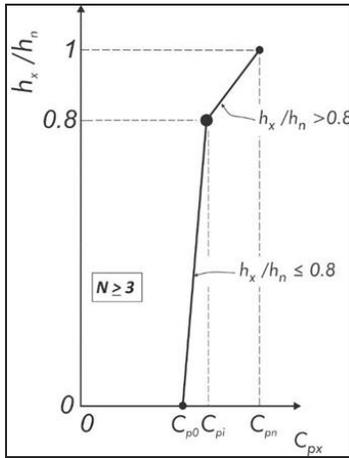
Equation and table numbers shown below are from ASCE 7-16.

$$N = 3$$

$z_s = 1.0$ (for wood shear wall buildings)

$R_s = 3.0$ (from Table 12.10.3.5-1)

Calculating the design acceleration coefficient C_{px} in buildings with $N \geq 3$

$$\Gamma_{m1} = 1 + 0.5 z_s \left(1 - \frac{1}{N}\right) \qquad\qquad \text{(Eq. 12.10.3 - 10)}$$

$$= 1 + 0.5 \times 1.00 \times \left(1 - \frac{1}{3}\right) = 1.33$$

$$\Gamma_{m2} = 0.9 z_s \left(1 - \frac{1}{N}\right)^2 = 0.9 \times 1.00 \times \left(1 - \frac{1}{3}\right)^2 = 0.4 \qquad\qquad \text{(Eq. 12.10.3-11)}$$

$$C_{p0} = 0.4 S_{DS} I_e = 0.4(1.0)(1.00) = 0.40 \qquad\qquad \text{(Eq. 12.10.3-3)}$$

$$C_{pi} = C_{p0} = 0.40 \qquad\qquad \text{(Eq. 12.10.3-5)}$$

$$C_{pi} = 0.9 \Gamma_{m1} \Omega_0 C_s = 0.9(1.33)(3.0)(0.154) = 0.55 \qquad\qquad \text{(Eq. 12.10.3-6)}$$

$$C_{s2} = (0.15N + 0.25) I_e S_{DS} = (0.15 \times 3 + 0.25) \times 1.0 \times 1.0 = 0.7 \qquad\qquad \text{(Eq. 12.10.3 - 7)}$$

$$C_{s2} = I_e S_{DS} = 1.0 \times 1.0 = 1.0 \qquad\qquad \text{(Eq. 12.10.3 - 8)}$$

$$C_{s2} = \frac{I_e S_{D1}}{0.03(N - 1)} = \frac{1.0 \times 0.6}{0.03 \times 2} = 10 \qquad\qquad \text{(Eq. 12.10.3 - 9)}$$

$$C_{pn} = \sqrt{(\Gamma_{m1}\Omega_0 C_s)^2 + (\Gamma_{m2}C_{s2})^2} = \sqrt{(1.33 \times 3 \times 0.154)^2 + (0.4 \times 0.7)^2} = 0.68 \qquad \text{(Eq. 12.10.3 - 4)}$$

Strength Level diaphragm design force:

$$F_{pr} = \frac{C_{pr}}{R_s} w_{pr} \qquad\qquad\qquad\qquad \text{(Eq.12.10.3-1)}$$

$$= \frac{0.68}{3.0} 194.1 = 44 \text{ kips} \quad \text{(transverse direction)}$$

$$= \frac{0.68}{3.0} 175.6 = 39.8 \text{ kips} \quad \text{(longitudinal direction)}$$

But not less than:

$$F_{pr} = 0.2 S_{DS} I_e w_{pr} \qquad\qquad\qquad\qquad \text{(Eq. 12.10.3-2)}$$

$$= 0.2(1.0)(1.0)(194.1) = 38.8 \text{ kips (transverse direction)}$$

$$= 0.2(1.0)(1.0)(175.6) = 35.1 \text{ kips (longitudinal direction)}$$

$$F_{p3} = \frac{C_{p3}}{R_s} w_{p3} \qquad\qquad\qquad\qquad \text{(Eq.12.10.3-1)}$$

$$= \frac{0.51}{3.0} 180.2 = 30.6 \text{ kips} \quad \text{(transverse direction)}$$

$$= \frac{0.51}{3.0} 143.2 = 24.3 \text{ kips} \quad \text{(longitudinal direction)}$$

But not less than:

$$F_{p3} = 0.2 S_{DS} I_e w_{p3} \qquad\qquad\qquad\qquad \text{(Eq. 12.10.3-2)}$$

$$= 0.2(1.0)(1.0)(180.2) = 36 \text{ kips (transverse direction)}$$

$$= 0.2(1.0)(1.0)(143.2) = 28.6 \text{ kips (longitudinal direction)}$$

$$F_{p2} = \frac{C_{p2}}{R_s} w_{p2} \qquad\qquad\qquad\qquad \text{(Eq.12.10.3-1)}$$

$$= \frac{0.46}{3.0} 180.2 = 27.6 \text{ kips} \quad \text{(transverse direction)}$$

$$= \frac{0.46}{3.0} 143.2 = 21.9 \text{ kips} \quad \text{(longitudinal direction)}$$

But not less than:

$$F_{p2} = 0.2 S_{DS} I_e w_{p2} \qquad\qquad\qquad\qquad \text{(Eq. 12.10.3-2)}$$

$$= 0.2(1.0)(1.0)(180.2) = 36 \text{ kips (transverse direction)}$$

$= 0.2(1.0)(1.0)(143.2) = 28.6$ kips (longitudinal direction)

<u>ASD Level diaphragm design force:</u>

$F_{px,\text{ASD}} = 0.7(F_{px,\text{Strength}})$

<u>Summary of diaphragm design force (kips):</u>

	Transverse Direction		Longitudinal Direction	
	Strength Level	ASD Level	Strength Level	ASD Level
Roof	44	30.8	39.8	27.9
3rd Floor	36	25.2	28.6	20.0
2nd Floor	36	25.2	28.6	20.0

ASCE 7-16 Roof Diaphragm Design - ASD

<u>Transverse - Roof</u>   <u>Longitudinal - Roof</u>

w_{ASD}= 30,800 lbs/192 ft.   = 160 plf w_{ASD} = 27,900 lbs/54 ft.   = 517 plf
R = V = 160plf (48 ft./2)   = 3840 lbs   R = V = 517 plf(24 ft./2)   = 6204 lbs
v = V/b = 3840/54 ft.   = 71 plf   v = V/b = 6204/192 ft.   = 32 plf

Sheathing Design per SDPWS - Table 4.2C - Unblocked Diaphragms:

5/16-inch Sheathing with 6d common nails at 6-inch supported edge, 12inch field
Transverse - Load Case 1 - capacity   = 300 plf/2   = 150 plf   > 71 plf OK
Longitudinal - Load Case 3 - capacity = 220 plf/2   = 110 plf   > 32 plf OK

Same sheathing OK for second and third floors by inspection, thicker than 5/16-inch sheathing will be used based on gravity load requirements.

2015 NEHRP *Provisions* Diaphragm Design Force

Equation and table numbers shown below are from the 2015 NEHRP *Provisions*.
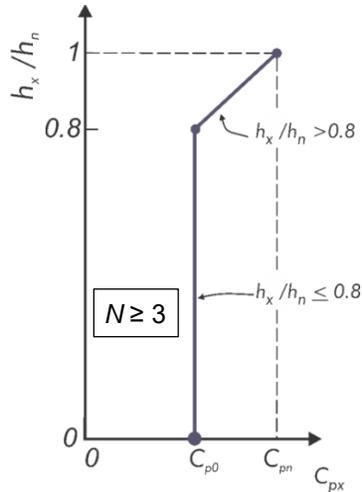
Calculating the design acceleration coefficient C_{px} in buildings with $N \geq 3$

$n = 3$

$z_s = 1.0$

$R_s = 3.0$

$$\Gamma_{m1} = 1 + \frac{z_s}{2}\left(1 - \frac{1}{n}\right) = 1 + \frac{1}{2}\left(1 - \frac{1}{3}\right) = 1.33 \tag{12.10-11}$$

$$\Gamma_{m2} = 0.9 z_s \left(1 - \frac{1}{n}\right)^2 = 0.9(1.0)\left(1 - \frac{1}{3}\right)^2 = 0.40 \tag{12.10-12}$$

$$C_{s2} = (0.15n + 0.25) I_e \, S_{DS} = (0.15 * 3 + 0.25)(1.00)(1.00) = 0.70 - controls \tag{12.10-8}$$

$$C_{s2} = I_e \, S_{DS} = 1.00(1.00) = 1.00 \tag{12.10-9}$$

$$C_{s2} = \frac{I_e \, S_{D1}}{0.03(n-1)} = \frac{1.00(1.00)}{0.03(3-1)} = 16.7 \qquad For\ n \geq 2 \tag{12.10-10a}$$

$$C_{p0} = 0.4 S_{DS} \, I_e = 0.4(1.0)(1.00) = 0.40 \tag{12.10-6}$$

$$C_{pn} = \sqrt{\left(\Gamma_{m1} \, \Omega_0 \, C_s\right)^2 + \left(\Gamma_{m2} \, C_{s2}\right)^2} = \sqrt{(1.33 * 3.0 * 0.154)^2 + (0.40 * 0.70)^2} = 0.672 \tag{12.10-7}$$

Roof - Strength Level:

$$F_{pr} = \frac{C_{pr}}{R_s} w_{pr} = \frac{0.68}{3.0} 194.1 = 44\ \text{kips} \tag{12.10-4}$$

But not less than:

$$F_{pr} = 0.2 S_{DS} I_e w_{pr} = 0.2(1.0)(1.0)(194.1) = 38.8\ \text{kips} \tag{12.10-5}$$

Roof - ASD Level:

$F_{pr} = 0.7(44\ \text{kips}) = 30.8\ \text{kips}$

3rd Floor - Strength Level:

$C_{p3} = 0.40$

$$F_{p3} = \frac{C_{p3}}{R_s} w_{p3} = \frac{0.4}{3.0} 180.2 = 24\ \text{kips} \tag{12.10-4}$$

But not less than:

$$F_{p3} = 0.2 S_{DS} I_e w_{p3} = 0.2(1.0)(1.0)(180.2) = 36\ \text{kips} \tag{12.10-5}$$

3rd Floor - ASD Level:
$F_{p3} = 0.7(36.0 \text{ kips}) = 25.2 \text{ kips}$

2nd Floor - Strength Level:
$C_{p2} = 0.40$

$$F_{p2} = \frac{C_{p2}}{R_s} w_{p2} = \frac{0.4}{3.0} 180.2 = 24 \text{ kips} \qquad (12.10\text{-}4)$$

But not less than:
$F_{p2} = 0.2 S_{DS} I_e w_{p2} = 0.2(1.0)(1.0)(180.2) = 36 \text{ kips}$ $\qquad$ (12.10-5)

2nd Floor - ASD Level:
$F_{p2} = 0.7(36.0 \text{ kips}) = 25.2 \text{ kips}$

Comparison Summary - ASD Level F_{px} Forces (#)

Level	ASCE 7-16	2015 NEHRP *Provisions*
Roof	30,800	30,800
3rd	25,200	25,200
2nd	25,200	25,200

6.4 COMPARISON OF DESIGN FORCE LEVELS

Comparisons of diaphragm seismic design force levels along the heights of a number of buildings of various materials and assigned to various SDC's are shown in this section.

4-Story Perimeter Wall Precast Concrete Parking Structure (SDC C, Knoxville)

The structure for Example 1 is a 4-story perimeter shear wall precast concrete parking garage. As seen in the plan view of Figure 6.4‑1a, the parking structure has three bays with a central ramp. The structural plan has a footprint of 300 ft × 180 ft, resulting in 300 ft × 60 ft dimensions for each sub-diaphragm. The floor-to-floor height is 10.5 ft for the typical story and 16 ft for the first story. The lateral force‑resisting system (LFRS) in the transverse direction is composed of four 25-ft long perimeter precast walls, two at each end of the structure. The LFRS in the longitudinal direction consists of 34 interior lite walls flanking the central ramp (see elevation in Figure 8.4-1b).

The comparison of diaphragm design force levels for the structure of Figure 6.4-1 by ASCE 7-16 Sections 12.10.1 and 12.10.2 (marked ASCE 7), by ASCE 7-16 Section 12.10.3 (marked ASCE 7 Alt., and by the 2015 NEHRP *Provisions* (labeled NEHRP), are illustrated in Figure 6.4-2. EDO, BDO, and RDO in the figure stand for Elastic, Basic, and Reduced Design Options, respectively.

(a) Typical floor plan

(b) Ramp elevation
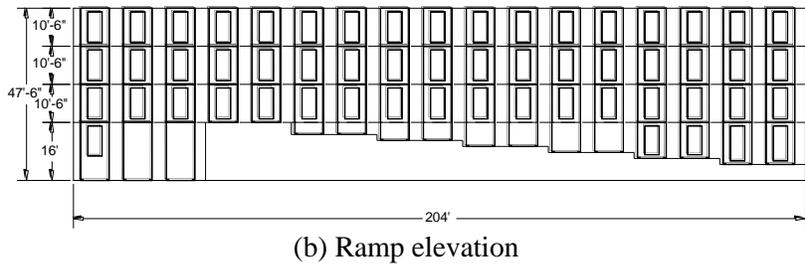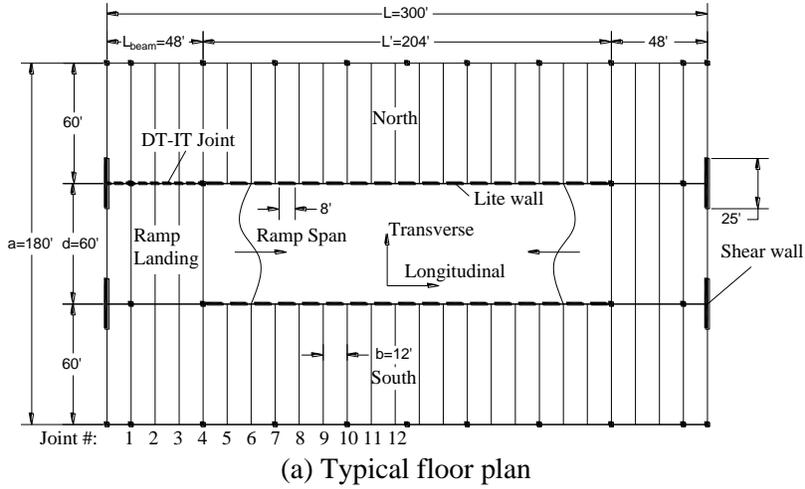
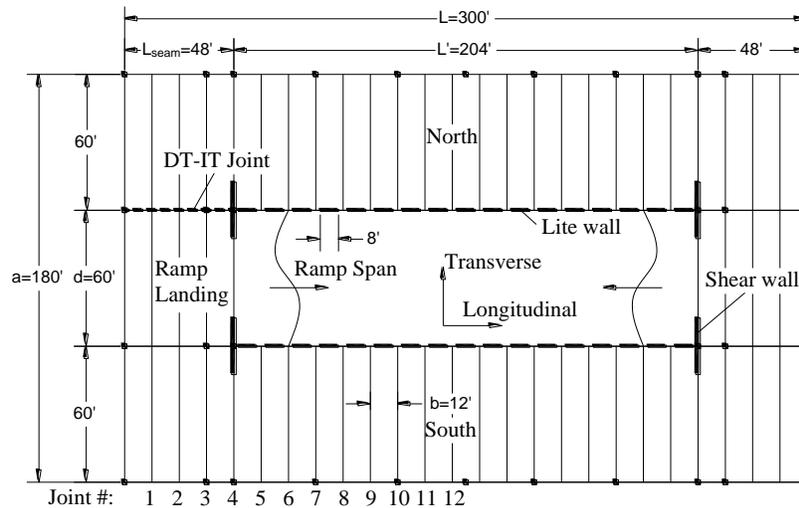**Figure 6.4-1 Example 1 : 4-story perimeter wall precast concrete parking structure**
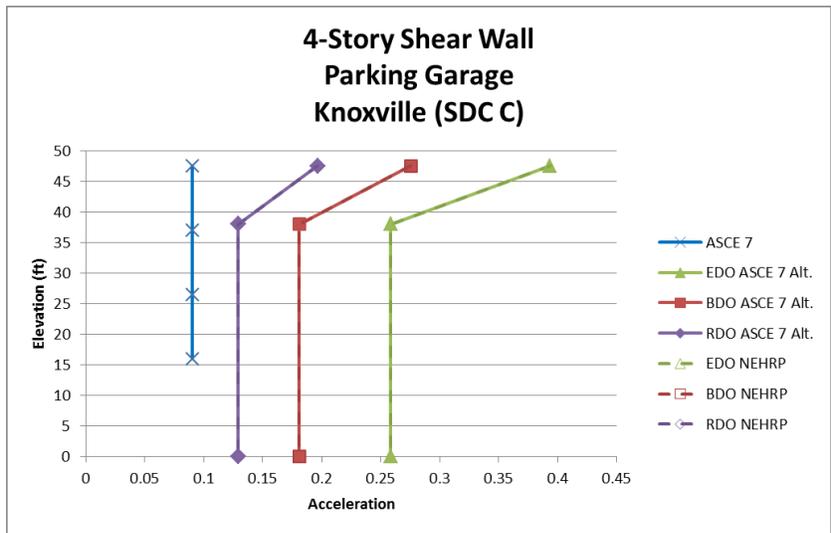
Figure 6.4-2 Design force level comparisons for Example 1 structure
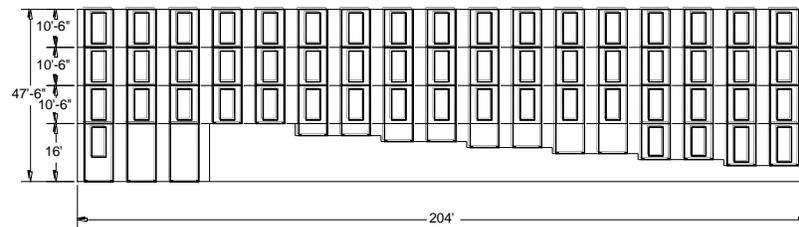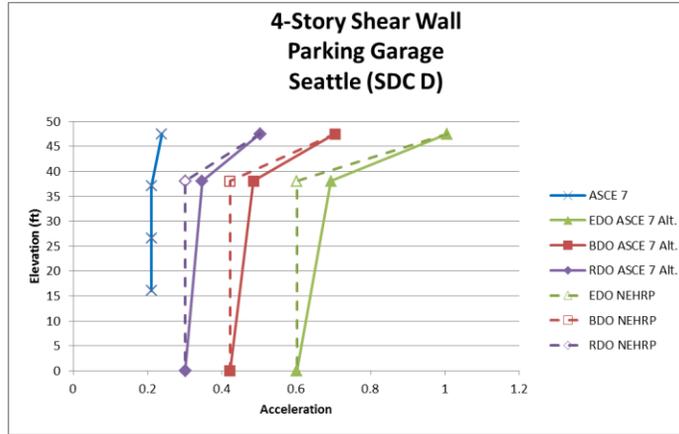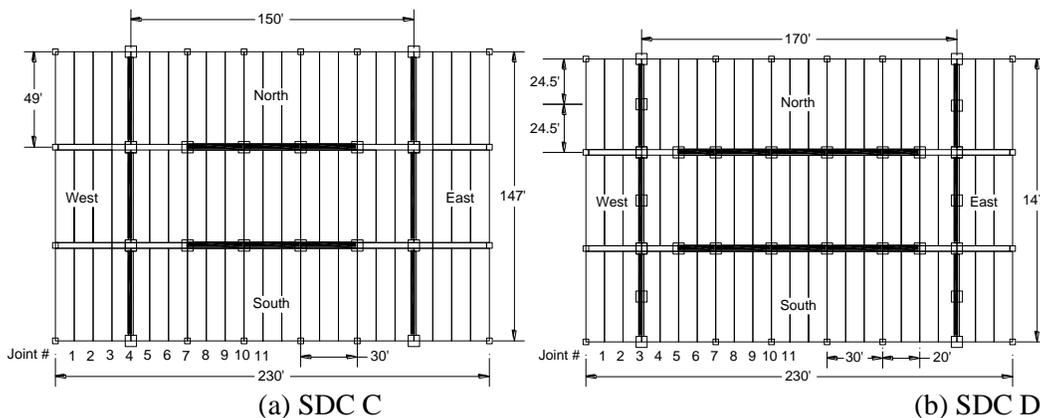(All references to ASCE 7 and NEHRP are to ASCE 7-16 and the 2015 NEHRP *Provisions*, respectively)

4-Story Interior Wall Precast Concrete Parking Structure (SDC D, Seattle)

The structure for example 2 is a 4-story interior wall precast concrete partaking garage. As seen in the plan view of Figure 6.4-3a, the parking structure has three bays with a central ramp. The structural plan has a footprint of 300 ft × 180 ft, resulting in 300 ft × 60 ft dimensions for each sub-diaphragm. The floor-to-floor height is 10.5 ft for the typical story and 16 ft at the first story. The LFRS in the transverse direction is composed of four 25-ft long interior reinforced concrete walls. The LFRS in the longitudinal direction consists of 34 interior lite walls flanking the central ramp (see elevation in Figure 6.4-3b).

The comparison of diaphragm design force levels for the structure of Figure 6.4-3 by ASCE 7-16 Sections 12.10.1 and 12.10.2 (marked ASCE 7), by ASCE 7-16 Section 12.10.3 (marked ASCE 7 Alt., and by the 2015 NEHRP *Provisions* (labeled NEHRP), are illustrated in Figure 6.4-4. EDO, BDO, and RDO in the figure stand for Elastic, Basic, and Reduced Design Options, respectively.


(a) Typical floor plan

(b) Ramp elevation

Figure 6.4-3 Example 2: 4-story interior wall precast concrete partaking structure
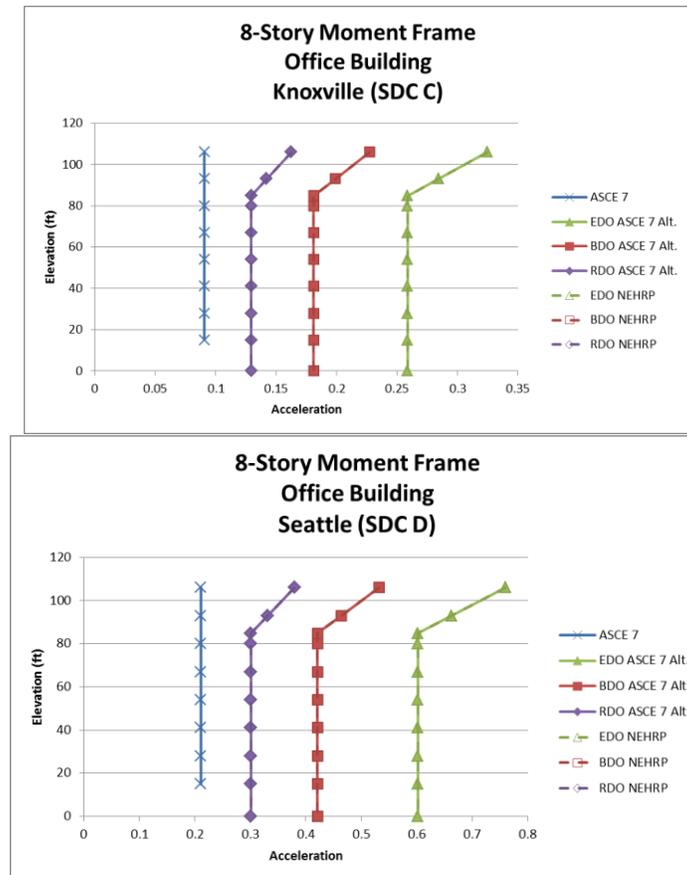
Figure 6.4-4 Design force level comparisons for Example 2 structure.
(All references to ASCE 7 and NEHRP are to ASCE 7-16 and the 2015 NEHRP *Provisions*, respectively)

8-Story Precast Concrete Moment Frame Office Building

The structure for example 3 is an 8-story precast concrete moment frame office building. As seen in Figure 6.4-5, the structure has three bays with a footprint of 230 ft × 147 ft. The story height is 13 ft for the typical floor and 15 ft for the first floor. The LFRS in the transverse as well as in the longitudinal direction is composed of intermediate moment frames for SDC C, Knoxville, and special moment frames for SDC D, Seattle. The precast floor system consists of double tees with a 3 in. toping.

The comparison of diaphragm design force levels for the structure of Figure 6.4‑5 by ASCE 7-16 Sections 12.10.1 and 12.10.2 (marked ASCE 7), by ASCE 7-16 Section 12.10.3 (marked ASCE 7 Alt., and by the 2015 NEHRP *Provisions* (labeled NEHRP), are illustrated in Figure 6.4-6. EDO, BDO, and RDO in the figure stand for Elastic, Basic, and Reduced Design Options, respectively.

(a) SDC C   (b) SDC D

(c) SDC C (d) SDC D
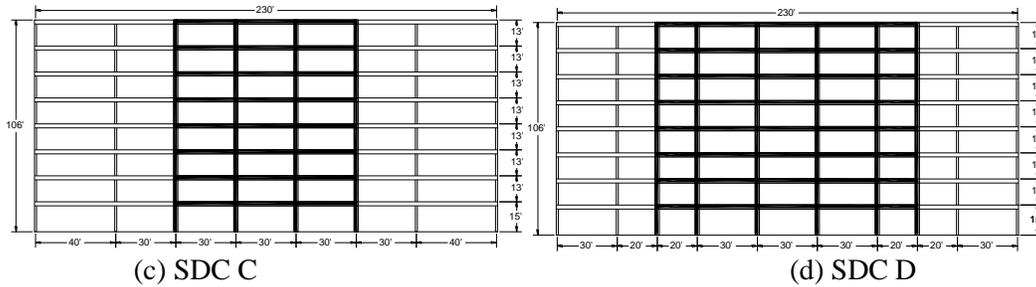
Figure 6.4-5 Example 3: 8-story moment frame office building of precast concrete

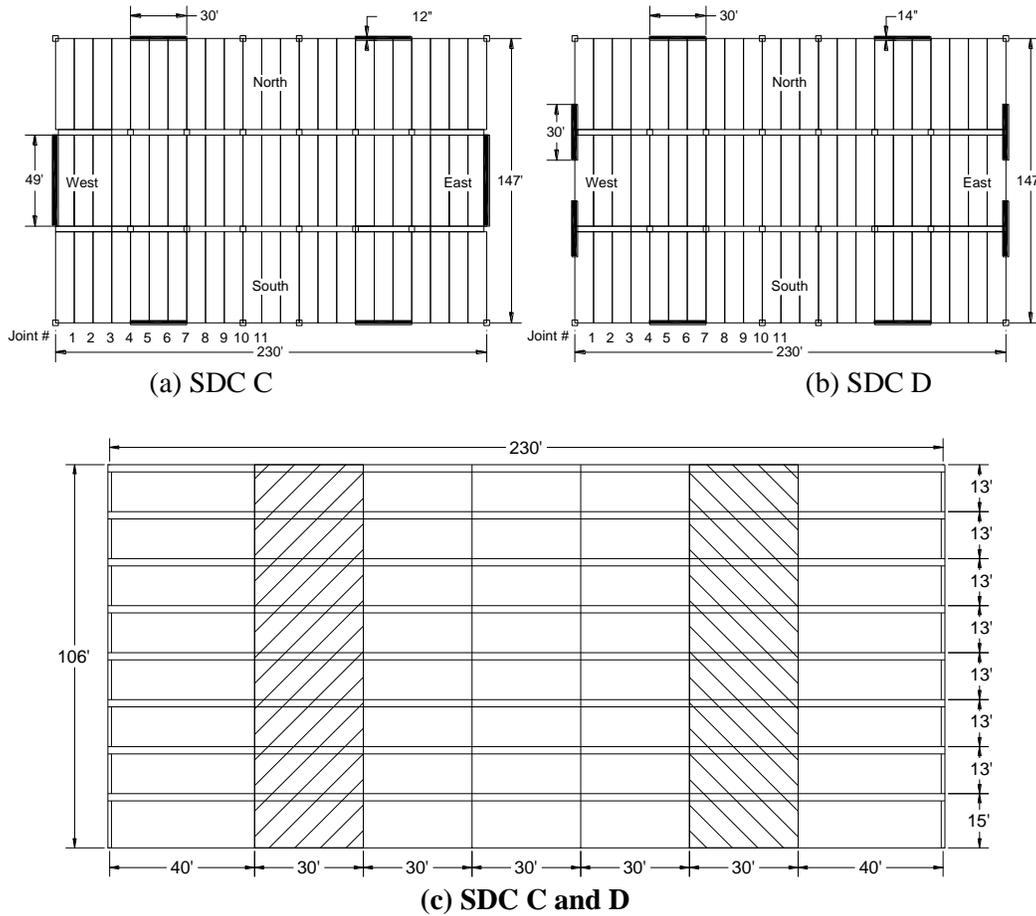**Figure 6.4-6 Design force level comparisons for Example 3 structures**
(All references to ASCE 7 and NEHRP are to ASCE 7-16 and the 2015 NEHRP *Provisions*, respectively)

### 8-Story Precast Concrete Shear Wall Office Building

The structure for example 4 is an 8-story precast concrete perimeter shear wall office building. As seen in Figure 6.4-7, the structure has three bays with a footprint of 230 ft × 147 ft. The story height is 13 ft for the typical story and 15 ft for the first story. The LFRS in the transverse direction is composed of two perimeter ordinary reinforced concrete shear walls for SDC C and four perimeter special reinforced concrete shear walls for SDC D. The LFRS in the longitudinal direction is composed of four perimeter ordinary reinforced

concrete shear walls for SDC C, Knoxville and 4 perimeter special reinforced concrete shear walls for SDC D, Seattle. The precast floor system consists of double tees with a 3-in. toping.

The comparison of diaphragm design force levels for the structure of Figure 6.4-7 by ASCE 7-16 Sections 12.10.1 and 12.10.2 (marked ASCE 7), by ASCE 7-16 Section 12.10.3 (marked ASCE 7 Alt., and by the 2015 NEHRP *Provisions* (labeled NEHRP), are illustrated in Figure 6.4-8. EDO, BDO, and RDO in the figure stand for Elastic, Basic, and Reduced Design Options, respectively.

(a) SDC C   (b) SDC D

(c) SDC C and D

Figure 6.4-7. Example 4: 8-story precast concrete shear wall office building
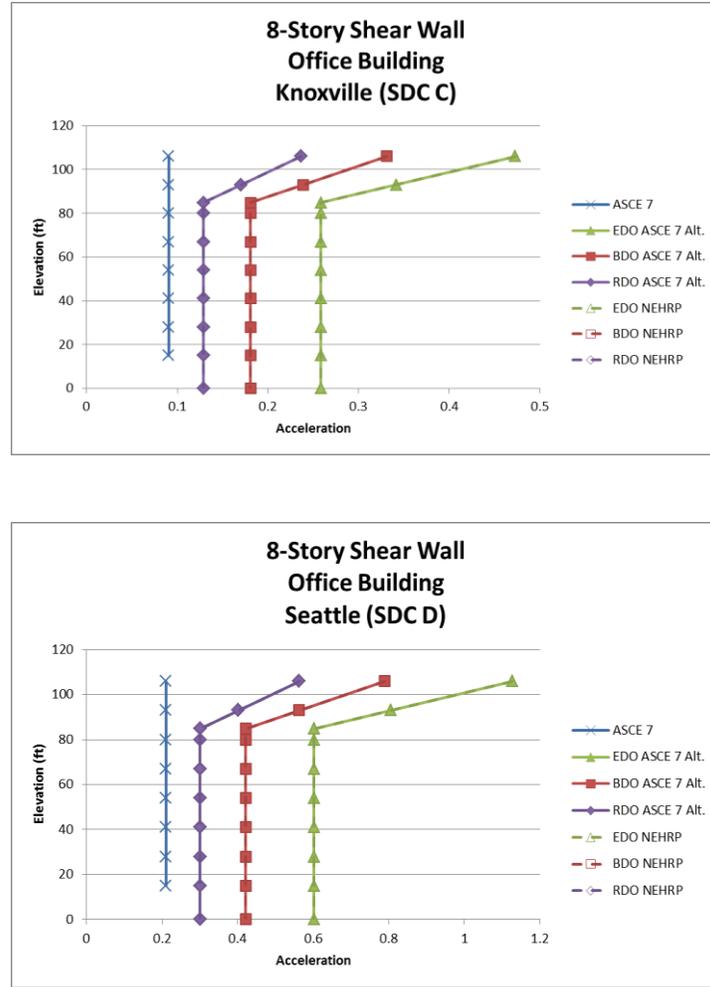
Figure 6.4-8 Design force level comparisons for Example 4 structures
(All references to ASCE 7 and NEHRP are to ASCE 7-16 and the 2015 NEHRP *Provisions*, respectively)

Steel-Framed Assembly Structure in Southern California

The structure for Example 5 is a 3-story buckling-restrained braced frame assembly structure in southern California. The following information is relevant.

Risk Category III
Seismic Design Category D
Base Shear Coefficient, $C_s = 0.212$
Design Base Shear, $V = 7,311$ kips
Building Height, $h_n = 60$ ft

The comparison of diaphragm design force levels for the structure by ASCE 7-16 Sections 12.10.1 and 12.10.2 (marked ASCE 7), by ASCE 7-16 Section 12.10.3 (marked ASCE 7 Alt., and by the 2015 NEHRP *Provisions* (labeled NEHRP), are illustrated in Figure 6.4-9. All three sets of requirements produce the same diaphragm design forces throughout the height of the structure, because the minimum diaphragm design force controls at every level.
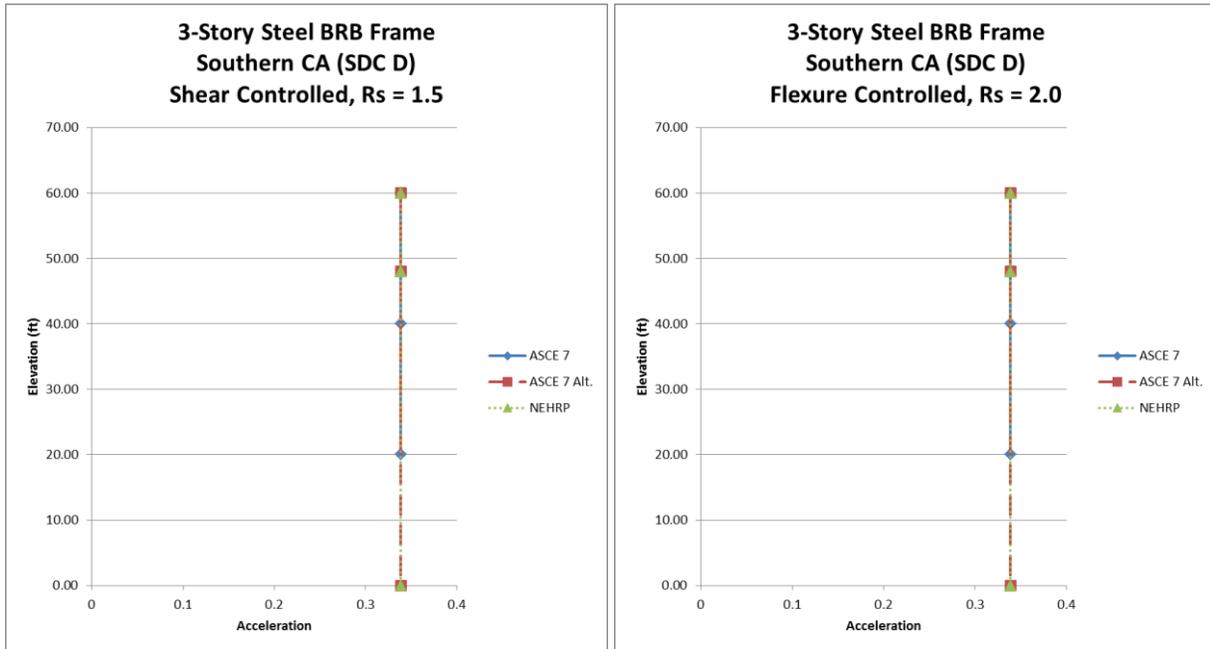
Figure 6.4-9. Design force level comparisons for 3-story steel-framed assembly structure
(References to ASCE 7 and NEHRP are to ASCE 7-16 and the 2015 NEHRP *Provisions*, respectively)

Steel-Framed Office Structure in Seattle, WA

The structure for Example 6 is a 12-story buckling-restrained braced frame office building in Seattle, WA. The following information is relevant.
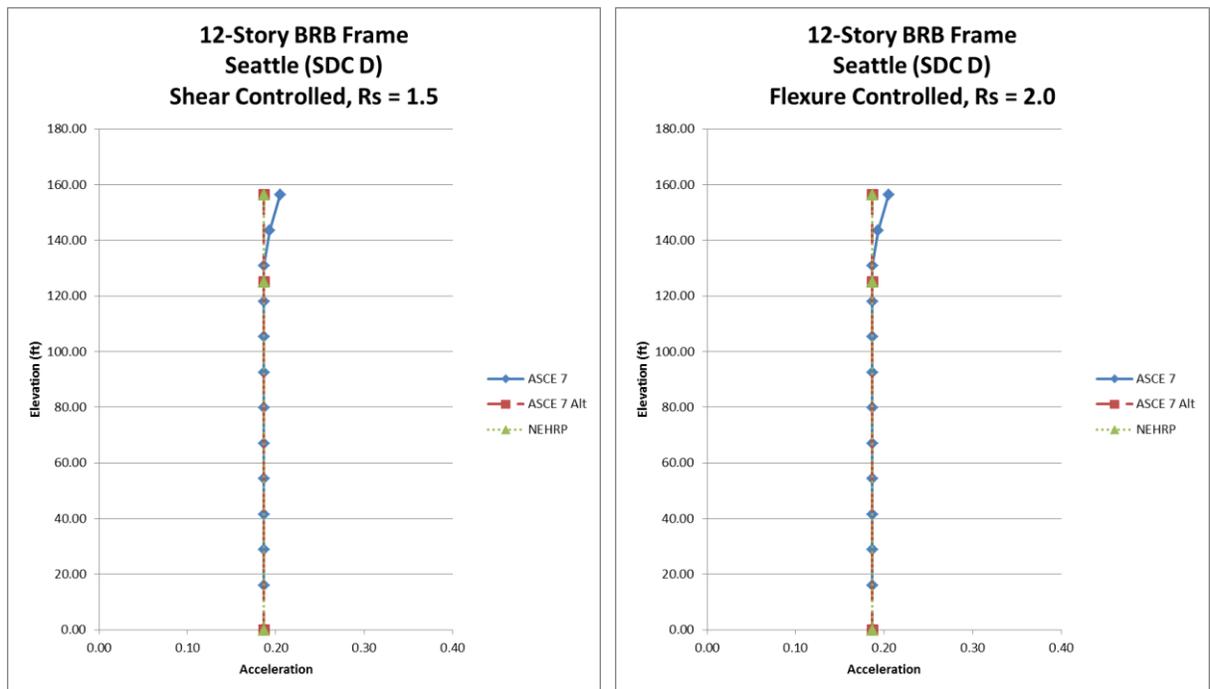
Risk Category II
Seismic Design Category D
Base Shear Coefficient, $C_s = 0.059$
Design Base Shear, $V = 3{,}150$ kips
Building Height, $h = 156$ ft

The comparison of diaphragm design force levels for the structure by ASCE 7-16 Sections 12.10.1 and 12.10.2 (marked ASCE 7), by ASCE 7-16 Section 12.10.3 (marked ASCE 7 Alt., and by the 2015 NEHRP *Provisions* (labeled NEHRP), are illustrated in Figure 6.4-10. All three sets of requirements produce the same diaphragm design forces through most of the height of the structure, because the minimum diaphragm design force controls, except that ASCE 7-16 Sections 12.10.1 and 12.10.2 produce slightly higher than minimum diaphragm design forces at and near the very top.

Figure 6.4-10. Design force level comparisons for 12-story steel-framed office structure
(References to ASCE 7 and NEHRP are to ASCE 7-16 and the 2015 NEHRP *Provisions*, respectively)

Cast-in-Place Concrete Framed Parking Structure in Southern California

The structure for Example 7 is a 3-story reinforced concrete special shear wall parking structure in southern California. The following information is relevant.
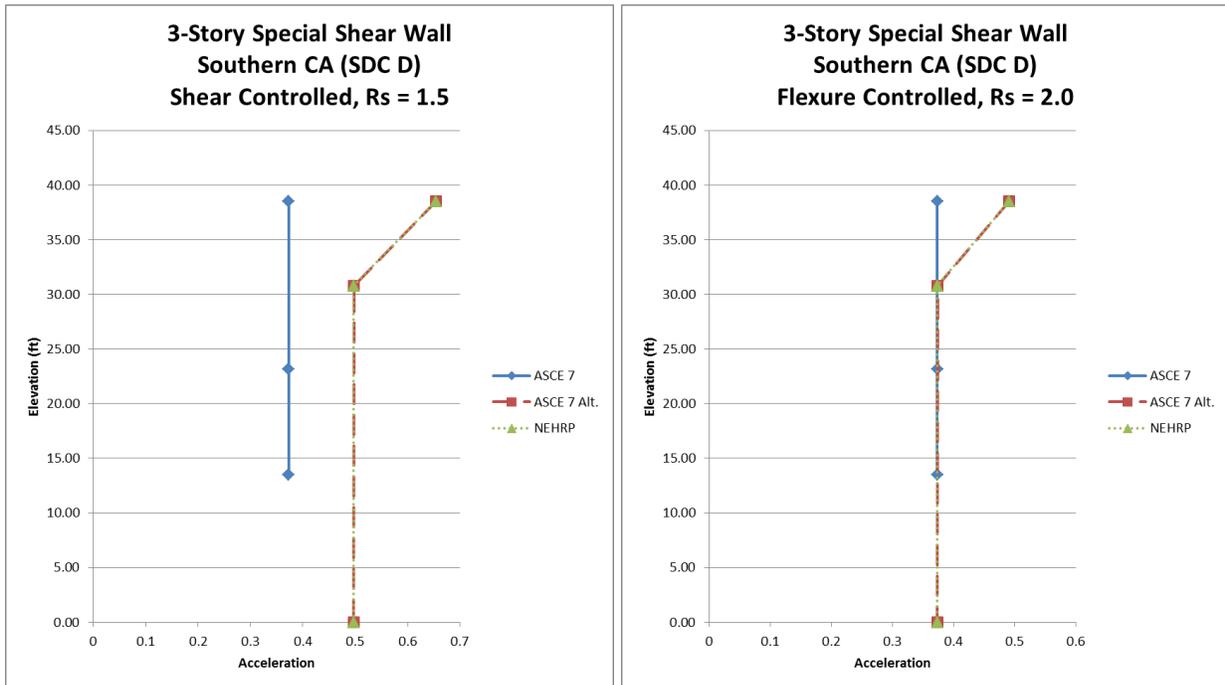
Risk Category II
Seismic Design Category D
Base Shear Coefficient, $C_s = 0.249$
Design Base Shear, $V = 7,145$ kips
Building Height, $h = 38.5$ ft

The comparison of diaphragm design force levels for the structure by ASCE 7-16 Sections 12.10.1 and 12.10.2 (marked ASCE 7), by ASCE 7-16 Section 12.10.3 (marked ASCE 7 Alt., and by the 2015 NEHRP *Provisions* (labeled NEHRP), are illustrated in Figure 6.4-11. By ASCE 7-16 Sections 12.10.1 and 12.10.2, the minimum diaphragm design force levels govern throughout the height for shear-controlled as well as flexure-controlled diaphragms. By ASCE 7-16 Section 12.10.3 and the *Provisions*, the diaphragm design force levels are the same at the first two floor levels and are higher at the roof level; they are higher than minimum for shear-controlled diaphragms. By ASCE 7-16 Section 12.10.3 and the *Provisions*, the diaphragm design force levels are the minimum values at all floor levels other than the roof, where they are higher, for flexure-controlled diaphragms.

Figure 6.4-11. Design force level comparisons for 3-story special shear wall parking structure
(References to ASCE 7 and NEHRP are to ASCE 7-16 and the 2015 NEHRP *Provisions*, respectively)

Cast-in-Place Concrete Framed Residential Structure in Northern California

The structure for Example 8 is a 15-story reinforced concrete special shear wall residential structure in northern California. The following information is relevant.
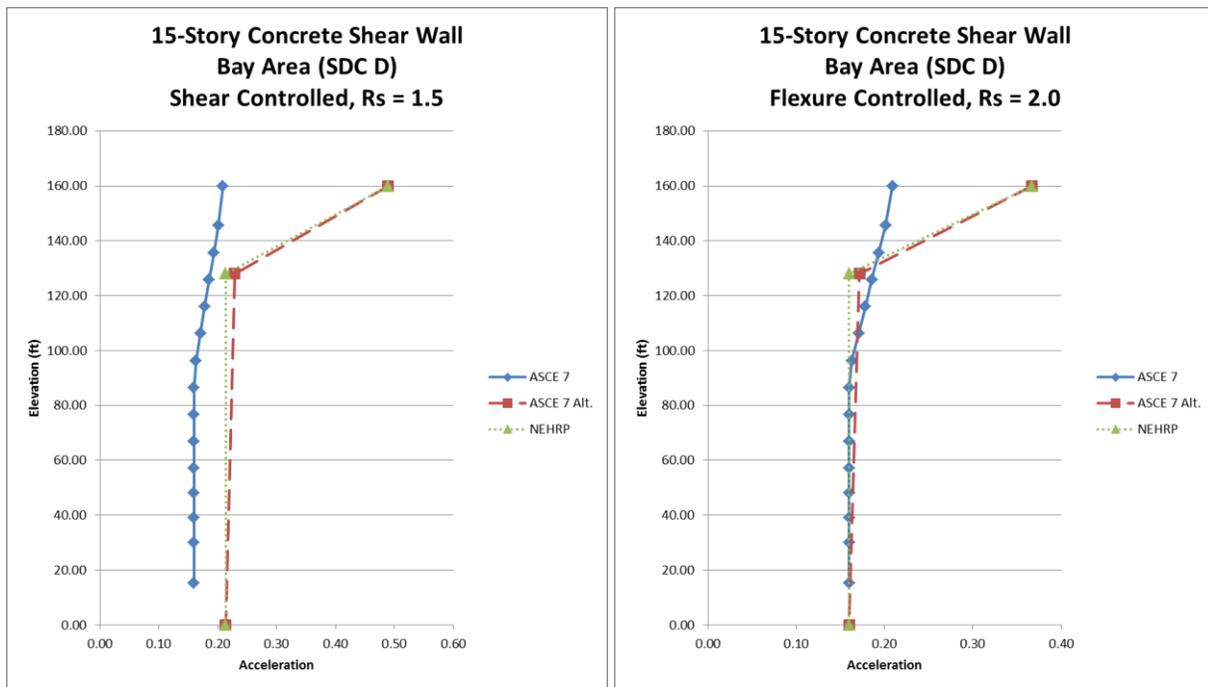
Risk Category II
Seismic Design Category D
Base Shear Coefficient, $C_s = 0.104$
Design Base Shear, $V = 4,439$ kips
Building Height, $h = 160$ ft

The comparison of diaphragm design force levels for the structure by ASCE 7-16 Sections 12.10.1 and 12.10.2 (marked ASCE 7), by ASCE 7-16 Section 12.10.3 (marked ASCE 7 Alt., and by the 2015 NEHRP *Provisions* (labeled NEHRP), are illustrated in Figure 6.4-12. There is very little difference between the design force levels by ASCE 7-16 Section 12.10.3 and the *Provisions*. These force levels are higher than those given by ASCE 7-10 Sections 12.10.1 and 12.10.2 – throughout the building height for shear-controlled diaphragms and only near the top for flexure-controlled diaphragms.

Figure 6.4-12. Design force level comparisons for 15-story concrete shear wall residential structure (References to ASCE 7 and NEHRP are to ASCE 7-16 and the 2015 NEHRP *Provisions*, respectively)

Cast-in-Place Concrete Framed Residential Structure in Seattle, WA

The structure for Example 9 is a 40-story reinforced concrete special shear wall residential structure in Seattle, WA. The following information is relevant.
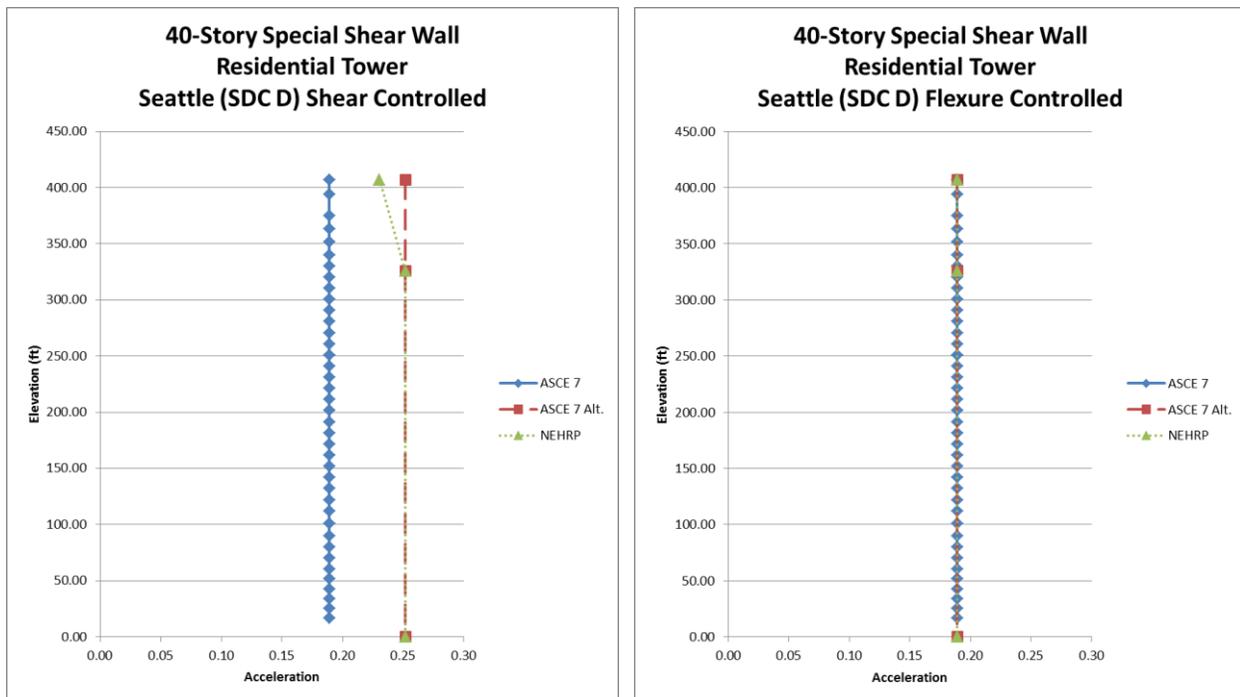
Risk Category II
Seismic Design Category D
Base Shear Coefficient, $C_s = 0.042$
Design Base Shear, $V = 3,696$ kips
Building Height, $h = 407$ ft

The comparison of diaphragm design force levels for the structure by ASCE 7-16 Sections 12.10.1 and 12.10.2 (marked ASCE 7), by ASCE 7-16 Section 12.10.3 (marked ASCE 7 Alt., and by the 2015 NEHRP *Provisions* (labeled NEHRP), are illustrated in Figure 6.4-13. The minimum design force level governs for all flexure-controlled shear walls by all three sets of requirements. It also controls for shear-controlled shear walls, when forces are calculated by ASCE 7-16 Sections 12.10.1 and 12.10.2. For shear-controlled walls, the design force levels are higher by ASCE 7-16 Section 12.10.3 and the *Provisions*. They are the same at every floor level by ASCE 7-16 Section 12.10.3, but turn a little lower at the top level by the *Provisions*. ASCE 7-16 Section 12.10.3 does not allow this to happen, because C_{pn} is restricted to be no lower than C_{pi}

Figure 6.4-13. Design force level comparisons for 40-story special shear wall residential structure
(References to ASCE 7 and NEHRP are to ASCE 7-16 and the 2015 NEHRP *Provisions*, respectively)

Cast-in-Place Concrete Framed Residential Structure in Hawaii

The structure for Example 10 is a 24-story reinforced concrete shear wall residential structure in Hawaii. The following information is relevant.
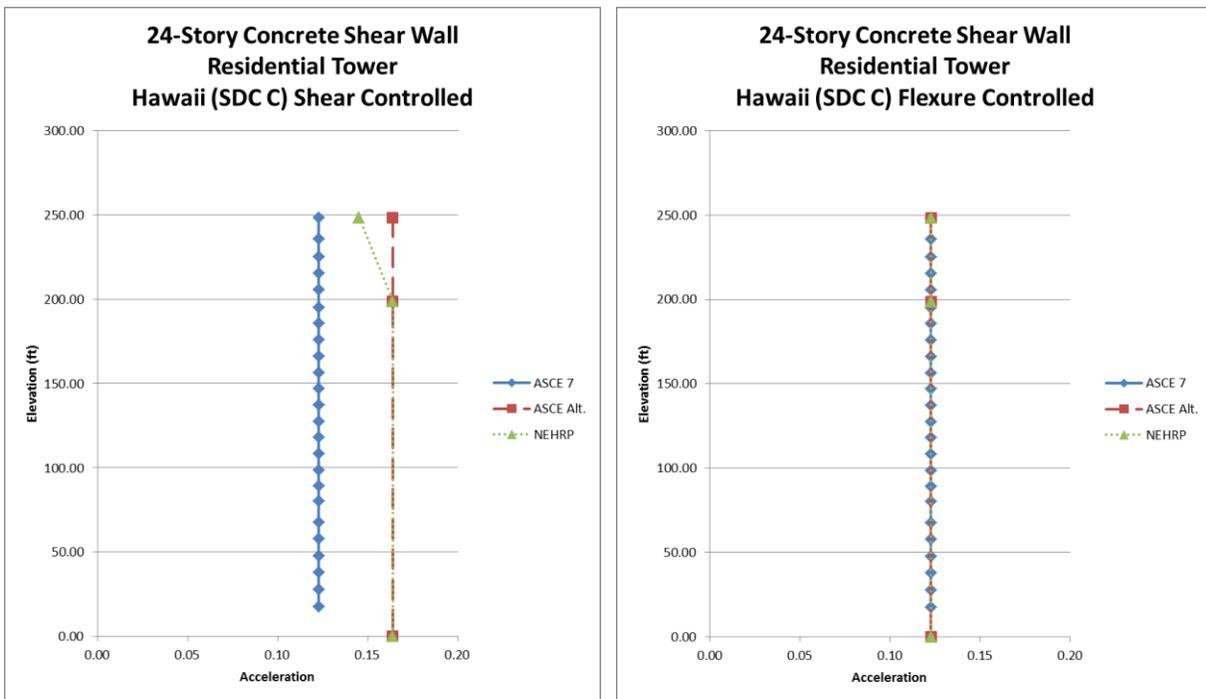
Risk Category II
Seismic Design Category C
Base Shear Coefficient, $C_s = 0.021$
Design Base Shear, $V = 2,982$ kips
Building Height, $h = 248$ ft

The comparison of diaphragm design force levels for the structureby ASCE 7-16 Sections 12.10.1 and 12.10.2 (marked ASCE 7), by ASCE 7-16 Section 12.10.3 (marked ASCE 7 Alt., and by the 2015 NEHRP *Provisions* (labeled NEHRP), are illustrated in Figure 6.4-14. The minimum design force level governs for all flexure-controlled shear walls by all three sets of requirements. It also controls for shear-controlled shear walls, when forces are calculated by ASCE 7-16 Sections 12.10.1 and 12.10.2. For shear-controlled walls, the design force levels are higher by ASCE 7-16 Section 12.10.3 and the *Provisions*, because of the low R_s-value assigned. They are the same at every floor level by ASCE 7-16 Section 12.10.3, but turn a little lower at the top level by the *Provisions*. ASCE 7-16 Section 12.10.3 does not allow this to happen, because C_{pn} is restricted to be no lower than C_{pi}

Figure 6.4-14. Design force level comparisons for 24-story concrete shear wall residential structure (References to ASCE 7 and NEHRP are to ASCE 7-16 and the 2015 NEHRP *Provisions*, respectively)

Steel Framed Office Structure in Southern California

The structure for Example 11 is a 3-story steel special moment frame office building in southern California. The following information is relevant.

Risk Category II
Seismic Design Category D
Base Shear Coefficient, $C_s = 0.062$
Design Base Shear, $V = 467$ kips
Building Height, $h = 47$ ft

The comparison of diaphragm design force levels for the structure by ASCE 7-16 Sections 12.10.1 and 12.10.2 (marked ASCE 7), by ASCE 7-16 Section 12.10.3 (marked ASCE 7 Alt., and by the 2015 NEHRP *Provisions* (labeled NEHRP), are illustrated in Figure 6.4-15. The minimum diaphragm design force governs throughout the height by all three sets of requirements for flexure-controlled as well as shear-controlled diaphragms.
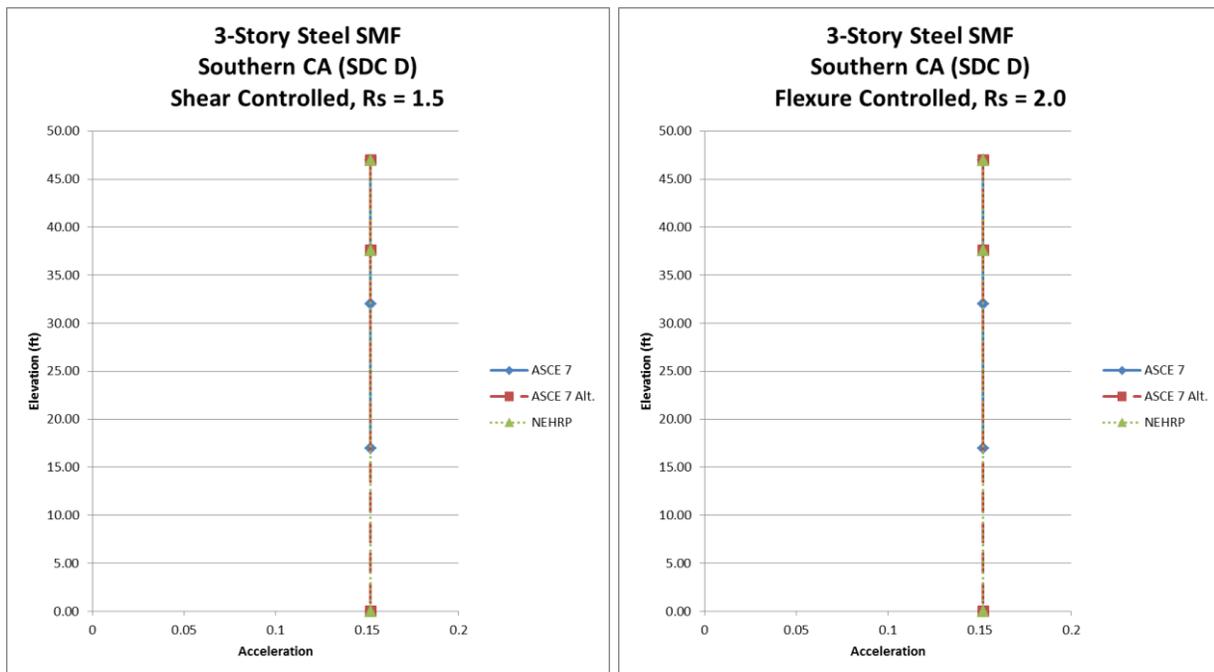
Figure 6.4-15. Design force level comparisons for 3-story steel SMF office building

6.5   SEISMIC DESIGN OF PRECAST CONCRETE DIAPHRAGMS

The following describes in a step-by-step fashion the seismic design of topped or untopped precast concrete diaphragms by ASCE 7-16 Section 14.2.4, Additional Design and Detailing Requirements for Precast Concrete Diaphragms. Seismic design by ASCE 7-16 Section 14.2.4 is required when the design force level of ASCE 7-16 Section 12.10.3 is used. For precast concrete diaphragms in buildings assigned to SDC C, D, E, or F, the design force level of ASCE 7-16 Section 12.10.3 is mandated. For precast concrete diaphragms in assigned to SDC B, the design force level of ASCE 7-16 Section 12.10.3 is

optional. These requirements are in addition to the seismic design requirements for reinforced concrete set forth in ASCE 7-16 and ACI 318-14 Section 18.12, Diaphragms and Trusses. The design methodology of ACE 7-16 Section 14.2.4 is illustrated in Chapter 8 of this publication. It is based on work by Fleischman et al., which was part of the extensive DSDM (Diaphragm Seismic Design Methodology) research effort (Pankow, 2014).

Step 1: Determine Diaphragm Seismic Demand Level

There are three "Diaphragm Seismic Demand Levels": low, moderate and high. The Diaphragm Seismic Demand Level is a function of the seismic design category a building is assigned to, the number of stories in the building, the diaphragm span as defined in Section 14.2.4.1.1, and the diaphragm aspect ratio as defined in Section 14.2.4.1.2. It leads to the selection of the Diaphragm Design Option. In fact, the Diaphragm Design Option cannot be chosen without the Diaphragm Seismic Demand Level. For structures assigned to SDCs B and C, the Diaphragm Seismic Demand Level is automatically designated as low. For structures assigned to SDC D, E, or F, the Diaphragm Seismic Demand Level is determined from Figure 14.2.4-1.
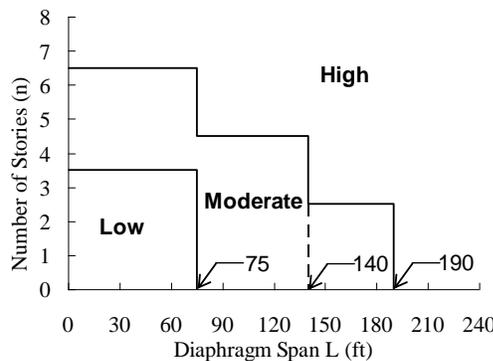
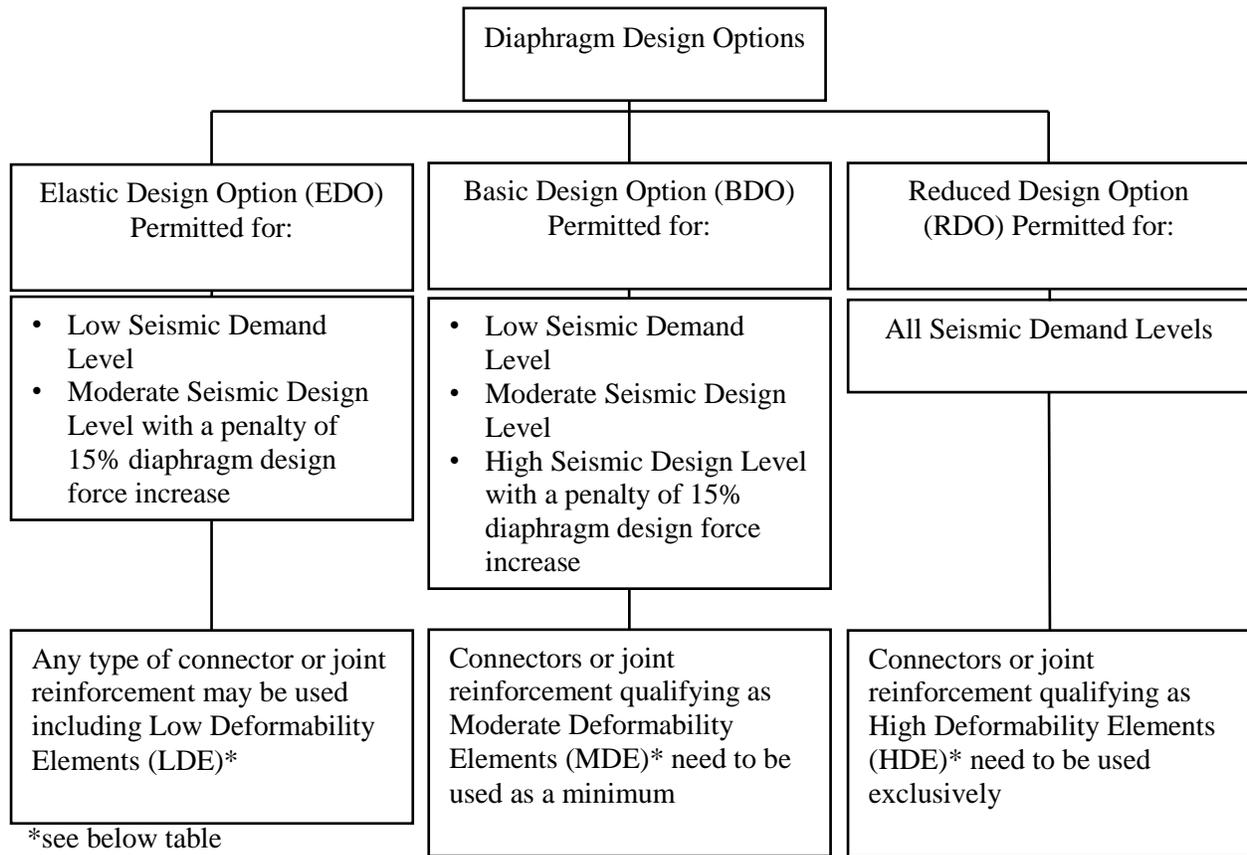*Standard* **Figure 14.2.4-1 Diaphragm seismic demand level**

1. If aspect ratio, *AR,* is greater than or equal to 2.5 and the Diaphragm Seismic Demand Level is *Low* according to Figure 14.2.4-1, the Diaphragm Seismic Demand Level needs to be changed from *Low* to *Moderate*.

2. If *AR* is less than 1.5 and the Diaphragm Seismic Demand Level is *High* according to Figure 14.2.4-1, the Diaphragm Seismic Demand Level can be changed from *High* to *Moderate*.

Diaphragm Seismic Demand Level	What does it mean?
Low	Low seismic vulnerability; automatically assigned to SDC B and C diaphragms
Moderate	Moderate seismic vulnerability
High	High seismic vulnerability

Step 2: Determine Diaphragm Design Option and Corresponding Connector or Joint Reinforcement Deformability Requirement

The Diaphragm Design Option addressed in Section 14.2.4.2 provides a mechanism for selecting the target performance of a diaphragm when subject to earthquake excitation. There are three diaphragm design options: Elastic, Basic, and Reduced. The Elastic Design Option (EDO) seeks to keep the diaphragm elastic in the MCE. The Basic Design Option (BDO) seeks to keep the diaphragm elastic in the design earthquake while permitting controlled inelastic behavior in the MCE. The Reduced Design Option (RDO) permits controlled inelastic behavior even in the design earthquake.

The flow chart below illustrates 1) which Diaphragm Design Option is permitted to be used when, and 2) the corresponding minimum precast concrete diaphragm connector or joint reinforcement classification that would need to be used per Section 14.2.4.3.

```
                         ┌────────────────────────────┐
                         │  Diaphragm Design Options  │
                         └────────────────────────────┘
```

Elastic Design Option (EDO) Permitted for:	Basic Design Option (BDO) Permitted for:	Reduced Design Option (RDO) Permitted for:
• Low Seismic Demand Level • Moderate Seismic Design Level with a penalty of 15% diaphragm design force increase	• Low Seismic Demand Level • Moderate Seismic Design Level • High Seismic Design Level with a penalty of 15% diaphragm design force increase	All Seismic Demand Levels
Any type of connector or joint reinforcement may be used including Low Deformability Elements (LDE)*	Connectors or joint reinforcement qualifying as Moderate Deformability Elements (MDE)* need to be used as a minimum	Connectors or joint reinforcement qualifying as High Deformability Elements (HDE)* need to be used exclusively

*see below table

Step 3: Comply with Qualification Procedure

This step is to ensure that the selected connector or joint reinforcement meets connector or joint reinforcement qualification requirements per Section 14.2.4.4.

See separate step-by-step instructions for Qualification Procedure.

Step 4: Amplify Required Shear Strength

Determine the diaphragm force reduction factor, R_s, from Table 12.10.3.5-1.

Amplify the required shear strength for the diaphragm by the diaphragm shear overstrength factor, Ω_v, which is to be taken equal to 1.4 R_s.

6.6 PRECAST CONCRETE DIAPHRAGM CONNECTOR AND JOINT REINFORCEMENT QUALIFICATION PROCEDURE

Precast concrete diaphragm connector or joint reinforcement is assigned a deformability classification based on tests. The testing is to establish the strength, stiffness, and deformation capacity of the element. As a minimum, in-plane shear tests and in-plane tension tests need to be conducted. The procedure is based on work by Naito et al., which was part of the extensive DSDM (Diaphragm Seismic Design Methodology) research effort (Naito et al., 2006, Naito et al., 2007, Ren and Naito, 2013).

Step 1: Construct test modules in conformance Section 14.2.4.4.1.

Step 2: Evaluate test results based on the number of tests in accordance with Section 14.2.4.4.2.

Step 3: Use test configuration as required by Section 14.2.4.4.3.

Step 4: Use instrumentation (displacement and force transducers) as required by Section 14.2.4.4.4.

Step 5: Conduct the following tests:

1. Monotonic and cyclic tests under displacement control as described in Section 14.2.4.4.5, Item 1.
2. A monotonic test to determine the reference deformation (as defined in Section 14.2.4.4.6, Item 2) in compliance with Section 14.2.4.4.5, Item 2.
3. In-plane cyclic shear test in accordance with Section 14.2.4.4.5, Item 3.
4. In-plane cyclic tension/compression tests in compliance with Section 14.2.4.4.5, Item 4.

Step 6: Construct an envelope of the cyclic force-deformation response from the force corresponding to the peak displacement applied during the first cycle of each increment of deformation. Simplify the envelope to a backbone curve consisting of four segments in accordance with Figure 14.2.4-2.
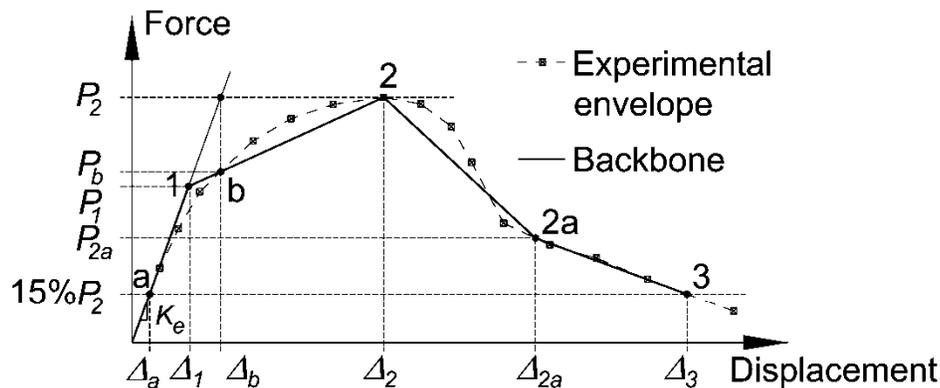
***Standard* Figure 14.2.4-2. Backbone qualification curve**

Step 7: Classify the backbone curve as one of the types indicated in *Standard* Figure 14.2.4-3.
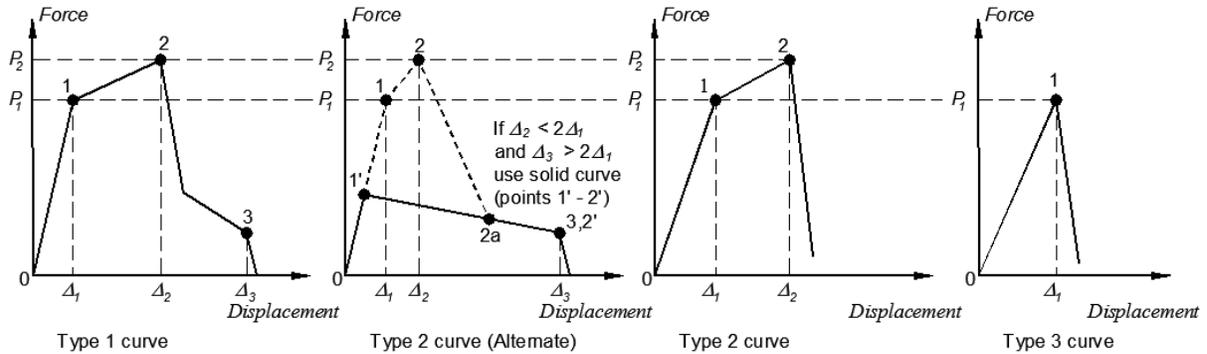
Standard **Figure 14.2.4-3 Deformation curve types**

Step 8: Determine if the connector being tested is a deformation-controlled or a force-controlled element.

Deformation-controlled elements conform to Type 1 or Type 2, but not Type 2 Alternate, response with Δ_2 larger than or equal to Δ_1. All other responses are classified as force-controlled.

Step 9: Quantify the following performance characteristics of the connector or joint reinforcement from the backbone curve:

1.   Effective yield (reference deformation)
2.   Tension deformation capacity
3.   Tensile strength
4.   Shear strength

Determine all quantities as the average of values obtained from the number of tests required by Section 14.2.4.4.2.

Determine the effective yield (reference deformation), Δ_1, corresponding to Point 1 on the backbone curve.

The tension deformation capacity corresponds to Point 2 for deformation-controlled connections. It corresponds to Point 1 for force-controlled connections except that for force-controlled connections exhibiting Type 2 Alternate response, tension deformation capacity corresponds to Point 1′.

The tensile strength of the connector or joint reinforcement is the force corresponding to Point 1.

If the shear deformation, Δ_1, is less than 0.25 inch, the shear strength is the force at the Point 1. If the shear deformation, Δ_1, is greater than or equal to 0.25 inch, the shear strength is the force at 0.25 inch of shear deformation. This shear strength is equal to the stiffness, K_e (see Figure 14.2.4-2), multiplied by 0.25 inch.

Step 10: Classify the connector or joint reinforcement as a Low Deformability Element (LDE), a Moderate Deformability Element (MDE), or a High Deformability Element (HDE) based on the tension deformation capacity ranges given Section 14.2.4.3 (see table below).

Type of Connector or Joint Reinforcement	Tension Deformation Capacity Determined per Section 14.2.4.4.7
Low Deformability Element (LDE)	< 0.3 inch
Moderate Deformability Element (MDE)	0.3 inch ≤ tension deformation capacity < 0.6 inch
High Deformability Element (LDE)	≥ 0.6 inch

6.7 ACKNOWLEDGEMENT

7

Foundation and Liquefaction Design

Ian McFarlane, S.E. and Stephen K. Harris, S.E.

Originally developed by Michael Valley, S.E.

Contents

This chapter illustrates application of the 2015 Edition of the *NEHRP Recommended Seismic Provisions* to the design of foundation elements. Example 5.1 completes the analysis and design of shallow foundations for two of the alternative framing arrangements considered for the building featured in Example 6.2. Example 5.2 illustrates the analysis and design of deep foundations for a building similar to the one highlighted in Chapter 7 of this volume of design examples. In both cases, only those portions of the designs necessary to illustrate specific points are included.

The force-displacement response of soil to loading is highly nonlinear and strongly time dependent. Control of settlement is generally the most important aspect of soil response to gravity loads. However, the strength of the soil may control foundation design where large amplitude transient loads, such as those occurring during an earthquake, are anticipated.

Foundation elements are most commonly constructed of reinforced concrete. As compared to design of concrete elements that form the superstructure of a building, additional consideration must be given to concrete foundation elements due to permanent exposure to potentially deleterious materials, less precise construction tolerances and even the possibility of unintentional mixing with soil.

Although the application of advanced analysis techniques to foundation design is becoming increasingly common (and is illustrated in this chapter), analysis should not be the primary focus of foundation design. Good foundation design for seismic resistance requires familiarity with basic soil behavior and common geotechnical parameters, the ability to proportion concrete elements correctly, an understanding of how such elements should be detailed to produce ductile response and careful attention to practical considerations of construction.

In addition to the *Standard* and the *Provisions* and *Commentary*, the following documents are either referenced directly or provide useful information for the analysis and design of foundations for seismic resistance:

AISC	American Institute of Steel Construction. 2011. *Steel Construction Manual, Fourteenth Edition.*
AISC 341	American Institute of Steel Construction. 2010. *Seismic Provisions for Structural Steel Buildings.*
ACI 318	American Concrete Institute. 2014. *Building Code Requirements and Commentary for Structural Concrete.*
Bowles	Bowles, J. E. 1988. *Foundation Analysis and Design.* McGraw-Hill.
CRSI	Concrete Reinforcing Steel Institute. 2008. *CRSI Design Handbook.* Concrete Reinforcing Steel Institute.
ASCE 41	ASCE. 2013. *Seismic Rehabilitation of Existing Buildings.*
Kramer	Kramer, S. L. 1996. *Geotechnical Earthquake Engineering.* Prentice Hall.
LPILE	Reese, L. C. and S. T. Wang. 2012. *Technical Manual for LPILE v2013 for Windows.* Ensoft.
NEHRP Tech Brief 7	Klemencic, R., McFarlane, I. S., Hawkins, N. M., and Nikolaou, S. (2012).

"Seismic design of reinforced concrete mat foundation: A guide for practicing engineerings." *NEHRP Seismic Design Technical Brief No. 7*, NIST GCR 12-917-22

Rollins et al. (a)   Rollins, K. M., Olsen, R. J., Egbert, J. J., Jensen, D. H., Olsen, K. G.and Garrett, B. H. (2006). "Pile Spacing Effects on Lateral Pile Group Behavior: Load Tests." *Journal of Geotechnical and Geoenvironmental Engineering*, ASCE, Vol. 132, No. 10, p. 1262-1271.

Rollins et al. (b)   Rollins, K. M., Olsen, K. G., Jensen, D. H, Garrett, B. H., Olsen, R. J.and Egbert, J. J. (2006). "Pile Spacing Effects on Lateral Pile Group Behavior: Analysis." *Journal of Geotechnical and Geoenvironmental Engineering*, ASCE, Vol. 132, No. 10, p. 1272-1283.

Wang & Salmon   Wang, C.-K. and C. G. Salmon. 1992. *Reinforced Concrete Design* . HarperCollins.

Several commercially available programs were used to perform the calculations described in this chapter. SAP2000 is used to determine the shears and moments in a concrete mat foundation; LPILE, in the analysis of laterally loaded single piles; and spColumn, to determine concrete pile section capacities.

7.1 SHALLOW FOUNDATIONS FOR A SEVEN-STORY OFFICE BUILDING, LOS ANGELES, CALIFORNIA

This example features the analysis and design of shallow foundations for two of the three framing arrangements for the seven-story steel office building described in Section 6.2 of this volume of design examples. Refer to that example for more detailed building information and for the design of the superstructure.

7.1.1 Basic Information

7.1.1.1 Description. The framing plan in Figure 7.1-1 shows the gravity load-resisting system for a representative level of the building. The site soils, consisting of medium dense sands, are suitable for shallow foundations. Table 7.1-1 shows the design parameters provided by a geotechnical consultant. Note that design parameters are presented in terms of nominal strength as rather than allowable stress to be consistent with changes made to ASCE 7-16 based on the 2015 NEHPR Provisions.

Foundation geotechnical capacities may be determined using either the strength design method defined in Section 12.13.5 of the *Standard*, or the more traditional approach of allowable stress design. The benefit of following the strength design method is that it permits a direct comparison of foundation capacities and supported structure capacities (determined using strength design). The strength design method utilizes strength reduction factors (phi factors) that reflect the uncertainty of site conditions and reliability of analysis methods. In order to describe the new strength design for foundation geotechnical capacity provisions in Section 12.13.5, this example focuses on that method.

Nominal strength values may be based on either a limitation of maximum expected foundation deformation at failure, or by the nominal strength that is associated with the anticipated failure mechanism. Given that limiting foundation movement (either total or differential settlement) under sustained loads is commonly an important performance objective, the example includes an additional serviceability verification using a lower level of loading than strength level and allowable bearing pressure less than the nominal strength values.
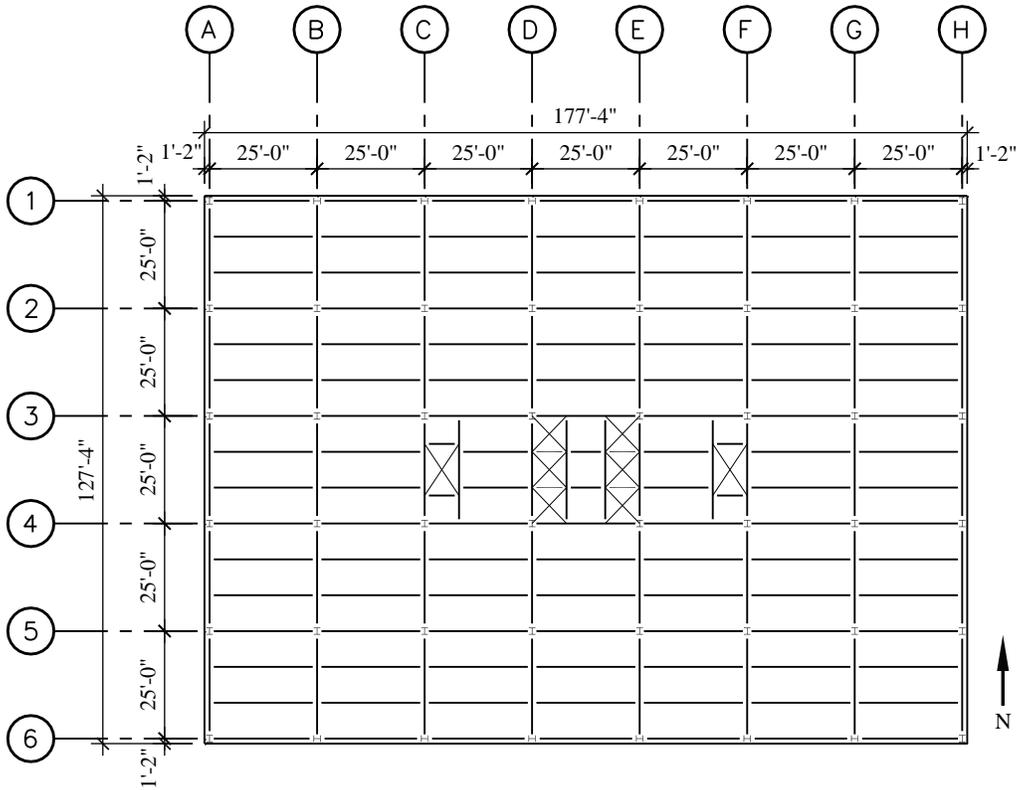
Figure 7.1-1 Typical framing plan

Because bearing capacities are generally expressed as a function of the minimum dimension of the loaded area and are applied as limits on the maximum pressure, foundations with significantly non-square loaded areas (tending toward strip footings) and those with significant differences between average pressure and maximum pressure (as for eccentrically loaded footings) have higher calculated bearing capacities. The recommended values are consistent with these expectations.

Table 7.1-1 Geotechnical Parameters

Parameter	Value
	Medium dense sand
	(SPT) $N = 20$
Basic soil properties	$\gamma = 125$ pcf
	Angle of internal friction = 33 degrees

Table 7.1-1 Geotechnical Parameters

Parameter	Value
Bearing capacity (Nominal foundation geotechnical capacity)	3,000B psf for concentrically loaded square footings 4,000B' psf for eccentrically loaded footings where B and B' are in feet, B is the footing width and B' is an average width for the compressed area. Resistance factor, $\phi = 0.45$ per Table 12.13-1 of the *Standard*
Lateral properties	Earth pressure coefficients: ▪ Active, $K_A = 0.3$ ▪ At-rest, $K_0 = 0.46$ ▪ Passive, $K_P = 3.3$ Sliding friction coefficient at base of footing = 0.65 Resistance factor, $\phi = 0.85$ per Table 12.13-1 of the *Standard*
Allowable soil bearing for sustained loads to control settlement (serviceability verification)	$\leq$ 2,000 psf for $B \leq 20$ feet $\leq$ 1,000 psf for $B \leq 40$ feet (may interpolate for intermediate dimensions)

The structural material properties assumed for this example are as follows:

▪ $f'_c = 4,000$ psi

▪ $f_y = 60,000$ psi

7.1.1.2 Seismic Parameters. The complete set of parameters used in applying the *Provisions* to design of the superstructure is described in Section 6.2.2.1 of this volume of design examples. The following parameters, which are used during foundation design, are duplicated here.

▪ Site Class = D

▪ $S_{DS} = 1.0$

▪ Seismic Design Category = D

7.1.1.3 Design Approach.

7.1.1.3.1 Selecting Footing Size and Reinforcement. Footing plan dimensions are first selected using the soil bearing capacity. Note that most foundation failures are related to excessive movement rather than loss of load-carrying capacity, and the soil bearing capacity may be based on either a limitation of maximum foundation deformation or the nominal strength associated with an anticipated failure mechanism. Maintaining a reasonably consistent level of service load-bearing pressures for all of the individual footings is encouraged since it will tend to reduce differential settlements, which are usually of more concern than are total settlements. Recommendations for limiting soil pressures for service loads are typically provided by geotechnical consultants.

The thickness of footings is selected to provide adequate shear capacity for the concrete section. The common design approach is to increase footing thickness as necessary to avoid the need for shear reinforcement, which is atypical in small shallow foundations.

Design requirements for concrete footings are found in Chapters 13 and 18 of ACI 318. Chapter 13 provides direction for the calculation of demands and includes detailing requirements. Section capacities are calculated in accordance with Chapter 22 (section strength). Figure 5.1-2 illustrates the critical sections (dashed lines) and areas (hatched) over which loads are tributary to the critical sections. For elements that are very thick with respect to the plan dimensions (as at pile caps), these critical section definitions become less meaningful and other approaches (such as strut-and-tie modeling) should be employed. Chapter 18 provides the minimum requirements for concrete foundations in Seismic Design Categories D, E and F, which are similar to those provided in prior editions of the *Provisions*.

For shallow foundations, reinforcement is designed to satisfy flexural demands. ACI 318 Section 13.3 defines how flexural reinforcement is to be distributed for footings of various shapes.

Assuming a two-way isolated spread footing will be used, Section 13.3.3 of ACI 318 references to Chapter 7 (one-way slabs) and 8 (two-way slabs) for applicable design and detailing provisions. Section 8.6.1.1 provides minimum requirements for temperature and shrinkage reinforcement that are applicable to footings of uniform thickness.

7.1.1.3.2 Additional Considerations for Eccentric Loads. The design of eccentrically loaded footings follows the typical design of a concentrically loaded spread footing with one significant addition: consideration of overturning stability. Stability calculations are sensitive to the characterization of soil behavior. For sustained eccentric loads, a linear distribution of elastic soil stresses is generally assumed and uplift is usually avoided. If the structure is expected to remain elastic when subjected to short-term eccentric loads (as for wind loading), uplift over a portion of the footing is acceptable to most designers. Where foundations will be subjected to short-term loads and inelastic response is acceptable (as for earthquake loading), plastic soil stresses may be considered. It is most common to consider stability effects on the basis of statically applied loads even where the loading is actually dynamic; that approach simplifies the calculations at the expense of increased conservatism. Figure 7.1-3 illustrates the distribution of soil stresses for the various assumptions. Most textbooks on foundation design provide simple equations to describe the conditions shown in Parts b, c and d of the figure; finite element models of those conditions are easy to develop. Simple hand calculations can be performed for the case shown in Part f. Practical consideration of the case shown in Part e would require modeling with inelastic elements, but that offers no advantage over direct consideration of the plastic limit. (All of the discussion in this section focuses on the common case in which foundation elements may be assumed to be rigid with respect to the supporting soil. For the interested reader, Chapter 4 of ASCE 41 provides a useful discussion of foundation compliance, rocking and other advanced considerations.)
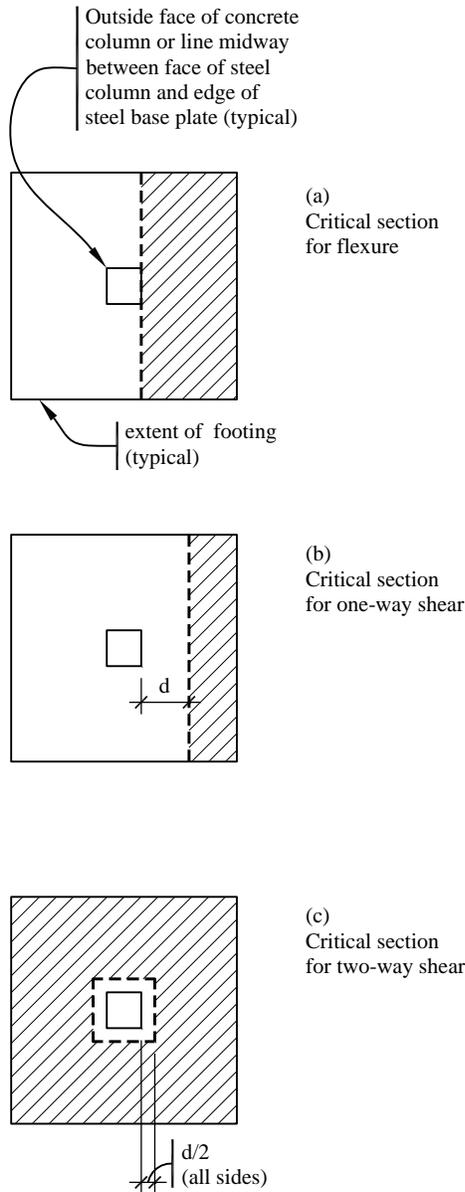
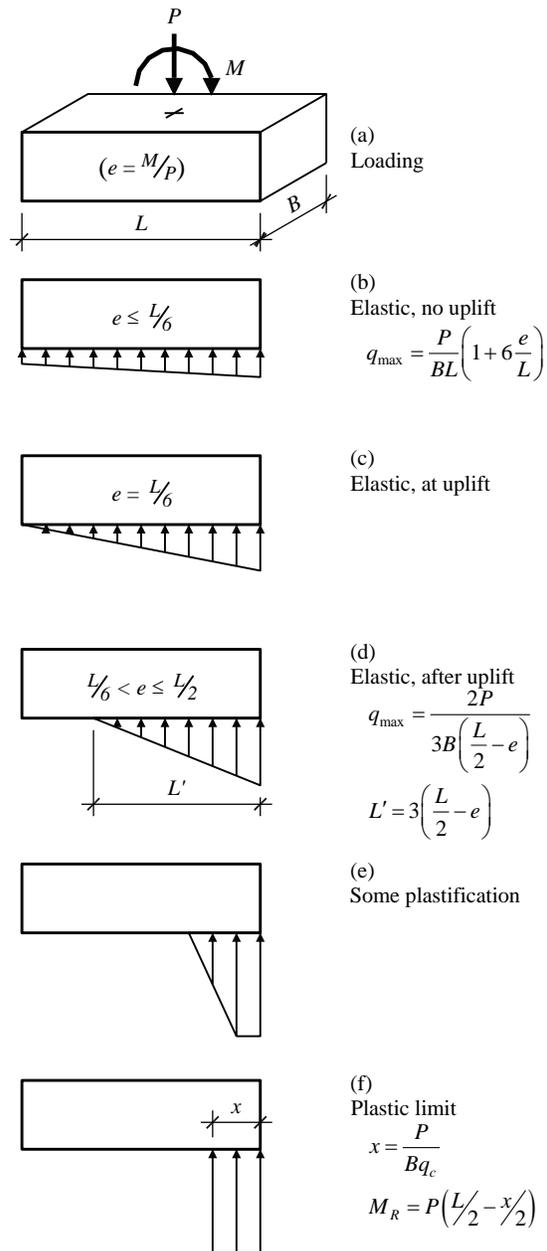**Figure 7.1-2 Critical sections for isolated footings**

Figure 7.1-3 Soil pressure distributions

7.1.2 Design for Moment-Resisting Frame System

Framing Alternate A in Section 6.2 of this volume of design examples includes a perimeter moment-resisting frame as the seismic force-resisting system. A framing plan for the system is shown in Figure 7.1-4. Detailed calculations are provided in this section for a combined footing at the corner including overturning and sliding checks, design of concrete sections, and long-term settlement checks. The results for all footing types are summarized in Section 7.1.3.4.
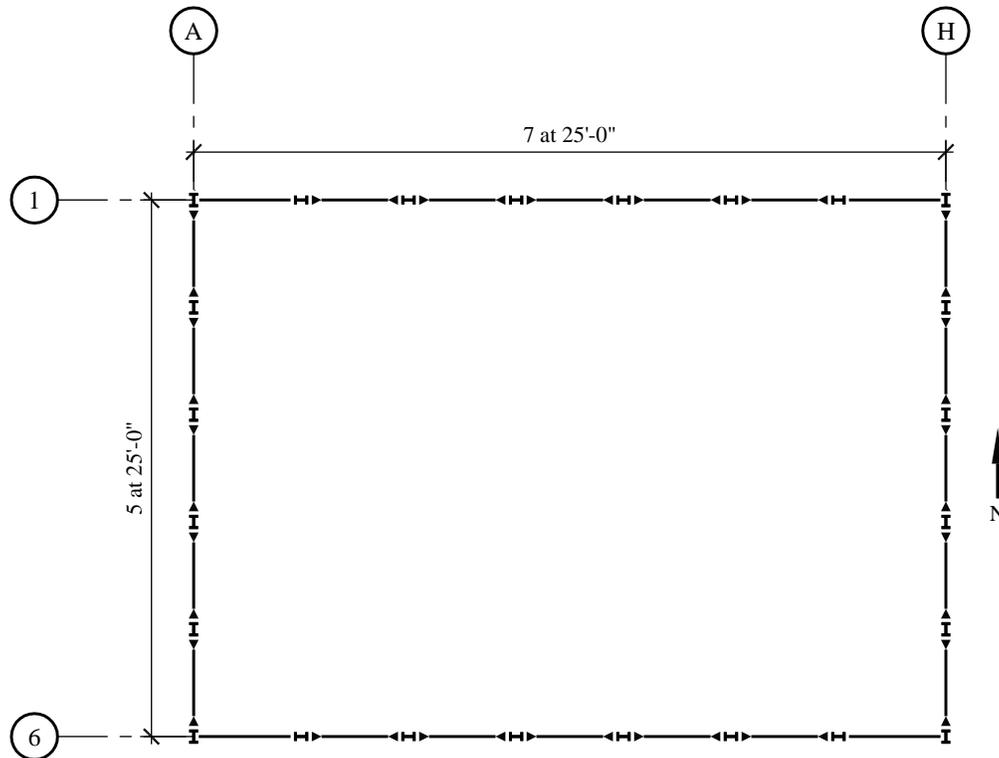
Figure 7.1-4 Framing plan for moment-resisting frame system

7.1.2.1 Demands. A three-dimensional analysis of the superstructure, in accordance with the requirements for the equivalent lateral force (ELF) procedure, is performed using the ETABS program. Foundation reactions at selected grids are reported in Table 7.1-3.

Table 7.1-3 Demands from Moment-Resisting Frame System

Location	Load	Fx	Fy	Fz	Mxx	Myy
A-5	D			-203.8		
	L			-43.8		
	Ex	-13.8	4.6	3.8	53.6	-243.1
	Ey	0.5	-85.1	-21.3	-1011.5	8.1
A-6	D			-103.5		
	L			-22.3		
	Ex	-14.1	3.7	51.8	47.7	-246.9
	Ey	0.8	-68.2	281.0	-891.0	13.4

Note: Units are kips and feet. Load *Ex* is for loads applied toward the east, including appropriately amplified counter-clockwise accidental torsion. Load *Ey* is for loads applied toward the north, including appropriately amplified clockwise accidental torsion.

Section 6.2.3.5 of this volume of design examples outlines the design load combinations, which include the redundancy factor as appropriate. A large number of load cases result from considering two senses of accidental torsion for loading in each direction and including orthogonal effects. The detailed calculations presented here are limited to two primary conditions, both for a combined foundation for columns at Grids A-5 and A-6: the downward case ($1.4D + 0.5L + 0.3Ex + 1.0Ey$) and the upward case ($0.7D + 0.3Ex + 1.0Ey$).

Note that the upward case is not required to include the vertical acceleration reduction of $0.2S_{DS}$ from the dead load component. In accordance with *Standard* Section 12.4.2.2, the vertical acceleration component is permitted to be taken as zero when it is subtracted from Equation 12.4-2 where determining demands on the soil-structure interface of foundations. The author has elected to include the vertical acceleration component in the design example for consistency of load combinations and to illustrate a condition of higher eccentricity with plastic soil pressure distribution.

Before loads can be computed, attention must be given to *Standard* Section 12.13.4. That Section states that "overturning effects at the soil-foundation interface are permitted to be reduced by 25 percent" where the ELF procedure is used and by 10 percent where modal response spectrum analysis is used. Because the overturning effect in question relates to the global overturning moment for the *system*, judgment must be used in determining which design actions may be reduced. If the seismic force-resisting system consists of isolated shear walls, the shear wall overturning moment at the base best fits that description. For a perimeter moment-resisting frame, most of the global overturning resistance is related to axial loads in columns. Therefore, in this example column axial loads (Fz) from load cases *Ex* and *Ey* are multiplied by 0.75 and all other load effects remain unreduced.

7.1.2.2 Downward Case ($1.4D + 0.5L + 0.3Ex + 1.0Ey$). In order to perform the overturning checks, a footing size must be assumed. Preliminary checks (not shown here) confirmed that isolated footings under single columns were untenable. Check overturning for a footing that is 9 feet wide by 40 feet long by 5 feet thick. Furthermore, assume that the top of the footing is 2 feet below grade (the overlying soil contributes to the resisting moment). (In these calculations the $0.2S_{DS}D$ modifier for vertical accelerations is used for the dead loads *applied to* the foundation but not for the weight of the foundation and soil. This is the author's interpretation of the *Standard*. The footing and soil overburden are not subject to the same potential for dynamic amplification as the dead load of the superstructure and it is not common practice to include the vertical acceleration on the weight of the footing and the overburden. Furthermore, for footings that resist significant overturning, this issue makes a significant difference in design.) Combining the loads from columns at Grids A-5 and A-6 and including the weight of the foundation and overlying soil produces the following loads at the foundation-soil interface:

P = applied loads + weight of foundation and soil
$\quad$ = 1.4(-203.8 - 103.5) + 0.5(-43.8 - 22.3) +0.75[0.3(3.8 + 51.8) + 1.0(-21.3 + 281)]
$\quad\quad$ - 1.2[9(40)(5)(0.15) + 9(40)(2)(0.125)]
$\quad$ = -688 kips.

M_{xx} = direct moments + moment due to eccentricity of applied axial loads
$\quad$ = 0.3(53.6 + 47.7) + 1.0(-1011.5 - 891.0)
$\quad\quad$ + [1.4(-203.8) + 0.5(-43.8) + 0.75(0.3)(3.8) + 0.75(1.0)(-21.3)](12.5)
$\quad\quad$ + [1.4(-103.5) + 0.5(-22.3) + 0.75(0.3)(51.8) + 0.75(1.0)(281)](-12.5)
$\quad$ = -6,717 ft-kips.

M_{yy} = 0.3(-243.1 - 246.9) + 1.0(8.1 + 13.4)
$\quad$ = -126 ft-kips. (The resulting eccentricity is small enough to neglect here, which simplifies the problem considerably.)

$V_x = 0.3(-13.8 - 14.1) + 1.0(0.5 + 0.8)$
   $= -7.11$ kips.

$V_y = 0.3(4.6 + 3.7) + 1.0(-85.1 -68.2)$
   $= -149.2$ kips.

Note that the above load combination does not yield the maximum downward load. Reversing the direction of the seismic load results in $P = -1,103$ kips and $M_{xx} = 2,964$ ft-kips. This larger axial load does not control the design because the moment is so much less that the resultant is within the kern and no uplift occurs.

The following soil calculations use a different sign convention than that in the analysis results noted above; compression is positive for the soil calculations. The eccentricity is as follows:

$e = |M/P| = 6,717/688 = 9.76$ ft

Figure 5.1-3 shows the elastic and plastic design conditions and their corresponding equations. Where e is less than $L/2$, a solution to the overturning problem exists; however, as e approaches $L/2$, the bearing pressures increase without bound. Since e is greater than $L/6 = 40/6 = 6.67$ feet, uplift occurs and the maximum bearing pressure is:

$$q_{max} = \frac{2P}{3B\left(\dfrac{L}{2} - e\right)} = \frac{2(688)}{3(9)\left(\dfrac{40}{2} - 9.76\right)} = 4.98 \text{ ksf}$$

and the length of the footing in contact with the soil is:

$$L' = 3\left(\frac{L}{2} - e\right) = 3\left(\frac{40}{2} - 9.76\right) = 30.7 \text{ ft}$$

The resulting bearing pressure diagram is shown in Figure 7.1-5.
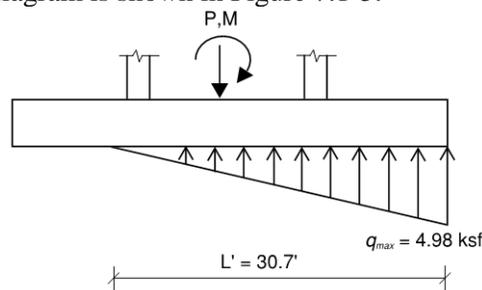
Figure 7.1-5: Elastic Bearing Pressure for Downward Load Case

The bearing capacity $Q_{ns} = 4,000B' = 4,000 \times \min(B, L'/2) = 4,000 \times \min(9, 30.7/2) = 36,000$ psf $= 36$ ksf. ($L'/2$ is used as an adjustment to account for the gradient in the bearing pressure in that dimension.)

The design bearing capacity $\phi Q_{ns} = 0.45(36 \text{ ksf}) = 16.2 \text{ ksf} > 4.98 \text{ ksf}$ OK

The foundation satisfies overturning and bearing capacity checks. The upward case, which follows, will control the sliding check.

7.1.2.3 Upward Case (0.7D + 0.3Ex + 1.0Ey). For the upward case the loads are:

P = -332 kips

M_{xx} = -5,712 ft-kips

M_{yy} = -126 ft-kips (negligible)

V_x = -7.1 kips

V_y = -149 kips

The eccentricity is:

$e = |M/P| = 5,712/332 = 17.2$ feet

Again, e is greater than $L/6$, so uplift occurs and the maximum bearing pressure is:

$$q_{max} = \frac{2(332)}{3(10)\left(\frac{40}{2} - 17.2\right)} = 8.82 \text{ ksf}$$

and the length of the footing in contact with the soil is:

$$L' = 3\left(\frac{40}{2} - 17.2\right) = 8.4 \text{ ft}$$

The bearing capacity $Q_{ns} = 4,000 \times \min(9, 8.4/2) = 16,800$ psf $= 16.8$ ksf.

The design bearing capacity $\phi Q_{ns} = 0.45(16.8 \text{ ksf}) = 7.56$ ksf < 8.82 ksf. \hfill NG

Using an elastic distribution of soil pressures, the foundation fails the bearing capacity check. Try the plastic distribution. Using this approach, the bearing pressure over the entire contact area is assumed to be equal to the design bearing capacity. In order to satisfy vertical equilibrium, the contact area times the design bearing capacity must equal the applied vertical load P. Because the bearing capacity used in this example is a function of the contact area and the value of P changes with the size, the most convenient calculation is iterative.

By iteration, the length of contact area is $L' = 4.54$ feet. See Figure 7.1-6 for illustration of both elastic and plastic distributions.
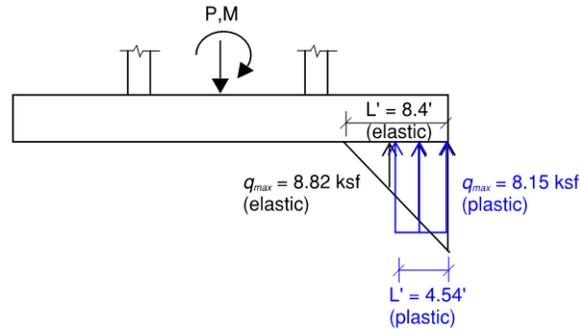
Figure 7.1-6: Elastic and Plastic Bearing Pressure for Upward Load Case

The bearing capacity $q_c = 4,000 \times$ min(9, 4.54) = 18,120 psf = 18.12 ksf. (No adjustment to *L'* is needed as the pressure is uniform.)

The design bearing capacity $\phi q_c = 0.45(18.12$ ksf) = 8.15 ksf.

   (8.15)(4.54)(9) = 332 kips = 332 kips, so equilibrium is satisfied.

The resisting moment, $M_R = P$ (*L*/2-*L'*/2) = 332 (40/2 - 4.54/2) = 5,896 ft-kip > 5,712 ft-kip.   OK

Therefore, using a plastic distribution of soil pressures, the foundation satisfies overturning and bearing capacity checks.

Concrete Section Design

The calculation of demands on concrete sections for strength checks should use the same soil stress distribution as the overturning check. Using a plastic distribution of soil stresses defines the upper limit of static loads for which the foundation remains stable, but the extreme concentration of soil bearing tends to drive up shear and flexural demands on the concrete section. It should be noted that the foundation may remain stable for larger loads if they are applied dynamically; even in that case, the strength demands on the concrete section will not exceed those computed on the basis of the plastic distribution.

Footing Thickness. Once the plan dimensions of the footing are verified, the thickness should be confirmed to satisfy the one-way and two-way shear demands without the addition of shear reinforcement. Demands are calculated at critical sections, shown in Figure 5.1-2, which depend on footing thickness.

One-way shear: Critical section is 3' from edge of footing, d = 56"
$V_u = (8.15$ ksf) (3 ft) (9 ft) = 220 kips
$\phi V_n = (0.75)\ 2\sqrt{4000}\ (9 \times 12)(56)(1/1000) = 574$ kips > 220 kips   OK

Two-way shear: For simplicity of calculation example check column A-5 for gravity load only in uplift condition. Column moment should be included with the appropriate load combination for complete check. For W14 columns used in this building, assume side dimension (halfway between face of column and edge of base plate) is 16 in.

Use gravity load combination of 1.2*D*+1.6*L*. For condition where footing is in uplift, there is no bearing pressure under critical perimeter therefore the full gravity load is used for punching shear check.

$V_u = 1.2D+1.6L = 1.2(203.8) + 1.6(43.8) = 314.6$ kips

$\phi V_n = \phi V_c = (0.75) \; 4\sqrt{4000} \; [4*(16+55.5)](55.5)(1/1000) = 3012 \text{ kips} > 314.6 \text{ kips}$ OK

Flexural Design: Critical section is 7' from edge of footing, d=56"
$M_u = (8.15 \text{ ksf}) (4.54 \text{ ft}) (7.0 \text{ ft} - 4.5 \text{ ft} /2) = 176 \text{ ft-kips / ft}$

Estimated minimum reinforcement: $\rho_{min} = 0.0018$, provide for bottom half of mat only
$A_{smin} = 0.0018 (84"/2)(12") = 0.648 \text{ in}^2/\text{ft}$, therefore use #8@10" oc (0.648 in²/ft)

The distance from extreme compression fiber to the center of the bottom layer of reinforcement, $d = t -$
cover $- 1.5 \; d_b = 60 - 3 - 1.5(1) = 55.5$ in.

$T = A_s f_y = (12/10) (0.79) (60) = 56.9 \text{ kips}$

Noting that $C = T$ and solving the expression $C = 0.85 \; f'_c \; b \; a$ for a produces $a = 1.39$ in
$\phi M_n = \phi T(d-a/2) = 0.9 (56.9 \text{ kips}) (55.5 - 1.39/2)(1/12) = 232 \text{ ft-kips / ft} > 176 \text{ ft-kips/ft}$ OK

Top Reinforcement for Uplift: For case where earthquake effects create uplift, minimum top reinforcement is required per ACI 318 18.13.2.4, which references 9.6.1.

A_{smin} shall be the greater of:
9.6.1.2(a): $3\sqrt{f'_c} \; / f_y \; b_w \; d = 3\sqrt{4000} \; (60,000) (12) (55.5) = 2.11 \text{ in}^2/\text{ft}$
9.6.1.2(b): $200/f_y \; b_w \; d = 200 / (60,000) (12) (55.5) = 2.22 \text{ in}^2/\text{ft}$ (controls)

Per Section 9.6.1.3, if A_s provided is at least one-third greater than A_s required by analysis, equations 9.6.1.2(a) and (b) need not be satisfied. Verify demand required by analysis. Consider demand at critical section for flexure at 7 feet from edge of footing. Demand is due to weight of footing and soil on top only for uplift condition.

$M_u = 1.2 \; [\; 5 \; (0.15) + 2 \; (0.125] \; (7) \;^2 / 2 = 29.4 \text{ ft-kips / ft}$

Assume minimum top reinforcement is provided for top half of mat depth, equal to bottom half consisting of #8 @ 10" oc.

Similar to flexural design check, $\phi M_n = 232 \text{ ft-kips/ft} > (4/3) (29.4) = 39.2 \text{ ft-kips/ft}$ OK

For the sliding check, initially consider base traction only. The sliding demand is:

$$V = \sqrt{V_x^2 + V_y^2} = \sqrt{(-7.11)^2 + (-149.2)^2} = 149.4 \text{ kips}$$

As calculated previously, the total compression force at the bottom of the foundation is 332 kips. The design sliding resistance is:

$\phi V_c = \phi \times \text{friction coefficient} \times P = 0.85(0.65)(332 \text{ kips}) = 183 \text{ kips} > 149.4 \text{ kips}$ OK

If base traction alone had been insufficient, resistance due to passive pressure on the leading face could be included. Section 5.2.2.2 below illustrates passive pressure calculations for a pile cap.

7.1.2.4 Long Term Settlement Verification

In order to verify adequate serviceability performance due to long term settlement effects, an additional check is performed to compare loading associated with a sustained load case and allowable bearing pressure. The allowable bearing pressure is determined by the geotechnical consultant to control long term settlement due to sustained loads to within acceptable limits. In this case, the limit of 2,000 psf has been specified per Table 7.1-1.

The load combination for the serviceability check should be a realistic sustained load case. Commentary for Appendix C of the *Standard* recommends a load combination for long-term settlement of D+0.5L. The footing axial load associated with this load combination is:

$P = (-203.8 + -103.5) + 0.5 (-43.8 + -22.3) = 340.4$ kips

The resulting uniform bearing pressure is calculated as:

$q_{sustained} = 340.4$ kips $/ (9$ ft x 40 ft$) = 0.945$ ksf $= 945$ psf

Compare to the allowable bearing pressure of 2,000 psf, the proposed footing is acceptable for the serviceability check.

7.1.3.4 Design Results. The calculations performed in Sections 7.1.3.2 and 7.1.3.3 are repeated for combined footings at middle and side locations. Figure 7.1-7 shows the results.
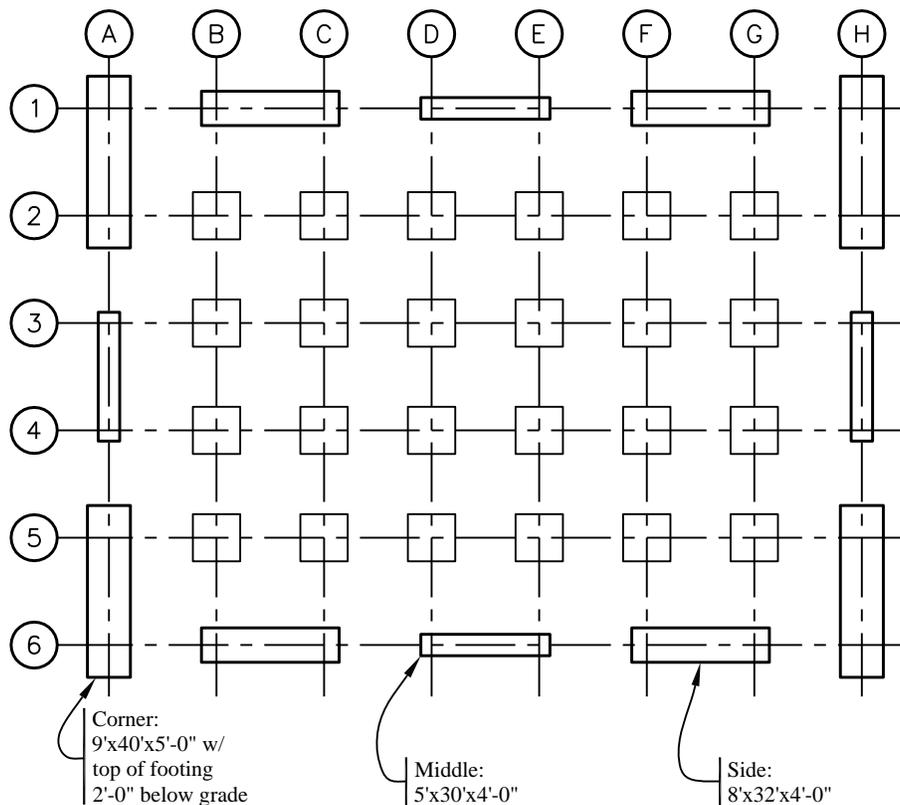

Figure 7.1-7 Foundation plan for moment-resisting frame system

One last check of interest is to compare the flexural stiffness of the footing with that of the steel column, which is needed because the steel frame design was based upon flexural restraint at the base of the columns. Using an effective moment of inertia of 50 percent of the gross moment of inertia and also using the distance between columns as the effective span, the ratio of *EI/L* for the smallest of the combined footings is more than five times the *EI/h* for the steel column. This is satisfactory for the design assumption.

7.1.3   Design for Concentrically Braced Frame System

Framing Alternate B in Section 6.2 of this volume of design examples employs a concentrically braced frame system at a central core to provide resistance to seismic loads. A framing plan for the system is shown in Figure 7.1-8.
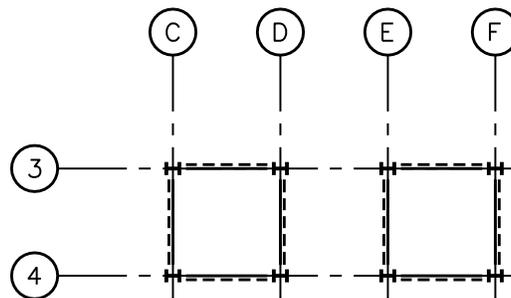
Figure 7.1-8 Framing plan for concentrically braced frame system

7.1.3.1 Check Mat Size for Overturning. Uplift demands at individual columns are so large that the only practical shallow foundation is one that ties together the entire core. The controlling load combination for overturning has minimum vertical loads (which help to resist overturning), primary overturning effects (M_{xx}) due to loads applied parallel to the short side of the core and smaller moments about a perpendicular axis (M_{yy}) due to orthogonal effects. Assume mat dimensions of 45 feet by 95 feet by 7 feet thick, with the top of the mat 3'-6" below grade. Combining the factored loads applied to the mat by all eight columns and including the weight of the foundation and overlying soil produces the following loads at the foundation-soil interface:

- P = -7,849 kips

- M_{xx} = -148,439 ft-kips

- M_{yy} = -42,544 ft-kips

- V_x = -765 kips

- V_y = -2,670 kips

Figure 7.1-8 shows the soil pressures that result from application in this controlling case, depending on the soil distribution assumed. In both cases the computed uplift is significant. In Part a of the figure, the contact area is shaded. The elastic solution shown in Part b was computed by modeling the mat in SAP2000 with compression only soil springs (with the stiffness of edge springs doubled as recommended

by Bowles). For the elastic solution, the average width of the contact area is 11.1 feet and the maximum soil pressure is 16.9 ksf.

The bearing capacity Q_{ns} = 4,000 × min(95, 11.1/2) = 22,200 psf = 22.2 ksf.

The design bearing capacity ϕQ_{ns} = 0.45(22.2 ksf) = 10.0 ksf < 16.9 ksf.   NG
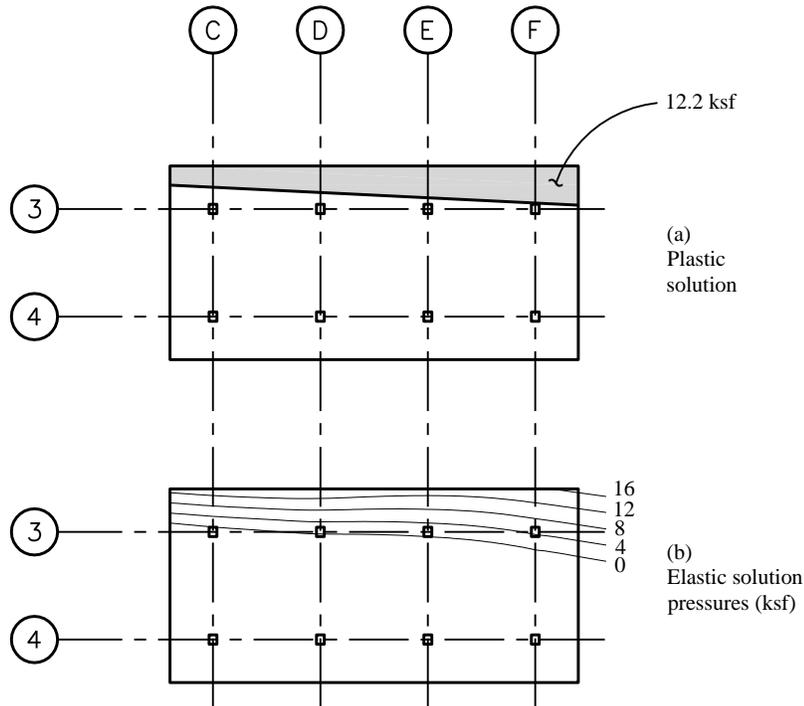
Figure 7.1-9 Soil pressures for controlling bidirectional case

As was done in Section 7.1.3.3 above, try the plastic distribution. The present solution has an additional complication as the off-axis moment is not negligible. The bearing pressure over the entire contact area is assumed to be equal to the design bearing capacity. In order to satisfy vertical equilibrium, the contact area times the design bearing capacity must equal the applied vertical load *P*. The shape of the contact area is determined by satisfying equilibrium for the off-axis moment. Again the calculations are iterative.

Given the above constraints, the contact area shown in Figure 7.1-8 is determined. The length of the contact area is 4.46 feet at the left side and 9.10 feet at the right side. The average contact length, for use in determining the bearing capacity, is (4.46 + 9.10)/2 = 6.78 feet. The distances from the center of the mat to the centroid of the contact area are as follows:

$\bar{x}$ =5.42 ft
$\bar{y}$ =18.97 ft

The bearing capacity is Q_{ns} = 4,000 × min(95, 6.78) = 27,120 psf = 27.12 ksf.

The design bearing capacity is $\phi Q_{ns} = 0.45(27.12 \text{ ksf}) = 12.21$ ksf.

$(12.21)(6.78)(95) = 7,864$ kips $\approx 7,849$ kips, confirming equilibrium for vertical loads.

$(7,849)(5.42) = 42,542$ ft-kips $\approx 42,544$ ft-kips, confirming equilibrium for off-axis moment.

The resisting moment, $M_{R,xx} = P\overline{y} = 7,849 (18.97) = 148,895$ ft-kips $> 148,439$ ft-kips   OK

So, the checks of stability and bearing capacity are satisfied. The mat dimensions are shown in Figure 7.1-10.
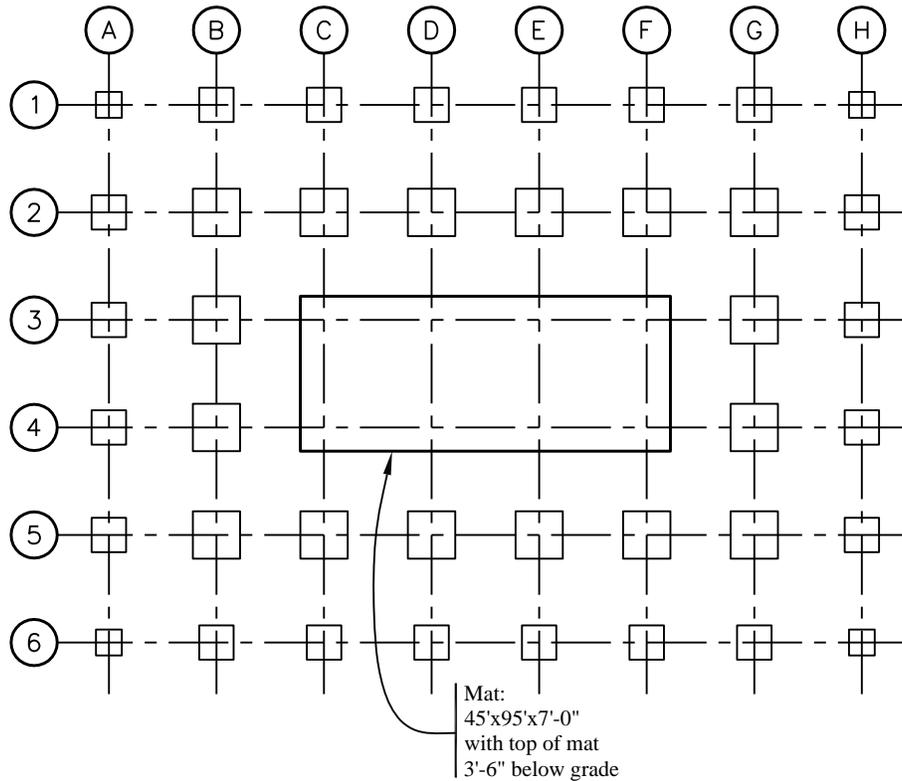
Figure 7.1-10 Foundation plan for concentrically braced frame system

7.1.3.2 Design Mat for Strength Demands. As was previously discussed, the computation of strength demands for the concrete section should use the same soil pressure distribution as was used to satisfy stability and bearing capacity. Because dozens of load combinations were considered and hand calculations were used for the plastic distribution checks, the effort required would be considerable. The same analysis used to determine elastic bearing pressures yields the corresponding section demands directly. One approach to this dilemma would be to compute an additional factor that must be applied to selected elastic cases to produce section demands that are consistent with the plastic solution. Rather than provide such calculations here, design of the concrete section will proceed using the results of the elastic analysis. This is conservative for the demand on the concrete for the same reason that it was

unsatisfactory for the soil: the edge soil pressures are high (that is, we are designing the concrete for a peak soil pressure of 16.9 ksf, even though the plastic solution gives 12.2 ksf).

Standard Section 12.13.3 requires consideration of parametric variation for soil properties where foundations are modeled explicitly. This example does not illustrate such calculations.

Concrete mats often have multiple layers of reinforcement in each direction at the top and bottom of their thickness. Use of a uniform spacing for the reinforcement provided in a given direction increases the ease of construction, although more refinement in layering/spacing may be more economical especially for larger mat foundations.

The minimum reinforcement requirements defined in Section 8.6.1.1 of ACI 318 were discussed in Section 7.1.1.3 above. Although all of the reinforcement provided to satisfy Section 8.6.1.1 of ACI 318 may be provided near one face, for thick mats it is best to compute and provide the amount of required reinforcement separately for the top and bottom halves of the section. Using a bar spacing of 10 inches for this 7-foot-thick mat and assuming one or two layers of bars, the section capacities indicated in Table 7.1-4 (presented in order of decreasing strength) may be precomputed for use in design. The amount of reinforcement provided for Marks B, C and D are less than the basic minimum for flexural members, so the demands should not exceed three-quarters of the design strength where those reinforcement patterns are used. The amount of steel provided for Mark D is the minimum that satisfies ACI 318 Section 8.6.1.1.

Table 7.1-4 Mat Foundation Section Capacities

Mark	Reinforcement	A_s (in.^{2} per ft)	ϕM_n (ft-kip/ft)
A	2 layers of #10 bars at 10 in. o.c.	3.05	1,018
B	2 layers of #9 bars at 10 in. o.c.	2.40	807
C	2 layers of #8 bars at 10 in. o.c.	1.90	641
D	#8 bars at 10 in. o.c.	0.95	340

To facilitate rapid design, the analysis results are processed in two additional ways. First, the flexural and shear demands computed for the various load combinations are enveloped. Then the enveloped results are presented (see Figure 7.1-11) using contours that correspond to the capacities shown for the reinforcement patterns noted in Table 7.1-4.
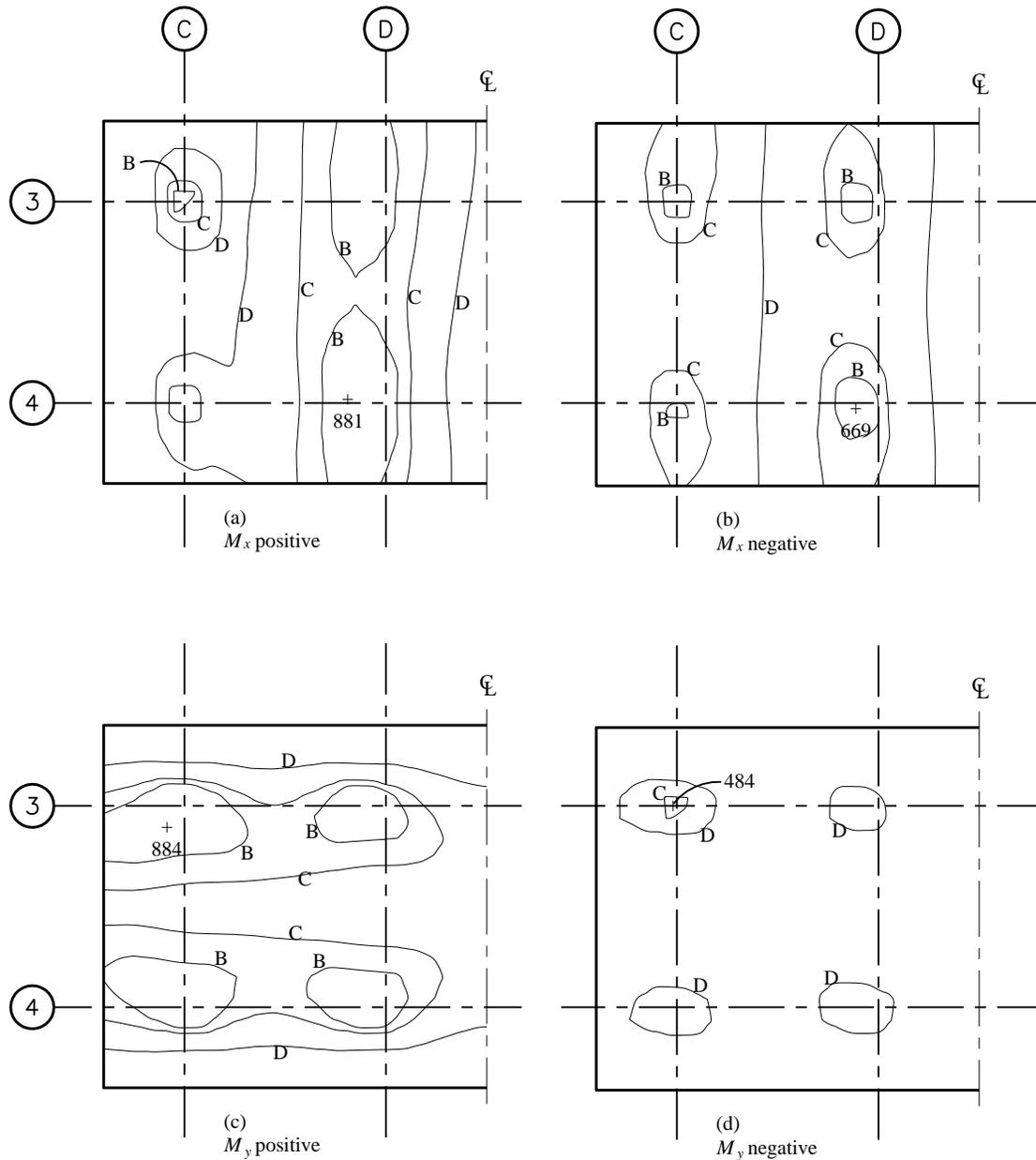
Figure 7.1-11 Envelope of mat foundation flexural demands

Using the noted contours permits direct selection of reinforcement. The reinforcement provided within a contour for a given mark must be that indicated for the next higher mark. For instance, all areas within Contour B must have two layers of #10 bars. Note that the reinforcement provided will be symmetric about the centerline of the mat in both directions. Where the results of finite element analysis are used in the design of reinforced concrete elements, averaging of demands over short areas is appropriate. In Figure 5.1-12, the selected reinforcement is superimposed on the demand contours. Figure 7.1-13 shows a section of the mat along Gridline C.
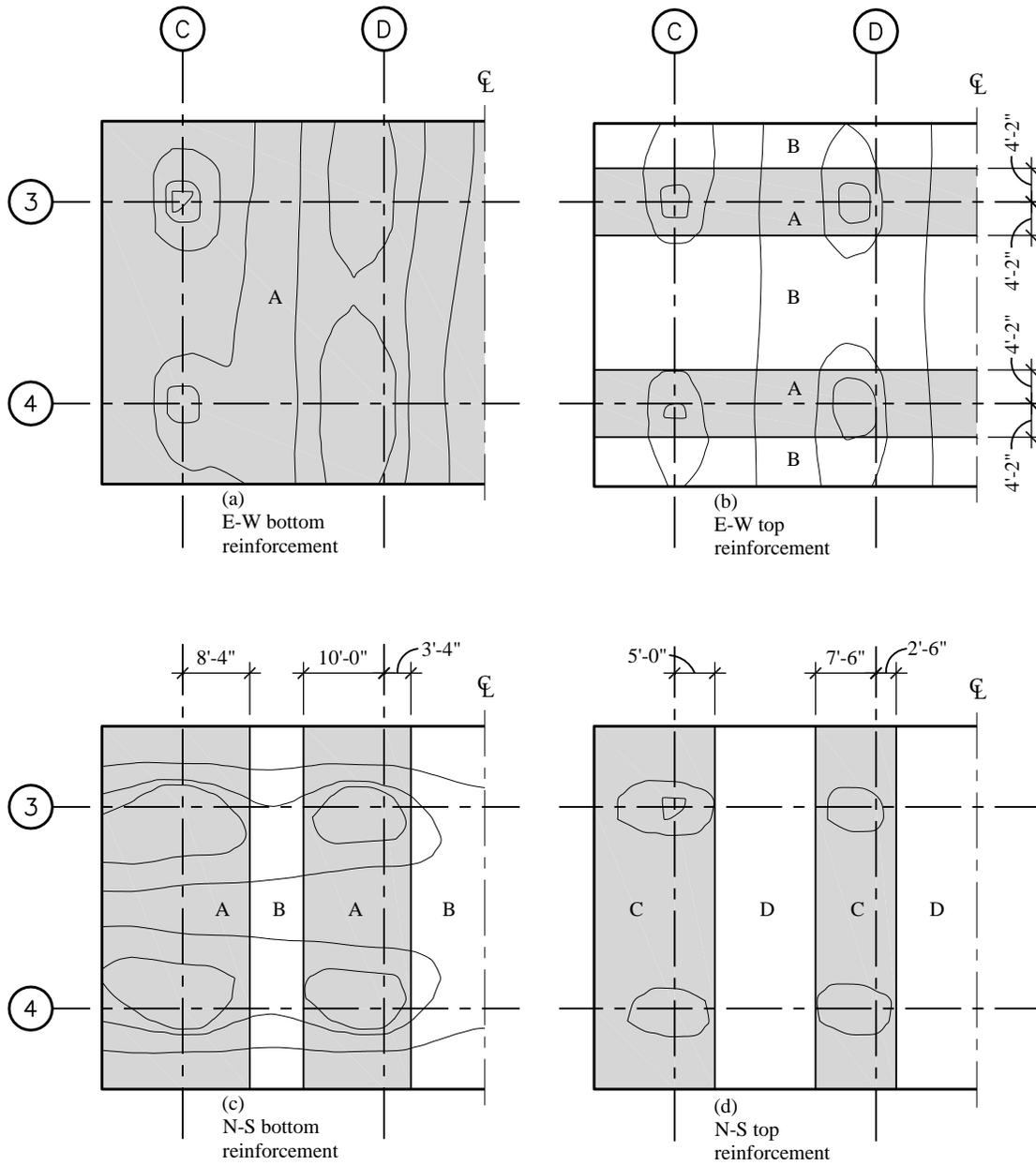
Figure 7.1-12 Mat foundation flexural reinforcement
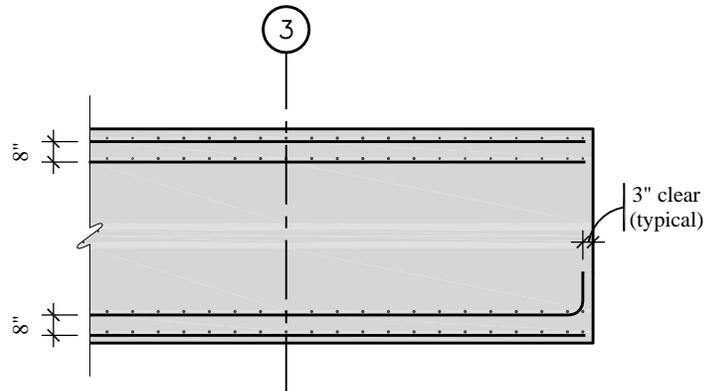
Figure 7.1-13 Section of mat foundation

Figure 7.1-14 presents the envelope of shear demands. The contours used correspond to the design strengths computed assuming $V_s = 0$ for one-way and two-way shear. In the hatched areas the shear stress exceeds $\phi 4\sqrt{f_c'}$ and in the shaded areas it exceeds $\phi 2\sqrt{f_c'}$. The critical sections for two-way shear (as discussed in Section 5.1.1.3) also are shown. The only areas that need more careful attention (to determine whether they require shear reinforcement) are those where the hatched or shaded areas are outside the critical sections. At the columns on Gridline D, the hatched area falls outside the critical section, so closer inspection is needed. Because the perimeter of the hatched area is substantially smaller than the perimeter of the critical section for punching shear, the design requirements of ACI 318 are satisfied.

One-way shears at the edges of the mat exceed the $\phi 2\sqrt{f_c'}$ criterion. Note that the high shear stresses are not produced by loads that create high bearing pressures at the edge. Rather, they are produced by loads that create large bending stresses parallel to the edge. The distribution of bending moments and shears is not uniform across the width (or breadth) of the mat, primarily due to the torsion in the seismic loads and the orthogonal combination. It is also influenced by the doubled spring stiffnesses used to model the soil condition. However, when the shears are averaged over a width equal to the effective depth (*d*), the demands are less than the design strength.

In this design, reinforcement for punching or beam shear is not required. If shear reinforcement cannot be avoided, vertical reinforcement should be introduced. This reinforcement should extend as close as possible to the tension and compression surfaces, and be anchored with a hook around the longitudinal reinforcement. Alternatively headed reinforcement may be used in order to improve constructability.

(a) V_x

Critical section
(typical)

(b) V_y
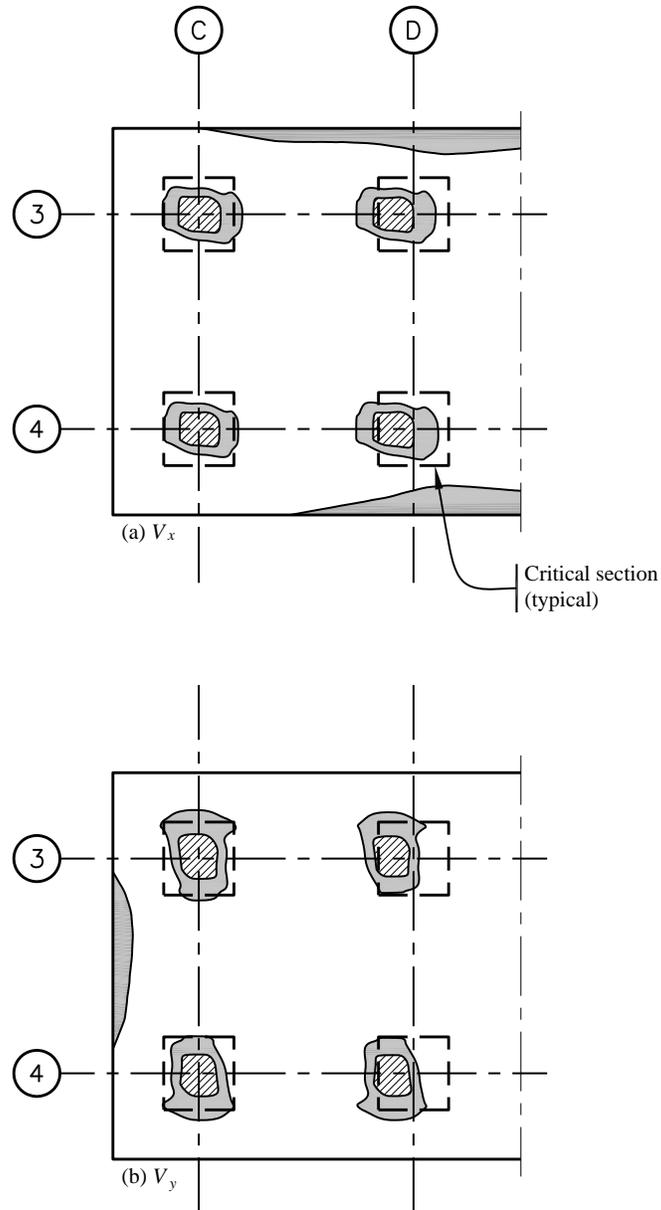
Figure 7.1-14 Critical sections for shear and envelope of mat foundation shear demands

7.2 DEEP FOUNDATIONS FOR A 12-STORY BUILDING, SEISMIC DESIGN CATEGORY D

This example features the analysis and design of deep foundations for a 12-story reinforced concrete moment-resisting frame building similar to that described in Chapter 7 of this volume of design examples.

7.2.1 Basic Information

7.2.1.1 Description. Figure 5.2-1 shows the basic design condition considered in this example. A 2×2 pile group is designed for four conditions: for loads delivered by a corner and a side column of a

moment-resisting frame system for Site Classes C and E. Geotechnical parameters for the two sites are given in Table 7.2-1. Design values are presented as nominal foundation geotechnical capacity, unless noted otherwise, in order to illustrate the strength design for nominal foundation geotechnical capacity provisions of *Standard* Section 12.13.5.
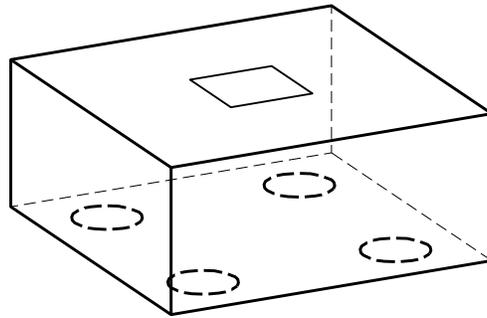
Figure 7.2-1 Design condition: Column of concrete moment-resisting frame supported by pile cap and cast-in-place piles

Table 7.2-1 Geotechnical Parameters

Depth	Class E Site	Class C Site
0 to 3 feet	Loose sand/fill $\gamma = 110$ pcf Angle of internal friction = 28 degrees Soil modulus parameter, $k = 25$ pci Neglect skin friction Neglect end bearing	Loose sand/fill $\gamma = 110$ pcf Angle of internal friction = 30 degrees Soil modulus parameter, $k = 50$ pci Neglect skin friction Neglect end bearing
3 to 30 feet	Soft clay $\gamma = 110$ pcf Undrained shear strength = 430 psf Soil modulus parameter, $k = 25$ pci Strain at 50 percent of maximum stress, $\quad \varepsilon_{50} = 0.01$ Skin friction (ksf) = 0.3 Neglect end bearing	Dense sand (one layer: 3- to 100-foot depth) $\gamma = 130$ pcf Angle of internal friction = 42 degrees Soil modulus parameter, $k = 125$ pci Skin friction (ksf)* $= 0.5 + 0.05/\text{ft} \le 3$ End bearing (ksf)* $= 100 + 1.0/\text{ft} \le 200$
30 to 100 feet	Medium dense sand $\gamma = 120$ pcf Angle of internal friction = 36 degrees Soil modulus parameter, $k = 50$ pci Skin friction (ksf)* $= 1.5 + 0.04/\text{ft} \le 3$ End bearing (ksf)* $= 60 + 0.8/\text{ft} \le 150$	
Pile cap resistance	300 pcf, ultimate passive pressure	575 pcf, ultimate passive pressure
Resistance factor, ϕ	0.45 for pile friction (tension or compression) 0.5 for lateral resistance	0.45 for pile friction (tension or compression) 0.5 for lateral resistance

*Nominal foundation geotechnical capacity values. Skin friction and end bearing values increase (up to the maximum value noted) for each additional foot of depth below the top of the layer. (The values noted assume a minimum pile length of 20 ft.)

The structural material properties assumed for this example are as follows:

- $f'_c = 3{,}000$ psi

- $f_y = 60{,}000$ psi

7.2.1.2 Seismic Parameters.

- Site Class = C and E (both conditions considered in this example)

- $S_{DS} = 1.1$

- Seismic Design Category = D (for both conditions)

7.2.1.3 Demands. The unfactored demands from the moment frame system are shown in Table 7.2-2.

Table 7.2-2 Gravity and Seismic Demands

Location	Load	Vx	Vy	P	Mxx	Myy
Corner	D			-460.0		
	L			-77.0		
	Vx	55.5	0.6	193.2	4.3	624.8
	Vy	0.4	16.5	307.5	189.8	3.5
	ATx	1.4	3.1	26.7	34.1	15.7
	ATy	4.2	9.4	77.0	103.5	47.8
Side	D			-702.0		
	L			-72.0		
	Vx	72.2	0.0	0.0	0.0	723.8
	Vy	0.0	13.9	181.6	161.2	1.2
	ATx	0.4	1.8	2.9	18.1	4.2
	ATy	1.2	5.3	8.3	54.9	12.6

Note: Units are kips and feet. Load *Vy* is for loads applied toward the east. *ATx* is the corresponding accidental torsion case. Load *Vx* is for loads applied toward the north. *ATy* is the corresponding accidental torsion case.

Using Load Combinations 5 and 7 from Section 12.4.2.3 of the *Standard* (with $0.2S_{DS}D = 0.22D$ and taking $\rho = 1.0$), considering orthogonal effects as required for Seismic Design Category D and including accidental torsion, the following 32 load conditions must be considered.

$1.42D + 0.5L \pm 1.0Vx \pm 0.3Vy \pm \max(1.0ATx, 0.3ATy)$

$1.42D + 0.5L \pm 0.3Vx \pm 1.0Vy \pm \max(0.3ATx, 1.0ATy)$

$0.68D \pm 1.0Vx \pm 0.3Vy \pm \max(1.0ATx, 0.3ATy)$

$0.68D \pm 0.3Vx \pm 1.0Vy \pm \max(0.3ATx, 1.0ATy)$

7.2.1.4 Design Approach. For typical deep foundation systems, resistance to lateral loads is provided by both the piles and the pile cap. Figure 7.2-2 shows a simple idealization of this condition. The relative contributions of these piles and pile cap depend on the particular design conditions, but often both effects

are significant. Resistance to vertical loads is assumed to be provided by the piles alone regardless of whether their axial capacity is primarily due to end bearing, skin friction, or both. Although the behavior of foundation and superstructure are closely related, they typically are modeled independently. Earthquake loads are applied to a model of the superstructure, which is assumed to have fixed supports. Then the support reactions are seen as demands on the foundation system. A similar substructure technique is usually applied to the foundation system itself, whereby the behavior of pile cap and piles are considered separately. This section describes that typical approach.
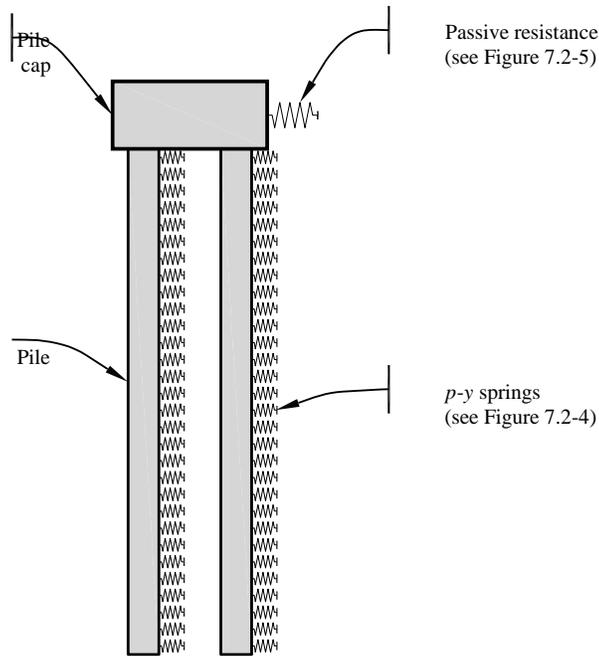
Figure 7.2-2 Schematic model of deep foundation system

7.2.1.4.1 Pile Group Mechanics. With reference to the free body diagram (of a 2×2 pile group) shown in Figure 7.2-3, demands on individual piles as a result of loads applied to the group may be determined as follows:

$$V = \frac{V_{group} - V_{passive}}{4}$$ and $M = V \times \ell$, where ℓ is a characteristic length determined from analysis of a laterally loaded single pile.

$$P_{ot} = \frac{V_{group}h + M_{group} + 4M - h_p V_{passive}}{2s}$$, where s is the pile spacing, h is the height of the pile cap and h_p is the height of $V_{passive}$ above Point O.

$$P_p = \frac{P_{group}}{4}$$ and $P = P_{ot} + P_p$
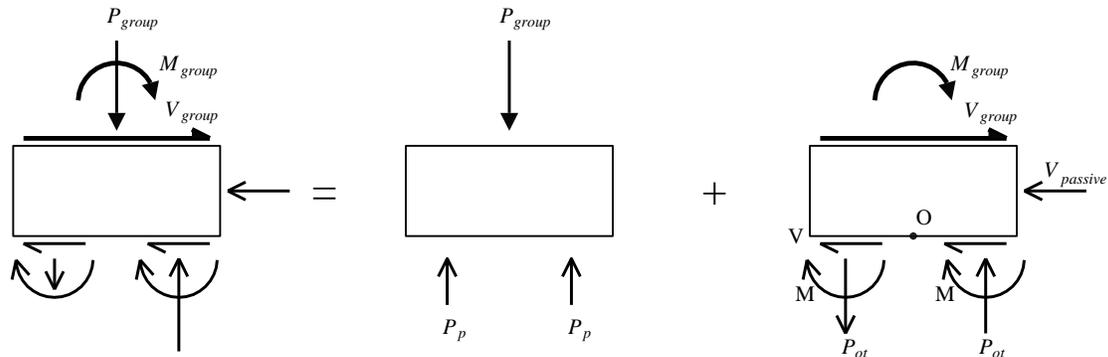
Figure 7.2-3 Pile cap free body diagram

7.2.1.4.2 Contribution of Piles. The response of individual piles to lateral loads is highly nonlinear. In recent years it has become increasingly common to consider that nonlinearity directly. Based on extensive testing of full-scale specimens and small-scale models for a wide variety of soil conditions, researchers have developed empirical relationships for the nonlinear *p-y* response of piles that are suitable for use in design. Representative *p-y* curves (computed for a 22-inch-diameter pile) are shown in Figure 7.2-4. The stiffness of the soil changes by an order of magnitude for the expected range of displacements (the vertical axis uses a logarithmic scale). The *p-y* response is sensitive to pile size (an effect not apparent in the figure, which is based on a single pile size); soil type and properties; and, in the case of sands, vertical stress, which increases with depth. Pile response to lateral loads, like the *p-y* curves on which the calculations are based, is usually computed using computer programs like LPILE.
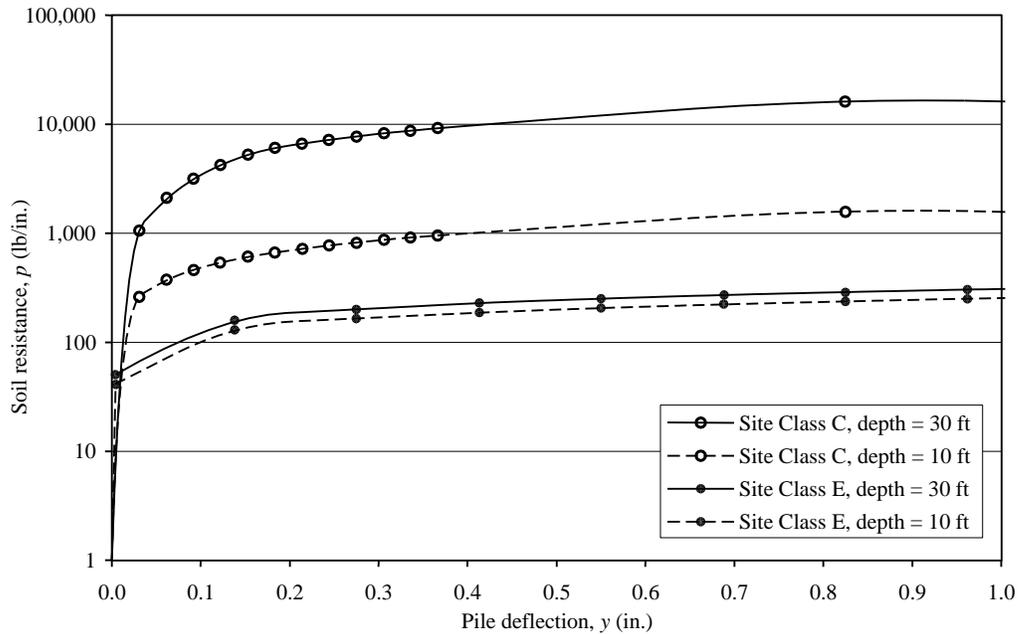
Figure 7.2-4 Representative *p-y* curves
(note that a logarithmic scale is used on the vertical axis)

7.2.1.4.3 Contribution of Pile Cap. Pile caps contribute to the lateral resistance of a pile group in two important ways: directly as a result of passive pressure on the face of the cap that is being pushed into the soil mass and indirectly by producing a fixed head condition for the piles, which can significantly reduce displacements for a given applied lateral load. Like the *p-y* response of piles, the passive pressure resistance of the cap is nonlinear. Figure 7.2-5 shows how the passive pressure resistance (expressed as a fraction of the ultimate passive pressure) is related to the imposed displacement (expressed as a fraction of the minimum dimension of the face being pushed into the soil mass).
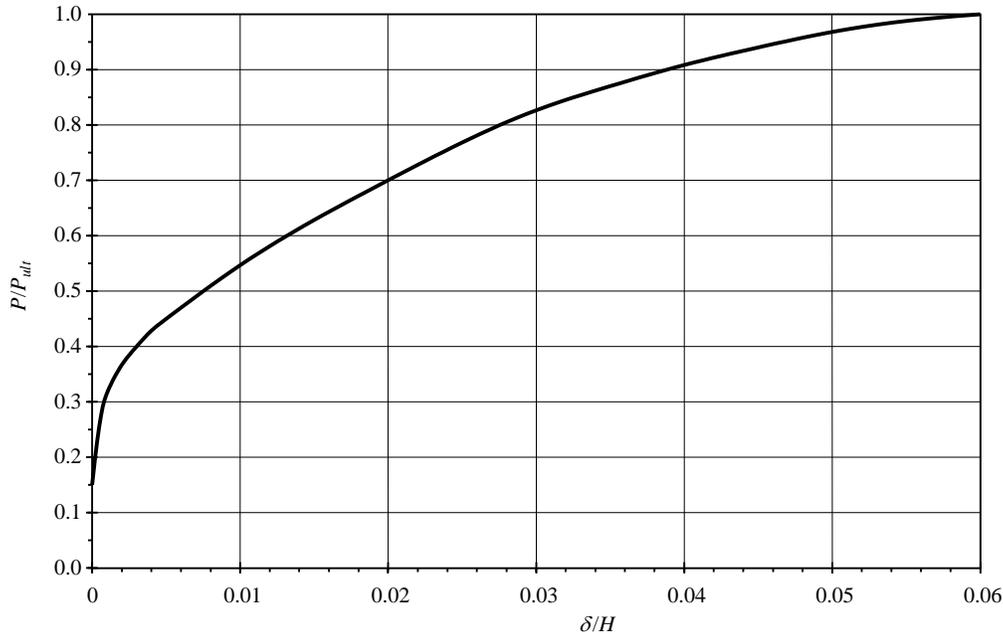
Figure 7.2-5 Passive pressure mobilization curve (after ASCE 41)

7.2.1.4.4 Group Effect Factors. The response of a group of piles to lateral loading will differ from that of a single pile due to pile-soil-pile interaction. (Group effect factors for axial loading of very closely spaced piles may also be developed but are beyond the scope of the present discussion.)

Full-size and model tests show that the lateral capacity of a pile in a pile group versus that of a single pile (termed "efficiency") is reduced as the pile spacing is reduced. The observed group effects are associated with shadowing effects. Various researchers have found that leading piles are loaded more heavily than trailing piles when all piles are loaded to the same deflection. The lateral resistance is primarily a function of row location within the group, rather than pile location within a row. Researchers recommend that these effects may be approximated by adjusting the resistance value on the single pile *p-y* curves (that is, by applying a *p*-multiplier).

Based on full-scale testing and subsequent analysis, Rollins et al. recommend the following *p*-multipliers (*f_m*), where *D* is the pile diameter or width and *s* is the center-to-center spacing between rows of piles in the direction of loading.

First (leading) row piles: $f_m = 0.26\ln\left(\frac{s}{D}\right) + 0.5 \leq 1.0$

Second row piles: $f_m = 0.52\ln\left(\frac{s}{D}\right) \leq 1.0$

Third or higher row piles: $f_m = 0.60\ln\left(\frac{s}{D}\right) - 0.25 \leq 1.0$

Because the direction of loading varies during an earthquake and the overall efficiency of the group is the primary point of interest, the average efficiency factor is commonly used for all members of a group in the analysis of any given member. In that case, the average *p*-reduction factor is as follows:

$$\bar{f}_m = \frac{1}{n}\sum_{i=1}^{n} f_{mi}$$

For a 2×2 pile group thus ③ ① ④ ② with *s* = 3*D*, the group effect factor is calculated as follows:

For piles 1 and 2, in the leading row, $f_m = 0.26\ln(3) + 0.5 = 0.79$.

For piles 3 and 4, in the second row, $f_m = 0.52\ln(3) = 0.57$.

So, the group effect factor (average *p*-multiplier) is $\bar{f}_m = \dfrac{0.79 + 0.79 + 0.57 + 0.57}{4} = 0.68$.

Figure 7.2-6 shows the group effect factors that are calculated for pile groups of various sizes with piles at several different spacings.
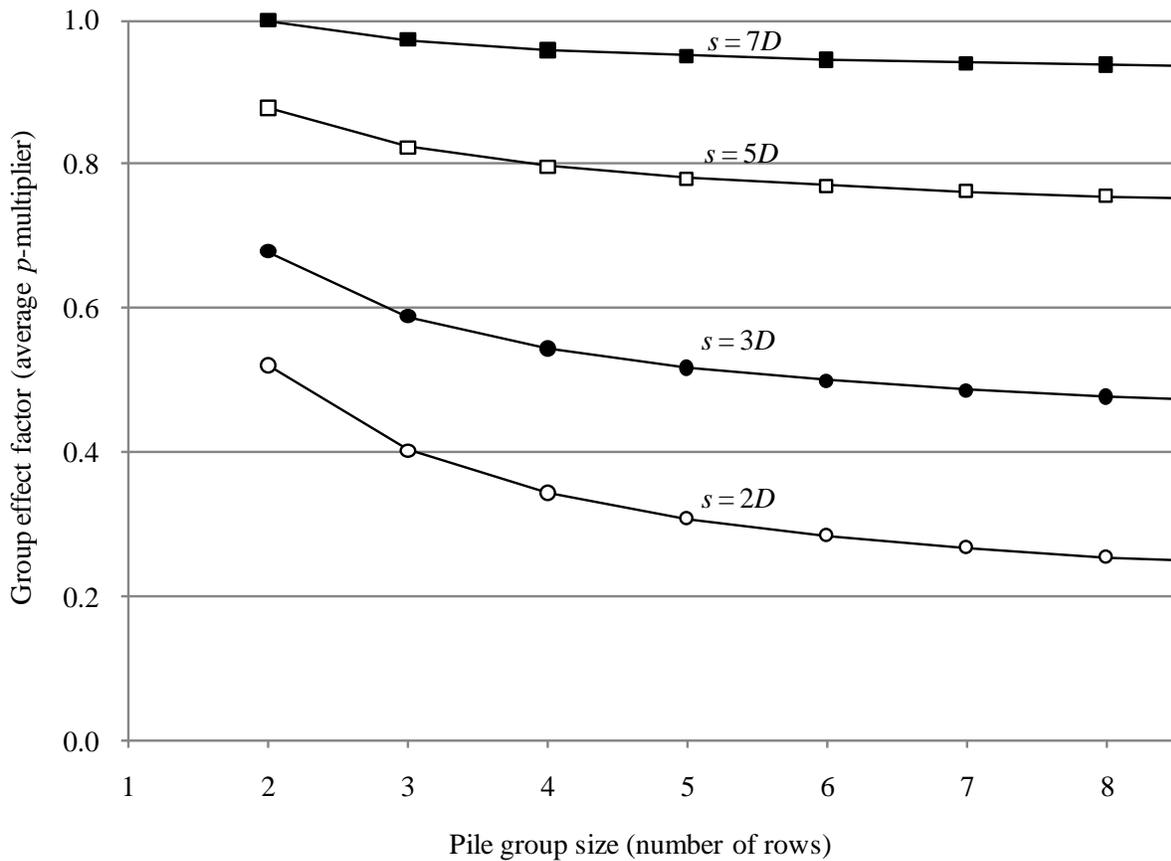

Figure 7.2-6 Calculated group effect factors

7.2.2 Pile Analysis, Design and Detailing

7.2.2.1 Pile Analysis. For this design example, it is assumed that all piles will be fixed-head, 22-inch-diameter, cast-in-place piles arranged in 2×2 pile groups with piles spaced at 66 inches center-to-center. The computer program LPILE v2013 is used to analyze single piles for both soil conditions shown in Table 7.2-1 assuming a length of 50 feet. Pile flexural stiffness is modeled using one-half of the gross moment of inertia because of expected flexural cracking. The response to lateral loads is affected to some degree by the coincident axial load. The full range of expected axial loads was considered in developing this example, but in this case the lateral displacements, moments and shears were not strongly affected; the plots in this section are for zero axial load. A *p*-multiplier of 0.68 for group effects (as computed at the end of Section 7.2.1.4) is used in all cases. Figures 7.2-7, 7.2-8 and 7.2-9 show the variation of shear, moment and displacement with depth (within the top 30 feet) for an applied lateral load of 15 kips on a single pile with the group reduction factor. It is apparent that the extension of piles to depths beyond 30 feet for the Class E site (or approximately 25 feet for the Class C site) does not provide additional resistance to lateral loading; piles shorter than those lengths would have reduced lateral resistance. The trends in the figures are those that should be expected. The shear and displacement are maxima at the pile head. Because a fixed-head condition is assumed, moments are also largest at the top of the pile. Moments and displacements are larger for the soft soil condition than for the firm soil condition.
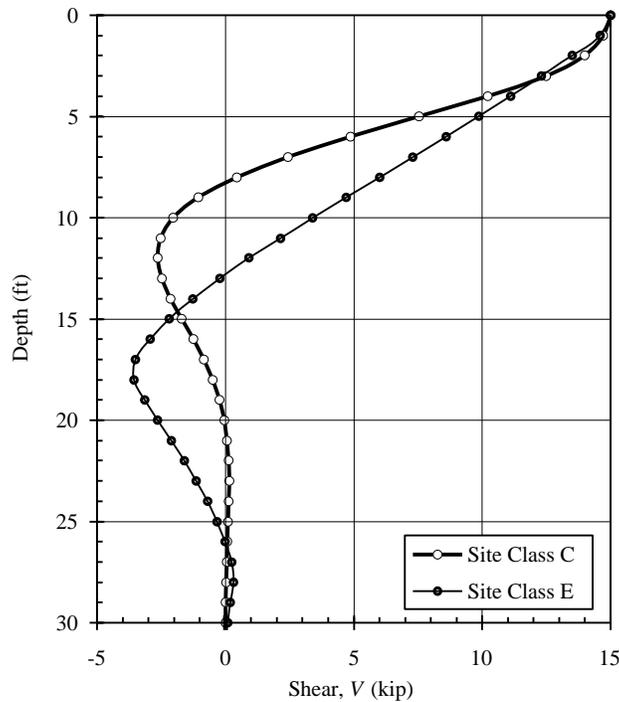
Figure 7.2-7 Results of pile analysis-shear versus depth
(applied lateral load is 15 kips)
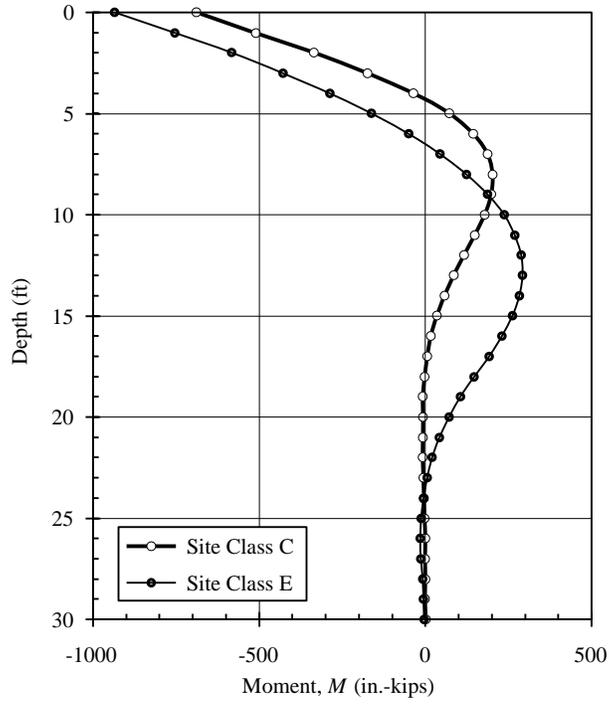
Figure 7.2-8 Results of pile analysis-moment versus depth
(applied lateral load is 15 kips)
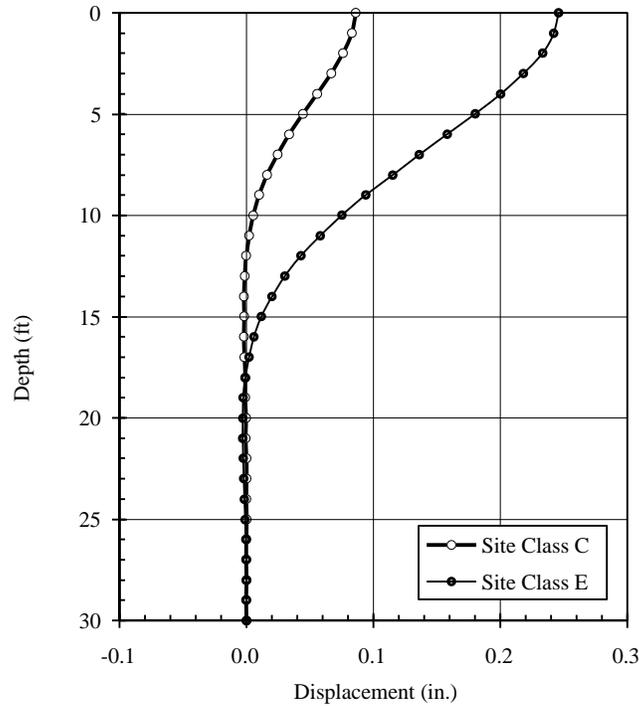
Figure 7.2-9 Results of pile analysis-displacement versus depth
(applied lateral load is 15 kips)

The analyses performed to develop Figures 7.2-7 through 7.2-9 are repeated for different levels of applied lateral load. Figures 7.2-10 and 7.2-11 show how the moment and displacement at the head of the pile are related to the applied lateral load. It may be seen from Figure 7.2-10 that the head moment is related to the applied lateral load in a nearly linear manner; this is a key observation. Based on the results shown, the slope of the line may be taken as a characteristic length that relates head moment to applied load. Doing so produces the following:

- $\ell = 46$ in. for the Class C site

- $\ell = 70$ in. for the Class E site
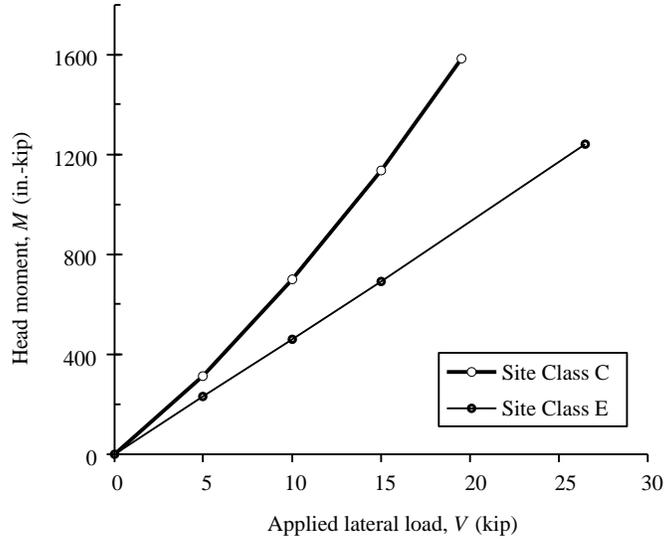
Figure 7.2-10 Results of pile analysis – applied lateral load versus head moment
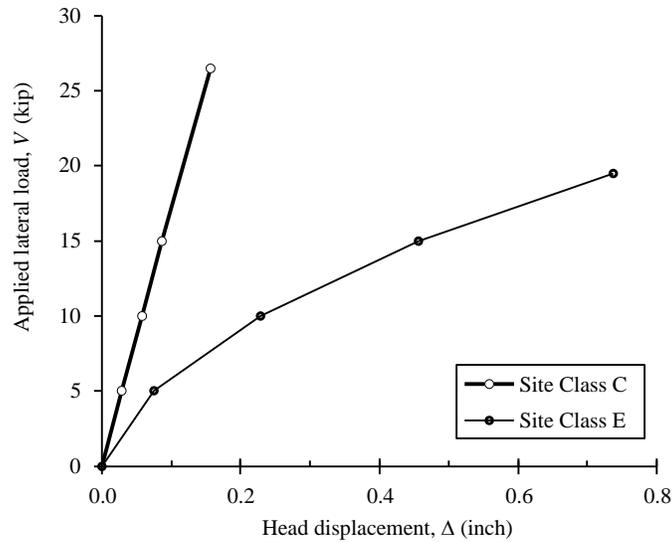
Figure 7.2-11 Results of pile analysis – head displacement versus applied lateral load

A similar examination of Figure 7.2-11 leads to another meaningful insight. The load-displacement response of the pile in Site Class C soil is essentially linear. The response of the pile in Site Class E soil is somewhat nonlinear, but for most of the range of response a linear approximation is reasonable (and useful). Thus, the effective stiffness of each individual pile is:

- $k = 175$ kip/in. for the Class C site

- $k = 40$ kip/in. for the Class E site

7.2.2.2 Pile Group Analysis. The combined response of the piles and pile cap and the resulting strength demands for piles are computed using the procedure outlined in Section 7.2.1.4 for each of the 32 load combinations discussed in Section 7.2.1.3. Assume that each 2×2 pile group has a 9'-2" × 9'-2" × 4'-0" thick pile cap that is placed 1'-6" below grade.

Check the Maximum Compression Case under a Side Column in Site Class C

Using the sign convention shown in Figure 7.2-3, the demands on the group are as follows:

- $P = 1{,}224$ kip

- $M_{yy} = 222$ ft-kips

- $V_x = 20$ kips

- $M_{yy} = 732$ ft-kips

- $V_y = 73$ kips

From preliminary checks, assume that the displacements in the x and y directions are sufficient to mobilize 30 percent and 35 percent, respectively, of the ultimate passive pressure:

$$V_{passive,x} = 0.30(575)\left(\frac{18}{12} + \frac{48}{2(12)}\right)\left(\frac{48}{12}\right)\left(\frac{110}{12}\right)\left(\tfrac{1}{1000}\right) = 22.1 \text{ kips}$$

and

$$V_{passive,y} = 0.35(575)\left(\frac{18}{12} + \frac{48}{2(12)}\right)\left(\frac{48}{12}\right)\left(\frac{110}{12}\right)\left(\tfrac{1}{1000}\right) = 25.8 \text{ kips}$$

and conservatively take $h_p = h/3 = 16$ inches. Note that by using a maximum mobilization factor of 0.35, this is conservative compared to calculating the ultimate passive resistance using ϕ=0.5. Therefore, ultimate lateral capacity is not limiting this case.

Since $V_{passive,x} > V_x$, passive resistance alone is sufficient for this case in the x direction. However, in order to illustrate the full complexity of the calculations, reduce $V_{passive,x}$ to 4 kips and assign a shear of 4.0 kips to each pile in the x direction. In the y direction, the shear in each pile is as follows:

$$V = \frac{73 - 25.8}{4} = 11.8 \text{kips}$$

The corresponding pile moments are:

$M = 4.0(46) = 186$ in.-kips for x-direction loading

and

$M = 11.8(46) = 543$ in.-kips for y-direction loading

The maximum axial load due to overturning for x-direction loading is:

$$P_{ot} = \frac{20(48) + 222(12) + 4(184) - 16(4)}{2(66)} = 32.5 \, \text{kips}$$

and for y-direction loading (determined similarly), $P_{ot} = 106.4$ kips.

The axial load due to direct loading is $P_p = 1224/4 = 306$ kips.

Therefore, the maximum load effects on the most heavily loaded pile are the following:

$P_u = 32.5 + 106.4 + 306 = 445$ kips

$M_u = \sqrt{(184)^2 + (543)^2} = 573 \, \text{in.-kips}$

The expected displacement in the y direction is computed as follows:

$\delta = V/k = 11.8/175 = 0.067$ in., which is 0.14 percent of the pile cap height (h)

Reading Figure 7.2-5 with $\delta/H = 0.0014$, $P/P_{ult} \approx 0.34$, so the assumption that 35 percent of P_{ult} would be mobilized was reasonable.

7.2.2.3 Design of Pile Section. The calculations shown in Section 7.2.2.2 are repeated for each of the 32 load combinations under each of the four design conditions. The results are shown in Figures 5.2-12 and 7.2-13. In these figures, circles indicate demands on piles under side columns and squares indicate demands on piles under corner columns. Also plotted are the ϕP-ϕM design strengths for the 22-inch-diameter pile sections with various amounts of reinforcement (as noted in the legends). The appropriate reinforcement pattern for each design condition may be selected by noting the innermost capacity curve that envelops the corresponding demand points. The required reinforcement is summarized in Table 7.2-4, following calculation of the required pile length.
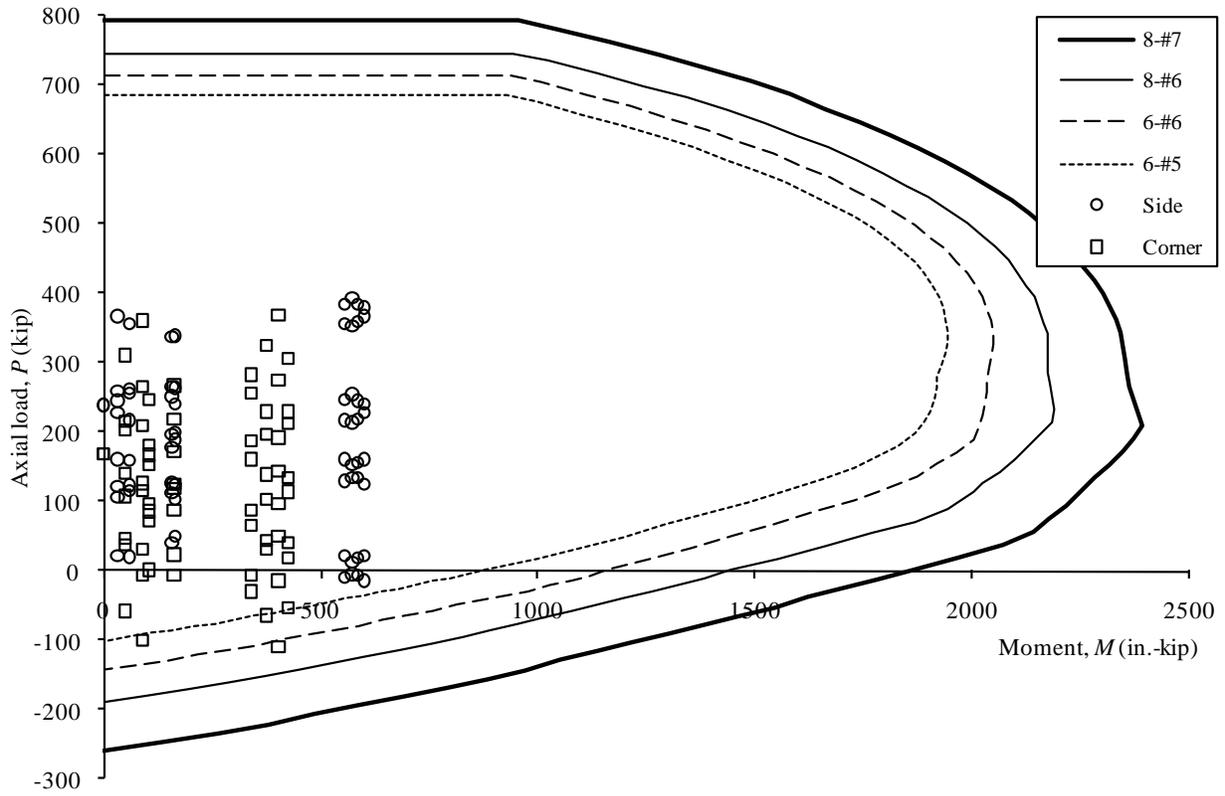
Figure 7.2-12 P-M interaction diagram for Site Class C
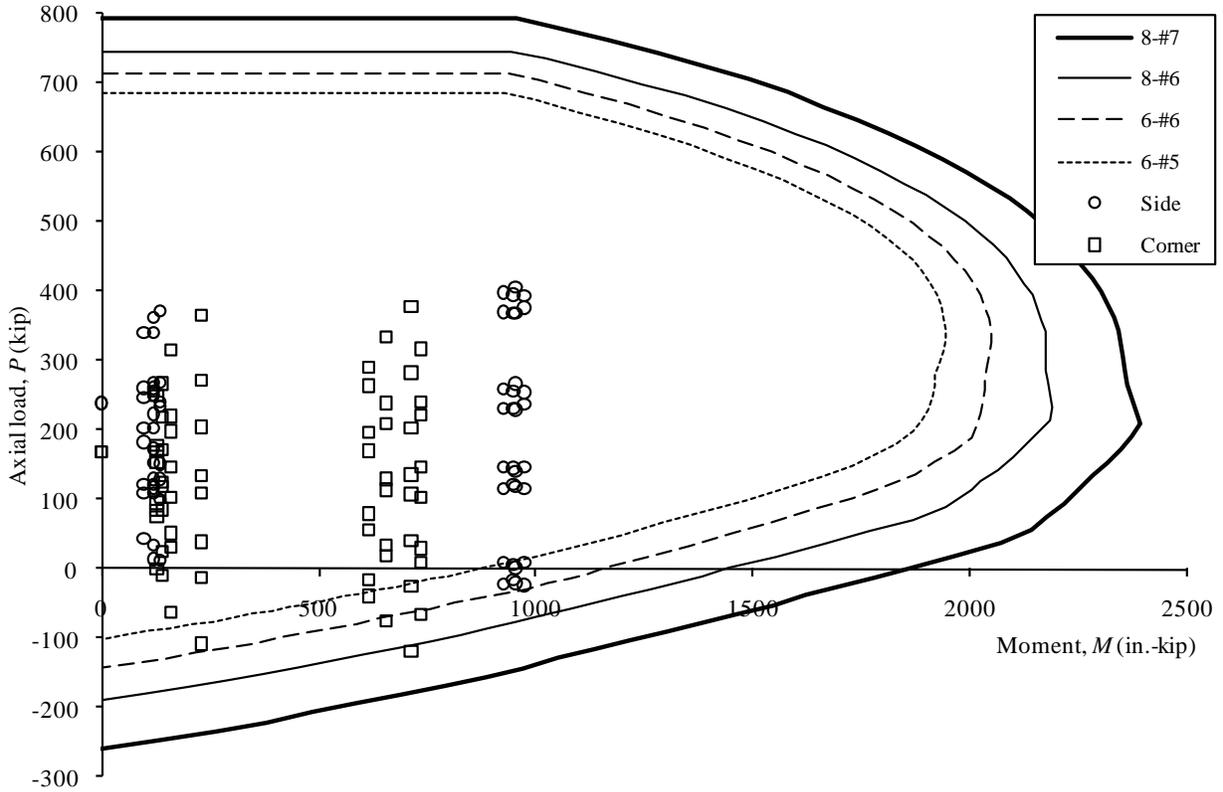
Figure 7.2-13 P-M interaction diagram for Site Class E

7.2.2.4 Pile Length for Axial Loads. For the calculations that follow, recall that skin friction and end bearing are neglected for the top 3 feet in this example. The design is based on having 1'-6" of soil over a 4'-0" deep pile cap.

Pile capacity for axial loads can be calculated by assuming a pile length. A more practical approach is to calculate the pile capacity as a function of length, or pre-calculate the capacity for each length increment using a spreadsheet format. This method lends itself to graphical expression. See Figures 7.2-14 and 7.2-15.
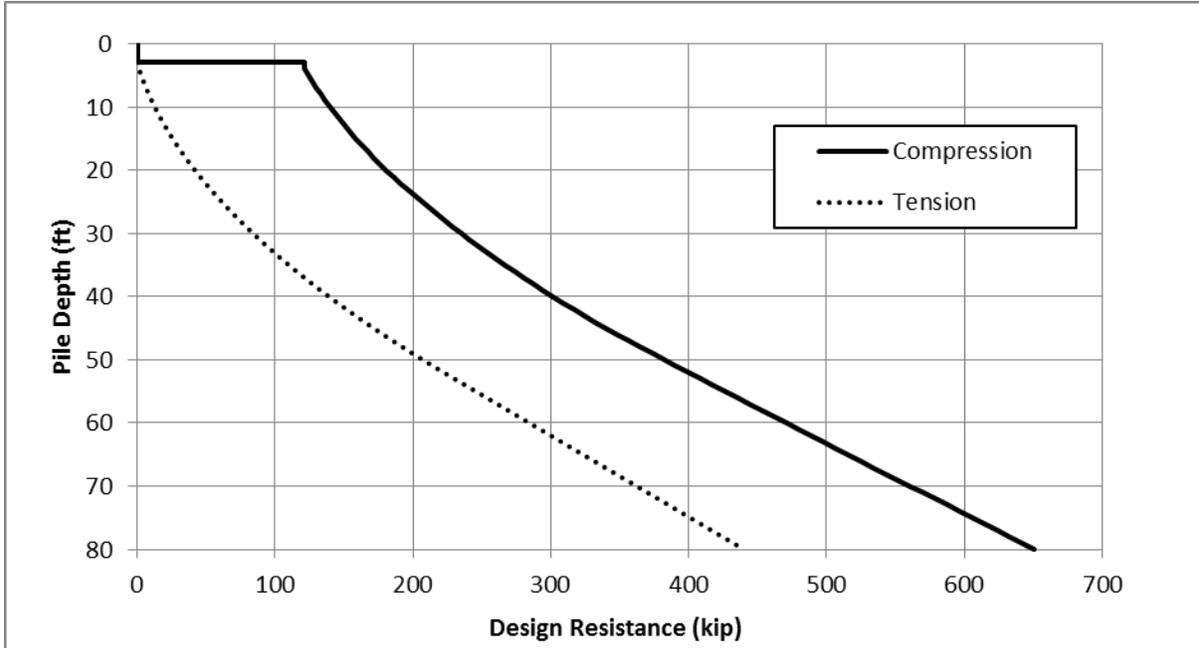
Figure 7.2-14 Pile axial capacity as a function of length for Site Class C
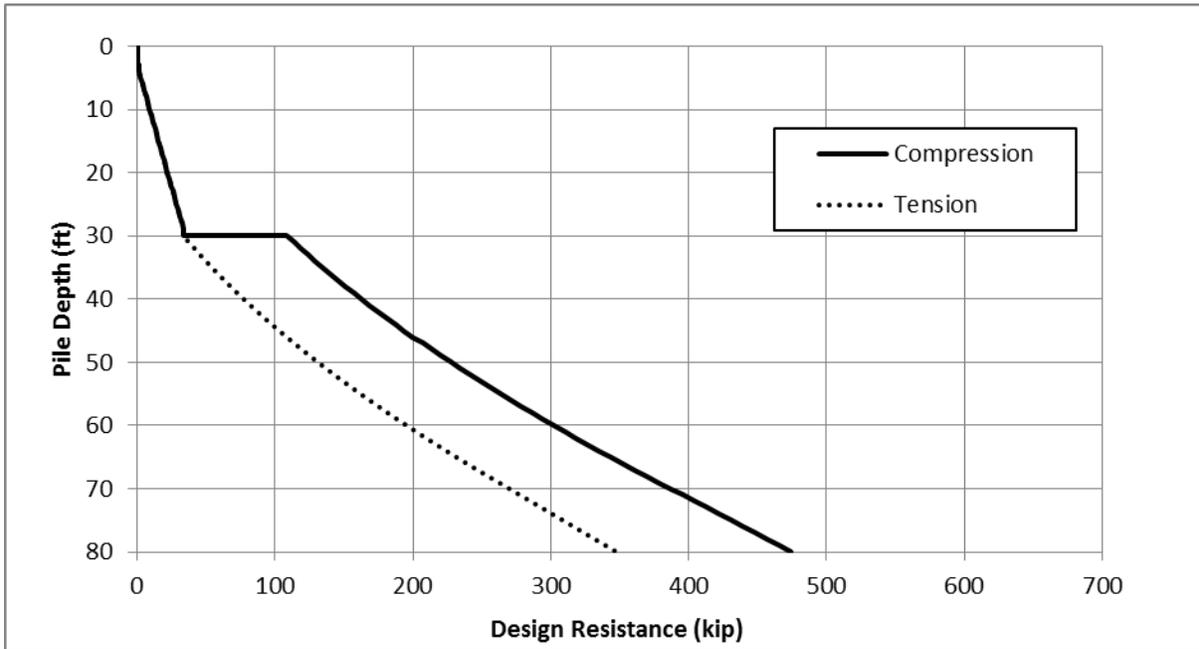
Figure 7.2-15 Pile axial capacity as a function of length for Site Class E

7.**2.2.4.1 Length for Compression Capacity.** All of the strength-level load combinations (discussed in Section 7.2.1.3) must be considered.

Check the pile group under the side column in Site Class C:

As seen in Figure 7.1-12, the maximum compression demand for this condition is $P_u = 394$ kips.

Determine length using Figure 7.2-14, resulting in $L = 52$ feet.

Calculate compression capacity to confirm for purposes of this example:

$P_{skin} = 0.5(0.5+3)\pi(22/12)(49) = 494$ kips
$P_{end} = [100+(49)(1)](\pi)(22/12)^2 = 393$ kips
$\phi P_n = \phi(P_{skin} + P_{end}) = 0.45(494 + 393) = 399$ kips > 394 kips   OK

Check the pile group under the corner column in Site Class E:

As seen in Figure 7.2-13, the maximum compression demand for this condition is $P_u = 390$ kips.

Determine length using Figure 7.2-15, resulting in $L = 70$ feet.

7.2.2.4.3 Length for Uplift Capacity. Again, all of the strength-level load combinations (discussed in Section 7.2.1.3) must be considered.

Check the pile group under side column in Site Class C:

As seen in Figure 7.2-12, the maximum tension demand for this condition is $P_u = -15$ kips.

Determine length using Figure 7.2-14, resulting in $L = 10$ feet.

Check the pile group under the corner column in Site Class E:

As seen in Figure 7.2-13, the maximum tension demand for this condition is $P_u = -120$ kips.

Determine length using Figure 7.2-15, resulting in $L = 48$ feet.

7.2.2.4.5 Results of Pile Length Calculations. Detailed calculations for the required pile lengths are provided above for two of the design conditions. Table 7.2-3 summarizes the lengths required to satisfy strength and serviceability requirements for all four design conditions.

Table 7.2-3 Pile Lengths Required for Axial Loads

	Piles Under Corner Column			Piles Under Side Column		
Site Class	Condition	Load	Min Length	Condition	Load	Min Length
Site Class C	**Compression**	**375 kip**	**48 ft**	**Compression**	**394 kip**	**52 ft**
	Uplift	115 kip	35 ft	Uplift	15 kip	10 ft
Site Class E	**Compression**	**390 kip**	**70 ft**	**Compression**	**420 kip**	**74 ft**
	Uplift	120 kip	48 ft	Uplift	20 kip	20 ft

7.2.2.5 Design Results. The design results for all four pile conditions are shown in Table 7.2-4. The amount of longitudinal reinforcement indicated in the table is that required at the pile-pile cap interface and may be reduced at depth as discussed in the following section.

Table 7.2-4 Summary of Pile Size, Length and Longitudinal Reinforcement

Site Class	Piles Under Corner Column	Piles Under Side Column
Site Class C	22 in. diameter by 48 ft long	22 in. diameter by 52 ft long
	8-#6 bars	6-#5 bars
Site Class E	22 in. diameter by 70 ft long	22 in. diameter by 74 ft long
	8-#7 bars	6-#6 bars

7.2.2.6 Pile Detailing. *Standard* Sections 12.13.5, 12.13.6, 14.2.3.1 and 14.2.3.2 contain special pile requirements for structures assigned to Seismic Design Category C or higher and D or higher. In this section, those general requirements and the specific requirements for uncased concrete piles that apply to this example are discussed. Although the specifics are affected by the soil properties and assigned site class, the detailing of the piles designed in this example focuses on consideration of the following fundamental items:

- All pile reinforcement must be developed in the pile cap (*Standard* Sec. 12.13.6.5).

- In areas of the pile where yielding might be expected or demands are large, longitudinal and transverse reinforcement must satisfy specific requirements related to minimum amount and maximum spacing.

- Continuous longitudinal reinforcement must be provided over the entire length resisting design tension forces (ACI 318 Sec. 18.13.4.1).

The discussion that follows refers to the detailing shown in Figures 7.2-16 and 7.2-17.

7.2.2.6.1 Development at the Pile Cap. Where neither uplift nor flexural restraint are required, the development length is the full development length for compression. Where the design relies on head fixity or where resistance to uplift forces is required (both of which are true in this example), pile reinforcement must be fully developed in tension unless the section satisfies the overstrength load condition or demands are limited by the uplift capacity of the soil-pile interface (*Standard* Sec. 12.13.6.5).

For both site classes considered in this example, the pile longitudinal reinforcement is extended straight into the pile cap a distance that is sufficient to fully develop the tensile capacity of the bars. In addition to satisfying the requirements of the *Standard*, this approach offers two advantages. By avoiding lap splices to field-placed dowels where yielding is expected near the pile head (although such would be permitted by the *Standard*), more desirable inelastic performance would be expected. Straight development, while it may require a thicker pile cap, permits easier placement of the pile cap's bottom reinforcement followed by the addition of the spiral reinforcement within the pile cap. Note that embedment of the entire pile in the pile cap facilitates direct transfer of shear from pile cap to pile but is not a requirement of the *Standard*. (Section 1810.3.11 of the 2015 *International Building Code* requires that piles be embedded at least 3 inches into pile caps.)

4" pile embedment

(6) #5

#4 spiral at 4.5 inch pitch

Section A

6'-4"

(6) #5

#4 spiral at 9 inch pitch

Section B

23'-0"

(4) #5

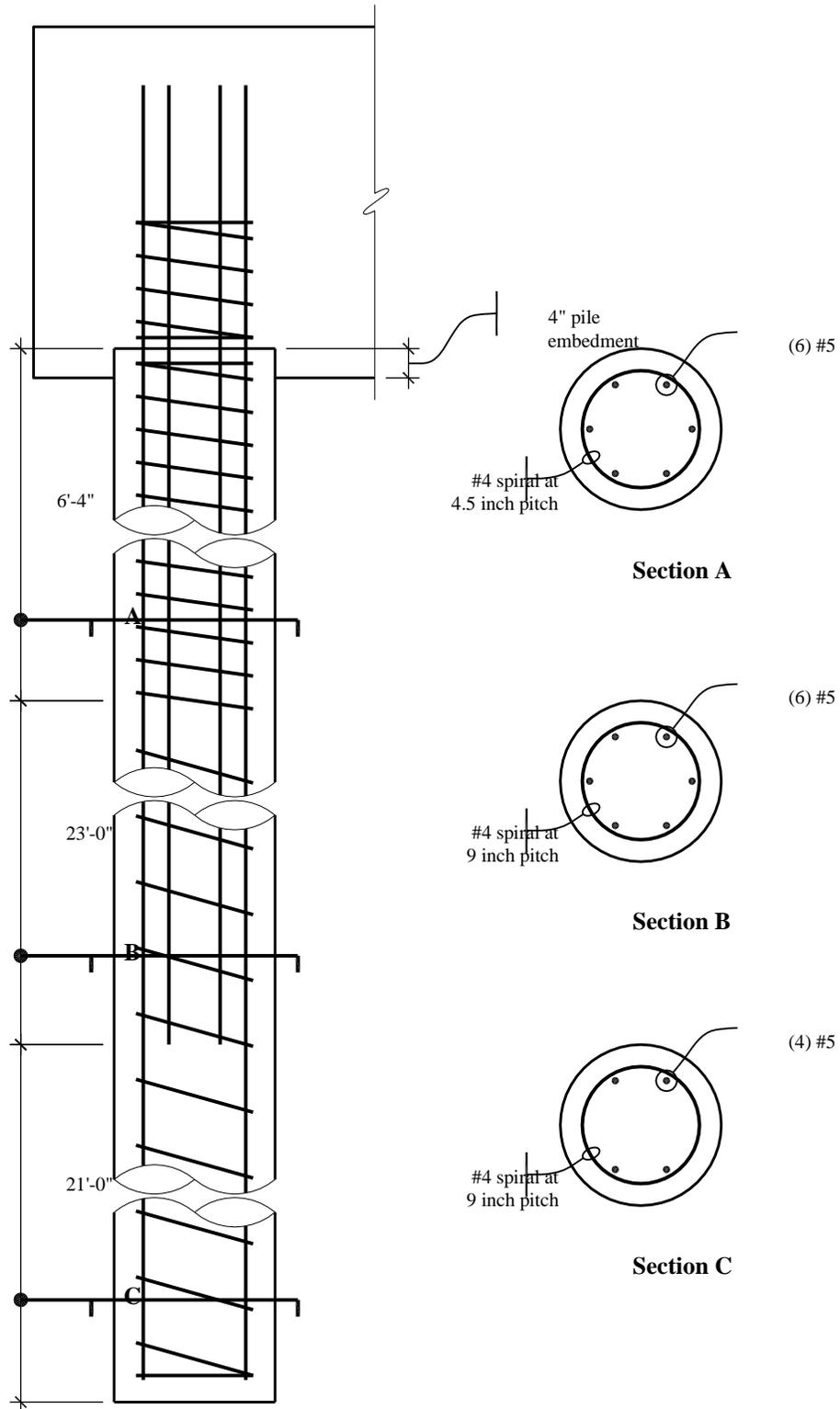#4 spiral at 9 inch pitch

Section C

21'-0"

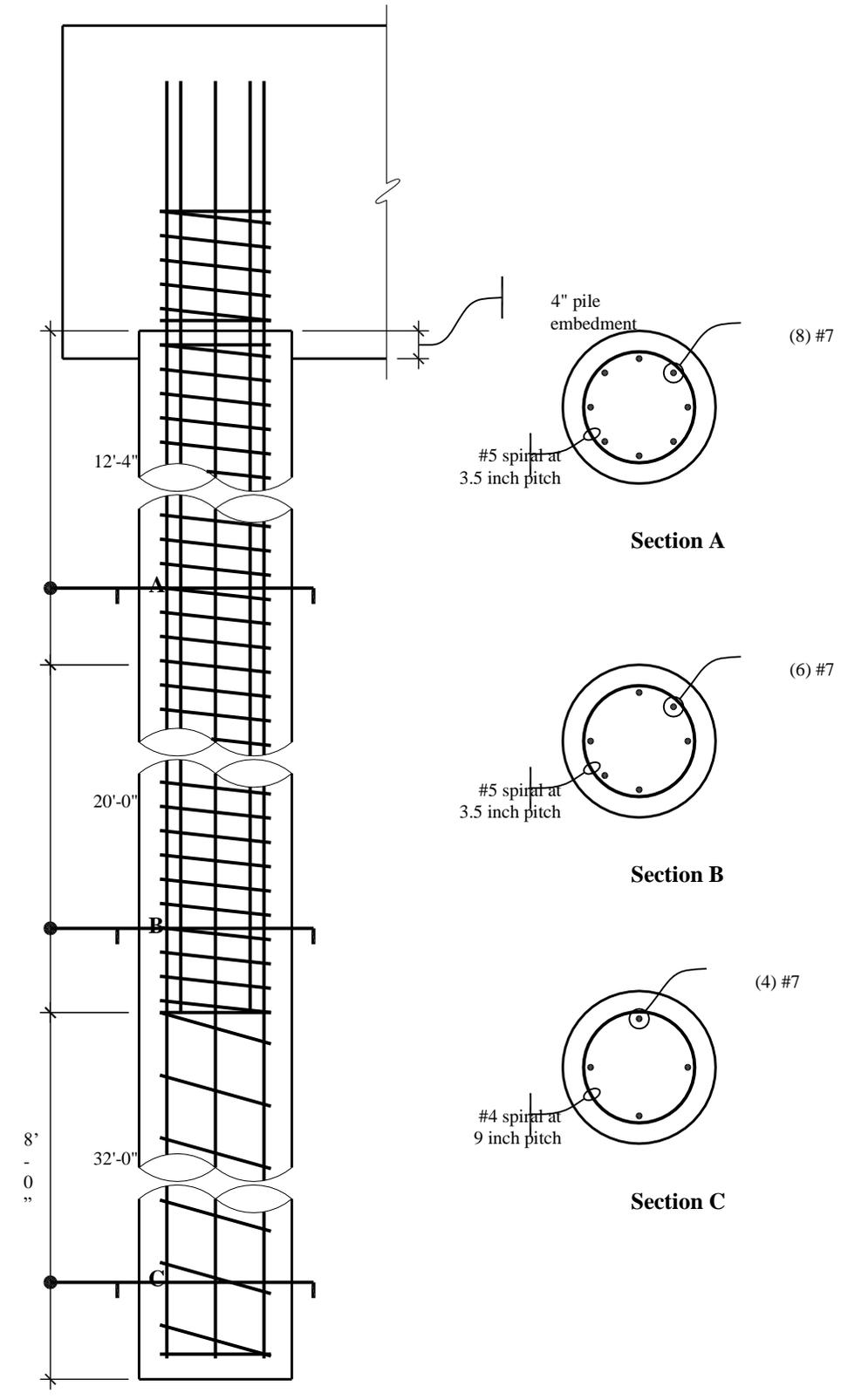**Figure 7.2-16 Pile detailing for Site Class C (under side column)**

Figure 7.2-17 Pile detailing for Site Class E (under corner column)

7.2.2.6.2 Longitudinal and Transverse Reinforcement Where Demands Are Large. Requirements for longitudinal and transverse reinforcement apply over the entire length of pile where demands are large. For uncased concrete piles in Seismic Design Category D, at least four longitudinal bars (with a minimum reinforcement ratio of 0.005) must be provided over the largest region defined as follows: the top one-half of the pile length, the top 10 feet below the ground, or the flexural length of the pile. The flexural length is taken as the length of pile from the cap to the lowest point where 0.4 times the concrete section cracking moment (see IBC 2015 Section 1810.3.9.1) exceeds the calculated flexural demand at that point. For the piles used in this example, one-half of the pile length governs. (Note that "providing" a given reinforcement ratio means that the reinforcement in question must be developed at that point. Bar development and cutoff are discussed in more detail in Chapter 10 of this volume of design examples.) Transverse reinforcement must be provided over the same length for which minimum longitudinal reinforcement requirements apply. Because the piles designed in this example are larger than 20 inches in diameter, the transverse reinforcement may not be smaller than 0.5 inch diameter. For the piles shown in Figures 7.2-16 and 7.2-17, the spacing of the transverse reinforcement in the top half of the pile length may not exceed the least of the following: $12d_b$ (7.5 in. for #5 longitudinal bars and 10.5 in. for #7 longitudinal bars), $22/2 = 11$ in., or 12 in.

Where yielding may be expected, even more stringent detailing is required. For the Class C site, yielding can be expected within three diameters of the bottom of the pile cap ($3D = 3 \times 22 = 66$ in.). Spiral reinforcement in that region must not be less that required by Section 18.7.5.4 of ACI 318 and the requirements of Sections 18.7.5.2 and 18.7.5.3 must be satisfied. Note that because the site is not Class E, Class F, or liquefiable, only one-half the spiral reinforcement required by Table 18.7.5.4(e) is necessary. Note that this equation will most commonly govern for deep foundation elements. In order to provide a reinforcement ratio of 0.01 for this pile section, a #4 spiral must have a pitch of no more than 4.8 inches, but the maximum spacing permitted by Section 21.4.4.2 is $22/4 = 5.5$ inches or $6d_b = 3.75$ inches, so a #4 spiral at 3.75-inch pitch is used. (Section 1810.3.2.1.2 of the 2015 *International Building Code* clarifies that ACI 318 Equation 25.7.3.3 and Table 18.7.5.4(d) need not be applied to piles.)

For the Class E site, the more stringent detailing must be provided "within seven diameters of the pile cap and of the interfaces between strata that are hard or stiff and strata that are liquefiable or are composed of soft to medium-stiff clay" (*Standard* Sec. 14.2.3.2.1). The author interprets "within seven diameters of ... the interface" as applying in the direction into the softer material, which is consistent with the expected location of yielding. Using that interpretation, the *Standard* does not indicate the extent of such detailing into the firmer material. Taking into account the soil layering shown in Table 7.2-1 and the pile cap depth and thickness, the tightly spaced transverse reinforcement shown in Figure 7.2-17 is provided within $7D$ of the bottom of pile cap and top of firm soil and is extended a little more than $3D$ into the firm soil. Because the site is Class E, the full amount of reinforcement indicated in ACI 318 Section 18.7.5.4 must be provided (Except that Table 18.7.5.4(d) need not be applied). In order to provide a reinforcement ratio of 0.02 for this pile section, a #5 spiral must have a pitch of no more than 3.7 inches. The maximum spacing permitted by Section 18.7.5.4.3 is $22/4 = 5.5$ inches or $6d_b = 5.25$ inches, so a #5 spiral at 3.5-inch pitch is used.

7.2.2.6.3 Continuous Longitudinal Reinforcement for Tension. Table 7.2-3 shows the pile lengths required for resistance to uplift demands. For the Site Class E condition under a corner column (Figure 7.2-17), longitudinal reinforcement must resist tension for at least the top 48 feet (being developed at that point). Extending four longitudinal bars for the full length and providing widely spaced spirals at such bars is practical for placement, but it is not a specific requirement of the *Standard*. For the Site Class C condition under a side column (Figure 7.2-16), design tension due to uplift extends only approximately 10 feet below the bottom of the pile cap. Therefore, a design with Section C of

Figure 7.2-16 being unreinforced would satisfy the *Provisions* requirements, but the author has decided to extend very light longitudinal and nominal transverse reinforcement for the full length of the pile.

7.2.3 Kinematic Interaction

Piles are subjected to curvature demands as a result of two different types of behavior: inertial interaction and kinematic interaction. The term *inertial interaction* is used to describe the coupled response of the soil-foundation-structure system that arises as a consequence of the mass properties of those components of the overall system. The structural engineer's consideration of inertial interaction is usually focused on how the structure *loads* the foundation and how such loads are transmitted to the soil (as shown in the pile design calculations that are the subject of most of this example) but also includes assessment of the resulting foundation movement. The term *kinematic interaction* is used to describe the manner in which the stiffness of the foundation system impedes development of free-field ground motion. Consideration of kinematic interaction by the structural engineer is usually focused on assessing the strength and ductility demands imposed directly on piles by movement of the soil. Although it is rarely done in practice, *Standard* Section 12.13.7.3 requires consideration of kinematic interaction for foundations of structures assigned to Seismic Design Category D, E, or F. Kramer (1996) discusses kinematic and inertial interaction and the methods of analysis employed in consideration of those effects and demonstrates "that the solution to the entire soil-structure interaction problem is equal to the sum of the solutions of the kinematic and inertial interaction analyses."

One approach that would satisfy the requirements of the *Standard* would be as follows:

- The geotechnical consultant performs appropriate kinematic interaction analyses considering free-field ground motions and the stiffness of the piles to be used in design.

- The resulting pile demands, which generally are greatest at the interface between stiff and soft strata, are reported to the structural engineer.

- The structural engineer designs piles for the sum of the demands imposed by the vibrating superstructure and the demands imposed by soil movement.

A more practical, but less rigorous, approach is to provide appropriate detailing in regions of the pile where curvature demands imposed directly by earthquake ground motions are expected to be significant. Where such a judgment-based approach is used, one must decide whether to provide only additional transverse reinforcement in areas of concern to improve ductility or whether additional longitudinal reinforcement should also be provided to increase strength. Section 18.10.2.4.1 of the 2015 *International Building Code* permits application of such deemed-to-comply detailing in lieu of explicit calculations and prescribes a minimum longitudinal reinforcement ratio of 0.005.

7.2.4 Design of Pile Caps

Design of pile caps for large pile loads is a very specialized topic for which detailed treatment is beyond the scope of this volume of design examples. CRSI notes that "most pile caps are designed in practice by various short-cut rule-of-thumb procedures using what are hoped to be conservative allowable stresses." Wang & Salmon indicates that "pile caps frequently must be designed for shear considering the member as a deep beam. In other words, when piles are located inside the critical sections d (for one-way action) or $d/2$ (for two-way action) from the face of column, the shear cannot be neglected." They go on to note that "there is no agreement about the proper procedure to use." Direct application of the special provisions for deep flexural members as found in ACI 318 is not possible since the design conditions are somewhat different. CRSI provides a detailed outline of a design procedure and tabulated solutions, but the procedure is developed for pile caps subjected to concentric vertical loads only (without applied overturning moments or pile head moments). Strut-and-tie models (as described in ACI 318 Chapter 23) may be employed, but their application to elements with important three-dimensional characteristics (such as pile caps for groups larger than 2×1) is so involved as to preclude hand calculations.

7.2.5 Foundation Tie Design and Detailing

Standard Section 12.13.6.2 requires that individual pile caps for structures in seismic design category C, D, E, or F be interconnected by ties. Additionally, Section 12.13.7.2 requires that individual spread footings founded on soil classified as Site Class E or F should also be interconnected by ties. Such ties are often grade beams, but the *Standard* would permit use of a slab (thickened or not) or calculations that demonstrate that the site soils (assigned to Site Class A, B, or C) provide equivalent restraint. For this example, a tie beam between the pile caps under a corner column and a side column is designed. The resulting section is shown in Figure 7.2-18.

For pile caps with an assumed center-to-center spacing of 32 feet in each direction and given P_{group} = 1,224 kips under a side column and P_{group} = 1,142 kips under a corner column, the tie is designed as follows.

As indicated in *Standard* Section 12.13.6.2, the minimum tie force in tension or compression equals the product of the larger column load times S_{DS} divided by 10 = 1224(1.1)/10 = 135 kips.

The design strength for six #6 bars is as follows

$$\phi A_s f_y = 0.9(6)(0.44)(60) = 143 \text{ kips} > 135 \text{ kips} \qquad \text{OK}$$

It should be noted that the longitudinal tie beam reinforcement (top and bottom) should be fully developed for tension into the pile cap or spread footing with either straight embedment or standard hooks in accordance with ACI 318 25.4.

According to ACI 318 Section 18.13.3.2, the smallest cross-sectional dimension of the tie beam must not be less than the clear spacing between pile caps divided by 20 = (32'-0" - 9'-2")/20 = 13.7 inches. Use a tie beam that is 14 inches wide and 16 inches deep. ACI 318 Section 18.13.3.2 further indicates that closed ties must be provided at a spacing of not more than one-half the minimum dimension, which is 14/2 = 7 inches.

Assuming that the surrounding soil provides restraint against buckling, the design strength of the tie beam concentrically loaded in compression is as follows:

$$\phi P_n = 0.8\phi[0.85f'_c(A_g - A_{st}) + f_y A_{st}]$$

$$= 0.8(0.65)[0.85(3)\{(16)(14) - 6(0.44)\} + 60(6)(0.44)] = 376 \text{ kips} > 135 \text{ kips} \qquad \text{OK}$$
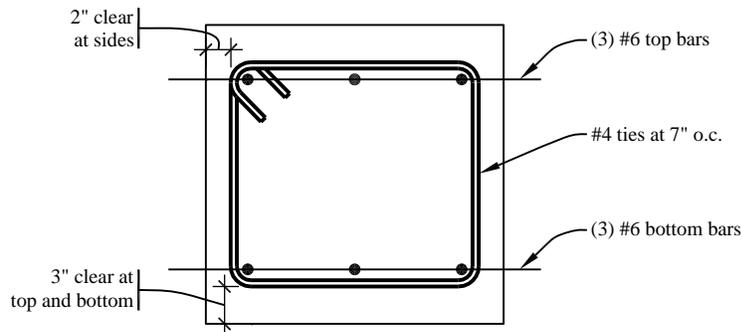
Figure 7.2-18 Foundation tie section

7.3 FOUNDATIONS ON LIQUEFIABLE SOIL

For Seismic Design Categories C, D, E and F, Standard Section 11.8.2 requires that the geotechnical report address potential hazards due to liquefaction. For Seismic Design Categories D, E and F, Standard Section 11.8.3 further requires that the geotechnical report describe the likelihood and potential consequences of liquefaction and soil strength loss (including estimates of differential settlement, lateral movement, lateral loads on foundations, reduction in foundation soil-bearing capacity, increases in lateral pressures on retaining walls and flotation of buried structures) and discuss mitigation measures.

Where the geotechnical investigation report indicates the potential for soil strength loss due to liquefaction in MCEg earthquake motions, the structure shall be designed to accommodate these effects in accordance with Standard Section 12.13.8.1 through 12.13.8.3. Section 12.13.8.1 requires that the foundations be designed to support gravity and Design Earthquake loads using soil bearing capacity utilizing any reductions necessary to consider liquefaction effects due. This capacity may include any mitigating effects of ground improvements.

Deep foundations on sites with liquefaction risk should be in accordance with the design and detailing requirements of Standard Section 12.13.8.3. Specifically, axial and lateral resistance should incorporate reductions as necessary to account for the effects of liquefaction. Liquefaction induced downdrag should also be incorporated by reducing the net ultimate geotechnical capacity and by including the downdrag load in the structural design of the pile section. Finally, the pile design should consider the effects of permanent ground displacement including nonlinear behavior of the piles such that gravity load carrying capacity is maintained in accordance with Section 12.13.8.3.4.

Standard Section 12.13.8.2 permits the use of shallow foundations to support a structure on a site with potential for liquefaction provided two criteria are met. First, Section 12.13.8.2(a) requires that the lateral spread ground displacement does not exceed a specific limit which is 18 inches for Risk Category II structures. Second, Section 12.13.8.2(b) requires that the structure be designed to accommodate differential settlements with limited loss of member and connection strength. As an alternative, if differential settlements are controlled to the limits specified in Table 12.13-3, explicit design beyond the detailing requirements identified below is not required. For the example problem of a multi-story braced

frame structure, permissible differential settlement limit is $\delta_v/L = 0.010$. With columns spaced at 25'-0" on center, permissible differential settlement between columns is 3 inches. In addition to requiring connection of the shallow foundations with ties in accordance with Section 12.13.7.2, these ties should be designed to accommodate differential settlement between footings. Where permanent ground displacement induced by lateral spreading exceeds 3 inches, the additional detailing requirements of 12.13.8.2.1.1 for should be followed consisting of an increased tie design force and a requirement to tie footings together with a nominal slab on grade.

This example includes illustration of two elements of the provisions in Section 12.13.8, Requirements for Structure Foundations on Liquefiable Sites. This is a new section of the Provisions addressing the design of foundations where the geotechnical investigation has identified the potential for strength loss due to liquefaction in MCE$_G$ earthquake motions. The Provisions place limits on the use of shallow foundations and provide design requirements for deep foundations. This example addresses two separate elements of the requirements: 1) Acceptability of shallow foundations for conditions outside the specified limit for differential settlement through a detailed structural evaluation; and 2) Design of a pile foundation for a site subject to lateral spreading.

7.3.1. Background. Liquefaction is assessed directly under MCE$_G$ earthquake motions. This differs from the seismic design approach in most of the Provisions, wherein designs are accomplished at MCE$_R$ earthquake motions that have been reduced for design by a factor of 2/3. The intent of the design is the same – to provide protection against collapse in the MCE – but the specifics of the approach are different. Because the design for liquefaction addresses higher levels of shaking directly, and its specific performance goal allows for more damage to occur, it becomes necessary to consider nonlinear effects. Such considerations are not common in designs based on these Provisions. Accordingly, these examples make use of the information in ASCE 41-13 and other resources in order to assess the acceptability of element demands and capacities. The Provisions do not require the use of any specific nonlinear procedures or criteria.

7.3.2. Acceptability of superstructure for support by shallow foundations. Structures on shallow foundations can experience lateral spreading or differential settlement when soils supporting foundations are subject to strength loss due to liquefaction. The Provisions specify limits on the conditions where shallow foundations are acceptable. These include upper limits on lateral displacement and differential settlement due to liquefaction (as specified in Tables 12.13-1 and 12.13-2 respectively). The Provisions are worded such that expected lateral displacement must be less than the upper limits indicated in Table 12.13-1 and the structure must be designed to accommodate the expected differential settlement, but an exception is provided: differential settlements less than those indicated in Table 12.13-2 are deemed to comply with the requirements. Differential settlement due to liquefaction occurs when soil densifies during an earthquake, decreasing in volume below shallow foundations. The effect of small differential settlements of shallow foundations is generally considered to be acceptable without explicit calculation. However, more significant differential settlement requires evaluation of the superstructure. This example considers design of a structure in compliance with Table 12.13-1 and not in compliance with Table 12.13-2, thus requiring structural analysis to demonstrate acceptability.

Differential settlement of foundations results in vertical column displacement and deformations in framing members (slab, beams, girders). Differential settlement induces additional shear, flexural, and displacement demands due to deformation compatibility. Figure 7.3-1 shows an elevation of a single-story moment frame subject to differential settlement. Depending on the severity of differential settlement, floor members or connections may yield as the structure deforms. The chord rotation due to settlement, indicated as δ_v/L in the Provisions, approximates rotation demand on floor framing members and their connections. If δ_v/L does not exceed the applicable value in Table 12.13-2, the differential

settlement is deemed acceptable. However, if δ_v/L exceeds the applicable value in the table, structural analysis is required to determine the acceptability of shallow foundations supporting the superstructure.
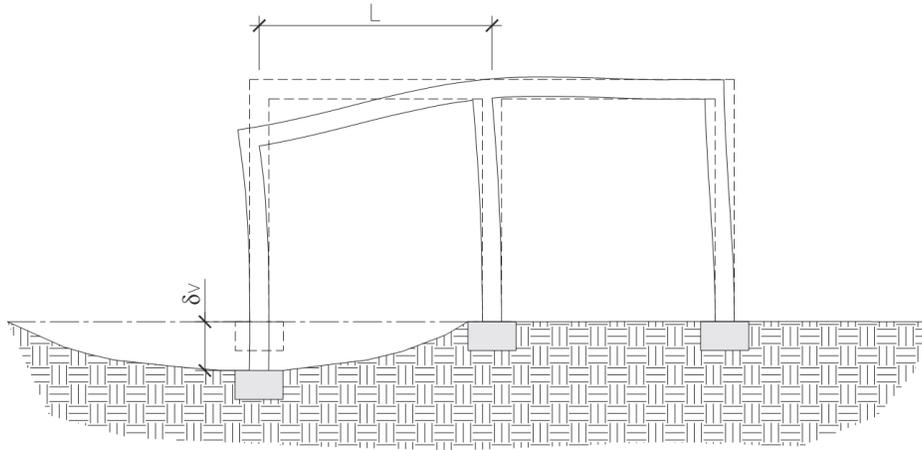
Figure 7.3-1. Elevation of single-story moment frame with differential settlement
(Note: Tie beams are not shown for clarity.)

A plan view of a typical floor in the subject building is shown in Figure 7.3-2. The following are the design requirements for this example:

- Seismic Force-Resisting System: Steel Special Moment Frames
- Moment Frame Beam: W27x94 (A992)
- Moment Frame Column: W14x605 (A992)
- Gravity System: Concrete fill over metal deck
          Steel beams, girders and columns
- Gravity Frame Beam: W16x36 (A992)
- Gravity Frame Girder: W24x62 (A992)
- Gravity shear tab connection plates: A36
- Gravity Load:
  - Floor Dead   85 psf
  - Floor Live   50 psf
  - Cladding   280 plf
- Typical bay width, L: 25 feet
- Expected differential settlement, δ_v: 8 inches
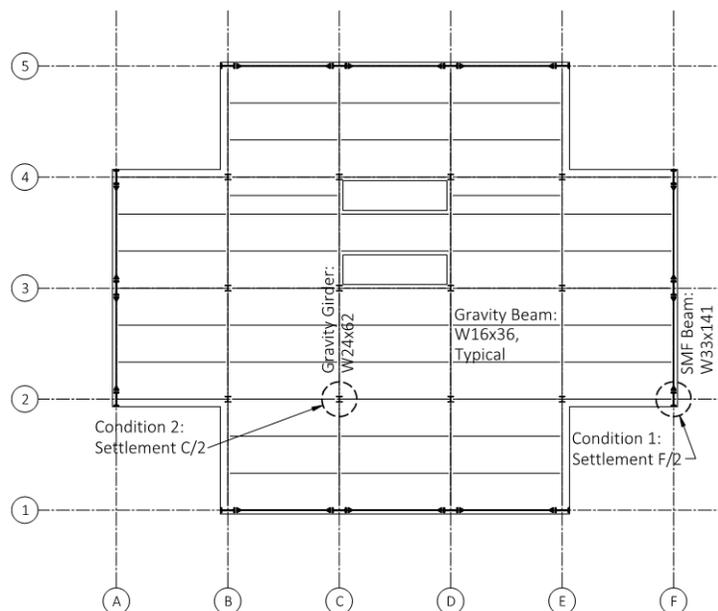
Figure 7.3-2. Floor framing plan with locations of assessment shown.

Because the potential differential settlement can occur at any location, we will assess two representative locations for settlement. In other buildings, many more locations may require assessment. The chord rotation due to differential settlement across one bay shown in Figure 7.3-2 is:

$$\delta_v/L = 8\ in/(25\ ft \times 12\ in/ft) = 0.027\ rad\ .$$

Table 12.13-3 of the Provisions indicates the acceptable chord rotation value for "other multi-story structures" in Risk Category II is 0.01 rad. The computed value exceeds the permissible limit, so analysis is required.

Provisions Section 12.13.8.2 (b) requires an analysis that incorporates the expected differential settlement to demonstrate that the structure is capable of undergoing settlement without loss of the ability to support gravity loads and that the residual strength of members and connections is not less than 67 percent of the undamaged nominal strength, considering nonlinear behavior in the structure, as necessary. If demands on all members and connections do not exceed any element's nominal strength when subjected to differential settlements, this requirement is satisfied. If nominal strengths are exceeded, we must demonstrate that their strength does not degrade beyond the required level.

The degraded strength limit of 67% in the Provisions is intended to ensure that elements and connections remain within the ductile range of the force-deformation (or moment-rotation) relationship. The residual strength of elements and connections experiencing significant strength degradation will fall below this value. Elements and connections beyond this limit may have little reserve strength to support gravity loads or further settlement following aftershocks. The intent of the provision is to maintain gravity support by avoiding significant strength degradation.

We will investigate two locations in the building: Condition 1 is located at Grid F/2. At this location, the girder is part of a special moment-resisting frame. The perpendicular beam at this location has a simple shear-tab connection. Both of these members frame into only one side of the column, so the settlement will cause moments in the column as well as the girder and beam due to the asymmetry.

Condition 2 is located at Grid C/2. This condition is symmetrically arranged, both in terms of the plan geometry and the member sizes. The beam-to-column condition here is the same as in Condition 1. The girder-to-column condition involves deeper members, which we will assess separately.

7.3.2.1 Condition 1 – Grid F/2.

SMF Beam along Grid F. Members and connections in special moment frame systems must comply with stringent member selection and connection detailing criteria, allowing them to sustain significant ductility demands while maintaining their strength. These elements will therefore provide sufficient ductility to satisfy the Provisions, provided that the rotation remains below the acceptable chord rotation specified in the applicable AISC documents. Members and connections in ordinary or intermediate moment resisting frame systems are less ductile and may require a more detailed evaluation. Braced frame and shear wall systems are stiffer than moment frame systems. Deformations within a braced frame bay or shear wall can approach rigid body behavior, resulting in significant rotation in secondary elements in adjacent bays. AISC 341-10 defines the minimum story drift angle a connection must be capable of providing to be an approved SMF connection in Section E3.6b. For the welded unreinforced flange-welded web (WUF-W) connection under consideration, the acceptable chord rotation is 0.04 rad.

At column at F/2, the SMF connection acceptable chord rotation exceeds the expected chord rotation, so the SMF members and connections are deemed acceptable.
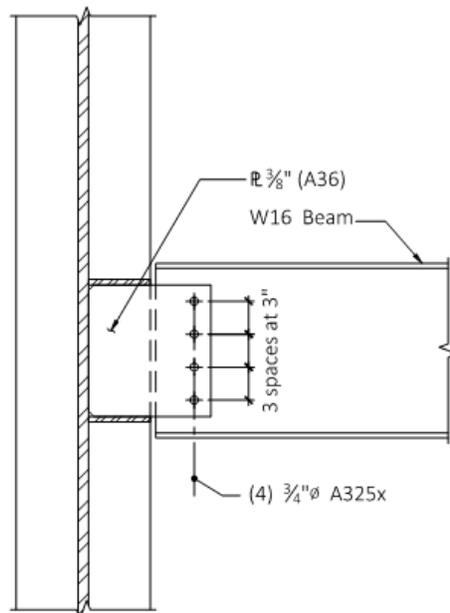
Figure 7.3-3. Gravity beam-to-column connection

Gravity Beam along Grid 2. A W16x36 beam frames into the weak axis of the column at F/2, as shown in Figure 7.3-3. Although we generally design gravity beams considering pinned end conditions, we recognize that there will be some fixity provided by the simple shear tab end connections and that the slab above the beam also contributes to end fixity. Therefore our initial assessment of this member will be to consider it as a beam that is fixed at both ends and subject to a vertical displacement at F/2 equal to the liquefaction-induced settlement of 8 inches. The shear will be uniform and the moment will have

opposing signs at the two ends. The resulting maximum shear and moment in the beam are computed as follows:

$$V_\Delta = 12EI\Delta/L^3 = (12)(29000ksi)(448in^4)(8in)/(25\,ft \times 12\,in/ft)^3 = 46\,kips$$
$$M_\Delta = 6EI\Delta/L^2 = (6)(29000ksi)(448in^4)(8in)/(25\,ft \times 12\,in/ft)^2 = 6,929\,kip - in$$
$$M_\Delta = 577\,kip - ft$$

We must also consider the applicable shear and moment due to the gravity loading on the beam. Considering the combination 1.2D + 0.5L, which is applicable in combination with seismic loading, we compute the tributary width as 4.17 ft. and the factored gravity uniform load as

$$w_{ug} = 1.2(4.17 \times 85 + 280) + 0.5(4.17 \times 50) = 0.866\,kip/ft$$

The resulting gravity shear and moment in the beam, again considering fixed ends, are computed as follows:

$$V_{ug} = w_{ug}l/2 = (.866)(25)/2 = 11\,kips$$
$$M_{ug} = w_{ug}l^2/12 = (0.866)(25)^2/12 = 45\,kip - ft$$

The maximum shear and moment are then

$$V_u = 46 + 11 = 57\,kips$$
$$M_u = 577 + 45 = 622\,kip - ft$$

We find the design flexural and shear strengths for the W16x36 beam in the AISC Manual

ϕM_n = 174 kip-ft (for negative moment, L_b = 12.5 ft. for bracing at mid-span, from Table 3-10)
ϕV_n = 141 kip (from Table 3-6)

The beam is adequate to resist induced shear demands due to differential settlement however the flexural demand exceeds the bending capacity. We find the shear strength of the single-plate connection in the AISC Manual:

ϕV_n = 78.3 kip (from Table 10-10a)

Since the shear strength of the connection is also adequate to resist the expected demand, either the beam or the connection will yield in flexure when subject to this deformation.

In order to determine whether the beam or the connection will yield, we compute the flexural strength of the connection. As a conservative first pass, we consider the pure moment strength of the bolt group, according to the AISC Manual.

$\varphi r_n = 22.5\,kips$, for 3/4" dia. A325-X bolts in single shear (Table 7-1)
$C' = 11.3$, from for 1 Row of (4) bolts (Table 7-6)
$$\varphi M_n = \varphi C' r_n = 254\,kip - in = 21\,kip - ft$$

Since the pure moment strength of the bolts in the connection is far less than the moment strength of the beam, we can be confident that the connection will yield first and the beam need not be checked for nonlinear behavior in bending.

Because the connection will be a yielding element, we must demonstrate that it has adequate ductility to resist the imposed chord rotation due to differential settlement. We employ the Single-Plate Connection Design Check in Chapter 10 of the AISC Manual. In this check, the thickness of the shear tab is limited to promote flexural yielding in the shear tab and minimize the likelihood of bolt fracture. Here, *d* is the depth of the shear tab. The maximum shear tab thickness is limited to:

$$t_{max} = \frac{6F_v(A_bC')}{0.90F_yd^2} = \frac{6(68ksi)(0.442in^2)(11.3)}{0.9(36\ ksi)(12)^2} = 0.44\ in.$$

The shear tab thickness is 3/8 inch, which satisfies the design check. Note that if the shear tab were constructed of grade 50 steel a thinner plate would be required to meet this check. Note also that this design check does not indicate an acceptable chord rotation for the connection; it only ensures the connection will yield in a ductile manner. We will employ Table 9-6 of ASCE 41-13 to obtain an acceptable plastic rotation capacity for simple shear connections, incorporating a value of d_{bg} = 9 inches for three bolts with 3-inch spacing. We consider the acceptable plastic rotation as the value stated in ASCE 41-13 for Collapse Prevention. Because the yield moment of this connection is so small, we take the plastic rotation equal to the total rotation.

$$\theta_{CP} = 0.15 - 0.0036d_{bg} = 0.117\ rad$$

The total acceptable chord rotation is exceeds the chord rotation due to differential settlement and the connection is deemed acceptable.

Bi-Axial Bending of Column at F/2. The moments induced in the beams due to the differential settlement will transfer to the column as well. In the case of the column at F/2, the column is part of the special moment-resisting frame. Because of the strong-column/weak-beam provisions for special moment frames, we can be assured that the column can withstand any moment that can be delivered by the SMF girder. The perpendicular W14 beam will also impart a moment, but because of the weakness of its connection (as indicated above) this moment is very small (unknown, but less than 11 kip-ft). As a result, we can safely consider that the weak-axis moment induced in the column is negligible and we may omit this check. In other structural configurations, it may be necessary to confirm numerically that the moments induced in the column are acceptable.

7.3.2.2 Condition 2 – Grid C/2

Interior gravity girders. Figure 7.3-4 shows the connection of the typical W24x62 gravity girder to the column. This check is similar to that for the W16 gravity beams, above. Please see the W16 gravity beam connection above for more a detailed discussion.
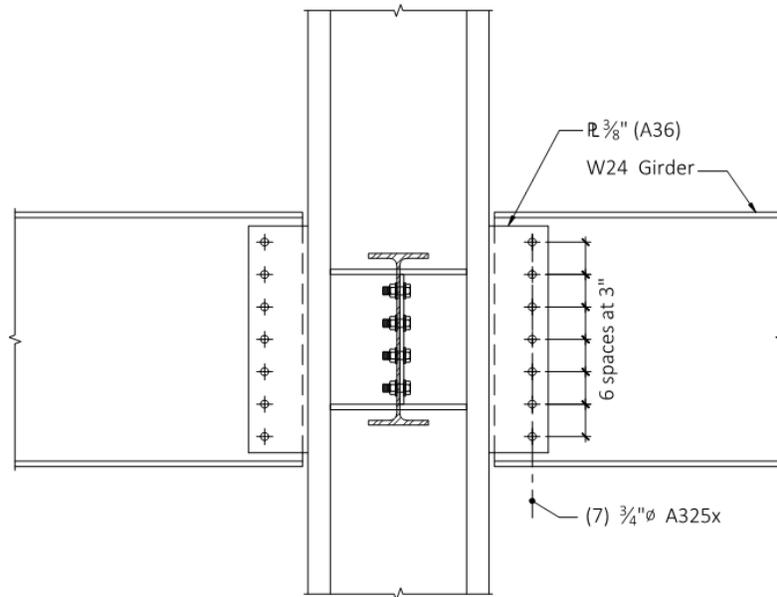
Figure 7.3-4. Gravity girder-to-column connection

The resulting maximum shear and moment in the beam due to the settlement are computed as follows:

$$V_\Delta = 12EI\Delta/L^3 = (12)(29000ksi)(1{,}550in^4)(8in)/(25\ ft \times 12\ in/ft)^3 = 160\ kips$$
$$M_\Delta = 6EI\Delta/L^2 = (6)(29000ksi)(1{,}550in^4)(8in)/(25\ ft \times 12\ in/ft)^2 = 23{,}973\ kip - in$$

$$M_\Delta = 1{,}998\ kip - ft$$

We must also consider the applicable shear and moment due to the gravity loading on the beam. Considering the combination 1.2D + 0.5L, which is applicable in combination with seismic loading, we compute the tributary area of each of two equal point loads as 208 sq. ft. and the factored gravity uniform load as

$$P_{ug} = 1.2(208 \times 85) + 0.5(208 \times 50) = 26\ kips$$

The resulting gravity shear and moment in the beam, again considering fixed ends, are computed as follows:

$$V_{ug} = P_{ug} = 26\ kips$$
$$M_{ug} = P_{ug}l/3 = (26)(25\ ft)/3 = 217\ kip - ft$$

The maximum shear and moment are then

$$V_u = 160 + 26 = 186\ kips$$
$$M_u = 1{,}998 + 217 = 2{,}215\ kip - ft$$

We find the design flexural and shear strengths for the W24x62 beam in the AISC Manual

ϕM_n = 482 kip-ft (for negative moment, L_b = 8.33 ft. for bracing at mid-span, from Table 3-10)
ϕV_n = 306 kip (from Table 3-6)

The beam is adequate to resist induced shear demands due to differential settlement however the flexural demand exceeds the bending capacity. We find the shear strength of the single-plate connection in the AISC Manual:

ϕV_n = 133 kip (from Table 10-10a)

Note that short-slotted holes are required by Table 10-10a for this condition for the 3/8" plate. The shear strength of the connection is less than the shear that could be developed if the connection did not yield in flexure when subject to this deformation.

We consider the pure moment strength of the bolt group, according to the AISC Manual.

$\varphi r_n = 22.5 \ kips$, for 3/4" dia. A325-X bolts in single shear (Table 7-1)
$C' = 33.8$, from for 1 Row of (7) bolts (Table 7-6)
$\varphi M_n = \varphi C' r_n = 761 \ kip - in = 63 \ kip - ft$

Since the pure moment strength of the bolts in the connection is far less than the moment strength of the beam, we can be confident that the connection will yield in flexure. Consequently, the shear strength of the connection will be adequate and the beam need not be checked for nonlinear behavior in flexure.

The maximum shear tab thickness is limited to:

$$t_{max} = \frac{6F_v(A_b C')}{0.90F_y d^2} = \frac{6(68ksi)(0.442in^2)(33.8)}{0.9(36 \ ksi)(21)^2} = 0.43 \ in.$$

The shear tab thickness is 3/8 inch, which satisfies the design check. We will employ Table 9-6 of ASCE 41-13 to obtain an acceptable plastic rotation capacity for simple shear connections, incorporating a value of d_{bg} = 18 inches for seven bolts with 3-inch spacing.

$$\theta_{CP} = 0.15 - 0.0036d_{bg} = 0.085 \ rad$$

The total acceptable chord rotation is exceeds the chord rotation due to differential settlement and the connection is deemed acceptable.

If the acceptable chord rotation were to be less than the rotation due to settlement, we could enlarge the standard bolt holes in the simple connection with long-slotted holes, such that under differential settlement, the bolts would not engage the ends of the slots -- thereby increasing connection's rotational capacity.

Conclusion. Based on the checks above, the superstructure can withstand the expected settlement without further modification and shallow foundations are an acceptable alternative.

7.3.2.3 Considerations for other structural systems.

The example above addressed assessment of settlement for a steel-frame structure. The assessment was primarily concerned with connection ductility. Other types of framing may require different

investigations in order to ensure that the structure can sustain the expected settlements while maintaining gravity support.

1. In concrete structures, particularly flat-slab structures, differential settlement can result in high shears near columns that are subject to settlement. Unlike the example above, these shears would need to be resisted by elastic (or nearly elastic) behavior, rather than relying on ductility.
2. In steel-frame structures incorporating moment connections that are not part of SMF systems, settlements can result in column yielding.
3. Potential load reversals due to settlements can result in the need for additional lateral bracing of beam flanges.

7.3.3. Design of pile foundation for a site subject to lateral spreading. Liquefaction can cause lateral spreading when the soils that are subject to liquefaction are free to displace laterally. These conditions can be found most commonly along banks of rivers and similar conditions where abrupt changes in ground elevation occur in the presence of saturated granular soils. The lateral spreading results in an extreme shear deformation in the affected soil layer. Pile foundations on sites subject to liquefaction are normally designed to support the structure vertically, incorporating liquefaction-induced downdrag as appropriate. Such designs generally include analysis of piles to sustain inertial lateral loading; piles are designed to remain elastic when subject to these demands. However, the large ground deformations that occur during lateral spreading will cause flexural demands in excess of the pile's nominal strength. The Provisions include requirements that place limits on the nonlinear behavior; with the intent of maintaining stability and gravity support.

When lateral spreading occurs, the head of the pile will displace laterally relative to the pile shaft embedded in competent soils below the liquefied layer. Figure 7.3-5 shows a schematic diagram of the pile and its behavior. Presuming fixed-head pile behavior, as would be provided in a typical multi-pile cap, the pile will develop two plastic hinges as the pile head displaces – one at the pile head and one near the interface between the liquefied layer and the competent soils below. The resulting displaced shape may be idealized as a single sloping line, with hinges at the top and bottom of the liquefiable layer. While a more complex analysis is possible – incorporating resistance provided by the liquefied soil and a hinge location somewhat below the interface between the liquefied layer and the competent soils below, the lack of precision in estimating the amount of lateral spread suggests a simple and conservative analysis of the pile's response to the deformation.

Downdrag will often occur in liquefied soils. However, it is not common for downdrag to occur in soils that are also subject to lateral spreading. In this example, we have not included vertical loading due to downdrag. In cases where downdrag occurs in combination with lateral spreading, the additional vertical loads should be included. The additional load would be applied in Figure 7.3-5 at the half-depth of the liquefiable soil and would impose an additional moment due to application of this load at half the lateral spreading deformation. Loads due to downdrag are considered as "E" loads and do not require additional load factors. The additional axial load will affect the P-delta demand, the pile flexural capacity and the pile ductility.
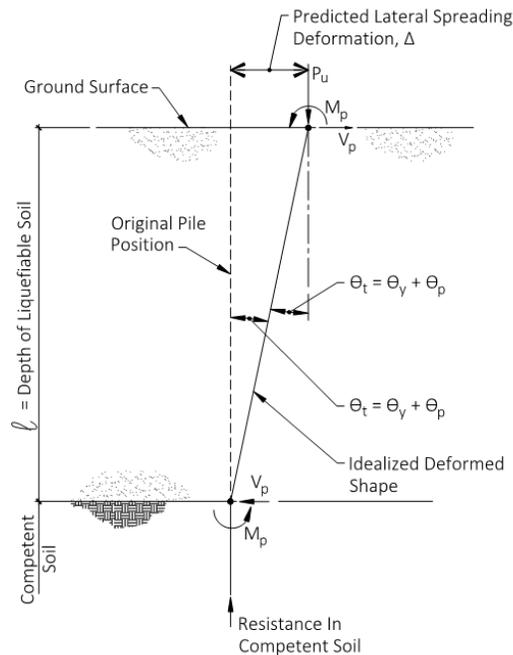
Figure 7.3-5. Schematic diagram of pile subject to lateral spreading

The following are the design requirements for this example:
▪ Expected lateral spreading displacement, Δ: 24 inches
▪ Depth of liquefiable layer, *l*: 30 feet
▪ Factored axial load per pile (1.2 D + 0.5 L)   250 kips (125 Tons)

We will employ the following material properties for this design example:
▪ f'_c = 5,000 psi
▪ f_y = 60,000 psi

Deep foundations subjected to lateral spreading must be designed according to Section 12.13.8.3. These requirements include an analysis incorporating the expected lateral deformation, the depth over which the deformation is expected to occur, and the nonlinear behavior of the piles. The Provisions include the following specific requirements for reinforced concrete piles subject to lateral spreading:

1. **Axial and Flexural Strength:** Pile deformations shall not exceed a value that results in loss of the pile's ability to carry gravity loads or in deterioration of the pile's lateral strength to less than 67 percent of the nominal strength.
2. **Detailing for Ductility:** Concrete piles shall be detailed to comply with Sections 18.7.5.2 through 18.7.5.4 of ACI 318-14 from the top of the pile to a depth exceeding that of the deepest liquefiable soil by at least 7 times the pile diameter.
3. **Shear Strength:** Nominal shear strength of piles shall exceed the maximum forces that can be generated due to pile deformations determined in the detailed analysis.

7.3.3.1 Figure 7.3-6 shows the pile foundation design under consideration, along with the soil profile subject to lateral spreading. The most important parameter in designing concrete piles for resistance to lateral spreading is the pile diameter. Selection of the pile diameter will affect many aspects of the behavior, including the following:

- Axial strength
- Flexural strength
- Ratio of shear strength to flexural strength
- Lateral stiffness
- Available flexural ductility.

Smaller pile diameters are advantageous in that they allow more elastic flexibility. However, larger pile diameters are advantageous in providing higher axial capacity, higher flexural capacity and higher shear strength.
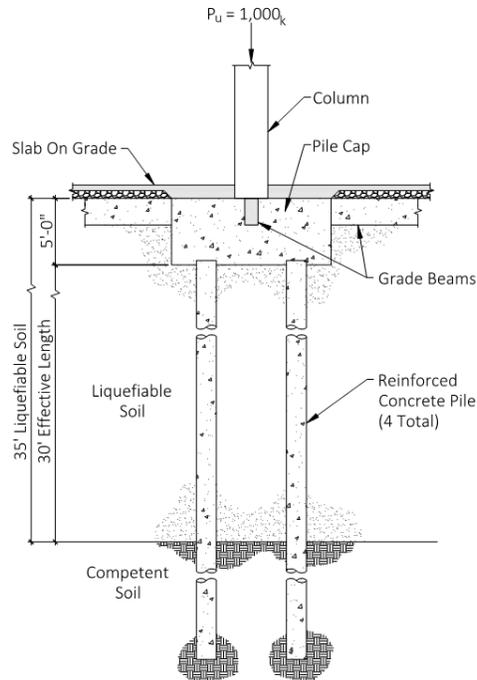
Figure 7.3-6. Foundation conditions for design

The 24 in. lateral spreading displacement exceeds the 18-inch limit in Table 12.13-2 for shallow foundations (for Risk Category 2), thus requiring the use of deep foundations.

When selecting the pile diameter, we will consider the requirement to avoid deterioration of the pile's lateral strength to less than 67 percent of the nominal strength. In this regard, we take note of the permissible plastic rotations and residual strength ratios indicated in Table 10-12 of ASCE 41-13 (Modeling parameters and numerical acceptance criteria for nonlinear procedures – reinforced concrete columns). We note that these parameters describing the behavior of reinforced concrete columns are highly dependent on the ratio of the column (or pile) axial load to its gross area and concrete strength.

Axial and Flexural Strength. Using ASCE 41-13 as a guideline for ductile behavior, we will select the pile diameter to ensure that the pile's axial load-to-axial strength ratio is less than 0.1. The lower axial load-to-capacity ratio provides significantly improved flexural ductility.

$$\frac{250k}{A_g f_c'} < 0.1;$$

$$Pile\ Diameter \geq 2 \sqrt{\frac{250k}{\pi(5ksi)(0.1)}} = 25.2\ in$$

Choose 30-inch diameter piles.

We must ensure that the pile will be able to support the axial loading when displaced laterally. Thus, the pile's flexural strength must be adequate to provide the restoring moments needed to counteract the P-Delta moment caused by the axial loading and the displacement. The two plastic moments combine to resist the P-Delta moment caused by the axial load and the displacement. The required flexural strength is computed as follows:

$$M_u = \frac{P_u\Delta}{2} = \frac{250k(24in)}{2} = 3,000\ kip - in$$

This assessment neglects any lateral resistance provided by the laterally spreading soil itself. It may be acceptable to incorporate this additional resistance, provided that the Geotechnical Investigation Report includes recommendations accordingly.

Although an Axial-Moment Diagram can be constructed by hand calculation or from tables, there are many commercially available software packages available to compute the axial-moment interaction capacity of a round pile section to facilitate design
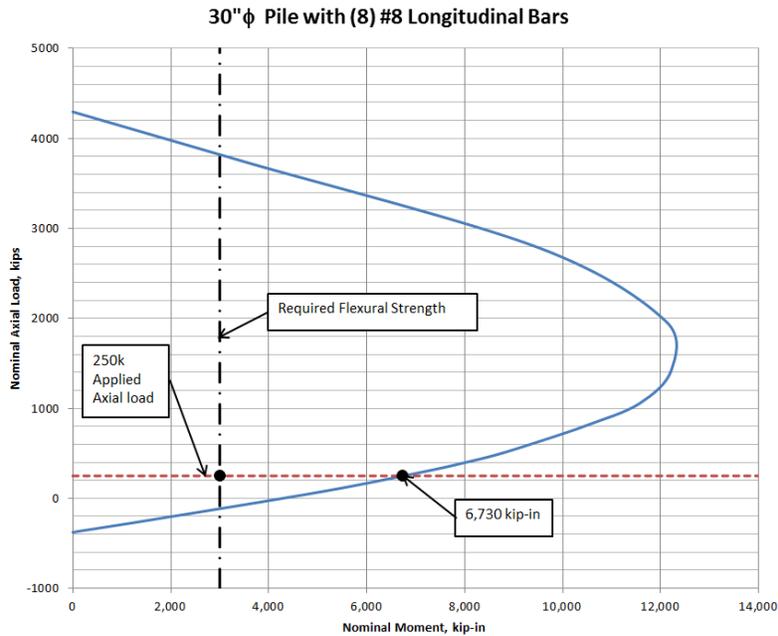
Figure 7.3-7. Nominal Axial–Moment Diagram for 30-in Pile reinforced with (8) #8 longitudinal bars

We can see from Figure 7.3-7 that a 30-inch pile reinforced with (8) #8 longitudinal bars has sufficient flexural strength (6,730 kip-in) to support the factored axial load and the P-Delta moment due to the 24-inch lateral spreading.

The flexural demand on the pile will be increased beyond the P-Delta moment as the pile bends to accommodate the displacement due to lateral spreading. The Provisions allow consideration of nonlinear behavior of the pile as this spreading occurs. The length over which bending occurs is the depth of the liquefiable layer. The total rotation produced by the lateral spreading is

$$\theta_t = \frac{24in}{360in} = 0.0667 \; rad.$$

In order to evaluate the adequacy of the pile, we must calculate the curvature of the cross section at θ_t. The section curvature depends on the length of the plastic hinge. Various methods exist for estimation of the plastic hinge length, l_p, depending on factors such as the effective length of the element, the section depth, and the size of the reinforcing bars. For the purpose of simplicity, we will use an estimate of half the section depth, in this case 15 inches. More detailed methods may result in longer lengths and thus smaller curvature. We then compute the curvature as

$$\varphi = \frac{\theta_t}{l_p} = \frac{0.0667 rad}{15in} = 0.0044 \; in^{-1}$$

We compare this value with the moment curvature relationship for the proposed pile section, under the design axial load. This relationship is shown in Figure 7.3-8. The computed curvature is less than the ultimate curvature (due to bar fracture). The moment strength at the design point exceeds the nominal strength (due to strain-hardening) thus meeting the requirement that the strength has not degraded to less than 67 percent of the nominal value.
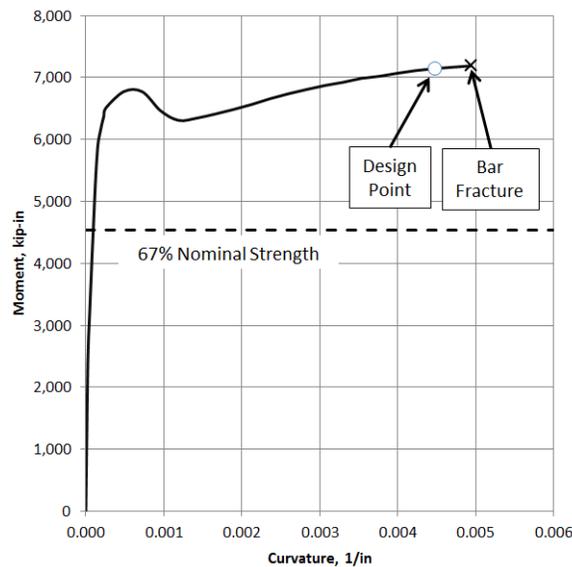
Figure 7.3-8. Moment-curvature relationship for pile under axial load of 250k

It is instructive to see how moment-curvature relationships vary with different values of applied axial load. Figure 7.3-9 shows several relationships for comparison. The higher values of axial load result in significantly smaller values of ultimate curvature, validating the need to keep the axial load-to-capacity ratio low.
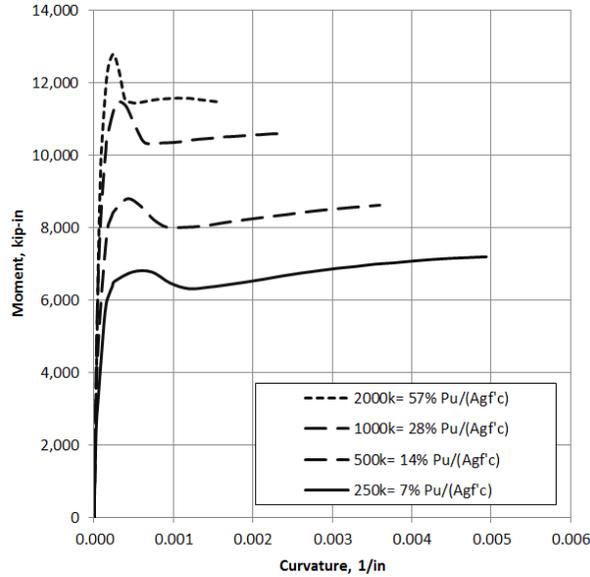
Figure 7.3-9. Moment-curvature relationship for pile under various axial loads

Detailing for ductility. ACI 318-14, Sections 18.7.5.2 through 18.7.5.4 make the following requirements on circular-section reinforced concrete elements:

1. Spiral spacing shall not exceed one-quarter of the member dimension, or six times the diameter of the smallest longitudinal bar, or six inches. Therefore the 6-inch maximum spacing controls.
2. The volumetric ratio of spirals shall not be less than the greater of the following:

$$\rho_s = 0.12 \, f_c'/f_{yt} = 0.01$$

and

$$\rho_s = 0.45 \left(\frac{A_g}{A_{ch}} - 1\right) \frac{f_c'}{f_{yt}} = 0.021$$

Note that Section 1810.3.2.1.2 of the 2015 *International Building Code* indicates that the second of these formulas need not be applied to piles. However, this formula does indeed apply to these requirements for piles subject to lateral spreading. The improved confinement provided by the heavier spiral reinforcing is critical to develop the degree of ductility necessary for proper performance.

We choose a spiral size of #5 and compute the required spacing. From the definitions of the volumetric confining steel ratio, we compute the spacing required.

$$\rho_s = V_s/V_{ch} = A_s \pi d_{ch}/s\pi \left(\frac{d_c}{2}\right)^2 = \frac{4A_s}{d_{ch}s}$$

$$s = \frac{4A_s}{d_{ch}\rho_s} = \frac{4(0.31)}{(24)0.021} = 2.5 \, in$$

Where the variables are as defined in ACI 318 and d_{ch} is the out-to-out diameter of the confined core. Considering 3 inches of clear cover, this is 6 inches less than the pile diameter: 24 inches. So, we use a #5 spiral at 2-1/2 inch pitch. Spirals of this size and pitch are required from the top of the pile to a depth at least 7 pile diameters (17'-6") below the interface of the liquefiable soil and the competent soil below.

Shear Strength. The pile must have shear strength at least sufficient to develop the double plastic hinge, in order to ensure ductile behavior in the pile. This shear demand is based on the probable moment occurring at the top of the pile and at the competent soil interface. The shear demand is

$$V_u = 2M_{pr}/l = 2(1.25 \times 6{,}730 \ kip - in)/360 \ in = 47 \ k.$$

Here, the probable moment capacity is taken as 1.25 times the nominal moment capacity. The shear capacity of the pile is computed according to ACI 318, with the effective section depth taken as 0.8 times the diameter (according to ACI 318-11, Section 11.2.3). Within the plastic hinge areas, the pile concrete may be less effective at resisting shear, due to the effects of repeated cyclic loading, so we check the shear neglecting the contribution of the concrete.

$$\varphi V_n = (0.75)(2)(0.31)(60ksi)\,(0.8 \times 30)/2.5 = 232k.$$

Shear capacity is sufficient.

Figure 7.3-10 shows a sectional detail of the proposed pile, showing the longitudinal bars and spirals.
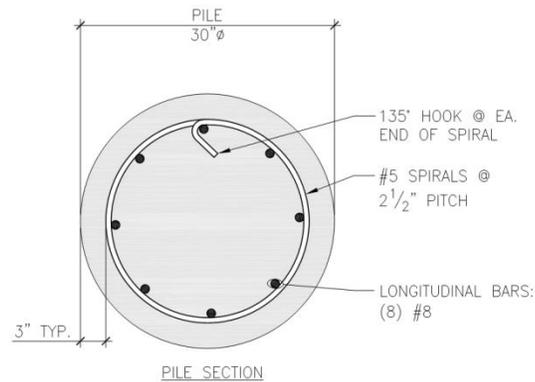
Figure 7.3-10. Sectional detail of pile

Soil-Structure Interaction

Robert Pekelnicky, P.E., S.E. and Insung Kim, P.E., S.E.

Contents

This chapter illustrates application of the 2015 Edition of the *NEHRP Recommended Seismic Provisions* (the *Provisions)* and ASCE 7-16 (the *Standard)* to incorporate soil structure interaction into the design of buildings and other structures. Section 8.1 presents a discussion of soil-structure interaction, the various types of soil-structure interaction and how those phenomena are incorporated into the *Provisions.* Because soil-structure interaction requires information not typically contained in the standard project geotechnical report, Section 8.2 discusses the information needed from a geotechnical engineer. Section 8.3 presents a discussion of foundation flexibility and provides an example illustrating how that can be incorporated into the analysis and design of a building or other structure. Section 8.4 discusses foundation damping and presents an example of how that can be incorporated into a linear analysis. Kinematic interaction, which is how the ground motion input to a structure can be altered by the characteristics of the structure is presented in Section 8.5 and an example is presented which shows how the foundation input motion is computed using kinematic interaction and its effect on a nonlinear analysis.

The *Provisions* and the *Standard* (henceforth simply referred to by the *Standard* unless there is a specific difference between the two) do not require the inclusion of soil-structure interaction in the analysis and design of a building or other structure. These provisions are optional. The decision to make use of these provisions is typically done when the soil conditions and building configuration are such that their inclusion in the analysis will show that the design forces or foundation input acceleration records can be reduced. Soil-structure interaction can be used with either the equivalent lateral force, modal response spectrum or linear response history analysis procedures of Chapter 12 or the nonlinear response history analysis procedures of Chapter 16 of the *Standard.* The reader is referred to Chapters 4 and 5 respectively of this document for discussion and examples of those procedures.

In addition to the *Standard*, the *Provisions* and associated commentary, the following documents are either referenced directly or provide useful information for the analysis and design of foundations for seismic resistance:

ACI 318   American Concrete Institute. 2014. *Building Code Requirements and Commentary for Structural Concrete*.

ASCE 41   American Society of Civil Engineers. 2013. *Seismic Rehabilitation of Existing Buildings*.

CBC   California Building Standards Commission, 2013, *California Building Code*.

FEMA 440   Applied Technology Council, 2005, *Improvement of Nonlinear Static Seismic Analysis Procedures*. Federal Emergency Management Agency.

NIST GCR 12-917-21   NEHRP Consultants Joint Venture. 2012. *Soil-Structure Interaction for Building Structures*. National Institute of Standards and Technology.

Several commercially available programs were used to perform the calculations described in this chapter. ETABS is used to determine the periods of the fixed-base and flexible base buildings, determine the shears and moments to perform the linear design and conduct a nonlinear response history analysis of the structure to show the effects of kinematic interaction.

8.1   SOIL-STRUCTURE INTERACTION OVERVIEW

The traditional approach taken in the design of buildings and other structure is to both inertial and kinematic. It is common design practice to apply forces to the structure and assume rigid restraint at the foundation. Section 12.7.1 of the *Standard* permits this idealization. In the Chapter 5 and 7 examples, the superstructure is analyzed and then the foundation is proportioned based on the reactions from the base.

There is no consideration of the flexibility of the foundation in the design, unless the foundation system is a structural mat, as illustrated in the mat foundation example in Chapter 7. In reality there is some, and potentially considerable, flexibility at the soil-foundation interface. This flexibility can be due to the soil, the foundation elements, or a combination of both. In short, stiff structures, the effect of foundation flexibility can be significant by making the system more flexible, increasing the fundamental period, and altering how the forces are distributed to elements.

One aspect of soil structure interaction is the damping in the system that can occur due to dynamic interaction at the soil-foundation interface. There are several ways that this damping can occur – soil and foundation yielding, soil hysteretic behavior and radiation of seismic waves away from the foundation caused by its dynamic response. Since the *Standard* does not require the soil actions of the foundation or the foundation itself to be stronger than the superstructure, there is the potential for yielding to occur in the foundation elements or in the soil directly adjacent to the foundation elements. This yielding contributes to inelastic dissipation of earthquake energy in a similar manner as yielding in the superstructure. For linear procedures, this energy dissipation is assumed to be inherent within the R-factor for the specific systems because the *Standard* does not require the design of the soil actions or the foundation elements for amplified seismic forces, E_m. For nonlinear response history analysis per Chapter 16 of the *Standard* and the *Provisions*, these actions can either be explicitly included in the nonlinear analysis model or can be treated as force controlled actions.

Damping of the structure response can be caused by hysteretic behavior of the soil as the earthquake waves move through the subsurface material. This effect is more pronounced on softer soils where the flexibility of the subsurface material significantly affects the stiffness and period of the soil-structure system. It is modeled in the provisions as a damping ratio that depends directly on the amplitude of the earthquake motions and the site class.

Radiation damping occurs when the movement of the structure creates waves in the subsurface material that interfere with the earthquake waves being transmitted through the material. As the earthquake waves move the structure, the structure responds to the movement by pushing laterally and vertically against the subsurface material. The transient shearing and compressing of the subsurface material generates waves which radiate out from the foundation. Those waves interfere with the waves from the earthquake shaking in a way that creates a damping effect on the earthquake waves affecting the foundation. It is also modeled as a damping ratio in the provisions, and it depends on the relative stiffness of the soil and the structure, with more radiation damping occurring for stiff structures on flexible soils than for flexible structures on stiff soils.

The last aspect of soil structure interaction covered by the *Standard* is kinematic soil-structure interaction and it accounts for the difference between the ground motion that would be recorded at a free filed site near the structure and the ground motion at the foundation of the structure. Typically all ground motion parameters, such as response spectrum ordinates and acceleration histories discussed in Chapter 3 of the *Design Examples*, are developed as free field motions. There are two main aspects of the structure's configuration that can cause a difference between the ground motion, the size and rigidity of the base of the structure and the depth of the foundation below the ground surface.

The ground shaking at any given point at the base of the structure may not be in phase with the shaking at another point. If the base of the structure is large in area and rigid with respect to horizontal shearing actions, then the out of phase nature of the ground shaking causes the base to filter some of the high frequency motion. This results in a foundation input ground motion that has lower spectral accelerations at the low periods. This effect is known as base-slab averaging.

Embedment of the foundation below the ground can have a similar effect as a large, rigid base in causing the high frequency motions to be reduced. Like base-slab averaging, this reduction can be significant in the lower period region of the response spectra.

The relationships in Chapter 19 of the *Standard* to account for soil-structure interaction effects are typically based on theoretically derived relationships for rigid structures situated on perfectly viscoelastic subsurface media. These theoretical formulas have been calibrated and corroborated with earthquake motions measured in actual buildings and in the adjacent free field. There are a number of limitations within each of the provisions based on structure and subsurface characteristics dissimilar to the theoretical idealizations. Consequently, limits were placed on maximum reductions in lateral loads due to soil-structure interaction. A more detailed discussion of the background behind all the material in the *Provisions* and the *Standard* can be found in commentary of the *Provisions* and the FEMA 440 and NIST GCR 12-917-21 reports.

8.2 GEOTECHNICAL ENGINEERING NEEDS

Proper consideration of soil structure interaction effects requires significant knowledge of the subsurface material and the dynamic characterizes of the soil-structure system. This requires information from a geotechnical engineering professional that is not often provided as part of a typical geotechnical report. Typical geotechnical reports provide the site class, the S_{DS} and S_{D1} parameters, and the foundation element design parameters such as allowable bearing capacity or pile strengths. Spring values to model the flexibility of the soil under the foundation elements are only provided for mat foundations.

To properly consider soil structure interaction the following information, in addition to the typical information above, should be obtained from a geotechnical engineer:

- The average small strain shear wave velocity of the soil under the foundation over a depth of approximately half the structure's smaller overall foundation footprint dimension and/or over the embedded depth of the structure.
- The effective shear wave velocity over the same depth at the design or maximum considered earthquake shaking intensity.
- The average small strain shear modulus of the soil under the foundation over a depth of approximately half the smallest structure's overall foundation footprint dimension.
- The effective shear modulus of the soil over the same depth at the design or maximum considered earthquake shaking intensity.
- Parameters to model the flexibility at the soil-foundation interface. These stiffness parameters should be at the design or maximum considered earthquake shaking intensity. The parameters should allow for modeling lateral, vertical, and rotational flexibility of the structure in the subsurface material.
- An estimate of Poisson's ratio for an effective layer of soil over a depth of approximately half the smallest structure's overall foundation dimension.

It is important that the parameters obtained from a geotechnical engineer are those at the design or maximum considered earthquake shaking intensity. Soil properties can be significantly different under the presence of earthquake shaking. The shear wave parameters obtained from in situ testing are usually the small strain vales and will be larger than those under earthquake shaking. Additionally, spring values given for mats may be based on settlement limitations and be less stiff than the earthquake shaking properties.

Due to the variability of subsurface material, Section 12.13.3 of the *Standard* requires the foundation stiffness properties be increased and decreased by 50%. Section 19.1 of the *Standard* requires that the more stiffness approximation that produces the more conservative soil structure interaction effects be used. This could mean that stiffer springs be used because they create a lower shift in period which generally leads to

lower force reductions due to inertial effects. However, using softer spring properties can result in increased deformations on other elements in the lateral force resisting system. The standard also permits lesser bounding values than 50% if the project geotechnical investigation provides for this.

If the parameters above are not provided by the geotechnical engineer, it is possible to approximate these values from other geotechnical information and empirical relationships. Chapter 8 of ASCE 41-13 provide equations to approximate the small strain shear modulus from small strain shear wave velocity, standard penetration test blow counts or effective vertical stress and void ratio. Tables in Chapter 19 provide factors to convert the small strain values of shear wave velocity and shear modulus based on approximations of the peak ground acceleration by dividing the S_{DS} value by 2.5. Caution should be exercised when developing geotechnical parameters from approximate methods for use with soil structure interaction and it is recommended to consult with a geotechnical engineer to confirm the appropriateness of those approximate methods.

It is tempting to use a shear wave velocity approximated from the site class, but this should not typically be done. There are several reasons for this. First, the default site class is often D, and sometimes C for short period structures. The shear wave velocity corresponding to site class D will often produce significant soil structure interaction effects because it corresponds to a softer site. While this is conservative in determine the general response spectra because greater site amplification is obtained from softer sites, it may overestimate the reductions from soil structure interaction.

While it is not explicitly required, site specific response spectra, is recommended for soil-structure interaction. Because the soil structure interaction effects alter the foundation input motion or seismic demands on a structure due to changes in damping, it is important to have an accurate representation of the free field motion at the site. Site specific response spectra can even be developed at the foundation depth, directly incorporating embedment effects instead of using the equations in Chapter 19 to estimate those effects.

8.3   FLEXIBLE BASE EXAMPLE

A four story reinforced concrete shear wall building with one basement will be used to illustrate the soil structure interaction provisions of the *Standard*. The building is located in a region of very high seismicity, within 5 miles of an active fault with subsurface material that would be characterized as Site Class D. The average shear wave velocity for 100 feet below the ground is 800 ft/s based on the geotechnical investigation at the site. A site specific response spectrum was developed in accordance with Chapter 21 of the *Standard* and shown below in Figure 8-1. *S_{DS} and S_{D1}* are 1.0 and 0.71 respectively, placing the building in Seismic Design Category E.
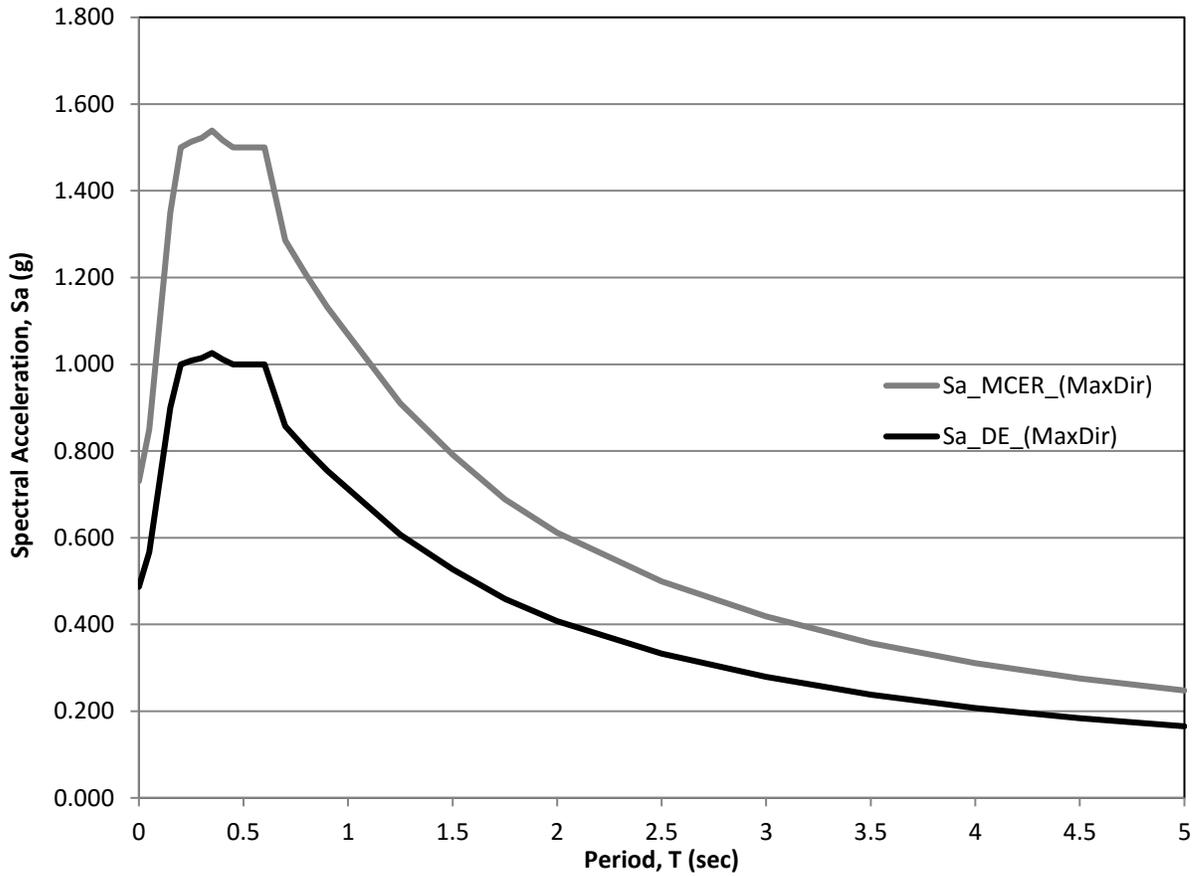
Figure 8.3-1: Site Specific Spectra

The building used for the example is approximately 53 feet tall and the basement is 15 feet below grade. Figure 8-2 shows an elevation of the building. The building is rectangular with a north south dimension of 180 feet and an east-west dimension of 150 feet. Floor slabs are reinforced concrete flat plates and the columns are rectangular cast-in-place concrete situated on spread footings. The lateral forces are resisted by cast-in-place special reinforced concrete shear walls. There is a reinforced concrete wall around the entire basement. The interior walls and columns are founded on spread footings and the basement wall is founded on a continuous strip footing. Figure 8-3 shows a foundation plan of the building.

The weight of each floor is summarized in Table 1.

Table 1: Story Weight

Story	Weight
Fourth	4,000 kips
Third	4,100 kips
Second	4,100 kips
First	4,400 kips
Basement	4,700 kips
Total	**21,200 kips**
Total without Basement	*16,500 kips*
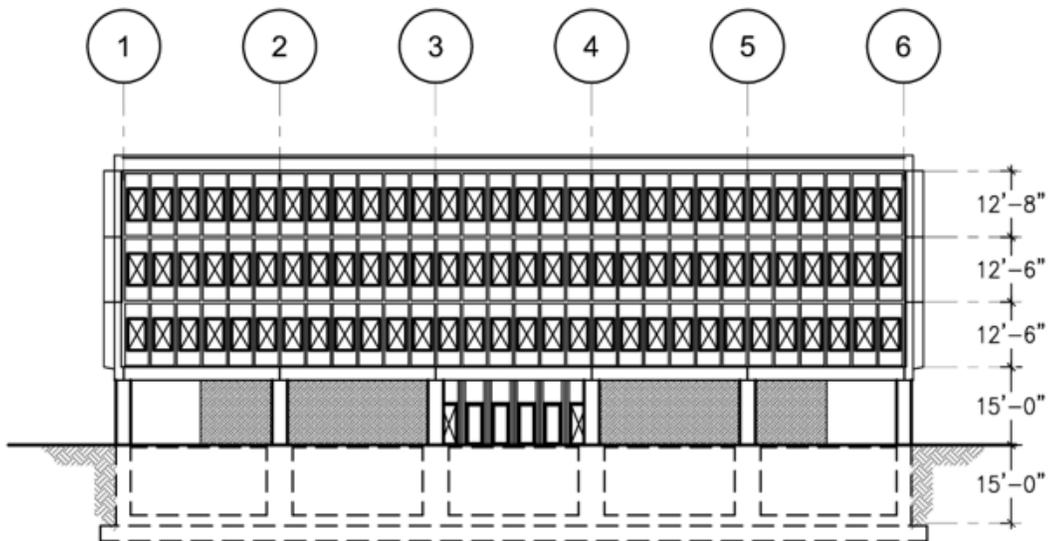
Figure 8.3-2: Building Elevation
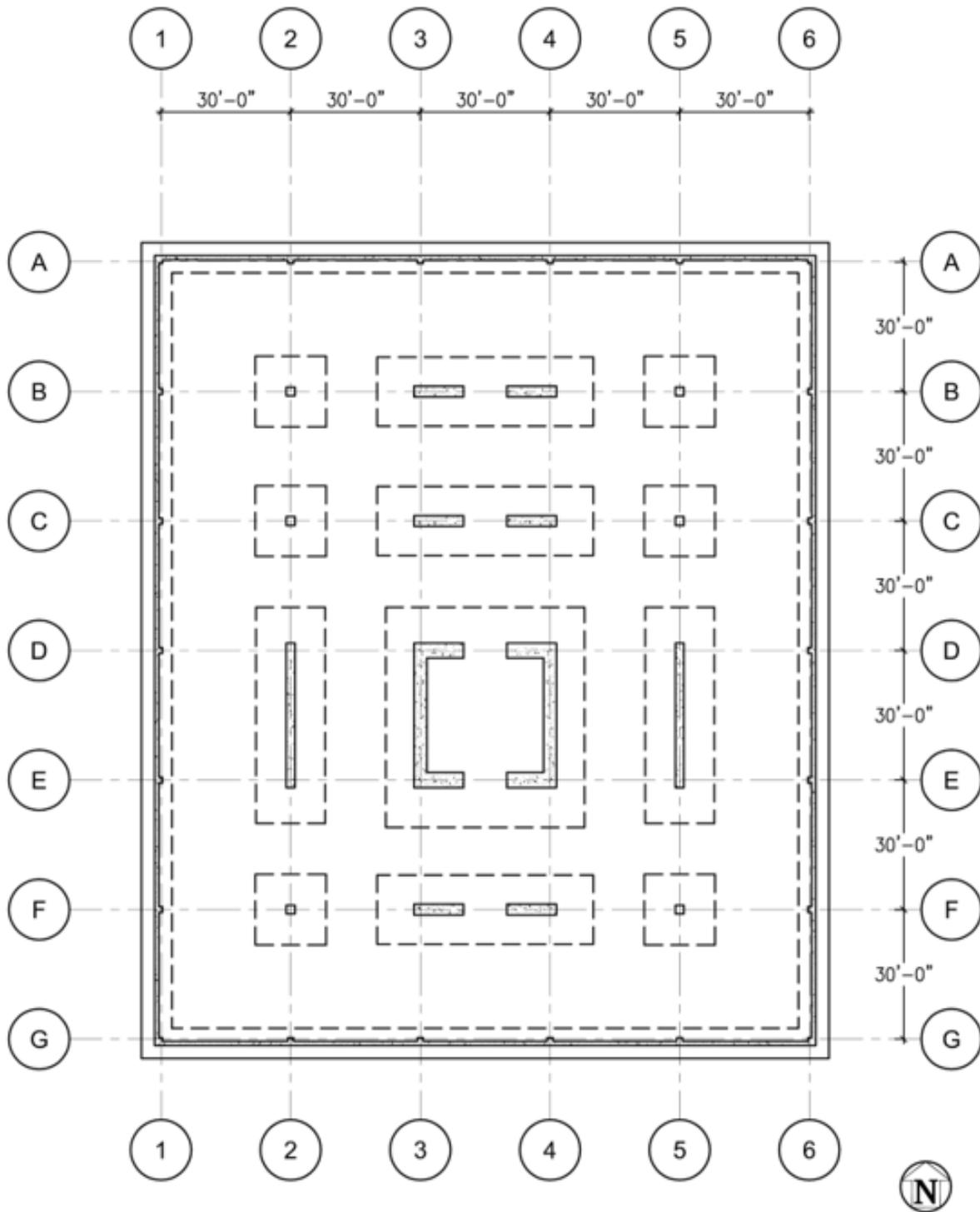
Figure 8.3-3: Foundation Plan

8.3.1 Fixed Base Building Design

The building was first designed assuming that it was pinned against vertical and lateral translation at the foundation. In addition the wall footings were assumed to be fixed against rotation as permitted in

Section 12.7.1 of the *Standard*. For the fixed base design, the base of the building can be taken at the first floor, as opposed to the basement. This idealization to eliminate the basement is commonly done in practice and is permitted by Section 12.2.3.2 of the *Standard*. In that section different portions of the structure can be decoupled based on one section being significantly more rigid than the upper portion provide the lower portion is designed for its inertial forces and the forces from the structure above. However, that section also requires that the period of the total building be less than 1.1 times the period of the upper portion alone. Based on a modal analysis performed in ETABS using a models without the basement and with the basement were 0.27 and 0.39 seconds. Since the period of the model with basement is 1.3 times the period of the model without the basement, the basement must be included in the model.

The reason that the model with the basement had a larger period than the 10% threshold in Section 12.2.3.2 was due in part to the choice to model first floor as a stiff instead of rigid diaphragm. This modeling choice was made because the effect that a stiff diaphragm and stiff basement walls will have on the loading in the main concrete walls. The stiffness of the first floor slab will affect how much load is transitioned out of the four story walls and transferred to the basement walls. Using a rigid diaphragm assumption will overestimate the amount of load that will transition out of the wall and will reduce the flexure demand on the four story walls footings.

The period calculated from the approximate period equation of (12.8-7) is

$$T_a = C_t h_n^x = 0.02*53^{0.75} = 0.39 \text{ s}$$

This is slightly smaller than the period for the modal analysis of the building with the basement, but since both periods are on the plateau of the response spectra, the Cs value will be the same

$$C_s = \frac{S_{S1}}{\left(\frac{R}{I_e}\right)} = \frac{1.0}{\left(\frac{5}{1.0}\right)} = 0.20$$

From that, the seismic base shear per Section 12.8.1 is

$$V = C_s W = 0.20*16,500 \text{ kips} = 3,300 \text{ kips}$$

The modal analysis base shear, V_t, is 2,700 kips, which being less than the seismic base shear means that the results of the modal analysis will need to be scaled up by 3,300/2,700 = 1.2.

The explicit design of the walls and foundation elements are not covered in detail in this chapter because the focus is on the soil structure interaction provisions. Refer to Chapters 7 and 10 for examples designing foundations and reinforced concrete shear walls.

For this example the effects of soil structure interaction will be illustrated by looking at the Line 2 wall. The Line 2 wall is 30 feet long by 14 inches thick. The horizontal reinforcement is #5 bars on each face at 12" on center. Boundary elements extending 44 inches at each end of the wall contain 12 #7 bars. The vertical reinforcing between the boundary are #5 bars at 12" on center. The foundation for the wall is 40 feet long by 18 feet wide and 2 feet 6 inches thick with 14 #7 bars top and bottom longitudinal reinforcement and #7 at 12 inches on center top and bottom transverse.

8.3.2   Flexible Base Design

Spring properties for the footings, the passive soil resistance along the basement walls, and for the shearing between the soil and the building base were provided by a geotechnical engineer. The properties provided are:

Vertical stiffness under footings   3.4 (kip/in)/ft^2

Horizontal stiffness under base   14 (kip/in)/ft^2

Horizontal stiffness under against basement wall   14 (kip/in)/ft^2

The vertical springs were placed as point springs under the columns and as distributed springs under the wall footings because the walls were modeled with shell elements. If the walls had been modeled with line elements, the vertical springs would also have to be coupled with rotational springs. The horizontal springs under the base were modeled as distributed springs along the perimeter of the base. The horizontal springs due to passive resistance along the basement walls were modeled as area springs over the basement walls.

When the soil springs were included in the model, the period of the building increased to 0.49 seconds. Using the plus and minus 50% bounding per 12.13.3, the upper bound spring model still had a period of 0.49 seconds and the lower bound stiffness had a period of 0.50 seconds. In this instance, the bounded periods do not affect the behavior of the model significantly. However, the inclusion of soil springs did affect the period significantly.

The flexible base period is still less than C_uT_a =1.4*0.39 = 0.54 seconds, so that cap does not apply. The flexible base period is still on the plateau, so the seismic base shear does not change. If the site specific spectrum had a more aggressive decrease after the short period peak, then the forces could have reduced due to the increase in the period.

8.3.3   Soil and Foundation Yielding

The foundation was proportioned based on the forces from the analysis. There was no consideration given to proportioning the foundation so actions like bending or shear in the footing would not occur before bearing capacity failure of the underlying soil or flexural yielding of the wall. The same is true for bearing capacity failure potentially occurring before flexural yielding of the wall. This means that there is the potential for the nonlinear actions of the structure to occur in the foundation or the soil as opposed to the intended mechanism in a special reinforced concrete bearing wall – flexure of the wall.

In the California Building Code sections for state owned buildings, schools, and hospitals, the foundation elements are required to be designed for the amplified seismic load, E_m, or the capacity of the structural elements or underlying soil. This is intended to provide a high degree of reliability that the yielding will occur in the soil or in the structural elements. In this example, that would cause the thickness of and reinforcement in the foundation to increase.

When performing a nonlinear analysis in accordance with Chapter 16 of the *Standard* foundation actions can be modeled as explicit nonlinear actions to capture yielding at the soil-foundation interface or those actions must be treated as force-controlled actions. If treaded as force-controlled actions the consequence of overstress will determine whether they should be classified as ordinary, critical, or non-critical. For example punching shear failure in a mat foundation may be considered a critical force controlled action if it leads to loss of support of the wall. Typically, most foundation actions can be treated as ordinary force controlled actions and many soil limit states can be treated as non-critical. However, if

excessive deformation in the soil causes deformation comparability issues with adjacent structural elements that action should either explicitly be modeled as nonlinear or be treated as ordinary or critical.

8.4 FOUNDATION DAMPING EXAMPLE

The provisions in Chapter 19 of the *Standard* provide a simplified method for assessing the amount of foundation damping in the soil-structure system. They account for foundation damping in linear procedures based on relationships which calculate factors to scale down the response spectral ordinates and reduce the seismic base shear. Those scale factors adjust the spectrum, which is typically developed with an effective damping ratio greater of 5% of critical, to a ratio greater than 5% that includes foundation damping estimated in the soil-structure system. This section illustrates how to calculate the additional damping due to radiation damping and soil damping.

In order to use these provisions there are several criteria the must be met. First, the foundation system must consist of shallow foundations, either spread or strip footings or a mat. The provisions do not apply to deep foundation systems. The second condition is that the shallow foundation elements must be interconnected with a slab or grade beams that provide a diaphragm that cannot be considered flexible. This requirement is to ensure the foundation behaves in a manner consistent with the idealizations that went in to the derivation of the relationships in this chapter. That is not to say that there is no foundation damping effects in structures with deep foundations or without stiff diaphragms connection the foundation elements, but rather the effects cannot be approximated with the provisions in Chapter 19 of the *Standard*.

The equations combine soil damping and radiation damping with the inherent structural damping. The effect of foundation damping is most pronounced in structures that are very stiff and situated on flexible soils. That is why the equations are based on the ratio of the flexible base period to the fixed base period of the structure. The total soil-structure system damping ratio, β_0, is calculated based on the equation:

$$\beta_0 = \beta_f + \frac{\beta}{\left(\tilde{T}/T\right)_{eff}^2} \leq 0.20$$

In this equation inherent structural damping ratio that the free-field response spectrum is based on, β, is divided by the effective lengthened period ratio of the structure. The period ratio of the flexible base period, $\tilde{T}$, to the fixed base period, T, is adjusted for structural yielding. This accounts for the contribution of elastic damping in the superstructure to the building response being reduced because of inelastic energy dissipation in the structure. The foundation damping is then added to the modified structural damping to provide a system damping. The total damping in the soil-structure system is limited to 20% because that is the upper bound damping ratio observed when correlating the theoretical formulations to actual structures studied.

The foundation damping is based on a combination of soil damping and radiation damping. They are added together based on the following equation:

$$\beta_f = \left[\frac{\left(\tilde{T}/T\right)^2 - 1}{\left(\tilde{T}/T\right)^2}\right]\beta_s + \beta_{rd}$$

The contribution of soil damping to the total foundation damping depends on the period shift between the fixed base and the flexible base of the structure. This is because the period shift indicate the effect of the soil and foundation deformations on the response of the structure. The greater the period shift the more significant the effect of the inertial soil-structure interaction effects

8.4.1   Radiation Damping

The radiation damping, β_{rd}, of the soil-structure system is calculated based on a combination of translational, β_y, and rotational, β_{xx}, damping. Both horizontal and vertical movement of the foundation in the subsurface media can produce waves that can interfere with the seismic waves being transmitted through the subsurface. The contribution of each direction is based on the flexibility of the soil-structure system to fictitious periods based on only foundation translation or rotation. That equation is:

$$\beta_{rd} = \left(\frac{1}{\left(\tilde{T}/T_y\right)^2}\right)\beta_y + \left(\frac{1}{\left(\tilde{T}/T_{xx}\right)^2}\right)\beta_{xx}$$

The following parameters will be needed to calculate radiation damping

B =   Half the shorter dimension of the structure's foundation footprint = 150 ft / 2 = 75 ft for this structure

L =   Half the longer dimension of the structure's overall foundation footprint = 180 ft / 2 = 90 ft for this structure

T =   Fixed base period = 0.39 s

$\tilde{T}$ =   Flexible base period = 0.49 s (typically the upper bound value since it will produce the least   reduction)

v_s =   Effective shear wave velocity over a depth equal to 'B' below the foundation = 570 ft/s

G =   Effective shear modulus over a depth equal to 'B' below the foundation = 1,200 k/ft^2

v =   Poisson's ratio of the soil = 0.3

M^*=   Fundamental mode effective mass = 14,500 kips (from the analysis model)

h^* =   Effective structure height at the fundamental mode = $h / (\Gamma\phi_{roof})$ = 41.5 ft (from the analysis model)

To determine the translational contribution to radiation damping, first the fictitious periods T_y is calculated.

$$T_y = 2\pi \sqrt{\frac{M^*}{K_y}} = 2 * 3.14 * \sqrt{\frac{\frac{14500}{32.2}}{537,000}} = 0.18 \ s$$

Where

$$K_y = \frac{GB}{2 - v}\left[6.8\left(\frac{L}{B}\right)^{0.65} + 0.8\left(\frac{L}{B}\right) + 1.6\right] =$$

$$\frac{1,200 * 75}{2 - 0.3}\left[6.8\left(\frac{90}{75}\right)^{0.65} + 0.8\left(\frac{90}{75}\right) + 1.6\right] = 537,000 \ k/ft^2$$

Then the translational contribution to radiation damping is computed as

$$\beta_y = \left[\frac{4(L/B)}{(K_y/GB)}\right]\left[\frac{a_0}{2}\right] = \left[\frac{4(90/75)}{(537,000/(1,200 * 75))}\right]\left[\frac{1.7}{2}\right] = 0.68$$

Where

$$a_0 = \frac{2\pi B}{\tilde{T} v_s} = \frac{2 * 3.14 * 75}{0.49 * 570} = 1.7$$

To determine the rotational contribution to radiation damping, first the fictitious periods T_{xx} is calculated.

$$T_{xx} = 2\pi\sqrt{\frac{M^*(h^*)^2}{\alpha_{xx}K_{xx}}} = 2 * 3.14 * \sqrt{\frac{\frac{14500}{32.2} * (41.5)^2}{0.68 * 3.33 \times 10^9}} = 0.12 \ s$$

Where

$$K_{xx} = \frac{GB^3}{1 - v}\left[3.2\left(\frac{L}{B}\right) + 0.8\right] =$$
$$\frac{1,200 * 75^3}{1 - 0.3}\left[3.2\left(\frac{90}{75}\right) + 0.8\right] = 3.33 \times 10^9 \frac{k}{ft^2}$$

and

$$\alpha_{xx} = 1.0 - \left[\frac{\left(0.55 + 0.01\sqrt{(L/B) - 1}\right)a_0}{\left(2.4 - \frac{0.5}{(L/B)^3}\right) + a_0}\right] =$$
$$\left[\frac{\left(0.55 + 0.01\sqrt{(90/75) - 1}\right) * 1.7}{\left(2.4 - \frac{0.5}{(90/75)^3}\right) + 1.7}\right] = 0.68$$

The rotational contribution to radiation damping is computed as

$$\beta_{xx} = \left[\frac{\left(^{4\psi}/_3\right)\left(^{L}/_B\right)a_0^2}{\left(^{K_{xx}}/_{GB^3}\right)\left[\left(2.2 - \frac{0.4}{\left(^{L}/_B\right)^3}\right) + a_0^2\right]}\right]\left[\frac{a_0}{2\alpha_{xx}}\right] =$$

$$\left[\frac{\left(^{(4*1.9)}/_3\right)\left(^{90}/_{75}\right)*1.7^2}{\left(3.33 \times 10^9/_{(1,200*75^3)}\right)\left[\left(2.2 - \frac{0.4}{\left(^{90}/_{75}\right)^3}\right) + 1.7^2\right]}\right]\left[\frac{1.7}{2*0.68}\right] = 0.34$$

Where

$$\psi = \sqrt{\frac{2(1-v)}{(1-2v)}} = \sqrt{\frac{2(1-0.3)}{(1-2*0.3)}} = 1.9 \le 2.5$$

The total radiation damping for the building's soil-structure system is

$$\beta_{rd} = \left(\frac{1}{(0.49/0.19)^2}\right)*0.68 + \left(\frac{1}{\left(\frac{0.49}{0.12}\right)^2}\right)*0.32 = 0.11$$

8.4.2   Soil Damping

Soil damping is proportional to the ground shaking intensity and the site class. Table 19.3-3 provides a means to estimate the soil damping, β_s, based on the site class and an approximate of the peak ground acceleration, $S_{DS}/2.5$. This structure is founded on site class D and the peak ground acceleration is approximated as $S_{DS}/2.5 = 1.0/2.5 = 0.4$. Therefore, $\beta_s = 0.07$.

8.4.3   Foundation Damping

The total foundation damping is a combination of radiation damping and soil damping. The soil damping contribution is based on the period ratio of the flexible base soil-structure system to the fixed base structural system. The radiation damping is also proportional to the period ratio. If the period shift is small, then the effect of flexibility at the soil-foundation interface does not affect the structural response significantly and that damping will not affect the system. If however the period shift is significant, the structural response is affected significantly by inertial soil-structure interaction.

$$\beta_f = \left[\frac{(0.49/0.39)^2 - 1}{(0.49/0.39)^2}\right]*0.07 + 0.11 = 0.14$$

8.4.4   Linear procedure

In order to determine the amount of force reduction that can be used in an equivalent lateral force analysis or a modal response spectrum analysis the effective damping of the soil-structure system must first be calculated. As discussed, that requires an approximation of the effective period ratio based on structural yielding. The *Standard* has the following equation to calculate that:

$$\left(\frac{\tilde{T}}{T}\right)_{eff} = \left\{1 + \frac{1}{\mu}\left[\left(\frac{\tilde{T}}{T}\right)^2 - 1\right]\right\}^{0.5}$$

In that equation a parameter to account for the amount of structural yielding, μ, can either be calculated as the maximum base shear divided by the elastic base shear or approximated as the R-factor divided by the overstrength factor, Ω_0. Typically determining the maximum base shear of the structure involves a nonlinear pushover or nonlinear dynamic analysis, which is generally not done as part of a linear design. Therefore this example approximates the value of μ as $R/\Omega_0 = 5/2.5 = 2$. Thus the effective period ratio is:

$$\left(\frac{\tilde{T}}{T}\right)_{eff} = \left\{1 + \frac{1}{2}\left[\left(\frac{0.49}{0.39}\right)^2 - 1\right]\right\}^{0.5} = 1.7$$

From that, the effective damping of the soil-structure system can be approximated as

$$\beta_0 = 0.11 + \frac{0.05}{1.7^2} = 0.16$$

For linear procedures, this means spectral response parameters based on 16% damping as opposed to 5% can be used. To determine those parameters, the *Standard* has the equation below to do so. A more accurate method would be have the geotechnical engineer develop the site specific spectra at 16% critical damping as opposed to 5%. In this example the approximate equation will be used to determine a factor, B_{SSI}, to divide the spectral response parameters by.

$$B_{SSI} = 4/[5.6 - \ln(100\beta_0)] = 4/[5.6 - \ln(100 * 0.16)] = 1.4$$

For the equivalent lateral force analysis, the seismic base shear calculated in accordance with Section 12.8 shall be reduced by ΔV, the difference between the C_s value calculated per Section 12.8 and the C_s value based on the flexible base period and reduced for foundation damping, $\tilde{C}_s$. There is, however, a maximum reduction in base shear due to foundation damping. That maximum reduction is dependent upon the R-factor, with higher R-factor systems receiving a lower amount of permitted foundation damping reduction. The reason for this is because the damping due to superstructure yielding, which is accounted for in the R-factor, is not completely additive to the damping cause by soil and radiation damping. If a structure is elastic or has little structural yielding, then the majority of the additional damping in the system will come from the foundation damping effects. On the other hand, if the majority of the added damping in the system is due to structural yielding, there will be little contribution from the foundation damping effects.

For this building, the seismic base shear including SSI effects is

$$\tilde{V} = V - \Delta V = 3{,}300 - 800 = 2{,}500 \text{ kips} = 0.15\text{W}$$

Where

$$\Delta V = \left(C_s - \frac{\tilde{C}_s}{B_{SSI}}\right)\overline{W} = \left(0.20 - \frac{0.20}{B_{SSI}}\right) * 14{,}500 = 800 \text{ kips}$$

In this equation $\tilde{C}_s$ is the same as C_s because the flexible base period is not large enough to place the structure on the descending portion of the response spectra in Figure 8-1. $\overline{W}$ is the effective weight in the fundamental mode, or can be taken as the effective seismic weight per Section 12.7.2. In this example, the effective weight of the first mode was used since it was slightly smaller than the effective seismic weight, 14,500 kips versus 16,500 kips.

The $\tilde{V}$ calculated above must then be checked against the equation below to confirm that it is greater than the permissible reduction.

$$\tilde{V} \ge \alpha V = 0.83 * 3{,}300 = 2{,}700 \text{ kips} = 0.17*\text{W}$$

Since R is greater than 3 and less than 6,

$$\alpha = 0.5 + R/15 = 0.5 + 5/15 = 0.83$$

Therefore, the maximum reduction governs and the SSI modified seismic base shear is 0.17W = 2,700 kips, an 18% reduction in design forces.

For the modal response spectrum analysis, the response spectrum should be reduced by B_{SSI} per Section 19.2.2. Figure 8.4-1 shows the foundation damping modified response spectrum and the design earthquake spectra. The modal analysis was re-run using the flexible base model and the modified response spectrum. The base shear from that analysis was 2,100 kips. Just like the fixed-base response spectrum base shear must be scaled to the seismic base shear calculated per Section 12.3, the SSI modified response spectrum base shear must be scaled to the SSI minimum base shear αV. Therefore the scale factor for the SSI response spectrum analysis is 2,700/2,100 = 1.3.
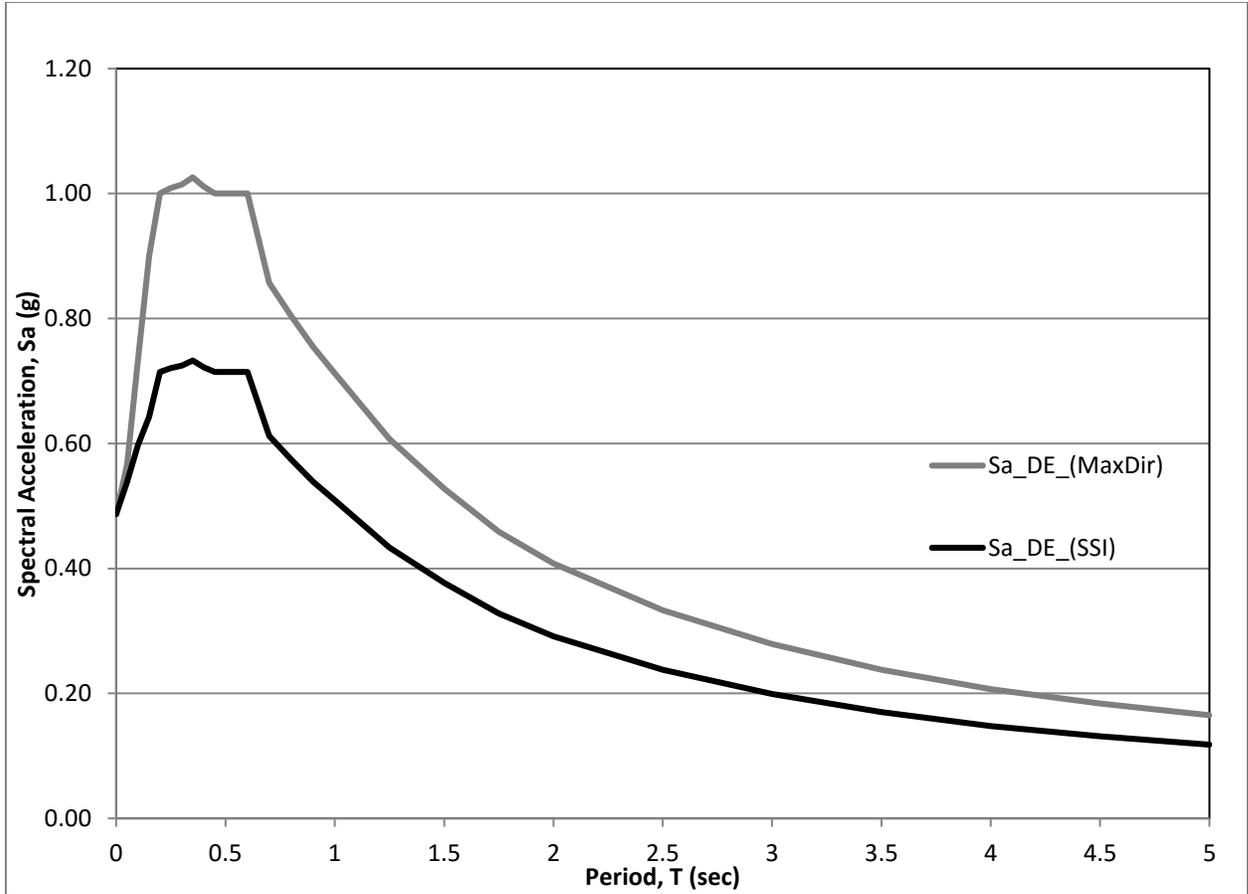
Figure 8.4-1: Design Earthquake Response Spectrum and SSI modified spectrum

The reduction in design forces for this example translates to some significant changes in the design. The shear wall thickness can be reduced from 14 inches to 12 inches and the need for confined boundary elements can be eliminated because the shear wall stress due to seismic moments is less than $0.2f'_c$ per Section 18.10.6.3 of ACI 318-14. The horizontal and vertical reinforcement can be adjusted to #4 @ 12" o.c. While the overall footing dimensions of the wall cannot be reduced, the reinforcement can be. Table 8.4-1 summarizes the change to the Line 2 shear wall based on to inclusion of foundation damping soil structure interaction.

Table 8.4-1: Building Design Comparison

Property	Fixed Base – No SSI	Flexible Base – SSI
Wall Thickness	14 inches	12 inches
Horizontal Reinf.	#5 @ 12" o.c.	#4 @ 12" o.c.
Vertical Reinf.	#5 @ 12" o.c.	#4 @ 12" o.c.
Boundary Region	14 - #7	None
Footing Dimensions	40-ft x 14-ft	40-ft x 14-ft
Footing Long. Reinf.	14 - #7 T&B	12 - #7 T&B
Footing Trans Reinf.	#7 @ 12" T&B	#7 @ 14" T&B

8.4.5   Nonlinear procedures

The inclusion of foundation damping in a nonlinear response history analysis is significantly more complex than the linear procedures. The equations to reduce the response spectrum cannot be used to modify the target spectra the ground acceleration histories are scaled to. Instead nonlinear spring and dashpot elements should be added to the model to capture the force-displacement relationship and damping at the soil-foundation interface. Guidance on how to develop the dashpots to represent foundation damping can be found in NIST GCR 12-917-21.

8.5   KINEMATIC INTERACTION

Kinematic soil structure interaction relates to how the configuration of the structure's foundation affect the ground motion input into the structure. The ground motion parameters given in the USGS maps or through a site specific response spectrum are for a free-field condition. The size of the foundation and how deep it is embedded in the ground can alter the ground motion such that the foundation input motion differs from the free field motion. There are two types of kinematic interaction covered in the *Standard* – base slab averaging and embedment.

For both types of kinematic soil-structural interaction, the *Standard* provides relationships derived from theoretical models that adjust the response spectrum parameters based on the base size, embedment depth, site class, and fundamental period of the soil-structure system. The adjustment factors are cumulative and result in a reduction of the response spectrum parameters, but that reduction is limited. For more thorough discussion of the theoretical background behind the reductions the reader is should refer to FEMA 440 and NIST GCR 12-917-21.

The limits of the reduction differ between the *Provisions* and the *Standard*, with the *Standard* providing for a higher floor on the reductions. In both the *Provisions* and the *Standard*, the product of the base-slab averaging and embedment reductions cannot reduce the response spectrum less than 80% of the site specific response spectrum or 70% of the general response spectrum based on the USGS mapped values. The difference is that the *Provisions* have a caveat that allows for no limit on the reduction with respect to the site specific spectrum and 60% of the general response spectrum based on the USGS mapped values if there is peer review. This was eliminated from *the Standard*, but on projects where peer review is already a part of the project, the *Provisions* criteria may be something the design team would propose. In the example following the difference between the *Standard* and the *Provisions* is illustrated.

While the response spectrum parameters are reduced, there is a prohibition of utilizing the kinematic interaction provisions in linear analyses. There are two main reasons for this. First, kinematic interaction provisions are highly dependent on the period of the building. Since most buildings designed to the *Standard* will undergo yielding in the superstructure and potentially at the foundation soil interface, the period of the soil-structure system will lengthen. If a reduction in response was calculated using the elastic period, it may overestimate the reduction because the reduction factors get smaller at longer periods. The

second reason is similar to the reason that foundation damping reductions are capped at a higher values when the R-factor is larger, at present there has not been sufficient study done on the cumulative reduction in response based on structural yielding, soil or foundation yielding, and kinematic interaction to postulate how the seismic base shear used for design should be reduced for that combination. Therefore, these provisions can only be used in a nonlinear analysis to reduce the target response spectrum that the ground motion acceleration histories are selected and scaled to and for the elastic design forces used for the Chapter 12 check of the structure per Section 16.1.

8.5.1 Base-slab averaging

Base-slab averaging refers to the phenomena where a base with significant in-plane rigidity acts to reduce the foundation input ground accelerations due to the ground acceleration response histories being out of phase at any two points on the base. Because the ground motions are out of phase, the high frequency motion is filtered out leading to a reduction in the short period response spectrum ordinates. Because there is very little reduction observed in theoretical models on rock sites and no measured response in buildings studied on those sites, the *Standard* does not permit kinematic interaction on Site Class A and B. Additionally, the *Standard* does not permit kinematic interaction reductions based on the equations in Chapter 19 on Site Class F. For that type of site the high degree on nolinearity and other site effects make this a significantly more complex issue and more detailed models are needed to understand the reduction.

Before the base-slab averaging provisions can be applied, it must be confirmed that the base is sufficiently rigid to allow this filtering to occur. This can be done by applying the diaphragm flexibility evaluation in Section 12.3.1 comparing the base slab or mat and the first floor above the base's in-plane stiffness between vertical lateral force resisting elements to the stiffness of those elements. If the base slab or the first floor slab cannot be classified as flexible, then the provisions can be used. In this example building, the presence of perimeter and interior walls, creates a rigid condition in the base slab and the first floor slab, so the provisions of Chapter 19 can be applied.

The two parameters ar needed to calculate the base slab averaging reduction – the effective foundation size and a period. The effective foundation size is the square root of the base area, but limited to 260 feet. That limit is placed on the equation because it is the extent to which the theoretical models have been verified through study of actual buildings. For this example, the effective foundation size is:

$$b_e = \sqrt{A_{base}} = \sqrt{150 * 180} = 164 \, ft$$

The equation to estimate the reduction due to base slab averaging is

$$RRS_{bsa} = 0.25 + 0.75 \times \left\{ \frac{1}{b_0^2} [1 - (exp(-2b_0^2) \times B_{bsa})] \right\}^{1/2}$$

Where

$$b_0 = 0.00071 \left(\frac{b_e}{T} \right)$$

and

$$B_{bsa} = \begin{cases} 1 + b_0^2 + b_0^4 + \dfrac{b_0^6}{2} + \dfrac{b_0^8}{4} + \dfrac{b_0^{10}}{12} & when\ b_0 \leq 1 \\[2mm] [exp(2b_0^2)] \times \left[\dfrac{1}{\sqrt{\pi}b_0}\left(1 - \dfrac{1}{16b_0^2}\right) \right] & when\ b_0 > 1 \end{cases}$$

Note that there is also a lower limitation on the period, T, of 0.20 s.

For this building, using the fundamental period of 0.49 s, the base slab averaging reduction is:

$$b_0 = 0.00071\left(\frac{164}{0.49}\right) = 0.24$$

$$B_{bsa} = 1 + 0.24^2 + 0.24^4 + \frac{0.24^6}{2} + \frac{0.24^8}{4} + \frac{0.24^{10}}{12} = 1.06$$

$$RRS_{bsa} = 0.25 + 0.75 \times \left\{ \frac{1}{0.24^2}[1 - (exp(-2*0.24^2)*1.06)] \right\}^{1/2} = 0.98$$

At the fundamental mode there is not significant reduction in the response due to base slab averaging. However, at the second mode of 0.11 s, the reduction factor due to base slab averaging, while capped at 0.20 s period values, is 0.91. Had the base been the maximum dimension of 260 feet, the reduction factors for the first and second modes would be 0.96 and 0.82.

8.5.2   Embedment

The ground acceleration at an embedded depth is different than the ground acceleration at the ground surface. The primary difference is in the lower acceleration at high frequency. The *Standard* provides the following equation to approximate the reduction in spectral response parameter:

$$RRS_e = 0.25 + 0.75 \times \cos\left(\frac{2\pi e}{T v_s}\right)$$

In the equations above, the embedment depth, e, is limited to a maximum of 20 feet because that is the extent that the equation has been verified against measured structures. There is also a requirement that at least 75% of the foundation footprint shall be present at the embedded depth. This is ensure that the majority of the base is at the depth where the modified ground acceleration is occurring. For sloping sites, the embedment depth used shall be the shallowest depth. The shear wave velocity used in this equation should be the effective average shear wave velocity over the embedment depth, which may be different than that used for determination of the site class and the foundation damping provisions.

For this building at the fundamental period, the reduction factor for embedment is:

$$RRS_e = 0.25 + 0.75 \times \cos\left(\frac{2*3.14*15}{0.49*440}\right) = 0.93$$

At the second mode of 0.11 s, the embedment reduction per the above equation is 0.61.

8.5.3   Nonlinear Example

To illustrate the application of kinematic interaction to the nonlinear response history analysis, the site specific risk targeted maximum considered earthquake shaking intensity response spectrum in Figure 8.3-1 is modified by the product of the reduction factors for base slab averaging and embedment calculated at each period. As can be seen, there is a significantly larger reduction when the period is less than 0.35 s. The dashed line shows the difference between the *Standard* and the *Provisions* due to the provisions allowing the reduction to be greater if a peer review is part of the design process.
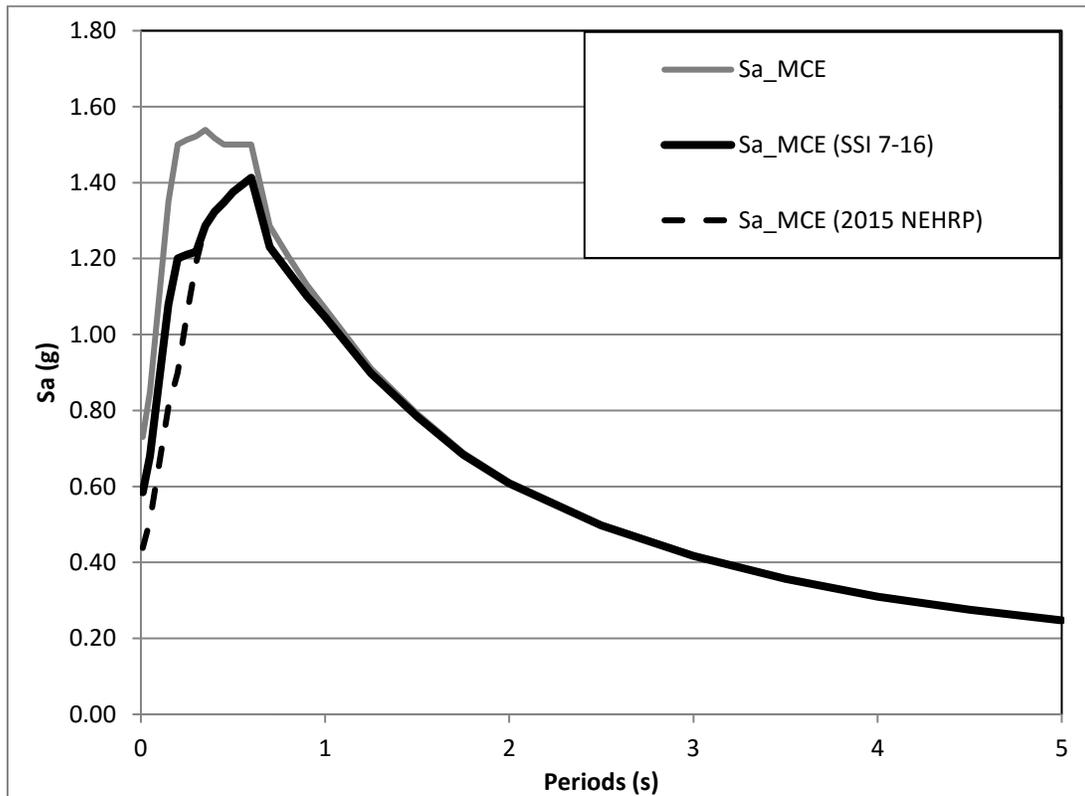
Figure 8.5-1: Risk Targeted Maximum Considered Earthquake Response Spectrum and Kinematic Interaction Modified Spectrum

For the nonlinear analysis, foundation damping is not included in analysis model. This is done to specifically illustrate the kinematic soil-structure interaction provisions. If both soil-structure interaction phenomena are included, it difficult to separate the influence of each.

As required by Section 16.1, the Chapter 12 linear analysis of the building could be performed with the response spectrum used in the modal analysis and the seismic base shear reduced by the product of the base slab averaging and embedment reduction factors. For this building, that seismic base shear would be 0.98*0.93*3,300 = 3,000 kips. This would result in minor changes in the building design.

One set of eleven ground motion acceleration records were selected and scaled per Section 16.2 of the *Standard* to each of the three target spectra. This resulted in three separate suites of eleven pairs of ground motion acceleration records.

A nonlinear analysis model of the building was developed, assuming yielding could occur in flexure at each of the walls or through soil bearing under the footing bases. The analysis was run three different times, with each different suite of scaled ground motion acceleration records. The average interstory drift and

story displacements for each suite of records are shown in Figures 8.5-2 and 8.5-3. From those plots, it is apparent that kinematic soil-structure interaction produces reduction in the response parameters of the structure.

Something to note is that the response for the motions scaled to the *Provision's* spectra with lower values in the very short period range, produces response slightly larger than that scaled to the *Standard.* The reason for this is the greater reduction in the second mode response spectrum ordinate means that modes contribution to the response of the structure is lessened. Because the second mode can act to reduce some of the first mode's response, using a lower value may increase the demands on the building.
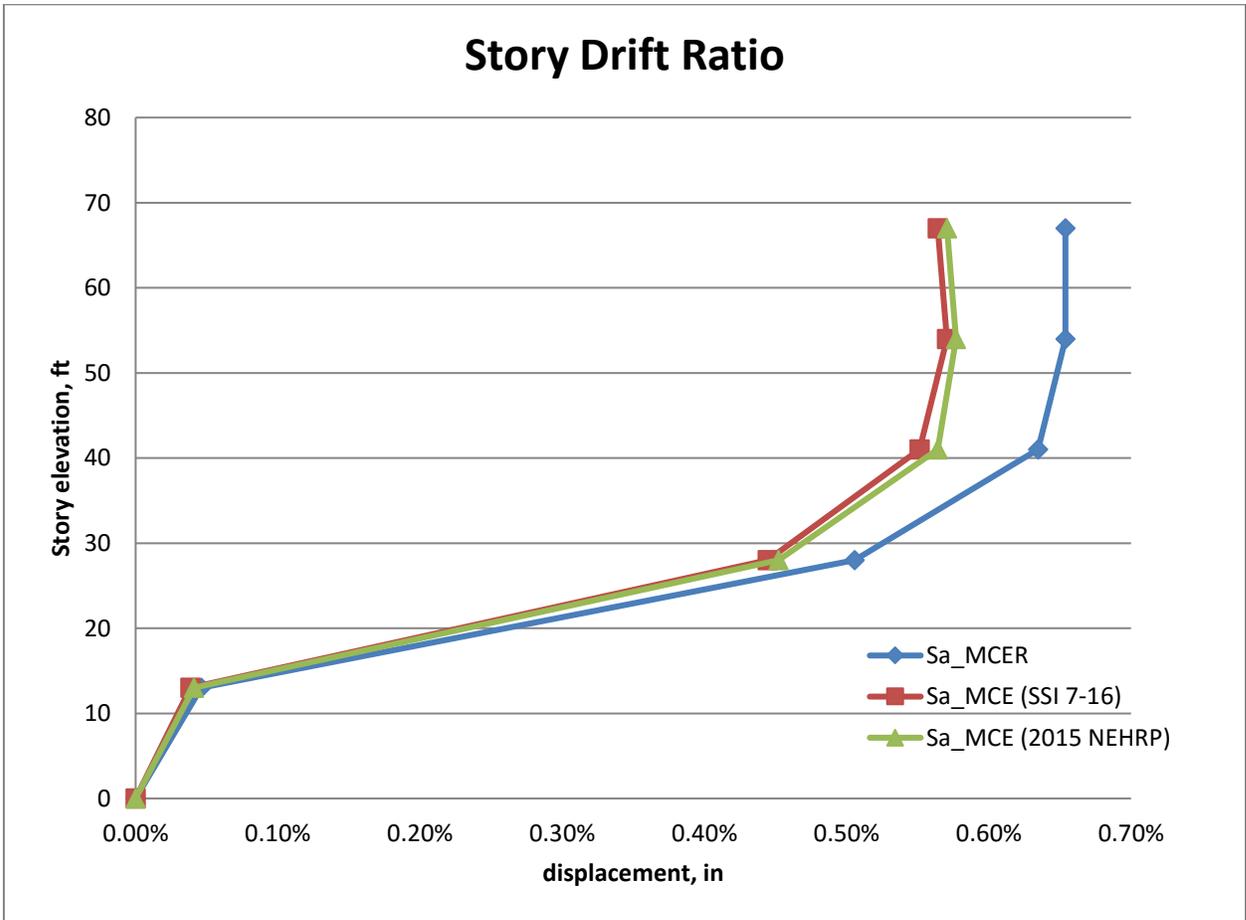
Figure 8.5-2: Nonlinear Analysis Average Story Drift
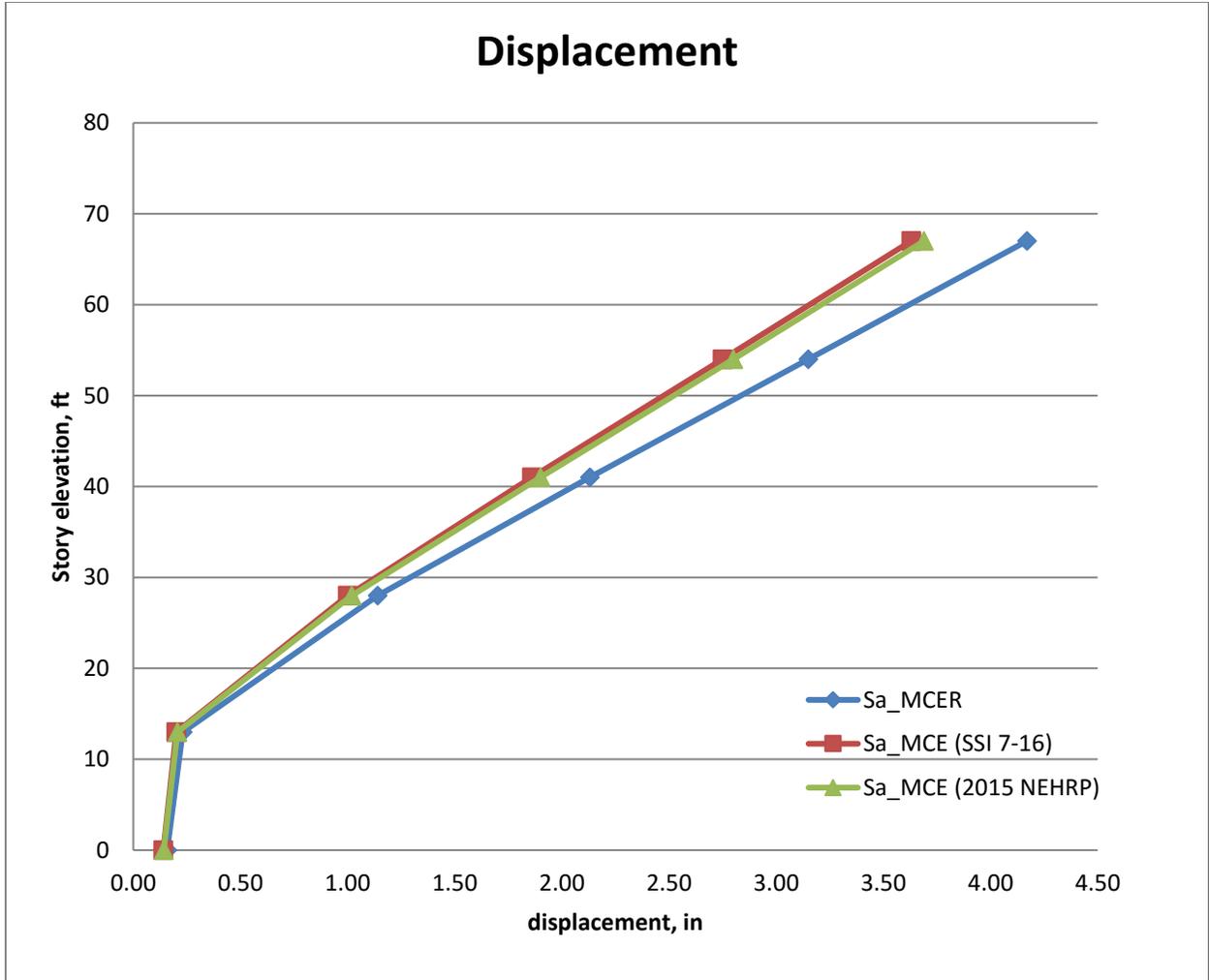
Figure 8.5-3: Nonlinear Analysis Average Floor Displacement

The reductions in the response obtained by kinematic interaction are slightly larger than predicted solely by the product of the reduction factors at the fundamental mode. The reductions observed were about 12% as opposed to the 10% calculated for the first mode. This is due to the higher modes being reduced by a greater reduction factor.

<div style="text-align: right; background: black; color: white; display: inline-block; padding: 1em;">

9

</div>

Structural Steel Design

Rafael Sabelli, S.E. and Brian Dean, P.E.

Contents

The intent of this example is to assist the reader in developing a better understanding of the design requirements in ASCE 7-16 Minimum Design Loads for Buildings and Other Structures (hereafter, the Standard), which incorporates the 2015 Edition of the NEHRP Recommended Seismic Provisions (hereafter, the Provisions).   In addition to the Standard, AISC 341 is the other main reference in this chapter. Except for very minor exceptions, the seismic force-resisting system design requirements of AISC 341 have been adopted in their entirety by the Standard. In addition to serving as a reference standard for seismic design, the Standard is also cited where discussions involve gravity loads, live load reduction, wind loads and load combinations. These examples were originally developed by James R. Harris, P.E., Ph.D., Frederick R. Rutz, P.E., Ph.D. and Teymour Manouri, P.E., Ph.D.

1. An industrial warehouse structure in Astoria, Oregon

2. A multistory office building in Los Angeles, California

The discussion examines the following types of structural framing for resisting horizontal forces:

- Ordinary concentrically braced frames (OCBF)

- Special concentrically braced frames

- Intermediate moment frames

- Special moment frames

The examples cover design for seismic forces in combination with gravity they are presented to illustrate only specific aspects of seismic analysis and design—such as lateral force analysis, design of concentric and eccentric bracing, design of moment resisting frames, drift calculations, member proportioning detailing.

All structures are analyzed using three-dimensional static or dynamic methods. ETABS (Computers & Structures, Inc., Berkeley, California, v.9.5.0, 2008) is used in Examples 9.1 and 9.2.

In addition to the 2015 *NEHRP Recommended Provisions*, the following documents are referenced:

AISC 341	American Institute of Steel Construction. 2016. *Seismic Provisions for Structural Steel Buildings*.
AISC 358	American Institute of Steel Construction. 2016. *Prequalified Connections for Special and Intermediate Steel Moment Frames for Seismic Applications*.
AISC 360	American Institute of Steel Construction. 2016. *Specification for Structural Steel Buildings*.
AISC Manual	American Institute of Steel Construction. 2011. *Manual of Steel Construction*, 14th Edition.
AISC SDM	American Institute of Steel Construction. 2012. *Seismic Design Manual*.
IBC	International Code Council, Inc. 2012. *2012 International Building Code*.

AISC SDGS-4   AISC Steel Design Guide Series 4. Second Edition. 2003. *Extended End-Plate Moment Connections*, 2003.

SDILuttrell, Larry D. 1981. *Steel Deck Institute Diaphragm Design Manual*. Steel Deck Institute.

Dowswell   Dowswell, B. (2014). "Gusset Plate Stability Using Variable Stress Trajectories," ASCE Structures Congress.

Hamburger et al.   Hamburger, Ronald O., Krawinkler, Helmut, Malley, James O., and Adan, Scott M. (2009). "Seismic design of steel special moment frames: a guide for practicing engineers," NEHRP Seismic Design Technical Brief No. 2, produced by the NEHRP Consultants Joint Venture, a partnership of the Applied Technology Council and the Consortium of Universities for Research in Earthquake Engineering, for the National Institute of Standards and Technology, Gaithersburg, MD, NIST GCR 09-917-3

Sabelli, et al.   Sabelli, Rafael. Roeder, Charles W., Hajjar, Jerome F. (2013). "*Seismic Design of Steel Special Concentrically Braced Frame Systems*," NEHRP Seismic Design Technical Brief No. 8, produced by the NEHRP Consultants Joint Venture, a partnership of the Applied Technology Council and the Consortium of Universities for Research in Earthquake Engineering, for the National Institute of Standards and Technology, Gaithersburg, MD, NIST GCR 13-917-24.

The symbols used in this chapter are from Chapter 11 of the *Standard*, the above referenced documents, or are as defined in the text. U.S. Customary units are used.

9.1   INDUSTRIAL HIGH-CLEARANCE BUILDING, ASTORIA, OREGON

This example utilizes a transverse intermediate steel moment frame and a longitudinal ordinary concentric steel braced frame. The following features of seismic design of steel buildings are illustrated:

- Seismic design parameters

- Equivalent lateral force analysis

- Three-dimensional analysis

- Drift check

- Check of compactness and spacing for moment frame bracing

- Moment frame connection design

- Proportioning of concentric diagonal bracing

9.1.1   Building Description
This building has plan dimensions of 180 feet by 90 feet and a clear height of approximately 30 feet. It includes a 12-foot-high, 40-foot-wide mezzanine area at the east end of the building. The structure consists

of 10 gable frames spanning 90 feet in the transverse (north-south) direction. Spaced at 20 feet on center, these frames are braced in the longitudinal (east-west) direction in two bays at the east end. The building is enclosed by nonstructural insulated concrete wall panels and is roofed with steel decking covered with insulation and roofing. Columns are supported on spread footings.

The elevation and transverse sections of the structure are shown in Figure 9.1-1. Longitudinal struts at the eaves and at the mezzanine level run the full length of the building and therefore act as collectors for the distribution of forces resisted by the diagonally braced bays and as weak-axis stability bracing for the moment frame columns.

The roof and mezzanine framing plans are shown in Figure 9.1-2. The framing consists of a steel roof deck supported by joists between transverse gable frames. The mezzanine represents both an additional load and additional strength and stiffness. Because all the frames resist lateral loading, the steel deck functions as a diaphragm for distribution of the effects of eccentric loading caused by the mezzanine floor when the building is subjected to loads acting in the transverse direction.

The mezzanine floor at the east end of the building is designed to accommodate a live load of 125 psf. Its structural system is composed of a concrete slab over steel decking supported by floor beams spaced at 10 feet on center. The floor beams are supported on girders continuous over two intermediate columns spaced approximately 30 feet apart and are attached to the gable frames at each end.

The member sizes in the main frame are controlled by serviceability considerations. Vertical deflections due to snow were limited to 3.5 inches, and lateral sway due to wind was limited to 2 inches.
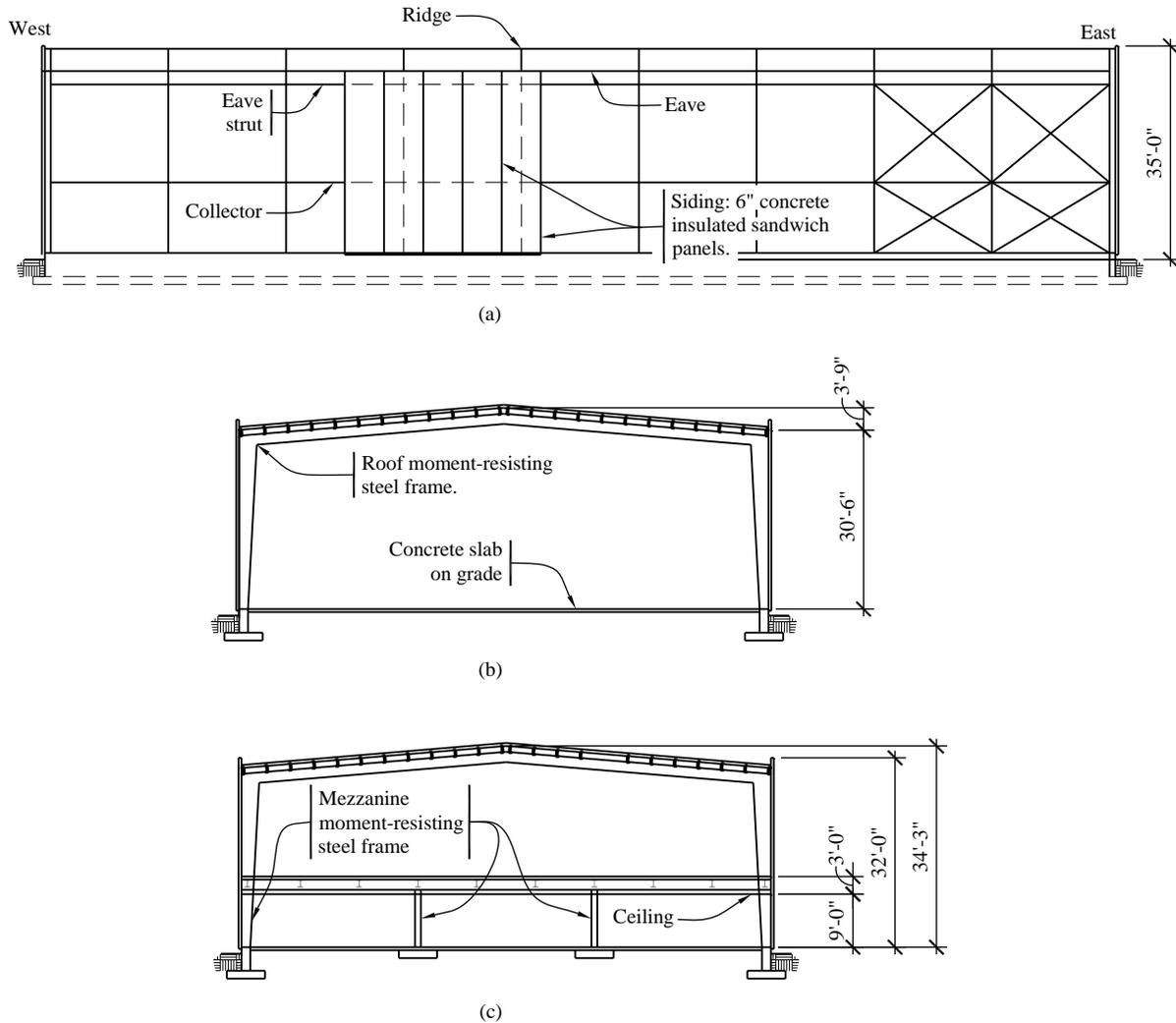
Figure 9.1-1 Framing elevation and sections
(1.0 ft = 0.3048 m; 1.0 in. = 25.4 mm)

Earthquake rather than wind governs the lateral design due to the mass of the insulated concrete panels. The panels are attached with long pins perpendicular to the concrete surface. These slender, flexible pins isolate the panels from acting as shear walls.

The building is supported on spread footings based on moderately deep alluvial deposits (i.e., medium dense sands). The foundation plan is shown in Figure 9.1-3. Transverse ties are placed between the footings of the two columns of each moment frame to provide restraint against horizontal thrust from the moment frames. Grade beams carrying the enclosing panels serve as ties in the longitudinal direction as well as across the end walls. The design of footings and columns in the braced bays requires consideration of combined seismic loadings. The design of foundations is not included here.
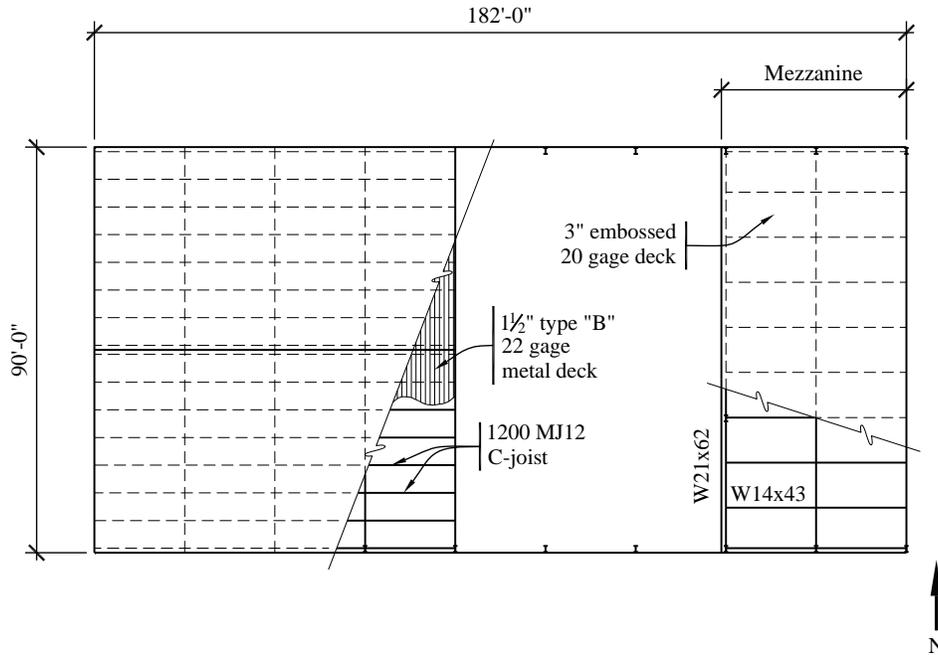
Figure 9.1-2 Roof framing and mezzanine framing plan
(1.0 ft = 0.3048 m; 1.0 in. = 25.4 mm)
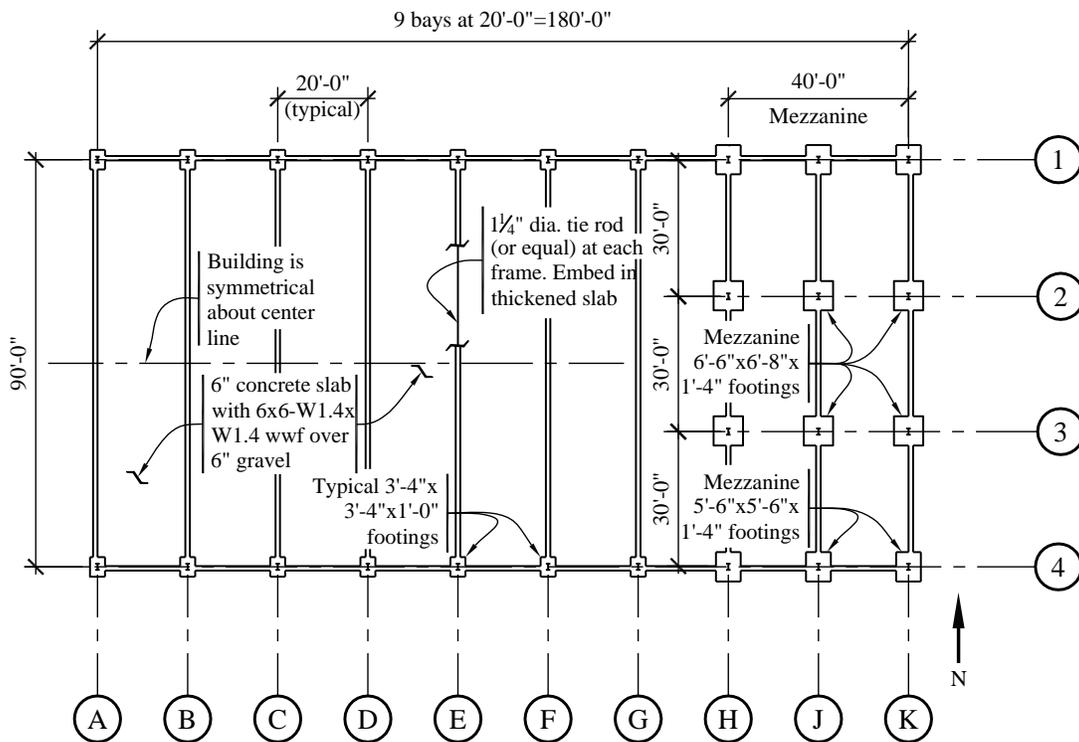
Figure 9.1-3 Foundation plan
(1.0 ft = 0.3048 m; 1.0 in. = 25.4 mm)

9.1.2   Design Parameters

9.1.2.1 Ground motion and system parameters. See Section 3.2 for an example illustrating the determination of design ground motion parameters. For this example the parameters are as follows.

$S_{DS} = 1.0$

$S_{D1} = 0.6$

Risk Category II

Seismic Design Category D

Note that *Standard* Section 12.2.5.6 permits an ordinary steel moment frame for buildings that do not exceed one story and 65 feet tall with a roof dead load not exceeding 20 psf. Intermediate steel moment frames with stiffened bolted end plates and ordinary steel concentrically braced frames are used in this example.

North-south (N-S) direction:

Moment-resisting frame system = intermediate steel moment frame (*Standard* Table 12.2-1)
$R = 4.5$
$\Omega_0 = 3$
$C_d = 4$

East-west (E-W) direction:

Braced frame system = ordinary steel concentrically braced frame (*Standard* Table 12.2-1)
$R = 3.25$
$\Omega_0 = 2$
$C_d = 3.25$

9.1.2.2 Loads

Roof live load (*L*), snow = 25 psf

Roof dead load (*D*) = 15 psf

Mezzanine live load, storage = 125 psf

Mezzanine slab and deck dead load = 69 psf

Weight of wall panels = 25 psf

Roof dead load includes roofing, insulation, metal roof deck, purlins, mechanical and electrical equipment, and the self-weight of that portion of the main frames that is tributary to the roof under lateral load. For determination of the seismic weights, the weight of the mezzanine will include the dead load plus 25 percent of the storage load (125 psf) in accordance with *Standard* Section 12.7.2. Therefore, the mezzanine seismic weight is $69 + 0.25(125) = 100$ psf.

9.1.2.3 Materials

Concrete for footings: $f_c' = 2.5$ ksi

Slabs-on-grade: $f_c' = 4.5$ ksi

Mezzanine concrete on metal deck: $f_c' = 3.0$ ksi

Reinforcing bars: ASTM A615, Grade 60

Structural steel (wide flange sections): ASTM A992, Grade 50

Plates (except continuity plates): ASTM A36

Bolts: ASTM A325

Continuity Plates: ASTM A572, Grade 50

9.1.3   Structural Design Criteria

9.1.3.1 Building configuration. Because there is a mezzanine at one end, vertical weight irregularities are considered to apply (*Standard* Sec. 12.3.2.2). However, the upper level is a roof and the *Standard* exempts roofs from weight irregularities. There also are no plan irregularities in this building (*Standard* Sec. 12.3.2.1).

9.1.3.2 Redundancy. In the N-S direction, the moment frames do not meet the requirements of *Standard* Section 12.3.4.2b since the frames are only one bay long. Thus, *Standard* Section 12.3.4.2a must be checked.

By inspection, the critical frames are at gridlines A and K. The effect of loss of a connection at either of these frames—one at a time—is evaluated to determine whether the system has sufficient redundancy. A copy of the three-dimensional model is made, with the moment frame beam at Gridline A pinned. The structure is checked to make sure that an extreme torsional irregularity (*Standard* Table 12.3-1) does not occur by comparing the maximum drift to 1.4 times the average drift:

$$1.4(\frac{\Delta_K + \Delta_A}{2}) \geq \Delta_A$$

$$1.4\left(\frac{4.17\,\text{in.} + 6.1\,\text{in.}}{2}\right) = 7.19\,\text{in.} \geq 6.1\,\text{in.}$$

where:

Δ_A = maximum displacement at knee along Gridline A, in.

Δ_K = maximum displacement at knee along gridline K, in.

The maximum drift is less than 1.4 times the average. Thus, the structure does not have an extreme torsional irregularity when a frame loses moment resistance.

Additionally, the structure must be checked in the N-S direction to ensure that the loss of moment resistance at Beam A has not resulted in more than a 33 percent reduction in story strength. This can be checked using elastic methods (based on first yield) as shown below, or using strength methods. The original model is run with the N-S load combinations to determine the member with the highest demand-capacity ratio. This demand-capacity ratio, along with the applied base shear, is used to calculate the base shear at first yield:

$$V_{yield} = \left(\frac{1}{(D/C)_{max}} \right) V_{base}$$

$$V_{yield} = \left(\frac{1}{0.89} \right) (223 \, \text{kips}) = 250.5 \, \text{kips}$$

where:

V_{base} = base shear from Equivalent Lateral Force (ELF) analysis

A similar analysis can be made using the model with no moment resistance at Frame A:

$$V_{yield,MFremoved} = \left(\frac{1}{0.951} \right) (223 \, \text{kips}) = 234.5 \, \text{kips}$$

$$\frac{V_{yield,MFremoved}}{V_{yield}} = \frac{234.5 \, \text{kips}}{250.5 \, \text{kips}} = 0.94$$

This evaluation is repeated for the loss of a moment connection at gridline K. (For brevity, those calculations are not presented.)

Thus, the loss of resistance at both ends of a single beam only results in a 6 percent reduction in story strength. The moment frames can be assigned a value of $\rho = 1.0$.

In the E-W direction, the OCBF system meets the prescriptive requirements of *Standard* Section 12.3.4.2a. As a result, no further calculations are needed and this system can be assigned a value of $\rho = 1.0$.

9.1.3.3 Orthogonal load effects. A combination of 100 percent seismic forces in one direction plus 30 percent seismic forces in the orthogonal direction must be applied to the columns of this structure in Seismic Design Category D (*Standard* Sec. 12.5.4). The *Standard* requires this in conditions in which the interaction of orthogonal ground motions is likely to have a significant effect. In this case, the columns that are shared by orthogonal frames require consideration of simultaneous accelerations in the orthogonal building axes.

9.1.3.4 Structural component load effects. The effect of seismic load (*Standard* Sec. 12.4.2) is:

$$E = \rho Q_E \pm 0.2 S_{DS} D$$

$S_{DS} = 1.0$ for this example. The seismic load is combined with the gravity loads as shown in *Standard* Sec. 12.4.2.3, resulting in the following:

$$1.4D + 1.0L + 0.2S + \rho Q_E$$

$$0.7D + \rho Q_E$$

Note that $1.0L$ is for the storage load on the mezzanine; the coefficient on L is 0.5 for many common live loads that do not exceed 100 psf.

9.1.3.5 Drift limits. For a building assigned to Risk Category II, the allowable story drift (*Standard* Table 12.12-1) is:

- $\Delta_a = 0.025h_{sx}$ in the E-W direction

- $\Delta_a/\rho = 0.025h_{sx}/1.0$ in the N-S direction

At the roof ridge, $h_{sx} = 34$ ft-3 in. and $\Delta_\alpha = 10.28$ in.

At the knee (column-roof intersection), $h_{sx} = 30$ ft-6 in. and $\Delta_a = 9.15$ in.

At the mezzanine floor, $h_{sx} = 12$ ft and $\Delta_a = 3.60$ in.

Footnote c in *Standard* Table 12.12-1 permits unlimited drift for single-story buildings with interior walls, partitions, etc., that have been designed to accommodate the story drifts. See Section 9.1.4.3 for further discussion. The main frame of the building can be considered to be a one-story building for this purpose, given that there are no interior partitions except below the mezzanine. (The definition of a story in building codes generally does not require that a mezzanine be considered a story unless its area exceeds one-third the area of the room or space in which it is placed; this mezzanine is less than one-third of the footprint of the building.)

9.1.3.6 Seismic weight. The weights that contribute to seismic forces are:

Roof $D = (0.015)(90)(180) =$	243 kips
Panels at sides $= (2)(0.0375)(32)(180)/2 =$	144 kips
Panels at ends $= (2)(0.0375)(35)(90)/2 =$	79 kips
Mezzanine slab and 25% LL $=$	360 kips
Mezzanine framing $=$	35 kips
Main frames $=$	27 kips
Seismic weight $=$	888 kips

The weight associated with the main frames accounts for only the main columns, because the weight associated with the remainder of the main frames is included in the roof dead load above. The computed seismic weight is based on the assumption that the wall panels offer no shear resistance for the structure. Additionally, snow load does not need to be included in the seismic weight per *Standard* Section 12.7.2 because it does not exceed 30 psf.

9.1.4 Analysis
Base shear will be determined using an ELF analysis.

9.1.4.1 Equivalent Lateral Force procedure. In the longitudinal direction where stiffness is provided only by the diagonal bracing, the approximate period is computed using *Standard* Equation 12.8-7:

$$T_a = C_r h_n^x = (0.02)\left(34.25^{0.75}\right) = 0.28 \text{sec}$$

where h_n is the height of the building, taken as 34.25 feet at the mid-height of the roof. In accordance with *Standard* Section 12.8.2, the computed period of the structure must not exceed the following:

$$T_{max} = C_u T_a = (1.4)(0.28) = 0.39 \text{sec}$$

The subsequent three-dimensional modal analysis finds the computed period to be 0.54 seconds. For purposes of determining the required base shear strength, T_{max} will be used in accordance with the *Standard*; drift will be calculated using the period from the model.

In the transverse direction where stiffness is provided by moment-resisting frames (*Standard* Eq. 12.8-7):

$$T_a = C_r h_n^x = (0.028)(34.25^{0.8}) = 0.47 \text{ sec}$$

and

$$T_{max} = C_u T_a = (1.4)(0.47) = 0.66 \text{ sec}$$

Also note that the dynamic analysis finds a computed period of 1.03 seconds. As in the longitudinal direction, T_{max} will be used for determining the required base shear strength.

The seismic response coefficient (C_s) is computed in accordance with *Standard* Section 12.8.1.1. In the longitudinal direction:

$$C_S = \frac{S_{DS}}{R / I_e} = \frac{1.0}{3.25 / 1.0} = 0.308$$

but need not exceed:

$$C_S = \frac{S_{D1}}{T\left(\dfrac{R}{I_e}\right)} = \frac{0.6}{0.39\left(\dfrac{3.25}{1.0}\right)} = 0.473$$

Therefore, use $C_s = 0.308$ for the longitudinal direction.

In the transverse direction:

$$C_S = \frac{S_{DS}}{R / I_e} = \frac{1.0}{4.5 / 1} = 0.222$$

but need not exceed:

$$C_S = \frac{S_{DS}}{T(R / I_e)} = \frac{0.6}{(0.66)(4.5 / 1)} = 0.202$$

Therefore, use $C_s = 0.202$ for the transverse direction.

In both directions the value of C_s exceeds the minimum value (*Standard* Eq. 12.8-5) computed as:

$$C_S = 0.044 I_e S_{DS} \geq 0.01 = (0.044)(1)(1.0) = 0.044$$

The seismic base shear in the longitudinal direction (*Standard* Eq. 12.8-1) is:

$$V = C_S W = (0.308)(888 \text{kips}) = 274 \text{kips}$$

The seismic base shear in the transverse direction is:

$$V = C_S W = (0.202)(888 \text{kips}) = 179 \text{kips}$$

Standard Section 12.8.3 prescribes the vertical distribution of lateral force in a multilevel structure. Even though the building is considered to be one story for some purposes, it is clearly a two-level structure. Using the data in Section 9.1.3.6 of this example and interpolating the exponent k as 1.08 for the period of 0.66 second, the distribution of forces for the N-S analysis is shown in Table 9.1-1.

Table 9.1-1 ELF Vertical Distribution for N-S Analysis

Level	Weight (w_x) (kips)	Height (h_x) (ft)	$w_x h_x{}^k$	$C_{vx} = \dfrac{w_x h_x^k}{\sum_{i=1}^{n} w_{ih_x^k}}$	$F_x = C_{vx} V$ (kips)
Roof	570	32.375	24,350	0.84	151
Mezzanine	318	12	4660	0.16	29
Total	888		29,010		179

It is not immediately clear whether the roof (a 22-gauge steel deck with conventional roofing over it) will behave as a flexible, semi-rigid, or rigid diaphragm. For this example, a three-dimensional model was created in ETABS including frame and diaphragm stiffness.

9.1.4.2 Three-dimensional ELF analysis. The three-dimensional analysis is performed for this example to account for the following:

The differing stiffness of the gable frames with and without the mezzanine level

The different centers of mass for the roof and the mezzanine

The flexibility of the roof deck

The significance of braced frames in controlling torsion due to N-S ground motions

The gabled moment frames, the tension bracing, the moment frames supporting the mezzanine and the diaphragm chord members are explicitly modeled using three-dimensional beam-column elements. The tapered members are approximated as short, discretized prismatic segments. Thus, combined axial bending checks are performed on a prismatic element, as required by AISC 360 Chapter H. The collector at the knee level is included, as are those at the mezzanine level in the two east bays. The mezzanine diaphragm is modeled using planar shell elements with their in-plane rigidity being based on actual properties and dimensions of the slab. The roof diaphragm also is modeled using planar shell elements, but their in-plane rigidity is based on a reduced thickness that accounts for compression buckling phenomena and for the fact that the edges of the roof diaphragm panels are not connected to the wall panels. SDI's *Diaphragm Design Manual* is used for guidance in assessing the stiffness of the roof deck. The analytical model includes elements with one-tenth the stiffness of a plane plate of 22 gauge steel.

The ELF analysis of the three-dimensional model in the transverse direction yields an important result: the roof diaphragm behaves as a rigid diaphragm. Accidental torsion is applied at the roof as a moment whose magnitude is the roof lateral force multiplied by 5 percent of 180 feet (9 feet). (This moment is distributed as a series of point loads on each of the moment frames.) A moment is also applied to the mezzanine level in a similar fashion. The resulting displacements are shown in Table 6.1-2.

Table 9.1-2 ELF Analysis Displacements in N-S Direction

Grid	Roof Displacement (in.)
A	4.98
B	4.92
C	4.82
D	4.68
E	4.56
F	4.46
G	4.34
H	4.19
J	4.05
K	3.92

The average of the extreme displacements is 4.45 inches. The displacement at the centroid of the roof is 4.51 inches. Thus, the deviation of the diaphragm from a straight line is 0.06 inch, whereas the average frame displacement is approximately 75 times that. Clearly, then, the diaphragm flexibility is negligible and the deck behaves as a rigid diaphragm.

Roof displacements are also used to determine if a torsional irregularity exists. The ratio of maximum to average displacement is:

$$\frac{4.98}{\frac{1}{2}(4.98 + 3.92)} = 1.11$$

This does not exceed the 1.2 limit given in *Standard* Table 12.3-1 and torsional irregularity is not triggered.

The same process needs to be repeated for the E-W direction.

Table 9.1-3 ELF Analysis Displacements in N-S Direction

Grid	Roof Displacement (in.)
1	0.88
2/3	0.82
4	0.75

The ratio of the maximum to average displacement is 1.07, well under the torsional irregularity threshold ratio of 1.2.

The demands from the three-dimensional ELF analysis are combined to meet the orthogonal combination requirement of *Standard* Section 12.5.3 for the columns:

E-W: (1.0)(E-W forces) + (0.3)(N-S forces)

N-S: (0.3)(E-W forces) + (1.0)(N-S forces)

9.1.4.3 Drift. The lateral deflection cited previously must be multiplied by $C_d = 4$ to find the transverse drift:

$$\delta_x = \frac{C_d \delta_e}{I_e} = \frac{(4)(4.51)}{1.0} = 18 \text{ in.}$$

This exceeds the limit of 10.28 inches computed previously. However, there is no story drift limit for single-story structures with interior wall, partitions, ceilings and exterior wall systems that have been designed to accommodate the story drifts. Detailing for this type of design may be problematic.

In the longitudinal direction, the lateral deflection is much smaller and is within the limits of *Standard* Section 12.12.1. The deflection computations do not include the redundancy factor.

9.1.4.4 P-delta effects. The P-delta effects on the structure may be neglected in analysis if the provisions of *Standard* Section 12.8.7 are followed. First, the stability coefficient maximum should be determined using *Standard* Equation 12.8-17. β may be assumed to be 1.0.

$$\theta_{max} = \frac{0.5}{\beta C_d} \leq 0.25$$

$$\theta_{max,N-S} = \frac{0.5}{(1.0)(4)} = 0.125$$

$$\theta_{max,E-W} = \frac{0.5}{(1.0)(3.25)} = 0.154$$

Next, the stability coefficient is calculated using *Standard* Equation 12.8-16. The stability coefficient is calculated at both the roof and mezzanine levels in both orthogonal directions. For purposes of illustration, the roof level check in the N-S direction will be shown as:

$$\theta = \frac{P_x \Delta I}{V_x h_{sx} C_d} \qquad \Delta = \frac{C_d \left(\delta_{e2} - \delta_{e1} \right)}{I}$$

$$\theta = \frac{P_x \left(\delta_{e2} - \delta_{e1} \right) C_d I}{V_x h_{sx} C_d I} = \frac{P_x \left(\delta_{e2} - \delta_{e1} \right)}{V_x h_{sx}}$$

$$P_{roof} = \text{Roof LL} + \text{Roof DL} + \text{Panels} + \text{Frames}$$

$$P_{roof} = 888 \, \text{kips}$$

$$\theta = \frac{888(4.51\text{in.})}{(179\,\text{kips})(32.375\,\text{ft})} = 0.069 < 0.1$$

The three other stability coefficients were all determined to be less than θ_{max}, thus allowing P-delta effects to be excluded from the analysis.

9.1.4.5 Force summary. The maximum moments and axial forces caused by dead, live and earthquake loads on the gable frames are listed in Tables 9.1-3 and 9.1-4. The frames are symmetrical about their ridge and the loads are either symmetrical or can be applied on either side on the frame because the forces are given for only half of the frame extending from the ridge to the ground. The moments are given in Table 9.1-4 and the axial forces are given in Table 9.1-5. The moment diagram for the combined load condition is shown in Figure 9.1-4. The load combination is $1.4D + L + 0.2S + \rho Q_E$, which is used throughout the remainder of calculations in this section, unless specifically noted otherwise.

The size of the members is controlled by gravity loads, not seismic loads. The design of connections will be controlled by the seismic loads.

Forces in the design of the braces are discussed in Section 9.1.5.5.

Table 9.1-4 Moments in Gable Frame Members

Location	D (ft-kips)	L (ft-kips)	S (ft-kips)	Q_E (ft-kips)	Combined* (ft-kips)
1 - Ridge	61	0	128	0	112
2 - Knee	161	0	333	162	447
3 - Mezzanine	95	83	92	137	79
4 - Base	0	0	0	0	0

* Combined Load = $1.4D + L + 0.2S + \rho Q_E$ (or $1.2D + 1.6S$). Individual maxima are not necessarily on the same frame; combined load values are maximum for any frame.
1.0 ft = 0.3048 m, 1.0 kip = 1.36 kN-m.

Table 9.1-5 Axial Forces in Gable Frame Members

Location	D (kips)	L (kips)	S (kips)	ρQ_E (kips)	Combined* (kips)
1 - Ridge	14	3.5	25	0.8	39
2 - Knee	16	4.5	27	7.0	37
3 - Mezzanine	39	39	23	26	127
4 - Base	39	39	23	26	127

Table 9.1-5 Axial Forces in Gable Frame Members

Location	D (kips)	L (kips)	S (kips)	ρQ_E (kips)	Combined* (kips)

* Combined Load = $1.4D + L + 0.2S + \rho Q_E$. Individual maxima are not necessarily on the same frame; combined load values are maximum for any frame.
1.0 ft = 0.3048 m, 1.0 kip = 1.36 kN-m.
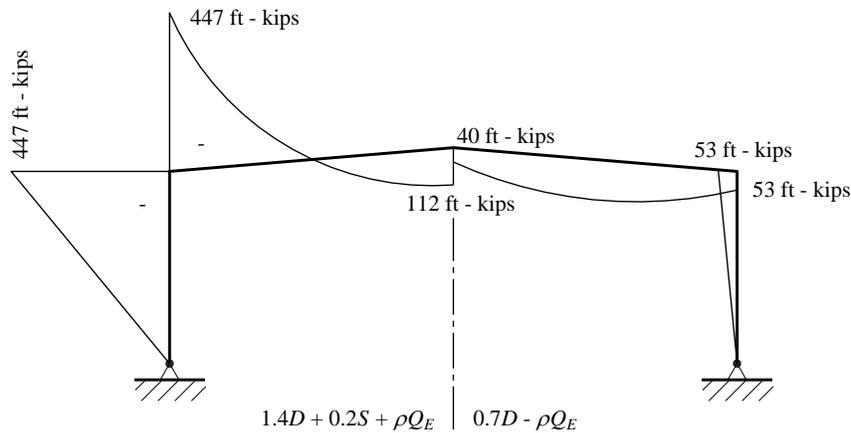
Figure 9.1-4 Moment diagram for seismic load combinations
(1.0 ft-kip = 1.36 kN-m)

9.1.5   Proportioning and Details
The gable frame is shown schematically in Figure 9.1-5. Using the load combinations presented in Section 9.1.3.4 and the loads from Tables 9.1-4 and 9.1-5, the proportions of the frame are checked at the roof beams and the variable-depth columns (at the knee). The mezzanine framing, also shown in Figure 9.1-1, was proportioned similarly. The diagonal bracing, shown in Figure 9.1-1 at the east end of the building, is proportioned using tension forces determined from the three-dimensional ELF analysis.
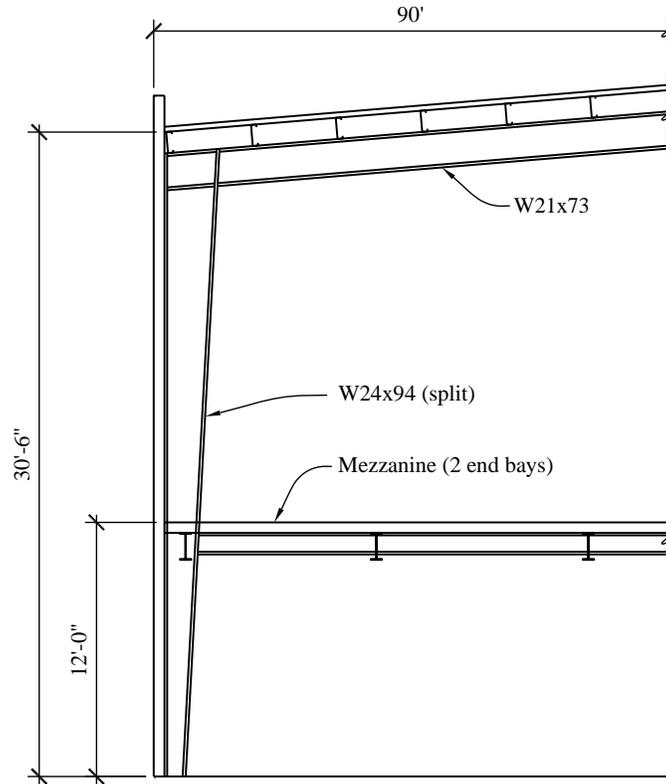
Figure 9.1-5 Gable frame schematic: Column tapers from 12 in. at base to 36 in. at knee; plate sizes are given in Figure 9.1-7
(1.0 in. = 25.4 mm)

Additionally, the bolted, stiffened, extended end-plate connections must be sized correctly to conform to the pre-qualification standards. AISC 358 Table 9.1 provides parametric limits on the beam and connection sizes for the 8-bolt stiffened end-plate connection. Table 9.1-6 shows these limits as well as the values used for design.

Table 9.1-6 Parametric Limits for Moment Frame Connection

Parameter	Minimum (in.)	As Designed (in.)	Maximum (in.)
t_p	3/4	1 1/4	2 1/2
b_p	9	9	15
g	5	5	6
p_{fi}, p_{fo}	1 5/8	1 3/4	2
p_b	3 1/2	3 1/2	3 3/4
d	18	36	36
t_{bf}	9/16	5/8	1
b_{bf}	7 1/2	8	12 1/4

9.1.5.1 Frame compactness and brace spacing. According to *Standard* Section 14.1.3, steel structures assigned to Seismic Design Category D, E, or F must be designed and detailed per AISC 341. For an intermediate moment frame (IMF), AISC 341, Section E2.1, "Scope," stipulates that those requirements are to be applied in conjunction with AISC 360. AISC 341 itemizes a few additional items beyond what is required by AISC 360 for intermediate moment frames, but otherwise the intermediate moment frames are to be designed per AISC 360.

AISC 341 requires IMFs to have compact width-thickness ratios for moderately ductile members per Table D1.1. The sections comply. (Refer to Table 1-3 of the *Seismic Design Manual*.)

. All P-M ratios (combined compression and flexure) are less than 1.00. This is based on proper spacing of lateral bracing.

Lateral bracing is provided by the roof joists. The maximum spacing of lateral bracing is determined using beam properties at the ends and AISC 341, Section D1.2a:

$$L_{b,max} \le 0.17 r_y \frac{E}{F_y}$$

$$L_{b,max} \le 0.17 (1.46 \text{ in.}) \left(\frac{29000 \text{ ksi}}{50 \text{ ksi}} \right) = 148 \text{ in.}$$

L_b is 48 inches; therefore, the spacing is OK.

Also, the required brace strength and stiffness are calculated per AISC 360, Equations A-6-7 and A-6-8:

$$P_{br} = \frac{0.02 M_r C_d}{h_o}$$

$$\beta_{br} = \frac{1}{\phi} \left(\frac{10 M_r C_d}{L_b h_o} \right)$$

where:

$$M_r = R_y Z F_y$$

$$C_d = 1.0$$

h_o = distance between flange centroids, in.

L_b = distance between braces or L_p (from AISC 360 Eq. F2-5), whichever is greater, in.

$$M_r = (1.1)(309 \text{ in.}^3)(50 \text{ ksi}) = 16,992 \text{ in.-kip} = 1,416 \text{ ft-kip}$$

$$P_{br} = \frac{0.02 (16,992 \text{ in.-kip})(1.0)}{(36 \text{ in.} - 5/8 \text{ in.})}$$

$P_{br} = 9.61$ kips

$$L_p = 1.76 r_y \sqrt{\frac{E}{F_y}}$$

$$L_p = 1.76(1.46 \text{ in.}) \sqrt{\frac{29,000 \text{ ksi}}{50 \text{ ksi}}} = 62 \text{ in.}$$

$$\beta_{br} = \frac{1}{(0.75)} \left(\frac{10(16,992 \text{ in.-kip})(1.0)}{(62 \text{ in.})(35.375 \text{ in.})} \right)$$

$\beta_{br} = 104$ kips/in.

Adjacent to the plastic hinge regions, lateral bracing must have additional strength as defined in AISC 341 D1.2c

$$P_u = \frac{0.06 M_u}{h_o}$$

$$P_u = \frac{0.06(16992 \text{ in - kip})}{(35.375 \text{ in.})}$$

$P_u = 28.8 \text{ kips}$

The C-joists used in this structure likely are not adequate to brace the moment frames. Instead, tube brace members will be used, but they are not analyzed in this example.

At the negative moment regions near the knee, lateral bracing is necessary on the bottom flange of the beams and inside the flanges of the columns (Figure 9.1-6).
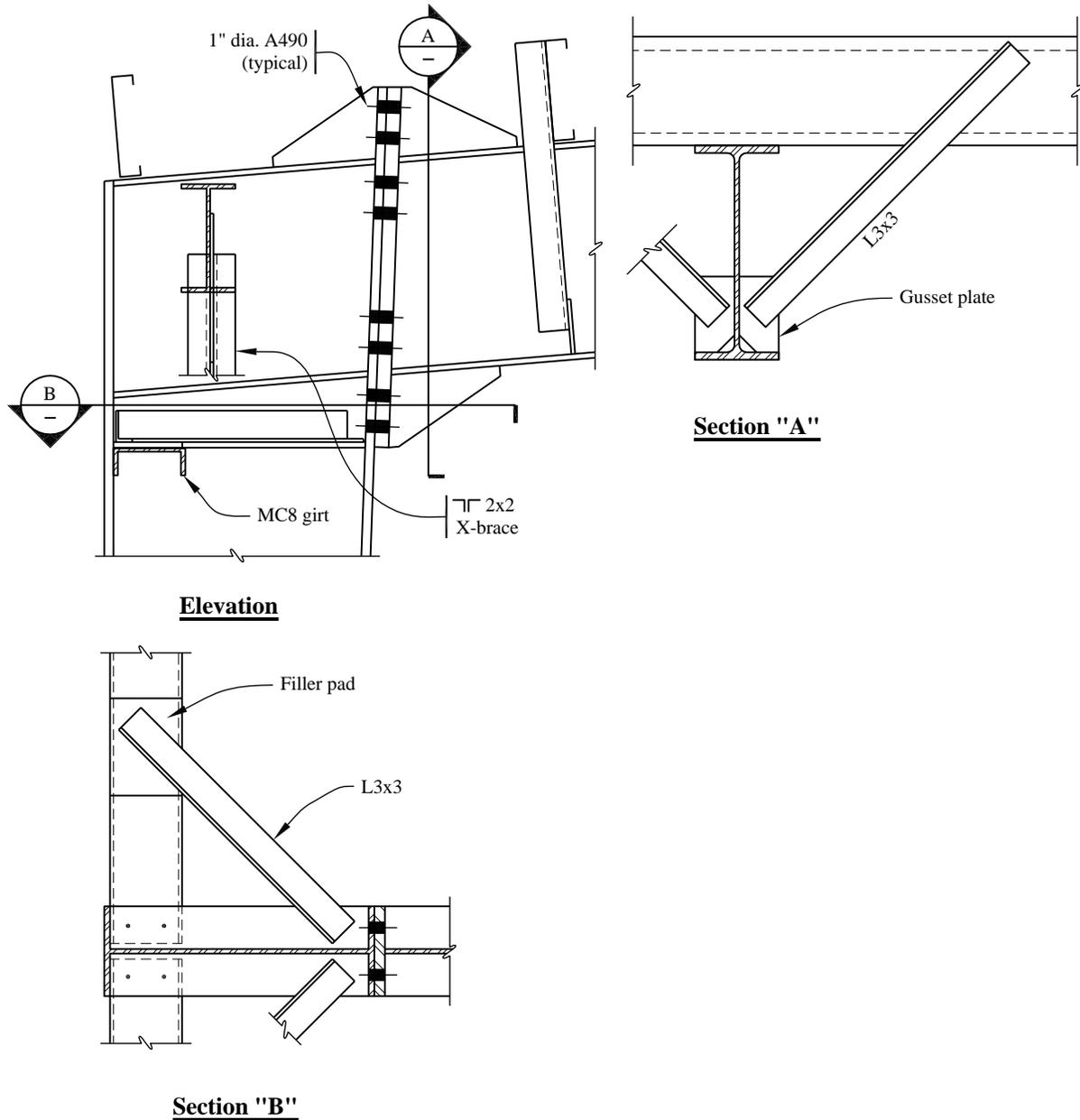
Figure 9.1-6 Arrangement at knee
(1.0 in. = 25.4 mm)

9.1.5.2 Knee of the frame. The knee detail is shown in Figures 9.1-6 and 9.1-7. The vertical plate shown near the upper left corner in Figure 9.1-6 is a gusset providing connection for X-bracing in the longitudinal direction. The beam-to-column connection requires special consideration. The method of AISC 358 for bolted, stiffened end plate connections is used. Refer to Figure 9.1-8 for the configuration. Highlights from this method are shown for this portion of the example. Refer to AISC 358 for a discussion of the entire procedure.
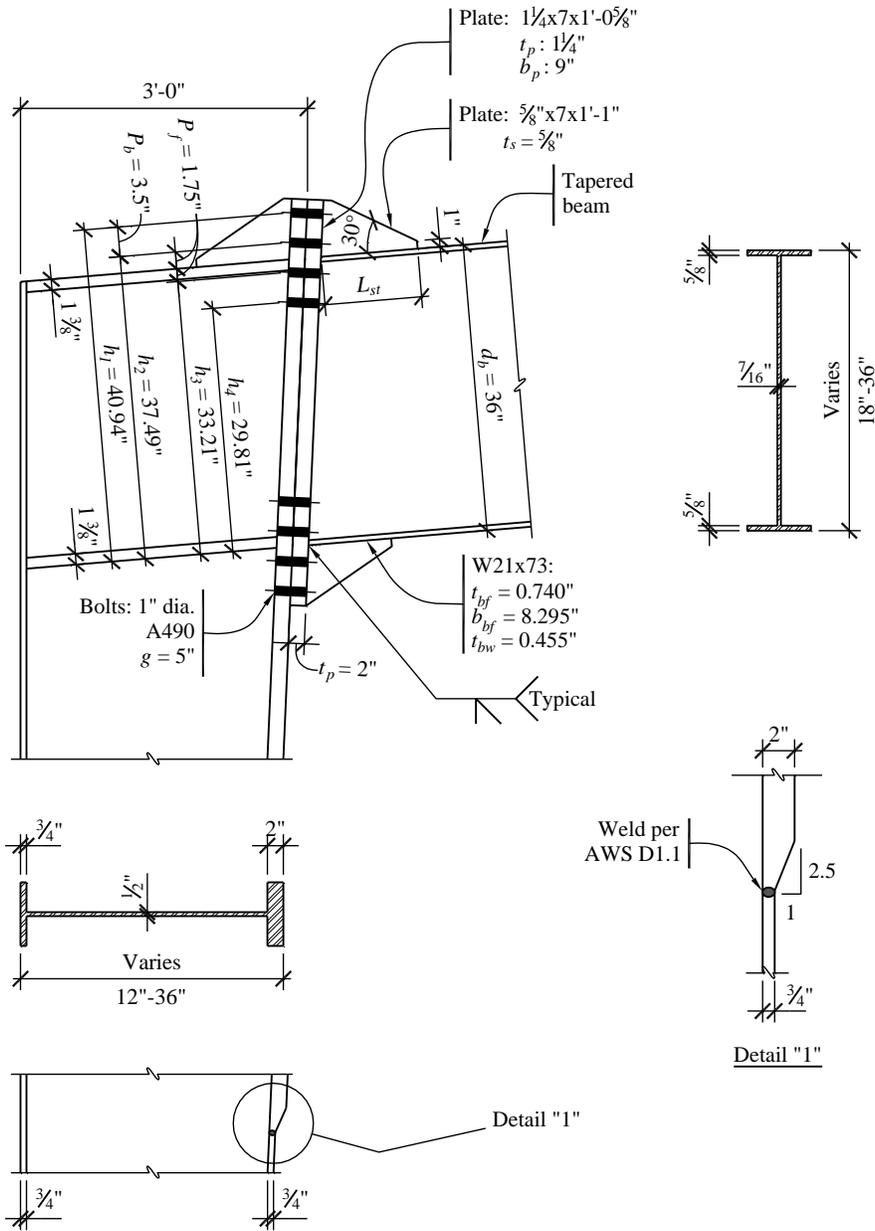
Figure 9.1-7 Bolted stiffened connection at knee
(1.0 in. = 25.4 mm)

The AISC 358 method for bolted stiffened end plate connection requires the determination of the maximum moment that can be developed by the beam. The steps in AISC 358 for bolted stiffened end plates follow:

Step 1.   Determine the maximum moment at the plastic hinge location. The end plate stiffeners at the top and bottom flanges increase the local moment of inertia of the beam, forcing the plastic hinge to occur away from the welds at the end of beam/face of column. The stiffeners should be long enough to force the plastic hinge to at least $d/2$ away from the end of the beam. With the taper of the section, the depth will be slightly less than 36 inches at the location of the hinge, but that reduction will be ignored here. The probable maximum moment, M_{pe}, at the plastic hinge is computed using AISC 358 Equation 2.4.3-1 as follows:

$$M_{pe} = C_{pr} R_y F_y Z_x$$

Where, per AISC 358 Equation 2.4.3-2:

$$C_{pr} = \frac{F_y + F_u}{2F_y} \le 1.2$$

$$C_{pr} = \frac{50 + 65}{2(50)}$$

$$C_{pr} = 1.15$$

where:

$R_y = 1.1$ from AISC 341 Table A.3-1

$Z_e = 309$ in.^{3}

$F_y = 50$ ksi

Therefore:

$$M_{pe} = (1.15)(1.1)(50 \text{ ksi})(309 \text{ in.}^3) = 19{,}541 \text{ in.-kip} = 1{,}628 \text{ ft-kip}$$

The moment at the column flange, M_f, which drives the connection design, is determined from AISC 358 Equation 6.10-1 as follows:

$$M_f = M_{pe} + V_u S_h$$

where:

V_u = shear at location of plastic hinge

L' = distance between plastic hinges

S_h = distance from the face of the column to the plastic hinge, ft.

$$S_h = L_{st} + t_p$$

where:

L_{st} = length of end-plate stiffener, as shown in AISC 358 Figure 6.4.

t_p = thickness of end plate, in.

$$L_{st} \geq \frac{h_{st}}{\tan 30°}$$

where:

h_{st} = height of the end-plate from the outside face of the beam flange to the end of the end-plate

$$L_{st} \geq \frac{(7\,\text{in.})}{\tan 30°}$$

$$L_{st} \geq 12.1 \text{ in.}$$

Use L_{st} = 13 in.

$$S_h = 13 \text{ in.} + 1.25 \text{ in.} = 14.3 \text{ in.}$$

$$L' = L_{out} - 2d_c - 2S_h$$

$$L' = (90\,\text{ft}) - 2(36\,\text{in.}) - 2(14.3\,\text{in.}) = 81.63 \text{ ft}$$

$$V_u = \frac{2M_{pe}}{L'} + V_{gravity}$$

$$V_u = \frac{2(1628\,\text{ft - kip})}{81.63\,\text{ft}} + 18.9\,\text{kips} = 58.8 \text{ kips}$$

$$M_f = 19{,}541 \text{ in.-kip} + (58.8 \text{ kips})(14.3 \text{ in.})$$

$$M_f = 1{,}698 \text{ ft-kip} = 20{,}379 \text{ in.-kip}$$

Step 2. Find bolt size for end plates. For a connection with two rows of two bolts inside and outside the flange, AISC 358 Equation 6.10-4 indicates the following:

$$d_{b\,req'd} = \sqrt{\frac{2M_f}{\pi \phi_n F_{nt} (h_1 + h_2 + h_3 + h_4)}}$$

where:

F_{nt} = nominal tensile stress of bolt, ksi

h_i = distance from the centerline of the beam compression flange to the centerline of the ith tension bolt row, in.

Try A490 bolts. See Figure 9.1-7 for bolt geometry.

$$d_{b\,req'd} = \sqrt{\frac{2(20{,}379 \text{ in.-kip})}{\pi(0.9)(113 \text{ ksi})(29.81 \text{ in.} + 33.31 \text{ in.} + 37.44 \text{ in.} + 40.94 \text{ in.})}} = 0.95 \text{ in.}$$

Use 1 in. diameter A490N bolts.

Step 3.   Determine the minimum end-plate thickness from AISC 358 Equation 6.10-5.

$$t_{p\,req'd} = \sqrt{\frac{1.11M_f}{\phi_d F_{yp} Y_p}}$$

where:

F_{yp} = specified minimum yield stress of the end plate material, ksi

Y_p = the end-plate yield line mechanism parameter from AISC 358 Table 6.4

ϕ_d = resistance factor for ductile limit states, taken as 1.0

From AISC 358 Table 6.4:

$$s = \frac{1}{2}\sqrt{b_p g}$$

where:

b_p = width of the end plate, in.

g = horizontal distance between bolts on the end plate, in.

$$s = \frac{1}{2}\sqrt{(9\text{ in.})(5\text{ in.})} = 3.35\text{in.}$$

$d_e = 7$ in. (see Figure 9.1-7)

Use Case 1 from AISC 358 Table 6.4, since $d_e > s$

$$Y_p = \frac{b_p}{2}\left[h_1\left(\frac{1}{2d_e}\right) + h_2\left(\frac{1}{p_{fo}}\right) + h_3\left(\frac{1}{p_{fi}}\right) + h_4\left(\frac{1}{s}\right) \right]$$

$$+ \frac{2}{g}\left[h_1\left(d_e + \frac{p_b}{4}\right) + h_2\left(p_{fo} + \frac{3p_b}{4}\right) + h_3\left(p_{fi} + \frac{p_b}{4}\right) + h_4\left(s + \frac{3p_b}{4}\right) + p_b^2 \right] + g$$

where:

p_{fo} = vertical distance between beam flange and the nearest outer row of bolts, in.

p_{fi} = vertical distance between beam flange and the nearest inner row of volts, in.

p_b = distance between the inner and our row of bolts, in.

$$Y_p = \frac{(9 \text{ in.})}{2} \left[(40.94 \text{ in.}) \left(\frac{1}{3.35 \text{ in.}} \right) + (37.44 \text{ in.}) \left(\frac{1}{1.75 \text{ in.}} \right) \right.$$

$$\left. + (33.31 \text{ in.}) \left(\frac{1}{1.75 \text{ in.}} \right) + (29.81 \text{ in.}) \left(\frac{1}{3.35 \text{ in.}} \right) \right]$$

$$+ \frac{2}{(5 \text{ in.})} \left[(40.94 \text{ in.}) \left(3.35 \text{ in.} + \frac{(3.5 \text{ in.})}{4} \right) + (37.44 \text{ in.}) \left(1.75 \text{ in.} + \frac{3(3.5 \text{ in.})}{4} \right) \right.$$

$$\left. + (33.31 \text{ in.}) \left(1.75 \text{ in.} + \frac{3.5 \text{ in.}}{4} \right) + (29.81 \text{ in.}) \left(3.35 \text{ in.} + \frac{3(3.5 \text{ in.})}{4} \right) + (3.5 \text{ in.})^2 \right]$$

$$+ (5 \text{ in.})$$

$$Y_P = 499 \text{ in.}$$

$$t_{p \, req'd} = \sqrt{\frac{1.11(20{,}379 \text{ in.-kip})}{(1.0)(36 \text{ ksi})(499 \text{ in.})}} = 1.12 \text{ in.}$$

Use 1.25-inch thick end-plates.

Step 4.   Calculate the factored beam flange force from AISC 358 Equation 6.10-6.

$$F_{fu} = \frac{M_f}{d - t_{bf}}$$

where:

d = depth of the beam, in.

t_{bf} = thickness of beam flange, in.

$$F_{fu} = \frac{20{,}379 \text{ in.-kip}}{36 \text{ in.} - 5/8 \text{ in.}} = 576 \text{ kips}$$

Step 5.   Determine the end-plate stiffener thickness from AISC 358 Equation 6.10-9.

$$t_s \geq t_{bw} \left(\frac{F_{yb}}{F_{ys}} \right)$$

where:

t_{bw} = thickness of the beam web, in.

F_{yb} = specified minimum yield stress of beam material, ksi

F_{ys} = specified minimum yield stress of stiffener material, ksi

$$t_s \geq (7/16 \text{ in.}) \left(\frac{50 \text{ ksi}}{36 \text{ ksi}} \right) = 0.61 \text{ in.}$$

Use 5/8-inch plates.

The stiffener width-thickness ratio must also comply with AISC 358 Equation 6.10-10.

$$\frac{h_{st}}{t_s} \leq 0.56 \sqrt{\frac{E}{F_{ys}}}$$

$$h_{st} \leq 0.56 \sqrt{\frac{(29000 \text{ ksi})}{(36 \text{ ksi})}} (5/8 \text{ in.})$$

$$h_{st} \leq 9.93 \text{in.}$$

$$h_{st} = 7 \text{ in.} \hspace{4cm} \text{OK}$$

Step 6.   Check bolt shear rupture strength at the compression flange by AISC 358 Equation 6.10-11.

$$V_u < \phi_n R_n = \phi_n \left(n_b \right) F_v A_b$$

where:

ϕ_n = resistance factor for non-ductile limit states, taken as 0.9

n_b = number of bolts at compression flange

F_v = nominal shear stress of bolts from AISC 360 Table J3.2, ksi

A_b = nominal bolt area, in.

$$\phi_n R_n = (0.9)(8)(68) \left(\pi \frac{1^2}{4} \right) = 385 \text{ kips} > 58.8 \text{ kips} \hspace{2cm} \text{OK}$$

Step 7.   Check bolt bearing/tear-out of the end-plate and column flange by AISC 358 Equation 6.10-12.

$$V_u < \phi_n R_n = \phi_n \left(n_i \right) r_{ni} + \phi_n \left(n_o \right) r_{no}$$

where:

n_i = number of inner bolts

n_o = number of outer bolts

$r_{ni} = 1.2 L_c t F_u < 2.4 d_b t F_u$ for each inner bolt

$r_{no} = 1.2 L_c t F_u < 2.4 d_b t F_u$ for each outer bolt

L_c = clear distance, in the direction of force, between the edge of the hole and the edge of the adjacent hole or edge of the material, in.

t = end-plate or column flange thickness, in.

F_u = specified minimum tensile strength of end-plate or column flange material, ksi

d_b = diameter of bolt, in.

$$L_{ci} = p_b - d_e$$

$$L_{co} = L_e - \frac{d_e}{2}$$

where:

d_e = effective area of bolt hole, in.

L_e = edge spacing of the bolts, in.

$$L_{ci} = 3.5 \text{ in.} - 1\tfrac{1}{8} \text{ in.} = 2.38 \text{ in.}$$

$$L_{co} = 1.75 \text{ in.} - \frac{1\tfrac{1}{8} \text{ in.}}{2} = 1.19 \text{ in.}$$

$$r_{ni} = 1.2(2.38 \text{ in.})(1.25 \text{ in.})(58 \text{ ksi}) < 2.4(1 \text{ in.})(1.25 \text{ in.})(58 \text{ ksi})$$

$$r_{ni} = 207 \text{ kips} < 174 \text{ kips}$$

$$r_{ni} = 174 \text{ kips}$$

$$r_{no} = 1.2 L_c t F_u < 2.4 d_b t F_u$$

$$r_{no} = 1.2(1.19 \text{ in.})(1.25 \text{ in.})(58 \text{ ksi}) < 2.4(1 \text{ in.})(1.25 \text{ in.})(58 \text{ ksi})$$

$$r_{no} = 103 \text{ kips} < 174 \text{ kips}$$

$$r_{no} = 103 \text{ kips}$$

$$V_u < \phi_n R_n = (1)(4)(174 \text{ kips}) + (1)(4)(103 \text{ kips})$$

$$\phi_n R_n = 998 \text{ kips} > 58.8 \text{ kips}$$

OK

Step 8.   Check the column flange for flexural yielding by AISC 358 Equation 6.10-13.

$$t_{cf\ req'd} = \sqrt{\frac{1.11M_f}{\phi_d F_{yc} Y_c}} \le t_{cf}$$

where:

F_{yc} = specified minimum yield stress of column flange material, ksi

Y_c = stiffened column flange yield line from AISC 358 Table 6.6

t_{cf} = column flange thickness, in.

$$Y_c = \frac{b_{cf}}{2}\left[h_1\left(\frac{1}{s}\right) + h_2\left(\frac{1}{p_{so}}\right) + h_3\left(\frac{1}{p_{si}}\right) + h_4\left(\frac{1}{s}\right) \right]$$
$$+ \frac{2}{g}\left[h_1\left(s + \frac{p_b}{4}\right) + h_2\left(p_{so} + \frac{3p_b}{4}\right) + h_3\left(p_{si} + \frac{p_b}{4}\right) + h_4\left(s + \frac{3p_b}{4}\right) + p_b^2 \right] + g$$

where:

b_{cf} = column flange width, in.

p_{si} = distance from column stiffener to inner bolts, in.

p_{so} = distance from column stiffener to outer bolts, in.

$$s = \frac{1}{2}\sqrt{b_{cf}\, g}$$

$$s = \frac{1}{2}\sqrt{(8\text{ in.})(5\text{ in.})} = 3.16\text{ in.}$$

$$Y_c = \frac{(8\text{ in.})}{2}\left[(40.94\text{ in.})\left(\frac{1}{3.16\text{ in.}}\right) + (37.44\text{ in.})\left(\frac{1}{1.75\text{ in.}}\right) \right.$$
$$\left. + (33.31\text{ in.})\left(\frac{1}{1.75\text{ in.}}\right) + (29.81\text{ in.})\left(\frac{1}{3.16\text{ in.}}\right) \right]$$
$$+ \frac{2}{(5\text{ in.})}\left[(40.94\text{ in.})\left(3.16\text{ in.} + \frac{(3.5\text{ in.})}{4}\right) + (37.44\text{ in.})\left(1.75\text{ in.} + \frac{3(3.5\text{ in.})}{4}\right) \right.$$
$$\left. + (33.31\text{ in.})\left(1.75\text{ in.} + \frac{3.5\text{ in.}}{4}\right) + (29.81\text{ in.})\left(3.16\text{ in.} + \frac{3(3.5\text{ in.})}{4}\right) + (3.5\text{ in.})^2 \right]$$
$$+ (5\text{ in.})$$

$$Y_c = 497\text{ in.}$$

$$t_{cf\ req'd} = \sqrt{\frac{1.11(20,379\ \text{in.-kip})}{(1)(50\ \text{ksi})(497\ \text{in.})}} \leq 2\ \text{in.}$$

$$t_{cf\ req'd} = 0.95\ \text{in.} \leq 2\ \text{in.}$$

Column flange of 2 inches is OK.

Step 9.   Determine the required stiffener force by AISC 358 Equation 6.10-14.

$$\phi_d M_{cf} = \phi_d F_{yc} Y_c t_{cf}^2$$

$$\phi_d M_{cf} = (1)(50\ \text{ksi})(497\ \text{in.})(2\ \text{in.})^2 = 99,344\ \text{in.-kip}$$

The equivalent column flange design force used for stiffener design by AISC 358 Equation 6. 10-15.

$$\phi_d R_n = \frac{\phi_d M_{cf}}{(d - t_{bf})}$$

$$\phi_d R_n = \frac{(99,690\ \text{in.-kip})}{(36\ \text{in.}) - (5/8\ \text{in.})} = 2,808\ \text{kips}$$

2,808 kips > 576 kips   OK

Step 10.   Check local column web yielding strength of the unstiffened column web at the beam flanges by AISC 358 Equations 6. 10-16and 6. 10-17.

$$\phi_d R_n \geq F_{fu}$$

$$\phi_d R_n = \phi_d C_t \left(6k_c + t_{bf} + 2t_p\right) F_{yc} t_{cw}$$

where:

$C_t = 0.5$ if the distance from the column top to the top of the beam flange is less than the depth of the column: otherwise 1.0

k_c = distance from outer face of the column flange to web toe of fillet weld, in.

t_p = end-plate thickness, in.

F_{yc} = specified yield stress of the column web material, ksi

t_{cw} = column web thickness, in.

t_{bf} = beam flange thickness, in.

$$\phi_d R_n = (1.0)(0.5)\left(6\left(2 \text{ in.} + \tfrac{5}{16} \text{ in.}\right)+(0.5 \text{ in.})+2(1.25 \text{ in.})\right)(50 \text{ ksi})(0.5 \text{ in.})$$

$$\phi_d R_n = 212 \text{ kips} \leq 576 \text{ kips}$$

The design is not acceptable. Column stiffeners need to be provided.

Step 11. Check the unstiffened column web buckling strength at the beam compression flange by AISC 358 Equations 6. 10-18and 6. 10-20.

$$\phi R_n \geq F_{fu}$$

$$\phi R_n = \phi \frac{12 t_{cw}^3 \sqrt{EF_{yc}}}{h}$$

where:

h = clear distance between flanges when welds are used for built-up shapes, in.

$$\phi R_n = (0.75)\frac{12(0.5 \text{ in.})^3 \sqrt{(29{,}000 \text{ ksi})(50 \text{ ksi})}}{(36 \text{ in.} - 2 \text{ in.} - 0.75 \text{ in.})} = 42 \text{ kips}$$

42 kips < 576 kips   NOT OK

Step 12. Check the unstiffened column web crippling strength at the beam compression flange by AISC 358 Equation 6-10-23.

$$\phi R_n \geq F_{fu}$$

$$\phi R_n = \phi 0.40 t_{cw}^2 \left[1 + 3\left(\frac{N}{d_c}\right)\left(\frac{t_{cw}}{t_{cf}}\right)^{1.5}\right]\sqrt{\frac{EF_{yc}t_{cf}}{t_{cw}}}$$

where:

N = thickness of beam flange plus 2 times the groove weld reinforcement leg size, in.

d_c = overall depth of the column, in.

$$R_n = (0.75)(0.80)(0.5 \text{ in.})^2 \left[1 + 3\left(\frac{3(\tfrac{5}{8} \text{ in.})}{36 \text{ in.}}\right)\left(\frac{0.5 \text{ in.}}{2 \text{ in.}}\right)^{1.5}\right]\sqrt{\frac{(29{,}000 \text{ ksi})(50 \text{ ksi})(2 \text{ in.})}{0.5 \text{ in.}}}$$

$$R_n = 184 \text{ kips}$$

184 kips < 576 kips   NOT OK

Step 13. Check the required strength of the stiffener plates by AISC 358 Equation 6-10-25.

9-30

$$F_{su} = F_{fu} - \min \phi R_n = 576 \text{ kips} - 42 \text{ kips} = 534 \text{ kips}$$

where:

$\min \phi R_n$ = the minimum design strength value from column flange bending check, column web yielding, column web buckling and column web crippling check

Although AISC 358 says to use this value of 534 kips to design the continuity plate, a different approach will be used in this example. In compression, the continuity plate will be designed to take the full force delivered by the beam flange, F_{su}. In tension, however, the compressive limit states (web buckling and web yielding) are not applicable and column web yielding will control the design instead. The tension design force can be taken as follows:

$$F_{su} = F_{fu} - \phi R_{n,web\ yielding} = 576 \text{kips} - 212 \text{ kips} = 364 \text{kips}$$

Step 14. Design the continuity plate for required strength by AISC 360 Section J10.

Find the cross-sectional area required by the continuity plate acting in tension:

$$A_{s,reqd} = \frac{F_{su}}{\phi F_y}$$

$$A_{s,reqd} = \frac{364 \text{ kips}}{(0.9)(50 \text{ ksi})} = 8.1 \text{ in.}^2$$

$$t_{s,reqd} = \frac{A_{s,reqd}}{b_{st}}$$

$$t_{s,reqd} = \frac{8.1 \text{ in.}^2}{8 \text{ in.}} = 1.01 \text{ in.}$$

Use a 1-3/8-inch continuity plate. As it will be shown later, net section rupture (not gross yielding) will control the design of this plate.

From AISC Section J10.8, calculate member properties using an effective length of $0.75h$ and a column web length of $12t_w = 6$ in.:

$$I_x = \frac{t_{cw}12t_{cw}^3}{12} + \frac{(b_{st} - t_{cw})t_{st}^3}{12}$$

$$I_x = \frac{(0.5 \text{ in.})(6 \text{ in.})^3}{12} + \frac{(8 \text{ in.} - 0.5 \text{ in.})(1.375 \text{ in.})^3}{12} = 10.6 \text{ in.}^4$$

$$I_y = \frac{t_{st}b_{st}^3}{12} + \frac{(12t_{cw} - t_{st})t_{cw}^3}{12}$$

$$I_y = \frac{(1.375 \text{ in.})(8 \text{ in.})^3}{12} + \frac{(6 \text{ in.} - 1.375 \text{ in.})(0.5 \text{ in.})^3}{12} = 58.7 \text{ in.}^4$$

$$J \cong \frac{b_{st} t_{st}^3}{3} + \frac{(12 t_{cw} - t_{st}) t_{cw}^3}{3}$$

$$J \cong \frac{(8 \text{ in.})(1.375 \text{ in.})^3}{3} + \frac{(6 \text{ in.} - 1.375 \text{ in.})(0.5 \text{ in.})^3}{3} = 7.13 \text{ in.}^4$$

$$A = b_{st} t_{st} + (12 t_{cw} - t_{st}) t_{cw}$$

$$A = (8 \text{ in.})(1.375 \text{ in.}) + (6 \text{ in.} - 1.375 \text{ in.})(0.5 \text{ in.}) = 13.3 \text{ in.}^2$$

$$r_y = \sqrt{\frac{I_y}{A}}$$

$$r_y = \sqrt{\frac{58.7 \text{ in.}^4}{13.3 \text{ in.}^2}} = 2.1 \text{ in.}$$

$$L = 0.75h = 0.75 (d_c - t_{f1} - t_{f2} - 2 t_{weld})$$

$$L = 0.75 (36 \text{ in.} - 2 \text{ in.} - 0.75 \text{ in.} - 2(5/16 \text{ in.})) = 24.5 \text{ in.}$$

Check the continuity plate in compression from AISC 360 Section J4.4:

$$\frac{KL}{r_y} = \frac{(1.0)(24.5 \text{ in.})}{2.1 \text{ in.}} = 11.65 \le 25$$

Strength in the other direction does not need to be checked because the cruciform section will not buckle in the plane of the column web.

Since *KL/r* is less than 25, use AISC 360 Equation J4-6 to determine compression strength:

$$\phi P_n = \phi F_y A_g$$

$$\phi P_n = (0.9)(50 \text{ ksi})(13.3 \text{ in.}^2) = 599 \text{ kips}$$

Check the continuity plate in tension. The continuity plate had been previously sized for adequacy to tensile yielding of the gross section. Now tensile rupture of the net section must be checked using AISC 360 Section D2-2. The critical section will be analyzed where the continuity plates are clipped adjacent to the k-region of the column.

$$A_e = (t_{st})(b_{st} - 2(t_{weld} + \text{clip}))$$

$$A_e = (1.375 \text{ in.})(8 \text{ in.} - 2(5/16 \text{ in.} + 0.5 \text{ in.})) = 8.77 \text{ in.}^2$$

$$\phi_t P_n = \phi_t F_u A_e = 381 \text{ kips} > 364 \text{ kips}$$

OK

Step 15.   Check the panel zone for required strength per AISC 360 Equation J10-9.

$$P_c = F_y A$$

where:

A = column cross sectional area, in^2.

$$P_c = (50 \text{ ksi})(38.6 \text{ in.}) = 1{,}931 \text{ kips}$$

The column axial force is:

$$P_r = 37 \text{ kips}$$

$$\frac{P_r}{P_c} = \frac{37 \text{ kips}}{1{,}931 \text{ kips}} = 0.02 < 0.75$$

Therefore, use AISC 360 Equation J10-11. Note that panel zone flexibility was accounted for in the ETABS model.

$$\phi R_n = \phi 0.60 F_y d_c t_{cw} \left(1 + \frac{3 b_{cf} t_{cf}^2}{d_b d_c t_{cw}} \right)$$

$$\phi R_n = (0.9)(0.60)(50 \text{ ksi})(36 \text{ in.})(0.5 \text{ in.}) \left(1 + \frac{3(8 \text{ in.})(2 \text{ in.})^2}{(36 \text{ in.})(36 \text{ in.})(0.5 \text{ in.})} \right)$$

$$\phi R_n = 558 \text{ kips} < 576 \text{ kips}$$

NOT OK

The column web is not sufficient to resist the panel zone shear. Although doubler plates can be added to the panel zone to increase strength, this may be an expensive solution. A more economical solution would be to simply upsize the column web to a sufficient thickness, such as 5/8 inch.

$$\phi R_n = \phi 0.60 F_y d_c t_{cw} \left(1 + \frac{3 b_{cf} t_{cf}^2}{d_b d_c t_{cw}} \right)$$

$$\phi R_n = (0.9)(0.60)(50 \text{ ksi})(36 \text{ in.})(5/8 \text{ in.}) \left(1 + \frac{3(8 \text{ in.})(2 \text{ in.})^2}{(36 \text{ in.})(36 \text{ in.})(5/8 \text{ in.})} \right)$$

$$\phi R_n = 680 \text{ kips} > 576 \text{ kips}$$

Note that changing the column member properties might affect the analysis results. In this example, this is not the case, although the slight difference in web thickness would result in marginally different values for some of the end-plate connection calculations. For simplicity, these changes are not undertaken in this example.

9.1.5.3 Frame at the ridge. The ridge joint detail is shown in Figure 9.1-8. A fully welded connection is selected.
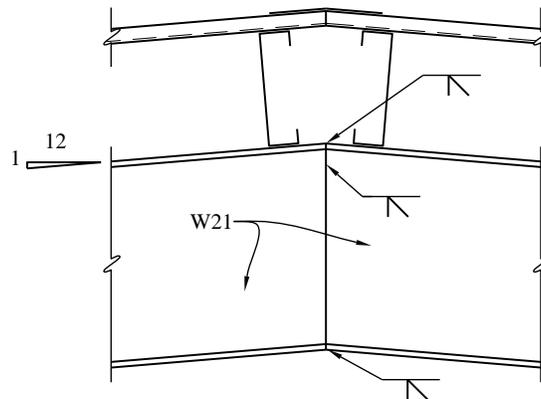
Figure 9.1-8 Connection at ridge

This connection is designed to the strength requirements of AISC 360.The proportioning requirements of AISC 358 (which ensure ductile behavior) are not applicable because there should not be a plastic hinge forming in this vicinity. Lateral seismic forces produce no moment at the ridge until yielding takes place at one of the knees. Vertical accelerations on the dead load do produce a moment at this point; however, the value is small compared to all other moments and does not appear to be a concern. Once seismic loads produce a plastic hinge at one knee, further lateral displacement produces positive moment at the ridge. Under the condition on which the AISC 358 design is based (a full plastic moment is produced at each knee), the moment at the ridge will simply be the static moment from the gravity loads less the horizontal thrust times the rise from knee to ridge. Analyzing this frame under the gravity load case $1.2D + 0.2S$, the static moment is 406 ft-kip and the reduction for the thrust is 128 ft-kip, leaving a net positive moment of 278 ft-kip, coincidentally close to the design moment for the factored gravity loads.

9.1.5.4 Design of mezzanine framing. The design of the framing for the mezzanine floor at the east end of the building is controlled by gravity loads. The concrete-filled 3-inch, 20-gauge steel deck of the mezzanine floor is supported on steel beams spaced at 10 feet and spanning 20 feet (Figure 9.1-2). The steel beams rest on three-span girders connected at each end to the portal frames and supported on two intermediate columns (Figure 9.1-1). The girder spans are approximately 30 feet each. Those lateral forces that are received by the mezzanine are distributed to the frames and diagonal bracing via the floor diaphragm. A typical beam-column connection at the mezzanine level is provided in Figure 9.1-9. The design of the end plate connection is similar to that at the knee, but simpler because the beam is horizontal and not tapered. Also note that demands on the end-plate connection will be less because this connection is not at the end of the column.

L3x3 strut

3" concrete slab

3" embossed 20 ga. deck

W14x43

Split W27x84

W21x62

MC8x18.7

(b)
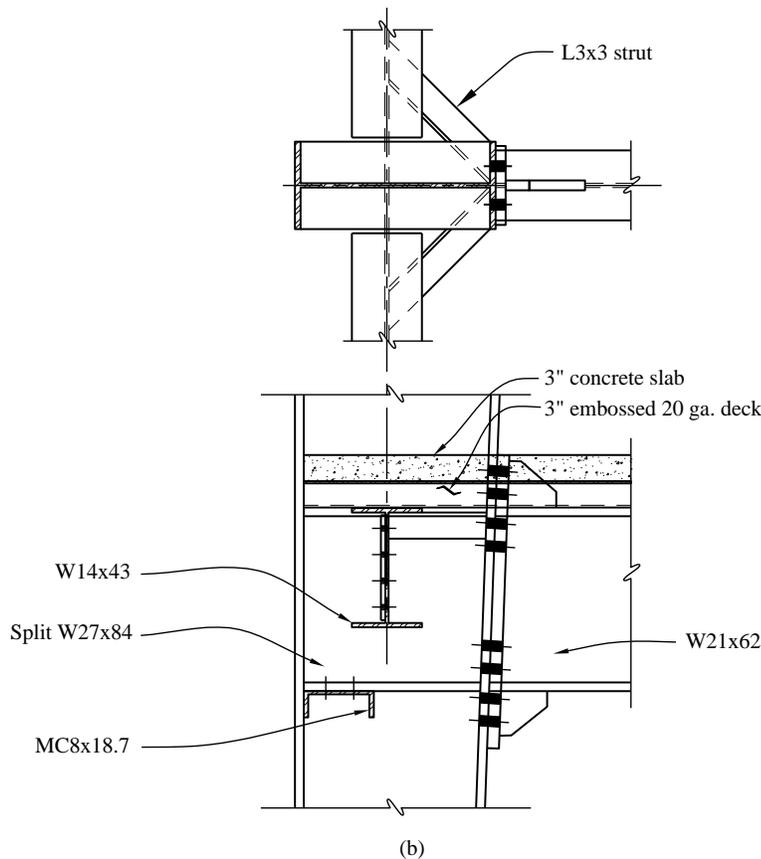
Figure 9.1-9 Mezzanine framing (1.0 in. = 25.4 mm)

9.1.5.5 Braced frame diagonal bracing

Although the force in the diagonal X-braces can be either tension or compression, only the tensile value is considered because it is assumed that the diagonal braces are capable of resisting only tensile forces.

See AISC 341 Section F1 for requirements on braces for OCBFs. The strength of the members and connections, including the columns in this area but excluding the brace connections, must be based on *Standard* Section 12.4.2.3:

$$1.4D + 1.0L + 0.2S + \rho Q_E$$

$$0.7D + \rho Q_E$$

Recall that a 1.0 factor is applied to *L* when the live load is greater than 100 psf (*Standard* Sec. 2.3.2). For the case discussed here, the "tension only" brace does not carry any live or dead load, so the load factor does not matter.

For simplicity, we can assume that the lateral force is equally divided among the roof level braces and is slightly amplified to account for torsional effects. Thus the brace force can be approximated using the following equation:

$$P_u = 0.55V \times \frac{1}{2} \times \frac{1}{\cos\theta}$$

$$P_u = 0.55(211 \text{ kips}) \times \frac{1}{2} \times \frac{1}{\cos 47°} = 85 \text{ kips}$$

All braces at this level will have the same design. Choose a brace member based on tensile yielding of the gross section by AISC 360 Equation D2-1:

$$\phi_t P_n = \phi_t F_y A_g$$

$$A_{g,reqd} = \frac{85 \text{ kips}}{(0.9)(36 \text{ ksi})} = 2.62 \text{ in.}^2$$

This also needs to be checked for tensile rupture of the net section. Demand will be taken as either the expected yield strength of the brace or the amplified seismic load. Try a 2L3½x3x 7/16, which is the smallest seismically compact angle shape available.

$$A_g = 5.34 \text{ in.}^2$$

The *Kl/r* requirement of AISC 341 Section F1.5b does not apply because this is not a V or an inverted V configuration.

Check net rupture by AISC 360 Equation D2-2 and D3-1:

$$\phi_t P_n = \phi_t F_u A_e$$

$$A_e = A_n U$$

Determine the shear lag factor, *U*, from AISC 360, Table D3.1, Case 2. In ordered to calculate *U*, the weld length along the double angles needs to be determined.

$$U = 1 - \frac{\bar{x}}{L}$$

Brace connection demand is given as the expected yield strength of the brace in tension per AISC 341 Section F1.6a.

$$R_y F_y A_g = (1.5)(36 \text{ ksi})(5.34 \text{ in.}^2) = 288 \text{ kips}$$

Expected yield strength of the brace is 288 kips. However, AISC 341 Section F1.6a limits the brace connection design force to the amplified seismic load.

$$\Omega_0 P_{QE} = (2)(85 \text{ kips}) = 170 \text{ kips}$$

Use four fillet welds, two on each angle. Try 1/4-inch welds using AISC 360 Equation J2-3:

$$\phi R_n = \phi F_w A_w$$

$$\phi R_n = \phi \left(0.60 F_{EXX} \right) \left(0.707 t_w \right) \left(L \right)$$

$$L = \frac{170 \text{ kips}}{4 \left(0.75 \right) \left(0.6 \right) \left(70 \text{ ksi} \right) \left(0.707 \right) \left(0.25 \text{ in.} \right)} = 7.63 \text{ in.}$$

Use four 1/4-inch fillet welds 8 inches long.

Check the base metal:

$$\phi R_n = \phi F_{BM} A_{BM}$$

Shear yielding from AISC 360 Equation J4-3:

$$\phi R_n = \phi 0.6 F_y A_g$$

$$\phi R_n = \left(1.0 \right) \left(0.6 \right) \left(36 \text{ ksi} \right) \left(0.25 \text{ in.} \right) (8 \text{ in.}) = 173 \text{kips}$$

OK

Shear rupture from AISC 360 Equation J4-4:

$$\phi R_n = \phi 0.6 F_u A_{nv}$$

$$\phi R_n = \left(0.75 \right) \left(0.6 \right) \left(58 \text{ ksi} \right) \left(0.25 \text{ in.} \right) (8 \text{ in.})$$

OK

Calculate the shear lag factor and the effective net area:

$$U = 1 - \frac{(0.846 \text{ in.})}{(9 \text{ in.})} = 0.89$$

$$A_e = \left(5.34 \text{ in.}^2 \right) (0.89) = 4.78 \text{ in.}^2$$

Calculate the tensile rupture strength:

$$\phi_t P_n = (0.9)(58 \text{ ksi}) \left(6.1 \text{in.}^2 \right) = 207 \text{ kips} > 170 \text{ kips}$$

OK

Additionally, the capacity of the eave strut at the roof must be checked. The eave strut, part of the braced frame, also acts as a collector element and must be designed using the overstrength factor per *Standard* Section 12.10.2.1.

9.1.5.6 Roof deck diaphragm. In the E-W direction, the base shear is 274 kips (Section 6.1.4.2) with 77 percent or 211 kips at the roof. Torsion is not significant, so a simple approximation is to take half the force to each side and divide by the length of the building, which yields (211,000/2)/180 feet = 586 plf.

In the N-S direction, the shear is highest just west of gridline I (the westernmost frame with the mezzanine) due to the higher stiffness of the frames with the mezzanine beams. A three-dimensional model or a rigid-diaphragm analysis is required to determine the diaphragm reactions at each frame, from which the diaphragm shears are determined. From the analysis, fames I, J, and K together resist 54% of the roof shear, while only 22% of the roof is east of line I. Thus approximately 31% of the roof shear must be

resisted by the diaphragm immediately west of line I. This is 42 kips, which, divided by 90 feet, gives a maximum shear of 470 plf.

9.2 SEVEN-STORY OFFICE BUILDING, LOS ANGELES, CALIFORNIA

The following example illustrates the preliminary design of a seven-story office building in an area of significant seismicity. Two alternative framing arrangements are developed for comparison: a Special Moment Frame with frames at the building perimeter, and a Special Concentrically Braced Frame, with braces located near a central core.

9.2.1 Building Description

9.2.1.1 General description. This seven-story office building of rectangular plan configuration is 177 feet, 4 inches long in the E-W direction and 127 feet, 4 inches wide in the N-S direction (Figure 9.2-1). The building has a penthouse. It is framed in structural steel with 25-foot bays in each direction. The typical story height is 13 feet, 4 inches; the first story is 22 feet, 4 inches high. The penthouse extends 16 feet above the roof level of the building and covers the area bounded by Gridlines C, F, 2 5 in Figure 9.2-1. Floors consist of 3-1/4-inch lightweight concrete over composite metal deck. The elevators and stairs are located in the central three bays.

9.2.1.2 Alternatives. This example includes two alternatives—a steel moment-resisting frame and a concentrically braced frame:

Alternative A: Seismic force resistance is provided by special moment frames (SMF) with prequalified Reduced Beam Section (RBS) connections located on the perimeter of the building (on Gridlines A, H, 1 6 in Figure 9.2-1, also illustrated in Figure 9.2-2). There are five bays of moment frames on each line.

Alternative B: Seismic force resistance is provided by four special concentrically braced frames (SCBF) in each direction. They are located in the elevator core walls between Columns 3C and 3D, 3E and 3F, 4C and 4D, 4E and 4F in the E-W direction and between Columns 3C and 4C, 3D and 4D, 3E and 4E, 3F and 4F in the N-S direction (Figure 9.2-1). The braced frames are in a two-story X configuration. The frames are identical in brace size and configuration, but there are some minor differences in beam and column sizes. Braced frame elevations are shown in Figures 9.2-10 through 9.2-12.

9.2.1.3 Scope. The example covers:

Seismic design parameters (Sec. 9.2.2.1)

Analysis of perimeter moment frames (Sec. 9.2.4.1)

Beam and column proportioning (Sec. 9.2.4.2.3)

Moment frame connection design (Sec. 9.2.4.2.5)

Analysis of concentrically braced frames (Sec. 9.2.5.1)

Proportioning of braces (Sec. 9.2.5.2.1)

Braced frame connection design (Sec. 9.2.5.2.5)
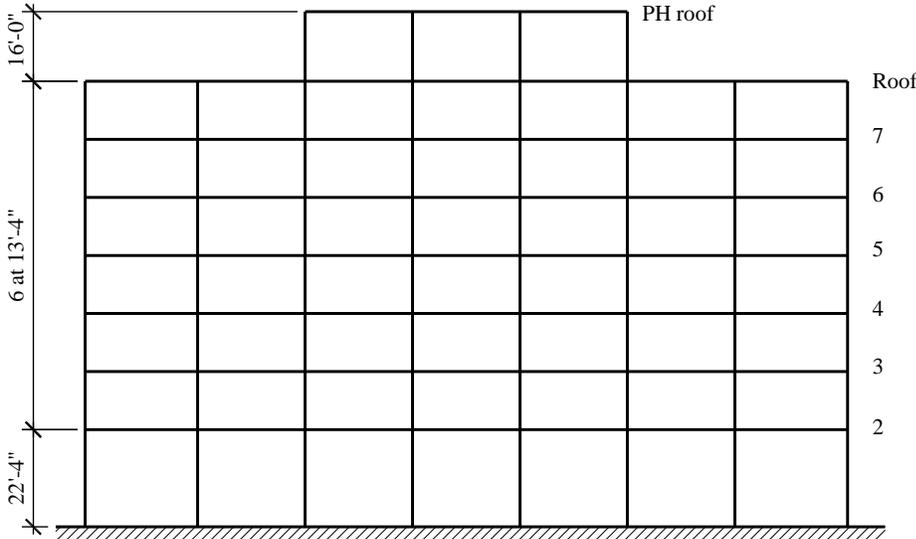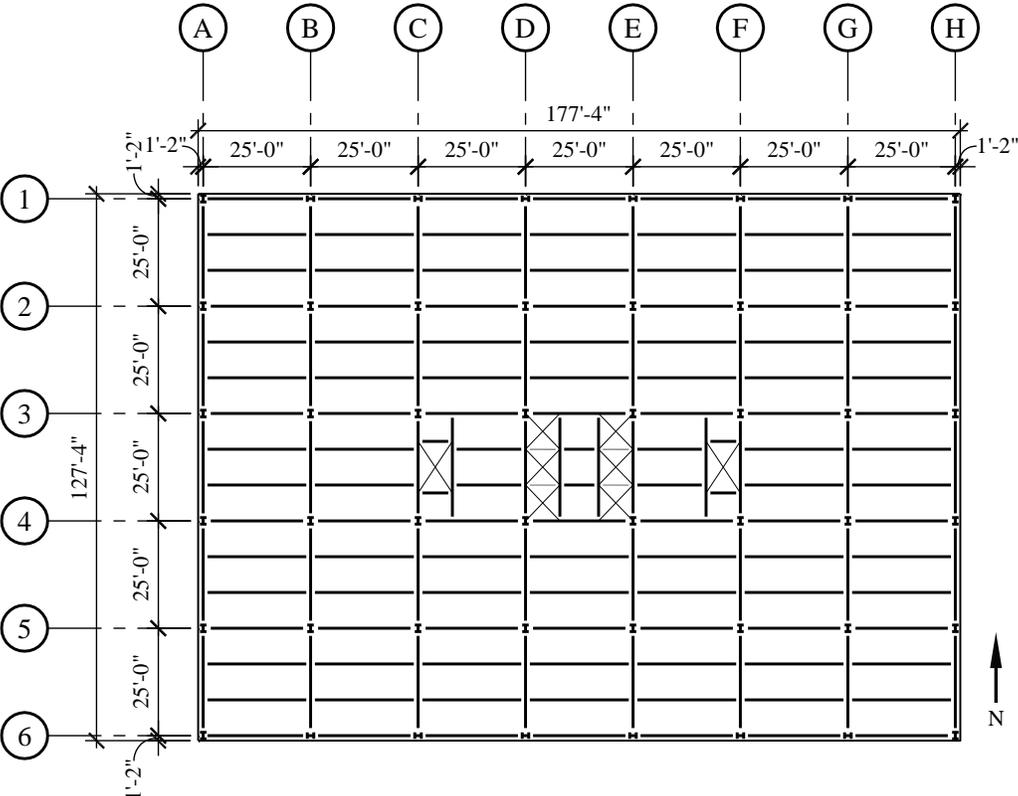
Figure 9.2-1 Typical floor framing plan and building section
(1.0 in. = 25.4 mm, 1.0 ft = 0.3048 m)

Figure 9.2-2 Framing plan for special moment frame and special concentrically braced frames
(1.0 in. = 25.4 mm, 1.0 ft = 0.3048 m)

9.2.2   Basic Requirements

9.2.2.1 *Provisions* **parameters.** See Section 3.2 for an example illustrating the determination of design ground motion parameters. For this example, the parameters are as follows

$S_{DS} = 1.0$

$S_{D1} = 0.6$

Risk Category II

Seismic Design Category D

For Alternative A, Steel Special Moment Frame (*Standard* Table 12.2-1)
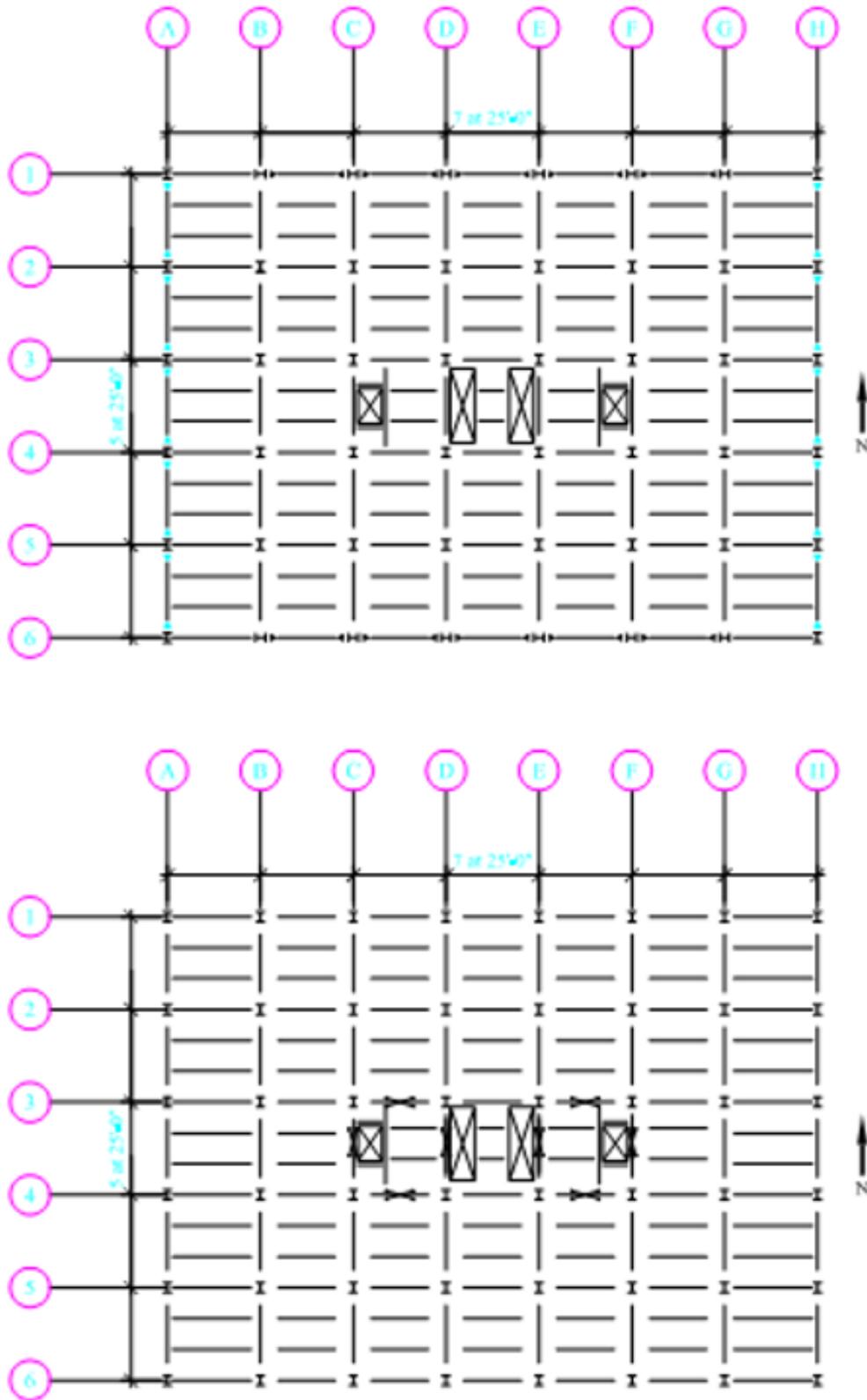
$R = 8$

$\Omega_0 = 3$

$C_d = 5.5$

For Alternative B, Steel Special Concentrically Braced Frame (*Standard* Table 12.2-1):

$R = 6$

$\Omega_0 = 2$

$C_d = 5$

9.2.2.2 Loads.

Roof live load (*L*): 25 psf

Penthouse roof dead load (*D*): 25 psf

Exterior walls of penthouse: 25 psf of wall

Roof *DL* (roofing, insulation, deck beams, girders, fireproofing, ceiling, mechanical, electrical plumbing): 55 psf

Exterior wall cladding: 25 psf of wall

Penthouse floor *D*: 65 psf

Penthouse Equipment: 39 psf

Floor *L*: 50 psf

Floor *D* (deck, beams, girders, fireproofing, ceiling, mechanical electrical, plumbing, partitions): 68 psf

Floor *L* reductions: per the IBC

9.2.2.3 Basic gravity loads.

Penthouse roof:

Roof slab = (0.025 ksf)(25 ft)(75 ft)	=	47 kips
Walls = (0.025 ksf)(8 ft)(200 ft)	=	40 kips
Columns = (0.110 ksf)(8 ft)(8 ft)	=	7 kips
Total	=	94 kips

Lower roof:

Roof slab = (0.055 ksf)[(127.33 ft)(177.33 ft) - (25 ft)(75 ft)	=	1139 kips
Penthouse floor = (0.065 ksf)(25 ft)(75 ft)	=	122 kips
Walls = 40 kips + (0.025 ksf)(609 ft)(6.67 ft)	=	142 kips
Columns = 7 kips + (0.170 ksf)(6.67 ft)(48 ft)	=	61 kips
Equipment = (0.039 ksf)(25 ft)(75 ft)	=	73 kips
Total		= 1,537 kips

Typical floor:

Floor = (0.068 ksf)(127.33 ft)(177.33 ft)	= 1,535 kips
Walls = (0.025 ksf)(609 ft)(13.33 ft)	= 203 kips
Columns = (0.285 ksf)(13.33 ft)(48 ft)	= 182 kips
Total	= 1,920 kips

Total weight of building = 94 kips + 1,537 kips + 6 (1,920 kips)   = 13,156 kips

9.2.2.4 Materials

Concrete for floors: $f_c' = 3$ ksi, lightweight (LW)

All other concrete: $f_c' = 4$ ksi, normal weight (NW)

Structural steel:
> Wide flange sections: ASTM A992, Grade 50
> HSS: ASTM A1085, Grade 50
> Plates: ASTM A36

9.2.3   Structural Design Criteria

9.2.3.1 Building configuration. The building has no vertical irregularities despite the relatively tall height of the first story. The exception of *Standard* Section 12.3.2.2 is taken, in which the drift ratio of adjacent stories are compared rather than the stiffness of the stories. In the three-dimensional analysis, the first story drift ratio is less than 130 percent of that for the story above. Because the building is symmetrical in plan, plan irregularities would not be expected. Analysis reveals that Alternative B is torsionally irregular (Irregularity Type 1a), which is not uncommon for core-braced buildings.

9.2.3.2 Orthogonal load effects. A combination of 100 percent of the seismic forces in one direction with 30 percent of the seismic forces in the orthogonal direction is required for structures in Seismic Design Category D for certain elements—namely, the shared columns at grid intersections 3C, 3E, 4C, and 4E in the SCBF (*Standard* Sec. 12.5.4). In using modal response spectrum analysis (MRSA), the bidirectional case is handled by using the square root of the sum of the squares (SRSS) of the forces corresponding to orthogonal spectra. In addition, AISC 341 requires that column axial forces in SCBF be calculated considering simultaneous yielding of braces in intersecting frames.

9.2.3.3 Structural component load effects. The effect of seismic load is defined by *Standard* Section 12.4.2 as:

$$E = \rho Q_E + 0.2 S_{DS} D$$

Using *Standard* Section 12.3.4.2, ρ is 1.0 for Alternative A and 1.3 for Alternative B. (For simplicity, ρ is taken as 1.3; the design does not comply with the prescriptive requirements of *Standard* Sec. 12.3.4.2. It is assumed that the design would fail the calculation-based requirements of *Standard* Sec. 12.3.4.2.) Substitute for ρ (and for $S_{DS} = 1.0$).

For Alternative A:

$$E = Q_E \pm 0.2D$$

Alternative B:

$$E = 1.3 Q_E \pm 0.2D$$

9.2.3.4 Load combinations. Load combinations from ASCE 7-10 are as follows:

$1.4D$

$1.2D + 1.6L + 0.5L_r$

$1.2D + L + 1.6L_r$

$(1.2 + 0.2S_{DS})D + 0.5L + \rho Q_E$

$(0.9 - 0.2\ S_{DS})D + \rho Q_E$

For each of these load combinations, substitute E as determined above, showing the maximum additive and minimum subtractive. Q_E acts both east and west (or north and south):

Alternative A:

$1.4D$
$1.2D + 1.6L + 0.5L_r$
$1.2D + L + 1.6L_r$
$1.4D + 0.5L + Q_E$
$0.7D + Q_E$

Alternative B"

$1.4D$
$1.2D + 1.6L + 0.5L_r$
$1.2D + L + 1.6L_r$
$1.4D + 0.5L + 1.3Q_E$
$0.7D + 1.3Q_E$

For both cases, six scaled response spectrum cases are used:

1) Spectrum in X direction

2) Spectrum in X direction with 5 percent mass eccentricity

3) Spectrum in Y direction

4) Spectrum in Y direction with 5 percent mass eccentricity

5) SRSS combined spectra in X and Y directions

6) SRSS combined spectra in X and Y directions with 5 percent mass eccentricity (X direction) .

9.2.3.5 Drift limits. The allowable story drift per *Standard* Section 12.12.1 is $\Delta_a = 0.02h_{sx}$.

The allowable story drift for the first floor is $\Delta_a = (0.02)(22.33 \text{ ft})(12 \text{ in./ft}) = 5.36 \text{ in.}$

The allowable story drift for a typical story is $\Delta_a = (0.02)(13.33 \text{ ft})(12 \text{ in./ft}) = 3.20 \text{ in.}$

Adjust calculated story drifts by the appropriate C_d factor from *Standard* Table 12.2-1.

9.2.4 Analysis and Design of Alternative A: SMF

9.2.4.1 Modal Response Spectrum Analysis. Determine the building period (T) per *Standard* Equation 12.8-7:

$$T_a = C_t h_n^x = (0.028)(102.3)^{0.8} = 1.14 \sec$$

where h_n, the height to the main roof, is conservatively taken as 102.3 feet. The height of the penthouse will be neglected since its seismic mass is negligible. $C_u T_a$, the upper limit on the building period, is determined per *Standard* Table 12.8-1:

$$T = C_u T_a = (1.4)(1.14) = 1.596 \sec$$

It is assumed that the calculated period will exceed $C_u T_a$; this is verified after member selection. The seismic response coefficient (C_s) is determined from *Standard* Equation 12.8-2 as follows:

$$C_s = \frac{S_{DS}}{R/I_e} = \frac{1}{8/1} = 0.125$$

However, *Standard* Equation 12.8-3 indicates that the value for C_s need not exceed:

$$C_s = \frac{S_{D1}}{T(R/I_e)} = \frac{0.6}{(1.596 \sec)(8/1)} = 0.047$$

and the minimum value for C_s per *Standard* Equation 12.8-5 is:

$$C_s = 0.044 I_e S_{DS} \geq 0.01 = (0.044)(1)(1) = 0.044$$

Therefore, use $C_s = 0.047$.

Seismic base shear is computed per *Standard* Equation 12.8-1 as:

$$V = C_S W = (0.047)(13{,}156\,\text{kips}) = 618\,\text{kips}$$

where W is the seismic mass of the building as determined above.

In evaluating the building in ETABS, twelve modes are analyzed, resulting in a total modal mass participation of 97 percent. The code requires at least 90 percent participation. A scaling factor is used to take the response spectrum to 100 percent of the ELF base shear, with a minimum scale factor for strength calculations of I_e/R. Typical software utilizes a spectrum presented as a coefficient of g, thus requiring scaling by g. Thus the scaling factor used here is $g/(R/I_e) = 386/(8/1) = 48.3$. For drift, results are scaled by $C_d/(R/I_e)$; for a spectrum using a coefficient times g, this factor is $gC_d/(R/I_e)$.

9.2.4.2 Size members. The method used is as follows:

1. Select preliminary member sizes

2. Check deflection and drift (*Standard* Sec. 12.12)

3. Check the column-beam moment ratio rule (AISC 341 Sec. E3.4a)

4. Check beam strength

5. Check connection design (AISC 341 Sec. E3.6b, AISC 358 Sec. 5.8)

6. Check shear requirement at panel-zone (AISC 341 Sec. E3.6e;)

After adjusting the weight and stiffness of the model by changing member sizes to meet the strength requirements and drift limits, the response spectrum must be rescaled for strength. The most significant criteria for the design are drift limits, relative strengths of columns and beams the panel-zone shear. Member strength must be checked but rarely governs for this system.

1. Select Preliminary Member Sizes: The preliminary member sizes are shown for the moment frame in the X-direction in Figure 9.2-3 and in the Y direction in Figure 9.2-4. These sections are selected from AISC SDM Table 1-2, ensuring that they are seismically compact. Members are sized to meet the prequalification limits of AISC 358 Section 5.3 for span-depth ratios, weight flange thickness. Members are also sized for drift limitations and to satisfy strong column–weak beam requirements by using a target ratio of:

$$\frac{\sum Z_c}{\sum Z_b} \geq 1.25$$

This proportioning does not guarantee compliance with AISC 341 Section E3.4a, but is a useful target that makes conformance likely. Using a ratio of 2.0 in lieu of 1.25 may save on detailing costs, such as continuity plates, doublers bracing.

Following recommendations by AISC (2016) the model uses the centerline-to-centerline beam length, with no rigid offsets. This introduces some additional flexibility, which is assumed to be roughly equivalent to the flexibility of the column panel zones (which are not modeled).

The software used accounts explicitly for the increase in beam flexibility due to the RBS cuts. For every beam, RBS parameters were chosen as follows:

$$a = 0.625b_f \quad b = 0.75d_b \quad c = 0.20b_f$$

In accordance with AISC 341 Table D1.1, beam flange slenderness ratios are limited to $0.3\sqrt{E/F_y}$ (7.22 for $F_y = 50$ ksi) beam web height-to-thickness ratios are limited to $2.45\sqrt{E/F_y}$ (59.0 for $F_y = 50$ ksi). Since all members selected are seismically compact per AISC SDM Table 1-2, they conform to these limits.

For columns in special steel moment frames such as this example, AISC 341 Table D1.1 Footnote b requires that where the ratio of column moment strength to beam moment strength is less than or equal to 2.0, the more stringent λ_{hd} requirements apply for b/t (given above) when $P_u/\phi_b P_y$ is greater than or equal to 0.125, the more stringent h/t requirements apply.

Per AISC 341 Table D1.1, consider the W14x132 column at Gridline B:

$$h/t_w \leq 1.49\sqrt{E/F_y} \quad = 22.8 \leq 35.9$$

Therefore, the column is seismically compact.

Strength checks are performed using ETABS; all members are satisfactory for strength
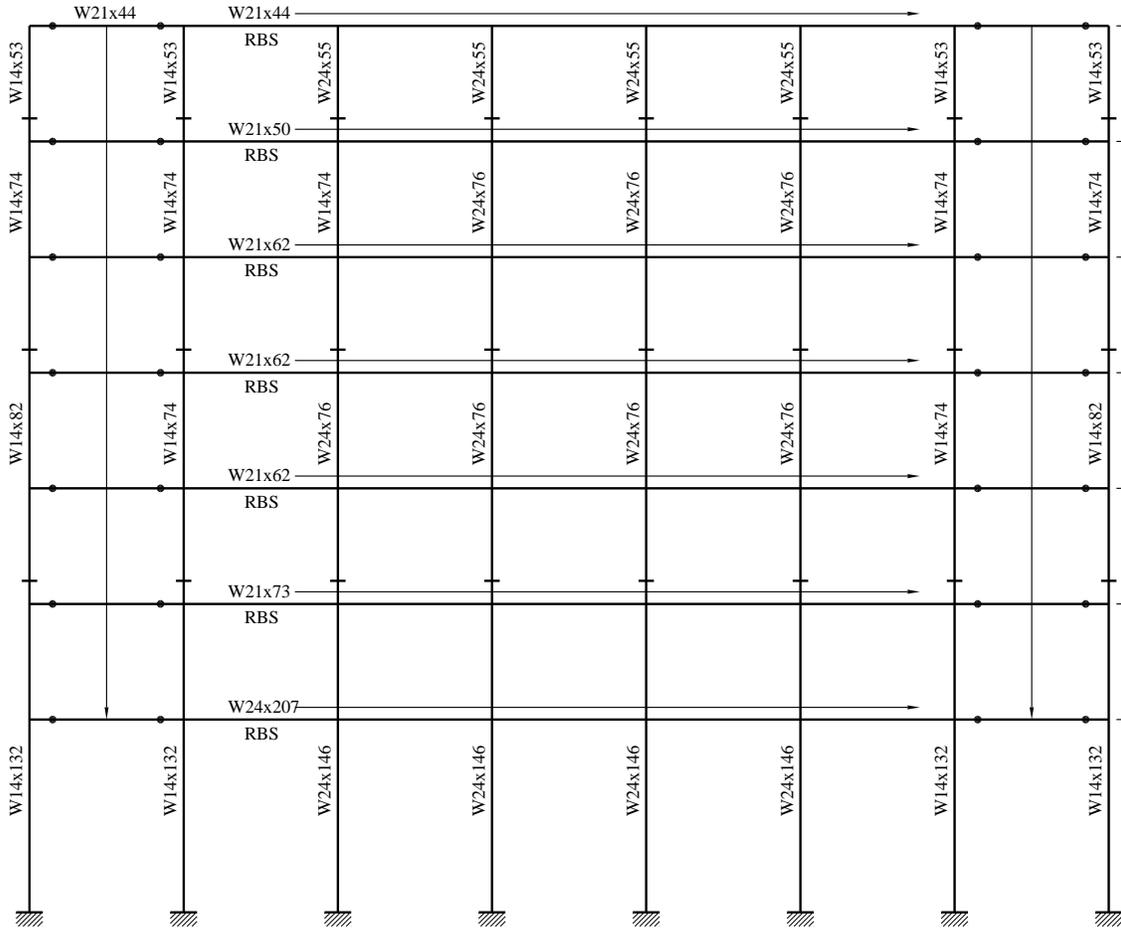
Figure 9.2-3 SMRF frame in E-W direction (penthouse not shown)

2. Check Drift: Check drift is in accordance with *Standard* Section 12.12.1. The building is modeled in three dimensions using ETABS. Displacements at the building corners under the 5 percent accidental torsion load cases are used here. Calculated story drifts, response spectrum scaling factors C_d amplification factors are summarized in Table 9.2-1 below. P-delta effects are included.

Sections are revised until the drift limits are met, while conforming to the compactness requirements and proportioning discussed earlier.

All story drifts are within the allowable story drift limit of $0.020h_{sx}$ per *Standard* Section 12.12 and Section 9.2.3.6 of this chapter.

Section 12.8.7 of the *Standard* also requires that this drift be used in the evaluation of P-delta effects against a maximum:

$$\theta = \frac{P_x \Delta I_e}{V_x h_{sx} C_d}$$

For the moment frame, this quantity is evaluated at the first floor thus:
$P_x = 0.5*50\text{psf}*125\text{ft}*175\text{ft}*6\text{stories}+13{,}156\text{kips}=16{,}400 \text{ kips}$

Assuming the maximum allowable drift:

$$\theta = \frac{16,400 kips(0.02 h_{sx})1}{(618 kips)\ h_{sx} 5.5} = 0.0967$$

The limit is:

$$\theta_{max} = \frac{0.5}{\beta C_d} \le 0.25$$

Assuming the demand-to-capacity ratio is 0.5 (which is reasonable for a Special Moment Frame) and neglecting overstrength, the limit is conservatively estimated as:

$$\theta_{max} = \frac{0.5}{0.5(5.5)} = 0.182$$
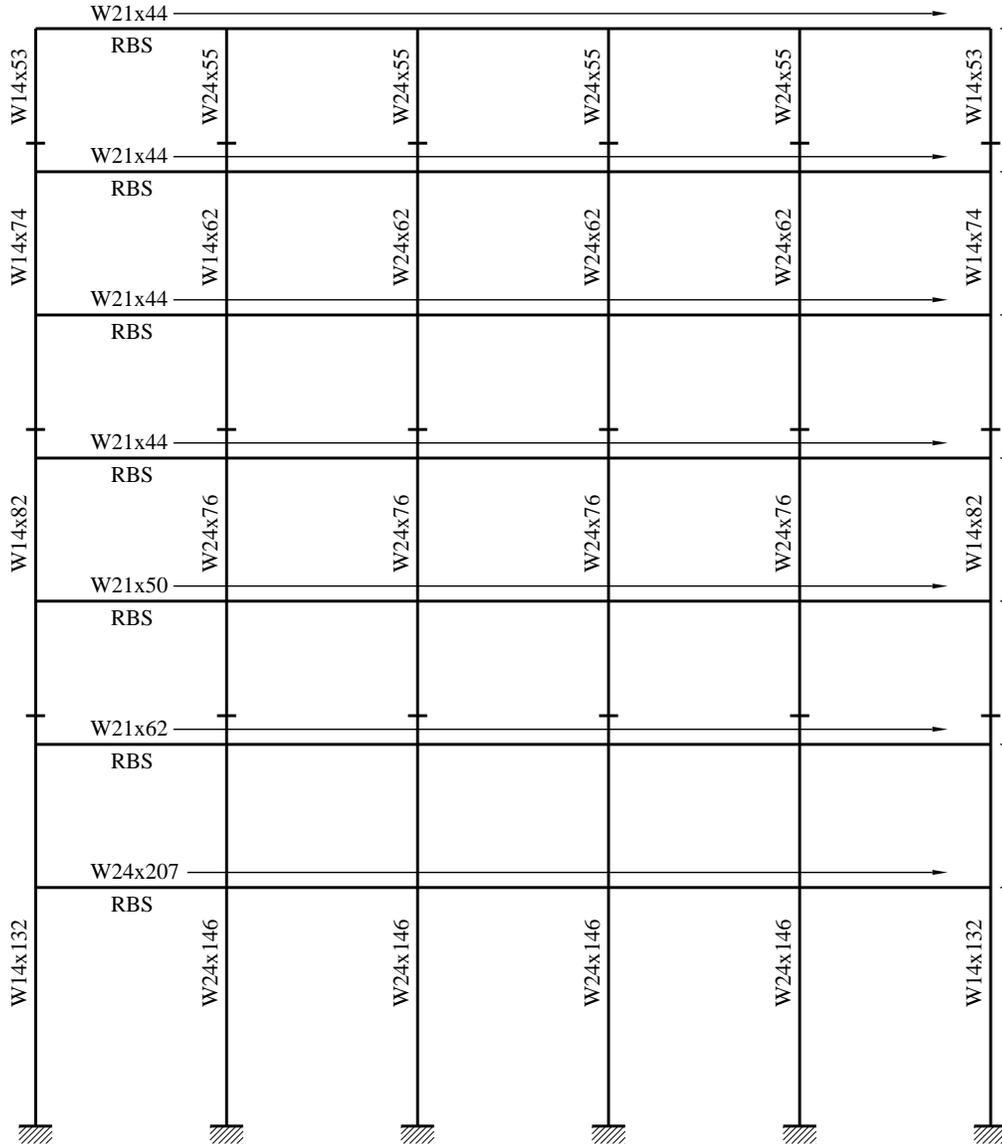
Figure 9.2-4 SMRF frame in N-S direction (penthouse not shown)

Table 9.2-1 Alternative A (Moment Frame) Story Drifts under Seismic Loads

| Level	Elastic Displacement at Building Corner, From Analysis		Expected Displacement $(=\delta_e C_d)$		Design Story Drift Ratio		Allowable Story Drift Ratio
	δ_e E-W (in.)	δ_e N-S (in.)	δ E-W (in.)	δ N-S (in.)	Δ E-W/h (%)	Δ N-S/h (%)	Δ/h (%)
Level 7	2.92	3.18	16.0	17.5	1.2	1.2	2.0
Level 6	2.66	2.89	14.7	15.9	1.4	1.7	2.0
Level 5	2.33	2.47	12.8	13.6	1.6	2.0	2.0
Level 4	1.91	1.95	10.5	10.7	1.9	2.0	2.0

Table 9.2-1 Alternative A (Moment Frame) Story Drifts under Seismic Loads

Level	Elastic Displacement at Building Corner, From Analysis		Expected Displacement ($=\delta_e C_d$)		Design Story Drift Ratio		Allowable Story Drift Ratio
	δ_e E-W (in.)	δ_e N-S (in.)	δ E-W (in.)	δ N-S (in.)	Δ E-W/h (%)	Δ N-S/h (%)	Δ/h (%)
Level 3	1.41	1.40	7.76	7.70	1.8	1.8	2.0
Level 2	0.90	0.88	4.96	4.85	1.2	1.2	2.0
Level 1	0.55	0.52	3.04	2.89	1.1	1.1	2.0

1.0 in. = 25.4 mm.

3. Check the Column-Beam Moment Ratio: Check the column-beam moment ratio per AISC 341 Section E3.4a. The expected moment strength of the beams is projected from the plastic hinge location to the column centerline. This is illustrated in Figure 9.2-5. For the columns, the moments at the location of the beam flanges are projected to the column-beam intersection as shown in Figure 9.2-6.
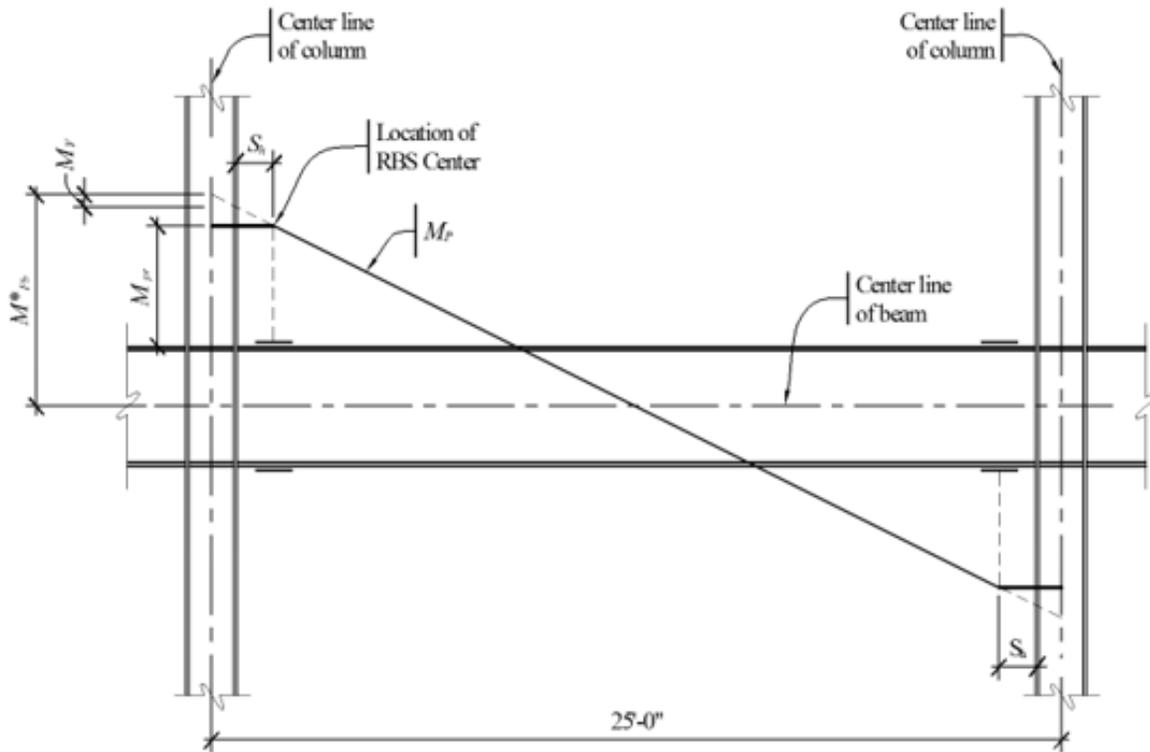
Figure 9.2-5 Projection of expected moment strength of beam
(1.0 in. = 25.4 mm, 1.0 ft = 0.3048 m)

The column-beam strength ratio calculation is illustrated for the lower level in the E-W direction, Level 2, at Gridline D (W24x146 column and W21x73 beam).

For the beams:

$$M^{\bullet}_{pb} = M_{pr} + V_e\left(S_h + \frac{d_c}{2}\right) \pm V_g\left(S_h + \frac{d_c}{2}\right)$$

where:

$M_{pr} = C_{pr}R_yF_y \, Z_e = (1.15)(1.1)(50) \, (122) = 7,361$ in.-kips

$R_y = 1.1$ for Grade 50 steel

$Z_e = Z_x \, -2ct_{bf}(d \, - \, t_{bf}) = 172 - 2(1.659)(0.74)(21.24\text{-}0.74) = 122$ in.^{3}

S_h = Distance from column face to centerline of plastic hinge (see Figure 9.2-9) = $a + b/2 = 13.2$ in. for the RBS

$V_e = 2M_{pr} / L^{'} \; V_g = w_u L^{'} / 2$

$L^{'}$ = Distance between plastic hinges = 248.8 in.

w_u = Factored uniform gravity load along beam
= $1.4D + 0.5L = 1.4[(0.068 \text{ ksf})(12.5 \text{ ft})+(0.025)(13.3 \text{ ft})] + 0.5(0.050 \text{ ksf})(12.5 \text{ ft})$
= 2.42 klf
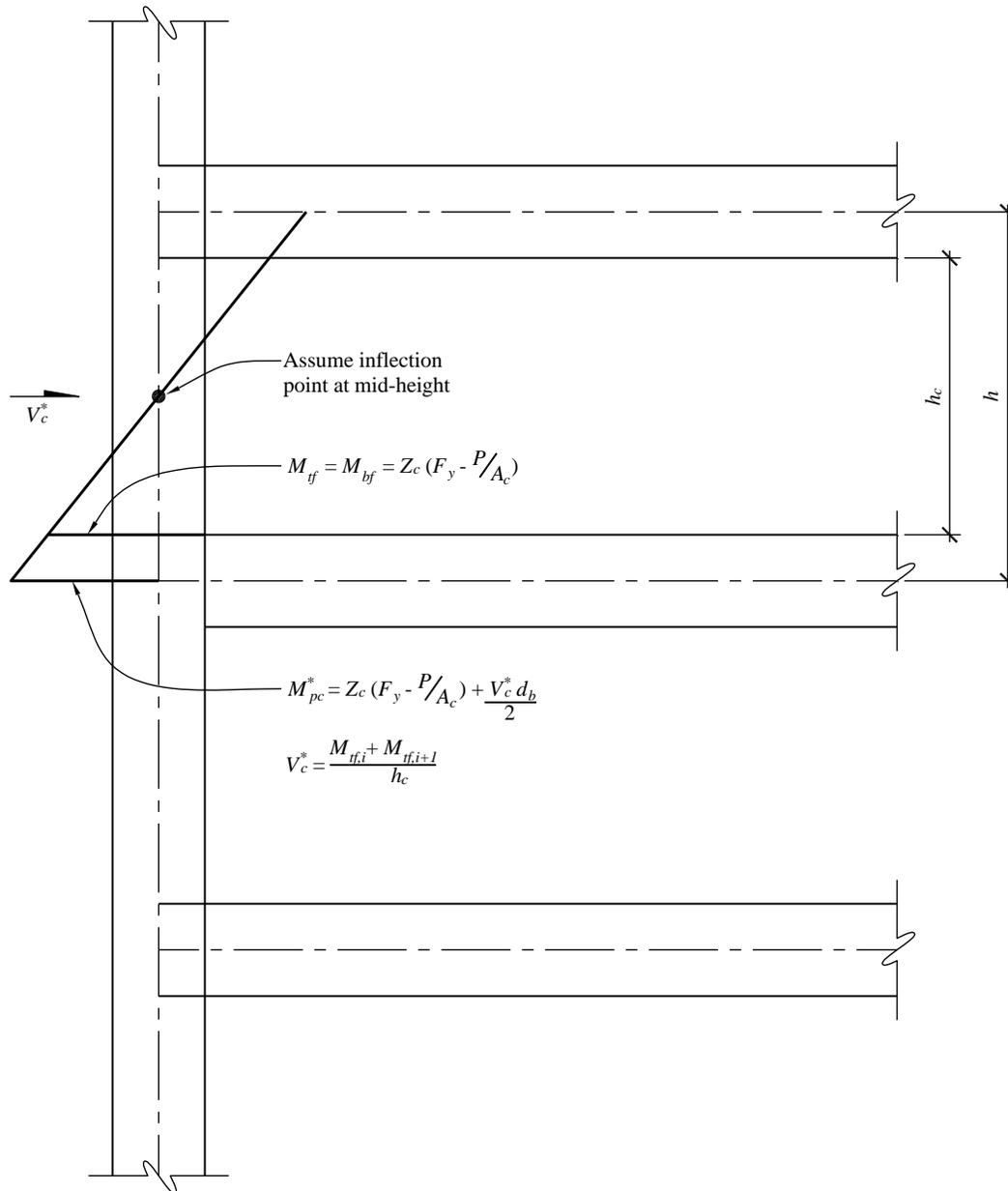
Figure 9.2-6 Moment in the column

The shear at the plastic hinge (Figure 9.2-7) is computed as:

$$V_p = V_e + V_g$$

where:

V_p = Shear at plastic hinge location
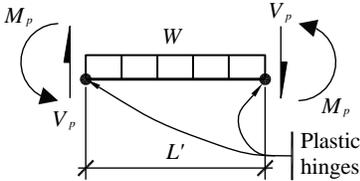
Figure 9.2-7 Free body diagram bounded by plastic hinges
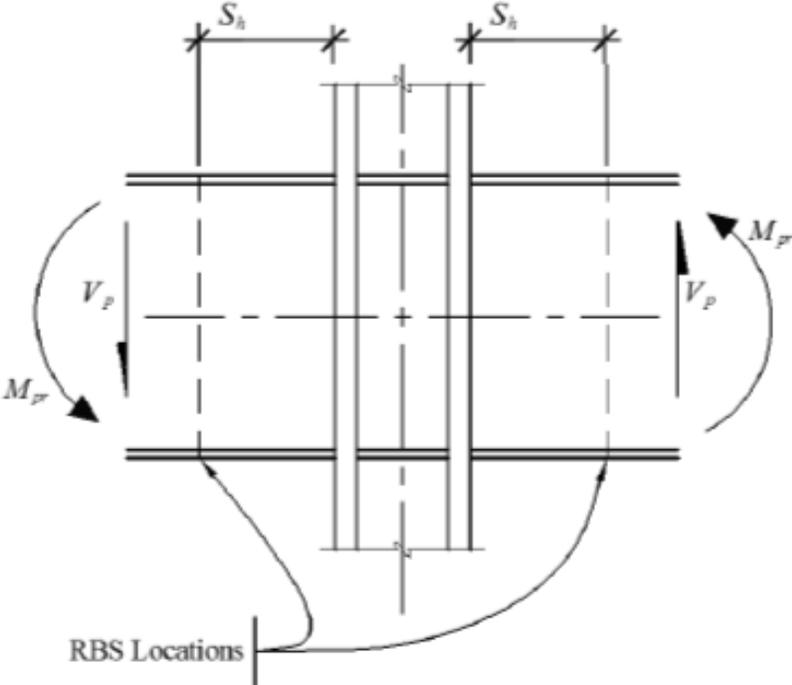
Figure 9.2-8 Forces at beam-column connection

$a = 0.625b_f = 0.625(8.3) = 5\tfrac{1}{4}''$

$b = 0.75d_b = 0.75(21.5) = 15\tfrac{3}{4}''$

$c = 0.20b_f = 0.20(8.3) = 1\tfrac{3}{4}''$
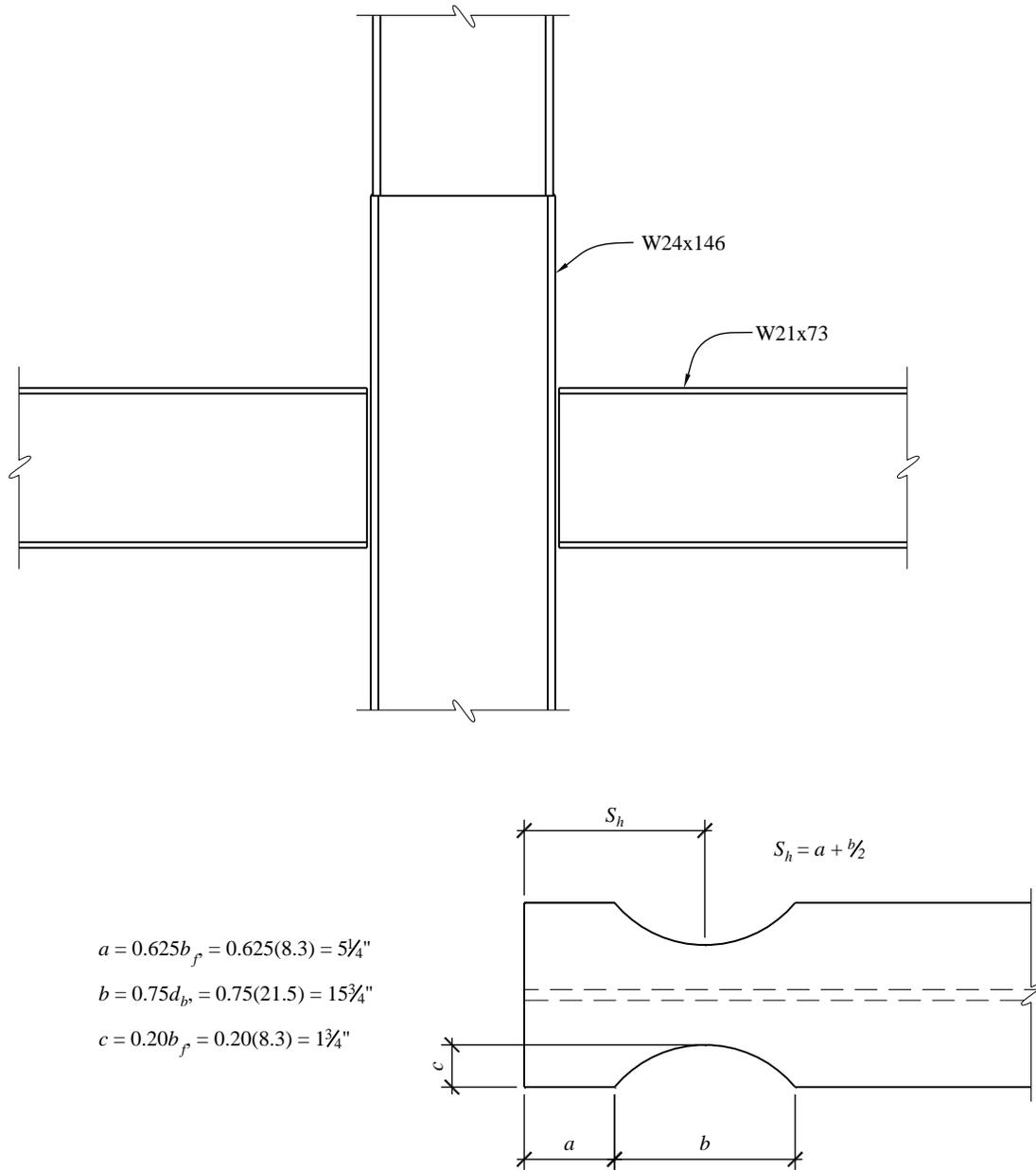
Figure 9.2-9 Reduced beam section dimensions
(1.0 in. = 25.4 mm)

Therefore:

$$V_e = 2M_{pr} / L' = 2(7361\text{in - kips}) / (248.8\text{in.}) = 59.2\text{kips}$$

$$V_g = w_u L' / 2 = (2.42\text{klf})(1/12)(248.8 \text{ in.}) / 2 = 25.1 \text{ kips}$$

$$V_p = 59.2\text{kips} + 25.1 \text{ kips} = 84.3\text{kips}$$

For the beam on the right, with gravity moments adding to seismic:

$$M^\bullet_{pb,r} = M_{pr} + V_e\left(S_h + \frac{d_c}{2}\right) + V_g\left(S_h + \frac{d_c}{2}\right)$$

$$= (7,361) + (59.2)\left((13.2) + \frac{(24.74)}{2}\right) + (25.1)\left((13.2) + \frac{(24.74)}{2}\right) = 9,517 \text{ in.-kips}$$

For the beam on the left, with gravity moments subtracting from seismic:

$$M^\bullet_{pb,r} = M_{pr} + V_e\left(S_h + \frac{d_c}{2}\right) - V_g\left(S_h + \frac{d_c}{2}\right)$$

$$= (7,361) + (59.2)\left((13.2) + \frac{(24.74)}{2}\right) - (25.1)\left((13.2) + \frac{(24.74)}{2}\right) = 8,233 \text{ in.-kips}$$

$$\sum M^\bullet_{pb} = M^\bullet_{pb,r} + M^\bullet_{pb,l} = 9,517 + 8,233 = 17,749 \text{ in.-kips}$$

Note that in most cases, the gravity moments cancel out and can be ignored for this check.

For the columns, the sum of the moments at the top and bottom flanges of the beam is:

$$\sum M_{BF} = \sum Z_c\left(F_{yc} - \frac{P_{uc}}{A_g}\right)$$

$$\sum M_{BF} = 2\left[418 \text{ in.}^3\left(50 \text{ ksi} - \frac{228 \text{ kips}}{43 \text{ in.}^2}\right)\right] = 37,367 \text{ in.-kips}$$

where:

M_{BF} = column moment at beam flange elevation

Referring to Figure 9.2-6, the moment at the beam centerline is:

$$\sum M^\bullet_{pc} = \sum M_{BF} + V^\bullet_c\frac{d_b}{2}$$

where:

$V^\bullet_c = \left[M_{BF_i} + M_{BF_{i+1}}\right]/h_c$, based on the expected yielding of the spliced column assuming an inflection point at column mid-height (e.g., a portal frame) and not the expected shear when the mechanism forms, which is:

$$V_c = \left[\frac{1}{2}\sum M^\bullet_{pb_i} + \frac{1}{2}\sum M^\bullet_{pb_{i+1}}\right]/h, \text{ where } h \text{ is the story height}$$

h_c = clear column height between beams = (13.33 ft)(12 in./ft) − 21.24 in. = 139 in.

$$V_c^* = \frac{(18{,}683 \text{ in.-kips}) + (7{,}964 \text{ in.-kips})}{(139 \text{ in.})} = 192 \text{ kips}$$

$$V_c = \left[\frac{1}{2}\sum M_{pb_i}^* + \frac{1}{2}\sum M_{pb_{i+1}}^*\right] / h = \left[\frac{1}{2}(17749) + \frac{1}{2}(14976)\right] / \left[(13.33)(12)\right]$$

$$= 102 \text{ kips}$$

Thus:

$$\sum M_{pc}^* = 37{,}367 \text{ in.-kips} + (192 \text{ kips})\frac{(21.24 \text{ in.})}{2} = 39{,}400 \text{ in.-kips}$$

The ratio of column moment strengths to beam moment strengths is computed as:

$$\text{Ratio} = \frac{\sum M_{pc}^*}{\sum M_{pb}^*} = \frac{39{,}400 \text{ in.-kips}}{17{,}749 \text{ in.-kips}} = 2.22 > 1$$

OK

Since the ratio is greater than 2, bracing is only required at the top flange per AISC 341 Section E3.4c.

4. Check the Beam Strength: Per AISC 358 Equation 5.8-4, the beam strength at the reduced section is:

$$\phi M_{pr} = \phi F_y Z_e = (0.9)(50\text{ksi})(122 \text{ in.}^3) = 5{,}490 \text{ in.-kips}$$

From analysis, $M_u = 4072$ in-kips. Therefore, $\phi M_{pr} \geq M_u$; the beam has adequate strength.

The moment at the column face is:

$$M_f = M_{pr} + V_e S_h \pm V_g S_h$$

$$M_{f,r} = 7{,}361 \text{ in.-kips} + (59.2 \text{ kips})(13.2 \text{ in.}) + (25.1 \text{ kips})(13.2 \text{ in.}) = 8{,}474 \text{ in.-kips}$$

$$M_{f,r} = 8{,}474 \text{ in.-kips} \leq \phi_d R_y F_y Z_x = (1.0)(1.1)(50)(172) = 9{,}460 \text{ in.-kips}$$

OK

To check the shear in the beam, first the appropriate equation must be selected:

$$2.24\sqrt{\frac{E}{F_{yw}}} = 2.24\sqrt{\frac{(29{,}000 \text{ ksi})}{(50 \text{ ksi})}} = 53.9$$

$$h/t_w = 46.6 \leq 53.9$$

Therefore:

$$V_n = 0.6 F_y A_w C_v$$

where $C_v = 1.0$.

$$V_n = 0.6(50\,\text{ksi})(21.2\,\text{in.})(0.455\text{ in.})(1.0) = 289 \text{ kips}$$

Comparing this to V_p:

$$\phi V_n = 289 \geq 84.3 = V_p$$

OK

Check the beam lateral bracing. Per AISC 341 Section E3.4b and Section D1.2b, the maximum spacing of the lateral bracing is:

$$L_b \leq 0.086 r_y E / F_y = 0.086(1.81 \text{ in.})(29{,}000 \text{ ksi}) / (50 \text{ ksi}) = 90 \text{ in.} = 7'\text{-}6''$$

The braces near the plastic hinges are required to have a minimum strength of:

$$P_{br} = \frac{0.06 M_u}{h_o}$$

$$= \frac{0.06(1.1)(50\,\text{ksi})(172\,\text{in.}^3)}{21.24 \text{ in.}^2 - 0.74 \text{ in.}^2} = 27.7 \text{ kips}$$

where:

$$M_u = R_y F_y Z$$

h_o = the distance between flange centroids

The required brace stiffness is:

$$\beta_{br} = \frac{10 M_u C_d}{\phi L_b h_o}$$

$$= \frac{10(1.1)(50\,\text{ksi})(172\,\text{in.}^3)(1.0)}{0.75(6.39\,\text{ft})(12 \text{ in.}/\text{ft})(21.24 \text{ in.}^2 - 0.74 \text{ in.}^2)} = 80.2 \text{ kips/in.}$$

L_b is taken as L_p. These values are for the typical lateral braces. No supplemental braces are required at the reduced section per AISC 358 Section 5.3.1 (7).

5. Check Connection Design:

   Check the need for continuity plates. Continuity plates are required per AISC 341 Section E3.6f unless both of the following conditions are met:

   $\phi R_n \geq R_u$ for applicable local limit states in the column

   Where

$$R_u = \frac{M_{f,r}}{d_b - t_f} = \frac{8,474 \text{ in.-kips}}{(21.24 \text{ in.}) - (0.74 \text{ in.})} = 413 \text{ kips}$$

And:

$$t_{cf} \geq \frac{b_{bf}}{6} = \frac{8.30 \text{ in.}}{6} = 1.38 \text{ in.}$$

Since t_{cf} = 1.09 inches, continuity plates are required. See below for the design of the plates.

Checking web crippling per AISC 360 Section J10.3:

$$R_n = 0.40t_w^2 \left[1 + 3\left(\frac{N}{d}\right)\left(\frac{t_w}{t_f}\right)^{1.5} \right] \sqrt{\frac{EF_{yw}t_f}{t_w}}$$

$$R_n = 0.80(0.65)^2 \left[1 + 3\left(\frac{(0.74 + 5/16)}{(24.74)}\right)\left(\frac{(0.65)}{(1.09)}\right)^{1.5} \right] \sqrt{\frac{(29,000)(50)(1.09)}{(0.65)}} = 558 \text{ kips}$$

$$\phi R_n = 0.75(558 \text{ kips}) = 419 \text{ kips} \geq 413 \text{ kips} = R_u \qquad\qquad \text{OK}$$

Checking web local yielding per *Specification* Section J10.2:

$$R_u = 413 \text{ kips}$$

$$\phi R_n = \phi(5k + N)F_{yw}t_w$$

$$\phi R_n = (1.00)\left(5(1.59 \text{ in.}) + (0.74 \text{ in.} + \tfrac{5}{16} \text{ in.})\right)(50 \text{ ksi})(0.65 \text{ in.}) = 293 \text{ kips}$$

Therefore, since $\phi R_n \leq R_u$, as well as due to the minimum column-flange-thickness check above, continuity plates are required. The force that the continuity plates must take is 413 - 293 = 120 kips. Therefore, each plate takes 60 kips. The minimum thickness of the plates is the thickness of the beam flanges, 0.74 inch. The minimum width of the plates per is taken to match the beam flange, minus the prescribed clip per AISC 341 Section I2.4:

$$b_{pl} = b_{f,b} - 2(k_{1,b} + \tfrac{1}{2} \text{ in.})$$

$$= 8.31 \text{ in.} - 2(0.875 \text{ in.} + 0.5 \text{ in.}) = 5.56 \text{ in.}$$

Checking the strength of the plate with minimum dimensions:

$$\phi R_n = \phi t_{pl} b_{pl} F_y$$

$$= (1.0)(0.74 \text{ in.})(5.56 \text{ in.})(50 \text{ ksi}) = 206 \text{ kips}$$

Therefore, since $\phi R_n = 206$ kips > 60 kips, the minimum continuity plates have adequate strength. Alternatively, a W24x192 section will work in lieu of adding continuity plates.

6. Check Panel Zone: The *Standard* defers to AISC 341 for the panel zone shear calculation.

    The panel zone shear calculation for Story 2 of the frame in the E-W direction at Grid C (column: W24x176; beam: W21x73) is from AISC 360 Section J10.6. Check the shear requirement at the panel zone in accordance with AISC 341 Section E3.6e. The factored shear R_u is determined from the flexural strength of the beams connected to the column. This depends on the style of connection. In its simplest form, the shear in the panel zone (R_u) is as follows for W21x73 beams framing into each side of a W24x146 column (such as Level 2 at Grid C):

$$R_u = \sum \frac{M_f}{d_b - t_{fb}} = \frac{16,285}{21.24 - 0.74} = 794 \text{ kips}$$

M_f is the moment at the column face determined by projecting the expected moment at the plastic hinge points to the column faces (see Figure 9.2-5):

$$M_f = M_{pr} + V_e S_h \pm V_g S_h$$

$$M_{f,r} = 7,361 \text{ in.-kips} + (59.2 \text{ kips})(13.2 \text{ in.}) + (25.1 \text{ kips})(13.2 \text{ in.}) = 8,474 \text{ in.-kips}$$

$$M_{f,l} = 7361 \text{ in - kips} + (59.2 \text{ kips})(13.2 \text{ in.}) - (25.1 \text{ kips})(13.2 \text{ in.}) = 7811 \text{ in - kips}$$

Note that in most cases, the gravity moments cancel out and can be ignored for this check. The total moment at the column face is:

$$\sum M_f = M_{f,r} + M_{f,l} = 8,474 \text{ in.-kips} + 7,811 \text{ in.-kips} = 16,285 \text{ in.-kips}$$

The shear transmitted to the joint from the story above, V_c, opposes the direction of R_u and may be used to reduce the demand. Previously calculated, this is 102 kips at this location. Thus the frame $R_u = 794 - 102 = 692$ kips.

The column axial force (Load Combination: $1.2D + 0.5L + \Omega_o E$) is $P_r = 228$ kips.

$$0.75 P_c = 0.75 F_y A_g = 0.75(50 \text{ ksi})(43 \text{ in.}^2) = 1,613 \text{ kips}$$

Since $P_r \leq 0.75 P_c$, using AISC 360 Equation J10-11:

$$R_n = 0.60 F_y d_c t_w \left(1 + \frac{3 b_{cf} t_{cf}^2}{d_b d_c t_w}\right)$$

$$R_n = 0.60(50)(24.74)(0.65)\left[1 + \frac{3(12.90)(1.09)^2}{(21.24)(24.74)(0.65)}\right] = 547 \text{ kips}$$

Since ϕ_v is 1, $\phi_v R_n = 547$ kips.

$$\phi_v R_n = 547 \text{ kips} < 692 \text{ kips} = R_u$$

Therefore, doubler plates are required. The required additional strength from the doubler plates is 692 - 547 = 145 kips. The strength of the doubler plates is:

$$\phi_v R_n = 0.6 t_{doub} d_c F_y$$

Therefore, to satisfy the demand the doubler plate must be at least 1/4 inch thick. Plug welds are required as:

$$t = 0.25 \text{ in.} < (d_z + w_z)/90 = \left[21.24 + 24.74 - 2(1.09)\right]/90 = 0.49 \text{ in.}$$

Use four plug welds spaced 12 inches apart. Alternatively, the use of a W24x192 column will not require doubler plates ($\phi_v R_n = 737$ kips).

9.2.5 Analysis and Design of Alternative B: SCBF

9.2.5.1 Modal Response Spectrum Analysis. As with the SMF, find the approximate building period (T_a) using *Standard* Equation 12.8-7:

$$T_a = C_t h_n^x = (0.02)(102.3)^{0.75} = 0.64 \text{ sec}$$

$C_u T_a$, the upper limit on the building period, is determined per *Standard* Table 12.8-1:

$$T = C_u T_a = (1.4)(0.64) = 0.896 \text{ sec}$$

It is assumed that the calculated period will exceed $C_u T_a$; this is verified after member selection. The seismic response coefficient (C_s) is determined from *Standard* Equation 12.8-2 as follows:

$$C_s = \frac{S_{DS}}{R/I_e} = \frac{1}{6/1} = 0.167$$

However, *Standard* Equation 12.8-3 indicates that the value for C_s need not exceed:

$$C_s = \frac{S_{D1}}{T(R/I_e)} = \frac{0.6}{(0.896 \text{ sec})(6/1)} = 0.112$$

and the minimum value for C_s per *Standard* Equation 12.8-5 is:

$$C_s = 0.044 I_e S_{DS} \geq 0.01 = (0.044)(1)(1) = 0.044$$

Use $C_s = 0.112$.

Seismic base shear is computed using *Standard* Equation 12.8-1 as:

$$V = C_S W = (0.112)(13,156 \text{kips}) = 1,473 \text{ kips}$$

where *W* is the seismic mass of the building as determined above.

In evaluating the building in ETABS, twelve modes are analyzed, resulting in a total modal mass participation of 99 percent. The *Standard* Sec. 12.9.1 requires at least 90 percent participation. As before with Alternative A, strength is scaled to 100 percent of the equivalent lateral force base shear and drift is scaled by $gC_d/(R/I)$.

9.2.5.2 Size members. There are two sets of strength requirements that apply to the SCBF frame. First, the entire frame must conform to the strength requirements of the *Standard*. Second, the beam and column members must have sufficient strength to resist the forces corresponding to two separate frame plastic mechanism cases specified in AISC 341 Section F2.3. In both cases the frame is considered to deform in a manner similar to the first mode, with all stories deflecting in the same direction.

In the first plastic mechanism, the frame is considered to have reached a lateral drift at which each brace in tension is at its maximum tension strength and each brace in compression is at its maximum compression strength. The maximum tension strength is taken as $R_y F_y A_g$. The maximum compression strength is taken as the lesser of $R_y F_y A_g$ and $1.14 F_{cre} A_g$ where $F_{cre} A_g$ is the compression strength based on expected material properties. This case corresponds to maximum overturning, as well as maximum tension and compression forces in connections. With respect to overturning, AISC 341 F2.3 allows the load combinations with overstrength to be used in lieu of this plastic mechanism analysis for end columns; this case therefore is significant for interior columns and for connection forces.

In the second plastic mechanism, the frame is considered to have reached a lateral drift at which each brace in tension is at its maximum tension strength and each brace in compression is at a reduced compression strength resulting from cyclic buckling. The maximum tension strength is taken as in the first mechanism, and the reduced compression strength is taken as 0.3 times the expected compression strength (The coefficient of 0.3 is an arbitrary value representing one point in a continual degradation of compression strength with each cycle of buckling and yielding, and thus the refinement of considering effective material properties is not meaningful; it is permitted as a potential simplification for engineers.) This case captures redistribution forces as braces degrade and is significant for beams and for interior columns.

The method used to size members is as follows:

1. Select brace sizes based on strength

2. Select column sizes based on special seismic load combinations (*Standard* Sec. 12.4.3.2)

3. Select beam sizes based on the load imparted by the expected strength of the braces

4. Check drift (*Standard* Sec. 12.12)

5. Design the connection

Re-proportion member sizes as necessary after each check. After the weight and stiffness have been modified by changing member sizes, the response spectrum must be rescaled. Torsional amplification is a significant consideration in this alternate.

1. Select Preliminary Member Sizes and Check Strength: The preliminary member sizes are shown for the braced frame in the E-W direction (seven bays) in Figure 9.2-10 and in the N-S direction (five bays) in Figures 9.2-11. The braces used are HSS A1085, a new specification that has higher strength and also tighter tolerance on wall thickness, such that the actual thickness may be used in design.
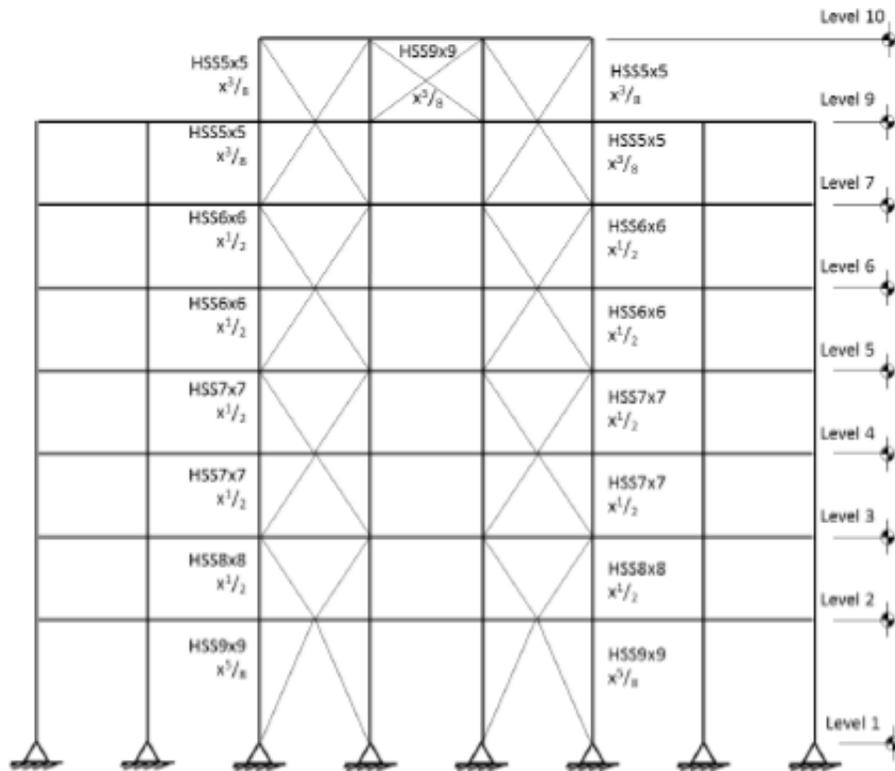
Figure 9.2-10 Braced frame in E-W direction (preliminary design)
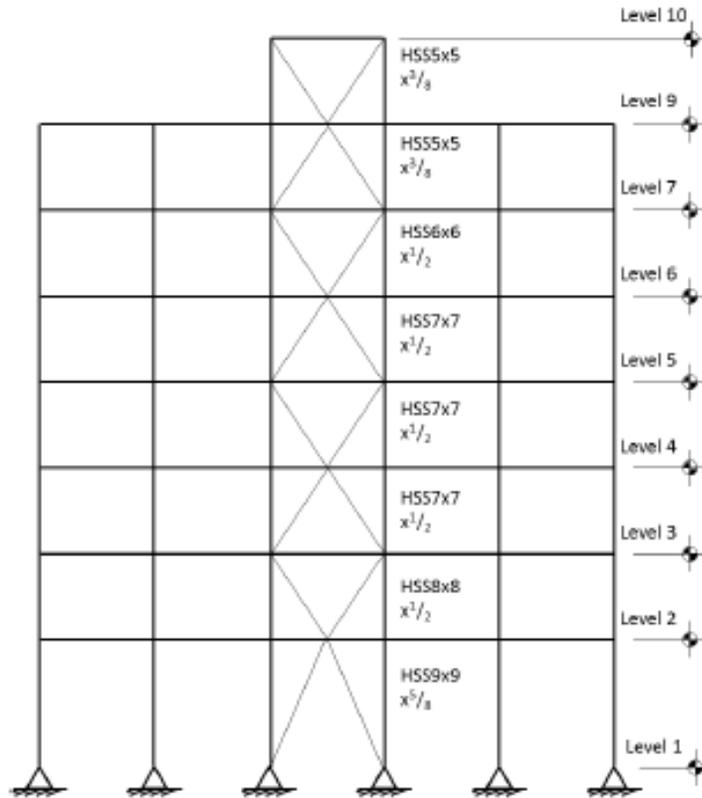
Figure 9.2-11 Braced frame in N-S direction on Gridlines C, D, E, and F (preliminary design)

Check slenderness and width-to-thickness ratios—the geometrical requirements for local stability. In accordance with AISC 341 Section C13.2a, bracing members must satisfy the following:

$$\frac{kl}{r} \leq 200$$

All members are seismically compact for SCBF per AISC SDM Table 1-2, thus satisfying slenderness requirements.

Columns: Wide flange members must comply with the width-to-thickness ratios contained in AISC 341 Table D1.1. Flanges must satisfy the following:

$$\frac{b}{t} \leq 0.30\sqrt{E / F_y} = 7.23$$

Webs in combined flexural and axial compression (where $P_u/\phi_b P_y = 0.385 > 0.125$) must satisfy the following:

$$\frac{h_c}{t_w} \le 1.12\sqrt{E/F_y}\left(2.33 - \frac{P_u}{\phi_b P_y}\right) = 52.5$$

Braces: Rectangular HSS members must satisfy the following:

$$\frac{b}{t} \le 0.55\sqrt{E/F_y} = 13.2$$

Using a redundancy factor of 1.3 on the earthquake loads, the braces are checked for strength using ETABS and found to be satisfactory.

2. Select Column and Beam Sizes: Columns and beams are sized to be able to resist the expected plastic and post-buckling capacity of the braces. In the computer model, the braces are removed and replaced with forces representing their capacities. These loads are applied for two general cases reflecting the expected mechanisms as defined in AISC 341 F2.3. In case 1, a direction of earthquake loading is assumed; the diagonal braces expected to be in tension under this loading are replaced with the force $R_y F_y A_g$ and the braces expected to be in compression are replaced with the force $1,14P_{ne}$, where P_{ne} is the compression strength based on expected material properties. In case 2, the diagonal braces expected to be in tension under this loading are replaced with the force $R_y F_y A_g$ and the braces expected to be in compression are replaced with the force $0.342P_{ne}$. Case 1 results in higher overturning and generally governs or the design of columns. Case 2 generally results in greater axial and flexural forces in beams.

The factor R_y for the A1085 material is 1.2, This value is not in the 2010 edition of AISC 341 but has been established for the 2016 edition.

Because the earthquake loading can act in any direction these two general cases become eight analytical cases:

1. T_{1x+} Case 1 acting in the positive x direction
2. T_{1x-} Case 1 acting in the negative x direction
3. T_{2x+} Case 2 acting in the positive x direction
4. T_{2x-} Case 2 acting in the negative x direction
5. T_{1y+} Case 1 acting in the positive y direction
6. T_{1y-} Case 1 acting in the negative y direction
7. T_{2y+} Case 2 acting in the positive y direction
8. T_{2y-} Case 2 acting in the negative y direction

For columns that form part of frames in both the principal building axes should be evaluated considering the simultaneous actions in both orthogonal directions (for example, applying T_{1x+} and T_{1y+} simultaneously).

Because of building symmetry, not every combination of cases (or even every case) needs to be explicitly examined. For design purposes the following combinations will be considered, with resulting designs applied in the symmetrical locations:

1. T_{1x+} and T_{1y+}
2. T_{2x+} and T_{2y+}

The load cases applied are as follows:

1. $\left(1.2 + 0.2 S_{DS}\right) D + 0.5 L + T$ (two combinations: T_{1x+} and T_{1y+}; and T_{2x+} and T_{2y+})

$\left(0.9 - 0.2 S_{DS}\right) D + T$ (two combinations)

Beam strength is checked for each of these load combinations using ETABS and found to be satisfactory. For illustration purposes, the explicit calculation of the seismic loads is presented below.

Chevron beam (floor 6):
This beam has vertical forces induced by the difference in tension strength and post buckling strength of braces. The pair of braces above (HSS6x6x½) have a net upward force, while the pair of braces below (HSS7x7x½) have a net downward force.

$$Q_V = [R_y F_y A_g - 0.342 F_{cre} A_g]_{i-1} \sin(\theta_{i-1}) - [R_y F_y A_g - 0.342 F_{cre} A_g]_i \sin(\theta_i)$$

$$= [744 \text{ kips} - 147 \text{ kips}] \sin(46.8 \text{ deg}) - [622 \text{ kips} - 104 \text{ kips}] \sin(46.8 \text{ deg})$$

$$= 21 \text{ kips}$$

The horizontal force on the beam is:

$$Q_H = [R_y F_y A_g + 0.342 F_{cre} A_g]_{i-1} \cos(\theta_{i-1}) - [R_y F_y A_g + 0.342 F_{cre} A_g]_i \cos(\theta_i)$$

$$= [744 \text{kips} + 147 \text{ kips}]\cos(46.8 \text{ deg}) - [622 \text{ kips} + 104 \text{ kips}]\cos(46.8 \text{ deg})$$

$$= 160 \text{ kips}$$

It is assumed that each beam segment resists 50% of this force.

Transfer beam (floor 7):
This beam has horizontal forces induced by the difference in tension strength and post buckling strength of braces. At each level the tension brace resists the majority of the force. The transfer force in the beam is determined by first solving for the collector forces corresponding to this mechanism. The pair braces above are HSS5x5x3/8 and the braces below are HSS6x6x½.

The total force collector force on level 6 corresponding to this mechanism is:
$$F = [R_y F_y A_g + 0.342 F_{cre} A_g]_{i-1} \cos(\theta_{i-1}) - [R_y F_y A_g + 0.342 F_{cre} A_g]_i \cos(\theta_i)$$

$$= [622 + 104]\cos(46.8 \text{ deg}) - [395 \text{kips} + 52 \text{ kips}]\cos(46.8 \text{ deg})$$
$$= 191 \text{ kips}$$

It is assumed that 50% of this force (95 kips) is delivered at each end of the frame. With this information, statics can be used to solve for the beam axial force:

$$P_u = \tfrac{1}{2} F + [0.342 F_{cre} A_g]_k \cos(\theta_k) - [R_y F_y A_g]_{i-1} \cos(\theta_{i-1})$$
-

$$= \tfrac{1}{2} F + [101 \text{ kips}] \cos(46.8 \text{ deg}) - [753 \text{ kips}] \cos(46.8 \text{ deg})$$

$$= -295 \text{ kips}$$

A similar approach can be taken for columns. For the columns case 1 (expected compression strength for the braces in compression, expected tension strength for the braces in tension) typically governs for the end columns of a braced frame. For the seismic axial force corresponding to this mechanism the vertical component of the brace forces is accumulated, along with the beam reaction due to the unbalanced force. Thus the column must resist the summation of these forces from the braces above, with the range of the levels contributing to the sum being determined by the bracing configuration.

$$E_m = \sum \left[\frac{R_y F_y A_g + 1.14 F_{cre} A_g}{2} \right] \sin \theta$$

For regular frames it is often simple to utilize a spreadsheet to compute the effect of all the braces on the column. For complex layouts, engineering software that allows imposing strain on elements may accomplish this calculation with less effort.

In this example, the column axial force must be computed considering the effects of the two intersecting orthogonal frames acting simultaneously.

The Final design of the frame on gridline C, D, E, and F is shown in Figure 9.2-12.
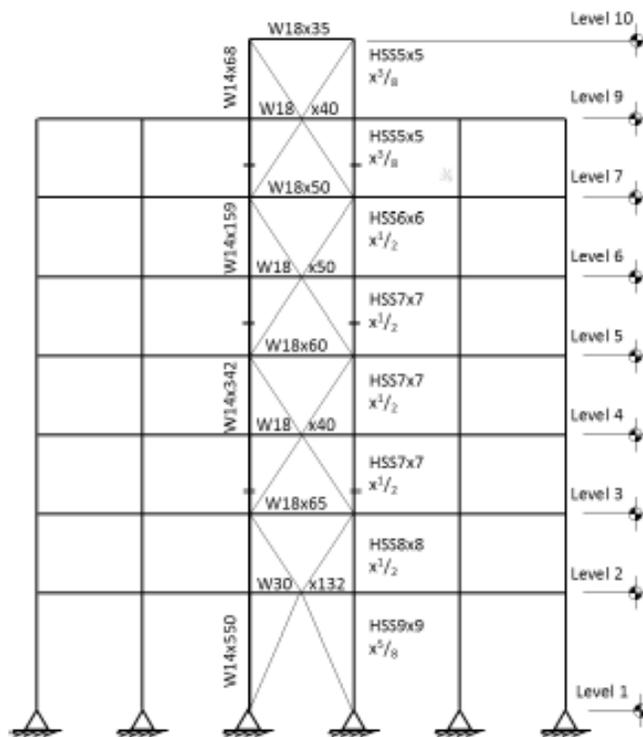

Figure 9.2-12 Braced frame in N-S direction on Gridlines C, D, E, and F (final design)

4. Check Story Drift: After designing the members for strength, the ETABS model is used to determine the design story drift. The story drifts are calculated without scaling to the equivalent lateral force base

shear. Displacements from the elastic analysis are amplified by the factor C_d (equal to 5.5 for this system). The maximum drift is determined at the corner of the structure.

All story drifts are within the allowable story drift limit of $0.020h_{sx}$ in accordance with *Standard* Section 12.12 and the allowable deflections for this building from Section 9.2.3.6 above. As these drifts are significantly smaller than those of the Special Moment Frame option, the P-Delta limits of Section 12.8.7 are considered to be satisfied by inspection.

5. Design the Connection: Figure 9.2-13 illustrates a typical connection design at a column.
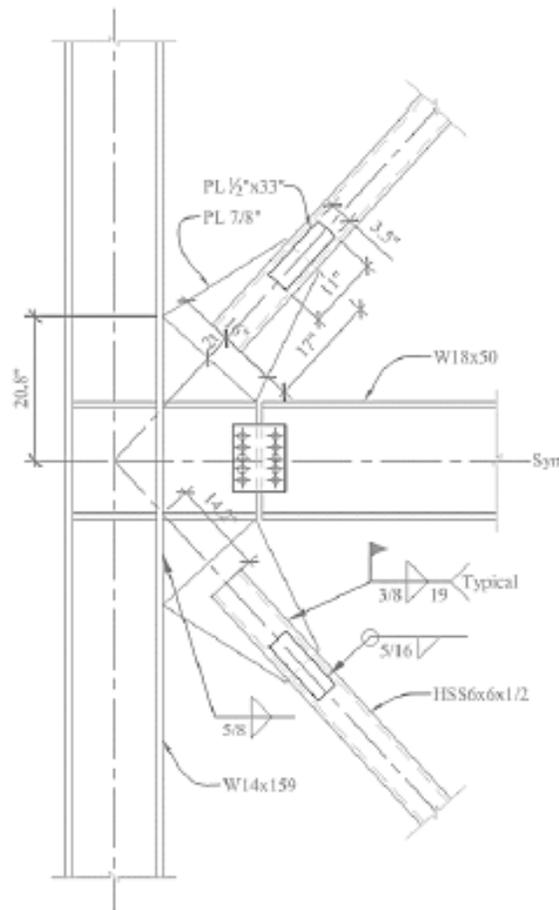
Figure 9.2-13 Bracing connection detail (1.0 in. = 25.4 mm, 1.0 ft = 0.3048 m)

The connection designed in this example is at the seventh floor on Gridline C. The required strength of the connection is to be the nominal axial tensile strength of the bracing member. For an HSS6x6x1/2, the expected axial tensile strength is computed using AISC 341 Section F2.6c:

$$R_u = R_yF_yA_g = (1.2)(50 \text{ ksi})(10.36 \text{ in.}^2) = 622 \text{ kips}$$

The area of the gusset is determined using the plate thickness and section width. See Figure 9.2-13 for the determination of this dimension. The thickness of the gusset is chosen to be 7/8 inch.

The gusset width is determined based on rupture in the net section:

$\phi T_n = \phi F_y A_n = (0.9)(50 \text{ ksi})(7/8 \text{ in.} \times w) = 622 \text{ kips}$

$w \geq 15.8 \text{ in.}$

A width of 16 in. will be used.

For a tube slotted to fit over a connection plate, there will be four welds. The demand in each weld will be 622 kips/4 = 156 kips. The design strength for a fillet weld per AISC 360 Table J2.5 is:

$\phi F_w = \phi(0.6 F_{exx}) = (0.75)(0.6)(70 \text{ ksi}) = 31.5 \text{ ksi}$

For a 3/8-inch fillet weld, the required length of weld is determined to be:

$$L_w = \frac{156}{(0.707)(0.375 \text{ in.})(31.5 \text{ ksi})} = 18.7 \text{ in.}$$

Therefore, use 19 inches of weld minimum.

In accordance with the exception of AISC 341 Section F2.6c (3), the design of brace connections must consider flexural forces or rotations associated with brace flexural buckling. Accommodation of rotations is often done by providing a "hinge zone"; the gusset plate is detailed such that it can form a plastic hinge over a distance of $2t$ (where t = thickness of the gusset plate) from the end of the brace. The gusset plate must be permitted to flex about this hinge, unrestrained by any other structural member. See also AISC 341 Section C-F2.6c. With such a pinned-end condition, the compression brace tends to buckle out-of-plane. During an earthquake, there will be alternating cycles of compression and tension in a single bracing member and its connections. Proper detailing is imperative so that tears or fractures in the steel do not initiate during the cyclic loading.

While the gusset is permitted to hinge, it must not buckle. To prevent buckling, the gusset compression strength must exceed the expected brace strength in compression per AISC 341 Section F2.6c (2). Determine the nominal compressive strength of the brace member. The effective brace length (kL) is the distance between the hinge zones on the gusset plates at each end of the brace member. This length is somewhat dependent on the gusset design. For the brace being considered, $kL = 161$ inches the expected compressive strength is determined using expected (not specified minimum) material properties per AISC 360 Section E3 using expected material strength:

$$P_n = 1.14 F_{cre} A_g$$

where:

A_g = gross area of the brace

F_{cre} = flexural buckling stress, determined as follows

When:

$$\frac{kL}{r} \leq 5.18\sqrt{E/R_y F_y} = 119$$

$$F_{cre} \leq \left[0.692^{\frac{R_y F_y}{F_e}} \right] R_y F_y$$

Otherwise,

$$F_{cre} \leq F_e$$

where:

$$F_e = \frac{\pi^2 E}{\left(\dfrac{kL}{r} \right)^2}$$

The equations have been recalibrated to use the expected stress rather than the specified minimum yield stress. Note that the 0.877 factor, which represents out-of-straightness, is not used here in order to calculate an upper bound brace strength and thereby ensure adequate gusset compression strength. Here, $kL/r = (1)(161)/(2.17) = 74.2$, thus:

$$F_e = \frac{\pi^2 (29{,}000 \text{ ksi})}{(81.8)^2} = 42.8 \text{ ksi}$$

$$F_{cre} = \left[0.692^{\frac{(1.2)(50 \text{ ksi})}{(42.8 \text{ ksi})}} \right] (1.2)(50 \text{ ksi}) = 33.4 \text{ ksi}$$

$$P_n = 1.14(33.4 \text{ ksi})(10.36 \text{ in.}^2) = 394 \text{ kips}$$

Now, using the expected compressive load from the brace of 394 kips, check the buckling capacity of the gusset plate using the section above. By this method, illustrated by Figure 9.2-13, the compressive force per unit length of gusset plate is (394 kips/16 in.) = 24.6 kips/in.

Try a plate thickness of 7/8 inch:

$f_a = P/A = 24.6$ kips/(7/8 in. × 1 in.) = 28.2 ksi

The length, from geometry, is 17.2 inches. Following Dowswell (2014), an effective length factor of 0.6 can be used in conjunction with a maximum width determined by:

$\tan(\theta) = 0.956 - 0.213 \lambda \geq 0.637$

$\lambda = KL/ \pi r \sqrt{(F_y/E)}$
$= 0.6*17.2 /3.14(7/8/\sqrt{12}) *\sqrt{(50/29{,}000)} = 0.541$

$\tan(\theta) = 0.956 - 0.213(0.541) = 0.841$

$\theta = 40.0$ deg

The maximum width is therefore:

$$w \le d + 2 \tan(\theta)L_w$$

$$w \le 6 \text{ in} + 2 \tan(40.0)14 \text{ in.} = 29.5 \text{ in.}$$

This exceeds the actual gusset width (14 in.), and thus the actual width will be used.

Per AISC 360 Section E3:

$$\frac{kL}{r} = \frac{(1.2)(17.2 \text{ in.})}{(0.252 \text{ in.})} = 81.7$$

$$F_e = \frac{\pi^2 (29,000 \text{ ksi})}{(71.2)^2} = 42.9 \text{ ksi}$$

$$F_{cr} = \left[0.658^{\frac{(50 \text{ ksi})}{(42.9 \text{ ksi})}} \right](50 \text{ ksi}) = 30.7 \text{ ksi}$$

$$F_{cr} = 30.7 \text{ ksi} > 24.6 \text{ ksi} = f_a \qquad\qquad\qquad \text{OK}$$

Next, check the reduced section of the tube, which has a 1-inch-wide slot for the gusset plate (the thickness of the gusset plus an extra 1/8 inch for ease of construction). The reduction in HSS6x6x1/2 section due to the slot is (0.5 in. × 1 in. × 2) = 1.0 in.² the net section, $A_{net} = (10.36 - 1.0) = 9.36$ in.²

To ensure gross section yielding governs, reinforcement is added over the area of the slot. The shear lag factor is computed per AISC 360 Table D3.1:

$$U = 1 - \frac{\bar{x}}{l}$$

where:

$$\bar{x} = \frac{B^2 + 2BH}{4(B+H)} = \frac{(6 \text{ in.})^2 + 2(6 \text{ in.})(6 \text{ in.})}{4(6 \text{ in.} + 6 \text{ in.})} = 2.25 \text{ in.}$$

and l is the length of the weld as determined above.

$$U = 1 - \frac{(2.25 \text{ in.})}{(14 \text{ in.})} = 0.839$$

Thus, the effective area of the section is:

$$A_e = UA_{net} = (0.839)(9.36 \text{ in.}^2) = 7.86 \text{ in.}^2$$

Try a reinforcing plate 1/2 inch thick and 3-1/2 inches wide on each side of the brace. (The necessary width can be computed from the effective area, but that calculation is not performed here.) Grade 50 material is used in order to match or exceed the brace material strength, thus allowing for treatment of the material as homogenous. The area of the section is $(2 \times 0.5 \text{ in.} \times 3.5 \text{ in.}) = 3.5 \text{ in.}^2$. The distance of its center of gravity from the center of gravity of the slotted brace is:

$$\bar{x} = \frac{B}{2} + \frac{t_{reinf}}{2} = \frac{(6 \text{ in.})}{2} + \frac{(0.5 \text{ in.})}{2} = 3.25 \text{ in.}$$

Thus, the area of the reinforced section is:

$$A = A_n + A_{reinf} = 9.4 \text{ in.}^2 + 3.5 \text{ in.}^2 = 12.9 \text{ in.}^2$$

The weighted average of the x's is 2.5 inches. Thus, the shear lag factor for the reinforced section is:

$$U = 1 - \frac{(2.5 \text{ in.})}{(14 \text{ in.})} = 0.82$$

Thus, the effective area of the section is:

$$A_e = UA_{net} = (0.82)(12.9 \text{ in.}^2) = 10.6 \text{ in.}^2$$

Now, check the effective area of the reinforced section against the original section of the brace per AISC 341 Section F2.6c (1):

$$\frac{A_g}{A_e} = \frac{(10.36 \text{ in.}^2)}{(10.6 \text{ in.}^2)} = 0.98 \leq 1 \qquad\qquad \text{OK}$$

The reinforcement is attached to the brace such that its expected yield strength is developed.

$$R_u = A_{reinf} R_y F_y = 3.5 \text{ in.}^2 (1.1)(50 \text{ ksi}) = 193 \text{ kips}$$

The plate will be developed with two 5/16-inch fillet welds, 14 inches long:

$$R_n = 2\phi 0.6 F_{exx} \frac{\sqrt{2}}{2} sL = 2(0.75)(0.6)(70 \text{ ksi})\frac{\sqrt{2}}{2}(\tfrac{5}{16} \text{ in.})(14 \text{ in.}) = 195 \text{ kips}$$

The force must be developed into the plate, carried past the reduced section developed out of the plate. To accomplish this, the reinforcement plate will be 33 inches: 14 inches on each side of the reduced section, 2 inches of anticipated over slot, plus 1 inch to provide erection tolerance.

The complete connection design includes the following checks (which are not demonstrated here):

Attachment of reinforcement to brace

Brace shear rupture

Brace shear yield

Gusset block shear

Gusset yield, tension rupture, shear rupture weld at both the column and the beam

Web crippling and yielding for both the column and the beam

Gusset edge buckling

Beam-to-column connection

10

Reinforced Concrete

By Peter W. Somers, S.E.

Contents

10.1   INTRODUCTION

In this chapter, a 12-story reinforced concrete office building with some retail shops on the first floor is designed for both high and moderate seismic loading. For the more extreme loading, it is assumed that the structure will be located in Berkeley, California and for the moderate loading, in Honolulu, Hawaii. These examples were originally developed by Finley Charney, Ph.D., P.E.

The basic structural configuration for both locations is illustrated in Figures 10-1 and 10-2, which show a typical floor plan and building section, respectively. The building has 12 stories above grade and one basement level. The typical bays are 30 feet long in the north-south (N-S) direction and either 40 or 20 feet long in the east-west (E-W) direction.

The main gravity framing system consists of seven continuous 30-foot spans of pan joists. These joists are spaced at 36 inches on center and have an average web thickness of 6 inches and a depth below slab of 16 inches. Due to fire code requirements, a 4-inch-thick floor slab is used, giving the joists a total depth of 20 inches. The joists are supported by concrete beams running in the E-W direction. The building is constructed of normal-weight concrete.

Concrete walls are located around the entire perimeter of the basement level.

For both locations, the seismic force-resisting system in the N-S direction consists of four 7-bay moment-resisting frames. At the Berkeley location, these frames are detailed as special moment-resisting frames. Due to the lower seismicity and lower demand for system ductility, the frames of the Honolulu building are detailed as intermediate moment-resisting frames as permitted by ASCE 7.

In the E-W direction, the seismic force-resisting system for the Berkeley building is a dual system composed of a combination of moment frames and frame-walls (walls integrated into a moment-resisting frame). Along Grids 1 and 8, the frames have five 20-foot bays. Along Grids 2 and 7, the frames consist of two exterior 40-foot bays and one 20-foot interior bay. At Grids 3, 4, 5 and 6, the interior bay consists of structural walls cast monolithically with the interior columns. The exterior bays of these frames are similar to Grids 2 and 7. For the Honolulu building, the structural walls are not necessary, so E-W seismic resistance is supplied by the moment frames along Grids 1 through 8. The frames on Grids 1 and 8 are five-bay frames and those on Grids 2 through 7 are three-bay frames with the exterior bays having a 40-foot span and the interior bay having a 20-foot span. Hereafter, frames are referred to by their gridline designation (e.g., Frame 1 is located on Grid 1).

The foundation system is not considered in this example, but it is assumed that the structure for both the Berkeley and Honolulu locations is founded on very dense soil (shear wave velocity of approximately 2,000 feet per second).
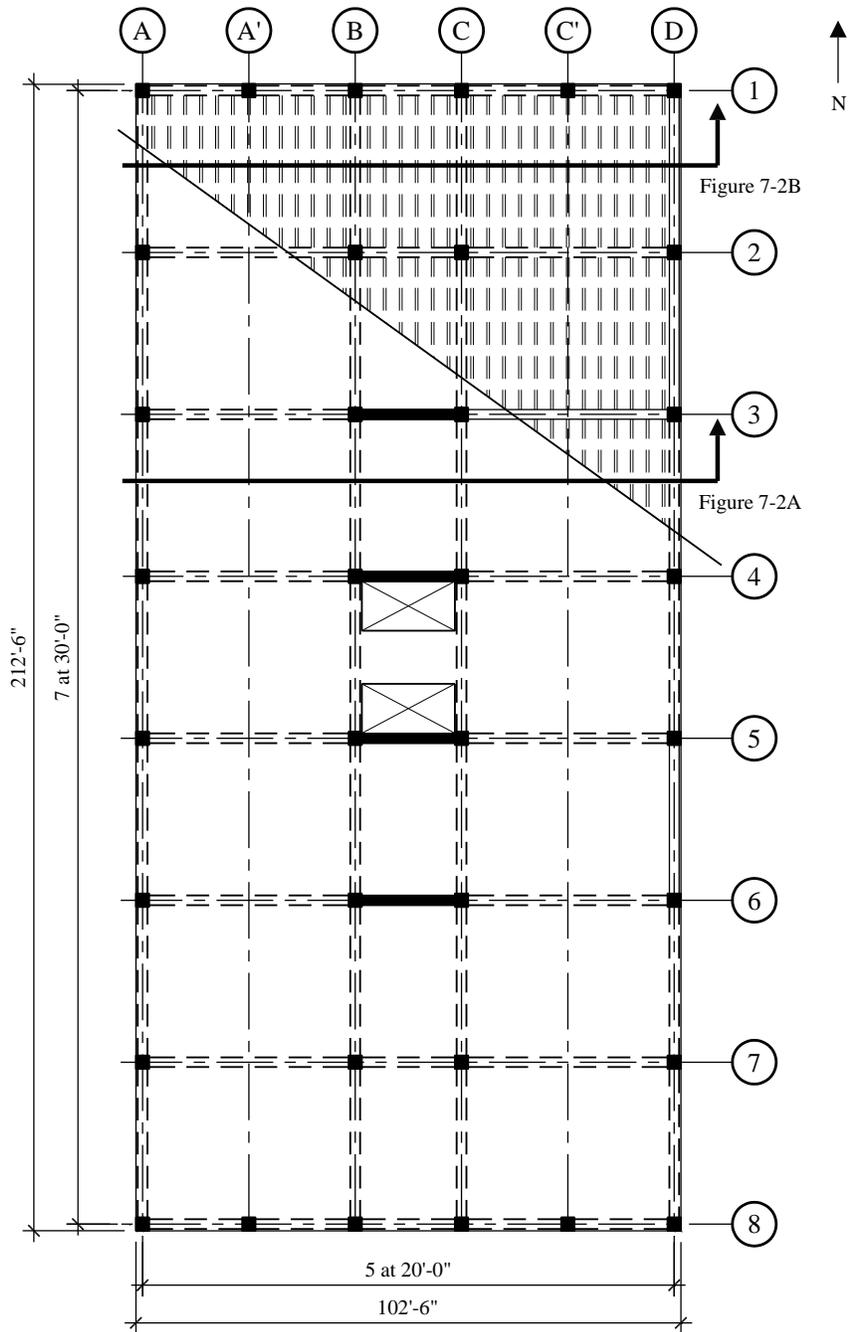
Figure 10-1 Typical floor plan of the Berkeley building; the Honolulu building is similar but without structural walls (1.0 ft = 0.3048 m)
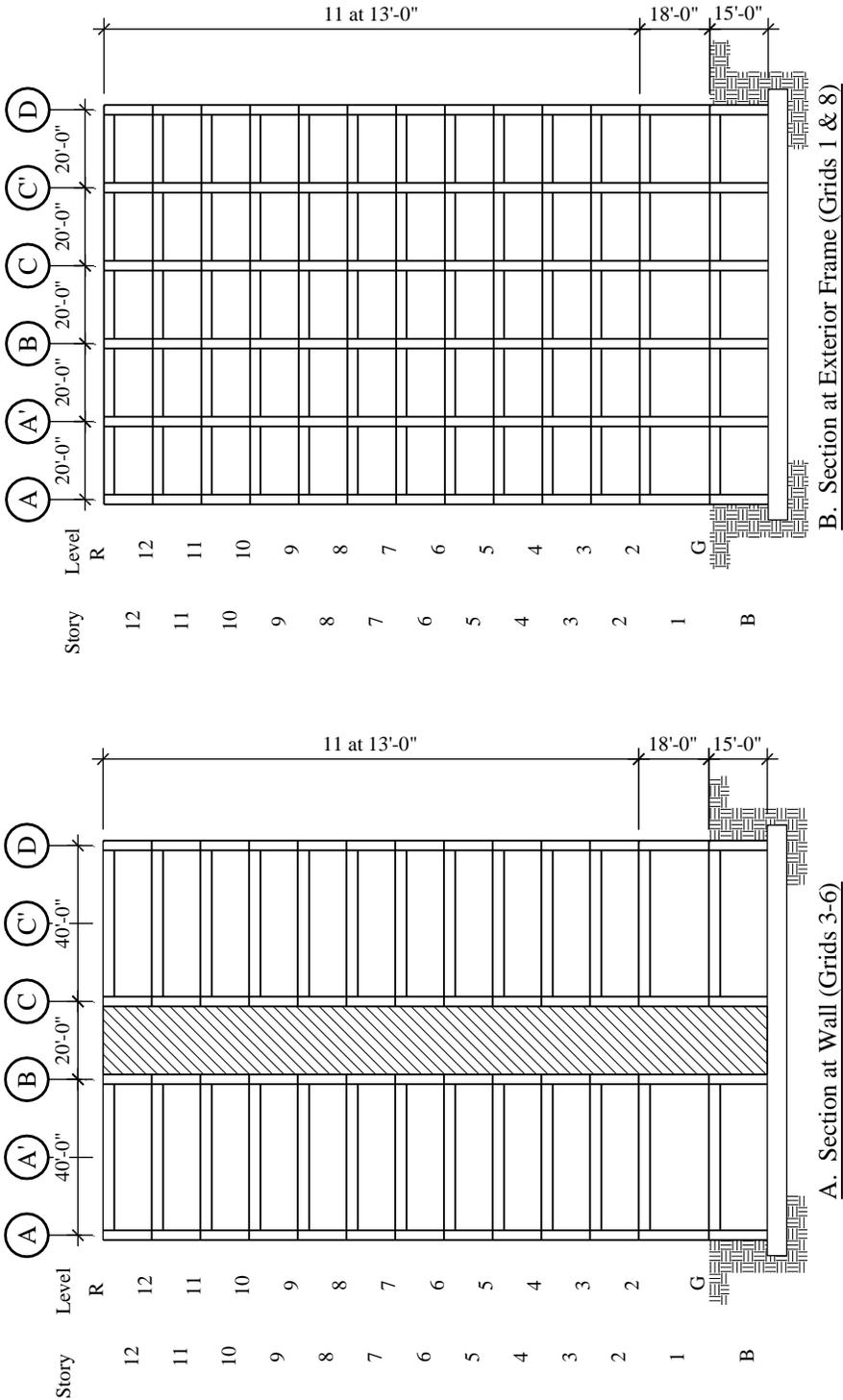
Figure 10-2 Typical elevations of the Berkeley building; the Honolulu building is similar but without structural walls (1.0 ft = 0.3048 m)

The intent of this example is to assist the reader in developing a better understanding of the design requirements in ASCE 7-10 *Minimum Design Loads for Buildings and Other Structures* (hereafter, the

Standard), which will be the primary reference document in the 2015 Edition of the *NEHRP Recommended Seismic Provisions* (hereafter, the *Provisions*). However, this chapter does not include any references to potential modifications to the *Standard* by the 2015 *Provisions*, which is still under development. In addition to the *Standard*, ACI 318-14 is the other main reference in this chapter. Except for very minor exceptions, the seismic force-resisting system design requirements of ACI 318 have been adopted in their entirety by the *Standard*. Cases where requirements of the *Standard* and ACI 318 differ are pointed out as they occur. (Note that the *Provisions* may further modify ACI 318, but these are not addressed in this chapter). In addition to serving as a reference standard for seismic design, the *Standard* is also cited where discussions involve gravity loads, live load reduction, wind loads and load combinations.

Because a single building configuration is designed for both high and moderate levels of seismicity, two different sets of calculations are required. Instead of providing one full set of calculations for the Berkeley building and then another for the Honolulu building, portions of the calculations are presented in parallel. For example, the development of seismic forces for the Berkeley and Honolulu buildings are presented before structural design is considered for either building. The design of representative elements then is given for the Berkeley building followed by the design of the Honolulu building. Each major section (development of forces, structural design, etc.) is followed by discussion. In this context, the following portions of the design process are presented in varying amounts of detail for each structure:

1. Seismic design criteria

2. Development and computation of seismic forces

3. Structural analysis and drift checks

4. Design of structural members including typical beams, columns and beam-column joints in Frame 1; and for the Berkeley building only, the design of the structural wall on Grid 3

The following are referenced in this chapter:

ACI 318   American Concrete Institute. 2014. *Building Code Requirements and Commentary for Structural Concrete*.

ASCE 7   American Society of Civil Engineers. 2010. *Minimum Design Loads for Buildings and Other Structures*.

ASCE 41   American Society of Civil Engineers. 2013. *Seismic Evaluation and Retrofit of Existing Buildings*.

Moehle (2008)   Moehle, Jack P., Hooper, John D and Lubke, Chris D. 2008. "Seismic Design of Reinforced Concrete Special Moment Frames: A Guide for Practicing Engineers," *NEHRP Seismic Design Technical Brief No. 1*, produced by the NEHRP Consultants Joint Venture, a partnership of the Applied Technology Council and the Consortium of Universities for Research in Earthquake Engineering, for the National Institute of Standards and Technology, Gaithersburg, MD., NIST GCR 8-917-1

Moehle (2011)   Moehle, Jack P., Ghodsi, Tony, Hooper, John D, Fields, David C., and Rajnikanth Gedhada. 2011. "Seismic Design of Cast-in-Place Concrete Special Structural Walls and Coupling Beams: A Guide for Practicing Engineers," *NEHRP Seismic Design Technical Brief No. 6*, produced by the NEHRP Consultants Joint Venture, a partnership of the Applied Technology Council and the Consortium of Universities for Research in Earthquake

Engineering, for the National Institute of Standards and Technology, Gaithersburg, MD., NIST GCR 11-917-11

The structural analysis for this chapter was carried out using the ETABS Building Analysis Program, version 9.7.4, developed by Computers and Structures, Inc., Berkeley, California. Axial-flexural interaction for column and structural wall design was performed using the spColumn program, version 4.6, developed by StructurePoint, LLC.

10.2 SEISMIC DESIGN REQUIREMENTS

10.2.1 Seismic Response Parameters

For Berkeley, California, the short period and one-second period spectral response acceleration parameters S_S and S_1 are 1.93 and 0.78, respectively. For the very dense soil conditions, Site Class C is appropriate as described in *Standard* Section 20.3. Using $S_S = 1.93$ and Site Class C, *Standard* Table 11.4-1 lists a short period site coefficient, F_a, of 1.0. For $S_1 > 0.5$ and Site Class C, *Standard* Table 11.4-2 gives a velocity based site coefficient, F_v, of 1.3. Using *Standard* Equation 11.4-1 and 11.4-2, the adjusted maximum considered spectral response acceleration parameters for the Berkeley building are:

$S_{MS} = F_a S_S = 1.0(1.93) = 1.93$

$S_{M1} = F_v S_1 = 1.3(0.78) = 1.014$

The design spectral response acceleration parameters are given by *Standard* Equation 11.4-3 and 11.4-4:

$S_{DS} = 2/3\ S_{MS} = 2/3\ (1.93) = 1.287$

$S_{D1} = 2/3\ S_{M1} = 2/3\ (1.014) = 0.676$

The transition period, T_s, for the Berkeley response spectrum is:

$$T_S = \frac{S_{D1}}{S_{DS}} = \frac{0.676}{1.287} = 0.525 \text{ sec}$$

T_s is the period where the horizontal (constant acceleration) portion of the design response spectrum intersects the descending (constant velocity or acceleration inversely proportional to T) portion of the spectrum. It is used later in this example as a parameter in determining the type of analysis that is required for final design.

For Honolulu, the short-period and one-second period spectral response acceleration parameters are 0.578 and 0.169, respectively. For Site Class C soils and interpolating from *Standard* Table 11.4-1, the F_a is 1.169 and from *Standard* Table 11.4-1, the interpolated value for F_v is 1.631. The adjusted maximum considered spectral response acceleration parameters for the Honolulu building are:

$S_{MS} = F_a S_S = 1.169(0.578) = 0.676$

$S_{M1} = F_v S_1 = 1.631(0.169) = 0.276$

and the design spectral response acceleration parameters are:

$S_{DS} = 2/3\ S_{MS} = 2/3\ (0.676) = 0.450$

$S_{D1} = 2/3\ S_{M1} = 2/3\ (0.276) = 0.184$

The transition period, T_s, for the Honolulu response spectrum is:

$$T_S = \frac{S_{D1}}{S_{DS}} = \frac{0.184}{0.450} = 0.409 \text{ sec}$$

10.2.2 Seismic Design Category

According to *Standard* Section 1.5, both the Berkeley and the Honolulu buildings are classified as Risk Category II. *Standard* Section 11.5.1 which refers to Table 1.5-2 assigns an importance factor, I_e, of 1.0 to all Risk Category II buildings.

According to *Standard* Section 11.6 and Tables 11.6-1 and 11.6-2, the Berkeley building is assigned to Seismic Design Category E and the Honolulu building is assigned to Seismic Design Category C.

10.2.3 Structural Systems

The seismic force-resisting systems for both the Berkeley and the Honolulu buildings consist of moment-resisting frames in the N-S direction. E-W loading is resisted by a dual frame-wall system in the Berkeley building and by a set of moment-resisting frames in the Honolulu building. For the Berkeley building, assigned to Seismic Design Category E, *Standard* Table 12.2-1 requires that all concrete moment-resisting frames be designed and detailed as special moment frames. Similarly, *Standard* Table 12.2-1 requires structural walls in dual systems to be detailed as special reinforced concrete structural walls. For the Honolulu building assigned to Seismic Design Category C, *Standard* Table 12.2-1 permits the use of intermediate moment frames for all building heights.

Standard Table 12.2-1 provides values for the response modification coefficient, R, the system overstrength factor, Ω_0 and the deflection amplification factor, C_d, for each structural system type. The values determined for the Berkeley and Honolulu buildings are summarized in Table 10-1.

Table 10-1 Response Modification, Overstrength and Deflection Amplification Coefficients for Structural Systems Used

Location	Response Direction	Building Frame Type	R	Ω_0	C_d
Berkeley	N-S	Special moment frame	8	3	5.5
	E-W	Dual system incorporating special moment frame and special structural wall	7	2.5	5.5
Honolulu	N-S	Intermediate moment frame	5	3	4.5
	E-W	Intermediate moment frame	5	3	4.5

For the Berkeley building dual system, *Standard* Section 12.2.5.1 requires that the moment frame portion of the system be designed to resist at least 25 percent of the total seismic force. As discussed below, this requires that a separate analysis of a frame-only system be carried out for loading in the E-W direction.

10.2.4 Structural Configuration

Based on the plan view of the building shown in Figure 10-1, the only potential horizontal irregularity is a Type 1a or 1b torsional irregularity (*Standard* Table 12.3-1). While the actual presence of such an irregularity cannot be determined without analysis, it appears unlikely for both the Berkeley and the Honolulu buildings because the lateral force-resisting elements of both buildings are distributed evenly over the floor. However, this will be determined later.

As for the vertical irregularities listed in *Standard* Table 12.3-2, the presence of a soft or weak story cannot be determined without analysis. In this case, however, the first story is suspect, because its height of 18 feet is well in excess of the 13-foot height of the story above. However, it is assumed (but verified later) that a vertical irregularity does not exist.

10.2.5 Load Combinations

The combinations of loads including earthquake effects are provided in *Standard* Section 12.4. Load combinations for other loading conditions are in *Standard* Chapter 2.

For the Berkeley structure, the basic strength design load combinations that must be considered are:

$1.2D + 1.6L$ (or $1.6L_r$)

$1.2D + 0.5L \pm 1.0E$

$0.9D \pm 1.0E$

In addition to the combinations listed above, for the Honolulu building wind loads govern the design of a portion of the building (as determined later), so the following strength design load combinations should also be considered:

$1.2D + 1.0L \pm 1.0W$

$0.9D \pm 1.0W$

The load combination including only 1.4 times dead load will not control for any condition in these buildings.

In accordance with *Standard* Section 12.4.2 the earthquake load effect, E, be defined as:

$$E = \rho Q_E + 0.2 S_{DS} D$$

where gravity and seismic load effects are additive and

$$E = \rho Q_E - 0.2 S_{DS} D$$

where the effects of seismic load counteract gravity.

The earthquake load effect requires the determination of the redundancy factor, ρ, in accordance with *Standard* Section 12.3.4. For the Honolulu building (Seismic Design Category C), $\rho = 1.0$ per *Standard* Section 12.3.4.1.

For the Berkeley building (Seismic Design Category E), ρ must be determined in accordance with *Standard* Section 12.3.4.2. For the purpose of the example, the method in *Standard* Section 12.3.4.2, Method b, will be utilized. Based on the preliminary design, it is assumed that $\rho = 1.0$ because the structure has a perimeter moment frame and is assumed to be regular based on the plan layout. As discussed in the previous section, this will be verified later.

For the Berkeley building, substituting E and with ρ taken as 1.0, the following load combinations must be used for seismic design:

$(1.2 + 0.2S_{DS})D + 0.5L \pm Q_E$

$(0.9 - 0.2\ S_{DS})D \pm Q_E$

Finally, substituting 1.287 for S_{DS}, the following load combinations must be used:

$1.46D + 0.5L \pm Q_E$

$0.64D \pm Q_E$

For the Honolulu building, substituting E and with ρ taken as 1.0, the following load combinations must be used for seismic design:

$(1.2 + 0.2S_{DS})D + 0.5L \pm Q_E$

$(0.9 - 0.2S_{DS})D \pm Q_E$

Finally, substituting 0.450 for S_{DS}, the following load combinations must be used:

$1.29D + 0.5L \pm Q_E$

$0.81D \pm Q_E$

The seismic load combinations with overstrength given in *Standard* Section 12.4.3.2 are not utilized for this example because there are no discontinuous elements supporting stiffer elements above them and collector elements are not addressed.

10.2.6 Material Properties

For the Berkeley building, normal-weight concrete of 5,000 psi strength is used everywhere (except as revised for the lower floor structural walls as determined later). All reinforcement has a specified yield strength of 60 ksi. As required by ACI 318 Section 20.2.2.5, the longitudinal reinforcement in the moment frames and structural walls either must conform to ASTM A706 or be ASTM A615 reinforcement, if the actual yield strength of the steel does not exceed the specified strength by more than 18 ksi and the ratio of actual ultimate tensile stress to actual tensile yield stress is greater than 1.25.

The Honolulu building also uses 5,000 psi concrete and ASTM A615 Grade 60 reinforcing steel. ASTM 706 reinforcing is not required for an intermediate moment frame.

10.3 DETERMINATION OF SEISMIC FORCES

The determination of seismic forces requires an understanding of the magnitude and distribution of structural mass and the stiffness properties of the structural system. Both of these aspects of design are addressed in the mathematical modeling of the structure.

10.3.1 Modeling Criteria

Both the Berkeley and Honolulu buildings will be analyzed with a three-dimensional mathematical model using the ETABS software. Modeling criteria for the seismic analysis is covered in *Standard* Section 12.7. This section covers how to determine the effective seismic weight (addressed in the next section) and provides guidelines for the modeling of the building. Of most significance in a concrete building is modeling realistic stiffness properties of the structural elements considering cracked sections in accordance with *Standard* Section 12.7.3, Item a. ACI 318 Sections 6.6.3.1 and R18.2.2 provide recommendations for

modeling cracked sections for seismic analysis. However, the effective stiffness values for the cracked sections in ACI 318 are not mandatory requirements and they can be selected based on results from the related research. This example utilizes the following effective moment of inertia, I_{eff}, for both buildings which are slightly different from those in ACI 318 :

Beams: $I_{eff} = 0.3I_{gross}$

Columns: $I_{eff} = 0.5I_{gross}$

Walls: $I_{eff} = 0.5I_{gross}$

The effective stiffness of the moment frame elements is based on the recommendations in Moehle (2008) and ASCE 41 Table 10-5 and account for the expected axial loads and reinforcement levels in the members. The value for the structural walls is based on the recommendations in Moehle (2011) and ASCE 41 Table 10-5 for cracked concrete structural walls. The effective moment of inertia values are in accordance with ACI 318 Sections 6.6.3.1 and R18.2.2 in general. A more accurate determination of cracked section properties could be determined by calculation, but this is not commonly done.

The following are other significant aspects of the mathematical model that should be noted:

1.The structure is modeled with 12 levels above grade and one level below grade. The perimeter basement walls are modeled as shear panels as are the main structural walls at the Berkeley building. The walls are assumed to be fixed at their base, which is at the basement level.

2.All floor diaphragms are modeled as infinitely rigid in plane and infinitely flexible out-of-plane, consistent with common practice for a regular-shaped concrete diaphragm (see *Standard* Section 12.3.1.2).

3.Beams and columns are represented by two-dimensional frame elements. The beams are modeled as T-beams using the effective slab width per ACI 318 Section 6.3.2, as recommended by Moehle (2008).

4.The structural walls of the Berkeley building are modeled as a combination of boundary columns and shear panels with composite stiffness.

5.Beam-column joints are modeled in accordance with Moehle (2008), which references the procedure in ASCE 41. Both the beams and columns are modeled with end offsets based on the geometry, but the beam offset is modeled as 0 percent rigid, while the column offset is modeled as 100 percent rigid. This provides effective stiffness for beam-column joints consistent with the expected behavior of the joint: strong column-weak beam condition. (While the recommendations in Moehle (2008) are intended for special moment frames, the same joint rigidities are used for Honolulu for consistency.)

6.P-delta effects are neglected in the analysis for the purposes of this example since they are unlikely to be significant for these buildings. This assumption is verified later in this example.

7.While the base of the model is located at the basement level, the seismic base for determination of forces is assumed to be at the first floor, which is at the exterior grade.

10.3.2 Building Mass

Before the building mass can be determined, the approximate size of the different members of the seismic force-resisting system must be established. For special moment frames, limitations on beam-column joint shear and reinforcement development length usually control. An additional consideration is the amount of vertical reinforcement in the columns. ACI 318 Section 18.7.4.1 limits the vertical steel reinforcing ratio to

6 percent for special moment frame columns; however, 3 to 4 percent vertical steel is a more practical upper-bound limit.

Based on a series of preliminary calculations (not shown here), it is assumed that for the Berkeley building all columns and structural wall boundary elements are 30 inches by 30 inches, beams are 24 inches wide by 32 inches deep and the panel of the structural wall is 16 inches thick. It has already been established that pan joists are spaced at 36 inches on center, have an average web thickness of 6 inches and, including a 4-inch-thick slab, are 20 inches deep. For the Berkeley building, these member sizes probably are close to the final sizes. For the Honolulu building (which does not have the weight of concrete walls and ends up with slightly smaller frame elements: 28- by 28-inch columns and 20- by 30-inch beams), the masses computed from the Berkeley member sizes are slightly high but are used for consistency.

In addition to the building structural weight, the following superimposed dead loads are assumed:

Roofing = 10 psf

Partition = 10 psf (see *Standard* Section 12.7.2, Item 2)

Ceiling and M/E/P = 10 psf

Curtain wall cladding = 10 psf (on vertical surface area)

Based on the above member sizes and superimposed dead load, the individual story weights and masses are listed in Table 10-2. These masses are used for the analysis of both the Berkeley and the Honolulu buildings (even though the structural walls in the Berkeley building would result in a slightly higher building mass). Note from Table 10-2 that the roof and lowest floor have masses slightly different from the typical floors. It is also interesting to note that the average density of this building is 12.4 pcf, which is in the range of typical concrete buildings with relatively high floor-to-floor heights.

Table 10-2 Story Weights and Masses

Level	Weight (kips)	Mass (kips-sec^2/in.)
Roof	3,352	8.675
12	3,675	9.551
11	3,675	9.551
10	3,675	9.551
9	3,675	9.551
8	3,675	9.551
7	3,675	9.551
6	3,675	9.551
5	3,675	9.551
4	3,675	9.551
3	3,675	9.551
2	3,817	9.879
Total	43,919	113.736

(1.0 kip = 4.45 kN, 1.0 in. = 25.4 mm)

In the ETABS model, these masses are applied as uniform distributed masses across the extent of the floor diaphragms in order to provide a realistic distribution of mass in the dynamic model as described below.

The structural framing is modeled utilizing massless elements since their mass is included with the floor mass. Note that for relatively heavy cladding systems, it would be more appropriate to model the cladding mass linearly along the perimeter in order to more correctly model the mass moment of inertia. This has little impact in relatively light cladding systems as is the case here, so the cladding masses are distributed across the floor diaphragms for convenience.

10.3.3 Analysis Procedures

The selection of analysis procedures is in accordance with *Standard* Table 12.6-1. Based on the initial review, it appears that the Equivalent Lateral Force (ELF) procedure is permitted for both the Berkeley and Honolulu buildings. However, as we shall see, the analysis demonstrates that the Berkeley building is torsionally irregular, meaning that the Model Response Spectrum Analysis (MRSA) procedure is required. Regardless of irregularities, it is common practice to use the MRSA for buildings in regions of high seismic hazard since the more rigorous analysis method tends to provide lower seismic forces and therefore more economical designs. For the Honolulu building, located in a region of lower seismic hazard and with wind governing in some cases, the ELF procedure will be used. However, a dynamic model of the Honolulu building is used for determining the structural periods.

It should be noted that even though the Berkeley building utilizes the MRSA, the ELF must be used for at least determining base shear for scaling of results as discussed below.

10.3.4 Development of Equivalent Lateral Forces

This section covers the ELF procedure for both the Berkeley and Honolulu buildings. Since the final analysis of the Berkeley building utilizes the MRSA procedure, the ELF is illustrated for determining base shear only. The complete ELF procedure is illustrated for the Honolulu building.

10.3.4.1 Period Determination. Requirements for the computation of building period are given in *Standard* Section 12.8.2. For the preliminary design using the ELF procedure, the approximate period, T_a, computed in accordance with *Standard* Equation 12.8-7 can be used:

$$T_a = C_t h_n^x$$

The method for determining approximate period will generally result in periods that are lower (hence, more conservative for use in predicting base shear) than those computed from a more rigorous mathematical model. If a more rigorous analysis is carried out, the resulting period may be too high due to a variety of possible modeling simplifications and assumptions. Consequently, the *Standard* places an upper limit on the period that can be used for design. The upper limit is $T = C_u T_a$ where C_u is provided in *Standard* Table 12.8-1.

For the N-S direction of the Berkeley building, the structure is a reinforced concrete moment-resisting frame and the approximate period is calculated according to *Standard* Equation 12.8-7 using $C_t = 0.016$ and $x = 0.9$ per *Standard* Table 12.8-2. For $h_n = 161$ feet, $T_a = 1.55$ seconds and $S_{D1} > 0.40$ for the Berkeley building, $C_u = 1.4$ and the upper limit on the analytical period is $T = 1.4(1.55) = 2.17$ seconds.

For E-W seismic activity in Berkeley, the structure is a dual system, so $C_t = 0.020$ and $x = 0.75$ for "other structures." The approximate period, $T_a = 0.90$ second and the upper limit on the analytical period is $1.4(0.90) = 1.27$ seconds.

For the Honolulu building, the $T_a = 1.55$ second period computed above for concrete moment frames is applicable in both the N-S and E-W directions. For Honolulu, S_{D1} is 0.192 and, from *Standard* Table 12.8-1, C_u can be taken as 1.52. The upper limit on the analytical period is $T = 1.52(1.55) = 2.35$ seconds.

For the detailed period determination at both the Berkeley and Honolulu buildings, computer models were developed based on the criteria in Section 7.3.1.

A summary of the Berkeley analysis is presented in Section 7.3.6, but the fundamental periods are presented here. The computed N-S period of vibration is 2.02 seconds. This is between the approximate period, T_a = 1.55 seconds and C_uT_a = 2.17 seconds. In the E-W direction, the computed period is 1.42 seconds, which is greater than both T_a = 0.90 second and C_uT_a = 1.27 seconds. Therefore, the periods used for the ELF procedure are 2.02 seconds in the N-S direction and 1.27 seconds in the E-W direction.

For the Honolulu building, the computed periods in the N-S and E-W directions are 2.40 seconds and 2.33 seconds, respectively. The N-S period is similar to the Berkeley building because there are no walls in the N-S direction of either building, but the Honolulu period is higher due to the smaller framing member sizes. In the E-W direction, the increase in period from 1.42 seconds at the Berkeley building to 2.33 seconds indicates a significant reduction in stiffness due to the lack of the walls in the Honolulu building. For both the E-W and the N-S directions, T_a for the Honolulu building is 1.55 seconds and C_uT_a is 2.35 seconds. Therefore, for the purpose of computing ELF forces, the periods are 2.35 seconds and 2.33 seconds in the N-S and E-W directions, respectively.
A summary of the approximate and computed periods is given in Table 10-3.

Table 10-3 Comparison of Approximate and Computed Periods (in seconds)

Method of Period Computation	Berkeley		Honolulu	
	N-S	E-W	N-S	E-W
Approximate T_a	1.55	0.90	1.55	1.55
Approximate $\times C_u$	2.17	**1.27**	**2.35**	2.35
ETABS	**2.02**	1.42	2.40	**2.33**

*Bold values should be used in the ELF analysis.

10.3.4.2 Seismic Base Shear. For the ELF procedure, seismic base shear is determined using the short period and 1-second period response acceleration parameters, the computed structural period and the system response modification factor (R).

Using *Standard* Equation 12.8-1, the design base shear for the structure is:

$$V = C_sW$$

where W is the total effective seismic weight of the building and C_s is the seismic response coefficient computed in accordance with *Standard* Section 12.8.1.1.

The seismic design base shear for the Berkeley is computed as follows:

For the moment frame system in the N-S direction with W = 43,919 kips (see Table 10-2), S_{DS} = 1.287, S_{D1} = 0.676, R = 8, I_e = 1.0 and T = 2.02 seconds:

$$C_{s,max} = \frac{S_{DS}}{R/I_e} = \frac{1.10}{8/1} = 0.161$$

$$C_s = \frac{S_{D1}}{T(R/I_e)} = \frac{0.676}{2.02(8/1)} = 0.042$$

$$C_{s,min} = 0.044S_{DS}I_e = 0.044(1.1)(1) = 0.057$$

10-14

Since S_1 exceeds 0.60, *Standard* Equation 12.8-6 also needs to be checked as follows:

$$C_{s,min} = \frac{0.5S_{D1}}{R/I_e} = \frac{0.5(0.676)}{8/1} = 0.042$$

Finally, in accordance with *Standard* Equation 12.8-5, the minimum lateral force cannot be less than 1 percent of the building weight, that is $C_{s,min} = 0.01$.

$C_{s,min} = 0.057$ controls, and the design base shear in the N-S direction is $V = 0.057 (43,919) = 2,486$ kips.

In the E-W direction with the dual system, $T = 1.27$ seconds and

$$C_{s,max} = \frac{S_{DS}}{R/I_e} = \frac{1.10}{7/1} = 0.184$$

$$C_S = \frac{S_{D1}}{T(R/I_e)} = \frac{0.676}{1.27(7/1)} = 0.076$$

$$C_{s,min} = 0.044S_{DS}I_e = 0.044(1.1)(1) = 0.057$$

$$C_{s,min} = \frac{0.5S_{D1}}{R/I_e} = \frac{0.5(0.676)}{7/1} = 0.048$$

In this case, $C_s = 0.076$ controls and $V = 0.076 (43,919) = 3,351$ kips.

For the Honolulu building, base shears are computed in a similar manner and are nearly the same for the N-S and the E-W directions. With $W = 43,919$ kips, $S_{DS} = 0.450$, $S_{D1} = 0.189$, $R = 5$, $I = 1$ and $T = 2.35$ seconds in the N-S direction:

$$C_{s,max} = \frac{S_{DS}}{R/I_e} = \frac{0.450}{5/1} = 0.090$$

$$C_S = \frac{S_{D1}}{T(R/I_e)} = \frac{0.0156}{2.35(5/1)} = 0.0156$$

$$C_{s,min} = 0.044S_{DS}I_e = 0.044(0.450)(1) = 0.0198$$

$$C_{s,min} = 0.01$$

$C_s = 0.0198$ controls, and $V = 0.0198 (43,919) = 870$ kips.

Due to rounding, the E-W base shear is also 870 kips. A summary of the Berkeley and Honolulu seismic design parameters are provided in Table 10-4.

Table 10-4 Comparison of Periods, Seismic Shears Coefficients and Base Shears for the Berkeley and Honolulu Buildings

Location	Response Direction	Building Frame Type	T (sec)	C_s	V (kips)
Berkeley	N-S	Special moment frame	2.02	0.0570	2,486
	E-W	Dual system incorporating special moment frame and structural wall	1.27	0.0760	3,351
Honolulu	N-S	Intermediate moment frame	2.35	0.0198	870
	E-W	Intermediate moment frame	2.33	0.0198	870

(1.0 kip = 4.45 kN)

10.3.4.3 Vertical Distribution of Seismic Forces. The vertical distribution of seismic forces for the ELF is computed from *Standard* Equations 12.8-11 and 12.8-12.:

$$F_x = C_{vx}V$$

$$C_{vx} = \frac{w_x h_x^k}{\sum_{i=1}^{n} w_i h_i^k}$$

where:

$k = 1.0$ for $T < 0.5$ second

$k = 2.0$ for $T > 2.5$ seconds

$k = 0.75 + 0.5T$ for $1.0 < T < 2.5$ seconds

For the Berkeley building with $T = 2.35$ seconds, $k = 1.92$.

Based on the equations above, the seismic story forces, shears and overturning moments are easily computed using a spreadsheet. Since the analysis of the Berkeley building utilizes the MRSA procedure, the vertical force distribution for the ELF procedure will not be used for the design and are not shown here. The vertical force distribution computations for the Honolulu building are shown in Table 10-5. The table is presented with as many significant digits to the left of the decimal as the spreadsheet generates but that should not be interpreted as real accuracy; it is just the simplest approach.

Table 10-5 Vertical Distribution of N-S and E-W Seismic Forces for the Honolulu Building

Level	Height h (ft)	Weight W (kips)	Wh^k	Wh^k/Σ	Force F_x (kips)	Story Shear V_x (kips)	Overturning Moment M_x (ft-k)
R	161.00	3,352	59,356,482	0.196	170.4	170.4	
12	148.00	3,675	55,336,431	0.183	158.9	329.3	2,215
11	135.00	3,675	46,360,685	0.153	133.1	462.4	6,496
10	122.00	3,675	38,150,481	0.126	109.5	571.9	12,508
9	109.00	3,675	30,711,664	0.101	88.2	660.1	19,943
8	96.00	3,675	24,050,797	0.079	69.1	729.2	28,524
7	83.00	3,675	18,175,345	0.060	52.2	781.3	38,003

6	70.00	3,675	13,093,962	0.043	37.6	818.9	48,161
5	57.00	3,675	8,816,911	0.029	25.3	844.3	58,807
4	44.00	3,675	5,356,779	0.018	15.4	859.6	69,782
3	31.00	3,675	2,729,786	0.009	7.8	867.5	80,958
2	18.00	3,817	995,719	0.003	2.9	870.3	92,235
Total		43,919	303,135,043	1.000	870.3		107,901

(1.0 ft = 0.3048 m, 1.0 kip = 4.45 kN, 1.0 ft-kip = 1.36 kN-m)

The computed seismic story shears for the Honolulu buildings are shown graphically in Figure 10-3. Also shown in this figure are the wind load story shears determined in accordance with the *Standard* based on a wind speed of 130 mph and Exposure Category B. Wind loads are determined using the Directional Procedure in *Standard* Chapter 27, which is permitted for this building in accordance with *Standard* Section 26.1.2.1. Since the *Standard* now uses strength design as a basis for determining wind loads, the wind loads are comparable to seismic loads without considering load factors (which are 1.0 for both types of loads).

As can be seen, the N-S seismic shears are significantly greater than the corresponding wind shears, but the E-W seismic and wind shears are closer. In the lower stories of the building, wind controls the strength demands and, in the upper levels, seismic forces control the strength demands. (A somewhat more detailed comparison is given later when the Honolulu building is designed.) With regards to detailing the Honolulu building, *all* of the elements must be detailed for inelastic deformation capacity as required by ACI 318 for intermediate moment frames.
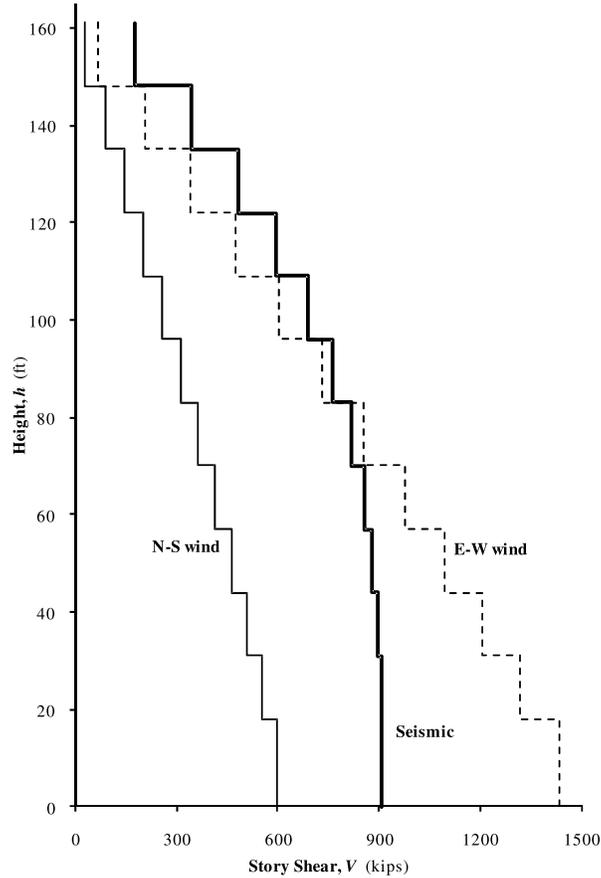
Figure 10-3 Comparison of wind and seismic story shears for the Honolulu building
(1.0 ft = 0.3048 m, 1.0 kip = 4.45 kN)

As expected, wind loads do not control the design of the Berkeley building based on calculations not presented here. (Note that the comparison between wind and seismic forces should be based on more than just the base shear values. For buildings where the wind and seismic loads are somewhat similar, it is possible that overturning moment for wind could govern even where the seismic base shear is greater, in which case a more detailed analysis of specific member forces would need to be performed to determine the controlling load case.)

10.3.4.4 Horizontal Force Distribution and Torsion. The story forces are distributed to the various vertical elements of the seismic force-resisting system based on relative rigidity using the ETABS model. As described previously, the buildings are modeled using rigid diaphragms at each floor. Since the structures are symmetric in both directions and the distribution of mass is assumed to be uniform, there is no inherent torsion (*Standard* Section 12.8.4.1) in either building. However, accidental torsion needs to be considered in accordance with *Standard* Section 12.8.4.2.

For this example, accidental torsion is applied to each level as a static moment equal to the story shear multiplied by 5 percent of the story width perpendicular to the direction of loading. The applied moment is based on the ELF forces for both the Berkeley building (analyzed using the MRSA) and Honolulu building (ELF). The computation of the accidental torsion moments for the Honolulu building is shown in Table 10-6.

10-18

Table 10-6 Accidental Torsion for the Honolulu Building

Level	Force F_x (kips)	N-S Building Width (ft)	N-S Torsion (ft-kips)	E-W Building Width (ft)	E-W Torsion (ft-kips)
R	170.4	103	873	216	1835
12	158.9	103	814	216	1712
11	133.1	103	682	216	1436
10	109.5	103	561	216	1183
9	88.2	103	452	216	953
8	69.1	103	354	216	747
7	52.2	103	267	216	566
6	37.6	103	193	216	408
5	25.3	103	130	216	275
4	15.4	103	79	216	168
3	7.8	103	40	216	86
2	2.9	103	15	216	31

(1.0 kip = 4.45 kN, 1.0 ft-kip = 1.36 kN-m)

Amplification of accidental torsion, which needs to be considered for buildings with torsional irregularities in accordance with *Standard* Section 12.8.4.3, will be addressed if required after the irregularities are determined.

10.3.5 Direction of Loading

For the initial analysis, the seismic loading is applied in two directions independently as permitted by *Standard* Section 12.5. This assumption at the Berkeley building will need to be verified later since *Standard* Section 12.5.4 requires consideration of multi-directional loading (the 100 percent-30 percent procedure) for columns that form part of two intersection systems and have a high seismic axial load.

Note that rather than checking whether or not multi-directional loading needs to be considered, some designers apply the seismic forces using the 100 percent-30 percent rule (or an SRSS combination of the two directions) as common practice when intersecting systems are utilized since today's computer analysis programs can make the application of multi-directional loading easier than checking each specific element. Since consideration of multi-directional loading for all elements is not a requirement of the *Standard*, the Berkeley building will be analyzed in two independent directions unless consideration of multi-directional effects is required for specific columns.

The Honolulu building, in Seismic Design Category C, does not require consideration of multi-directional loading since it does not contain the nonparallel system (Type 5 Horizontal) irregularity (*Standard* Section 12.5.3).

10.3.6 Modal Analysis Procedure

The Berkeley building will be analyzed using the MRSA procedure of *Standard* Section 12.9 and the ETABS software. The building is modeled based on the criteria discussed in Section 10.3.1 and analyzed using a response spectrum generated by ETABS based on the seismic response parameters presented in Section 10.2.1. The modal parameters were combined using the complete quadratic combination (CQC) method per *Standard* Section 12.9.3.

The computed periods and the modal response characteristics of the Berkeley building are presented in Table 10-7. In order to capture higher mode effects, 12 modes were selected for the analysis, and with 12 modes, the accumulated modal mass in each direction is more than 90 percent of the total mass as required by *Standard* Section 12.9.1.

Table 10-7 Periods and Modal Response Characteristics for the Berkeley Building

Mode	Period (sec)	% of Effective Mass Represented by Mode[*]		Description
		N-S	E-W	
1	2.02	83.62 (83.62)	0.00 (0.00)	First Mode N-S
2	1.46	0.00 (83.62)	0.00 (0.00)	First Mode Torsion
3	1.42	0.00 (83.62)	74.05 (74.05)	First Mode E-W
4	0.66	9.12 (92.74)	0.00 (74.05)	Second Mode N-S
5	0.38	2.98 (95.72)	0.00 (74.05)	Third Mode N-S
6	0.35	0.00 (95.72)	16.02 (90.07)	Second Mode E-W
7	0.25	1.36 (97.08)	0.00 (90.07)	Fourth Mode N-S
8	0.18	0.86 (97.94)	0.00 (90.07)	Fifth Mode N-S
9	0.17	0.00 (97.94)	0.09 (90.16)	Second Mode Torsion
10	0.15	0.00 (97.94)	5.28 (95.44)	Third Mode E-W
11	0.10	0.59 (98.53)	0.00 (95.44)	Sixth Mode N-S
12	0.08	0.00 (98.53)	3.14 (98.58)	Fourth Mode E-W

[*]Accumulated modal mass in parentheses.

One of the most important aspects of the MRSA procedure is the scaling requirement. In accordance with *Standard* Section 12.9.4, the seismic base shear computed using the MRSA cannot be less than 85 percent of the base shear using the ELF. This is commonly accomplished by running the MRSA to determine the modal base shear. If the modal base shear is more than 85 percent of the ELF base shear in each direction, then no scaling is required. However, if the model base shear is less than the ELF base shear, then the response spectrum is scaled upward so that the modal base shear is equal to 85 percent of the ELF base shear. This is illustrated in Table 10-8. Note that this scaling is typically not applicable to the determination of drifts.

Table 10-8 Scaling of MRSA results for the Berkeley Building

Direction	V_{ELF} (kips)	$0.85V_{ELF}$ (kips)	V_{MRSA} (kips)	Scale Factor
N-S	2,486	2,113	1,598	1.32
E-W	3,351	2,849	2,583	1.10

(1.0 kip = 4.45 kN)

Therefore, the response spectrum functions for the Berkeley analysis will be scaled by 1.32 and 1.10 in the N-S and E-W directions, respectively, which will result in the modal base shears being equal to 85 percent of the static base shears.

As discussed previously, the accidental torsion requirement for the model analysis will be satisfied by applying at each story the torsional moments computed using the ELF procedure as a static load case. These torsional forces will be combined with the dynamic load case for the MRSA forces.

10.4 DRIFT AND P-DELTA EFFECTS

The checks of story drift and P-delta effect are contained in this section, but first, deflection-related configuration checks are performed for each building. As discussed previously, these structures could contain torsional or soft-story irregularities. The output from the drift analysis will be used to determine if either of these irregularities is present in the buildings. It should be noted, however, that the presence of a soft story irregularity impacts only the analysis procedure limitations for the Berkeley building (requiring the MRSA procedure which is being used anyway) and has no impact on the design procedures for the Honolulu building. Therefore, the check is performed here for illustrative purposes only.

10.4.1 Torsion Irregularity Check for the Berkeley Building

In Section 10.2.4 it was mentioned that torsional irregularities are unlikely for the Berkeley building because the elements of the seismic force-resisting system were well distributed over the floor area. This will now be verified by comparing the story drifts at each end of the building in accordance with *Standard* Table 12.3-1. For this check, drifts are computed using the ETABS program using the ELF procedure (to avoid having to obtain modal combinations of drifts at multiple points) and including accidental torsion with $A_x = 1.0$ in accordance with Standard Table 12.3-1. Note that since this check is only for relative drifts, the C_d factor would cancel out and therefore is not included in this computation.

The drift computations and torsion check for the E-W direction are shown in Table 10-9. The drift values are shown only for one direction of accidental torsion (positive torsion moment) since the other direction is the opposite due to symmetry.

Table 10-9 Torsion Check for Berkeley Building Loaded in the E-W Direction

Story	Story Drift North End (in)	Story Drift South End (in)	Average Story Drift (in)	Max Drift / Average Drift
12	0.233	0.301	0.267	1.13
11	0.237	0.321	0.279	1.15
10	0.241	0.338	0.290	1.17
9	0.244	0.356	0.300	1.19
8	0.244	0.369	0.307	1.20
7	0.241	0.377	0.309	1.22
6	0.234	0.378	0.306	1.24
5	0.221	0.369	0.295	1.25
4	0.202	0.350	0.276	1.27
3	0.176	0.318	0.247	1.29
2	0.142	0.271	0.206	1.31
1	0.119	0.229	0.174	1.32

(1.0 in = 25.4 mm)

As can be seen from the table, a torsional irregularity (Type 1a) does exist at Story 8 and below because the ratio of maximum to average drift exceeds 1.2. This is counterintuitive for a symmetric building but can happen for a building in which the lateral elements are located towards the center of a relatively long floor plate, as occurs here. This configuration results in a relatively large accidental torsion load but relatively low torsional resistance.

For loading in the N-S direction, similar computations (not shown here) demonstrate that the structure is torsionally regular.

The presence of the torsional irregularity in the E-W direction has several implications for the design:

The qualitative determination for using the redundancy factor, ρ, equal to 1.0 is not applicable per *Standard* Section 12.3.4.2, Item b, as previously assumed in Section 7.2.5. For the purposes of this example, we will assume $\rho = 1.0$ based on *Standard* Section 12.3.4.2, Item a, which references Table 12.3-3. Due to the number of structural walls and moment frames in the E-W direction, the loss of an individual moment frame element would still satisfy the criteria of *Standard* Table 12.3-3. Note that since the height-to-length ratio of the structural walls is less than 1.0, removal of a structural wall element is not required. This redundancy check would have to be verified independently and if those criteria were not met, then analysis would have to be revised with $\rho = 1.3$.

The ELF procedure is not permitted per *Standard* Table 12.6-1. This does not change the analysis since we are utilizing the MRSA procedure.

The amplification of accidental torsion needs to be considered per *Standard* Section 12.8.4.3. The A_x factor is computed for each floor in this direction and the analysis is revised. See below.

Story drifts need to be checked at both ends of the building rather than at the floor centroid, per *Standard* Section 12.12.1. This is covered in Section 10.4.2 below.

The initial determination of accidental torsion was based on $A_x = 1.0$. Due to the torsional irregularity, accidental torsion for the E-W direction of loading needs to be computed again with the amplification factor.

This is shown in Table 10-10. Note that while the determination of the torsional irregularity is based on story drifts, the computation of the torsional amplification factor is based on story displacements.

Table 10-10 Accidental Torsion for the Berkeley Building

Level	Force F_x (kips)	E-W Building Width (ft)	E-W Torsion (ft-k)	Max Displ (in)	Ave Displ (in)	A_x	E-W Torsion, $A_x M_{ta}$ (ft-k)
Roof	544.6	213	5787	4.03	3.3	1.04	6012
12	531.5	213	5647	3.73	3.0	1.05	5947
11	468.0	213	4973	3.41	2.7	1.07	5308
10	406.9	213	4323	3.07	2.5	1.08	4677
9	348.2	213	3699	2.71	2.2	1.10	4058
8	292.1	213	3104	2.34	1.9	1.11	3452
7	238.9	213	2538	1.97	1.5	1.13	2864
6	188.7	213	2005	1.59	1.2	1.15	2298
5	142.1	213	1509	1.22	0.9	1.16	1758
4	99.3	213	1055	0.87	0.7	1.18	1250
3	61.2	213	650	0.55	0.4	1.20	783
2	30.0	213	318	0.28	0.2	1.21	386

(1.0 kip = 4.45 kN, .0 ft = 0.3048 m, 1.0 ft-kip = 1.36 kN-m)

With the revised accidental torsion values for the E-W direction of loading, the ETABS model is rerun for the drift checks and member design in subsequent sections.

10.4.2 Drift Check for the Berkeley Building

Story drifts are computed in accordance with *Standard* Section 12.9.2 and then checked for acceptance based on *Standard* Section 12.12.1. According to *Standard* Table 12.12-1, the story drift limit for this Risk Category II building is $0.020h_{sx}$, where h_{sx} is the height of story x. This limit may be thought of as 2 percent of the story height. Quantitative results of the drift analysis for the N-S and E-W directions are shown in Tables 10-11a and 10-11b, respectively. The story drifts are taken directly from the modal combinations in ETABS. Due to the torsional irregularity in the E-W direction, drifts are checked at both ends of the structure, while N-S drifts are checked at the building centroid. Note that in Table 10-11b the drifts at each end of the building are taken as the maximum drifts considering the enveloped cases of accidental torsion. Since this building is perfectly symmetric, the drift values are the same at both ends, which would rarely be the case in actual buidings.

In neither case does the computed drift ratio (amplified story drift divided by h_{sx}) exceed 2 percent of the story height. Therefore, the story drift requirement is satisfied. A plot of the total deflection in both the N-S and E-W directions is shown in Figure 10-4 and a plot of story drifts is in Figure 10-5.

An example calculation for drift in Story 4 loaded in the N-S direction is given below. Note that the relevant row is highlighted bold in Table 10-11a.

Story drift = Δ_{4e} = 0.262 inch
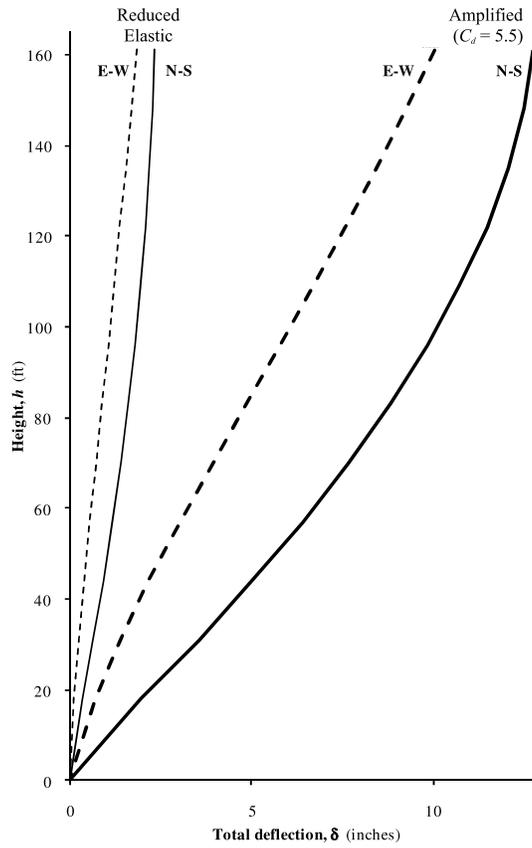Deflection amplification factor, C_d = 5.5
Importance factor, I_e = 1.0
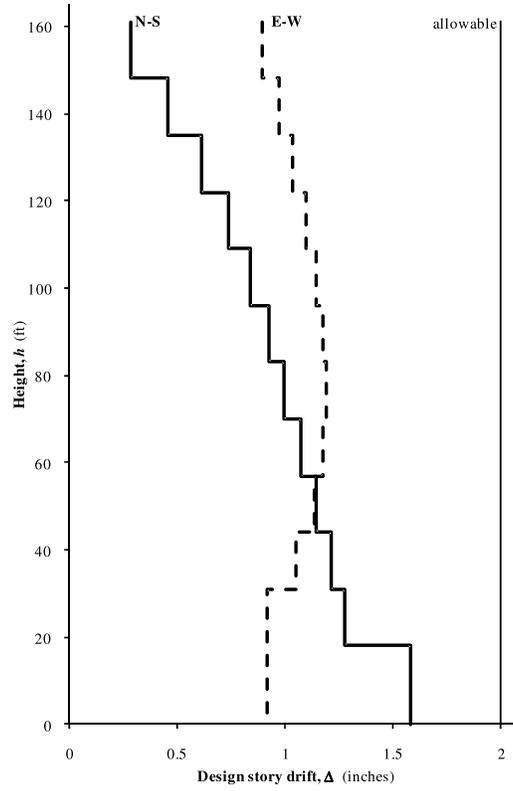Amplified story drift = $\Delta_4 = C_d \Delta_{4e}/I_e = 5.5(0.262)/1.0 = 1.44$ inches

Amplified drift ratio = Δ_4/h_4 = (1.44/156) = 0.00923 = 0.923% < 2.0%   OK

Figure 10-4 Deflected shape for Berkeley building
(1.0 ft = 0.3048 m, 1.0 in = 25.4 mm)

Figure 10-5 Drift profile for Berkeley building
(1.0 ft = 0.3048 m)

Table 10-11a Drift Computations for the Berkeley Building Loaded in the N-S Direction

Story	Story Drift (in)	Story Drift $\times C_d^*$ (in)	Drift Ratio[**] (%)
12	0.068	0.37	0.239
11	0.106	0.58	0.373
10	0.141	0.77	0.496
9	0.169	0.93	0.596
8	0.192	1.06	0.677
7	0.212	1.16	0.746
6	0.229	1.26	0.808
5	0.246	1.35	0.866
4	**0.262**	**1.44**	**0.923**
3	0.277	1.52	0.977
2	0.289	1.59	1.018
1	0.342	1.88	0.871

[*]C_d = 5.5 for loading in this direction.
[**]Story height = 156 inches for Stories 2 through roof and 216 inches for Story 1.
(1.0 in = 25.4 mm)

Table 10-11b Drift Computations for the Berkeley Building Loaded in the E-W Direction

Story	Story Drift North End (in)	Story Drift South End (in)	Max Story Drift $\times$ C_d^* (in)	Max Drift Ratio[**] (%)
12	0.208	0.208	1.14	0.733
11	0.224	0.224	1.23	0.788
10	0.237	0.237	1.30	0.835
9	0.249	0.249	1.37	0.879
8	0.259	0.259	1.43	0.914
7	0.266	0.266	1.46	0.937
6	0.268	0.268	1.47	0.944
5	0.264	0.264	1.45	0.931
4	0.254	0.254	1.40	0.894
3	0.234	0.234	1.29	0.826
2	0.204	0.204	1.12	0.718
1	0.200	0.200	1.10	0.509

[*]C_d = 5.5 for loading in this direction.
[**]Story height = 156 inches for Stories 2 through roof and 216 inches for Story 1.
(1.0 in = 25.4 mm)

The story deflection information will be used to determine whether or not a soft story irregularity exists. As indicated previously, a soft story irregularity (Vertical Irregularity Type 1a) would not impact the design since we are utilizing the MRSA. However, an extreme soft story irregularity (vertical irregularity Type 1b) is prohibited in Seismic Design Category E building per *Standard* Section 12.3.3.1.

However, *Standard* Section 12.3.2.2 lists an exception:

> Structural irregularities of Types 1a, 1b, or 2 in Table 12.3-2 do not apply where no story drift ratio under design lateral load is less than or equal to 130 percent of the story drift ratio of the next story above…. The story drift ratios of the top two stories of the structure are not required to be evaluated.

To determine whether the exception applies to the Berkeley building, the ratio of the drift ratios are reported in Table 10-11c.

Table 10-11c Drift Ratio Comparisons for Stiffness Irregularity Check

Story	North-South Drift Ratio	Ratio to Story Above	East-West Drift Ratio	Ratio to Story Above
12	0.239	-	0.743	-
11	0.373	1.56	0.796	1.07
10	0.496	1.33	0.843	1.06
9	0.596	1.20	0.890	1.06
8	0.677	1.14	0.929	1.04
7	0.746	1.10	0.957	1.03
6	0.808	1.08	0.969	1.01
5	0.866	1.07	0.960	0.99
4	0.923	1.07	0.925	0.96
3	0.977	1.06	0.856	0.93
2	1.018	1.04	0.746	0.87
1	0.871	0.86	0.510	0.68

As can be seen the vertical irregularity does not apply in the E-W direction since the ratio is less than 1.3 at all stories. In the N-S direction, however, the ratio exceeds 1.3 at the two upper stories. While the top stories are excluded from this check, the ratio of 1.35 at Story 11 means that the story stiffness's need to be evaluated to determine whether there is a stiffness irregularity based on *Standard* Table 12.3-2.

Since this controlling ratio of drift ratios is at an upper floor and just exceeds the 1.3 limit, it could be reasonable to conclude that a stiffness irregularity does not exist. For the purposes of this example, as long as an extreme stiffness irregularity is not present (which seems highly unlikely given the relative drift ratios), the presence of a non-extreme stiffness irregularity does not have a substantive impact on the design since this example utilizes the MRSA procedure anyway. In accordance with *Standard* Table 12.6-1, the ELF procedure would not be permitted if there were to be a stiffness irregularity. Therefore, the required stiffness checks for the N-S direction are not shown in this example.

10.4.3   P-delta Check for the Berkeley Building

In accordance with *Standard* Section 12.8.7 (as referenced by *Standard* Section 12.9.6 for the MRSA), P-delta effects need not be considered in the analysis if the stability coefficient, θ, is less than 0.10 for each story. However, the *Standard* also limits θ to a maximum value determined by *Standard* Equation 12.8-17 as:

$$\theta_{max} = \frac{0.5}{\beta C_d} \le 0.25$$

Taking β as 1.0 (see *Standard* Section 12.8.7), the limit on stability coefficient for both directions is 0.5/(1.0)5.5 = 0.091.

The P-delta analysis for each direction of loading is shown in Tables 10-12a and 10-12b. For this P-delta analysis a story live load of 20 psf (50 psf for office occupancy reduced to 40 percent per *Standard* Section 4.8.1) was included in the total story load calculations. Deflections and story shears are based on the MRSA with no upper limit on period in accordance with *Standard* Sections 12.9.6 and 12.8.6.2. As can be seen in the last column of each table, θ does not exceed the maximum permitted value computed above and P-delta effects can be neglected for both drift and strength analyses.

An example P-delta calculation for the Story 4 under N-S loading is shown below. Note that the relevant row is highlighted bold in Table 10-12a.

Amplified story drift = Δ_4 = 1.440 inches
Story shear = V_4 = 1,336 kips
Accumulated story weight P_4= 36,532 kips
Story height = h_{s4}= 156 inches
I_e = 1.0
C_d = 5.5
$\theta = (P_4 I_e \Delta_4 / (V_4 h_{s4} C_d) = (36{,}532)(1.0)(1.44)/(6.5)(1{,}336)(156) = 0.0459 < 0.091$ OK

Table 10-12a P-Delta Computations for the Berkeley Building Loaded in the N-S Direction

Story	Story Drift (in)	Story Shear (kips)	Story Dead Load (kips)	Story Live Load (kips)	Total Story Load (kips)	Accum. Story Load (kips)	Stability Coeff, θ
12	0.372	291	3,352	420	3,772	3,772	0.0056
11	0.582	544	3,675	420	4,095	7,867	0.0098
10	0.774	729	3,675	420	4,095	11,962	0.0148
9	0.929	870	3,675	420	4,095	16,057	0.0200
8	1.056	984	3,675	420	4,095	20,152	0.0252
7	1.164	1,081	3,675	420	4,095	24,247	0.0305
6	1.260	1,169	3,675	420	4,095	28,342	0.0356
5	1.351	1,253	3,675	420	4,095	32,437	0.0408
4	**1.440**	**1,336**	**3,675**	**420**	**4,095**	**36,532**	**0.0459**
3	1.524	1,423	3,675	420	4,095	40,627	0.0507
2	1.587	1,507	3,675	420	4,095	44,722	0.0549
1	1.881	1,575	3,817	420	4,237	48,959	0.0492

(1.0 in = 25.4 mm, 1.0 kip = 4.45 kN)

Table 10-12b P-Delta Computations for the Berkeley Building Loaded in the E-W Direction

Story	Story Drift (in)	Story Shear (kips)	Story Dead Load (kips)	Story Live Load (kips)	Total Story Load (kips)	Accum. Story Load (kips)	Stability Coeff, θ
12	1.114	539	3,352	420	3,772	3,772	0.0091
11	1.194	969	3,675	420	4,095	7,867	0.0113
10	1.264	1,252	3,675	420	4,095	11,962	0.0141
9	1.334	1,426	3,675	420	4,095	16,057	0.0175
8	1.394	1,547	3,675	420	4,095	20,152	0.0212
7	1.436	1,667	3,675	420	4,095	24,247	0.0243
6	1.453	1,808	3,675	420	4,095	28,342	0.0265
5	1.440	1,964	3,675	420	4,095	32,437	0.0277
4	1.387	2,129	3,675	420	4,095	36,532	0.0277
3	1.284	2,307	3,675	420	4,095	40,627	0.0264
2	1.119	2,471	3,675	420	4,095	44,722	0.0236
1	1.101	2,577	3,817	420	4,237	48,959	0.0176

(1.0 in = 25.4 mm, 1.0 kip = 4.45 kN)

10.4.4 Torsion Irregularity Check for the Honolulu Building

A test for torsional irregularity for the Honolulu building can be performed in a manner similar to that for the Berkeley building. Based on computations not shown here, the Honolulu building is not torsionally irregular. This is the case because the walls, which draw the torsional resistance towards the center of the Berkeley building, do not exist in the Honolulu building. Therefore, the torsional amplification factor, $A_x = 1.0$ for all levels and the accidental torsion moments used for the analysis do not need to be revised.

10.4.5 Drift Check for the Honolulu Building

The story drift computations for the Honolulu building deforming under the N-S and E-W seismic loading are shown in Tables 10-13a and 10-13b. Note that although *Standard* Equation 12.8-5 controls the base shear determination, that minimum base shear need not be considered for drift determination in accordance with *Standard* Section 12.8.6.1.

These tables show that the story drift at all stories is less than the allowable story drift of $0.020h_{sx}$ (*Standard* Table 12.12-1). Even though it is not pertinent for Seismic Design Category C buildings, a soft first story does not exist for the Honolulu building because the ratio of first story drift to second story drift does not exceed 1.3.

Table 10-13a Drift Computations for the Honolulu Building Loaded in the N-S Direction

Story	Total Drift (in)	Story Drift (in)	Story Drift $\times C_d$ * (in)	Drift Ratio (%)
12	1.559	0.039	0.176	0.113
11	1.520	0.064	0.288	0.185
10	1.456	0.088	0.397	0.255
9	1.368	0.109	0.490	0.314
8	1.259	0.126	0.565	0.362
7	1.133	0.139	0.625	0.400
6	0.994	0.149	0.669	0.429
5	0.846	0.156	0.701	0.449
4	0.690	0.160	0.722	0.463
3	0.530	0.163	0.735	0.471
2	0.366	0.165	0.743	0.477
1	0.201	0.200	0.899	0.416

*C_d = 4.5 for loading in this direction; total drift is at top of story, story height = 156 inches for Stories 2 through roof and 216 inches for Story 1.
(1.0 in. = 25.4 mm)

Table 10-13b Drift Computations for the Honolulu Building Loaded in the E-W Direction

Story	Total Drift (in)	Story Drift (in)	Story Drift $\times C_d$ * (in)	Drift Ratio (%)
12	1.485	0.044	0.199	0.127
11	1.441	0.067	0.300	0.192
10	1.374	0.088	0.396	0.254
9	1.286	0.106	0.477	0.306
8	1.180	0.121	0.543	0.348
7	1.059	0.132	0.593	0.380
6	0.928	0.140	0.629	0.403
5	0.788	0.145	0.654	0.419
4	**0.642**	**0.149**	**0.669**	**0.429**
3	0.494	0.150	0.675	0.433
2	0.344	0.151	0.681	0.437
1	0.192	0.190	0.853	0.395

C_d = 4.5 for loading in this direction; total drift is at top of story, story height = 156 inches for Stories 2 through roof and 216 inches for Story 1.
(1.0 in = 25.4 mm)

A sample calculation for Story 4 of Table 10-13b (highlighted in the table) is as follows:

Deflection at top of story = δ_{4e} = 0.642 inches
Deflection at bottom of story = δ_{3e} = 0.494 inch
Story drift = $\Delta_{4e} = \delta_{4e} - \delta_{3e}$ = 0.642 - 0.494 = 0.149 inch
Deflection amplification factor, C_d = 4.5
Importance factor, I_e = 1.0
Amplified story drift = $\Delta_5 = C_d \Delta_{4e}/I_e$ = 4.5(0.149)/1.0 = 0.669 inch
Amplified drift ratio = Δ_4 / h_4 = (0.669/156) = 0.00429 = 0.429% < 2.0%   OK

Therefore, story drift satisfies the drift requirements.

10.4.6 P-Delta Check for the Honolulu Building

Calculations for P-delta effects are shown in Tables 10-14a and 10-14b for N-S and E-W loading, respectively.

Table 10-14a P-Delta Computations for the Honolulu Building Loaded in the N-S Direction

Story	Story Drift (in)	Story Shear (kips)	Story Dead Load (kips)	Story Live Load (kips)	Total Story Load (kips)	Accum. Story Load (kips)	Stability Coeff, θ
12	0.176	170.4	3,352	420	3,772	3,772	0.0056
11	0.288	329.3	3,675	420	4,095	7,867	0.0098
10	0.397	462.4	3,675	420	4,095	11,962	0.0146
9	0.490	571.9	3,675	420	4,095	16,057	0.0196
8	0.565	660.1	3,675	420	4,095	20,152	0.0246
7	0.625	729.2	3,675	420	4,095	24,247	0.0296
6	0.669	781.3	3,675	420	4,095	28,342	0.0346
5	0.701	818.9	3,675	420	4,095	32,437	0.0395
4	0.722	844.2	3,675	420	4,095	36,532	0.0445
3	0.735	859.6	3,675	420	4,095	40,627	0.0495
2	0.743	867.5	3,675	420	4,095	44,722	0.0546
1	0.899	870.3	3,817	420	4,237	48,959	0.0520

(1.0 in = 25.4 mm, 1.0 kip = 4.45 kN)

Table 10-14b P-Delta Computations for the Honolulu Building Loaded in the E-W Direction

Story	Story Drift (in)	Story Shear (kips)	Story Dead Load (kips)	Story Live Load (kips)	Total Story Load (kips)	Accum. Story Load (kips)	Stability Coeff, θ
12	0.199	170.4	3,352	420	3,772	3,772	0.0063
11	0.300	329.3	3,675	420	4,095	7,867	0.0102
10	0.396	462.4	3,675	420	4,095	11,962	0.0146
9	0.477	571.9	3,675	420	4,095	16,057	0.0191
8	0.543	660.1	3,675	420	4,095	20,152	0.0236
7	0.593	729.2	3,675	420	4,095	24,247	0.0281
6	0.629	781.3	3,675	420	4,095	28,342	0.0325
5	0.654	818.9	3,675	420	4,095	32,437	0.0369
4	**0.669**	**844.2**	**3,675**	**420**	**4,095**	**36,532**	**0.0412**
3	0.675	859.6	3,675	420	4,095	40,627	0.0454
2	0.681	867.5	3,675	420	4,095	44,722	0.0500
1	0.853	870.3	3,817	420	4,237	48,959	0.0494

(1.0 in = 25.4 mm, 1.0 kip = 4.45 kN)

The stability ratio at Story 4 from Table 10-14b is computed as follows:

Amplified story drift = Δ_4 = 0.669 inch
Story shear = V_4 = 844.2 = kips
Accumulated story weight P_4 = 36,532 kips
Story height = h_{s4} = 156 inches
I_e = 1.0
C_d = 4.5
$\theta = (P_4 I_e \Delta_4 / (V_4 h_{s4} C_d) = (36{,}532)(1.0)(0.669)/(844.2)(156)(4.5) = 0.0412$

The requirements for maximum stability ratio ($0.5/C_d$ = 0.5/4.5 = 0.111) are satisfied. Because the stability ratio is less than 0.10 at all floors, P-delta effects need not be considered (*Standard* Section 12.8.7).

10.5   STRUCTURAL DESIGN OF THE BERKELEY BUILDING

Frame-wall interaction plays an important role in the behavior of the structure loaded in the E-W direction. This behavior has the following attributes:

1. For frames without walls (Frames 1, 2, 7 and 8), the shears developed in the beams (except for the first story) do not differ greatly from story to story. This allows for uniformity in the design of the beams.

2. For frames containing structural walls (Frames 3 through 6), the overturning moments in the structural walls are reduced as a result of interaction with the remaining frames (Frames 1, 2, 7 and 8).

3. For the frames containing structural walls, the 40-foot-long girders act as outriggers further reducing the overturning moment resisted by the structural walls.

4. A significant load reversal occurs at the top of frames with structural walls. This happens because the structural wall pulls back on (supports) the top of Frame 1. The deflected shape of the structure loaded in the E-W direction also shows the effect of frame-wall interaction because the shape is neither a cantilever mode (wall alone) nor a shear mode (frame alone). It is the "straightening out" of the deflected shape of the structure that causes the story shears in the frames without walls to be relatively equal.

Some of these attributes are shown graphically in Figure 10-6, which illustrates the total story force resisted by Frames 1, 2 and 3.
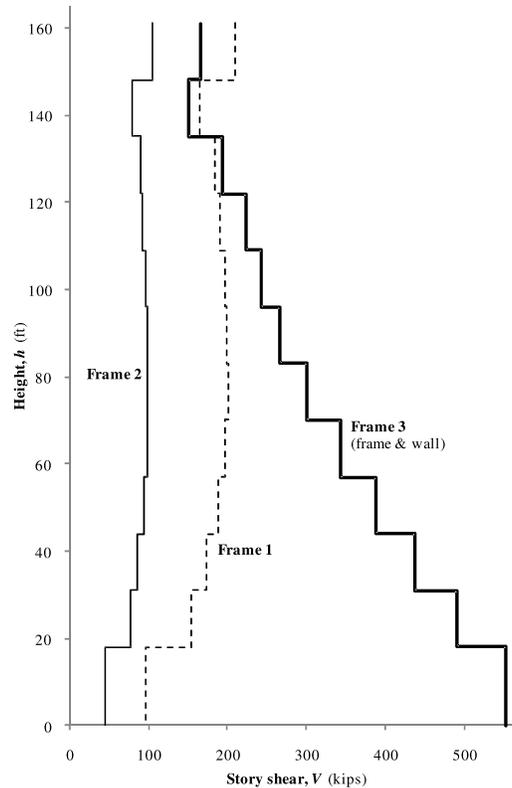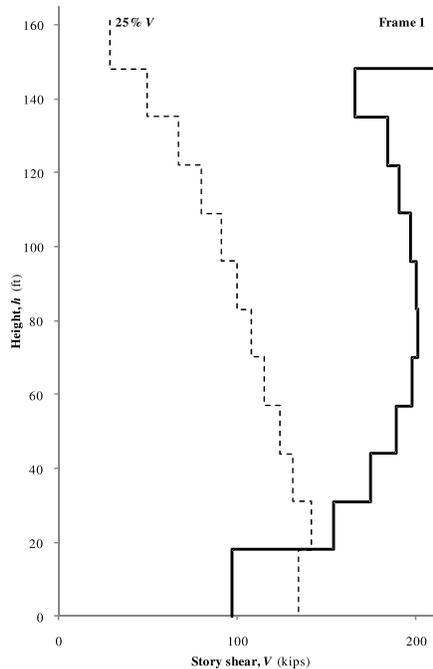

Figure 10-6 Story shears in the E-W direction
(1.0 ft = 0.3048 m, 1.0 kip = 4.45 kN)

### 10.5.1 Analysis of Frame-Only Structure for 25 Percent of Lateral Load

Where a dual system is utilized, *Standard* Section 12.2.5.1 requires that the moment frames themselves are designed to resist at least 25 percent of the total base shear. This provision ensures that the dual system has sufficient redundancy to justify the increase from $R = 6$ for a special reinforced concrete structural wall to $R = 7$ for a dual system (see *Standard* Table 12.2-1). This 25 percent analysis was carried out using the ETABS program with the mathematical model of the building being identical to the previous version except that the panels of the structural walls were removed. The boundary elements of the walls were retained in the model so that behavior of the interior frames (Frames 3, 4, 5 and 6) would be analyzed in a rational way. It could be argued that keeping the boundary columns in the 25 percent model violates the intent of the provision since they are an integral part of the structural walls as well as the moment frames. However, in this condition, the columns are needed for the moment frames adjacent to the walls and those in longitudinal direction (which resist a small amount of torsion). Since these eight boundary columns resist only a small portion (just over 15 percent) the total base shear for the 25 percent model, the intent of the dual system requirements is judged to be satisfied. It should be noted that it is not the intent of the *Standard* to allow dual systems of co-planar and integral moment frames and structural walls. It may be preferable to establish a dual system layout that maintains a separation between the elements of the structural walls and moment frames, but that was not practical for the structure of this particular design example.

The seismic demands for this frame-only analysis were scaled such that the spectra base shear is equal to 25 percent of the design base shear for the dual system. In this case, the response spectrum was scaled such that the frame-only base shear is equal to $(0.25)(0.85)V_{ELF}$. While this global scaling may not result in story forces exactly equal to 25 percent of the story forces from the MRSA of the dual system (because the model response may be slightly different), the method used is assumed to meet the intent of this provision of the *Standard.*

The results of the analysis are shown in Figures 10-7, 10-8 and 10-9 for the frames on Grids 1, 2 and 3, respectively. The frames on Grids 6, 7 and 8 are similar by symmetry and Grids 4 and 5 are similar to Grid 3. In these figures, the original analysis (structural wall included) is shown by a heavy line and the 25 percent (frame-only) analysis is shown by a light, dashed line. As can be seen, the 25 percent rule controls only at the lower level of the building. Therefore, for the design of the beams and columns at the lower two levels (not part of this example), the greater of the dual system and frame-only analysis should be used. For the purposes of this example, which includes representative designs for the framing at a middle level, design forces from the dual system analysis will satisfy the 25 percent requirement.

Figure 10-7 25 percent story shears, Frame 1 E-W direction
(1.0 ft = 0.3048 m, 1.0 kip = 4.45 kN)
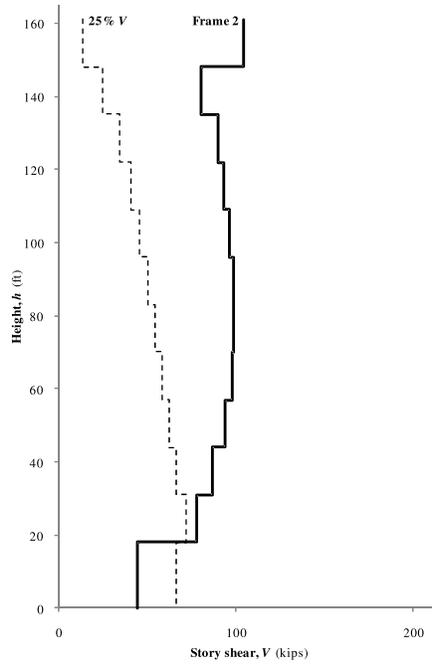
Figure 10-8 25 percent story shears, Frame 2 E-W direction
(1.0 ft = 0.3048 m, 1.0 kip = 4.45 kN)
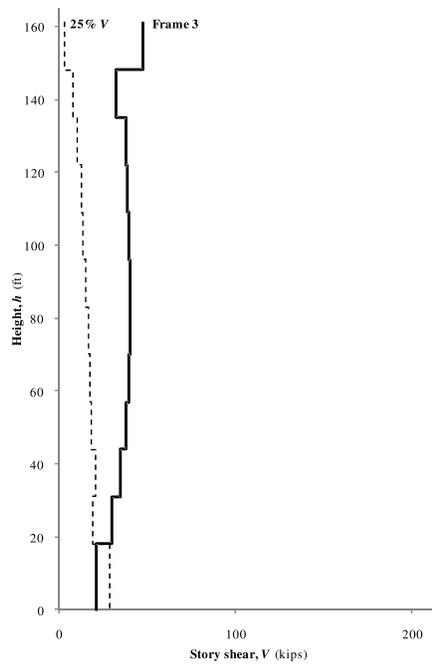
Figure 10-9 25 percent story shear, Frame 3 E-W direction
(1.0 ft = 0.3048 m, 1.0 kip = 4.45 kN)

10.5.2 Design of Moment Frame Members for the Berkeley Building

For this part of the example, the design and detailing of five beams and one interior column along Grid 1 on Level 5 are presented in varying amounts of detail. The beams are designed first because the flexural

10-35

capacity of the as-designed beams is a factor in the design and detailing of the column and the beam-column joint.

Before continuing with the example, it should be mentioned that the design of ductile reinforced concrete moment frame members is controlled by the flexural reinforcement in the beams. The percentage and placement of beam flexural reinforcement governs the flexural rebar cutoff location, the size and spacing of beam shear reinforcement, the cross-sectional characteristics of the column, the column flexural reinforcement and the column shear reinforcement. The beam reinforcement is critical because the basic concept of ductile frame design is to force most of the energy-dissipating deformation to occur through inelastic rotation in plastic hinges at the ends of the beams.

In carrying out the design calculations, three different flexural strengths are used for the beams. These capacities are based on the following:

- Design strength: ϕ = 0.9, tensile stress in reinforcement at $1.00 f_y$

- Nominal strength: ϕ = 1.0, tensile stress in reinforcement at $1.00 f_y$

- Probable strength: ϕ = 1.0, tensile stress in reinforcement at $1.25 f_y$

Various aspects of the design of the beams and other members depend on the above capacities are as follows:

- Beam rebar cutoffs: Design strength

- Beam shear reinforcement: Probable strength of beam

- Beam-column joint strength: Probable strength of beam

- Column flexural strength: $6/5 \times$ nominal strength of beam

- Column shear strength: Probable strength of column or beam

In addition, beams in ductile frames will always have top and bottom longitudinal reinforcement throughout their length. In computing flexural capacities, only the tension steel will be considered. This is a valid design assumption because reinforcement ratios are quite low, yielding a depth to the neutral axis similar to the depth of the compression reinforcement.

Finally, a sign convention for bending moments is required in flexural design. In this example, where the steel at the top of a beam section is in tension, the moment is designated as a negative moment. Where the steel at the bottom is in tension, the moment is designated as a positive moment. All moment diagrams are drawn using the reinforced concrete or tension-side convention. For beams, this means negative moments are plotted on the top and positive moments are plotted on the bottom. For columns, moments are drawn on the tension side of the member.

10.5.2.1 Preliminary Calculations. Before the quantity and placement of reinforcement is determined, it is useful to establish, in an overall sense, how the reinforcement will be distributed. The preliminary design established that the moment frame beams would be 24 inches wide by 32 inches deep and the columns would be 30 inches by 30 inches. Note that the beam widths were selected to consider the beam-column joints "confined" per ACI 318 Section 18.8.4.2, which requires beam widths of at least 75 percent of the column width.

In order to determine the effective depth used for the design of the beams, it is necessary to estimate the size and placement of the reinforcement that will be used. In establishing this depth, it is assumed that #8 bars will be used for longitudinal reinforcement and that hoops and stirrups will be constructed from #4 bars. In all cases, clear cover of 1.5 inches is assumed. Since this structure has beams spanning in two orthogonal directions, it is necessary to layer the flexural reinforcement as shown in Figure 10-10. The reinforcement for the E-W spanning beams was placed in the upper and lower layers because the strength demand for these members is somewhat greater than that for the N-S beams. Note that the quantity of longitudinal reinforcing and stirrups indicated in Figure 10-10 is conceptual, and the final quantities and details may vary.
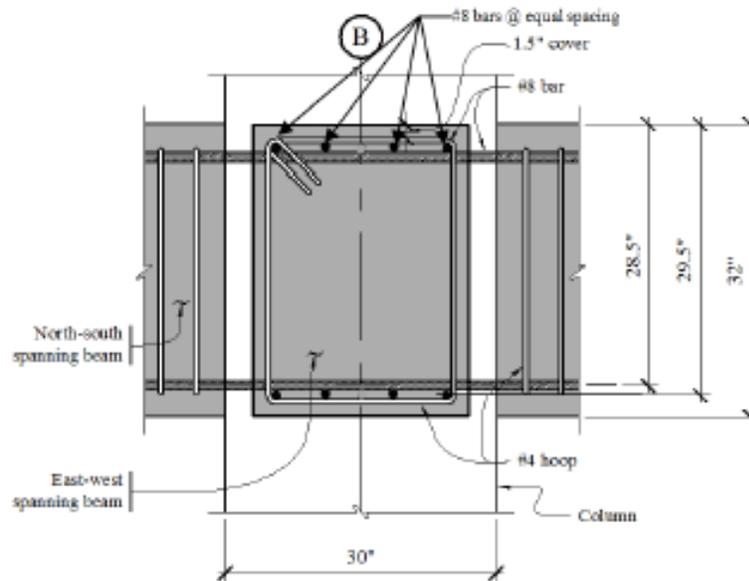
Figure 10-10 Layout for beam reinforcement
(1.0 ft = 0.3048 m, 1.0 in. = 25.4 mm)

Given Figure 10-10, compute the effective depth for both positive and negative moment as follows:

Beams spanning in the E-W direction, d = 32 - 1.5 - 0.5 - 1.00/2 = 29.5 inches

Beams spanning in the N-S direction, d = 32 - 1.5 - 0.5 - 1.0 - 1.00/2 = 28.5 inches

For negative moment bending, the effective width is 24 inches for all beams. For positive moment, the slab is in compression and the effective T-beam width varies according to ACI 318 Section 6.3.2. The effective widths for positive moment are as follows (with the parameter controlling effective width shown in parentheses):

20-foot beams in Frames 1 and 8: b = 24 + 20(12)/12 = 44 inches (span length)

20-foot beams in Frames 2 and 7: b = 20(12)/4 = 60 inches (span length)

40-foot beams in Frames 2 through 7: b = 24 + 2[8(4)] = 88 inches (slab thickness)

30-foot beams in Frames A and D: b = 24 + [6(4)] = 48 inches (slab thickness)

30-foot beams in Frames B and C: b = 24 + 2[8(4)] = 88 inches (slab thickness)

ACI 318 Section 18.6.3.1 controls the longitudinal reinforcement requirements for beams. The minimum reinforcement to be provided at the top and bottom of any section is as follows:

$$A_{s,min} = greater\ of\ \frac{3\sqrt{f'_c}}{f_y} b_w\ d = \frac{3\sqrt{5000}}{60,0000}(24)(29.5) = 2.50\ in^2$$

$$and\ \frac{200}{f_y} b_w\ d = \frac{200}{60,0000}(24)(29.5) = 2.36\ in^2$$

$$A_{s,min} = 2.50\ in^2$$

This amount of reinforcement can be supplied by four #8 bars with $A_s = 3.16\ in^2$. Since the four #8 bars will be provided continuously top and bottom, reinforcement required for strength will include these #8 bars.

Before getting too far into member design, it is useful to check the required tension development length for hooked bars since the required length may control the dimensions of the exterior columns and the boundary elements of the structural walls.

From Equation 18.8.5.1 of ACI 318 Section 18.8.5.1, the required development length is as follows:

$$l_{dh} = \frac{f_y d_b}{65\sqrt{f'_c}}$$

For normal-weight (NW) concrete, the computed length cannot be less than 6 inches or $8d_b$.

For straight typical bars, $l_d = 2.5l_{dh}$ and for straight "top" bars, $l_d = 3.25l_{dh}$ (ACI 318 Sec. 18.8.5.3). These values are applicable only where the bars are anchored in well-confined concrete (e.g., column cores and plastic hinge regions with confining reinforcement). The development length for the portion of the bar extending into unconfined concrete must be increased by a factor of 1.6 per ACI 318 Section 18.8.5.4. Development length requirements for hooked and straight bars are summarized in Table 10-15.

Where hooked bars are used, the hook must be 90 degrees and be located within the confined core of the column or boundary element. For bars hooked into 30-inch-square columns with 1.5 inches of cover and #4 ties, the available development length is 30 - 1.50 - 0.5 = 28.0 inches. With this amount of available length, there will be no problem developing hooked bars in the columns.

Table 10-15 is applicable to bars anchored in joint regions only. For development of bars outside of joint regions, ACI 318 Chapter 25 should be used.

Table 10-15 Tension Development Length Requirements for Hooked Bars and Straight Bars in 5,000 psi NW Concrete

Bar Size	d_b (in)	l_{dh} hook (in)	l_d typ (in)	l_d top (in)
#4	0.500	6.5	16.3	21.2
#5	0.625	8.2	20.4	26.5
#6	0.750	9.8	24.5	31.8
#7	0.875	11.4	28.6	37.1
#8	1.000	13.1	32.6	42.4
#9	1.128	14.7	36.8	47.9
#10	1.270	16.6	41.4	53.9
#11	1.410	18.4	46.0	59.8

(1.0 in = 25.4 mm)

Another requirement to consider prior to establishing column sizes is ACI 318 Section 18.8.2.3 which sets a minimum ratio of 20 for the column width to the diameter of the largest longitudinal beam bar passing through the joint. This requirement is easily satisfied for the 30-inch columns in this example.

10.5.2.2 Design of Representative Frame 1 Beams. The preliminary design of the beams of Frame 1 was based on members with a depth of 32 inches and a width of 24 inches. The effective depth for positive and negative bending is 29.5 inches and the effective widths for positive and negative bending are 44 and 24 inches, respectively. This assumes the stress block in compression is less than the 4.0-inch flange thickness.

The layout of the geometry and gravity loading on the three eastern-most spans of Level 7 of Frame 1 as well as the unfactored gravity and seismic moments are illustrated in Figure 10-11. The seismic and gravity moments are taken directly from the ETABS program output. The seismic forces are from the E-W spectral load case plus the controlling accidental torsion case (the torsional moment where translation and torsion are additive). The values of the seismic forces are taken from the MSRA analysis, but the signs and moment diagram are equivalent to a static lateral load in order to combine the seismic and gravity moments. Note that all negative moments are given at the face of the column and that seismic moments are considerably greater than those due to gravity.

Factored bending moment envelopes are shown in Figure 10-11. Negative moment at the supports is controlled by the $1.46D + 0.5L + 1.0E$ load combination and positive moment at the support is controlled by $0.64D - 1.0E$. Mid-span positive moments are based on the load combination $1.2D + 1.6L$.
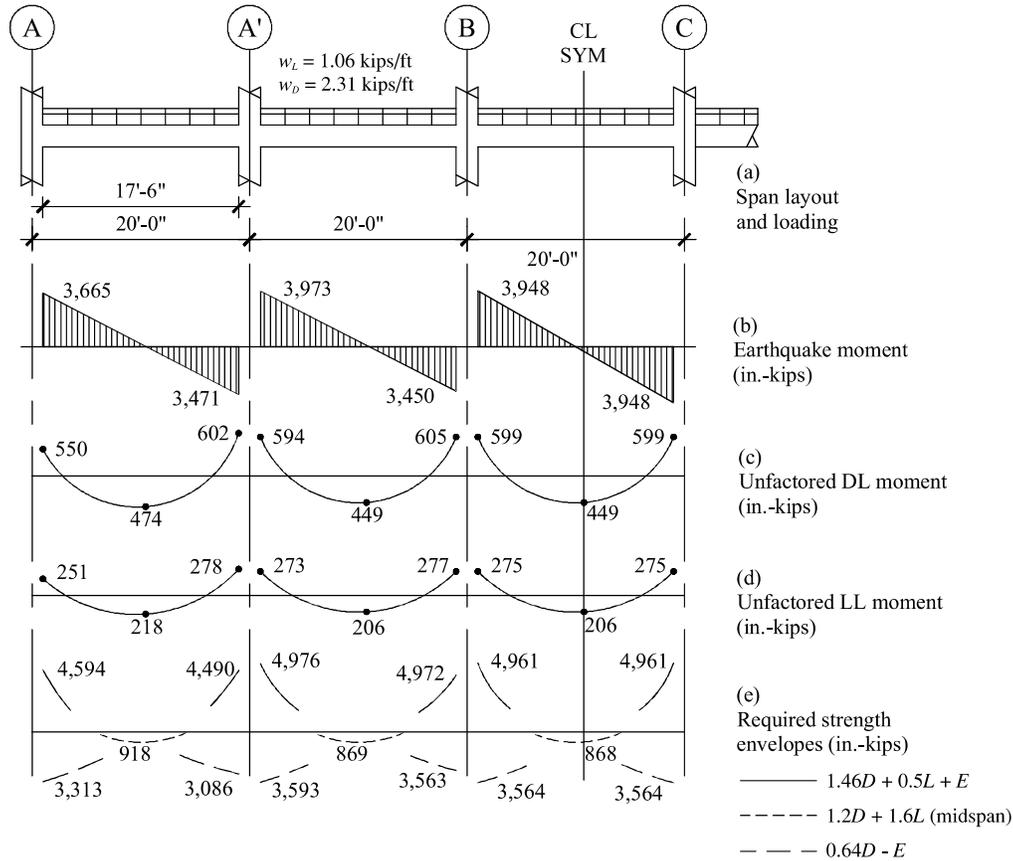
Figure 10-11 Bending moments for Frame 1
(1.0 ft = 0.3048 m, 1.0 in-kip = 0.113 kN-m)

10.5.2.2.1 Longitudinal Reinforcement. The design process for determining longitudinal reinforcement is illustrated as follows for Span A-A'.

1. Design for Negative Moment at the Face of the Exterior Support (Grid A):

M_u = 1.46(-550) + 0.5(-251) + 1.0(-3,664) = -4,594 inch-kips

Try four #8 bars required for minimum steel:

A_s = 4(0.79) = 3.16 in^2
f_c' = 5,000 psi
f_y = 60 ksi
Width b for negative moment = 24 inches
d = 29.5 in.
Depth of compression block, $a = A_s f_y / 0.85 f_c' b$
a = 3.16 (60)/[0.85 (5) 24] = 1.86 inches
Design strength, $\phi M_n = \phi A_s f_y (d - a/2)$

10-40

$\phi M_n = 0.9(3.16)60(29.5 - 1.86/2) = 4,875$ inch-kips $> 4,594$ inch-kips   OK

2. Design for Positive Moment at Face of Exterior Support (Grid A):

$M_u = [-0.64(550)] + [1.0(3,664)] = 3,313$ inch-kips

Try the four #8 bars required for minimum steel:

$A_s = [4(0.79)] = 3.16$ in^2
Width b for positive moment = 44 inches
$d = 29.5$ inches
$a = [3.16(60)]/[0.85(5)44] = 1.01$ inch
$\phi M_n = 0.9(3.16) 60(29.5 - 1.01/2) = 4,948$ inch-kips $> 3,313$ inch-kips   OK

3. Positive Moment at Midspan:

$M_u = [1.2(474)] + [1.6(218)] = 918.1$ inch-kips

Minimum reinforcement (four #8 bars) controls by inspection.

4. Design for Negative Moment at the Face of the Interior Support (Grid A'):

$M_u = 1.46(-602) + 0.5(-278) + 1.0(-3,973) = -4,976$ inch-kips

Try one #7bars in addition to the four #8 bars required for minimum steel:

$A_s = 4(0.79) + 1(0.60) = 3.76$ in^2
$a = 3.76 (60)/[0.85 (5) 24] = 2.21$ inches
$\phi M_n = 0.9(3.76)60(29.5 - 2.21/2) = 5,765$ inch-kips $> 4,976$ inch-kips
OK

5. Design for Positive Moment at Face of Interior Support (Grid A'):

$M_u = [-0.64(602)] + [1.0(3,973)] = 3,593$ inch-kips

Four #8 bars similar to the exterior support location are adequate by inspection.

Similar calculations can be made for the Spans A'-B and B-C and then the remaining two spans are acceptable via symmetry. A summary of the preliminary flexural reinforcing is shown in Table 10-16.

In addition to the computed strength requirements and minimum reinforcement ratios cited above, the final layout of reinforcing steel also must satisfy the following from ACI 318 Section 18.6.3:

Minimum of two bars continuous top and bottom	OK (four #8 bars continuous top and bottom)
Positive moment strength greater than 50 percent negative moment strength at a joint	OK (at all joints)
Minimum strength along member greater than 0.25 maximum strength	OK (A_s provided = four #8 bars is more than 25 percent of reinforcement provided at joints)

The preliminary layout of reinforcement is shown in Figure 10-12. The arrangement of bars is based on the above computations and Table 10-16 summary of the other spans. Note that a slightly smaller amount of reinforcing could be used at the top of the exterior spans, but #8 bars are selected for consistency. In addition, the designer could opt to use four #8 bars continuous throughout the span for uniformity and ease of placement.
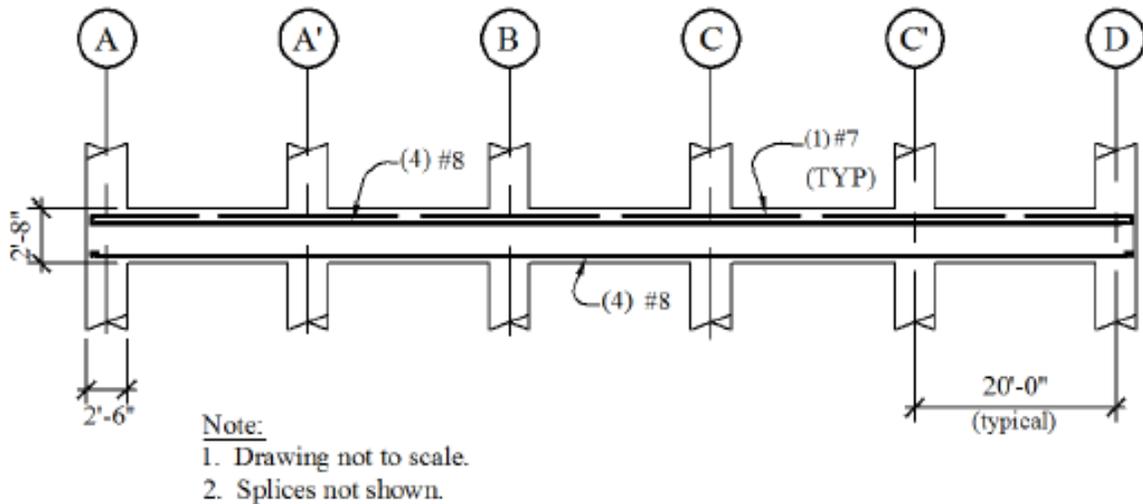
Figure 10-12 Preliminary rebar layout for Frame 1
(1.0 ft = 03.048 m)

As mentioned above, later phases of the frame design will require computation of the design strength and the maximum probable strength at each support. The results of these calculations are shown in Table 10-16.

Table 10-16 Design and Maximum Probable Flexural Strength For Beams in Frame 1

Item		A	A'	B	C	C'	D
				Location*			
Negative Moment	Moment Demand (inch-kips)	4,594	4,976	4,972	4,972	4,976	4,594
	Reinforcement	four #8	four #8 + one#7	four #8 + one#7	four #8 + one#7	four #8 + one#7	four #8
	Design Strength (inch-kips)	4,875	5,765	5,765	5,765	5,765	4,875
	Probable Strength (inch-kips)	7,042	7,929	7,929	7,929	7,929	7,042
Positive Moment	Moment Demand (inch-kips)	3,313	3,593	3,564	3,564	3,593	3,313
	Reinforcement	four #8	four #8	four #8	four #8	four #8	four #8
	Design Strength (inch-kips)	4,948	4,948	4,948	4,948	4,948	4,948
	Probable Strength (inch-kips)	6,841	6,841	6,841	6,841	6,841	6,841

*Moment demand is taken as the larger of the beam moments on each side of the column.

(1.0 in-kip = 0.113 kN-m)

As an example of computation of probable strength, consider the case of four #8 top bars plus the portion of slab reinforcing within the effective beam flange width computed above, which is assumed to be 0.002(4 inches)(44-24)=0.16 square inches. (The slab reinforcing, which is not part of this example, is assumed to be 0.002 for minimum steel.)

$A_s = 4(0.79) + 0.16 = 3.32$ in^2
Width b for negative moment $= 24$ inches
$d = 29.5$ inches
Depth of compression block, $a = A_s(1.25f_y)/0.85f_c'b$
$a = 3.32(1.25)60/[0.85(4)24] = 2.44$ inches
$M_{pr} = 1.0A_s(1.25f_y)(d - a/2)$
$M_{pr} = 1.0(3.32)1.25(60)(29.6 - 2.44/2) = 7,042$ inch-kips

For the case of four #8 bottom bars:

$A_s = 4(0.79) = 3.16$ in^2
Width b for positive moment $= 44$ inches
$d = 29.5$ inches
$a = 3.16(1.25)60/[0.85(5)44] = 1.2$ inch
$M_{pr} = 1.0(3.16)1.25(60)(29.5 - 1.27/2) = 6,841$ inch-kips

At this point in the design process, the layout of reinforcement has been considered preliminary because the quantity of reinforcement placed in the beams has a direct impact on the magnitude of the stresses developed in the beam-column joint. If the computed joint stresses are too high, the only remedies are increasing the concrete strength, increasing the column area, changing the reinforcement layout, or increasing the beam depth. The complete check of the beam-column joint is illustrated in Section 10.5.2.3 below, but

preliminary calculations indicate that the joint is adequate, so the design can progress based on the reinforcing provided.

Because the arrangement of steel is acceptable from a joint strength perspective, the cutoff locations of the various bars may be determined (see Figure 10-12 for a schematic of the arrangement of reinforcement). The four #8 bars (top and bottom) required for minimum reinforcement are supplied in one length that runs continuously across the two end spans and are spliced in the center span. An one #7 top bars are placed at each column.

To determine where added top bars should be cut off in each span, it is assumed that theoretical cutoff locations correspond to the point where the continuous top bars develop their design flexural strength. Cutoff locations are based on the members developing their design flexural capacities ($f_y = 60$ ksi and $\phi = 0.9$). Using calculations similar to those above, it has been determined that the design flexural strength supplied by a section with only four #8 bars is 4,875 inch-kips for negative moment.

Sample cutoff calculations are given for Span B-C. To determine the cutoff location for negative moment, both the additive and counteractive load combinations must be checked to determine the maximum required cutoff length. In this case, the $1.46D + 0.5L \pm Q_E$ load combination governs. Loading diagrams for determining cutoff locations are shown in Figure 10-13.

For negative moment cutoff locations, refer to Figure 10-14, which is a free body diagram of the left end of the member in Figure 10-13. Since the goal is to develop a negative moment capacity of 4,875 inch-kips in the continuous #8 bars, summing moments about Point A in Figure 10-14 can be used to determine the location of this moment demand. The moment summation is as follows:

$$4,961 + \frac{0.325x^2}{2} - 71.7x = 4,875$$

In the above equation, 4,961 (inch-kips) is the negative moment demand at the face of column, 0.325 (kips/inch) is the factored gravity load, 71.7 kips is the end shear and 3,686 inch-kips is the design strength of the section with three #8 bars. Solving the quadratic equation results in $x = 1.2$ inches. ACI 318 Section 7.7.3.3 requires an additional length equal to the effective depth of the member or 12 bar diameters (whichever is larger). Consequently, the total length of the bar beyond the face of the support is $1.2 + 29.5 = 35.4$ inches and a 4'-0" extension beyond the face of the column could be used at this location. Similar calculations should be made for the other ends of the beam.
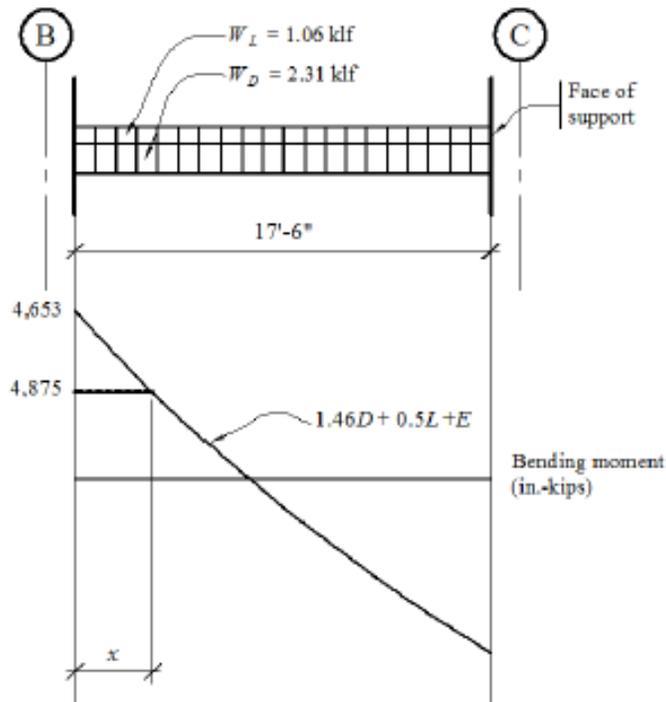
Figure 10-13 Loading for determination of rebar cutoffs
(1.0 ft = 0.3048 m, 1.0 klf = 14.6 kN/m, 1.0 in-kip = 0.113 kN-m)
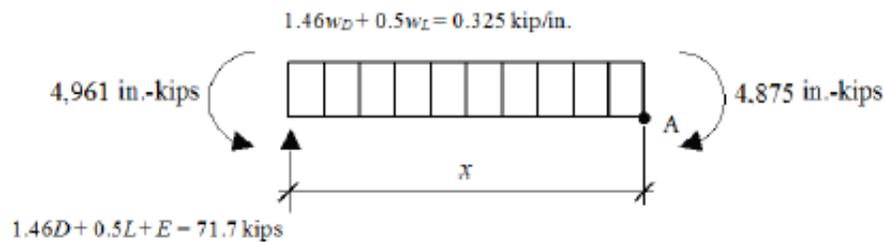
Figure 10-14 Free body diagram
(1.0 kip = 4.45kN, 1.0 klf = 14.6 kN/m, 1.0 in-kip = 0.113 kN-m)

As shown in Figure 10-15, another requirement in setting cutoff length is that the bar being cut off must have sufficient length to develop the strength required in the adjacent span. From Table 10-15, the required development length of the #7 top bars in tension is 37.1 inches if the bar is anchored in a confined joint region. The confined length in which the bar is developed is shown in Figure 10-15 and consists of the column depth plus twice the depth of the beam (the length for beam hoops per ACI 318 Section 18.6.4.1). This length is 30 + 32 + 32 = 94 inches, which is greater than the 37.1 inches required. The column and beam are considered confined because of the presence of closed hoop reinforcement as required by ACI 318 Sections 18.6.4 and 18.7.5.
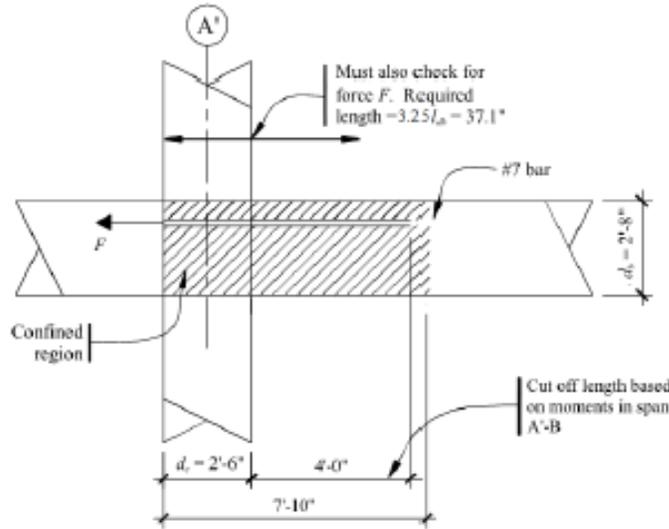
Figure 10-15 Development length for top bars
(1.0 ft = 0.3048 m, 1.0 in. = 25.4 mm)

The continuous top bars are spliced at the center of Span B-C and the bottom bars at Spans A'-B and C-C' as shown in Figure 10-16. The splice length is taken as Class B splice length for #8 bars. These splice locations satisfy the requirements of ACI 318 Section 18.6.3.3 for permitted splice locations.

The splice length is determined in accordance with ACI 318 Section 25.5.2, which indicates that the splice length is 1.3 times the development length. From ACI 318 Section 25.4.2, the development length, l_d, is computed as:

$$l_d = \left(\frac{3}{40} \frac{f_y}{\lambda\sqrt{f_c'}} \frac{\psi_t\psi_e\psi_s}{\left(\dfrac{c_b + K_{tr}}{d_b} \right)} \right) d_b$$

using $\psi_t = 1.3$ (top bar), $\psi_e = 1.0$ (uncoated), $\psi_s = 1.0$ (#8 bar), $\lambda = 1.0$ (NW concrete) and taking $(c + K_{tr}) / d_b$ as 2.5 (based on clear cover and confinement), the development length for one #8 top bar is:

$$l_d = \left(\frac{3}{40} \left(\frac{60,000}{(1.0)\sqrt{5,000}} \right) \frac{(1.3)(1.0)(1.0)}{(2.5)} \right)(1.0) = 33.1 \text{ inches}$$

The splice length = 1.3(33.1) = 43 inches. Therefore, use a 43-inch contact splice for the top bars. Computed in a similar manner, the required splice length for the #8 bottom bars is 34 inches. According to ACI 318 Section 18.6.3.3, the entire region of the splice must be confined by closed hoops spaced at the smaller of d/4 or 4 inches.

The final bar placement and cutoff locations for all five spans are shown in Figure 10-16.
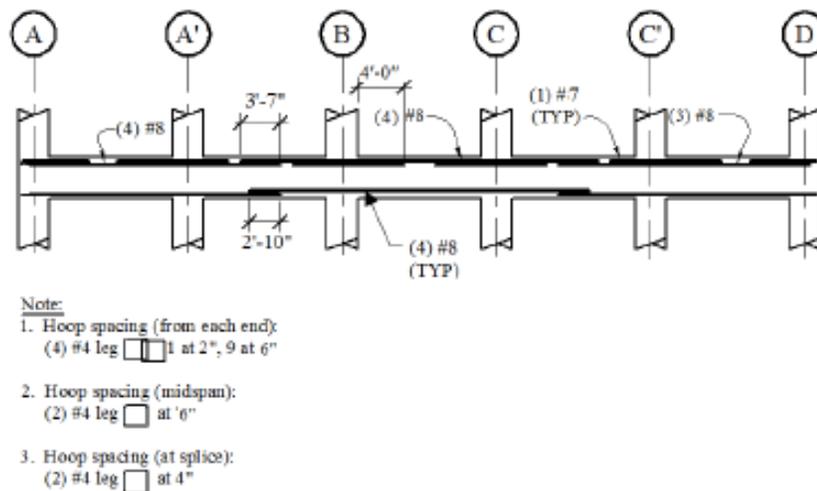
Figure 10-16 Final bar arrangement
(1.0 ft = 0.3048 m, 1.0 in. = 25.4 mm)

10.5.2.2.2 Transverse Reinforcement. The requirements for transverse reinforcement in special moment frame beams, include shear strength requirements (ACI 318 Sec. 18.6.5) covered here first and then detailing requirements (ACI 318 Sec. 18.6.4).

To avoid nonductile shear failures, the shear strength demand is computed as the sum of the factored gravity shear plus the maximum earthquake shear. The maximum earthquake shear is computed based on the maximum probable beam moments described and computed previously. The probable moment strength at each support is shown in Table 10-16.

Figure 10-17 illustrates the development of the design shear strength envelopes for Spans A-A', A'-B and B-C. In Figure 10-17a, the maximum probable earthquake moments are shown for seismic forces acting to the east (solid lines) and to the west (dashed lines). The moments shown occur at the face of the supports.

The earthquake shears produced by the maximum probable moments are shown in Figure 10-17b. For Span B-C, the values shown in the figure are:

$$V_E = \frac{M^-_{pr} + M^+_{pr}}{l_{clear}}$$

where l_{clear} = 17 feet-6 inches = 210 inches

Note that the magnitude of the earthquake shear can vary with direction (if the beam moment capacities are different at each end). However, in this case the shears are the same in both directions and are computed as:

V_E = (7,929 + 6,841) / 210 = 70.3 kips
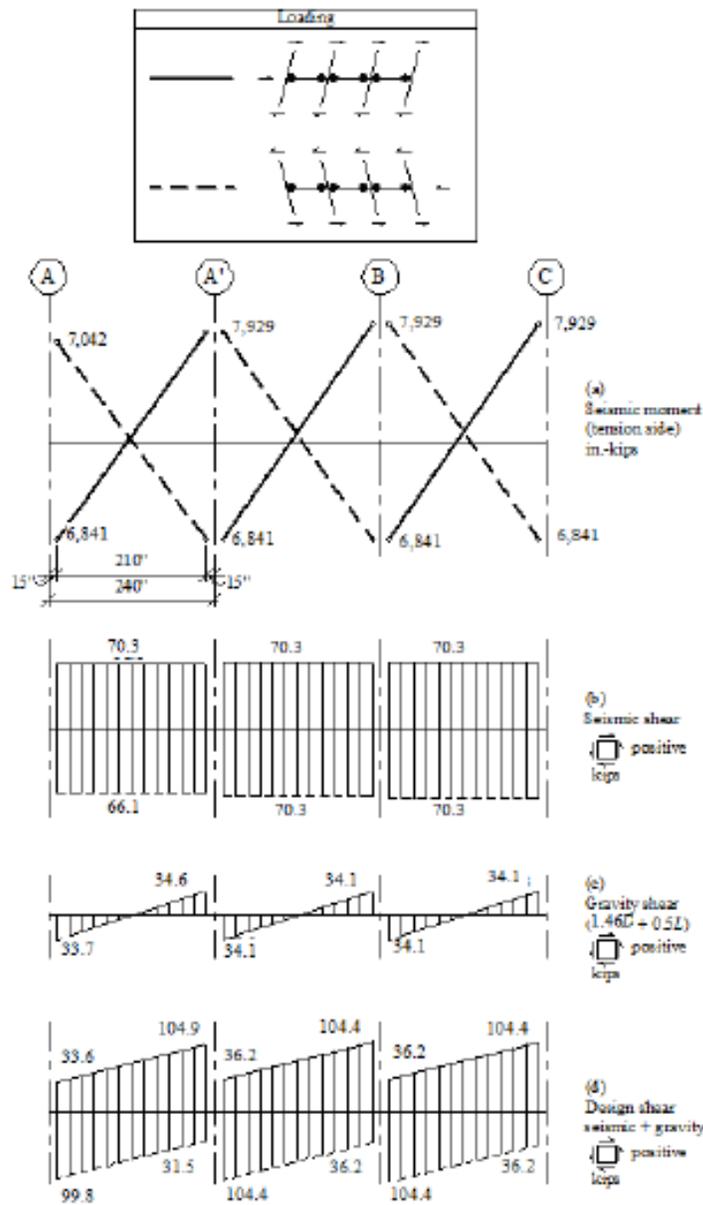
Figure 10-17 Shear forces for transverse reinforcement
(1.0 in. = 25.4 mm, 1.0 kip = 4.45kN, 1.0 in-kip = 0.113 kN-m)

The gravity shears shown in Figure 10-17c are taken from the ETABS model:

Factored gravity shear $= V_G = 1.46V_{dead} + 0.5V_{live}$
$V_{dead} = 20.2$ kips
$V_{live} = 9.3$ kips
$V_G = 1.46(20.2) + 0.5(9.3) = 34.1$ kips

Total design shears for each span are shown in Figure 10-17d. The strength envelope for Span B-C is shown in detail in Figure 10-18, which indicates that the maximum design shears is 70.3 + 34.1 = 104.4 kips. While this shear acts at one end, a shear of 70.3 – 34.1 = 36.2 kips acts at the opposite end of the member. In the figure the sloping lines indicate the shear demands along the beam and the horizontal lines indicate the shear capacities at the end and center locations.
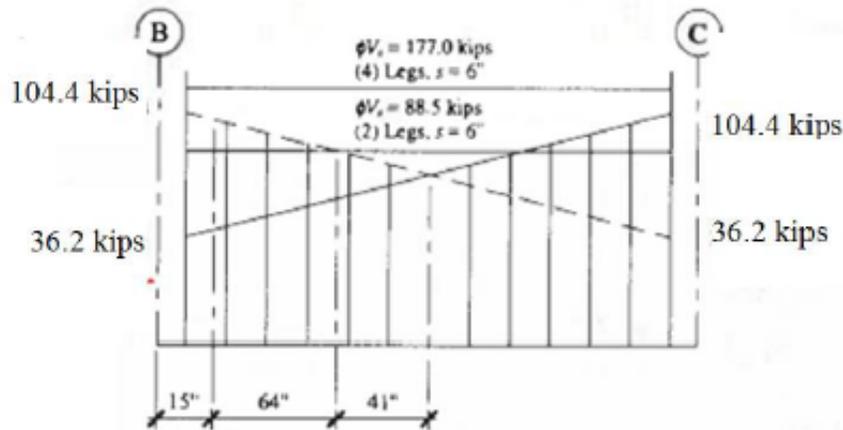
Figure 10-18 Detailed shear force envelope in Span B-C
(1.0 in. = 25.4 mm, 1.0 kip = 4.45kN)

In designing shear reinforcement, the shear strength can consist of contributions from concrete and from steel hoops or stirrups. However, according to ACI 318 Section 18.6.5.2, the design shear strength of the concrete must be taken as zero where the axial force is small ($P_u/A_g f'_c < 0.05$) and the ratio V_E/V_u is greater than 0.5. From Figure 10-17, this ratio is $V_E/V_u = 70.3/104.4 = 0.67$, so concrete shear strength must be taken as zero.

Compute the required shear strength provided by reinforcing steel at the face of the support:

$V_u = \phi V_s = 104.4$ kips
$V_s = A_v f_y d/s$

For reasons discussed below, assume four #4 vertical legs ($A_v = 0.8$ in^2), $f_y = 60$ ksi and $d = 29.5$ inches and compute the required spacing as follows:

$s = \phi A_v f_y d/V_u = 0.75[4(0.2)](60)(29.5/104.4) = 10.2$ inches

At midspan, the design shear $V_u = (104.4 + 36.2)/2 = 70.3$ kips, which is the same as the earthquake shear since gravity shear is nominally zero. Compute the required spacing assuming two #4 vertical legs:

$s = 0.75[2(0.2)](60)(29.5/70.3) = 7.55$ inches

In terms of detailing requirements, ACI 318 Section 18.6.4.1 states that closed hoops at a reduced spacing compared to the midspan locations are required over a distance of twice the member depth from the face of the support and ACI 318 Section 18.6.4.6 indicates that stirrups are permitted away from the ends.

Therefore, the shear strength requirements at this transition point should be computed. At a point equal to twice the beam depth, or 64 inches from the support, the shear is computed as:

$V_u = 104.4 - (64/210)(104.4 - 36.2) = 83.6$ kips

Compute the required spacing assuming two #4 vertical legs:

$s = 0.75[2(0.2)](60)(29.5/83.6) = 6.35$ inches

Before the final layout can be determined, the detailing requirements need to be considered. The first hoop must be placed 2 inches from the face of the support and the maximum hoop spacing at the beam ends is per ACI 318 Section 18.6.4.4 as follows:

$d/4 = 29.5/4 = 7.4$ inches
$6d_b = 6(1.0) = 6.0$ inches
6.0 inches

Outside of the region at the beam ends, ACI 318 Section 18.6.4.6 permits stirrups with seismic hooks to be spaced at a maximum of $d/2$.

Therefore, at the beam ends, overlapped close hoops with four legs will be spaced at 6 inches and in the middle, closed hoops with two legs will be spaced at 6 inches. This satisfies both the strength and detailing requirements and results in a fairly simple pattern. Note that hoops are being used along the entire member length. This is being done because the earthquake shear is a large portion of the total shear, the beam is relatively short and the economic premium is negligible.

This arrangement of hoops will be used for Spans A-A', B-C and C'-D. In Spans A'-B and C-C', the bottom flexural reinforcement is spliced and hoops must be placed over the splice region at $d/4$ or a maximum of 4 inches on center per ACI 318 Section 18.6.3.3.

One additional requirement at the beam ends is that where hoops are required (the first 64 inches from the face of support), longitudinal reinforcing bars must be supported as specified in ACI 318 Section 25.7.2.3 as required by ACI 318 Section 18.6.4.2. Hoops should be arranged such that every corner and alternate longitudinal bar is supported by a corner of the hoop assembly and such that the maximum spacing between transversely supported reinforcing is 14 inches. This will require overlapping hoops with four vertical legs as assumed previously. Details of the transverse reinforcement layout for all spans of Level 5 of Frame 1 are shown in Figure 10-16.

10.5.2.3 Check Beam-Column Joint at Frame 1. Prior to this point in the design process, preliminary calculations were used to check the beam-column joint, since the shear force developed in the beam-column joint is a direct function of the beam longitudinal reinforcement. These calculations are often done early in

the design process because if the computed joint shear is too high, the only remedies are increasing the concrete strength, increasing the column area, changing the reinforcement layout, or increasing the beam depth. At this point in the design, the joint shear is checked for the final layout of beam reinforcing.

The design of the beam-column joint is based on the requirements of ACI 318 Section 18.8. While ACI 318 provides requirements for joint shear strength, it does not specify how to determine the joint shear demand, other than to indicate that the joint forces are computed using the probable moment strength of the beam (ACI 318 Sec. 18.8.2.1). This example utilizes the procedure for determining joint shear demand contained in Moehle (2008). The shear in the joint is a function of the shear in the column and the tension/compression couple contributed by the beam moments. The method for determining column shear is illustrated in Figure 10-19. In this free-body diagram, the column shear, V_{col}, is determined from equilibrium as follows:

$$V_{col} = \frac{\left[\left(M_{pr,L} + M_{pr,R}\right) + \left(V_{e,L} + V_{e,R}\right)\frac{h}{2}\right]}{l_c}$$
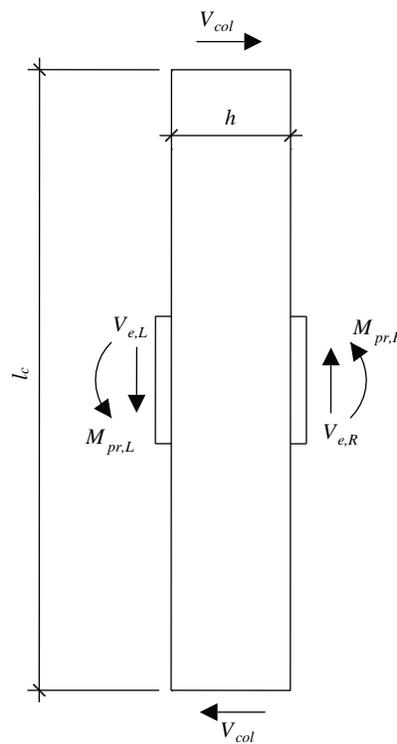
Figure 10-19 Column shear free body diagram

The determination of the forces in the joint of the column on Grid C of Frame 1 is based on Figure 10-16a, which shows how plastic moments are developed in the various spans for equivalent lateral forces acting to the east. An isolated sub-assemblage from the frame showing moments is shown in Figure 10-20b. The beam shears shown in Figure 10-20c are based on the probable moment strengths shown in Table 10-16.

For forces acting from west to east, compute the earthquake shear in Span B-C as follows:

$V_E = (M_{pr}^- + M_{pr}^+)/l_{clear} = (7{,}929 + 6{,}841)/(240 - 30) = 70.3$ kips

For Span C-C', the earthquake shear is the same since the probable moments are equal and opposite.
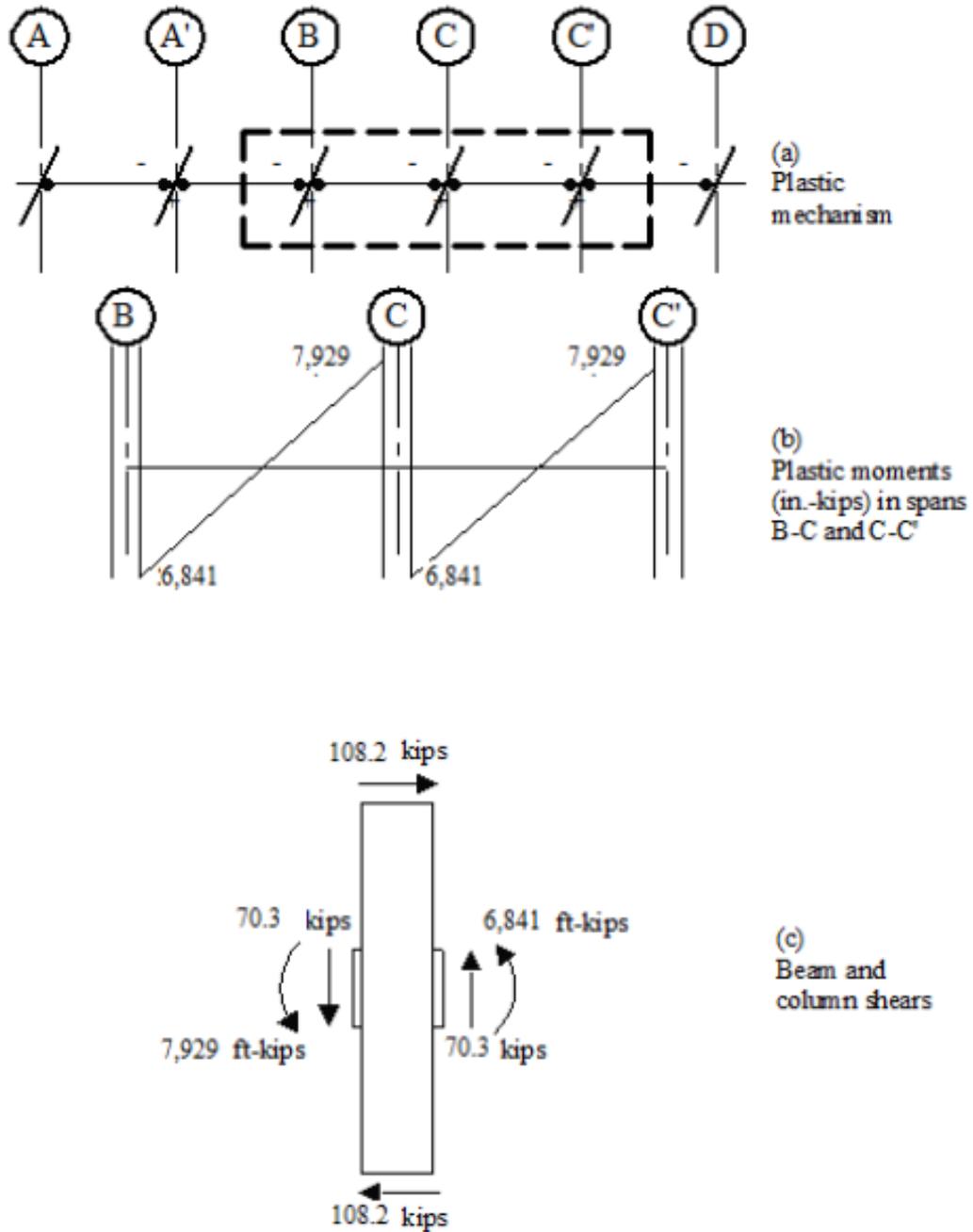
Figure 10-20 Diagram for computing column shears
(1.0 ft = 0.3048 m, 1.0 kip = 4.45kN, 1.0 in-kip = 0.113 kN-m)

With $h = 30$ inches and $l_c = 156$ inches, the column shear is computed as follows:

$$V_{col} = \frac{\left[(7,929+6,841)+(70.3+70.3)\dfrac{30}{2}\right]}{156} = 108.2 \text{ kips}$$

With equal spans, gravity loads do not produce significant column shears, except at the end column, where the seismic shear is much less. Therefore, gravity loads are not included in this computation.

The forces in the beam reinforcement for negative moment are based on four #8 plus one #7 bars at 1.25 f_y:

$T = C = 1.25(60)[4(0.79)+1(0.60)] = 282.0$ kips

For positive moment, four #8 bars also are used, assuming $C = T$, $C = 237.0$ kips.

As illustrated in Figure 10-21, the joint shear force V_j is computed as follows:

$V_j = T + C - V_{col}$
    $= 282.0 + 237.0 - 108.2$
    $= 410.8$ kips
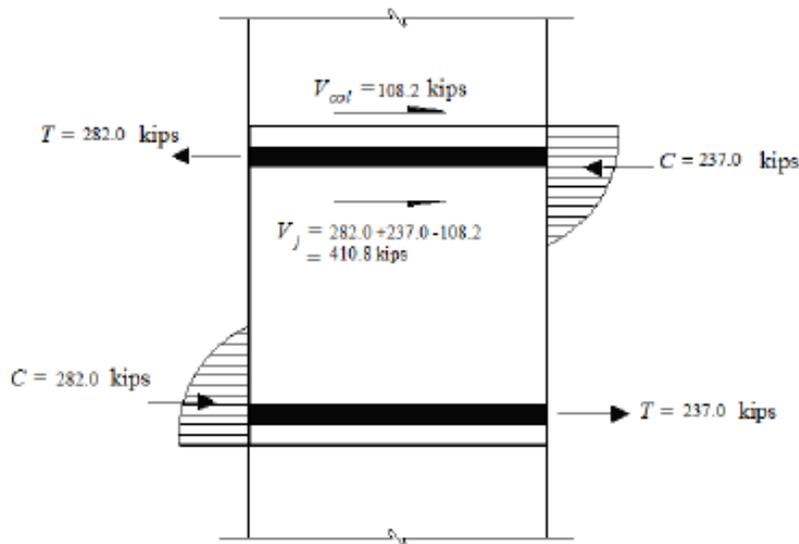
Figure 10-21 Computing joint shear stress (1.0 kip = 4.45kN)

For joints confined on three faces or on two opposite faces, the nominal shear strength is based on ACI 318 Section 18.8.4.1 as follows:

$V_n = 15\sqrt{f_c'}A_j = 15\sqrt{5,000}(30)^2 = 954.6$ kips

For joints of special moment frames, ACI 318 Section 21.2.4.3 permits $\phi = 0.85$, so $\phi V_n = 0.85(954.6$ kips) = 811.4 kips, which exceeds the computed joint shear, so the joint is acceptable. Joint stresses would be checked for the other columns in a similar manner.

ACI 318 Section 18.8.3.1 specifies the amount of transverse reinforcement required in the joint. Since the joint is not confined on all four sides by a beam, the total amount of transverse reinforcement required by ACI 318 Section 18.7.5.4 will be placed within the depth of the joint. As shown later, this reinforcement consists of four-leg #4 hoops at 4 inches on center.

10.5.2.4 Design of a Typical Interior Column of Frame 1. This section illustrates the design of a typical interior column on Gridline A'. The column, which supports Level 7 of Frame 1, is 30 inches square and is constructed from 5,000 psi concrete and 60 ksi reinforcing steel. An isolated view of the column is shown in Figure 10-22. The flexural reinforcement in the beams framing into the column is shown in Figure 10-16. Using simple tributary area calculations (not shown), the column supports an unfactored axial dead load of 367 kips and an unfactored axial reduced live load of 78 kips. The ETABS analysis indicates that the maximum axial earthquake force is 33.7 kips, tension or compression. The load combination used to compute this force consists of the full earthquake force in the E-W direction plus amplified accidental torsion. Since this column is not part of an N-S moment frame, orthogonal effects need not be considered per *Standard* Section 12.5.4. Hence, the column is designed for axial force plus uniaxial bending.
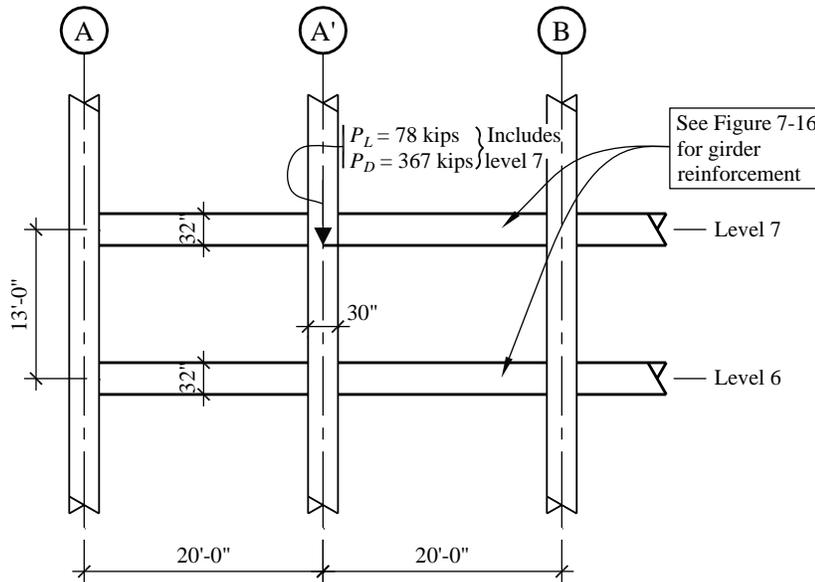
Figure 10-22 Layout and loads on column of Frame A'
(1.0 ft = 0.3048 m, 1.0 in. = 25.4 mm, 1.0 kip = 4.45kN)

10.5.5.3.1 Longitudinal Reinforcement. To determine the axial design loads, use the controlling basic load combinations:

$1.46D + 0.5L + 1.0E$

$0.64D - 1.0E$

The combination that results in maximum compression is:

$P_u = 1.46(367.2) + 0.5(78.0) + 1.0(33.7) = 608$ kips (compression)

The combination for minimum compression (or tension) is:

$P_u = 0.64(367.2) - 1.0(33.7) = 201$ kips (compression)

The maximum axial compression force of 608 kips is greater than $0.1f_c'A_g = 0.1(5)(30^2) = 450$ kips, so the design is based on ACI 318-11 Section 21.6 for columns. However, note that this section has been revised in ACI 318-14 to apply column requirements for special moment frames regardless of axial load. (see ACI 318 Sec. 18.7.1). According to ACI 318 Section 18.7.3, the sum of nominal column flexural strengths at the joint must be at least 6/5 of the sum of nominal flexural strength of the beams framing into the column. Beam moments at the face of the support are used for this computation. These capacities are provided in Table 10-16.

Nominal (negative) moment strength at end A' of Span A-A' = 5,765/0.9 = 6,406 inch-kips

Nominal (positive) moment strength at end A' of Span A' B = 4,948/0.9 = 5,498 inch-kips

Sum of beam moment at the joint = 6,406 + 5,498 = 11,904 inch-kips

Required sum of column design moments = 6/5 × 11,904 = 14,285 inch-kips.

Individual column design moment = 14,285/2 = 7,142 inch-kips

Knowing the factored axial load and the required design flexural strength, a column with adequate capacity must be selected. Figure 10-23 shows a P-M interaction curve for a 30- by 30-inch column with longitudinal reinforcing consisting of twelve #8 bars (1.05 percent steel). Computed using spColumn, the curve is based on a ϕ factor of 1.0 as required for nominal strength. At axial forces of 608 kips and 201 kips, solid horizontal lines are drawn. The dots on the lines represent the required average nominal flexural strength (7,142 inch-kips) at each axial load level. These dots must lie to the left of the curve representing the nominal column strengths. Since the dots are within the capacity curve for both design and nominal moments strengths at both the minimum and maximum axial forces, this column design is clearly adequate.
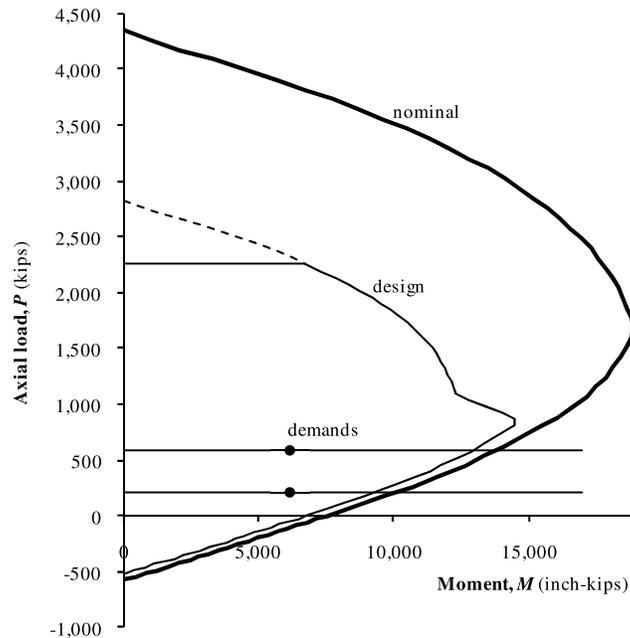
Figure 10-23 Design interaction diagram for column on Gridline A'
(1.0 kip = 4.45kN, 1.0 ft-kip = 1.36 kN-m)

10.5.2.4.2 Transverse Reinforcement. The design of transverse reinforcement for columns of special moment frames must consider confinement requirements (ACI 318 Sec. 18.7.5) and shear strength requirements (ACI 318 Sec. 18.7.6). The confinement requirements are typically determined first.

Based on ACI 318 Section 18.7.5.1, tighter spacing of confinement is generally required at the ends of the columns, over a distance, l_o, equal to the larger of the following:

Column depth = 30 inches
One-sixth of the clear span = (156-32)/6 = 20.7 inches
18 inches

There are both spacing and quantity requirements for the reinforcement. ACI 318 Section 18.7.5.3 specifies the spacing as the minimum of the following:

One-fourth the minimum column dimension = 30/4=7.5 inches

Six longitudinal bar diameters = 6(1.0) = 6.0 inches

Dimension $s_o = 4 + (14 - h_x) / 3$, where s_o is between 4 inches and 6 inches and h_x is the maximum horizontal spacing of hoops or cross ties.

For the column with twelve #8 bars and #4 hoops and cross ties, $h_x = 8.833$ inches and $s_o = 5.72$ inches, which controls the spacing requirement.

ACI 318 Section 18.7.5.4 gives the requirements for minimum transverse reinforcement. f_c' is less than 10,000 psi and the maximum axial compression force of 608 kips is less than $0.1f_c'A_g = 0.3(5)(30^2) = 1350$

kips so the following two equations in ACI 318 Section 18.7.5.4 shall be satisfied for rectangular sections with hoops:

$$A_{sh} = 0.3 \left(\frac{sb_c f_c'}{f_{yt}} \right) \left(\frac{A_g}{A_{ch}} - 1 \right)$$

$$A_{sh} = 0.09 \left(\frac{sb_c f_c'}{f_{yt}} \right)$$

Note that this section has been revised in ACI 318-14. For a column with high axial load, $\underline{P_u > 0.3 f_c' A_g}$, or high strength concrete, $\underline{f_c' > 10{,}000}$ psi, there is another equation to be satisfied other than two equations above.

The first of these equations controls when $A_g/A_{ch} > 1.3$. For the 30- by 30-inch columns:

$A_{ch} = (30 - 1.5 - 1.5)^2 = 729$ in^2
$A_g = 30 (30) = 900$ in^2
$A_g/A_{ch} = 900/729 = 1.24$

Therefore, the second equation controls. Try hoops with four #4 legs:

$b_c = 30 - 1.5 - 1.5 = 27.0$ inches
$s = [4 (0.2)(60{,}000)]/[0.09 (27.0)(5{,}000)] = 3.95$ inches

This spacing controls the design, so hoops consisting of four #4 bars spaced at 4 inches will be considered acceptable.

ACI 318 Section 18.7.5.5 specifies the maximum spacing of transverse reinforcement in the region beyond the l_o zones. The maximum spacing is the smaller of 6.0 inches or $6d_b$, which for #8 bars is also 6 inches. Hoops and crossties with the same details as those placed in the critical regions of the column will be used.

10.5.2.4.3 Check Column Shear Strength. The amount of transverse reinforcement computed in the previous section is the minimum required for confinement. The column also must be checked for shear strength in based on ACI 318 Sec. 18.7.6. According to that section, the column shear is based on the probable moment strength of the columns, but need not be more than what can be developed into the column by the beams framing into the joint. However, the design shear cannot be less than the factored shear determined from the analysis.

The shears computed based on the probable moment strength of the column can be conservative since the actual column moments are limited by the moments that can be delivered by the beams. For this example, however, the shear from the column probable moments will be checked first and then a determination will be made if a more detailed limit state analysis should be used.

As determined from spColumn, the maximum probable moment of the column in the range of factored axial load is 14,940 in.-kips. With a clear height of 124 inches, the column shear can be determined as $2(14{,}940)/124 = 241$ kips. This shear will be compared to the capacity provided by the 4-leg #4 hoops spaced at 6 inches on center. If this capacity is in excess of the demand, the columns will be acceptable for shear.

For the design of column shear capacity, the concrete contribution to shear strength may be considered because the minimum $P_u > A_g f'_c/20$. The design shear strength contributed by concrete and reinforcing steel are as follows:

$$V_c = 2\sqrt{f'_c}bd = 2\sqrt{5,000}(30)(27.5) = 116.7 \text{ kips}$$
$$V_s = A_v f_y d/s = (4)(0.2)(60)(27.5)/6 = 220.0 \text{ kips}$$
$$\phi V_n = \phi(V_c + V_s) = 0.75(116.7 + 220.0) = 252.5 \text{ kips} > 241 \text{ kips} \qquad\qquad \text{OK}$$

The column with the minimum transverse steel is therefore adequate for shear. The final column detail with both longitudinal and transverse reinforcement is given in Figure 10-24. The spacing of reinforcement through the joint has been reduced to 4 inches on center. This is done for practical reasons only. Column bar splices, where required, should be located in the center half of the column and must be proportioned as Class B tension splices.
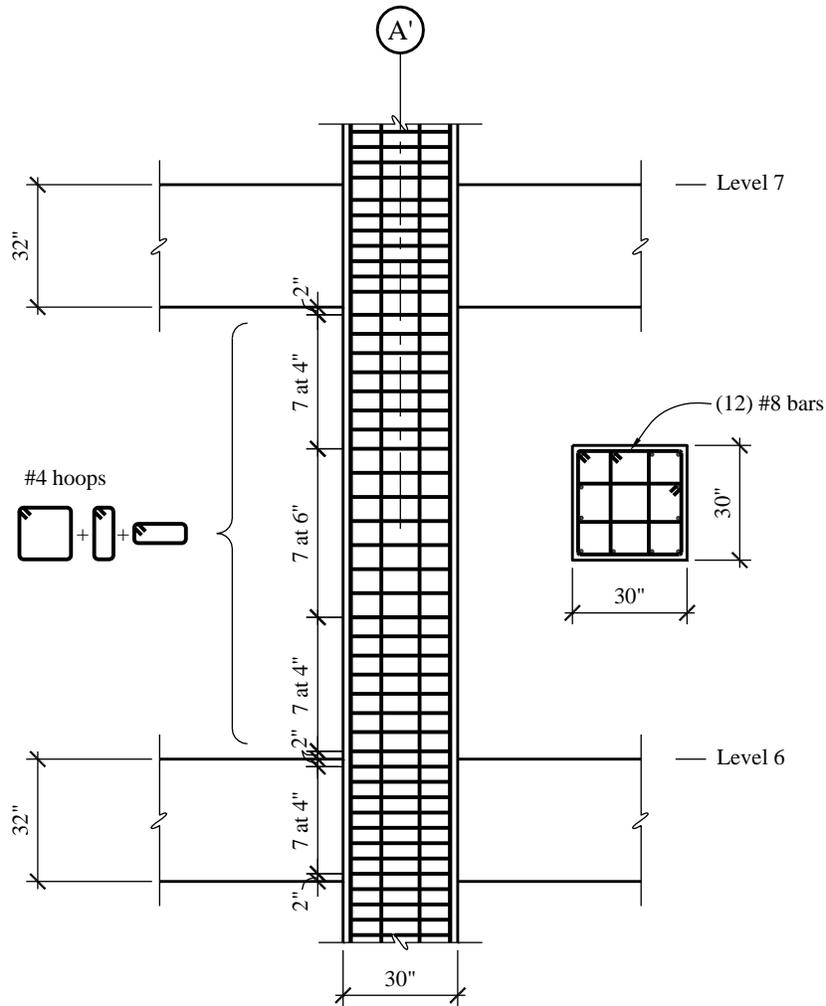
Figure 10-24 Details of reinforcement for column
(1.0 in. = 25.4 mm)

10.5.3 Design of Frame 3 Structural Wall

This section addresses the design of a representative structural wall. The structural wall includes the 16-inch wall panel in between two 30- by 30-inch columns. The design includes shear, flexure-axial interaction and boundary elements.

The factored forces acting on the structural wall of Frame 3 are summarized in Table 10-17. The axial compressive forces are based on the self-weight of the wall, a tributary area of 1,800 square feet of floor area for the entire wall (includes column self-weight), an unfactored floor dead load of 139 psf and an unfactored (reduced) floor live load of 20 psf. Based on the assumed 16-inch wall thickness, the wall between columns weighs (1.33 feet)(17.5 feet)(13 feet)(150 pcf) = 45.4 kips per floor. The total axial force for a typical floor is:

$P_u = 1.46D + 0.5L = 1.46[1,800(0.139) + 45,400] + 0.5[1,800(0.02)] = 468$ kips for maximum compression

$P_u = 0.64D = 0.64[1,800(0.139) + 45,400] = 189$ kips for minimum compression

The bending moments come from the ETABS analysis, using a section cut to combine forces in the wall panel and end columns.

Note that the gravity moments and the earthquake axial loads on the structural wall are assumed to be negligible given the symmetry of the system, so neither of these load effects is considered in the structural wall design.

Table 10-17 Design Forces for Grid 3 Structural wall

Supporting Level	Axial Compressive Force P_u (kips)		Shear V_u (kips)	Moment M_u (inch-kips)
	1.46D + 0.5L	0.64D		
R	432	189	206	41,008
12	89	378	170	59,429
11	1,367	568	194	76,999
10	1,835	757	235	91,920
9	2,303	956	263	102,872
8	2,770	1,135	299	109,891
7	3,238	1,325	348	116,039
6	3,706	1,514	406	131.578
5	4,173	1,703	475	168,242
4	4,641	1,892	556	222,352
3	5,109	2,082	651	297,514
2	5,577	2,271	769	441,592
1	6,044	2,460	712 (use 769)	310,641

(1.0 kip = 4.45 kN, 1.0 inch-kip = 0.113 kN-m)

10.5.3.1 Design for Shear Loads. First determine the required shear reinforcement in the wall panel and then design the wall for combined bending and axial force. The nominal shear strength of the wall is given by ACI 318 Equation 18.10.4.1:

$$V_n = A_{cv}(\alpha_c \lambda \sqrt{f_c'} + \rho_t f_y)$$

where $\alpha_c = 2.0$ because $h_w/l_w = 161/22.5 = 7.15 > 2.0$, where the 161 feet is the wall height and 22.5 feet is the overall wall length from the edges of the 30-inch boundary columns.

Using $f_c' = 5,000$ psi, $f_y = 60$ ksi, $\lambda = 1.0$, $A_{cv} = (22.5)(12)(16) = 4,320$ in^2, the required amount of shear reinforcement, ρ_t, can be determined by setting $\phi V_n = V_u$. In accordance with ACI 318 Section 21.2.4, the ϕ factor for shear is 0.60 for special structural walls unless the wall is specifically designed to be governed by flexure yielding. If the walls were designed to be flexure-critical, then the ϕ factor for shear would be 0.75, consistent with typical shear design. Unlike special moment frames, shear-critical special structural walls are permitted (with the reduced ϕ), although it should be noted that in areas of high seismic hazard many practitioners recommend avoiding shear-critical structural walls where practical. In this case, $\phi = 0.60$ will be used for design.

The required reinforcement ratio for strength at Level 1 is determined as:

$$\rho_t = \frac{\left(\dfrac{769,000}{0.60}\right) - \left(2\sqrt{5,000}(4,320)\right)}{4,320(60,000)} = 0.00258$$

This is slightly more than the minimum ratio of 0.0025 required by ACI 318 Section 18.10.2.1, but that minimum will apply to all walls above Level 2. (This is a good indication that the actual wall thickness can be reduced, but this example will proceed with the 16-inch wall thickness.) Above Level 2, assuming two curtains of #5 bars spaced at 15 inches on center, $\rho_t = 0.0026$ and $\phi V_n = 768$ kips, which exceeds the required shear capacity at all these levels. For Level 1, provide two curtains of #5 bars spaced at 12 inches on center, $\rho_t = 0.0032$ and $\phi V_n = 869$ kips.

Vertical reinforcing will be the same as the horizontal reinforcing based on the minimum reinforcing ratio requirements of ACI 318 Section 18.10.2.1.

10.5.3.2 Design for Flexural and Axial Loads. The flexural and axial design of special structural walls includes two parts: design of the wall for flexural and axial loads and the design of boundary elements where required. This section covers the design loads and the following section covers the boundary elements.

The wall analysis was performed using spColumn and considers the wall panel plus the boundary columns. For axial and flexural loads, $\phi = 0.65$ and 0.90, respectively. Figure 10-25 shows the interaction diagram for the wall section below Level 2, considering the range of possible factored axial loads. The wall panel is 16 inches thick and has two curtains of #5 bars at 15 inches on center, except at the lower two levels where the reinforcing two curtains of #5 bars at 12 inches on center. The boundary columns are 30 by 30 inches with twelve #9 bars at this location. The section is clearly adequate because the interaction curve fully envelopes the design values.
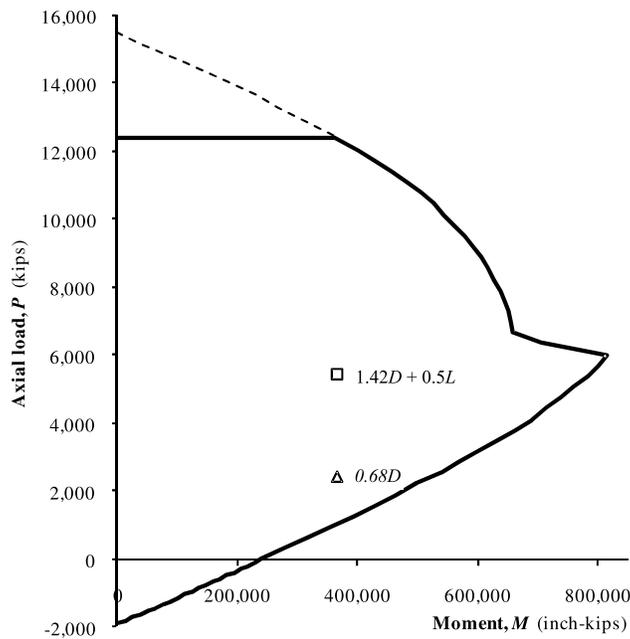
Figure 10-25 Interaction diagram for structural wall
(1.0 kip = 4.45kN, 1.0 in-kip = 0.113 kN-m)

10.5.3.3 Design of Boundary Elements. An important consideration in the ductility of special reinforced concrete structural walls is the determination of where boundary elements are required and the design of them where they are required. ACI 318 provides two methods for this. The first approach, specified in ACI 318 Section 18.10.6.2, uses a displacement based procedure. The second approach, described in ACI 318 Section 18.10.6.3 uses a stress-based procedure and will be illustrated for this example.

In accordance with ACI 318 Section 18.10.6.3 special boundary elements are required where the maximum extreme fiber compressive stress exceeds $0.2f'_c$ and they can be terminated where the stress is less than $0.15f'_c$. The stresses are determined based on the factored axial and flexure loads as shown in Table 10-18. The stresses are determined using a wall area of 5,160 in^2, a section modulus of 284,444 in^3 and $f'_c = 5,000$ psi.

Table 10-18 Grid 3 Structural wall Boundary Element Check

Supporting Level	Axial Force P_u (kips)	Moment M_u (inch-kips)	Maximum stress		Boundary Element Required?
			(ksi)	($\times f_c'$)	
R	432	41,008	0.228	0.05	No
12	899	59,429	0.383	0.08	No
11	1,367	76,999	0.536	0.11	No
10	1,835	91,920	0.679	0.14	No
9	2,303	102,872	0.808	0.16	Yes
8	2,770	109,891	0.923	0.18	Yes
7	3,238	116,039	1.035	0.21	Yes
6	3,706	131,578	1,181	0.24	Yes
5	4,173	168,242	1.400	0.28	Yes
4	4,641	222,352	1.681	0.34	Yes
3	5,109	297,514	2.036	0.41	Yes
2	5,577	441,592	2.633	0.53	Yes
1	6,044	310,641	2.263	0.45	Yes

(1.0 kip = 4.45 kN, 1.0 in-kip = 0.113 kN-m)

As can be seen, special boundary elements are required at the base of the wall and can be terminated above Level 9.

Where they are required, the detailing of the special boundary element is based on ACI 318 Section 18.10.6.4.

According to ACI 318 Section 18.10.6.4 Item (a), the special boundary elements must have a minimum plan length equal to the greater of c - $0.1l_w$, or $c/2$, where c is the neutral axis depth and l_w is the wall length. The neutral axis depth is a function of the factored axial load and the nominal (ϕ = 1.0) flexural capacity of the wall section. This value is obtained from the spColumn analysis for the wall section and range of axial loads. For the Level 2 wall with twelve #9 vertical bars at each boundary column and two curtains of #5 bars at 15 inches at vertical bars, the computed neutral axis depths are 31.2 inches and 72.6 inches for axial loads of 5,577 and 2,271 kips, respectively. For the governing case of 72.6 inches and a wall length of 270 inches, the boundary element length is the greater of 72.6 - 0.1(270) = 50.6 inches and the second is 72.6/2 = 38.8 inches.

It is clear, therefore, that the special boundary element needs to extend beyond the 30-inch edge columns at least at the lower levels. For the wall below Level 5 where the maximum factored axial load is 4,173 kips, c = 55.3 inches and the required length is 28.3 inches, which fits within the boundary column. For the walls from the basement to below Level 4, the boundary element can be detailed to extend into the wall panel, or the concrete strength could be increased. Based on the desire to simply the reinforcing, the wall concrete strength could be increased to f_c' = 7,000 psi and the required boundary element length below Level 2 is 28.7 inches. Figure 10-26 illustrates the variation in neutral axis depth based on factored axial load and concrete strength. Although there is a cost premium for the higher strength concrete, this is still in the range of commonly supplied concrete and will save costs by allowing the column rebar cage to serve as the boundary element and have only distributed reinforcing in the wall panel itself. The use of 7,000 psi concrete at the lower levels will impact the calculations for maximum extreme fiber stress per Table 10-18, but since the 7,000 psi concrete extends up to Level 4, not Level 8, the vertical extent of the boundary elements is unchanged.

It is expected that the increase in concrete strength (and thus the modulus of elasticity) at the lower floors will have a slight impact on the overall building stiffness, but this will not impact the overall design. However, this should be verified.
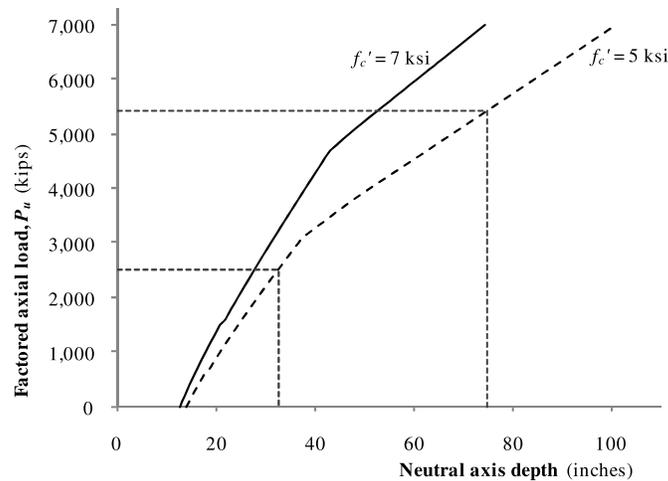
Figure 10-26 Variations of neutral axis depth
(1.0 in. = 25.4 mm, 1.0 kip = 4.45 kN)

Where special boundary elements are required, transverse reinforcement must conform to ACI 318 Section 18.10.6.4. Note that this section has been revised in ACI 318-14. ACI 318 Section 18.10.6.4 (e), which refers to ACI 318 Sections 18.7.5.2 (a) through (e) and 18.7.5.3 . In addition, the transverse reinforcing spacing limit of ACI 318 Section 18.7.5.3(a) can be one-third of the least dimension of the element. Similar to columns of special moment frames, there are requirements for spacing and total area of transverse reinforcing.

The spacing is determined as follows:

One-third of least dimension = 30/3 = 10 inches

Six longitudinal bar diameters = 6(1.125) = 6.75 inches

Dimension $s_o = 4 + (14 - h_x) / 3$, where s_o is between 4 inches and 6 inches and h_x is the maximum horizontal spacing of hoops or cross ties which shall not exedd the lesser of 14 inches and two-thirds of the boundary element thickness.

In addition, where hoops are used, the transverse reinforcement must satisfy ACI 318 Table 18.10.6.4 (f):

$$A_{sh} = 0.3 \left(\frac{sb_c f'_c}{f_{yt}} \right) \left(\frac{A_g}{A_{ch}} - 1 \right)$$

$$A_{sh} = 0.09 \left(\frac{sb_c f'_c}{f_{yt}} \right)$$

The first of these equations controls when $A_g/A_{ch} > 1.3$. For the 30- by 30-inch boundary element:

$A_{ch} = (30 - 1.5 - 1.5)^2 = 729 \text{ in}^2$

10-63

$A_g = 30\ (30) = 900\ \text{in}^2$
$A_g/A_{ch} = 900/729 = 1.24$

Therefore, the second equation controls. If #4 hoops with two crossties in each direction are used similar to the moment frame columns, $A_{sh} = 0.80\ \text{in}^2$ and $b_c = 27$ inches. For $f_c' = 7{,}000$ psi and $f_{yt} = 60$ ksi,

$s = [(0.8)(60{,}000)]/[0.09(27.0)(7{,}000)] = 2.82$ inches

which is impractical. Therefore, use #5 hoops and cross ties for the 7,000 psi concrete below Level 4, so A_{sh} = 4(0.31) = 1.24 in^2 and $s = 4.4$ inches.

Where the concrete strength is 5,000 psi above Level 4, use #4 hoops and cross ties and the spacing, $s = 3.95$ inches.

Therefore, for the special boundary elements, use hoops with two cross ties spaced at 4 inches. The hoops and cross ties are #5 below Level 4 and #4 above Level 4. ACI 318 Section 18.10.6.4(g) also requires that the boundary element transverse reinforcement be extended beyond the base of the wall a distance equal to the tension development length of the longitudinal reinforcement in the boundary elements unless there is a mat, footing or pile cap, in which case the transverse reinforcement extends down at least 12 inches unless a great extension is required by ACI 318 Section 18.13.2.3.

Details of the boundary element and wall panel reinforcement are shown in Figures 10-27 and 10-28, respectively. The vertical reinforcement in the boundary elements will be spliced as required using either Class B lap splices or Type 2 mechanical splices at all locations. According to Table 10-15 (prepared for 5,000 psi concrete), there should be no difficulty in developing the horizontal wall panel steel into the 30- by 30-inch boundary elements.

* #4 Hoops and Cross Ties above Level 4.
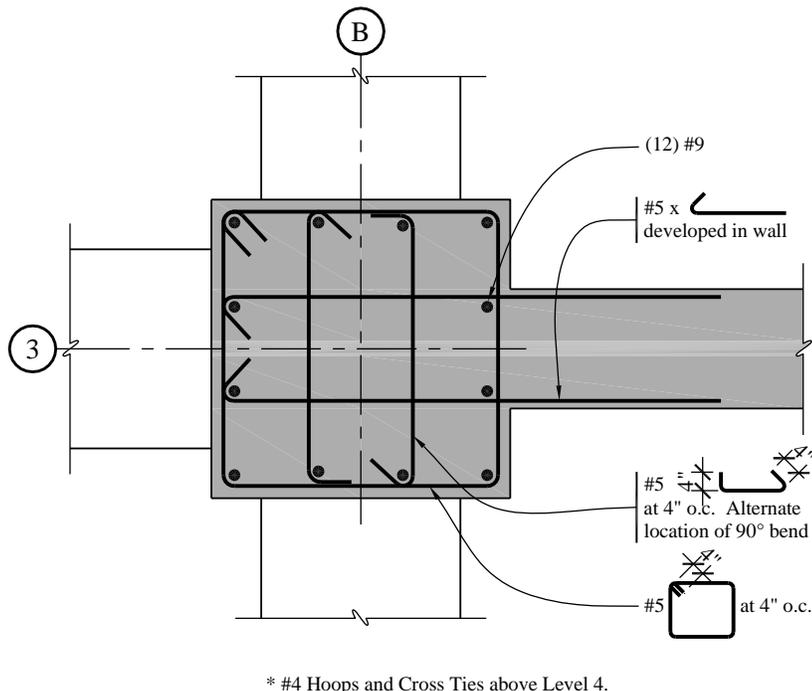
Figure 10-27 Details of structural wall boundary element
(1.0 in. = 25.4 mm)
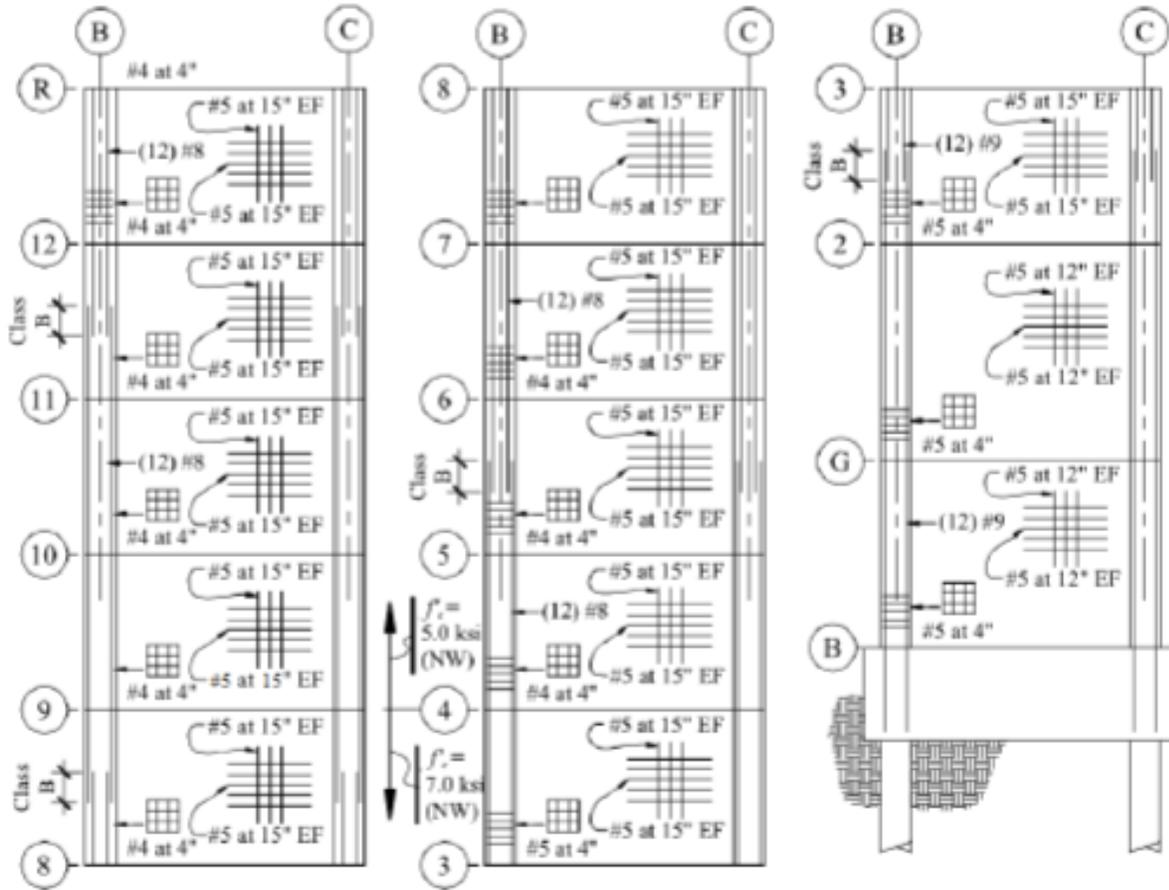
Figure 10-28 Overall details of structural wall
(1.0 in. = 25.4 mm)

10.6   STRUCTURAL DESIGN OF THE HONOLULU BUILDING

The structure illustrated in Figures 10-1 and 10-2 is now designed and detailed for the Honolulu building. Because of the relatively moderate level of seismicity, the lateral load-resisting system will consist of a series of intermediate moment-resisting frames in both the E-W and N-S directions. This is permitted for Seismic Design Category C buildings in accordance with *Standard* Table 12.2-1. Design guidelines for the reinforced concrete framing members are provided in ACI 318 Section 18.4.

As noted previously, the beams are assumed to be 30 inches deep by 20 inches wide and the columns are 28 inches by 28 inches. These are slightly smaller than the Berkeley building, reflecting the lower seismicity.

10.6.1 Compare Seismic Versus Wind Loading
As has been discussed and as illustrated in Figure 10-3, wind forces appear to govern the strength requirements of the structure at the lower floors and seismic forces control at the upper floors. The seismic

and wind shears, however, are so close at the middle levels of the structure that a careful evaluation must be made to determine which load governs for strength. This determination requires consideration of several load cases for both wind and seismic loads.

Because the Honolulu building is in Seismic Design Category C and does not have a Type 5 horizontal irregularity (*Standard* Table 12.3-1); orthogonal loading effects need not be considered per *Standard* Section 12.5.3. However, as required by *Standard* Section 12.8.4.2, accidental torsion must be considered. Torsional amplification is not required per *Provisions* Section 12.8.4.3 because the building does not have a torsional irregularity as determined previously.

For wind, the *Standard* requires that buildings over 60 feet in height be checked for four loading cases under the Directional Procedure of *Standard* Chapter 27. The required load cases are shown in Figure 10-29, which is reproduced directly from *Standard* Figure 27.4-8. In Cases 1 and 2, load is applied separately in the two orthogonal directions, but Case 2 adds a torsional component. Cases 3 and 4 involve wind loads in two directions simultaneously and Case 4 adds a torsional component.
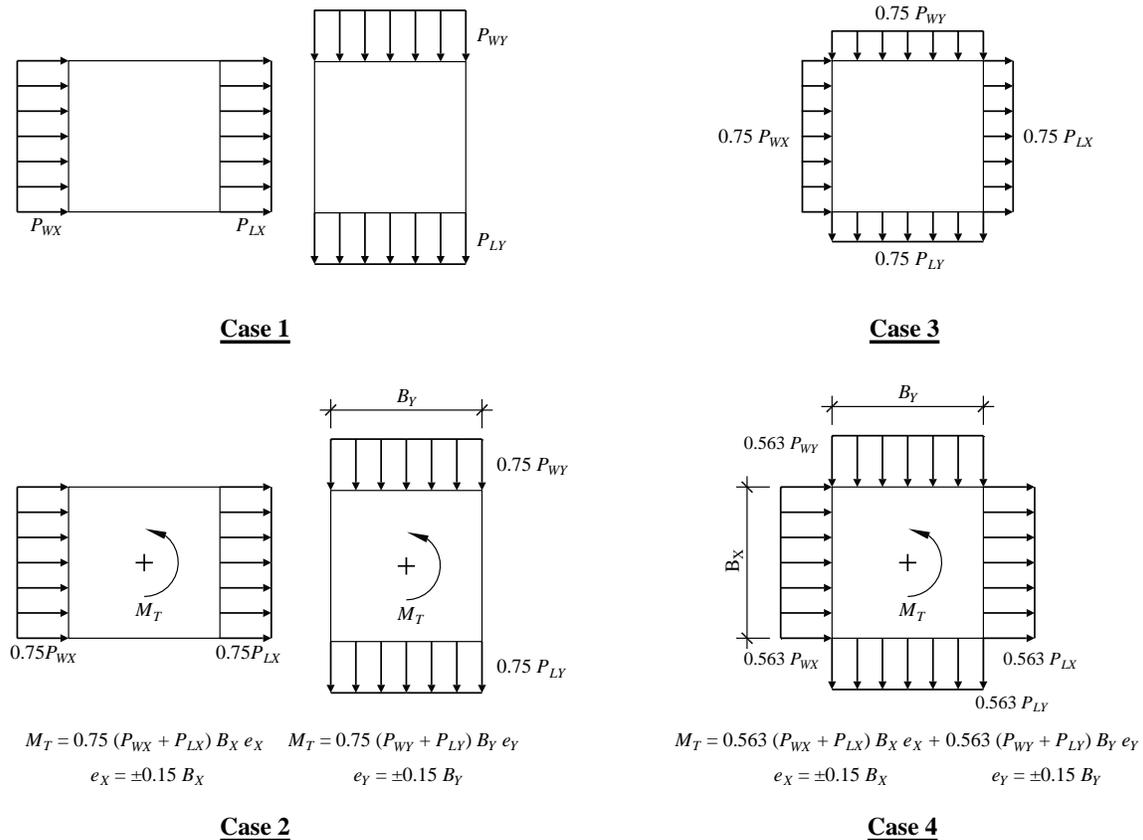
Figure 10-29 Wind loading requirements from ASCE 7

In this example, only loading in the E-W direction is considered. Hence, the following lateral load conditions are applied to the ETABS model:

E-W seismic with accidental torsion

Wind Case 1 applied in E-W direction only

Wind Case 2 applied in E-W direction only

Wind Case 3

Wind Case 4

All cases with torsion are applied in such a manner as to maximize the shears in the elements of Frame 1, for whose members the design is illustrated in the following section.

A simple method for determining which load case is likely to govern is to compare the beam shears for each story. For the five load cases indicated above, the beam shears produced from seismic effects control at the sixth level, with the next largest forces coming from direct E-W wind Case 1. This is shown graphically in Figure 10-30, where the beam shears at the center bay of Frame 1 are plotted versus story height. Wind controls load at the lower four stories and seismic controls for all other stories. This is somewhat different from that shown in Figure 10-3, wherein the total story shears are plotted and where wind controlled for the lower five stories. A basic difference between Figures 10-3 and 10-30 is that Figure 10-30 includes torsion effects.
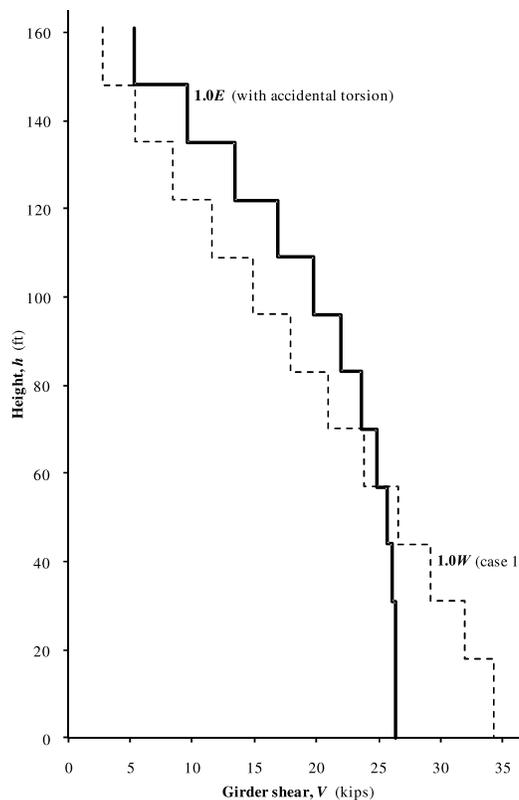
Figure 10-30 Wind versus seismic shears in center bay of Frame 1
(1.0 ft = 0.3048 m, 1.0 kip = 4.45kN)

10.6.2 Design and Detailing of Members of Frame 1

In this section, the beams and a typical interior column of Level 6 of Frame 1 are designed and detailed.

10.6.2.1 Initial Calculations. The girders of Frame 1 are 30 inches deep and 20 inches wide. For positive moment bending, the effective width of the compression flange is taken as $20 + 20(12)/12 = 40.0$ inches. Assuming 1.5-inch cover, #4 stirrups and #9 longitudinal reinforcement, the effective depth for computing flexural and shear strength is $30 - 1.5 - 0.5 - 1.125 / 2 = 27.4$ inches.

10.6.2.2 Design of Representative Beams. ACI 318 Section 18.4.2 provides the minimum requirements for longitudinal and transverse reinforcement in the beams of intermediate moment frames. The requirements for longitudinal steel are as follows:

1. The positive moment strength at the face of a joint shall be at least one-third of the negative moment strength at the same joint.

2. Neither the positive nor the negative moment strength at any section along the length of the member shall be less than one-fifth of the maximum moment strength supplied at the face of either joint.

The second requirement has the effect of requiring top and bottom reinforcement along the full length of the member. The minimum reinforcement ratio at any section is taken from ACI 318 Section 9.6.1.2 as greater of $\dfrac{3\sqrt{f'_c}}{f_y} = 0.0035$ or $200/f_y = 0.0033$ for $f_y = 60$ ksi $f'_c = 5,000$ psi. However, according to ACI 318 Section 10.5.3, the minimum reinforcement provided need not exceed 1.33 times the amount of reinforcement required for strength.

The gravity loads and design moments for the first three spans of Frame 1 are shown in Figure 10-31. The seismic and gravity moments are determined from ETABS analysis, similar to the Berkeley building. All moments are given at the face of the support. The gravity moments shown in Figures 10-31c and 10-31d are slightly different from those shown for the Berkeley building (Figure 10-11) because the beam self-weight is less and the clear span is longer due to the reduction in column size.
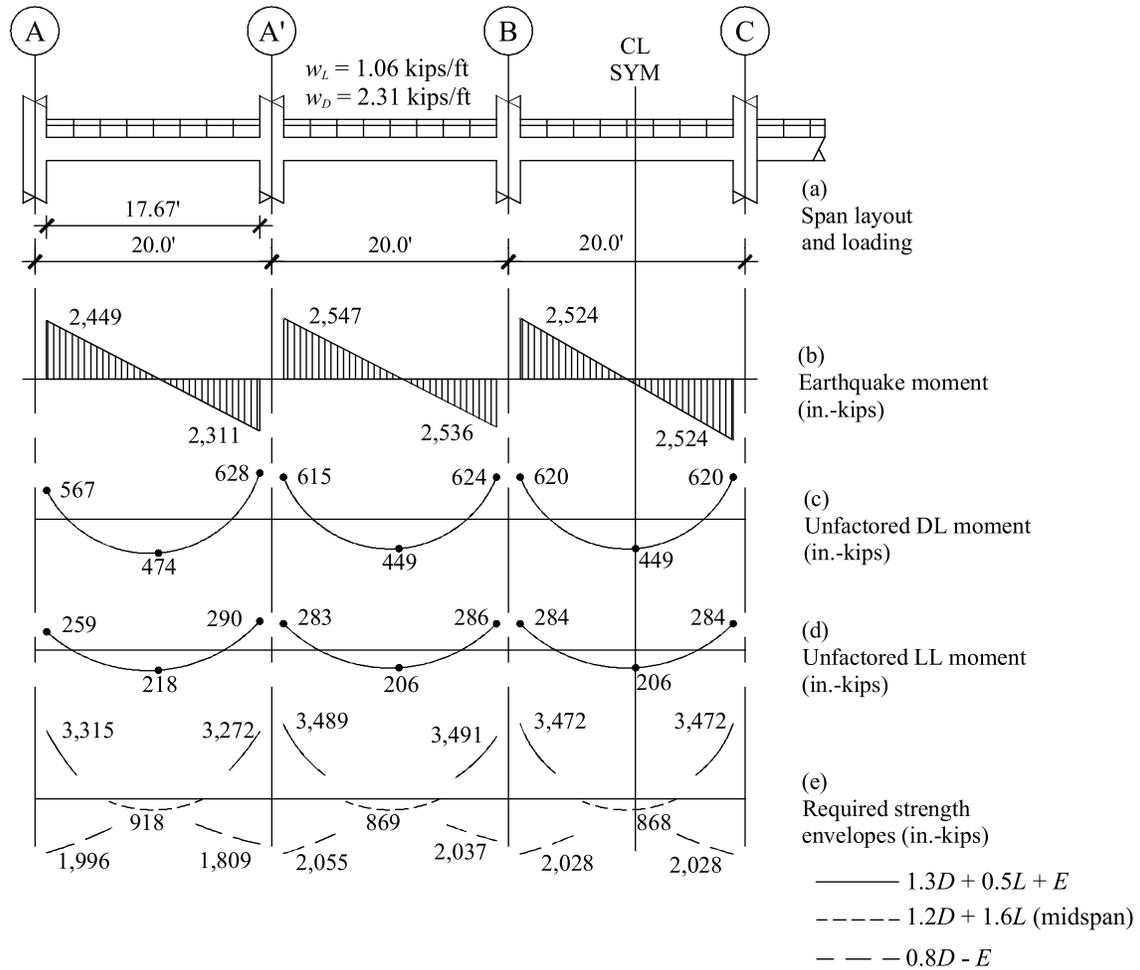
Figure 10-31 Bending moment envelopes at Level 6 of Frame 1
(1.0 ft = 0.3048 m, 1.0 kip/ft = 14.6 kN/m, 1.0 in-kip = 0.113 kN-m)

10.6.2.2.1 Longitudinal Reinforcement. Based on a minimum amount of longitudinal reinforcing of $0.0035b_wd = 0.0035(20)(27.4)=1.92$ in^2, provide two #9 bars continuous top and bottom as a starting point and provide additional reinforcing as required.

1. Design for Negative Moment at the Face of the Interior Support Grid A'

   $M_u = -1.29 (615) - 0.5 (283) - 1.0 (2,547) = -3,484$ inch-kips

Try two #9 bars plus one #7 bar.

   $A_s = 2 (1.00) + 0.60 = 2.60$ in^2
   Depth of compression block, $a = [2.6 (60)]/[0.85 (5) 20] = 1.83$ inches
   Nominal strength, $M_n = [2.60 (60)] [27.4 - 1.83/2] = 4,131$ inch-kips
   Design strength, $\phi M_n = 0.9 (4,131) = 3,718$ inch-kips $> 3,484$ inch-kips   OK

This reinforcement also will work for negative moment at all other supports.

2. Design for Positive Moment at the Face of the Interior Support Grid A'

$M_u = -0.8\,(615) + 1.0\,(2{,}536) = 2{,}055$ inch-kips

Try the minimum of two #9 bars.

$A_s = 2\,(1.00) = 2.00$ in^2
$a = 2.00\,(60)/[0.85\,(5)\,40] = 0.71$ inch
$M_n = [2.00\,(60)]\,[27.4 - 0.71/2] = 3{,}246$ inch-kips
$\phi\ M_n = 0.9\,(3{,}246) = 2{,}921$ inch-kips $> 2{,}055$ inch-kips   OK

This reinforcement also will work for positive moment at all other supports.

The layout of flexural reinforcement layout is shown in Figure 10-32. The top short bars are cut off 5 feet-0 inch from the face of the support. The bottom bars are spliced in Spans A'-B and C-C' with a Class B lap length of 37 inches. Unlike special moment frames, there are no requirements that the spliced region of the bars in intermediate moment frames be confined by hoops over the length of the splice. Note that the steel clearly satisfies the detailing requirements of ACI 318 Section 18.4.2.2.
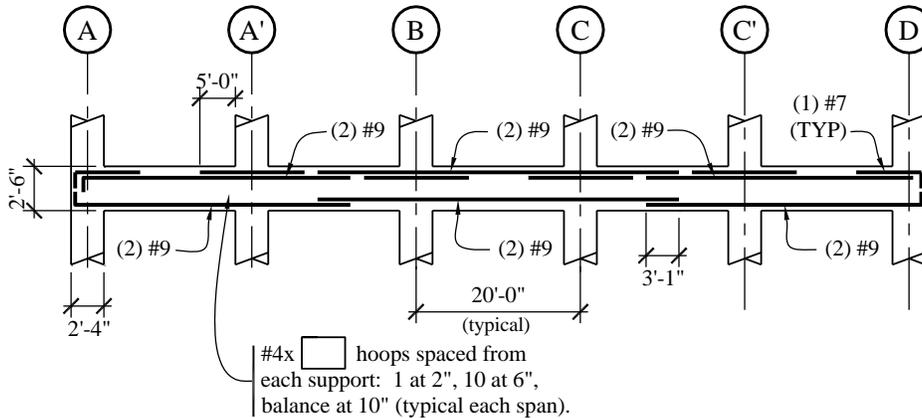
Figure 10-32 Longitudinal reinforcement layout for Level 6 of Frame 1
(1.0 in. = 25.4 mm, 1.0 ft = 0.3048 m)

10.6.2.2.2 Transverse Reinforcement. The requirements for transverse reinforcement in intermediate moment frames are somewhat different from those in special moment frames, both in terms of detailing and shear design. The shear strength requirements will be covered first, followed by the detailing requirements.

In accordance with ACI 318 Section 18.4.2.3, the design earthquake shear for the design of intermediate moment frame beams must be larger than the smaller of the following:

a. The sum of the shears associated with the nominal moment strength at the ends of the members.
    Nominal moment strengths are computed with a flexural reinforcement tensile strength of $1.0f_y$
    and a flexural ϕ factor of 1.0.

b. Two times the factored earthquake shear force determined from the structural analysis.

In either case, the earthquake shears are combined with the factored gravity shears to determine the total design shear.

Consider the interior span between Grids A' and B. For determining earthquake shears per Item a above, the nominal strengths at the ends of the beam were computed earlier as 3,246 inch-kips for positive moment at Support B and 4,131 inch-kips for negative moment at Support A'. Compute the design earthquake shear V_E:

$$V_E = \frac{3,246 + 4,131}{212} = 34.8 \text{ kips}$$

where 212 inches is the clear span of the member. The shear is the same for earthquake forces acting in the other direction.

For determining earthquake shears per Item b above, the shear is taken from the ETABS analysis as 23.4 kips. The design earthquake shear for this method is 2(21.2 kips) = 42.4 kips.

Since the design shear using Item a is the smaller value, it is used for computing the design shear.

The gravity load shears are taken from the ETABS model. Since the gravity shears at Grid A' are similar but slightly larger than those at Grid A, Grid A' will be used for the design. From the ETABS analysis, V_D = 20.7 kips and V_L = 9.5 kips.

The factored design shear V_u = 1.29(20.7) + 0.5(9.5) + 1.0(34.8) = 66.5 kips. This shear force applies for earthquake forces coming from either direction as shown in the shear strength design envelope in Figure 10-33.

The design shear force is resisted by a concrete component, V_c and a steel component, V_s. Note that the concrete component may be used regardless of the ratio of earthquake shear to total shear. The required design strength is:

$$V_u \leq \phi V_c + \phi V_s$$

where ϕ = 0.75 for shear.

$$V_c = \frac{2\sqrt{5,000}(20)(27.4)}{1,000} = 77.5 \text{ kips}$$

The shear to be resisted by reinforcing steel, assuming two #4 vertical legs (A_v = 0.4) and f_y = 60 ksi is:

$$V_s = \frac{V_u - \phi V_c}{\phi} = \frac{66.5 - 0.75(77.5)}{0.75} = 11.2 \text{ kips}$$

Using $V_s = A_v f_y d / s$:

$$s = \frac{(0.4)(60)(27.4)}{11.2} = 58.7 \text{ inches}$$

Minimum transverse steel requirements are given in ACI 318 Section 18.4.2.4. At the ends of the beam, hoops are required. The first hoop must be placed 2 inches from the face of the support and within a

distance $2h$ from the face of the support, the spacing should be not greater than $d/4$, eight times the smallest longitudinal bar diameter, 24 times the hip bar diameter, or 12 inches. For the beam under consideration $d/4$ controls minimum transverse steel, with the maximum spacing being $27.4/4 = 6.8$ inches, which is less than what is required for shear strength.

In the remainder of the span, stirrups are permitted and must be placed at a maximum of $d/2$ (ACI 318 Sec. 18.4.2.5).

Because the earthquake shear (at midspan where the gravity shear is essentially zero) is greater than 50 percent of the shear strength provided by concrete alone, the minimum requirements of ACI 318 Section 9.6.3.1 and 9.6.3.3 must be checked:

$$s_{max} = \frac{A_v f_{yt}}{0.75\sqrt{f_c'}b_w} = \frac{0.4(60,000)}{0.75\sqrt{5,000}(20)} = 20.8 \text{ inches}$$

This spacing does not control over the $d/2$ requirement. The layout of transverse reinforcement for the beam is shown in Figure 10-32. This spacing is used for all other spans as well.
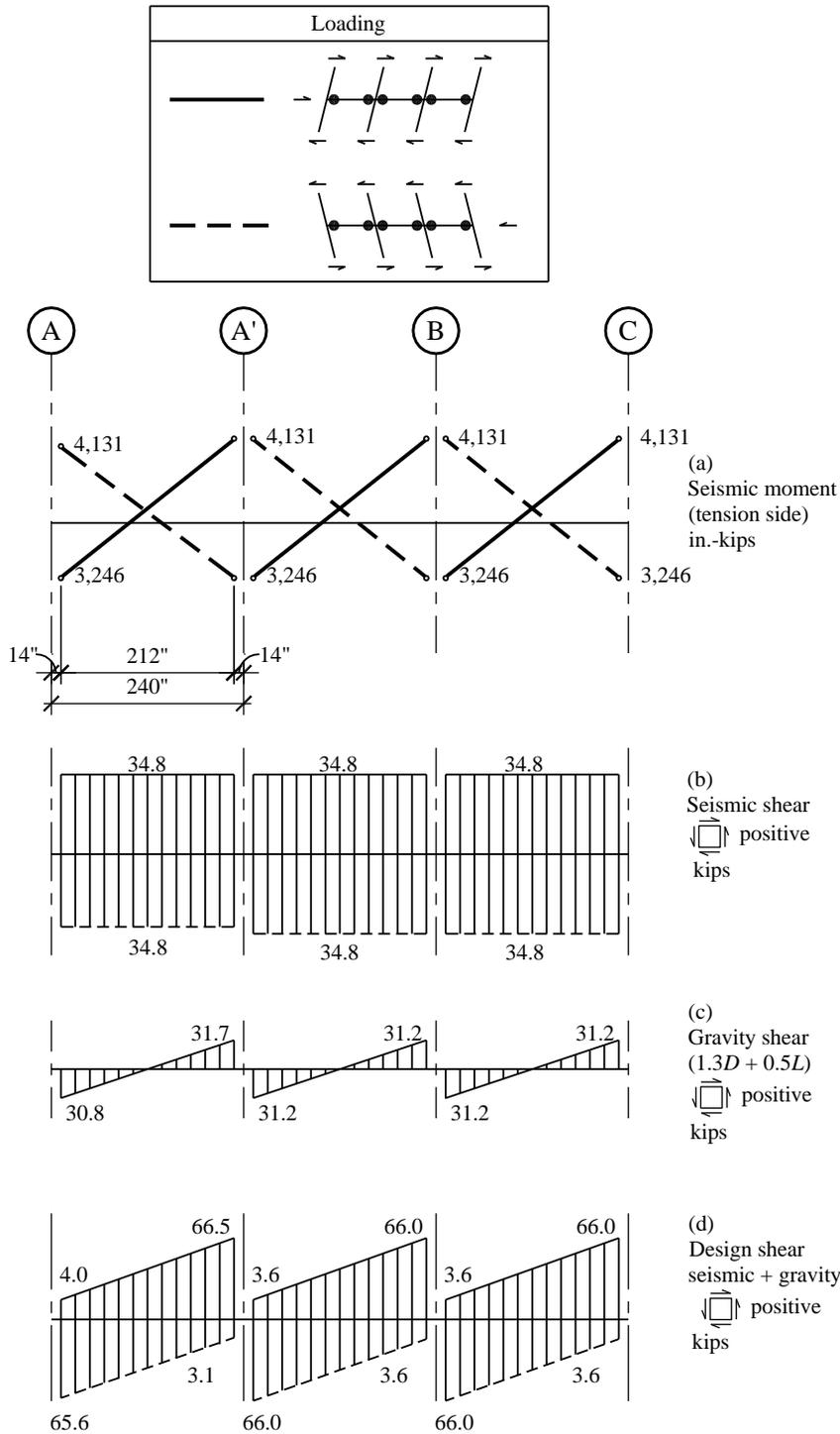
Figure 10-33 Shear strength envelopes for Span A-A' of Frame 1
(1.0 in. = 25.4 mm, 1.0 kip = 4.45kN, 1.0 in-kip = 0.113 kN-m)

10.6.2.3 Design of Representative Column of Frame 1. This section illustrates the design of a typical interior column on Gridline A'. The column, which supports Level 6 of Frame 1, is 28 inches square and is constructed from 5,000 psi concrete and 60 ksi reinforcement. An isolated view of the column is shown in Figure 10-34.

The column supports an unfactored axial dead load of 506 kips and an unfactored axial live load (reduced) of 117 kips. The ETABS analysis indicates that the axial earthquake force is ±17.6 kips, the earthquake shear force is ±34.4 kips and the earthquake moments at the top and the bottom of the column are ±2,222 and ±2,218 inch-kips, respectively. Moments and shears due to gravity loads are assumed to be negligible.
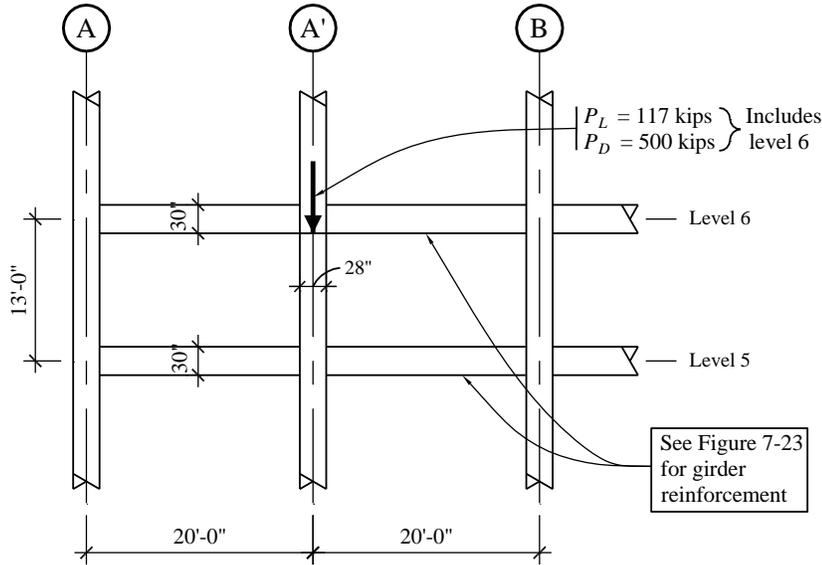
Figure 10-34 Isolated view of Column A'
(1.0 ft = 0.3048 m, 1.0 kip = 4.45kN)

10.6.2.3.1 Longitudinal Reinforcement. The factored gravity force for maximum compression (without earthquake) is:

$P_u = 1.2(506) + 1.6(117) = 794$ kips

This force acts with no significant gravity moment.

The factored gravity force for maximum compression (including earthquake) is:

$P_u = 1.29(506) + 0.5(117) + 17.6 = 734$ kips

The factored gravity force for minimum compression (including earthquake) is:

$P_u = 0.81(506) - 17.6 = 387$ kips

Before proceeding with the flexural strength calculations, first determine whether or not slenderness effects need to be considered. For a frame that is unbraced against sideway, ACI 318 Section 6.2.5 allows slenderness effects to be neglected where $kl_u/r < 22$. For a 28- by 28-inch column with a clear unbraced length, $l_u = 126$ inches, $r = 0.3(28) = 8.4$ inches (ACI 318 Sec. 6.2.5.1) and $l_u/r = 126/8.4 = 15.0$. Therefore, as long as the effective length factor k for this column is less than $22/15.0 = 1.47$, then slenderness effects can be ignored. It is reasonable to assume that k is less than 1.47 and this can be confirmed using the commentary to ACI 318 Section 6.2.5.

Continuing with the design, an axial-flexural interaction diagram for a 28- by 28-inch column with 12 #8 bars ($\rho = 0.0121$) is shown in Figure 10-35. The column clearly has the strength to support the applied loads (represented as solid dots in the figure).
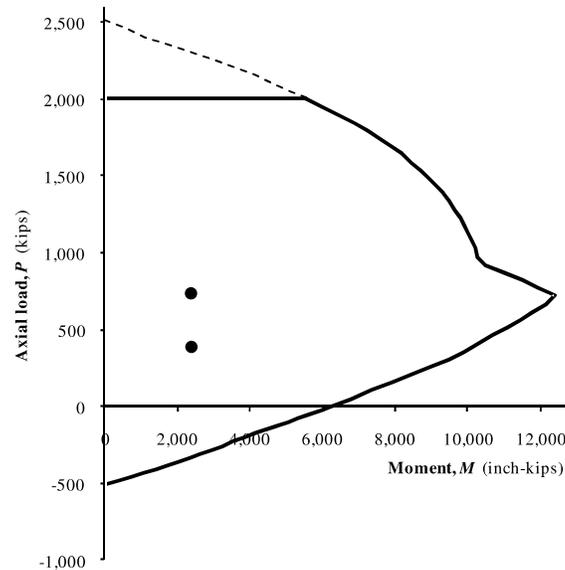
Figure 10-35 Interaction diagram for column
(1.0 kip = 4.45kN, 1.0 ft-kip = 1.36 kN-m)

10.6.2.3.2 Transverse Reinforcement. The design earthquake shear for columns in determined in accordance with ACI 318 Section 18.4.3.1 as the lesser of the shear associated with the development of the beam nominal moment strength or the shear from analysis times Ω_0. Assuming Ω_0 times the shear from analysis will produce the smaller design shear, the ETABS analysis indicates that the shear force is 34.4 kips and the design shear is 3(34.4) = 103.2 kips.

The concrete supplies a capacity of:

$$\phi V_c = 0.75(2\sqrt{5,000}(28)(25.6)) = 76.0 \text{ kips } < 103.2 \text{ kips}$$

Therefore, steel reinforcement is required for strength. First, however, determine the detailing requirements for transverse reinforcement in intermediate moment frame columns in accordance ACI 318 Section 18.4.3.

Within a region l_o from the face of the support, the tie spacing must not exceed:

$8d_b = 8(1.0) = 8.0$ inches (using #8 longitudinal bars)
$24d_{tie} = 24 (0.5) = 12.0$ inches (using #4 ties)
1/2 the smallest dimension of the frame member = 28/2 = 14 inches
12 inches

The 8-inch maximum spacing controls. Ties at this spacing are required over a length l_o of:

1/6 clearspan of column = 126/6 = 21 inches

Maximum cross section dimension = 28 inches
18 inches

Given the above, try a four-legged #4 tie spaced at 8 inches over a depth of 28 inches. The top and bottom ties will be provided at 4 inches from the beam soffit and floor slab.

Beyond the end regions, ACI 318 Section 18.4.3.5 requires that tie spacing satisfy ACI 318 Sections 10.7.6.5.2, which requires ties at $d/2$ maximum spacing. Therefore, consider a 12-inch maximum tie spacing in the middle region of the column.

Next, determine the shear reinforcing required for strength. Since contribution of concrete is 76.0 kips, the required contribution of the shear reinforcing is:

$$V_s = \frac{V_u - \phi V_c}{\phi} = \frac{102.3 - 0.75(76.0)}{0.75} = 36.3 \, \text{kips}$$

Using #4 ties with four legs and d = 28 – 1.5 – 0.5 – 0.5 = 25.5 inches,

$$V_s = \frac{4(0.4)(60)(25.5)}{12} = 102 \, \text{kips} > 36.3 \, \text{kips}$$

The layout of the transverse reinforcing for the subject column is shown in Figure 10-36
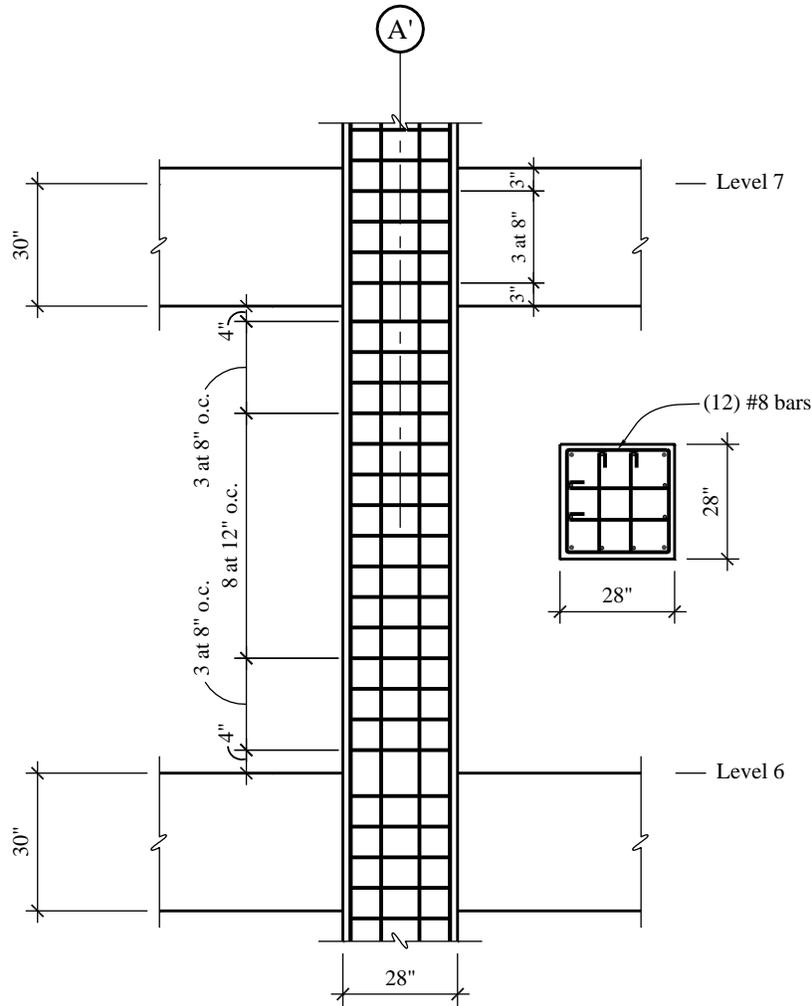
Figure 10-36 Column reinforcement
(1.0 in. = 25.4 mm)

10.6.2.4 Design of Beam-Column Joint. Joint reinforcement for intermediate moment frames is addressed in ACI 318 Section 18.4.4.1, which refers to ACI 318 Chapter 15. ACI 318 Section 15.4 requires that all beam-column connections have a minimum amount of transverse reinforcement through the beam-column joints. The only exception is in non-seismic frames where the column is confined on all four sides by beams framing into the column. The amount of reinforcement required is given by ACI 318 Section 15.4.2:

$$A_{v,\min} = 0.75\sqrt{f_c'}\,\frac{b_w s}{f_{yt}}$$

This is the same equation used to proportion minimum transverse reinforcement in beams. Assuming A_v is supplied by four #4 ties and $f_y = 60$ ksi:

$$s = \frac{4(0.2)(60,000)}{0.75\sqrt{5,000}(28)} = 32.4 \text{ inches}$$

This essentially permits no ties to be located in the joint. Since it is good practice to provide transverse reinforcing in moment frame joints, ties will be provided at the same 8-inch spacing as at the ends of the columns. The arrangement of ties within the beam-column joint is shown in Figure 10-36.

<div style="text-align: right;">**11**</div>

Precast Concrete Design

S. K. Ghosh, PhD

Originally developed by
Suzanne Dow Nakaki, S.E., Gene R. Stevens, P.E., and James Robert Harris, P.E., PhD

Contents

This chapter illustrates the seismic design of precast concrete members using the *NEHRP Recommended Provisions* (referred to herein as the *Provisions*) for buildings in several different seismic design categories. The 2015 *Provisions* adopts the seismic design requirements of ASCE 7-10 (referred to herein as the *Standard*) and makes a small number of modifications to them in Part 1 of the *Provisions*. In the 2015 *Provisions,* there are significant new developments with regard to diaphragms – see Chapter 6 of this volume of design examples. Part 1 of the 2015 *Provisions* adds a Section 12.10.3 to ASCE 7-16,[2] which provides a diaphragm design force level that is different from the design force level of Sections 12.10.1 and 12.10.2. The alternative design force level of Section 12.10.3 is mandatory for precast concrete diaphragms in buildings assigned to SDC C, D, E, or F and is permitted for other precast concrete diaphragms, cast-in-place concrete diaphragms, and wood diaphragms. Part 1 of the 2015 *Provisions* also adds a precast diaphragm design procedure including a connector qualification protocol to ASCE 7-16 Section 14.2. In addition to the requirements for reinforced concrete set forth in ASCE 7-16 and Section 18.12 of ACI 318-14, design, detailing and construction of diaphragms constructed with precast concrete components in SDC C, D, E, and F, or in SDC B and using the requirements of ASCE 7-16 Section 12.11, must conform to the requirements of this section.

ASCE 7-16 Chapter 14 adopts ACI 318-14 for concrete design and construction. ACI 318-14, as modified by ASCE 7-16 Section 14.2, sets forth the following requirements for precast concrete structural systems.

> Precast seismic systems used in structures assigned to Seismic Design Category C must be intermediate or special moment frames, or intermediate precast or special structural walls.

> Precast seismic systems used in structures assigned to Seismic Design Category D must be special moment frames, or intermediate precast (up to 40 feet) or special structural walls.

> Precast seismic systems used in structures assigned to Seismic Design Category E or F must be special moment frames or special structural walls.

> Prestress provided by prestressing steel resisting earthquake-induced flexural and axial loads in beams of special moment frames must be limited to 500 psi or $f'_c/10$ in plastic hinge regions (ACI 318 Section 18.6.3.5).

> An ordinary precast structural wall is defined as one that satisfies ACI 318 Chapters 1-13, 15, 16, and 19 through 26.

> An intermediate precast structural wall must meet additional requirements for its connections beyond those defined in ACI 318 Section 18.5. These are given in Section 14.2.2.4 of ASCE 7-16.

> ▪ A special structural wall constructed using precast concrete must satisfy ACI 318 Section 18.10 and 18.5.2. In other words, it must meet the requirements of a special cast-in-place concrete shear wall and an intermediate precast shear wall at the same time. Special shear walls constructed using precast concrete and unbonded post-tensioning tendons and not satisfying the above requirements are permitted, provided they satisfy the requirements of ACI ITG-5.1 *Acceptance Criteria for Special Unbonded Post-Tensioned Precast Structural Walls Based on Validation Testing.*

---

[2] The 2015 NEHRP modifications are to ASCE 7-10, but they have been approved for inclusion in ASCE 7-16. So ASCE 7-16 section numbers are used here.

Examples are provided for the following concepts:

The example in Section 11.1 illustrates the design of untopped and topped precast concrete floor and roof diaphragms of the five-story masonry buildings described in Section 13.2 of this volume of design examples. The two untopped precast concrete diaphragms of Section 11.1.1 show the requirements for Seismic Design Categories B and C using 8-inch-thick hollow core precast, prestressed concrete planks. Section 11.1.2 shows the requirements for the same precast planks with a 2-1/2-inch-thick composite lightweight concrete topping serving as diaphragms for the same five-story masonry building of Section 13.2, now assigned to Seismic Design Category D . Untopped diaphragms are commonly used in regions of low seismic hazard.. Untopped precast concrete diaphragms in high-seismic applications have been discussed in (Cleland and Ghosh, 2002).

The example in Section 11.2 illustrates the design of an intermediate precast concrete shear wall building in a region of low or moderate seismicity, which is where many precast concrete seismic force-resisting systems are constructed. The precast concrete walls in this example resist the seismic forces for a three-story office building assigned to Seismic Design Category B. ACI 318 requires that in connections that are expected to yield, the yielding be restricted to steel elements or reinforcement. The *Standard* also requires that connections that are designed to yield be capable of maintaining 80% of their design strength at the deformation induced by the design displacement, as defined in ACI 318, unless Type 2 mechanical splices are used.

The example in Section 11.3 illustrates the design of a special precast concrete shear wall for a single-story industrial warehouse building in a region of high seismicity. For buildings assigned to Seismic Design Category D, the *Standard* requires that the precast seismic force-resisting system be designed and detailed to meet the requirements for either an intermediate (permitted only up to a height limit of 40 feet) or a special precast concrete structural wall.

The example in Section 11.4 is a partial example for the design of a special moment frame constructed using precast concrete per ACI 318 Section 18.9. Concepts for ductile and strong connections are presented and a detailed description of the calculations for a strong connection located at the beam-column interface is presented.

Tilt-up concrete wall buildings in all seismic zones have long been designed using the precast wall panels as concrete shear walls for the seismic force-resisting system. Such designs usually have been performed using design force coefficients and strength limits as if the precast walls emulated the performance of cast-in-place reinforced concrete shear walls, which they usually do not. Tilt-up buildings assigned to Seismic Design Category C or higher should be designed and detailed as intermediate or special precast structural wall systems as defined in ACI 318. Also see Resource Paper 5, *One-Story, Flexible Diaphragm Buildings with Stiff Vertical Elements*, in the 2015 NEHRP *Provisions* and FEMA Publication P-1026.

In addition to the *Provisions*, the following documents are either referred to directly or are useful design aids for precast concrete construction:

ACI 318   American Concrete Institute. 2014. *Building Code Requirements for Structural Concrete*.

ACI 374.1   American Concrete Institute. 2005. *Acceptance Criteria for Moment Frames based on Structural Testing*.

ACI ITG-5.1   American Concrete Institute. 2007. *Acceptance Criteria for Special Unbonded Post-Tensioned Precast Structural Walls Based on Validation Testing*.

AISC 360	American Institute of Steel Construction. 2010. *Specification for Structural Steel Buildings*.
AISC Manual	American Institute of Steel Construction. 2010. *Manual of Steel Construction,* Thirteen Edition.
Cleland and Ghosh	Cleland, N. M., and Ghosh, S. K. 2002. "Untopped Precast Concrete Diaphragms in High-Seismic Applications." *PCI Journal*, Vol. 47, No.6, (November – December).
FEMA P-1026	Federal Emergency Management Agency. 2015. *Seismic Design of Rigid Wall – Flexible Diaphragm Buildings: An Alternate Procedure*.
Moustafa	Moustafa, Saad E. 1981 and 1982. "Effectiveness of Shear-Friction Reinforcement in Shear Diaphragm Capacity of Hollow-Core Slabs." *PCI Journal*, Vol. 26, No. 1 (January - February, 1981) and the discussion contained in *PCI Journal*, Vol. 27, No. 3 (May-June, 1982).
PCI Handbook	Precast/Prestressed Concrete Institute. 2010. *PCI Design Handbook,* Seventh Edition.
PCI Details	Precast/Prestressed Concrete Institute. 1988. *Design and Typical Details of Connections for Precast and Prestressed Concrete,* Second Edition.
PCI Connections	Precast/Prestressed Concrete Institute. 2008.PCI Connections Manual for Precast & Prestressed Concrete Construction, 1st Edition
PCI Seismic Connections	Precast/Prestressed Concrete Institute. 1986.Design of Connections for precast prestressed concrete buildings for the Effects of Earthquake
PCI Hollow Core	PCI Hollow Core Precast/Prestressed Concrete Institute. 1998. *Manual for the Design of Hollow Core Slabs*, 2nd Edition.

11.1 HORIZONTAL DIAPHRAGMS

Structural diaphragms are horizontal or nearly horizontal elements, such as floor and roof slabs, that transfer seismic inertial forces to the vertical elements of the seismic force-resisting system. Precast concrete diaphragms may be constructed using topped or untopped precast elements depending on the Seismic Design Category. Reinforced concrete diaphragms constructed using untopped precast concrete elements are not addressed explicitly in the *Standard*, in the *Provisions*, or in ACI 318. Topped precast concrete diaphragms, which act compositely or noncompositely for gravity loads, are designed using the requirements of ACI 318 Section 18.12.

11.1.1 Untopped Precast Concrete Units for Five-Story Masonry Buildings Assigned to Seismic Design Categories B and C

This example illustrates floor and roof diaphragm design for five-story masonry buildings in Seismic Design Category B and in Seismic Design Category C on soft rock. The example in Section 13.2 provides design parameters used here. The floors and roofs of these buildings are to be untopped 8-inch-thick hollow-core precast, prestressed concrete plank. Figure 13.2-1 shows the typical floor plan of the diaphragms.

11.1.1.1 General Design Requirements. In accordance with ACI 318, untopped precast diaphragms are permitted only in Seismic Design Categories A through C. Static rational models are used to determine shears and moments on joints as well as shear and tension/compression forces on connections. Dynamic modeling of seismic response is not required. Per ACI 318 Section 18.2.1.5, diaphragms in Seismic Design Categories D through F are required to meet ACI 318 Section 18.12, which does not allow untopped diaphragms. A relevant publication on this topic is (Cleland and Ghosh, 2002). In the 2003 *Provisions*, an appendix provided a framework for the design of untopped diaphragms in higher Seismic Design Categories, in which diaphragms with untopped precast elements were designed to remain elastic and connections were designed for limited ductility. However, in the 2009 *Provisions*, that appendix was discontinued. Instead, a Resource Paper describing emerging procedures for the design of such diaphragms was included in Part 3 of the *Provisions*.

The difficulty of evaluation of precast concrete diaphragms is the jointed nature of the construction. With hollow core slabs, mechanical connections using plate anchorage and welded plates is not practical because the components are most commonly made by an extrusion process. Diaphragm connections in untopped floors are limited to reinforcement in joints, or in cores that are broken open so the bars can be grouted in. When planks intersect with orthogonal orientation, as occurs in the example building layout, it may be necessary to break the top of a plank so that reinforcing with hooks can be placed and grouted in to match joints in the intersecting planks.

Reference should now be made to Section 6.5, which provides a step-by-step guide to the seismic design of precast concrete diaphragms. For the SDC C example below, the Diaphragm Seismic Demand Level is Low. So all diaphragm design options are allowed; the Basic Design Option (BDO) is chosen. The issue of connector deformability is moot, because there are no connectors involved. $R_s = 1$; therefore, the shear overstrength factor is $1.4R_s = 1.4$.

For the SDC D example, the Reduced Design Option (RDO) is chosen, $R_s = 1.4$ and the shear overstrength factor is $1.4R_s = 2.0$.

The design method used here follows Moustafa (1981 and 1982) and makes use of the shear friction provisions of ACI 318 with the friction coefficient, μ, being equal to 1.0. To use $\mu = 1.0$, ACI 318 requires grout or concrete placed against hardened concrete that has clean, laitance-free, and intentionally roughened surfaces with a total amplitude of approximately 1/4 inch (peak to valley). Roughness for formed edges is provided either by sawtooth keys along the length of the plank or by hand-roughening with chipping hammers. Details from the PCI Hollow Core Manual are used to develop the connection details. Note that grouted joints with edges not intentionally roughened can be used with $\mu = 0.6$.

The terminology used is defined in ACI 318 Section 2.3.

11.1.1.2 In-Plane Seismic Design Forces for Untopped Diaphragms. For precast concrete diaphragms including chords and collector in structures assigned to SDC C through F, *Standard* Section 12.10.3 defines the diaphragm seismic design force.

All other diaphragms and their chords and collectors can be designed for the seismic design forces given in *Standard* Sections 12.10.1 and 12.10.2 or Section 12.10.3, except that Section 12. 10.3 does not apply to the design of steel deck diaphragms.

When designing by *Standard* Sections 12.10.1 and 12.10.2, for Seismic Design Categories C through F, *Standard* Section 12.10.2.1 requires that collector elements, collector splices and collector connections to the vertical seismic force-resisting members be designed in accordance with *Standard* Section 12.4.3, which amplifies design forces by the overstrength factor, Ω_o. When designing by *Standard* Section 12.10.3, the

same forces are required to be amplified by a factor of 1.5, with three exceptions (*Standard* Section 12.10.3.4).

When designing by *Standard* Sections 12.10.1 and 12.10.2, *Standard* Section 12.10.1.1 requires that the overstrength factor, Ω_o, be used only on transfer forces where the vertical seismic force-resisting system is offset and the diaphragm is required to transfer forces between vertical seismic force-resisting elements above and below the diaphragm; it need not be applied to inertial forces given by *Standard* Equations 12.10-1 through 12.10-3. When designing by *Standard* Sections 12.10.3, the requirement is the same, except that the inertial forces are now given by Equations (12.10.3-1) and (12.10.3-2). Parameters from the example in Section 13.2 used to calculate in-plane seismic design forces for the diaphragms are provided in Table 11.1-1.

Table 11.1-1 Design Parameters from Example 13.2

Design Parameter	SDC B	SDC C
Ω_o	2.5	2.5
C_s	0.105	0.106
w_i (roof)	861 kips	869 kips
w_i (floor)	963 kips	978 kips
S_{DS}	0.21	0.37
S_{D1}	0.12	0.15
I_e	1.0	1.0
SDC	B	C

1.0 kip = 4.45 kN.

11.1.1.3 Diaphragm Forces for Building in SDC B. The weight tributary to the roof and floor diaphragms (w_{px}) is the total story weight (w_i) at Level i minus the weight of the walls parallel to the direction of loading.

Compute diaphragm weight (w_{px}) for the roof and floor as follows:

Roof:

Total weight	=	861 kips
Walls parallel to force = (45 psf)(277 ft)(8.67 ft / 2)	=	-54 kips
w_{px}	=	807 kips

Floors:

Total weight	=	963 kips
Walls parallel to force = (45 psf)(277 ft)(8.67 ft)	=	-108 kips
w_{px}	=	855 kips

Since the building is assigned to SDC B, the diaphragm design forces are permitted to be determined from the provisions of *Standard* Sections 12.10.1 and 12.10.2, or Section 12.10.3. Both calculations are shown below for comparison purposes.

A. Computation of diaphragm forces in accordance with *Standard* Sections 12.10.1 and 12.10.2:

From Equation 12.10-1,

$$F_{px} = \frac{\sum_{i=x}^{n} F_i}{\sum_{i=x}^{n} w_i} w_{px}$$

Calculations for F_{px} are provided in Table 11.1-2A.

Table 11.1-2A F_{px} Calculations for Building in SDC B

Level	w_i (kips)	$\sum_{i=x}^{n} w_i$ (kips)	F_i (kips)	$\sum_{i=x}^{n} F_i = V_i$ (kips)	w_{px} (kips)	F_{px} (kips)
Roof	861	861	175	175	807	164
4	963	1,824	156	331	855	155
3	963	2,787	117	448	855	137
2	963	3,750	78	526	855	120
1	963	4,713	39	565	855	103

1.0 kip = 4.45 kN.

The values for F_i and V_i used in Table 11.1-2A are listed in Table 13.2-2.

The minimum value of $F_{px} = 0.2S_{DS}I_e w_{px}$ 　　　$= 0.2(0.21)1.0(807 \text{ kips})$ 　　　$= 33.9$ kips (roof)
　　　　　　　　　　　　　　　　　　　　　　　$= 0.2(0.21)1.0(855 \text{ kips})$ 　　　$= 35.9$ kips (floors)

The maximum value of $F_{px} = 0.4S_{DS}I_e w_{px}$ 　　　$= 2(33.9 \text{ kips})$ 　　　$= 67.8$ kips (roof)
　　　　　　　　　　　　　　　　　　　　　　　$= 2(35.9 \text{ kips})$ 　　　$= 71.8$ kips (floors)

Note that the calculated F_{px} in Table 11.1-2A is substantially larger than the specified maximum limit value of F_{px}. This is generally true at upper levels if the R-factor is less than 5.

To simplify the design, the diaphragm design force used for all levels will be the maximum force at any level, 72 kips.

B. Computation of diaphragm forces in accordance with *Standard* Section 12.10.3:

Step 1: Determine R_s, Diaphragm Design Force Reduction Factor (*Standard* Table 12.10.3.5-1)

ASCE 7-16 Table 12.10.3.5-1 Diaphragm design force reduction factor, R_s

Diaphragm System		Shear-Controlled[a]	Flexure-Controlled[a]
Cast-in-place concrete designed in accordance with Section 14.2 and ACI 318	-	1.5	2
Precast concrete designed in accordance with Section 14.2.4 and ACI 318	EDO[1, b]	0.7	0.7
	BDO[2, b]	1.0	1.0
	RDO[3, b]	1.4	1.4
Wood sheathed designed in accordance with Section 14.5 and AF&PA (now AWC) Special Design Provisions for Wind and Seismic	-	3.0	NA

[1] EDO is precast concrete diaphragm Elastic Design Option.
[2] BDO is precast concrete diaphragm Basic Design Option.
[3] RDO is precast concrete diaphragm Reduced Design Option.
[a] Flexure-controlled and Shear-controlled diaphragms are defined in ASCE 7-16 Section 11.2.
[b] Elastic, basic, and reduced design options are defined in ASCE 7-16 Section 11.2.

The Basic Design Option (BDO) is adopted in the design of this precast diaphragm. As a result, $R_s = 1.0$.

Step 2: Determine C_{px}, Diaphragm Design Acceleration (Force) Coefficient at Level x (*Standard* Section 12.10.3.2)

In order to determine C_{px}, three parameters - C_{p0}, C_{pi}, and C_{pn}, need to be determined first.

$$C_{p0} = 0.4 S_{DS} I_e = 0.4 \times 0.21 \times 1.0 = 0.084$$

C_{pi} is the greater of the values given by:

$$C_{pi} = C_{p0} = 0.084, \text{ and}$$

$$C_{pi} = 0.9 \Gamma_{m1} \Omega_0 C_s$$

where:

Γ_{m1} is first mode contribution factor

$$\Gamma_{m1} = 1 + 0.5 z_s \left(1 - \frac{1}{N}\right)$$

where z_s = modal contribution coefficient modifier dependent on seismic force-resisting system (see Table below).

Modal Contribution Coefficient Modifier, z_s

Description	z_s - value
Buildings designed with Buckling Restrained Braced Frame systems defined in Table 12.2-1	0.30
Buildings designed with Moment-Resisting Frame systems defined in Table 12.2-1	0.70
Buildings designed with Dual Systems defined in Table 12.2-1 with Special or Intermediate Moment Frames capable of resisting at least 25% of the prescribed seismic forces	0.85
Buildings designed with all other seismic force-resisting systems	1.00

The building being designed consists of bearing wall system of reinforced masonry. As a result,

$$z_s = 1.00$$

$$\Gamma_{m1} = 1 + 0.5 z_s \left(1 - \frac{1}{N}\right) = 1 + 0.5 \times 1.00 \times \left(1 - \frac{1}{5}\right) = 1.4$$

$C_{pi} = 0.9 \Gamma m1\, \Omega_0\, Cs = 0.9 \times 1.4 \times 2.5 \times 0.105 = 0.331$ Governs

$$C_{pn} = \sqrt{(\Gamma_{m1}\Omega_0 C_s)^2 + (\Gamma_{m2} C_{s2})^2}$$

where:

Γ_{m2} is higher mode contribution factor

$$\Gamma_{m2} = 0.9 z_s \left(1 - \frac{1}{N}\right)^2 = 0.9 \times 1.00 \times \left(1 - \frac{1}{5}\right)^2 = 0.576$$

C_{s2} is higher mode seismic response coefficient. C_{s2} is the smallest of the values given by
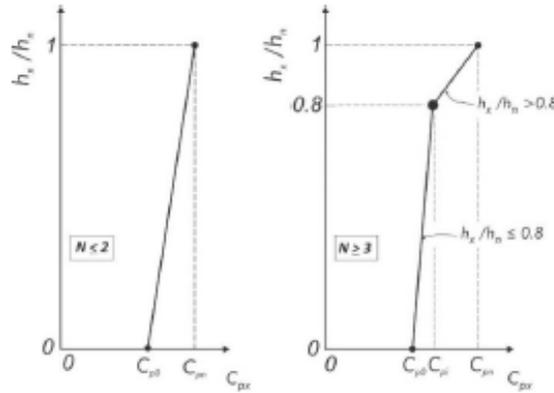
$$C_{s2} = (0.15 N + 0.25) I_e S_{DS} = (0.15 \times 5 + 0.25) \times 1.0 \times 0.21 = 0.21 \quad \text{Governs}$$

$$C_{s2} = I_e S_{DS} = 1.0 \times 0.21 = 0.21 \quad \text{Governs}$$

$$C_{s2} = \frac{I_e S_{D1}}{0.03(N-1)} = \frac{1.0 \times 0.12}{0.03(5-1)} = 1.00 \quad \text{For } N \geq 2$$

$$C_{pn} = \sqrt{(\Gamma_{m1}\Omega_0 C_s)^2 + (\Gamma_{m2} C_{s2})^2} = 0.387$$

Using *Standard* Figure 12.10.3-1, C_{px} is determined at various floor levels, as shown in Table 11.1-2B

ASCE 7-16 Figure 12.10.3-1 Calculating the design acceleration coefficient
C_{px} in buildings with $N \leq 2$ and in buildings with $N \geq 3$

Step 3: Determine F_{px}, Diaphragm Design Force at Level x

$$F_{px} = \frac{C_{px}}{R_s} w_{px} \geq 0.2 S_{DS} I_e w_{px}$$

Table 11.1-2B F_{px} Calculations for Building in SDC B

Level	h_x (ft)	w_{px} (kips)	C_{px}	F_{px} (kips)
Roof	43.34	807	0.39	312
4	34.67	855	0.33	283
3	26.00	855	0.27	230
2	17.33	855	0.21	177
1	8.67	855	0.15	125

1.0 kip = 4.45 kN.

The minimum value of $F_{px} = 0.2 S_{DS} I_e w_{px}$ = 0.2(0.21)1.0(807 kips) = 33.90 kips (roof)
= 0.2(0.21)1.0(855 kips) = 35.90 kips (floors)

11.1.1.4 Diaphragm Design Forces for Building Assigned to SDC C. The weight tributary to the roof and floor diaphragms (w_{px}) is the total story weight (w_i) at Level i minus the weight of the walls parallel to the force.

Compute diaphragm weight (w_{px}) for the roof and floor as follows:

Roof:

Total weight = 870 kips
Walls parallel to force = (48 psf)(277 ft)(8.67 ft / 2) = -58 kips
w_{px} = 812 kips

Floors:

Total weight	=	978 kips
Walls parallel to force = (48 psf)(277 ft)(8.67 ft)	=	-115 kips
w_{px}	=	863 kips

Since the building is assigned to SDC C, the precast concrete diaphragm design forces are required to be determined by the provisions of *Standard* Section 12.10.3.

Step 1: Determine R_s, Diaphragm Design Force Reduction Factor (*Standard* Table 12.10.3.5-1)

The Basic Design Option (BDO) is adopted in the design of this precast diaphragm. As a result, $R_s = 1.0$.

Step 2: Determine C_{px}, Diaphragm Design Acceleration (Force) Coefficient at Level x (*Standard* Section 12.10.3.2)

In order to determine C_{px}, three parameters - C_{p0}, C_{pi}, and C_{pn}, need to first be determined.

$C_{p0} = 0.4S_{DS}I_e = 0.4 \times 0.37 \times 1.0 = 0.148$

C_{pi} is the greater of the values given by:

$C_{pi} = C_{p0} = 0.148$, and

$C_{pi} = 0.9\Gamma_{m1} \Omega_0 C_s$

where:

Γ_{m1} is first mode contribution factor

$$\Gamma_{m1} = 1 + 0.5z_s\left(1 - \frac{1}{N}\right)$$

where z_s = modal contribution coefficient modifier dependent on seismic force-resisting system.

The building being designed consists of bearing wall system of reinforced masonry. As a result,

$z_s = 1.00$

$$\Gamma_{m1} = 1 + 0.5z_s\left(1 - \frac{1}{N}\right) = 1 + 0.5 \times 1.00 \times \left(1 - \frac{1}{5}\right) = 1.4$$

$C_{pi} = 0.9\Gamma_{m1} \Omega_0 C_s = 0.9 \times 1.4 \times 2.5 \times 0.106 = 0.334$ Governs

$$C_{pn} = \sqrt{\left(\Gamma_{m1}\Omega_0 C_s\right)^2 + \left(\Gamma_{m2}C_{s2}\right)^2}$$

where:

Γ_{m2} is higher mode contribution factor

11-11

$$\Gamma_{m2} = 0.9 z_s \left(1 - \frac{1}{N}\right)^2 = 0.9 \times 1.00 \times \left(1 - \frac{1}{5}\right)^2 = 0.576$$

C_{s2} is higher mode seismic response coefficient. C_{s2} is the smallest of the values given by

$$C_{s2} = (0.15N + 0.25)I_e S_{DS} = (0.15 \times 5 + 0.25) \times 1.0 \times 0.37 = 0.37 \quad \text{Governs}$$

$$C_{s2} = I_e S_{DS} = 1.0 \times 0.37 = 0.37 \quad \text{Governs}$$

$$C_{s2} = \frac{I_e S_{D1}}{0.03(N-1)} = \frac{1.0 \times 0.15}{0.03(5-1)} = 1.25 \quad \text{For } N \geq 2$$

$$C_{s2} = 0 \quad \text{For } N = 1$$

$$C_{pn} = \sqrt{(\Gamma_{m1} \Omega_0 C_s)^2 + (\Gamma_{m2} C_{s2})^2} = 0.428$$

Using *Standard* Figure 12.10.3-1, C_{px} is determined at various floor levels, as shown in Table 11.1-3

Step 3: Determine F_{px}, Diaphragm Design Force at Level x

$$F_{px} = \frac{C_{px}}{R_s} w_{px} \geq 0.2 S_{DS} I_e w_{px}$$

Table 11.1-3 F_{px} Calculations for Building in SDC C

Level	h_x (ft)	w_{px} (kips)	C_{px}	F_{px} (kips)
Roof	43.34	812	0.43	347
4	34.67	863	0.33	288
3	26.00	863	0.29	248
2	17.33	863	0.24	208
1	8.67	863	0.19	168

1.0 kip = 4.45 kN.

The minimum value of $F_{px} = 0.2 S_{DS} I_e w_{px}$ $\quad = 0.2(0.37)1.0(812 \text{ kips}) \quad = 60.10 \text{ kips (roof)}$
$\quad = 0.2(0.37)1.0(863 \text{ kips}) \quad = 63.90 \text{ kips (floors)}$

11.1.1.5 Static Analysis of Diaphragms. The balance of this example will use the controlling diaphragm seismic design force of 347 kips for the building in SDC C.

The joints in the floor plan for this example include longitudinal joints between adjacent planks, located in the two orthogonal directions, transverse joints between the ends of planks, transverse joint between the ends of planks at masonry walls, end joints at masonry wall bearings, and joints at the intersection of longitudinal and transverse planks at masonry walls. Force demands for loads crossing or within these joints include chord forces, shear friction forces, and integrity tie forces. ACI 318 does not recognize dowel

behavior of reinforcement embedded in concrete nor friction in grouted joints without shear friction tension strength. The steel requirements for friction transfer come only from shear friction calculations. The shear transfer, however, is actually through the grout in the longitudinal joint.

A common approach to diaphragm design is to consider the horizontal plane of the floor as a beam, and to calculate force and moment demands on joints based on their locations within that beam. This is the approach followed here. The beam analogy may, however, miss deep beam effects, the effects of service core (stair and elevator) voids, and the discontinuities created by the joints. Finite element analysis of the diaphragm using continuous plate elements can be used to capture the deep beam and interior void effects, but the effects of load transfer across joints are not identified by this approach.

In the transverse direction, the diaphragm seismic design force of 347 kips will be distributed as shown in Figure 11.1-1.
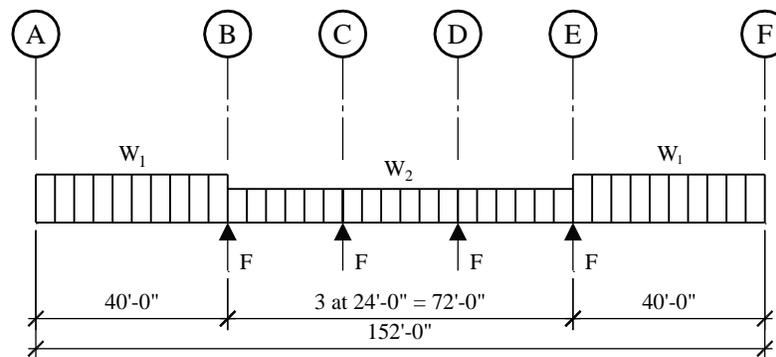
Figure 11.1-1 Diaphragm force distribution and analytical model
(1.0 ft = 0.3048 m)

The *Standard* requires that structural analysis consider the relative stiffness of the diaphragms and the vertical elements of the seismic force-resisting system. Since a pretopped precast diaphragm doesn't satisfy the conditions of either the flexible or the rigid diaphragm conditions identified in the *Standard*, maximum in-plane deflections of the diaphragm must be evaluated. However, that analysis is beyond the scope of this document. Therefore, with a rigid diaphragm assumption, assuming the four shear walls have the same stiffness and ignoring torsion, the diaphragm reactions at the transverse shear walls (*F* as shown in Figure 11.1-1) are computed as follows:

F = 347 kips/4 = 86.8 kips

The uniform diaphragm demands are proportional to the distributed weights of the diaphragm in different areas (see Figure 11.1-1).

W_1 = [67 psf (72 ft) + 48 psf (8.67 ft)4](347 kips / 863 kips) = 2,610 lb/ft

W_2 = [67 psf (72 ft)](347 kips / 863 kips) = 1,940 lb/ft

Figure 11.1-2 identifies critical regions of the diaphragm to be considered in this design. These regions are:

Joint 1: Maximum transverse shear parallel to the panels at panel-to-panel joints

Joint 2: Maximum transverse shear parallel to the panels at the panel-to-wall joint

Joint 3: Maximum transverse moment and chord force

Joint 4: Maximum longitudinal shear perpendicular to the panels at the panel-to-wall connection (exterior longitudinal walls) and anchorage of exterior masonry wall to the diaphragm for out-of-plane forces

Joint 5: Collector element and shear for the interior longitudinal walls
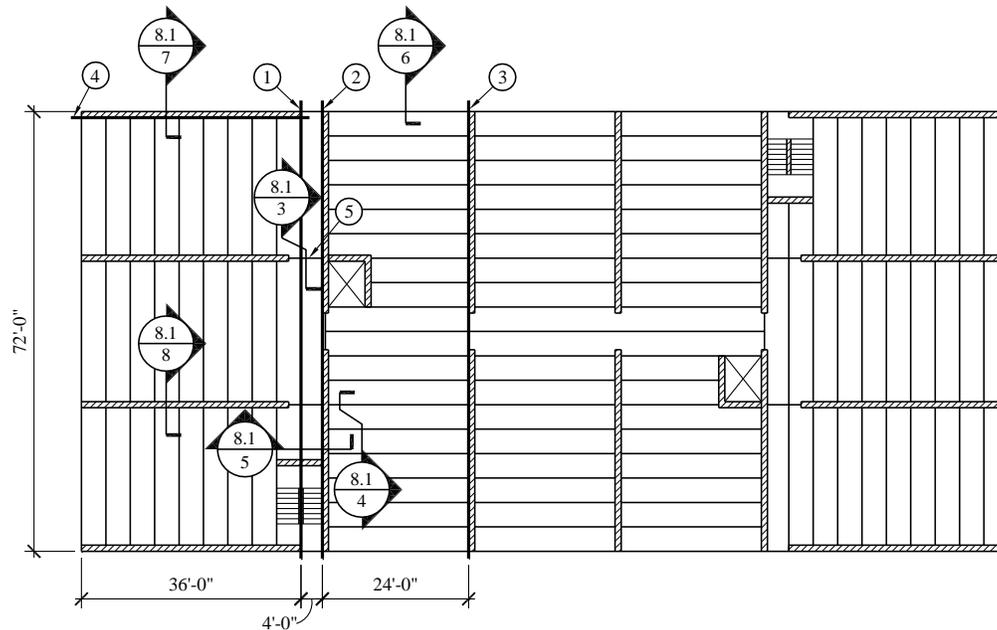
Figure 11.1-2 Diaphragm plan and critical design regions
(1.0 ft = 0.3048 m)

Joint forces are determined as shown below. Since the building is assigned to SDC C, collector elements will be designed for 1.5 times the diaphragm force per *Standard* Section 12.10.3.4.

Joint 1 – Transverse forces:

Shear, V_{u1} = 2.61 kips/ft (36 ft) = 94 kips
Moment, M_{u1} = 94 kips (36 ft / 2) = 1692 ft-kips
Chord tension force, T_{u1} = M/d = 1692 ft-kips / 71 ft = 23.8 kips

Joint 2 – Transverse forces:

Shear, V_{u2} = 2.61 kips/ft (40 ft) = 104.4 kips
Moment, M_{u2} = 104.4 kips (40 ft / 2) = 2088 ft-kips
Chord tension force, T_{u2} = M/d = 2088 ft-kips / 71 ft = 29.4 kips

Joint 3 – Transverse forces:

Shear, V_{u3} = 104.4 kips + 1.94 kips/ft (24 ft) – 86.8 kips = 64.2 kips
11-14

Moment, $M_{u3} = 104.4$ kips (44 ft) + 46.6 kips (12 ft) - 86.8 kips (24 ft) = 3070 ft-kips
Chord tension force, $T_{u3} = M/d = 3070$ ft-kips / 71 ft = 43.2 kips

Joint 4 – Longitudinal forces:

Wall force, $F = 347$ kips / 8 = 43.4 kips
Wall shear along wall length, $V_{u4} = 43.4$ kips (36 ft)/(152 ft /2) = 20.6 kips
Design collector force at wall end, $1.5T_{u4} = 1.5C_{u4} = 1.5(43.4$ kips - 20.6) kips = 34.2 kips

Joint 4 – Out-of-plane forces:

The *Standard* has several requirements for out-of-plane forces. None are unique to precast diaphragms and all are less than the requirements in ACI 318 for precast construction regardless of seismic considerations. Assuming the planks are similar to beams and comply with the minimum requirements of *Standard* Section 1.4.4, the required out-of-plane horizontal force is:

$0.05(D+L)_{plank} = 0.05(67$ psf + 40 psf)(24 ft / 2) = 64.2 plf

According to *Standard* Section 12.11.2.1 (Seismic Design Category B and greater), structural wall anchorage must be designed for a force computed as:

$F_p = 0.4(S_{DS})(k_a)(I_e)(W_{wall}) = 0.4(0.37)(1.0)(1.0)$ [(48 psf)(8.67 ft)] = 61.6 plf

where

$k_a = 1.0 + L_f/100 = 1.0$ for rigid diaphragms

Due to its geometry, this diaphragm is likely to be classified as rigid. However, the relative deformations of the wall and diaphragm must be checked in accordance with *Standard* Section 12.3.1.3 to validate this assumption.

The force requirements in ACI 318 Section 16.2.1.8 will be described later.

Joint 5 – Longitudinal forces:

Wall force, $F = 347$ kips / 8 = 43.4 kips
Wall shear along each side of wall, $V_{u5} = 43.4$ kips [2(36 ft) / 152 ft]/2 = 10.3 kips
Design collector force at wall end, $1.5T_{u5} = 1.5C_{u5} = 1.5[43.4$ kips - 2(10.3 kips)] = 34.2 kips

Joint 5 – Shear flow due to transverse forces:

Shear at Joint 2, $V_{u2} = 104.4$ kips
$Q = A\ d$
  $A = (0.67$ ft) (24 ft) = 16 ft^2
  $d = 24$ ft
$Q = (16$ ft^2) (24 ft) = 384 ft^3
$I = (0.67$ ft) (72 ft)^3 /12 = 20,840 ft^4
$V_{u2}Q/I = (104.4$ kip) (384 ft^3) /20,840 ft^4 = 1.923 kip/ft maximum shear flow
Joint 5 length = 40 ft
Total transverse shear in joint 5, $V_{u5} = (1.923$ kip/ft) (40 ft)/2 = 38.5 kips

ACI 318 Section 16.2.1.8 also has minimum connection force requirements for structural integrity in accordance with 16.2.4 or 16.2.5. ACI 318 Section 16.2.4.1 reads: "Except where the provisions of 16.2.5 govern, longitudinal and transverse integrity ties shall connect precast members to a lateral-force-resisting system, and vertical integrity ties shall be provided in accordance with 16.2.4.3 to connect adjacent floor and roof levels." ACI 318 Section 16.2.5 has the title "*Integrity tie requirements for precast concrete bearing wall structures three stories or more in height*." The structure being designed is a masonry bearing wall structure with precast concrete slabs acting as diaphragms; it is 5-stories tall. It has been decided to apply Section 16.2.5 requirements to the precast slabs, in which case, Sections 16.2.4.2 and 16.2.4.3 do not apply. Section 16.2.4.3 would not apply anyway since the bearing walls are made of masonry. According to ACI 318 Section 16.2.5.1, the horizontal tie force requirements for a precast bearing wall structure three or more stories in height are:

> 1500 pounds per foot parallel and perpendicular to the span of the floor members. The maximum spacing of ties parallel to the span is 10 feet. The maximum spacing of ties perpendicular to the span is the distance between supporting walls or beams.

> 16,000 pounds parallel to the perimeter of a floor or roof located within 4 feet of the edge at all edges.

11.1.1.6 Diaphragm Design and Details. The phi factors used for this example are as follows:

Tension control (bending and ties): $\phi = 0.90$

Shear: $\phi = 0.75$

Compression control in tied members: $\phi = 0.65$

The required shear strength of the diaphragm is amplified by a factor of $1.4R_s = 1.4 \times 1.0 = 1.4$, as required by *Standard* Section 14.2.4.1.3. The minimum tie force requirements given in ACI 318 Section 16.2.5 are specified as nominal values, meaning that $\phi = 1.00$ for those forces.

Note that although buildings assigned to Seismic Design Category C are not required to meet ACI 318 Section 18.12, some of the requirements contained therein are applied below as good practice but shown as optional.

11.1.1.6.1 Joint 1 Design and Detailing. The design must provide sufficient reinforcement for chord forces as well as shear friction connection forces, as follows:

Chord reinforcement, $A_{s1} = T_{u1}/\phi f_y = (23.8 \text{ kips})/[0.9(60 \text{ ksi})] = 0.44 \text{ in}^2$ (The collector force from Joint 4 calculations of 34.2 kips is not directly additive.)

Shear friction reinforcement, $A_{vf1} = 1.4V_{u1}/\phi \mu f_y = (1.4)(94 \text{ kips})/[(0.75)(1.0)(60 \text{ ksi})] = 2.92 \text{ in}^2$

Total reinforcement required $= 2(0.44 \text{ in}^2) + 2.92 \text{ in}^2 = 3.80 \text{ in}^2$

ACI tie force $= (1.5 \text{ kips/ft})(72 \text{ ft}) = 108 \text{ kips}$; reinforcement $= (108 \text{ kips})/(60 \text{ ksi}) = 1.80 \text{ in}^2$

Provide four #6 bars (two at each of the outside edges) plus four #7 bars (two each at the interior joint at the ends of the plank) for a total area of reinforcement of $4(0.44 \text{ in}^2) + 4(0.60 \text{ in}^2) = 4.16 \text{ in}^2$.

Because the interior joint reinforcement acts as the collector reinforcement in the longitudinal direction for the interior longitudinal walls, the cover and spacing of the two #7 bars in the interior joints will be provided to meet the requirements of ACI 318 Section 18.12.7.6 (optional):

Minimum cover = 2.5(7/8) = 2.19 in., but not less than 2.00 in.

Minimum spacing = 3(7/8) = 2.63 in., but not less than 1.50 in.

Figure 11.1-3 shows the reinforcement in the interior joints at the ends of the plank, which is also the collector reinforcement for the interior longitudinal walls (Joint 5). The two #6 bars extend along the length of the interior longitudinal walls as shown in Figure 11.1-3.
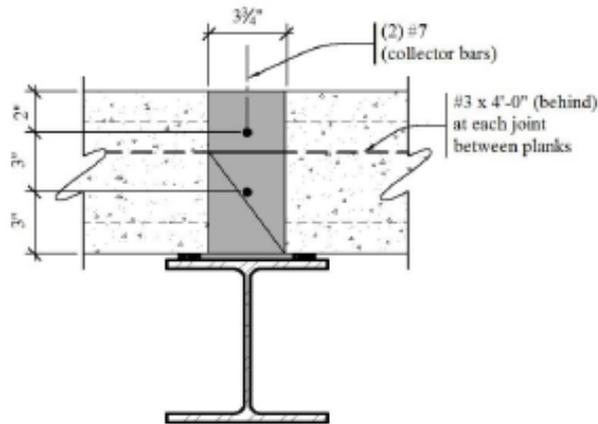
Figure 11.1-3 Interior joint reinforcement at the ends of plank and collector reinforcement at the end of the interior longitudinal walls - Joints 1 and 5
(1.0 in. = 25.4 mm)

Figure 11.1-4 shows the extension of the two #7 bars of Figure 11.1-3 into the region where the plank is parallel to the bars (see section cut on Figure 11.1-2). The bars will need to be extended the full length of the diaphragm unless supplemental plank reinforcement is provided. This detail makes use of this
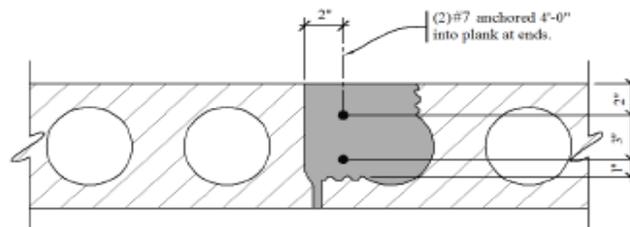
Figure 11.1-4 Anchorage region of shear reinforcement for Joint 1 and collector reinforcement for Joint 5
(1.0 in. = 25.4 mm)

supplemental plank reinforcement (two #7 bars or an equal area of strand) and shows the bars anchored at each end of the plank. The anchorage length of the #7 bars is calculated using ACI 318 Chapter 25:

$$l_d = \left(\frac{f_y \psi_t \psi_e}{25\lambda\sqrt{f_c'}} \right) d_b = \left(\frac{60,000\,\text{psi}\,(1.0)(1.0)}{25(1.0)\sqrt{4,000}\,\text{psi}} \right) d_b = 37.9 d_b$$

Using #7 bars, the required l_d = 37.9(7/8 in.) = 33.16 in. Therefore, use l_d = 4 ft, which is the width of the plank.

11.1.1.6.2 Joint 2 Design and Detailing. The chord design is similar to the previous calculations:

Chord reinforcement, $A_{s2} = T_{u2}/\phi f_y$ = (29.4 kips)/[0.9(60 ksi)] = 0.55 in.^{2}

The shear force may be reduced along Joint 2 by the shear friction resistance provided by the supplemental chord reinforcement ($2A_{chord} - A_{s2}$) and by the four #7 bars projecting from the interior longitudinal walls across this joint. The supplemental chord bars, which are located at the end of the walls, are conservatively excluded here. The shear force along the outer joint of the wall where the plank is parallel to the wall is modified as follows:

$$V_{u2}^{Mod} = 1.4 V_{u2} - \phi f_y \mu A_{4\#7}$$

$$= 1.4 \times 104.4 - 0.75(60)(1.0)(4 \times 0.60) = 38.16 \,\text{kips}$$

This force must be transferred from the planks to the wall. Using the arrangement shown in Figure 11.1-5, the required shear friction reinforcement (A_{vf2}) is computed as:

$$A_{vf2} = \frac{V_{u2}^{Mod}}{\phi f_y \left(\mu \sin\alpha_f + \cos\alpha_f \right)} = \frac{38.16}{0.75 \times 60(1.0 \times \sin 26.6° + \cos 26.6°)} = 0.63 \,\text{in.}^2$$

Use two #3 bars placed at 26.6 degrees (2-to-1 slope) across the joint at 6 feet from the ends of the plank (two sets per plank). The angle (α_f) used above provides development of the #3 bars while limiting the grouting to the outside core of the plank. The total shear reinforcement provided is 6(0.11 in.^{2}) = 0.66 in.^{2}. Note that the spacing of these connectors will have to be adjusted at the stair location.

The shear force between the other face of this wall and the diaphragm is:

$$V_{u2}\text{-}F = 1.4 \times (104.4 - 86.8) = 24.64 \,\text{kips}$$

The shear friction resistance provided by #3 bars in the grout key between each plank (provided for the 1.5 klf requirement of ACI 318) is computed as:

$$\phi A_{vf} f_y \mu = (0.75)(10 \,\text{bars})(0.11 \,\text{in.}^2)(60 \,\text{ksi})(1.0) = 49.5 \,\text{kips}$$

The development length of the #3 bars will now be checked. For the 180 degree standard hook, use ACI 318 Section 25.4.3, l_{dh} times the factors of ACI 318 Section 25.4.3.2, but not less than $8d_b$ or 6 inches. Side cover exceeds 2-1/2 inches and cover on the bar extension beyond the hook is provided by the grout and the planks, which is close enough to 2 inches to apply the 0.7 factor of ACI 318 Section 25.4.3.2. For the #3 hook:

$$l_{dh} = 0.7 \left(\frac{0.02 \psi_e f_y}{\sqrt{f_c'}} \right) d_b = 0.7 \left(\frac{0.02(1.0)(60,000\,\text{psi})}{\sqrt{4,000}\,\text{psi}} \right) 0.375 = 4.98 \text{ in. } (\leq 6 \text{ in. minimum})$$

The available distance for the perpendicular hook is approximately 5-1/2 inches. The bar will not be fully developed at the end of the plank because of the 6-inch minimum requirement. The full strength is not required for shear transfer. By inspection, the diagonal #3 hook will be developed in the wall as required for the computed diaphragm-to-shear-wall transfer. The straight end of the #3 bar will now be checked. The standard development length of ACI 318 Section 25.4.2 is used for l_d.

$$l_d = \frac{f_y d_b}{25\sqrt{f_c'}} = \frac{60,000(0.375)}{25\sqrt{4,000}} = 14.2 \text{ in.}$$

Figure 11.1-5 shows the reinforcement along each side of the wall on Joint 2.
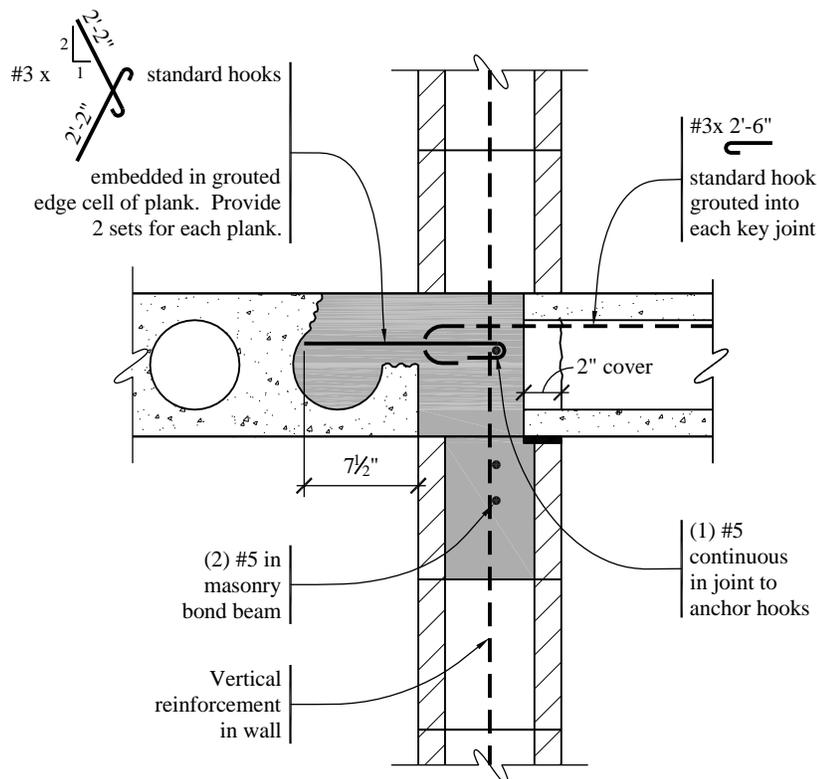
Figure 11.1-5 Joint 2 transverse wall joint reinforcement
(1.0 in. = 25.4 mm, 1.0 ft = 0.3048 m)

11.1.1.6.3 Design and Detailing at Joint 3. Compute the required amount of chord reinforcement at Joint 3 as:

$$A_{s3} = T_{u3}/\phi f_y = (43.2 \text{ kips})/[0.9(60 \text{ ksi})] = 0.8 \text{ in.}^2$$

Use two #6 bars, A_s = 2(0.44) = 0.88 in.^{2} along the exterior edges (top and bottom of the plan in Figure 11.1-2). Required cover for chord bars and spacing between bars at splices and anchorage zones per ACI 318 Section 18.12.7.6 (optional).

Minimum cover = 2.5(6/8) = 1.875 in., but not less than 2.00 in.

Minimum spacing = 3(6/8) = 2.25 in., but not less than 1.50 in.

Figure 11.1-6 shows the chord element at the exterior edges of the diaphragm. The chord bars extend along the length of the exterior longitudinal walls and act as collectors for these walls in the longitudinal direction (see Joint 4 collector reinforcement calculations and Figure 11.1-7).
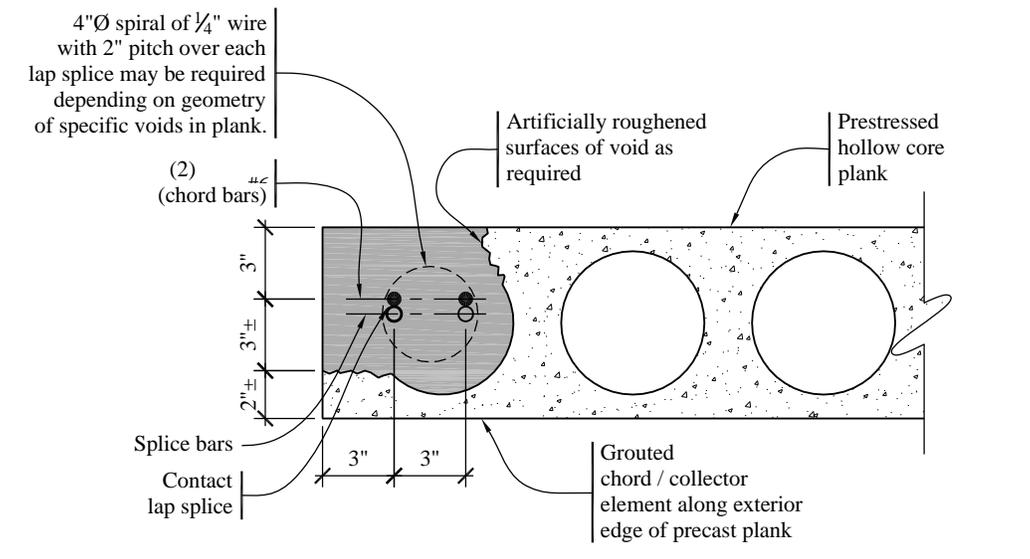
Figure 11.1-6 Joint 3 chord reinforcement at the exterior edge
(1.0 in. = 25.4 mm)

Joint 3 must also be checked for the minimum ACI tie forces. The chord reinforcement obviously exceeds the 16 kip perimeter force requirement. To satisfy the 1.5 kips per foot requirement, a 6 kip tie is needed at each joint between the planks, which is satisfied with a #3 bar in each joint (0.11 in.^{2} at 60 ksi = 6.6 kips). This bar is required at all bearing walls and is shown in subsequent details.

11.1.1.6.4 Joint 4 Design and Detailing. The required shear friction reinforcement along the wall length is computed as:

$A_{vf4} = 1.4V_{u4}/\phi\mu f_y$ = (1.4×20.6 kips)/[(0.75)(1.0)(60 ksi)] = 0.64 in.^{2}

Based upon the ACI tie requirement, provide #3 bars at each plank-to-plank joint. For eight bars total, the area of reinforcement is 8(0.11) = 0.88 in.^{2}, which is more than sufficient even considering the marginal development length, which is less favorable at Joint 2. The bars are extended 2 feet into the grout key, which is more than the development length and equal to half the width of the plank.
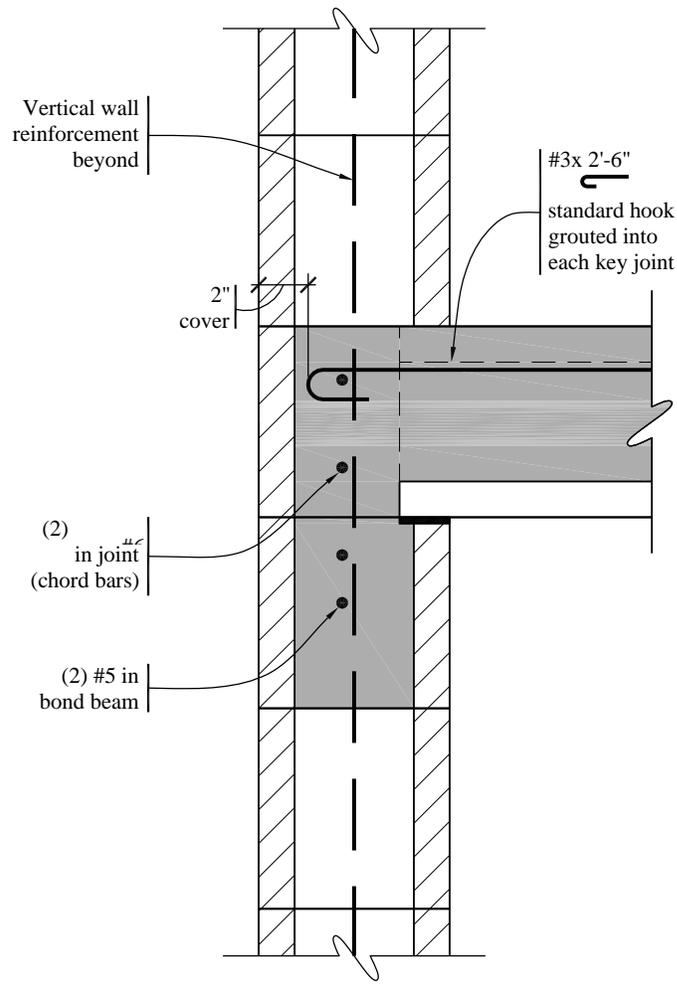
The required collector reinforcement is computed as:

$$A_{s4} = 1.5T_{u4}/\phi f_y = (34.2 \text{ kips})/[0.9(60 \text{ ksi})] = 0.63 \text{in.}^2$$

The two #6 bars, which are an extension of the transverse chord reinforcement, provide an area of reinforcement of 0.88 in.[2].

The reinforcement required by the *Standard* for out-of-plane force (62 plf) is far less than the ACI 318 requirement.

Figure 11.1-7 shows this joint along the wall.

**Figure 11.1-7 Joint 4 exterior longitudinal walls to diaphragm reinforcement
and out-of-plane anchorage**
(1.0 in. = 25.4 mm, 1.0 ft = 0.3048 m)

11.1.1.6.5 Joint 5 Design and Detailing. The required shear friction reinforcement along the wall length is computed as:
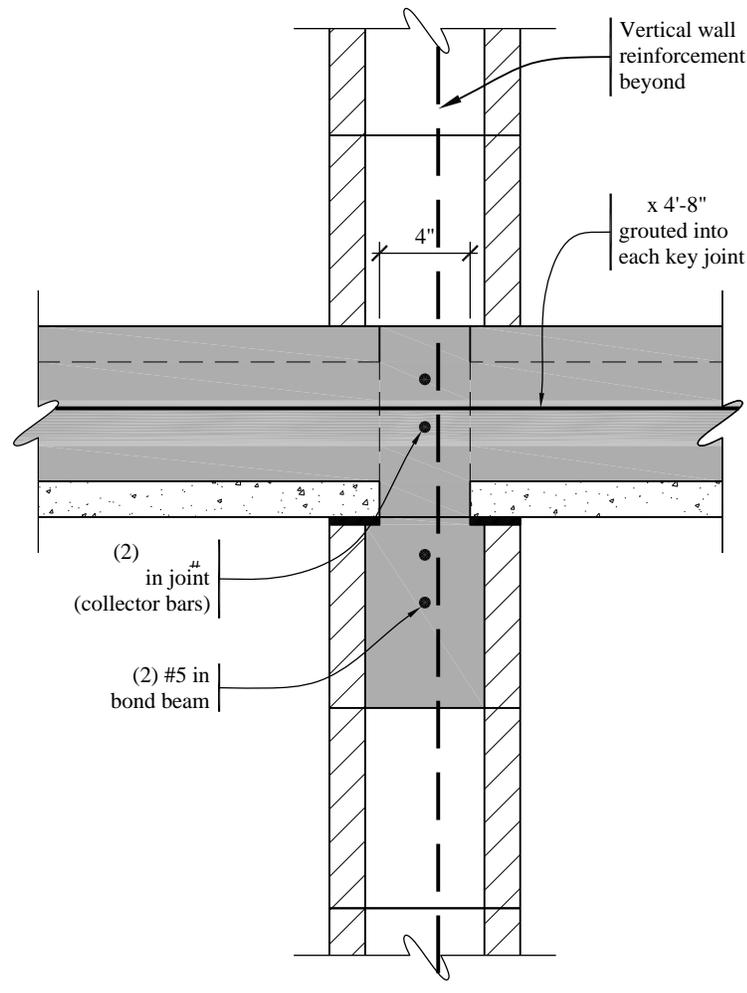
$$A_{vf5} = 1.4V_{u5}/\phi \mu f_y = (1.4 \times 38.5 \text{ kips})/[(0.75)(1.0)(0.85)(60 \text{ ksi})] = 1.41 \text{ in.}^2$$

Provide #4 bars at each plank-to-plank joint for a total of 8 bars.

The required collector reinforcement is computed as:

$A_{s5} = 1.5T_{u5}/\phi f_y = (34.2 \text{ kips})/[0.9(60 \text{ ksi})] = 0.63 \text{ in.}^2$

Two #7 bars specified for the design of Joint 1 above provide an area of reinforcement of 1.20 in.^{2}. Figure 11.1-8 shows this joint along the wall.

Figure 11.1-8 Wall-to-diaphragm reinforcement along interior longitudinal walls - Joint 5
(1.0 in. = 25.4 mm, 1.0 ft = 0.3048 m)

11.1.2 Topped Precast Concrete Units for Five-Story Masonry Building Assigned to Seismic Design Category D

This design shows the floor and roof diaphragms using topped precast units in the five-story masonry building when it is assigned to SDC D (see Section 13.2). The topping thickness exceeds the minimum thickness of 2 inches as required for composite topping slabs by ACI 318 Section 18.12.6. The topping is lightweight concrete (weight = 115 pcf) with a 28-day compressive strength (f'_c) of 4,000 psi and is to act

compositely with the 8-inch-thick hollow-core precast, prestressed concrete plank. Design parameters are provided in Section 13.2. Figure 13.2-1 shows the typical floor and roof plan.

11.1.2.1 General Design Requirements. Topped diaphragms may be used in any Seismic Design Category. ACI 318 Section 18.12 provides design provisions for topped precast concrete diaphragms. *Standard* Section 12.10.3 specifies the forces to be used in designing the precast concrete diaphragms in buildings assigned to SDC C or higher.

11.1.2.2 In-Plane Seismic Design Forces for Topped Diaphragms. The in-plane diaphragm seismic design force (F_{px}) is calculated in accordance with *Standard* Section 12.10.3. V_x must be added to F_{px} calculated using Equation 12.10.3-1 where:

V_x = the portion of the seismic shear force required to be transferred to the components of the vertical seismic force-resisting system due to offsets or changes in stiffness of the vertical resisting member at the diaphragm being designed

For Seismic Design Category C and higher, *Standard* Section 12.10.3.4 requires that collector elements, collector splices and collector connections to the vertical seismic force-resisting members be designed for diaphragm forces amplified by a factor of 1.5, with three exceptions:

1. Any transfer force increased by the overstrength factor of Section 12.4.3 need not be further amplified by 1.5.

2. For moment frame and braced frame systems, collector forces need not exceed the lateral strength of the corresponding frame line below the collector, considering only the moment frames or braced frames. In addition, diaphragm design forces need not exceed the forces corresponding to the collector forces so determined.

3. In structures or portions thereof braced entirely by light-frame shear walls, collector elements and their connections including connections to vertical elements need only be designed to resist the diaphragm seismic design forces without the 1.5 multiplier.

The parameters from the example in Section 13.2 used to calculate in-plane seismic design forces for the diaphragms are provided in Table 11.1-4.

Table 11.1-4 Design Parameters from Section 13.2

Design Parameter	Value
Ω_o	2.5
C_s	0.2
w_i (roof)	1166 kips
w_i (floor)	1302 kips
S_{DS}	1.0
S_{D1}	0.6
I_e	1.0
SDC	D

1.0 kip = 4.45 kN.

11.1.2.3 Diaphragm Design Forces. As indicated previously, the weight tributary to the roof and floor diaphragms (w_{px}) is the total story weight (w_i) at Level i minus the weight of the walls parallel to the force.

Compute diaphragm weight (w_{px}) for the roof and floor as follows:

Roof:

Total weight	= 1,166 kips
Walls parallel to force = (60 psf)(277 ft)(8.67 ft / 2)	= -72 kips
w_{px}	= 1,094 kips

Floors:

Total weight	= 1,302 kips
Walls parallel to force = (60 psf)(277 ft)(8.67 ft)	= -144 kips
w_{px}	= 1,158 kips

Since the building is assigned to SDC D, the precast concrete diaphragm design forces are required to be determined by the provisions of *Standard* Section 12.10.3.

Step 1: Determine R_s, Diaphragm Design Force Reduction Factor (*Standard* Table 12.10.3.5-1)

The Reduced Design Option (RDO) is adopted in the design of this precast diaphragm. As a result, $R_s = 1.4$.

Step 2: Determine C_{px}, Diaphragm Design Acceleration (Force) Coefficient at Level x (*Standard* Section 12.10.3.2)

In order to determine C_{px}, three parameters - C_{p0}, C_{pi}, and C_{pn}, need to first be determined.

$C_{p0} = 0.4S_{DS}I_e = 0.4 \times 1.0 \times 1.0 = 0.4$

C_{pi} is the greater of the values given by:

$C_{pi} = C_{p0} = 0.4$, and

$C_{pi} = 0.9\Gamma_{m1}\,\Omega_0\,C_s$

where:

Γ_{m1} is first mode contribution factor

$$\Gamma_{m1} = 1 + 0.5z_s\left(1 - \frac{1}{N}\right)$$

where z_s = modal contribution coefficient modifier dependent on seismic force-resisting system.

The building being designed consists of a bearing wall system of reinforced masonry. As a result,

$z_s = 1.00$

$$\Gamma_{m1} = 1 + 0.5 z_s \left(1 - \frac{1}{N}\right) = 1 + 0.5 \times 1.00 \times \left(1 - \frac{1}{5}\right) = 1.4$$

$C_{pi} = 0.9 \Gamma_{m1} \Omega_o C_s = 0.9 \times 1.4 \times 2.5 \times 0.2 = 0.63$ Governs

$$C_{pn} = \sqrt{\left(\Gamma_{m1} \Omega_0 C_s\right)^2 + \left(\Gamma_{m2} C_{s2}\right)^2}$$

where:

Γ_{m2} is higher mode contribution factor

$$\Gamma_{m2} = 0.9 z_s \left(1 - \frac{1}{N}\right)^2 = 0.9 \times 1.00 \times \left(1 - \frac{1}{5}\right)^2 = 0.576$$

C_{s2} is higher mode seismic response coefficient. C_{s2} is the smallest of the values given by

$$C_{s2} = (0.15 N + 0.25) I_e S_{DS} = (0.15 \times 5 + 0.25) \times 1.0 \times 1.0 = 1.0 \qquad \text{Governs}$$

$$C_{s2} = I_e S_{DS} = 1.0 \times 1.0 = 1.0 \qquad \text{Governs}$$

$$C_{s2} = \frac{I_e S_{D1}}{0.03(N-1)} = \frac{1.0 \times 0.60}{0.03(5-1)} = 5.0 \qquad \text{For N} \geq 2$$

$$C_{s2} = 0 \qquad \text{For N} = 1$$

$$C_{pn} = \sqrt{\left(\Gamma_{m1} \Omega_0 C_s\right)^2 + \left(\Gamma_{m2} C_{s2}\right)^2} = 0.428$$

Using *Standard* Figure 12.10.3-1, C_{px} is determined at various floor levels, as shown in Table 11.1-5

Step 3: Determine F_{px}, Diaphragm Design Force at Level x

$$F_{px} = \frac{C_{px}}{R_s} w_{px} \geq 0.2 S_{DS} I_e w_{px}$$

Table 11.1-5 F_{px} Calculations for Building in SDC D

Level	h_x (ft)	w_{px} (kips)	C_{px}	F_{px} (kips)
Roof	43.34	1094	0.91	708
4	34.67	1158	0.63	521
3	26.00	1158	0.57	474
2	17.33	1158	0.51	426
1	8.67	1158	0.46	378

1.0 kip = 4.45 kN.

The minimum value of $F_{px} = 0.2 S_{DS} I_e w_{px}$ $= 0.2(1.0)1.0(1094 \text{ kips})$ $= 218.80 \text{ kips (roof)}$
                                          $= 0.2(1.0)1.0(1158 \text{ kips})$ $= 231.60 \text{ kips (floors)}$

11.1.2.4 Static Analysis of Diaphragms. The seismic design force of 708 kips is distributed as in Section 11.1.1.6 (Figure 11.1-1 shows the distribution). The force is twice that used to design the untopped diaphragm for the design of the building in SDC C due to the higher seismic demand. Figure 11.1-2 shows critical regions of the diaphragm to be considered in this design. Collector elements will be designed for 1.5 times the diaphragm force per *Standard* Section 12.10.3.4.

Joint forces taken from Section 11.1.1.5 times 2.0 are as follows:

    Joint 1 – Transverse forces:

        Shear, $V_{u1} = 94 \text{ kips} \times 2.0 = 188 \text{ kips}$
        Moment, $M_{u1} = 1692 \text{ ft-kips} \times 2.0 = 3384 \text{ ft-kips}$
        Chord tension force, $T_{u1} = M/d = 3384 \text{ ft-kips} /71 \text{ ft} = 47.7 \text{ kips}$

    Joint 2 – Transverse forces:

        Shear, $V_{u2} = 104.4 \text{ kips} \times 2.0 = 208.8 \text{ kips}$
        Moment, $M_{u2} = 2088 \text{ ft-kips} \times 2.0 = 4176 \text{ ft-kips}$
        Chord tension force, $T_{u2} = M/d = 4176 \text{ ft-kips} / 71 \text{ ft} = 58.8 \text{ kips}$

    Joint 3 – Transverse forces:

        Shear, $V_{u3} = 64.2 \text{ kips} \times 2.0 = 128.4 \text{ kips}$
        Moment, $M_{u3} = 3070 \text{ ft-kips} \times 2.0 = 6140 \text{ ft-kips}$
        Chord tension force, $T_{u3} = M/d = 6140 \text{ ft-kips} /71 \text{ ft} = 86.5 \text{ kips}$

    Joint 4 – Longitudinal forces:

        Wall force, $F = 64.9 \text{ kips} \times 2.0 = 129.8 \text{ kips}$
        Wall shear along wall length, $V_{u4} = 20.6 \text{ kips} \times 2.0 = 41.2 \text{ kips}$
        Collector force at wall end, $1.5 T_{u4} = 1.5(22.8 \text{ kips})(2.0) = 68.4 \text{ kips}$

    Joint 4 – Out-of-plane forces:

        Just as with the untopped diaphragm, the out-of-plane forces are controlled by ACI 318 Section 16.2.5.1, which requires horizontal ties of 1.5 kips per foot from floor to walls.

    Joint 5 – Longitudinal forces:

        Wall force, $F = 708 \text{ kips} / 8 \text{ walls} = 88.5 \text{ kips}$
        Wall shear along each side of wall, $V_{u5} = 10.3 \text{ kips} \times 2.0 = 20.6 \text{ kips}$
        Collector force at wall end, $1.5 T_{u5} = 1.5(22.8 \text{ kips})(2.0) = 68.4 \text{ kips}$

    Joint 5 – Shear flow due to transverse forces:

        Shear at Joint 2, $V_{u2} = 208.8 \text{ kips}$
        $Q = A\ d$

$$A = (0.67 \text{ ft}) (24 \text{ ft}) = 16 \text{ ft}^2$$
$$d = 24 \text{ ft}$$
$$Q = (16 \text{ ft}^2) (24 \text{ ft}) = 384 \text{ ft}^3$$
$$I = (0.67 \text{ ft}) (72 \text{ ft})^3 / 12 = 20,840 \text{ ft}^4$$
$$V_{u2}Q/I = (208.8 \text{ kip}) (384 \text{ ft}^3) / 20,840 \text{ ft}^4 = 3.85 \text{ kips/ft maximum shear flow}$$
Joint 5 length = 40 ft

Total transverse shear in joint 5, V_{u5} = 3.85 kips/ft) (40 ft)/2 = 77 kips

11.1.2.5 Diaphragm Design and Details

11.1.2.5.1 Minimum Reinforcement for 2.5-inch Topping. ACI 318 Section 18.12.7.1 references ACI 318 Section 24.4, which requires a minimum $A_s = 0.0018bd$ for Grade 60 welded wire reinforcement. For a 2.5-inch topping, the required $A_s = 0.054$ in.^{2}/ft. WWR 10×10 - W4.5×W4.5 provides 0.054 in.^{2}/ft. However, as is shown later in Section 11.1.2.5.4, WWR 10×10 – W8×W8 ($A_s = 0.096$ in.^{2}) must be provided as minimum. The minimum spacing of wires is 10 inches and the maximum spacing is 18 inches. Note that the ACI 318 Section 24.4 limit on spacing of five times thickness is interpreted such that the topping thickness is not the pertinent thickness.

11.1.2.5.2 Boundary Members. Joint 3 has the maximum bending moment and is used to determine the boundary member reinforcement of the chord along the exterior edge. The need for transverse boundary member reinforcement is reviewed using ACI 318 Section 18.12.7.5. Calculate the compressive stress in the chord with the ultimate moment using a linear elastic model and gross section properties of the topping. It is conservative to ignore the precast units, but this is not necessary since the joints between precast units are grouted. The chord compressive stress is:

$$6M_{u3}/hd^2 = 6(6140 \times 12)/(2.5)(72 \times 12)^2 = 237 \text{ psi}$$

The chord compressive stress is less than $0.2f'_c = 0.2(4000) = 800$ psi. Transverse reinforcement in the boundary member is not required.

The required chord reinforcement is:

$$A_{s3} = T_{u3}/\phi f_y = (86.5 \text{ kips})/[0.9(60 \text{ ksi})] = 1.6 \text{ in.}^2$$

11.1.2.5.3 Collectors. The design for Joint 4 collector reinforcement at the end of the exterior longitudinal walls and for Joint 5 at the interior longitudinal walls is the same.

$$A_{s4} = A_{s5} = 1.5T_{u4}/\phi f_y = (68.4 \text{ kips})/[0.9(60 \text{ ksi})] = 1.27 \text{ in.}^2$$

Use two #8 bar ($A_s = 2 \times 0.79 = 1.58$ in.^{2}) along the exterior edges, along the length of the exterior longitudinal walls and along the length of the interior longitudinal walls. Provide cover for chord and collector bars and spacing between bars per ACI 318 Section 18.12.7.6.

Minimum cover = 2.5(8/8) = 2.5 in., but not less than 2.0 in.

Minimum spacing = 3(8/8) = 3.0 in., but not less than 1.5 in.

Figure 11.1-9 shows the diaphragm plan and section cuts of the details and Figure 11.1-10 shows the boundary member and chord/collector reinforcement along the edge. Given the close margin on cover, the transverse reinforcement at lap splices also is shown.
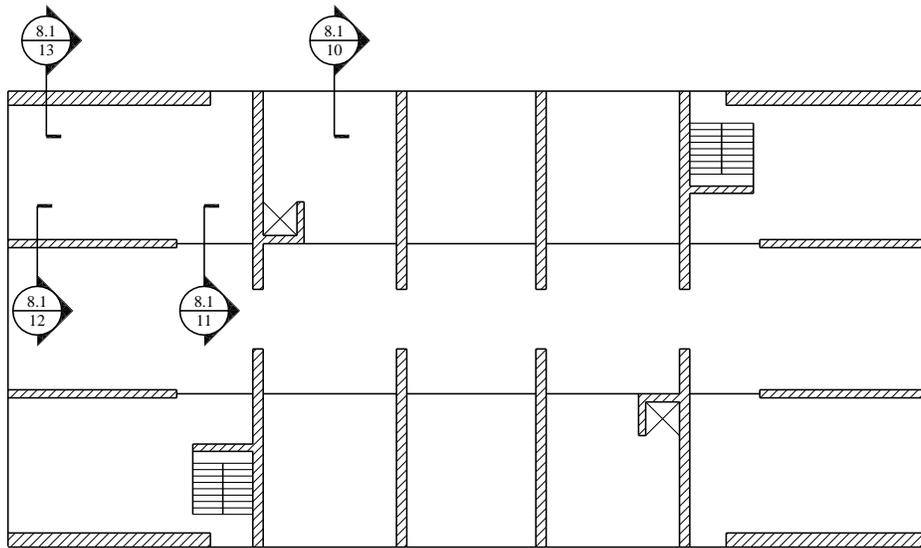
Figure 11.1-9 Diaphragm plan and section cuts
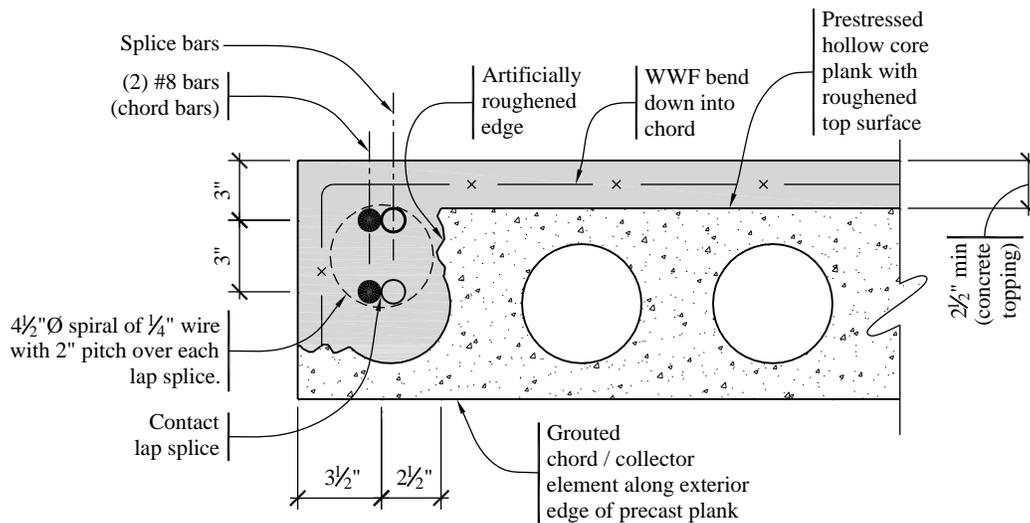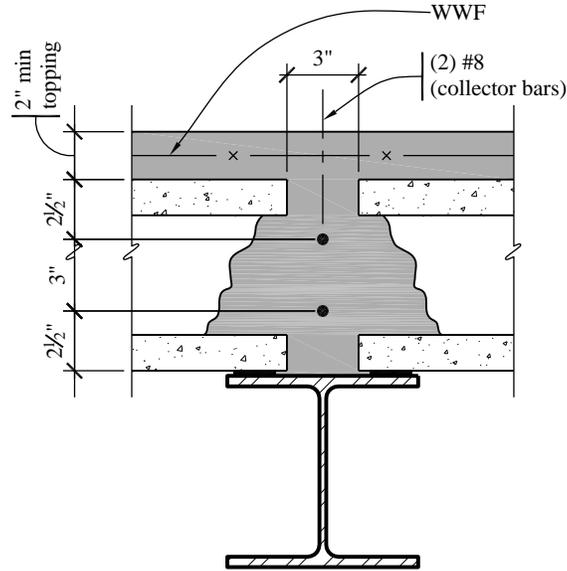

Figure 11.1-10 Boundary member and chord and collector reinforcement
(1.0 in. = 25.4 mm)

Figure 11.1-11 shows the collector reinforcement for the interior longitudinal walls. The side cover of 2-1/2 inches is provided by casting the topping into the cores and by the stems of the plank. A minimum space of 1 inch is provided between the plank stems and the sides of the bars.

Figure 11.1-11 Collector reinforcement at the end of the interior longitudinal walls - Joint 5
(1.0 in. = 25.4 mm, 1.0 ft = 0.3048 m)

11.1.2.5.4 Shear Resistance. In thin composite and noncomposite topping slabs on precast floor and roof members, joints typically are tooled during construction, resulting in cracks forming at the joint between precast members. Therefore, the shear resistance of the topping slab is limited to the shear friction strength of the reinforcing crossing the joint.

ACI 318 Section 18.12.9.1 provides an equation for the shear strength of the diaphragm, which includes both concrete and reinforcing components. However, for noncomposite topping slabs on precast floors and roofs where the only reinforcing crossing the joints is the field reinforcing in the topping slab, the shear friction capacity at the joint will always control the design. ACI 318 Section 18.12.9.3 defines the shear strength at the joint as follows:

$$\phi V_{n,WWR} = \phi A_{vf}f_y\mu = 0.75(0.096 \text{ in.}^2/\text{ft})(60 \text{ ksi})(1.0)(0.85) = 3.67 \text{ kips/ft}$$

Note that $\mu = 1.0\lambda$ is used since the joint is assumed to be pre-cracked.

The shear resistance in the transverse direction is:

3.67 kips/ft (72 ft) = 264 kips

Shear friction from the collector reinforcement (4#8) at the interior longitudinal walls:

$$\phi V_{n,collector} = \phi A_{vf}f_y\mu = 0.75(4\times0.79)(60 \text{ ksi})(1.0)(0.85) = 120 \text{ kips}$$

Total shear resistance: $\phi V_n = 264 \text{ kips} + 120 \text{ kips} = 384 \text{ kips}$

The required shear strength on the diaphragm is amplified by a factor of $1.4R_s = 1.4\times1.4 = 2.0$, as required by *Standard* Section 14.2.4.1.3.

So, required shear in Joint 1, $2.0V_{u1} = 2\times188 \text{ kips} = 376 \text{ kips}$

At the plank adjacent to Joint 2, the shear strength of the diaphragm in accordance with ACI 318 Section 18.12.9.1 is:

$$\phi V_n = \phi A_{cv}\left(2\lambda\sqrt{f_c'} + \rho_t f_y\right)$$
$$= 0.75(2.5 \times 72 \times 12)\left(2(1.0)\sqrt{4000} + (0.0032 + 0.0014) \times 60{,}000\right)$$
$$= 652\,\text{kips} > 2V_{u2}(= 2 \times 208.8 = 418\,\text{kips})$$

Number 3 dowels are used to provide continuity of the topping slab welded wire reinforcement across the masonry walls. The topping is to be cast into the masonry walls as shown in Figure 11.1-12 and the spacing of the #3 bars is set to be modular with the CMU.
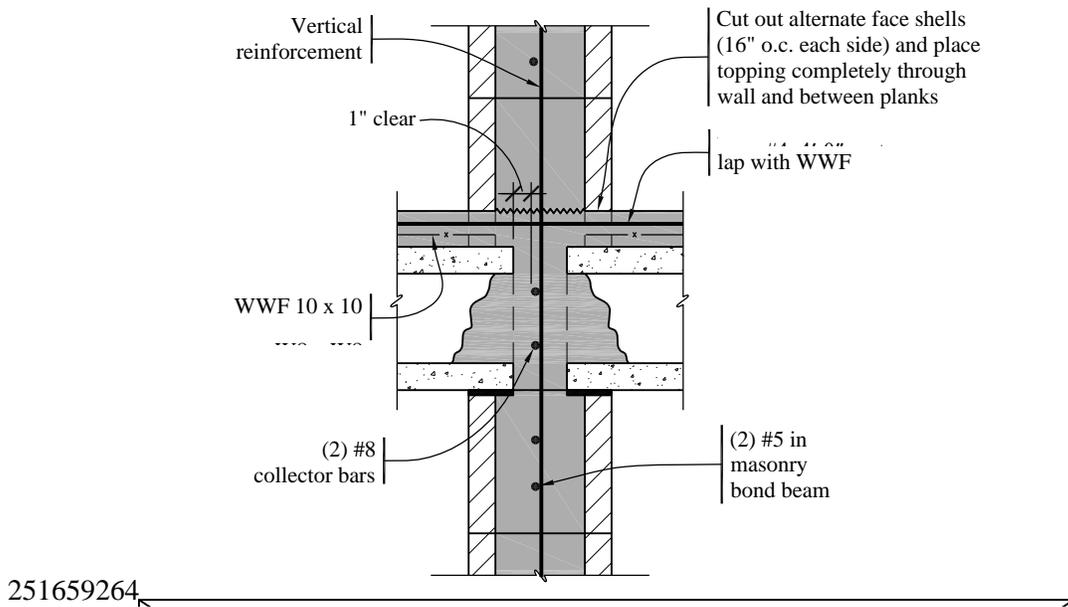
Figure 11.1-12 Wall-to-diaphragm reinforcement along interior longitudinal walls - Joint 5
(1.0 in. = 25.4 mm, 1.0 ft = 0.3048 m)

The required shear reinforcement along the exterior longitudinal wall (Joint 4) is:

$A_{vf4} = 2V_{u4}/\phi\mu f_y = (2{\times}41.2 \text{ kips})/[(0.75)(1.0)(0.85)(60 \text{ ksi})] = 2.15 \text{ in.}^2$

Number 5 dowels spaced at 48 inches o.c. provide

$A_v = (0.31 \text{ in.}^2)\ (36 \text{ ft x } 12 \text{ in./ft}) / 48 \text{ in.} = 2.79 \text{ in.}^2$

The required shear reinforcement along the interior longitudinal wall (Joint 5) is:

$A_{vf5} = 2V_{u5}/\phi\mu f_y = (2{\times}77 \text{ kips})/[(0.75)(1.0)(0.85)(60 \text{ ksi})] = 4.03 \text{ in.}^2$

Number 4 dowels spaced at 16 o.c. provide

11-30

$A_v = (0.20 \text{ in}^2)(40 \text{ ft x } 12 \text{ in/ft}) / 16 \text{ in} = 6.0 \text{ in}^2$

11.1.2.5.5 Check of Out-of-Plane Forces. At Joint 4, the out-of-plane forces are checked as follows:

$F_p = 0.4(S_{DS})(k_a)(I_e)(W_{wall}) = 0.4(1.0)(1.0)(1.0) [(60 \text{ psf})(8.67 \text{ ft})] = 208 \text{ plf}$

where

$k_a = 1.0 + L_f/100 = 1.0$ for rigid diaphragms

With bars at 4 feet on center, $F_p = 4$ ft (208 plf) = 0.83 kips.

The required reinforcement, $A_s = 0.83 \text{ kips}/(0.9)(60\text{ksi}) = 0.015 \text{ in.}^2$. Provide #5 bars at 4 feet on center, which provides a nominal strength of $0.31 \times 60/4 = 4.65$ klf. This detail satisfies the tie force of 1.5 klf required by ACI 318 Section 16.2.5.1. The bars are extended 2 feet into the grout key, which is more than the development length. Using #5 bars at 4 feet on center will be adequate and the detail is shown in Figure 11.1-13. The detail at Joint 2 is similar.
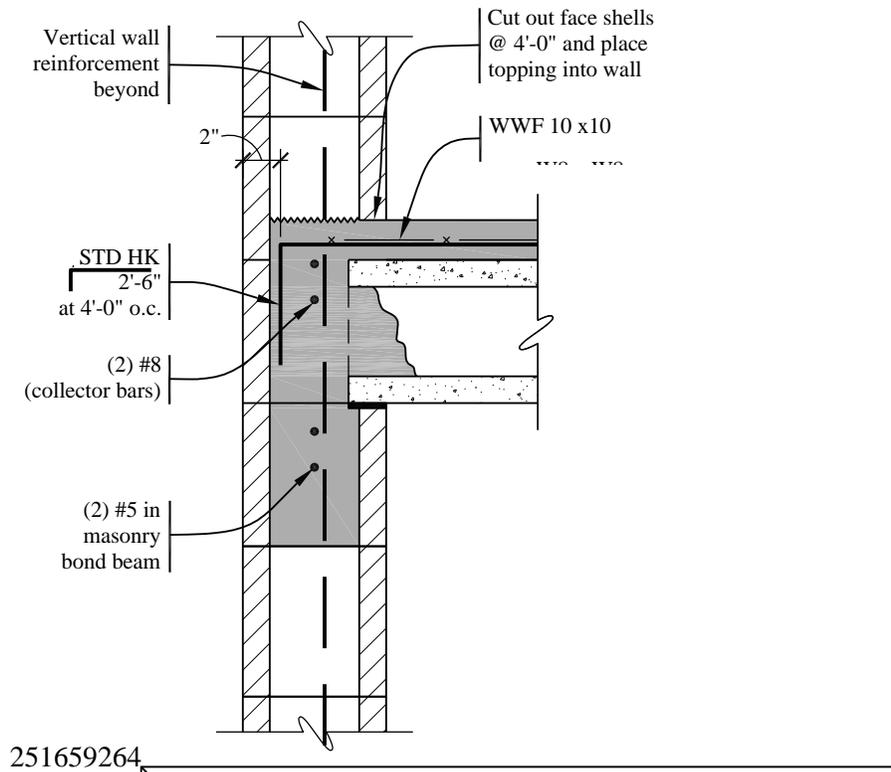
Figure 11.1-13 Exterior longitudinal wall-to-diaphragm reinforcement and out-of-plane anchorage - Joint 4
(1.0 in. = 25.4 mm, 1.0 ft = 0.3048 m).

11.2 THREE-STORY OFFICE BUILDING WITH INTERMEDIATE PRECAST CONCRETE SHEAR WALLS

This example illustrates the seismic design of intermediate precast concrete shear walls. These walls can be used up to any height in Seismic Design Categories B and C but are limited to 40 feet for Seismic Design Categories D, E, and F. An increase in structural height to 45 feet is permitted for "single story storage warehouse facilities" – see Footnote k to *Standard* Table 12.2-1.

ACI 318 Section 18.5.2.1 requires that yielding between wall panels or between wall panels and the foundation be restricted to steel elements or reinforcement. However, the *Standard* is more specific concerning the means to accomplish the objective of providing reliable post-elastic performance. *Standard* Section 14.2.2.4 (in a modification to ACI 318 Section 18.5) requires that connections that are designed to yield be capable of maintaining 80 percent of their design strength at the deformation induced by the design displacement. Alternatively, they can use Type 2 mechanical splices.

Additional requirements are contained in the *Provisions* for intermediate precast walls with wall piers in structures assigned to SDC D, E, or F (*Standard* Section 14.2.2.4 [ACI 318 Section 18.5.2.4]); however, irrespective of SDC, these requirements do not apply to the solid wall panels used for this example.

11.2.1 Building Description

This precast concrete building is a three-story office building (Risk Category II) on Site Class D soils. The structure utilizes 10-foot-wide by 18-inch-deep prestressed double tees (DTs) spanning 40 feet to prestressed inverted tee beams for the floors and the roof. The DTs are to be constructed using lightweight concrete. Each of the above-grade floors and the roof are covered with a 2-inch-thick (minimum), normal-weight cast-in-place concrete topping. The vertical seismic force-resisting system is to be constructed entirely of precast concrete walls located around the stairs and elevator/mechanical shafts. The only features illustrated in this example are the rational selection of the seismic design parameters and the design of the reinforcement and connections of the precast concrete shear walls. The diaphragm design is not shown.

As shown in Figure 11.2-1, the building has a regular plan. The precast shear walls are continuous from the ground level to 12 feet above the roof. The walls of the elevator/mechanical pits are cast-in-place below grade. The building has no vertical irregularities. The story height is 12 feet.
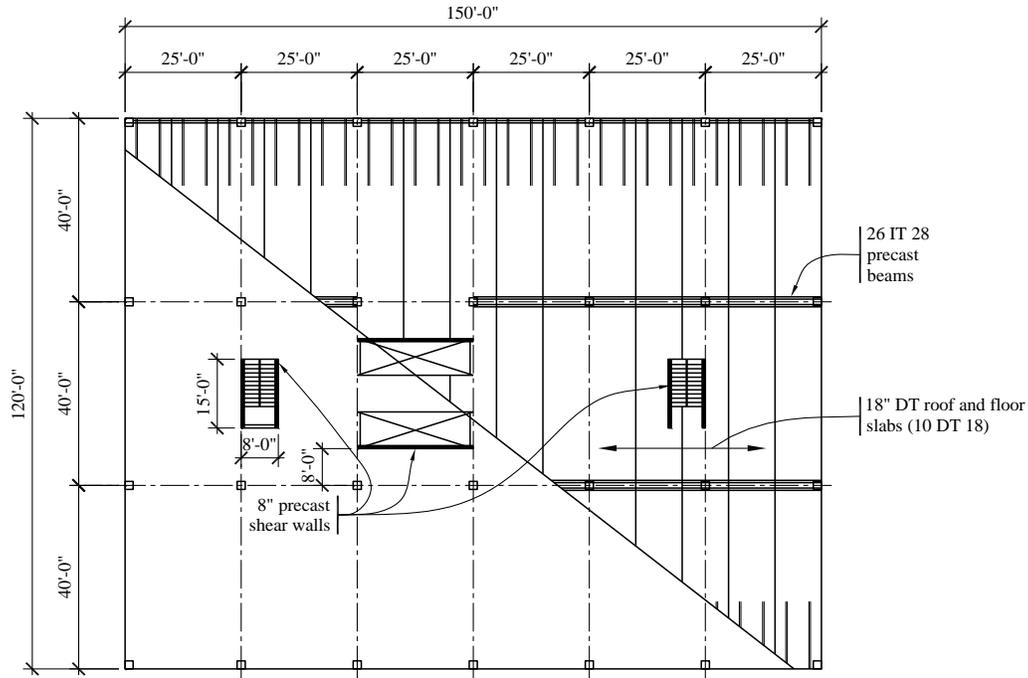
Figure 11.2-1 Three-story building plan
(1.0 in. = 25.4 mm, 1.0 ft = 0.3048 m)

The precast walls are estimated to be 8 inches thick for building mass calculations. These walls are normal-weight concrete with a 28-day compressive strength, f'_c, of 5000 psi. Reinforcing bars used at the ends of the walls and in welded connectors are ASTM A706 (60 ksi yield strength). The concrete for the foundations and below-grade walls has a 28-day compressive strength, f'_c, of 4000 psi.

11.2.2 Design Requirements

11.2.2.1 Seismic Parameters. The basic parameters affecting the design and detailing of the building are shown in Table 11.2-1.

Table 11.2-1 Design Parameters

Design Parameter	Value
Risk Category II	$I_e = 1.0$
S_S	0.266
S_1	0.08
Site Class	D
F_a	1.59
F_v	2.4
$S_{MS} = F_a S_S$	0.425
$S_{M1} = F_v S_1$	0.192
$S_{DS} = 2/3\ S_{MS}$	0.283

Table 11.2-1 Design Parameters

$S_{D1} = 2/3\ S_{M1}$	0.128
Seismic Design Category	B
Basic Seismic Force-Resisting System	Bearing Wall System
Wall Type	Intermediate Precast Shear Walls
R	4
Ω_0	2.5
C_d	4

A Bearing Wall System is defined in the *Standard* as "A structural system with bearing walls providing support for all or major portions of the vertical loads. Shear walls or braced frames provide seismic force resistance." A concrete Bearing Wall is one which "supports more than 200 pounds per linear foot of vertical load in addition to its own weight." Note that if a Building Frame System with Intermediate Precast Shear Wall were used, the design would be based on $R=5$, $\Omega_o=2\ \frac{1}{2}$ and $C_d=4\frac{1}{2}$.

Note that in Seismic Design Category B an ordinary precast shear wall could be used to resist seismic forces. However, the design forces would be 33 percent higher, since they would be based on $R = 3$, $\Omega_o = 2.5$, and $C_d = 3$. Ordinary precast structural walls need not satisfy any provisions in ACI 318 Chapter 18.

11.2.2.2 Structural Design Considerations

11.2.2.2.1 Precast Shear Wall System. This system is designed to yield in bending at the base of the precast shear walls without shear slip at any of the joints. The remaining connections (shear connectors and flexural connectors away from the base) are then made strong enough to ensure that the inelastic action is forced to the intended location.

Although it would be desirable to force yielding to occur in a significant portion of the connections, it frequently is not possible to do so with common configurations of precast elements and connections. The connections are often unavoidable weak links. Careful attention to detail is required to assure adequate ductility in the location of first yield and to preclude premature yielding of other connections. For this particular example, the vertical bars at the ends of the shear walls (see Figure 11.2-6) act as flexural reinforcement for the walls and are selected as the location of first yield. The yielding will not propagate far into the wall vertically due to the unavoidable increase in flexural strength provided by unspliced reinforcement within the panel. The issue of most significant concern is the performance of the shear connections (see Figure 11.2-7) at the same joint. The connections are designed to provide the necessary shear resistance and avoid slip without providing increased flexural strength at the connection, since such an increase would also increase the maximum shear force on the joint. At the base of the panel, welded steel angles are designed to be flexible for uplift but stiff for in-plane shear.

11.2.2.2.2 Building System. No height limits are imposed, since SDC is B (*Standard* Table 12.2-1).

For structural design, the floors are assumed to act as rigid horizontal diaphragms to distribute seismic inertial forces to the walls parallel to the motion. Because the building is assigned to SDC B, according to *Standard* Table 12.6-1, use of the Equivalent Lateral Force (ELF) procedure (*Standard* Section 12.8) is permitted.

Orthogonal load combinations are not required for this building (*Standard* Section 12.5.2).

Ties, continuity, and anchorage must be considered explicitly when detailing connections between the floors and roof and the walls and columns.

This example does not include consideration of nonstructural elements.

Collector elements are required due to the short length of shear walls as compared to the diaphragm dimensions, but they are not designed in this example.

Diaphragms need to be designed for the required forces (*Standard* Section 12.10), but that design is not shown here.

The bearing walls must be designed for a force perpendicular to their plane (*Standard* Section 12.11), but design for that requirement is not shown for this building.

The drift limit is $0.025h_{sx}$ (*Standard* Table 12.12-1, Row 1), but drift is not computed here.

ACI 318 Section 16.2.5 requires minimum strengths for connections between elements of precast building structures. The horizontal forces were described in Section 11.1 above; the vertical forces will be described in this example.

11.2.3 Load Combinations

The basic load combinations require that seismic forces and gravity loads be combined in accordance with the factored load combinations presented in *Standard* Section 12.4.2.3. Vertical seismic load effects are described in *Standard* Section 12.4.2.2.

According to *Standard* Section 12.3.4.1, $\rho = 1.0$ for structures in Seismic Design Categories A, B and C, even though this seismic force-resisting system is not particularly redundant.

The relevant load combinations from ASCE 7 are as follows:

$$(1.2 + 0.2S_{DS})D \pm \rho Q_E + 0.5L$$

$$(0.9 - 0.2S_{DS})D \pm \rho Q_E$$

Substituting S_{DS} as determined above, these load combinations become:

$$1.26D + Q_E + 0.5L$$

$$0.843D - Q_E$$

These load combinations are for loading in the plane of the shear walls.

11.2.4 Seismic Force Analysis

11.2.4.1 Weight Calculations. For the roof and two floors:

18-inch double tees (32 psf) + 2-inch topping (24 psf)	= 56.0 psf
Precast beams at 40 feet	= 12.5 psf
16-inch square columns	= 4.5 psf
Ceiling, mechanical, miscellaneous	= 4.0 psf
Exterior cladding (per floor area)	= 5.0 psf

Partitions $= 10.0$ psf
Total $= 92.0$ psf

Note that since the design snow load is 30 psf, it can be ignored in calculating the seismic weight (*Standard* Section 12.7.2). The weight of each floor including the precast shear walls is:

(120 ft)(150 ft)(92 psf / 1,000) + [(15 ft)4 + (25 ft)2](12 ft)(0.10 ksf) = 1788 kips

Considering the roof to be the same weight as a floor, the total building weight is $W = 3(1788$ kips) = 5364 kips.

11.2.4.2 Base Shear. The seismic response coefficient, C_s, is computed using *Standard* Equation 12.8-2:

$$C_S = \frac{S_{DS}}{R/I_e} = \frac{0.283}{4/1} = 0.0708$$

except that it need not exceed the value from *Standard* Equation 12.8-3 computed as:

$$C_S = \frac{S_{D1}}{T(R/I_e)} = \frac{0.128}{0.29(4/1)} = 0.110$$

where T is the fundamental period of the building computed using the approximate method of *Standard* Equation 12.8-7:

$$T_a = C_t h_n^x = (0.02)(36)^{0.75} = 0.29 \text{ sec}$$

Therefore, use $C_s = 0.0708$, which is larger than the minimum specified in *Standard* Equation 12.8-5:

$$C_s = 0.044(S_{DS})(I_e) \geq 0.01 = 0.044(0.283)(1.0) = 0.012$$

The total seismic base shear is then calculated using *Standard* Equation 12.8-1 as:

$$V = C_s W = (0.0708)(5364) = 380 \text{ kips}$$

Note that this force is substantially larger than a design wind would be. If a nominal 30 psf were applied to the long face, the result would be less than half this seismic force already reduced by an R factor of 4.

11.2.4.3 Vertical Distribution of Seismic Forces. The seismic lateral force, F_x, at any level is determined in accordance with *Standard* Section 12.8.3:

$$F_x = C_{vx} V$$

where:

$$C_{vx} = \frac{w_x h_x^k}{\sum_{i=1}^{n} w_i h_i^k}$$

Since the period, T, is less than 0.5 seconds, $k = 1$ in both building directions. With equal weights at each floor level, the resulting values of C_{vx} and F_x are as follows:

11-36

Roof: $C_{vr} = 0.50$; $F_r = 190$ kips

Third Floor: $C_{v3} = 0.333$; $F_3 = 127$ kips

Second Floor: $C_{v2} = 0.167$; $F_2 = 63$ kips

11.2.4.4 Horizontal Shear Distribution and Torsion

11.2.4.4.1 Longitudinal Direction. Design each of the 25-foot-long walls at the elevator/mechanical shafts for half the total shear. Since the longitudinal walls are very close to the center of rigidity, assume that torsion will be resisted by the 15-foot-long stairwell walls in the transverse direction. The forces for each of the longitudinal walls are shown in Figure 11.2-2.
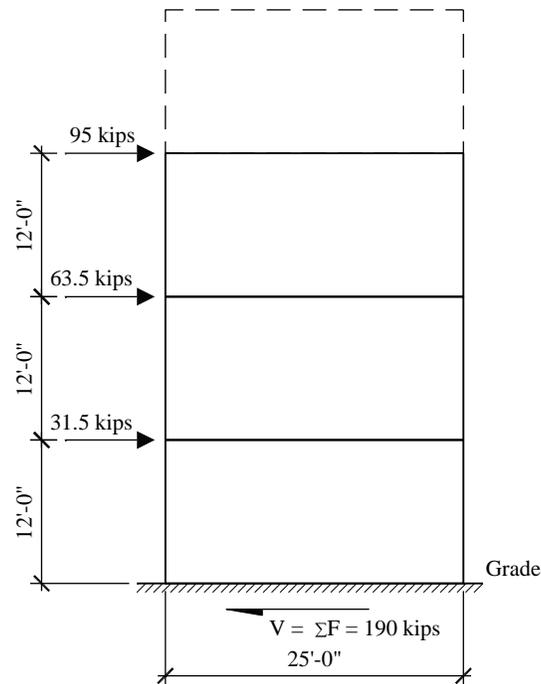
Figure 11.2-2 Forces on the longitudinal walls
(1.0 kip = 4.45 kN, 1.0 ft = 0.3048 m)

11.2.4.4.2 Transverse Direction. Design the four 15-foot-long stairwell walls for the total shear including 5 percent accidental torsion (*Standard* Section 12.8.4.2). A rough approximation is used in place of a more rigorous analysis considering all of the walls. The maximum force on the walls is computed as follows:

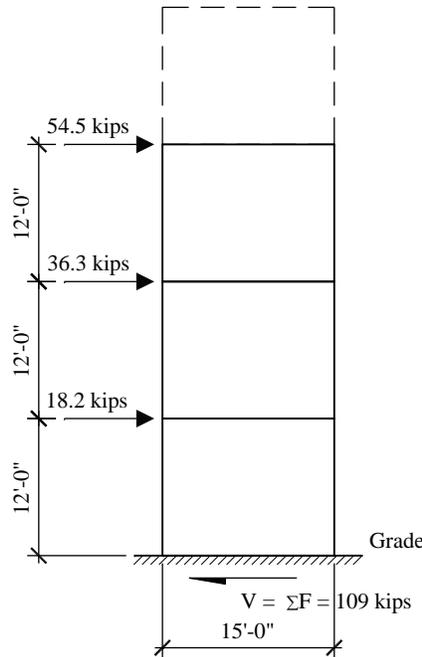$V = 380/4 + 380(0.05)(150)/[(100 \text{ ft moment arm}) \times (2 \text{ walls in each set})] = 109$ kips

Thus:

$F_r = 109(0.50) = 54.5$ kips

$F_3 = 109(0.333) = 36.3$ kips

$F_2 = 109(0.167) = 18.2$ kips

Seismic forces on the transverse walls of the stairwells are shown in Figure 11.2-3.

Figure 11.2-3 Forces on the transverse walls
(1.0 kip = 4.45 kN, 1.0 ft = 0.3048 m)

11.2.5 Proportioning and Detailing

The strength of members and components is determined using the strengths permitted and required in ACI 318 Chapters 1 through 17 and 19 through 26, plus Sections 18.2.2 and 18.5.

11.2.5.1 Overturning Moment and End Reinforcement. Design shear panels to resist overturning by means of reinforcing bars at each end with a direct tension coupler at the joints. A commonly used alternative is a threaded post-tensioning (PT) bar inserted through the stack of panels, but the behavior is different than assumed by ACI 318 Section 18.5 since the PT bars do not yield. If PT bars are used, the system should be designed as an Ordinary Precast Shear Wall (allowed in SDC B.) For a building in a higher seismic design category, a post-tensioned wall would need to be qualified as a Special Precast Structural Wall Based on Validation Testing per 14.2.4.

11.2.5.1.1 Longitudinal Direction. The free-body diagram for the longitudinal walls is shown in Figure 11.2-4. The tension connection at the base of the precast panel to the below-grade wall is governed by the seismic overturning moment and the dead loads of the panel and supported floors and roof. In this example, the weights for an elevator penthouse, with a floor and equipment load at 180 psf between the shafts and a roof load at 20 psf, are included. The weight for the floors includes double tees, ceiling and partitions (total load of 70 psf) but not beams and columns. Floor live load is 50 psf, except 100 psf is used in the elevator lobby. Roof snow load is 30 psf. (The elevator penthouse is so small that it was ignored in computing the gross seismic forces on the building, but it is not ignored in the following calculations.)
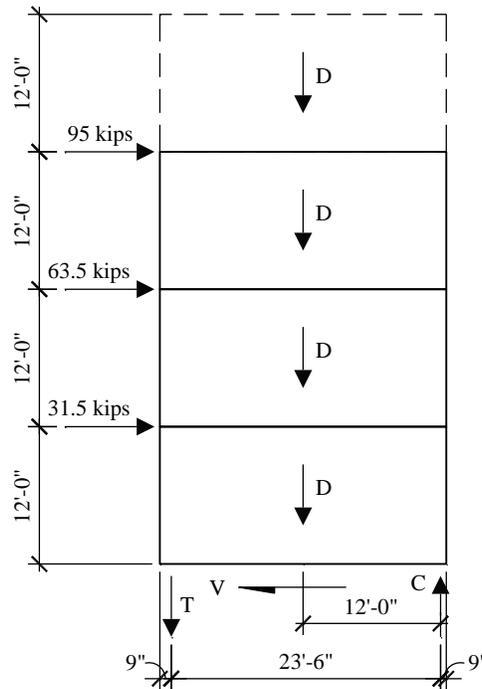
Figure 11.2-4 Free-body diagram for longitudinal walls
(1.0 kip = 4.45 kN, 1.0 ft = 0.3048 m)

At the base:

M_E = (95 kips)(36 ft) + (63.5 kips)(24 ft) + (31.5 kips)(12 ft) = 5320 ft-kips

$\sum D$ = wall + exterior floors/roof + lobby floors + penthouse floor + penthouse roof
  = (25 ft)(48 ft)(0.1 ksf) + (25 ft)(48 ft / 2)(0.070 ksf)(3) + (25 ft)(8 ft / 2)(0.070 ksf)(2)
    + (25 ft)(8 ft / 2)(0.18 ksf) + (25ft)(24 ft / 2)(0.02 ksf)
  = 120 + 126 + 14 + 18 + 6 = 284 kips

$\sum L$ = (25 ft)(48 ft / 2)(0.05 ksf)(2) + (25 ft)(8 ft / 2)(0.1 ksf) = 60 + 10 = 70 kips

$\sum S$ = (25ft)(48 ft + 24 ft)(0.03 ksf)/2 = 27 kips

Using the load combinations described above, the vertical loads for combining with the overturning moment are computed as:

P_{max} = 1.26D + 0.5L + 0.2S = 397 kips

P_{min} = 0.843D = 239 kips

The axial load is quite small for the wall panel. The average compression P_{max}/A_g = 0.165 ksi (3.3 percent of f'_c). Therefore, the tension reinforcement can easily be found from the simple couple shown in Figure 11.2-4.

The effective moment arm is:

$$jd = 25 - 1.5 = 23.5 \text{ ft}$$

and the net tension on the uplift side is:

$$T_u = \frac{M_E}{jd} - \frac{P_{min}}{2} = \frac{5320}{23.5} - \frac{239}{2} = 107 \text{ kips}$$

The required reinforcement is:

$$A_s = T_u/\phi f_y = (107 \text{ kips})/[0.9(60 \text{ ksi})] = 1.98 \text{ in.}^2$$

Use two #9 bars ($A_s = 2.0$ in.^{2}) at each end with Type 2 couplers for each bar at each panel joint. Since the flexural reinforcement must extend a minimum distance, d, (the flexural depth) beyond where it is no longer required, use both #9 bars at each end of the panel at all three levels for simplicity. Note that if it is desired to reduce the bar size up the wall, the design check of ACI 318 Section 18.5.2.2 must be applied to the flexural strength calculation at the upper wall panel joints.

At this point a check per ACI 318 Section 16.2.5 will be made. Bearing walls must have vertical ties with a nominal strength exceeding 3 kips per foot and there must be at least two ties per panel. With one tie at each end of a 25-foot panel, the demand on the tie is:

$$T_u = (3 \text{ kip/ft})(25 \text{ ft})/2 = 37.5 \text{ kips}$$

The two #9 bars are more than adequate for the ACI requirement.

Although no check for confinement of the compression boundary is required for intermediate precast shear walls, it is shown here for interest.

Since the h_w/ℓ_w ratio is less than 2.0 for this wall, the displacement based check in ACI 318 Section 18.10.6.2 does not apply. Using the alternative check from ACI 318 Section 18.10.6.3 with the compression stress as an index:

$$\sigma = \frac{P}{A} + \frac{M}{S} = \frac{389}{8(25)12} + \frac{6(5320)}{8(25)^2(12)} = 694 \text{ psi}$$

The limiting stress is $0.2f'_c$, which is 1000 psi, so no specially confined boundary zone is required at the ends of the longitudinal walls.

11.2.5.1.2 Transverse Direction. The free-body diagram of the transverse walls is shown in Figure 11.2-5. The weight of the precast concrete stairs is 100 psf and of the roof over the stairs is 70 psf.
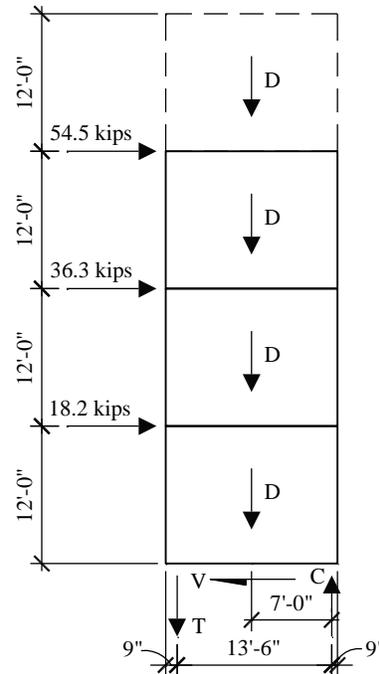
Figure 11.2-5 Free-body diagram of the transverse walls
(1.0 kip = 4.45 kN, 1.0 ft = 0.3048 m)

The transverse wall is similar to the longitudinal wall.

At the base:

M_E = (54.5 kips)(36 ft) + (36.3 kips)(24 ft) + (18.2 kips)(12 ft) = 3052 ft-kips

$\sum D$ = (15 ft)(48 ft)(0.1 ksf) + 2(12.5 ft / 2)(10 ft / 2)(0.07 ksf)(3) + (15 ft)(8 ft / 2)[(0.1 ksf)(3) + (0.07 ksf)]
    = 72 + 13 + 18 + 4 = 107 kips

$\sum L$ = 2(12.5 ft / 2)(10 ft / 2)(0.05 ksf)(2) + (15 ft)(8 ft / 2)(0.1 ksf)(3)
    = 6 + 18 = 24 kips

$\sum S$ = [2(12.5 ft / 2)(10 ft / 2) + (15 ft)(8 ft / 2)](0.03 ksf) = 3.7 kips

P_{max} = 1.26(107) + 0.5(24) + 0.2(4) = 148 kips

P_{min} = 0.843(107) = 90.5 kips

jd = 15 - 1.5 = 13.5 ft

T_u = (M_E/jd) - $P_{min}/2$ = (3052/13.5) - 90.5/2 = 181 kips

A_s = $T_u/\phi f_y$ = (181 kips)/[0.9(60 ksi)] = 3.35 in.^{2}

Use two #10 and one #9 bars (A_s = 3.54 in.^{2}) at each end of each wall with a Type 2 coupler at each bar for each panel joint. All three bars at each end of the panel will also extend up through all three levels for simplicity.

As done with the longitudinal wall, a check for confinement of the compression boundary is performed with this wall as well, even though the check is not required for intermediate walls. Since, h_w/ℓ_w ratio for the transverse wall is greater than 2.0, the displacement based check from ACI 318 Section 18.10.6.2 can be performed.

Total compression force, $A_s f_y + P_{max}$ = (3.54)(60) + 148 = 360 kips

Compression block, a = (360 kips)/[(0.85)(5 ksi)(8 in. width)] = 10.6 in.

Neutral axis depth, $c = a/(0.80)$ = 13.3 in.

The maximum depth (c) with no boundary member per ACI 318 Equation 18.10.6.2 is:

$$c < \frac{\ell_w}{600\left(1.5\delta_u / h_w\right)}$$

where the term (δ_u/h_w) shall not be taken as less than 0.005.

Once the base joint yields, it is unlikely that there will be any flexural cracking in the wall more than a few feet above the base. An analysis of the wall for the design lateral forces using 50 percent of the gross moment of inertia, ignoring the effect of axial loads and applying the C_d factor of 4 to the results gives a ratio (δ_u/h_w) less than 0.005. Using the 0.005 value in the equation above results in a c of 40 inches, far in excess of the neutral axis depth of 13.3 inches. Thus, ACI 318 would not require specially confined boundary zones even if this wall were designed as a special reinforced concrete shear wall. For those used to checking the compression stress as an index:

$$\sigma = \frac{P}{A} + \frac{M}{S} = \frac{140}{8(15)12} + \frac{6(2930)}{8(15)^2(12)} = 951 \text{ psi}$$

Since σ < 1000 psi, no transverse reinforcement is required at the ends of the transverse walls. Note how much closer to the criterion this transverse wall is by the compression stress check.

The overturning reinforcement and connection are shown in Figure 11.2-6.

8"

Direct tension
coupler-(typical)

1" shim and drypack
(typical)

8" precast wall

(2) #9 ea. end, full height
of 25' longitudinal
wall panel

(2) #10 & (1) #9 ea. end,
full ht. of 15' transverse
wall panel

Longitudinal Wall

8"

Transverse Wall

Reinforced foundation
not designed in the
example

Standard hook to develop
overturning reinforcement

25" min for #9

28" min for 10"

3" min

Development at Foundation

Figure 11.2-6 Overturning connection detail at the base of the walls
(1.0 in = 25.4 mm, 1.0 ft = 0.3048 m)

ACI 318 Section 18.5.2.2 requires that elements of the connection that are not designed to yield develop at least $1.5S_y$ of the yielding portion of the connection. This requirement applies to the anchorage of the coupled bars.

The bar in the panel is made continuous to the roof; therefore, no calculation of development length is necessary in the panel. The dowel from the foundation will be hooked; otherwise the depth of the foundation would be more than required for structural reasons. The size of the foundation will provide adequate cover to allow the 0.7 factor on ACI's standard development length for hooked bars. For the #9 bar:

$$1.5l_{dh} = \frac{1.5(0.7)(1,200)d_b}{\sqrt{f_c^{'}}} = \frac{1,260(1.128)}{\sqrt{4,000}} = 22.5 \text{ in.}$$

Similarly, for the #10 bar, the length is 25.3 inches.

Like many shear wall designs, this design does concentrate a demand for overturning resistance on the foundation. In this instance, the resistance may be provided by a large footing (on the order of 20 feet by 28 feet by 3 feet thick) under the entire stairwell or by deep piers or piles with an appropriate cap for load transfer. Refer to Chapter 7 for examples of design of each type of foundation, although not for this particular example. Note that the *Standard* permits the overturning effects at the soil-foundation interface to be reduced under certain conditions.

11.2.5.2 Shear Connections and Reinforcement. Panel joints often are designed to resist the shear force by means of shear friction, but that technique is not used for this example because the joint at the foundation will open due to flexural yielding. This opening would concentrate the shear stress on the small area of the dry-packed joint that remains in compression. This distribution can be affected by the shims used in construction. With care taken to detail the grouted joint, shear friction can provide a reliable mechanism to resist this shear. Alternatively, the joint can be designed with direct shear connectors that will prevent slip along the joint. That concept is developed here.

11.2.5.2.1 Longitudinal Direction. The design shear force is based on the yield strength of the flexural connection. The flexural strength of the connection can be approximated as follows:

$$\frac{M_n}{M_u} = \frac{A_s f_y jd + P_{max}(jd/2)}{M_E} = \frac{(2.0 \text{ in.}^2)(60 \text{ ksi})(23.5 \text{ ft}) + (397 \text{ kip})(23.5 \text{ ft}/2)}{5320 \text{ ft - kips}} = 1.41$$

Therefore, the design shear, V_u, at the base is 1.5(1.41)(190 kips) = 402 kips.

The base shear connection is shown in Figure 11.2-7 and is to be flexible vertically but stiff horizontally in the plane of the panel. The vertical flexibility is intended to minimize the contribution of these connections to overturning resistance, which would simply increase the shear demand.

(b) Side elevation

(a) Section through connection

(c) Section through embeded assembly
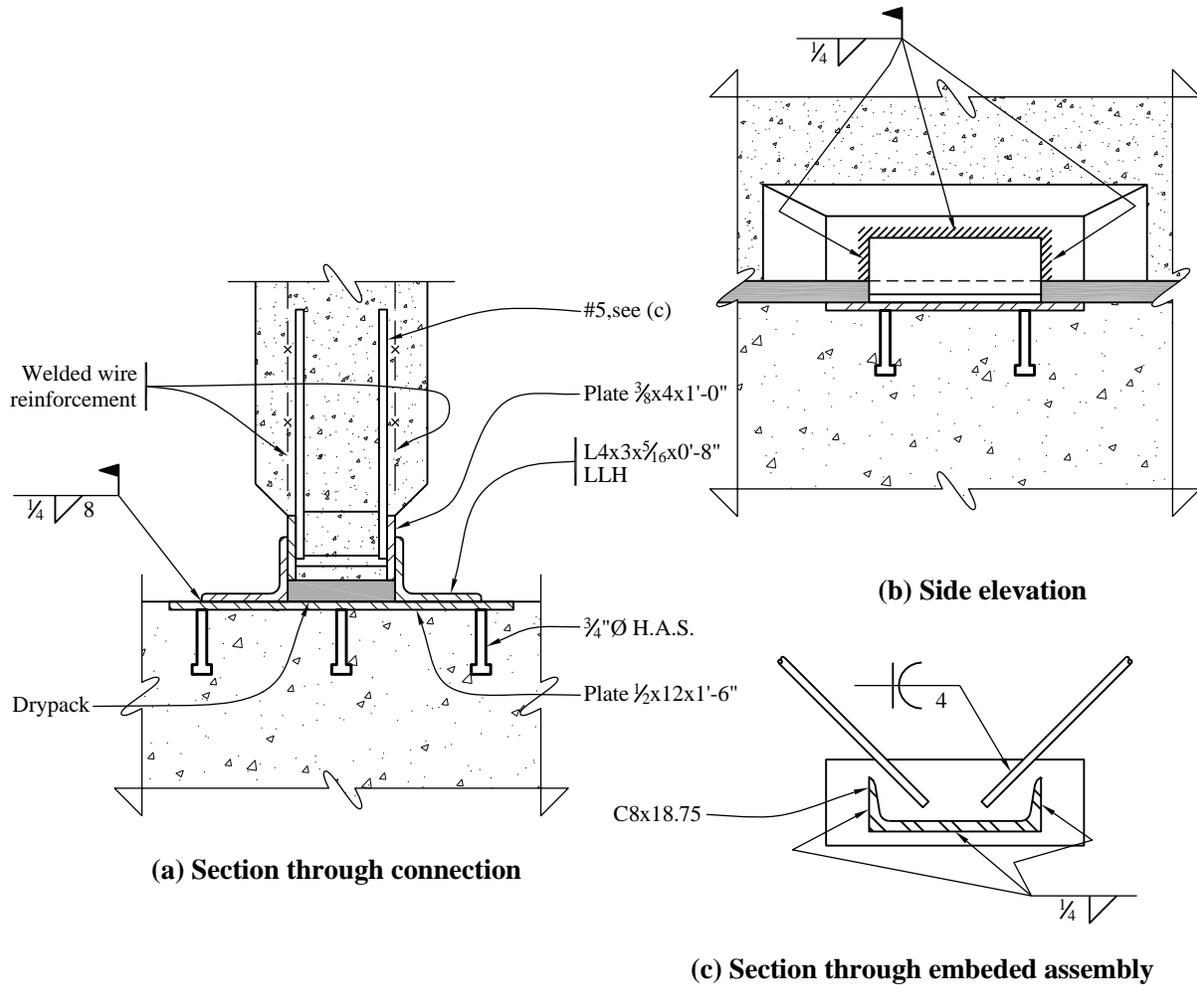
Figure 11.2-7 Shear connection at base
(1.0 in = 25.4 mm, 1.0 ft = 0.3048 m)

In the panel, provide an assembly with two face plates measuring 3/8" × 4" × 12" connected by a C8x18.75 and with diagonal #5 bars as shown in the figure. In the foundation, provide an embedded plate 1/2" × 12" × 1'-6" with six 3/4-inch-diameter headed anchor studs as shown. In the field, weld an L4×3×5/16 × 0'-8", long leg horizontal, on each face. The shear capacity of this connection is checked as follows:

Shear in the two loose angles:

$\phi V_n = \phi(0.6F_u)tl(2) = (0.75)(0.6)(58 \text{ ksi})(0.3125 \text{ in.})(8 \text{ in.})(2) = 130.5$ kips

Weld at toe of loose angles:

$\phi V_n = \phi(0.6F_u)t_el(2) = (0.75)(0.6)(70 \text{ ksi})(0.25 \text{ in. } / \sqrt{2})(8 \text{ in.})(2) = 89.1$ kips

Weld at face plates, using Table 8-8 in AISC Manual (14th edition):

$\phi V_n = \phi CC_1Dl$ (2 sides)
$\phi \quad = 0.75$

C_1 = 1.0 for E70 electrodes
L = 8 in.
D = 4 (sixteenths of an inch)
K = 2 in. / 8 in. = 0.25
a = eccentricity, summed vectorially: horizontal component is 4 in.; vertical component is 2.67 in.; thus, al = 4.80 in. and a = 4.8 in. / 8 in. = 0.6 from the table. By interpolation, C = 1.73
ϕV_n = 0.75(1.73)(1.0)(4)(8)(2) = 83.0 kips

Weld from channel to plate has at least as much capacity, but less demand.

Bearing of concrete at steel channel:

$$f_c = \phi(0.85f'_c) = 0.65(0.85)(5 \text{ ksi}) = 2.76 \text{ ksi}$$

The C8 has the following properties:

t_w = 0.487 in.
b_f = 2.53 in.
t_f = 0.39 in. (average)

The bearing will be controlled by bending in the web (because of the tapered flange, the critical flange thickness is greater than the web thickness). Conservatively ignoring the concrete's resistance to vertical deformation of the flange, compute the width (b) of flange loaded at 2.76 ksi that develops the plastic moment in the web:

$$M_p = \phi F_y t_w^2/4 = (0.9)(50 \text{ ksi})(0.487^2 \text{ in.}^2)/4 = 2.67 \text{ in-kip/in.}$$

$$M_u = f_c[(b-t_w)^2/2 - (t_w/2)^2/2] = 2.76[(b - 0.243 \text{ in.})^2 - (0.243 \text{ in.})^2]/2$$

setting the two equal results in b = 1.65 inches.

Therefore, bearing on the channel is:

$$\phi V_c = f_c(2 - t_w)(l) = (2.76 \text{ ksi})[(2(1.65) - 0.487 \text{ in.}](6 \text{ in.}) = 46.6 \text{ kips}$$

To the bearing capacity on the channel is added the four #5 diagonal bars, which are effective in tension and compression; ϕ = 0.75 for shear is used here:

$$\phi V_s = \phi f_y A_s \cos\alpha = (0.75)(60 \text{ ksi})(4)(0.31 \text{ in}^2)(\cos 45°) = 39.5 \text{ kips}$$

Thus, the total capacity for transfer to concrete is:

$$\phi V_n = \phi V_c + \phi V_s = 46.6 + 39.6 = 86.1 \text{ kips}$$

The capacity of the plate in the foundation is governed by the headed anchor studs. ACI 318 Chapter 17 has detailed information on calculating the strength of headed anchor studs. ACI 318 Section 17.2.3 has additional requirements for anchors resisting seismic forces in Seismic Design Categories C through F. Capacity in shear for anchors located far from an edge of concrete, such as these and with sufficient embedment to avoid the pryout failure mode is governed by the capacity of the steel, which is given by ACI 318 Section 17.5.1:

$\phi V_{sa} = \phi\, n\, A_{se}\, f_{uta} = (0.65)(6\text{ studs})(0.44\text{ in.}^2\text{ per stud})(60\text{ ksi}) = 103\text{ kips}$

In summary, the various shear capacities of the connection are as follows:

Shear in the two loose angles: 130.5 kips

Weld at toe of loose angles: 89.1 kips

Weld at face plates: 83.0 kips

Transfer to concrete: 86.1 kips

Headed anchor studs at foundation: 103 kips

The number of embedded plates (n) required for a panel is:

$n = 402/83.0 = 4.8$

Use five connection assemblies, equally spaced along each side (4'-0" on center works well to avoid the end reinforcement). The plates are recessed to position the #5 bars within the thickness of the panel and within the reinforcement of the panel.

It is instructive to consider how much moment capacity is added by the resistance of these connections to vertical lift at the joint. The vertical force at the tip of the angle that will create the plastic moment in the leg of the angle is:

$T = M_p/x = F_y l t^2/4\,/\,(l\text{-}k) = (36\text{ ksi})(8\text{ in.})(0.3125^2\text{ in.}^2)/4]/(4\text{ in. - }0.69\text{ in.}) = 2.12\text{ kips}$

There are five assemblies with two loose angles each, giving a total vertical force of 21 kips. The moment resistance is this force times half the length of the panel, which yields 265 ft-kips. The total demand moment, for which the entire system is proportioned, is 5320 ft-kips. Thus, these connections will add approximately 5 percent to the resistance and ignoring this contribution is reasonable. If a straight plate measuring 1/4 inch by 8 inches (which would be sufficient) were used and if the welds and foundation embedment did not fail first, the tensile capacity would be 72 kips each, a factor of 34 increase over the angles and the shear connections would have the unintended effect of more than doubling the flexural resistance, which would require a much higher shear resistance to develop a plastic hinge at the wall base.

Using ACI 318 Section 11.5.4, check the shear strength of the precast panel at the first floor:

$\phi V_c = \phi 2 A_{cv} \sqrt{f_c'}\, hd = 0.75(2)\sqrt{5000}\,(8)(23.5)(12) = 239\text{ kips}$

Because $\phi V_c \ge V_u = 190$ kips, the wall is adequate for shear without even considering the reinforcement. Note that the shear strength of the wall itself is not governed by the overstrength required for the connection. However, since $V_u \ge 0.5\phi V_c = 120$ kips, ACI 318 Section 11.6.2 requires minimum wall reinforcement as shown below:

$\rho_t = 0.0025$

ρ_ℓ = the greater of 0.0025, and
$\qquad 0.0025 + 0.5(2.5 - h_w/\ell_w)(\rho_t - 0.0025) = 0.0025,$

For the minimum required $\rho_t = \rho_\ell = 0.0025$, the required reinforcement is:

   $A_v = 0.0025(8)(12) = 0.24$ in²/ft

As before, use two layers of welded wire reinforcement, WWF 4×4 - W4.0×W4.0, one on each face. The shear reinforcement provided is:

   $A_v = 0.12(2) = 0.24$ in.²/ft

Next, compute the required connection capacity at Level 2. Even though the end reinforcing at the base extends to the top of the shear wall, the connection still needs to be checked for flexure in accordance with *Standard* Section 14.2.2.4 (ACI 318 Section 18.5). At Level 2:

   $M_E = (95$ kips$)(24$ ft$) + (63.5$ kips$)(12$ ft$) = 3,042$ ft-kips

There are two possible approaches to the design of the joint at Level 2.

First, if Type 2 couplers are used at the Level 2 flexural connection, then the connection can be considered to have been "designed to yield," and no overstrength is required for the design of the flexural connection. In this case, the bars are designed for the moment demand at the Level 2 joint.

Alternately, if a non-yielding connection is used at the Level 2 connection, then to meet the requirements of *Standard* Section 14.2.2.4 (ACI 318 Section 18.5), the flexural strength of the connection at Level 2 must be $1.5S_y$ of the yielding portion of the connection or:

   $M_u = 1.5(1.41)M_E = 1.5(1.41)(3,042$ ft-kips$) = 6,433$ ft-kips

At Level 2, the gravity loads on the wall are:

   $\sum D$ = wall + exterior floors/roof + lobby floors + penthouse floor + penthouse roof
       $= (25$ ft$)(36$ ft$)(0.1$ ksf$) + (25$ ft$)(48$ ft $/ 2)(0.070$ ksf$)(2) + (25$ ft$)(8$ ft $/ 2)(0.070$ ksf$)(1) +$
       $(25$ ft$)(8$ ft $/ 2)(0.18$ ksf$) + (25$ ft $)(24$ ft $/ 2)(0.02$ ksf$)$
       $= 90 + 84 + 7 + 18 + 6 = 205$ kips

   $\sum L = (25$ ft $)(48$ ft $/ 2)(0.05$ ksf$)(1) + (25$ ft$)(8$ ft $/ 2)(0.1$ ksf$) = 30 + 10 = 40$ kips

   $\sum S = (25$ft$)(48$ ft $+ 24$ ft$)(0.03$ ksf$)/2 = 27$ kips

   $P_{max} = 1.26(205) + 0.5(40) + 0.2(27) = 285$ kips

   $P_{min} = 0.843(205) = 173$ kips

Note that since the maximum axial load was used to determine the maximum yield strength of the base moment connection, the maximum axial load is used here to determine the nominal strength of the Level 2 connection. For completeness, the base moment overstrength provided should be checked using the minimum axial load as well and compared to the moment strength at Level 2 using the minimum axial load.

   $\phi M_n = 0.9\left[A_s f_y jd + P_{max}(jd/2)\right] = 0.9\left[(2.0 \text{ in.}^2)(60 \text{ ksi})(23.5 \text{ ft}) + (285 \text{ kips})(23.5 \text{ ft}/2)\right] = 5552$ ft - kips

Therefore, the non-yielding flexural connection at Level 2 must be strengthened.

Provide:
   11-48

$$T_u = \frac{M_u}{jd} - \frac{P_{min}}{2} = \frac{6433}{23.5} - \frac{285}{2} = 131 \text{ kips}$$

The required reinforcement is:

$$A_s = T_u / \phi f_y = (131 \text{ kips})/[0.9(60 \text{ ksi})] = 2.43 \text{ in.}^2$$

In addition to the two #9 bars that extend to the roof, provide one #6 bar developed into the wall panel above and below the joint. Note that no increase on the development length for the #6 bar is required for this connection since the connection itself has been designed for the loads to promote base yielding per Standard Section 14.2.2.4 (ACI 318 Section 18.5).

Since the Level 2 connection is prevented from yielding, shear friction can reasonably be used to resist shear sliding at this location. Also, because of the lack of flexural yield at the joint, it is not necessary to make the shear connection flexible with respect to vertical movement should an embedded plate detail be desired.

The design shear for this location is:

$$V_{u,Level\,2} = 1.5(1.41)(95+63.5) = 335 \text{ kips}$$

Using the same recessed embedded plate assemblies in the panel as at the base, but welded with a straight plate, the number of plates, *n, is* 335/83.0 = 4.04. Use four plates, equally spaced along each side.

Figure 11.2-8 shows the shear connection at the second and third floors of the longitudinal precast concrete shear wall panels.
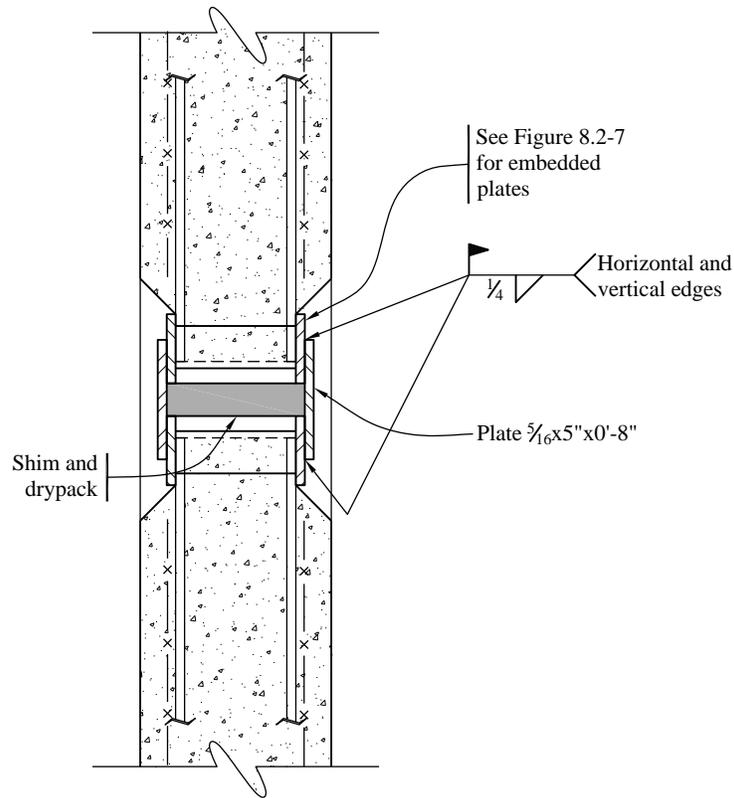
Figure 11.2-8 Shear connections on each side of the wall at the second and third floors
(1.0 in = 25.4 mm)

11.3 ONE-STORY PRECAST SHEAR WALL BUILDING

This example illustrates the design of a precast concrete shear wall for a single-story building in a region of high seismicity. For buildings assigned to Seismic Design Category D, ACI 318 Section 18.11 requires that special structural walls constructed of precast concrete meet the requirements of ACI 318 Section 18.10, in addition to the requirements for intermediate precast structural walls. Alternately, special structural walls constructed using precast concrete are allowed if they satisfy the requirements of ACI ITG-5.1, *Acceptance Criteria for Special Unbonded Post-Tensioned Precast Structural Walls Based on Validation Testing (ACI ITG 5.1-07)*. Design requirements for one such type of wall have been developed by ACI ITG 5 and have been published by ACI as *Requirements for Design of a Special Unbonded Post-Tensioned Precast Shear Wall Satisfying ACI ITG-5.1 (ACI ITG 5.2-09)*. ITG 5.1 and ITG 5.2 describe requirements for precast walls for which a self-centering mechanism is provided by post-tensioning located concentrically within the wall.

11.3.1 Building Description

The precast concrete building is a single-story industrial warehouse building (Risk Category II) on Site Class C soils. The structure has 8-foot-wide by 12.5-inch-deep prestressed double tee (DT) wall panels. The roof is light gage metal decking spanning to bar joists that are spaced at 4 feet on center to match the location of the DT legs. The center supports for the joists are joist girders spanning 40 feet to steel tube columns. The vertical seismic force-resisting system is the precast/prestressed DT wall panels located around the perimeter of the building. The average roof height is 20 feet and there is a 3-foot parapet. Figure 11.3-1 shows the plan of the building, which is regular.
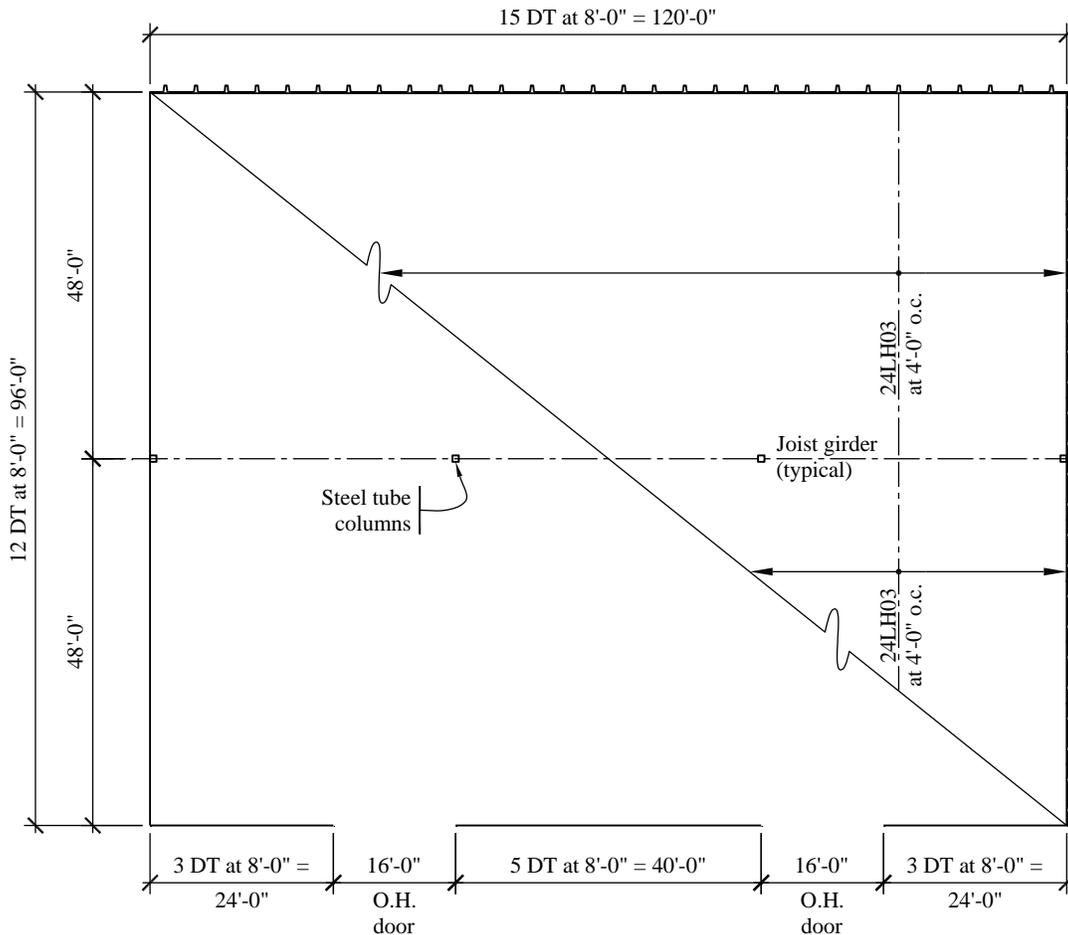
Figure 11.3-1 Single-story industrial warehouse building plan
(1.0 ft = 0.3048 m)

The precast wall panels used in this building are typical DT wall panels commonly found in many locations but not normally used in southern California. For these wall panels, an extra 1/2 inch has been added to the thickness of the deck (flange). This extra thickness is intended to reduce cracking of the flanges and provide cover for the bars used in the deck at the base. The use of thicker flanges is addressed later.

The wall panels are normal-weight concrete with a 28-day compressive strength of $f'c$ = 5000 psi. Reinforcing bars used in the welded connections of the panels and footings are ASTM A706 (60 ksi). The concrete for the foundations has a 28-day compressive strength of $f'c$ = 4,000 psi.

In *Standard* Table 12.2-1 the values for special reinforced concrete shear walls are for both cast-in-place and precast walls. In Section 2.3, ACI 318 defines a special structural wall as "a cast-in-place structural wall in accordance with 18.2.3 through 18.2.8 and 18.10; or a precast structural wall in accordance with 18.2.3 through 18.2.8 and 18.11." ACI 318 Section 18.11 defines requirements for special structural walls constructed using precast concrete, including that the wall must satisfy all of the requirements of ACI 318 Section 18.10.

Unfortunately, several of the requirements of ACI 318 Section 18.10 are problematic for a shear wall system constructed using DT wall panels. These include the following:

1.   ACI 318 Section 18.10.2.1 requires reinforcement to be spaced no more than 18 inches on center and be continuous. This would require splices to the foundation along the DT flange.

2.   ACI 318 Section 21.9.2.2 requires two curtains of reinforcement for walls with shear stress greater than $2\lambda\sqrt{f'c}$ or for walls with $h_w/\ell_w \geq 2.0$. When a wall meets any of these conditions, placing two layers of reinforcing in a DT flange would be a challenge.

3.   ACI 318 Section 18.2.6, by referencing Section 20.2.2, allows only nonprestressing steel in the special precast shear walls, and excludes the use of prestressing steel. The only exception to this is found in ACI 318 Section 18.11.2.2.

Therefore, these walls will be designed using the ACI category of intermediate precast structural walls.

11.3.2 Design Requirements

11.3.2.1 Seismic Parameters of the *Provisions*. The basic parameters affecting the design and detailing of the building are shown in Table 11.3-1.

11.3.2.2 Structural Design Considerations

11.3.2.2.1 Intermediate Precast Structural Walls Constructed Using Precast Concrete. The intent of the intermediate precast structural wall requirements is to provide yielding in a dry connection in flexure at the base of each precast shear wall panel while maintaining significant shear resistance in the connection. The flexural connection for a wall panel at the base is located in one DT leg while the connection at the other leg is used for compression. Per ACI 318 Section 18.5, these connections must yield only in steel elements or reinforcement and all other elements of the connection (including shear resistance) must be designed for 1.5 times the force associated with the flexural yield strength of the connection.

Yielding will develop in the dry connection at the base by bending in the horizontal leg of the steel angle welded between the embedded plates of the DT and footing. The horizontal leg of this angle is designed in a manner to resist the seismic tension of the shear wall due to overturning and then yield and deform inelastically. The connections on the two legs of the DT are each designed to resist 50 percent of the shear. The anchorage of the connection into the concrete is designed to satisfy the $1.5S_y$ requirements of ACI 318 Section 18.5.2.2. Careful attention to structural details of these connections is required to ensure tension ductility and resistance to large shear forces that are applied to the embedded plates in the DT and footing.

11.3.2.2.2 Building System. The height limit in Seismic Design Category D (*Standard* Table 12.2-1) is 40 feet.

Table 11.3-1 Design Parameters

Design Parameter	Value
Risk Category II	$I_e = 1.0$
S_S	1.5
S_1	0.60
Site Class	C
F_a	1.0
F_v	1.3
$S_{MS} = F_a S_S$	1.5
$S_{M1} = F_v S_1$	0.78
$S_{DS} = 2/3\ S_{MS}$	1.0
$S_{D1} = 2/3\ S_{M1}$	0.52
Seismic Design Category	D
Basic Seismic Force-Resisting System	Bearing Wall System
Wall Type	Intermediate Precast Structural Wall
R	4
Ω_0	2.5
C_d	4

The metal deck roof acts as a flexible horizontal diaphragm to distribute seismic inertia forces to the walls parallel to the direction of earthquake motion *(Standard* Section 12.3.1.1).

The building is regular both in plan and elevation.

The redundancy factor, ρ, is determined in accordance with *Standard* Section 12.3.4.2. For this structure, which is regular and has more than two perimeter wall panels (bays) on each side in each direction, $\rho = 1.0$.

The structural analysis to be used is the ELF procedure *(Standard* Section 12.8) as permitted by *Standard* Table 12.6-1.

Orthogonal load combinations are not required for flexible diaphragms in Seismic Design Category D *(Standard* Section 12.5.4).

This example does not include design of the foundation system, the metal deck diaphragm, or the nonstructural elements.

Ties, continuity and anchorage *(Standard* 12.11) must be considered explicitly when detailing connections between the roof and the wall panels. This example does not include the design of those connections, but sketches of details are provided to guide the design engineer.

There are no drift limits for single-story buildings as long as they are designed to accommodate predicted lateral displacements *(Standard* Table 12.12-1, Footnote c).

Load Combinations

The basic load combinations (*Standard* Section 12.4.2.3) require that seismic forces and gravity loads be combined in accordance with the following factored load combinations:

$(1.2 + 0.2S_{DS})D \pm \rho Q_E + 0.5L + 0.2S$

$(0.9 - 0.2S_{DS})D \pm \rho Q_E + 1.6H$

At this flat site, both S and H equal 0. Note that roof live load need not be combined with seismic loads, so the live load term, L, can be omitted from the equation. Therefore:

$1.4D + \rho Q_E$

$0.7D - \rho Q_E$

These load combinations are for the in-plane direction of the shear walls.

11.3.3 Seismic Force Analysis

11.3.4.1 Weight Calculations. Compute the weight tributary to the roof diaphragm:

Roofing	=	2.0 psf
Metal decking	=	1.8 psf
Insulation	=	1.5 psf
Lights, mechanical, sprinkler system, etc.	=	3.2 psf
Bar joists	=	2.7 psf
Joist girder and columns	=	0.8 psf
Total	=	12.0 psf

The total weight of the roof is computed as:

$(120 \text{ ft} \times 96 \text{ ft})(12 \text{ psf} / 1000) = 138 \text{ kips}$

The exterior DT wall weight tributary to the roof is:

$(20 \text{ ft} / 2 + 3 \text{ ft})[42 \text{ psf} / 1000](120 \text{ ft} + 96 \text{ ft})2 = 236 \text{ kips}$

Total building weight for seismic lateral load, $W = 138 + 236 = 374 \text{ kips}$

11.3.4.2 Base Shear. The seismic response coefficient (C_s) is computed using *Standard* Equation 12.8-2 as:

$$C_S = \frac{S_{DS}}{R/I_e} = \frac{1.0}{4/1} = 0.25$$

except that it need not exceed the value from *Standard* Equation 12.8-3, as follows:

$$C_S = \frac{S_{D1}}{T(R/I_e)} = \frac{0.52}{0.189(4/1)} = 0.69$$

where T is the fundamental period of the building computed using the approximate method of *Standard* Equation 12.8-7:

11-54

$$T_a = C_r h_n^x = (0.02)(20.0)^{0.75} = 0.189 \text{ sec}$$

Therefore, use $C_s = 0.25$, which is larger than the minimum specified in *Standard* Equation 12.8-5:

$$C_s = 0.044(S_{DS})(I_e) \geq 0.01 = 0.044(1.0)(1.0) = 0.044$$

The total seismic base shear is then calculated using *Standard* Equation 12.8-1, as:

$$V = C_s W = (0.25)(374) = 93.5 \text{ kips}$$

11.3.4.3 Horizontal Shear Distribution and Torsion. Torsion is not considered in the shear distribution in buildings with flexible diaphragms. The shear along each side of the building will be equal, based on a tributary area force distribution.

11.3.4.3.1 Longitudinal Direction. The total shear along each side of the building is $V/2 = 46.75$ kips. The maximum shear on longitudinal panels (at the side with the openings) is:

$$V_{lu} = 46.75/11 = 4.25 \text{ kips}$$

On each side, each longitudinal wall panel resists the same shear force as shown in the free-body diagram of Figure 11.3-2, where D_1 represents roof joist reactions and D_2 is the panel weight.

11.3.4.3.2 Transverse Direction. Seismic forces on the transverse wall panels are all equal and are:

$$V_{tu} = 46.75/12 = 3.90 \text{ kips}$$

Figure 11.3-3 shows the transverse wall panel free-body diagram.

Note the assumption of uniform distribution to the wall panels in a line requires that the roof diaphragm be provided with a collector element along its edge. The chord designed for diaphragm action in the perpendicular direction will normally be capable of fulfilling this function, but an explicit check should be made in the design.
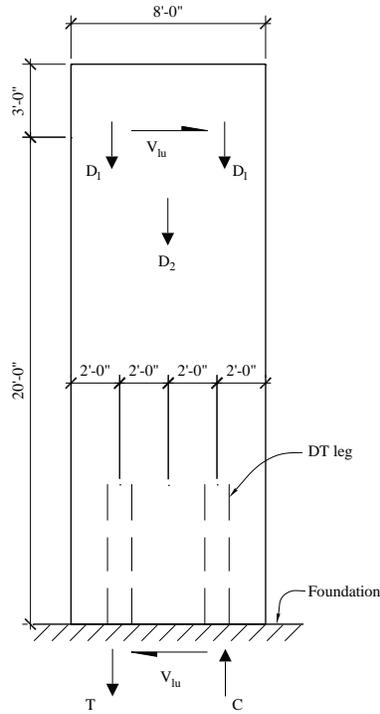
Figure 11.3-2 Free-body diagram of a panel in the longitudinal direction
(1.0 ft = 0.3048 m)
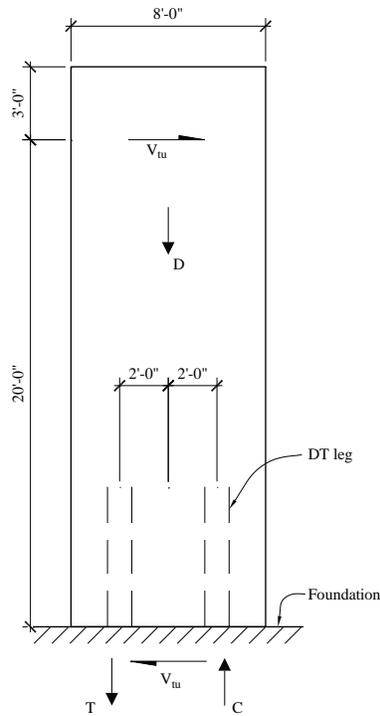
Figure 11.3-3 Free-body diagram of a panel in the transverse direction
(1.0 ft = 0.3048 m)

11.3.5 Proportioning and Detailing

The strength of members and components is determined using the strengths permitted and required in ACI 318 including Chapter 18.

11.3.5.1 Tension and Shear Forces at the Panel Base. Design each precast shear panel to resist the seismic overturning moment by means of a ductile tension connector at the base of the panel. A steel angle connector will be provided at the connection of each leg of the DT panel to the concrete footing. The horizontal leg of the angle is designed to yield in bending as needed in an earthquake. ACI 318 Section 18.5 requires that dry connections at locations of nonlinear action comply with applicable requirements of monolithic concrete construction and satisfy both of the following:

1. Where the moment action on the connection is assumed equal to $1.5M_y$, the co-existing forces on all other components of the connection other than the yielding element shall not exceed their design strength.

2. The nominal shear strength for the connection shall not be less than the shear associated with the development of $1.5M_y$ at the connection.

11.3.5.1.1 Longitudinal Direction. Use the free-body diagram shown in Figure 11.3-2. The maximum tension for the connection at the base of the precast panel to the concrete footing is governed by the seismic overturning moment and the dead loads of the panel and the roof. The weight for the roof is 11.2 psf, which excludes the joist girders and columns.

At the base:

$$M_E = (4.25 \text{ kips})(20 \text{ ft}) = 85.0 \text{ ft-kips}$$

Dead loads:

$$D_1 = \left(11.2/1000\right)\left(\frac{48}{2}\right)4 = 1.08 \text{ kips}$$

$$D_2 = 0.042(23)(8) = 7.73 \text{ kips}$$

$$\Sigma D = 2(1.08) + 7.73 = 9.89 \text{ kips}$$

$$1.4D = 13.8 \text{ kips}$$

$$0.7D = 6.92 \text{ kips}$$

Compute the tension force due to net overturning based on an effective moment arm, d, of 4.0 feet (the distance between the DT legs). The maximum is found when combined with $0.7D$:

$$T_u = M_E/d - 0.7D/2 = 85.0/4 - 6.92/2 = 17.8 \text{ kips}$$

11.3.5.1.2 Transverse Direction. For the transverse direction, use the free-body diagram of Figure 11.3-3. The maximum tension for connection at the base of the precast panel to the concrete footing is governed by the seismic overturning moment and the dead loads of just the panel. No load from the roof is included, since it is negligible.

At the base:

$M_E = (3.90 \text{ kips})(20 \text{ ft}) = 78.0 \text{ ft-kips}$

The dead load of the panel (as computed above) is $D_2 = 7.73$ kips and $0.7D = 5.41$ kips.

The tension force is computed as above for $d = 4.0$ feet (the distance between the DT legs):

$T_u = 78.0/4 - 5.41/2 = 16.8 \text{ kips}$

This tension force is less than that at the longitudinal wall panels. Use the tension force of the longitudinal wall panels for the design of the angle connections.

11.3.5.2 Size the Yielding Angle. The angle, which is the ductile element of the connection, is welded between the plates embedded in the DT leg and the footing. This angle is an L5×3-1/2×3/4 × 0'-6-1/2" with the long leg vertical. The steel for the angle and embedded plates will be ASTM A572, Grade 50. The horizontal leg of the angle needs to be long enough to provide significant displacement at the roof, although this is not stated as a requirement in a code or standard. This will be examined briefly here. The angle and its welds are shown in Figure 11.3-4.
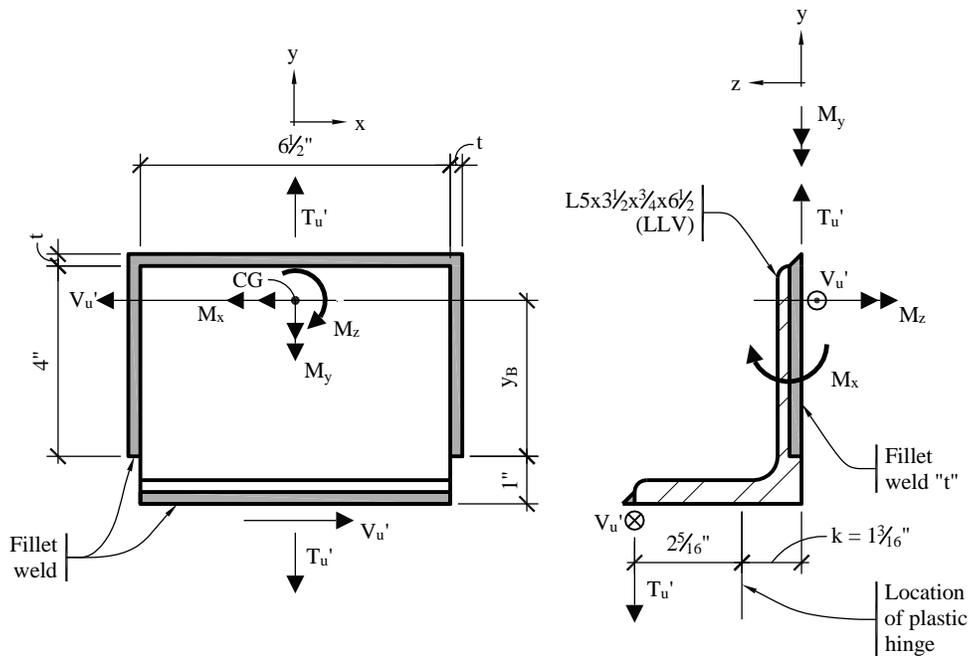
Figure 11.3-4 Free-body of the angle and the fillet weld connecting the embedded plates in the DT and the footing (elevation and section)
(1.0 in = 25.4 mm)

The location of the plastic hinge in the angle is at the toe of the fillet (at a distance, *k,* from the heel of the angle.) The bending moment at this location is:

$M_u = T_u(3.5 - k) = 17.8(3.5 - 1.1875) = 41.2 \text{ in.-kips}$

$$\phi_b M_n = 0.9 F_y Z = 0.9(50) \left[\frac{6.5(0.75)^2}{4} \right] = 41.1 \text{ in.-kips}$$

Provid
of the assembly. Using ACI 318 Section 18.5.2.2, the tension force for the remainder of this connection and the balance of the wall design are based upon a probable strength equal to 150 percent of the yield strength. Thus:

$$T_{pr} = \frac{M_n(1.5)}{3.5 - k} = \frac{(50)(6.5)(0.75)^2 / 4}{0.9(3.5 - 1.1875)} \times 1.5 = 27.0 \text{ kips}$$

The amplifier, required for the design of the balance of the connection, is:

$$\frac{T_{pr}}{T_u} = \frac{27.0}{17.8} = 1.52$$

The shear on the connection associated with this force in the angle is:

$$V_{pr} = V_E \frac{T_{pr}}{T_u} = 4.25 \times 1.52 = 6.46 \text{ kips}$$

Check the welds for the tension force of 27.0 kips and a shear force 6.46 kips.

The *Provisions* Section 14.2.2.4 (ACI 318 Section 18.5) requires that connections that are designed to yield be capable of maintaining 80 percent of their design strength at the deformation induced by the design displacement. For yielding of a flat bar (angle leg), this can be checked by calculating the ductility capacity of the bar and comparing it to C_d. Note that the element ductility demand (to be calculated below for the yielding angle) and the system ductility, C_d, are only equal if the balance of the system is rigid. This is a reasonable assumption for the intermediate precast structural wall system described in this example.

The idealized yield deformation of the angle can be calculated as follows:

$$P_y = \frac{M_n}{L} = \frac{50(6.5)(0.75^2) / 4}{2.25} = 19.8 \text{ kips}$$

$$\Delta_{y,idealized} = \frac{P_y L^3}{3EI} = \frac{19.83(2.31^3)}{3(29,000)(6.5 \times 0.75^3 / 12)} = 0.012 \text{ in.}$$

It is conservative to limit the maximum strain in the bar to $\varepsilon_{sh} = 15\varepsilon_y$. At this strain, a flat bar would be expected to retain all its strength and thus meet the requirement of maintaining 80 percent of its strength.

Assuming a plastic hinge length equal to the section thickness:

$$\phi_p = \frac{15\varepsilon_y}{d / 2} = \frac{15(50 / 29,000)}{0.75 / 2} = 0.06897$$

$$\Delta_{sh} = \phi_p L_p \left(L - \frac{L_p}{2} \right) + \Delta_y = 0.06897(0.75) \left(2.31 - \frac{0.75}{2} \right) + 0.012 \ = 0.112 \text{ in.}$$

Since the ductility capacity at strain hardening is $0.112/0.012 = 9.3$ is larger than $C_d = 4$ for this system, the requirement of *Provision* Section 14.2.2.4 (ACI 318 Section 18.5) is met.

11.3.5.3 Welds to Connection Angle. Welds will be fillet welds using E70 electrodes.

For the base metal, $\phi R_n = \phi(F_y)A_{BM}$.

For which the limiting stress is $\phi F_y = 0.9(50) = 45.0$ ksi.

For the weld metal, $\phi R_n = \phi(F_y)A_w = 0.75(0.6)70(0.707)A_w$.

For which the limiting stress is 22.3 ksi.

Size a fillet weld, 6.5 inches long at the angle to the embedded plate in the footing. Using an elastic approach:

Resultant force $= \sqrt{V_{pr}^2 + T_{pr}^2} = \sqrt{6.46^2 + 27.0^2} = 27.8$ kips

$A_w = 27.8/22.3 = 1.24$ in.^{2}

$t = A_w/l = 1.24$ in.^{2} / 6.5 in. $= 0.19$ in.

For a 3/4 inch angle leg, use a 5/16-inch fillet weld. Given the importance of this weld, increasing the size to 3/8 inch would be a reasonable step. With ordinary quality control to avoid flaws, increasing the strength of this weld by such an amount should not have a detrimental effect elsewhere in the connection.

Now size the weld to the plate in the DT. Continue to use the conservative elastic method to calculate weld stresses. Try a fillet weld 6.5 inches long across the top and 4 inches long on each vertical leg of the angle. Using the free-body diagram of Figure 11.3-4 for tension and Figure 11.3-5 for shear, the weld moments and stresses are:

$M_x = T_{pr}(3.5) = 27.0(3.5) = 94.5$ in.-kips
$M_y = V_{pr}(3.5) = (6.46)(3.5) = 22.6$ in.-kips
$M_z = V_{pr}(y_b + 1.0)$
    $= 6.46(2.77 + 1.0) = 24.4$ in.-kips
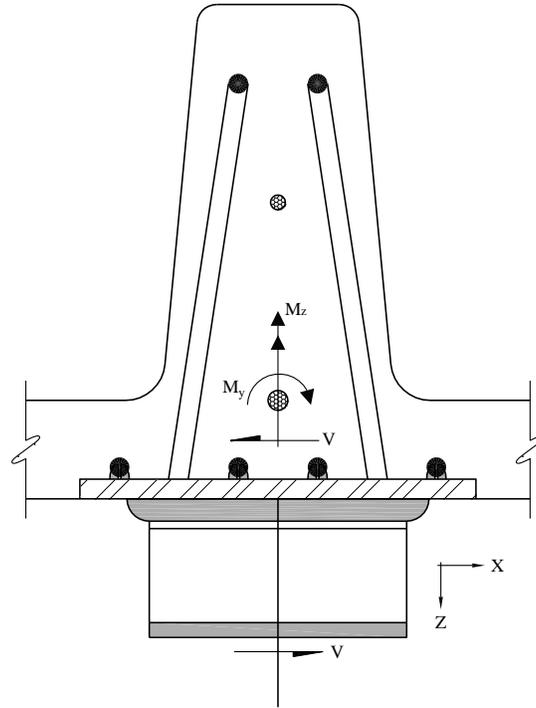
Figure 11.3-5 Free-body of angle with welds, top view, showing only shear forces and resisting moments

For the weld between the angle and the embedded plate in the DT as shown in Figure 11.3-5, the section properties for a weld leg (t) are:

$A = 14.5t$ in.^{2}

$I_x = 25.0t$ in.^{4}

$I_y = 107.4t$ in.^{4}

$I_p = I_x + I_y = 132.4t$ in.^{4}

$y_b = 2.90$ in.

$x_L = 3.25$ in.

To check the weld, stresses are computed at all four ends (and corners). The maximum stress is at the lower right end of the inverted "U" shown in Figure 11.3-4.

$$\sigma_x = \frac{V_{pr}}{A} + \frac{M_z y_b}{I_p} = \frac{6.46}{14.5t} + \frac{(24.4)(2.90)}{132.4t} = \frac{0.98}{t} \text{ ksi}$$

$$\sigma_y = -\frac{T_{pr}}{A} + \frac{M_z x_L}{I_p} = -\frac{27.0}{14.5t} + \frac{(24.4)(3.25)}{132.4t} = \frac{-1.26}{t} \text{ ksi}$$

$$\sigma_z = -\frac{M_y x_L}{A} - \frac{M_z y_b}{I_p} = -\frac{(22.6)(3.25)}{107.4t} - \frac{(94.5)(2.90)}{25.0t} = \frac{-11.8}{t} \text{ ksi}$$

$$\sigma_R = \sqrt{\sigma_x^2 + \sigma_y^2 + \sigma_z^2} = \frac{1}{t}\sqrt{0.98^2 + 1.26^2 + 11.8^2} = \frac{11.9}{t} \text{ ksi}$$

Thus, $t = 11.9/22.3 = 0.53$ inch, which can be taken as 9/16 inch. Field welds are conservatively sized with the elastic method for simplicity and to minimize construction issues.

11.3.5.4 Panel Reinforcement. Check the maximum compressive stress in the DT leg. Note that for an intermediate precast structural wall, ACI 318 Section 18.10.6 does not apply and transverse boundary element reinforcing is not required. However, the cross section must be designed for the loads associated with 1.5 times the moment that yields the base connectors.

Figure 11.3-6 shows the cross section used. The section is limited by the area of dry-pack under the DT at the footing.
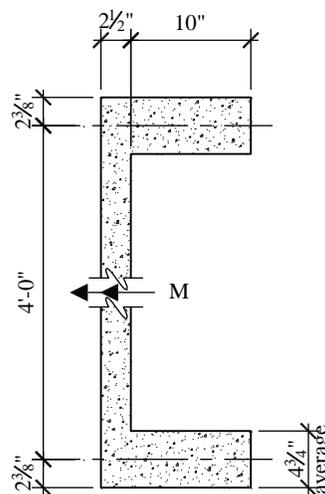
Figure 11.3-6 Cross section of the DT dry-packed at the footing
(1.0 in = 25.4 mm, 1.0 ft = 0.3048 m)

The reason to limit the area of dry-pack at the footing is to locate the boundary elements in the legs of the DT, at least at the bottom of the panel. The flange between the legs of the DT is not as susceptible to cracking during transportation as are the corners of DT flanges outside the confines of the legs. The compressive stress due to the overturning moment at the top of the footing and dead load is:

$A = 227 \text{ in.}^2$

$S = 3240 \text{ in.}^3$

$$\sigma_z = \frac{P}{A} + \frac{M_E}{S} = \frac{13,800}{227} + \frac{1.52(85,000 \times 12)}{3240} = 539 \text{ ksi}$$

Roof live loads need not be included as a factored axial load in the compressive stress check, but the force from the prestressing steel will be added to the compression stress above because the prestress force will be effective a few feet above the base and will add compression to the DT leg. Each leg of the DT will be reinforced with one 1/2-inch-diameter strand and one 3/8-inch-diameter strand. Figure 11.3-7 shows the location of these prestressed strands.
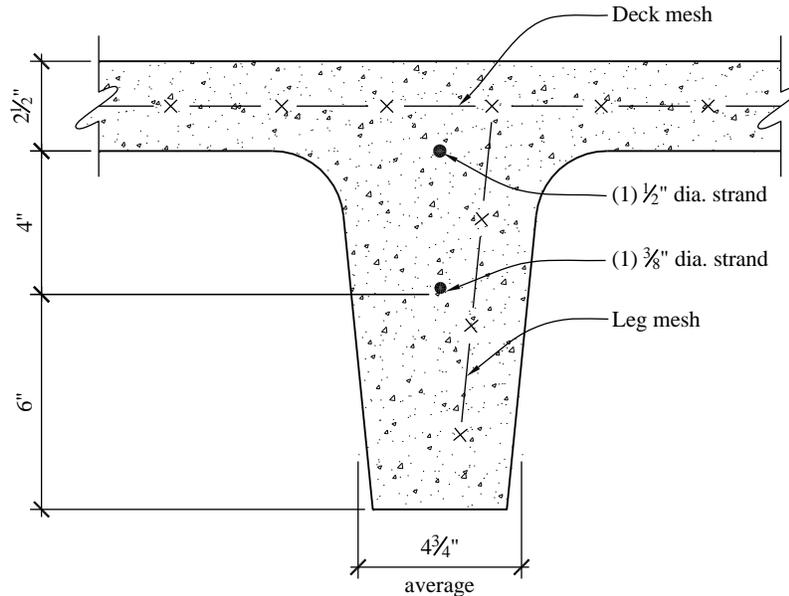
**Figure 11.3-7 Cross section of one DT leg showing the location of
the bonded prestressing tendons or strand**
(1.0 in = 25.4 mm, 1.0 ft = 0.3048 m)

Next, compute the compressive stress resulting from these strands. Note that the moment at the height of strand development above the footing, about 26 inches for the effective stress (f_{se}), is less than at the top of footing. This reduces the compressive stress by:

$$\frac{(4.25)(26)}{3240} \times 1000 = 34 \text{ psi}$$

In each leg, use:

$P = 0.58f_{pu}A_{ps} = 0.58(270 \text{ ksi})[0.153 + 0.085] = 37.3 \text{ kips}$

$A = 168 \text{ in.}^2$

$e = y_b - CG_{Strand} = 9.48 - 8.57 = 0.91 \text{ in.}$

$S_b = 189 \text{ in.}^3$

$$\sigma = \frac{P}{A} + \frac{Pe}{S} = \frac{37,300}{168} + \frac{0.91(37,300)}{189} = 402 \text{ psi}$$

Therefore, the total compressive stress is approximately 539 + 402 - 34 = 907 psi.

Since yielding is restricted to the steel angle and the DT is designed to be 1.5 times stronger than the yield force in the steel angle, the full strength of the strand can be used to resist axial forces in the DT stem, without concern for yielding in the strand.

$D_2 = (0.042)(20.83)(8) = 7.0$ kips

$P_{min} = 0.7(7.0 + 2(1.08)) = 6.41$ kips

$M_E = (1.52)(4.25)(17.83) = 115.2$ ft-kips

$T_{u,stem} = M_E/d - P_{min}/2 = 25.5$ kips

The area of tension reinforcement required is:

$A_{ps} = T_{u,stem}/\phi f_{py} = (25.5 \text{ kips})/[0.9(270 \text{ ksi})] = 0.10 \text{ in.}^2$

The area of one 1/2-inch-diameter strand and one 3/8-inch-diameter strand is 0.153 in.^{2} + 0.085 in.^{2} = 0.236 in.^{2}. The mesh in the legs is available for tension resistance but is not required in this check.

To determine the nominal shear strength of the concrete for the connection design, complete the shear calculation for the panel in accordance with ACI 318 Chapter 11. The demand on each panel is:

$V_u = V_{pr} = 6.46$ kips

Only the deck between the DT legs is used to resist the in-plane shear (the legs act like flanges, meaning that the area effective for shear is the deck between the legs). First, determine the minimum required shear reinforcement based on ACI 318 Sections 11.5 and 11.6.

$$\phi V_c = \phi 2\lambda\sqrt{f_c'}\,hd = 0.75(2)(1.0)\sqrt{5000}\,(2.5)(48) = 12.7 \text{ kips}$$

Since V_u of 6.46 kips exceeds $\phi V_c/2$ of 6.36 kips, provide minimum reinforcement per ACI 318 Section 11.6.2. Using welded wire reinforcement, the required areas of reinforcement are:

$\rho_t = 0.0025$

$\rho_\ell =$ the greater of 0.0025, and
$\quad\quad 0.0025 + 0.5(2.5 - h_w/\ell_w)(\rho_t - 0.0025) = 0.0025$,

$A_v = A_{vh} = (0.0025)(2.5)(12) = 0.075 \text{ in.}^2/\text{ft}$

Provide 6×6 – W4.0×W4.0 welded wire reinforcement.

$A_{sv} = A_{sh} = 0.08 \text{ in.}^2/\text{ft}$

The prestress force and the area of the DT legs are excluded from the calculation of the nominal shear strength of the DT wall panel. The prestress force is not effective at the base, where the connection is and the legs are like the flanges of a channel, which are not effective in shear.

11.3.5.5 Tension and Shear at the Footing Embedment. Reinforcement to anchor the embedded plates is sized for the same tension and shear. Reinforcement in the DT leg and in the footing will be welded to embedded plates as shown in Figure 11.3-8.

The welded reinforcement is sloped to provide concrete cover and to embed the bars in the central region of the DT leg and footing. The tension reinforcement area required in the footing is:

$$A_{s,Sloped} = \frac{T_{u,stem}}{\phi f_y \cos\theta} = \frac{27.0}{(0.9)(60)\cos 26.5°} = 0.56 \text{ in.}^2$$

Use two #5 bars ($A_s = 0.62$ in^2) at each embedded plate in the footing.

The shear bars in the footing will be two #4 bars placed on an angle of two-to-one. The resultant shear resistance is:

$$\phi V_n = 0.75(0.2)(2)(60)(\cos 26.5°) = 16.1 \text{ kips}$$

11.3.5.6 Tension and Shear at the DT Embedment. The area of reinforcement for the welded bars of the embedded plate in the DT, which develops tension as the angle bends through cycles, is:

$$A_s = \frac{T_{u,stem}}{\phi f_y \cos\theta} = \frac{27.0}{(0.9)(60)\cos 6.3°} = 0.503 \text{ in.}^2$$

Two #5 bars are adequate. Note that the bars in the DT leg are required to extend upward the development length of the bar, which would be 22 inches. In this case, they will be extended 22 inches past the point of development of the effective stress in the strand, which totals approximately 48 inches.

The same embedded plate used for tension will also be used to resist one-half the nominal shear. This shear force is 6.46 kips. The transfer of direct shear to the concrete is easily accomplished with bearing on the sides of the reinforcing bars welded to the plate. Two #5 and two #4 bars (explained later) are welded to the plate. The available bearing area is approximately $A_{br} = 4(0.5 \text{ in.})(5 \text{ in.[available]}) = 10$ in.^{2} and the bearing capacity of the concrete is $\phi V_n = (0.65)(0.85)(5 \text{ ksi})(10 \text{ in.}^2) = 27.6$ kips, which is greater than the 6.46-kips demand.

The weld of these bars to the plate must develop both the tensile demand and this shear force. The weld is a flare bevel weld, with an effective throat of 0.2 times the bar diameter along each side of the bar. (Refer to the PCI Handbook.) Using the weld capacity for the #5 bar:

$$\phi V_n = (0.75)(0.6)(70 \text{ ksi})(0.2)(0.625 \text{ in.})(2) = 7.9 \text{ kips/in.}$$
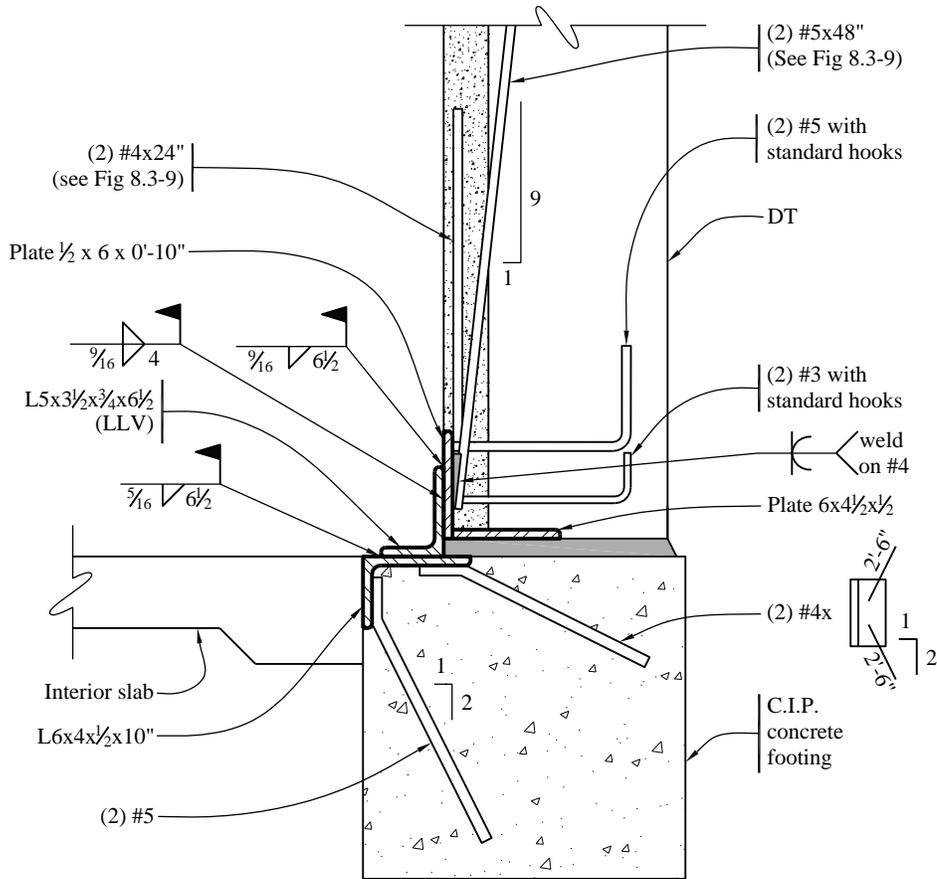
**Figure 11.3-8 Section at the connection of the precast/prestressed shear wall panel
and the footing**
(1.0 in = 25.4 mm)

The shear demand is prorated among the four bars as (6.46 kip)/4 = 1.6 kips. The tension demand is $T_{u,stem}/2$(13.5 kips). The vectorial sum of shear and tension demand is 13.6 kips. Thus, the minimum length of weld is 13.6/7.9 = 1.7 inches.

11.3.5.7 Resolution of Eccentricities at the DT Embedment. Check the twisting of the embedded plate in the DT for M_z. Use $M_z = 24.4$ in-kips.

$$A_s = \frac{M_z}{\phi f_y (jd)} = \frac{24.4}{0.9(60)(9.0)} = 0.05 \text{ in.}^2$$

Use one #4 bar on each side of the vertical embedded plate in the DT as shown in Figure 11.3-9. This is the same bar used to transfer direct shear in bearing.

Check the DT embedded plate for M_y (equal to 22.6 in.-kips) and M_x (equal to 94.5 in.-kips) using the two #4 bars welded to the back side of the plate near the corners of the weld on the loose angle and the two #3 bars welded to the back side of the plate near the bottom of the DT leg (as shown in Figure 11.3-9). It is relatively straightforward to compute the resultant moment magnitude and direction, assume a triangular compression block in the concrete and then compute the resisting moment. It is quicker to make a reasonable assumption as to the bars that are effective and then compute resisting moments about the X and

Y axes. That approximate method is demonstrated here. The #5 bars are effective in resisting M_x and one each of the #3 and #5 bars is effective in resisting M_y. For M_y, assume that the effective depth extends 1 inch beyond the edge of the angle (equal to twice the thickness of the plate). Begin by assigning one-half of the "corner" #5 bar to each component.

With $A_{sx} = 0.31 + 0.31/2 = 0.47$ in.^{2}:

$$\phi M_{nx} = \phi A_s f_y jd = (0.9)(0.47 \text{ in.}^2)(60 \text{ ksi})(0.95)(5 \text{ in.}) = 120 \text{ in.-kips} (> 94.5 \text{ in.-kips})$$

With $A_{sy} = 0.11 + 0.31/2 = 0.27$ in.^{2}:

$$\phi M_{ny} = \phi A_s f_y jd = (0.9)(0.27 \text{ in.}^2)(60 \text{ ksi})(0.95)(5 \text{ in.}) = 69 \text{ in-kips} (> 22.6 \text{ in.-kips})$$

Each component is strong enough, so the proposed bars are satisfactory.

Figure 11.3-9 Details of the embedded plate in the DT at the base
(1.0 in = 25.4 mm)

Figure 11.3-10 Sketch of connection of non-load-bearing DT wall panel at the roof
(1.0 in = 25.4 mm, 1.0 ft = 0.3048 m)
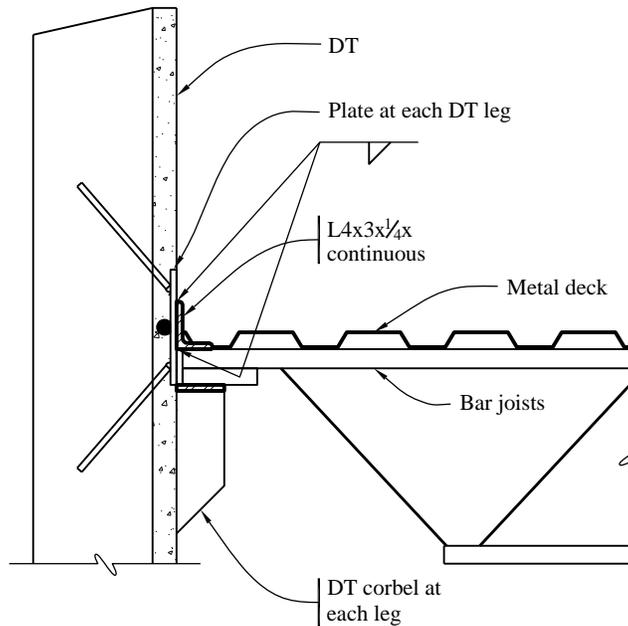
Figure 11.3-11 Sketch of connection of load-bearing DT wall panel at the roof
(1.0 in = 25.4 mm)

11.3.5.8 Other Connections. This design assumes that there is no in-plane shear transmitted from panel to panel. Therefore, if connections are installed along the vertical joints between DT panels to control the out-of-plane alignment, they should not constrain relative movement in-plane. In a practical sense, this means the chord for the roof diaphragm should not be a part of the panels. Figures 11.3-10 and 11.3-11 show the

connections at the roof and DT wall panels. These connections are not designed here. Note that the continuous steel angle would be expected to undergo vertical deformations as the panels deform laterally.

Because the diaphragm supports concrete walls out of their plane, *Standard* Section 12.11.2.1 requires specific force minimums for the connection and requires continuous ties across the diaphragm. Also, it specifically prohibits use of the metal deck as the ties in the direction perpendicular to the deck span. In that direction, the designer may wish to use the top chord of the bar joists, with an appropriate connection at the joist girder, as the continuous cross ties. In the direction parallel to the deck span, the deck may be used, but the laps should be detailed accordingly.

In precast DT shear wall panels with flanges thicker than 2-1/2 inches, consideration may be given to using vertical connections between the wall panels to transfer vertical forces resulting from overturning moments and thereby reduce the overturning moment demand. These types of connections are not considered here, since the uplift force is small relative to the shear force and cyclic loading of bars in thin concrete flanges is not always reliable in earthquakes.

11.4 SPECIAL MOMENT FRAMES CONSTRUCTED USING PRECAST CONCRETE

As for special concrete walls, the *Standard* does not distinguish between a cast-in-place and a precast concrete special moment frame in Table 12.2-1. However, ACI 318 Section 18.9 provides requirements for special moment frames constructed using precast concrete. That section provides requirements for designing special precast concrete frame systems using either ductile connections (ACI 318 Section 18.9.2.1) or strong connections (ACI 318 Section 18.9.2.2). ACI 318 Section 18.9.2.3 also explicitly allows precast moment frame systems that meet the requirements of ACI 374.1, *Acceptance Criteria for Moment Frames based on Structural Testing*.
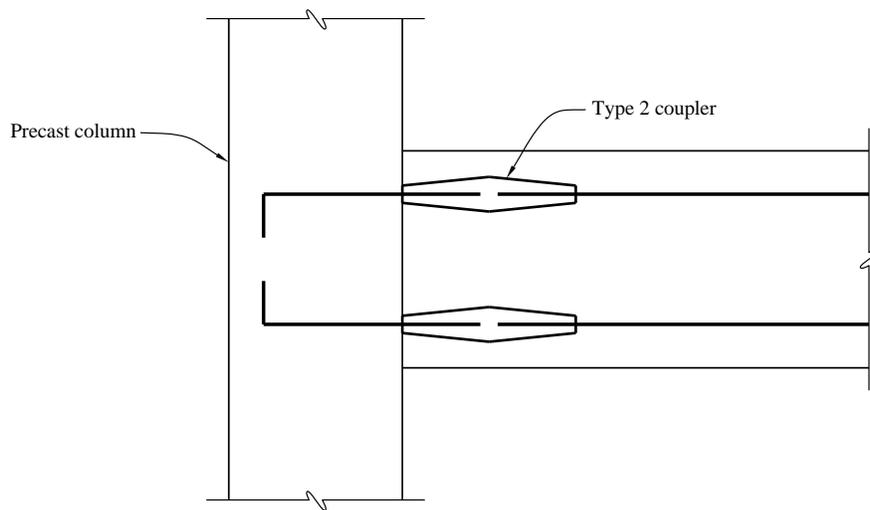
11.4.1 Ductile Connections

For moment frames constructed using ductile connections, ACI 318 allows plastic hinges to form in the connection region. All of the requirements for special moment frames must still be met, plus there is a factor larger than one that must be applied in computing the shear demand at the joint.

It is interesting to note that while Type 2 connectors can be placed anywhere (including in a plastic hinge region) in a cast-in-place frame or a precast frame with strong connections, these same connectors cannot be placed closer than $h/2$ from the joint face in a precast frame with ductile connections. The objective of a Type 2 connector is that it directs yielding away from the connector, into the bar itself. In a precast frame with ductile connections, inelastic deformations take place within the region between a joint face and the connector at least $h/2$ away from it. The minimum distance of $h/2$ is intended to avoid strain concentrations over the short length of reinforcement between the joint face and the adjacent splice device.

If a Type 2 connector is used at the face of a column as shown in Figure 11.4-1 and the bar size is the same in both the column and the beam, yielding will occur at the joint at the face of the column but not be able to spread into the beam to develop a plastic hinge, due to the strength of the connector. This concentrates the yielding in the bar to the left of the connector and likely will fracture the bar when significant rotation is imposed on the beam. To prevent this from happening, there are two options open to the designer. (1) Increase the flexural strength of the beam at least over the length of the connectors, compared to the flexural strength of the beam away from the column face and the connectors, so that hinging will occur away from the connectors. This is the strong connection concept (see ACI 318-14 Figure R18.9.2.2). Alternatively, (2) the connector may be separated from the column face by a minimum distance, over which hinging can take place. This is the concept of the ductile connection.

In a ductile connection, frame yielding takes place within the connection. This is most easily accomplished by extending the reinforcement out of the precast column element and coupling these reinforcing bars at the end of the precast beam. Since the couplers have to be located a minimum distance of $h/2$ from the column

face, the resulting gap between the precast beam and the precast column is filled with cast-in-place concrete as shown in Figure 11.4-2.

Figure 11.4-1 Type 2 coupler location in a strong connection
(1.0 in = 25.4 mm, 1.0 ft = 0.3048 m)
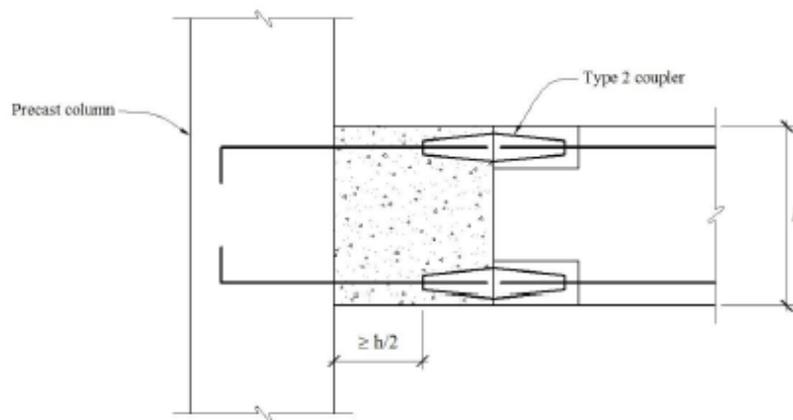
Figure 11.4-2 Type 2 coupler location in a ductile connection
(1.0 in = 25.4 mm, 1.0 ft = 0.3048 m)

11.4.2 Strong Connections

ACI 318 also provides design rules for strong connections used in special moment frames. The concept is to provide connections that are strong enough to remain elastic when a plastic hinge forms in the beam away from the connections. Thus the frame behavior is the same as would occur if the connection were monolithic.

Using the frame in Figure 11.4-3 (ignoring gravity forces for simplicity), design forces for the plastic hinge region and the associated forces on the precast connection are computed. Assuming inflection points at mid-height of the columns and a seismic shear force of V_{col} on each column:

11-70

$$V_b = V_{col} \frac{2H_{col}}{L_b}$$
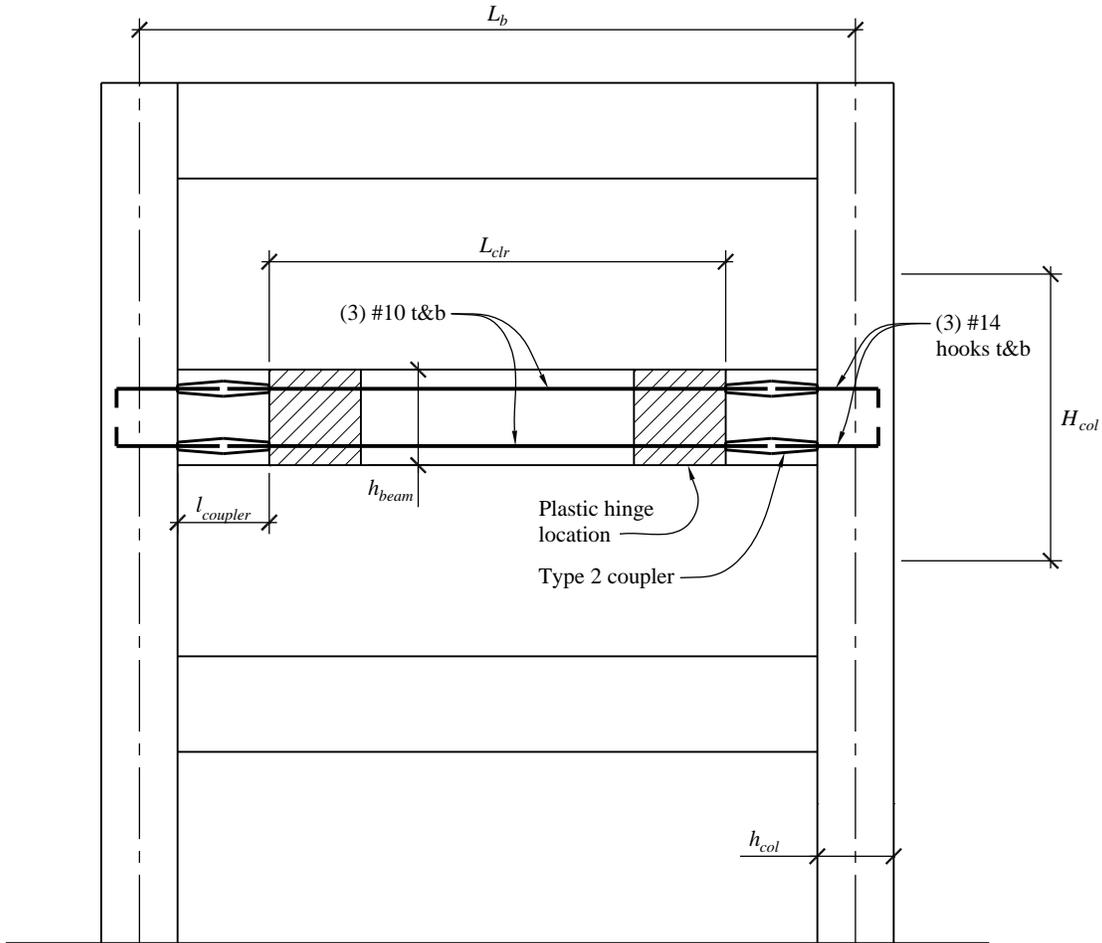
Figure 11.4-3 Moment frame geometry
(1.0 in = 25.4 mm, 1.0 ft = 0.3048 m)

Under seismic loads alone, the shear is constant along the beam length. Therefore, the moment at the joint between the end of the beam and the column is:

$$M_{joint} = V_b \frac{L_b - h_{col}}{2}$$

The plastic hinge, however, will be relocated to the side of the Type 2 coupler away from the column. With a coupler length of $l_{coupler}$, the moment at the end of the coupler is:

$$M_b = M_{joint} - V_b l_{coupler}$$

In order to ensure that the hinge forms at the intended location (away from the precast connection), the connection needs to be designed to be stronger than the moment associated with the development of the plastic hinge. This is done by upsizing the bar that is anchored into the column.

11.4.2.1 Strong Connection Example. In the following numerical example, a single-bay frame is designed to meet the requirements of a precast frame using strong connections at the beam-column interface. Using Figure 11.4-3 and the following geometry:

$H_{col} = 12$ ft

$h_{col} = 36$ in.

$L_b = 30$ ft (column centerline to column centerline)

$l_{coupler} = 18$ in.

$L_{clr} = L_b - h_{col} - 2l_{coupler} = 24$ ft (distance between plastic hinge locations)

$h_{beam} = 42$ in.

Reinforcing the beam with three #10 bars top and bottom, the design moment strength of the beam is:

$$a = \frac{A_s f_y}{0.85 f_c' b} = \frac{3(1.27)(60)}{0.85(5)(18)} = 3.0 \text{ in.}$$

$$\phi M_n = \phi A_s f_y \left(d - \frac{a}{2} \right) = 0.9(3)(1.27)(60)\left(33 - \frac{3.0}{2} \right)/12 = 540 \text{ ft-kips}$$

This is the moment strength at the plastic hinge location. The strong precast connection must be designed for the loads that occur at the connection when the beam at the plastic hinge location develops its probable strength.

Therefore, the moment strength at the beam-column interface (which also is the precast joint location) must be at least:

$$M_{u, joint} = M_{pr} \frac{L_b - h_{col}}{L_{clr}}$$

Where:

$$M_{pr} = \phi M_n \frac{1.25}{\phi} = 540 \frac{1.25}{0.9} = 750 \text{ ft-kips}$$

Therefore, the design strength of the connection must be at least:

$$M_{u, joint} = 750 \frac{30 - 36/12}{24} = 843 \text{ ft-kips}$$

Using #14 bars to the column side of the Type 2 coupler:

$$a = \frac{A_s f_y}{0.85 f'_c b} = \frac{3(2.25)(60)}{0.85(5)(18)} = 5.3 \text{ in.}$$

$$\phi M_n = \phi A_s f_y \left(d - \frac{a}{2} \right) = 0.9(3)(2.25)(60)\left(33 - \frac{3.0}{2} \right)/12 = 921 \text{ ft-kips}$$

which is greater than the moment at the connection (843 ft-kips) when the plastic hinge develops.

If column-to-column connections are required, ACI 318 Section 18.9.2.2(e) requires a 1.4 amplification factor, in addition to loads associated with the development of the plastic hinge in the beam. Locating the column splice near the point of inflection, while difficult for construction, can help to make these forces manageable.

The beam shear, when the plastic hinge location reaches its design strength, is:

$$V_b = \frac{\phi M_n}{L_{clr}/2} = \frac{540}{24/2} = 20 \text{ kips}$$

Assuming inflection points at the mid-span of the beam and mid-height of the column, the column shear is:

$$V_{col} = V_b \frac{L_b}{2H_{col}} = 20 \frac{30}{2(12)} = 25 \text{ kips}$$

However, the column shear must be amplified to account for the development of the plastic hinge.

$$V_u = V_{col} \frac{M_{pr}}{\phi M_n} = 25 \frac{750}{540} = 34.5 \text{ kips}$$

The column design moment is:

$$M_u = V_u \frac{(H_{col} - h_{beam})}{2} = 34.5 \frac{12 - 42/12}{2} = 147 \text{ ft-kips}$$

At the connection, this moment is amplified by 1.4 for a strong connection design moment of 205 ft-kips. ACI 318 Section 18.9.2.2(e) requires that this moment shall be at least $0.4M_{pr}$ for the column within the story height. M_{pr} must be determined as the largest value that is consistent with the axial forces that may result in the column from the various applicable load combinations. $1.4M_u$ as determined above or $0.4M_{pr}$, whichever is larger, must be combined with the factored axial load on the connection from both gravity loads and amplified seismic forces.

The balance of the design is the same as for a cast-in-place special moment frame.

12

Composite Steel and Concrete

Clinton O. Rex, P.E., PhD

Originally developed by
James Robert Harris, P.E., PhD and Frederick R. Rutz, P.E., PhD

Contents

The 2015 *NEHRP Recommended Provisions* for the design of a composite building using a "Composite Partially Restrained Moment Frame" (C-PRMF) as the lateral force-resisting system is illustrated in this chapter by means of an example design. The C-PRMF lateral force-resisting system is recognized in *Standard* Section 12.2 and in AISC 341 Section G4; and it is an appropriate choice for buildings in low to moderate Seismic Design Categories (SDC A to D). There are other composite lateral force-resisting systems recognized by the *Standard* and AISC 341; however, the C-PRMF is the only one illustrated in this set of design examples.

The design of a C-PRMF is different from the design of a more traditional steel moment frame in three important ways. First, the design of a Partially Restrained Composite Connection (PRCC) differs in that the connection itself is not designed to be stronger than the beam it is connecting. Consequently, the lateral system typically will hinge within the connections and not within the associated beams or columns. Second, because the connections are neither simple nor rigid, their stiffness must be accounted for in the frame analysis. Third, because the connections are weaker than fully restrained moment connections, the lateral force-resisting system requires more frames with more connections, resulting in a highly redundant system.

In addition to the 2015 *NEHRP Recommended Provisions* (referred to herein as the *Provisions*), the following documents are referenced throughout the example:

ACI 318   American Concrete Institute. 2014. *Building Code Requirements for Structural Concrete*.

AISC 341   American Institute of Steel Construction. 2016. *Seismic Provisions for Structural Steel Buildings*, including Supplement No. 1.

AISC 360   American Institute of Steel Construction. 2016. *Specification for Structural Steel Buildings*.

AISC Manual   American Institute of Steel Construction. 2011. *Steel Construction Manual*. 14th Edition.

AISC SDGS-8   American Institute of Steel Construction. 1996. *Partially Restrained Composite Connections*, Steel Design Guide Series 8. Chicago: AISC.

AISC SDM   American Institute of Steel Construction. 2012. *Seismic Design Manual.*

Arum (1996)   Mayangarum, Arum, 12-5-1996. Design, Analysis and Application of Bolted Semi-Rigid Connections for Moment Resisting Frames, MS Thesis, Lehigh University.

ASCE TC   American Society of Civil Engineers Task Committee on Design Criteria for Composite Structures in Steel and Concrete. October 1998. "Design Guide for Partially Restrained Composite Connections," *Journal of Structural Engineering* 124(10).

RCSC   Research Council on Structural Connections. 2004. *Specification for Structural Joints Using ASTM A325 or A490 Bolts.*

Standard   American Society of Civil Engineers, 2016, ASCE/SEI 7-16 Minimum Design Loads for Buildings and other Structures

Yura (2006)   Yura, Joseph A and Helwig, Todd A. (2-8-2006) Notes from SSRC/AISC Short Course 2 on "Beam Buckling and Bracing"The short-form designations presented above for each citation are used throughout.

The PRCC used in the example has been subjected to extensive laboratory testing, resulting in the recommendations of AISC SDGS-8 and ASCE TC. ASCE TC is the newest of the two guidance documents and is referenced here more often; however, AISC SDGS-8 provides information not in ASCE TC, which is still pertinent to the design of this type of frame. While both of these documents provide guidance for design of PRCC, the method presented in this design example deviates from that guidance based on more recent code requirements for stability and on years of experience in designing C-PRMF systems.

The structure is analyzed using three-dimensional, static, nonlinear methods. The SAP 2000 analysis program, (Computers and Structures, Inc., Berkeley, California) is used in the example.

The symbols used in this chapter are from Chapter 2 of the *Standard* or the above referenced documents, or are as defined in the text. U.S. Customary units are used.

12.1   BUILDING DESCRIPTION

The example building is a four-story steel framed medical office building located in Denver, Colorado (see Figures 12.1-1 through 12.1-3). The building is free of plan and vertical irregularities. Floor and roof slabs are 4.5-inch normal-weight reinforced concrete on 0.6-inch form deck (total slab depth of 4.5 inches.). Typically slabs are supported by open web steel joists which are supported by composite steel girders. Composite steel beams replace the joists at the spandrel locations to help control cladding deflections. The lateral load-resisting system is a C-PRMF in accordance with *Standard* Table 12.2-1 and AISC 341 Section G4. The C-PRMF uses PRCCs at almost all beam-to-column connections. A conceptual detail of a PRCC is presented in Figure 12.1-4. The key advantage of this type of moment connection is that it requires no welding. The lack of field welding results in erection that is quicker and easier than that for more traditional moment connections with CJP welding and the associated inspections.
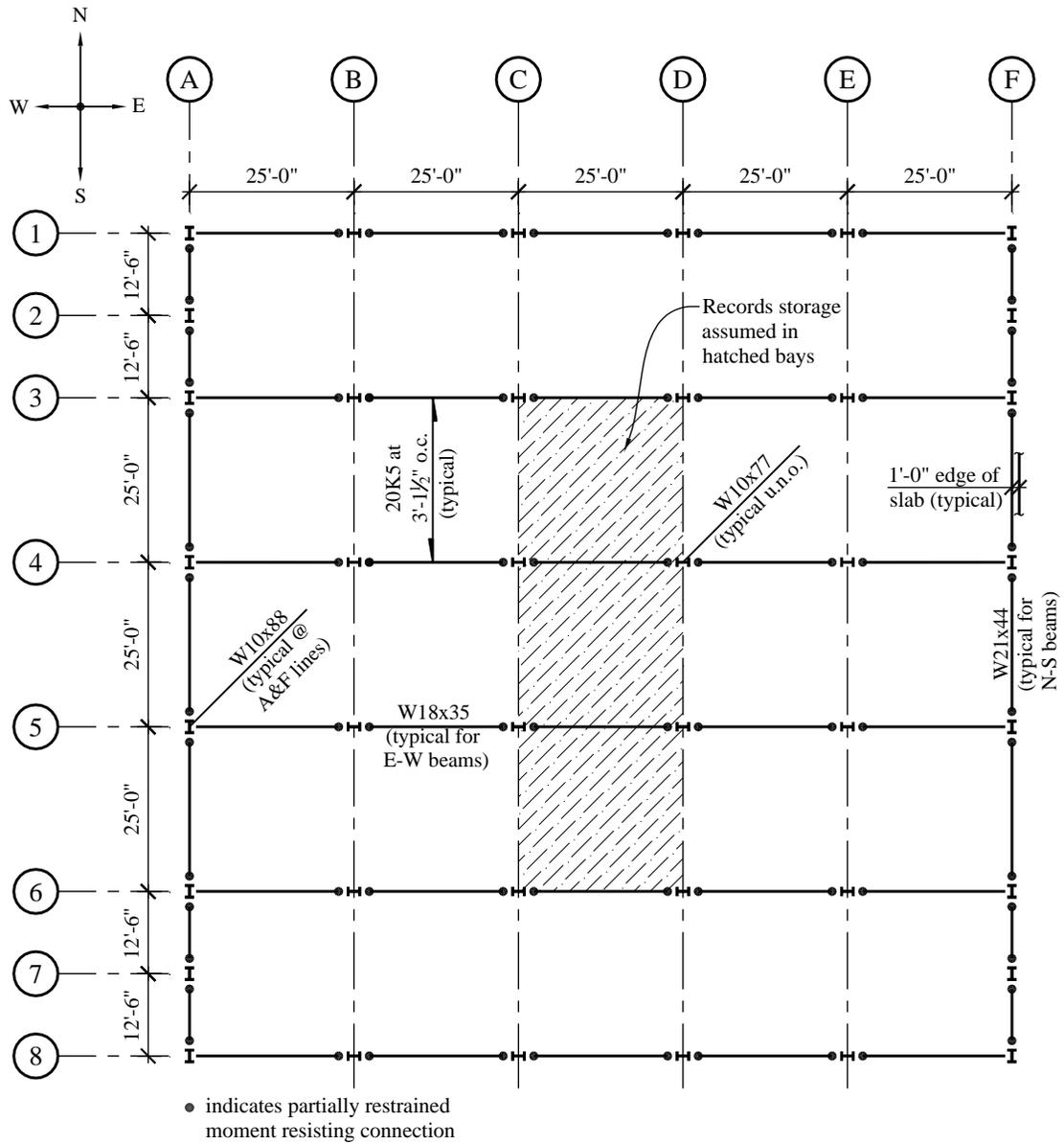
Figure 12.1-1 Typical floor and roof plan

Typical North Elevation
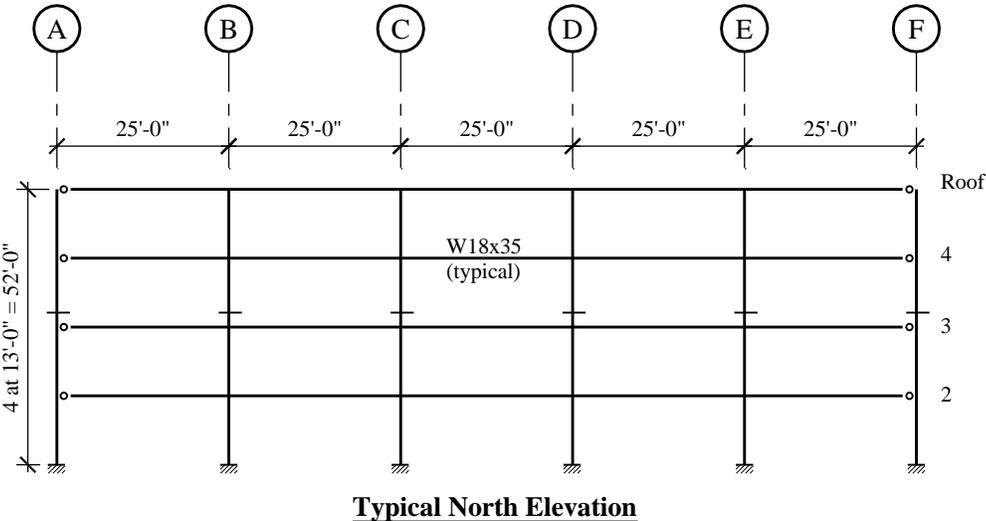
Figure 12.1-2 Building end elevation

East and West Side Elevation
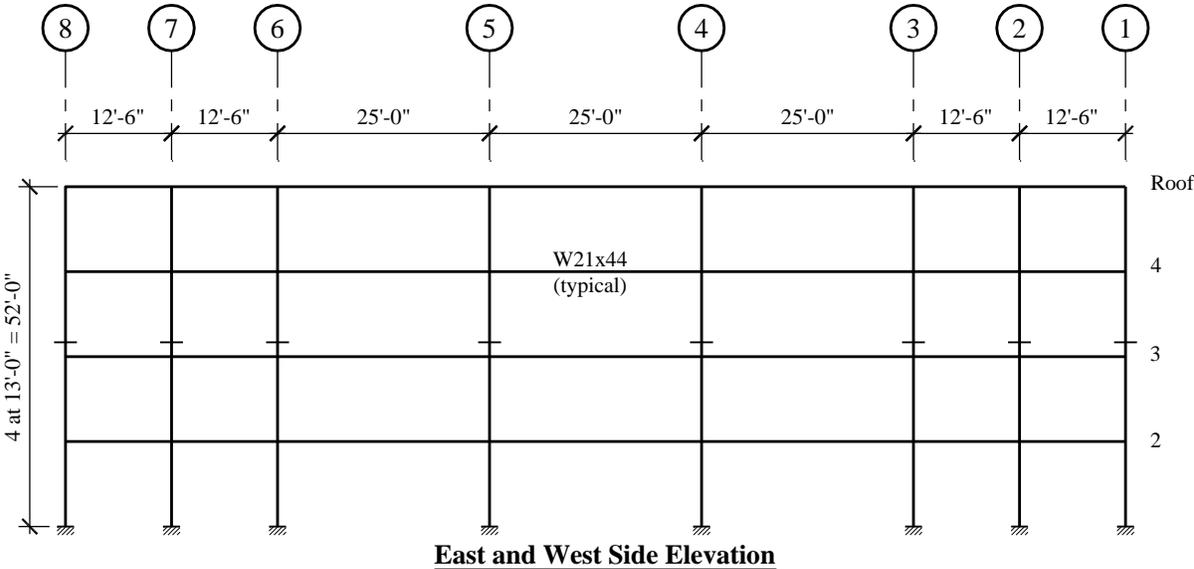
Figure 12.1-3 Building side elevation

The building is located in a relatively low seismic hazard region, but localized internal storage loading and Site Class E are used in this example to provide somewhat higher seismic design forces for purposes of illustration and to push the example building into Seismic Design Category C.
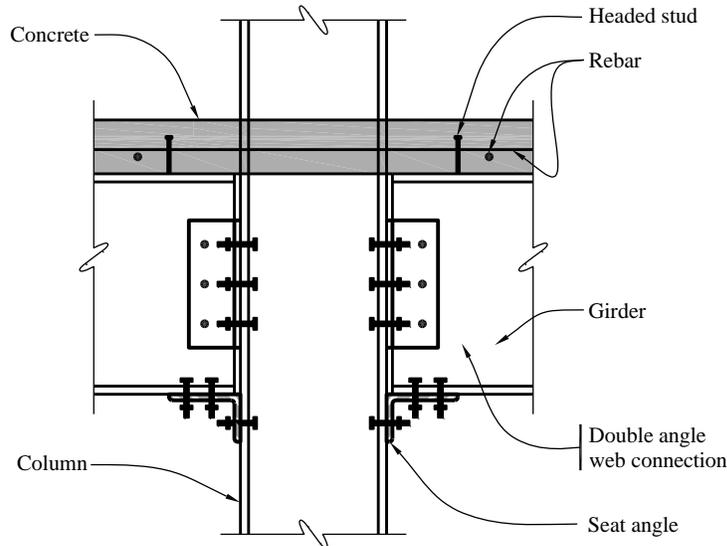
Figure 12.1-4 Conceptual partially restrained composite connection (PRCC)

There are no foundations designed in this example. For this location and system, the typical foundation would be a drilled pier and voided grade beam system, which would provide flexural restraint for the strong axis of the columns at their base (very similar to the foundation for a conventional steel moment frame). The main purpose here is to illustrate the procedures for the PRCCs. The floor and roof slabs serve as horizontal diaphragms distributing the seismic forces and by inspection they are stiff enough to be considered as rigid.

The typical bay spacing is 25 feet. Architectural considerations allowed an extra column at the end bay of each side in the north-south direction, which is useful in what is the naturally weaker direction. The exterior frames in the north-south direction have moment-resisting connections at all columns. The frames in each bay in the east-west direction have moment-resisting connections at all columns except the end columns. Composite connections to the weak axis of the column are feasible, but they are not used for this design. The PRCC connection locations are illustrated in Figure 12.1-1.

Material properties in this example are as follows:

- Structural steel beams and columns (ASTM A992): $F_y = 50$ ksi

- Structural steel connection angles and plates (ASTM A36): $F_y = 36$ ksi

- Concrete slab (4.5 inches thick on form deck, normal weight): $f_c' = 3,000$ psi

- Steel reinforcing bars (ASTM A615): $F_y = 60$ ksi

12.2 PARTIALLY RESTRAINED COMPOSITE CONNECTIONS

12.2.1 Connection Details

The type of PRCC used for this example building consists of a reinforced composite slab, a double-angle bolted web connection and a bolted seat angle. In real partially restrained building design, it is

advantageous to select and design the complete PRCC simply based on beam depth and element capacities. Generally it is impractical to "tune" connections to beam plastic moment capacities and/or lateral load demands. This allows the designer to develop an in-house suite of PRCC details and associated behavior curves for each nominal beam depth ahead of time. Slight adjustments can be made later to account for real versus nominal beam depth.

It is considered good practice (particularly for capacity-based seismic design) to provide substantial rotation capacity at connections while avoiding non-ductile failure modes. This requirement for ductile rotation capacity is expressed in AISC 341 Section G4 as a requirement for story drift of 0.02 radians. Because much of the drift in a partially restrained building comes from connection rotation, this story drift requirement implies a connection rotation ductility requirement. In short, connections must be detailed to allow ductile modes to dominate over non-ductile failure modes.

Practical detailing is limited by commonly available components. For instance, the largest angle leg commonly available is 8 inches, which can reasonably accommodate four 1-inch-diameter bolts. As a result, the maximum shear that can be delivered from the beam flange to the seat angle is limited by shear in four A490-X bolts. Bolt shear failure is generally considered to be non-ductile, so the rest of the connection design and detailing aims to maximize moment capacity of the connection while avoiding this limit state.

The connection details chosen for this example are illustrated in Figures 12.2-1, 12.2-2, 12.2-3 and 12.2-4.
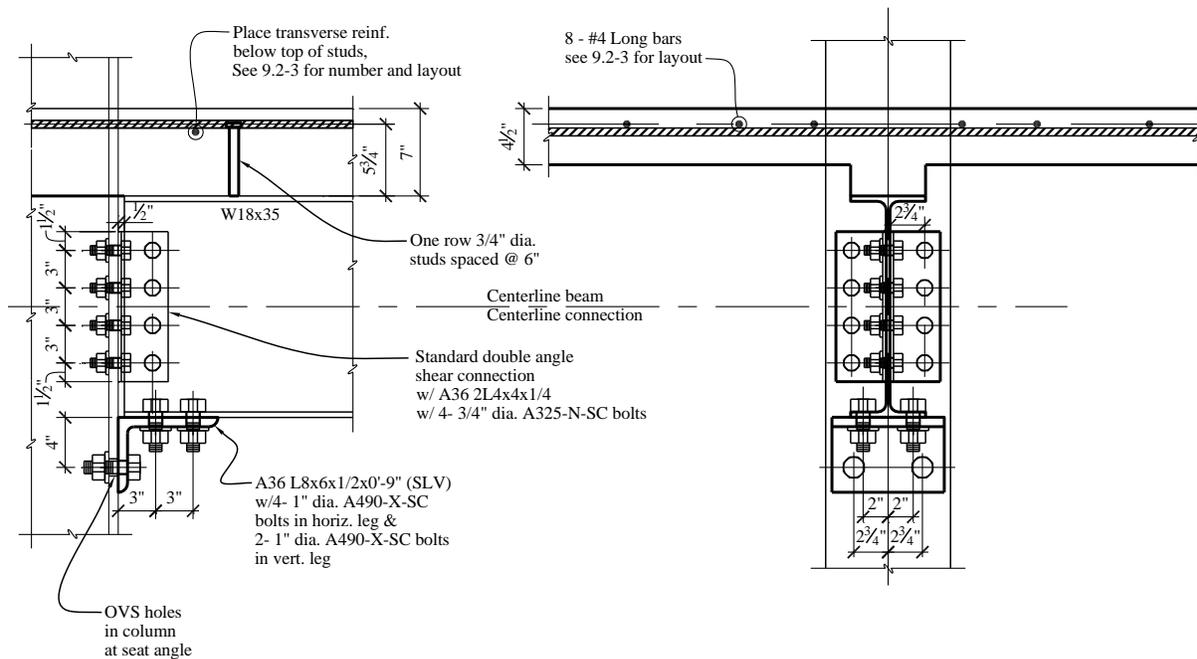
Figure 12.2-1 Typical interior W18x35 PRCC
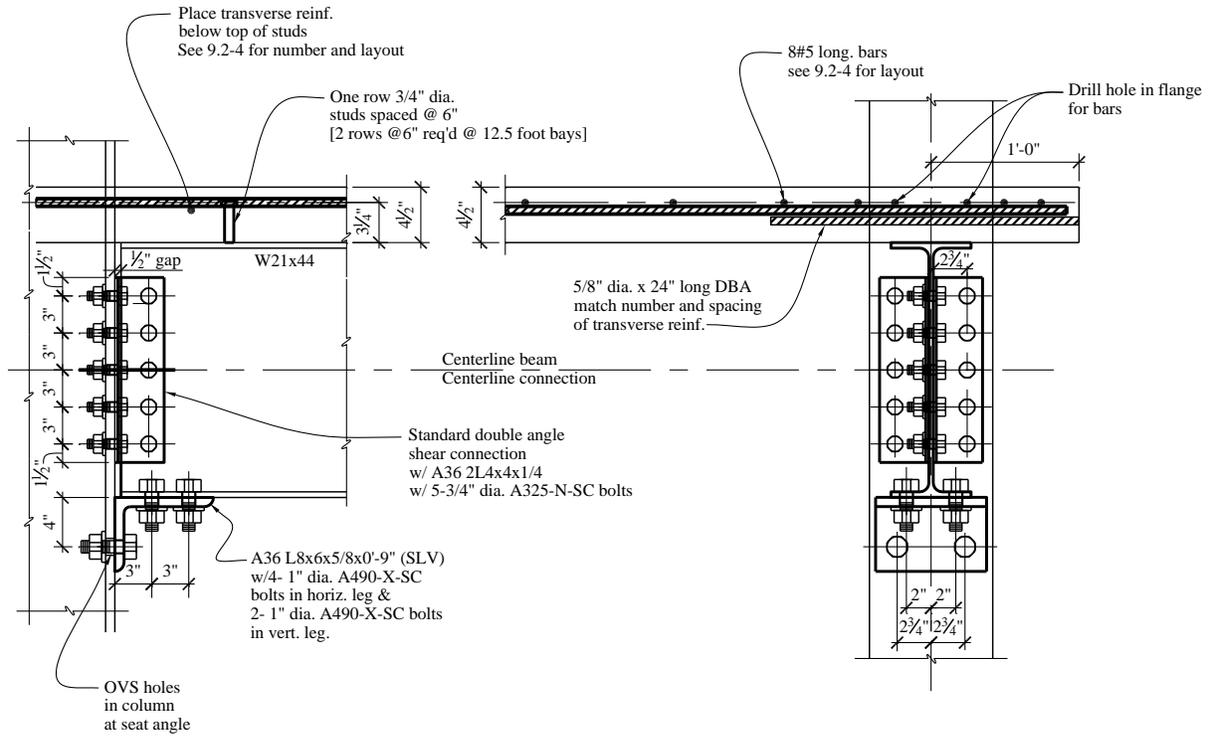
Figure 12.2-2 Typical spandrel W21x44 PRCC
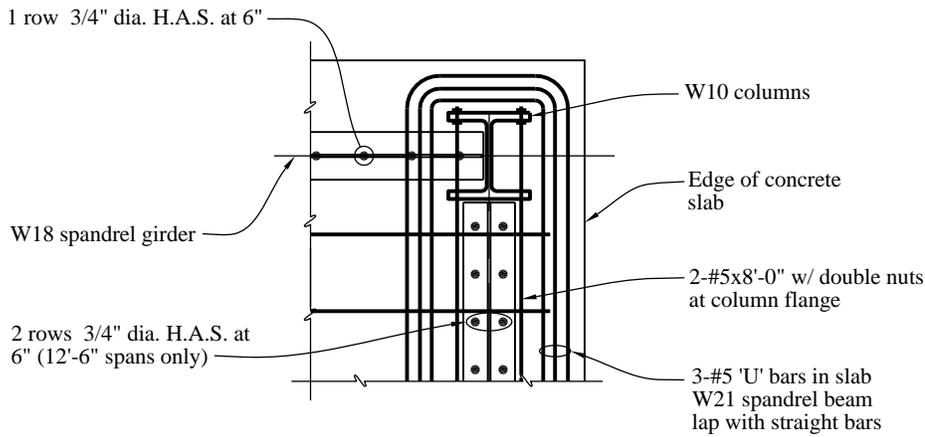
Figure 12.2-3 Typical corner PRCC
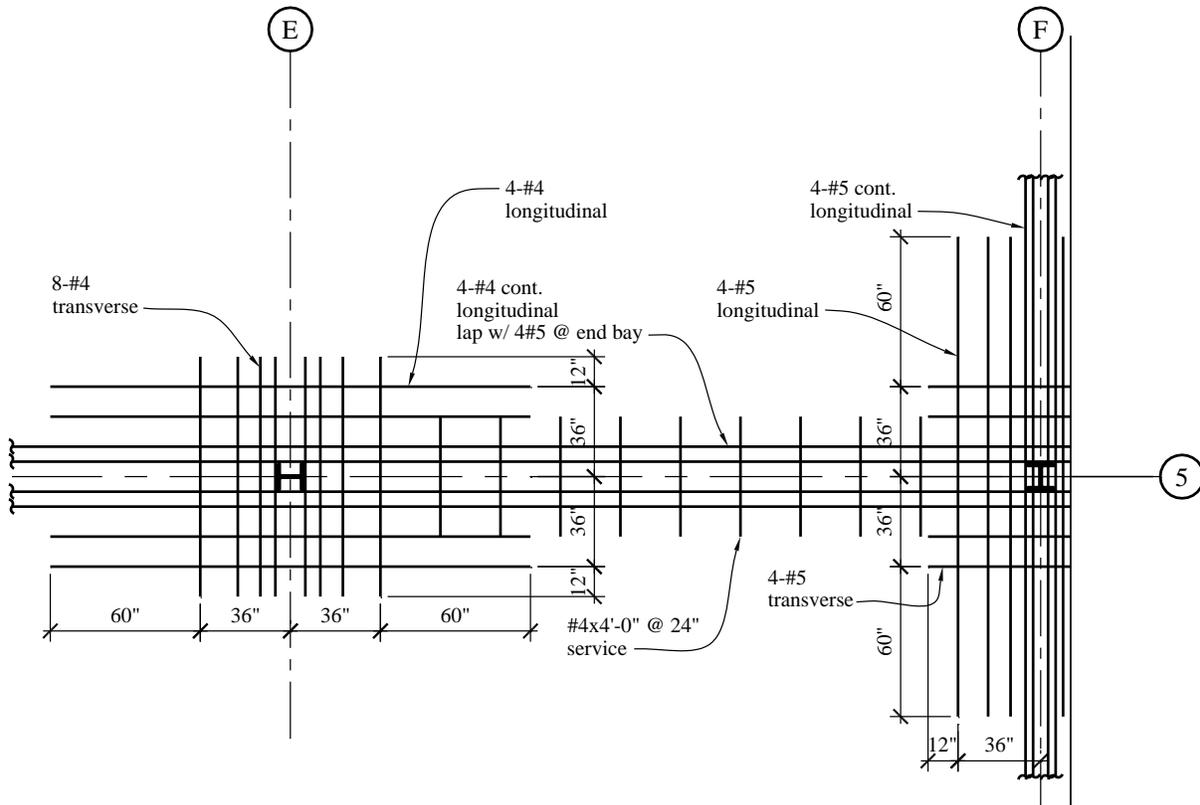
Figure 12.2-4 Typical PRCC reinforcing plan

12.2.2 Connection Moment-Rotation Curves

Two connection moment-rotation curves are required for the design of partially restrained buildings: the nominal moment-rotation curve and the modified moment-rotation curve.

The nominal moment-rotation curve, obtained from connection test data or from published moment-rotation prediction models, is used for service-level load design. For this example, the published moment-rotation prediction model given in ASCE TC is used to define the moment-rotation curve for the PRCC.

Negative moment-rotation behavior (slab in tension):

$$M_c^- = C_1\left(1 - e^{-C_2\theta}\right) + C_3\theta$$

<div align="right">(ASCE TC, Eq. 4)</div>

Where:

$C_1 = 0.18(4 \times A_{rb}F_{yrb} + 0.857A_{sa}F_{ya})(d + Y_3)$, kip-in.
$C_2 = 0.775$
$C_3 = 0.007(A_{sa} + A_{wa})F_{ya}(d + Y_3)$, kip-in.
θ = connection rotation (mrad = radians $\times$ 1,000)
d = beam depth, in.

Y_3 = distance from top of beam to the centroid of the longitudinal slab reinforcement, in.
A_{rb} = area of longitudinal slab reinforcement, in^2
A_{sa} = gross area of seat angle leg, in^2
   (For use in these equations, A_{sa} is limited to a maximum of $1.5A_{rb}$)
A_{wa} = gross area of double web angles for shear calculations, in^2
   (For use in these equations, A_{wa} is limited to a maximum of $2.0A_{sa}$)
F_{yrb} = yield stress of reinforcing, ksi
F_{ya} = yield stress of seat and web angles, ksi

Positive moment-rotation behavior (slab in compression):

$$M_c^+ = C_1\left(1 - e^{-C_2\theta}\right) + (C_3 + C_4)\theta$$

<div align="right">(ASCE TC, Eq. 3)</div>

Where:

$C_1 = 0.2400[(0.48A_{wa}) + A_{sa}](d + Y_3)F_{ya}$, kip-in.
$C_2 = 0.0210(d + Y_3/2)$
$C_3 = 0.0100(A_{wL} + A_L)(d + Y_3)F_{ya}$, kip-in.
$C_4 = 0.0065\ A_{wL}(d + Y_3)F_{ya}$, kip-in.

The modified moment-rotation curve is used for strength level load design. The Direct Analysis Method requires two modifications to the nominal moment-rotation curve: an elastic stiffness reduction and a strength reduction. AISC 360 Section 7.3(3) requires an elastic stiffness reduction of 0.8, which is accomplished by translating the connection rotation by an elastic stiffness reduction offset. This translation can be shown as follows:

$$\theta_{cDAM} = \theta_c + \frac{M_c}{4 \times K_{ci}}$$

Where:

M_c = connection moment from the nominal moment-rotation curve, kip-in.
K_{ci} = connection initial stiffness, kip-in./mrad; because the moment-rotation curve is nonlinear, it is necessary to define how the initial stiffness will be measured. For this example, the initial stiffness will be taken as the secant stiffness to the moment-rotation curve at $\theta = 2.5$ mrad as suggested in ASCE TC. Note that this will be different values for the positive and negative moment-rotation portions of the connection behavior.

$$K_{ci} = \frac{M_{c@2.5\,mrad}}{2.5\,mrad}$$

The second modification to the nominal moment-rotation curve is a strength reduction associated with ϕ. ASCE TC recommends using ϕ equal to 0.85. The associated connection strength is given by:

$M_{cDAM} = 0.85\ M_c$

From these equations, curves for M-θ can be developed for a particular connection. The moment-rotation curves for the typical connections associated with the W18x35 girder and the W21x44 spandrel beam are presented in Figures 12.2-5 and 12.2-6, respectively.
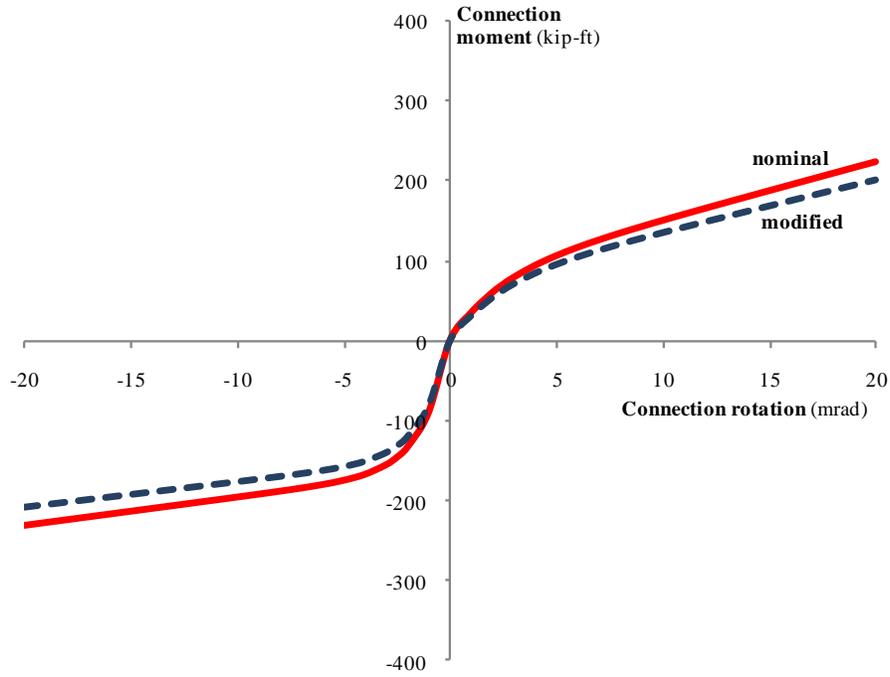
Figure 12.2-5 Typical interior W18x35 PRCC M-θ curves
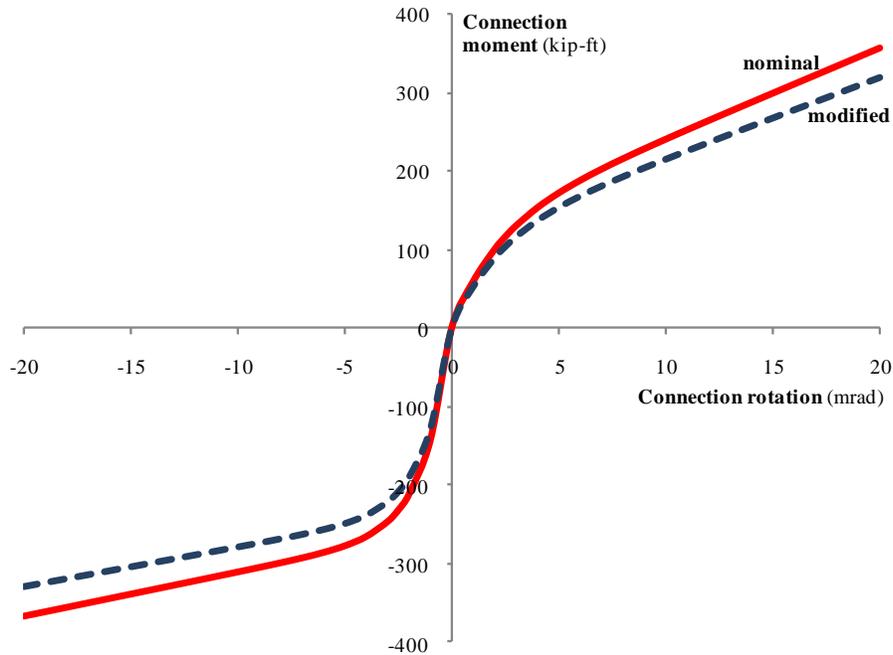
Figure 12.2-6 Typical spandrel W21x44 PRCC *M-θ* curves

Important key values from the above connection curves are summarized in Table 12.2-1 for reference in later parts of the example design.

Table 12.2-1 Key Connection Values From Moment-Rotation Curves

	W18x35 PRCC	W21x44 PRCC
K_{ci}^- (kip-in/rad) (nominal)	704,497	1,115,253
K_{ci}^+ (kip-in/rad) (nominal)	338,910	554,498
M_c^- @ 20 mrad (kip-ft) (nominal/modified)	232/206	367/326
M_c^+ @ 10 mrad (kip-ft) (nominal/modified)	151/127	240/202

These curves and the corresponding equations do not reproduce the results of any single test. Rather, they are averages fitted to real test data using numerical methods and they smear out the slip of bolts into bearing. Articles in the *AISC Engineering Journal* (Vol. 24, No.2; Vol. 24, No.4; Vol. 27, No.1; Vol. 27, No. 2; and Vol. 31, No. 2) describe actual test results. Those tests demonstrate clearly the ability of the connection to satisfy the rotation requirements of AISC 341 Section G4.

12.2.3 Connection Design
This section illustrates the detailed design decisions and checks associated with the typical W21x44 spandrel beam connection. A complete design would require similar checks for each different connection

type in the building. Design typically involves iteration on some of the chosen details until all the design checks are within acceptable limits.

12.2.3.1 Longitudinal Reinforcing Steel. The primary negative moment resistance derives from tensile yielding of slab reinforcing steel. Since ductile response of the connection requires that the reinforcing steel yield and elongate prior to failure of other connection components, providing too much reinforcing is not a good thing. The following recommendations are from ASCE TC.

A minimum of six bars (three bars each side of column), #6 or smaller, should be used (eight #5 bars have been used in this example). The bars should be distributed symmetrically within a total effective width of seven column flange widths (36 inches at each side of the column has been used in this example). For edge beams, the steel should be distributed as symmetrically as possible, with at least one-third (minimum three bars) of the total reinforcing on the exterior side of the column. Bars should extend a minimum of one-fourth of the beam length or 24 bar diameters past the assumed inflection point at each side of the column. For seismic design a minimum of 50 percent of the reinforcing steel should be detailed continuously. Continuous reinforcing should be spliced with a Class B tension lap splice and minimum cover should be in accordance with ACI 318.

12.2.3.2 Transverse Reinforcing Steel. The purpose of the transverse reinforcing steel is to help promote the force transfer from the tension reinforcing to the column and to prevent potential shear splitting of the slab over the beams, thus allowing the beam studs to transfer the reinforcing tension force into the beam. ASCE TC recommends the following.

Provide transverse reinforcement, consistent with a strut-and-tie model as shown in Figure 12.2-7. In the limit (maximum), this amount will be equal to the longitudinal reinforcement. The transverse reinforcing should be placed below the top of the studs to prevent a cone-type failure over the studs. The transverse bars should extend at least 12 bar diameters or 12 inches, whichever is larger, on either side of the outside longitudinal bars.
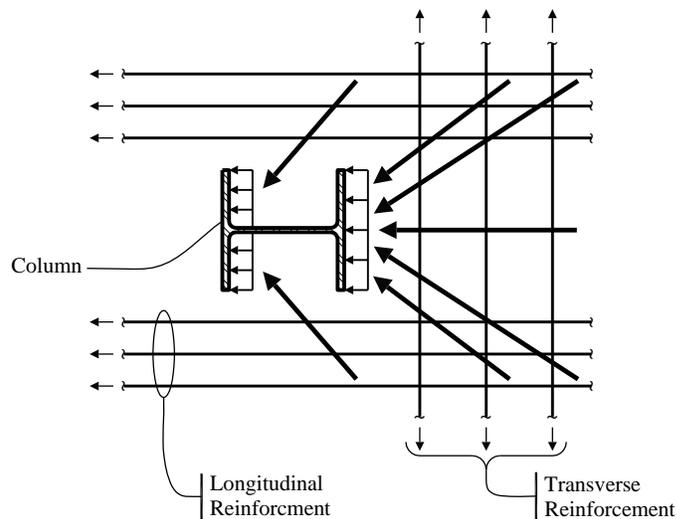
Figure 12.2-7 Force transfer mechanism from slab to column

Concrete bearing stresses on the column flange should be limited to $1.8f'_c$ per the ASCE TC recommendations. For the W21x44 PRCC, the sum of the positive and negative moment capacity is 607 kip-ft. The moment arm is approximately 22.95 inches (20.7 + 4.5/2). So the maximum possible transfer of force from the slab to the column, if each connection is at maximum and opposite strengths on each side of the column, is 607 ft-kip/22.95 inches = 317 kips. A W10x88 column has a 10.3-inch-wide flange. Assuming uniform bearing of the concrete on each flange, the bearing stress would be 317 kips / 2 flanges / 4.5-inch-thick slab / 10.3-inch-wide flange = 3.42 ksi, which is less than the recommended limit of $1.8f'_c$. It is also necessary to check this force against the flange local bending and web local yielding limit states given in Chapter J of AISC 360. It is important to have concrete filling the gap between column flanges; otherwise, the force must be transferred by a single column flange.

12.2.3.3 Connection Moment Capacity Limits. AISC 341 Section G4 requires that the PRCC have a nominal strength that is at least equal to 50 percent of the nominal M_p for the connected beam ignoring composite action. ASCE TC recommends 75 percent as a good target, with 50 percent as a lower limit and 100 percent as an upper limit. ASCE TC also recommends using the moment capacity at 20 mrad for negative moment and 10 mrad for positive moment to determine the nominal connection moment capacity. From the W21x44 PRCC connection curve, the negative moment capacity at 20 mrad is 367 kip-ft and the positive moment capacity at 10 mrad is 240 kip-ft. With M_p of the beam being 398 kip-ft, the ratio of connection-to-beam moment capacity is 0.922 and 0.603 for negative and positive moments, respectively.

12.2.3.4 Seat Angle. The typical gage for the bolts attaching the seat angle to the column is 5.5 inches to allow sufficient room for bolt tightening on the inside of the column. For a 1-inch bolt diameter and a 1.75-inch minimum edge distance to a sheared edge, the minimum angle length is 9 inches. Per ASCE TC, the minimum area of the outstanding angle leg should be:

$$A_{samin} = 1.33 \times F_{yrd} \times A_{rb} / F_{ya} = 5.497 \text{ in}^2$$

A 5/8-inch thick angle with the 9-inch angle length results in A_{sa} equal to 5.625 in^2.

The outstanding angle dimension is controlled by the number of bolts attaching the angle to the beam flange. As previously discussed, a minimum 8-inch dimension is desired here to allow room for four 1-inch-diameter bolts.

The vertical angle dimension has to be sufficient both to allow room for bolts to the column flange and to permit yielding when the seat angle is in tension. The ductility of the connection, when in positive bending, is derived from angle hinging, as shown in Figure 12.2-8.
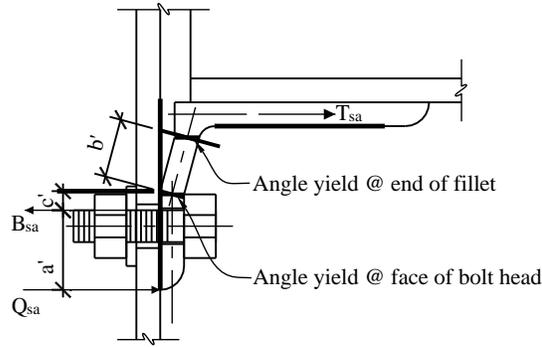
Figure 12.2-8 Typical angle tension hinging mechanism

This mechanism is based on research by Arum (1996). The following equations can be used to determine the associated angle tension, prying forces and bolt forces associated with the angle hinging mechanism.

$a' = L_{vsa} - g_{sa} + d_{bsa} / 2 = 2.500$ in.

$c' = (W_{sa} - d_{bsa}) / 2 = 0.313$ in.

$b' = L_{vsa} - a' - c' - k_{sa} = 2.062$ in.

$M_{psa} = F_{ya} \times t_{sa}^2 \times L_{sa} / 4 = 31.641$ kip-in

$T_{sa} = 2 \times M_{psa} / b' = 30.682$ kips

$Q_{sa} = M_{psa} / a' \times (1 + 2 \times c' / b') = 16.491$ kips

$B_{sa} = T_{sa} + Q_{sa} = 47.173$ kips

The above equations were derived in the same fashion as the prying action equations currently given in Section 9 of the AISC Manual with the same limitations applied to a'. The nomenclature in the above equations is shown in Figure 12.2-9.
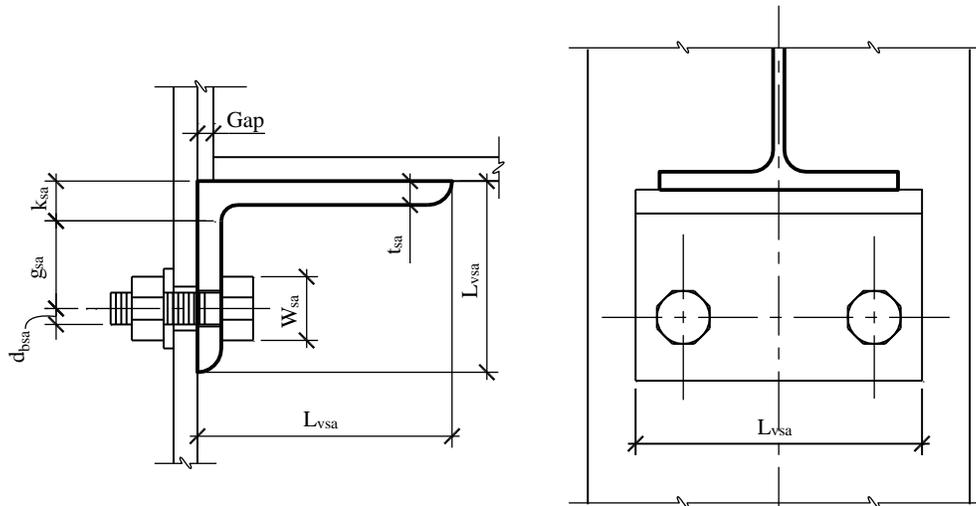
Figure 12.2-9 Seat angle nomenclature

The author recommends that the ratio of t_{sa}/b' be limited to no more than 0.5, so that the angle can properly develop the assumed hinges. For the example detail, the ratio is 0.303.

12.2.3.5 Bolts in Vertical Seat Angle Leg. The bolts in the vertical seat angle leg are designed primarily to resist tension in the case of connection positive moment. To protect against premature tension failure, the bolt force calculated in the previous section should be magnified by R_y from AISC 341 Table I-6-1.

$$R_y \times B_{sa} = 1.5 \times 47.173 \text{ kips} = 70.76 \text{ kips}$$

The tension capacity for two 1-inch-diameter A490 bolts is 133 kips.

12.2.3.6 Bolts in Outstanding Seat Angle Leg. The bolts in the outstanding leg of the seat angle must be designed for the shear transfer between the beam flange and the seat angle. For positive moments, this force is limited by tension hinging of the seat angle as calculated previously. For negative moments, this force is the sum of tension from the reinforcing steel and tension developed from hinging of the web angles. In general, the latter will be significantly more than the former. The tension hinging capacity of the web angles, T_{wa}, is calculated in the same way as the tension hinging of the seat angle. Again, to protect against premature shear failure of bolts, the tension capacity of the web angle and the reinforcing steel is magnified by an appropriate R_y. ASCE TC recommends $R_y = 1.25$ for the reinforcing steel.

$$R_y \times T_{wa} + R_y \times F_{yrd} \times A_{rb} = 1.5 \times 22.5 \text{ kips} + 1.25 \times 60 \text{ ksi} \times 2.48 \text{ in}^2 = 220 \text{ kips}$$

The published shear capacity for four 1-inch-diameter A490-X bolts is 177 kips; however, this capacity includes a 0.8 reduction to account for joint lengths up to 50 inches per the RCSC. The RCSC further states that this reduction does not apply in cases where the distribution of force is essentially uniform along the joint. When one increases the published shear capacity by 1/0.8, the revised shear capacity is 221 kips. Bolt bearing at the beam flange and at the seat angle should also be checked.

12.2.3.7 Double Angle Web Connection. The primary purpose of the double angle web connection is to resist shear. Therefore, it can be selected directly from the AISC Manual; the specific design limits will not be addressed here. The required shear force is determined by adding the seismic demand to the

gravity demand. The seismic demand for the W21x44 PRCC is the sum of the positive and negative moment capacity (607 kip-ft) divided by the appropriate beam length. For the typical 25-foot beam length, the seismic shear is approximately 25 kips.

12.3 LOADS AND LOAD COMBINATIONS

12.3.1 Gravity Loads and Seismic Weight

The design gravity loads and the associated seismic weights for the example building are summarized in Table 12.3-1. The seismic weight of the storage live load is taken as 50 percent of the design gravity load (a minimum of 25 percent is required by *Standard* Section 12.7.2). To simplify this design example, the roof design is assumed to be the same as the floor design and floor loads are used rather than considering special roof and snow loads.

Table 12.3-1 Gravity Load and Seismic Weight

	Gravity Load	Seismic Weight
Non-Composite Dead Loads (D_{nc})		
4.5-in. Slab on 0.6-in. Form Deck (4.5-in. total thickness) plus Concrete Ponding	58 psf	58 psf
Joist and Beam Framing	6 psf	6 psf
Columns	2 psf	2 psf
Total:	66 psf	66 psf
Composite Dead Loads (D_c)		
Fire Insulation	4 psf	4 psf
Mechanical and Electrical	6 psf	6 psf
Ceiling	2 psf	2 psf
Total:	12 psf	12 psf
Precast Cladding System	800 plf	800 plf
Live Loads (L)		
Typical Area Live and Partitions (Reducible)	70 psf	10 psf
Records Storage Area Live (Non-Reducible)	200 psf	100 psf

The reason for categorizing dead loads as non-composite and composite is explained in Section 9.4.2.

Live loads are applied to beams in the analytical model, with corresponding live load reductions appropriate for beam design. Column live loads are adjusted to account for different live load reduction factors, including the 20 percent reduction on storage loads for columns supporting two or more floors per *Standard* Section 4.8.2.

12.3.2 Seismic Loads

The basic seismic design parameters are summarized in Table 12.3-2

Table 12.3-2 Seismic Design Parameters

Parameter	Value
S_s	0.20
S_1	0.06
Site Class	E
F_a	2.5
F_v	3.5
$S_{MS} = F_a S_s$	0.50
$S_{M1} = F_v S_1$	0.21
$S_{DS} = 2/3 S_{MS}$	0.33
$S_{D1} = 2/3 S_{M1}$	0.14
Occupancy Category	II
Importance Factor	1.0
Seismic Design Category (SDC)	C
Frame Type per *Standard* Table 12.2-1	Composite Partially Restrained Moment Frame
R	6
Ω_0	3
C_d	5.5

For Seismic Design Category C, the height limit is 160 feet, so the selected system is permitted for this 52-foot-tall example building. The building is regular in both plan and elevation; consequently, the Equivalent Lateral Force Procedure of Section 12.8 is permitted in accordance with *Standard* Table 12.6-1. The seismic weight, W, totals 7,978 kips. The approximate period is determined to be 0.66 seconds using Equation 12.8-7 and the steel moment-resisting frame parameters of Table 12.8-2. The coefficient for upper limit on calculated period, C_u, from Table 12.8-1 is 1.62, resulting in T_{max} of 1.07 seconds for purposes of determining strength-level seismic forces.

A specific value for PRCC stiffness must be selected in order to conduct a dynamic analysis to determine the building period. It is recommended that the designer use K_{ci} of the negative moment-rotation behavior given in Section 12.2.2 above for this analysis. This should result in the shortest possible analytical building period and thus the largest seismic design forces. For the example building, the computed periods of vibration in the first modes are 2.13 and 1.95 seconds in the north-south and east-west directions, respectively. These values exceed T_{max}, so strength-level seismic forces must be computed using T_{max} for the period. The seismic response coefficient is then given by:

$$C_s = \frac{S_{D1}}{T\left(\dfrac{R}{I}\right)} = \frac{0.14}{1.07\left(\dfrac{6}{1.0}\right)} = 0.022$$

The total seismic forces or base shear is then calculated as:

$V = C_s\,W = (0.022)(7{,}978) = 174 \text{ kips}$ (*Standard* Eq. 12.8-1)

The distribution of the base shear to each floor (by methods similar to those used elsewhere in this volume of design examples) is:

Roof	(Level 4):	77 kips
Story 4	(Level 3):	53 kips
Story 3	(Level 2):	31 kips
Story 2	(Level 1):	13 kips
	Σ:	174 kips

For Seismic Design Category C, the value of ρ is permitted to be taken as 1.0 per *Standard* Section 12.3.4.1, so the above story shears are applied as E_h without any additional magnification.

12.3.3 Wind Loads

From calculations not illustrated here, the gross service-level wind force following ASCE 7 is 83 kips (assuming 90 mph, 3-second-gust wind speed). Including the directionality effect and the strength load factor, the design wind force is less than the design seismic base shear. The wind force is not distributed in the same fashion as the seismic force, thus the story shears and the overturning moments for wind are considerably less than for seismic. The distribution of the wind base shear to each floor is:

Roof	(Level 4):	13 kips
Story 4	(Level 3):	25 kips
Story 3	(Level 2):	23 kips
Story 2	(Level 1):	22 kips
	Σ:	83 kips

Because the wind loads are substantially below the seismic loads, they are not considered in subsequent strength design calculations; however, wind drift is considered in the design.

12.3.4 Notional Loads

AISC 360 now requires that notional loads be included in the building analysis. As shown later, the example building qualifies for application of notional loads to gravity-only load combinations. The notional load at level i is $N_i = 0.002Y_i$, where Y_i is the gravity load applied at level i. For our example building, these values are as follows:

$ND_{nc} = 4{,}258 \text{ kips} \times 0.002 = 8.516 \text{ kips} / 4 \text{ floors} = 2.13 \text{ kips/floor}$

$ND_c = 2{,}393 \text{ kips} \times 0.002 = 4.786 \text{ kips} / 4 \text{ floors} = 1.20 \text{ kips/floor}$

$NL = 4{,}469 \text{ kips} \times 0.002 = 8.938 \text{ kips} / 4 \text{ floors} = 2.23 \text{ kips/floor}$

The notional loads are applied in the same manner as the seismic and wind loads in each orthogonal direction of the building and they are factored by the same load factors that are applied to their corresponding source (such as 1.2 or 1.4 for dead loads). It is important to note that, in general, notional loads should be determined, at a minimum, on a column-by-column basis rather than for an entire floor as done above. This will allow the design to capture the effect of gravity loads that are not symmetric about the center of the building. The example building happens to have gravity loads that are concentric with the center of the building, so it does not matter in this case.

12.3.5 Load Combinations

Three load combinations (from *Standard* Section 2.3.2) are considered in this design example.

Load Combination 2: $1.2D + 1.6L$

Load Combination 5: $1.2D + 0.5L + 1.0E$

Load Combination 7: $0.9D + 1.0E$

Expanding the combinations for vertical and horizontal earthquake effects, breaking D into D_{nc} and D_c (defined in Section 12.3.1) and including notional loads, results in:

Load Combination 2: $1.2(D_{nc} + ND_{nc}) + 1.2(D_c + ND_c) + 1.6(L + NL)$

Load Combination 5:
$1.2D_{nc} + 1.2D_c + 0.5L + 1.0E_h + 1.0E_v$
$E_v = 0.2S_{DS}(D_{nc} + D_c) = 0.2(0.33)(D_{nc} + D_c) = 0.067(D_{nc} + D_c)$
$1.267D_{nc} + 1.267D_c + 0.5L + 1.0E_h$

Load Combination 7:
$0.9\ D_{nc} + 0.9\ D_c + 1.0\ E_h - 1.0\ E_v$
$0.833\ D_{nc} + 0.833\ D_c + 1.0\ E_h$

D_{nc} has to be applied separately to the columns and beams because of the two-stage connection behavior (discussed later). D_{ncc} is for column loading and D_{ncb} is for beam loading. This breakout of the loading results in the following combinations:

Stage 1 Analysis:

Load Combinations 2 and 5: $1.2\ D_{ncb}$

Load Combination 7: $0.9\ D_{ncb}$

Stage 2 Analysis:

Load Combination 2: $1.2(D_{ncc} + ND_{nc}) + 1.2(D_c + ND_c) + 1.6(L + NL)$

Load Combination 5: $1.2D_{ncc} + 0.067D_{ncb} + 1.267D_c + 0.5L + 1.0E_h$

Load Combination 7: $0.9D_{ncc} - 0.067D_{ncb} + 0.833D_c + 1.0E_h$

The columns are designed from the Stage 2 Analysis and the beams are designed from the linear combination of the Stage 1 and Stage 2 Analyses.

Because partially restrained connection behavior is nonlinear, seismic and wind drift analyses must be carried out for each complete load combination, rather than for horizontal loads by themselves. Note that *Standard* Section 12.8.6.2 allows drifts to be checked using seismic loads based on the analytical building period.

Seismic Drift: $1.0D_{ncc} + 0.067D_{ncb} + 1.0D_c + 0.5L + 1.0E_h$

Wind Drift: $1.0D_{ncc} + 1.0D_c + 0.5L + 1.0W$

The typical permeations of the above combinations have to be generated for each orthogonal direction of the building; however, orthogonal effects need not be considered for Seismic Design Category C provided the structure does not have a horizontal structural irregularity (*Standard* Sec. 12.5.3).

12.4 DESIGN OF C-PRMF SYSTEM

12.4.1 Preliminary Design

The goal of an efficient partially restrained building design is to have a sufficient number of beams, columns and connections participating in the lateral system so that the forces developed in any of these elements from lateral loads is relatively small compared to the gravity design. In other words, design for gravity as if the connections are pinned; add the connections and check to see if any beams or columns must be upsized to handle the lateral loads. The author cautions designers against trying to reduce beam sizes below the initial gravity sizes unless a full inelastic, path-dependent analysis accounting for potential shakedown of the connections is conducted. At this time, such an analysis typically is relegated to academic study and is not applied in real building design. The analysis methods described below do not go to that level of detail.

Once the building has been designed for gravity, a preliminary lateral analysis can be made to assess whether the proposed steel framing sizes may be suitable for lateral loads in combination with gravity loads. Typically this is done assuming all the PRCCs are rigid connections. Two basic checks can be based on this preliminary analysis. First, review connection moments that come from the lateral load cases alone (earthquake moments and wind moments) without gravity. If these moments (at strength levels) exceed approximately 75 percent of the negative moment capacity of the PRCC then either additional beams, columns and connections need to be added to the lateral system or existing beams need to be upsized to provide larger PRCCs with higher capacities. Second, perform a preliminary assessment of the building drift. While there is no simple, reliable relationship between rigid frame drift and C-PRMF drift, the author typically assumes that the partially restrained system will drift approximately twice as much as a fully rigid analysis indicates. Keep in mind that these preliminary checks are made to establish basic system proportions before extensive modeling efforts are made to include the real partially restrained behavior of the building.

Using this preliminary design method, initial floor framing was selected. In accordance with the ASCE TC, the beams are designed to be 100 percent composite; no partial composite design is used.

The W18x35 typical interior girder is determined from a simple beam design. This typical size would work for all locations with the exception of the girders that support storage load on both sides (Grids 4 and 5 between Grids C and D). For simplicity, the example design was not further refined. The W18x35 size would also work as the Grid Line A and F spandrel beams; however, a W21x44 spandrel beam is used to help control drift in the north-south direction and help equalize the building periods in both directions. Note that the W21x44 improves drift more due to the increase in beam depth, which increases PRCC moment-rotation stiffness, rather than because of the increase in the moment of inertia of the steel beam section.

12.4.2 Application of Loading

PRCC do not develop substantial beam end restraint until after the concrete has hardened (since the reinforcing steel cannot be mobilized without the concrete). At the time of concrete casting, the bare steel elements of the connection are all that are present to resist rotation at the beam ends. The degree of restraint provided by the bare steel connection varies depending on the details; however, for purposes of design, the connection stiffness prior to concrete hardening typically is assumed to be zero (a pinned beam end). Consequently, the connection actually has two stages of behavior that need to be accounted for in the analysis. These two stages are the pre-composite stage, when the connection is assumed to

behave as a pin and the post-composite stage, when the connection is assumed to have the full moment-rotation behavior determined in Section 12.2.2. In a building where the complete lateral system is provided by PRCCs, temporary bracing may be required to provide lateral stability prior to concrete hardening.

The above two-stage connection behavior requires separation of dead load into portions consistent with each stage. This is why the dead loads in Section 12.3.1 are separated into D_{nc} and D_c. The D_{nc} load is placed on the beams during the Stage 1 analysis (when the connections are pins) but is not placed on the beams (other than the seismic fraction) during the Stage 2 analysis (when the connections have PRCC stiffness). In Stage 2 analysis, the D_{nc} loads are placed directly on the columns so that their destabilizing effects are accounted for properly in the nonlinear P-delta analysis. That is why D_{nc} loads are further broken down into D_{ncc} and D_{ncb}. The Stage 2 load combinations are presented graphically in Figures 12.4-1 and 12.4-2.
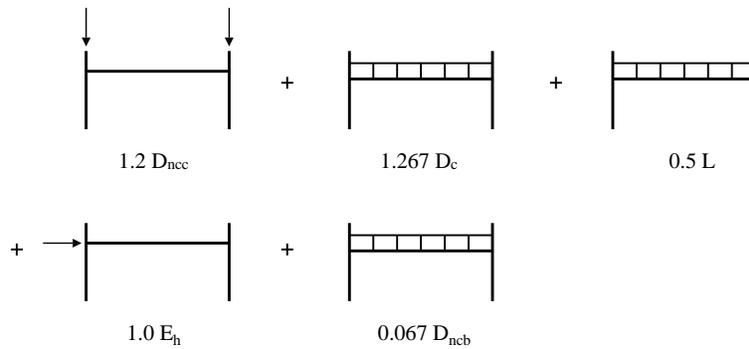
Figure 12.4-1 Stage 2 Load Combination 5
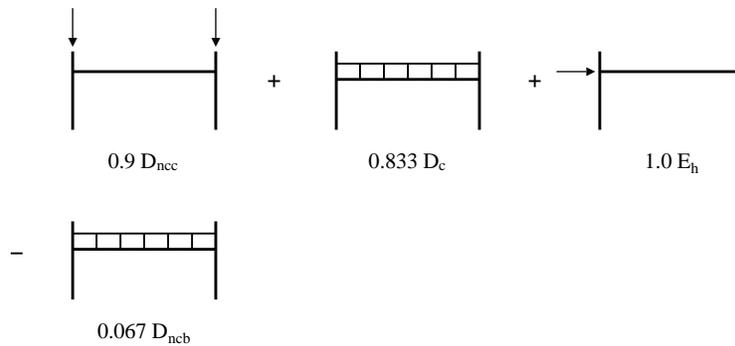
Figure 12.4-2 Stage 2 Load Combination 7

12.4.3 Beam and Column Moment of Inertia

ASCE TC recommends that the beam moment of inertia used for frame analysis be increased to account for the stiffening effect that the composite slab has on the beam moment of inertia. The use of the increased moment of inertia is also required by AISC 341 Section G4. The following equivalent moment of inertia is recommended:

$$I_{eq} = 0.6I_{LB+} + 0.4I_{LB-} \qquad \text{(Eq. 5, ASCE TC)}$$

I_{LB+} and I_{LB-} are the lower bound moments of inertia in positive and negative bending, respectively. I_{LB+} can be determined from Table 3-20 in the AISC Manual as 1,594 in^4 for the W18x35 interior girder and 1,570 in^4 for the W21x44 spandrel beam once composite beam design values are known. Note that the W21x44 spandrel 100 percent composite design is limited by the effective slab capacity, which is why its composite moment of inertia is so close to that of the W18x35 interior girder. I_{LB-} can be assumed as the bare steel moment of inertia, as 510 in^4 for the W18x35 interior girder and 843 in^4 for the W21x44 spandrel beam. It is permitted to account for the transformed area of the reinforcing steel in calculating I_{LB-}, but the bare steel beam property has been used in this example. The equivalent moment of inertia is then calculated as:

W18x35 Interior Girder: $I_{eq} = 0.6(1,594) + 0.4(510) = 1,160$ in^4

W21x44 Spandrel Beam: $I_{eq} = 0.6(1,570) + 0.4(843) = 1,279$ in^4

The bare steel moment of inertia values in the building analysis are revised to these values, which are suitable for service-level limit state checks. Use of a 0.8 reduction factor on the beam moment of inertia is required by AISC 360 Section 7.3(3) for strength-level checks from direct analysis.

The bare steel moment of inertia for the columns is appropriate for service-level checks. For strength-level checks, the same 0.8 reduction factor on the moment of inertia used on beams would apply to the columns. A further reduction on the column moment of inertia for strength-level checks is required if P_r/P_y exceeds 0.5. A quick scan of the column loads from the building analysis results indicates that the only columns that exceed this value are the first-story columns at Grids C-4, C-5, D-4 and D-5 for Load Combination 2 only. The adjustment factor is calculated to be:

$\tau_b = 4[P_r/P_y(1-P_r/P_y)] = 4[612 \text{ kips}/1130 \text{ kips } (1- 612 \text{ kips}/1130 \text{ kips})] = 0.99$

In the author's judgment, the above reduction on so few columns will have little or no effect on the building analysis results and it is ignored for this example.

12.4.4 Connection Behavior Modeling

For each connection type (such as W18 PRCC or W21 PRCC), there are four different connection behavior models used, as developed in Section 12.2.2. First, the connection is modeled as a linear spring with nominal stiffness K_{ci}. This is done for the dynamic analysis of the building needed to determine the building period. Second, a service-level analysis is conducted using the full nonlinear nominal service moment-rotation behavior. Third, a connection Stage 1 building analysis is done with the connections having no moment resistance (analytical pins) so the beam pre-composite loads can be applied. Finally, a Stage 2 building strength analysis under factored loads is performed with the full modified nonlinear moment-rotation behavior.

The multi-linear elastic link option provided in SAP2000 is used to model the connection springs for all stages. This nonlinear spring model allows user-defined behavior for two types of analysis, linear and nonlinear, for each spring type. This is helpful to handle the various connection behaviors because the dynamic analysis and the Stage 1 pre-composite beam load analysis can both be linear analysis which automatically switches the connection spring to the defined linear behavior. Another important point is that this particular spring model stays on the defined connection curve in a nonlinear-elastic manner. That is, the analysis simply rides up and down always converging at moment-rotation points on the connection backbone curve. This allows what is known as a path independent analysis; the order of the loading does not matter. This is in contrast with a spring model with different connection unloading

behavior, such as might be used to model the full hysteric connection behavior. If the connection unloading behavior is considered, the analysis is no longer path independent because the answer will depend on the sequence of loads that are applied. This path-dependent analysis is more accurate and allows consideration of connection shakedown to be captured in the model; however, it is also much more complicated when compared to the path-independent analysis. Since the simpler, path-independent connection modeling approach does not capture connection shakedown behavior, the author does not recommend reducing beam sizes from the pure simple pinned gravity design discussed in Section 12.4.1.

12.4.5 Building Drift and P-delta Checks

Drifts should be checked using the service moment-rotation curves along with the full moment of inertias for the beams and columns (no 0.8 reduction). Because of the nonlinear connection behavior, the analysis is nonlinear. Though optional, the author recommends including P-delta effects in the service drift checks for partially restrained building designs. Drifts are computed for the nonlinear load combinations developed in Section 12.3.5.

12.4.5.1 Torsional Irregularity Check. *Standard* Table 12.3-1 defines torsional irregularities. The story drift values at the each end of the example building and their average story drift values including *P*-delta are presented in Table 12.4-1. Since the ratio of maximum drift to average drift does not exceed 1.2, no torsional irregularity exists, accidental torsion need not be amplified and drift may be checked at the center of the building (rather than at the corners).

Table 12.4-1 Torsional Irregularity and Seismic Drift Checks

Story	North-south Direction (in.)						East-west Direction (in.)					
	Displacement		Story Drift				Displacement		Story Drift			
	A-1	F-1	A-1	F-1	avg	max/avg	F-1	F-8	F-1	F-8	avg	max/avg
1	0.40	0.45	0.40	0.45	0.43	1.06	0.31	0.37	0.31	0.37	0.34	1.08
2	0.91	1.03	0.51	0.58	0.55	1.06	0.72	0.84	0.41	0.47	0.44	1.07
3	1.32	1.49	0.41	0.46	0.43	1.06	1.05	1.22	0.33	0.38	0.35	1.08
4	1.55	1.76	0.23	0.27	0.25	1.06	1.23	1.44	0.19	0.22	0.20	1.08

12.4.5.2 Seismic Drift and P-delta Effect. The allowable seismic story drift is taken from *Standard* Table 12.12-1 as $0.025h_{sx} = (0.025)(13 \text{ ft} \times 12 \text{ in./ft}) = 3.9$ in. With C_d of 5.5 and I of 1.0, this corresponds to a story drift limit of 0.71 inch under the equivalent elastic forces (see *Standard* Section 12.8.6 for story drift determination). Review of the average drift values in Table 12.4-1 shows that all drifts are within the 0.71-inch limit.

Table 12.4-2 P-delta Effect Checks

| | North-south Direction (in.) | | | | | | East-west Direction (in.) | | | | | |
| | Displacement | | Story Drift | | | | Displacement | | Story Drift | | | |
Story	w/o P-Δ	w/ P-Δ	w/o P-Δ	w/ P-Δ	$P\Delta_{amp}$	θ	w/o P-Δ	w/ P-Δ	w/o P-Δ	w/ P-Δ	$P\text{-}\Delta_{amp}$	θ
1	0.38	0.43	0.38	0.43	1.14	0.12	0.30	0.34	0.30	0.34	1.12	0.10
2	0.86	0.97	0.48	0.55	1.14	0.12	0.70	0.78	0.40	0.44	1.12	0.10
3	1.25	1.41	0.39	0.43	1.10	0.09	1.02	1.13	0.32	0.35	1.09	0.08
4	1.48	1.66	0.24	0.25	1.06	0.06	1.22	1.33	0.19	0.20	1.05	0.04

Separate analyses are conducted to determine seismic drifts with and without P-delta effects. Due to the nonlinear connection behavior, all of the analyses are nonlinear. The ratio of these two drifts ($P\text{-}\Delta_{amp}$) is compared to the 1.5 limit for ratio of second-order drift to first-order drift set forth in AISC 360 Section 7.3(2). Because the ratios are all below the 1.5 limit, it is permissible to apply the notional loads as a minimum lateral load for the gravity-only combination and not in combination with other lateral loads. The results of these analyses are given in Table 12.4-2.

Provisions Section 12.8.7 now defines the stability coefficient (θ) as follows:

$$\theta = \frac{P_x \Delta I}{V_x h_{sx} C_d}$$

The story drift (Δ) is defined in *Standard* Section 12.8.6 as:

$$\Delta = \frac{C_d \delta_{xe}}{I}$$

Replacing Δ in the stability coefficient equation results in:

$$\theta = \frac{P_x \delta_{xe}}{V_x h_{sx}}$$

This value of θ can also be calculated from the P-delta amplifier presented in Table 9.4-2 by the following:

$$\theta = 1 - \frac{1}{P\Delta_{amp}}$$

The stability coefficients presented in Table 12.4-2 were calculated in this manner. Review of the values shows that θ varies from 0.04 to 0.12. *Provisions* Section 12.8.7 now requires that θ not exceed 0.10 unless the building satisfies certain criteria when subjected to either nonlinear static (pushover) analysis or nonlinear response history analysis. Because θ for the building in the north-south direction exceeds 0.10 in the lower stories, the designer would have to either increase the building stiffness in that direction or conduct an approved nonlinear analysis. Such nonlinear analysis is beyond the scope of this example.

12.4.5.3 Wind Drift. A wind drift limit of $h_{sx}/400$ was chosen based on typical office practice for this type of building. This gives a story drift limit of $13 \times 12 / 400 = 0.39$ inch. The wind drift values presented in Table 12.4-3 were determined for the 50-year return interval wind loads previously determined in Section 12.3.3 above. Review of the drift values indicates that all drifts are within the 0.39-inch limit.

Table 12.4-3 Wind Drift Results

Story	North-south Direction (in.)		East-west Direction (in.)	
	Displacement	Story Drift	Displacement	Story Drift
1	0.19	0.19	0.15	0.15
2	0.39	0.20	0.32	0.17
3	0.52	0.13	0.42	0.11
4	0.57	0.05	0.47	0.04

12.4.6 Beam Design

AISC 341 Section G4 requires that composite beams be designed in accordance with AISC 360 Chapter I. The beams are designed for 100 percent composite action and sufficient shear studs to develop 100 percent composite action are provided between the end and midspan. They do not develop 100 percent composite action between the column and the inflection point, but it may be easily demonstrated that they are more than capable of developing the full force in the reinforcing steel within that distance. Composite beam design is not unique to this example; however, composite beams acting as part of the lateral load-resisting system is unique and deserves further attention. When proportioning the shear connectors for the steel beam used in a composite lateral force resisting system, AISC 341 Section D2.8 requires that shear connector capacity be reduced by 25%. This means that 33% more connectors are required.

As a result of connection restraint, negative moments will develop at beam ends. These moments must be considered when checking beam strength. The inflection point cannot be counted on as a brace point, so it may be necessary to consider the full beam length as unbraced for checking lateral-torsional buckling and comparing that capacity to the negative end moments. Note that there are C_b equations in the literature that do a better job (as compared to the standard C_b equation in AISC 360) of predicting the lateral-torsional buckling strength of beams that are continuously attached to a composite slab floor system (Yura, 2006)

AISC 341 Section G4 specifically addresses compactness criteria for beams; by requiring beams meet the requriements of AISC 341 Section D1.1 for highly ductile members. A quick check in Table 1-2 of the AISC SDM indicates that both W18x35 and W21x44 are compact for flexure.

12.4.7 Column Design

Requirements for column design are found in AISC 341 and AISC 360. AISC 341 Section G4 requires that columns meet the requirements of AISC 341 Section D1.1 for highly ductile members. W10 columns of A992 steel meet all Section D1.1 material requirements.

AISC 341 Section D1.4 requires columns in moment frames be designed for axial load from the amplified seismic load combination (Ω_0) neglecting applied moments, provided the moments are not caused by loads applied to the column between supports.   .

The nominal strength of the columns is determined using $K = 1.0$ in accordance with AISC 360 Section 7.1. The associated column strength unity checks are presented in Table 12.4-4. The unity checks 12presented are for the first story of the center four columns in the building.

Table 12.4-4 Column Strength Check for W10x77

	Seismic Load Combination	Gravity Load Combination
Axial force, P_u	734 kip	612 kip
Moment, M_u	Neglected	35 ft-kip
Interaction	0.94	0.866

AISC SDM Table 1-2 indicates that the W10x77 meets compactness requirements for a highly ductile member for flexure (beam) and for axial loads (column) and is therefore an acceptable section.

The equivalent of the weak-beam–strong-column concept for the C-PRMF lateral system is a weak connection-strong column. This is not specifically addressed in AISC 341; however, ASCE TC recommends the following check, where Pu is calculated using the regular seismic load combination (without Ω_0):

$$\sum M_{p,col}\left(1-\frac{P_u}{P_y}\right) \geq 1.25\left(M_{cu}^- + M_{cu}^+\right)$$

For the same lower level interior W10x77 one gets:

$$2 \times 50 \times 97.6\left(1-\frac{370 \text{ kips}}{50 \times 22.6}\right) = 547 \text{ ft-kips} \geq 1.25(232 + 151) = 479 \text{ ft-kips}$$

12.4.8 Connection Design

There is really little to do with the connection design at this stage because the full nonlinear connection behavior is being used in the analysis. This means that the connection moments will never exceed the connection capacity during the analysis. This is in contrast to any analysis method that models the connections with linear behavior. When the connections are modeled with linear behavior, it is up to the designer to confirm that the final connection results are consistent with the expected connection behavior. This might be very easy for building designs where connection moments are small; however, when the connections are being pushed close to their capacity, that sort of independent connection check by the designer can be problematic.

Although not entirely necessary, it is useful to check where the connections are along the expected behavior curves for any given analysis so one can see just how hard the connections are being pushed. The connection moment demand versus design capacities (including ϕ) are presented in Table 12.4-5. The demand values are from different load combinations. A quick check of this table indicates that this building design is not being pushed particularly hard and that there is likely significant reserve capacity in the lateral system.

Table 12.4-5 Connection Moment Demand vs. Capacity (kip-ft)

	W21 PRCC		W18 PRCC	
	(-) M-θ	(+) M-θ	(-) M-θ	(+) M-θ
Demand	136	87.0	126	37.0
Capacity	312	204	197	128
Ratio	0.44	0.43	0.64	0.29

12.4.9 Column Splices

Column splice design would be in accordance with AISC 341 Section D1.5 but is not illustrated in this example.

12.4.10   Column Base Design

Column base design would be in accordance with AISC 341 Section D2.6 but is not illustrated in this example.

13

Masonry

David G. Sommer, PE

Originally developed by
James Robert Harris, PE, PhD and Frederick R. Rutz, PE, PhD

Contents

This chapter illustrates application of the 2015 *NEHRP Recommended Provisions* (the *Provisions*) and *ASCE 7-10 Minimum Design Loads for Buildings and Other Structures* (the *Standard*) to the design of a variety of reinforced masonry structures in regions with different levels of seismicity. Example 13.1 features a single-story masonry warehouse building with tall, slender walls, and Example 13.2 presents a five-story masonry hotel building with a bearing wall system designed in areas with different seismicities. Selected portions of each building are designed to demonstrate specific aspects of the design provisions.

Masonry is a discontinuous and heterogeneous material. The design philosophy of reinforced grouted masonry approaches that of reinforced concrete; however, there are significant differences between masonry and concrete in terms of restrictions on the placement of reinforcement and the effects of the joints. These physical differences create significant differences in the design criteria.

All structures were analyzed using two-dimensional (2D) static methods using the RISA 2D program, V.5.5 (Risa Technologies, Foothill Ranch, California). Example 13.2 also uses the SAP 2000 program, V6.11 (Computers and Structures, Berkeley, California) for dynamic analyses to determine the structural periods.

All examples are for buildings of concrete masonry units (CMU); clay unit masonry shear walls, prestressed masonry shear walls, and autoclaved aerated concrete masonry shear walls are not included.

In addition to the *Provisions* and the *Standard*, the following documents are referenced in this chapter:

ACI 318   American Concrete Institute. 2014. *Building Code Requirements for Structural Concrete*.

TMS 402   The Masonry Society. 2013. *Building Code Requirements for Masonry Structures*, TMS 402/ACI 530/ASCE 5.

IBC   International Code Council. 2012. *International Building Code*.

NCMA   National Concrete Masonry Association. *A Manual of Facts on Concrete Masonry*, NCMA-TEK is an information series from the National Concrete Masonry Association, various dates. NCMA-TEK 10-3, *Control Joints for Concrete Masonry Walls – Alternative Engineered Method*, NCMA-TEK 14-1B, *Section Properties of Concrete Masonry Walls*, NCMA-TEK 14-3A, *Designing Concrete Masonry Walls for Wind Loads,* and NCMA-TEK 14-11B, *Strength Design of Concrete Masonry Walls for Axial Load & Flexure*, are referenced here.

USGS   United States Geological Survey. *Seismic Design Maps* web application.

The short form designations for each citation are used throughout. The citation to the IBC is because one of the designs employees a tall, slender wall that is partially governed by wind loads and the IBC provisions are used for that design.

Regarding TMS 402:

  The 2010 edition of the *Standard* refers to the 2008 edition of TMS 402.

  The 2015 edition of the *Provisions* refer to the 2013 edition of TMS 402.

  The examples herein are prepared according to the 2013 edition of TMS 402.

13.1 WAREHOUSE WITH MASONRY WALLS AND WOOD ROOF, AREA OF HIGH SEISMICITY

This example features a one-story building with reinforced masonry bearing walls and shear walls.

13.1.1 Building Description

This simple rectangular warehouse is 100 feet by 200 feet in plan (Figure 13.1-1). The masonry walls are 30 feet high on all sides, with the upper 2 feet being a parapet. The wood roof structure slopes slightly higher towards the center of the building for drainage. The walls are 8 inches thick on the long side of the building, for which the slender wall design method is adopted, and 12 inches thick on both ends. The masonry is grouted in the cells containing reinforcement, but it is not grouted solid. Local trade groups should be consulted for typical practices as masons in some areas fully grout masonry walls almost exclusively, while in other areas only build partially grouted walls. The specified strength of masonry is 2,000 psi. Normal-weight CMU with Type S mortar are assumed.
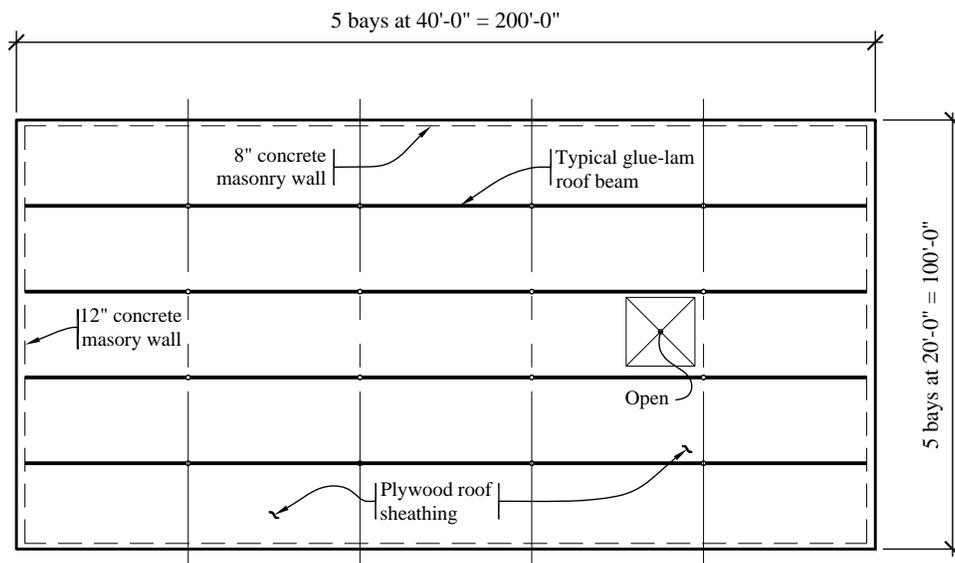
Figure 13.1-1 Roof plan
(1.0 in. = 25.4 mm, 1.0 ft = 0.3048 m)

The long side walls are solid (no openings). The end walls are penetrated by several large doors, which results in more highly stressed piers between the doors (Figure 13.1-2); thus, the greater thickness for the end walls.
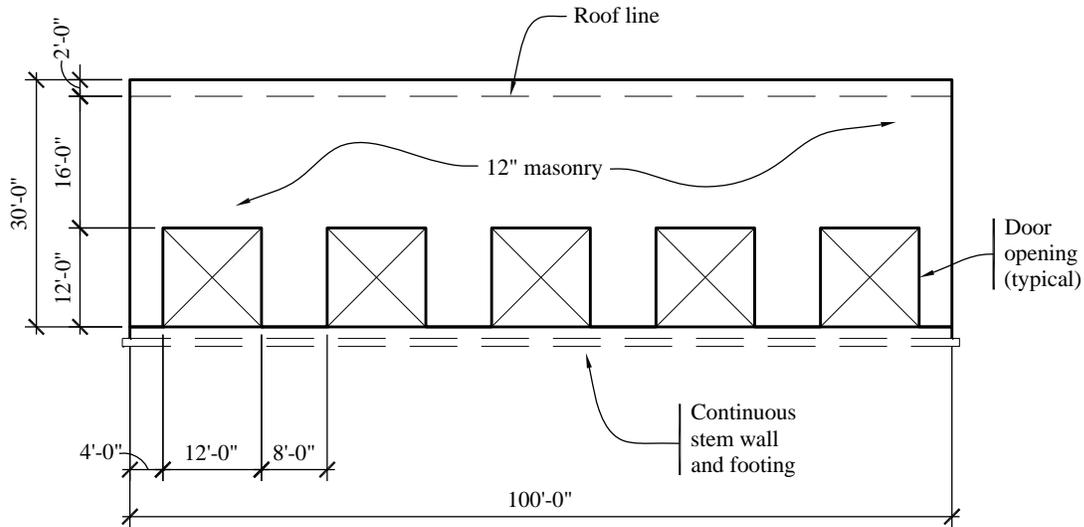
Figure 13.1-2 End wall elevation
(1.0 in. = 25.4 mm, 1.0 ft = 0.3048 m)

The floor is concrete slab-on-grade construction. Conventional spread footings are used to support the interior steel columns. The soil at the site is a dense, gravelly sand.

The roof structure is wood and acts as a diaphragm to carry lateral loads in its plane from and to the exterior walls. The roofing is ballasted, yielding a total roof dead load of 20 psf. There are no interior walls for seismic resistance. This design results in a highly stressed diaphragm with large calculated deflections. The design of the wood roof diaphragm and the masonry wall-to-diaphragm connections is illustrated in Sec. 14.2.

In this example, the following aspects of the structural design are considered:

Design of reinforced masonry walls for seismic loads

Computation of *P-delta* effects.

13.1.2 Design Requirements
This building could qualify for the simplified approach in *Standard* Section 12.14, although the "long" method per *Standard* Section 11.4-11.6 has been followed.

13.1.2.1 Seismic parameters. The ground motion response coefficients are found from USGS based upon latitude and longitude. The site class is taken from a site-specific geotechnical report and is typical for dense sands and gravels. The warehouse is not designated for hazardous materials and does not house any essential facility, thus the occupancy category is "all other".

Site Class = C

$S_S = 2.14$

$S_1 = 0.74$

Occupancy Category (*Standard* Sec. 1.5.1) = II

The remaining basic parameters depend on the ground motion adjusted for site conditions.

13.1.2.2 Response parameter determination. The mapped spectral response factors must be adjusted for site class in accordance with *Standard* Section 11.4.3. The adjusted spectral response acceleration parameters are computed according to *Standard* Equations 11.4-1 and 11.4-2 for the short period and one-second period, respectively, as follows:

$S_{MS} = F_a S_S = 1.0(2.14) = 2.14$

$S_{M1} = F_v S_1 = 1.3(0.74) = 0.96$

Where F_a and F_v are site coefficients defined in *Standard* Tables 11.4-1 and 11.4-2, respectively. The design spectral response acceleration parameters (*Standard* Sec. 11.4.4) are determined in accordance with *Standard* Equations 11.4-3 and 11.4-4 for the short-period and one-second period, respectively:

$$S_{DS} = \frac{2}{3} S_{MS} = \frac{2}{3}(2.14) = 1.43$$

$$S_{D1} = \frac{2}{3} S_{M1} = \frac{2}{3}(0.96) = 0.64$$

The Seismic Design Category may be determined by the design spectral acceleration parameters combined with the Occupancy Category. For buildings assigned to Seismic Design Category D, masonry shear walls must satisfy the requirements for special reinforced masonry shear walls in accordance with *Standard* Section 12.2. A summary of the seismic design parameters follows:

Seismic Design Category (*Standard* Sec. 11.6): D

Seismic Force-Resisting System (*Standard* Table 12.2-1)   : Special Reinforced Masonry Shear Wall

Response Modification Factor, *R:* 5

Deflection Amplification Factor, C_d: 3.5

System Overstrength Factor, Ω_0: 2.5

Redundancy Factor, ρ (*Standard* Sec. 12.3.4.2): 1.0

(Determination of ρ is discussed in Section 13.1.3 below.)

13.1.2.3 Structural design considerations. With respect to the lateral load path, the roof diaphragm supports approximately the upper 16 feet of the masonry walls (half the clear span plus the parapet) in the out-of-plane direction, transferring the lateral force to in-plane masonry shear walls. This is more precisely calculated in Section 13.1.4.1.

Soil structure interaction is not considered.

The building is of bearing wall construction.

Other than the opening in the roof, the building is symmetric about both principal axes, and the vertical elements of the seismic force-resisting system are arrayed entirely at the perimeter. The opening is not large enough to be considered an irregularity (per *Standard* Table 12.3-1); thus, the building is regular, both horizontally and vertically. *Standard* Table 12.6-1 permits several analytical procedures to be used; the equivalent lateral force (ELF) procedure (*Standard* Sec. 12.8) is selected for use in this example. The direction of loading requirements of *Standard* Section 12.5 are for walls that act in both principal directions, which is not the case for this structure, as will be discussed in more detail.

There is no inherent torsion because the building is symmetric. The effects of accidental torsion and its potential amplification, need not be included because the roof diaphragm is flexible (*Standard* Sec. 12.8.4.2).

The masonry bearing walls also must be designed for forces perpendicular to their plane (*Standard* Sec. 12.11.1).

For in-plane loading, the walls are treated as cantilevered shear walls. For out-of-plane loading, the walls are treated as simply supported at top and bottom. The assumption of a pinned connection at the base is deemed appropriate because the foundation is shallow and narrow, which permits rotation near the base of the wall.

13.1.3 Load Combinations

The basic load combinations are the same as specified in *Standard* Section 2.3.2. The seismic load effect, *E*, is defined by *Standard* Equations 12.4-1, 12.4-3 and 12.4-4, as follows:

$$E = E_h + E_v = \rho Q_E \pm 0.2 S_{DS} D = (1.0) Q_E \pm 0.2 (1.43) D = Q_E \pm 0.286 D$$

This assumes $\rho = 1.0$ as will be confirmed in the following section.

13.1.3.1 Redundancy Factor. In accordance with *Standard* Section 12.3.4.2, the redundancy factor, ρ, applies to the in-plane load direction.

In order to achieve $\rho = 1.0$, the two conditions in *Standard* Section 12.3.4.2 must be met. In the long direction there are no walls with height-to length ratios exceeding 1.0; thus $\rho = 1.0$ in the long direction. In the short direction the pier heights do exceed the length; thus their conditions must be checked. For our case, both are met.

Although the calculation is not shown here, note that a single 8-foot-long pier carries approximately 23 percent (determined by considering the relative rigidities of the piers) of the in-plane load for each end wall. Thus, failure of a single pier results in less than 33 percent reduction in base shear resistance.

Loss of a single pier will not result in extreme torsional irregularity because the diaphragm is flexible.

Even if the diaphragm were rigid, an extreme torsional irregularity would not be created. The lateral deflection of end wall with all piers in place is approximately 0.018 inch (determined by RISA analysis). Lateral deflection of end wall with one pier removed is 0.024 inch. The larger deflection divided by the average of both deflections is less than 1.4:

$$\frac{0.024}{\left(\dfrac{0.018+0.024}{2}\right)}=1.14<1.4$$

Therefore, even if the diaphragm were rigid, there is no extreme torsional irregularity as per *Standard* Table 12.3-1.

13.1.3.2 Combination of load effects. Load combinations for the in-plane loading direction from *Standard* Section 2.3.2 are:

$1.2D + 1.0E + 0.5L + 0.2S$

and

$0.9D + 1.0E + 1.6H$

L, S and H do not apply for this example (roof live load, L_r, is not floor live load, *L*) so the load combinations become:

$1.2D + 1.0E$

and

$0.9D + 1.0E$

For this case, $E = E_h \pm E_v = \rho Q_E \pm 0.2 \, S_{DS}D = (1.0)Q_E \pm (0.2)(1.43)D = Q_E \pm 0.286D$

Where the effect of the earthquake determined above, $1.2D + 1.0(Q_E \pm 0.286D)$, is inserted in each of the load combinations, the controlling cases are $1.486D + Q_E$ when gravity and seismic are additive and $0.614D - Q_E$ when gravity and seismic counteract.

These load combinations are for the in-plane direction of loading. Load combinations for the out-of-plane direction of loading are similar except that the redundancy factor, ρ, is not applicable. Thus, for this example (where $\rho = 1.0$), the load combinations for both the in-plane and the out-of-plane directions are $1.486D + Q_E$ and $0.614D - Q_E$.

The combination of earthquake motion (and corresponding loading) in two orthogonal directions as per *Standard* Section 12.5.3.a need not be considered. *Standard* Section 12.5.4 for Seismic Design Category D refers to Section 12.5.3 for Category C, which requires consideration of direction to produce maximum effect where horizontal irregularity Type 5 exists ("non-parallel systems"); this building does not have that irregularity. *Standard* Section 12.5.4 also requires consideration of direction for maximum effect for elements that are part of intersecting systems *if* those elements receive an axial load from seismic action that exceeds 20 percent of their axial strength; axial loads are less than that for this building.

If a masonry control joint is provided at the corner, there are no elements acting in two directions. The short pier at the corner can be designed as an "L" shaped element, which means that it does participate in both directions. The vertical seismic force in that pier, generated by frame action, is small and easily less than 20 percent of its capacity. Therefore, no element of the seismic force-resisting system is required to be checked for the direction of load that produces the maximum effect. Although it is not required, the

typical pier in the end wall will be checked using the method of *Standard* Section 12.5.3.a. to illustrate the *Standard's* method for design to account for orthogonal effects.

13.1.4 Seismic Forces

Seismic base shear, diaphragm force and wall forces are discussed below.

13.1.4.1 Base Shear. Base shear is computed using the parameters determined previously. The *Standard* does not recognize the effect of long, flexible diaphragms on the fundamental period of vibration. The approximate period equations, which limit the computed period, are based only on the height. Since the structure is relatively short and stiff, short-period response will govern the design equations. Refer to the *Provisions* Part 3 Resource Paper 5 for discussion of rigid-wall flexible-diaphragm building behavior. According to *Standard* Section 12.8 (for short-period structures):

$$V = C_s W = \left[\frac{S_{DS}}{R / I} \right] W = \left[\frac{1.43}{5 / 1} \right] W = 0.286 \, W$$

The seismic weight for forces in the long direction is as follows:

Roof = (20 psf)(100 ft)(200 ft)	=	400 kips
End walls = (103 psf) (2 walls)[(30 ft)(100 ft) – (5)(12 ft)(12 ft)](17.8 ft/28 ft)*	=	299 kips
Side walls = (65 psf) (30ft)(200ft)(2 walls)	=	780 kips
Total	=	1,479 kips

*Only the portion of the end walls that is distributed to the roof contributes to seismic weight in the long direction.

(The initial estimates of 65 psf for 8-inch CMU and 103 psf for 12-inch CMU are slightly higher than normal-weight CMU with grouted cells at 24 inches on center. However, grouted bond beams at 4 feet on center will be included, as will certain additional grouted cells.)

Note that the centroid of the end walls is determined to be 17.8 feet above the base, so the portion of the weight distributed to the roof is approximately the total weight multiplied by 17.8 feet/28 feet (weights and section properties of the walls are described subsequently).

Therefore, the base shear to each of the long walls is as follows:

V_u = (0.286)(1,479 kips)/2 = 211 kips

The seismic weight for forces in the short direction is:

Roof = (20 psf)(100 ft)(200 ft)	=	400 kips
Side walls = (65 psf)(2 walls)(30ft)(200ft)(15ft/28ft)*	=	418 kips
End walls = (103 psf)(2 walls)[(30ft)(100ft)-5(12ft)(12ft)]	=	470 kips
Total	=	1,288 kips

*Only the portion of the side walls that is distributed to the roof contributes to seismic weight in the short direction.

The base shear to each of the short walls is as follows:

$V_u = (0.286)(1,288 \text{ kips})/2 = 184 \text{ kips}$

13.1.4.2 Diaphragm force. See Section 11.2 for diaphragm forces and design.

13.1.4.3 Wall forces. Because the diaphragm is flexible with respect to the walls, shear is distributed to the walls on the basis of beam theory, ignoring walls perpendicular to the motion (this is the "tributary" basis).

The building is symmetric. Given the previously explained assumption that accidental torsion need not be applied, the force to each wall becomes half the force on the diaphragm.

All exterior walls are bearing walls and, according to *Standard* Section 12.11.1, must be designed for a normal (out-of-plane) force of $0.4S_{DS}IW_w$ where W_w = weight of wall. The out-of-plane design is shown in Sections 13.1.5.2 and 13.1.6.3.

13.1.5 Side Walls

The total base shear is the design force. *Standard* Section 14.4, which cites TMS 402, is the reference for design strengths. The compressive strength of the masonry, f_m', is 2,000 psi. TMS 402 Section 4.2.2.2.1 gives $E_m = 900f_m' = (900)(2 \text{ ksi}) = 1,800 \text{ ksi}$.

For 8-inch-thick CMU with vertical cells grouted at 24 inches on center and horizontal bond beams at 40 inches on center, the weight is conservatively taken as 65 psf (recall the CMU are normal weight) and the net bedded area is 51.3 in.^{2}/ft based on tabulations in NCMA-TEK 14-1B.

13.1.5.1 Horizontal reinforcement – side walls. As determined in Section 13.1.4.1, the design base shear tributary to each longitudinal wall is 211 kips. Based on TMS 402 Section 7.3.2.6.1.1, the design shear strength must exceed either the shear corresponding to the development of 1.25 times the nominal flexure strength of the wall (which is very unlikely in this example due to the length of wall) or 2.5 times V_u, which in this case is 2.5(211) = 528 kips.

From TMS 402 Section 9.3.4.1.2.1, the masonry component of the shear strength capacity for reinforced masonry is as follows:

$$V_{nm} = \left[4.0 - 1.75 \left(\frac{M_u}{V_u d_v} \right) \right] A_n \sqrt{f_m'} + 0.25\, P_u$$

For a single-story cantilever wall, $M_u/V_u d_v = h/d$, which is (28/200) = 0.14 for this case assuming no control joints. For the long walls and conservatively treating P as 0.614 times the weight of the wall only, without considering the roof weight contribution:

$$V_{nm} = [4.0 - 1.75(0.14)](51.3)(200)\sqrt{2,000} + 0.25\big[(0.614)(390)\big] = 1,783 \text{ kips}$$

Shear strength of masonry walls is given in TMS 402 Equation 9-21 as:

$$V_n = \left(V_{nm} + V_{ns} \right) \gamma_g$$

Where $\gamma_g = 0.75$ for partially grouted shear walls, which is the case for this wall. Therefore,
$\phi V_m = 0.8(1,783)(0.75) = 1,070 \text{ kips} > 528 \text{ kips}$ OK

where $\phi = 0.8$ is the strength reduction factor for shear from TMS 402 Section 9.1.4.5.

Horizontal reinforcement therefore is not required for shear strength but is required if the wall is to qualify as a Special Reinforced Masonry Wall (TMS 402 Sec. 7.3.2.6(b)). *Standard* Table 12.2-1 does not permit lower quality masonry walls in Seismic Design Category D.

According to TMS 402 Section 7.3.2.6(c), minimum horizontal reinforcement is $0.0007A_g = (0.0007)(7.625 \text{ in.})(8 \text{ in.}) = 0.043 \text{ in.}^2$ per course, but the author believes it prudent to use more horizontal reinforcement for shrinkage in this very long wall and then use minimum reinforcement in the vertical direction [this concept applies even though this wall requires far more than the minimum reinforcement (also $0.0007A_g$) in the vertical direction due to its large height-to-thickness ratio]. Two #5 bars at 40 inches on center provide 0.186 in.^{2} per foot. This amounts to 0.35 percent of the area of masonry plus the grout in the bond beams. NCMA-TEK 10-3 calculates the amount of reinforcing required to effectively restrain shrinkage cracks and eliminate control joints as 0.2 percent of the net area of masonry, so the reinforcing is deemed adequate for shrinkage. However, the actual shrinkage properties of the masonry and the grout as well as local experience should be considered in deciding how much reinforcement to provide. For long walls that have no control joints, as in this example, providing more than minimum horizontal reinforcement is appropriate.

13.1.5.2 Out-of-plane flexure – side walls. The design demand for seismic out-of-plane flexure is $0.4S_{DS}Iw_w$ (*Standard* Sec. 12.11.1). For a wall weight of 65 psf for the 8-inch-thick CMU side walls, this demand is $0.4(1.43)(1)(65 \text{ psf}) = 37 \text{ psf}$.

Calculations for out-of-plane flexure become somewhat involved and include the following:

1. Select a trial design.

2. Investigate to ensure ductility (i.e., check maximum reinforcement limit).

3. Make sure the trial design is suitable for wind (or other nonseismic) lateral loadings using the wind provisions of the *Standard* (which satisfies the IBC) (this is not illustrated in this example).

4. Calculate mid-height deflection due to wind by TMS 402 (not illustrated in this example) (note that while the *Standard* has story drift requirements, it does not impose a mid-height deflection limit for walls).

5. Calculate seismic demand. This computation requires consideration of *P-delta* effects because of the wall slenderness (seismic demand is greater than wind for this wall).

6. Determine seismic resistance and compare to the demand determined in Step 5.

7. Calculate mid-height deflection due to seismic loads by TMS 402.

Proceed with these steps as follows:

13.1.5.2.1 Trial design. A trial design of #7 bars at 24 inches on center is selected. See Figure 13.1-3.
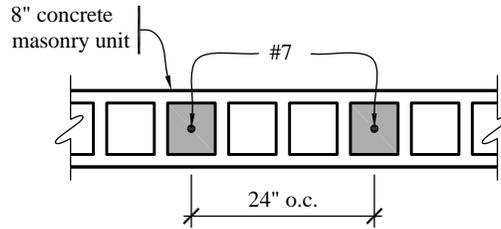
Figure 13.1-3 Trial design for 8-inch-thick CMU wall
(1.0 in. = 25.4 mm)

13.1.5.2.2 Investigate to ensure ductility. The critical strain condition corresponds to a strain in the extreme tension reinforcement (which is a single #7 centered in the wall in this example) equal to α times the strain at yield stress. α is the tension reinforcement strain factor (equal to 1.5 for out-of-plane flexure; see TMS 402 9.3.3.5).

Based on TMS 402 Section 9.3.3.5.1(a) for this case:

$t = 7.63$ in.

$d = t/2 = 3.81$ in.

$\varepsilon_m = 0.0025$

$\varepsilon_s = 1.5\varepsilon_y = 1.5(f_y/E_s) = 1.5(60 \text{ ksi} / 29{,}000 \text{ ksi}) = 0.0031$

$$c = \left[\frac{\varepsilon_m}{(\varepsilon_m + \varepsilon_s)}\right]d = 1.70 \text{ in.}$$

$a = 0.8c = 1.36$ in.

The Whitney compression stress block, $a = 1.36$ inches for this strain distribution, is greater than the 1.25-inch face shell width. Thus, the compression stress block is broken into two components: one for full compression against solid masonry (the face shell), and another for compression against the webs and grouted cells but accounting for the open cells. These are shown as C_1 and C_2 in Figure 13.1-4:

$C_1 = 0.80f_m'$ (1.25 in.)$b = (0.80)(2 \text{ ksi})(1.25)(24) = 48$ kips (for a 24-inch length)

$C_2 = 0.80\,f_m'$ (a-1.25 in.)(8 in.) $= (0.80)(2 \text{ ksi})(1.36\text{-}1.25)(8) = 1.41$ kips (for a 24-inch length)

The 8-inch dimension in the C_2 calculation is for the combined width of the grouted cell and the adjacent mortared webs over a 24-inch length of wall. The actual width of one cell plus the two adjacent webs will vary with various block manufacturers and may be larger or smaller than 8 inches. The 8-inch value has the benefit of simplicity (and is correct for solidly grouted walls).
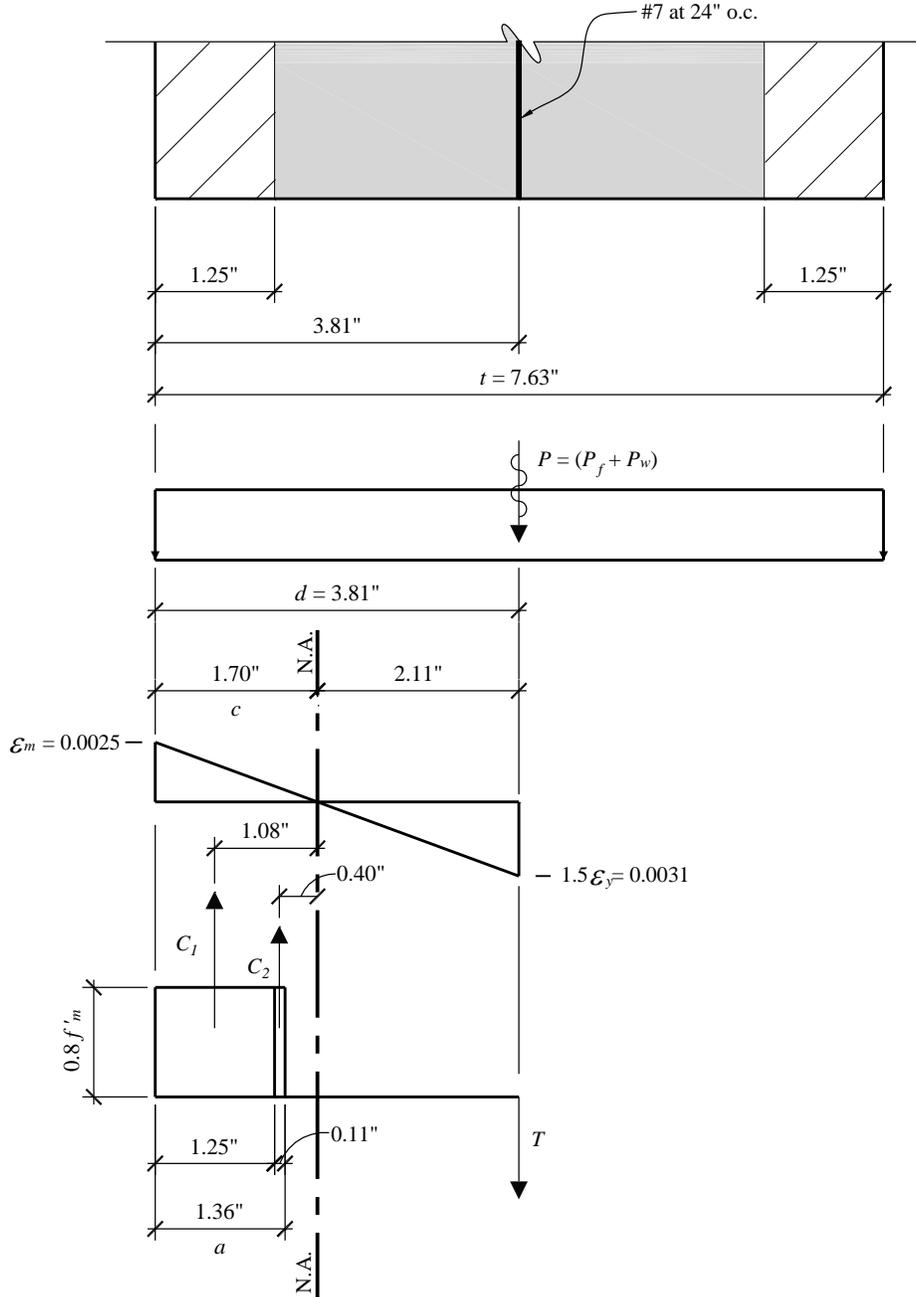
Figure 13.1-4 Investigation of out-of-plane ductility for the 8-inch-thick CMU side walls
(1.0 in. = 25.4 mm)

T is based on $F_y A_s$ (TMS 402 Sec. 9.3.3.5.1(c)):

$T = F_y A_s = (1.0)(60 \text{ ksi})(0.60 \text{ in.}^2) = 36 \text{ kips (for a 24-inch length)}$

P is based on the load combination of $D + 0.75L + 0.525Q_E$ (TMS 402 Sec. 9.3.3.5.1(d)).

Q_E is the effect of horizontal seismic motions, and P is a vertical force. Q_E produces overturning forces, but because this is such a long wall, the vertical force due to horizontal seismic motion is not significant, so the net total vertical force is taken as zero here. Therefore Q_E is zero in determining P for this wall.

Conservatively neglecting the roof weight:

$$Q_E = F_p = 0.2S_{DS}D = (0.2)(1.43)\left[(65\text{ psf})\left(\frac{28\text{ ft}}{2}+2\text{ ft}\right)\left(\frac{24\text{ in}}{12\text{ in}}\right)\right] = 595\text{ lb/24 in. length}$$

$$P = (65\text{ psf})\left(\frac{28\text{ ft}}{2}+2\text{ ft}\right)\left(\frac{24\text{ ft}}{12\text{ in}}\right)+(0.75)(0)\pm(0.525)(0\text{ lb}) = 2.08\text{ kips/24 in. length}$$

Check $C_1 + C_2 > T + P$ (all for 24-inch length):

$T + P = 36 + 2.08 = 38.1$ kips

$C_1 + C_2 = 49.4$ kips > 38.1 kips OK

The compression capacity is greater than the tension capacity; therefore, the ductile failure mode criterion is satisfied.

13.1.5.2.3 Check for wind load. The wind design check is beyond the scope of this seismic example, so it is not presented here. Both strength and deflection need to be ascertained in accordance with a building code; most are based on the *Standard*, which we are using. For our example, a check on strength to resist wind was found to conform to the *Standard* and is not shown here.

13.1.5.2.4 Calculate mid-height deflection due to wind by *Standard*. Deflection due to wind was found to conform to the *Standard* and is not shown here.
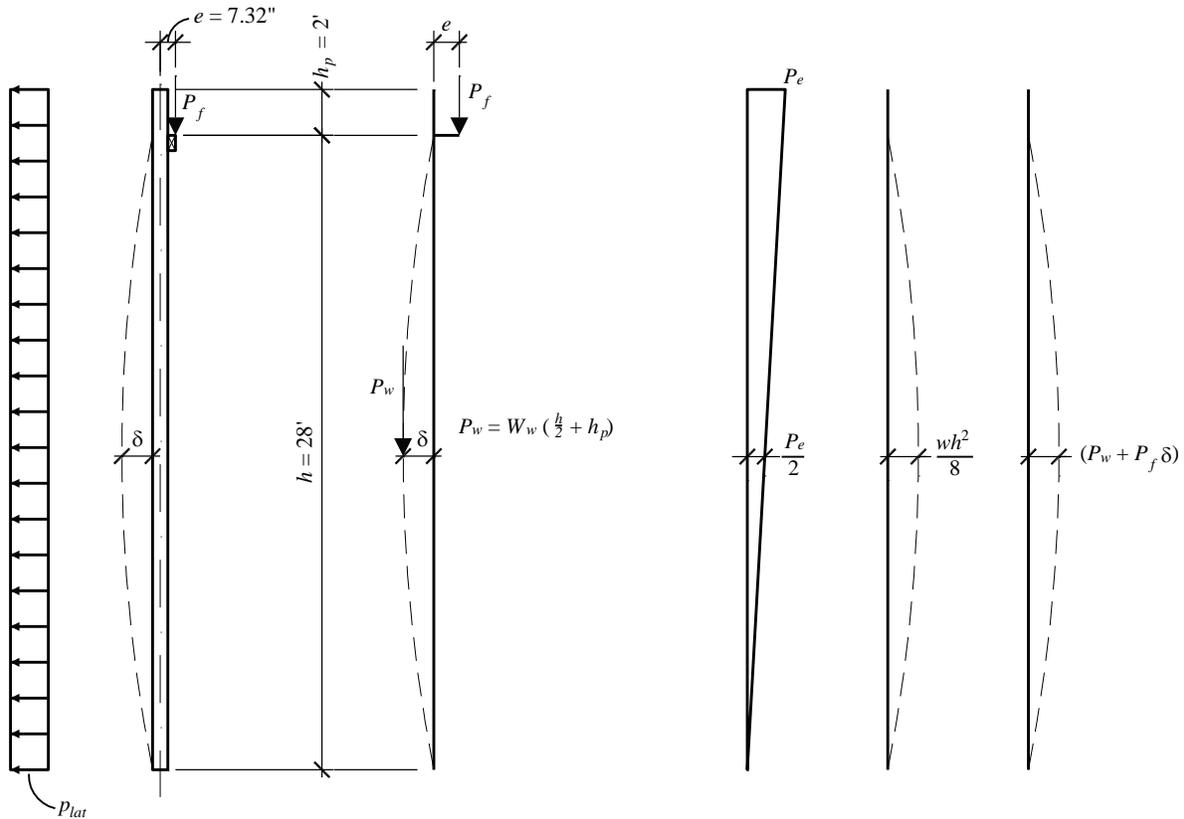
Figure 13.1-5 Basis for out-of-plane deflection calculation

13.1.5.2.5 Calculate seismic demand. For this case, the two load factors for dead load apply: 0.614*D* and 1.486*D*. Conventional wisdom holds that the lower dead load will result in lower moment-resisting capacity of the wall, so the 0.614*D* load factor would be expected to govern. However, the lower dead load also results in lower *P-delta,* so both cases should be checked. (As it turns out, the higher factor of 1.486*D* controls).

$w_u = 37$ psf (from Sec. 13.1.5.3)

Check moment capacity for 0.614*D*: TMS 402 Section 9.3.5.4 requires consideration of the secondary moment from the axial force acting through the deflection. TMS 402 Section 9.3.5.4.2 gives an equation that is essentially bilinear (two straight lines joined at the point of cracking). NCMA TEK 14-4B illustrates that determining the final moment by this method requires iteration.

Roof load, $P_f = (20 \text{ psf})(10 \text{ ft}) = 200$ plf

Wall load (at mid-height), $P_w = (65 \text{ psf})(16 \text{ ft}) = 1,040$ plf

$P = P_f + P_w = 1,240$ plf

$P_{uf} = (0.614)(200 \text{ plf}) = 123$ plf

$P_{uw} = (0.614)(1,040 \text{ plf}) = 638$ plf

13-14

$P_u = P_{uf} + P_{uw} = 761$ plf

Eccentricity, $e = 7.32$ in. (distance from wall centerline to roof reaction centerline)

Modulus of elasticity, $E_m = 1{,}800{,}000$ psi

$f_m' = 2000$ psi

Modular ratio, $n = \dfrac{E_s}{E_m} = 16.1$

The modulus of rupture, f_r, is found from TMS 402 Table 9.1.9.2. The values given in the table are for either hollow CMU or fully grouted CMU. Values for partially grouted CMU are not given; Footnote a indicates that interpolation between these values must be performed. As illustrated in Figure 13.1-6, and shown below, the interpolated value for this example is based on relative areas of hollow and grouted cells:

$$f_r = 84 + (163 - 84)\left[\frac{(103 - 60)}{(183 - 60)}\right] = 112 \text{ psi}$$

Another method for making the interpolation, while approximate, is simpler. It is based on 2/3 of the cells being hollow and 1/3 of the cells being grouted for the case of grouted cells at 24 inches on center:

$$f_r = 84\left(\frac{2}{3}\right) + 163\left(\frac{1}{3}\right) = 110 \text{ psi}$$

For this example, the value of $f_r = 112$ psi will be used.

From NCMA TEK 14-1B:

$I_n = 355$ in.^{4}/ft

$S_n = 93.2$ in.^{3}/ft

$A_n = 51.3$ in.^{2}/ft

$M_{cr} = S_n(f_r + P/A_n) = 93.2(112 + 1240/51.3) = 12{,}691$ in-lb/ft. Use $M_{cr} = 12{,}700$ in.-lb/ft. Note: this equation for M_{cr} is not in TMS 402; however, it is valid based on mechanics.

CASE 1
All cells open
$A = 60$ in.^{2}
$f_r = 63$ psi

CASE 2
(1) Cell grouted
$A = 103$ in.^{2}
$f_r = 98$ psi *

CASE 3
Fully grouted
$A = 183$ in.^{2}
$f_r = 163$ psi
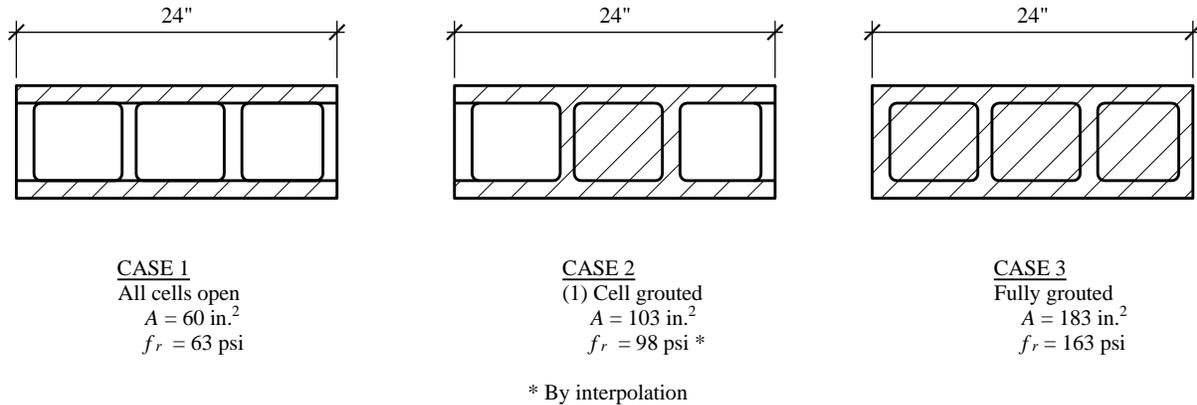
* By interpolation

Figure 13.1-6 Basis for interpolation of modulus of rupture, f_r
(1.0 in. = 25.4 mm, 1.0 psi = 6.89 kPa).

Axial load does enter the computation of the neutral axis. The equations for location of the neutral axis and cracked moment of inertia are given in TMS 402 Section 9.3.5.4.5. Thus:

$$c = \frac{A_s f_y + P_u}{0.64 f'_m b} = \frac{0.60 \text{ in.}^2 / 2 \text{ ft} (60 \text{ ksi}) + 1.240 \text{ klf}}{0.64 (2.0 \text{ ksi})(12 \text{ in./ft})} = 1.25 \text{ in.}$$

$A_s = 0.30$ in.^{2}/ft

Note: The 1.25 in dimension for the neutral axis is still within the face shell of a standard 8" unit. If the reinforcing were greater or the axial load significantly higher, the neutral axis would most likely be within the cells, which would necessitate more involved calculations for the moment capacity and cracked moment of inertia. As it is, the equations for uniform rectangular sections may be used.

$$I_{cr} = n\left(A_s + \frac{P_u}{f_y} \frac{t_{sp}}{2d} \right)(d - c)^2 + \frac{bc^3}{3}$$

$= 16.1(0.30 \text{ in.}^2/\text{ft} + 1.240 \text{ klf}/60 \text{ ksi} *1)(3.81 \text{ in. } - 1.25 \text{ in.})^2 + (12 \text{ in./ft})(1.25 \text{ in.})^3/3$

$= 42.1$ in.^{4}/ft

Note that I_{cr} could be recomputed for $P_u = 0.614D$ and $P_u = 1.486D$, but that refinement is not pursued in this example. In the opinion of the author, the most correct method for computing the cracked section properties is to use P_u. This will necessitate two sets of cracked section properties for this example. For purposes of illustration, one set of cracked section properties, with $P = 1.0D$, is computed.

The seismic force acting on the parapet, if in the same direction as the force acting on the wall, will lower the maximum moment at mid-height of the wall. Common practice is to ignore any seismic loading at the parapet for the design of the wall reinforcing and the story height is treated as a simple span. The computation of the secondary moment in an iterative fashion is shown below:

First iteration:

$$M_{u1} = w_u h^2 / 8 + P_{uf} e_u + (P_{uf} + P_{uw})\delta_u$$

$$M_{u1} = \frac{(37 \text{ psf}/12)(336 \text{ in.})^2}{8} + (123 \text{ plf})\left(\frac{7.32 \text{ in.}}{2}\right) + (761 \text{ plf})(0)$$

$M_{u1} = 43{,}512 + 450 + 0 = 43{,}962$ in.-lb/ft $> M_{cr} = 12{,}700$ in.-lb/ft

$$\delta_{s1} = \frac{5M_{cr}h^2}{48EI_n} + \frac{5(M_{u1} - M_{cr})h^2}{48EI_{cr}}$$

$$\delta_{s1} = \frac{5(12{,}700)(336)^2}{48(1{,}800{,}000)(355)} + \frac{5(43{,}962 - 12{,}700)(336)^2}{48(1{,}800{,}000)(42.1)} = 0.234 + 4.85 = 5.08 \text{ in.}$$

Second iteration:

$$M_{u2} = 43{,}512 + 450 + (761)(5.08) = 47{,}831 \text{ in.-lb}$$

$$\delta_{s2} = 0.234 + \frac{5(47{,}831 - 12{,}700)(336)^2}{48(1{,}800{,}000)(42.1)} = 0.234 + 5.452 = 5.69 \text{ in.}$$

Third iteration

$$M_{u3} = 43{,}512 + 450 + (761)(5.69) = 48{,}289 \text{ in.-lb/ft}$$

$$\delta_{s3} = 0.234 + \frac{5(48{,}289 - 12{,}700)(336)^2}{48(1{,}800{,}000)(42.1)} = 0.234 + 5.523 = 5.76 \text{ in.}$$

Convergence check:

$$\frac{5.76 - 5.69}{5.69} = 1.2\% < 5\%$$

$M_u = 48{,}289$ in.-lb/ft (for the $0.614D$ load case)

Using the same procedure, find M_u for the $1.486D$ load case. The results are summarized below:

First iteration:

$P_u = 1.486 (P_f + P_w) = 1.486(200 + 1{,}040) = 297 + 1{,}545 = 1{,}843$ plf

$M_{u1} = 44{,}600$ in.-lb/ft

$\delta_{u1} = 5.18$ in.

Second iteration:

$M_{u2} = 54,154$ in.-lb/ft

$\delta_{u2} = 6.67$ in.

Third iteration:

$M_{u3} = 56,887$ in.-lb/ft

$\delta_3 = 7.09$ in.

Fourth iteration:

$M_{u4} = 57,670$ in.-lb/ft

$\delta_{u4} = 7.21$ in.

Check convergence:

$$\frac{7.21 - 7.09}{7.09} = 1.7\% < 5\%$$

$M_u = 57,670$ in.-lb/ft (for the $1.486D$ load case)

The iterative method described above is consistent with NCMA TEK 14-11B. The 2013 edition of TMS 402 Section 9.3.5.4.3 now includes alternate provisions for the design of slender walls using a moment magnifier approach. For the computation of deflection at nominal strength, the cracked stiffness is conservatively used over the entire height of the wall. The absence of the bilinear relation is much closer to deflection computations by other methods, such as given in TMS 402, Section 5.2.1.4.2. The absence of bilinear relations allows direct computation of the final deflection and moment, rather than iteration. For illustration, moment demand using the moment magnifier provisions is shown here:

$$M_u = \psi M_{u,0} = M_{u,0} \left(\frac{1}{1 - \dfrac{P_u}{P_e}} \right)$$

Where:

$$P_e = \frac{\pi^2 E_m I_{eff}}{h^2} = \frac{\pi^2 (1{,}800 \text{ ksi})(42.1 \text{ in.}^4)}{(28 \text{ ft x } 12)^2} = 6.62 \text{ k/ft}$$

Therefore, for the $1.486D$ case:

$$M_u = 44.6 \text{ in.-k/ft} \left(\cfrac{1}{1 - \cfrac{1.84 \text{ k/ft}}{6.62 \text{ k/ft}}} \right) = 61.8 \text{ in.-k/ft}$$

which is approximately 7 percent larger than $M_u = 57.7$ in.-k/ft by the iterative method above.

13.1.5.2.6 Determine flexural strength of wall. Refer to Figure 13.1-7. As in the case for the ductility check, a strain diagram is drawn. Unlike the ductility check, the strain in the steel is not predetermined. Instead, as in conventional strength design of reinforced concrete, a rectangular stress block is computed first and then the flexural capacity is checked.

$T = A_s f_y = (0.30 \text{ in.}^2/\text{ft})60 \text{ ksi} = 18.0 \text{ klf}$

The results for the two axial load cases are shown in Table 13.1-2 below.

Table 13.1-2 Flexural Strength of Side Wall

Load Case	$0.614D + E$	$1.486D + E$
P_u, klf	0.761	1.843
$C = T + P_u$, klf	18.76	19.84
$a = C / (0.8f'_m b)$, in.	0.978	1.03
$M_n = C (d - a/2)$, in.-kip/ft	62.3	65.35
$\phi M_n = 0.9M_n$, in.-kip/ft	56.1	58.8
M_u, in.-kip/ft	48.3	57.7*
Acceptance	OK	OK

*The M_u from the alternative direct computation is approximately 5% higher than the design strength.
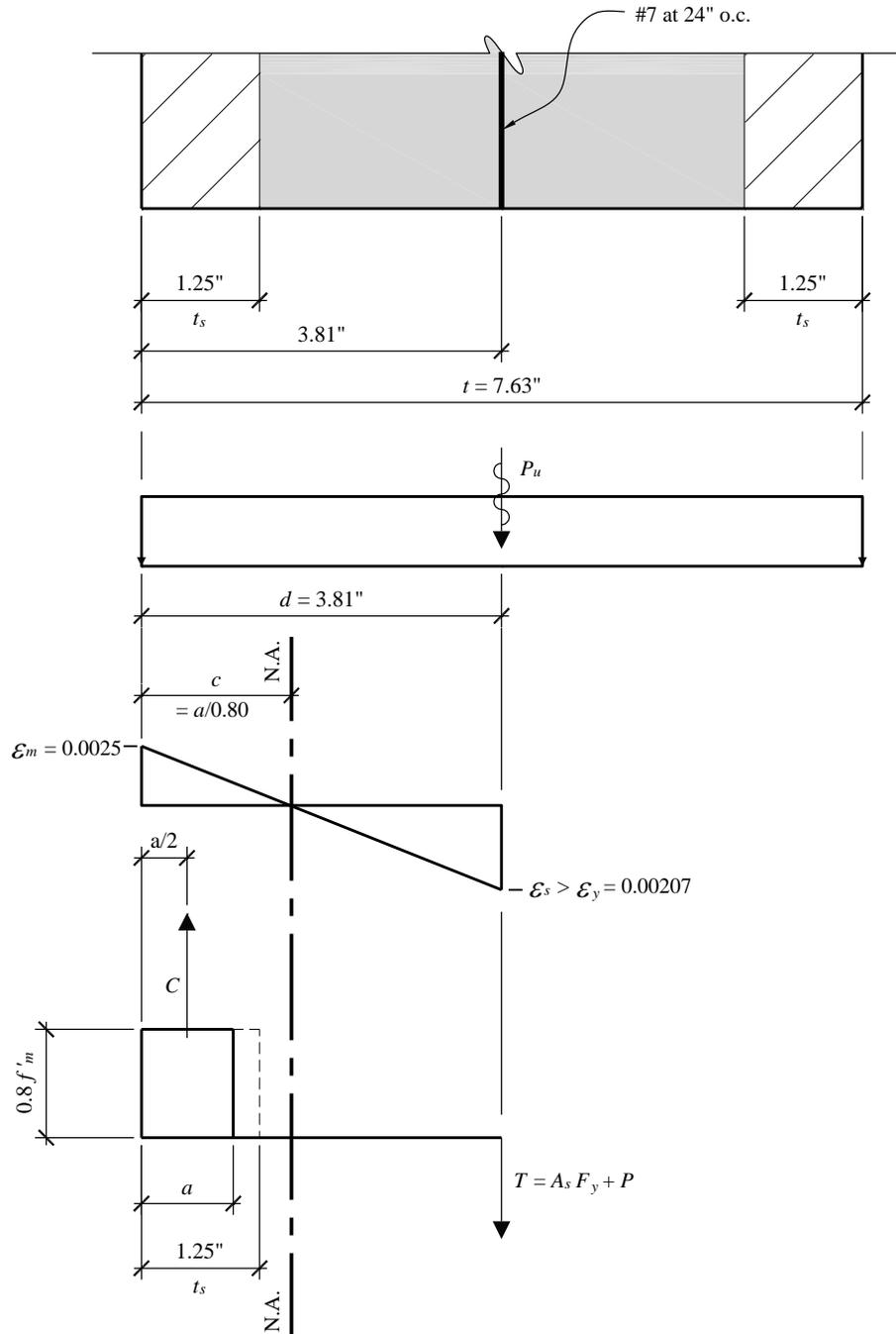
Figure 13.1-7 Out-of-plane strength for 8-inch-thick CMU walls
(1.0 in. = 25.4 mm)

Note that either wind or earthquake may control the stiffness and strength out-of-plane; earthquake controls for this example. A careful reading of *Standard* Section 12.5 should be made to see if the orthogonal loading combination will be called for; as discussed earlier, the orthogonal combination is not

required for this example (although an orthogonal combination check will be made for illustration purposes later).

13.1.5.2.7 Calculate mid-height deflection due to seismic loads by TMS 402. As in the calculation of out-of-plane flexural demand, the maximum deflection of the wall will be decreased if the seismic force acting on the parapet is in the same direction as the force acting on the wall. Though not common practice, the parapet loading can be taken as acting in the opposite direction as that of the wall below, increasing the maximum deflection. For the purposes of this example, the parapet loading is ignored and the story height is treated as a simple span.

P-Δ effects are required to be considered for mid-height deflection of the wall per TMS 402 Section 9.3.5.5. The same approaches (iterative or moment magnifier) can be used to account for P-Δ effects on deflection as were used for maximum moment demand. For expediency, the magnifier approach is shown here per Section 9.3.5.5.2. Note that as the previous calculation for I_{cr} was performed using $P = 1.0D$, the cracked moment of inertia is unchanged from before.

P = 1.240 klf

w = 0.7w_u = 0.7(37 psf) = 26 psf

$$I_{cr} = n\left(A_s + \frac{P}{f_y}\frac{t_{sp}}{2d}\right)(d-c)^2 + \frac{bc^3}{3} = 42.1 \text{ in.}^4/\text{ft}$$

$$M_a = \frac{w_a L^2}{8} + Pe = \frac{(26\,plf)(28\,ft)^2}{8} + 200\left(\frac{7.32}{2}\right) = 2,609\,ft-k/ft = 31,308\,in-k/ft$$

$$\delta_{ASD,0} = \frac{5M_{cr}h^2}{48EI_n} + \frac{5(M_a - M_{cr})h^2}{48EI_{cr}} = 0.234 + \frac{5(31,308-12,700)(336)^2}{48(1,800,000)(42.1)} = 3.13in$$

$$P_e = \frac{\pi^2 E_m I_{eff}}{h^2} = \frac{\pi^2(1,800\text{ ksi})(42.1\text{ in.}^4)}{(28\text{ ft x }12)^2} = 6.62\text{ k/ft}$$

$$\delta_s = \delta_{ASD,0}\left(\frac{1}{1-\dfrac{P}{P_e}}\right) = 3.85\text{ in.}$$

The allowable deflection at mid-height is given by Equation 9-36 in TMS 402 as

$$\delta_s \le 0.007h = 0.007(336\text{ in.}) = 2.35\text{ in.}$$

The maximum deflection is greater than the allowable deflection. To decrease deflections, the thickness of blocks can be increased or pilasters can be added to increase the stiffness of the wall. For this example, pilasters will be designed to stiffen the wall.

Assume pilaster spacing of 40 ft on center. The wall will span in two directions – between pilasters with a fixed boundary condition and between the roof and stem wall with a simply supported boundary

condition (rotation not restrained). Using the methodology in NCMA TEK note 14-3A, approximately 55% of the lateral load will span horizontally and the remaining 45% will span vertically.

Verify that the wall can span horizontally between pilasters. No axial load is present in the horizontal span, so a simple moment capacity can be calculated similar to reinforced concrete.

$$M_{u,H} = \frac{w_{u,H} h^2}{12} = \frac{0.55(37\,psf)(40\,ft)^2}{12} = 2{,}713\,ft - lb = 32{,}560in - lb$$

$$d = 3.81in$$

$$a = \frac{A_s f_y + P_u}{0.8 f_m' b} = \frac{(0.186in^2)(60{,}000\,psi) + 0}{0.8(2{,}000\,psi)(12in)} = 0.58in$$

$$\phi M_{n,H} = \phi A_s f_y (d - a/2) = 0.9(0.186in^2)(60{,}000\,psi)(3.81" - 0.58"/2) = 35{,}374in - lb$$

Wall is okay to span horizontally with (2) #5 at 40" on center. Try 16" x 16" pilaster built integrally with the wall with (4) #6 bars and #3 ties, one vertical bar in each corner (see Figure 13.1-8).
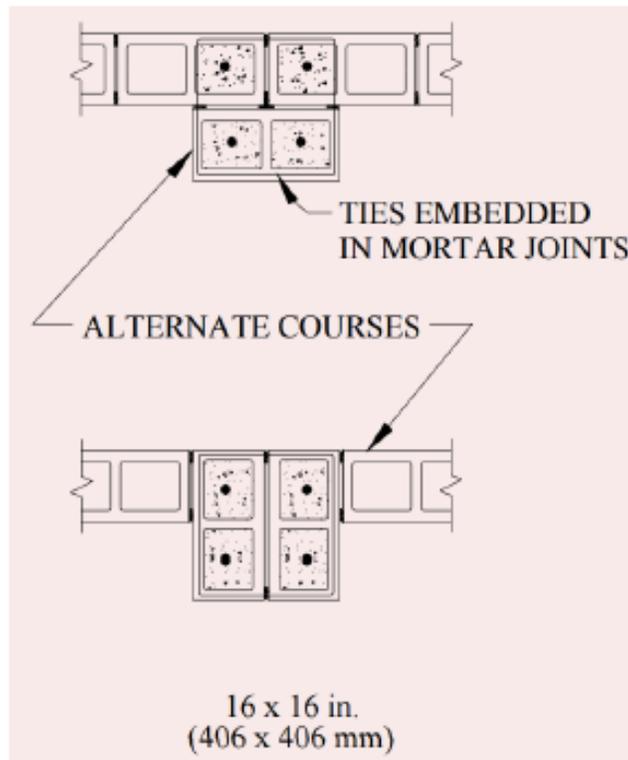
Figure 13.1-8 16" Square Pilaster Section

As the pilaster is not slender (h/t = 21), and the only dead load being resisted is self-weight with no eccentricity, increases to the moment demand due to *P-delta* effects are not likely to offset the increase of

moment capacity by the dead load. It would then be conservative to ignore the effects of dead load on the pilaster and treat it as a simply supported beam with transverse loading.

$$M_u = \frac{w_u h^2}{8} = \frac{0.55(37\,psf \times 20\,ft)(28\,ft)^2}{8} = 39,886\,ft - lb = 478,632\,in - lb$$

$$d = 15.625" - 1.25" \text{ face shell} - 1.5" \text{ clr} - 3/8" - 1/2(3/4") = 12.125" \rightarrow \text{Use } 12"$$

$$a = \frac{A_s f_y + P_u}{0.8 f_m' b} = \frac{2(0.44\,in^2)(60,000\,psi) + 0}{0.8(2,000\,psi)(15.625\,in)} = 2.11\,in$$

A 1.5" clear distance from the reinforcing to the face shell is used for constructability, in excess of the grout clear spacing requirement of 0.5" for course grout per TMS 402 Section 6.1.3.5. In one direction the masonry walls on either side of the pilaster can help resist the tensile or compressive forces per TMS 402 Section 5.4, giving increased moment capacity. However, it is conservative to neglect these flanges and design the pilaster as a rectangular element. In this situation, no issues with ductility or overstrength would be anticipated by neglecting the increased strength.

$$\phi M_{n,H} = \phi A_s f_y (d - a/2) = 0.9(0.88\,in^2)(60,000\,psi)(12" - 2.11"/2) = 520,059\,in - lb$$

Pilaster is okay for strength as designed. Check combined deflections of the pilaster and the wall.

$$f_r = 163\,psi$$

$$M_{cr} = S_x \times f_r = \frac{bh^2}{6} \times f_r = \frac{(15.625\,in)^3}{6}(163\,psi) = 103,633\,in - lb$$

$$M_{ASD} = \frac{w_{ASD} h^2}{8} = \frac{0.55(26\,psf \times 20\,ft)(28\,ft)^2}{8} = 27,920\,ft - lb = 335,042\,in - lb$$

$$I_n = \frac{bh^3}{12} = \frac{(15.625)^4}{12} = 4,967\,in^4$$

$$c = a/0.8 = 2.11/0.8 = 2.64\,in$$

$$I_{cr} = n\left(A_s + \frac{P}{f_y}\frac{t_{sp}}{2d}\right)(d-c)^2 + \frac{bc^3}{3} = 16.1(0.88+0)(12-2.64)^2 + \frac{15.625(2.64)^3}{3} = 1337.1\,in^4$$

$$\delta_{ASD,Pilaster} = \frac{5M_{cr}h^2}{48EI_n} + \frac{5(M_a - M_{cr})h^2}{48EI_{cr}}$$

$$= \frac{5(103,633)(336)^2}{48(1,800,000)(4,967)} + \frac{5(335,042 - 103,633)(336)^2}{48(1,800,000)(1337.1)} = 0.136 + 1.131 = 1.267\,in$$

Add the out of plane wall deflection to the pilaster deflection. The modulus of rupture for flexural tensile stress parallel to bed joints (masonry spanning horizontal) for partially grouted construction is taken from TMS 402 Table 9.1.9.2.

$$f_r = 167\,psi$$

$$M_{cr} = S_x \times f_r = \frac{bh^2}{6} \times f_r = \frac{(12in)(7.625in)^2}{6}(167\,psi) = 19,419in - lb$$

$$M_{ASD,H} = \frac{w_{ASD,H}h^2}{12} = \frac{0.55(26\,psf)(40\,ft)^2}{12} = 1,907\,ft - lb = 22,880in - lb$$

$$I_{cr} = n\left(A_s + \frac{P}{f_y}\frac{t_{sp}}{2d}\right)(d-c)^2 + \frac{bc^3}{3} = 16.1(0.186+0)(3.81-0.58/0.8)^2 + \frac{12(0.58/0.8)^3}{3} = 30.0in^4$$

$$\delta_{ASD,Wall} = \frac{M_{cr}h^2}{48EI_n} + \frac{(M_a - M_{cr})h^2}{48EI_{cr}}$$

$$= \frac{(19,419)(480)^2}{48(1,800,000)(357)} + \frac{(22,880-19,419)(480)^2}{48(1,800,000)(30.0)} = 0.145 + 0.308 = 0.453in$$

Total deflection is thus 1.267 + 0.453 = 1.72in which is less than the allowable deflection of 2.35in. Wall design with pilasters at 40 ft on center is adequate for out of plane forces.

The force in the wall that spans vertically decreases with the addition of pilasters. The vertical reinforcing likely could be reduced for the lower demand, but for brevity the vertical reinforcing will remain the same for this example.

Note that if control joints were used, joint spacing would need to match a multiple of the pilaster spacing, and the boundary conditions for the horizontal span would change. Detailing would also need to ensure that force transfer across the control joint can take place without in plane restraint of the wall.

13.1.5.3 In-plane flexure – side walls. In-plane calculations for flexure in masonry walls include two items per the *Provisions*:

Ductility check

Strength check

It is recognized that this wall is very strong and stiff in the in-plane direction. Many engineers would not even consider these checks as necessary in ordinary design. The ductility check is illustrated here to show a method of implementing the requirement.

13.1.5.3.1 Ductility check. For this case, with $M_u/V_ud_v < 1$ and $R > 5$, TMS 402 Section 9.3.3.5.4 refers to Section 9.3.3.5.1, which stipulates that the critical strain condition corresponds to a strain in the

extreme tension reinforcement equal to 1.5 times the strain associated with F_y. This calculation uses unfactored gravity loads (See Figure 13.1-9.).

$$c = \left(\frac{\varepsilon_m}{\varepsilon_m + \varepsilon_s}\right)d = \left(\frac{0.0025}{0.0025 + 0.0031}\right)200 \text{ ft} = 89.29 \text{ ft}$$

$$a = 0.8c = 71.43 \text{ ft}$$

$$C_m = 0.8f'_m ab_{avg} = (0.8)(2 \text{ ksi})(71.43 \text{ ft})(51.3 \text{ in.}^2/\text{lf}) = 5{,}862 \text{ kips}$$

Where b_{avg} is taken from the average area used earlier, 51.3 in.^{2}/ft results; see Figure 13.1-9 for locations of tension steel and compression steel (the rebar in the compression zone will act as compression steel). From this it can be seen that:

$$T_{s1} = f_y\left(\frac{73.80}{(2)(2 \text{ ft o.c.})}\right)(0.60) = 664 \text{ kips}$$

$$T_{s2} = f_y\left(\frac{36.91}{2 \text{ ft}}\right)(0.60) = 664 \text{ kips}$$

$$C_{s1} = f_y\left(\frac{15.42}{2 \text{ ft o.c.}}\right)(0.60) = 278 \text{ kips}$$

$$C_{s2} = f_y\left(\frac{73.87}{(2)(2 \text{ ft})}\right)(0.60) = 665 \text{ kips}$$
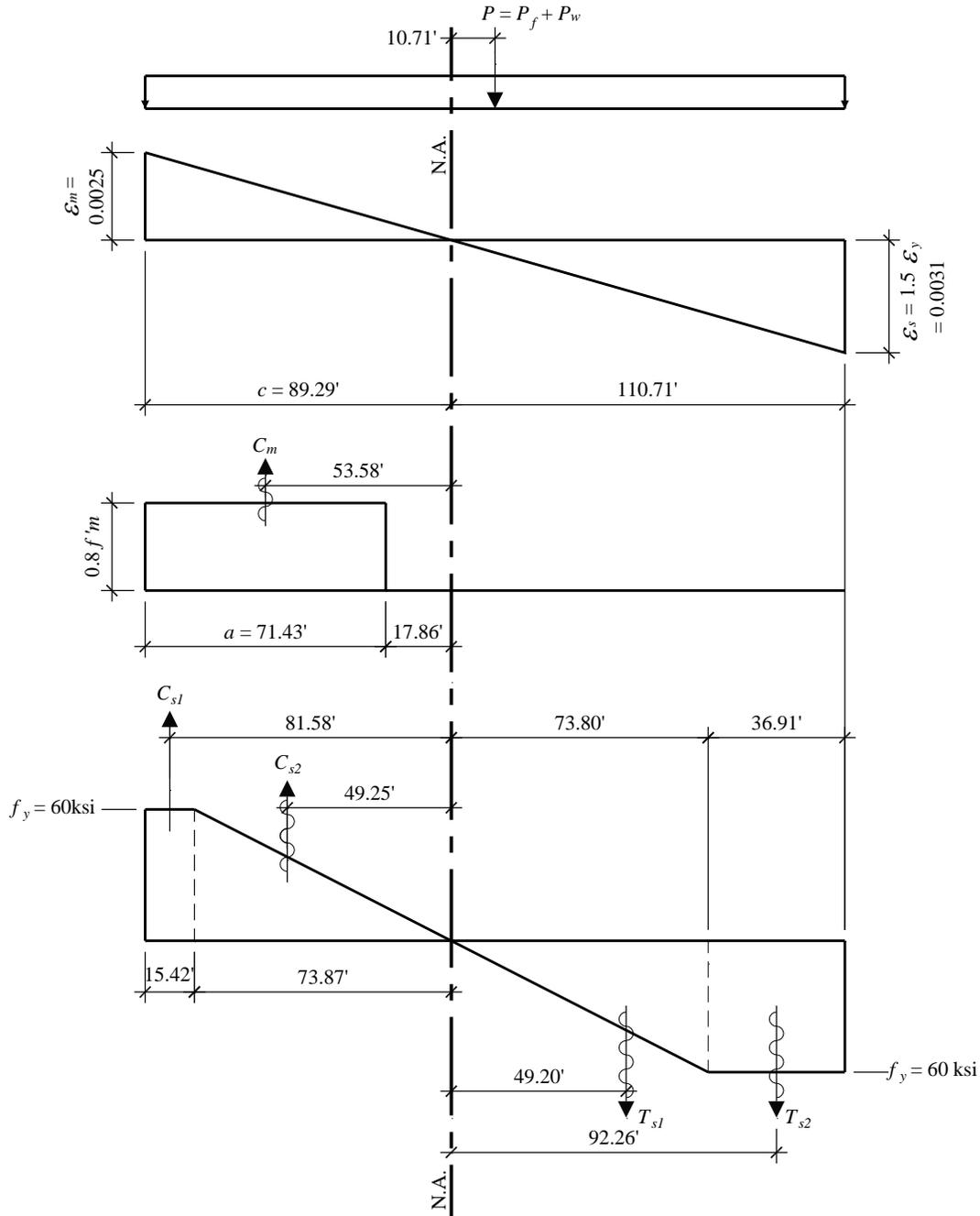
Figure 13.1-9 In-plane ductility check for side walls
(1.0 in. = 25.4 mm, 1.0 ksi = 6.89 MPa)

Some authorities would not consider the compression resistance of reinforcing steel that is not confined within ties. In one location (Section 9.3.2(e)) TMS 402 clearly requires transverse reinforcement (ties) for any steel used in compression, except as permitted in the maximum tensile reinforcement check (Section 9.3.3.5.1(e)) where it explicitly permits inclusion of compression reinforcement with or without lateral restraining reinforcement. TMS 402 Commentary 9.3.3.5 explains that confinement reinforcement

is not required because the maximum masonry compressive strain will be less than ultimate values. This inconsistency does not usually have a significant effect on computed results. The author has taken credit for unconfined compression reinforcement for strength and included it in ductility checks (though per the letter of TMS 402 unconfined compression reinforcement should be neglected for strength).

In the author's opinion, there are two approaches to the determination of P, one following TMS 402 and the other following the *Standard*:

P is at the base of the wall rather than at the mid-height:

TMS 402 Section 9.3.3.5.1(d):

$D + 0.75L + 0.525\ Q_E$

Since Q_E represents the effect of horizontal seismic forces, which equals zero for our case, and roof live load is not combined with seismic loads, this reduces to D:

$P = P_w + P_f = [(0.065\ \text{ksf})\ (30\ \text{ft}) + (0.02\ \text{ksf})(10\ \text{ft})](200\ \text{ft}) = 430\ \text{kips}$

Standard Section 12.4.2.3:

$(1.2 + 0.2\ S_{DS})D + \rho Q_E + L + 0.2S$

which reduces to:

$[1.2 + (0.2)(1.43)]D + 0 + 0 + 0$

$P_u = (1.486)(P_f + P_w) = (1.486)(480\ \text{kips}) = 713\ \text{kips}$

Continuing with the in-plane ductility check:

$\Sigma C > P + \Sigma T$

$C_m + C_{s1} + C_{s2} > P + T_{s1} + T_{s2}$

And conservatively using the higher of the two values for P,

$5{,}862 + 278 + 665 > 713 + 664 + 664$ $6{,}805 > 2{,}041$ OK

Therefore, there is enough compression capacity to ensure ductile failure. Note that either of the two values for P brings us to the same conclusion for this case.

It should also be noted that even if the compression reinforcement were neglected, there would still be enough compression capacity to ensure ductile failure.

In the opinion of the author, flexural yield is feasible for walls with $M_u/V_u d_v$ in excess of 1.0; this criterion limits the compressive strain in the masonry, which leads to good performance in strong ground shaking. For walls with $M_u/V_u d_v$ substantially less than 1.0, the wall will fail in shear before a flexural yield is possible. Therefore, the criterion does not affect performance. Well distributed and well developed reinforcement to control the shear cracks is the most important ductility attribute for such walls.

13.1.5.3.2 Strength check. The wall is so long with respect to its height that in-plane strength for flexure is acceptable by inspection. Shear strength was checked in Section 13.1.5.1.

13.1.6 End Walls

The transverse walls are designed in a manner similar to the longitudinal walls. Complicating the design of the transverse walls are the door openings, which leave a series of masonry piers between the doors.

13.1.6.1 Horizontal reinforcement – end walls. The minimum reinforcement, per TMS 40*2* Section 7.3.2.6, is $0.0007A_g = (0.0007)(11.625$ in.$)(8$ in.$) = 0.065$ in.^{2} per course. The maximum spacing of horizontal reinforcement is 48 inches, for which the minimum reinforcement is 0.39 in.^{2}. Two #4 in bond beams at 48 inches on center would satisfy the requirement. The large amount of vertical reinforcement would combine to satisfy the minimum total reinforcement requirement. However, given the 100-foot length of the wall, a larger amount is desired for control of restrained shrinkage as discussed in Section 13.1.5.1. Two #5 at 40 inches on center will be used to match the reinforcing of the side walls (adequate per Table 3 in NCMA TEK 10-3).

13.1.6.2 Vertical reinforcement – end walls. The area for each bay subject to out-of-plane wind is 20 feet wide by 30 feet high because wind load applied to the doors is transferred to the masonry piers. However, the area per bay subject to both in-plane and out-of-plane seismic forces is reduced by the area of the doors. This is because the doors are relatively light compared to the masonry. See Figures 13.1-11 and 13.1-12.

13.1.6.3 Out-of-plane flexure – end walls. Out-of-plane flexure is considered in a manner similar to that illustrated in Section 13.1.5.2. The design of this wall must account for the effect of door openings between a row of piers. The steps are the same as identified previously and are summarized here for convenience:

1. Select a trial design.

2. Investigate to ensure ductility.

3. Make sure the trial design is suitable for wind (or other non-seismic) lateral loadings using the wind provisions of the *Standard.*

4. If wind controls over seismic (it does not in this example), then calculate the mid-height deflection due to wind by TMS 402.

5. Calculate the seismic demand.

6. Determine the seismic resistance and compare to the demand determined in Step 5.

7. Calculate mid-height deflection due to seismic loads by TMS 402.

13.1.6.3.1 Trial design. A trial design of 12-inch-thick CMU reinforced with two #6 bars at 24 inches on center is selected. The self-weight of the wall, accounting for horizontal bond beams at 4 feet on center, is taken as 103 psf. Adjacent to each door jamb, the vertical reinforcement is placed into two cells. See Figure 13.1-10.
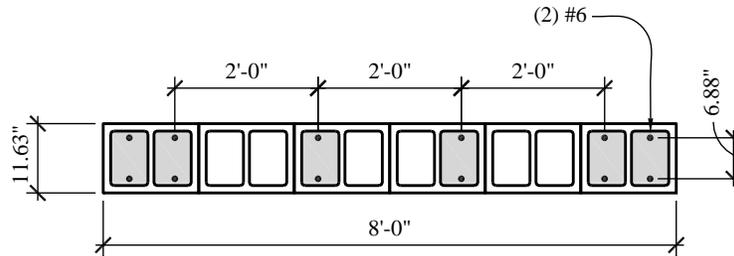
Figure 13.1-10 Trial design for piers on end walls
(1.0 in. = 25.4 mm, 1.0 ft = 0.3048 m)

Next, determine the design load locations. The centroid for seismic loads, out-of-plane, is the centroid of the mass of the wall and, accounting for the door openings, is determined to be 17.8 feet above the base. See Figures 13.1-11 and 13.1-12.

13.1.6.3.2 Investigate to ensure ductility. The critical strain condition corresponds to a strain in the extreme tension reinforcement (which is a pair of #6 bars in the end cell in this example) equal to α times the strain at yield stress. As for the side walls, $\alpha = 1.5$ for out-of-plane flexure (TMS 402 Section 9.3.3.5). See Figure 13.1-13.

For this case:

$t = 11.63$ in.

$d = 11.63 - 2.38 = 9.25$ in.

$\varepsilon_m = 0.0025$ (TMS Sec. 402 9.3.2(c))

$\varepsilon_s = 1.5\ \varepsilon_y = 1.5\ (f_y/E_s) = 1.5\ (60$ ksi $/29{,}000$ ksi$) = 0.0031$ (TMS 402 Sec. 9.3.3.5.1(a) and 9.3.3.5.3)

$$c = \left[\frac{\varepsilon_m}{(\varepsilon_m + \varepsilon_s)}\right]d = 4.13 \text{ in.}$$

$a = 0.8c = 3.30$ in. (TMS 402 Sec. 9.3.2(g))
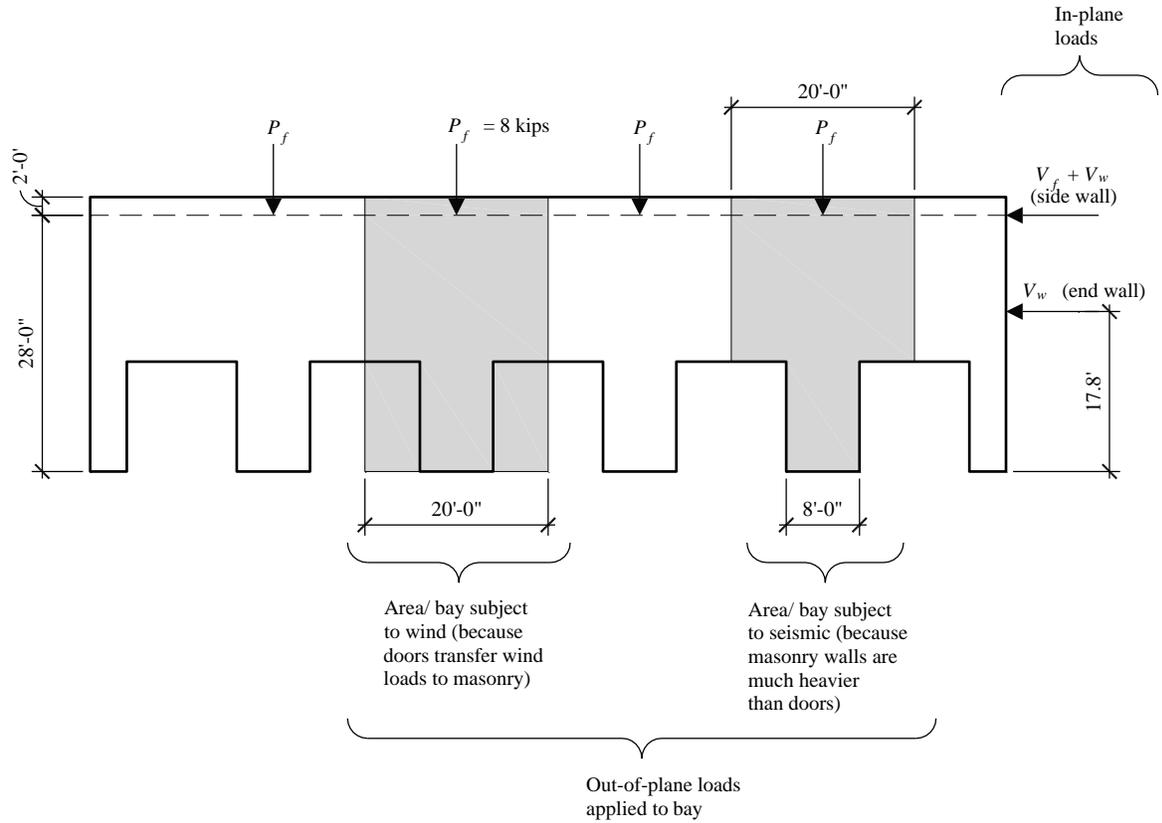
Figure 13.1-11 In-plane loads on end walls
(1.0 ft = 0.3048 m)

w_{top} = (0.4) (1.43) (103 psf) (20') = 1200 plf/bay out-of-plane

R_{top} = 17.5 kips/bay out-of-plane

2'

16'

H_1

H_r

21'

17.8'

H_2

12'

6'

R_{bot} = 9.8 kips /bay out-of-plane

w_{bot} = (0.4) (1.43) (103) (8') = 480 plf/bay out-of-plane
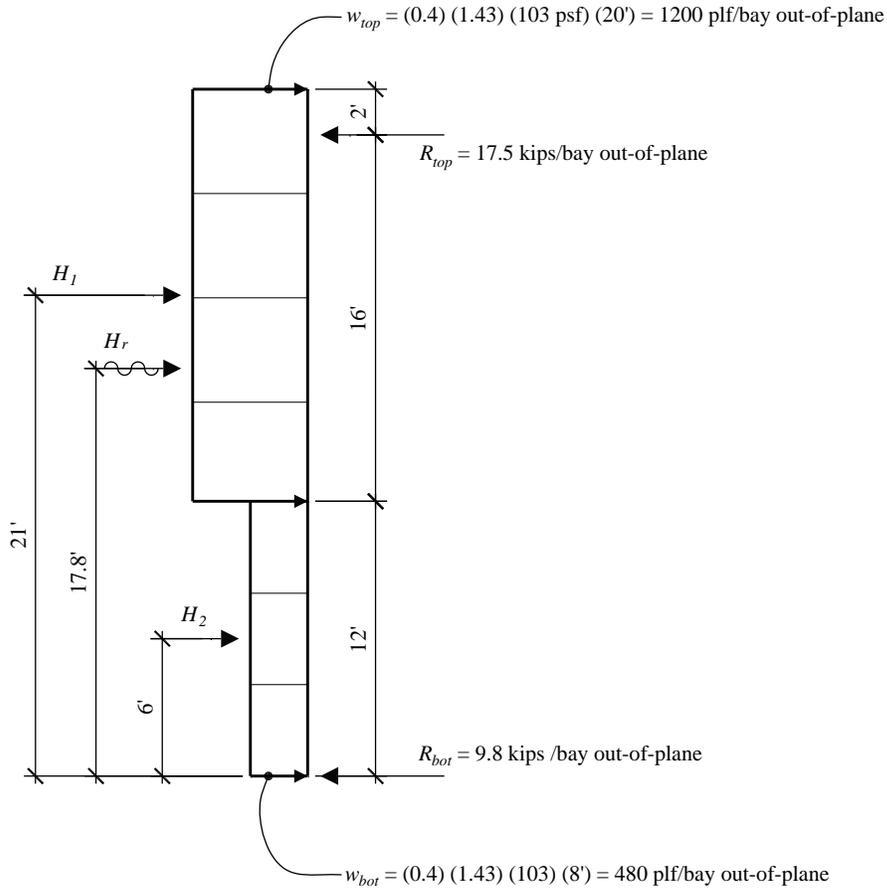
Figure 13.1-12 Out-of-plane load diagram and resultant of seismic lateral loads
(1.0 ft = 0.3048 m, 1.0 lb = 4.45 N, 1.0 kip = 4.45 kN)
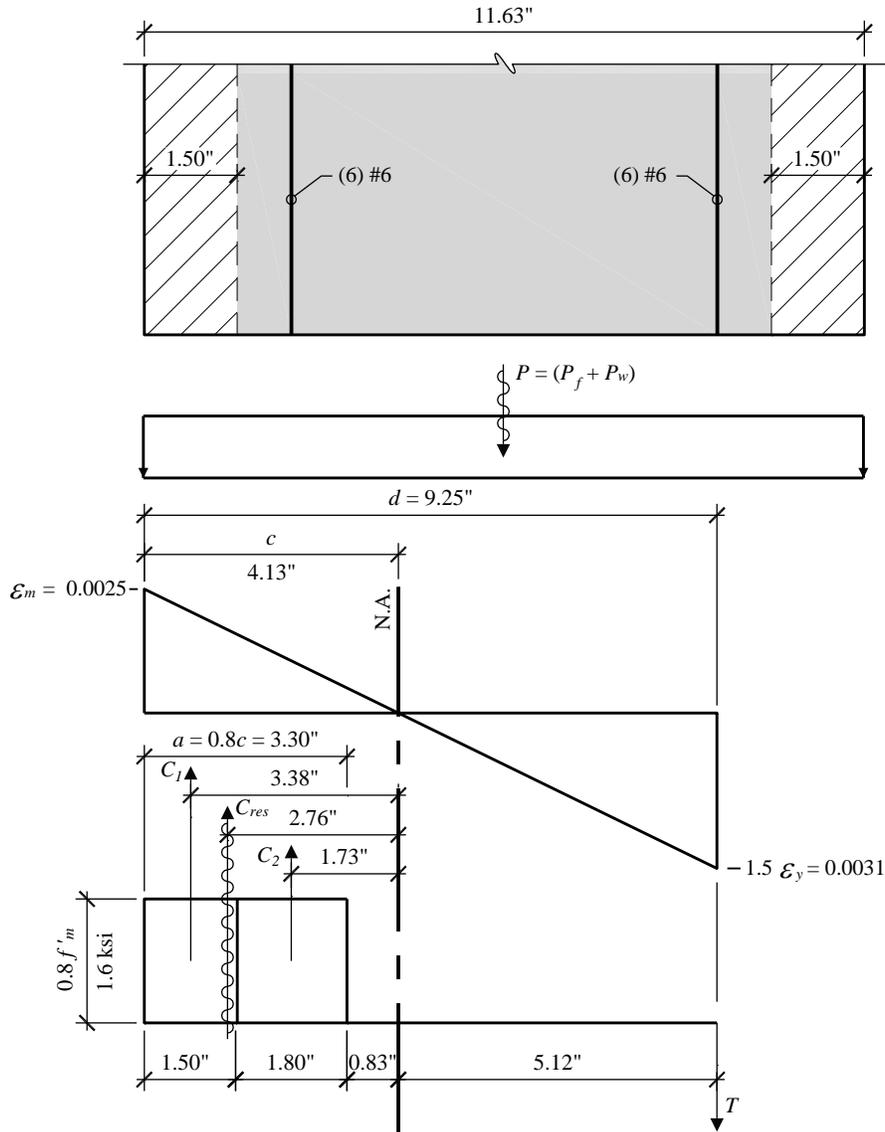
Figure 13.1-13 Investigation of out-of-plane ductility for end wall
(1.0 in. = 25.4 mm, 1.0 ksi = 6.89 MPa)

Note that the Whitney compression stress block, $a = 3.30$ inches deep, is greater than the 1.50-inch face shell thickness. Thus, the compression stress block is broken into two components: one for full compression against solid masonry (the face shell) and another for compression against the webs and grouted cells but accounting for the open cells. These are shown as C_1 and C_2 in Figure 13.1-14. The values are computed using TMS 402 Section 9.3.2(g):

$C_1 = 0.80f_m'$ (1.50 in.)$b = (0.80)(2$ ksi$)(1.50)(96) = 230$ kips (for full length of pier)

$C_2 = 0.80f_m'$ (a - 1.50 in.)(6(8 in.)) = $(0.80)(2$ ksi$)(3.30 - 1.50)(48) = 138$ kips

The 48-inch dimension in the C_2 calculation is the combined width of grouted cell and adjacent mortared webs over the 96-inch length of the pier.

$T = F_y A_s = (60 \text{ ksi})(6 \times 0.44 \text{ in.}^2) = 158 \text{ kips/pier}$

P is computed at the head of the doors. The dead load component of P is:

$P = (P_f + P_w) = (0.020 \text{ ksf})(20 \text{ ft})(20 \text{ ft}) + (0.103 \text{ ksf})(18 \text{ ft})(20 \text{ ft}) = 8.0 + 37.1$

$P = 45.1 \text{ kips/pier}$

From TMS 402 Section 9.3.3.5.1(d), axial forces are taken from the load combination of the following:

$P = D + 0.75L + 0.525Q_E$ with $Q_E = F_p = 0.2S_{DS}D = (0.2)(1.43)(45.1) = 12.9 \text{ kips/pier}$

$P = 45.1 \text{ kips/pier} + (0.75)(0) + (0.525)(12.9 \text{ kips/pier})$

$P = 51.9 \text{ kips/pier}$

$C_1 + C_2 > P + T$

$368 \text{ kip} > 210 \text{ kips}$

The compression capacity is greater than the tension capacity, so the ductility criterion is satisfied.

13.1.6.3.3 Check for wind loading. Wind pressure per bay is over the full 20-foot-wide by 30-foot-high bay, as discussed above, and is based on the *Standard*. While both strength and deflection need to be ascertained per a building code (the IBC was used), the calculations are not presented here.
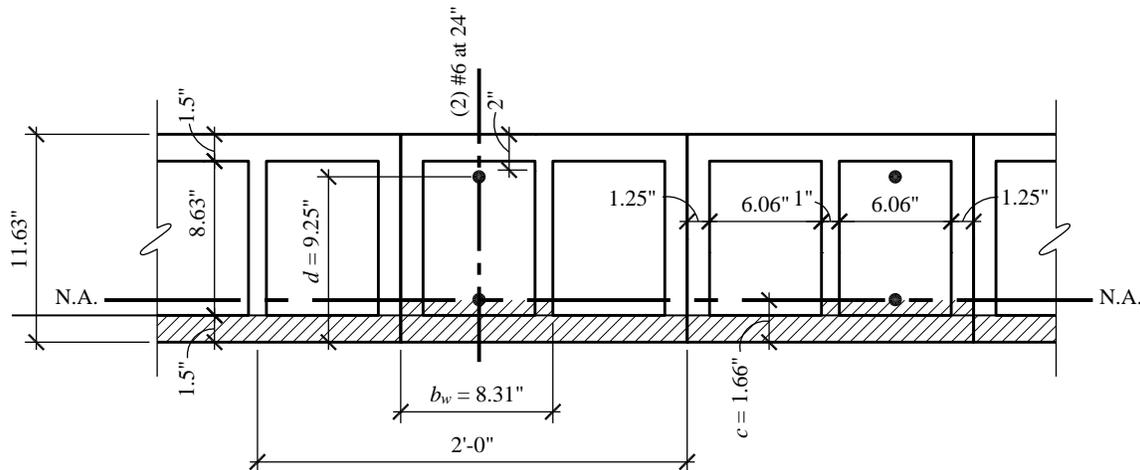
Figure 13.1-14 Cracked moment of inertia (I_{cr}) for end walls
Dimension "c" depends on calculations shown for Figure 13.1-15.
(1.0 in. = 25.4 mm, 1.0 ft = 0.3048 m)

13.1.6.3.4 Calculate mid-height deflection due to wind loads by TMS 402. Wind pressures do not control the design of the end wall piers. Deflection will be checked for the controlling load case of seismic forces in Section 13.1.6.3.7 below.

13.1.6.3.5 Calculate out-of-plane seismic demand. For this example, the load combination $0.614D$ has been used, and for this calculation, forces and moments over a single pier (width = 96 in.) are used. This does not violate the $b > 6t$ rule (TMS 402 Sec. 9.3.4.3.3(d)) because the pier is reinforced at 24 inches on center. The use of the full width of the pier instead of a 24-inch width is simply for calculation convenience.

For this example, a *P-delta* analysis using RISA-2D was run, resulting in the following:

Maximum moment, M_u = 95.6 ft-kips/bay = 95.6/20 ft = 4.78 klf   (does not control)

Moment at top of pier, M_u = 89.3 ft-kips/pier = 89.3 / 8 ft = 11.2 klf   (controls)

Shear at bottom of pier, V_u = 9.61 kips/pier

Reaction at roof, V_u = 17.5 kips/bay

Axial force at base, R_u = 31.2 kips/pier (includes load factor on D of 0.614)

13.1.6.3.6 Determine moment resistance at the top of the pier. See Figure 13.1-15.

A_s = 6-#6 = 2.64 in.^{2}/pier

d = 9.25 in.

T = 2.64(60) = 158.4 kip/pier

$C = T + P$ = 184.1 kip/pier (P is based on D of (0.614)(37.1 + 8 kip) = 27.7 kip/pier at top of pier)

$a = C / (0.8f'_mb)$ = 184.1 / [(0.8)(2)96] = 1.20 in.

Because a is less than the face shell thickness (1.50 in.), compute as for a rectangular beam. Moments are computed about the centerline of the wall.

$M_n = C\ (t/2 - a/2) + P\ (0) + T\ (d - t/2)$

$\quad$ = 184.1(5.81 - 1.20/2) + 158.4(9.25-5.81) = 1,504 in.-kip = 125.4 ft-kip

φM_n = 0.9(125.4) = 112.8 ft-kip

Because moment capacity at the top of the pier, φM_n = 112.8 ft-kips, exceeds the maximum moment demand at top of pier, M_u = 89.3ft-kips, the condition is acceptable.

Figure 13.1-15 Out-of-plane seismic strength of pier on end wall
(1.0 in. = 25.4 mm, 1.0 ksi = 6.89 MPa)

13.1.6.3.7 Calculate mid-height deflection due to seismic loads by TMS 402. The wall is non-prismatic over its height due to the door openings. As a conservative check, the wall is analyzed as an 8 ft. wall over the entire height, with the load distribution shown in Figure 13.1-12, reduced to ASD level loads.

$n = E_s / E_m = 16.1$

$A_s = 2.64$ in.^{2}/pier

$P = 1.0D = 45.1$ kips/pier

$t_{sp} = 11.63$ in.

$d = 9.25$ in.

$$c = \frac{A_s f_y + P}{0.64 f'_m b} = \frac{2.64(60) + 45.1}{0.64(2)(8*12)} = 1.66 \text{ in.}$$

The neutral axis location is inside of the face shell, but it is judged that the 0.16" of ungrouted area will not make a significant difference in the deflection calculations, so the formula for a rectangular section is used.

$$I_{cr} = n\left(A_s + \frac{P}{f_y}\frac{t_{sp}}{2d}\right)(d-c)^2 + \frac{bc^3}{3} = 3033 \text{ in.}^4/\text{pier}$$

Analyze loading as the seismic load over the 8 ft. width over the full height plus additional load over the height above the opening, ignoring loading on the parapet:

$w_{uniform} = 0.7w_{u,bot} = 0.7(480 \text{ plf}) = 336 \text{ plf}$

$w_{partial} = 0.7(w_{u,top} - w_{u,bot}) = 0.7(1,200 \text{ plf} - 480 \text{ plf}) = 504 \text{ plf}$

Check deflection at mid-height of the wall:

a = 16 ft. = 192 in. for use in the deflection formula below.

x = 14 ft. (mid-height of wall) = 168 in.

L = 28 ft. = 336 in.

$$\delta_{ASD,0} = \frac{5}{384}\frac{w_{uniform}L^4}{E_m I_{cr}} + \frac{w_{partial}x}{24 E_m I_{cr} L}\left(a^2(2L-a)^2 - 2ax^2(2L-a) + Lx^3\right)$$

$$\delta_{ASD,0} = 0.851 + 0.783 = 1.63 \text{ in.}$$

$$P_e = \frac{\pi^2 E_m I_{eff}}{h^2} = \frac{\pi^2(1,800 \text{ ksi})(3033 \text{ in.}^4)}{(28 \text{ ft x } 12)^2} = 477 \text{ kips/pier}$$

$$\delta_s = \delta_{ASD,0}\left(\frac{1}{1-\dfrac{P}{P_e}}\right) = 1.80 \text{ in.}$$

The allowable deflection at mid-height is given by Equation 9-36 in TMS 402 as

$$\delta_s \leq 0.007h = 0.007(336 \text{ in.}) = 2.35 \text{ in.}$$

The maximum deflection is below the allowable limit. The stiffness of the wall piers is sufficient for out of plane deflections under seismic loading.

13.1.6.4 In-plane flexure – end walls. There are several possible methods to compute the shears and moments in the individual piers of the end wall. For this example, the end wall was modeled using RISA-2D. The horizontal beam was modeled at the top of the opening, rather than at its mid-height. The in-plane lateral loads (see Figure 13.1-11) were applied at the 12-foot elevation and combined with joint moments representing transfer of the horizontal forces from their point of action down to the 12-foot

elevation. Vertical load due to roof beams and the self-weight of the end wall were included. The input loads are shown in Figure 13.1-16. For this example:

$w = (18 \text{ ft})(103 \text{ psf}) + (20 \text{ ft})(20 \text{ psf}) = 2.254 \text{ klf}$

$H = (184 \text{ kip})/5 = 36.8 \text{ kip}$

$M = C_s[(V_{f\,long} + V_{w\,long})h_{long} + (V_{w\,short})(h_{short})]$ (refer to Fig. 13.1-11).

$M = 0.286[(400 + 418)(28 \text{ ft} - 12 \text{ ft}) + 470(17.8 \text{ ft} - 12 \text{ ft})] = 452 \text{ ft-kip}$
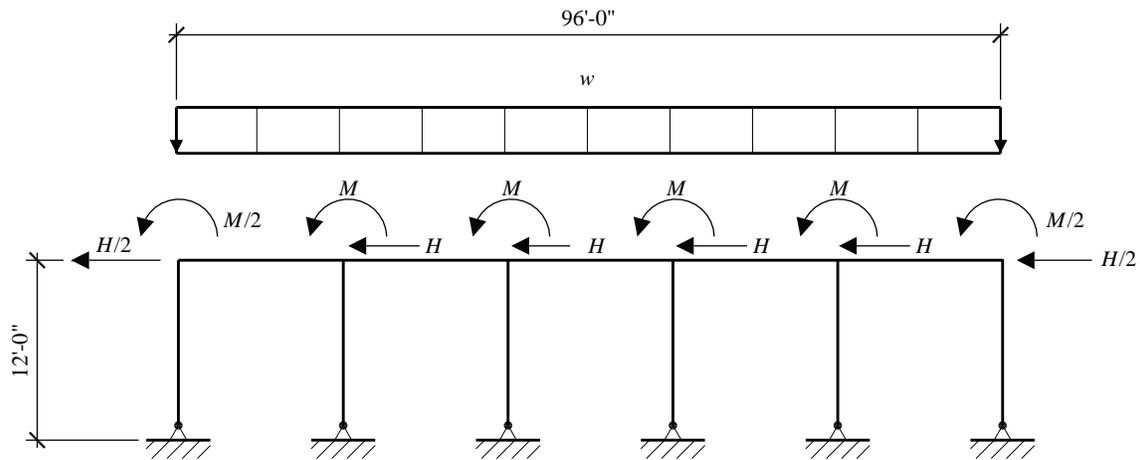
Figure 13.1-16 Input loads for in-plane end wall analysis
(1.0 ft = 0.3048 m)

The input forces at the end wall are distributed over all the piers to simulate actual conditions. The RISA-2D frame analysis accounts for the relative stiffnesses of the 4-foot- and 8-foot-wide piers (continuity of the 4-foot-wide piers at the corners was not considered). The final distribution of forces, shears and moments for an interior pier is shown on Figure 13.1-17.
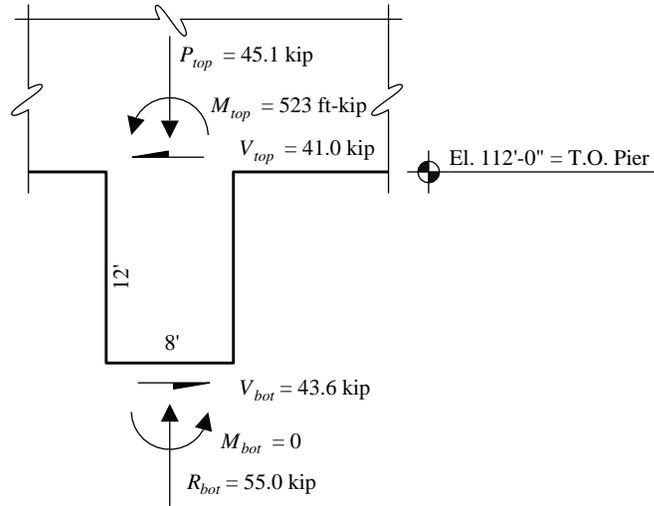
Figure 13.1-17 In-plane design condition for 8-foot-wide pier
(1.0 ft = 0.3048 m)

Continuing with the trial design for in-plane pier design, use two #6 bars at 24 inches on center supplemented by adding two #6 bars in the cells adjacent to the door jambs (see Figures 13.1-10 and

13.1-18).
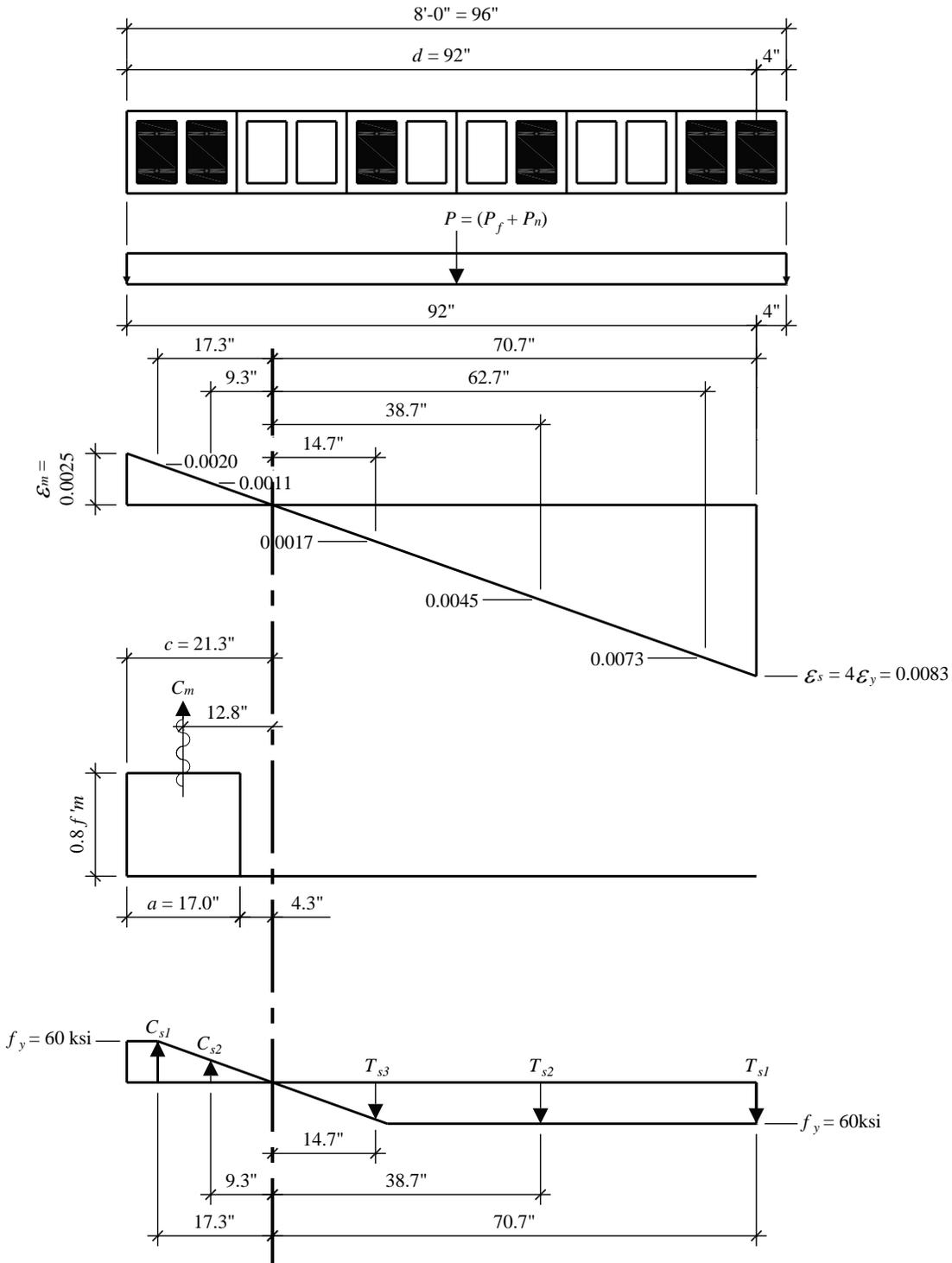
Figure 13.1-18 In-plane ductility check for 8-foot-wide pier
(1.0 in. = 25.4 mm, 1.0 ksi = 6.89 MPa)

The design values for in-plane design at the top of the pier are:

Table 13.1-3 In-plane Design Values at Pier Top

Unfactored	$0.614D + 1.0E$	$1.486D + 1.0E$
$P = 45.1$ kips	$P_u = 41.2$ kips	$P_u = 67.0$ kips
$V = 43.6$ kips	$V_u = 43.6$ kips	$V_u = 43.6$ kips
$M = 523$ ft-kips	$M_u = 523$ ft-kips	$M_u = 523$ ft-kips
M_u/V_ud_v	1.50	1.50

The ductility check is illustrated in Figure 13.1-18. Because $M_u/V_ud_v > 1$ for this special reinforced masonry shear wall subject to in-plane loads, $\alpha = 4$:

$\varepsilon_m = 0.0025$

$\varepsilon_s = 4\varepsilon_y = (4)(60/29{,}000) = 0.0083$

$d = 92$ in.

From the strain diagram (Fig. 13.1-18), the strains at the rebar locations from left to right are:

$\varepsilon = 0.0020$
$\varepsilon = 0.0011$
$\varepsilon = 0.0017$
$\varepsilon = 0.0045$
$\varepsilon = 0.0073$
$\varepsilon = 0.0083$

To check ductility, use unfactored loads (from Section 13.1.6.3.2):

$P = P_f + P_w = 8$ kips $+ 37.1$ kips $= 45.1$ kips

$a = 0.8c = 17.0$ in.

$C_m = (0.8f_m')ab = (1.6$ ksi$)(17.0$ in.$)(11.63$ in.$) = 315.5$ kips

$T_{s1} = T_{s2} = F_yA_s = (60$ ksi$)(2 \times 0.44$ in.$^2) = 52.8$ kips

$T_{s3} = \varepsilon EA_s = (0.0017)(29{,}000$ ksi$)(2 \times 0.44$ in.$^2) = 43.4$ kip

$C_{s1} = \varepsilon EA_s = (0.0021)(29{,}000$ ksi$)(2 \times 0.44$ in.$^2) = 53.6$ kip

$C_{s2} = \varepsilon EA_s = (0.0011)(29{,}000$ ksi$)(2 \times 0.44$ in.$^2) = 28.1$ kip

$\Sigma C > \Sigma T + P$

$C_m + C_{s1} + C_{s2} > T_{s1} + T_{s2} + T_{s3} + P$

$315.5 + 53.6 + 28.1 > 52.8 + 52.8 + 43.4 + 45.1$

397 kips > 194 kips   OK

Because compression capacity exceeds tension capacity, the requirement for ductile behavior is OK.

Note that maximum P for the wall to remain ductile is $P_{max} = \Sigma C - \Sigma T = 248$ kips. Thus, $\phi P_{max} = 223$ kips in order to assure ductility.

For the strength check, see Figure 13.1-19.
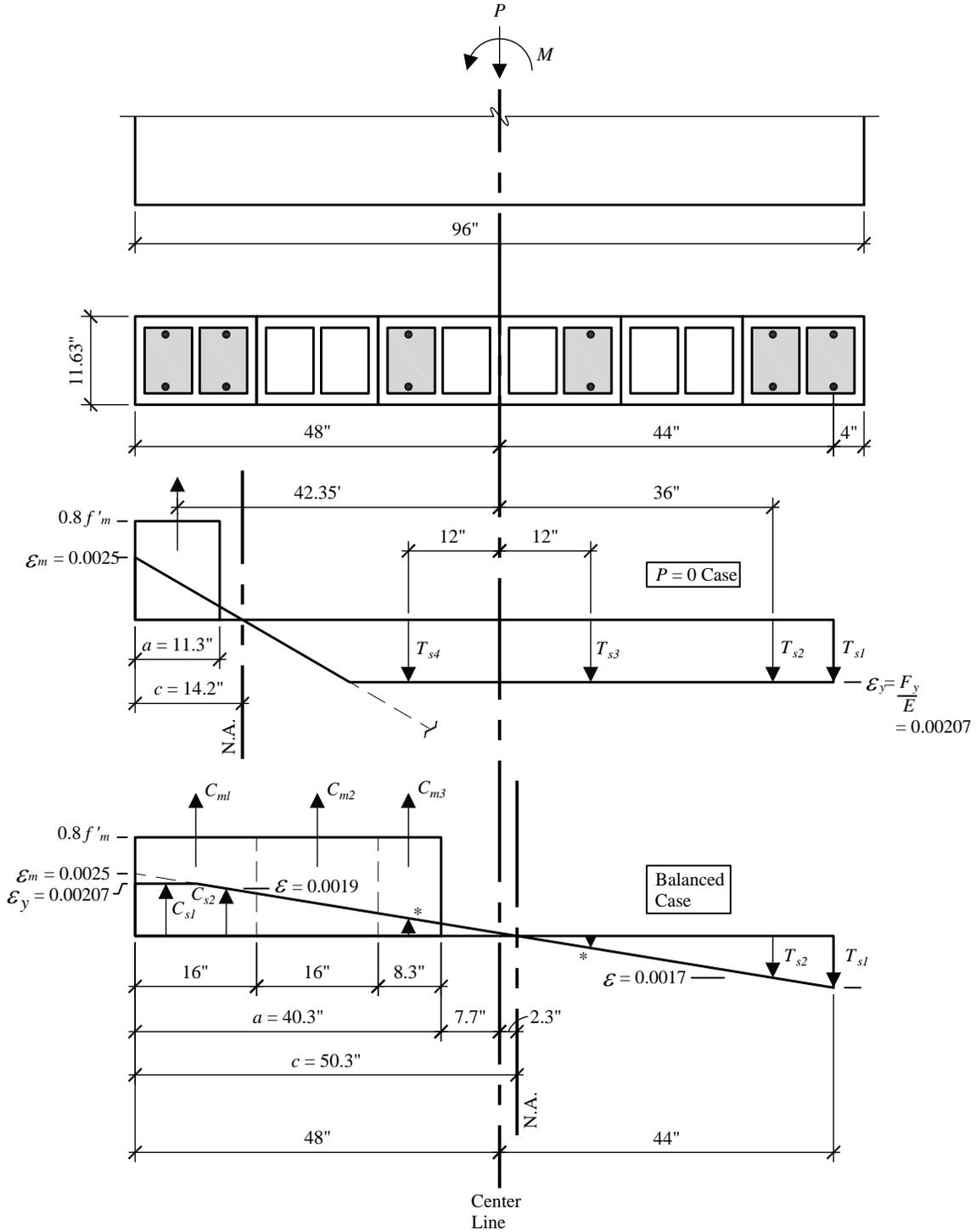
Figure 13.1-19 In-plane seismic strength of pier.
Strain diagram superimposed on strength diagram for both cases.
Note that locations with low force in reinforcement, marked by *, are neglected.
(1.0 in. = 25.4 mm)

To ascertain the strength of the pier, a ϕP_n - ϕM_n curve is developed. Only the portion below the "balance point" is examined since that portion is sufficient for the purposes of this example. (Ductile failures occur only at points on the curve that are below the balance point, so this is consistent with the overall approach).

For the $P = 0$ case, assume all bars in tension reach their yield stress and neglect compression steel (a conservative assumption):

$T_{s1} = T_{s2} = T_{s3} = T_{s4} = (2)(0.44 \text{ in.}^2)(60 \text{ ksi}) = 52.8$ kips

$C_m = \Sigma T_s = (4)(52.8) = 211.2$ kips

$C_m = 0.8f'_m ab = (0.8)(2 \text{ ksi})a(11.63 \text{ in.}) = 18.6a$

Thus, $a = 11.3$ inches and $c = a/0.8 = 11.3 / 0.8 = 14.2$ inches.

$\Sigma M_{cl} = 0$

$M_n = 42.35 \, C_m + 44T_{s1} + 36T_{s2} + 12T_{s3} - 12T_{s4} = 13,168$ in.-kips

$\phi M_n = (0.9)(13,168) = 11,851$ in.-kips $= 988$ ft-kips

For the balanced case:

$d = 92$ in.

$\varepsilon = 0.0025$

$\varepsilon_y = 60/29,000 = 0.00207$

$c = \left(\dfrac{\varepsilon_m}{\varepsilon_m + \varepsilon_y} \right) d = 50.3$ in.

$a = 0.8c = 40.3$ in.

Compression values are determined from the Whitney compression block adjusted for fully grouted cells or ungrouted cells:

$C_{m1} = (1.6 \text{ ksi})(16 \text{ in.})(11.63 \text{ in.}) = 297.8$ kips

$C_{m2} = (1.6 \text{ ksi})(16 \text{ in.})(2 \times 1.50 \text{ in.}) = 76.8$ kips

$C_{m3} = (1.6 \text{ ksi})(8.3 \text{ in.})(11.63 \text{ in.}) = 154.4$ kips

$C_{s1} = (0.88 \text{ in.}^2)(60 \text{ ksi}) = 52.8$ kips

$C_{s2} = (0.88 \text{ in.}^2)(60 \text{ ksi})(0.0019 / 0.00207) = 48.5$ kips

T_{s1} = (0.88 in.^{2})(60 ksi) = 52.8 kips

T_{s2} = (0.88 in.^{2})(60 ksi)(0.0017 / 0.00207) = 43.4 kips

ΣF_y = 0:

$P_n = \Sigma C - \Sigma T$ = 297.8 + 76.8 + 154.4 + 52.8 + 48.5 -52.8 - 43.4 = 534 kips

ϕP_n = (0.9)(534) = 481 kips

ΣM_{cl} = 0:

$M_n = 40C_{m1} + 24C_{m2} + 11.85C_{m3} + 44C_{s1} + 36C_{s2} + 44T_{s1} + 36T_{s2}$ = 23,540 in.-kips

ϕM_n = (0.9)(23,540) = 21,186 in.-kips = 1,765 ft-kips

The two cases are plotted in Figure 13.1-20 to develop the ϕP_n - ϕM_n curve on the pier. The demand (P_u, - M_u) also is plotted. As can be seen, the pier design is acceptable because the demand is within the ϕP_n - ϕM_n curve. (See the Low Seismicity SDC B Building example in Section 13.2 for additional discussion of ϕP_n - ϕM_n curves.) By linear interpolation, ϕM_n at the maximum axial load is 1,096 ft- kip.

The author notes that the use of $\phi = 0.9$ on P_n at the balance point is consistent with TMS 402, but, because of the ductility requirement, the balance point will never be reached. The maximum P_n for this pier, as per the ductility requirement (from Sec. 13.1.6.4), would be (397 kips - 149 kips) = 248 kips (as discussed above), well below the 481 kips at P_b. To illustrate the point, this maximum expressed as ϕP_{nmax} = 223 kips, is illustrated in Figure 13.1-20.
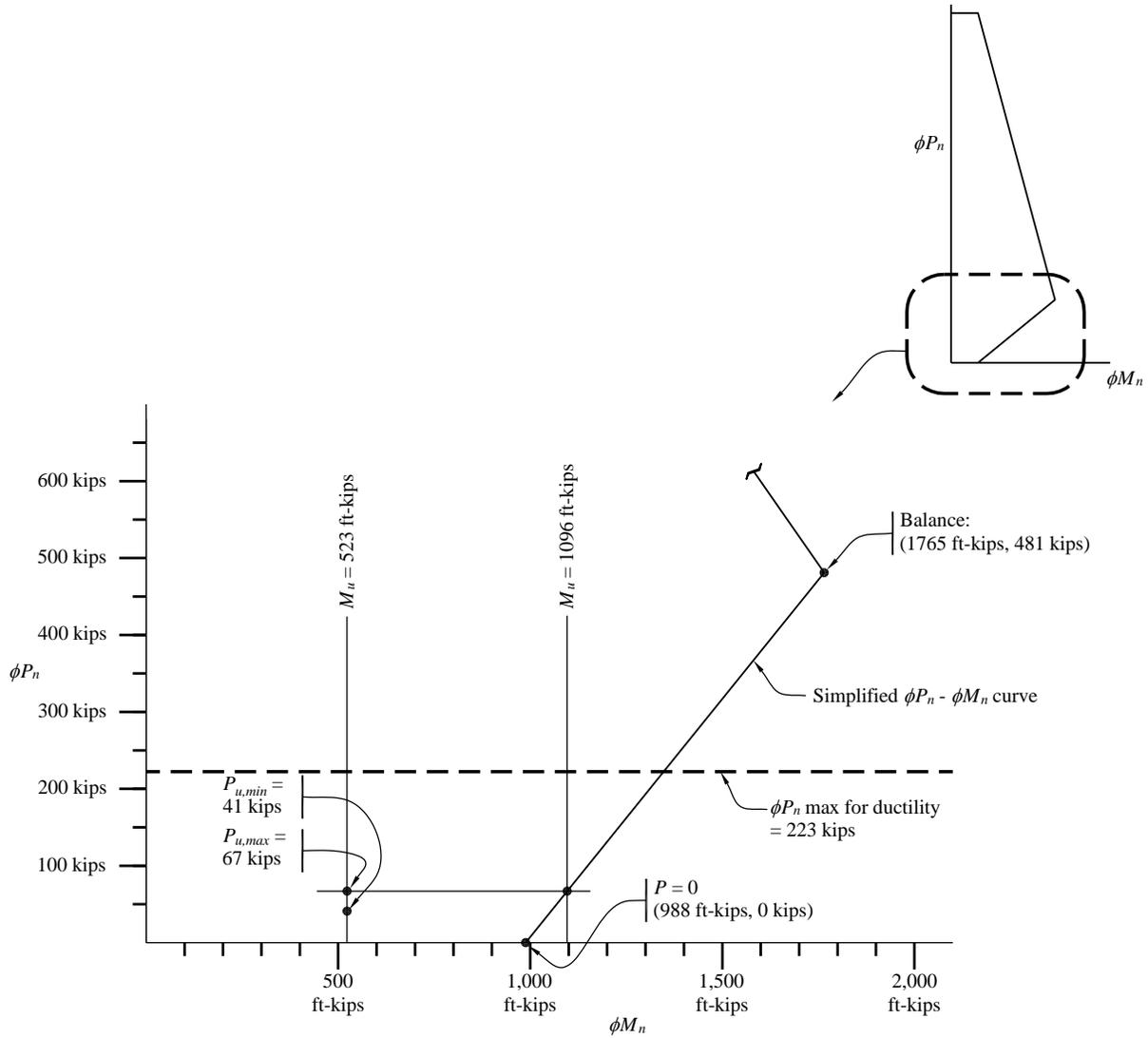
Figure 13.1-20 In-plane ϕP_n - ϕM_n diagram for pier
(1.0 kip = 4.45 kN, 1.0 ft-kip = 1.36 kN-m)

13.1.6.5 Combined loads. Although it is not required by the *Standard*, it is educational to illustrate the orthogonal combination of seismic loads for this pier (as if *Standard* Section 12.5.3.a were required), shown in Table 13.1-4:

Table 13.1-4 Combined Loads for Flexure in End Wall Pier

0.614D	Out-of-Plane		In-Plane		Total	
Case 1	1.0(89.3/112.8)	+	0.3(523/1026)	=	0.94 < 1.00	OK
Case 2	0.3(89.3/112.8)	+	1.0(523/1026)	=	0.75 < 1.00	OK

Values are in kips; 1.0 kip = 4.45 kN.

13.1.6.6 Shear – In-plane shear at end wall piers.

The in-plane shear at the base of the pier is 43.6 kips per bay. At the head of the opening where the moment demand is highest, the in-plane shear is slightly less (based on the weight of the pier). There, V = 43.6 kips - (0.286)(8 ft)(12 ft)(0.103 ksf) = 40.8 kips. Per TMS 402 Section 7.3.2.6.1.1, the design shear strength, ϕV_n, must exceed the shear corresponding to the development of 1.25 times the nominal flexural strength, M_n, or $2.5V_u$, whichever is smaller. Using the results in Figure 13.1-20, the 125 percent implies a factor on shear by analysis of:

$$1.25\left(\frac{\phi M_n}{M_u}\right)\left(\frac{1}{\phi}\right)(V_u)=1.25\left(\frac{1096}{523}\right)\left(\frac{1}{0.9}\right)V_u = 2.91\ V_u$$

But $2.91V_u > 2.5V_u$; therefore, $2.5V_u$ controls (TMS 402 Sec. 7.3.2.6.1.1).

Therefore, the required shear capacities at the base and head of the pier are (2.5)(43.6 kips) = 109 kips and (2.5)(40.8) = 102 kips, respectively.

The in-plane shear capacity is computed as follows where the net area, A_n, of the pier is the area of face shells plus the area of grouted cells and adjacent webs:

$$V_m = \left[4.0 - 1.75\left(\frac{M_u}{V_u d_v}\right)\right] A_n \sqrt{f'_m} + 0.25 P_u$$

As discussed previously, $M_u/V_u d_v$ need not exceed 1.0 in the above equation.

A_n = (96 in. × 1.50 in. × 2) + (6 cells × 8 in. × 8.63 in.) = 702 in.^{2}/ bay

Recall that horizontal reinforcement is 2-#5 at 40 inches in bond beams:

$$V_{ns} = 0.5\left(\frac{A_v}{s}\right)f_y d_v$$

$$= 0.5\left(\frac{0.62\ \text{in.}^2}{40\ \text{in.}}\right)(60\ \text{ksi})(96\ \text{in.})$$

$$= 44.6\ \text{kips/bay}$$

At the base of the pier:

V_m = [4.0 - 1.75(0)](702 in.^{2})(0.0447 ksi) + (0.25)(0.614 × 55.0 kips)

V_m = 134.0 kips/bay

ϕV_n = (0.8)(134.0 + 44.6)(0.75) = 107.2 kips/bay < 109 kips/bay = 2.5 V_u N.G.

At the head of the pier:

V_m = [4.0 - 1.75(1.0)](702 in.^{2})(0.0447 ksi) + (0.25)(0.614 × 45.1 kips) = 77.5 kips/bay

$\phi V_n = (0.8)(77.5 + 44.6)(0.75) = 73.3$ kips/bay < 102 kips/bay $= 2.5\ V_u$ N.G.

This non-ductile situation can be addressed by fully grouting the cells in the pier. The penalty for partially grouted walls is removed and the area of masonry resisting shear is increased to $A_n = b_w d_v = (11.63$ in.$)(96$ in.$) = 1116$ in.^{2}. At the bottom of the pier, this results in $V_m = 119.2$ kips and $\phi V_n = 131$ kips > 102 kips $= 2.5\ V_u$ which is OK.

Note: The design of the piers in the end walls of this example will remain the same without iteration to reflect the additional grouted cells. Note also that there is no additional vertical reinforcement; only grout has been added to the cells.

13.1.7 In-Plane Deflection – End Walls
Deflection of the end wall (short wall) has two components as illustrated in Figure 13.1-21.
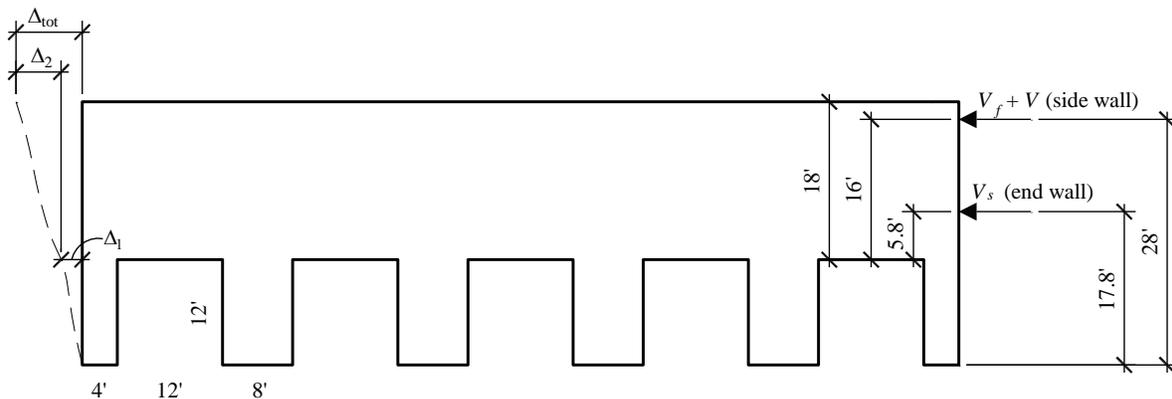
Figure 13.1-21 In-plane deflection of end wall
(1.0 ft = 0.3048 m)

As obtained from the RISA-2D analysis of the piers, $\Delta_1 = 0.047$ in.:

$$\Delta_2 = \sum \frac{\alpha V L}{AG}$$

where α is the form factor equal to 6/5 and:

$G = E_m/2(1 + \mu) = 1{,}800$ ksi $/ 2(1 + 0.15) = 782$ ksi

$A = A_n =$ area of face shells + area of grouted cells

$= (100$ ft $\times 12$ in./ft $\times 2 \times 1.50$ in.$^2) + (50)(8$ in.$)(8.63$ in.$) = 7{,}050$ in.^{2}

Note: Contribution to base shear of end walls (above the doors) is C_s (end wall weight) = $(0.286)[(470$ kips$/2) - (103$ psf$)(5)(8$ ft$)(12$ ft$)] = 53$ kips. Contribution to base shear of long walls plus roof is C_s (long wall + roof weight) = $(0.286)[(400+418)/2] = 117$ kips.

Therefore:

$$\Delta_2 = \left(\frac{6}{5}\right)\frac{(53)(5.8\times12)}{(7,050)(782)} + \left(\frac{6}{5}\right)\frac{(117)(16\times12)}{(7,050)(782)} = 0.0008 + 0.0049 = 0.006 \text{ in.}$$

TMS 402 Section 9.1.5.2 requires the consideration of cracked section properties on the effective flexural and shear stiffnesses. The effective stiffnesses can be taken as 0.5 times the gross section properties (I_g and A). As both terms are linear and in the denominator, the deflection will be twice that of the deflection calculated with gross section properties. The total deflection is thus:

$$\Delta_{total} = C_d(0.047 + 0.006)(2) = 3.5(0.053 \text{ in.})(2) = 0.37 \text{ in.} < 2.35 \text{ in.} \qquad \text{OK}$$

where $(2.35 = 0.007h_n = 0.01h_{sx})$ (TMS 402 Sec. 9.3.5.4).

Note that the drift limits for masonry structures are smaller than for other types of structure. It is possible to interpret *Standards* Table 12.12-1 to give a limit of $0.007h_n$ for this structure, but that limit also is easily satisfied. The real displacement in this structure is in the roof diaphragm; see Sec. 14.2.4.2.3.

13.1.8 Bond Beam – Side Walls (and End Walls)

Reinforcement for the bond beam located at the elevation of the roof diaphragm can be used for the diaphragm chord. The uniform lateral load for the design of the chord is the lateral load from the long wall plus the lateral load from the roof and is equal to 1.17 klf. The maximum tension in rebar is equal to the maximum moment divided by the diaphragm depth:

$$M = \frac{(1.17 \text{ klf})(200\text{ft})^2}{8} = 5,850 \text{ ft-kips}$$

$M/d = 5,850$ ft-kips/100 ft $= 58.5$ kips

The seismic load factor is 1.0. The required reinforcement is:

$$A_{reqd} = T/\phi F_y = 58.5/(0.9)(60) = 1.081 \text{ in.}^2$$

This will be satisfied by two #7 bars, $A_s = (2 \times 0.60 \text{ in.}^2) = 1.20 \text{ in.}^2$

In Sec. 14.2.4.2.2, the diaphragm chord is designed as a wood member utilizing the wood ledger member. Using either the wood ledger or the bond beam is considered acceptable.

13.2 FIVE-STORY MASONRY RESIDENTIAL BUILDINGS IN LOCATIONS OF VARYING SEISMICITY

13.2.1 Building Description

In plan, this five-story residential building has bearing walls at 24 feet on center (see Figures 13.2-1 and 13.2-2). All structural walls are of 8-inch-thick concrete masonry units (CMU). The floor is of 8-inch-thick hollow core precast, prestressed concrete planks. To demonstrate the incremental seismic requirements for masonry structures, the building is partially designed for four locations: two adjacent sites in an area of low seismicity; a site in an area of moderate seismicity; and a site in an area of high seismicity. The two adjacent sites have been selected to illustrate the influence of different soil profiles at the same location. The building is designed for Site Classes C and E in the area of low seismicity.
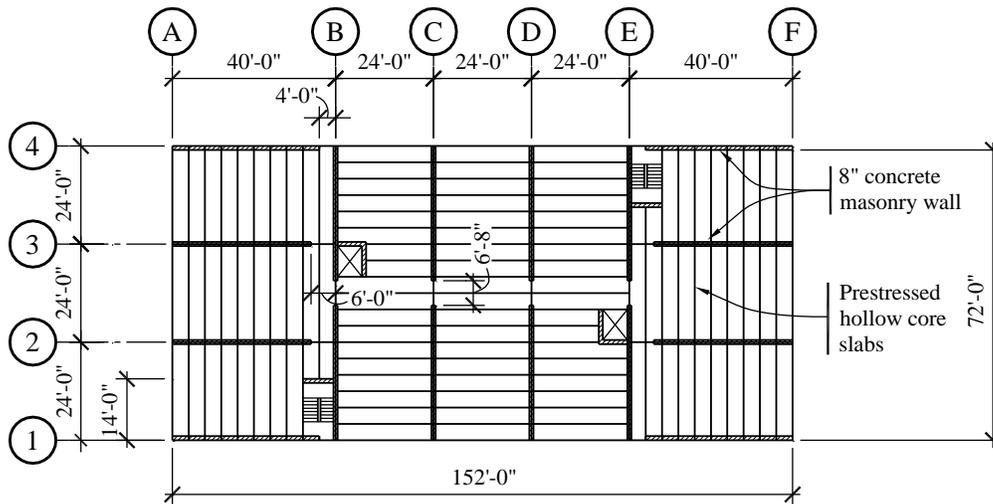
Figure 13.2-1 Typical floor plan
(1.0 in. = 25.4 mm, 1.0 ft = 0.3048 m)
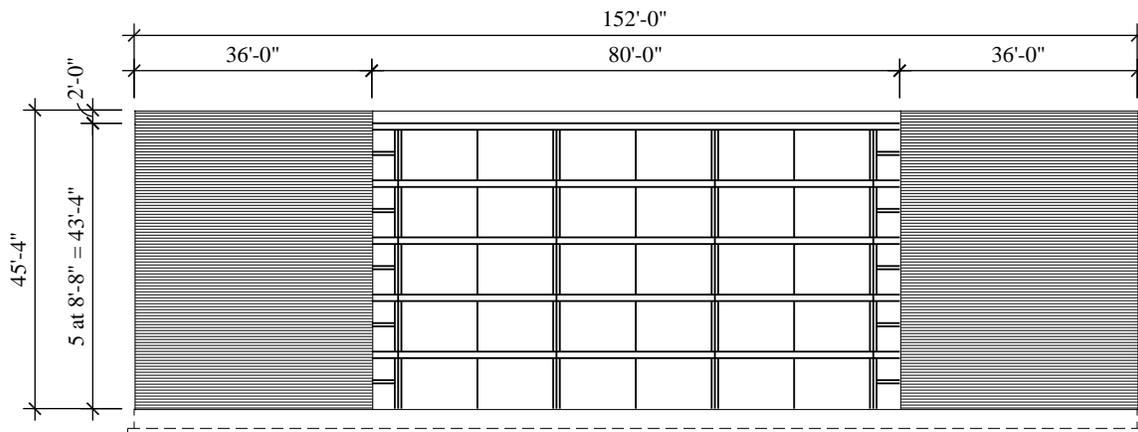
Figure 13.2-2 Building elevation

(1.0 in. = 25.4 mm, 1.0 ft = 0.3048 m)

For the sites in areas of low and moderate seismicity, it is assumed that shear friction reinforcement in the joints of the diaphragm planks is sufficient to resist seismic forces, so no topping is used. For the site in the area of high seismicity, a cast-in-place 2½-inch-thick reinforced lightweight concrete topping is applied to all floors. The structure is free of irregularities both in plan and elevation. ACI 318, Sections 18.2.1.5 and 18.12.1, require reinforced cast-in-place toppings as diaphragms in Seismic Design Category D and higher. Thus, the building in an area of low seismicity example in Site Class E / Seismic Design Category D would require a topping, although that is not included in this example.

The design of an untopped diaphragm (for Seismic Design Categories A, B and C) is not addressed explicitly in ACI 318. The designs of both untopped and topped diaphragms for these buildings are described in Chapter 8 of this volume using ACI 318 for the topped diaphragm in the building in the area of high seismicity.   The *Provisions* provide guidance for the design of untopped precast plank diaphragms in Part 3, RP3-4.

For the purpose of determining the site class coefficient (*Standard* Sec. 11.4.2 and 20.3), a stiff soil profile with standard penetration test results of $15 < N < 50$ is assumed for the high seismicity site resulting in a Site Class D for this location. The sites at one of the buildings in the area of low seismicity and the building in the area of moderate seismicity have soft rock with $N > 50$, resulting in Site Class C. The site at the other building in the area of low seismicity has soft clay with $N < 15$, which results in Site Class E. The two low seismicity sites are presented to illustrate how different soil conditions at the same location (same seismicity) can result in different Seismic Design Categories. No foundations are designed in this example. The foundation systems are assumed to be able to carry the superstructure loads including the overturning moments.

The masonry walls in two perpendicular directions act as bearing and shear walls with different levels of axial loads. The geometry of the building in plan and elevation results in nearly equal lateral resistance in both directions. The walls are constructed of CMU and typically are minimally reinforced in all locations. Figure 13.2-3 illustrates the wall layout.
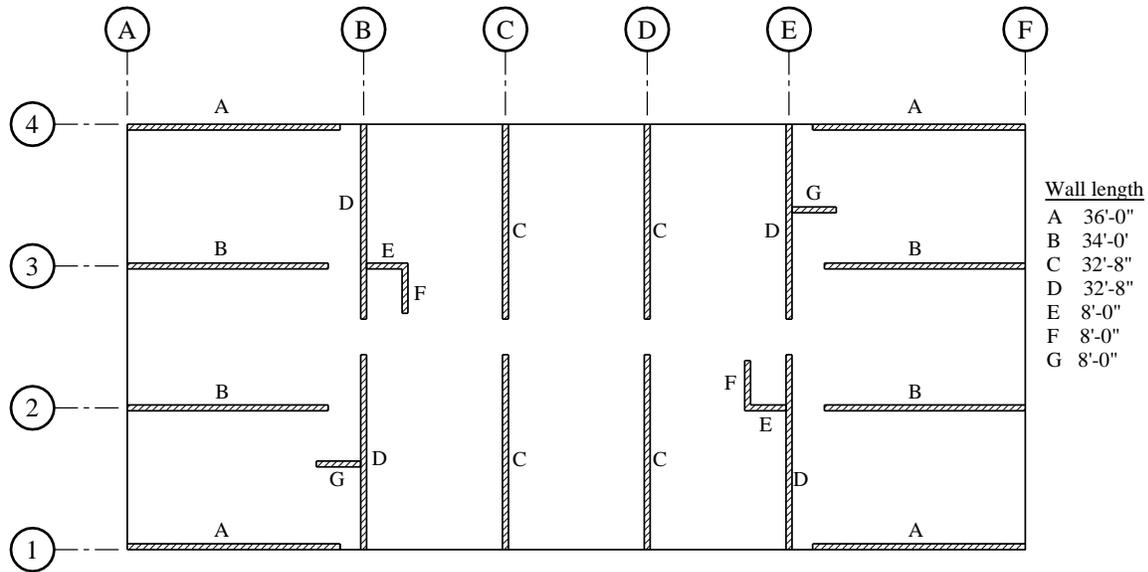
Figure 13.2-3 Plan of walls
(1.0 ft = 0.3048 m)

Wall length
A   36'-0"
B   34'-0'
C   32'-8"
D   32'-8"
E   8'-0"
F   8'-0"
G   8'-0"

The floors serve as horizontal diaphragms distributing the seismic forces to the walls and are assumed to be stiff enough to be considered rigid. There is little information about the stiffness of untopped precast diaphragms. The design procedure in Section RP3-4 of Part 3 of the *Provisions* results in a diaphragm intended to remain below the elastic limit until the walls reach an upper bound estimate of strength; therefore, it appears that the assumption is reasonable.

Material properties are as follows:

The compressive strength of masonry, f'_m, is taken as 2,000 psi, and the steel reinforcement has a yield limit of 60 ksi.

The design snow load (on an exposed flat roof) is less than the roof live load for all locations.

This example covers the following aspects of a seismic design:

Determining the equivalent lateral forces

Design of selected masonry shear walls for their in-plane loads

Computation of drifts

The story heights are small enough that the design of the masonry walls for out-of-plane forces is nearly trivial. In-plane response governs both the reinforcement in the wall and the connections to the diaphragms.

13.2.2 Design Requirements

13.2.2.1 Seismic parameters. The basic parameters affecting the design and detailing of the buildings are shown in Table 13.2-1. The Seismic Design Category for the building in an area of low seismicity with soft clay deserves special comment. The value of S_{DS} would imply a Seismic Design Category of C, while the value of S_{D1} would imply Seismic Design Category D, per Tables 11.6-1 and 11.6-2 of the *Standard,* where in Section 11.6 a provision permits the use of Table 11.6-1 alone if $T < 0.8 \, S_{D1}/S_{DS}$ and the floor diaphragm is considered rigid or has a span of less than 40 feet. As will be shown for this building, $T_a = 0.338$ seconds and $0.8 \, S_{D1}/S_{DS} = 0.446$. In the author's opinion, the untopped diaphragm may not be sufficiently rigid and thus Table 11.6-2 is considered, resulting in Seismic Design Category D.

13.2.2.2 Structural design considerations. The floors act as horizontal diaphragms, and the walls parallel to the motion act as shear walls for all four buildings.

The system is categorized as a bearing wall system (*Standard* Sec. 12.2). For Seismic Design Category D, the bearing wall system has a height limit of 160 feet and must comply with the requirements for special reinforced masonry shear walls. Note that the structural system is one of uncoupled shear walls. Crossing beams over the interior doorways (their design is not included in this example) will need to continue to support the gravity loads from the deck slabs above during the earthquake, but are not designed to provide coupling between the shear walls.

The building is symmetric and appears to be regular both in plan and elevation. It will be shown, however, that the building is torsionally irregular. *Standard* Table 12.6-1 permits use of the ELF procedure in accordance with *Standard* Section 12.8 for the buildings in Seismic Design Categories B and C. By the same table, the Seismic Design Category D buildings must use a dynamic analysis for design. A careful reading of *Standard* Table 12.6-1 for Seismic Design Category D reveals that all of the rows do not apply to our building except the last, "all other structures"; thus, ELF analysis is not permitted, but modal analysis is permitted.

Table 13.2-1 Design Parameters

Design Parameter	Value for Building in Area of Low Seismicity on Soft Rock	Value for Building in Area of Low Seismicity on Soft Clay	Value for Building in Area of Moderate Seismicity	Value for Building in Area of High Seismicity
S_s (Map 1)	0.266	0.266	0.456	1.5
S_1 (Map 2)	0.105	0.105	0.137	0.6
Site Class	C	E	C	D
F_a	1.2	2.45	1.2	1
F_v	1.7	3.49	1.66	1.5
$S_{MS} = F_a S_s$	0.32	0.65	0.55	1.5
$S_{M1} = F_v S_1$	0.18	0.37	0.23	0.9
$S_{DS} = 2/3 \, S_{MS}$	0.21	0.43	0.37	1
$S_{D1} = 2/3 \, S_{M1}$	0.12	0.24	0.15	0.6
Seismic Design Category	B	D	C	D
Diaphragm Topping req'd per ACI 318?	No	Yes*	No	Yes

Table 13.2-1 Design Parameters

Design Parameter	Value for Building in Area of Low Seismicity on Soft Rock	Value for Building in Area of Low Seismicity on Soft Clay	Value for Building in Area of Moderate Seismicity	Value for Building in Area of High Seismicity
Masonry Wall Type	Ordinary Reinforced	Special Reinforced	Intermediate Reinforced	Special Reinforced
Standard Design Coefficients (Table 12.2-1)				
R	2.0	5	3.5	5
Ω_0	2.5	2.5	2.5	2.5
C_d	1.75	3.5	2.25	3.5

*For this masonry example, Low Seismicity SDC D Building is designed without topping on the precast planks. It is assumed that the precast planks at floors and roof have connections sufficiently rigid to permit the idealization of rigid horizontal diaphragms.

The type of masonry shear wall is selected to illustrate the various requirements as well as to satisfy Table 12.2-1 of the *Standard*. Note that "Ordinary Reinforced Masonry Shear Walls" could be used for Seismic Design Category C at this height.

The orthogonal direction of loading combination requirement (*Standard* Sec. 12.5) needs to be considered for structures assigned to Seismic Design Category D. However, the arrangement of this building is not particularly susceptible to orthogonal effects; the walls are not subject to axial force from horizontal seismic motions, only bending and shear.

The walls are all solid, and there are no significant discontinuities, as defined by *Standard* Section 12.3.2.2, in the vertical elements of the seismic force-resisting system.

Ignoring the short walls at stairs and elevators, there are eight shear walls in each direction; therefore, the system appears to have adequate redundancy (*Standard* Sec. 12.3.4.2). The redundancy factor, however, will be computed.

Tie and continuity requirements (*Standard* Sec. 12.11) must be addressed when detailing connections between floors and walls (see Chapter 11 of this volume).

Nonstructural elements (*Standard* Chapter 18) are not considered in this example.

Collector elements are required in the diaphragm for longitudinal response (*Standard* Sec. 12.10). Rebar in the longitudinal direction, spliced into bond beams, is used for this purpose (see Chapter 11 of this volume).

Diaphragms must be designed for the required forces (*Standard* Sec. 12.10 and *Provisions* Part 3, Sec. RP3).

The structural walls must be designed for the required out-of-plane seismic forces (*Standard* Sec. 12.11) in addition to out-of-plane wind on exterior walls and 5 psf differential air pressure on interior walls.

Each wall acts as a vertical cantilever in resisting in-plane forces. The walls are classified as masonry cantilever shear wall structures in *Standard* Table 12.12-1, which limits story drift to 0.01 times the story height.

13.2.3 Load Combinations

The basic load combinations are those in *Standard* Section 2.3.2. The seismic load effect, E, is defined by *Standard* Section 12.4, as follows:

$$E = E_h + E_v = \rho Q_E \pm 0.2 S_{DS} D$$

13.2.3.1 Redundancy Factor. The Redundancy Factor, ρ, is a multiplier on design force effects and applies only to the in-plane direction of the shear walls. For structures in Seismic Design Categories A, B and C, $\rho = 1.0$ (*Standard* Sec. 12.3.4.1). For structures in Seismic Design Category D, ρ is determined per *Standard* Section 12.3.4.2.

For a shear wall building assigned to Seismic Design Category D, $\rho = 1.0$ as long as it can be shown that failure of a shear wall or pier with a height-to-length ratio greater than 1.0 would not result in more than a 33 percent reduction in story strength or create an extreme torsional irregularity. The intent is that the aspect ratio is based on story height, not total height.

$$\frac{\text{height}}{\text{length}} = \frac{8'}{32.67'} = 0.24 < 1.0$$

Because no walls have a ratio exceeding 1.0, none have to be removed to check for redundancy and $\rho = 1.0$. If one were to consider the removal of one shear wall in either direction, 1/8 or 12.5 percent resistance would be removed. 12.5% < 33%, so $\rho = 1.0$. Therefore, for this example, the redundancy factor is 1.0 for the buildings assigned to Seismic Design Category D.

13.2.3.2 Combination of load effects. The seismic load effect, E, determined for each of the buildings is as follows:

Low Seismicity SDC B: $E = (1.0)Q_E \pm (0.2)(0.21)D = Q_E \pm 0.04D$

Low Seismicity SDC D: $E = (1.0)Q_E \pm (0.2)(0.43)D = Q_E \pm 0.09D$

Moderate Seismicity SDC C: $E = (1.0)Q_E \pm (0.2)(0.37)D = Q_E \pm 0.07D$

High Seismicity SDC D: $E = (1.0)Q_E \pm (0.2)(1.00)D = Q_E \pm 0.20D$

The applicable load combinations from *Standard* Sections 2.3.2 and 12.4.2.3 are:

$1.2D + 1.0E + 0.5L + 0.2S$

where the effects of gravity and seismic loads are additive, and

$0.9D + 1.0E + 1.6H$

where the effects of gravity and seismic loads are counteractive. H is the effect of lateral pressures of soil and water in soil. The 0.5 factor on L is because $L_0 < 100$ psf for these residential buildings. Per the *Standard*, corridors are "same as occupancy served", except for the first floor.

Load effect H does not apply for this design, and the snow load effect, S, does not exceed the minimum roof live load at any of the buildings. Consideration of snow loads is not required in the effective seismic weight, W, of the structure where the design snow load does not exceed 30 psf (*Standard* Sec. 12.7.2).

The basic load combinations are combined with E as determined above, and the load combinations representing the extreme cases are as follows:

Low Seismicity SDC B:	$1.24D + Q_E + 0.5L$
	$0.86D - Q_E$
Low Seismicity SDC D:	$1.29D + Q_E + 0.5L$
	$0.81D - Q_E$
Moderate Seismicity SDC C:	$1.27D + Q_E + 0.5L + 0.2S$
	$0.83D - Q_E$
High Seismicity SDC D:	$1.40D + Q_E + 0.5L$
	$0.70D - Q_E$

These combinations are for the in-plane direction. Load combinations for the out-of-plane direction are similar except that the redundancy factor (1.0 in all cases for in-plane loading) is not applicable.

13.2.4 Seismic Design for Low Seismicity SDC B Building

13.2.4.1 Low Seismicity SDC B Building weights. This site is assigned to Seismic Design Category B, and the walls are designed as ordinary reinforced masonry shear walls (*Standard* Table 12.2-1), which stipulates that the minimum reinforcement requirements of TMS 402 Section 7.3.2.3.1 be followed. Given the length of the walls, vertical reinforcement of #4 bars at 8 feet on center works well for detailing reasons and will be used here (10 feet is the maximum spacing per TMS 402). For this example, 45 psf will be used for the 8-inch-thick lightweight partially grouted CMU walls. The 45 psf value includes grouted cells, as well as bond beams in the course just below the floor planks.

67 psf is used for 8-inch-thick, normal-weight hollow core plank plus the non-masonry partitions. 67 psf is also used for the roof plank plus roofing.

Story weight, w_i, is computed as follows.

For the roof:

Roof slab (plus roofing) = (67 psf) (152 ft)(72 ft) = 733 kips

Walls = (45 psf)(589 ft)(8.67 ft/2) + (45 psf)(4)(36 ft)(2 ft) = 128 kips

Total = 861 kips

Note that there is a 2-foot-high masonry parapet on four walls and the total length of masonry wall, including the short walls not used in the seismic force-resisting system, is 589 feet.

For a typical floor:

Slab (plus partitions) = 733 kips

Walls = (45 psf)(589 ft)(8.67 ft) = 230 kips

Total = 963 kips

Total effective seismic weight, $W = 861 + (4)(963) = 4,713$ kips.

This total excludes the lower half of the first story walls, which do not contribute to seismic loads that are imposed on CMU shear walls.

13.2.4.2 Low Seismicity SDC B Building base shear calculation. The seismic response coefficient, C_s, is computed using *Standard* Section 12.8.

Per *Standard* Equation 12.8-2:

$$C_s = \frac{S_{DS}}{R/I} = \frac{0.21}{2/1} = 0.105$$

The value of C_s need not be greater than *Standard* Equation 12.8-3:

$$C_s = \frac{S_{D1}}{T(R/I)} = \frac{0.12}{0.338(2/1)} = 0.178$$

where T is the fundamental period of the building approximated per *Standard* Equation 12.8-7 as follows:

$$T_a = C_t h_n^x = (0.02)(43.33^{0.75}) = 0.338 \text{ sec}$$

where $C_t = 0.02$ and $x = 0.75$ are from *Standard* Table 12.8-2 (the approximate period, based on building system and building height, is the same for all locations).

The value for C_s is taken as 0.105 (the lesser of the two computed values). This value is larger than the minimum specified in *Standard* Equation 12.8-5 (Sup. 2):

$$C_s = 0.044 I S_{DS} \geq 0.010$$

$$= (0.044)(1.0)(0.21) = 0.00924 = 0.010 \qquad\qquad \text{(0.105 controls)}$$

The total seismic base shear is then calculated using *Standard* Equation 12.8-1 as follows:

$$V = C_s W = (0.105)(4,713) = 495 \text{ kips}$$

13.2.4.3 Low Seismicity SDC B Building vertical distribution of seismic forces. *Standard* Section 12.8.3 stipulates the procedure for determining the portion of the total seismic load assigned to each floor level. The story force, F_x, is calculated using *Standard* Equations 12.8-11 and 12.8-12 as follows:

$$F_x = C_{vx} V$$

and

$$C_{vx} = \frac{w_x h_x^k}{\sum\limits_{i=1}^{n} w_i h_i^k}$$

where C_{vx} is a vertical distribution factor which has the effect of distributing more of the base shear to the upper levels to mimic the dynamic response of the structure.

For $T = 0.338$ sec < 0.5 sec, $k = 1.0$.

The seismic design shear in any story is determined from *Standard* Equation 12.8-13:

$$V_x = \sum_{i=x}^{n} F_i$$

Although not specified in the *Standard* or used in design, story overturning moment may be computed using the following equation:

$$M_x = \sum_{i=x}^{n} F_i (h_i - h_x)$$

The application of these equations for this building is shown in Table 13.2-2.

Table 13.2-2 Low Seismicity SDC B Building Seismic Forces and Moments (i.e., Seismic Demand) by Level

Level x	w_x (kips)	h_x (ft)	$w_x h_x^k$ (ft-kips)	C_{vx}	F_x (kips)	V_x (kips)	$M_{(x-1)}$ (ft-kips)
5	861	43.34	37,310	0.3089	153	153	1,326
4	963	34.67	33,384	0.2764	137	290	3,840
3	963	26.00	25,038	0.2073	103	393	7,245
2	963	17.33	16,692	0.1382	68	461	11,240
1	963	8.67	8,346	0.0691	34	461	15,530
Σ	4,715		120,770	1.0000	495	495	

1.0 kips = 4.45 kN, 1.0 ft = 0.3048 m.

Note that F_x, V_x and M_x are all factored loads.

A note regarding locations of V and M: the vertical weight at the roof (fifth level), which includes the upper half of the wall above the fifth floor (fourth level), produces an inertial force that contributes to the shear, V, in the walls supporting the fifth level. That shear in turn generates a moment that increases towards the level below (fourth level). Resisting this moment is the rebar in the wall combined with the wall weight above the fourth level. The story overturning moment is tabulated for the level below the level that receives the story force. This is illustrated in Figure 13.2-4.
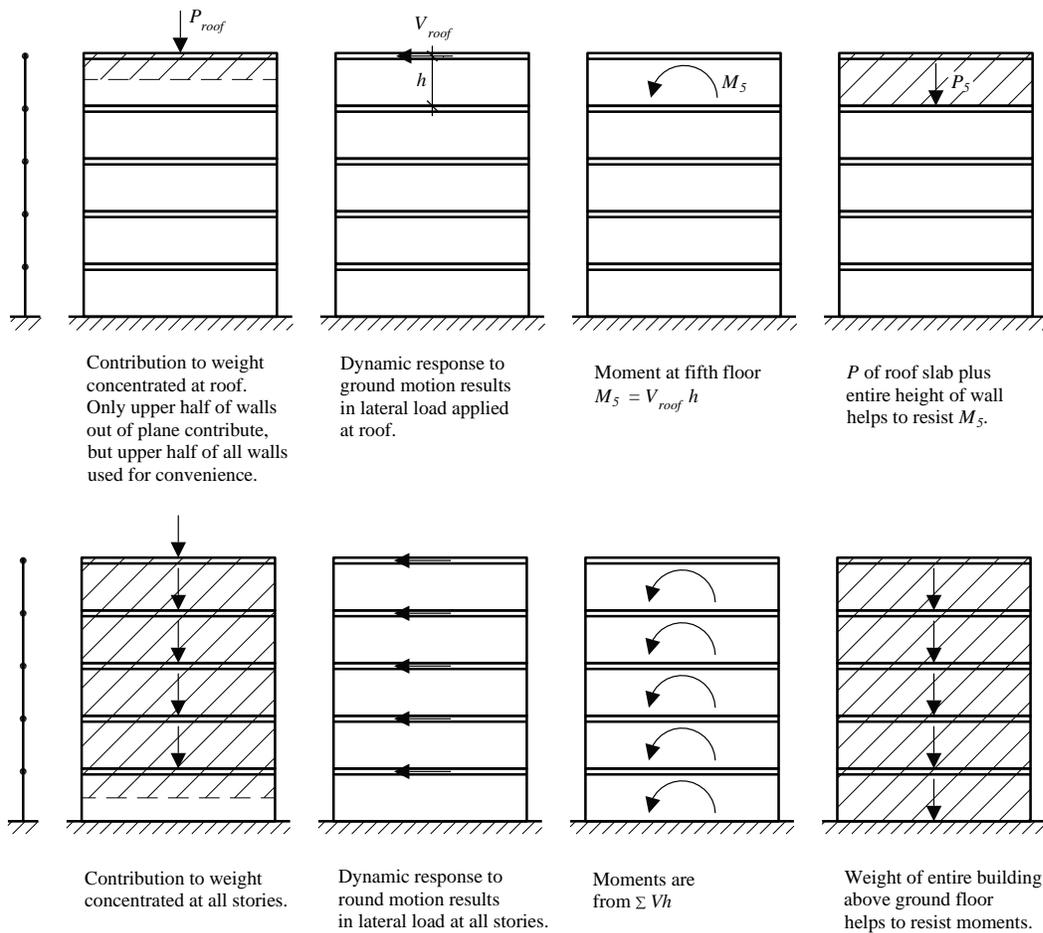
Figure 13.2-4 Location of moments due to story shears

13.2.4.4 Low Seismicity SDC B Building horizontal distribution of forces. The wall lengths are shown in Figure 13.2-3. The initial grouting pattern is essentially the same for Walls A, B, C and D. Because of a low relative stiffness, the effects Walls E, F and G are ignored in this analysis. Walls A, B, C and D are so nearly the same length that their stiffnesses are assumed to be the same for this example.

Torsion is considered according to *Standard* Section 12.8.4. For a symmetric plan, as in this example, the only torsion to be considered is the accidental torsion, M_{ta}, caused by an assumed eccentricity of the mass each way from its actual location by a distance equal to 5 percent of the dimension of the structure perpendicular to the direction of the applied loads.

Dynamic amplification of the torsion need not be considered for Seismic Design Category B per *Standard* Section 12.8.4.3.

For this example, the building is analyzed in the transverse direction only. The evaluation of Wall D is selected for this example. The rigid diaphragm distributes the lateral forces into walls in both directions. Two components of force must be considered: direct shear and shear induced by torsion.

The direct shear force carried by each Wall D is one-eighth of the total story shear (eight equal walls). The torsional moment per *Standard* Section 12.8.4.2 is as follows:

$$M_{ta} = 0.05bV_x = (0.05)(152 \text{ ft})V_x = 7.6V_x$$

The torsional force per wall, V_t, is:

$$V_t = \frac{M_t Kd}{\sum Kd^2}$$

where K is the stiffness (rigidity) of each wall. Note that all the walls in both directions are included.

Because all the walls in this example are assumed to be equally long, then they are equally stiff:

$$V_t = M_t \left[\frac{d}{\sum d^2} \right]$$

where d is the distance from each wall to the center of twisting.

$$\sum d^2 = 4(36)^2 + 4(12)^2 + 4(36)^2 + 4(12)^2 = 11{,}520 \text{ ft}^2$$

The maximum torsional shear force in Wall D, therefore, is:

$$V_t = \frac{(7.6V)(36 \text{ ft})}{11{,}520 \text{ ft}^2} = 0.0238V$$

The total shear in Wall D is:

$$V_{tot} = 0.125V + 0.0238V = 0.149V$$

The total story shear and overturning moment may now be distributed to Wall D and the wall proportions checked. The wall capacity is checked before considering deflections.

13.2.4.5 Low Seismicity SDC B Building transverse wall (Wall D). The *Provisions* and the *Standard* define the seismic load as a strength or limit state design level effect. TMS 402 Chapter 9 defines strength design for masonry. Strength design of masonry, as defined in TMS 402, is illustrated here. It is also permissible to use the allowable stress design method of TMS 402 by factoring the seismic load effects, but that will not be illustrated here.

The required strength is derived from the load combinations defined previously.

13.2.4.5.1 Low Seismicity SDC B Building shear strength. TMS 402 Section 9.1.3 states that the design strength must be greater than the required strength. The design strength is equal to the nominal strength times a strength-reduction factor:

$$V_u \leq \phi V_n$$

The strength reduction factor, ϕ, for shear is 0.8 (TMS 402 Sec. 9.1.4.5).

The nominal shear strength, V_n, is:

$$V_n = (V_{nm} + V_{ns})\gamma_g$$

Likewise:

$$\phi V_n = \phi(V_{nm} + V_{ns})\,\gamma_g$$

The shear strength provided by masonry (TMS 402 Sec. 9.3.4.1.2.1) is as follows:

$$V_{nm} = \left[4.0 - 1.75\left(\frac{M_u}{V_u d_v}\right)\right] A_n \sqrt{f'_m} + 0.25\,P_u$$

For grouted cells at 8 feet on center:

$$A_n = (2 \times 1.25 \text{ in.} \times 32.67 \text{ ft} \times 12 \text{ in./ft}) + (8 \text{ in.} \times 5.13 \text{ in.} \times 5 \text{ cells}) = 1{,}185 \text{ in.}^2$$

The shear strength provided by reinforcement (given by TMS 402 Sec. 9.3.4.1.2.2) is as follows:

$$V_{ns} = 0.5\left(\frac{A_v}{s}\right) F_y d_v$$

The wall will have a bond beam with two #4 bars at each story to bear the precast floor planks and wire joint reinforcement at alternating courses. Common joint reinforcement with 9-gauge wires at each face shell will be used; each wire has a cross-sectional area of 0.017 in.^{2}. With six courses of joint reinforcement and two #4 bars, the total area per story is 0.60 in.^{2} or 0.07 in.^{2}/ft. Given that the story height is less than half the wall length, the author believes that it is acceptable to treat the distribution of horizontal reinforcement as if being uniformly distributed for shear resistance.

$$V_{ns} = 0.5(0.07 \text{ in.}^2/\text{ft})(60 \text{ ksi})(32.67 \text{ ft}) = 68.3 \text{ kips}$$

The maximum nominal shear strength of the member (Wall D in this case) for $M/Vd_v > 1.00$ is given by TMS 402 Section 9.3.4.1.2(b):

$$V_n(\text{max}) = \left(4 A_n \sqrt{f'_m}\right)\gamma_g$$

The coefficient 4 becomes 6 for $M/Vd_v < 0.25$ (TMS 402 Sec. 9.3.4.1.2(a)). Interpolation between yields the following:

$$V_n\ (\text{max}) = \left[\left(6.67 - 2.67\left(\frac{M_u}{V_u d_v}\right)\right) A_n \sqrt{f'_m}\right]\gamma_g$$

The factor g_g is 0.75 for partially grouted shear walls per TMS 402 Section 9.3.4.1.2. The shear strength of Wall D, based on the equations listed above, is summarized in Table 13.2-3. Note that V_x and M_x in this table are values from Table 13.2-2 multiplied by 0.149 (which represents the portion of direct and torsional shear assigned to Wall D). P_u is the dead load of the roof or floor times the tributary area for

Wall D, taken as 0.86*D* for the minimum (conservative) P_u. (Note that there is a small load from the floor plank parallel to the wall.)

Table 13.2-3 Shear Strength Calculations for Low Seismicity SDC B Building Wall D

Story	V_x (kips)	M_x (ft-kips)	M_x/V_xd_v	$V_u = V_x$ (kips)	P_u (kips)	V_{nm} (kips)	V_{ns} (kips)	V_n (kips)	V_n (max) (kips)	ϕV_n (kips)
5	22.8	198	0.266	22.8	35.3	196	68	**198**	237	158
4	43.2	572	0.405	43.2	76.5	193	68	**196**	222	157
3	58.6	1080	0.564	58.6	118	189	68	**193**	206	154
2	68.7	1675	0.746	68.7	158	182	68	188	**186**	149
1	73.8	2314	0.960	73.8	200	173	68	181	**164**	131

1.0 kip = 4.45 kN, 1.0 ft-kip = 1.36 kN-m.

Values shown in **bold** are the controlling values for V_n

For all levels, $\phi V_n > V_u$, so it is OK for this Ordinary Reinforced Masonry Shear Wall.

13.2.4.5.2 Low Seismicity SDC B Building axial and flexural strength. All the walls in this example are bearing shear walls since they support vertical loads as well as lateral forces. In-plane calculations include:

Strength check

Ductility check

13.2.4.5.2.1 Strength check. The wall demands, using the load combinations determined previously, are presented in Table 9.2-4 for Wall D. In the table, Load Combination 1 is $1.245D + Q_E + 0.5L$ and Load Combination 2 is $0.86D + Q_E$.

Table 13.2-4 Demands for Low Seismicity SDC B Building Wall D

Story	P_D (kips)	P_L (kips)	Load Combination 1		Load Combination 2	
			P_u (kips)	M_u (ft-kips)	P_u (kips)	M_u (ft-kips)
5	49	0	61	198	42	198
4	98	15	129	572	84	572
3	147	25	195	1,080	126	1,080
2	196	34	260	1,675	168	1,675
1	245	41	324	2,314	210	2,314

1.0 kip = 4.45 kN, 1.0 ft-kip = 1.36 kN-m.

P_D and P_L are based on floor tributary area of 540 ft². P_L has been reduced per *Standard* Section 4.8 using $K_{LL} = 2$.

Strength at the bottom story (where *P*, *V* and *M* are the greatest) is examined here. (For a real design, all levels should be examined). As will be shown, Load Combination 2 from Table 13.2-4 is the controlling case because it has the same lateral load as Load Combination 1, but with lower values of axial force.

For the base of the shear walls:

$$P_{u_{min}} = 210 \text{ kips}$$

$$P_{u_{max}} = 324 \text{ kips}$$

$$M_u = 2{,}314 \text{ ft-kips}$$

Try one #4 bar in each end cell and a #4 bar at 8 feet on center for the interior cells. A curve of ϕP_n - ϕM_n representing the wall strength envelope, are developed and used to evaluate P_u and M_u determined above. Three cases are analyzed and their results are used in plotting the ϕP_n - ϕM_n curve.

In accordance with TMS 402 Section 9.3.2, the strength of the section is reached as the compressive strains in masonry reach their maximum usable value of 0.0025 for CMU. The force equilibrium in the section is attained by assuming an equivalent rectangular stress block of $0.8f'_m$ over an effective depth of $0.8c$, where c is the distance of the neutral axis from the fibers of maximum compressive strain. Stress in all steel bars is taken into account. The strains in the bars are proportional to their distance from the neutral axis. For strains above yield, the stress is independent of strain and is taken as equal to the specified yield strength, F_y. See Figure 13.2-5 for strains and stresses for all three cases selected.

Case 1 ($P = 0$)

Assume all tension bars yield (which can be verified later):

$$T_{s1} = (0.20 \text{ in.}^2)(60 \text{ ksi}) = 12.0 \text{ kips}$$

$$T_{s2} = (0.20 \text{ in.}^2)(60 \text{ ksi}) = 12.0 \text{ kips each}$$

Because the neutral axis is close to the compression end of the wall, compression steel, C_{s1}, is neglected (it would make little difference anyway) for Case 1:

$$\Sigma F_y = 0:$$

$$C_m = \Sigma T$$

$$C_m = (4)(12.0) = 48.0 \text{ kips}$$

The compression block is entirely within the first grouted cell:

$$C_m = 0.8 f'_m ab$$

$$48.0 = (0.8)(2.0 \text{ ksi})a(7.625 \text{ in})$$

$$a = 3.9 \text{ in.} = 0.33 \text{ ft}$$

$c = a/0.8 = 0.33/0.8 = 0.41$ ft

Thus, the neutral axis is determined to be 0.41 feet from the compression end on the wall, which is within the first grouted cell:

$\Sigma M_{cl} = 0$: (The math is a little easier if moments are taken about the wall centerline.)

$M_n = (16.33\text{-}0.33/2 \text{ ft})C_m + (16.00 \text{ ft})T_{s1} + (0.00 \text{ ft})\Sigma T_{s2} + (0.00 \text{ ft})P_n$

$M_n = (16.17)(48.0) + (16.00)(12) + 0 + 0 = 968$ ft-kips

$\phi M_n = (0.9)(968) = 871$ ft-kips
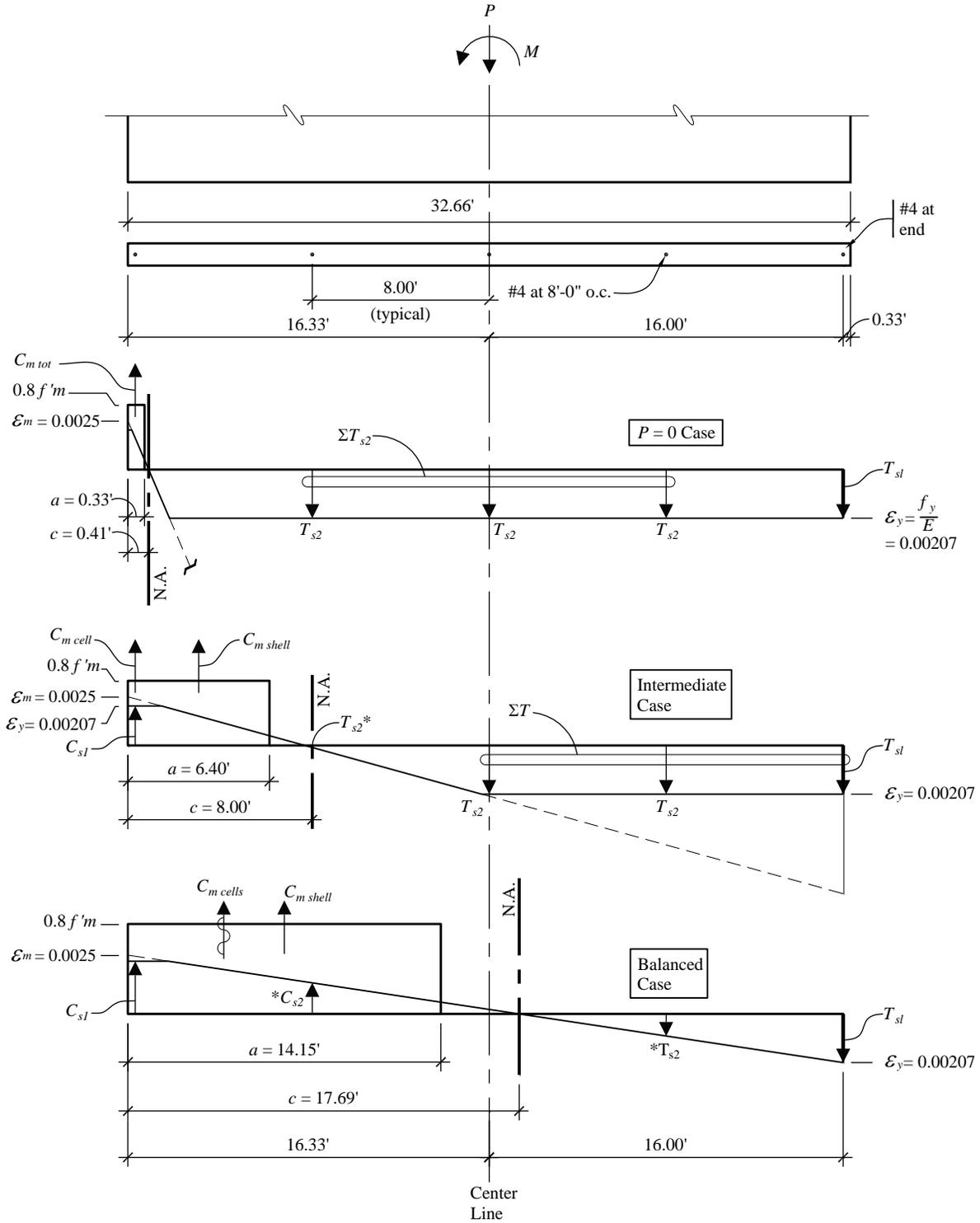
Figure 13.2-5 Strength of Low Seismicity SDC B Building Wall D.
Strain diagram superimposed on strength diagram for the three cases.
*The low force in the selected reinforcement is neglected in the calculations.
(1.0 ft = 0.3048 m)

To summarize, Case 1:

$\phi P_n = 0$ kips

$\phi M_n = 871$ ft-kips

Case 2 (Intermediate case between $P = 0$ and P_{bal})

Let $c = 8.00$ feet (this is an arbitrary selection). Thus, the neutral axis is defined at 8 feet from the compression end of the wall:

$a = 0.8c = (0.8)(8.00) = 6.40$ ft

$C_{m\ shells} = 0.8f'_m(2\text{ shells})(1.25\text{ in. / shell})(6.40\text{ ft } (12\text{ in./ft}) = 307.2$ kips

$C_{m\ cells} = 0.8\,f'_m(41\text{ in.}^2) = 65.6$ kips

$C_{m\ tot} = C_{m\ shells} + C_{m\ cells} = 307.2 + 65.6 = 373$ kips

$C_{s1} = (0.20\text{ in.}^2)(60\text{ ksi}) = 12$ kips (Compression steel is not enclosed by a lateral tie, take $C_{s1} = 0$)

$T_{s1} = (0.20\text{ in.}^2)(60\text{ ksi}) = 12$ kips

$T_{s2} = (0.20\text{ in.}^2)(60\text{ ksi}) = 12$ kips each

TMS 402 Section 9.3.2 states that the compression resistance of reinforcing steel that is not enclosed within ties be neglected. Compression reinforcement without lateral ties may be considered for the specific check of maximum tensile reinforcement (ductility check) per TMS 402 Section 9.3.3.5.1(e). For this example, the compression reinforcement is neglected.

$\Sigma F_y = 0$:

$C_{m\ tot} = P_n + T_{s1} + \Sigma T_{s2}$

$373 = P_n + (3)(12.0)$

$P_n = 337$ kips

$\phi P_n = (0.9)(337) = 303$ kips

$\Sigma M_{cl} = 0$:

$M_n = (13.13\text{ ft})C_{m\ shell} + (16.00\text{ ft})(C_{m\ cell}) + (16.00\text{ ft})T_{s1} + (8.00\text{ ft})T_{s2}$

$M_n = (13.13)(307.2) + (16.00)(65.6) + (16.00)(12.0) + (8.00\text{ ft})(12.0) = 5,371$ ft-kips

$\phi M_n = (0.9)(5,371) = 4,834$ ft-kips

To summarize Case 2:

$\phi P_n = 303$ kips

$\phi M_n = 4{,}834$ ft-kips

Case 3 (Balanced case)

In this case, T_{s1} just reaches its yield stress:

$$c = \left[\frac{0.0025}{(0.0025 + 0.00207)} \right] (32.33 \text{ ft}) = 17.69 \text{ ft}$$

$a = 0.8c = (0.8)(17.69) = 14.15$ ft

$C_{m \text{ shells}} = 0.8f'_m(2 \text{ shells})(1.25 \text{ in./shell})(14.15 \text{ ft}) (12 \text{ in./ft}) = 679.2$ kips

$C_{m \text{ cells}} = 0.8f'_m(2 \text{ cells})(41 \text{ in.}^2/\text{cell}) = 131.2$ kips

$C_{m \text{ tot}} = C_{m \text{ shells}} + C_{m \text{ cells}} = 810.4$ kips

$C_{s1} = (0.20 \text{ in.}^2)(60 \text{ ksi}) = 12.0$ kips (Again take $C_{s1} = 0$)

$T_{s1} = (0.20 \text{ in.}^2)(60 \text{ ksi}) = 12.0$ kips

C_{s2} and T_{s2} are neglected because they are small.

$\Sigma F_y = 0$:

$P_n = \Sigma C - \Sigma T$

$P_n = C_{m \text{ tot}} - T_{s1} = 810.4 - 12.0 = 798.4$ kips

$\phi P_n = (0.9)(798.4) = 719$ kips

$\Sigma M_{cl} = 0$:

$M_n = 9.26 \, C_{m \text{ shells}} + ((16 + 8)/2) \, C_{m \text{ cells}} + + 16 \, T_{s1}$

$M_n = (9.26)(679.2) + (12.0)(131.2) + (16.0)(12.0) = 8{,}056$ kips

$\phi M_n = (0.9)(8{,}056) = 7{,}250$ ft-kips

To summarize Case 3:

$\phi P_n = 719$ kips

$\phi M_n = 7{,}250$ ft-kips

Using the results from the three cases above, the ϕP_n - ϕM_n curve shown in Figure 13.2-6 is plotted. Although the portion of the ϕP_n - ϕM_n curve above the balanced failure point could be determined, it is not necessary here. Thus, only the portion of the curve below the balance point is examined. This is the region of high moment capacity.

Similar to reinforced concrete beam-columns, in-plane compression failure of the cantilevered shear wall will occur if $P_u > P_{bal}$ and yield of tension steel will occur first if $P_u < P_{bal}$. A ductile failure mode is essential to the design, so the portion of the curve above the "balance point" is not useable. In fact, the ductility (maximum reinforcement) requirement prevents P_u from approaching P_{bal}.

As can be seen, the points for ($P_{u\ min}$, M_u) and ($P_{u\ max}$, M_u) are within the ϕP_n - ϕM_n envelope; thus, the strength design is acceptable with the minimum reinforcement. Figure 13.2-6 shows two schemes for determining the design flexural resistance for a given axial load. One interpolates along the straight line between pure bending and the balanced load. The second makes use of intermediate points for interpolation. This particular example illustrates that there can be a significant difference in the interpolated moment capacity between the two schemes for axial loads midway between the balanced load and pure bending.
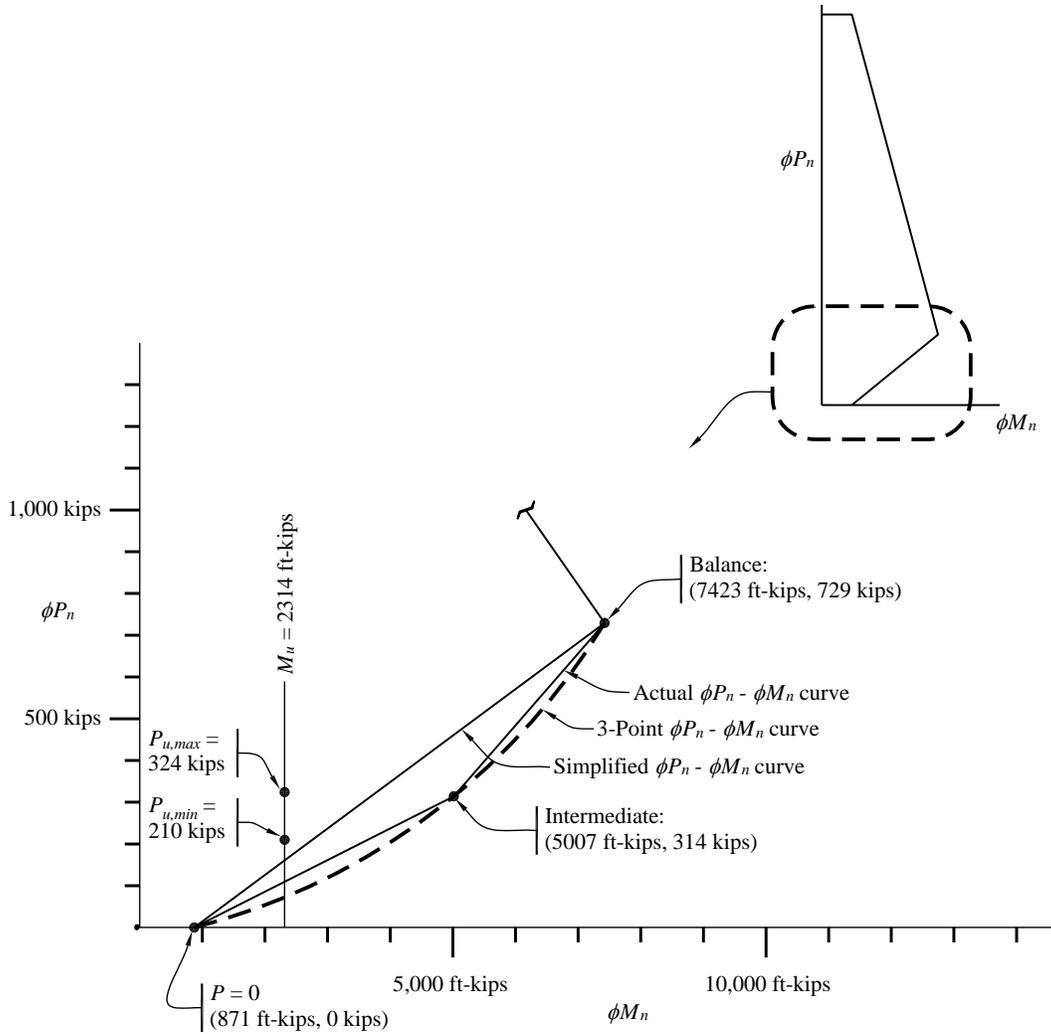
Figure 13.2-6 ϕP_n - ϕM_n Diagram for Low Seismicity SDC B Building Wall D
(1.0 kip = 4.45 kN, 1.0 ft-kip = 1.36 kN-m)

13.2.4.5.3 Ductility check. For this case, with $M_u/V_u d_v < 1$ and $R > 1.5$, TMS 402 Section 9.3.3.5.4 refers to Section 9.3.3.5.1, which stipulates that the critical strain condition correspond to a strain in the extreme tension reinforcement equal to 1.5 times the strain associated with F_y. This calculation uses unfactored gravity loads. Refer to Figure 13.2-7 and the following calculations which illustrate this use of loads at the bottom story (highest axial loads). Calculations for other stories are not presented in this example.
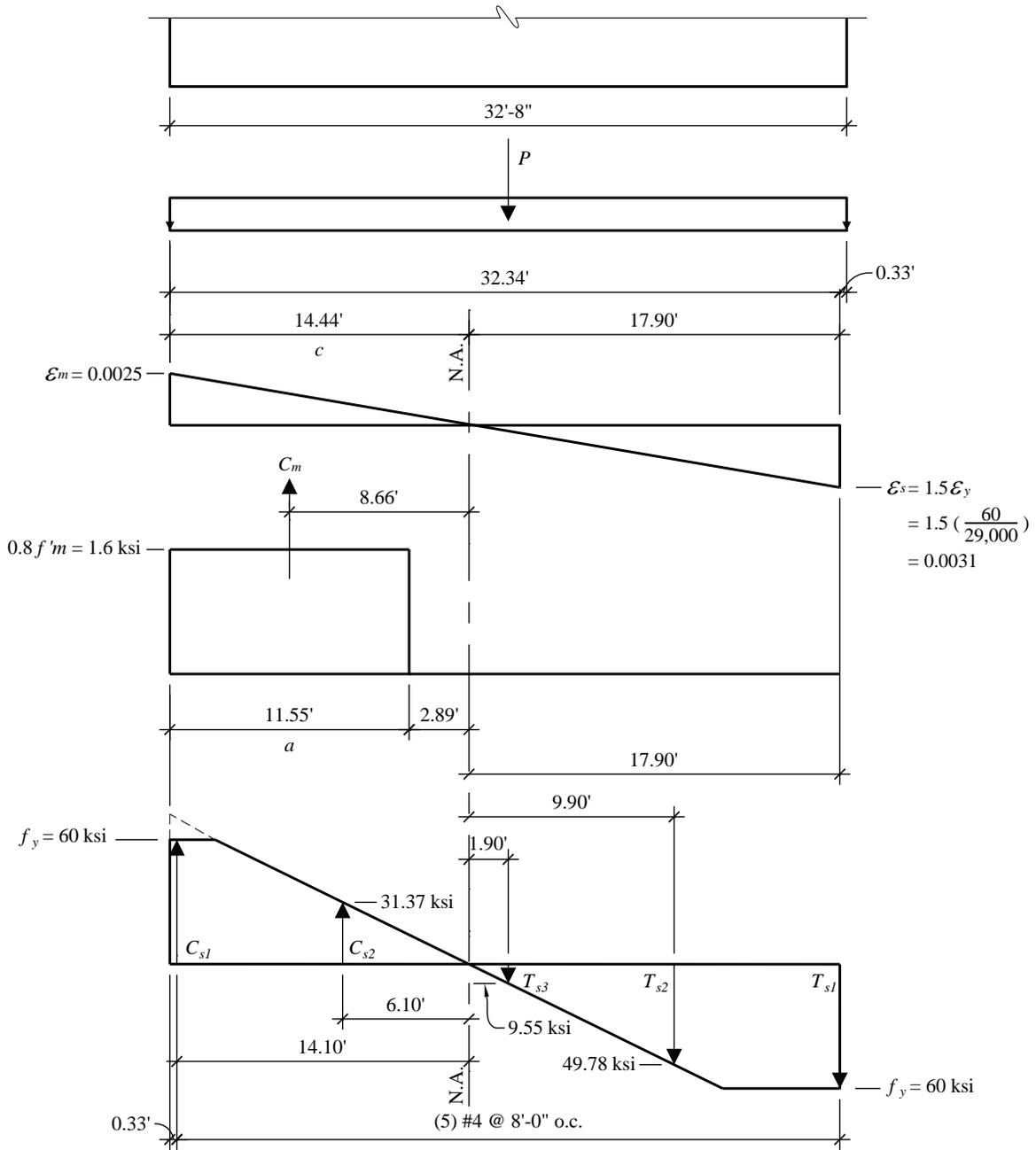
Figure 13.2-7 Ductility check for Low Seismicity SDC B Building Wall D
(1.0 ft = 0.3048 m, 1.0 ksi = 6.89 MPa)

For Level 1 (bottom story), the unfactored axial loads are:

$P = 245$ kips

Refer to Figure 13.2-7:

$C_m = 0.8 f'_m(ab + 2A_{cell}) = (1.6 \text{ ksi})[(0.8 \times 14.44 \text{ ft} \times 12 \text{ in./ft})(2)(1.25 \text{ in.}) + (2)(41 \text{ in.}^2)] = 686 \text{ kips}$

$C_{s1} = F_y A_s = (60 \text{ ksi})(0.20 \text{ in.}^2) = 12.0 \text{ kips}$

$C_{s2} = (31.37 \text{ ksi})(0.20 \text{ in.}^2) = 6.3 \text{ kips}$

$T_{s1} = (60 \text{ ksi})(0.20 \text{ in.}^2) = 12.0 \text{ kips}$

$T_{s2} = (49.78 \text{ ksi})(0.20 \text{ in.}^2) = 10.0 \text{ kips}$

$T_{s3} = (9.55 \text{ ksi})(0.20 \text{ in.}^2) = 1.9 \text{ kips.}$

$\sum C > \sum P + T$

$C_m + C_{s1} + C_{s21} > P + T_{s1} + T_{s2} + T_{s3}$

$686 + 12.0 + 6.3 > 245.0 + 12.0 + 10.0 + 1.9$

704 kips > 269 kips   OK

There is more compression capacity than required, so the ductile failure condition controls.

13.2.4.6 Low Seismicity SDC B Building deflections. The calculations for deflection involve many variables and assumptions, and it must be recognized that any calculation of deflection is approximate at best.

The *Standard* requires that deflections be calculated and compared with the prescribed limits set forth by *Standard* Table 12.12-1. Furthermore, *Standard* Section 12.7.3 requires that the effect of cracking be considered in establishing the elastic stiffness of masonry elements. In contrast, TMS 402 has two provisions that contradict the *Standard*: Section 7.2.4 effectively dismisses the drift requirement for all masonry shear walls except Special Reinforced Masonry Shear Walls, and Section 4.3.2 permits the use of uncracked stiffness. However, the commentary to Section 4.3.2 states that for reinforced masonry, cracked stiffness should be considered, and Section 9.1.5.2 requires cracked stiffness of no more than $0.5I_g$ for deflection calculations of reinforced masonry. Cracked section properties are considered for this example. Elastic deflections are calculated considering cracking and then increased by C_d to account for non-linear response during the design earthquake. Recognizing that *P-delta* effects are minor for the in-plane direction, we solve for $\delta_{total} = \delta_{flexural} + \delta_{shear}$ for elastic and increase that value by C_d. The story drift, Δ, is the difference between δ_{total} for adjacent stories.

The following procedure is used for calculating deflections:

1. For purpose of illustration, moments and cracking moments in each story are computed and are shown in Table 13.2-5.

2. Cracking moment is determined from $M_{cr} = S(f_r + P_{u \ min} / A_n)$.

3. Compute deflection for each level.

While I_{cr} can be determined from principles of mechanics, the author prefers to consider the following:

$I_{cr} < I_g$

For walls with no compression, the calculation for I_{cr} is straightforward.

For walls with compression, one can adjust A_s to account for the effect of compression, resulting in A_{se}.

ACI 318 permits $I_{cr} = 0.35I_g$ for cracked, reinforced concrete walls (ACI 318 Table 6.6.3.1.1(a)).

Alternatively, a (complicated) equation for I can be used (ACI 318 Table 6.6.3.1.1(b)).

TMS 402 Section 9.1.5.2 permits up to one-half of gross section properties for use in deflection calculations when considering effects of cracking on reinforced masonry members.

NEHRP Seismic Design Technical Brief No. 9, Seismic Design of Special Reinforced Masonry Shear Walls, recommends using $I_{cr} = 0.15I_g$ for unflanged walls and $I_{cr} = 0.40I_g$ for flanged walls.

For this example, the effect of cracking is recognized by taking I_{eff} as 35 percent of the gross moment of inertia, as recommended for reinforced concrete walls in ACI 318. Other approximations can be used. In the author's opinion, the approximations pale in uncertainty in comparison to the approximation of nonlinear deformation using C_d.

For the Low Seismicity SDC B Building:

b_e = effective masonry wall width, averaged over the entire wall length

$b_e = [(2 \times 1.25 \text{ in.})(32.67 \text{ ft} \times 12) + (5 \text{ cells})(41 \text{ in.}^2/\text{cell})]/(32.67 \text{ ft} \times 12) = 3.02 \text{ in.}$

$S = b_e \, l^2/6 = (3.02)(32.67 \times 12)^2/6 = 77,434 \text{ in.}^3$

$f_r = (0.084 \text{ ksi })(11 \text{ cells}/12 \text{ cells}) + (0.163 \text{ ksi}) (1 \text{ cell}/12 \text{ cells}) = 0.091 \text{ ksi}$
(for CMU with every 12th cell grouted)

$A_n = b_e \, l = (3.02 \text{ in.})(32.67 \text{ ft} \times 12) = 1,185 \text{ in.}^2$

P_u is calculated using 1.00D (see Table 13.2-4). 1.00D is considered to be a reasonable value for axial load for this admittedly approximate analysis. If greater conservatism is desired, P_u could be calculated using 0.86D. (Recall that the 0.86 factor accounts for E_v in the upward direction [i.e., 0.9 - 0.2 S_{DS}], leading to a lower bound on P_u).

The results are shown in Table 13.2-5.

Table 13.2-5 Low Seismicity SDC B Building Cracked Wall Determination

Level	$P_{u_{min}}$ (kips)	M_{cr} (ft-kips)	M_u (ft-kips)	Status
5	49	851	198	Uncracked
4	98	1,118	572	Uncracked
3	147	1,385	1,080	Uncracked

Table 13.2-5 Low Seismicity SDC B Building Cracked Wall Determination

Level	$P_{u_{min}}$ (kips)	M_{cr} (ft-kips)	M_u (ft-kips)	Status
2	196	1,652	1,675	Cracked
1	245	1,919	2,314	Cracked

1.0 kip = 4.45 kN, 1.0 ft-kip = 1.36 kN-m.

For uncracked walls:

$I_n = I_g = bl^3/12 = (3.02 \text{ in.})(32.67 \times 12)^3 /12 = 1.52 \times 10^7 \text{ in.}^4$

$I_{eff} = 0.35 \, I_g = 0.532 \times 10^7 \text{ in.}^4$

The calculation of δ considers flexural and shear deflections. For the final determination of deflection, a RISA-2D analysis is made. The result is summarized Table 13.2-6 below. Figure 13.2-8 illustrates the deflected shape of the wall.
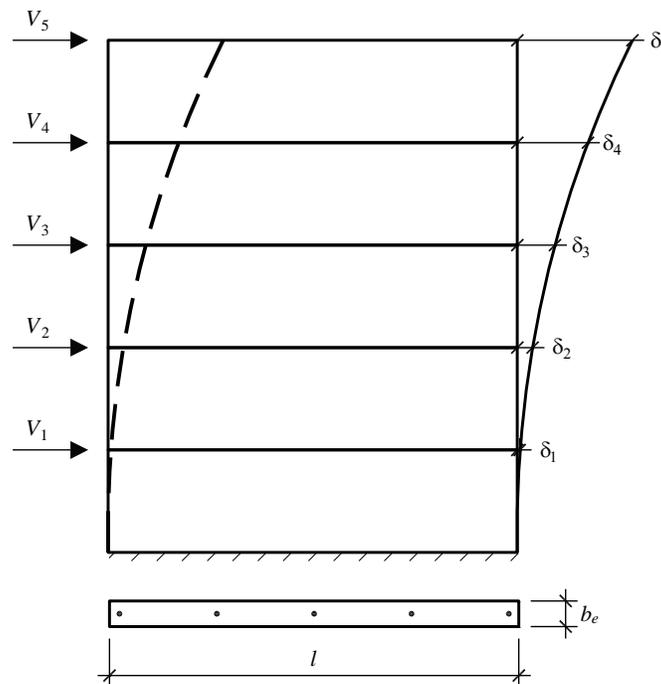
Figure 13.2-8 Shear wall deflections

Table 13.2-6 Deflections, Low Seismicity SDC B Building

Level	F (kips)	I_{eff} (in.^{4})	$\delta_{flexural}$ (in.)	δ_{shear} (in.)	δ_{total} (in.)	$C_d \delta_{total}$ (in.)	Δ (in.)
5	22.8	1.52×10^7	0.201	0.032	0.233	0.408	0.096
4	20.4	1.52×10^7	0.150	0.028	0.178	0.312	0.097
3	15.3	1.52×10^7	0.099	0.024	0.123	0.215	0.096
2	10.1	0.532×10^7	0.051	0.017	0.068	0.119	0.079
1	5.1	0.532×10^7	0.014	0.009	0.023	0.040	0.040

1.0 kip = 4.45 kN, 1.0 in. = 25.4 mm.
$F = 0.149 F_x$, for F_x from Table 13.2-2.
Δ = story drift.

The maximum story drift occurs at Levels 3 and 4 (*Standard* Table 12.12-1):

Δ_{max} = 0.097 in.

The drift limit = $0.01 h_n$ (TMS 402 Sec. 7.2.4 and *Standard* Table 12.12-1).

Δ_{max} = 0.097 in. < 1.04 in. = $0.01 h_n$ OK

13.2.4.7 Low Seismicity SDC B Building out-of-plane forces. The *Standard* Section 12.11.1 requires that the bearing walls be designed for out-of-plane loads determined as follows:

$w = 0.40 S_{DS} I W_w \geq 0.1 W_w$

$w = (0.40)(0.24)(1)(45 \text{ psf}) = 4.3 \text{ psf} < 4.5 \text{ psf} = 0.1 W_w$

where:

W_w = weight of wall

The calculated seismic load, w = 4.5 psf, is much less than wind pressure for exterior walls and is also less than the 5 psf required by the IBC for interior walls. Thus, seismic loads do not control the design of any of the walls for loading in the out-of-plane direction.

13.2.4.8 Low Seismicity SDC B Building orthogonal effects. Orthogonal effects do not have to be considered for Seismic Design Category B (*Standard* Section 12.5.2).

This completes the design of Transverse Wall D.

13.2.4.9 Summary of Design for Low Seismicity SDC B Building Wall D.

8-inch CMU

f'$_m$ = 2,000 psi

Reinforcement:

One vertical #4 bar at wall end cells.

> > Vertical #4 bars at 8 feet on center at intermediate cells throughout.
>
> > Bond beam with two #4 bars at each story just below the floor and roof slabs.
>
> > Horizontal joint reinforcement at 16 inches.
>
> Grout at cells with reinforcement and at bond beams.

13.2.5 Seismic Design for Moderate Seismicity SDC C Building

This example focuses on differences from the design for the Low Seismicity SDC B Building site. The walls are designed as Intermediate Reinforced Masonry Shear Walls even though the *Standard* would permit Ordinary Masonry Shear Walls. While the maximum reinforcement, and thus the grout, is increased, the change in *R* factor is advantageous in that the required strength is less.

This site is assigned to Seismic Design Category C, and the walls will be designed as intermediate reinforced masonry shear walls (*Standard* Table 12.2-1. Intermediate reinforced masonry shear walls have a minimum of #4 bars at 4 feet on center (TMS 40*2* Sec. 7.3.2.5).

13.2.5.1 Moderate Seiscmicity SDC C Building Weights

As before, use 67 psf for 8-inch-thick normal-weight hollow core plank plus the non-masonry partitions. For this example, 48 psf will be assumed for the 8-inch partially grouted CMU walls. The 48 psf value includes grouted cells as well as bond beams in the course just below the floor planks. It will be shown that this symmetric building, with a seemingly well distributed lateral force-resisting system, has "extreme torsional irregularity" by the *Standard*.

Story weight, w_i:

> Roof:

> > Roof slab (plus roofing) = (67 psf) (152 ft)(72 ft) = 733 kips
> > Walls = (48 psf)(589 ft)(8.67 ft/2) + (48 psf)(4)(36 ft)(2 ft) = 136 kips
> > Total = 869 kips

> There is a 2-foot-high masonry parapet on four walls, and the total length of masonry wall is 589 feet.

> Typical floor:

> > Slab (plus partitions) = 733 kips
> > Walls = (48 psf)(589 ft)(8.67 ft) = 245 kips
> > Total = 978 kips

Total effective seismic weight, $W = 869 + (4)(978) = 4{,}781$ kips.

This total excludes the lower half of the first-story walls, which do not contribute to seismic loads that are imposed on CMU shear walls.

13.2.5.2 Moderate Seismicity SDC C Building base shear calculation.

The seismic response coefficient, C_s, is computed from *Standard* Section 12.8:

$$C_s = \frac{S_{DS}}{R/I} = \frac{0.37}{3.5/1} = 0.106$$

The value of C_s need not be greater than:

$$C_s = \frac{S_{DI}}{T(R/I)} = \frac{0.15}{0.338(3.5/1)} = 0.127$$

where T is the same as found in Section 13.2.4.2.

The value for C_s is taken as 0.106 (the lesser of the two computed values). This value is still larger than the minimum specified in *Standard* Equation 12.8-5 (Sup. 2):

$$C_s = 0.044IS_{DS} \geq 0.01$$

$$= 0.044(1.0)(0.37) = 0.0163 \geq 0.01 \qquad \text{(0.106 controls)}$$

Note that this is essentially the same as the value for the Low Seismicity SDC B Building, even though S_{DS} is 71 percent larger. This is because we are using a system with an R factor that is 75 percent larger. We continue with this example because we will find an unexpected result arising from a requirement which applies in Seismic Design Category C but not in Seismic Design Category B.

The total seismic base shear is then calculated using *Standard* Equation 12.8-1:

$$V = C_sW = (0.106)(4,781) = 507 \text{ kips}$$

13.2.5.3 Moderate Seismicity SDC C Building vertical distribution of seismic forces

The vertical distribution of seismic forces is determined in accordance with *Standard* Section 12.8.3, which was described in Section 13.2.4.3. Note that for the *Standard*, $k = 1.0$ because T is less than 0.5 seconds (similar to the Low Seismicity SDC B Building).

The application of the *Standard* equations for this building is shown in Table 13.2-7:

Table 13.2-7 Moderate Seismicity SDC C Building Seismic Forces and Moments by Level

Level x	w_x (kips)	h_x (ft)	$w_x h_x{}^k$ (ft-kips)	C_{vx}	F_x (kips)	V_X (kips)	M_x (ft-kips)
5	869	43.34	37,657	0.3076	156	156	1,350
4	978	34.67	33,904	0.2770	141	297	3,930
3	978	26.00	25,428	0.2077	105	402	7,410
2	978	17.33	16,949	0.1385	70	472	11,500
1	978	8.67	8,476	0.0692	35	507	15,900
$\sum$	4,781		122,414	1.0000	507		

1.0 kip = 4.45 kN, 1.0 ft = 0.3048 m, 1.0 ft-kip = 1.36 kN-m.

13.2.5.4 Moderate Seismicity SDC C Building horizontal distribution of forces

The initial distribution is the same as Low Seismicity SDC B Building. See Section 13.2.4.4 and Figure 13.2-3 for wall designations.

Total shear in Wall D:

$$V_{tot} = 0.125V + 0.0238V = 0.149V$$

For Seismic Design Category C structures, *Standard* Section 12.8.4.3 requires a check of torsional irregularity using the ratio of maximum displacement at the end of the structure, including accidental torsion, to the average displacement of the two ends of the building. For this simple and symmetric structure, the actual displacements do not have to be computed to find the ratio. Relying on symmetry and the assumption of rigid diaphragm behavior used to distribute the forces, the ratio of the maximum displacement of Wall D to the average displacement of the floor will be the same as the ratio of the wall shears with and without accidental torsion:

$$\frac{F_{max}}{F_{ave}} = \frac{0.149V}{0.125V} = 1.190$$

This can be extrapolated to the end of the rigid diaphragm:

$$\frac{\delta_{max}}{\delta_{ave}} = 1 + 0.190\left(\frac{152/2}{36}\right) = 1.402$$

Standard Table 12.3-1 defines a building as having a "Torsional Irregularity" if this ratio exceeds 1.2 and as having an "Extreme Torsional Irregularity" if this ratio exceeds 1.4. Thus, an important result of the Seismic Design Category C classification is that the total torsion must be amplified by the factor (*Standard* Eq. 12.8-14):

$$A_x = \left(\frac{\delta_{max}}{1.2\delta_{ave}}\right)^2 = \left(\frac{1.402}{1.2}\right)^2 = 1.365$$

Therefore, the portion of the base shear for design of Wall D is increased to:

$$V_{tot} = 0.125V + 1.365(0.0238V) = 0.158V$$

which is a 6 percent increase from before considering torsional irregularity.

The total story shear and overturning moment may now be distributed to Wall D and the wall proportions checked. The wall capacity will be checked before considering deflections.

13.2.5.5 Moderate Seismicity SDC C Building Transverse Wall D

The strength or limit state design concept is used from TMS 402 Chapter 9.

13.2.5.5.1 Moderate Seismicity SDC C Building shear strength. Similar to the design for Low Seismicity SDC B Building, the shear wall design is governed by the following:

$$V_u \leq \phi V_n$$

$$V_n = (V_{nm} + V_{ns})\gamma_g$$

$$V_{n\,max} = \left((4 \text{ to } 6)A_n\sqrt{f_m'}\right)\gamma_g \quad \text{depending on } M_u/V_u d_v$$

$$V_{nm} = \left[4 - 1.75\left(\frac{M_u}{V_u d_v}\right)\right]A_n\sqrt{f_m'} + 0.25\,P_u$$

$$V_{ns} = 0.5\left(\frac{A_v}{s}\right)f_y d_v$$

$\gamma_g = 0.75$ for partially grouted shear walls

where:

$A_n = (2 \times 1.25 \text{ in.} \times 32.67 \text{ ft} \times 12 \text{ in.}) + (41 \text{ in.}^2 \times 9 \text{ cells}) = 1{,}349 \text{ in.}^2$

The shear strength of each Wall D, based on the aforementioned formulas and the strength reduction factor of $\phi = 0.8$ for shear from TMS 402 Section 9.1.4.5, is summarized in Table 13.2-8. Note that V_x and M_x in this table are values from Table 13.2-7 multiplied by 0.158 (representing the portion of direct and indirect shear assigned to Wall D), and P_u is the dead load of the roof or floor times the tributary area for Wall D.

Table 13.2-8 Moderate Seismicity SDC C Building Shear Strength Calculation for Wall D

Story	V_x (kips)	M_x (ft-kips)	$M_x/V_x d_v$	2.5 V_x (kips)	P_u (kips)	V_{nm} (kips)	V_{ns} (kips)	V_n (kips)	V_n (max) (kips)	ϕV_n (kips)
5	24.6	213	0.266	24.6	35	222	68	**218**	269	174
4	46.9	621	0.405	47.0	75	217	68	**214**	253	171
3	63.5	1,171	0.564	63.5	115	211	68	**209**	234	167
2	74.6	1,817	0.746	74.6	156	202	68	**203**	212	162
1	80.1	2,512	0.960	80.1	196	189	68	193	**186**	149

1.0 kip = 4.45 kN, 1.0 ft-kip = 1.36 kN-m.

Values shown in **bold** are the controlling values for V_n

For all levels, $\phi V_n > V_{u,}$, so this Intermediate Reinforced Masonry shear wall is OK.

13.2.5.5.2 Moderate Seismicity SDC C Building axial and flexural strength. The walls in this example are all load-bearing shear walls because they support vertical loads as well as lateral forces. In-plane calculations include the following:

Strength check

Ductility check

13.2.5.5.2.1 Strength check. Wall demands, using load combinations determined previously, are presented in Table 9.2-9 for Wall D. In the table, Load Combination 1 is $1.27D + Q_E + 0.5L$ and Load Combination 2 is $0.83D + Q_E$.

Table 13.2-9 Demands for Moderate Seismicity SDC C Building Wall D

Level	P_D (kips)	P_L (kips)	Load Combination 1		Load Combination 2	
			P_u (kips)	M_u (ft-kips)	P_u (kips)	M_u (ft-kips)
5	50	0	64	213	42	213
4	100	15	135	621	83	612
3	149	25	202	1,171	124	1,171
2	199	34	270	1,817	165	1,817
1	249	41	337	2,512	207	2,512

1.0 kip = 4.45 kN, 1.0 ft-kip = 1.36 kN-m.

As in Section 13.2.4.5.2, the strength at the bottom story (where *P*, *V* and *M* are the greatest) is examined. The strength design considers Load Combination 2 from Table 13.2-9 to be the governing case because it has the same lateral load as Load Combination 1 but with lower values of axial force. Refer to Figure 13.2-9 for notation and dimensions.
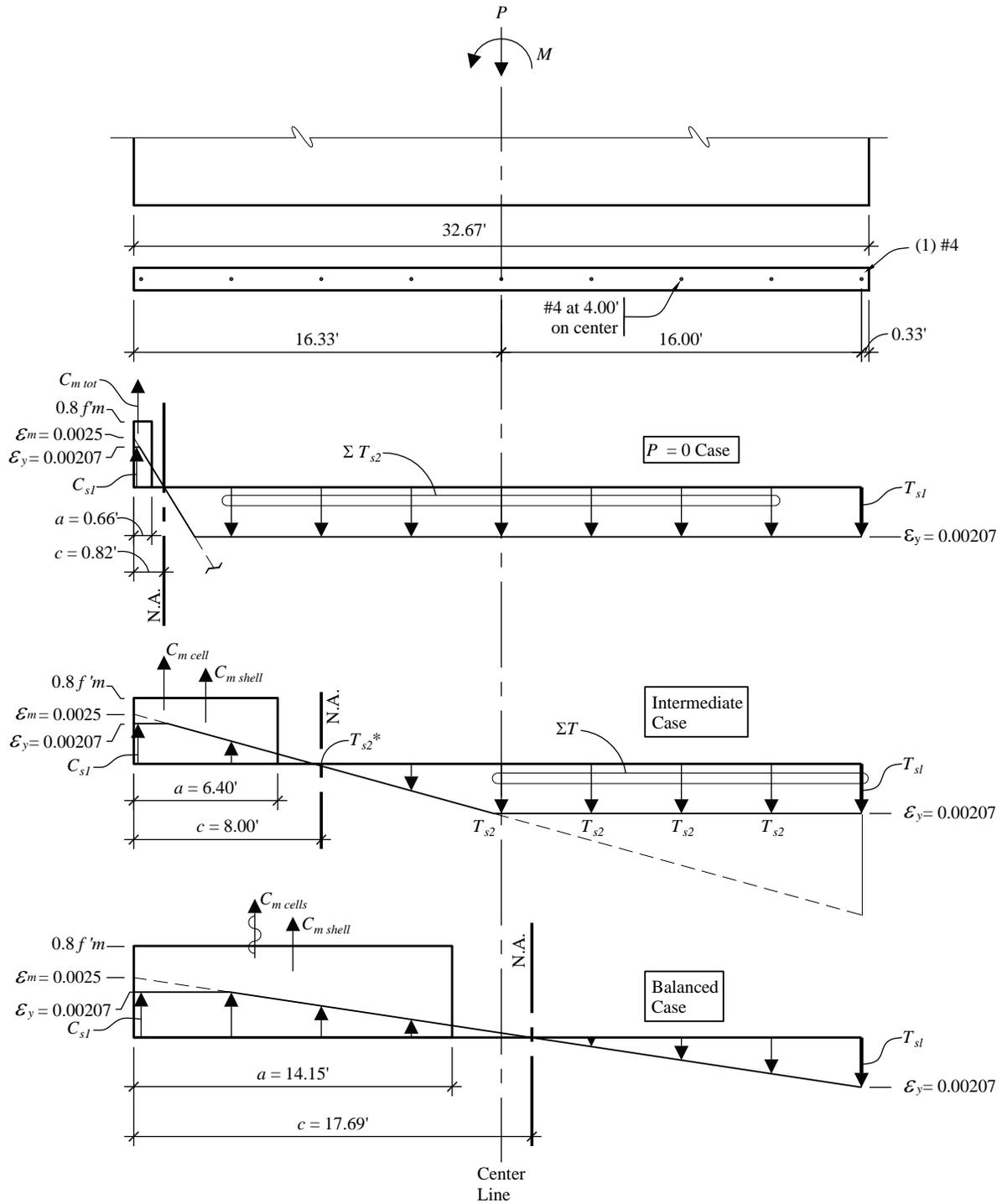
**Figure 13.2-9 Strength of Moderate Seismicity SDC C Building Wall D
Strain diagram superimposed on strength diagram for the three cases.
Low forces in the reinforcement are neglected in the calculations**
(1.0 ft = 0.3048 m)

Examine the strength of Wall D at Level 1:

$P_{u\ min.}$ = 207 kips

$P_{u\ max}$ = 337 kips

M_u = 2,512 ft-kips

Because intermediate reinforced masonry shear walls are used (Seismic Design Category C), vertical reinforcement is required at 4 feet on center in accordance with TMS 402 Section 7.3.2.5. Therefore, try one #4 bar in each end cell and #4 bars at 4 feet on center at all intermediate cells.

The calculation procedure is similar to that for the Low Seismicity SDC B Building presented in Section 13.2.4.5.2. The results of the calculations (not shown) for the Moderate Seismicity SDC C Building are summarized below and shown in Figure 13.2-9.

$P = 0$ case:

$\phi P_n = 0$

ϕM_n = 1,562 ft-kips

Intermediate case:

$c = 8.0$ ft

ϕP_n = 349 kips

ϕM_n = 5,929 ft-kips

Balanced case:

ϕP_n = 854

ϕM_n = 8,697 ft-kips

With the intermediate case, it is simple to use the three points to make two straight lines on the interaction diagram. Use the simplified ϕP_n - ϕM_n curve shown in Figure 13.2-10. The straight line from pure bending to the balanced point is conservative and can easily be used where the design is not as close to the criterion. It is the nature of lightly reinforced and lightly loaded masonry walls that the intermediate point is frequently useful.

Use one #4 bar in each end cell and one #4 bar at 4 feet on center throughout the remainder of the wall.
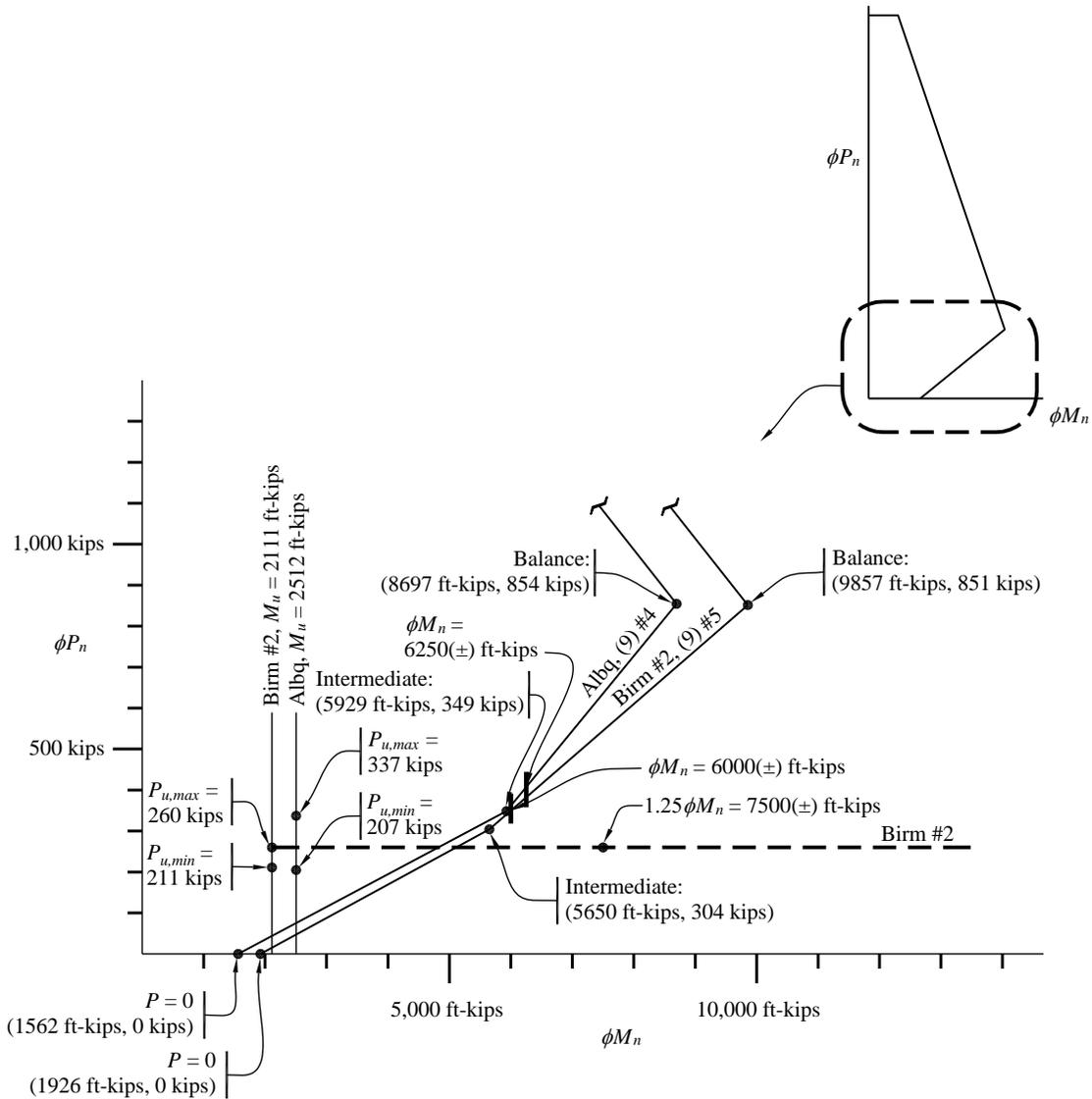
Figure 13.2-10 ϕP_n - ϕM_n Diagram for Moderate Seismicity SDC C Building and Low Seismicity SDC D Building Wall D
(1.0 kip = 4.45 kN, 1.0 ft-kip = 1.36 kN-m)

While Low Seismicity SDC D Building has a lesser demand than Moderate Seismicity SDC C Building, more robust reinforcement is required prescriptively because it is Seismic Design Category D. The greater flexural resistance will also necessitate a design to resist greater shear, a requirement that applies to special reinforced masonry shear walls (TMS 402, Sec. 7.3.2.6.1), which are required for Seismic Design Category D.

13.2.5.5.2.2 Ductility check. Refer to Section 13.2.4.5.2, Item 2, for explanation. The strain distribution is shown in Figure 13.2-11. If M/Vd equals or exceeds 1.0, the multiplier on steel yield strain for intermediated reinforced masonry walls (TMS 402 Sec. 9.3.3.5.2) is 3.0, not 1.5. For this design $M/Vd =$ 0.96. For Level 1 (bottom story), the unfactored loads are as follows:

$P = 249$ kips

$C_m = 0.8\ f_m'\ [(a)(b) + A_{cells}]$
      where b = face shells = $(2 \times 1.25$ in.$)$ and $A_{cell} = 41$ in.^{2}

$C_m = (1.6$ ksi$)[(11.55$ ft $\times 12)(2.5$ in.$) + (3)(41)] = 751$ kips

$C_{s1} = F_y A_s = (60$ ksi$)(0.20$ in.$^2) = 12$ kips

$C_{s2} = (51.9$ ksi$)(0.20$ in.$^2) = 10.4$ kips

$C_{s3} = (31.4$ ksi$)(0.20$ in.$^2) = 6.3$ kips

C_{s4} and T_{s5} are small, so are neglected

$T_{s1} = T_{s2} = = (60$ ksi$)(0.20$ in.$^2\ ) = 12$ kips

$T_{s3} = (49.8$ ksi$)(0.20$ in.$^2) = 10.0$ kips

$T_{s4} = (29.7$ ksi$)(0.20$ sq. in.$) = 5.9$ kips

$\sum C > \sum P + T$

$C_m + C_{s1} + C_{s2} + C_{s3} > P + T_{s1} + T_{s2} + T_{s3} + T_{s4}$

$751 + 12 + 10.4 > 249 + 12 + 12 + 10.0 + 5.9$

773 kips > 289 kips   OK

There is more compression capacity than required, so a ductile failure condition controls.
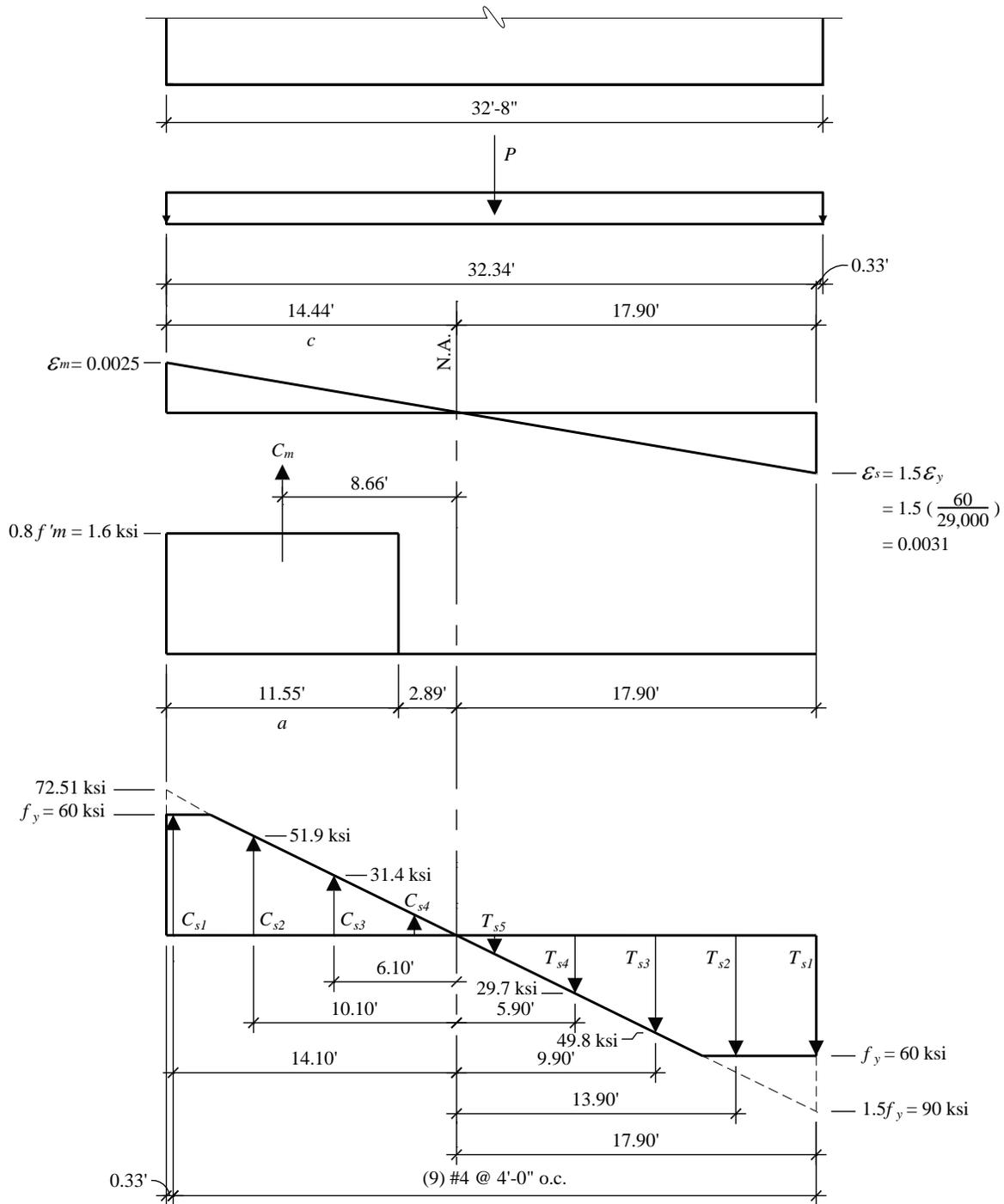
Figure 13.2-11 Ductility check for Moderate Seismicity SDC C Building
(1.0 kip = 4.45 kN, 1.0 ft-kip = 1.36 kN-m)

13.2.5.6 Moderate Seismicity SDC C Building deflections. Refer to Section 13.2.4.6 for more explanation. For the Moderate Seismicity SDC C Building, the determination of whether the walls will be cracked is as follows:

b_e = effective masonry wall width

$b_e = [(2 \times 1.25 \text{ in.})(32.67 \text{ ft} \times 12) + (9 \text{ cells})(41 \text{ in.}^2/\text{cell})]/(32.67 \text{ ft} \times 12) = 3.44 \text{ in.}$

$A_n = b_e\, l = (3.44 \text{ in.})(32.67 \times 12) = 1,349 \text{ in.}^2$

$S = b_e\, l^2/6 = (3.44)(32.67 \times 12)^2/6 = 88,100 \text{ in.}^3$

$f_r = (0.084 \text{ ksi})(5 \text{ cells}/6 \text{ cells}) + (0.163 \text{ ksi})(1 \text{ cell}/6 \text{ cells}) = 0.097 \text{ ksi}$

P_u is calculated using $1.00D$ (see Table 13.2-9 for values and refer to Sec. 13.2.4.6 for discussion). Table 13.2-10 summarizes these calculations.

Table 13.2-10 Moderate Seismicity SDC C Building Cracked Wall Determination

Level	P_u (kips)	M_{cr} (ft-kips)	M_x (ft-kips)	Status
5	50	979	213	Uncracked
4	100	1,245	621	Uncracked
3	149	1,512	1,171	Uncracked
2	199	1,779	1,817	Cracked
1	249	2,046	2,512	Cracked

1.0 kip = 4.45 kN, 1.0 ft-kip = 1.36 kN-m.

For the uncracked walls:

$I_n = I_g = bl^3/12 = (3.44 \text{ in.})(32.67 \times 12)^3/12 = 1.73 \times 10^7 \text{ in.}^4$

For the cracked wall:

$I_{eff} = 0.35\, I_g = 0.606 \times 10^7 \text{ in.}^4$

The calculation of δ should consider shear deflection in addition to flexural deflection. This example uses a RISA 2D analysis. The results are summarized in Table 13.2-11.

Table 13.2-11 Moderate Seismicity SDC C Building Deflections

Level	F (kips)	I_{eff} (in.^{4})	$\delta_{flexural}$ (in.)	δ_{shear} (in.)	δ_{total} (in.)	$C_d\,\delta_{total}$ (in.)	Δ (in.)
5	23.2	1.73×10^7	0.181	0.032	0.213	0.479	0.110
4	21.0	1.73×10^7	1.134	0.030	0.164	0.369	0.115
3	15.6	1.73×10^7	0.089	0.024	0.113	0.254	0.112
2	10.4	0.61×10^7	0.046	0.017	0.063	0.142	0.092
1	5.2	0.61×10^7	0.013	0.009	0.022	0.050	0.052

1.0 kip = 4.45 kN, 1.0 in. = 25.4 mm.
$F = 0.149\, F_x$, for F_x from Table 13.2-7.
Δ = story drift.

The maximum story drift occurs between Levels 4 and 3:

$\Delta_4 = 0.115$ in. < 1.04 in. $= 0.01\ h_n$ (*Standard* Table 12.2-1)   OK

13.2.5.7 Moderate Seismicity SDC C Building out-of-plane forces. *Standard* Section 12.11.1 requires that bearing walls be designed for out-of-plane loads, determined as follows:

$w = 0.40\ S_{DS}\ IW_w \geq 0.1W_w$

$w = (0.40)(0.37)(1)(48\text{ psf}) = 7.1\text{ psf} > 4.8\text{ psf} = 0.1W_w,$

So the equivalent normal pressure due to the design earthquake is 7.1 psf. This is greater than the design differential air pressure of 5 psf. However, the lateral pressure is sufficiently low for this short wall that the author considers it acceptable by inspection, without further calculation. So, seismic loads do not govern the design of Wall D for loading in the out-of-plane direction.

13.2.5.8 Moderate Seismicity SDC C Building orthogonal effects. According to *Standard* Section 12.5.3, orthogonal interaction effects have to be considered for Seismic Design Category C where the ELF procedure is used (as it is here). However, the out-of-plane component of only 30 percent of 7.1 psf on the wall does not produce a significant effect where combined with the in-plane direction of loads, so no further calculation is made.

This completes the design of the transverse Wall D for the Moderate Seismicity SDC C Building.

13.2.5.9 Summary of Moderate Seismicity SDC C Building Wall D design

8-inch CMU

f'$_m$ = 2,000 psi

Reinforcement:

Vertical #4 bars at 4 feet on center throughout the wall.

Bond beam with two #4 at each story just below the floor or roof slabs.

Horizontal joint reinforcement at alternate courses.

13.2.6 Low Seismicity SDC D Building Seismic Design
The emphasis here is on differences from the previous two locations for the same building. *Standard* Table 12.6-1 requires that design of a Seismic Design Category D building with torsional irregularity be based on a dynamic analysis. Although it is not explicitly stated, the implication is that the analytical model should be three-dimensional in order to capture the torsional response. This example compares both the ELF procedure and the modal response spectrum analysis procedure.

13.2.6.1 Low Seismicity SDC D Building weights. The floor weight for this example uses the same 67 psf for 8-inch-thick, normal-weight hollow core plank plus roofing and the nonmasonry partitions as used in the prior examples (see Sec. 13.2.1). This site is assigned to Seismic Design Category D, and the walls are designed as special reinforced masonry shear walls (*Standard* Table 12.2-1). Special reinforced masonry shear walls have a maximum spacing of rebar at 4 feet on center both horizontally and vertically (TMS 402 Sec. 7.3.2.6). Also, the total area of horizontal and vertical reinforcement must exceed 0.002 times the gross area of the wall and neither direction may have a ratio of less than 0.0007. The vertical #4 bars at 48 inches used for the Moderate Seismicity SDC C Building design yield a ratio of 0.00055, so it must be increased. #5 bars at 48 inches (yielding 0.00085) is selected. The latter is chosen in order to avoid unnecessarily increasing the shear demand. Therefore, the horizontal reinforcement must be (0.0020 - 0.00085)(7.625 in.)(12 in./ft) = 0.105 in.^{2}/ft Two #5 bars in bond beams at 48 inches on center will be adequate. For this example, 56 psf weight for the 8-inch-thick partially grouted CMU walls will be assumed. The 56 psf value includes grouted cells and bond beams.

Story weight, w_i:

> Roof:

>> Roof slab (plus roofing) = (67 psf) (152 ft)(72 ft) = 733 kips
>> Walls = (56 psf)(589 ft)(8.67 ft/2) + (56 psf)(4)(36 ft)(2 ft) = 159 kips
>> Total = 892 kips

> There is a 2-foot-high masonry parapet on four walls, and the total length of masonry wall is 589 feet.

> Typical floor:

>> Slab (plus partitions) = 733 kips
>> Walls = (56 psf)(589 ft)(8.67 ft) = 286 kips
>> Total = 1,019 kips

Total effective seismic weight, W = 892 + (4)(1,019) = 4,968 kips.

This total excludes the lower half of the first story walls, which do not contribute to seismic loads that are imposed on CMU shear walls.

13.2.6.2 Low Seismicity SDC D Building base shear calculation. The ELF analysis proceeds as described for the previous locations. The seismic response coefficient, C_s, is computed using *Standard* Section 12.8:

$$C_s = \frac{S_{DS}}{R/I} = \frac{0.43}{5/1} = 0.086$$

(Controls)

$$C_s = \frac{S_{D1}}{T(R/I)} = \frac{0.24}{0.338(5/1)} = 0.142$$

The fundamental period of the building, based on *Standard* Equation 12.8-7 is approximately 0.338 seconds as computed previously (the approximate period, based on building system and building height, is the same for all locations). The value for C_s is taken as 0.086 (the lesser of the two values). This value is still larger than the minimum specified in *Standard* Equation 12.8-5, which is:

$C_s = 0.044 S_{D1}I = (0.044)(0.24)(1) = 0.011$

The total seismic base shear is calculated using *Standard* Equation 12.8-1:

$V = C_s W = (0.086)(4,968) = 427$ kips

This is somewhat less than the 507 kips computed for the Moderate Seismicity SDC C Building design, due to the larger *R* factor.

A three-dimensional (3D) model is created in SAP2000 for the modal response spectrum analysis. The masonry walls are modeled as shell bending elements, and the floors are modeled as an assembly of beams and shell membrane elements. The beams have very little mass and a large flexural moment of inertia to avoid consideration of modes of vertical vibration of the floors. The flexural stiffness of the beams is released at the bearing walls in order to avoid a wall-slab frame that would inadvertently increase the torsional resistance. The mass of the floors is captured by the shell membrane elements. Table 13.2-12 shows data on the modes of vibration used in the analysis.

Standard Section 11.4.5 is used to create the response spectrum for the modal analysis. The key points that define the spectrum are as follows:

$T_S = S_{D1}/S_{DS} = 0.21/0.43 = 0.56$ sec

$T_0 = 0.2\ T_S = 0.11$ sec

at $T = 0$, $S_a = 0.4\ S_{DS}/R = 0.034\ g$

from $T = T_0$ to T_S, $S_a = S_{DS}/R = 0.086\ g$

for $T > T_S$, $S_a = S_{D1}/(RT) = 0.042/T$

The computed fundamental period is less than the approximate period. The transverse direction base shear from the SRSS combination of the modes is 293 kips, which is considerably less than that obtained using the ELF method.

Standard Section 12.8.2 requires that the modal base shear be compared with the ELF base shear computed using a period no larger than $C_u T_a$. As shown in Section 13.2.4.2, $T_a = 0.338$ seconds. Per *Standard* Table 12.8-1, $C_u = 1.46$. Thus, $C_u T_a = 0.49$ seconds. However, the computed period, *T*, is only 0.2467 seconds (as shown in Table 13.2-12), which is less than $C_u T_a$ so the ELF base shear must be computed at that period. Since *T* is less that T_S/S_{DS}, the ELF base shear for comparison is 427 kips as just computed. Because the base shear from the modal analysis is less than 100 percent of 427 kips, the *Provisions* Section 12.9.4.1 dictates that all the results of the modal analysis be multiplied by the following:

$$\frac{V_{ELF}}{V_{Modal}} = \frac{427}{293} = 1.46$$

Both analyses are carried forward as discussed in the subsequent sections.

Table 13.2-12   Low Seismicity SDC D Building Periods, Mass Participation Factors and Modal Base Shears in the Transverse Direction for Modes Used in Analysis

Mode Number	Period, (seconds)	Individual Mode (percent)			Cumulative Sum (percent)			Trans. Base Shear
		Long.	Trans.	Vert.	Long.	Trans.	Vert.	
1	0.2467	0.00	0.00	0.00	0.00	0.00	0.00	0.0
2	0.1919	0.00	70.18	0.00	0.00	70.18	0.00	339.6
3	0.1915	70.55	0.00	0.00	70.55	70.18	0.00	0.0
4	0.0579	0.00	18.20	0.00	70.55	88.39	0.00	55.6
5	0.0574	17.86	0.00	0.00	88.41	88.39	0.00	0.0
6	0.0535	0.00	4.09	0.00	88.41	92.48	0.00	12.1
7	0.0532	4.17	0.00	0.00	92.58	92.48	0.00	0.0
8	0.0413	0.00	0.01	0.00	92.58	92.48	0.00	0.0
9	0.0332	1.50	0.24	0.00	94.08	92.72	0.00	0.6
10	0.0329	0.30	2.07	0.00	94.38	94.79	0.00	5.3
11	0.0310	1.28	0.22	0.00	95.66	95.01	0.00	0.6
12	0.0295	0.22	1.13	0.00	95.89	96.14	0.00	2.8
13	0.0253	1.97	0.53	0.00	97.86	96.67	0.00	1.3
14	0.0244	0.53	1.85	0.00	98.39	98.52	0.00	4.5
15	0.0190	1.05	0.36	0.00	99.44	98.89	0.00	0.8
16	0.0179	0.33	0.94	0.00	99.77	99.82	0.00	2.1
17	0.0128	0.19	0.07	0.00	99.95	99.90	0.00	0.1
18	0.0105	0.03	0.10	0.00	99.99	99.99	0.00	0.2

1 kip = 4.45 kN.

13.2.6.3 Low Seismicity SDC D Building vertical distribution of seismic forces. The dynamic analysis is revisited for the horizontal distribution of forces in the next section but, as stated there, the ELF procedure will be used in this example for more direct comparison to the other sites. The purpose of this analysis is to study amplification of accidental torsion. Note that Mode 1 has no net base force in the longitudinal, transverse, or vertical directions. The mode shape confirms that it is purely torsional.

The vertical distribution of seismic forces for the ELF analysis is determined in accordance with *Standard* Section 12.8.3, which was described in Section 13.2.4.3, in which $k = 1.0$ because $T < 0.5$ seconds (similar to the Low Seismicity SDC B Building and Moderate Seismicity SDC C Buildings). It should be noted that the response spectrum analysis (modal analysis) may result in moments that are different than those calculated using the ELF method; however, because of its relative simplicity, the ELF is used in this example.

Application of the *Standard* equations for this building is shown in Table 13.2-13:

Table 13.2-13 Low Seismicity SDC D Building Seismic Forces and Moments by Level

Level x	w_x (kips)	h_x (ft)	$w_x h_x$ (ft-kips)	C_{vx}	F_x (kips)	V_x (kips)	M_x (ft-kips)
5	892	43.34	38,659	0.3045	130	130	1,130
4	1,019	34.67	35,329	0.2782	119	249	3,290
3	1,019	26.00	26,494	0.2086	89	338	6,220
2	1,019	17.33	17,659	0.1391	59	397	9,660
1	1,019	8.67	8,835	0.0695	30	427	13,360
$\sum$	4,968		126,976	1.000	427		

1.0 kip = 4.45 kN, 1.0 ft = 0.3048 m, 1.0 ft-kip = 1.36 kN-m.

13.2.6.4 Low Seismicity SDC D Building horizontal distribution of forces. The ELF analysis for Low Seismicity SDC D Building is the same as that for the Moderate Seismicity SDC C Building location; see Section 13.2.5.4.

Total shear in Wall D:

$$V_{tot} = 0.125V + 1.365(0.0238)V = 0.158V = 67.4 \text{ kips}$$

The fact that the fundamental mode is torsional does confirm, to an extent, that the structure is torsionally sensitive. This modal analysis does not show any significant effect of the torsion, however, because of the symmetry. The pure symmetry of this structure is somewhat idealistic. Real structures usually have some real eccentricity between mass and stiffness and dynamic analysis then yields coupled modes, which contribute to computed forces.

The *Standard* does not require that the accidental eccentricity be analyzed dynamically. For illustration, however, this is approximated by adjusting the mass of the floor elements to generate an eccentricity of 5 percent of the 152-foot length of the building. Table 13.2-14 shows the results of such an analysis. (Accidental torsion could also be considered using a linear combination of the dynamic results and a statically applied moment equal to the accidental torsional moment.)

The transverse direction base shear from the SRSS combination of the modes with dynamic torsion is 258.4 kips, less than the 293 kips for the symmetric model. The amplification factor for this base shear is 427/258 = 1.66. This smaller base shear from modal analysis of a model with an artificially introduced eccentricity is normal for two primary reasons: First, the mass participates in more modes. The participation in the largest mode generally is less, and the combined result is dominated by the largest single mode. Second, the period for the fundamental mode generally increases, because there is more flexibility between the mass and the foundation. The increase in period will reduce the spectral response except for structures with short periods (such as this one).

Let us consider torsional effects based on modal analysis in greater detail than required by the *Standard*: The base shear in Wall D is computed by adding the in-plane reactions. For the symmetric model the result is 36.6 kips, which is 12.5 percent of the total of 293 kips, as would be expected. Amplifying this by the 1.46 factor (to bring the modal result to 100 percent of the ELF result) yields 53 kips. Application of a static horizontal torsion equal to the 5 percent eccentricity times a base shear of 427 kips adds 12 kips, for a total of 65 kips. If the static horizontal torsion is amplified by 1.365, as found in the analysis for the Moderate Seismicity SDC C Building location, the total becomes 69 kips, which is greater than the 64 kips (0.149V) or 67 kips (0.158V) computed in the ELF analysis without and with,

respectively, the amplification of accidental torsion. The Wall D base shear from the modal analysis with the eccentric model was 42 kips (SRSS); with the amplification of base shear equal to 1.66 (to reach 100 percent of the ELF), this becomes 70 kips. Note that this value is again greater than the shear from the ELF model including amplified static torsion (67 kips). The conclusion is that for buildings with irregularities as defined in the *Standard*, dynamic analysis should be used to get the force demands. However, for ease of comparison to the previous examples on other sites, the remainder of the example designs for this building are completed using the ELF.

Table 13.2-14   Low Seismicity SDC D Building Periods, Mass Participation Factors and Modal Base Shears in the Transverse Direction for Modes Used in Approximate Accidental Torsion Analysis

Mode Number	Period (sec)	Individual Mode (percent)			Cumulative Sum (percent)			Trans. Base Shear
		Long.	Trans.	Vert.	Long.	Trans.	Vert.	
1	0.2507	0.0	8.8	0.0	0.0	8.8	0.0	42.4
2	0.1915	70.5	0.0	0.1	70.5	8.8	0.1	0.0
3	0.1867	0.0	61.4	0.0	70.5	70.2	0.1	297.3
4	0.0698	0.0	2.9	0.0	70.5	73.1	0.1	9.5
5	0.0613	1.1	0.0	23.0	71.6	73.1	23.1	0.0
6	0.0575	19.2	0.0	0.0	90.9	73.1	23.2	0.0
7	0.0570	0.0	13.7	0.0	90.9	86.8	23.2	41.8
8	0.0533	0.0	5.6	0.0	90.9	92.4	23.2	16.6
9	0.0480	1.2	0.0	12.8	92.0	92.4	35.9	0.0
10	0.0380	1.4	0.0	0.0	93.5	92.4	35.9	0.0
11	0.0374	0.0	0.4	0.0	93.5	92.8	35.9	0.9
12	0.0327	1.7	0.0	0.2	95.2	92.8	36.1	0.0
13	0.0322	0.0	3.1	0.0	95.2	95.9	36.1	7.9
14	0.0263	2.8	0.0	0.1	98.0	95.9	36.2	0.0
15	0.0243	0.0	3.0	0.0	98.0	98.8	36.2	7.2
16	0.0201	1.6	0.0	0.1	99.6	98.8	36.3	0.0
17	0.0164	0.0	1.1	0.0	99.6	100.0	36.3	2.6
18	0.0141	0.4	0.0	0.1	100.0	100.0	36.3	0.0

The "extreme torsional irregularity" has an additional consequence for Seismic Design Category D: *Standard* Section 12.3.3.4 requires that the design forces for connections between diaphragms, collectors and vertical elements (walls) be increased by 25 percent. For this example, the diaphragm of precast elements is designed using the different requirements of the *Provisions*, Part 3, RP3-4.

13.2.6.5 Low Seismicity SDC D Building transverse wall (Wall D). The total story shear and overturning moment (from the ELF analysis) may now be distributed to Wall D and the wall proportions checked. The wall capacity is checked before considering deflections.

The design demands are slightly smaller than for the Moderate Seismicity SDC C Building design, largely due to an *R* of 5 instead of 3.5, yet there is more reinforcement, both vertical and horizontal in the walls, because of the prescriptive detailing requirements for Seismic Design Category D. This illustration will focus on those items where the additional reinforcement has special significance.

13.2.6.5.1 Low Seismicity SDC D Building shear strength. Refer to Section 13.2.5.5.1 for most quantities. Compared to the Moderate Seismicity SDC C Building, the additional horizontal reinforcement raises V_s *and* the additional grouted cells raises A_n and therefore both V_{nm} and V_n(max).

$A_v/s = (4)(0.31 \text{ in.}^2)/(8.67 \text{ ft}) = 0.1431 \text{ in.}^2/\text{ft}$

$V_{ns} = 0.5(0.1431)(60 \text{ ksi})(32.67 \text{ ft}) = 140.2 \text{ kips}$

$A_n = (2 \times 1.25 \text{ in.} \times 32.67 \text{ ft} \times 12 \text{ in.}) + (41 \text{ in.}^2 \times 9 \text{ cells}) = 1{,}349 \text{ in.}^2$

The shear strength of Wall D is summarized in Table 13.2-15 below. (V_x and M_x in this table are values from Table 13.2-13 multiplied by 0.158, the portion of direct and torsional shear assigned to the wall.) Note that the minimum configuration as shown suffices to resist forces from the ELF analysis or the modal analysis. Note also that the format of Table 13.2-15 differs from that of its counterparts for the Low Seismicity SDC B Building and the Moderate Seismicity SDC C Building: a column for $2.5V_x$ is included here because, for special reinforced masonry shear walls, TMS 402 Section 7.3.2.6.1.1 requires the shear capacity to exceed the lesser of the shear corresponding to $1.25M_n$ or $2.5V_x$. The intent is to require response controlled by flexure in most cases, but to permit non-ductile shear response if the shear capacity is 2.5 times the demand from analysis. The walls are partially grouted, so V_n, V_n(max) and ϕV_n are all multiplied by $\gamma_g = 0.75$.

Table 13.2-15 Low Seismicity SDC D Building Shear Strength Calculation for Wall D

Story	V_x (kips)	M_x (ft-kips)	M_x/V_xd_v	$2.5V_x$ (kips)	P_u (kips)	V_{nm} (kips)	V_{ns} (kips)	V_n (kips)	V_n(max) (kips)	ϕV_n (kips)
5	20.5	178	0.265	51.2	42	224	140	273	**271**	217
4	39.3	520	0.405	98.3	84	220	140	270	**253**	202
3	53.4	983	0.563	134	126	213	140	265	**234**	187
2	62.7	1,526	0.745	157	168	205	140	259	**212**	169
1	67.5	2,111	0.957	169	210	193	140	250	**186**	149

1.0 kip = 4.45 kN, 1.0 ft-kip = 1.36 kN-m.
Values shown in **bold** are the controlling values for V_n

V_n(max) is less than V_n at all levels, so it controls in the determination of ϕV_n. $\phi V_n > 2.5V_x$ for all levels except the first story, so the shear corresponding to $1.25M_n$ should be checked. While the calculations are not shown in this example, the shear corresponding to $1.25M_n$ is also greater than ϕV_n at the first story. Shear reinforcing needs to be increased by a minimum of 0.034 in.^{2}/ft, and vertical reinforcing should also be increased to meet TMS 402 Section 7.3.2.6(c) provisions. Use two #6 horizontal bars in bond beams at 48" on center and #6 vertical bars at 48" on center in lieu of the #5 bars.

13.2.6.5.2 Low Seismicity SDC D Building axial and flexural strength. Once again, the similarities to the design for the Moderate Seismicity SDC C Building location are exploited. The in-plane calculations include the following:

Strength check

Ductility check

13.2.6.5.2.1 Strength check. The wall demands, using the load combinations determined previously, are presented in Table 13.2-16 for Wall D. In the table, Load Combination 1 is $1.29D + Q_E + 0.5L$ and Load Combination 2 is $0.81D + Q_E$.

Table 13.2-16 Low Seismicity SDC D Building Demands for Wall D

Level	P_D (kips)	P_L (kips)	Load Combination 1		Load Combination 2	
			P_u (kips)	M_u (ft-kips)	P_u (kips)	M_u (ft-kips)
5	53	0	68	178	43	178
4	104	15	134	520	84	520
3	156	25	201	983	126	983
2	208	34	268	1526	168	1526
1	260	41	335	2111	211	2111

1.0 kip = 4.45 kN, 1.0 ft-kip = 1.36 kN-m.

Strength at the bottom story (where *P*, *V* and *M* are the greatest) is less than required for the Moderate Seismicity SDC C Building design. The demands for Low Seismicity SDC D Building are plotted on Figure 13.2-10 along with those for Moderate Seismicity SDC C Building (showing that the design for Moderate Seismicity SDC C Building has sufficient axial and flexural capacity for this Low Seismicity SDC D Building location).

13.2.6.5.2.2 Ductility check. The requirements for ductility are described in Sections 13.2.4.5.3 and 13.2.5.5.3. While the reinforcing is increased per Section 13.2.6.5.1, it is still similar to the reinforcing for the Moderate Seismicity SDC C Building, and the computations are not repeated here. A brief review of the Moderate Seismicity SDC C Building ductility calculations (Sec. 13.2.5.5.3) reveals that the Low Seismicity SDC D Building reinforcement should satisfy the ductility provisions.

13.2.6.6 Low Seismicity SDC D Building deflections. The calculations for deflection would be similar to that for the Moderate Seismicity SDC C Building location. The calculation is not repeated here; refer to Sections 13.2.4.6 and 13.2.5.6. While the C_d factor is larger, 3.5 versus. 2.25, the resulting maximum story drift is still less than the 0.01 h_n allowable and therefore is OK.

13.2.6.7 Low Seismicity SDC D Building out-of-plane forces. *Standard* Section 12.11 requires that the bearing walls be designed for out-of-plane loads, determined as follows:

$w = 0.40 \, S_{DS} \, IW_w \geq 0.1W_w$

$w = (0.40)(0.43)(1)(56 \text{ psf}) = 9.6 \text{ psf} \geq 0.1W_w$

The calculated seismic load, $w = 9.6$ psf, is less than wind pressure for exterior walls. This is larger than the design differential pressure of 5 psf across an interior wall (per the IBC). Given the story height for either interior or exterior walls, the out-of-plane seismic force is sufficiently low that it is considered acceptable by inspection without further calculation.

13.2.6.8 Low Seismicity SDC D Building orthogonal effects. According to *Standard* Section 12.5.3, orthogonal interaction effects should be considered for Seismic Design Category D where the ELF procedure is used (as it is here). However, the out-of-plane component of only 30 percent of 9.6 psf on the wall does not produce a significant effect where combined with the in-plane direction of loads, so no further calculation is made.

This completes the design of Transverse Wall D.

13.2.6.9 Summary of Low Seismicity SDC D Building Wall D

  8-inch CMU

  $f'_m = 2,000$ psi

  Reinforcement:

    9 vertical #6 bars per wall at 4'-0" on center.

    Two bond beams with two #6 at each story, at bearing for the planks and at 4 feet above each floor.

    Horizontal joint reinforcement at alternate courses is recommended, but not required.

13.2.7 Seismic Design for High Seismicity SDC D Building

Once again, the differences from the designs for the other locations are emphasized. As explained for the Low Seismicity SDC D Building, the *Standard* would require a dynamic analysis for the design of this building. As in Section 13.2.6.4, this design is illustrated using the ELF procedure.

13.2.7.1 High Seismicity SDC D Building weights. Use 91 psf for 8-inch-thick, normal-weight hollow core plank, 2.5-inch lightweight concrete topping (115 pcf), plus the non-masonry partitions. This building is in Seismic Design Category D, and the walls will be designed as special reinforced masonry shear walls (*Standard* Table 12.2-1), which requires prescriptive seismic reinforcement (TMS 402 Section 7.3.2.6). Special reinforced masonry shear walls have a minimum spacing of vertical reinforcement of 4 feet on center. The demand is considerably larger than that for the other Seismic Design Category D building, so more reinforcement is required. Trial reinforcement is selected as nine #7 bars at 4'-0" on center. For this example, a 60 psf weight for the 8-inch partially grouted CMU walls is assumed. The 60 psf value includes grouted cells and bond beams in the course just below the floor planks and in the course 4 feet above the floors. (Note that the wall is 43.33 feet high, not 8 feet high, for purpose of determining the maximum spacing of vertical and horizontal reinforcement.)

A typical wall section is shown in Figure 13.2-12.
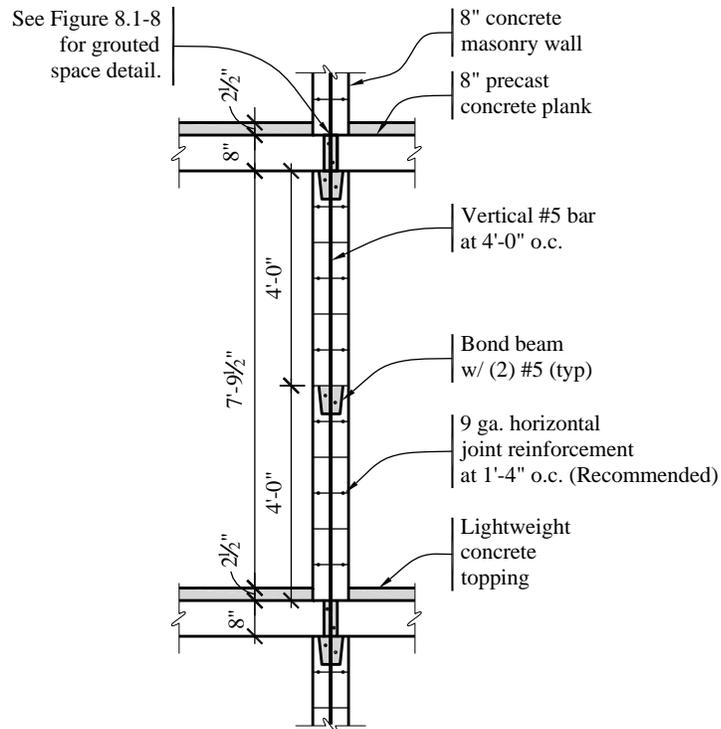
Figure 13.2-12 Typical wall section for the High Seismicity SDC D Building location
(1.0 in. = 25.4 mm, 1.0 ft = 0.3048 m)

Story weight ,w_i:

Roof weight:

Roof slab (plus roofing) = (91 psf) (152 ft)(72 ft) = 996 kips
Walls = (60 psf)(589 ft)(8.67 ft/2) + (60 psf)(4)(36 ft)(2 ft) = 170 kips
Total = 1,166 kips

There is a 2-foot-high masonry parapet on four walls, and the total length of masonry wall is 589 feet.

Typical floor:

Slab (plus partitions) = 996 kips
Walls = (60 psf)(589 ft)(8.67 ft) =306 kips
Total = 1,302 kips

Total effective seismic weight, W = 1,166 + (4)(1,302) = 6,374 kips.

This total excludes the lower half of the first story walls, which do not contribute to the seismic loads that are imposed on the CMU shear walls.

13.2.7.2 High Seismicity SDC D Building base shear calculation. The seismic response coefficient, C_s, is computed using *Standard* Section 12.8:

$$C_s = \frac{S_{DS}}{R/I} = \frac{1.00}{5/1} = 0.20 \qquad\qquad\qquad\qquad \text{(Controls)}$$

$$C_s = \frac{S_{D1}}{T(R/I)} = \frac{0.60}{0.338(5/1)} = 0.355$$

where T is the fundamental period of the building, which is 0.338 seconds as computed previously. The value for C_s is taken as 0.20 (the lesser of these two). This value is still larger than the minimum specified in *Standard*, Section 12.8-5, which is:

$$C_s = 0.044S_{D1}I = (0.044)(0.60)(1) = 0.026$$

The total seismic base shear is then calculated using *Standard* Equation 12.8-1:

$$V = C_sW = (0.20)(6,374) = 1,275 \text{ kips}$$

13.2.7.3 High Seismicity SDC D Building vertical distribution of seismic forces. The vertical distribution of seismic forces is determined in accordance with *Standard* Section 12.8.3, which is described in Section 13.2.4.3. Note that for the *Standard*, $k = 1.0$ because $T = 0.338$ seconds, which is less than 0.5 seconds (similar to the previous example buildings).

The application of the *Provisions* equations for this building is shown in Table 13.2-17:

Table 13.2-17 High Seismicity SDC D Building Seismic Forces and Moments by Level

Level x	w_x (kips)	h_x (ft)	$w_xh_x{}^k$ (ft-kips)	C_{vx}	F_x (kips)	V_x (kips)	M_x (ft-kips)
5	1,166	43.34	50,534	0.309	394	394	3,420
4	1,302	34.67	45,140	0.276	353	747	9,890
3	1,302	26.00	33,852	0.207	264	1,011	18,660
2	1,302	17.33	22,564	0.138	176	1,187	28,950
1	1,302	8.67	11,288	0.069	88	1,275	40,000
$\sum$	6,374		163,378	1.000	1,275		

1.0 kip = 4.45 kN, 1.0 ft = 0.3048 m, 1.0 ft-kip = 1.36 kN-m

13.2.7.4 High Seismicity SDC D Building horizontal distribution of forces. This is the same as for the Low Seismicity SDC D Building design; see Section 13.2.6.4.

Total shear in Wall D:

$$V_{tot} = 0.125V + 1.365(0.0238)V = 0.158V = 201.5 \text{ kips}$$

13.2.7.5 High Seismicity SDC D Building Transverse Wall D. This design continues to illustrate ELF analysis and, as explained for the Low Seismicity SDC D Building design, slightly larger demands would be derived from dynamic analysis, however the difference would likely not change the design results for this building. All other parameters are similar to those for Low Seismicity SDC D Building except the following:

$$A_n = (2 \times 1.25 \text{ in.} \times 32.67 \text{ ft} \times 12 \text{ in.}) + (41 \text{ in.}^2 \times 9 \text{ cells}) = 1,349 \text{ in.}^2$$

The shear strength of each Wall D, based on the aforementioned formulas and data, are summarized in Table 13.2-18.

Table 13.2-18 High Seismicity SDC D Building Shear Strength Calculations for Wall D

Story	V_x (kips)	M_x (ft-kips)	M_x/V_xd_v	$2.5V_x$ (kips)	P_u (kips)	V_{nm} (kips)	V_{ns} (kips)	V_n (kips)	V_n (max) (kips)	ϕV_n (kips)
5	62.3	540	0.265	156	46.3	225	163	291	**270**	216
4	118	1,563	0.405	295	92.6	222	163	289	**253**	202
3	160	2,948	0.564	400	161	222	163	289	**233**	187
2	188	4,574	0.745	470	185	209	163	279	**211**	169
1	201	6,320	0.962	503	231	197	163	270	**185**	148

1.0 kip = 4.45 kN, 1.0 ft-kip = 1.36 kN-m.

The maximum on V_n controls over the sum of V_m and V_s at all stories. Since ϕV_n does not exceed $2.5V_x$ except at the top story it is necessary to check the shear corresponding to $1.25M_n$, (as discussed below in Section 13.2.7.5.3). It will be learned, once M_n is determined below, that an increase in shear capacity is required. However, as we are not there yet, let us proceed in a sequence similar to a real design and continue with the flexural design.

13.2.7.5.2 Axial and flexural strength. The basics of flexural design are demonstrated for the previous locations. The demand is much higher at this location, which introduces issues about the amount and distribution of reinforcement in excess of the minimum requirements. Therefore, both strength and ductility checks are examined.

13.2.7.5.2.1 Strength check. Load combinations, using factored loads, are presented in Table 13.2-19 for Wall D. In the table, Load Combination 1 is $1.4D + Q_E + 0.5L$ and Load Combination 2 is $0.7D + Q_E$.

Table 13.2-19 High Seismicity SDC D Building Load Combinations for Wall D

Level x	P_D (kips)	P_L (kips)	Load Combination 1		Load Combination 2	
			P_u (kips)	M_u (ft-kips)	P_u (kips)	M_u (ft-kips)
5	66	0	92	540	46	540
4	132	15	185	1563	92	1563
3	198	25	277	2948	139	2948
2	265	34	371	4574	186	4574
1	331	41	463	6320	232	6320

1.0 kip = 4.45 kN, 1.0 ft-kip = 1.36 kN-m.

Strength at the bottom story (where P, V and M are the greatest) is examined. This example considers Load Combination 2 from Table 13.2-19 to be the governing case, because it has the same lateral load as Load Combination 1 but lower values of axial force.

Refer to Figure 13.2-13 for notation and dimensions.
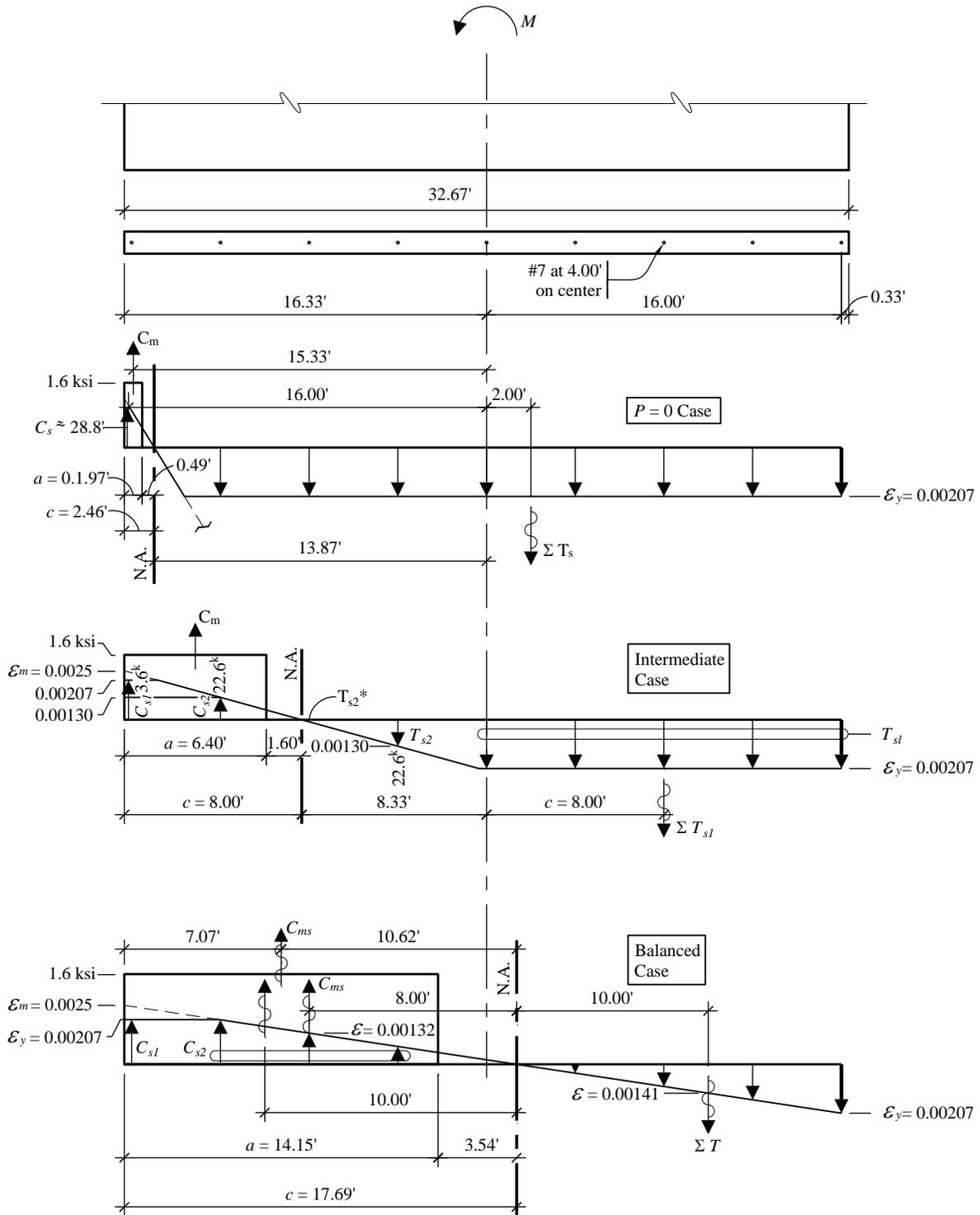
**Figure 13.2-13 High Seismicity SDC D Building: Strength of Wall D
Strength diagrams superimposed on strain diagrams for the three cases**
(1.0 ft = 0.3048 m)

Examine the strength of Wall D at Level 1:

$P_{u_{min}} = 232$ kips

$P_{u_{max}} = 463$ kips

$M_u = 6{,}320$ ft-kips

Because special reinforced masonry shear walls are used (Seismic Design Category D), vertical reinforcement at 4 feet on center and horizontal bond beams at 4 feet on center are prescribed (TMS 402, Sec. 7.3.2.6). For this bending moment, the #5 bars at 4'-0" on center used at Low Seismicity SDC D Building will not suffice (refer to the ϕP_n - ϕM_n diagram for Low Seismicity SDC D Building in Figure 13.2-10). It is desirable to limit the reinforcement to as small an amount as necessary to keep ϕM_n relatively low, such that the required shear capacity is at a minimum when the check for shear corresponding to $1.25M_n$ is made.

The calculation procedure is similar to that presented in Section 13.2.4.5.2. The strain and stress diagrams are shown in Figure 13.2-14 and the results are as follows:

$P = 0$ case:

$\phi P_n = 0$

$\phi M_n = 4{,}492$ ft-kips

Intermediate case (setting $c = 8.0$ ft):

$\phi P_n = 265$ kips

$\phi M_n = 7{,}261$ ft-kips

Balanced case:

$\phi P_n = 852$ kips

$\phi M_n = 10{,}364$ ft-kips

The simplified ϕP_n - ϕM_n curve is shown in Figure 13.2-14 and indicates that the design with nine #7 bars is satisfactory.
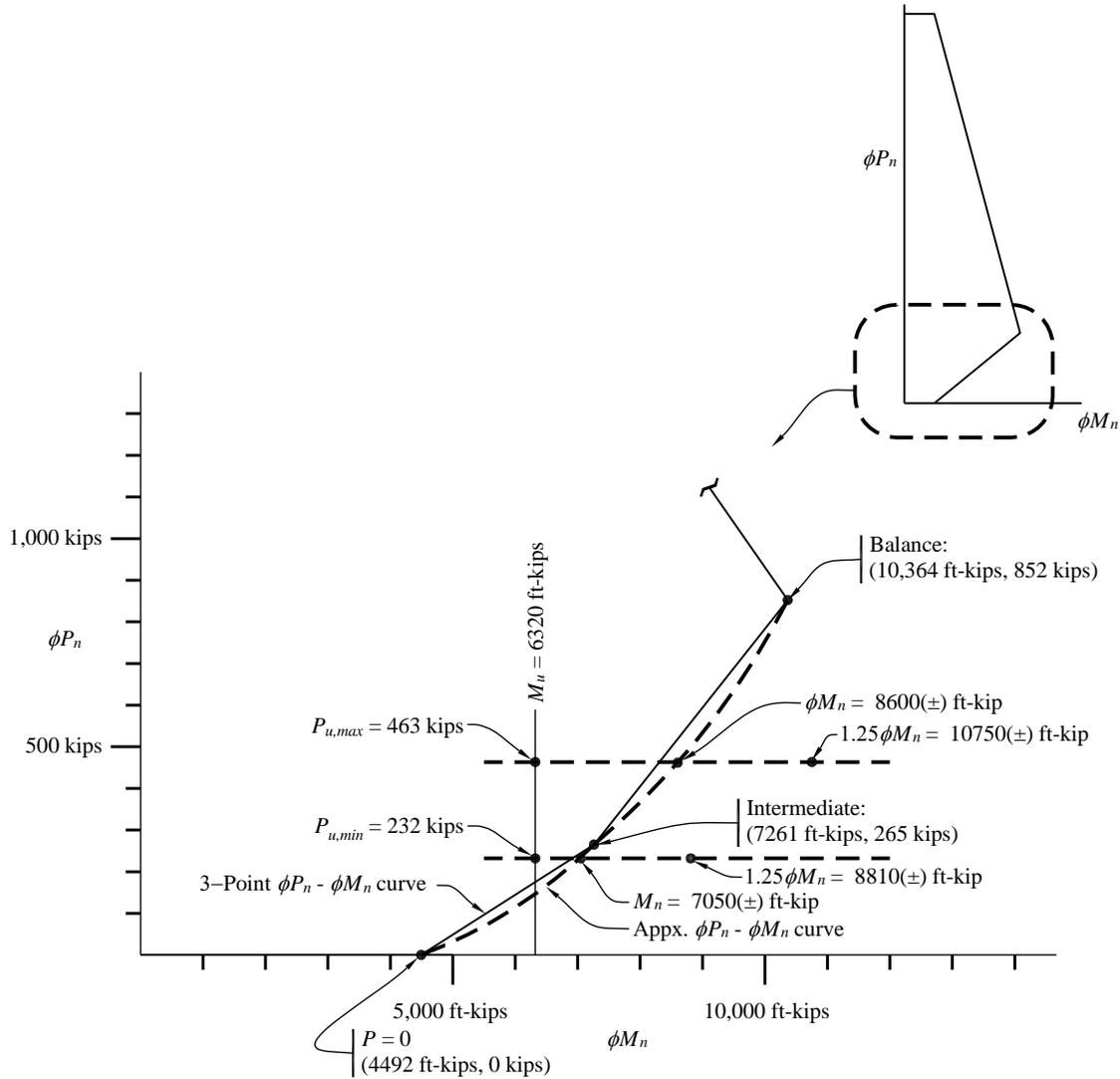
Figure 13.2-14 ϕP_n - ϕM_n Diagram for High Seismicity SDC D Building Wall D
(1.0 kip = 4.45 kN, 1.0 kip-ft = 1.36 kN-m)

13.2.7.5.2.2 Ductility check. TMS 402 Section 9.3.3.5.4 is illustrated in the prior designs. Recall that this calculation uses factored gravity axial loads (based on the *Standard*) to result in the minimum P_u value instead of load combination $D + 0.75L + 0.525Q_E$ per TMS 402 Section 9.3.3.5.1(d). Refer to Figure 13.2-15 and the following calculations which illustrate this using loads at the bottom story (highest axial loads).
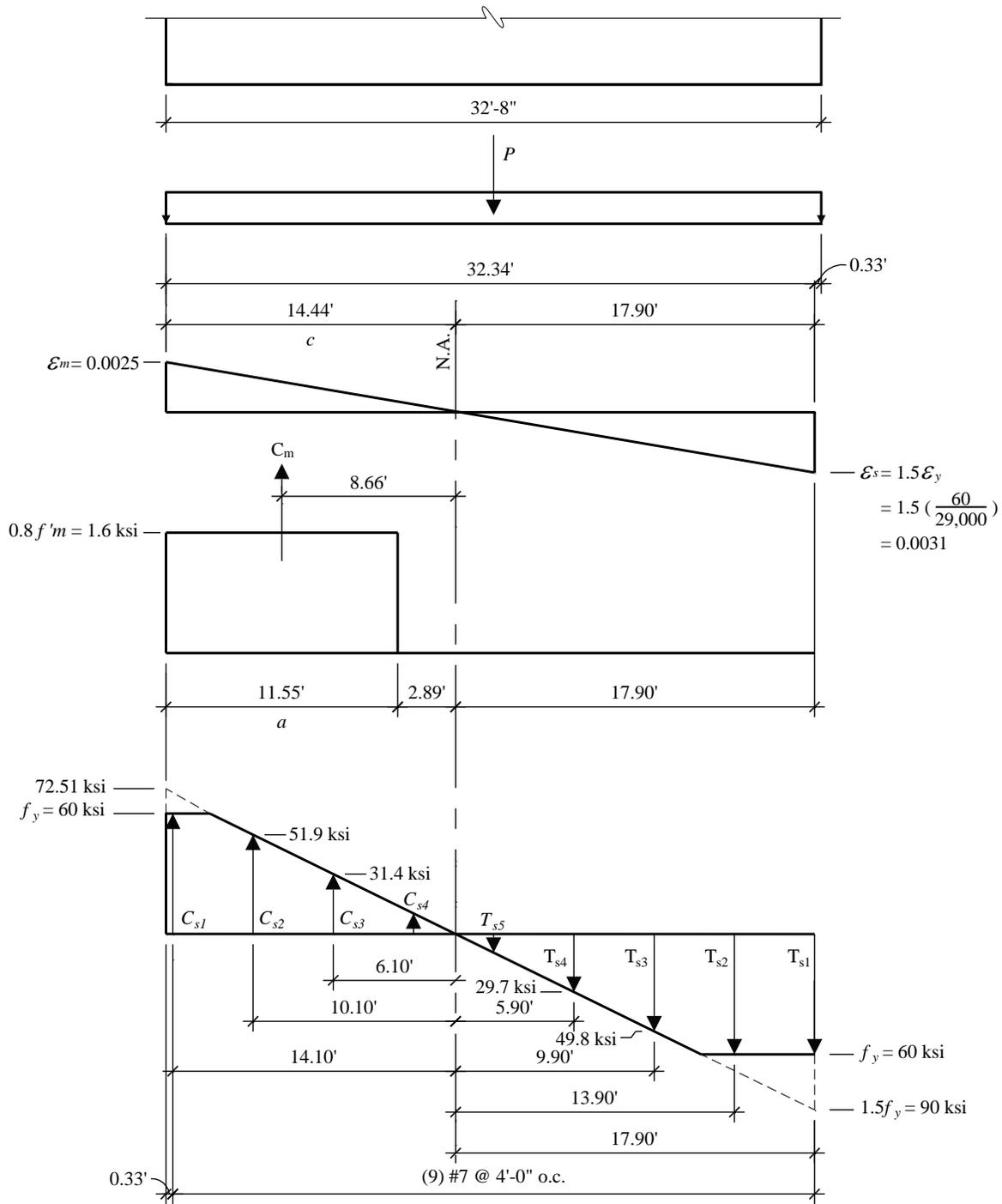
Figure 13.2-15 Ductility Check for High Seismicity SDC D Building Wall D
(1.0 ft = 0.3048 m, 1.0 ksi = 6.89 MPa)

For Level 1 (the bottom story), the unfactored loads are as follows:

$P = 331$ kips

$C_m = 0.8f'_m[(2.5 \text{ in.})(11.55 \text{ ft})(12) + (3 \text{ cells})(41 \text{ in.}^2)] = 751 \text{ kips}$

$C_{s1} = (0.60 \text{ in.}^2)(60 \text{ ksi}) = 36 \text{ kips}$

$C_{s2} = (0.60 \text{ in.}^2)(51.9 \text{ ksi}) = 31 \text{ kips}$

$C_{s3} = (0.60 \text{ in.}^2)(31.4 \text{ ksi}) = 19 \text{ kips}$

C_{s4} is neglected.

$\sum C = 837 \text{ kips}$

$T_{s1} = T_{s2} = (0.60 \text{ in.}^2)(60 \text{ ksi}) = 36 \text{ kips}$

$T_{s3} = (0.60 \text{ in.}^2)(49.8 \text{ ksi}) = 30 \text{ kips}$

$T_{s4} = (0.60 \text{ in.}^2)(18 \text{ ksi}) = 18 \text{ kips}$

T_{s5} is neglected.

$\sum T = 120 \text{ kips}$

$\sum C > \sum P + T$

837 kips > 451 kips   OK

The compression capacity is larger than the tension capacity, so ductile failure is assured. The maximum area of flexural tensile reinforcement requirement of TMS 402 Section 9.3.3.5 is satisfied.

13.2.7.5.3 Check for Shear Corresponding to $1.25\phi M_n$. From Figure 13.2-14, values for $1.25M_n$ can be obtained:

Load Combination 1:

   $P_u \text{ max} = 463 \text{ kips}$

   $1.25M_n = 12{,}000 \text{ ft-kips}$

Load Combination 2:

   $P_u \text{ min} = 232 \text{ kips}$

   $1.25\phi M_n = 9{,}800 \text{ ft-kips}$

Both cases need to be checked. As our example focuses on Load Combination 2, only that case is discussed below.

$$1.25\left(\frac{M_n}{M_u}\right) = 1.25\frac{(9800)}{6320} = 1.94 \text{ , which is less than the 2.5 upper bound.}$$

Therefore, the shear demand is 1.94 times the value from analysis. Referring to Table 13.2-18, $V_u = (1.94)(201 \text{ kips}) = 390 \text{ kips} > 148 \text{ kips} = \phi V_n$. There is more shear demand than allowed; this can be addressed by adding grouted cells.

$$\text{Additional grouted cells} = \left(\frac{390 - 148}{(1.6 \text{ ksi})(41 \text{ in.}^2/\text{cell})} \right) = 3.7 \text{ cells}$$

If the four cells adjacent to the end cells of the wall are grouted (for a total of eight additional grouted cells), the shear requirement is satisfied. The additional grout will add to the building weight slightly. The author recommends that another design iteration be performed to address significant increases in building weight; however, another iteration is not presented here. Note that the above shear check is just for Load Combination 2. Load Combination 1 also needs to be checked; it may necessitate even more grouted cells.

13.2.7.6 High Seismicity SDC D Building deflections. Recall the assertion that the calculations for deflection involve many variables and assumptions and that any calculation of deflection is approximate at best. The requirements and procedures for computing deflection are provided in Section 13.2.4.6.

For the High Seismicity SDC D Building, the determination of whether the walls will be cracked is as follows:

b_e = effective masonry wall width

$b_e = [(2 \times 1.25 \text{ in.})(32.67 \text{ ft} \times 12) + (17 \text{ cells})(41 \text{ in.}^2/\text{cell})]/32.67 \text{ ft} \times 12 = 6.45 \text{ in.}$

$A_n = b_e \, l = (6.45 \text{ in.})(32.67 \times 12) = 2{,}523 \text{ in.}^2$

$S = b_e \, l^2/6 = (6.45)(32.67 \times 12)^2/6 = 165{,}189 \text{ in.}^3$

$f_r = 0.084(32 \text{ cells}/49 \text{ cells}) + 0.163(17 \text{ cells}/49 \text{ cells}) = 0.111 \text{ ksi}$

P_u is calculated using $1.00D$ (see Table 13.2-19 for values and refer to Section 13.2.4.6 for discussion). Table 13.2-20 provides a summary of these calculations.

Table 13.2-20 High Seismicity SDC D Building Cracked Wall Determination

Level	$P_{u_{min}}$ (kips)	M_{cr} (ft-kips)	M_x (ft-kips)	Status
5	66	1888	540	Uncracked
4	132	2248	1563	Uncracked
3	198	2608	2948	Cracked
2	265	2974	4574	Cracked
1	331	3334	6320	Cracked

1.0 kip = 4.45 kN, 1.0 ft-kip = 1.36 kN-m.

For the uncracked wall:

$I_n = I_g = b_e l^3/12 = (6.45$ in.$)(32.67 \times 12)^3/12 = 3.24 \times 10^7$ in.^{4}

As in the three previous examples, I_{cr} will be taken as $0.35 I_g$ for the wall deflection calculation.

The results from a RISA 2D analysis, in which both flexural and shear deflections are included, are shown in Table 13.2-21 and are approximately 50 percent higher than the use of I_{eff} over the full height.

Table 13.2-21 High Seismicity SDC D Building Deflections

Level	F (kips)	I_{eff} (in.^{4})	$\delta_{flexural}$ (in.)	δ_{shear} (in.)	δ_{total} (in.)	$C_d \delta_{total}$ (in.)	Δ (in.)
5	62.3	3.24×10^7	0.431	0.067	0.498	1.743	0.406
4	55.8	3.24×10^7	0.321	0.062	0.382	1.337	0.420
3	41.7	1.13×10^7	0.212	0.050	0.262	0.917	0.409
2	27.8	1.13×10^7	0.110	0.035	0.145	0.508	0.336
1	13.9	1.13×10^7	0.030	0.019	0.049	0.172	0.172

kip = 4.45 kN, 1.0 in. = 25.4 mm.

$F = F_x$ for level (from Table 13.2-17) $\times$ 0.158

The maximum drift occurs at Level 4; per *Provisions* Table 5.2.8 it is:

$\Delta = 0.420$ in. < 1.04 in. $= 0.01 h_n$ (*Standard* Table 12.12-1)   OK

13.2.7.7 High Seismicity SDC D Building out-of-plane forces. *Standard* Section 12.11 requires that bearing walls be designed for out-of-plane loads determined as follows:

$w = 0.40\ S_{DS}\ IW_w \geq 0.1 W_w$

$w = (0.40)(1.00)(1)(60$ psf$) = 24$psf ≥ 6.0 psf $= 0.1 W_w$

The out-of-plane bending moment, using the strength design method for masonry, for the pressure $w = 24$ psf and considering the P-delta effect, is computed to be 2,232 in.-lb/ft. This compares to a computed strength of the wall of 30,000 in.-lb/ft, considering the #7 bars at 4 feet on center. Thus, the wall is loaded to approximately 7 percent of its capacity in flexure in the out-of-plane direction. (See Section 13.1.5.2.5 for a more detailed discussion of strength design of masonry walls, including the *P-delta* effect.)

13.2.7.8 High Seismicity SDC D Building orthogonal effects According to *Standard* Section 12.5.3, orthogonal interaction effects have to be considered for Seismic Design Category D where the ELF procedure is used (as it is here).

The out-of-plane effect is 7 percent of capacity, as discussed in Section 13.2.7.7. Where considering the 0.3 combination factor, the out-of-plane action adds approximately 2 percent overall to the interaction effect. For the lowest story of the wall, this could conceivably require a slight increase in capacity for in-plane actions. In the author's opinion, this is on the fringe of requiring real consideration (in contrast to the end walls of Example 13.1).

This completes the design of the transverse Wall D.

13.2.7.9 Summary of High Seismicity SDC D Building Wall D.

8-inch CMU

f'_m = 2,000 psi

Reinforcement:

Vertical #7 bars at 4 feet on center at intermediate cells.

Two bond beams with two #5 bars at each story, at floor bearing and at 4 feet above each floor.

Horizontal joint reinforcement at alternate courses recommended but not required.

Grout:

All cells with reinforcement and bond beams, plus grout at eight additional cells.

13.2.8 Summary of Wall D Design for All Four Locations

Table 13.2-22 compares the reinforcement and grout for Wall D designed for each of the four locations.

Table 13.2-22 Variation in Reinforcement and Grout by Location for Wall D

	Low Seismicity SDC B Building	Moderate Seismicity SDC C Building	Low Seismicity SDC D Building	High Seismicity SDC D Building
Vertical bars	5 - #4	9 - #4	9 - #6	9 - #7
Horizontal bars	10 - #4 + jt. reinf.	10 - #4 + jt. reinf.	20 - #6	20 - #5
Grout (cu. ft)	91	122	152	172

1 cu. ft = 0.0283 m³.

14

Wood Design

Kelly Cobeen, S.E. & Peter W. Somers, P.E., S.E.

Contents

This chapter examines the design of a variety of wood building elements. Section 14.1 features a three-story, wood-frame apartment building. Section 14.2 illustrates the design of the roof diaphragm and wall-to-roof anchorage for the masonry building featured in Section 13.1. In both cases, only those portions of the designs necessary to illustrate specific points are included.

Wood framing members have significant overstrength, making connections and fasteners the primary sources of ductility and energy dissipation. Nailed plywood shear panels develop considerable ductility through yielding of nails that attach the sheathing to the framing and crushing of the sheathing and framing under the nail shank. Because wood structures are composed of many elements that must act as a whole, the interconnection of elements must be considered carefully to ensure that the load path is complete. Tying the structure together is essential to good earthquake-resistant construction.

Wood elements are often used in low-rise masonry and concrete wall buildings. The same basic principles apply to the design of these wood elements, but certain aspects of the design (for example, wall-to-diaphragm anchorage) are more critical in mixed systems than in all-wood construction.

Wood structural panel sheathing is referred to as "plywood" in this chapter. However, sheathing can include plywood and other products, such as oriented-strand board (OSB), that conform to the appropriate materials standards.

The calculations herein are intended to provide a reference for the direct application of the design requirements presented in the 2015 *NEHRP Recommended Provisions* (hereafter, the *Provisions*), as adopted into ASCE 7-16 *Minimum Design Loads for Buildings and Other Structures* (hereafter, the *Standard*), and to assist the reader in developing a better understanding of the principles behind the *Provisions* and the *Standard*. In addition to the *Provisions*, the documents below are referenced in this chapter; the editions noted are consistent with the *Standard*.

ACI 318	American Concrete Institute. 2014. *Building Code Requirements and Commentary for Structural Concrete.*
ANSI/AITC A190.1	American Institute of Timber Construction. 2007. *Structural Glued-Laminated Timber.*
ASCE 7	American Society of Civil Engineers. 2016. *Minimum Design Loads for Buildings and Other Structures.*
AF&PA Guideline	American Forest & Paper Association 1996. *Manual for Engineered Wood Construction (LRFD), Pre-Engineered Metal Connectors Guideline.*
AWC NDS & Supplement	American Wood Council. 2015. *National Design Specification and Design Values for Wood Construction.*
AWC SDPWS	American Wood Council. 2015. *Special Design Provisions for Wind and Seismic.*
IBC	International Code Council. 2015. *International Building Code.*

TMS 402/ACI 530/ASCE 5   The Masonry Society, American Concrete Institute, and American Society of Civil Engineers. 2013. *Building Code Requirements for Masonry Structures.*

14.1   THREE-STORY WOOD APARTMENT BUILDING

This example features a wood-frame building with plywood diaphragms and shear walls.

14.1.1 Building Description

This three-story wood-frame apartment building has a double-loaded central corridor. The building is typical stick-frame construction consisting of wood joists and stud bearing walls supported by a concrete foundation wall and strip footing system. The seismic force-resisting system consists of plywood floor and roof diaphragms and plywood shear walls. Figure 14.1-1 shows a typical floor plan and Figure 14.1-2 shows a longitudinal section and elevation. The building is located in a residential neighborhood a few miles north of downtown Seattle.

The shear walls in the longitudinal direction are located on the exterior faces of the building and along the corridor. The entire solid (non-glazed) area of the exterior walls has plywood sheathing, but only a portion of the corridor walls will require sheathing. In the transverse direction, the end walls and one line of interior shear walls provide lateral resistance. It should be noted that while plywood sheathing generally is used at the exterior walls for reasons beyond just lateral load resistance, the interior longitudinal (corridor) and transverse shear walls could be designed using gypsum wallboard as permitted by AWC SDPWS Section 4.3.7.5. However, the corridor shear walls are not included in this example and the interior transverse walls are designed using plywood sheathing, largely due to the required shear capacity.

The floor and roof systems consist of wood joists supported on bearing walls at the perimeter of the building, the corridor lines, plus one post-and-beam line running through each bank of apartments. Exterior walls are framed with 2×6 studs for the full height of the building to accommodate insulation. Interior bearing walls require 2×6 or 3×4 studs on the corridor line up to the second floor and 2×4 studs above the second floor. Apartment party walls are not load-bearing; however, they are double walls and are constructed of staggered 2×4 studs at 16 inches on center. Surfaced, dry (seasoned) lumber is used for all framing to minimize shrinkage. Floor framing members are assumed to be composed of Douglas Fir-Larch material and wall framing is Hem-Fir No. 2, as graded by the WWPA Rules. The material and grading of other framing members associated with the lateral design is as indicated in the example. The lightweight concrete floor fill is for sound isolation and is interrupted by the party walls, corridor walls and bearing walls.

The building is founded on interior footing pads, continuous strip footings and concrete foundation (stem) walls (Figure 14.1-3). The depth of the footings and the height of the walls are sufficient to provide crawlspace clearance beneath the first floor. The concrete stem walls extend to the underside of the first floor framing; as a result the first floor is treated as the building base for purposes of seismic design.
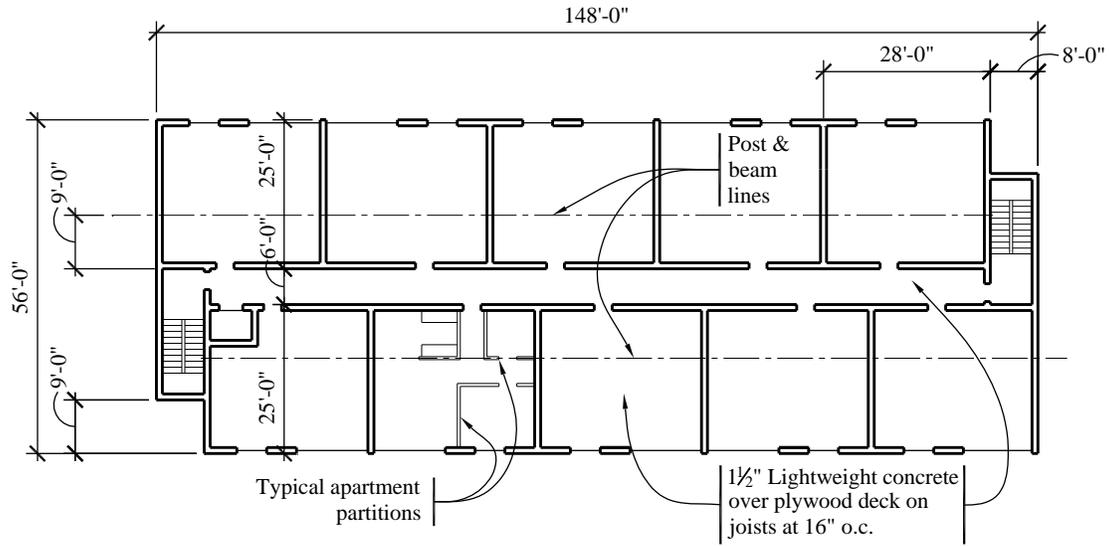
Figure 14.1-1 Typical floor plan
(1.0 ft = 0.3048 m)
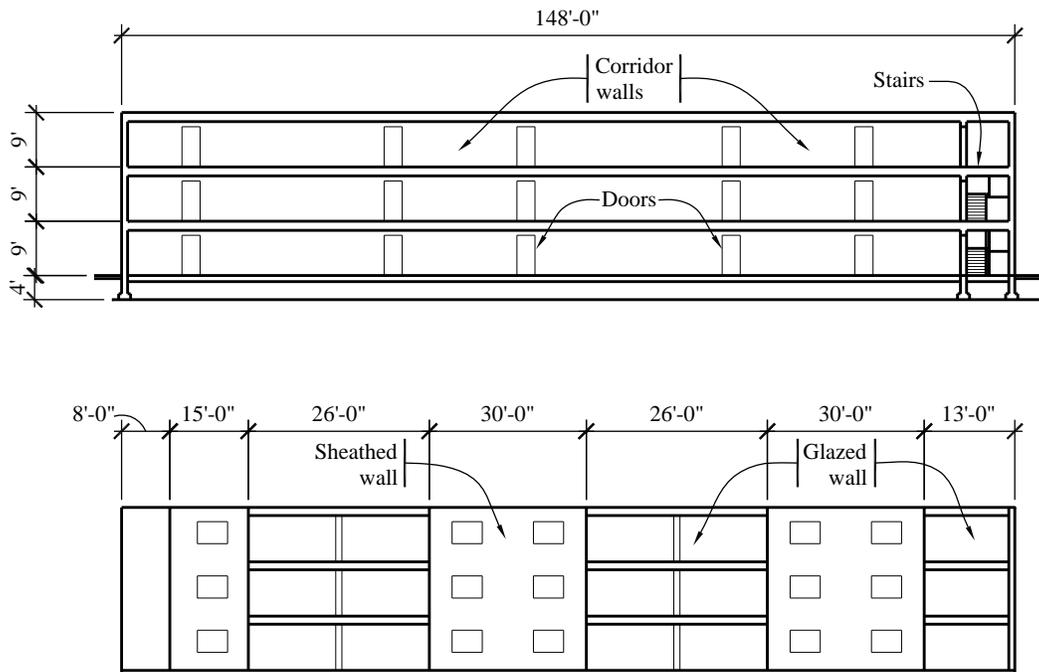
Figure 14.1-2 Longitudinal section and elevation
(1.0 ft = 0.3048 m)
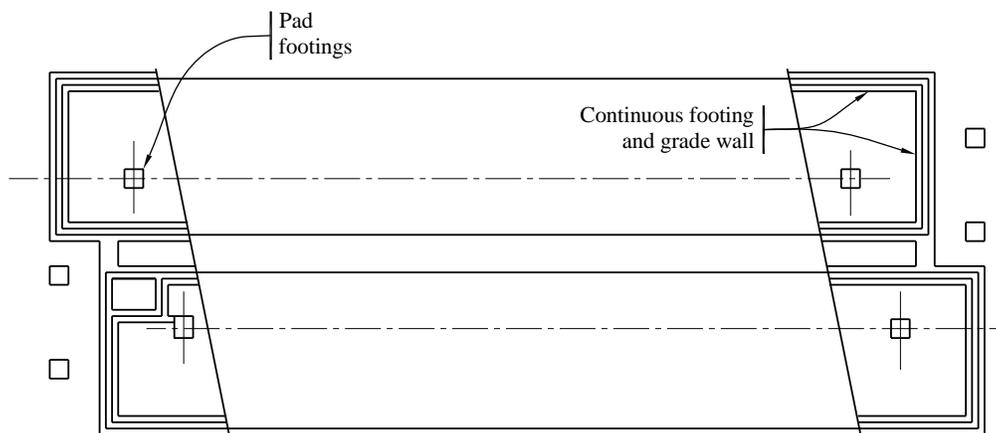
Figure 14.1-3 Foundation plan

14.1.1.1 Scope. In this example, the structure is designed and detailed for forces acting in the transverse and longitudinal directions, including the following:

Development of seismic loads using the Simplified Alternative Structural Design Criteria (herein referred to as the "simplified procedure") contained in Standard Section 12.14.

Design and detailing of transverse plywood walls for shear and overturning moment.

Design and detailing of plywood floor and roof diaphragms.

Design and detailing of wall and diaphragm chord members.

Design and detailing of longitudinal plywood walls using the requirements for perforated shear walls.

The simplified procedure, first introduced in the 2005 edition of the *Standard* and revised in subsequent editions, is permitted for relatively short, simple and regular structures utilizing shear walls or braced frames. The seismic analysis and design procedure is much less involved than a building utilizing a seismic force resisting system analyzed using one of the procedures listed in *Standard* Section 12.6. See Section 14.1.2.2 for a more detailed discussion of what is and is not required for the seismic design. In accordance with *Standard* Section 12.14.1.1, the subject building qualifies for the simplified procedure because of the following attributes:

- Risk Category II (residential occupancy)

- Three stories above grade plane in height

- Bearing wall lateral system

- At least two lines of lateral force-resisting elements in both directions, at least one on each side of the center of weight

- Center of weight located not further from geometric centroid than 10% of the length of the diaphragm parallel to the eccentricity

- Flexible diaphragm idealization permitted

- Lines of resistance at 90 degrees to each other

- Simplified method used in both orthogonal directions

- No in-plane or out-of-plane offsets

- No reduction in seismic resistance at lower floors.

14.1.2 Basic Requirements
14.1.2.1 Seismic Parameters

Table 14.1-1 Seismic Parameters

Design Parameter	Value
Risk Category (*Standard* Sec. 1.5.1)	II
Short-Period Response, S_S	1.34
Site Class (*Standard* Sec. 11.4.2)	D
Seismic Design Category (*Standard* Sec. 11.6)	D
Seismic Force-Resisting System (*Standard* Table 12.14-1)	Wood Structural Panel Shear Walls
Response Modification Coefficient, *R*	6.5

14.1.2.2 Structural Design Criteria

14.1.2.2.1 Ground Motion Parameter. Unlike the typical design procedures in *Standard* Chapter 12, the simplified procedure requires consideration of just one spectral response parameter, S_{DS} (except as noted in Section 14.1.2.2.2 below). This is because the behavior of short, stiff buildings for which the simplified procedure is permitted will always be governed by short-period response. In accordance with *Standard* Section 12.14.8.1:

$$S_{DS} = 2/3 F_a S_S$$

The site coefficient, F_a, can be determined using *Standard* Section 12.14.8.1 with simple default values based on soil type or using *Standard* Table 11.4-1 if the site class is known. Since *Standard* Table 11.4-1 generally will result in more favorable value, that method is used for this example. Using $S_S = 1.34$ and Site Class D, *Standard* Table 11.4-1 lists a short-period site coefficient, F_a, of 1.0. Therefore, in accordance with *Standard* Equation:

$$S_{DS} = 2/3(1.0)(1.34) = 0.89$$

Note that $F_a = 1.0$ is applicable only when the site class is specifically determined to be D; Section 11.4 of the 2016 edition of ASCE 7 has introduced additional requirements where the site class is assigned to be D as a default.

14.1.2.2.2 Seismic Design Category (Standard Sec. 11.6). Where the simplified procedure is used, *Standard* Section 11.6 permits the Seismic Design Category to be determined based on *Standard* Table 11.6-1 only. Based on the Risk Category and the design spectral response acceleration parameter, the subject building is assigned to Seismic Design Category D. Note that *Standard* Section 12.14.1.1 requires that the Seismic Design Category be assigned as E where S_1 is greater than or equal to 0.75.

14.1.2.2.3 Seismic Force-Resisting Systems (Standard Sec. 12.14.4). See Figure 14.1-4. For both directions, the load path for seismic loading consists of plywood floor and roof diaphragms and plywood shear walls. Because the lightweight concrete floor topping is discontinuous at each partition and wall, it is not considered to be a structural diaphragm. In accordance with *Standard* Table 12.14-1, building has a bearing wall system comprised of light-framed walls sheathed with wood structural panels. The response modification factor, *R,* is 6.5 for both directions.
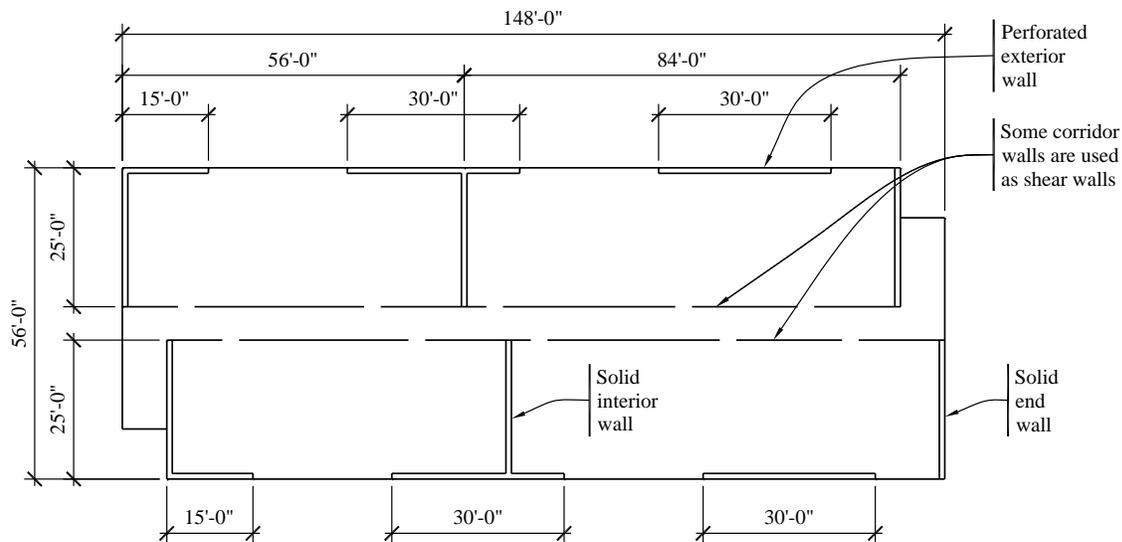
Figure 14.1-4 Load path and shear walls
(1.0 ft = 0.3048 m)

14.1.2.2.4 Diaphragm Flexibility (Standard Sec. 12.14.5). *Standard* Section 12.14.5 defines a diaphragm comprised of wood structural panels as flexible. Because the lightweight concrete floor topping is discontinuous at each partition and wall, it is not considered to be a structural diaphragm. Note that AWC SDPWS Section 4.2.5 imposes additional requirements new to the 2015 edition and applicable to cantilevered diaphragms. In this example the diaphragms need not be considered to be cantilevered if appropriate collectors are provided.

14.1.2.2.5 Application of Loading (Standard Sec. 12.14.6). For the simplified procedure, seismic loads are permitted to be applied independently in two orthogonal directions.

14.1.2.2.6 Design and Detailing Requirements (Standard Sec. 12.14.7). The plywood diaphragms are designed for the forces prescribed in *Standard* Section 12.14.7.4. The design of foundations is per

Standard Section 12.13 and wood design requirements are based on *Standard* Section 14.4 as discussed in greater detail below.

14.1.2.2.7 Analysis Procedure (Standard Sec. 12.14.8). For the simplified procedure, only one analysis procedure is specified and it is described in greater detail in Section 14.1.3.1 below.

14.1.2.2.8 Drift Limits (Standard Sec. 12.14.8.5). Where the simplified procedure is used, there are not any specific drift limitations because the types of structures for which the simplified procedure is applicable are generally not drift-sensitive. As specified in *Standard* Section 12.14.8.5, if a determination of expected drift is required (for the design of cladding for example), then drift is permitted to be computed as 1 percent of the building height unless a more detailed analysis is performed.

14.1.2.2.9 Combination of Load Effects (Standard Sec. 12.14.3). The basic design load combinations are as stipulated in *Standard* Chapter 2. Seismic load effects according to the *Standard* Equations 12.14-3 through 12.14-6 are as follows:

$$E = Q_E + 0.2S_{DS}D$$

$$E = Q_E - 0.2S_{DS}D$$

Where seismic and gravity are additive and counteractive, respectively.

For $S_{DS} = 0.89$, the strength level design load combinations are as follows:

$$(1.2 + 0.2S_{DS})D + 1.0Q_E + 0.5L + 0.2S = 1.38D + 1.0Q_E + 0.5L + 0.2S$$

$$(0.9 - 0.2S_{DS})D - 1.0Q_E = 0.72D - 1.0Q_E$$

Note that there is no redundancy factor for the simplified procedure.

14.1.2.3 Basic Gravity Loads

Roof:

Table 14.1-2 Roof Gravity Loads

Load Type	Value
Live/Snow Load (in Seattle, snow load governs over roof live load; in other areas this may not be the case)	25 psf
Dead Load (including roofing, sheathing, joists, insulation and gypsum ceiling)	15 psf

Floor:

Table 14.1-3 Floor Gravity Loads

Load Type	Value
Live Load	40 psf
Dead Load (1-1/2-in. lightweight concrete, sheathing, joists and gypsum ceiling. At first floor, omit ceiling but add insulation.)	20 psf
Interior Partitions and Corridor Walls (8 ft high at 11 psf)	7 psf distributed floor load
Exterior Frame Walls (wood siding, plywood sheathing, 2×6 studs, batt insulation and 5/8-in. gypsum wallboard)	15 psf of wall surface
Exterior Double Glazed Window Wall	9 psf of wall surface
Party Walls (double-stud sound barrier)	15 psf of wall surface
Stairways	20 psf
Typical Footing (10 in. by 1 ft-6 in.) and Stem Wall (10 in. by 4 ft-0 in.)	690 plf
Applicable Seismic Weights at Each Level	
W_{roof} = Area (roof dead load + interior partitions + party walls) + End Walls + Longitudinal Walls	182.8 kips
$W_3 = W_2$ = Area (floor dead load + interior partitions + party walls) + End Walls + Longitudinal Walls	284.2 kips
Effective Total Building Weight, W	751 kips

For modeling the structure, the first floor is assumed to be the seismic base, because the short crawlspace with concrete foundation walls is stiff compared to the superstructure.

14.1.3 Seismic Force Analysis

The analysis is performed manually following a step-by-step procedure for determining the base shear (*Standard* Sec. 12.14.8.1), vertical distribution of forces (*Standard* Sec. 12.14.8.2) and horizontal distribution of forces (*Standard* Sec. 12.14.8.3). For a building with flexible diaphragms, *Standard* Section 12.14.8.3.1 allows the horizontal distribution of forces to be based on tributary areas and accidental torsion need not be considered for the simplified procedure.

14.1.3.1 Base Shear Determination. According to *Standard* Equation 12.14-12:

$$V = \frac{FS_{DS}}{R}W$$

Where $F = 1.2$ for a three-story building, $R = 6.5$ and $W = 751$ kips as determined previously. Therefore, the base shear is computed as follows:

$$V = \frac{(1.2)(0.89)}{6.5}(751) = 123.4 \text{ kips (both directions)}$$

14.1.3.2 Vertical Distribution of Forces. Forces are distributed as shown in Figure 14.1-5, where the story forces are calculated according to *Standard* Equation 12.14-13 as follows:

$$F_x = \frac{w_x}{W} V$$

This results in a uniform vertical distribution of forces, where the story force is based on the relative seismic weight of the story with all stories at the same seismic acceleration (as opposed to the triangular or parabolic vertical distribution used in the Equivalent Lateral Force procedure of *Standard* Sec. 12.8)
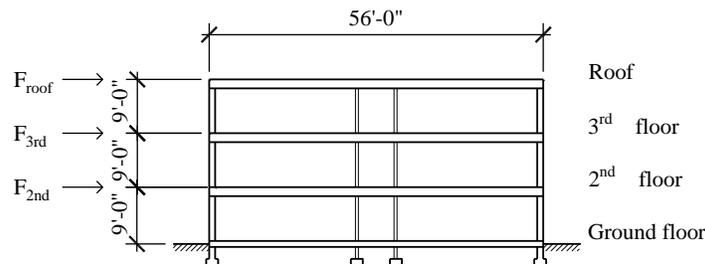
Figure 14.1-5 Vertical shear distribution
(1.0 ft = 0.3048 m)

The story force at each floor is computed as:

F_{roof} = [182.8/751](123.4)	=	30.0 kips
F_{3rd} = [284.2/751](123.4)	=	46.7 kips
F_{2nd} = [284.2/751](123.4)	=	46.7 kips
Σ	=	123.4 kips

14.1.3.3 Horizontal Distribution of Shear Forces to Walls. Since the diaphragms are defined as flexible by *Standard* Section 12.14.5, the horizontal distribution of forces is based on tributary area to the individual shear walls in accordance with *Standard* Section 12.14.8.3.1. For this example, forces are distributed as described below.

14.1.3.3.1 Longitudinal Direction. In this direction, there are four lines of resistance, but only the exterior walls are considered in this example. The total story force tributary to the exterior wall is determined as follows:

$(25/2)/56F_x = 0.223F_x$

The distribution to each individual shear wall segment along this exterior line is discussed in Section 14.1.4.7 below.

14.1.3.3.2 Transverse Direction. Again, based on the flexible diaphragm assumption, force is to be distributed based on tributary area. As shown in Figure 14.1-4, there are three sets of two shear walls, each offset in plan by 8 feet. For the purposes of this example, each set of walls is assumed to be in alignment, resisting the same tributary width. The result is that the building is modeled with a diaphragm

consisting of two simple spans, which provides a more reasonable horizontal distribution of force than a pure tributary area distribution.

For a two-span, flexible diaphragm, the central walls will resist one-half of the total load, or $0.50F_x$. The other walls resist story forces in proportion to the width of diaphragm between them and the central walls. The left set of walls in Figure 14.1-4 resists $(60/2)/148F_x = 0.203F_x$ and the right set resists $(88/2)/148F_x = 0.297F_x$, where 60 feet and 88 feet represent the dimension from the ends of the building to the centroid of the two central walls. Note that this does not exactly match the existing diaphragm spans, but is a reasonable simplification to account for the three sets of offset shear walls at the ends and middle of the building.

14.1.3.4 Diaphragm Design Forces. As specified in *Standard* Section 12.14.7.4, the design forces for floor and roof diaphragms are the same forces as computed for the vertical distribution in Section 14.1.3.2 above plus any force due to offset walls (not applicable for this example).

The weight tributary to the diaphragm, w_{px}, need not include the weight of walls parallel to the force. For this example, however, since the shear walls in both directions are relatively light compared to the total tributary diaphragm weight, the diaphragm force is computed based on the total story weight, for convenience. Therefore, the diaphragm forces are exactly the same as the story forces shown above.

14.1.4 Basic Proportioning
Designing a plywood diaphragm and plywood shear wall building principally involves the determination of sheathing thicknesses and nailing patterns to accommodate the applied loads. This is especially the case where the simplified procedure is utilized, since there are not any deflection checks and possible subsequent design iterations.

In addition to the wall and diaphragm design, this design example features framing member and connection design for elements including shear wall end posts and hold-downs, foundation anchorage and diaphragm chords.

Nailing patterns in diaphragms and shear walls have been established on the basis of tabulated requirements included in the AWC SDPWS. It is important to consider the framing requirements for a given nailing pattern and capacity as indicated in the notes following the tables. In addition to strength requirements, AWC SDPWS Section 4.2.4 places aspect ratio limits on plywood diaphragms (L/W must not exceed 3:1 for unblocked diaphragms or 4:1 for blocked diaphragms) and AWC SDPWS Section 4.3.4 places similar limits on plywood shear walls (h/b must not exceed 2:1 for full design capacities or 3.5:1 with reduced capacities).

14.1.4.1 Strength of Members and Connections. The *Standard* references the AWC NDS and AWC SDPWS for engineered wood structures. These reference standards support both Allowable Stress Design (ASD) and Load and Resistance Factor Design (LRFD) as permitted by the *Standard*. For this example, LRFD is utilized. The AWC NDS and AWC Supplement contains the material design values for framing members and connections, while the AWC SDPWS contains the diaphragm and shear wall tables as well as detailing requirements for shear wall and diaphragm systems.

Throughout this example, the resistance of members and connections subjected to seismic forces, acting alone or in combination with other prescribed loads, is determined in accordance with the AWC NDS and AWC SDPWS. The methodology is somewhat different between the AWC NDS for framing members and connections and the AWC SDPWS for shear walls and diaphragms.

For framing members and connections, the AWC NDS incorporates the notation F_b, F_t, Z, etc., for reference design values, which are then modified using standard wood adjustment factors, C_M, C_r, C_F, etc. (used for both ASD and LRFD) and then for LRFD are modified by a format conversion factor, K_F, a resistance factor, ϕ and a time effect factor, λ, to compute an adjusted design resistance, F_b', F_t', Z'. These factors are defined in AWC NDS Appendix N.

For shear walls and diaphragms, the AWC SDPWS contains tabulated unit shear values, v_s, which are multiplied by a resistance factor, ϕ_D, equal to 0.8 for LRFD design or divided by a reduction factor of 2 for ASD. The tabulated design values are applicable to Douglas Fir-Larch or Southern Pine framing. Additional modification in accordance with the footnotes to the tabular values in the AWC SDPWS is required for the Hem-Fir framing species used for wall framing in this example.

For pre-engineered connection elements, the AWC NDS does not contain a procedure for converting the manufacturer's cataloged values (typically as ASD values) to LRFD. However, such a procedure is contained in a guideline published with the 1996 edition of the LRFD wood standard (AWC Guideline). The AWC Guideline contains a method for converting allowable stress design values for cataloged metal connection hardware (for example, tie-down anchors) into ultimate capacities for use with strength design. The procedure, which is used for this example, can generally be described as taking the catalog ASD value, multiplying by 2.88 and dividing the by the load duration factor on which the cataloged value is based (typically 1.33 or 1.60 for pre-engineered connection hardware often used for wind or seismic design).

14.1.4.2 Transverse Shear Walls. The design will focus on the more highly loaded interior walls; the end walls would be designed in a similar manner.

14.1.4.2.1 Load to Interior Transverse Walls. As computed in Section 14.1.3.3.2, the total story force resisted by the central walls is $0.50F_x$. Since the both walls are the same length and material, each individual wall will resist one-half of the total or $0.25F_x$. Therefore:

$F_{roof} = 0.25(30.0)$	=	7.50 kips
$F_{3rd} = 0.25(46.7)$	=	11.68 kips
$F_{2nd} = 0.25(46.7)$	=	11.68 kips
Σ	=	30.86 kips

The story forces and story shears resisted by the individual wall segment is illustrated in Figure 14.1-6.
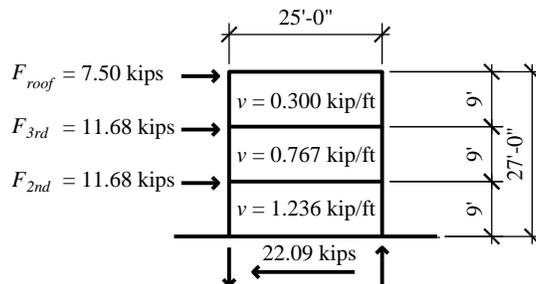
Figure 14.1-6 Transverse section: end wall
(1.0 ft = 0.3048 m, 1.0 kip = 4.45 kN, 1.0 kip/ft = 14.6 kN/m)

14.1.4.2.2 Roof to Third Floor Shear Wall Sheathing

V = 7.50 kips

v = 7.50/25 = 0.300 klf

Try a 15/32-inch plywood rated sheathing (not Structural I) on blocked 2× Hem-Fir members at 16 inches on center with 8d common nails at 6 inches on center at panel edges and 12 inches on center at intermediate framing members. From AWC SDPWS Table 4.3A, this shear wall assembly has a nominal unit shear capacity, v_s, of 0.520 klf. However, according to Note 3 of AWC SDPWS Table 4.3A, the design shear resistance values are for Douglas Fir-Larch or Southern Pine and must be adjusted for Hem-Fir wall framing. The specific gravity adjustment factor equals 1-(0.5-SG) where SG is the specific gravity of the framing lumber. From AWC NDS Table 12.3.3A, the SG for Hem-Fir is 0.43. Therefore, the adjustment factor is 1-(0.5-0.43) = 0.93. The adjusted shear capacity is computed as follows:

$0.93\phi_D v_s = 0.93(0.8)(0.520) = 0.387$ klf > 0.300 klf   OK

14.1.4.2.3 Third Floor to Second Floor Shear Wall Sheathing

V = 7.50 + 11.68 = 19.18 kips

v = 19.18/25 = 0.767 klf

Try 15/32-inch plywood rated sheathing (not Structural I) on blocked 2× Hem-Fir members at 16 inches on center with 10d nails at 3 inches on center at panel edges and at 12 inches on center at intermediate framing members. From AWC SDPWS Table 4.3A, this shear wall assembly has a nominal unit shear capacity, v_s, of 1.200 klf. The adjusted shear capacity is computed as follows:

$0.93\phi_D v_s = 0.93(0.8)(1.200) = 0.893$ klf > 0.767 klf   OK

For this shear wall assembly, the width of framing at panel edges needs to be checked relative to AWC SDPWS Section 4.3.7.1. In accordance with Item 5 of that section, 3× framing is required at adjoining panel edges since the wall has 10d nails spaced at 3 inches or less and because the unit shear capacity exceeds 0.700 klf for a building assigned to Seismic Design Category D.

However, an exception to this section permits double 2× framing to be substituted for the 3× member, provided that the 2× framing is adequately stitched together in accordance with AWC SDPWS Section 4.3.6.1.1. Since the double 2× framing is often preferred over the 3× member, this procedure will be utilized for this example. The exception requires the double 2× members to be connected to "transfer the induced shear between members." For the purposes of this example, the induced shear along the vertical plane between adjacent panels will be conservatively taken as the adjusted design shear of 0.893 klf. Note that 0.767 could be used, but using 0.893 assures that the transfer nailing calculated can be used anywhere that this combination of sheathing and edge nailing is used.

Using 16d common wire nails and 2× Hem-Fir framing, AWC NDS Table 12N specifies a lateral design value, Z, of 0.122 kips per nail. The adjusted design capacity is:

$Z' = ZK_F\phi\lambda = (0.122)(3.32)(0.65) = 0.264$ kips per nail

and the number of nails per foot is 0.893/0.264 = 3.4, so provide 4 nails per foot. Therefore, use double 2× framing at panel edges fastened with 16d at 3 inches on center and staggered (as required by the exception where the nail spacing is less than 4 inches).

14.1.4.2.4 Second Floor to First Floor Shear Wall Sheathing

19.18 + 11.68 = 30.86 kips

v = 30.86/25 = 1.236 klf

Try 19/32-inch plywood rated sheathing (not Structural I) on blocked 2-inch Hem-Fir members at 16 inches on center with 10d common nails at 2 inches on center at panel edges and 12 inches on center at intermediate framing members. From AWC SDPWS Table 4.3A, this shear wall assembly has a nominal unit shear capacity, v_s, of 1.740 klf. The adjusted shear capacity is computed as follows:

$0.93\phi_D v_s = 0.93(0.8)(1.740) = 1.294$ klf > 1.236 klf   OK

This shear wall assembly also requires 3× or stitched double 2× framing at panel edges. In this case, 3× framing is recommended, since the tight nail spacing required to stitch the double 2× members could lead to splitting and bolts or lag screws would not be economical.

Rather than increasing the plywood thickness at this level, adequate capacity could be achieved by using Structural I sheathing, Douglas Fir-Larch framing members, or 15/32-inch plywood on both sides of the shear wall framing.

14.1.4.3 Transverse Shear Wall Anchorage. AWC SDPWS Section 4.3.6.4.2 requires tie-down (hold-down) anchorage at the ends of shear walls where net uplift is induced. Net uplift is computed as the combination of the seismic overturning moment and the dead load counter-balancing moment using the load combination $0.72D - 1.0Q_E$. For the full height shear wall segments used in the transverse shear walls, the overturning and resisting moments are calculated for global shear wall turning, based on the diaphragm shown in Figure 14.1-6.

AWC SDPWS requires the tie-down devices (Sec. 4.3.6.4.2) and end posts (Sec. 4.3.6.1.2) to be designed for a tension or compression force. The uplift force over the height of a shear wall is taken as the unit shear, v, times the clear height, h, as defined in AWC SDPWS Section 2.3. This uplift force is combined with the uplift forces from stories above, if applicable, and reduced by the tributary dead load acting to counter the uplift.

14.1.4.3.1 Tie-down Anchors at Third Floor. For the typical 25-foot interior wall segment, the overturning moment at the third floor is:

M_0 = (8 ft)(7.50 kips) = 60.0 ft-kip = Q_E

Where the wall clear height is eight feet. For the counter-balancing moment, it is assumed that the interior transverse walls will engage a certain length of exterior and corridor bearing wall for uplift resistance. The width of floor is taken as the length of solid wall panel at the exterior, or 10 feet. See Figures 14.1-1 and 14.1-13. For convenience, the same length is used for the longitudinal walls. The designer should take care to assume a reasonable amount of tributary dead loads that can be engaged considering the connections and stiffness of the cross wall elements. In this situation, considering that the exterior and corridor walls are plywood-sheathed shear walls, the assumption noted above is considered reasonable.

The weight of interior wall, 11 psf, is used for both conditions.

Shear wall self-weight = (8 ft)(25 ft)(11 psf)/1,000   = 2.20 kips
Tributary roof = (10 ft)(25 ft)(15 psf)/1,000   = 3.75 kips
Tributary longitudinal walls = (8 ft)(10 ft)(11 psf)(2)/1,000   = <u>1.76 kips</u>
Σ = 7.71 kips

$0.72Q_D = 0.72(7.71)(12.5) = 69.4$ ft-kip

Since the dead load stabilizing moment exceeds the overturning moment, uplift anchorage is not required at the third floor. An end post for shear wall boundary compression is required, but since the design is similar to the second floor end post, it is not illustrated here.

14.1.4.3.2 Tie-down Anchors at Second Floor. The total overturning moment at the second floor is:

$M_0 = 8(7.50) + 8(7.50+11.68) = 213$ ft-kip

The total counter-balancing moment is computed using the same assumptions as for the third floor.

Shear wall self weight = (8+8 ft)(25 ft)(11 psf)/1,000	= 4.40 kips
Tributary roof +floor = (10 ft)(25 ft)(15+20 psf)(2)/1,000	= 8.75 kips
Tributary longitudinal walls = (8+8 ft)(10 ft)(11 psf)(2)/1,000	= 3.52 kips
Σ	= 16.67 kips

$0.72Q_D = 0.72(16.67)(12.5) = 150$ ft-kips

M_0 (net) = 213 - 150 = 63 ft-kips

As would be expected, uplift anchorage is required.

It is assumed that the tie-down post is installed approximately six inches from the end of the shear wall, making the effective moment arm 25.0 ft - 0.5 ft = 24.5 ft. Therefore, the design uplift force at the second floor is:

$T = 63$ ft-kips/ 24.5 ft = 2.6 kips

Use a tie-down anchor to connect the end posts. For ease of construction, select a tie-down device that screws to the end post. See Figure 14.1-7. A tie-down with a 5/8-inch threaded rod and fourteen 1/4-inch screws has a cataloged ASD capacity of 5.645 kips for Douglas Fir-Larch framing based on a load duration factor of 1.6. Using the AWC Guideline procedure for pre-engineered connections described in Section 14.1.4.1 ($K_F = 2.88/1.60$), the LRFD capacity is determined as follows:

$ZK_F\phi\lambda = (5.645)(2.88/1.60)(0.65)(1.0) = 6.60$ kips > 2.6 kips   OK
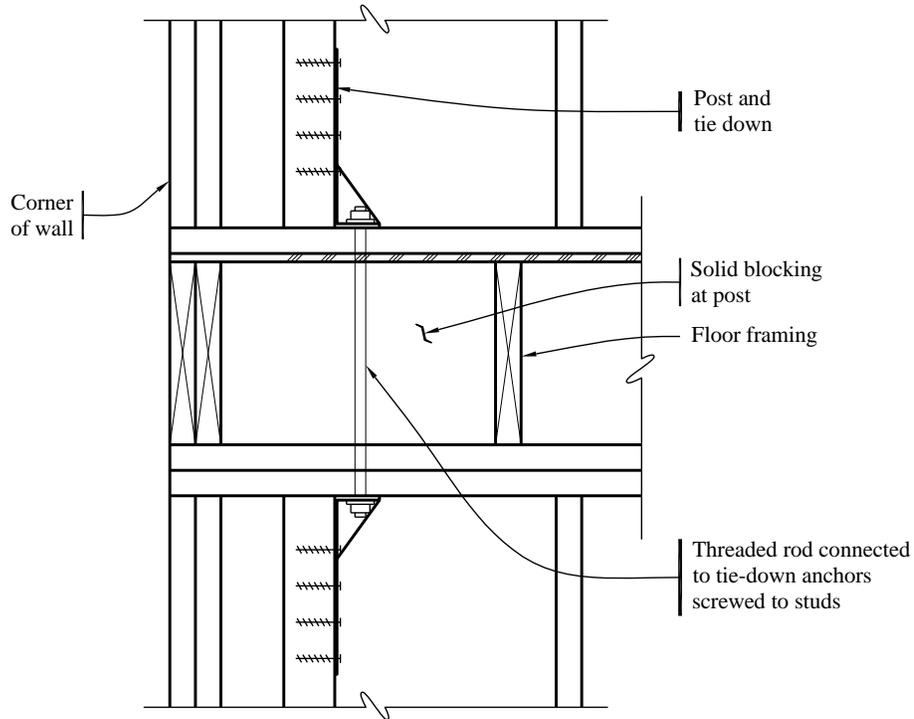
Figure 14.1-7 Shear wall tie down at suspended floor framing

14.1.4.3.3 Tie-down Anchors at First Floor. The overturning moment at the first floor is:

$M_0 = 8(7.50) + 8(7.50+11.68) + 8(7.50+11.68+11.68) = 460$ ft-kip $= Q_E$

The counter-balancing moment is computed using the same assumptions as for the second floor.

Shear wall self-weight = (8+8+8 ft)(25 ft)(11 psf)/1,000	=	6.60 kips
Tributary floor = (10 ft)(25 ft)(15+20+20 psf)/1,000	=	13.75 kips
Tributary longitudinal walls = (8+8+8 ft)(10 ft)(11 psf)(2)/1,000	=	5.28 kips
Σ	=	25.63 kips

$0.72Q_D = 0.72(25.63)12.5 = 230$ ft-kip

M_0 (net) $= 460-230 = 230$ ft-kip

A 24.5 ft moment arm for the tie-down is again used. The total design uplift force at the first floor is:

$T = 230/24.5 = 9.4$ kips

Use a tie-down anchor that extends down into the foundation with an anchor bolt. Tie-downs with a 7/8-inch threaded rod anchor and three 1-inch bolts through a 6×6 Douglas Fir-Larch end post have a cataloged capacity of 12.1 kips based on a load duration factor of 1.6. The LRFD capacity of the tie down is computed as follows:

$2ZK_F\phi\lambda = (12.1)(2.88/1.60)(0.65)(1.0) = 14.2$ kips > 9.4 kips   OK

Next, check the LRFD capacity of the bolts in shear. For the three bolts, the AWC NDS gives the following equation:

$3ZK_F\phi\lambda = 3(2.86)(3.32)(0.65)(1.0) = 18.5$ kips > 9.4 kips   OK

The strength of the end post, based on failure across the net section, must also be checked. Try a 6×6 Douglas Fir-Larch No. 1 end post. Accounting for 1-1/16-inch bolt holes, the net area of the post is 24.4 in^2. Using $\phi = 1.0$ for nominal strength, according to the AWC NDS Supplement:

$F_t' = F_tK_F\phi\lambda = (0.825)(2.70)(1.0)(1.0) = 2.228$ ksi

$T' = F_t'A = 2.228(24.4) = 54.4$ kips > 9.4 kips   OK

Not shown here but recommended, AWC NDS non-mandatory Appendix E provides a check for tear-out of a group of bolts and a row of bolts.

For the maximum compressive load at the end post, combine the maximum gravity load plus the seismic overturning load. Using the load combination that has been used for the tension force, C is calculated as:

$C = 9.4 + 0.72(25.63) = 27.85$ kips

The compression load also needs to be checked using the other applicable combination with $1.2D + 1.0$ $Q_E + 0.5L + 0.2S$. When this equation is used, the resisting moment needs to be recalculated. Using D=25.63, L=15.00 and S=6.25, the resisting moment is:

$(1.38(25.63)+0.5(15.00)+0.2(6.25))(12.5) = 552$ ft-kips.

This is larger than the overturning moment of 460 ft-kips, so there is no net uplift. The minimum dead load that needs to be mobilized to resist the overturning moment is 460 ft-kips/ 12.5 ft = 36.8 kips. Using a free body diagram that balances overturning and resisting moments, this will be the vertical reaction, C. And so the controlling value of C is 36.8 kips

Due to the relatively short clear height of the post, the governing condition is bearing perpendicular to the grain on the bottom plate. Check the bearing of the 6×6 end post on a 3×6 Douglas Fir-Larch No. 2 plate, per the AWC NDS Supplement:

$F'_{c\perp} = F_{c\perp}K_F\phi\lambda = (0.625)(1.67)(0.9)(1.0) = 0.94$ ksi

$C' = F'_{c\perp}A = 0.94(5.5)(5.5) = 28.4$ kips < 36.8 kips   NG

While the 6x6 post alone does not have the required compression capacity, when installed in the framed wall it will have one or two 2x6 studs in the immediate vicinity that can share this compression load. Alternately a single 6x8 or two 4x6 posts could be provided.

14.1.4.3.4 Check Overturning at the Soil Interface. A summary of the overturning forces is shown in Figure 14.1-8. An overturning calculation at the soil to structure interface is usually used to check that soil bearing pressures do not exceed those permitted by the geotechnical report. As a first pass the soil bearing can be checked considering only the strip of footing immediately below the shear wall; if this

results in unacceptably high bearing stresses, the contribution of foundations on perpendicular walls can be considered. To compute the overturning at the soil interface, the overturning moment must be increased for the 4-foot foundation height:

$M_0 = 460 + 30.9(4.0) = 584$ ft-kip
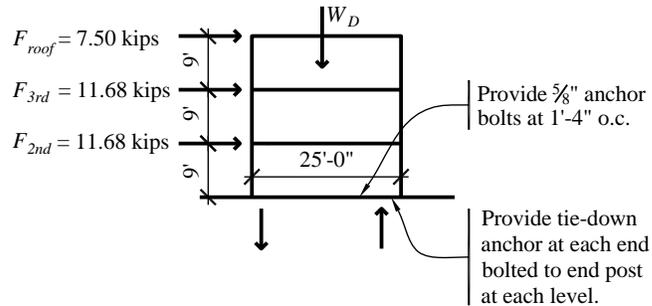
Figure 14.1-8 Transverse wall: overturning
(1.0 ft = 0.3048 m, 1.0 in. = 25.4 mm, 1.0 kip = 4.45 kN)

However, it then may be reduced in accordance with *Standard* Section 12.14.8.4:

$M_0 = 0.75(584) = 436$ ft-kip

To determine the total resistance, combine the weight above with the dead load of the first floor and foundation.

Load from first floor = (25 ft) (10 ft) (20-4+1) psf / 1,000 = 4.25 kips

where 4 psf is the weight reduction due to the absence of a ceiling and 1 psf is the weight of insulation.

The length of the longitudinal foundation wall included is a conservative approximation of the amount that can be engaged assuming minimum nominal reinforcement in the foundation.

Foundation weight = (690 plf [10 ft +10 ft + 25 ft])/1,000 = 31.05 kips
First floor = 4.25 kips
Structure above = 25.63 kips
Σ = 60.93 kips

An exception to Standard Section 12.14.3.1.2 permits the vertical component of earthquake loading to be taken as zero when checking the soil-structure interface, so the resisting weight is multiplied by 0.9, consistent with the basic load combination. Therefore, $0.9D - 1.0Q_E = 0.9(60.93)(12.5$ ft$) - 1.0(436) = 249$ ft-kips. The centroid and soil bearing pressures can be calculated as:

$x = 249/ 60.93 = 4.1$ ft

$f_{SOIL} = 2(60.93)/3(4.1) = 9.9$ klf

With a foundation width of 3.0 ft, this would give a soil bearing pressure of 3.3 ksf, which can be checked against the geotechnical report allowable. Note that this bearing pressure was calculated using strength level forces, and should therefore be checked against strength level soil allowable pressures.

14.1.4.3.5 Anchor Bolts for Shear. At the first floor, the unit shear demand, *v,* is 1.236 klf.

Try 5/8-inch bolts in a 3×6 Douglas Fir-Larch sill plate, in single shear, parallel to the grain. In accordance with the AWC NDS:

$ZK_F\phi\lambda = (1.18)(3.32)(0.65)(1.0) = 2.54$ kips per bolt

The required bolt spacing is 2.54/(1.236/12) = 24.7 in. Therefore, provide 5/8-inch bolts at 16 inches on center to match the joist layout.

AWC SDPWS Section 4.3.6.4.3 requires plate washers at all shear wall anchor bolts and where the nominal unit shear capacity exceeds 400 plf, the plate washer needs to extend within 1/2 inch of the edge of the plate on the side with the sheathing. For sill plates greater than four-inch nominal width, this can either be accomplished by offsetting the anchor bolts and using standard 3-inch square plate washers, or by centering the anchor bolts and using larger 4.5-inch-square plate washers.

Note that the IBC Section 1905.1.8 permits use of 5/8-inch anchor bolts in wood sills based on the AWC NDS capacity, without requiring bolt capacity in the concrete foundation wall to be checked based on ACI 318 Appendix D.

14.1.4.6 Remarks on Shear Wall Connection Details. In typical platform frame construction, details must be developed that will transfer the lateral loads through the floor system and, at the same time, accommodate normal material sizes and the cross-grain shrinkage in the floor system. The connections for wall overturning in Section 14.1.4.5 are an example of one of the necessary force transfers. The transfer of diaphragm shear to supporting shear walls is another important transfer, as is the transfer from a shear wall on one level to the level below.

The floor-to-floor height is 9 feet with approximately 1 foot occupied by the floor framing. Using standard 8-foot-long plywood sheets for the shear walls, a gap occurs over the depth of the floor framing. It is common to use the floor framing to transfer the lateral shear force. Figures 14.1-9 and 14.1-10 depict this accomplished by nailing the plywood to the bottom plate of the shear wall, which is nailed through the floor plywood to the double 2×12 chord in the floor system.

Wall edge nailing

Floor edge nailing

2-2x12 chord for diaphragm

Where shear forces are small, sheet metal framing clips may be replaced by toe-nailing the 2-2x12 chord to the wall top plate

Bottom plate nailing to develop capacity of shear wall

Joists at 16" o.c. toe-nailed to wall plate with 2-8d

2x12 blocking between joists toe-nailed to wall plate with 2-16d and to 2-2x12 chord with 2-16d

Provide sheet metal framing clips (under blocking) to connect 2-2x12 chord to wall top plate

Figure 14.1-9 Bearing wall
(1.0 in = 25.4 mm)

Wall and floor nailing as in bearing wall detail (Figure 11.1-9)

Framing clip or alternate toe nailing as in bearing wall detail (Figure 11.1-9)

8d at 6" o.c. into blocking

2x12 joists

Sheet metal strap connecting blocks across bottom of joists

2x12 blocking between joists at 4'-0" o.c. extending inward from wall to third joist and toe-nailed to each joist with 2-8d and to wall plate with 2-16d. Connect across joist with sheet metal strap and 2-10d each side. Remainder of blocking at plywood joists to be 2x3 lumber.

Figure 14.1-10 Nonbearing wall
(1.0 in. = 25.4 mm)

The top plate of the lower shear wall also is connected to the double 2×12 by means of sheet metal framing clips to the double 2×12 to transfer the force back out to the lower plywood. (Where the forces

are small, toe nails between the double 2×12 and the top plate may be used for this connection.) This technique leaves the floor framing free for cross-grain shrinkage.

The floor plywood is nailed directly to the framing at the edge of the floor, before the plate for the upper wall is placed. Also, the floor diaphragm is connected directly to framing that spans over the openings between shear walls. The axial strength and the connections of the double 2×6 top plates, allows them to function as collectors to move the force from the full length of the diaphragm to the discrete shear walls. It is also common to use the top plates as diaphragm chords. (According to *Standard* Sec. 12.14.7.3, the design of collector elements in wood shear wall buildings need not consider increased seismic demands due to overstrength.)

The floor joist is toe nailed to the wall below for forces normal to the wall. Likewise, full-depth blocking is provided adjacent to walls that are parallel to the floor joists, as shown in Figure 14.1-10. (Elsewhere, the blocking for the floor diaphragm (where required) only need be small pieces, flat 2×4s for example.) The connections at the foundation are similar (see Figure 14.1-11).

Labels in figure:
- Bottom plate nailing
- Wall edge nailing
- Flashing, sheathing, and finish siding not shown
- 2x12 joist toe-nailed to sill with 3-16d
- 2x12 blocking between joists. Connect to sill with sheet metal framing clips.
- 3x6 sill, dense, treated
- ⅝" dia. anchor bolt at 2'-8" or 1'-4" o.c. w/ plate washer
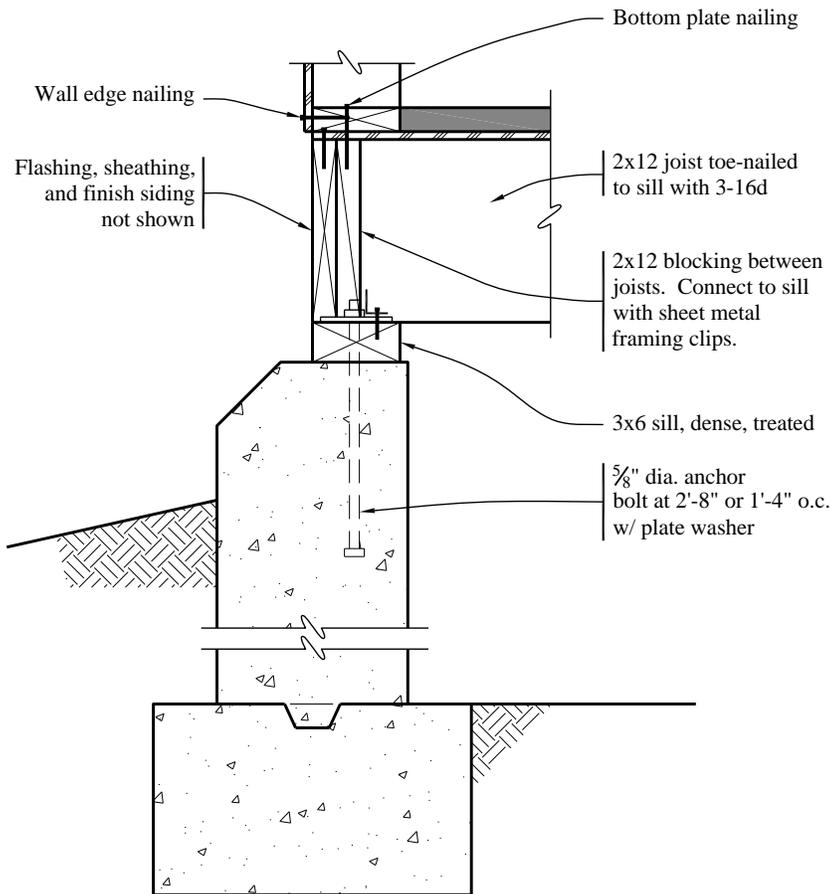
Figure 14.1-11 Foundation wall detail
(1.0 in. = 25.4 mm)

The particular combinations of nails and bent steel framing clips shown in Figures 14.1-9, 14.1-10 and 14.1-11 to accomplish the necessary force transfers are not the only possible solutions. A great amount of leeway exists for individual preference, as long as the load path has no gaps. Common carpentry practices often will provide most of the necessary transfers, but careful attention to detailing and inspection is an absolute necessity to ensure a complete load path.

14.1.4.5 Roof Diaphragm. Common practice is to design plywood diaphragms as simply supported beams spanning between shear walls. The design will be based on the shears associated with the tributary area distribution of force to the shear walls.

From Section 14.1.3.4, the diaphragm design force at the roof is the same as the roof story force, so $F_{P,roof}$ = 30.0 kips.

As discussed previously, the design force computed in this example includes the internal force due to the weight of the walls parallel to the motion. Particularly for concrete or masonry wall buildings, it is common practice to remove that portion of the design force. It is conservative to include it, as is done here.

14.1.4.5.1 Diaphragm Nailing. For transverse loading, idealizing the building as a two-span diaphragm with three sets of walls as described previously, the maximum diaphragm shear occurs at the ends of the 88-foot diaphragm span. Assuming a uniform distribution of the diaphragm force across the building, the maximum shear over the entire diaphragm width is computed as follows:

$V = (30.0)(88/148)/2 = 8.93$ kips

$v = 8.93 / 56$ ft $= 0.160$ klf

Try 15/32-inch plywood rated sheathing (not Structural I) on unblocked 2-inch Douglas Fir-Larch members at 16 inch on center, with 8d nails at 6 inches on center at all boundaries and panel edges and 12 inches on center at intermediate framing members, and Case 1 for sheathing layout. From AWC SDPWS Table 4.2C, this diaphragm assembly has a nominal unit shear capacity, v_s, of 0.480 klf. The adjusted shear capacity is computed as follows:

$\phi_D v_s = 0.8(0.480) = 0.384$ klf > 0.160 klf   OK

14.1.4.5.2 Chord and Splice Connection. Diaphragm continuity is an important factor in the design of the chords. The design must consider the tension/compression forces, due to positive moment at the middle of the span. It is common to design the chord for the positive moment assuming a simply supported beam. The positive moment is $wl^2/8$, where w is the unit diaphragm force and l is the length of the governing diaphragm span. It is also common practice to provide this chord capacity over the full length of the chord, allowing for the possibility of negative moment in the diaphragm where supported by interior shear walls.

For $w = 30.0$ kips $/ 148$ ft $= 0.203$ klf, the maximum positive moment is:

$0.203(88)^2 / 8 = 197$ ft-kip

The design chord force is 197/56 = 3.51 kips. Try the double 2×6 Hem-Fir No. 2 top plates. Due to staggered splices, compute the tension capacity based on a single 2×6, with an area of $A_n = 8.25$ in^2. According to the AWC NDS Supplement:

$F_t' = F_t C_F K_F \phi \lambda = (0.525)(1.3)(2.70)(0.8)(1.0) = 1.47$ ksi

$T' = F_t'A = 1.47(8.25) = 12.1$ kips > 3.51 kips   OK

For chord splices, use 16d nails in the staggered chord members. According to the AWC NDS, the capacity of one 16d common wire nail in single shear with two 2× Hem-Fir members is 0.122 kips. The adjusted strength per nail is:

$Z' = ZK_F \phi \lambda = (0.122)(3.32)(0.65)(1.0) = 0.263$ kips

The number of required nails at the splice is 3.51/0.263 = 13.3, so use 14 16d nails. Assuming a 4-foot splice length, provide two rows of 16d nails at 6 inches on center each row at each lap in the top plate. A typical chord splice connection is shown in Figure 14.1-12.
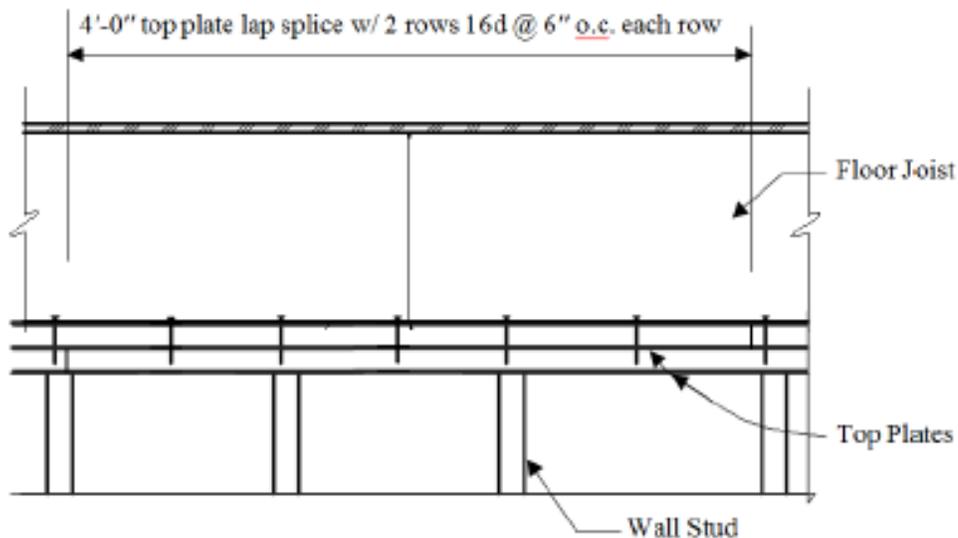
Figure 14.1-12 Diaphragm chord splice
(1.0 ft = 0.3048 m, 1.0 in. = 25.4 mm)

14.1.4.6 Second- and Third-Floor Diaphragm. The design of the second- and third-floor diaphragms follows the same procedure as for the roof diaphragm. From Section 10.1.3.4, the diaphragm design force for both floors is $F_{p,3rd} = F_{p,2nd} = 46.7$ kips.

14.1.4.6.1 Diaphragm Nailing. The maximum diaphragm shear is computed as follows:

$V = (46.7)(88/148)/2 = 13.88$ kips

$v = 13.88 / 56$ ft $= 0.248$ klf

With an adjusted capacity of 0.384 klf, the same diaphragm as at the roof also works for the floors. Note that the floor sheathing is not likely to be less than 19/32-inch for gravity load purposes.

14.1.4.6.2 Chord and Splice Connection. Computed as described above for the roof diaphragm, the maximum positive moment is 306 ft-kips and the design chord force is 5.48 kips.

By inspection, a double 2×6 top plate chord spliced with 16d nails similar to the roof level is adequate. The number of nails at the floors is 5.48/0.263 = 22 nails, so for the 4-foot splice length, provide two rows of nine 16d nails at 3 inches on center on each side of the splice joint.

14.1.4.7 Longitudinal Direction. Only one exterior shear wall section will be designed here. The design of the corridor shear walls would be similar to that of the transverse walls. For loads in the longitudinal direction, diaphragm stresses are negligible and the nailing provided for the transverse direction is more than adequate.

AWC Section 4.3.5 identifies three distinct types of shear walls. The type to be used in a particular design must be selected and the wall designed consistent with the requirements of the chosen type. The design of the exterior wall utilizes the provisions for perforated shear walls as defined in AWC SDPWS Section 4.3.5.3. The procedure for perforated shear walls applies to walls that encompass openings and that have not been specifically designed and detailed for force transfer around the openings (as per Section 4.3.5.2). Essentially, a perforated wall is treated in its entirety rather than as a series of discrete wall piers. The use of this design procedure is limited by several conditions as specified in AWC SDPWS Section 4.3.5.3.

The main aspects of the perforated shear wall design procedure are as follows. The design shear capacity of the shear wall is the sum of the capacities of each segment (all segments must have the same sheathing and nailing) reduced by an adjustment factor that accounts for the geometry of the openings. Uplift anchorage (tie-down) is required only at the ends of the wall (not at the ends of all wall segments), but all wall segments must resist a specified unit uplift force per foot of wall length (using anchor bolts at the foundation and strapping or other means at upper floors). Requirements for shear anchorage and collectors (drag struts) across the openings are also specified. It should be taken into account that the design capacity of a perforated shear wall is less than that of a standard segmented wall with all segments fully restrained against overturning (as per Section 4.3.5.1). However, the procedure is useful in eliminating interior hold downs for specific conditions and thus is illustrated in this example. In the perforated shear wall methodology, the end pier that has a tie-down is effectively fully restrained for overturning, while other interior piers are partially restrained and therefore have lower unit shears.

The portion of the story force resisted by each exterior wall was computed previously as $0.223F_x$. The exterior shear walls are composed of three separate perforated shear wall segments (two at 30 feet long and one at 15 feet long, all with the same relative length of full-height sheathing), as shown in Figure 14.1-2. This section will focus on the design of a 30-foot section. Assuming that load is distributed to the wall sections based on relative length of the shear panel, then the total story force to the 30-foot section is $(30/75)0.223F_x = 0.089F_x$ per floor. The load per floor is:

$$F_{roof} = 0.089(30.0) \quad = \quad 2.67 \text{ kips}$$
$$F_{3rd} = 0.089(46.7) \quad = \quad 4.16 \text{ kips}$$
$$F_{2nd} = 0.089(46.7) \quad = \quad \underline{4.16 \text{ kips}}$$
$$\Sigma \quad\quad\quad\quad\quad\quad = 10.99 \text{ kips}$$

This approach is consistent with the concept of AWC SDPWS Section 4.3.3.4, Exception 2, which within limits allows seismic force to be distributed amongst shear walls in a line in proportion to shear capacity.

14.1.4.7.1 Perforated Shear Wall Resistance. The design shear capacity for perforated shear walls is computed as the factored shear resistance for the sum of the wall segments, multiplied by an adjustment factor that accounts for the percentage of full-height (solid) sheathing and the ratio of the maximum

opening to the story height as described in AWC SDPWS Section 4.3.3.5. At each level, the design shear capacity, V_{wall}, is:

$$V_{wall} = (vC_0)\Sigma L_i$$

where:

> v = factored shear resistance (AWC SDPWS Table 4.3A)
> C_0 = shear capacity adjustment factor (AWC SDPWS Table 4.3.3.5)
> ΣL_i = sum of shear wall segment lengths

For the subject wall, the widths of perforated shear wall segments are 4+10+4 = 18 feet, the percent of full-height sheathing is 18/30 = 0.60 and the maximum opening height is 4 feet. Therefore, per AWC SDPWS Table 4.3.3.5, $C_0 = 0.83$.
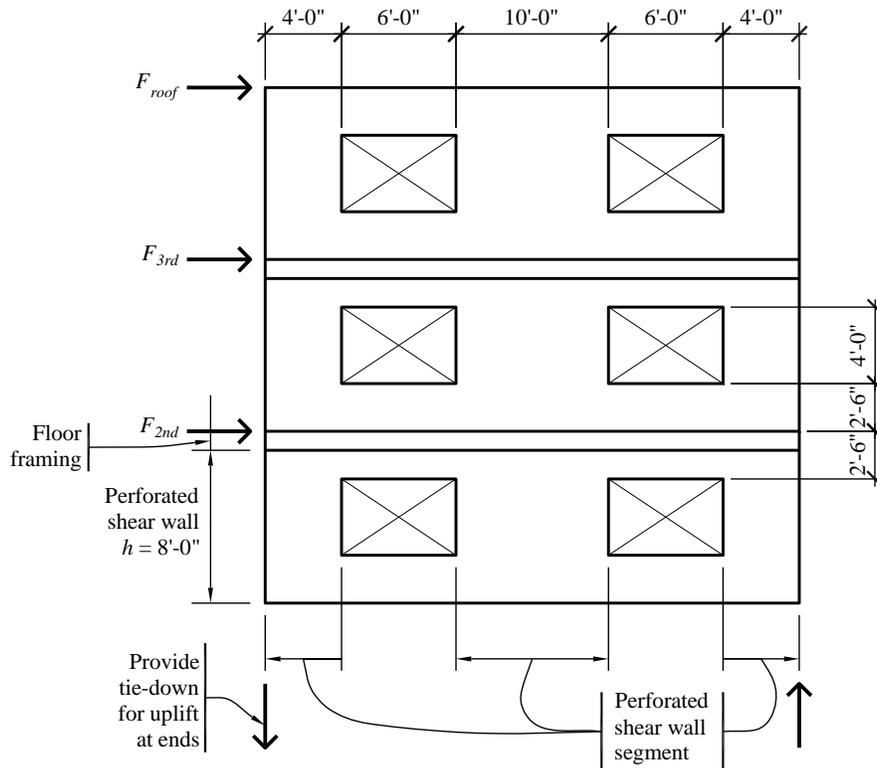
Figure 14.1-13 Perforated shear wall at exterior
(1.0 ft = 0.3048 m, 1.0 in. = 25.4 mm)

The wall geometry (and thus the adjustment factor and total length of wall segments) is the same at all three levels, as shown in Figure 14.1-13. Perforated shear wall plywood and nailing are determined below.

> Roof to third floor:

$V = 2.67$ kips

Required $v = 2.67/0.83(18) = 0.179$ klf

Try 15/32-inch plywood rated sheathing (not Structural I) on blocked 2× Hem-Fir members at 16 inches on center with 8d nails at 6 inches on center at panel edges and at 12 inches on center at intermediate framing members. From AWC SDPWS Table 4.3A, this shear wall assembly has a nominal unit shear capacity, v_s, of 0.520 klf. Adjusting for framing material, the shear capacity is computed as follows:

$0.93\phi_D v_s = 0.93(0.8)(0.520) = 0.387$ klf > 0.179 klf   OK

Third floor to second floor:

$V = 2.67 + 4.16 = 6.83$ kips

Required $v = 6.83/0.83(18) = 0.457$ klf

Try 15/32-inch plywood rated sheathing (not Structural I) on blocked 2× Hem-Fir members at 16 inches on center with 8d nails at 4 inches on center at panel edges and at 12 inches on center at intermediate framing members. From AWC SDPWS Table 4.3A, this shear wall assembly has a nominal unit shear capacity, v_s, of 0.760 klf. Adjusting for framing material, the shear capacity is computed as follows:

$0.93\phi_D v_s = 0.93(0.8)(0.760) = 0.565$ klf > 0.457 klf   OK

Second floor to first floor:

$V = 6.83 + 4.16 = 10.99$ kips
Required $v = 10.99/0.83(18) = 0.735$ klf

Try 15/32-inch plywood rated sheathing (not Structural I) on blocked 2× Hem-Fir members at 16 inches on center with 10d nails at 3 inch on center at panel edges and at 12 inch on center at intermediate framing members. From AWC SDPWS Table 4.3A, this shear wall assembly has a nominal unit shear capacity, v_s, of 1.200 klf. Adjusting for framing material, the shear capacity is computed as follows:

$0.93\phi_D v_s = 0.93(0.8)(1.200) = 0.893$ klf > 0.735 klf   OK

Note that the nominal unit shear capacity of 1.200 klf is less than the maximum permitted nominal shear capacity of 1.740 klf in accordance with AWC SDPWS Section 4.3.5.3, Item 3.

14.1.4.7.2 Perforated Shear Wall Tension Chord. According to AWC SDPWS Section 4.3.6.1.2, compression chords and associated anchorage must be evaluated at the ends of the wall only. Compression chords are required to be provided at each end of each wall segment. Uplift anchorage at each wall segment is treated separately as described later. The tension and compression forces due to overturning uplift forces at the wall ends are determined per AWC SDPWS Equation 4.3-8 as follows:

$$T = C = \frac{Vh}{C_0 \sum L_i}$$

where:

V = design shear force in the shear wall
h = shear wall height (per floor)
C_0 = shear capacity adjustment factor
ΣL_i = sum of widths of perforated shear wall segments

Unlike the transverse shear wall that is designed considering global overturning and resisting dead load, each wall pier on the perforated shear wall overturns locally with varying degrees of overturning restraint provided by sheathing above and below openings and by the wall unit tension anchorage. Although it is conservative to neglect overturning resistance, it is reasonable to credit some local overturning restraint due to dead load.

For this example, the tension chord and tie-down will be designed at the first floor only; the other floors would be computed similarly and tie-down devices, as shown in Figure 14.1-7, would be used. For h = 8 ft, C_0 = 0.83 and ΣL_i = 18 ft, the tension force is computed as follows:

Third floor: $T = 2.67(8)/(0.83 \times 18)$	= 1.42 kips
Second floor: $T = (2.67 + 4.16)(8)/(0.83 \times 18)$	= 3.66 kips
First floor: $T = (2.67 + 4.16 + 4.16)(8)/(0.83 \times 18)$	= 6.42 kips
Σ	= 11.50 kips

For the dead load to resist the tension chord uplift at the shear wall end, assume a tributary width of 4 feet and the tributary joist span is 8 feet. Rather than distributed load over the length of the wall, as used in the transverse wall calculations, this is simply a concentrated load acting at the tie-down post, and based on judgement of what dead load will be mobilized when this post uplifts. The tributary weight is computed as follows:

Exterior wall weight = (8+8+8 ft)(4 ft)(9 psf)/1,000	= 0.86 kips
Tributary roof = (8 ft)(4 ft)(15 psf)/1,000	= 0.48 kips
Tributary floor = (8 ft)(4 ft)(20 psf)(2)/1,000	= 1.28 kips
Σ	= 2.62 kips

The net uplift is computed as follows, simply subtracting the mobilized dead load:

0.72D - 1.0E = 0.72(2.62) - 11.5 = 9.61 kips

Therefore, uplift anchorage is required per AWC SDPWS Section 4.3.6.4.2. Since the chord member resists the perforated shear wall compression load and supports the window header as well, use a 6×6 Douglas Fir-Larch No. 1, similar to the transverse walls. The post has ample tension capacity. For the anchorage, try a double tie-down device with a 7/8-inch anchor bolt and twenty 1/4-inch screws into the post. Using the method described above for computing the strength of a pre-engineered tie-down, the capacity is computed as follows:

$ZK_F\phi\lambda$ = 2(7.87)(3.32)(0.65)(1.0) = 18.4 kips > 9.61 kips   OK

The design of the tie-downs at the second and third floors is similar.

14.1.4.7.3 Perforated Shear Wall Compression Chord. Again, just the chord at the first floor will be designed here; the design at the upper floors would be similar. The force in the compression chord can be

most simply taken equal to the gross uplift of 11.5 kips at the first floor if a post is provided for this reaction in addition to the framing that carries gravity loads. If the uplift critical equation is used, C can be computed as:

C = 9.61 + 0.72(2.62) = 11.5 kips

Using the load combination $1.38D + 1.0Q_E + 0.5L + 0.2S$, with live load and snow load as 1.92 kips and 0.60 kips, respectively, the resisting load, tension load and compression loads are calculated as:.

1.38(2.62) + 0.5(1.92) + 0.2(0.60) = 4.69 kips

T = 11.5 - 4.69 = 6.81 kips

C = 6.81 + 4.69 = 11.5 kips

The bearing capacity on the bottom plate was computed previously as 28.4 kips, which is greater than 11.5 kips. Note that where end posts are loaded in both directions, the simplified method exempts the design from complying with the orthogonal effects of Standard Section 12.5.

14.1.4.7.4 Anchorage at Shear Wall Segments. The anchorage at the base of a shear wall segment (bottom plate to floor framing or foundation wall) is designed per AWC SDPWS Section 4.3.6.4. This section requires two types of anchorage: in-plane shear anchorage (AWC SDPWS Sec. 4.3.6.4.1.1) and distributed uplift anchorage (AWC SDPWS Sec. 4.3.6.4.1.2). While both types of anchorage need only be provided at the full-height sheathing, the shear anchorage is usually extended at least over the entire length of the perforated shear wall to simplify the detailing and reduce the possibility of construction errors.

The in-plane shear anchorage is required to resist the following:

$$v = \frac{V}{C_0 \sum L_i}$$

where:

V = design shear force in the shear wall
C_0 = shear capacity adjustment factor
ΣL_i = sum of widths of perforated shear wall segments

This equation is the same as was previously used to compute unit shear demand on the wall segments. Therefore, the in-plane anchorage will be designed to meet the following unit, in-plane shear forces:

Third floor: $v = 0.179$ klf

Second floor: $v = 0.457$ klf

First floor: $v = 0.735$ klf

The required distributed uplift force, t, is equal to the in-plane shear force, v. Per AWC SDPWS Section 4.3.6.4, this uplift force must be provided with a complete load path to the foundation. That is,

the uplift force at each level must be combined with the uplift forces at the levels above (similar to the way overturning moments are accumulated down the building).

At the foundation level, the unit in-plane shear force, v and the unit uplift force, t, are combined for the design of the bottom plate anchorage to the foundation wall. The design unit forces are as follows:

Shear: $v = 0.735$ klf

Tension: $t = 0.179 + 0.457 + 0.735 = 1.371$ klf

Assuming that stresses on the wood bottom plate govern the design of the anchor bolts, the anchorage is designed for shear (single shear, wood-to-concrete connection) and tension (plate washer bearing on bottom plate). The interaction between shear and tension need not be considered in the wood design for this configuration of loading.

Try a 5/8-inch bolt at 32 inches on center with a 4.5-inch square plate washer (AWC SDPWS Section 4.3.6.4.3 requires plate washer to extend within 1/2 inch of the 5.5-inch-wide bottom plate). As computed previously, the shear capacity of a 5/8-inch bolt in a 3×6 Douglas Fir-Larch sill plate is 2.54 kips. The demand per bolt is 0.735 klf (32/12) = 1.96 kips, so the 32-inch spacing is adequate for shear.

For anchor bolts at 32 inches on center, the tension demand per bolt is 1.371 klf (32/12) = 3.66 kips. Bearing capacity of the plate washer (using a Douglas Fir No. 2 bottom plate) is computed per AWC NDS Supplement as follows:

$F'_{c\perp} = F_{c\perp}K_F\phi\lambda = (0.625)(1.67)(0.9)(1.0) = 0.94$ ksi

$C' = F'_{c\perp}A = 0.94(4.5)(4.5) = 19.0$ kips > 3.66 kips   OK

In addition to designing the anchor bolts for uplift, a positive load path must be provided to transfer the uplift forces into the bottom plate. One method for providing this load path continuity is to use metal straps nailed to the studs and lapped around the bottom plate, as shown in Figure 14.1-14. Attaching the studs directly to the foundation wall (using embedded metal straps) for uplift and using the anchor bolts for shear only is an alternative approach.

Nail to stud

Metal strap used to resist uplift, lapped under sill plate.

$\frac{5}{16}$x4$\frac{1}{2}$x4$\frac{1}{2}$ steel plate washer at anchor bolt

$\frac{5}{8}$" dia. anchor bolt at 2'-8" o.c. (Used to resist shear and tension)
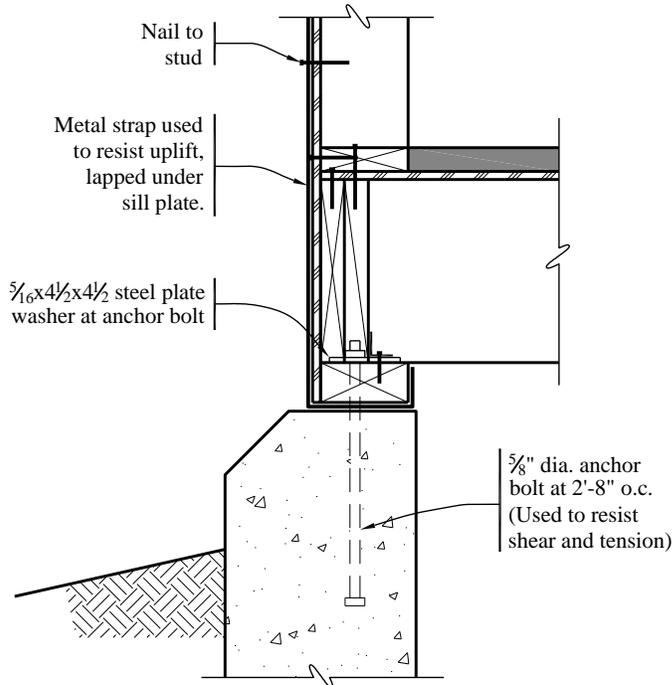
Figure 14.1-14 Perforated shear wall detail at foundation
(1.0 ft = 0.3048 m, 1.0 in. = 25.4 mm)

At the upper floors, the load transfer for in-plane shear is accomplished by using nailing or framing clips between the bottom plates, rim joists and top plates in a manner similar to that for standard shear walls. The uniform uplift force can be resisted either by using the nails in withdrawal (for small uplift demand), providing screws in withdrawal, or by providing vertical metal strapping between studs above and below the level considered. This type of connection is shown in Figure 14.1-15. For this type of connection (and the one shown in Figure 14.1-14) to be effective, shrinkage of the floor framing must be minimized using dry or manufactured lumber.
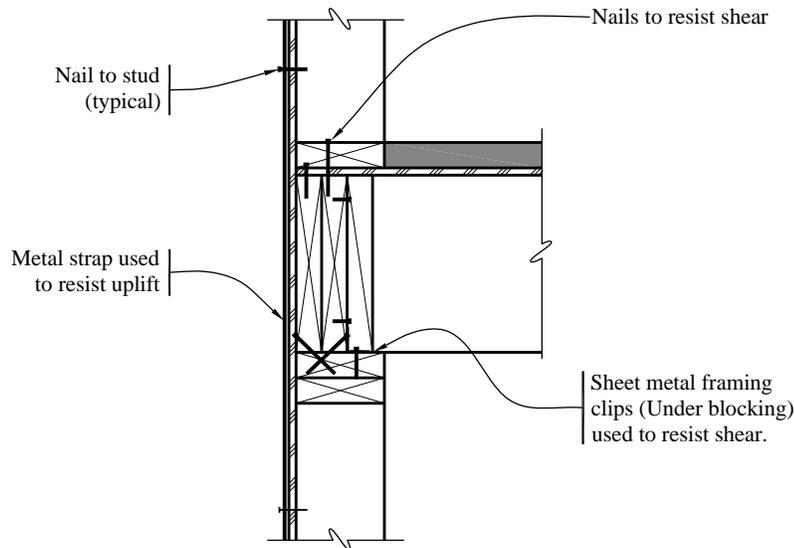
Figure 14.1-15 Perforated shear wall detail at floor framing

For example, consider the second floor. The required uniform uplift force, $t = 0.244+0.496 = 0.740$ klf. Place straps at every other stud, so the required strap force is $0.740(32/12) = 1.97$ kips. Provide an 18-gauge strap with twelve 10d nails at each end.

14.2 WAREHOUSE WITH MASONRY WALLS AND WOOD ROOF

This example features the design of the wood roof diaphragm and wall-to-diaphragm anchorage for the one-story masonry building described in Section 13.1 of this volume of design examples. Refer to that example for more detailed building information and the design of the masonry walls.

14.2.1 Building Description

This is a very simple rectangular warehouse, 100 feet by 200 feet in plan (see Figure 14.2-1), with a roof height of 28 feet. The wood roof structure slopes slightly, but it is nominally flat. The long walls (side walls) are 8 inches thick and solid and the shorter end walls are 12 inches thick and penetrated by several large openings.
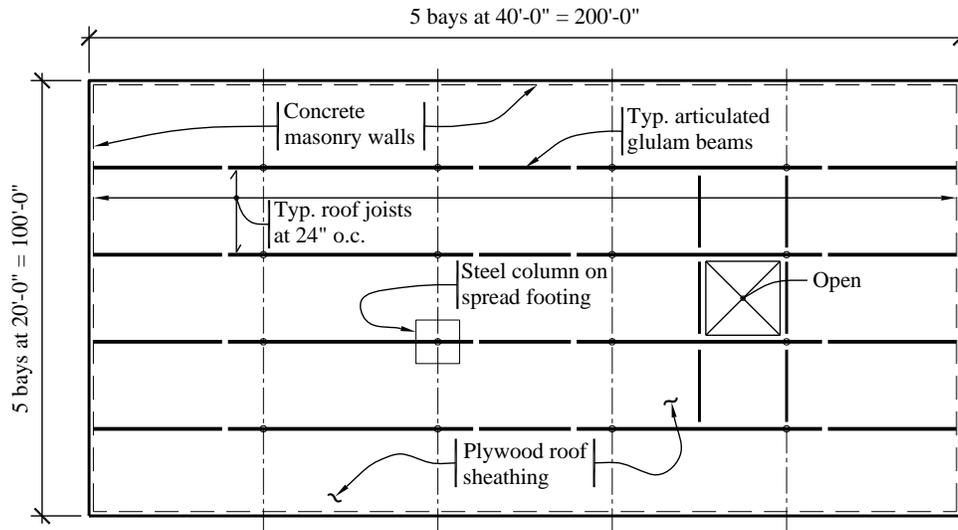
Figure 14.2-1 Building plan
(1.0 ft = 0.3048 m, 1.0 in. = 25.4 mm)

Based on gravity loading requirements, the roof structure consists of wood joists, supported by 8-3/4-inch-wide by 24-inch-deep glued-laminated timber beams on steel columns. The joists span 20 feet and the beams span 40 feet, as an articulated system. Typical roof framing is assumed to be Douglas Fir-Larch No 1 as graded by the WWPA Rules. The glued-laminated timber beams meet the requirements of Combination 24F-V4 per AITC A190.1.

The plywood roof deck acts as a diaphragm to carry lateral loads to the exterior walls. There are no interior walls for seismic resistance. The roof contains a large opening that interrupts the diaphragm continuity. The diaphragm contains continuous cross ties in both principal directions that serve as part of the wall anchorage system.

The following aspects of the structural design are considered in this example:

Development of diaphragm forces based on the Equivalent Lateral Force Procedure used for the masonry wall design (Sec. 13.1)

Design and detailing of a plywood roof diaphragm with a significant opening

Computation of drift and P-delta effects

Anchorage of masonry walls to diaphragm and roof joists

Design of continuous ties and subdiaphragms as part of the wall anchorage system

14.2.2 Basic Requirements
14.2.2.1 Seismic Parameters

Table 14.2-1 Seismic Parameters

Design Parameter	Value
S_S	2.14
S_1	0.74
Site Class (*Standard* Sec. 11.4.2)	C
Occupancy Category (*Standard* Sec. 1.5.1)	II
Seismic Design Category (*Standard* Sec. 11.6)	D
Seismic Force-Resisting System (*Standard* Table 12.2-1)	Special Reinforced Masonry Shear Walls
Response Modification Factor, R	5
System Overstrength Factor, Ω_0	2.5
Deflection Amplification Factor, C_d	3.5

14.2.2.2 Structural Design Criteria. A complete discussion on the criteria for ground motion, seismic design category, load path, structural configuration, redundancy, analysis procedure and shear wall design is included in Section 13.1 of this volume of design examples.

14.2.2.2.1 Design and Detailing Requirements. Since this building has a wood structural panel diaphragm with masonry shear walls, the diaphragm can be considered flexible in accordance with *Standard* Section 12.3.1.1. There are not any irregularities (*Standard* Sec. 12.3.2) that would impact the diaphragm design and the diaphragm and wall anchorage system is permitted to be designed with the redundancy factor equal to 1.0 per *Standard* Section 12.3.4.1.

The design of the diaphragm is based on *Standard* Section 12.10. This example will first illustrate diaphragm forces using the traditional method of Sections 12.10.1 and 12.10.2, and then illustrate the alternative provisions for diaphragms of Section 12.10.3. The large opening in the diaphragm must be provided with boundary elements (*Standard* Sections 12.10.1 and 12.10.3). However, the diaphragm does not require any collector elements that would have to be designed for the special load combinations (*Standard* Section 12.10.2.1).

The requirements for anchorage of masonry walls to flexible diaphragms (*Standard* Section 12.11.2) are of great significance in this example.

14.2.2.2.2 Seismic Load Effects and Combinations. The basic design load combinations for the seismic design, as stipulated in *Standard* Section 12.4.2.3, were computed in Section 13.1 of this volume of design examples, as follows:

$$1.486D + 1.0Q_E$$

where gravity and earthquake are additive and

$0.614D - 1.0Q_E$

where gravity and earthquake counteract.

The roof live load, L_r, is not combined with seismic loads (see *Standard* Chapter 2) and the design snow load is zero for the location of the structure.

14.2.2.2.3 Deflection and Drift Limits. In-plane deflection and drift limits for the masonry shear walls are considered in Section 13.1.

As illustrated below, the diaphragm deflection is much greater than the shear wall deflection. According to *Standard* Section 12.12.2, in-plane diaphragm deflection must not exceed the permissible deflection of the attached elements. Because the walls are essentially pinned at the base and simply supported at the roof, they are capable of accommodating large deflections at the roof diaphragm.

For illustrative purposes, story drift is determined and compared to the requirements of *Standard* Table 12.12-1. However, according to this table, there is essentially no drift limit for a single-story structure as long as the architectural elements can accommodate the drift (assumed to be likely in a warehouse structure with no interior partitions). As a further check on the deflection, P-delta effects (*Standard* Sec. 12.8.7) are evaluated.

14.2.3 Seismic Force Analysis

14.2.3.1 Diaphragm Design Forces (Traditional Method Section 12.10.1 and 12.10.2). Building weights and base shears are as computed in Section 13.1. (The building weights used in this example are based on a preliminary version of Example 13.1 and thus minor numerical differences may exist between the two examples). *Standard* Section 12.10.1.1 specifies that floor and roof diaphragms be designed to resist a force, F_{px}, computed in accordance with *Standard* Equation 12.10-1 as follows:

$$F_{px} = \frac{\sum\limits_{i=x}^{n} F_i}{\sum\limits_{i=x}^{n} w_i} w_{px}$$

plus any force due to offset walls (not applicable for this example). For one-story buildings, the first term of this equation will be equal to the seismic response coefficient, C_s, which is 0.286. The effective diaphragm weight, w_{px}, is equal to the weight of the roof plus the tributary weight of the walls perpendicular to the direction of the motion. The tributary weights acting at the roof for seismic forces are as follows:

Roof = 20(100)(200) = 400 kips

Side walls = 2(65)(200 ft)(15 ft/28 ft.) = 418 kips

End walls = 2(105)(100 ft)(17.8 ft/28 ft) = 393 kips

The diaphragm design force for this building simplifies to:

Transverse: $F_{p,roof}$ = 0.286(400+418) = 234 kips

Longitudinal: $F_{p,roof}$ = 0.286(400+393) = 226 kips

These forces equal the minimum diaphragm design forces given in *Standard* Section 12.10.1.1, because C_s equals the minimum factor of $0.2S_{DS} = 0.2(1.43) = 0.286$.

14.2.3.1 Diaphragm Design Forces (Alternative Method Section 12.10.3). In accordance with Section 12.10 Exception 2, wood sheathed diaphragms supported by wood diaphragm framing are permitted to be designed in accordance with the alternative provisions of Section 12.10.3. This section illustrates use of those alternative provisions. As stated in Section 12.10.3.1, the provisions of Section 12.10.3 apply to diaphragms, chords, collectors and their connections to vertical elements.

The diaphragm design force F_{px} is defined in Equation 12.10-4 as:

$$F_{px} = \frac{C_{px}}{R_s} w_{px}$$

Where C_{px} is defined as C_{pn} in accordance with the left hand portion of *Provisions* Figure 12.10-2 for this one story structure ($N \leq 2$ where N is the number of stories above the base):
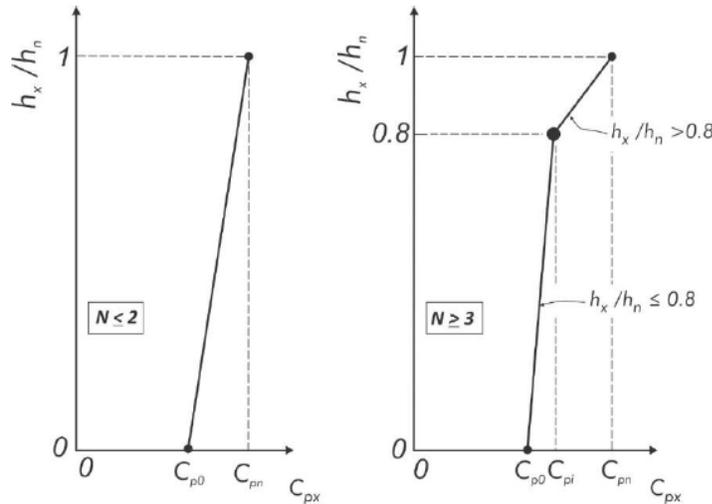
Provisions FIGURE 12.10-2 **Calculating the Design Acceleration Coefficient C_{px} in Buildings with $N \leq 2$ and in Buildings with $N \geq 3$**

It may be noted that, although *Provisions* Figure 12.10-2 differs from the corresponding ACE 7-16 Figure 12.10.3-1 for buildings with $N \geq 3$, there is no difference for buildings with $N \leq 2$.

The variable C_{pn} is defined by Equation 12.10.7 as:

$$C_{pn} = \sqrt{\left(\Gamma_{m1} \Omega_0 C_s\right)^2 + \left(\Gamma_{m2} C_{s2}\right)^2}$$

In order to calculate C_{pn}, the designer must define z_s, Γ_{m1}, and Γ_{m2} in accordance with Sec. 12.10.3.2.1:

$z_s = 1.0$ (for buildings with seismic force-resisting systems other than Buckling Restrained Braced Frame systems, Moment-Resisting Frame systems, and Dual systems)

$$\Gamma_{m1} = 1 + \frac{z_s}{2}\left(1 - \frac{1}{N}\right)$$

14-36

$$\Gamma_{m2} = 0.9\, z_s \left(1 - \frac{1}{N}\right)^2$$

For this $N=1$ structure, and $z_s = 1.0$, Γ_{m1} is 1 and Γ_{m2} is zero. These answers reflect that there is no higher mode influence on the vertical distribution of forces in a one-story structure, so the full first mode contribution is included by setting Γ_{m1} to 1, while setting Γ_{m2} to zero avoids higher mode contributions.

Finally, in order to determine C_{pn}, the overstrength factor Ω_0 needs to be determined. This was identified at the beginning of this example as 2.5. Note that in accordance with ASCE 7-16, it is no longer permitted to reduce this value by subtracting 0.5 for flexible diaphragms. This was permitted by footnote g to ASCE 7-10 Table 12.2-1.

Using these values, C_{pn} can then be calculated as

$$C_{pn} = \sqrt{\left(\Gamma_{m1}\,\Omega_0\, C_s\right)^2 + \left(\Gamma_{m2}\, C_{s2}\right)^2} = \Gamma_{m1}\Omega_0 C_s = 1.0(2.5)(0.286) = 0.715$$

This diaphragm seismic coefficient represents the seismic demand for near-elastic diaphragm behavior.

The diaphragm force is then calculated based on this value of C_{pn}, and the diaphragm design force reduction factor, R_s, from Table 12.10-1. For wood sheathed diaphragms designed in accordance with AWC's *Special Design Provisions for Wind and Seismic* (SDPWS), the diaphragm is recognized as shear controlled and assigned an R_s factor of 3.0. The R_s factor recognizes the ductility and displacement capacity of wood structural panel diaphragms. Because of overstrength factors inherent in wood design, the development of a flexure-controlled diaphragm is not anticipated. This results in:

$$
\begin{aligned}
F_{px} &= \frac{C_{px}}{R_s} w_{px} \\
&= (0.715 / 2.5)\ w_{px} \\
&= 0.286\ w_{px}
\end{aligned}
$$

For this structure, the diaphragm design force using the alternative procedure results in the same design force as the traditional procedure. The minimum design force for the alternative procedure is the same as for the traditional procedure: $0.2\ S_{DS} = 0.286$.

14.2.4 Basic Proportioning of Diaphragm Elements (Traditional Method, Sec. 12.10.1 and 12.101.2)

The design of plywood diaphragms primarily involves the determination of sheathing sizes and nailing patterns to accommodate the applied loads. Large openings in the diaphragm and wall anchorage requirements, however, can place special requirements on the diaphragm capacity. Diaphragm deflection is also a consideration.

Nailing patterns for diaphragms are established on the basis of tabulated requirements included in the AWC SDPWS. It is important to consider the framing requirements for a given nailing pattern and capacity as indicated in the notes following the tables. In addition to strength requirements, AWC SDPWS Section 4.2.4 places aspect ratio limits on plywood diaphragms (length-to-width must not exceed 4/1 for blocked diaphragms). However, it should be taken into consideration that compliance with this aspect ratio does not guarantee that drift limits will be satisfied.

While there is no specific limitation on deflection for this example, the diaphragm has been analyzed for deflection as well as for shear capacity.

14.2.4.1 Strength of Members and Connections. As described in more detail in Section 14.1.4.1, the *Standard* references the AWC NDS and AWC SDPWS for engineered wood structures. Diaphragm design is based on AWC SDPWS Section 4.2, which provides design criteria for both ASD and LRFD methods. This example utilizes LRFD as the design basis, so the diaphragm design is based on the tabulated unit shear values, v_s, which are multiplied by a resistance factor, ϕ_D, equal to 0.80.

Refer to Section 14.1.4.1 for a summary of the design methodology in the AWC NDS for framing members and connections.

14.2.4.2 Roof Diaphragm Design for Transverse Direction

14.2.4.2.1 Plywood and Nailing. The diaphragm design force is $F_{p,roof} = 234$ kips and the maximum end shear is $0.5F_{p,roof} = 117$ kips. This corresponds to a unit shear force of $v = (117/100) = 1.17$ klf. (Note that per *Standard* Sec. 12.8.4.2, accidental torsion need not be considered for flexible diaphragms.)

Due to the relatively high diaphragm shears, closely spaced nailing will be required, so in accordance with AWC SDPWS Section 4.2.7.1.1, Item 3, 3-inch nominal framing will be provided. Assuming 3-inch nominal framing, try blocked 1/2-inch (15/32) Structural I wood structural panel sheathing with 10d common nails at 2 inches on center at diaphragm boundaries and continuous panel edges and at 3 inches on center at other panel edges. The use of 2×4 flat blocking at continuous panel edges satisfies the requirements for blocked diaphragms. Note that extra care may be required to avoid splitting of the 2x4 flat blocking during edge nail installation. Use of 3x or 4x blocking may reduce this splitting. From AWC SDPWS Table 4.2A:

$$\phi_D v_s = 0.80(1.640) = 1.31 \text{ klf} > 1.17 \text{ klf} \hspace{3cm} \text{OK}$$

Because the diaphragm shear decreases towards the midspan of the diaphragm, the diaphragm capacity may be reduced towards the center of the building. A reasonable configuration for the interior of the building utilizes 2-inch nominal framing and 1/2-inch (15/32) Structural I wood structural panel sheathing with 10d at 4 inches on center at diaphragm boundaries and continuous panel edges and 6 inches on center nailing at other panel edges. Determine the distance, X, from the end wall where the transition can be made, as follows:

$$\phi_D v_s = 0.80(0.850) = 0.68 \text{ klf (AWC SDPWS Table 4.2A)}$$

Shear capacity = $0.68(100) = 68.0$ kips

Uniform diaphragm demand = $233/200 = 1.17$ klf

$X = (117-68)/1.17 = 42.1$ ft (assumed as 50 ft from the diaphragm edge)

In a building of this size, it may be beneficial to further reduce the diaphragm nailing towards the middle of the roof. However, due to the requirements for subdiaphragms (see below) and diaphragm capacity in the longitudinal direction and for simplicity of design, no additional nailing pattern is used.

Table 14.2-1 contains a summary of the diaphragm framing and nailing requirements (all nails are 10d common). See Figure 14.2-2 for designation of framing and nailing zones and Figure 14.2-3 for typical sheathing layout.

Table 14.2-2 Roof Diaphragm Framing and Nailing Requirements

Zone[*]	Framing	Structural 1 Sheathing	Nail Spacing (in.)			Capacity (kip/ft)
			Boundaries and Cont. Panel Edges	Other Panel Edges	Intermediate Framing Members	
A	3×12	15/32 in.	2	3	12	1.31
B	2×12	15/32 in.	4	6	12	0.68

1.0 in. = 25.4 mm, 1.0 kip/ft = 14.6 kN/m.

* Refer to Figure 14.2-2 for zone designation.
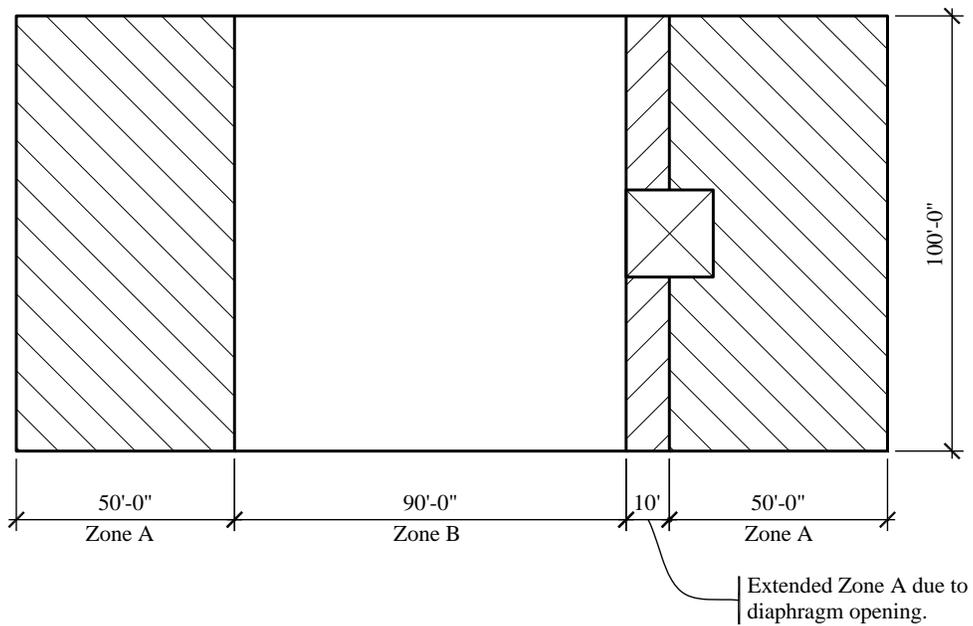
Figure 14.2-2 Diaphragm framing and nailing layout
(1.0 ft = 0.3048 m)
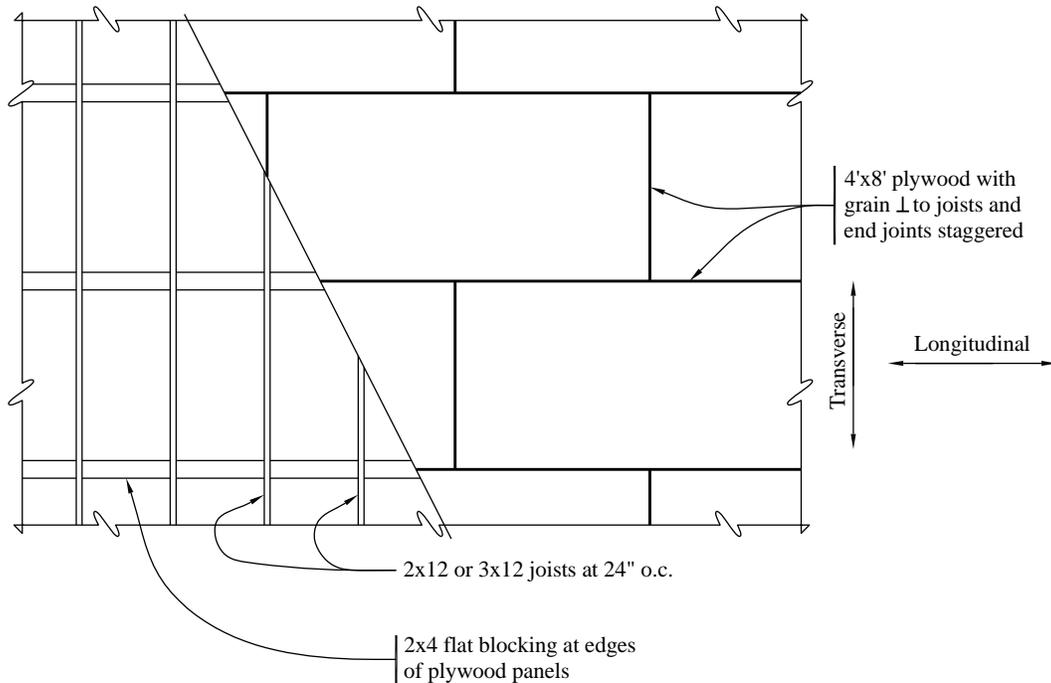
Figure 14.2-3 Typical diaphragm sheathing layout
(1.0 ft = 0.3048 m, 1.0 in = 25.4mm)

14.2.4.2.2 Chord Design. Although the bond beam at the masonry wall is commonly used as a diaphragm chord, this example illustrates the design of the wood ledger member as a chord. Chord forces are computed using a simply supported beam analogy, where the design force is the maximum moment divided by the diaphragm depth.

Diaphragm moment, $M = wL^2/8 = F_{p,roof}L/8 = 234(200/8) = 5,850$ ft-kips

Chord force, $T = C = 5,850/(100 - 16/12) = 59.2$ kips

Try a select structural Douglas Fir-Larch 4×12 for the chord. Assuming two 1-1/16-inch bolt holes (for 1-inch bolts) at splice locations, the net chord area is 31.9 in^2. Tension strength (parallel to wood grain), per the AWC NDS, is as follows:

$F_t' = F_tC_FK_F\phi\lambda = (1,000 \text{ psi})(1.0)(2.16/0.8)(0.8)(1.0) = 2,160$ psi

$T' = F_t'A = 2,160(31.9)/1000 = 68.9$ kips > 59.2 kips   OK

Design the splice for the maximum chord force of 59.2 kips. Try bolts with steel side plates using 1-inch A307 bolts, with a 3-1/2-inch length in the main member. The capacity, according to the AWC NDS, is as follows:

$Z' = ZK_F\phi\lambda = (4.90)(2.16/0.65)(0.65)(1.0) = 10.6$ kips per bolt

The number of bolts required (at each side of the splice joint) is 59.2/10.6 = 5.6.

Use two rows of three bolts. The edge distance, end distance and spacing meet the AWC NDS requirements to avoid capacity reductions and the reduction for multiple bolts (group action factor) is negligible. The net area of the 4×12 chord with two rows of 1-1/16-inch holes is 31.9 in.[2] as assumed above. Therefore, use six 1-inch A307 bolts on each side of the chord splice (see Figure 14.2-4).

In addition to the bolt checks, the steel splice plates would need to be checked for tension. Although it is shown for illustration, this type of chord splice may not be the preferred splice against a masonry wall since the bolts and side plate would have to be recessed into the wall.
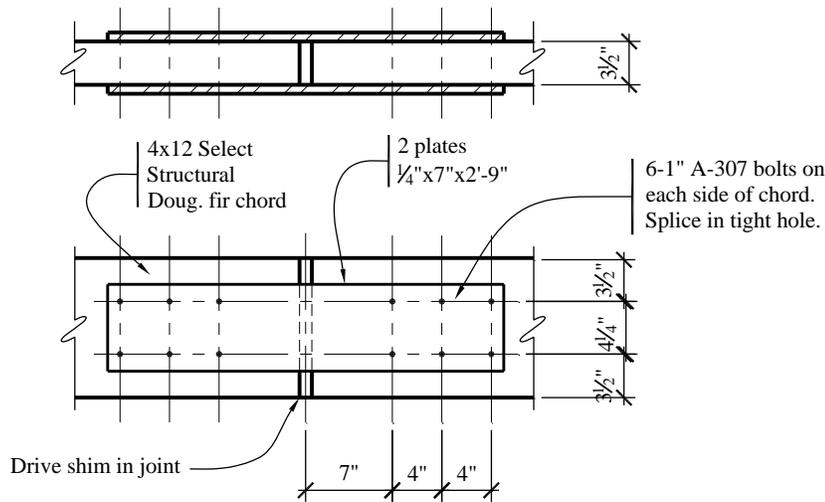
Figure 14.2-4 Chord splice detail
(1.0 ft = 0.3048 m, 1.0 in. = 25.4 mm)

In addition to the above criteria, NDS Appendix E includes non-mandatory but highly recommended criteria for bolted connections to avoid row tear-out and group tear out, similar to tear-out considerations in steel design.

Row tear-out capacity for one row of bolts is calculated as:

$Z'_{RTi} = n_i F'_v t S_{critical}$

Where:

n_i = 3 bolts in a row
$F_v' = F_v K_F \phi \lambda = (180 \text{ psi})(1.0)(2.88)(0.75)(1.0) = 389 \text{ psi}$
t = 3.5 inches
$S_{critical}$ = 4 inches, center-to-center spacing of bolts in row

$Z'_{RTi} = (3) (389) (3.5) (4) = 16,340$ lb per row, 32,700 lb for 2 rows.

Group tear-out can be similarly calculated using Appendix E. Note that the resulting capacity of 37.2 kips is notably less than the demand of 59.2 kips. It is recommended that row tear-out capacity be increased by

increasing the bolt end and center-to-center distances to 7-1/4 inches. This distance will keep row tear-out from controlling connection capacity.

14.2.4.2.3 Diaphragm Deflection and P-delta Check. Based on the procedure in AWC SDPWS Section 4.2.2, diaphragm deflection is computed as follows:

$$\delta_{dia} = \frac{5vL^3}{8EAW} + \frac{0.25vL}{1000G_a} + \frac{\sum(x\Delta_c)}{2W}$$

The equation produces the midspan diaphragm displacement in inches and the individual variables *must* be entered in the force or length units as described below. A small increase in diaphragm deflection due to the large opening is neglected and the effects of the variable nail spacing are neglected for simplicity.

The variables above and associated units used for computations are as follows:

v = (234/2)/100 = 1,170 plf (shear per foot at boundary)

L = 200 ft (diaphragm length)

W = 100 ft (diaphragm width)

A = effective area of 4×12 chord
= 39.38 in.^{2}

E = 1,900,000 psi (for Douglas Fir-Larch select structural chord)

G_a = 1.2(18) = 21.6 kips/in. (apparent diaphragm shear stiffness from AWC SDPWS Table 4.2A accounting for nail slip and panel shear deformation, based on sheathing and nailing at the outer zone and increased by 1.2 per Footnote 3, assuming four-ply minimum sheathing)

Δ_c = diaphragm chord splice slip in inches at the induced unit shear in diaphragm. This will be assumed to be 1/8-inch based on typical bolt installation tolerances

x = distance from chord splice to nearest supporting shear wall in feet. It will be assumed that 4x12's are 20 feet long, and two splices occur at 20, 40, 60 and 80 feet from the support, as well as one at 100 feet.

Bending deflection = $5vL^3/8EAW$ = 0.78 in.

Shear/nail slip deflection = $0.25vL/1000G_a$ = 2.71 in.

Deflection due to chord slip at splices = $\Sigma(x\Delta_c)/2W \approx$ (2(20+40+60+80)+100)(0.125)/ 2(100) = 0.31 in.

Total for diaphragm:

δ_{dia} = 0.78+2.71+0.31 = 3.80 in.

End wall deflection = 0.037 in. (see Sec. 13.1 of this volume of design examples)

14-42

Therefore, the total elastic deflection $\delta_{xe} = 3.80+0.037 = 3.84$ in.

Total deflection, $\delta_x = C_d\,\delta_{xe}/I_e = 3.5(3.84)/1.0 = 13.4$ in.

For one-story buildings, *Standard* Table 12.12-1, Footnote c permits unlimited drift, provided that the structural elements and finishes can accommodate the drift. In addition, the limit for masonry cantilever shear wall structures (0.007) should only be applied to the in-plane movement of the end walls ($0.13/h = 0.0004 < 0.007$). This masonry wall structure meets all drift requirements. The diaphragm deflection is not regulated by the code, except that vertical elements supporting gravity loads must be able to withstand this seismic deflection. The construction of the out-of-plane walls allows them to accommodate very large diaphragm deflections.

P-delta effects are computed according to *Standard* Section 12.8.7 for determining the stability coefficient, θ, per *Provisions* Equation 12.8-16:

$$\theta = \frac{P_x \Delta I}{V_x h_{sx} C_d}$$

Because the midspan diaphragm deflection is substantially greater than the deflection at the top of the masonry end walls, it would be overly conservative to consider the entire design load at the maximum deflection. Therefore, the stability coefficient is computed by splitting the P-delta product into two terms: one for the diaphragm and one for the end walls.

For the diaphragm, consider the weight of the roof and side walls at the maximum displacement. (This overestimates the P-delta effect. The computation could consider the average displacement of the total weight, which would lead to a reduced effective delta. Also, the roof live load need not be included.)

$P = 400+418 = 818$ kips

$\Delta = 13.4$ in.

$V = 234$ kips (diaphragm force)

For the end walls, consider the weight of the end walls at the wall displacement:

$P = 330$ kips

$\Delta = (3.5)(0.037) = 0.13$ in.

$V = 264$ kips (additional base shear for wall design)

For story height, $h = 28$ feet, the stability coefficient is:

$$\theta = \left(\frac{P\Delta}{V} + \frac{P\Delta}{V}\right)\Big/ hC_d = \left(\frac{818(13.4)}{234} + \frac{330(0.13)}{264}\right)\Big/(28)(12)(3.5) = 0.040$$

For $\theta < 0.10$, P-delta effects need not be considered based on *Provisions* Section 12.8.7.

Since the P-delta effects are not significant for this structure and the *Standard* does not impose drift limitations for this type of structure, the computed diaphragm deflections appear acceptable.

14.2.4.2.4 Detail at Opening. Consider diaphragm strength at the roof opening as required by *Standard* Section 12.10.1. The diaphragm nailing must be checked for the reduced total width of diaphragm sheathing and the chords must be checked for bending forces at the opening.

Check diaphragm nailing for the shear in the diaphragm at edge of opening. The maximum shear at the exterior-side edge of the opening is computed as follows:

Shear = 117 - [40(1.165)] = 69.9 kips

v = 69.9/(100-20) = 0.874 klf

Because the opening is centered in the width of the diaphragm, half the force to the diaphragm must be distributed on each side of the opening.

Diaphragm capacity in this area is 0.680 klf as computed previously (see Table 14.2-1 and Figure 14.2-2). Because the diaphragm demand at the reduced section exceeds the capacity, the extent of the Zone A nailing and framing should be increased. For simplicity, extend the Zone A nailing to the interior edge of the opening (60 feet from the end wall). The diaphragm strength is now adequate for the reduced overall width at the opening.

14.2.4.2.5 Framing around Opening. The opening is located 40 feet from one end of the building and is centered in the other direction (Figure 14.2-5). This does not create any panels with very high aspect ratios.

In order to develop the chord forces, continuity will be required across the glued-laminated beams in one direction and across the roof joists in the other direction.
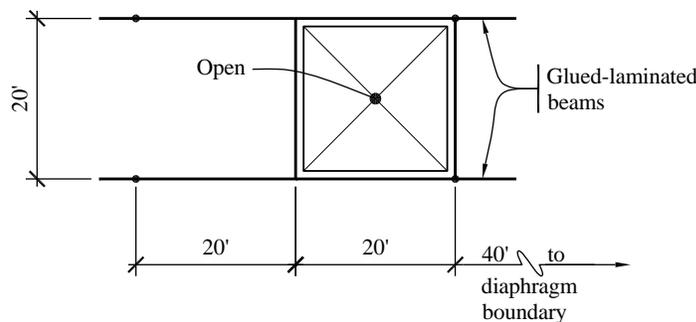
Figure 14.2-5 Diaphragm at roof opening
(1.0 ft = 0.3048 m)

14.2.4.2.6 Chord Forces at Opening. To determine the chord forces on the edge joists, split the diaphragm into smaller free-body sections, assume the inflection points will be at the midpoint of the elements (Figure 14.2-6) and compute the forces at the opening using a uniformly distributed diaphragm demand of 233/200 = 1.165 klf.

For Element 1 (shown in Figure 14.2-7):

$w_1 = 1.165/2 = 0.582$ kips/ft (assuming half the diaphragm load on each side of the opening)

$V_{1B} = 0.5[116.5-(40)(1.165)] = 35.0$ kips (based on diaphragm unit shear on right side of opening)

$V_{1A} = 35.0-20(0.582) = 23.3$ kips (based on diaphragm unit shear on left side of opening)

$M_1 = (1/2)[35.0(10) + 23.3(10)] = 291$ ft-kips (assuming equal moments at each edge of the section)

The chord force due to $M_1 = 291/40 = 7.28$ kips. This is only 35 psi on the glued-laminated beam on the edge of the opening. This member is adequate by inspection. On the other side of this diaphragm element, the chord force is much less than the maximum global chord force (59.0 kips), so the ledger and ledger splice are adequate.
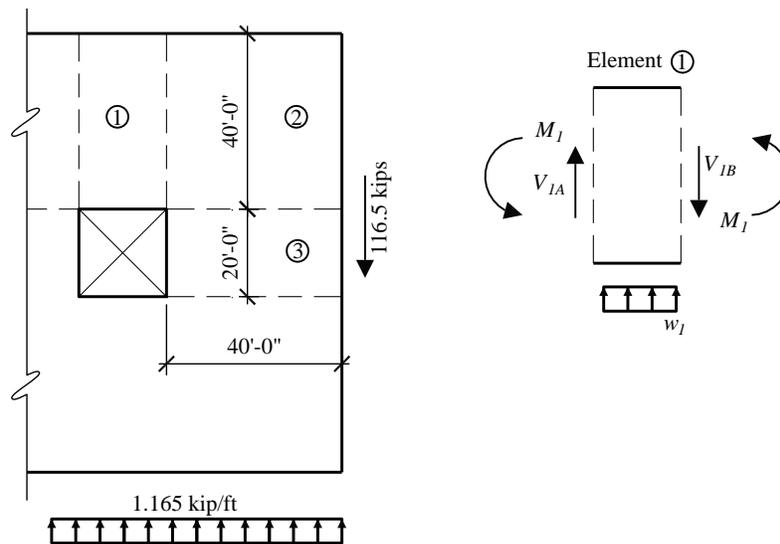
Figure 14.2-6 Chord forces and Element 1 free-body diagram
(1.0 ft = 0.3048 m, 1.0 kip = 4.45 kN, 1.0 kip/ft = 14.6 kN/m)

For Element 3, analyze Element 2 (shown in Figure 14.2-7) in the same manner as Element 1:

$w_2 = 1.165(40/100) = 0.466$ kips/ft

$V_3 = 116.5(40/100) = 46.6$ kips

$V_{1B} = 35.0$ kips

$M_1 = 291$ ft-kips.

T_{1B} is the chord force due to moment on the total diaphragm:

$M = 116.5(40) - 1.165(40^2/2) = 3{,}728$ ft-kips

$T_{1B} = 3{,}728/100 = 37.3$ kips

$\Sigma M_0 : M_3 = M_1 + 40V_3 - 40T_{1B} - w_2 40^2/2 = 291$ ft-kips

Therefore, the chord force on the roof joist $= 291/40 = 7.26$ kips
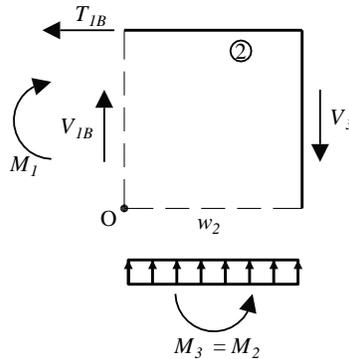
Figure 14.2-7 Free-body diagram for Element 2

Alternatively, the chord design should consider the wall anchorage force interrupted by the opening. As described in Section 14.2.4.4.1, the edge members on each side of the opening are used as continuous cross-ties, with maximum cross-tie force of 16.6 kips. Therefore, the cross-tie will adequately serve as a chord at the opening.

14.2.4.3 Roof Diaphragm Design for Longitudinal Direction.

Force $= 226$ kips

Maximum end shear $= 0.50(226) = 113$ kips

Diaphragm unit shear, $v = 113/200 = 0.565$ klf

For this direction, the plywood layout is Case 3 in AWC SDPWS Table 4.2A. Using 1/2-inch Structural I wood structural panel sheathing, blocked, with 10d common nails at 4 inches on center at diaphragm boundaries and continuous panel edges parallel to the load (ignoring the capacity of the extra nails in the outer zones), per AWC SDPWS Table 4.2A:

$\phi_D v_s = 0.80(0.850) = 0.68$ klf > 0.565 klf   OK

Therefore, use the same nailing designed for the transverse direction. Compared with the transverse direction, the diaphragm deflection and P-delta effects will be satisfactory.

14.2.5 Basic Proportioning of Diaphragm Elements (Alternative Method, Sec. 12.10.3)
Because the diaphragm design force for the example structure for the alternative method of Sec. 12.10.3 is the same as that for the traditional method, all of the diaphragm proportioning described in Section 14.2.4 of this example problem is equally applicable for the alternative method. One difference to note is

that if collectors were to be provided within the diaphragm, Section 12.10.3.4 would require that the collector be designed for 1.5 times the force calculated using the diaphragm design forces. This is instead of requiring that the collector force be multiplied by the overstrength factor Ω_0, as would be required when using the traditional provisions.

14.2.6 Masonry Wall Anchorage to Roof Diaphragm

As stipulated in *Standard* Section 12.11.2.1, walls must be anchored to flexible diaphragms to resist out-of-plane forces computed per *Standard* Equation 12.11-1 as follows:

$F_P = 0.4S_{DS}K_aI_eW_p$

Side walls:
$L_f = 200$ ft
$K_a = 1.0 + L_f/100 + 1.0 + 2.0 = 3.0$, but need not exceed 2.0
$F_P = 0.4S_{DS}K_aI_eW_p = 0.8(1.14)(2.0)(1.0)W_p = 1.14\ W_p$
$F_P = 1.14(65\text{psf})(2+28/2)/1{,}000 = 1.19$ klf

End walls:
$L_f = 100$ ft
$K_a = 1.0 + L_f/100 + 1.0 + 1.0 = 2.0$
$F_P = 0.4S_{DS}K_aI_eW_p = 0.8(1.14)(2.0)(1.0)W_p = 1.14\ W_p$
$F_P = 1.14(103\text{psf})(2+28/2)/1{,}000 = 1.89$ klf

14.2.6.1 Anchoring Joists Perpendicular to Walls (Side Walls). The roof joists are spaced at 2 feet on center, so as a preliminary design, consider a connection at every other joist that will develop 4(1.19) = 4.76 kips/joist. Note that 4 feet is the maximum anchor spacing allowed without having to check the walls for resistance to bending between anchors (*Standard* Sec. 12.11.2).

A common connection for this application is a metal tension tie-down or hold-down device that is anchored to the masonry wall with an embedded bolt and is either nailed, screwed, or bolted to the roof joist. Other types of anchors include metal straps that are embedded in the wall and nailed to the top of the joist. The ledger is not used for this force transfer because the eccentricity between the anchor bolt and the plywood creates tension perpendicular to the grain in the ledger (cross-grain bending), which is prohibited. Also, using the edge nails to resist tension perpendicular to the edge of the plywood is not permitted.

Try a tension tie with a 3/4-inch headed anchor bolt, embedded in the bond beam and with 26 10d nails into the side of the joist (Figure 14.2-8). The cataloged ASD tension capacity of this connector is 4.35 kips based on a load duration factor of 1.60. Modifying the allowable values using the procedure in Section 14.1.4.5 results in a design LRFD capacity of:

$Z'K_F\phi\lambda = (4.35)(2.88/1.60)(0.65)(1.0) = 5.09$ kips per anchor > 4.76 kips   OK

The joists anchored to the masonry wall must also be adequately connected to the diaphragm sheathing. Sheathing edge nailing is commonly provided to joists at wall anchors. The edge nail spacing is not greater than 4 inches and the joist length is 20 feet, so there are 20 nails per joist. From the AWC NDS, the LRFD capacity of a single 10d common nail in 1/2-inch plywood is:

$Z'K_F\phi\lambda = (0.090)(2.16/0.65)(0.65) = 0.194$ kips per nail

20(12 in./4 in.)(0.194) = 11.64 kips > 4.76 kips   OK

The embedded anchor bolt also serves as the ledger connection, for both gravity loading and in-plane shear transfer at the diaphragm. Therefore, the strength of the anchorage to masonry and the strength of the bolt in the wood ledger must be checked.

For the anchorage to masonry, check the combined tension and shear resulting from the out-of-plane seismic loading (3.32 kips per bolt) and the vertical gravity loading. Assuming 20 psf dead load (roof live load need not be combined with seismic loads), a 10-foot tributary roof width and ledger bolts at 2 feet on center (at tension ties and in between) the vertical load per bolt = (20 psf)(10 ft)(2 ft)/1,000 = 0.40 kip. Using the load combinations described previously, the design horizontal tension and vertical shear on the bolt are as follows:

$$b_{af} = 1.0Q_E = 4.76 \text{ kips}$$

$$b_{vf} = 1.486D = 1.486(0.40) = 0.59 \text{ kip}$$

The anchor bolts in masonry are designed according to TMS 402/ACI 530/ ASCE 5 as adopted by the *Standard* (Sec. 14.4) and as modified by *Standard* Sections 14.4.7.6 and 14.4.7.7. *Standard* Section 14.4.7.6 requires the strength of the anchorage connecting diaphragms to other parts of the seismic force-resisting system to be governed by steel tensile or shear yielding unless the anchorage is designed for 2.5 times the required forces. For this example, the anchorage is proportioned such that the steel governs the capacity. *Standard* Section 14.4.7.7 modifies the shear strength requirements for anchorage, requiring that the shear capacity is not more than 2 times the strength due to masonry pry-out.

Using 3/4-inch headed anchor bolts with an effective embedment depth of 6 inches, both tensile strength, B_{an} and shear strength, B_{vn}, will be computed assuming the masonry strength, f''_m, is 2,000 psi and the steel strength, f_y, is 36,000 psi. Tensile strength per ACI 530 Section 9.1.6.3.1.1 is taken as the lesser of the following:

$$B_{ans} = A_b f_y = 0.44(36) = 15.8 \text{ kips}$$

$$B_{anb} = 4A_{pt}\sqrt{f'_m} = 4(113)\sqrt{2,000} = 20.2 \text{ kips}$$

where A_{pt} is the projected area of the right cone and is equal to $\pi(l_b)^2$, where l_b is the effective embedment depth. Therefore, $A_{pt} = \pi(6)^2 = 113 \text{ in}^2$.

Since the steel strength governs, per ACI 530 Section 9.1.4.1, $\phi = 0.9$. Therefore the design strength in tension is 0.9(15.8) = 14.2 kips.

Shear strength per ACI 530 Section 9.1.6.3.2 is taken as the lesser of the following:

$$B_{av} = 0.6A_b f_y = 0.6(0.44)(36) \quad B_{vns} = 0.6A_b f_y = 0.6(0.44)(36) = 9.50 \text{ kips}$$

$$B_{vnb} = 4A_{pv}\sqrt{f'_m} = 4(56.5)\sqrt{2,000} = 10.1 \text{ kips}$$

$$B_{vnc} = 1050\sqrt[4]{f'_m A_b} = 1050\sqrt[4]{(2,000)(0.44)} = 5.72 \text{ kips}$$

$$B_{vnpry} = 8A_{pt}\sqrt{f'_m} = 8(113)\sqrt{2,000} = 40.4 \text{ kips}$$

where A_{pv} is one half of the projected area of the right cone and is equal to $113/2 = 56.5$ in^2. Since the governing strength is from masonry crushing, per ACI 530 Section 9.1.4.1, $\phi = 0.5$. Therefore, the design strength in shear is $0.5(5.72) = 2.86$ kips.

Shear and tension are combined per ACI 530 Section 3.1.6.4 as:

$$\frac{b_{af}}{\phi B_{an}} + \frac{b_{vf}}{\phi B_{vn}} = \frac{4.76}{14.2} + \frac{0.59}{2.86} = 0.54 < 1.0 \qquad \text{OK}$$

Figure 14.2-8 summarizes the details of the connection. In-plane seismic shear transfer (combined with gravity) and orthogonal effects are considered in a subsequent section.
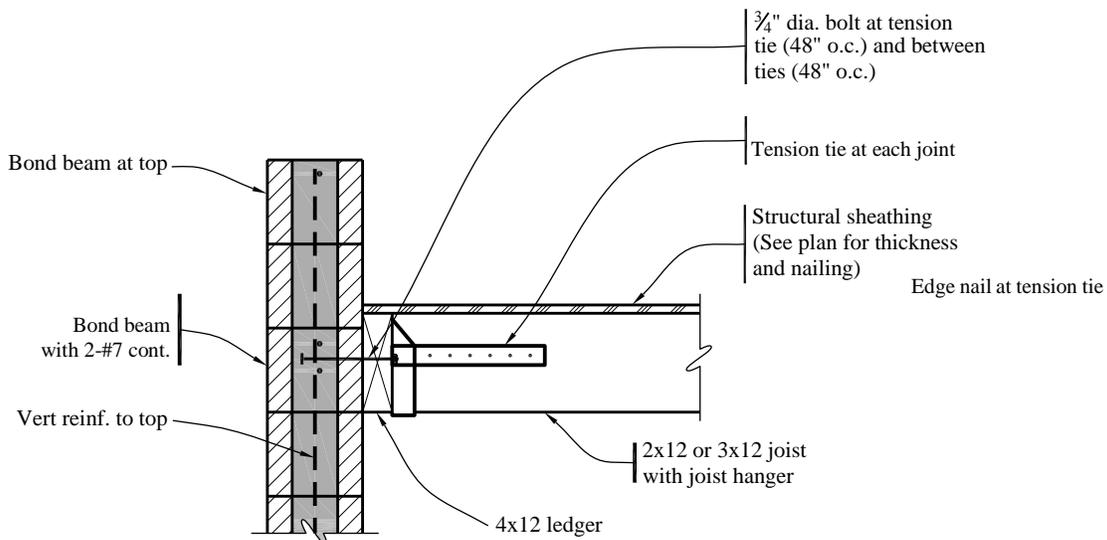
Figure 14.2-8 Anchorage of masonry wall perpendicular to joists
(1.0 in. = 25.4 mm)

According to *Standard* Section 12.11.2.2.1, diaphragms must have continuous cross-ties to distribute the anchorage forces into the diaphragms. Although the *Standard* does not specify a maximum spacing, 20 feet is common practice for this type of construction and seismic design category.

For cross-ties at 20 feet on center, the wall anchorage force per cross-tie is:

(1.19 klf)(20 ft) = 23.8 kips

Try a 3×12 Douglas Fir-Larch No. 1 as a cross-tie. Assuming one row of 1-1/8-inch bolt holes, the net area of the section is 25.3 in^2. Tension strength (parallel to wood grain) per the AWC NDS Supplement is:

$F'_T = F_t K_F \phi \lambda = (0.675)(2.16/0.8)(0.8) = 1.46$ ksi

$T' = F'_t A = (1.46)(25.3) = 36.9$ kips > 23.8 kips   OK

However, the cross-tie must be checked for combined gravity and lateral loads. The governing case for combined loads is midspan where the maximum gravity moment is combined with seismic tension. The 3×12 cross-tie has the following properties:

$A = 28.1$ in^2

$S = 52.7$ in^3

$F'_t = 1.46$ ksi

$F'_b = F_b C_r K_F \phi \lambda = (1.000)(1.15)(2.16/0.85)(0.85) = 2.48$ kips

The factored dead load moment is computed using the load combinations described above as:

$M_u = 1.4(20 \text{ psf})(2 \text{ ft})(20 \text{ ft})^2/8 = 2.80$ ft-kips

The factored stresses are computed as:

$f_t = 23.8/28.1 = 0.85$ ksi

$f_b = (2.80)(12)/52.7 = 0.638$ ksi

Combined stresses are checked in accordance with AWC NDS Section 3.9.1 as follows:

$$\frac{f_t}{F'_t} + \frac{f_b}{F^t_b} = \frac{0.85}{1.46} + \frac{0.638}{2.48} = 0.84 < 1.0$$ OK

At the splices, try a double tie-down device with three 1-inch bolts in double shear through the 3×12 member (Figure 14.2-9). Product catalogs provide design capacities for single tie-downs only; the design of double hold-downs requires two checks. First, consider twice the capacity of one tie-down and, second, consider the capacity of the bolts in double shear.

For the double tie-down, use the procedure in Section 14.1.4.5 to modify the allowable values:

$2ZK_F \phi \lambda = 2(10.33)(2.88/1.60)(0.65)(1.0) = 24.2$ kips > 23.8 kips   OK

For the four bolts, the AWC NDS gives:

$4ZK_F \phi \lambda = 4(3.50)(2.16/0.65)(0.65)(1.0) = 30.2$ kips > 23.8 kips   OK
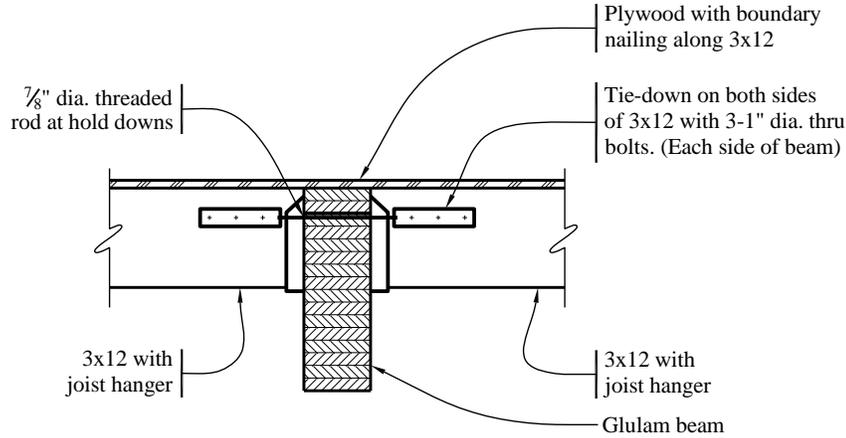
Figure 14.2-9 Chord tie at roof opening
(1.0 in. = 25.4 mm)

In order to transfer the wall anchorage forces into the cross-ties, the subdiaphragms between these ties must be checked per *Standard* Section 12.11.2.2.1. There are several ways to perform these subdiaphragm calculations. One method is illustrated in Figure 14.2-10. The subdiaphragm spans between cross-ties and utilizes the glued-laminated beam and ledger as its chords. The 1-to-1 aspect ratio meets the requirement of 2.5 to 1 for subdiaphragms per *Standard* Section 12.11.2.2.1.

For the typical subdiaphragm (Figure 14.2-10):

$F_p = 1.19$ klf

$v = (1.19)(20/2)/20 = 0.595$ klf.

The subdiaphragm demand is less than the minimum diaphragm capacity (0.68 klf along the center of the side walls). In order to develop the subdiaphragm strength and boundary nailing must be provided along the cross-tie beams.
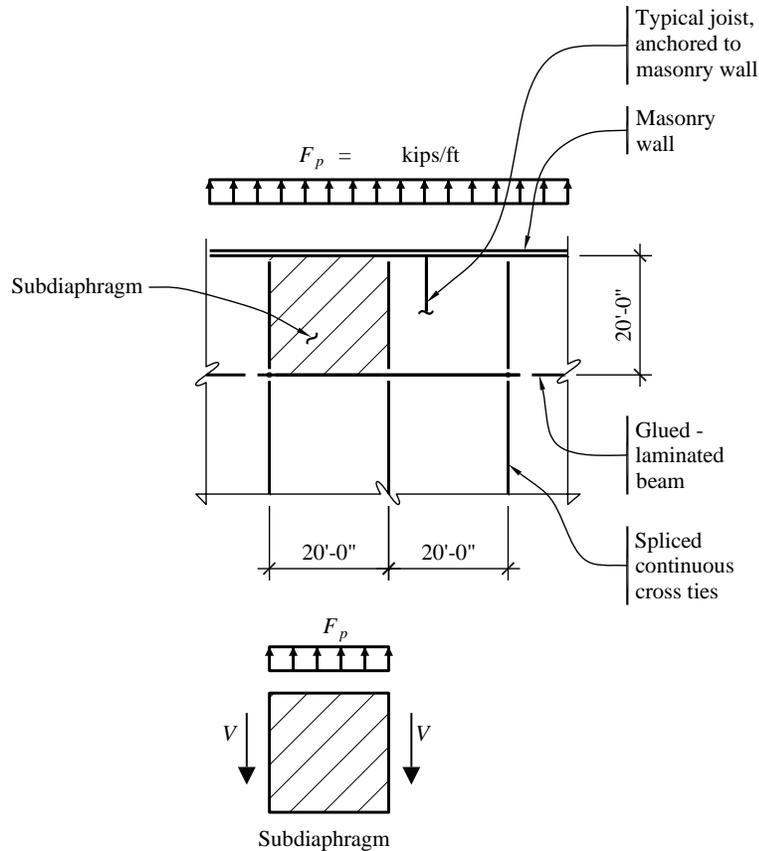
Figure 14.2-10 Cross tie plan layout and subdiaphragm free-body diagram for side walls
(1.0 ft = 0.3048 m, 1.0 kip/ft = 14.6 kN/m)

14.2.6.2 Anchorage at Joists Parallel to Walls (End Walls). Where the joists are parallel to the walls, tied elements must transfer the forces into the main body of the diaphragm, which can be accomplished by using either metal strapping and blocking or metal rods and blocking. This example uses threaded rods that are inserted through the joists and coupled to the anchor bolt (Figure 14.2-11). Blocking is added on both sides of the rod to transfer the force into the plywood sheathing. The tension force in the rod causes a compression force on the blocking through the nut and on the bearing plate at the innermost joist.
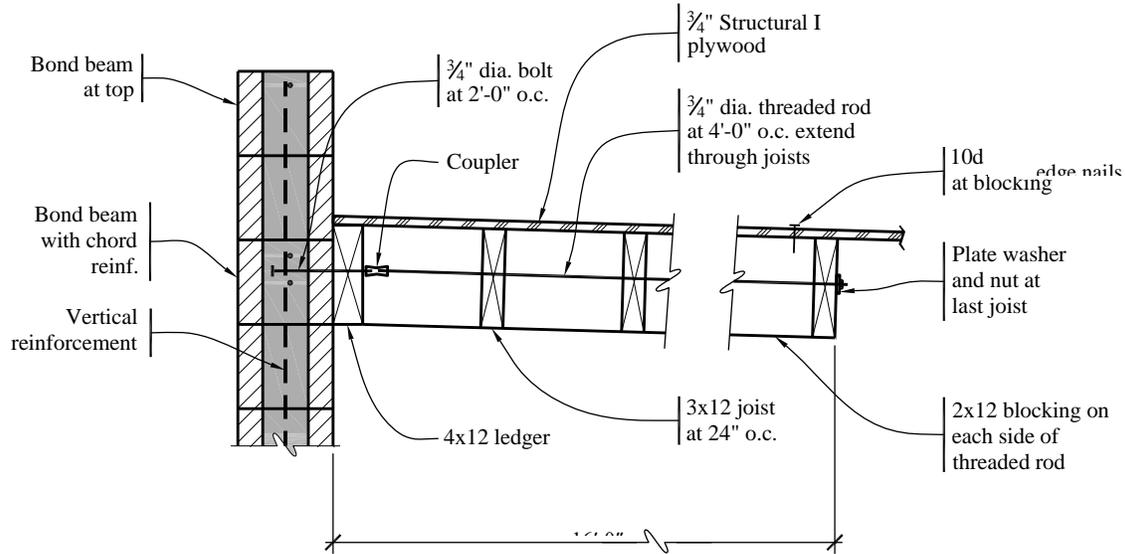
Figure 14.2-11 Anchorage of masonry wall parallel to joists
(1.0 ft = 0.3048 m, 1.0 in. = 25.4 mm)

The anchorage force at the end walls is 1.89 klf. Space the connections at 4 feet on center so that the wall need not be designed for flexure. Thus, the anchorage force is 7.56 kips per anchor.

Try a 3/4-inch headed anchor bolt, embedded into the masonry. In this case, gravity loading on the ledger is negligible and can be ignored and the anchor can be designed for tension only. (In-plane shear transfer and orthogonal effects are considered later.)

As computed for 3/4-inch headed anchor bolts (with 6 inch embedment), the design axial strength is $\phi B_{an} = 14.2$ kips > 7.56 kips. Therefore, the bolt is acceptable.

Using couplers rated for 125 percent of the strength of the rod material, the threaded rods are then coupled to the anchor bolts and extend eight joist spaces (16 feet) into the roof framing. (This length of 16 feet is required for the subdiaphragm force transfer discussed below.)

Nailing the blocking to the plywood sheathing is determined using nail capacities from the AWC NDS. As computed previously, the LRFD capacity of a single 10d common nail, $Z'K_F\phi\lambda = 0.194$ kips per nail. Thus, 39 nails are required (7.56/0.194). This corresponds to a nail spacing of approximately 5 inches for two 12-foot rows of blocking. Edge nail spacing at not more than 4 inches will meet this requirement.

Use the glued-laminated timber beams (at 20 feet on center) to provide continuous cross-ties and check the subdiaphragms between the beams to provide adequate load transfer to the beams per *Standard* Section 12.11.2.2.1:

Design tension force on beam = (1.89 klf)(20 ft) = 37.8 kips

The stress on the beam is $f_t = 37,800/[8.75(24)] = 180$ psi, which is small. The beam is adequate for combined moment due to gravity loading and axial tension.

At the beam splices, try 3/4-inch bolts with steel side plates. Per the AWC NDS:

$ZK_F\phi\lambda = (3.34)(3.32)(0.65)(1.0) = 7.21$ kips per bolt

The number of bolts required (on each side of the splice joint) is 37.8/7.21 = 5.2
Use six bolts in a single row at mid-height of the beam, with 1/4-inch by 4-inch steel side plates. The reduction (group action factor) for multiple bolts is negligible. Although not included in this example, the steel side plates should be checked for tension capacity on the gross and net sections. There are pre-engineered hinged connectors for glued-laminated beams that could provide sufficient tension capacity for the splices.

In order to transfer the wall anchorage forces into the cross-ties, the subdiaphragms between these ties must be checked per *Provisions* Section 12.11.2.2.1. The procedure is similar to that used for the side walls as described previously. The end wall condition is illustrated in Figure 14.2-12. The subdiaphragm spans between beams and utilizes a roof joist as its chord. In order to adequately engage the subdiaphragm, the wall anchorage ties must extend back to this chord. Since the maximum aspect ratio for subdiaphragms is 2.5 to 1, the minimum depth is 20/2.5 = 8 feet.
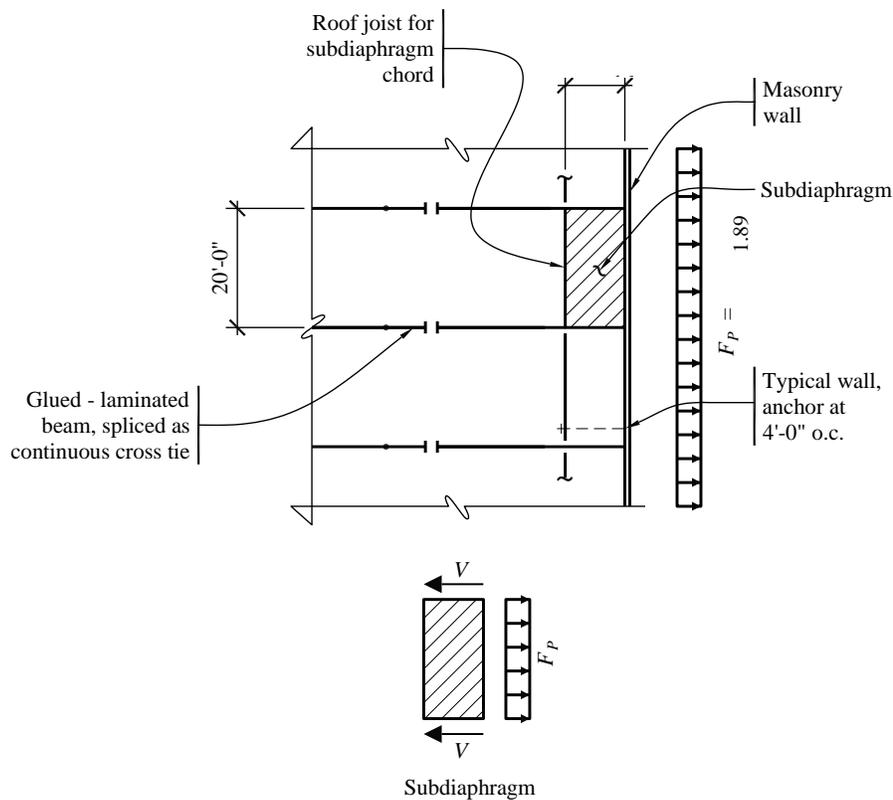
Figure 14.2-12 Cross tie plan layout and subdiaphragm free-body diagram for end walls
(1.0 ft = 0.3048 m, 1.0 kip/ft = 14.6 kN/m)

For the typical subdiaphragm (Figure 14.2-12):

$F_p = 1.89$ klf

$v = (1.89)(20/2)/8 = 2.36$ klf

As computed previously (see Table 14.2-1 and Figure 14.2.2), the diaphragm strength in this area is 1.17 klf < 1.65 klf. Therefore, increase the subdiaphragm depth to 16 feet (eight joist spaces):

$v = (1.89)(20/2)/16 = 1.18$ klf $= 1.17$ klf   OK

In order to develop the subdiaphragm strength, boundary nailing must be provided along the cross-tie beams. There are methods of refining this analysis using multiple subdiaphragms so that all of the tension anchors need not extend 16 feet into the building.

14.2.4.4.3 Transfer of Shear Wall Forces. The in-plane diaphragm shear must be transferred to the masonry wall by the ledger, parallel to the wood grain. The connection must have sufficient capacity for the diaphragm demands as follows:

Side walls: 0.523 klf

End walls: 1.165 klf

For each case, the capacity of the bolted wood ledger and the capacity of the anchor bolts embedded into masonry must be checked. Because the wall connections provide a load path for both in-plane shear transfer and out-of-plane wall forces, the bolts must be checked for orthogonal load effects in accordance with *Standard* Section 12.5. That is, the combined demand must be checked for 100 percent of the lateral load effect in one direction (e.g., shear) and 30 percent of the lateral load effect in the other direction (e.g., tension).

At the side walls, the wood ledger with 3/4-inch bolts (Figure 14.2-8) must be designed for gravity loading (0.56 kip per bolt as computed above) as well as seismic shear transfer. The seismic load per bolt (at 2 feet on center) is $0.523(2) = 1.05$ kips.

Combining gravity shear and seismic shear produces a resultant force of 1.19 kips at an angle of 28 degrees from the axis of the wood grain. The bolt capacity in the wood ledger can be determined using the formulas for bolts at an angle to the grain per the AWC NDS (either adjusting for dowel bearing strength per Section 12.3.4 or adjusting the tabulated bolt values per Appendix J). The resulting design value, $Z = 1.41$ kips and the LRFD capacity is determined as follows:

$ZK_F\phi\lambda = (1.41)(3.32)(0.65)(1.0) = 3.05$ kips > 1.19 kips   OK

This bolt spacing also satisfies the load combination for gravity loading (dead and roof live) only.

For the check of the embedded anchor bolts, the factored demand on a single bolt is 1.05 kips in horizontal shear (in-plane shear transfer), 4.76 kips in tension (out-of-plane wall anchorage) and 0.56 kip in vertical shear (gravity). Orthogonal effects are checked, using the following two equations:

$$\frac{0.3(4.76)}{8.75} + \frac{\sqrt{1.05^2 + 0.56^2}}{2.66} = 0.61$$

and

$$\frac{4.76}{8.75} + \frac{\sqrt{(0.3 \times 1.05)^2 + 0.56^2}}{2.66} = 0.78 \text{ (controls)} < 1.0 \qquad\qquad \text{OK}$$

At the end walls, the ledger with 3/4-inch bolts (Figure 14.2-11) need only be checked for in-plane seismic shear because gravity loading is negligible. For bolts spaced at 4 feet on center, the demand per bolt is 1.165(4) = 4.66 kips parallel to the grain of the wood. Per the AWC NDS:

$$ZK_F\phi\lambda = (1.61)(3.32)(0.65)(1.0) = 3.48 \text{ kips} < 4.66 \text{ kips} \qquad\qquad \text{NG}$$

Therefore, add 3/4-inch headed bolts evenly spaced between the tension ties such that the bolt spacing is 2 feet on center and the demand per bolt is 1.165(2) = 2.33 kips. These added bolts are used for in-plane shear only and do not have coupled tension tie rods.

For the check of the embedded bolts, the factored demand on a single bolt is 2.33 kips in horizontal shear (in-plane shear transfer), 7.56 kips in tension (out-of-plane wall anchorage), 0 kip in vertical shear (gravity is negligible). Orthogonal effects are checked using the following two equations:

$$\frac{0.3(7.56)}{8.75} + \frac{2.33}{2.66} = 1.14 \text{ (controls)} > 1.0 \qquad\qquad \text{NG}$$

$$\frac{7.56}{8.75} + \frac{0.3(2.33)}{2.66} = 1.12$$

Since the equations are slightly more than unity, the bolt capacity can be increased by using a larger bolt or more embedment depth, or more bolts can be added. With this minor revision, the wall connections satisfy the requirements for combined gravity and seismic loading, including orthogonal effects.

15

Seismically Isolated Structures

William McVitty, M.S., Andrew Taylor, S.E., Ph.D.

Based in part on materials originally developed by
Charles A. Kircher, P.E., Ph.D.

Contents

Chapter 17 of ASCE/SEI 7-16 (hereafter the *Standard*) addresses the design of buildings that incorporate a seismic isolation system. It defines load, design and testing requirements specific to the isolation system and interfaces with the other chapters of the *Standard* for design of the structure above the isolation system and of the foundation and structural elements below.

The *Standard* has evolved over the years to reflect the state of art and practice in the field. The latest evolution of the *Standard* incorporates a number of major revisions including:

- Added a new section titled *Isolation System Properties* for the explicit development of property modification (λ) factors which are used to account for the variation in a bearing's nominal mechanical properties.
- Revised provisions to reflect a MCE_R-only basis for analysis and design.
- Expanded the range of applicability of the equivalent lateral force (ELF) procedure.
- Incorporated a more realistic distribution of shear force over the building height considering the period of the superstructure and the effective damping of the isolation system.
- Revised and clarified the seismic ground motion selection and scaling criteria.
- Made a number of additions and changes to the testing requirements, such as dynamic testing sequences, criteria for bearings to be classified as similar, and requirements for quality testing of 100% of production bearings.
- Expanded commentary to compliment the provisions.

This example uses the *Standard* to analyze and design a three-story emergency operations center (EOC) located in a region of high seismicity, classified as Seismic Design Category D. The building is base-isolated to achieve a higher level of seismic performance in a major earthquake. The focus of this example is given to the analysis and design of the isolation system with two common types considered: 1) elastomeric bearings and 2) sliding bearings. Arbitrarily, the elastomeric isolation system is carried through to final design, however generally the analysis is similar for sliding systems. Although the facility is hypothetical, it is of comparable size and configuration to actual base-isolated EOCs and is generally representative of base-isolated buildings.

In addition to the *Standard*, the following documents are either referenced directly, provide background, or are useful aids for the analysis and design of isolated structures:

Constantinou et al.   Constantinou, M. C., Kalpakidis, I., Filiatrault, A. and Ecker Lay, R. A. (2011). *LRFD-Based Analysis and Design Procedures for Bridge Bearings and Seismic Bearings*, Technical Report MCEER-11-0004, Multidisciplinary Center for Earthquake Engineering Research, Buffalo, New York.

Constantinou et al.   Constantinou, M. C., Whittaker, A. S., Kalpakidis, Y., Fenz, D. M. and Warn, G. P. (2007). *Performance of Seismic Isolation Hardware under Service and Seismic Loading*, Technical Report MCEER-07-0012, Multidisciplinary Center for Earthquake Engineering Research, Buffalo, New York.

Fenz and Constantinou   Fenz, D. M., Constantinou, M. C. (2006). "Behavior of Double Concave Friction Pendulum Isolator", Earthquake Engineering and Structural Dynamics 2006, 35:1403-1421.

Fenz and Constantinou   Fenz, D. M., Constantinou, M. C. (2008). "Development, Implementation and Verification of Dynamic Analysis Models for Multi-Spherical Sliding Isolators", Technical Report MCEER-08-0018, Multidisciplinary Center for Earthquake Engineering Research, Buffalo, New York.

Kalpakidis and Constantinou	Kalpakidis, I. V., Constantinou, M. C., (2008). "Effects of Heating and Load History on the Behavior of Lead-Rubber Bearings", Technical Report MCEER-08-0027, Multidisciplinary Center for Earthquake Engineering Research, Buffalo, New York.
McVitty and Constantinou	McVitty, W. J., Constantinou, M. C. (2015). *Property Modification Factors for Seismic Bearings: Design Guidance for Buildings*, Technical Report MCEER-15-0005, Multidisciplinary Center for Earthquake Engineering Research, Buffalo, New York.
NEHRP	NEHRP (2015). *Recommended Seismic Provisions for New Buildings and Other Structures*, FEMA P-1050.
NIST	NIST (2011). *Selecting and Scaling Earthquake Ground Motions for Performing Response-History Analyses*, NIST GCR 11-917-15.
Sarlis and Constantinou	Sarlis A. A. S., Constantinou, M. C. (2010). *Modeling Triple Friction Pendulum Bearings in Program SAP2000*, Technical Report released to the engineering community.
Sarkisian et al.	Sarkisian et al. (2012). *Property Verification of Triple Pendulum^{TM} Seismic Isolation Bearings.*20th Analysis and Computation Specialty Conference, ASCE.
SEAOC	Structural Engineers Association of California (2014). *2012 IBC SEAOC Structural/Seismic Design Manual*, Volume 5: Examples for Seismically Isolated Buildings and Buildings with Supplemental Damping, Published January 2014.
Thompson et al.	Thompson, A. C. T., Whittaker, A. S., Fenves, G. L., and Mahin, S. A. (2000). "Property modification factors for elastomeric seismic isolation bearings." Proc., 12th World Conf. on Earthquake Engineering, Auckland, New Zealand, 1–8.
Warn and Whittaker	Warn G. P., Whittaker, A. S. (2007). *Performance Estimates for Seismically Isolated Bridges*, Technical Report MCEER-07-0024, Multidisciplinary Center for Earthquake Engineering Research, Buffalo, New York.
Wolff et al.	Wolff, E. D., Ipek, C., Constantinou, M. C., Morillas, L. (2014). *Torsional Response of Seismically Isolated Structures Revisited* Engineering Structures 59, 462-468
York and Ryan	York, K., Ryan, K. (2008). *Distribution of Lateral Forces in Base-Isolated Buildings Considering Isolation System Nonlinearity*. Journal of Earthquake Engineering.

15.1 BACKGROUND

15.1.1 Concept of Seismic Isolation

The concept of seismic isolation involves increasing the fundamental period of the structure away from dominate frequencies of earthquake ground motion as well as providing damping to reduce response. It can be likened to introducing an engineered soft-story in the structure, whereby a majority of the inelastic action and displacement is concentrated at a single level (the isolation level) therefore protecting the building above.

The potential advantages of seismic isolation and the advancements in isolation system products led to the design and construction of a number of isolated buildings and bridges in the early 1980s. This activity, in turn, identified a need to supplement existing seismic codes with design requirements developed specifically for such structures. The application of the technology in the United States is now regulated by building codes which invariably refer to ASCE 7 (the *Standard*) for analysis and design requirements. These requirements assure the public that isolated buildings are safe, they provide engineers with a basis for preparing designs and they provide building officials with minimum standards for regulating construction.

Seismic isolation is a high-performance system that provides greatly improved seismic performance compared to most other conventional seismic force resisting systems. That is, a seismically isolated building and a conventional fixed-base building, designed to the respective minimum requirements of the *Standard* will exhibit widely differing performance in a major earthquake. A seismically isolated building is expected to have considerably better performance, with limited damage, whereas a conventional building may be damaged to the point where it is uneconomical to rehabilitate. This is due to the inherent nature of isolation, for example it reduces both displacements and accelerations in the superstructure. Although not explicitly seeking damage control as an objective, indirectly the minimum requirements of the *Standard* will give limited damage as a consequence of ensuring proper isolation achieved. For example, the *Standard* limits the amount of inelastic action and drift that may occur in the superstructure to avoid detrimental coupling with the isolation system. Moreover, the *Standard* requires that the isolation devices be designed and tested to be functional under the effects of the Maximum Considered Earthquake (MCE_R).

15.1.2 Types of Isolation Systems

The *Standard* requirements are intentionally broad, accommodating all types of acceptable isolation systems. To be acceptable, the *Standard* requires the isolation system to:
- Remain stable for maximum earthquake displacements.
- Provide increasing resistance with increasing displacement.
- Have limited degradation under repeated cycles of earthquake load.
- Have well-established and repeatable mechanical properties (effective stiffness and damping).

The *Standard* recognizes that the properties of an isolation system, such as effective stiffness and damping, can change during repeated cycles of earthquake response. This variability is acceptable provided that the design is based on analyses that conservatively bound (limit) the range of possible values of design parameters.

The first seismically isolated buildings in the United States were composed of either high-damping rubber (HDR) or lead-rubber (LR) elastomeric bearings. Other types of isolation systems now include sliding systems, such as the friction pendulum system, or some combination of elastomeric and sliding bearings. Furthermore, at sites with very strong ground shaking there has been the application of supplementary fluid viscous dampers in parallel with the bearings to control displacement. While generally applicable to

all types of systems, certain requirements of the *Standard* (in particular, prototype testing criteria) were originally developed for isolation systems with elastomeric bearings tested at slow-speeds.

Isolation systems typically provide only horizontal isolation and are rigid or semi-rigid in the vertical direction. A rare exception to this rule is the full (horizontal and vertical) isolation of a building in southern California, isolated by large helical coil springs and viscous dampers. Three-dimensional seismic isolation platforms are also currently being designed and implemented for earthquake protection of sensitive computer equipment.   While the basic concepts of the *Standard* can be extended to full isolation systems, the requirements are only for horizontal isolation systems. The design of a full isolation system requires special analyses that explicitly include vertical ground shaking and the potential for rocking response.

15.1.3 Design Process Summary

The following design process is specific for elastomeric isolation systems however the process is similar for sliding isolation systems.

Recommended[3] design steps include:

1) Determine the site response spectrum using the USGS website and check if a site-specific ground motion hazard analysis is required. Determine proximity to faults for use in the selection and scaling of motions (i.e. near fault, high velocity pulse motions). Engage specialist expertise, as appropriate, for the selection and scaling of motions for response history analysis.

2) Select bearing dimensions and properties and quickly assess adequacy using the equivalent lateral force (ELF) procedure for estimating displacement and the stability criterion (see Section 15.3.1). Be sure to include the effects of additional axial load due to vertical earthquake and overturning moment effects, and additional displacement due to torsion. The design may be conservative at this stage as the analysis is not yet refined. Use lower bound properties of the isolation system and the MCE_R earthquake.

3) When a bearing design appears promising, proceed with a formal determination of the isolation system properties (see Section 15.4) and conduct the ELF procedure for lower bound and upper bound bearing properties on a three-dimensional mathematical model of the building (see Section 15.5). At this point the designer may want to think about distribution of bearing types (e.g. some with and some without lead cores) so that torsion is minimized. Calculate bearing displacement demands, story shear forces, story drifts and additional axial bearing loads. Note that for the calculations of the axial loads the designer will have to perform a static analysis of the frame, including torsion effects.

4) Perform an analysis to assess the vertical earthquake effects. This could be by simply adding $\pm$ $0.2S_{MS}D$ or by more refined calculations. For example, constructing a representative vertical response spectrum and performing a vertical response spectrum analysis (see Section15.6.4). This could be done with an ETABS (or similar) comprehensive model or by simply treating the structure as a rigid block with vertical stiffness derived from the vertical stiffness of the bearings. This analysis will give the peak vertical load on each bearing due to the vertical ground motion. This can be combined with the horizontal earthquake effects by combining 100% vertical + 30% horizontal or 30% vertical +100% horizontal (this is consistent with the ASCE 7-10 philosophy

---

[3] Adapted from a design steps list created by SUNY Dist. Prof. Michael Constantinou, University at Buffalo.

for combining loads in orthogonal directions, but a statement to this effect is not clearly made in ASCE 7-10).

5) Assess the adequacy of the bearings using the results of the ELF analysis. Determine if uplift/tension is a problem. If so, modify the structure to reduce uplift/tension to acceptable levels (for an elastomeric bearing, negative pressure not more than *3G*, where *G* is the shear modulus of the elastomer). The model for static analysis in step 3 above is useful in this step. If not possible to modify the structure to achieve the desired effect, you may consider other options, including modifying the isolation system to further reduce the shear force, replacing some elastomeric bearings with another type of bearing or accepting damage to a limited number of bearings provided the resulting structure response is acceptable.

6) Check requirements to see if a response spectrum or response history analysis is required. For a response history analysis, model and analyze the structure in the lower and the upper bound conditions for the MCE_R (see Section 15.6). The designer needs to decide on how to include vertical earthquake effects. Options are to include nothing and simply add later the axial load effect due to the vertical earthquake determined in Step 4, or add a $+ag$ or $–ag$ constant vertical earthquake in the dynamic analysis where a is a portion of the acceleration determined in the vertical earthquake response spectrum analysis (say if the peak value was 1.2g, then $a = 0.3 \times 1.2 = 0.36$). Also, the designer needs to consider torsion. The best approach is to model only the actual eccentricities (none in this example, because the building above the bearings and the isolation system is symmetric) and not artificially shift the center of mass. Accidental torsion is instead added using the same approach as in the ELF procedure or by using amplification factors.

7) Compare response history and ELF results on peak resultant bearing displacement, story shear force and drifts (along the two principal building directions). Decide on the final values for bearing displacements and forces to use in assessing adequacy of the bearings. These values will be from the response history analysis values if its values are larger than the ELF values; otherwise the values for evaluation cannot be less than a certain portion of the ELF values per the *Standard §17.6.4*.

15.2 PROJECT INFORMATION

15.2.1 Building Description

This Emergency Operations Centre (EOC) is a three story, steel frame structure with a large, centrally located mechanical penthouse. Story heights are 14 feet at the first floor to accommodate computer access flooring and other architectural and mechanical systems and 12 feet at the second, third and penthouse floors. The roof and penthouse roof decks are designed for significant live load to accommodate a helicopter landing pad and to meet other functional requirements of the EOC. Figure 15.2-1 shows the three-dimensional model of the structural system.
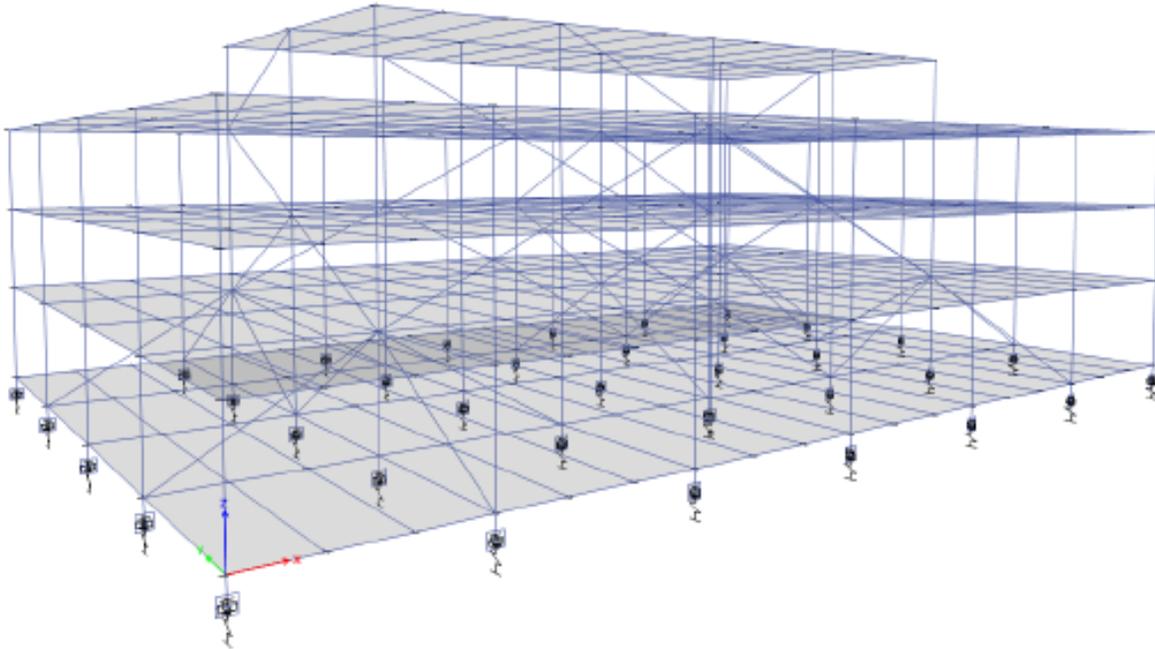
Figure 15.2-1 Three-dimensional Model of the Structural System

The structure (which is regular and symmetrical in configuration) has plan dimensions of 100 feet by 150 feet at all floors except for the penthouse, which is approximately 50 feet by 100 feet in plan. Columns are spaced at 25 feet in both directions. Figures 15.2-2 and 15.2-3 are framing plans for the typical floor levels (but with beam sizes for the first level) and the penthouse roof, respectively. The X-direction is termed the longitudinal direction and the Y-direction is the transverse direction
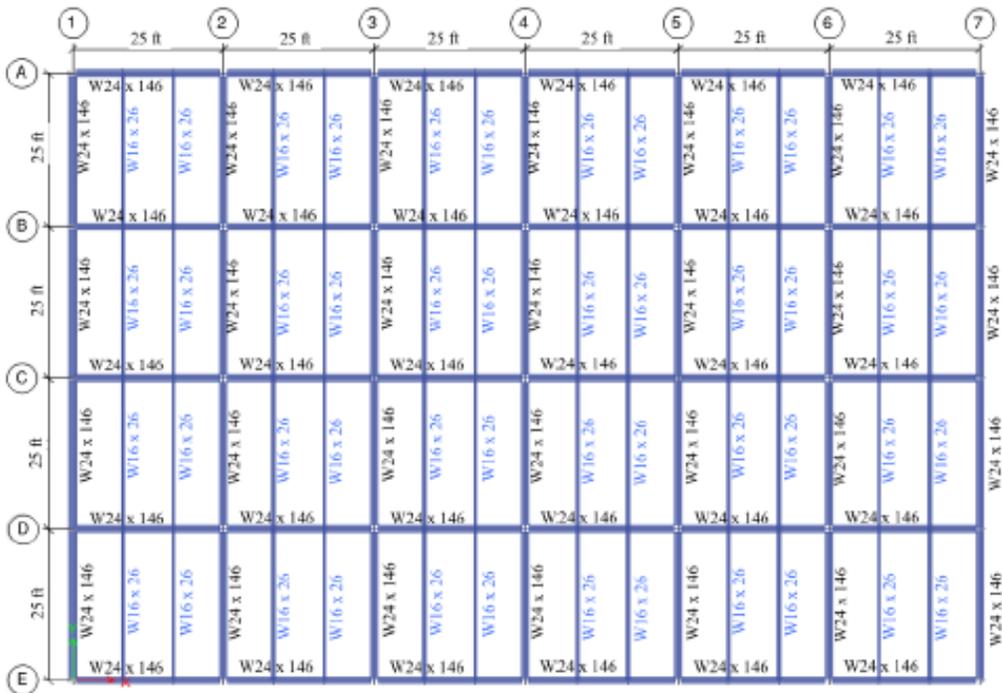
Figure 15.2-2 Typical Floor Layout with First Floor Framing
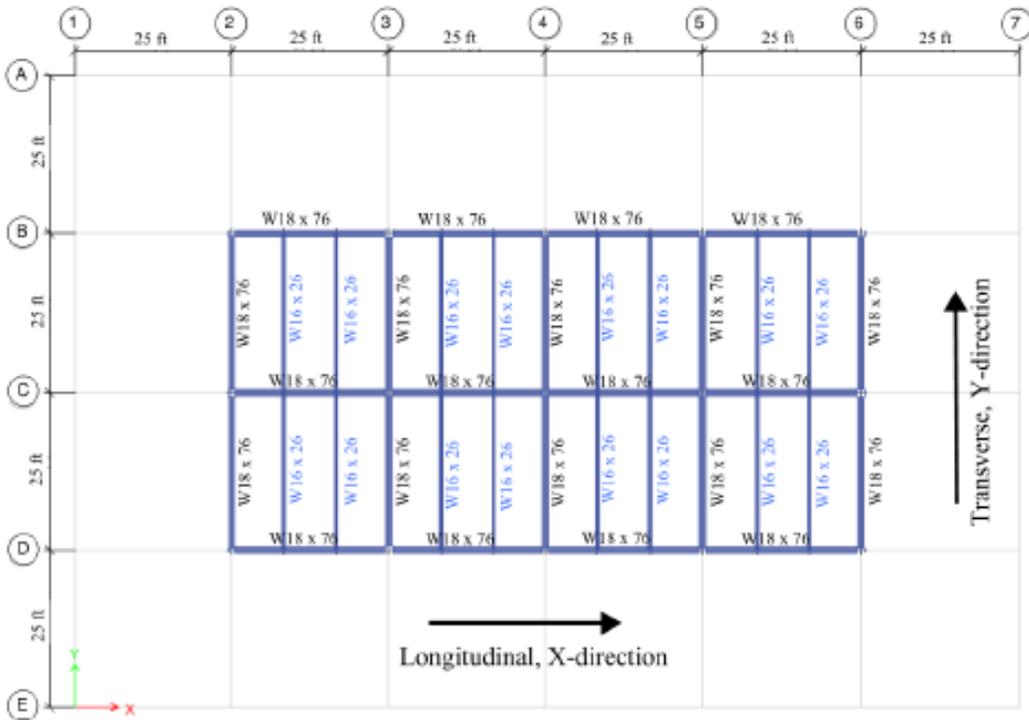
Figure 15.2-3 Penthouse Roof Framing Plan

The vertical load-carrying system consists of concrete fill on ribbed steel deck floors, supported by steel beams at 8.3 feet on center and steel girders at gridlines. Isolation devices (also referred to as isolators or bearings) support each column below the first floor. The foundation consists of concrete spread footings.

The lateral force resisting system consists of a roughly symmetrical pattern of concentrically braced frames. These frames are located on Gridlines B and D in the longitudinal direction and on Gridlines 2, 4 and 6 in the transverse direction. Figures 15.2-4, 15.2-5 and 15.2-6 show elevations of the longitudinal and transverse framing. This framing is specifically configured to reduce the concentration of earthquake overturning and uplift (tension) loads on the bearings. This is achieved by:

Increasing the number of bays with bracing at lower stories.

Locating braces at interior (rather than perimeter) gridlines since they have greater gravity loading.

Avoiding common end columns for bracing in the transverse and longitudinal directions.

Figure 15.2-4 Longitudinal Bracing Elevation, Gridlines B and D
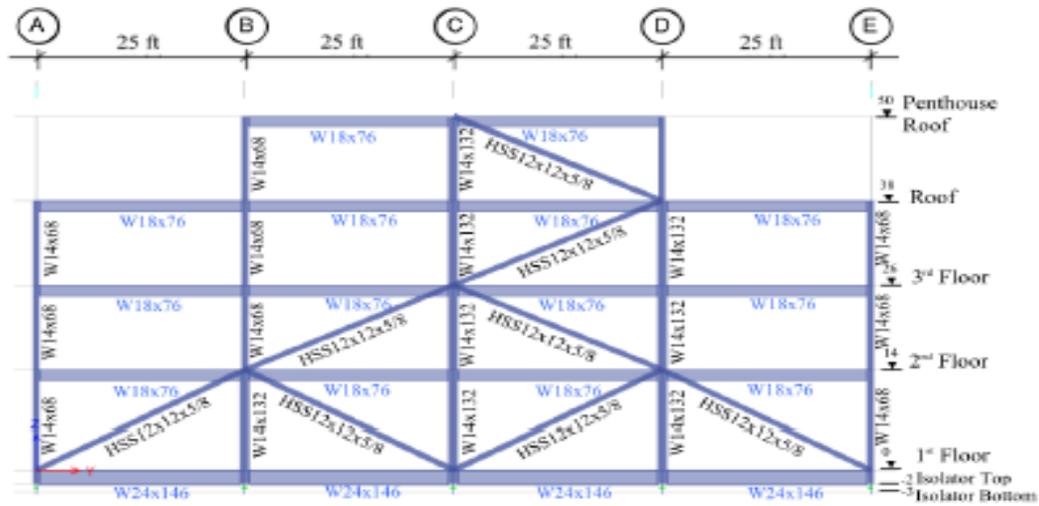
Figure 15.2-5 Transverse Bracing Elevation, Gridlines 2 and 6:
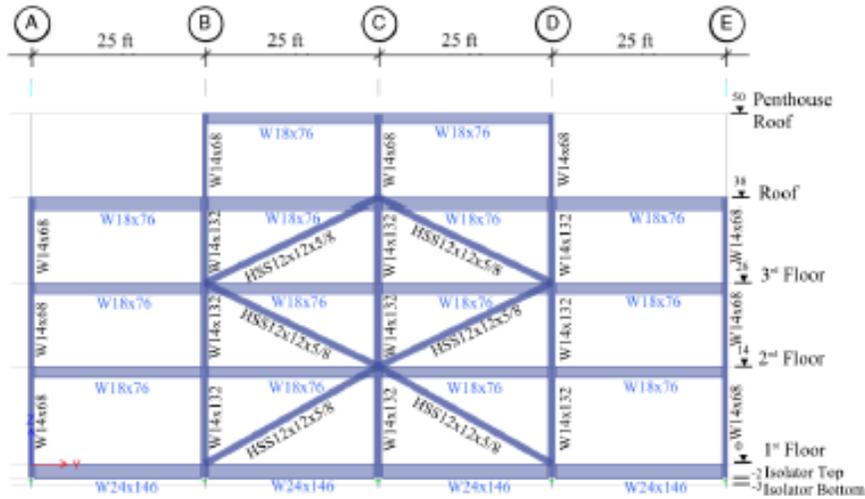
Figure 15.2-6 Transverse Bracing Elevations, Gridline 4:

The isolation system has 35 identical lead rubber bearings located below each column. The first floor is just above grade and the bearings are approximately 3 feet below grade to provide clearance below the first floor for construction and maintenance personnel. A short retaining wall borders the perimeter of the facility and provides approximately 2 feet of "moat" clearance for lateral displacement of the isolated structure. Access to the EOC is provided at the entrances by segments of the first floor slab, which cantilever over the moat.

Girders at the first-floor gridlines are much heavier than the girders at other floor levels and have moment-resisting connections to columns. These girders stabilize the bearings by resisting moments due to both vertical P-delta effects and horizontal shear loads. Column extensions from the first floor to the top plates of the bearings are stiffened in both horizontal directions to resist these moments and to serve as stabilizing haunches for the beam-column moment connections. The typical detailing of this connection is shown in Figure 15.2-7.
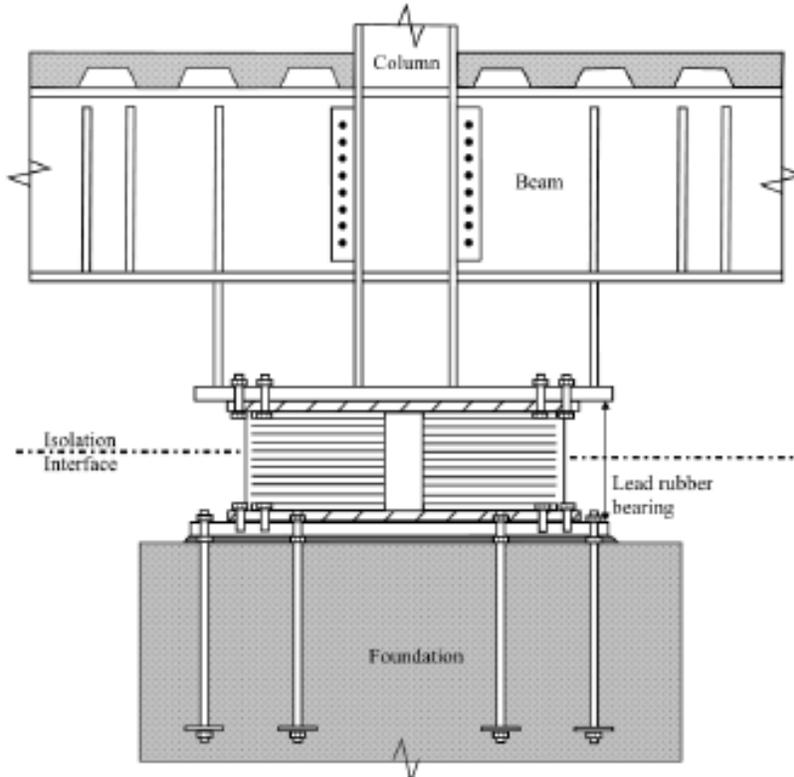
Figure 15.2-7 Typical Detailing of Isolation System at Columns
(for clarity, some elements are not shown)

15.2.2 Building Weights

The gravity loadings include the main structural framing (composite floor and framing), architectural facades, partitions and superimposed dead loads (i.e. MEP, ceiling systems). A summary of the EOC dead loads and live loads without reduction for each level are:

Penthouse roof	D_{PR}	= 800 kips	L_{PR}	=	250 kips
Roof (penthouse floor)	D_R	= 2250 kips	L_R	=	750 kips
Third floor	D_3	= 1950 kips	L_3	=	1500 kips
Second floor	D_2	= 1900 kips	L_2	=	1500 kips
First floor (base level)	D_1	= 2200 kips	L_1	=	1500 kips
Total EOC Dead Load	D	= 9100 kips	L_{unred}	=	5500 kips

The 2012 IBC Section 1607.10 permits an area-based live load reduction of not more than 60 percent for elements with live loads from multiple stories. Therefore the axial component of live load on columns at lower levels and on bearings have a total reduced live load (L) of $L = 2,200$ kips.

The effective seismic weight is taken as the dead load plus half the reduced life load, equal to 10,200 kips. Alternatively, the seismic weight could be calculated in accordance with *Standard §12.7.2*, which gives an effective seismic weight equal to the dead load plus a provision for partitions and the weight of permanent fixtures. For this example the seismic weight is taken as the former case, D + 0.5L, to be consistent with vertical load combination 1 specified in *§17.2.7.1*.

15.2.3 Seismic Design Parameters

Performance criteria. The performance criteria are determined according to *Standard §1.5.1*:

Designated Emergency Operation Center: Occupancy Category IV

Occupancy Importance Factor: $I = 1.5$ (for a conventional structure)

Occupancy Importance Factor (*Standard Chapter 17*): $I = 1.0$ (for an isolated structure)

Note: *Standard Chapter 17* does not require use of the occupancy importance factor to determine the design loads on the structural system of an isolated building (i.e., $I = 1.0$). However, the component importance factor is still required by Chapter 13 to determine seismic forces on nonstructural components of isolated structures ($I_p = 1.5$ for Occupancy Category IV facilities).

Design spectral accelerations. Chapters 11 and 21 of the *Standard* are used to determine the design spectral accelerations. The *Standard* incorporates changes to the ground motions (new USGS spectral accelerations and site coefficients) and new site-specific analysis requirements. Section 11.4.7 requires that a ground hazard analysis be performed in accordance with Section 22.2 on sites with an S_1 greater than or equal to 0.6. For the purpose of this example, a generic site has been selected with details as follows:

Site Hazard and Soil Conditions:

Seismic Design Category (*Standard §11.6*): D

Nearest active fault: greater than 3 miles away

Site soil type: Site Class D

Short-Period Design Parameters:

Short-period MCE$_R$ spectral acceleration: $S_S = 1.4$

Site coefficient (*Standard* Table 11.4-1): $F_a = 1.0$

Short-period MCE$_R$ spectral acceleration adjusted for site class (F_aS_S): $S_{MS} = 1.4$

1-Second Design Parameters:

1-Second MCE$_R$ spectral acceleration: $S_1 = 0.50$

Site coefficient (*Standard* Table 11.4-2): $F_v = 1.8$

1-Second MCE$_R$ spectral acceleration adjusted for site class (F_vS_1): $S_{M1} = 0.9$

15.2.4 Structural Design Criteria

Design basis.

Seismic force-resisting system (< 160 feet): Ordinary steel concentrically braced frames (OCBF)

Although *Table 12.2-1* of the *Standard* limits the height of fixed-base OCBFs to 35 feet for this Seismic Design Category D building, new provisions (*§17.2.5.4*) permit the use of OCBFs in seismic isolation applications for heights up to 160 feet. This is permitted provided 1) the OCBF remains elastic for the MCE_R event and 2) the displacement capacity to which the isolation system lock-up or impact the moat wall shall be increased by a factor of 1.2.

Response modification factor for design of the superstructure: $R_I = 1.0$

Note: *Standard §17.5.4.2* gives $R_I = 3/8R \leq 2$, $R_I = 1.2$ however R_I is limited to 1.0 in *§17.2.5.4* since it is an OCBF.

Horizontal irregularity (of superstructure) (*Standard Table 12.3-1:* Type 1b): None

Vertical irregularity (of superstructure) (*Standard Table 12.3-2:* Type 1a, 1b, 5a, 5b): None

Redundancy factor (*Standard §17.2.3*): $\rho = 1.0$

Earthquake load effects (*Standard* Chapters 12 and 17).

The *Standard* has been revised so that analysis and design need only be considered for the MCE_R event. The horizontal, vertical and torsional earthquake effects are taken as follows:

Maximum considered earthquake ($Q_E \pm 0.2S_{MS}D$): $E = \rho Q_E \pm 0.28D$

Mass eccentricity - actual plus accidental: $0.05b = 5$ ft (X direction); $0.05d = 7.5$ ft (Y direction)

where Q_E are the effects of horizontal seismic forces and $0.2S_{MS}D$ is the vertical seismic load effect. For the ELF procedure, the combination of the horizontal earthquake effects in the X and Y directions are:

- $Q_E = $ Max $(1.0Q_{EX} + 0.3Q_{EY}, 0.3Q_{EX} + 1.0Q_{EY})$

For the response history analysis, two perpendicular components of horizontal ground motion are simultaneously applied in the model and therefore the combination of orthogonal effects is directly accounted for.

Superstructure design load combinations (*Standard §2.3.2*, using $R_I = 1$).

Gravity loads (dead load and reduced live load): $1.4D$ and $1.2D + 1.6L$

Maximum gravity and reduced earthquake loads ($1.2D + 0.5L + 1.0E$): $1.48D + 0.5L + Q_E/R_I$

Minimum gravity and reduced earthquake loads ($0.9D - 1.0E$): $0.62D - Q_E/R_I$

Note the load factor on *L* is taken as 0.5 for this example since the live load is not greater than 100 psf.

15.2.4.6 Isolation system and foundation design load combinations

Gravity loads (for example, long term load on bearings): $1.4D$ and $1.2D + 1.6L$

Standard §17.2.7.1:

1. Average gravity loads

    $(1.0D + 0.5L)$: $1.0D + 0.5L$ (15.2-1)

2. Maximum gravity and unreduced earthquake loads

    $(1.2D + 0.5L + 1.0E)$: $1.48D + 0.5L + Q_E$ (15.2-2)

3. Minimum gravity and unreduced earthquake loads

    $(0.9D - 1.0E)$: $0.62D - Q_E$ (15.2-3)

15.3 PRELIMINARY DESIGN OF ISOLATION SYSTEM

The preliminary design of both an elastomeric isolation system, consisting of lead-rubber bearings, and a sliding isolation system, consisting of double concave sliding bearings, is illustrated.

The preliminary design requires the determination of the isolation system properties (e.g., effective period and damping), which depend on the type and size of the isolation bearings and the type and size of supplementary dampers if they are also incorporated into the isolation system. The size of the bearings is related to the amount of vertical load that they support and the maximum lateral displacement. This displacement is a function of both the MCE_R ground motions at the building site and the effective period and damping of the isolation system. Thus, preliminary design tends to be an iterative process.

A common approach is to perform parametric studies to get a theoretical understanding of the tradeoff between forces and displacements. However the engineer must be mindful of specifying details (i.e. a friction coefficient or a stiffness) of bearings not previously manufactured and tested as this will give uncertainty in performance and potential for further iterations later in design. Furthermore, atypical bearings may be more expensive and take longer to manufacture, test and deliver. A recommended approach is to make contact with manufacturers early in the design process to view qualification test data (*§17.8.1.1* of the *Standard*) and use this data along with the details of the similar bearings as a basis for design.

The preliminary designs are based on the approach presented in Constantinou et al. (2011). This method uses the ELF procedure and gives guidance for estimating the dynamic nominal properties of lead-rubber and friction pendulum bearings based on the assumption that the manufacturer is unknown or qualification test data is not available.

15.3.1 Elastomeric Isolation System

The elastomeric isolation system will consists of 35 lead-rubber (LR) bearings of the same size. This section illustrates how to estimate the diameter of the bearing D_B, the diameter of lead core D_L and the total rubber thickness T_r. By determining these three variables, along with manufacturer specific or default properties from Constantinou et al. (2011), one can calculate the force-displacement behavior of the bearings and in turn the effective stiffness and effective damping of the isolation system.

Force-displacement behavior. The hysteretic force-displacement behavior of LR bearings can be idealized as bilinear as illustrated in Figure 15.3-1. The two key parameters that characterize behavior are the characteristic strength Q_d, which is primarily dependent on the mechanical properties of lead, and the post-elastic stiffness k_d, which is primarily dependent on the mechanical properties of rubber. The value of the yield displacement Y is in the range 0.25 to 1.0 inch and, although it may affect the in-structure accelerations and residual displacements of the isolation system, is of minor significance.
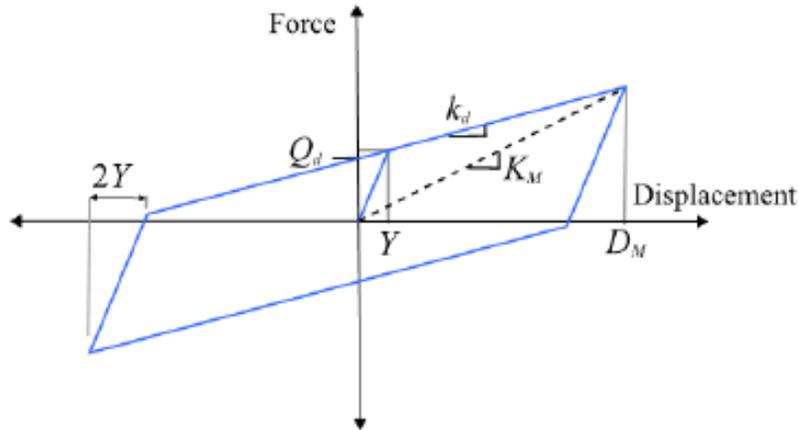
Figure 15.3-1 Bilinear Force-Deflection Behavior of LR Bearings

The characteristic strength Q_d is the strength of the bearing at zero displacement and can be idealized as being related to the diameter of the lead core D_L and the effective yield stress of lead σ_{YL}:

$$Q_d = \frac{\pi D_L^2 \sigma_{YL}}{4} \qquad\qquad (15.3\text{-}1)$$

Equation 15.3-1 implies that any contribution to the strength from rubber is included in σ_{YL}, which is a reasonable simplification for low-damping rubbers used in LR bearings.

The post-elastic stiffness k_d is related to the shear modulus of rubber G, the bonded rubber area (which is a function of the diameter of the bearing and the lead core) and the thickness of rubber T_r (sum of the individual rubber layers):

$$k_d = \frac{G f_L \pi (D_B^2 - D_L^2)}{4 T_r} \qquad\qquad (15.3\text{-}2)$$

The parameter f_L accounts for the effect of the lead core on the k_d and ranges in value from 1.0 to about 1.2. Only after repeated cycling is the value of f_L close to unity.

Nominal properties and bounding. The two important properties to determine are the effective yield stress of lead σ_{YL} and the shear modulus of rubber G. These properties are dependent on a variety of parameters and are manufacturer specific.

There is uncertainty in σ_{YL} as it is dependent on the speed of motion, size and confinement of the lead core (i.e. vertical load, manufacturer details with steel plates and installation of the lead core), and degrades from cycle to cycle due to heating effects. Constantinou et al. (2011) provide guidance on a range of properties based on high velocity, large amplitude testing of LR bearings. The dynamic nominal value (which is the average of properties over 3-cycles of loading) of σ_{YL} may be in the range of 1.45 to 1.75 ksi. The upper bound

is taken as the first cycle properties, recommended as 1.35 times the nominal properties. The lower bound is assumed to be the nominal properties, which are close to the second cycle properties. Hence the values of σ_{YL} taking into account uncertainty in the nominal value, scragging, speed of motion and heating effects is:

- Upper bound $\quad\quad\quad \sigma_{YL,max} = 1.75 \times 1.35 = 2.36$ ksi

- Lower bound $\quad\quad\quad \sigma_{YL,min} = 1.45$ ksi

The shear modulus of rubber G depends on the rubber compound and manufacturing processes, which are proprietary, as well as the on the frequency and conditions of loading. Constantinou et al. (2011) recommend a nominal value in the range of 65 to 125 psi. Lower values of G are possible however few manufacturers can reliably achieve this without experiencing significant scragging effects (temporary degradation of properties with repeated cycling). For this example we seek the lowest shear modulus and consider a range of 60-75psi for a competent bearing manufacturer. The associated scragging and aging effects are taken as 1.1 and 1.1, respectively, times the nominal value. Hence the values of G are calculated as:

- Upper bound $\quad\quad G_{max} = 75 \times 1.1 \times 1.1 = 91$ psi
- Lower bound $\quad\quad G_{min} = 60$ psi

If the manufacturer is inexperienced then these values may not be conservative and it is recommended the engineer use a wider range to account for uncertainties.

Preliminary design procedure. This procedure is based on examples in Constantinou et al. (2011) and involves assessing the bearing stability, which is a critical check for preliminary sizing of elastomeric bearings. Other adequacy checks are necessary but can be done later in design or by the bearing manufacturer.

The bearing stability is critical at maximum displacements and large compression loads. Hence the lower bound properties will be used for this analysis (lower bound on lateral stiffness) with a conservative (high) estimate on the vertical load. An upper bound analysis (upper bound on lateral stiffness) may also be conducted at the preliminary design stage as it typically results in the maximum forces on the structure and maximum uplift demands on the bearings. This upper bound analysis can also be done after a mathematical (e.g. ETABS) model is created, so as to better understand the distribution of inertial forces over the height of the structure.

To enable iteration, the process is best executed using a spreadsheet and can be summarized as follows:
1. Approximate values for the variables D_L, D_B and/or T_r
2. Conduct the ELF procedure to calculate the maximum displacement D_M
3. Increase D_M for torsion and make a conservative estimate of the vertical compression load due to dead, live, vertical earthquake and overturning effects.
4. Calculate the required individual rubber layer thickness to maintain stability of the bearing. An acceptable design is typically one where the rubber layer thickness is in the range of 0.25 to 0.75 inches and where the shear strain (total displacement D_M divided by T_r) is in the 200-250% range. If this is not achieved then perform another iteration by altering the values in Step 1

A step-by-step illustration of this process with further guidance is provided below:

- **Step 1**
The first step involves sizing the lead core so that the strength of the isolation system is some desirable proportion of the building weight W. In general $Q_{d,total}/W$ should be about 0.05 or greater in the lower bound analysis. A ratio of 0.08 gives a system strength $Q_{d,total}$ of 816 kips and, by Equation 15.3-1, a lead core diameter of $D_L = 4.5$ inches for 35 LR bearings. As will be seen later, it is necessary to increase D_L in order to reduce displacements and maintain stability of the bearing. Guidance from Constantinou et al. (2011) on the selection of D_B and T_r is as follows:

- D_B should be in the range of $3D_L$ to $6D_L$
- T_r should be about equal to or larger than D_L

Furthermore, the configuration of the isolation system may be altered, for example by arranging a mixture of LR bearings and low-damping elastomeric bearings, or by installing supplementary dampers that act in parallel with the isolation bearings. For simplicity, these options are not explored in this example.

- **Step 2**

Using the LR bearing dimensions in Step 1 and properties in Section 15.3.1.2, construct a bilinear force-displacement model of the isolation system. This is simply the sum of individual bearings strengths and stiffnesses since the bearings are acting in parallel across the isolation plane. The ELF procedure (per Section 15.5.1) is then conducted to calculate the maximum bearing displacement D_M.

- **Step 3**

This step involves estimating the critical combination of displacement (including torsion) and vertical load for the stability calculation. Since this is preliminary design, conservative assumptions can be made by calculating the displacement for a corner bearing and combining with the maximum vertical load which occurs at any interior bearing. Since the *Standard* does not permit the total maximum displacement D_{TM} to be taken less than $1.15D_M$, and considering that the building is rectangular and has a uniform distribution of bearing properties (i.e. not purposely configured to increase the torsion resistance), D_{TM} of the corner bearing is taken as 1.2 times D_M calculated in Step 2. The vertical load from dead and live loads can be roughly calculated based on tributary area, giving 380 kip and 90 kip, respectively, and the vertical load from earthquake overturning can be approximated by taking the base shear $K_M D_M$, applying it as a vertical triangular distribution over the height of the structure, distributing it to the braced frames and then calculating the resistance to this overturning by the reaction from each bearing support. This crude and conservative calculation gives a maximum overturning load of about 550 kip for the lower bound analysis.

Therefore from load combination Equation (15.2-2) the maximum compression load from preliminary calculations is 1200 kips which is used for the stability calculation in Step 4.

- **Step 4**

The empirical equations that follow, for assessing the required rubber layer thickness, are from Constantinou et al. (2011). For a deformed hollow (assuming the lead core does not to contribute to stability) circular bearing which is bolted to base plates top and bottom, the maximum thickness of rubber layers, t, to maintain stability is calculated as follows:

$$t \le 0.218 \frac{G D_B^4}{T_r} \frac{\left(1 - \dfrac{D_L}{D_B}\right)\left(1 - \dfrac{D_L^2}{D_B^2}\right)}{\left(1 - \dfrac{D_L^2}{D_B^2}\right)} \frac{(\delta - \sin \delta)}{\phi \pi P_u} \qquad (15.3\text{-}3)$$

where G is the nominal shear modulus of rubber (ksi), D_B is the diameter of the bearing (inch), D_L is the lead core diameter (inch), T_r is the total thickness of rubber (inch), P_u is the factored ultimate compression load (kip), the factor of safety ϕ is taken as 1.1 and δ is calculated as follows:

$$\delta = 2\cos^{-1}\left(\frac{D_{TM}}{D_B}\right) \qquad (15.3\text{-}4)$$

A summary of the preliminary design calculations is provided in Table 15.3-1. The first design iteration required a rubber thickness of 0.072 of an inch and had a shear strain of over 300%, which is not practical

to construct. Therefore the size of the lead core and diameter of the bearing were increased to get a rubber layer that is practical to construct and to reduce the shear strain.

Table 15.3-1   Preliminary Design Calculations for LR Bearings

Properties (Section 15.4.1.2)		1st Iteration	Lower Bound	Upper Bound	Units
Effective Yield Stress of Lead	σ_{YL}	1.45	1.45	2.36	ksi
Rubber Shear Modulus	G	60	60	91	psi
Bearing Dimensions (Step 1)					
Lead Core Diameter	D_L	4.5	5.125	5.125	inch
Bonded Rubber Diameter	D_B	22.5	26.5	26.5	inch
Total Thickness of Rubber	T_r	4.5	5.125	5.125	inch
Yield Displacement	Y	0.60	0.60	0.60	inch
Isolation System Force-Displacement Behavior (Step 2)					
System Post-elastic Stiffness	$k_{d,Total}$	178	218	330	kip/in
System Characteristic Strength	$Q_{d,Total}$	807	1047	1704	kip
Equivalent Lateral Force Procedure (MCE$_R$) (Step 2)					
Maximum Displacement	D_M	13.6	11.2	7.7	inch
Effective Stiffness	k_M	237	311	551	kip/in
Effective Period	T_M	2.10	1.83	1.38	second
Effective Damping	β_M	0.15	0.18	0.24	
Required Rubber Layer Thickness (Steps 3 and 4)					
$(1.2 + 0.2S_{MS})D + 0.5 L + Q_E$	P_u	1156	1199	1328	kip
Displacement with Torsion	D_{TM}	16.3	13.4	9.2	inch
Rubber thickness for stability	t	0.072	0.274	0.553	inch
Rubber Shear Strain	D_M/T_r	302	219	150	%
Strength at Yield	Q_d/W	8	10	17	%
Base Shear	V_b/W	32	34	42	%

Uplift assessment. At this point in design it is also worthwhile to assess the potential for uplift at bearings. Using preliminary estimates of axial loads along with the minimum vertical load combination, Equation 15.2-3, the uplift demand is about -350 kip (in tension). Tension in elastomeric bearings should be avoided, nevertheless, Constantinou et al. (2007) states that high quality manufacturers can sustain tensile pressure of about $3G$ before cavitation occurs (where G is the shear modulus of the elastomer). The issue however is that this cannot be known without testing of the production bearings and testing may damage the bearings. Accordingly, it is recommended to avoid large tension demands that are close to the capacity of $3GA_r$ (~100 kip for this preliminary sized bearing using lower bound properties).

There are various solutions to consider for mitigating the effects of uplift:

1. Change the structural system to eliminate or reduce the bearing tension to an acceptable level, by:
   a. Increasing the number of bays with braced frames.
   b. Moving the braced frame location to where the columns have high dead loads or artificially increasing the dead load (i.e. localized thickening of slabs or heavy facades).
   c. Stiffening the beams above the bearings to distribute the tension over a larger number of bays.

2. Alter the bearing connection details to allow for limited and controlled uplift. This will be for the small number of bearings experiencing uplift. Options include:
   a. Have one end of the bearing bolted and the other end recessed/slotted (or with a "loose-nut" condition) to allow limited and controlled uplift.
   b. Use of an uplift restraining system.

   These options require explicit modeling of the uplift behavior to quantify the effects of bearing uplift, and testing under these conditions may also be required.

3. Perform more refined calculations for uplift, using a 3-dimensional mathematical model and by using NLRHA.

Local uplift of individual elements is permitted (*Standard §17.2.4.7*), provided the resulting deflections do not cause overstress or instability of the isolated structure. For this example, the braced frames are well distributed and there is not scope to alter the structural system. Therefore a more refined calculation of the uplift demands will be made using a three dimensional building model and using nonlinear response history analysis. This is expected to reduce the calculated uplift demand.

Uplift on sliding bearings also needs careful consideration however there are examples where controlled uplift of sliding bearings have been accepted on projects, for example the Mills-Peninsula Bay Hospital and the new San Bernardino Court facility, Sarkisian et al. (2012).

15.3.2 Sliding Isolation System

The sliding isolation system will consists of 35 double concave sliding bearings of the same size. Double concave bearings offer many benefits over the single concave configuration, such as more compact bearings, increased displacement capacity, decreased sliding velocities (approximately halved) and therefore reduced frictional heating and associated problems with wear.

The preliminary design involves determining the dynamic friction coefficient of the sliding interface μ and the post-elastic stiffness k_d. This stiffness is simply a function of the radius of curvature of the concave plates. By determining these two variables, one can calculate the force-displacement behavior of the bearing and in turn the effective stiffness and effective damping of the isolation system.

Force-displacement behavior. Sliding bearings are available in a number of different configurations, with a number of different sliding interfaces. The key dimensions of a double concave sliding bearing are illustrated in Figure 15.3-2, where R is the radius of curvature of the concave plates, μ is the coefficient of friction, d is the nominal displacement capacity and h is height to the pivot point. Although double concave bearings may be designed for a range of frictional and geometrical properties (Fenz and Constantinou 2006), this example assumes the bearing has identical properties about the mid-height. That is $R_1 = R_2$, $d_1 = d_2$, $h_1 = h_2$ and $\mu_1 = \mu_2 = \mu$ (note: technically an articulated slider is not required is this scenario).
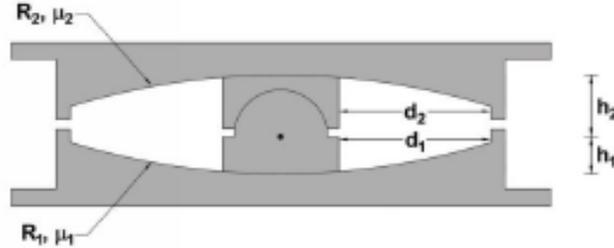
Figure 15.3-2 Section View of Double-concave Sliding Bearing

Single, double and triple concave sliding bearings, with identical friction coefficients and identical radii of curvature on the outer concave plates, can all be idealized by the rigid-linear model shown in Figure 15.3-3. The rigid-linear model will give a reasonable estimate of the global response of the structure for triple concave sliding bearings. However, if in-structure accelerations and residual displacements, or behavior beyond the MCE$_R$ are of interest to the RDP then it may be appropriate to adopt a more sophisticated force-displacement model. The formulation, implementation and validation of the triple concave sliding force-deflection behavior, as well as for other configurations of multi-spherical bearings, can be found in Fenz and Constantinou (2008).
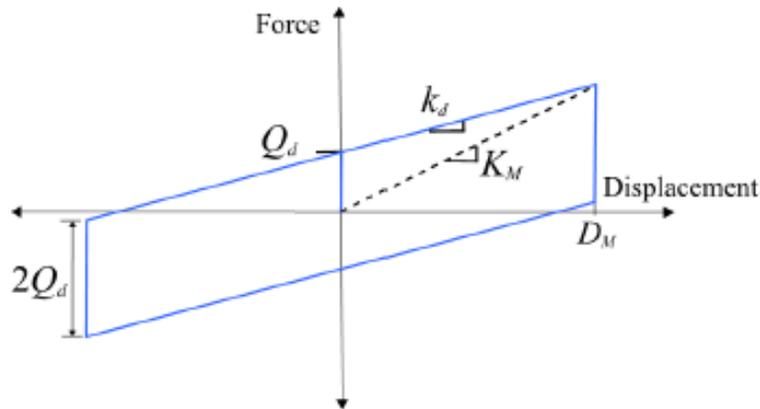
Figure 15.3-3 Rigid-linear Force-Deflection Behavior of Sliding Bearings

The characteristic strength Q_d of the sliding bearing is calculated as μ times the weight on the bearing:

$$Q_d = \mu W \qquad\qquad\qquad (15.3\text{-}5)$$

The post-elastic stiffness k_d for the double concave bearing with $R_1 = R_2$ and $h_1 = h_2$ is calculated as:

$$k_d = \frac{W}{2(R_1 - h_1)} = \frac{W}{2R_{eff}} \qquad\qquad\qquad (15.3\text{-}6)$$

where R_{eff} if the effective radius of curvature equal to (R_1-h_1). Furthermore the actual displacement capacity d^* for $R_1 = R_2$, $d_1=d_2$ and $h_1=h_2$ is given by:

$$d^* = \frac{2(R_1 - h_1)}{2R_1} 2d_1 = \frac{R_{eff}}{R_1} 2d_1 \qquad (15.3\text{-}7)$$

   Nominal properties and bounding. It is recommended to make contact with bearing manufacturers in order to help select a range of trial design friction coefficients and available radii of curvature and diameters (i.e. displacement capacity) of concave plates.

As shown in Equation 15.3-6, k_d is purely based on the geometry of the bearing. Since this can be constructed with a high degree of tolerance by most manufacturers, the bounding of k_d is not required for sliding bearings. k_d is largely dependent on the value of R_1 and therefore this is the parameter the engineer can optimize. Other bearing dimensions can be determined by the manufacturer. A partial list of previously manufactured concave plates, from Constantinou et al. (2011), is R_1 of 61, 88, 120, 156 and 238 inches. Increasing R_1 gives a lower post-elastic stiffness. This typically results in a lower structural shear at the cost of a larger displacement. Although there are greater P-delta moments and the bearing may require more material (i.e. thicker top and bottom plates), this extra displacement can be readily accommodated by increasing the displacement capacity, or by relation d_1, with no change in the force-displacement behavior.

For this example, it is assumed that the manufacturer has already produced and tested bearings with an R_1 of 88 inches, and that this will be used as a basis for design.

The coefficient of friction μ is affected by a number of factors, of which the sliding velocity, bearing pressure (axial load divided by the contact area of the slider) and temperature are the most important. Furthermore μ depends on the type and construction of the sliding interface, which is manufacturer specific and proprietary. As such, a range of default μ values is not listed here for sliding bearings. Rather it is recommended to view dynamic test data from the manufacturer without any effects of aging, contamination and history of loading, that is, for a fresh bearing tested at normal temperature.

For example, Constantinou et al. (2011) approximate the nominal (three-cycle average) coefficient of friction for concave sliding bearings of a particular manufacturer that uses a polytetrafluoroethylene (PTFE) and stainless steel sliding interface, as follows:

$$\mu = 0.122 - 0.01p \qquad (15.3\text{-}8)$$

where p is the contact pressure of the slider. Equation 15.3-8 is applicable for pressures of 2 to 8 ksi, with a slider diameter of 11 inches, and tested amplitudes of 12 to 28 inches. Furthermore testing at velocities of the order of 39 inch/s will have a lower μ than those predicted by Equation (15.3-8) by amounts of about 0.01 to 0.02.

Hence for our preliminary design the average vertical load (D+0.5L) for all bearings is 290 kips, which for a 12 inch diameter slider gives a bearing pressure of 2.6 ksi and μ of 0.096 less 0.015 (for high velocities) = 0.081. This value is further adjusted for uncertainty in the nominal value by a factor of 0.80 to give a nominal coefficient of 0.065 rounded down to 6%. This value is also taken as the lower bound. The upper bound value may be taken as the first cycle value, equal to 1.2 μ, multiplied by aging and contamination effects taken as $(1+0.75(1.1 \times 1.1\text{-}1)) = 1.16$ for an internal environment and a 1.2 factor for uncertainty in the nominal value. Therefore the friction coefficient from preliminary design, accounting for aging, contamination, velocity and heating effects, and uncertainty in the nominal value are:

- Upper bound μ_{max} = $1.2 \times 1.16 \times 1.2 \times 0.065 = 0.11$

- Lower bound $\mu_{,min}$ =   0.06

Preliminary design procedure. The selection of the double concave sliding bearing dimensions, as depicted in Figure 15.3-2, are explained in the preceding sections and are taken as:

- Radius of curvature of plates, $R_1 = R_2 =$ 88   inches

- Internal slider height, $h_1 = h_2 =$ 4.5   inches

- Nominal displacement capacity $d_1 = d_2 =$ 15   inches

Using Equations 15.3-5 and 15.3-6 to construct the force-displacement behavior, the ELF procedure (per Section 15.5.1) is conducted to calculate the maximum bearing displacement D_M and maximum base shear using the upper and lower bound properties determined in 15.3.2.2.

Table 15.2-2   Sliding Isolation System Preliminary Design Calculations

Properties		Lower Bound	Upper Bound	Units
Friction coefficient	μ	0.06	0.11	
Weight	W	10200	10200	kip
Bearing Dimensions				
Radius of Curvature of Plates	$R_1 = R_4$	88	88	inch
Half height of internal slider	$h_1 = h_2$	4.5	4.5	inch
Nominal displacement capacity	$d_1 = d_4$	15	15	inch
Isolation System Force-Displacement Behavior				
System Post-elastic Stiffness	$k_{d,Total}$	61	61	kip/in
System Characteristic Strength	$Q_{d,Total}$	612	1122	kip
Equivalent Lateral Force Procedure (MCE$_R$)				
Maximum Displacement	D_M	19.2	12.5	inch
Effective Stiffness	k_M	93	151	kip/in
Effective Period	T_M	3.35	2.63	second
Effective Damping	β_M	0.22	0.38	
Total Maximum Displacement and Base Shear				
Displacement with Torsion	D_{TM}	23.0	15.0	inch
Strength at Yield	Q_d/W	6	11	%
Base Shear	V_b/W	17	18	%

Using Equation 15.3-7, the actual displacement capacity is 28.5 inches, which is greater than the lower bound total maximum displacement of 23 inches. This displacement includes torsion taken as 1.2 times D_M. Therefore the displacement capacity of the bearings is adequate.

15.4 ISOLATION SYSTEM PROPERTIES

15.4.1 Overview

The materials used in bearings (i.e. composites, lead, elastomers) differ somewhat from conventional civil engineering materials, in that their properties may vary considerably due to temperature, aging, contamination, history of loading, among other factors. There are no standards which govern how a bearing must be produced and assembled. These details vary by manufacturer and are usually proprietary. Furthermore, in the United States there is no official certification required of manufactures before they start supplying bearings for construction. Consequently, there can be a considerable difference in the quality and performance of bearings, even for identical bearings produced by different manufactures.

Given the importance of the isolation system, and uncertainty in the quality of different manufacturers, the *Standard* has taken the approach of requiring the registered design professional (RDP) to determine (in consultation with the manufacturer) the nominal design properties and to account for the likely variation in those properties on a product- and project-specific basis. This is achieved through incorporating new provisions (*§17.2.8*) for calculating the upper- and lower-bound force-deflection behavior of the isolation system.

The following sections give guidance on interpreting test data and procedures for determining the nominal mechanical properties of the bearings. To account for the variation in these properties, property modification or λ factors are used to modify the nominal properties to an appropriate upper- or lower-bound.

The concept of property modification factors was originally presented in Constantinou et al. (1999) and is already implemented in bridge design codes. The approach is to assess the impact of a particular effect on the bearing properties (e.g. heating, aging, velocity, etc), and if the effect is appreciable then assigning it a λ-factor and accounting for the effect in analysis and design. Therefore the λ-factors encompass many different effects and describe the deviation in properties their nominal value. For example, if an effect causes a 10% increase in a nominal property than it is assigned a λ value of 1.10 and contributes to the overall λ_{max} factor. The λ-factors are determined through testing, rational analysis and engineering judgment and are categorized in the *Standard* into three groups:

- $\lambda_{ae.max}$ and $\lambda_{ae.min}$ which account for aging and environmental effects.

- $\lambda_{test,max}$ and $\lambda_{test.min}$ which account for scragging, hysteretic heating and speed of loading.

- $\lambda_{spec,max}$ and $\lambda_{spec.min}$ which account for manufacturing variations.

The *Standard* then combines the λ-factors using *Equations 17.2-1* and *17.2-2* as follows:

$$\lambda_{max} = (1 + f_a(\lambda_{ae,max} - 1)) \times \lambda_{test,max} \times \lambda_{spec,max} \geq 1.8$$
$$\lambda_{min} = (1 - f_a(1 - \lambda_{ae,min})) \times \lambda_{test,min} \times \lambda_{spec,min} \leq 0.6$$

The λ_{max} and λ_{min} factors are applied to each nominal mechanical property of interest and therefore set the upper- and lower- bound force-displacement behavior, respectively. For the LR bearing the shear modulus of rubber G and the effective yield stress of lead σ_{YL} are the important properties. For the sliding bearing, it is the friction coefficient μ. Each of these properties requires determination of property specific λ_{max} and λ_{min} factors.

In *Equations 17.2-1* and *17.2-2* the *Standard* presumes a system property adjustment factor f_a of 0.75, to account for the conservative assumption of having full aging and environmental effects when the governing earthquake occurs. However the RDP has discretion to increase f_a based on the contributing factors to λ_{ae} and/or based on the significance of the structure.

The limits of *Equations 17.2-1* and *17.2-2* do not apply when either:
   a) qualification test data per *§17.8.1.2*, (i.e. satisfying *Items 2, 4, 7 and 8* of the similarity requirements of *§17.8.2.7*), is approved by the RDP and is used to establish λ-factors.
   b) project-specific dynamic prototype testing is conducted per *§17.8.2.3*, and that data is used establish λ-factors.

Therefore the limits of *Equations 17.2-1* and *17.2-2* are rarely expected to apply and are intentionally wide. Caution is advised, however, as they may not be conservative for inexperienced manufacturers with no, or limited test data. Regardless, it is implied by the *Standard* that dynamic testing is required in such a case.

Furthermore, to supplement theses new provisions on isolation system properties, the *Standard* incorporates a new clause: *§17.8.1.1 Qualification Tests* as well as new criteria in *§17.8.2.7 Testing Similar Units* for when a bearing may be classified as similar. *§17.8.2.3* has also been renamed *Dynamic Testing* and implies that prototype testing shall be conducted dynamically.

The RDP has the flexibility and authority to determine what data is accepted as qualification test data. However it is generally the responsibility of the manufacturer to conduct qualification testing. These tests may be used to aid in the establishment of nominal properties and λ-factors, to characterize the longevity of the bearing, and to develop models of the bearing for analysis. In practice it is assumed that manufacturers have comprehensive databases of properties, based on research projects and past prototype and production testing. This is already the case for two suppliers in the United States which have compiled large databases.

The intent of the *Standard* is not that dynamic testing of bearings be conducted on every project. This can be expensive and can only be performed at a limited number of facilities. The change in language in *§17.8.2.3* is identifying that most bearing types exhibit velocity dependence, and that the nominal properties (average over three cycles) calculated from slow-speed testing will be different from the nominal properties calculated from dynamic testing. The nominal properties are typically underestimated by slow-speed testing, due to speed of loading effects, and furthermore the variation in those properties, or bounds ($\lambda_{test,max}$ and $\lambda_{test,min}$), are also underestimated by slow-speed testing due to less heating effects. Therefore it is important to account for dynamic effects in the analysis and design.

15.4.2 Nominal Properties and Testing λ-Factors

Interpreting Test Data from Lead-Rubber Bearings. For this example, dynamic testing per *§17.8.2.2, Item 3* is conducted at a vertical load equal to D + 0.5L on two virgin (unscragged) bearings tested at a normal temperature of 20°C. This test consists of three fully-reversed cycles at a displacement amplitude of D_M conducted dynamically at the effective period T_M determined from the upper-bound properties. Therefore the speed of loading effects and heating effects are directly accounted for by the testing, since it is conducted at approximate peak earthquake velocities (i.e. 30-40 inch/sec).

Figure 15.4-1 illustrates the force-displacement behavior of a LR bearing tested at high-speed, with the test data for two prototype bearings documented in Table 15.5-1. Table 15.5-1 gives the maximum measured force and maximum measured displacement in the positive and negative directions, F$^+$ and F$^-$ and Δ^+ and Δ^- respectively, as well as the measured energy dissipated per cycle E_{loop}. E_{loop} is calculated by

numerical integration of the test loop. Although this test data is fictitious, it is generally representative of high-speed test results from large LR bearings.
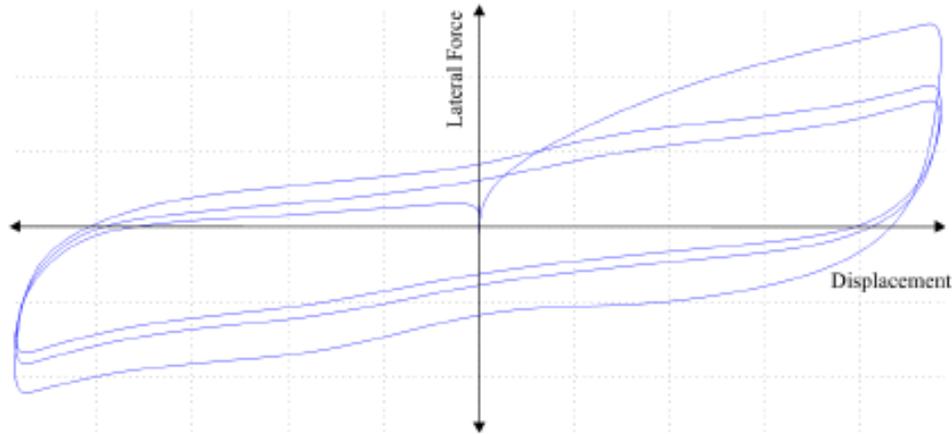
Figure 15.4-1 Representative Dynamic Testing of a LR Bearing

Table 15.4-1 Fictitious Test Data for two Prototype LR Bearings

Measure	F+	F-	Δ+	Δ-	E_{loop}
Units	kip	kip	inch	inch	kip-inch
Bearing 1					
Cycle 1	175	-143	15	-15	2705
Cycle 2	126	-122	15	-15	1861
Cycle 3	116	-116	15	-15	1482
Bearing 2					
Cycle 1	173	-141	15	-15	2688
Cycle 2	124	-120	15	-15	1844
Cycle 3	114	-114	15	-15	1464

The test data in Table 15.4-1 is sufficient to determine the isolation system properties. Before calculating the nominal properties, a few comments and recommendations are noted as follows:

- The first cycle shows a distinctly higher strength and stiffness. This is due primarily to heating effects on the lead core and also scragging effects of the rubber if the test is on a virgin/not previously tested bearing (i.e. unscragged).

- Sequential prototype testing with a small rest time for cooling may give an underestimate of the strength of lead in the first cycle. Therefore it is recommended to determine properties for analysis from only the initial test(s), of a regime of many tests.

- The post-elastic stiffness k_d is influenced by the lead core. Only after the first few cycles are its effect negligible (i.e. in Equation 15.3-2 f_L is equal to 1.0). Therefore it is recommended that the first cycle is not used in the calculation in the shear modulus of rubber.

- The shear modulus of rubber shall not be determined from a coupon test specimen that has a low shape factor (bonded area divided by the area free to bulge). LR bearings used in buildings typically have a shape factor greater than 10 and often larger than 20, and the rubber deforms purely in shear. For coupon tests the rubber may be deforming in shear and bending, which

results in an artificially low estimate of the shear modulus and consequently an unrealistically low calculated effective stiffness of the actual bearing.

▪ It is not possible to determine the scragging effects of rubber from lead rubber bearing test data as the effects in the first cycle are completely masked by heating effect on the lead core. Data from bearings tested from a virgin state without the lead core, or using data from plain natural rubber bearings (if such bearings are also used in parallel in the isolation system) may be suitable. Coupon tests may also be used to estimate scragging effects as the scragging effects are expected to be similar on the bending response (coupon test) and shear stiffnesses (full size bearing test). However size effects shall be taken into consideration since large bearings may exhibit variable zones of curing through the volume of the bearing whereas small coupon samples are generally uniformly cured throughout their thickness.

▪ The stiffness of rubber is dependent on the shear strain; hence the post-elastic stiffness is displacement-dependent. Although dynamic test data are only shown for the maximum displacement, this is somewhat in conflict with the *Standard* which requires that properties envelope $\pm 0.5 D_M$ up to and including $\pm D_M$. This implies that tests at other displacement amplitudes must also be used in determining properties. Enveloping the post-elastic stiffness at different strains may result in a multi-linear force-deflection loop (say, high post-elastic stiffness at smaller strains, which is reduced at medium strains and increased again at large strains). It is the authors' opinion that the post-elastic stiffness should be a best-fit representation of the strains from $\pm 0.5 D_M$ to $\pm D_M$ from the dynamic test data in Figure15.4-1, using only a bilinear model, and that test cycles at other displacement amplitudes (i.e. $0.5 D_M$ and $0.67 D_M$) be viewed to verify consistency with this best-fit. The reason for this is that, under the current Standards provisions, analyses are carried out only at MCE$_R$ conditions. Furthermore the bilinear representation is fitted to the test loop such that it has the same values of effective stiffness at the maximum displacement.

The calculation of the mechanical properties for the two similar/prototype lead rubber bearings is given in Table 15.4-2. The effective stiffness k_{eff} is calculated using *Equation 17.8-1* of the *Standard*. The characteristic strength Q_d (fitted loop force at zero displacement) is determined using Equation 15.4-1, using the energy dissipated E_{loop}, the displacement amplitude D_M, and by assuming a yield displacement Y, taken as 0.6 inches for all cycles.

$$E_{loop} = 4Q_d(D_M - Y)$$ (15.4-1)

Assuming that this strength is all from the lead core, per Equation 15.4-1, one can calculate the effective yield stress of lead. It is noted that rubber may contribute small amount to E_{loop} (by relation, say 0.02 to 0.05 effective damping), and the interested reader is referred to Kalapakidis et al. (2008) for more information.

The post-elastic stiffness can be determined directly by a straight-line fit, or can be calculated based on the Q_d and k_{eff} by the following relationship:

$$k_{eff} = k_M = \frac{Q_d}{D_M} + k_d$$ (15.4-2)

The shear modulus of rubber is then calculated by Equation 15.3-2, assuming the contribution to the post-elastic stiffness from the lead core is negligible ($f_L = 1$) after the first cycle. As noted above, the first cycle properties cannot be used, since the effects of heating on the lead core mask behavior of the rubber.

Table 15.4-2 Mechanical Properties of LR Bearings

Measure	k_{eff}	D_M	Y	Q_d	σ_{YL}	k_d	f_L	G	β_{eff}
Calculation Method	Std[1]. Eq. 17.8-1	Average	Assumed	Eq. 15.4-1	Eq. 15.3-1	Eq. 15.4-2	Assumed	Eq. 15.3-2	Std. Eq. 17.8-2
Units	kip/in	inch	inch	kip	ksi	kip/in		psi	
Cycle 1	10.6	15	0.6	47.0	2.28	Cannot be determined			0.18
Cycle 2	8.3	15	0.6	32.3	1.57	6.11	1	59	0.16
Cycle 3	7.7	15	0.6	25.7	1.25	6.01	1	58	0.14
Average	**8.9**				**1.70**			**58.5**	
Cycle 1	10.5	15	0.6	46.7	2.26	Cannot be determined			0.18
Cycle 2	8.1	15	0.6	32.0	1.55	6.01	1	58	0.16
Cycle 3	7.6	15	0.6	25.4	1.23	5.90	1	57	0.14
Average	**8.7**				**1.68**			**57.5**	
Average of Two	**8.8**				**1.69**			**58**	

1. Std = ASCE 7-2016 *Standard*

Fortuitously, the two prototype bearings have near identical properties. The nominal mechanical properties are calculated as the average among the three cycles, and averaged for the two bearings. Therefore the nominal properties are $G = 58$ psi and $\sigma_{YL} = 1.69$ ksi.

The next step is to determine the associated test λ-factors. The *Standard* requires $\lambda_{test,max}$ and $\lambda_{test,min}$ to include variation from *Item 2 of §17.8.2.2*, which for the *Item 2b* dynamic testing consists of the following sequence: continuous loading of one fully-reversed cycle at each of the following increments of maximum displacement D_M: 1.0, 0.67, 0.5, 0.25 followed by continuous loading of one fully-reversed cycles at each of the following increments of D_M: 0.25, 0.5, 0.67 and 1.0.

For the effective yield stress of lead σ_{YL} the upper bound is taken as the first cycle properties divided by the nominal value, giving $\lambda_{test,max}$=2.27/1.69=1.34. What to take for the lower bound is not so clear. In the initial cycles of loading the lead loses strength due to hysteretic heating effects. This reduction in strength is temporary and recoverable with adequate cooling time. The representative values in Table 15.5-2 show a large difference between the σ_{YL} in the first and third cycles, which is not uncommon for large-scale bearings tested at high-speed. It is the opinion of the authors that the lower bound should be based on considerations of the seismic hazard and nominal isolation system properties (strength and stiffness). Response history analysis studies by Warn and Whittaker (2007) demonstrate that about two (and less than three) fully-reversed cycles at the maximum displacement are expected for isolation systems with a yield strength to supported weight ratio (Q_d/W) of 0.06 or larger and period based on a post-elastic stiffness of 2.5 seconds or greater. Therefore the lower bound will be taken as the second cycle properties, giving $\lambda_{test,min}$=1.56/1.69=0.92.

A validated theory from Kalpakidis et al. (2008) can be used to quantify these heating effects, thus reducing the need for extensive testing. For example, the tested bearing had a displacement amplitude of 15 inches whereas the preliminary design only required a 11.2 inch amplitude. Examples of using simplified heating calculations are illustrated in McVitty and Constantinou (2015).

The process described above is believed to be consistent with the intent of the *Standard,* even though it uses a different test sequence. Simplified heating calculations by Kalpakidis et al. (2008) show that the reduction in σ_{YL} can be related to the total travel of the bearing. After two cycles of loading at D_M the tested bearing has experienced 2×4 $D_M = 120$ inches of travel and σ_{YL} has reduced to a value of 1.56 ksi. Had the *Item 2b* test been conducted, with a D_M of 11.2 inches, the total travel for bounding would be $(1+0.67+0.5+0.25) \times 4$ $D_M = 108$ inches, which is less than 120 inches. Therefore the effects of heating

are adequately captured by testing to two full cycles at a displacement of D_M. It is also noted that the effective damping β_{eff} in Table 15.4-2 is under-predicted when compared to the preliminary design values, as the bearings were tested to a larger displacement.

For the shear modulus of rubber G, the scragging effects need to be determined from other tests, and are assumed in this example to be minor at $\lambda_{test,max}$=1.1 and increased to 1.15 since the nominal value is based on the last two cycles only. Data presented by Thompson et al. (2000) demonstrate that these scragging effects are recoverable within a short period of time (see Constantinou et al. 2007 for more references). Therefore the full effects of scragging should be incorporated in design, even though the bearing is scragged in the production tests.

In summary, the nominal properties and associated test λ-factors, are:
- Nominal Shear Modulus of Rubber, G =   58 psi
- Maximum test λ-factor $\lambda_{test,max}$ =   1.15
- Minimum test λ-factor $\lambda_{test,min}$ =   1.0

- Nominal Effective Yield Stress of Lead, σ_{YL} =   1.7 ksi
- Maximum test λ-factor $\lambda_{test,max}$ =   1.34
- Minimum test λ-factor $\lambda_{test,min}$ =   0.92

Sliding bearings. Representative high-speed dynamic force-displacement behavior for a sliding bearing is illustrated in Figure 15.4-2. The test sequence is not too dissimilar from first half of the *§17.8.2.2, Item 2b* testing. It is noted that this data is for a triple concave sliding bearing, which is why there is a slope (apparent yield displacement) upon reversal of the direction of displacement. For the double concave sliding bearing described in this example the behavior would be more likened to the rigid-linear model of Figure 15.3-3 (i.e. yield displacement Y=0 in Equation 15.4-1).
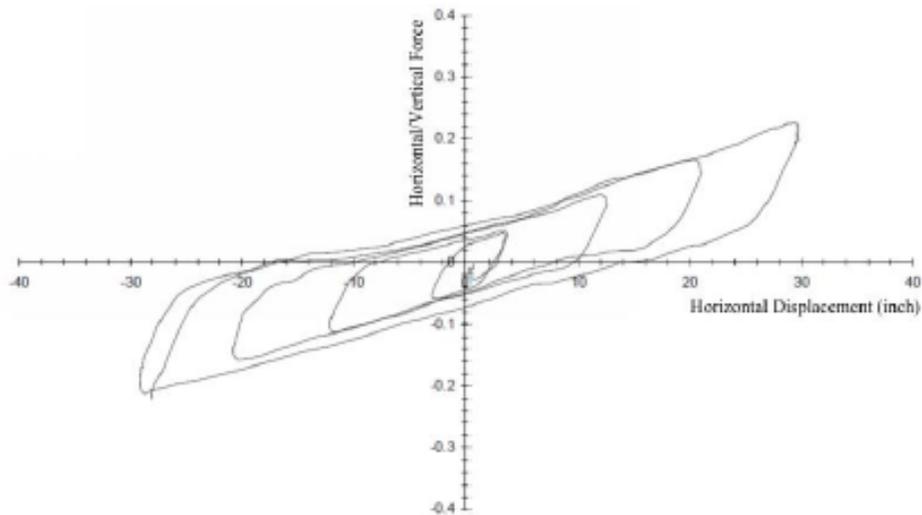
Figure 15.4-2 Representative Dynamic Testing of a Sliding Bearing

The process of determining the nominal mechanical properties and fitting a rigid-linear loop is a similar process to that described in Section 15.4.2.1, with some important points to note:

- The dynamic friction coefficient μ is the most important parameter to determine. It can be calculated directly from the measured energy dissipated per cycle, using Equation 15.4-1 and assuming a yield displacement $Y = 0$. The utility of this calculation is that it can be readily

obtained without determination/judgment of other parameters (say, for a triple concave sliding bearing).

▪ It is recommended to calculate the post-elastic stiffness based on the geometry of the bearing, per Equation15.3-6. This is because the geometry can be constructed by most manufacturers with a high degree of tolerance and theory predicts behavior very accurately. Any observed difference between the fitted loop k_d (based on Equation 15.3-6) and the test data k_d may be due to (a) fluctuations of the vertical load during the test, which affects the instantaneous value of the friction coefficient, and (b) heating effects on the friction coefficient which are more pronounced in high-velocity, large-amplitude cycles. Therefore the approach recommended is to accept that the post-elastic stiffness does not vary and to assign any variability from cycle to cycle to the frictional properties.

▪ The hysteretic heating effects on sliding bearings are dependent on the friction coefficient (which in turn is dependent on temperature), pressure and sliding velocity, as well as size of the bearing components. Therefore the heating effects on sliding bearings are different from that explained above for LR bearings, however the studies by Warn and Whittaker (2004), with regard to the equivalent number of cycles of two at the maximum displacement, are still considered applicable.

15.4.3 Aging and Environmental λ-Factors

The aging and environmental λ factors $\lambda_{ae,max}$ and $\lambda_{ae,min}$ account for the change in properties that occur over the design life of the bearing. Effects include aging, creep, contamination, fatigue, effects of ambient temperature and cumulative travel. For the bearings considered in this example, aging and contamination are the relevant considerations. This is assuming there is little/no movement in the bearings due to service loads (i.e. wind) and that for this application the bearings are not exposed to extreme temperatures or damaging substances. In many cases the effects of aging and contamination are greater than unity (that is $\lambda_{ae,max}$ >1.0 and $\lambda_{ae,min} = 1.0$). Cumulative travel, fatigue and low temperatures are more an issue for bridges. Creep may be an issue for improperly designed bearings. The interested reader may see Constantinou et al. (2007) for further discussion on these effects.

The following sections list typical $\lambda_{ae,max}$ and $\lambda_{ae,min}$ expected of experienced manufacturers, and are adopted for this example.

Elastomeric bearings. The aging and environmental factors for the shear modulus of rubber *G* are:

▪ $\lambda_{ae,max,G} = \lambda_{aging,G} \times \lambda_{contamination,G} = 1.1 \times 1.0$ **= 1.1**

▪ $\lambda_{ae,min,G}$ **= 1.0**

The aging and environmental factors for the effective yield stress of lead σ_{YL} of 99.99% purity are:

▪ $\lambda_{ae,max,\sigma}$ **= 1.0**

▪ $\lambda_{ae,min,\sigma}$ **= 1.0**

Sliding bearings. The aging and environmental factors for the friction coefficient μ for an unlubricated PTFE-stainless steel sliding interface are:

▪ $\lambda_{ae,max,\mu} = \lambda_{aging,\mu} \times \lambda_{contamination,\mu} = 1.1 \times 1.1$ **= 1.21**

- $\lambda_{ae,min,\mu}$ **= 1.0**

15.4.4 Specification λ-Factors

The specification λ-factors; $\lambda_{spec,max}$ and $\lambda_{spec,min}$ are a manufacturing tolerance assumed for design and usually written into specifications. It is recommended that the bearing manufacturer be consulted when establishing these tolerance values.

This tolerance is required because the testing of a small number of prototype bearings may not necessarily provide the best estimate of the nominal design properties. This potential discrepancy occurs because the average of two prototype test results may be at the upper or lower end of the range of a larger population. Alternatively, if past test data is used to establish nominal properties, there may be differences due to the natural variability in properties and manufacturing variations.

For this example the specification tolerance on the average properties of all bearings, for each property of interest (i.e. G, σ_{YL} or μ), is ±10%. That is:

- $\lambda_{spec,max}$ **= 1.10**

- $\lambda_{spec,min}$ **= 0.90**

Variations in individual bearing properties from the nominal design properties may be greater than the tolerance on the average properties of all bearings, say ±15%. The wider specification tolerance for individual bearings is not used for analysis of the isolation system but should be taken into account for bearing connection design by amplifying the upper-bound analysis forces by the ratio of the λ-factors, e.g., 1.15/1.10 for the example values here.

15.4.5 Upper- and Lower-Bound Force-Deflection Behavior

 LR bearings force-displacement behavior. The maximum and minimum λ factors for the shear modulus of rubber and effective yield stress of lead are calculated based on *Equations 17.2-1* and *17.2-2*, as follows:

$$\lambda_{max,G} = (1 + 0.75(1.10 - 1)) \times 1.15 \times 1.10 = 1.4$$

$$\lambda_{min,G} = (1 - 0.75(1 - 1.0)) \times 1.0 \times 0.90 = 0.9$$

$$\lambda_{max,\sigma_{YL}} = (1 + 0.75(1.0 - 1)) \times 1.34 \times 1.10 = 1.5$$

$$\lambda_{min,\sigma_{YL}} = (1 - 0.75(1 - 1.0)) \times 0.92 \times 0.90 = 0.8$$

The upper- and lower- bound force-displacement behavior of the preliminary sized elastomeric isolation system, based on the nominal values and λ-factors in Sections 15.4.2 through 15.4.4, is illustrated in Figure 15.4-3.
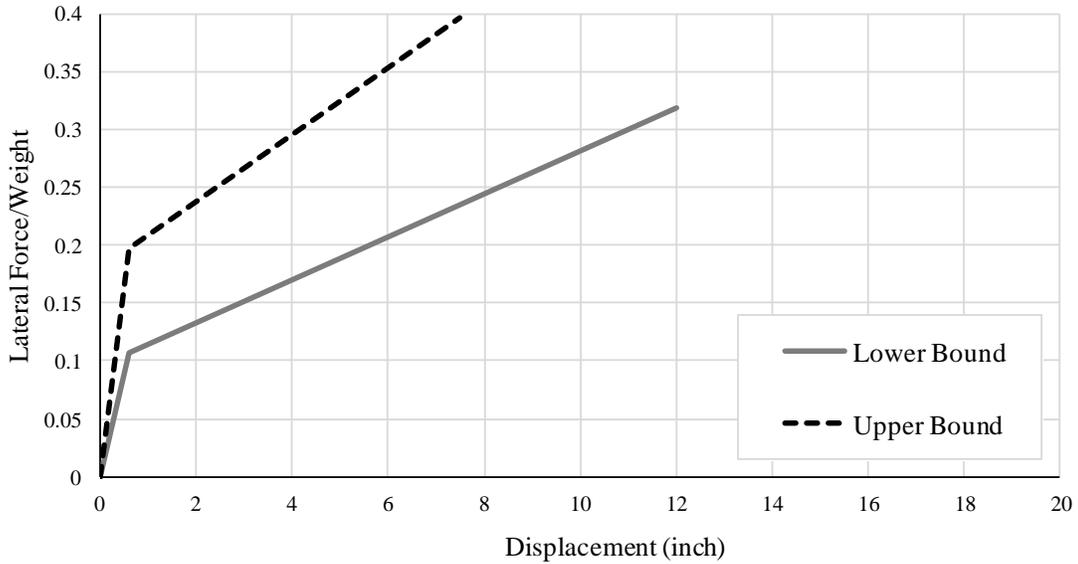
Figure 15.4-3 Force-Deflection Behavior of Preliminary Sized Elastomeric Isolation System

Sliding bearings force-displacement behavior. The upper- and lower- bound force-displacement behavior of the sliding isolation system, based on the preliminary design, is illustrated in Figure 15.4-4.
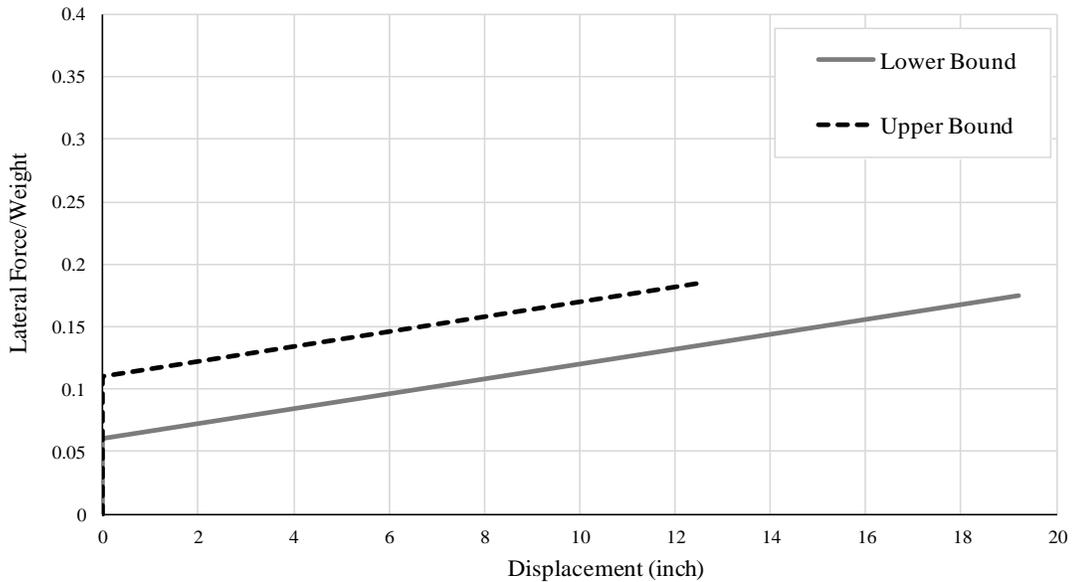
Figure 15.4-4 Preliminary Design Force-Deflection Behavior of Sliding Isolation System

A check of the minimum restoring force, per *§17.2.4.4*, gives a difference between the force at 0.5 D_M and 1.0D_M of 0.037W for the upper-bound properties and difference of 0.057W for the lower-bound properties. Hence the *Standards* minimum limit of 0.025W is satisfied.

15.5 EQUIVALENT LATERAL FORCE PROCEDURE

The equivalent lateral force (ELF) procedure is a single-degree-of freedom displacement-based method that uses simple equations to determine an isolated structures response. The equations are based on ground shaking defined by 1-second spectral acceleration and the assumption that the shape of the design response spectrum at long periods is inversely proportional to period. Although the ELF procedure is considered a linear method of analysis, the equations incorporate amplitude-dependent values of effective stiffness and effective damping to account implicitly for the nonlinear properties of the isolation system. The equations assume that the superstructure is rigid and lateral displacements occur primarily in the isolation system.

The following calculations are illustrated, arbitrarily, for the elastomeric isolation system. The calculation process for the sliding isolation system would be similar.

15.5.1 Procedure

The ELF procedure is an iterative process and is illustrated in the following equations for the preliminary design bearing dimensions and lower bound properties. The terms below are defined in Section 15.3.

1. Assume a maximum displacement, say $D_M = 11.2$ inch

2. Calculate the effective stiffness k_M

$$k_M = k_{d,total} + \frac{Q_{d,total}}{D_M} \qquad (15.5\text{-}1)$$

$$= 218 + \frac{1047}{11.3} = 311 \text{ kip/inch}$$

3. Calculate the effective period T_M (*Equation 17.5-2*):

$$T_M = 2\pi\sqrt{\frac{W}{k_M g}} \qquad (15.5\text{-}2)$$

$$= 2\pi\sqrt{\frac{10200}{311\times386}} = 1.83 \text{ seconds}$$

4. Calculate the effective damping β_M. The yield displacement Y is assumed to be 0.6inch

$$\beta_M = \frac{4Q_{d,total}(D_M - Y)}{2\pi k_M D_M{}^2} \qquad (15.5\text{-}3)$$

$$= \frac{4\times1047\times(11.2-0.6)}{2\pi\times311\times11.2^2} = 0.18$$

5. Interpolate the damping coefficient B_M from *Table 17.5-1*

$$B_M = 1.44$$

6. Check the displacement matches what was initially assumed in Step 1 (*Equation 17.5-1*):

$$D_M = \frac{gS_{M1}T_M}{4\pi^2 B_M} \qquad\qquad (15.5\text{-}4)$$

$$= \frac{386 \times 0.9 \times 1.83}{4 \times \pi^2 \times 1.44} = 11.18 \text{ inch} \approx 11.2 \text{ inch} \therefore O.K$$

15.5.2 Structural Analysis

The *Standard* requires that two parallel analyses are performed, one using the isolation system upper-bound properties and one using the lower-bound properties, with the governing case for each response parameter of interest being used for design.

Modeling assumptions. To expedite calculation of loads on bearings and other elements of the seismic-force-resisting system, a three-dimensional mathematical model of the building is developed and analyzed using the computer program ETABS (CSI, 2013).

The vertical load on each bearing depends on their relative vertical compression stiffness K_v and soil stiffness, the rigidity of the base level diaphragm/framing and the mass distribution. The compression stiffness of a multi-layered elastomeric bearing can be approximated accordingly:

$$K_v = A\left[\sum_i t_i \left(\frac{1}{E_{ci}} + \frac{4}{3K}\right)\right]^{-1} \qquad\qquad (15.5\text{-}5)$$

where A is the bonded rubber area, t_i is the individual rubber layers thickness, K is the bulk modulus of rubber, assumed as 290 ksi and E_{ci} is the compression modulus for incompressible material behavior which is dependent on the rubber shear modulus, shape factor and the bearing geometry (see Constantinou et al., 2007 for details). The compression stiffness for the LR bearings was calculated as about 10,000 kip/in. The soil stiffness is taken as 150 pci and for a 5ft square footing beneath each bearing column gives and vertical soil spring stiffness of 540 kip/in.

Since the ELF analysis is a linear-elastic method, the lateral effective stiffness of the bearings at the maximum displacement is input into the model. For each bearing the effective stiffness is simply the isolation systems effective stiffness, from Section 15.5.1 calculations, divided by the number of bearings. A modal analysis of the structure shall be used to verify that the first two modes of vibration are translational with a period similar to Section 15.5.1 calculations, with the third mode of vibration being the torsional isolated mode.

Bearing dimensions and properties. The preliminary sizing of the bearing, per Section 15.3.1, used quick but conservative calculations. Using the more refined calculations that are set out in the following sections, it was decided to further optimize the sizing of the bearings to reduce structural shear. The final dimensions of all the 35 LR bearings and their properties (as determined in Section 15.4) are as follows:

Table 15.5-1   Final Lead-Rubber Bearing Dimensions and Properties

Parameter	Symbol	Value	Units
Lead Core Diameter	D_L	4.75	inch
Bonded Rubber Diameter	D_B	25.75	inch
Total Thickness of Rubber	T_r	5.225	inch
Yield Displacement	Y	0.6	inch
Nominal Effective Yield Stress of Lead	σ_{YL}	1.7	ksi
Maximum Variation	$\lambda_{max,\sigma}$	1.5	
Minimum Variation	$\lambda_{min,\sigma}$	0.8	
Lower-, Upper-Bound	$\sigma_{YL,min}, \sigma_{YLmax}$	1.36, 2.55	ksi
Nominal Shear Modulus of Rubber	G	58	psi
Maximum Variation	$\lambda_{max,G}$	1.4	
Minimum Variation	$\lambda_{min,G}$	0.9	
Lower-, Upper-Bound	G_{min}, G_{max}	52, 81	ksi

Using Equations 15.3-1 and 15.3-2 and details in Table 15.5-1, the ELF force-displacement behavior of the isolation system can be constructed, as illustrated in Figure 15.5-1:
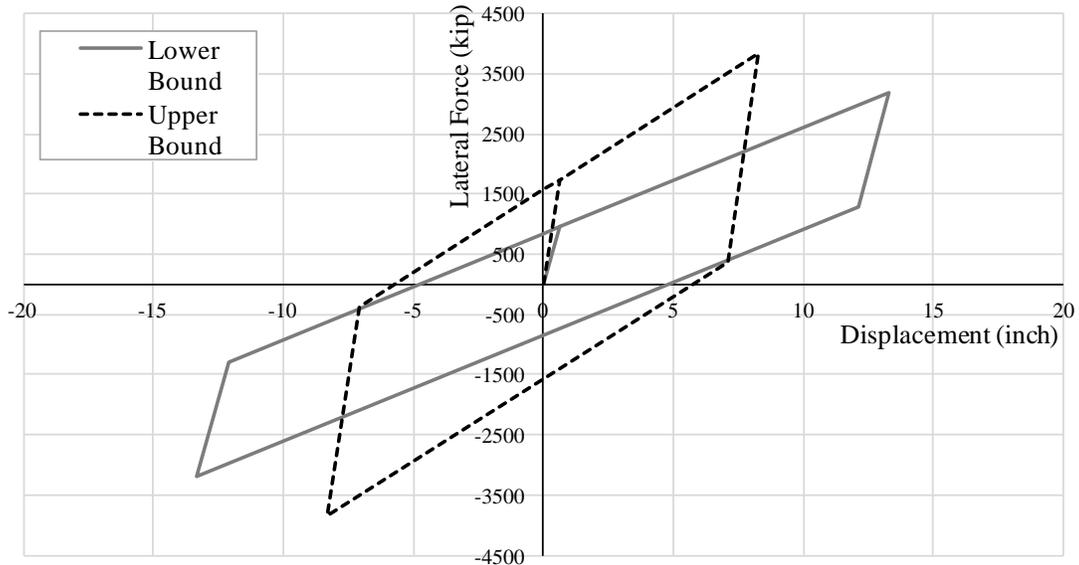
Figure 15.5-1 Force-Deflection Behavior of Elastomeric Isolation System

  Maximum displacement and effective period. The maximum displacement D_M and effective period at the maximum displacement T_M is calculated using the ELF procedure in Section 15.5.1, which is consistent with *§17.5.3.1 and §17.5.3.2* of the *Standard* . The calculations for the upper- and lower-bound properties are documented in Table 15.5-2.

Table 15.5-2   ELF Procedure for Upper- and Lower-Bound

Parameter	Symbol	Upper-Bound	Lower-Bound	Units
Maximum Displacement	D_M	8.3	13.3	inch
Effective Stiffness	k_M	464	239	kip/inch
Effective Period	T_M	1.50	2.09	seconds
Effective Damping	β_M	0.24	0.16	
System Post-elastic Stiffness	$k_{d,Total}$	274	176	kip/inch
System Characteristic Strength	$Q_{d,Total}$	1582	843	kip
System Strength	Q_d/W	0.16	0.08	
Base Shear	V_b/W	0.38	0.31	

Lateral seismic forces and vertical distribution. The lateral shear force required for the design of the isolation system, foundation and other structural elements below the isolation system is given by V_b in *Equation 17.5-5*. The overturning loads (i.e. axial loads) from the superstructure, which are used for the design of the isolation system, foundation, and elements below the isolation system is given by the unreduced lateral force V_{st} in *Equation 17.5-7*. Subject to the limits of *§17.5.4.3*, the base shear, V_s, for the design of superstructure above the isolation level is taken as V_{st} reduced by the R_I factor in accordance with *Equation 17.5-6*. The results from these calculations for the upper- and lower- bound analysis are given in Table 15.5-3.

Table 15.5-3   ELF Lateral Design Forces

Parameter	Symbol	Upper-Bound	Lower-Bound	Units
Lateral force for elements below the isolation system	V_b	3853	3183	kip
Unreduced lateral force for elements above the isolation system and for overturning loads	V_{st}	3449	2691	kip
Reduced lateral force for elements above the isolation system	V_s	3449[1]	2691[1]	kip

1.   Uses an $R_I = 1.0$.

The minimum lateral design force for structural elements above the isolation system V_s is initially calculated as 3449 kip. However the value of V_s shall also be checked against *§17.5.4.3* to ensure it meets the minimum requirements. As shown in Table 15.5-4, the value of V_s is not governed by the minimum requirements.

Table 15.5-4   Minimum Requirements of §17.5.4.3 for Reduced Lateral Force V_s

Item No.	Requirement	Check
1	The lateral seismic force required by *Standard §12.8* for a fixed-base structure of the same effective seismic weight, W_S, and a period equal to the period of the isolation system using the upper bound properties T_M.	$C_s = \dfrac{\frac{2}{3} S_{M1}}{T\left(\dfrac{R}{I_e}\right)} = \dfrac{\frac{2}{3} \times 0.9}{1.5\left(\dfrac{3.25}{1.5}\right)} = 0.19$ $C_S \geq 0.044 \times \frac{2}{3} \times S_{MS} \times I_e \geq 0.01$ ≥ 0.06 $V_S \geq C_S W = 1940 \text{ kip O.K.}$
2	The base shear corresponding to the factored design wind load.	O.K.
3	The lateral seismic force, V_{st}, calculated using Eq. 17.5-7, and with V_b set equal to the force required to fully activate the isolation system utilizing the upper bound properties.	$F_y = Q_d + k_d Y = 1582 + 274 \times 0.6$ $= 1746 \text{ kip O.K.}$
3a	1.5 times the nominal properties, for the yield level of a softening system	N/A
3b	the ultimate capacity of a sacrificial wind-restraint system	N/A
3c	the break-away friction force of a sliding system, or	N/A
3d	the force at zero displacement of a sliding system following a complete dynamic cycle of motion at D_M.	N/A

The *Standard* has been revised to incorporate a more realistic distribution of lateral forces over the buildings height (York and Ryan 2008) with details of the method explained in the *Standard* commentary. Because the superstructure is much stiffer laterally than the isolation system, it tends to move as a rigid body in the first mode, with a pattern of lateral seismic forces that is typically more uniformly distributed over the height of the building. This is rather than an inverted triangular distribution, which is representative of the first mode for a fixed-base building.

The method calculates the force of the base level, immediately above the isolation plane, then distributes the remainder of the base shear among the other levels. The vertical distribution of the unreduced lateral forces is given in Table 15.5-5. It is noted that *§17.5.4.2* has an exception which recommends a more conservative exponent term be used in *Equation 17.5-7* when the hysteretic behavior of the isolation system is characterized by an abrupt transition from pre-yield to post-yield. For an elastomeric isolation system the transition is typically rounded and therefore the (1-2.5β) exponent is relevant.

Table 15.5-5   Vertical Distribution of Earthquake Forces

Floor level, x (Story)	Seismic floor weight	Cum. weight (kips)	Height above isolation	Vertical Distribution Factor Upper-, Lower-Bound	Story force, *(Cum. Shear)* Upper-Bound	Story force, *(Cum. Shear)* Lower-Bound
Symbol (units)	w_x (kips)	(kips)	h_x (ft)	C_{vx}	F_x, (kips)	F_x, (kips)
PH Roof	850		53			
(Penthouse)		850		0.22, 0.18	761	486
Roof	2400		41		*(761)*	*(486)*
(Third)		3250		0.43, 0.40	1477	1070
Third Floor	2250		29		*(2238)*	*(1556)*
(Second)		5500		0.24, 0.27	836	717
Second Floor	2200		17		*(3074)*	*(2273)*
(First)		7700		0.11, 0.16	375	418
First Floor	2500		3		*(3449)*	*(2691)*
(Isolation/Base Level)		10200		N/A	404	492
Total	10200			1.0	3853	3183

Bearing vertical loads. The vertical/axial load on the bearings was calculated using the ETABS model for both the upper- and lower-bound properties. In this case the upper-bound properties gave the critical earthquake demands and are reported in Table 15.5-6 and 15.5-7. This table documents the loadings from dead and reduced live loadings, as well as the envelope of the maximum and minimum demands from horizontal earthquake and torsion actions. The X and Y directions referred to in the tables are illustrated in Figure15.3-2. A negative sign denotes tension loading.

Since the isolation system and lateral-force resisting system have a symmetrical layout (in two directions), only the critical demands are reproduced in the Table 15.5-6 through 15.5-9. That is, loads and displacements at Gridlines 5, 6 and 7 (not shown) are similar to those at Gridlines 3, 2 and 1, respectively; and loads and displacements at Gridlines D and E (not shown) are similar to those at Gridlines B and A, respectively.

Table 15.5-6   ELF Vertical Loads on Bearings, Upper-Bound Properties

Gridline	1	2	3	4
Summary of dead (*D*) and reduced live loads (*L*) on bearings: *D*, *L* (kips)				
A	105, 21	224, 58	170, 38	161, 36
B	239, 56	325, 80	370, 93	386, 97
C	196, 45	345, 86	411, 104	396, 100
Summary of ELF (X-direction) loads on bearings: *Max*, *Min* (kips)				
A	50, -51	44, -47	10, -11	1, 1
B	179, -184	110, -118	52, -60	23, 22
C	83, -85	89, -96	25, -27	19, 19
Summary of ELF (Y-direction) loads on bearings: *Max*, *Min* (kips)				
A	56, -52	248, -232	78, -74	49, -49
B	83, -73	189, -164	165, -152	240, -233
C	-5, -5	-61, -65	-7, -7	4, 4
Summary of accidental torsion loads on bearings: *Max*, *Min* (kips)				
A	1, -1	21, -21	4, -4	0, 0
B	7, -7	10, -10	2, -2	1, -1
C	0, 0	7, -7	1, -1	0, 0

Using the load combinations in Section 15.2.4, which incorporate vertical earthquake actions using $\pm 0.2S_{MS}D$, Table 15.5-7 shows the maximum and minimum downward forces for design of the bearings. These forces result from the simultaneous application of gravity loads and unreduced earthquake story forces (see Table 15.5-5) to the ETABS model. It is noted that tension stresses are developed in a number of locations. This tension stress is acceptable for a high-quality elastomeric bearing if it is less than three times the shear modulus of rubber. For the LR bearing in this example the capacity for the upper- and lower bound properties is $3GA$, equal to 80 and 120 kip, respectively. Hence there are four bearing locations (Gridline A2, E2, A6 and E6) where there is a potential uplift issue. This issue is discussed further in Section 15.7.1, after the vertical response spectrum and response history analyses.

Table 15.5-7   ELF Maximum and Minimum Vertical Loads on Bearings, Upper-Bound Properties

Maximum Loads $1.48D + 0.5L + \max(Q_{EX}+0.3Q_{EY}, 0.3Q_{EX}+Q_{EY}) + \max(Q_{E,Torsion})$ (kips)				
Gridline	1	2	3	4
A	237	640	356	306
B	592	752	776	**867**
C	395	631	683	657
Minimum Loads $0.62D + \min(Q_{EX}+0.3Q_{EY}, 0.3Q_{EX}+Q_{EY}) + \min(Q_{E,Torsion})$ (kips)				
Gridline	1	2	3	4
A	-4	**-129**	24	52
B	-65	-8	57	12
C	35	92	225	255

Total maximum displacement. The maximum design displacement D_M calculated previously represents the peak earthquake displacement at the center of mass of the building without the additional displacements that can occur at other locations due to actual or accidental mass eccentricity. The additional displacements due to torsion can be calculated from the ETABS model with the application of the torsional moment. However, the resultant total maximum displacement D_{TM} may not be taken less than that calculated in *Equation 17.5-3*. This equation now includes a new term P_T which is the ratio of the effective translational period to the effective torsional period of the isolation system. Work by Wolff et al. (2014) give the background theory for this revision of the amplification factor, which offers an improvement by relaxing the assumption of equal translation and torsional periods.

Using the modal analysis from the ETABS model, the ratio of the 1ˢᵗ and 3ʳᵈ modes, which are the translational and torsional modes, respectively, for the lower-bound properties are 2.14sec/1.83sec or $P_T =$ 1.17. There could be a further reduction in the amplification factor (or increase in P_T) by placing LR bearings around the perimeter and plain elastomeric or sliding bearings on the interior of the building to increase the torsional resistance. However the *Standard* places a minimum amplification factor of $1.15D_M$ for the corner bearings, regardless of how torsionally stiff the isolation system is. Part of the reason behind increasing this minimum factor is that past experimental tests used to quantify the isolation systems torsional response was on unrealistically torsionally stiff isolation systems (i.e. only four bearings located on the perimeter).

The *Standard* minimum torsional amplification factor and total maximum displacements for various bearing locations is given in Table 15.5-8. The minimum amplification factor is calculated using *Equation 17.5-3* with the greater of the amplification for and X- or Y-direction reported in the table. It is noted that the total maximum displacement calculated using the ETABS model (i.e. with the application of the torsional moment at each floor level) gives similar values for this example.

Table 15.5-8   Minimum Amplification Factors and ELF Total Maximum Displacement

Gridline	1	2	3	4
	Minimum Torsional Amplification Factor			
A	1.15	1.10	1.07	1.07
B	1.15	1.10	1.05	1.03
C	1.15	1.10	1.05	1.00
	Upper-Bound Total Maximum Displacements, D_{TM} (inches)			
Gridline	1	2	3	4
A	9.6	9.1	8.9	8.9
B	9.6	9.1	8.7	8.6
C	9.6	9.1	8.7	8.3
	Lower-Bound Total Maximum Displacements, D_{TM} (inches)			
Gridline	1	2	3	4
A	15.3	14.6	14.2	14.2
B	15.3	14.6	14.0	13.7
C	15.3	14.6	14.0	13.3

Bearing stability and shear strain assessment. A more refined calculation of the minimum required individual rubber layer thickness for stability (per Equation 15.3-3), with compatible combinations of maximum axial loads and total maximum displacements, for each bearing location are documented in Table 15.5-9. The critical bearing location is Gridlines B4 and D4 which require a rubber thickness less than 0.28 inches which is at the lower limit for what can be satisfactorily constructed by manufactures. This would give a final bearing with 5.225/0.275 = 19 rubber layers each 0.275 inches (7 mm) thick. The rubber shear strains due to lateral displacements are high at 294% in the corner locations, but are achievable for a quality manufacturer.

The stability check is illustrated in this example since it is typically a governing criterion for the design of the lead-rubber bearings. However, the design checks of the bearing stability, rubber shear strains, and other components of the bearing (i.e. steel shim plates and end plate design) are typically the responsibility of the manufacturer.

Table 15.5-9   Minimum Individual Rubber Thickness and Rubber Shear Strain

	Upper-Bound Minimum Individual Rubber Layer Thickness, t_i (inches)			
Gridline	1	2	3	4
A	1.54	0.56	1.02	1.17
B	0.71	0.49	0.47	0.43
C	1.07	0.69	0.54	0.57
	Lower-Bound Minimum Individual Rubber Layer Thickness, t_i (inches)			
Gridline	1	2	3	4
A	0.88	0.36	0.63	0.71
B	0.40	0.30	0.30	**0.28**
C	0.57	0.38	0.32	0.36
	Lower-Bound Rubber Shear Strain, D_{TM}/T_r (%)			
Gridline	1	2	3	4
A	**294**	281	268	263
B	294	281	272	272
C	294	281	268	263

Story drifts. The *Standard* permits more liberal drift limits where the design of the superstructure is based on a nonlinear response history analysis (NLRHA). The ELF procedure and response spectrum drift limits are $0.015h_{sx}$ for the reduced MCE$_R$ level forces, which are increased to $0.020h_{sx}$ for a NLRHA (where h_{sx} is the story height at level x). Usually a stiff system (e.g., braced frame) is selected for the superstructure to limit damage to nonstructural components sensitive to drift and therefore the drift demand is typically less than about $0.005h_{sx}$. *Standard §17.6.4.4* requires an explicit check of superstructure stability at the MCE$_R$ displacement if the earthquake story drift ratio exceeds $0.010/R_I$.

The maximum story displacement of the structure above the isolation system is calculated by *Equation 12.8-5* with C_d equal to R_I ($C_d = 1$) and using $I_e = 1.0$. The upper-bound properties give the greater story shear and therefore greater drift. The story drift in each direction, including accidental eccentricity, are given in Table 15.5-10. Since the structure has braced frames, the calculated maximum story drift ratio is well below the limit of 1.5%.

Table 15.5-10   Maximum story drift from ELF procedure

Floor level, x (Story)	Story height	Maximum story drift X-direction[1]	Maximum story drift Y-direction[1]
Symbol (units)	(feet)	%	%
Penthouse	12	0.23	0.45
Third	12	0.30	0.39
Second	12	0.27	0.32
First	14	0.22	0.21

1. Includes torsion

15.5.3 Limitation Checks

The ELF calculations in the preceding sections are permitted to be used for the final design since all the items of *§17.4.1* are satisfied. These checks are reproduced in Table 15.5-11.

If any of the items were not satisfied, then a dynamic analysis would be required. If items number 1, 2, 3, 4, 6 and 7(sic) are satisfied, then the response spectrum procedure is permitted. The ELF and response spectrum procedures are both linear-elastic analyses, where the bearings behavior is represented by an effective stiffness and effective damping at the maximum displacement D_M. The response history analysis, on the other hand, directly accounts for the nonlinear bearing behavior and is permitted for all seismically isolated structures.

Table 15.5-11   Restrictive Requirements for ELF (and Response Spectrum) Analysis

Item No.	Requirement	Upper-bound	Lower-bound	Check
1	The structure is located on a Site Class A, B, C and D.	Site Class D		O.K.
2	The effective period of the isolated structure at the maximum displacement, D_M, is less than or equal to 5.0s.	1.5 sec	2.1 sec	O.K.
3	The structure above the isolation interface is less than or equal to 4 stories or 65 ft (19.8m) in structural height measured from the base level. Exception: These limits are permitted to be exceeded if there is no tension/uplift on the bearings.	4 stories with 50 ft height.		O.K.
4	The effective damping of the isolation system at the maximum displacement, D_M, is less than or equal to 30%.	24%	16%	O.K.
5	The effective period of the isolated structure T_M is greater than three times the elastic, fixed-base period of the structure above the isolation system determined using a rational modal analysis.	$T_M = 1.5$sec	$T_M = 2.1$ sec	$T_{fb}=0.43$s $3T_{fb}=1.3$s O.K.
6	The structure above the isolation system does not have a structural irregularity, as defined in Section 17.2.2.	No structural irregularity, see Section 15.2.4.1		O.K.
7a	The effective stiffness of the isolation system at the maximum displacement, D_M, is greater than one-third of the effective stiffness at 20 percent of the maximum displacement.	$464 > 409$	$239 > 164$	O.K.
7b	The isolation system is capable of producing a restoring force such that the lateral force at the corresponding maximum displacement is at least $0.025W$ greater than the lateral force at 50 percent of the corresponding maximum displacement.	$0.11W$	$0.12W$	O.K.
7c	The isolation system does not limit maximum earthquake displacement to less than the total maximum displacement, D_{TM}.	Assumed to have no restrictions less than D_{TM}		O.K.

15.6 DYNAMIC ANALYSES

15.6.1 Background

There are two dynamic analyses illustrated in this section: 1) a vertical response spectrum analysis to obtain a better estimate of the vertical earthquake effects and 2) and nonlinear response history analysis (NLRHA) for more refined estimates of the building horizontal earthquake response.

The NLRHA gives the most realistic estimate of an isolated buildings response. Typically the superstructure is modeled as elastic with nonlinear behavior confined to the isolation level. Two models are required, one with the isolator units upper-bound force-deflection properties and one using the lower-bound properties. Each model is subjected to at least seven different ground motion sets, where the values used in design (for each response parameter of interest) are taken as the average of the seven ground motion analyses maxima. The ELF analysis is still necessary to evaluate results of the dynamic analysis and to obtain minima of response quantities.

In this example the NLRHA is used only to determine the final design displacements of the isolation system, to assess the overturning loads and uplift, and to verify that ELF-based story forces used for design of the superstructure are valid. If the NLRHA procedure were used as the primary basis for superstructure design, then response results would be required for design of individual elements, rather than for checking a limited number of global response parameters.

15.6.2 Structural Analysis and Modeling

The NLRHA was undertaken in the program ETABS using the Fast Nonlinear Analysis procedure. ETABS internally calculates modal damping based on the hysteretic properties of the nonlinear elements (isolators) and an additional amount of user-specified modal damping. Inherent damping was specified as 2% (as the superstructure remains elastic) in each mode of vibration with override such that the damping in the first six (isolated) modes were specified as zero per procedures described in Sarlis and Constantinou (2010).

The nonlinear force-deflection characteristics of isolator units are modeled explicitly (rather than using effective stiffness and damping, as in the ELF procedure). For most types of isolators, force-deflection properties can be approximated by bilinear, hysteretic curves that can be modeled using commercially available nonlinear structural analysis programs. The initial stiffness, yield strength and post yield stiffness ratio of a single bearing for the upper- and lower-bound properties specified in ETABS is given in Table 15.6-1. These properties give an isolation system response (for 35 bearings) matching that shown in Figure 15.5-1.

Table 15.6-1   Nonlinear Properties of Individual Bearings for Analysis

	Upper-bound	Lower-bound
Initial stiffness (kip/inch)	83.1	45.2
Yield strength (kip)	49.9	27.1
Post-yield stiffness ratio	0.094	0.111

Note: ETABS also asks for linear properties which are used in the nonlinear modal history analysis. It is recommended to specify a low effective stiffness, say equal to the post-elastic stiffness, and zero effective damping.

More sophisticated nonlinear models may be necessary to accurately represent the response of isolators with complex configurations or properties (e.g., triple pendulum sliding bearings), to capture stiffening effects at very large displacements (e.g., of elastomeric bearings), to model rate-dependent effects explicitly (Sarlis 2010, Kalapakidis 2008) or to model uplift behavior.

Special modeling concerns for isolated structures include two important and related issues: uplift of isolator units and P-delta effects on the isolated superstructure and the substructure. Typically, isolator units have little or no ability to resist tension forces and can uplift when earthquake overturning (upward) loads exceed factored gravity (downward) loads. To model uplift effects, gap elements may be used in nonlinear models or tension may be released manually in linear models. For this example the uplift forces from NLRHA do not exceed $3GA$ (see Section 15.7.1.1 for details) therefore uplift is not modeled explicitly.

The vertical earthquake effects were not explicitly considered in the NLRHA model (i.e. only two horizontal ground motion components are applied to the model) but are accounted for in the results later.

The effects of P-delta loads on the isolation system and adjacent elements of the structure can be quite significant. The compression load, P, can be large due to earthquake overturning (and factored gravity loads) at the same time that large displacements occur in the isolation system. Computer analysis programs (most of which are based on small-displacement theory) may not correctly calculate P-delta moments at the isolator level in the structure above or in the foundation below. Figure 15.6-1 illustrates moments due to P-delta effects (and horizontal shear loads) for an elastomeric bearing and a flat sliding bearing. The same concept applies for multi-spherical sliding bearings. For the elastomeric bearing, the P-delta moment is split one-half up and one-half down. For the flat and single-concave sliding bearings, the full P-delta moment is applied to the foundation below (due to the orientation of the sliding surface). A reverse (upside down) orientation of the flat and single-sided sliding bearings would apply the full P-delta moment on the structure above. For the double-concave sliding bearing, P-delta moments are split one-half up and one-half down, in a manner similar to an elastomeric bearing, provided that the friction (and curvature) properties of the top and bottom concave dishes are the same.
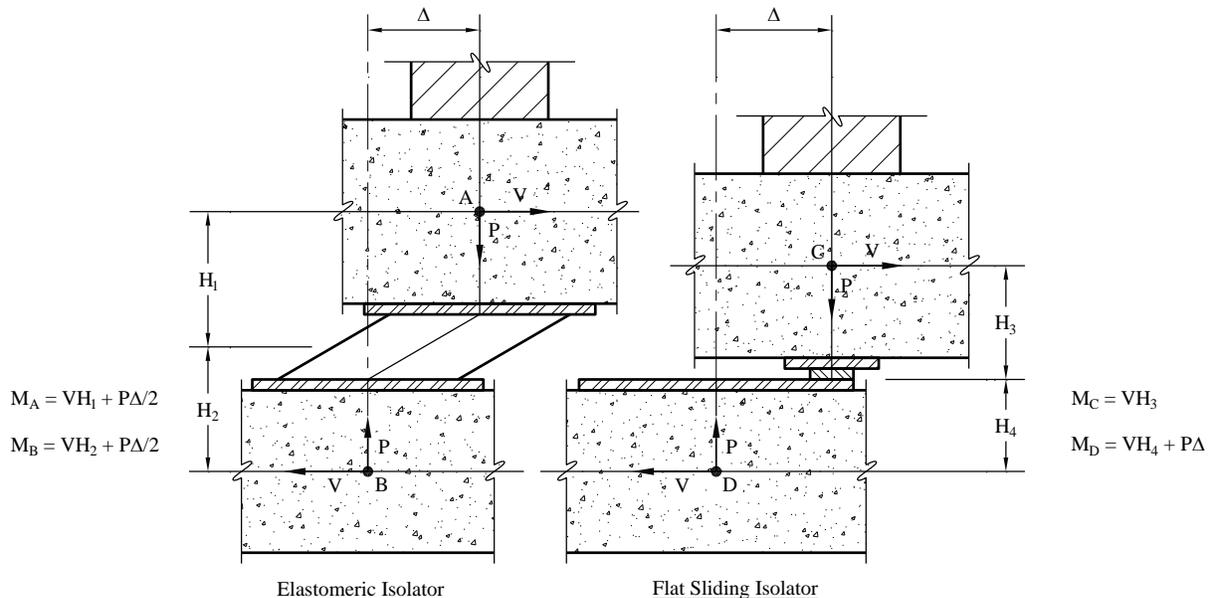

$M_A = VH_1 + P\Delta/2$

$M_B = VH_2 + P\Delta/2$

$M_C = VH_3$

$M_D = VH_4 + P\Delta$

Elastomeric Isolator

Flat Sliding Isolator

Figure 15.6-1 Moments due to Horizontal Shear and P-delta Effects

15.6.3 Ground Motion Records

Selection and scaling of ground motions. The *Standard* requires that ground motions be scaled to match maximum spectral response in the horizontal plane. In concept, at a given period of interest, the maximum spectral response of scaled records should, on average, be the same as that defined by the MCE_R spectrum. The ground motion acceleration histories selection and scaling are illustrated in Chapter 3 of these NEHRP Design Examples.

For NLRHA, *Standard §17.3* requires at least seven pairs of horizontal ground motion acceleration histories be selected from actual earthquake records and scaled to match the MCE_R spectrum. Where the required number of recorded pairs is not available, then the *Standard* permits the use of simulated ground motion records. Selection and scaling of appropriate ground motions should be performed by a ground motion expert experienced in earthquake hazard of the region, considering site conditions, earthquake magnitudes, fault distances and source mechanisms that influence ground motion hazard at the building site.

Standard §17.3.4 recognizes two types of scaling methods: amplitude scaling and spectrally matching, and has different requirements for each. There are also different requirements if the site is within 3 miles (5 km) of an active fault. For this example, the site is greater than 3 miles away from an active fault, and amplitude scaling is the selected scaling method. In this case, the *Standard* requires that the earthquake records are scaled to match a target spectrum over the period range of interest, defined as $0.75T_M$ determined using upper-bound isolator properties to $1.25T_M$ using lower-bound isolator properties. This gives a period range of interest of 1.1 to 2.6 seconds for the elastomeric isolation system. For each period in this range, the average of seven square-root-of-the-sum-of-the-squares (SRSS) combinations (of each pair of horizontal components of scaled ground motion) should be equal to or greater than 1.0 times the MCE_R spectrum.

The scaling factors are shown in Table 15.6-2 and reflect the total amount that each as-recorded ground motion is scaled for NRLHA. Also shown are associated parameters which are useful for NLRHA. Further illustration of selection and scaling of ground motion records is illustrated in Chapter 3 of these NEHRP Design Examples.

Table 15.6-2 Selected and Scaled Ground Motions[1]

GM No.	Earthquake name	Duration (seconds)	Time step (seconds)	Unscaled PGA (g) X-component	Unscaled PGA (g) Y-component	Scale factor (SF)	ETABS SF (inch/sec^2)
1	Tokachi-oki, Japan	247.0	0.01	0.14	0.10	3.00	1158
2	Tokachi-oki, Japan	269.0	0.01	0.62	0.44	1.20	463
3	Tokachi-oki, Japan	120.0	0.02	0.24	0.30	1.65	637
4	Western Washington	89.2	0.02	0.16	0.26	2.95	1139
5	Loma Prieta	40.0	0.005	0.51	0.33	1.65	637
6	Duzce, Turkey	25.9	0.005	0.40	0.51	1.10	425
7	Kobe, Japan	41.0	0.01	0.48	0.46	1.75	676

2.   Directly adopted from Chapter 3.4 of these NEHRP Design Examples.

Orientation of ground motion components for analysis. Only for sites within 3 miles of an active fault does the *Standard* specify how the two scaled components of each record should be applied to a three-dimensional model (i.e., how the two components of each record should be oriented with respect to the axes of the model). For other sites, the *Standards* commentary states that individual pairs of horizontal ground motion components need not be applied in multiple orientations. Guidance on the orientation of components of ground motions by NIST (2011) state that there is no systematic directional dependence to ground motions at distant sites and that each pair of motions need only be applied to the model in one orientation.

Since this example building is symmetrical in both directions and the site is further than 3 miles from an active fault, the earthquake records were applied randomly to the model in one orientation only. The post-processing of results per Section 15.6.4 accounts for whether the maximum response occurs in the positive or negative direction.

On some projects, lack of guidance sometimes caused engineers to perform an unnecessarily large number of response history analyses with each pair of ground motion records oriented in four or even more different orientations. It is the author's experience that these additional analyses have diminishing returns. However, multiple orientations may still be necessary depending on project, and should be assessed on a case-by-case basis (i.e. jurisdictional requirements or as requested for design verification).

15.6.4 Vertical Response Spectrum Analysis

Vertical Earthquake Spectrum. In the ELF procedure the vertical earthquake effects are accounted for by simply adding or subtracting $0.2S_{MS}D$ or $0.2 \times 1.4 = 0.28g$. The 0.2 factor is derived by multiplying the horizontal spectrum at short periods by 2/3 and then using a 30% combination with horizontal earthquake effects. This crude approach is also valid for NLRHA; however a more thorough method is illustrated herein.

The *Standard* does not give explicit guidance of how to account for vertical motions, however commentary has been added to address the matter. In *§C17.3.3* one recommended approach to compute the vertical design spectrum is to use the 2009 NEHRP Provisions in Chapter 23 where S_{DS} is replaced with S_{MS}. The vertical spectra are a strong function of the natural period, source-to-site distance and local site conditions, and relatively weak function of magnitude and faulting mechanisms. The 2009 Provisions have simplified this so that the vertical spectrum can be calculated through the parameter S_S (short-period horizontal spectral acceleration for the site), as well as the site class classification. Using the 2009 Provisions the vertical coefficient C_v was calculated to be 1.38 for the D site class. The resulting vertical response spectrum, along with horizontal spectra for comparison (both for the MCE$_R$ event) is given in Figure 15.6-2. There is a limit that the vertical response spectrum acceleration shall not be less than one-half (1/2) of the corresponding horizontal spectral acceleration, which is why there is a "kink" in the vertical spectra to be used for design.

For the design vertical spectrum the period refers to the vertical period and the spectral acceleration is in the upwards or downwards direction.
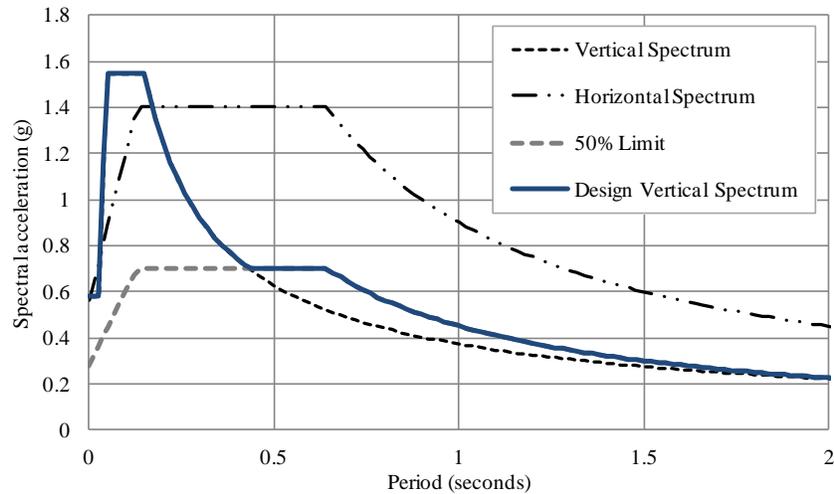
Figure 15.6-2 MCE$_R$ Vertical Spectrum for Design

Analysis and Bearing Axial Loads. A vertical earthquake analysis requires careful modeling considerations. These are outlined in the *Standard* commentary *§C17.6.2,* such as including all structural elements in the model and adding more degrees of freedom (i.e. nodes along a beam or slab) so that the mass is realistically distributed across the building footprint. Consideration of the soil-structure interaction is also necessary and will require input from a geotechnical engineer. The modal analysis must also capture the vertical excitation of the building, which may require hundreds of modes to obtain 90-100% of the mass participation in the vertical direction.

A single degree of freedom analysis should be used initially to estimate the vertical period and resulting vertical base reaction. The stiffness of the building in the vertical direction is calculated as the vertical stiffness of the bearing (10,000 kip/in) and soil stiffness below (540 kip/in) acting in series, which gives a total vertical stiffness of 35 bearings multiplied by 512 kip/in (1/512 = 1/10000 + 1/540), which is 17,920 kip/in. The corresponding vertical period would be:

$$T = 2\pi \sqrt{\frac{10,200}{17920 \times 386}} = 0.24 \text{ seconds}$$

The vertical spectral acceleration for a period of 0.24 seconds is 1.09g. However the multi-degree of freedom ETABS model shows that the longest period for a vertical mode shape is around 0.34 seconds, so we would expect a lower base reaction than 1.09g using the vertical response spectrum analysis.

The vertical response spectrum analysis resulted in a total reaction in the upwards/downwards direction of 7174 kip, which is equivalent to 7174/10200 = 0.7g. This corresponds to about 0.15S_{MS} (i.e. 0.7× 30%/1.4) which is less than the 0.2S_{MS} used in Section 15.5 to account for vertical earthquake effects. The response spectrum analysis also gives a more realistic distribution of vertical earthquake loads over the building footprint. These bearing axial loads are given in Table15.6-3 and can be acting either in the upward (tension) or downward (compression) directions. These maximum vertical earthquake loads can be combined with the maximum vertical reactions due to horizontal earthquake loads using orthogonal combinations corresponding to the 100%-30% rule per *§C17.2*.

Table 15.6-3   Bearings Axial Loads due to Vertical Earthquake Effects, E_v

Gridline	1	2	3	4
A	70	160	129	128
B	165	247	314	342
C	140	262	434	369

15.6.5 Nonlinear Response History Analysis

 Introduction. The two independent ETABS models, which represent upper- or lower-bound bearing properties, are analyzed for the set of seven pairs of horizontal ground motion records applied to the model in the one orientation only (i.e. are not rotated). The post-processing in this section takes the absolute maximum (i.e. maximum whether in the positive or negative directions) response for each ground motion. The average of these absolute maxima responses over the seven ground motions is then used for design.

Due to the many inputs required for NLRHA it is important to carry out verification checks. For example, Figure 15.6-3 shows the NLRHA hysteretic response (base shear vs. displacement) of the isolation system in the X and Y directions from ground motion 5, which compares well to the ELF procedure.
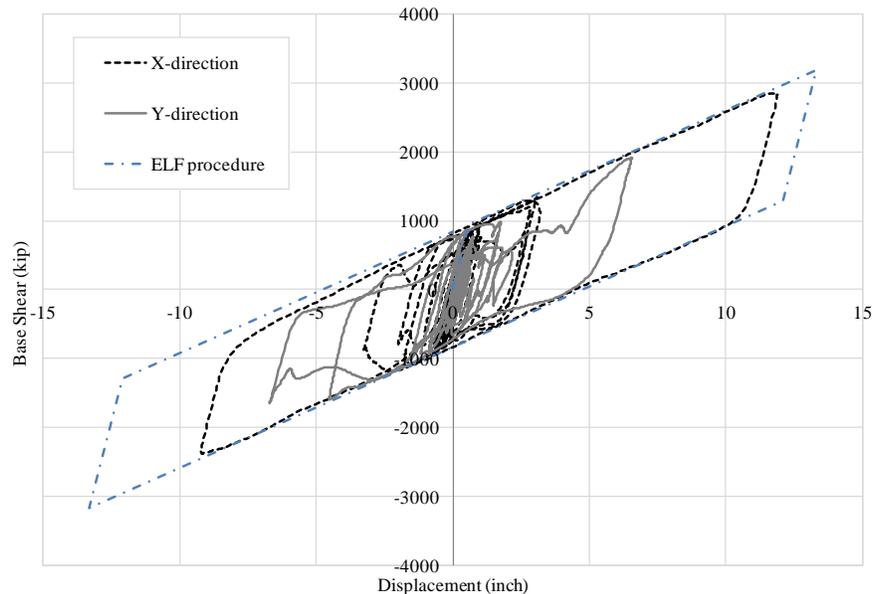
Figure 15.6-3 Base Shear Force-Displacement Behavior of Isolation System for Lower Bound Properties, comparison of ELF and NLRHA for Ground Motion 5.

**Torsion.** The *Standard §17.6.2.1* requires that the effect of torsion above the isolation interface, considering the most disadvantageous position of eccentric mass, be considered. There are two components of eccentric mass, the inherent eccentricity between the center of mass and center of rigidity and the accidental eccentricity. This accidental eccentricity approach is used to indirectly account for various effects, including: plan distributions of mass that differ from those assumed in design, variations in the mechanical properties of structural components, non-uniform yielding of the lateral system, and torsional and rotational ground motions.

Different models could be used to explicitly evaluate various locations of accidental mass eccentricity. However, this approach would require multiple additional models to consider the most disadvantageous location of accidental eccentric mass. To avoid doing an unnecessarily larger number of analyses, the *Standard §17.6.3.4.1* now permits the use of amplification factors to account for the effects of accidental mass eccentricity.

In the NLRHA of this example, only the actual eccentricities (none in this case since the superstructure and isolation system are symmetric) were modeled, with the calculated displacements and forces being increased for accidental eccentricity effects during post-processing of the results. The resultant maximum displacement, D_M was multiplied by the amplification factor given in *Standard Equation 17.5-3* (see Table 15.5-8). This procedure of amplifying D_M by a factor is the recommended method to account for accidental torsion in NLRHA since it can be problematic to artificially alter the mass and/or center of stiffness of the model because it changes the dynamic characteristics of the model and may unintentionally improve performance. Furthermore it significantly reduces computational effort. For shear and axial forces, the effects of accidental eccentricities were accounted for by using the ELF procedure. That is, applying the torsion statically to the model and superimposing the results on the NLRHA results to give the worst effect.

Peak isolation system displacement and base shear. The isolation system displaces simultaneously in the X- and Y-directions at each increment in time with the resultant displacement being the vectorial (SRSS) combination of these two components. Simply taking the maximum X or Y displacement over the whole ground motion record and calculating their SRSS combination may be overly conservative. For example, Figure 15.6-4 shows the displacement history of the isolation system in the X and Y directions for ground motion 5, Loma Prieta, using lower-bound properties. The peak X, Y and SRSS displacements were 11.9, 6.5 and 12.0 inches, respectively. The SRSS of the maximum X and Y displacements is overly conservative at $(11.9^2 + 6.5^2)^{1/2} = 13.6$ inches.
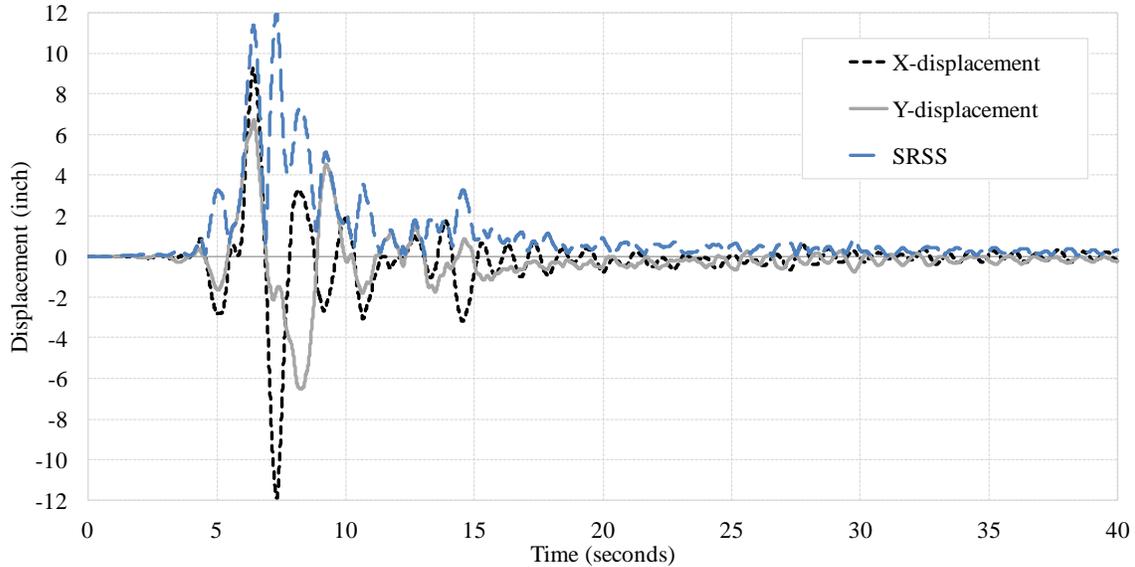
Figure 15.6-4 Displacement Histories of Isolation System, Ground Motion 5, Lower Bound Properties

Table 15.6-4 summarizes peak SRSS combinations of isolation system displacements and base shears for each ground motion from the NLRHA. The ELF calculated displacement and base shear are also given for comparison. The displacements are calculated at the center of mass of the isolation system and do not include the effects of accidental mass eccentricity. This is accounted for by using the amplification factors in Table15.5-8.

Table 15.6-4 NLRHA Peak SRSS Displacement and Base Shear of the Isolation System

Ground Motion	Upper Bound		Lower Bound	
	SRSS Max Displacement (inch)	SRSS Max Base Shear (kip)	SRSS Max Displacement (inch)	SRSS Max Base Shear (kip)
GM 1	3.6	2300	7.5	2047
GM 2	6.7	3041	6.6	1905
GM 3	6.5	3162	9.1	2048
GM 4	4.4	2140	6.7	1991
GM 5	9.1	3846	12.0	2858
GM 6	8.0	2561	12.5	2947
GM 7	4.9	2789	7.4	2120
NLRHA Average	6.2	2834 (28%)	8.9	2273 (22%)
ELF	8.3	3853 (38%)	13.3	3183 (31%)

To avoid possible under-design, the *Standard* establishes lower-bound limits on results of dynamic analysis to be used for design. These limits are established as a percentage of the corresponding parameter calculated using the ELF procedure equations.

The total maximum displacement of the isolation system shall not be taken less than 80 percent of D_{TM} calculated in Section 15.5, where D_M may be replaced with D'_M per *Standard Equation 17.6-1*.

- Minimum displacement limit:

$$D_{TM,LB} = 80\% \times Equation\ 17.5\text{-}3 \times \frac{1}{\sqrt{1+(T/T_M)}} = 0.8 \times (1.15 \times 13.3) \times \frac{1}{\sqrt{1+(0.43/2.09)}} = 12.0\ \text{inch}$$

$$D_{TM,UB} = 0.8 \times (1.15 \times 8.3) \times \frac{1}{\sqrt{1+(0.43/1.50)}} = 6.7\ \text{inch}$$

- NLRHA total maximum displacement:

$$D_{TM,LB} = 1.15 \times 8.9 = 10.2\ \text{inches} < 12.0\ \therefore\ \text{use}\ 12.0\ \text{inches}$$

$$D_{TM,UB} = 1.15 \times 6.2 = 7.1\ \text{inches} > 6.7\ \therefore\ \text{use}\ 7.1\ \text{inches}$$

Therefore the displacement used to design the bearings shall be no less than $D_{TM} = \textbf{12.0 inches}$ for lower bound properties, as the minimum limit governs, and $D_{TM} = \textbf{7.1 inches}$ for upper bound properties.

Since an OCBF structural system has been used the moat clearance and all elements crossing the isolation interface shall designed for a displacement increased by a factor of 1.2 per *§17.2.5.4*:

- Displacement capacity of moat/seismic gap:

$$D_{TM} = 1.2 \times 12.0 = 14.4\ \text{inches, rounded up to 15 inches around the building perimeter.}$$

The isolation system, foundation and all structural elements below the isolation system shall be designed for lateral force no less than $0.9V_b$. Therefore the NLRHA forces below the isolation system would need to be scaled up by a factor of:

- Scale factor for forces below the isolation level $= 0.9 \times 3853/2834 = 1.2$

and further increased to account for accidental eccentricity.

Story forces. Table 15.6-5 summarizes average (of seven ground motions) absolute maximum (maximum whether in the positive or negative direction) story shear force results at each level in the X and Y directions from the NLRHA and compares these values with story shear forces calculated by ELF formulas for unreduced design earthquake loads. The upper-bound isolation system properties gave the greater shear forces. Figure 15.6-5 shows story shears calculated by ELF formulas and by the NLRHA.

Table 15.6-5   Summary of Peak Design Story Shear Forces and Comparison with Story Shear Values Calculated Using ELF Methods, Upper Bound Properties

Response Parameter	Method of Analysis		
	ELF formulas	Peak NLRHA Result	
		X-direction	Y-direction
Penthouse	761	803	807
Third Story	2238	1787	1915
Second Story	3074	2392	2277
First Story	3449	2620	2230
V_b (Isolators)	3853	2834	2410
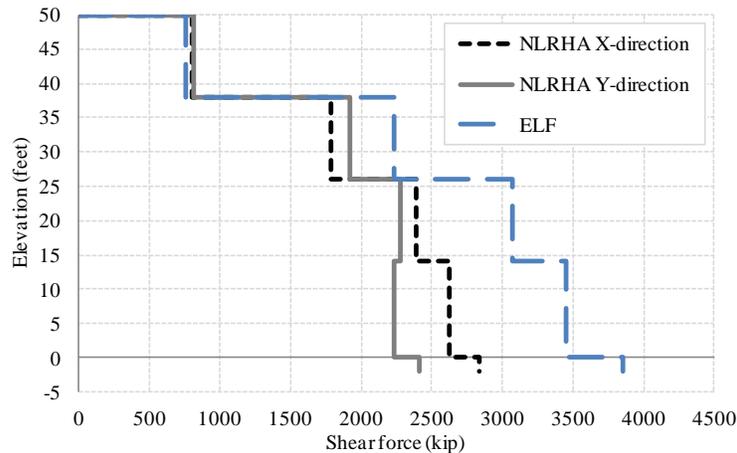
Figure 15.6-5 Comparison of Story Shear Force based on NLRHA Average and ELF Procedures, Upper-bound Properties

The minimum requirements of the *Standard* are that the base shear, V_b, shall not be taken less than 80 percent of that determined from the ELF procedure (for this regular structure) and that V_s shall not be taken less than the limits in Table 15.5-4.

Therefore if the NLRHA demands are used for superstructure design, all demands on structural elements above the isolation level need to be scaled up by the following factors:

- X-direction scale factor: $0.8 \times 3853/2834 = 1.09$

Checking X-direction minimum structural shear $V_s = 1.09 \times 2620$ kip >1940 kip (Table15.5-4) O.K.

- Y-direction scale factor: $0.8 \times 3853/2410 = 1.28$

Checking Y-direction minimum structural shear $V_s = 1.28 \times 2230$ kip >1940 kip (Table15.5-4) O.K.

Bearing vertical loads. The combination of vertical/axial loads on the bearings to be used for design consist of static dead and live loads, torsion (from the ELF procedure per Table 15.5-6), vertical earthquake loads per the response spectrum analysis and given in Table 15.6-3, as well as the vertical effects of horizontal earthquake loads from the NLRHA per this section.

The earthquake horizontal/overturning forces are calculated to be smaller in the NLRHA compared to the ELF procedure. These force need to be increased by the ratio of the NLRHA base shear to the minimum limit given by §17.6.4. This gives a scale factor of 1.2, per Section 15.6.5.3, on the earthquake overturning load. The scaled and factored minimum axial loads on the bearings, which were critical for upper bound properties, are given in Table 15.6-6.

Table 15.6-6 Maximum and Minimum Bearing Vertical Loads, Upper-Bound Properties

Maximum Loads $1.2D + 0.5L + \max(Q_E)^a + \max(Q_{E,Torsion})^b + 0.3(E_V)^c$ (kips)				
Gridline	1	2	3	4
A	215	568	325	287
B	535	702	736	**829**
C	369	651	698	665

Maximum Loads $1.2D + 0.5L + \max(0.3Q_E) + \max(0.3Q_{E,Torsion}) + E_V$ (kips)				
Gridline	1	2	3	4
A	223	522	371	351
B	531	736	850	918
C	419	753	**986**	903

Minimum Loads $0.9D + \min(Q_E) + \min(Q_{E,Torsion}) - 0.3E_V$ (kips)				
Gridline	1	2	3	4
A	14	**-74**	51	70
B	-16	31	79	30
C	62	119	208	219

Minimum Loads $0.9D + \min(0.3Q_E) + \min(0.3Q_{E,Torsion}) - E_V$ (kips)				
Gridline	1	2	3	4
A	6	-27	5	6
B	-4	-11	-29	-59
C	15	15	**-74**	-20

a. NLRHA average of maximum or minimum value from each of the seven ground motion records and scaled by a factor of 1.2
b. Calculated per the ELF procedure
c. Vertical response spectrum analysis per Section15.6.4, Table 15.6-3

The vertical loads in Table 15.6-6 and displacements per Section 15.6.4.3 are slightly less critical than that calculated from the ELF procedure (see Tables 15.5-7 and 15.5-8, respectively). Therefore the sizing of the bearing from the ELF procedure is adequate, however and could be further optimized with another design iteration.

15.7 DESIGN AND TESTING REQUIREMENTS

Detailed design of the bearings typically is the responsibility of the manufacturer subject to the design and testing (performance) criteria included in the construction documents (drawings and/or specifications). Performance criteria typically include a basic description and size(s) of isolator units; design life, durability, environmental loads and fire-resistance criteria; quality assurance and quality control requirements (including QC testing of production units); design criteria (loads, displacements, effective stiffness and damping); and prototype testing requirements. This section summarizes the design criteria and prototype testing requirements for the LR bearings of the example EOC.

15.7.1 Design Requirements

Bearing design loads.
For stability checking of the bearing:
    Maximum Long-Term Load (from Table 15.5-6, Col. C3):
        $1.2D + 1.6L$ =   665 kips

    Maximum Short-Term Load (from Tables 15.6-6 Col. C3):
        $1.2D + 0.5L + 0.3|Q_E| + E_V$ =   986 kips
        for a displacement 30% times the upper bound displacement $= 0.3 \times 7.1 = 2.1$ inches.

    Maximum Short-Term Load (from Tables 15.6-6 Col. B4):
        $1.2D + 0.5L + |Q_E| + 0.3E_V$ =   829 kips
        conservatively for the lower bound displacement = 12.0 inches. In lieu of this envelope (i.e. maximum load from upper-bound isolator properties and maximum displacement from lower-bound isolator properties), it is permitted to use two combinations of vertical load and horizontal displacement, as shown in Section 15.5.2.7.

    Minimum Short-Term Load (from Table 15.6-6, Col. A2):
        $0.9D + 0.5L + |Q_E| - 0.3E_V$ =   -74 kips
        conservatively for the lower bound displacement = 12.0 inches, or use load combinations compatible with upper- and lower-bound isolator properties.

Although tension in elastomeric bearings is discouraged, high quality bearings can sustain significant tensile deformation and this characteristic can be utilized if tension is unavoidable. Constantinou et al. (2007) observes that the bearing have approximately the same stiffness in tension and compression up to cavitation (where small cracks develop in the volume of rubber). Cavitation occurs at a negative pressure over about 3G, where G is the shear modulus of rubber. Hence the bearing per Table 15.5-1, and using nominal properties, can sustain a tension load of about 88 kip which is greater than 74 kip (which results from upper bound properties). Therefore theoretically this is achievable; however the tension capacity of the manufacturers' isolator should be verified to the satisfaction of the RDP.

For cyclic-load testing (*Standard §17.8.2.2*):
   ▪   Typical Load (Table 15.5-6, average all bearings):
        $1.0D + 0.5L$ =   290 kips

   ▪   Maximum Load (Table 15.5-6, average all bearings):
        $1.2D + 0.5L + E$ =   590 kips

   ▪   Minimum Load (Table 15.5-6, average all bearings):
        $0.9D - E$ =   30 kips

The *Standard §17.8.2.2* requires that cyclic tests at different displacement amplitudes be performed for typical vertical load (1.0D + 0.5L) and for maximum and minimum values of vertical load which are based on the load combinations of *Standard §17.2.7.1*. For this example, maximum and minimum values of vertical load are based on average of all the bearings peak earthquake response load (critical for upper bound properties), as defined by the loads in Table 15.6-6. The test displacement is conservatively based on the isolation system lower bound properties. This range of vertical load, from 30 kips to 590 kips, addresses the intent of the cyclic testing requirements (i.e., to measure possible variation in effective stiffness and damping properties).

Bearing design displacements.

Maximum considered earthquake displacement: $D_M = 10.4$ in.

Total maximum considered earthquake displacement: $D_{TM} = 12.0$ in.

Bearing force-displacement behavior and bounds.

Nominal effective stiffness (average over three cycles) for typical vertical load tested at high-speed (or tested at low speed and adjusted for high speed response) and with a displacement amplitude of $1.0D_M$:

$$k_M = \frac{G_{nom}\pi(D_B^2 - D_L^2)}{4T_r} + \frac{0.25\pi D_L^2 \sigma_{YL,Nom}}{D_M} = \frac{0.058 \times \pi(25.75^2 - 4.75^2)}{4 \times 5.225} + \frac{0.25\pi \times 4.75^2 \times 1.7}{10.4}$$

$k_M = 8.5$ kips/inch

Nominal energy dissipated per cycle (average over three cycles), E_{loop} or EDC, for typical vertical load tested at high-speed (or tested at low speed and adjusted for high speed response) and with a displacement amplitude of $1.0D_M$:

$$E_{loop} = 4A_L \sigma_{YL,Nom}(D_M - D_Y) = 4 \times 0.25 \times 4.75^2 \times \pi \times 1.7 \times (10.4 - 0.6)$$

$E_{loop} = 1180$ kip-inch

The range in this effective stiffness and EDC shall fall within the limits specified by the RDP, as defined by the λ-factors determined in Section 15.4.

15.7.2 Prototype Bearing Testing Criteria

Standard Section 17.8 prescribes a series of prototype tests to establish and validate design properties used for design of the isolation system and defines "generic" acceptance criteria *(§17.8.4)* with respect to force-deflection properties of test specimens. Table 15.7-1 summarizes one approach of the sequence and cycles of prototype testing found in *Standard §17.8.2*, applicable to the LR bearing of the example EOC.

Table 15.7-1   Example Prototype Test Requirements[1]

No. of Cycles	Standard Criteria		Example EOC Criteria	
	Vertical Load	Lateral Load	Vertical Load	Lateral Load
Production Set of Tests, Performed Quasi-Statically on a Virgin Bearing				
3 cycles	Typical	$0.67D_M$	290 kips	7.0 in.
Cyclic Load Tests to Establish Force-Deflection Behavior, Performed Dynamically				
1 cycle at each increment of displacement	Typical	1.0, 0.67, 0.5, $0.25D_M$	290 kips	10.4, 7.0, 5.2, 2.6 in.
1 cycle at each increment of displacement	Typical	0.25, 0.5, 0.67, $1.0D_M$	290 kips	2.6, 5.2 7.0, 10.4 in.
1 cycle at each increment of displacement	Maximum	1.0, 0.67, 0.5, $0.25D_M$	590 kips	10.4, 7.0, 5.2, 2.6 in.
1 cycle at each increment of displacement	Maximum	0.25, 0.5, 0.67, $1.0D_M$	590 kips	2.6, 5.2 7.0, 10.4 in.
1 cycle at each increment of displacement	Minimum	1.0, 0.67, 0.5, $0.25D_M$	30 kips	10.4, 7.0, 5.2, 2.6 in.
1 cycle at each increment of displacement	Minimum	0.25, 0.5, 0.67, $1.0D_M$	30 kips	2.6, 5.2 7.0, 10.4 in.
3 cycles	Typical	$1.0D_M$	290 kips	10.4 in.
3 cycles	Maximum	$1.0D_M$	590 kips	10.4 in.
3 cycles	Minimum	$1.0D_M$	30 kips	10.4 in.
Cyclic Load Tests to Check Durability				
14 cycles[2]	Typical	$0.75D_M$	290 kips	7.8 in.
Load Test of Isolator Stability[3]				
1 cycle	Maximum	$1.0D_{TM}$	830 kips	12.0 in.
1 cycle	Minimum	$1.0D_{TM}$	-75 kips[4]	12.0 in.

1. Item 1 of *Standard §17.8.2.2* is omitted.
2. $30S_{M1}/S_{MS}B_M$ = 14 cycles and may be performed in 3 sets of tests (5 cycles each) if tests are dynamic.
3. The exception of *Standard §17.8.2.5* may be used to have load and displacement combinations compatible with upper- and lower-bound isolator properties.
4. This is an unusual case and should be coordinated with the bearing manufacturer. It is uncommon to test LR isolators in tension as design should ideally avoid tension.

15.7.3 Production Testing

Production testing is intended to verify the quality of the individual production isolators and is commonly referred to as quality control testing. The *Standard* now requires that 100% of the project's isolators to be tested in compression and shear, and gives the RDP flexibility to determine the manufacturing quality control test program and acceptance criteria. The requirement for production testing of all isolation hardware has been the result of recent observation of failures or unacceptable behavior of hardware that has not been tested with two notable examples being:

1) Elastomeric isolators for the Kunming Airport in China were installed in 2011 without testing. As construction progressed and loads increased on the isolators, several showed signs of delamination. Hundreds of isolators were removed and replaced.
2) Sliding isolators for a project in Italy in which production testing would have disclosed defects in manufacturing.

Furthermore, production testing shall be used to confirm that the isolation system properties are appropriate and within the specification tolerance assumed for analysis and design. As discussed in Section 15.4.4, variations in individual isolator properties from the nominal design properties may be greater than the tolerance (λ_{spec}) on the average properties of all isolators, provided the individual tolerance is taken into account for isolator connection design and structure in vicinity of the bearing.

Quasi-static production testing is assumed to be the common practice for most manufacturers at present. Therefore to evaluate the consistency of the nominal values measured from production testing, there must be a relationship established between properties determined under quasi-static and to behavior under dynamic conditions. Typically, this requires that the prototype isolators are tested under the same conditions as the production testing to establish the criteria for acceptance of the production isolators, and to be tested under dynamic conditions for obtaining the nominal values and related property modification factors for analysis.

A recommended approach, which is now written into the *Standard §17.8.2*, is to perform the production set of tests on the prototype bearings (these are the bearings which are used to calculate the dynamic properties and bounds for analysis) prior to the sequence and cycles in *§17.8.2.2*. This testing is recommended first as it represents the test conditions of productions bearings. That is, a virgin state and not previously tested. Therefore the calculated nominal properties (average over three cycles), which are multiplied by λ_{spec} to give the acceptable range, will include scragging/first-cycle effects and will not be influenced by heating effects from previous testing. Hence, the acceptance criteria of the average of all production bearings are:

$$\lambda_{spec.min} \times Nom_{Proto.} \leq Nom_{Prod,Avg} \leq \lambda_{spec.max} \times Nom_{Proto.}$$

where:

Nom_{Proto} = Nominal property average over three cycles from testing specified in Table 15.7-1 from prototype isolator units not previously tested (virgin state).

$Nom_{Prod,Avg}$ = Nominal property average over three cycles from testing specified in Table 15.7-2 from production isolator units not previously tested (virgin state), averaged for all production bearings of a common type.

Table 15.7-2   Example Production Test Requirements[1]

No. of Cycles	*Standard* Criteria		Example EOC Criteria	
	Vertical Load	Lateral Load	Vertical Load	Lateral Load
3 cycles	Typical	$0.67D_M$	290 kips	7 in.

1. Testing performed quasi-statically

16

Structures with Supplemental Energy Dissipation Devices

William McVitty, M.S., Andrew Taylor, S.E., Ph.D.

Contents

Chapter 18 of ASCE/SEI 7-16 (hereafter the *Standard*) addresses the design of structures that incorporate supplemental energy dissipation devices. These devices cannot be used as the primary load path to resist earthquake loads. Instead, they <u>supplement</u> a seismic force resisting system and are typically used to improve the seismic performance.

This *Standard* defines load, design and testing requirements specific to structures with supplemental energy dissipation devices and interfaces with other chapters of the *Standard* for design of the structure. The latest evolution of the *Standard* (2016) incorporates revisions that reflect the state of practice, some of which include:

- Revised the requirements for selection and scaling of ground motions for response history analysis.
- Added new sections for the determination of the maximum and minimum damper properties for use in analysis and design.
- Revised the testing requirements for more realistic combinations of intensities and cycles.
- Clarified and revised the design review criteria, where only one registered design professional is adequate to perform the review.
- Reordered the sections to show that the current and preferred practice for analysis procedures is nonlinear response history. This involved moving the linear elastic procedures to the end of the chapter and placing them under the title "alternative procedures".
- Added commentary to compliment the provisions.

This example uses the *Standard* to design a seven-story office building located in a region of high seismicity, classified as Seismic Design Category D. The building has steel special moment resisting frames (SMRF) around the perimeter and fluid viscous dampers (FVD) in interior frames. The design of the SMRF without energy dissipation devices, for a comparable area of seismicity, is illustrated in Chapter 9 of these NEHRP design examples. The details of that building are directly adopted as a starting point for this example.

In addition to the *Standard*, the following documents are either referenced directly, provide background, or are useful aids for the analysis and design of structures with supplemental energy dissipation devices.

AISC	American Institute of Steel Construction (2010). *Seismic Provisions for Structural Steel Buildings*. Standard AISC 341-10
Basu et al	Basu, D., Constantinou, M. C., Whittaker, A. S. (2014). *An equivalent accidental eccentricity to account for the effects of torsional ground motion on structure*, Eng. Struct. Vol. 69
CERC	Canterbury Earthquakes Royal Commission Final Report (2012), *Volume 3 Low Damage Building Technologies*. http://canterbury.royalcommission.govt.nz/Final-Report-Volume-Three-Contents.
Charney and McNamara	Charney, F. A., and McNamara, R. J. (2008). *A comparison of methods for computing equivalent viscous damping ratios of structures with added viscous damping*. J. Struct. Eng., 134, 32–44.
Christopoulos and Filiatrualt	Christopoulos, C., Filiatrault, A. (2006) *Principles of Passive Supplemental Damping and Seismic Isolation*. IUSS Press.
Constantinou et al	Constantinou, M. C., Whittaker, A. S., Kalpakidis, Y., Fenz, D. M. and Warn, G. P. (2007). *Performance of Seismic Isolation Hardware under Service and Seismic Loading*, Technical Report MCEER-07-0012, Multidisciplinary Center for Earthquake Engineering Research, Buffalo, New York.

Constantinou et al	Constantinou, M. C., Tsopelas, P., Hammel, W., and Sigaher, A. N. (2001). *Toggle-brace-damper seismic energy dissipation systems.* J.Struct. Eng., 1272, 105–112.
FEMA	Federal Emergency Management Agency FEMA 273 (1997) *Prestandard and Commentary for the Seismic Rehabilitation of Buildings.*
FEMA	Federal Emergency Management Agency FEMA 356 (2000) *NEHRP Guidelines for the Seismic Rehabilitation of Buildings.*
Hamburger et al	Hamburger, R. O, Krawinkler, H., Malley, J. O., Adan, S. C., (2009) *Seismic Design of Steel Special Moment Frames: A Guide for Practicing Engineers.* NIST GCR 09-917-3.
Pavlou and Constantinou	Pavlou, E., and Constantinou, M. C. (2004). *Response of elastic and inelastic structures with damping systems to near-field and soft-soil ground motions.* Eng. Struct., 269, 1217–1230.
Pavlou and Constantinou	Pavlou, E. and Constantinou, M.C. (2006), *Response of Nonstructural Components in Structures with Damping Systems*, Journal of Structural Engineering, ASCE, Vol. 132, No. 7, 1108-1117.
Ramirez et al	Ramirez, O. M., Constantinou, M. C,, Kircher, C. A., Whittaker, A. S., Johnson, M. W., Gomez, J. D., Chrysostomou C. Z. (2001) *Development and Evaluation of Simplified Procedures for Analysis and Design of Buildings with Passive Energy Dissipation Systems.* MCEER-00-0010, Multidisciplinary Center for Earthquake Engineering Research, Buffalo, New York.
SEAOC	Structural Engineers Association of California (2014). *2012 IBC SEAOC Structural/Seismic Design Manual*, Volume 5: Examples for Seismically Isolated Buildings and Buildings with Supplemental Damping, Published January 2014.
Symans et al	Symans M. D., Charney, F. A., Whittaker, A. S., Constantinou, M. C., Kircher, C. A., Johnson, M. W., McNamara, R. J. (2008) *Energy Dissipation Systems for Seismic Applications: Current Practice and Recent Developments.* ASCE Journal of Structural Engineering.
Taylor	Taylor, D. P. (1999). *Buildings: Design for Damping.* http://taylordevices.com/Tech-Paper-archives/literature-pdf/56-BuildingsDesignforDamping.pdf
Whittaker et al	Whittaker, A. S., Aiken, I. D., Bergman, D., Clark, P. W., Cohen, J., Kelly, J. M., and Scholl, R. E. (1993). *Code requirements for design and implementation of passive energy dissipation systems.* Proc., ATC-17–1 Seminar on Seismic Isolation, Passive Energy Dissipation, and Active Control, Vol. 2, ATC, Redwood City, Calif., 497–508.
Wolff and Constantinou	Wolff, E.D. and Constantinou, M.C. (2004), *Experimental Study of Seismic Isolation Systems with Emphasis on Secondary System Response and Verification of Accuracy of Dynamic Response History Analysis Methods*, Report No. MCEER-04-0001.

16.1 BACKGROUND

16.1.1 Energy Dissipation Devices

Passive energy dissipation devices (widely known, and referred to hereafter, as dampers) absorb and dissipate vibration energy through relative movement across the damper and can be implemented in buildings to achieve a higher level of seismic performance. These dampers supplement the seismic force resisting system (SFRS) and are primarily used to reduce displacements. Dampers can also reduce force in the structure, provided the structure is responding elastically, but would not necessarily be expected to reduce force in structures that are responding inelastically.

The dampers are termed 'passive' to differentiate them from semi-active or active dampers which require a computerized control system and an external power source to adjust the engagement and/or properties of the energy dissipation devices. These latter systems have yet to gain confidence in the United States for seismic applications. Passive dampers are divided into three categories: displacement-dependent/activated devices, velocity-dependent/activated devices, and other. Examples of displacement-dependent devices include metallic yielding, friction and lead-extrusion dampers which exhibit hysteretic force-displacement behavior. Examples of velocity-dependent devices include dampers consisting of visco-elastic solid materials, dampers operating by deformation of visco-elastic fluids (e.g. viscous shear walls), and dampers operating by forcing fluid through an orifice (e.g. viscous fluid dampers). Systems categorized as 'other' have characteristics that cannot be classified into the former two categories (see Constantinou et al. 2007).

This example uses the fluid viscous damper (FVD) since it is a predominate type of damper used in seismic applications and has been implemented in structures in the United States since the early 1990s. One manufacturer of FVDs lists over 400 civil structures worldwide that have incorporated FVDs to improve the seismic performance[4]. These types of devices were originally developed for military applications dating back over 40 years.

Structures that contain damping systems must have a SFRS that confirms to one of the types in *Standard Table 12.2-1*. Or conversely, Chapter 18 applies to structural systems that dissipated earthquake energy but are not listed as a SFRS in *Table 12.2-1*. For example, prior to the development of the Buckling-Restrained Brace (BRB) frame, one could have designed the system using Chapter 18 where the BRB is a displacement-dependent damper that supplements a SMRF. However to foster implementation, proponents of the BRB have progressed the system such that it is regarded as the primary lateral load path and designed in a similar manner to a conventional braced frame using its own response modification factor, *R*.

16.1.2 Intent of Seismic Provisions

The design philosophy of the current *Standard* can be traced back to earlier SEAONC, FEMA and NEHRP guidelines. Key concepts which are relevant to the current *Standard* are outlined in Symans et al. (2008) as follows:

1. The *Standard* is applicable to all types of damping systems, including displacement-dependent damping devices, hysteretic or friction systems, and velocity-dependent viscous or viscoelastic systems;

---

[4] http://taylordevices.com/pdf/2011-StructuralApp.pdf

2. The *Standard* provides minimum design criteria with performance objectives comparable to those for a structure with a conventional seismic-force-resisting system but also permits design criteria that will achieve higher performance levels;

3. The *Standard* requires that the damping system also have a SFRS (see *Standard Table 12.2-1*) that provides a complete load path. The SFRS must comply with the requirements of the *Standard* (i.e. minimum base shear), except that the damping system may be used to meet drift limits. Thus, the detailing requirements that are in place for structures without damping systems may not be relaxed for structures which include damping systems;

4. The *Standard* requires design of damping devices and prototype testing of damper units for displacements, velocities, and forces corresponding to those of the maximum considered earthquake; and

5. The *Standard* provides linear static and response spectrum analysis methods for design of structures that meet certain configuration and other limiting criteria. For example, at least two damping devices at each story configured to resist torsion, a S_1 value for the site less than 0.6, among other requirements. These procedures are listed under "alterative procedures" since nonlinear response history analysis is the preferred design tool.

With regard to point 2, although the requirements of the *Standard* are intended to produce a performance comparable to that for a structure with a conventional SFRS system, it is common practice for the structures to be designed to achieve a much higher performance. This is achieved by designing the SFRS to remain essentially elastic at the MCE_R level with a majority of the earthquake energy dissipated by the damping system.

The intent of initial guidelines (Whittaker et al. 1993) was to direct dissipation of earthquake-induced energy into damping systems not part of the vertical load resisting structure, thereby improving performance by reducing repair costs and business interruption. However since severe earthquakes are very rare events and limiting damage may be costly for conventional SFRS, the building codes only enforce a design philosophy intended to provide safety by avoiding collapse, while permitting extensive structural and nonstructural damage. The reality with this design approach was notably demonstrated by the Canterbury earthquakes in New Zealand 2010/2011. The business disruption and economic impacts were considerable. The central business district was cordoned off for nearly two years to allow for the demolition or repair of buildings, with damage estimated at NZ$20 billion (Royal Commission 2012), or 8% of GDP. Simply directing the dissipation of earthquake energy into elements that are readily replaceable (or do not require replacement at all) is a wise progression for the seismic design of structures.

With regard to point 3, the design philosophy of the *Standard* is centered on the independent design of the SFRS and the damping system (i.e. dampers and connected elements), where these two systems may or may not have common elements. The SFRS must provide a complete lateral load path, as if the dampers where disconnected, so as to provide safety in the event of the dampers malfunctioning. The presence of the dampers is accounted for by modifying the characteristics of the SFRS, foremost its damping, and in the case of hysteretic and viscoelastic dampers, also its lateral stiffness characteristics. The *Standard* specifies minimum base shear criteria for the design of SFRS which may be more critical than that calculated from analysis but, on the other hand, allows the damping system to be used when assessing the *Standard's* drift limits.

With regard to point 5, the elastic procedures for analysis and design are largely based on studies by Ramirez et al. 2001. These methods have been shown to give a reasonable estimate of responses, however are not straightforward to apply and have their limitations. Current practice and computing power has evolved such that nonlinear response history analysis is the common and preferred analysis tool used to calculate peak responses. One complication over the ELF and response spectrum procedures is that a suite

of ground motions is required, which is typically unavailable at the preliminary design stage. Hence elastic methods may be useful for the initial sizing of damping devices but are rarely used as a basis for the final design requirements.
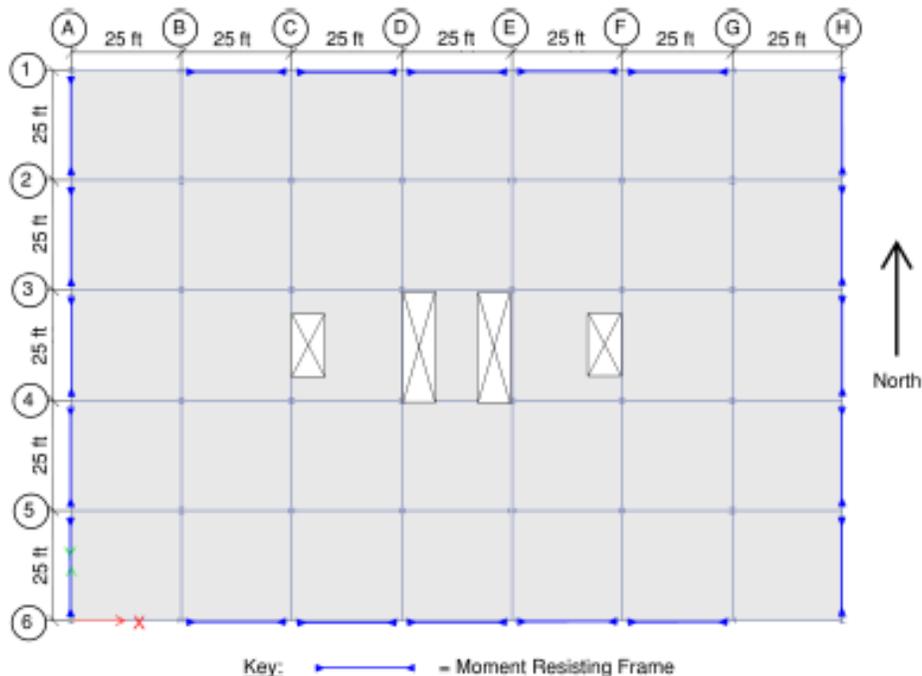
16.2 PROJECT INFORMATION

16.2.1 Building Description

The example building is a seven story steel framed office building located in a region of high seismicity, classified as Seismic Design Category D. The building has a rectangular plan configuration measuring 175 feet, in the E-W direction and 125 feet wide in the N-S direction (Figure 16.2-1). The typical story height is 13 feet, 4 inches but with a first story height of 22 feet, 4 inches (Figure 16.2-2). The building has a penthouse that extends 16 feet above the roof level of the building and covers the area bounded by Gridlines C, F, 3 and 4 in Figure16.2-1. The floors consist of 3-1/4-inch lightweight concrete over composite metal deck. The elevators and stairs are located in the central three bays.

The seismic force resisting system consists of steel special moment resisting frames (SMRF) with prequalified Reduced Beam Section (RBS) connections located on the perimeter bays of the building along Gridlines A, H, 1 and 6 as shown in Figure 16.2-1. Each SMRF line has five bays of moment resisting frames. The elevations and member sizes are directly adopted from the Chapter 9 analysis and are given in Figures 16.2-3 and 16.2-4 for Gridlines 1 and 6, and A and H, respectively. To meet the architect's requirement of having no diagonal bracing members around the perimeter of the building, supplemental damping devices are located on gravity framing lines on the interior of the structure on Gridlines B, G, 2, and 5. The number and layout of these dampers is determined in the preliminary design and is shown later in Figures 16.3-1 and 16.3-2 in Section 16.3.

The foundations elements are designed and detailed with adequate strength and stiffness to provide fixity such that the column bases of the SMRF can be modeled assuming fixed bases.

Figure 16.2-1 Typical Floor Framing Plan with SMRF Locations

Figure 16.2-2 Typical North-South Building Elevation

Figure 16.2-3 Steel Special Moment Frame on Gridlines 1 and 6

Figure 16.2-4 Steel Special Moment Frame on Gridlines A and H

16.2.2 General Parameters

16.2.1.1 Seismic design parameters. See Chapter 3 of these NERHP design examples for illustration of calculating design ground motion parameters. For this example, the parameters adopted are:

$S_{DS} = 0.93$

$S_{D1} = 0.6$

Risk Category II

$I_e = 1.0$

Seismic Design Category D

Site Class D

Site is located greater than 3 miles from an active fault. Therefore the scaling and orientation requirements for sites located near an active fault do not apply.

For a Steel Special Moment Frame (*Standard* Table 12.2-1)

$R = 8$

$\Omega_0 = 3$

$C_d = 5.5$

Gravity loads.

Dead Loads:

Penthouse roof dead load:	25 psf
Exterior walls of penthouse:	25 psf

Roof dead load (roofing, insulation, deck beams, girders, fireproofing, ceiling, mechanical, electrical plumbing):   55 psf

Exterior wall cladding:	25 psf
Penthouse floor dead load:	65 psf
Penthouse permanent equipment:	39 psf

Floor dead load (deck, beams, girders, fireproofing, ceiling, mechanical electrical, plumbing, partitions):   68 psf

Reducible Live Loads:

Roof live load:	25 psf
Floors live load:	50 psf

Live load reduction: 2012 IBC Section 1607.10 permits area-based live load reduction of not more than 50 percent for elements with live loads from a single story (girders) and not more than 60 percent for elements with live loads from multiple stories (axial component of live load on columns at lower levels).

Seismic weight calculation. The seismic weight calculation assumes a 14 inch overhang of the slab around the perimeter of the building. The total seismic weight of building is 94 kips + 1,537 kips + 6×(1,920 kips) = 13,151 kips

Penthouse roof:

Roof slab = (0.025 ksf)(25 ft)(75 ft)	=	47 kips
Walls = (0.025 ksf)(8 ft)(200 ft)	=	40 kips
Columns = (0.110 ksf)(8 ft)(8 ft)	=	7 kips
Total	=	94 kips

Lower roof:

Roof slab = (0.055 ksf)[(127.33 ft)(177.33 ft) - (25 ft)(75 ft)]	=	1139 kips
Penthouse floor = (0.065 ksf)(25 ft)(75 ft)	=	122 kips
Walls = 40 kips + (0.025 ksf)(609 ft)(6.67 ft)	=	142 kips
Columns = 7 kips + (0.170 ksf)(6.67 ft)(48 ft)	=	61 kips
Equipment = (0.039 ksf)(25 ft)(75 ft)	=	73 kips
Total	=	1,537 kips

Typical floor:

Floor = (0.068 ksf)(127.33 ft)(177.33 ft)	=	1,535 kips
Walls = (0.025 ksf)(609 ft)(13.33 ft)	=	203 kips
Columns = (0.285 ksf)(13.33 ft)(48 ft)	=	182 kips
Total	=	1,920 kips

16.2.3 Structural Design Criteria

Structural component load effects. The effect of seismic load is defined by *Standard §12.4.2* as:

$$E = \rho Q_E \pm 0.2 S_{DS} D$$

where Q_E is the horizontal seismic load and $0.2 S_{DS} D$ is the vertical seismic load effects. Using *Standard §12.3.4.2*, ρ is 1.0. The value of S_{DS} is taken as 0.93 for the design earthquake, whereas S_{DS} is replaced by S_{MS} and taken as 1.4 for the MCE$_R$ event.

Design Earthquake: $\quad E = Q_E \pm 0.19 D$
MCE$_R$: $\qquad\qquad\quad E = Q_E \pm 0.28 D$

Load combinations. Load combinations from ASCE 7-10 are as follows:

$1.4D$

$1.2D + 1.6L + 0.5L_r$

$1.2D + L + 1.6L_r$

For the design earthquake level:

$(1.2 + 0.2 S_{DS})D + 0.5L + \rho Q_E \qquad = 1.39D + 0.5L \ \pm \ Q_E$

$(0.9 - 0.2 \ S_{DS})D + \rho Q_E \qquad\qquad = 0.71D \ \pm \ Q_E$

For the MCE$_R$ event:

$(1.2 + 0.2 S_{MS})D + 0.5L + \rho Q_E \qquad = 1.48D + 0.5L \ \pm \ Q_E$

$(0.9 - 0.2 \ S_{MS})D + \rho Q_E \qquad\qquad = 0.62D \ \pm \ Q_E$

Response history analysis combinations. The NLRHA can generate a large amount of data considering there are seven ground motions, each with two components that may be applied in multiple orientations, multiplied by maximum and minimum dampers properties, and with various load combination cases. This number of analyses may also be magnified by considering different cases of accidental eccentricity.

The post-processing approach to determine the critical demands for the design of structural members depends on a number of factors, such as whether the site is near a fault, the complexity of the buildings geometry, the importance of the structure, and the reviewing jurisdiction. For this example building, the authors consider the following approach practical and appropriate:
- Since the building is greater than 3 miles from an active fault the two horizontal components of each ground motion are applied randomly to the building model parallel to the principal axes of the building. The ground motions are not rotated to their fault-normal and fault-parallel components nor are the components rotated. The ground motions are applied in one orientation only.
- The maximum and minimum demands are calculated for each ground motion.
- In Section 16.4.4.2 the absolute maximum of the maximum and minimum demands is taken for each ground motion and then averaged for the seven ground motions.
- In Section 16.5, the average of the maximum demands and average of the minimum demands is taken for the seven ground motions. This is so that the maximum tension in the frame columns can be calculated. Therefore, since the absolute maximum is not taken from each ground motion, the average results are slightly less than the average results calculated in the step above (by about 5-10% or less in this example).

16-10

16.3 DESIGN CONSIDERATIONS

16.3.1 Advantages of Using Dampers in New Construction

One primary reason to use dampers in the seismic design of new construction is to limit damaging deformations in structural components and therefore achieve a higher performance level. The inclusion of FVD within the a steel SMRF is effective in reducing seismic drifts, and therefore can lead to a number of benefits as explained in Symans et al. 2008:

1. A reduction in the size of framing members of the SMRF, which may offset the cost of the added damping elements.

2. A reduction in overturning moment and foundation sizes when compared to a conventional braced frame system.

3. A reduction in yielding, and hence damage, to the SMRF. The structure may be designed to achieve an operational performance level following a severe earthquake. In comparison, both a conventional SMRF and braced frame may have significant damage, to the point where it is uneconomical to repair.

16.3.2 Early Design Decisions

Performance goals. Typical practice is to use the FVD devices in new construction to reduce damage. Therefore the office building will be designed to achieve a higher performance level than the minimum requirements of the *Standard*. This will be achieved by sizing the seismic force resisting system (SFRS) such that all the structural members remain "essentially" elastic at the MCE_R level, with virtually all earthquake energy dissipated by the FVDs.

Added damping. Added damping of 20 percent of critical in the fundamental mode of vibration is targeted for the initial sizing of the dampers. The optimal amount of added damping depends on the structure and excitation. Generalized damping levels from previous projects are as follows (Taylor 1999):
- Building 1-15 floors   =   15-25% added damping
- Tall buildings   =   5-15% added damping

A reduction in ductility demand in the SFRS is facilitated through displacement reductions, which come from increased damping provided by the FVD. However with increased damping typically comes increased base shear (depending on the FVD properties), which will need to be accommodated in the design of the structure and foundations. Nevertheless, in some cases the structural analysis may show benefits from higher damping ratios, greater than 35-45 percent. However at these high damping levels the damper costs starts going past the point of diminishing returns.

Other considerations are that the equivalent lateral force (ELF) and response spectrum procedures are only permitted by the *Standard* if the damping ratio is less than 35 percent of critical. Also the *Standard* states that the seismic base shear of the SFRS shall be taken no less than 75 percent of the seismic base shear of the un-damped frame, *V*, determined in accordance with *Standard §12.8*. Hence at high damping ratios, there may be limited benefit from adding more damping to reduce the base shear on the independent SFRS, as the 75 percent base shear limit of the *Standard* will govern the design of the SFRS.

Placement and configuration of dampers. The design of the SFRS and/or damping system may be affected by requirements in the *Standard* which refer to the number and location of dampers. These include:

- *§18.2.1.1*: The base shear of the SFRS may be taken no less than 1.0*V* if, in the direction of interest, the damping system has less than two damping devices configured to resist torsion on each floor level.
- *§18.2.3*: The ELF and response spectrum procedures are permitted only if there are two or more damping devices configured to resist torsion on each floor level.
- *§18.2.4.6*: If there are fewer than four damping devices provided in each principal direction at each floor level or less than two damping devices are configured to resist torsion in either principal direction, the maximum calculated velocity for the FVD under the MCE$_R$ earthquake shall be penalized by a factor of 1.3.

In the upper stories the example building has two bays installed with dampers in the north-south direction and two bays installed with dampers in the east-west direction, as shown in Figure 16.3-1. Dampers are located at every story apart from the penthouse roof level. This level is a minor attachment at the top of the building, at only 6 percent of the weight of the floor below. Therefore it can be assumed that the structure has damping devices over its full height. The center of stiffness is located at the center of the floor plate at every story and coincides with the center of mass. The dampers are configured to resist torsion by placing the two bays of dampers on gridlines which are at an equal distance either side of the center of stiffness.

The configuration in Figure 16.3-1 satisfies the first two requirements of the *Standard* as noted above, that is: the SFRS base shear is permitted to be taken as small as 0.75*V* and both the ELF and response spectrum analysis procedures are allowed. However the damping system does not meet the redundancy criterion. The redundancy criterion of *Standard §18.2.4.6* is the most demanding, as it requires more damping devices to be located in each story. The interpretation of the *Standard* is that it is referring to the number of bays with damping devices, not the number of damping devices themselves. For example, a configuration with chevron bracing and two dampers located horizontally either side of the chevron apex gives a total number of four dampers in each principal direction for each story, but is only in two bays of framing. This example does not increase the number of bays with damping devices in the upper stories to avoid the penalty factor of 1.3 as: a) the architect wants to minimize diagonal members in the occupied areas of the floor plate and b) it typically is not difficult or costly to design the FVD itself for the additional displacement (i.e. stroke) and force demands required by the *Standard*.

The effectiveness of each FVD is a function of the velocity and damper design properties. For each mode of vibration, the effectiveness of the dampers can be maximized by positioning the devices in accordance with the largest story displacements in that mode. For this example the dampers are installed at the largest distance from the center of stiffness as the architect's requirements allow. This is to improve the effectiveness of dampers over the first few fundamental modes of vibrations, which typically contribute the most to seismic response. If the dampers were instead installed in the core of the building, although they would still be effective in the first and second modes of vibration (which are translational modes), they would provide little damping in the torsional modes, such as the third mode for the example structure.

The dampers may also be strategically placed and damping values optimized to remedy irregularities in the building such as soft-stories and torsional irregularities. For the example, the dampers in the first level of the example building would experience significant deformations and thus produce significant damping forces to mitigate the potential soft-story P-delta effects. Furthermore the effectiveness of dampers may be enhanced, particularly for stiff structures, by using configurations that geometrically amplify the

relative displacement. Examples include toggle and scissor-jack bracing as described by Constantinou et al. 2001.

Analysis procedure selection. A nonlinear response history analysis (NLRHA) will be used to calculate the maximum displacement, velocities and forces at the MCE$_R$ level which are used for the design of the damping system and to calculate frame moments, shears and axial forces at the design earthquake level for the design of the SFRS.

A NLRHA is adopted because a) it is typically common practice in design firms and preferred by the *Standard*, b) it may be required by peer review, and c) the computational effort is not notably more than elastic methods. Above all the NLRHA gives the most realistic prediction of seismic response. This is because the degree to which a damped structure is able to accomplish its performance goals depends on the inherent properties of the structure, the properties of the dampers and its connecting elements, the characteristics of the ground motion, and the limit state being investigated. Given the potentially large variation in each of these parameters, it is usually necessary to perform an extensive suite of nonlinear response-history analyses.

Viscous damper velocity exponent. The force output of a linear and nonlinear fluid viscous damper is specified as follows:

$$F = C\left|v\right|^{\alpha} \text{sgn}(v) \qquad\qquad (16.3\text{-}1)$$

where v is the velocity, C is the damping coefficient, α is the velocity exponent in the range of 0.1 to 2.0 and sgn is the signum function (i.e. sign of the velocity, whether positive of negative). An α value of 1.0 gives linear behavior. The difference in force-velocity and force-displacement behavior of a linear and nonlinear FVD is illustrated in Figures 16.3-5 and 16.3-6.

Nonlinear fluid viscous dampers, with exponents in the range of 0.3 to 0.5 are often used in design for the following reasons: (a) force output increments are small at large velocities, therefore limiting the force output of the damper for velocities in excess of the design velocity (b) energy dissipation per cycle is more than that of comparable linear viscous dampers and the dampers are more effective for smaller magnitude earthquakes, and (c) such devices are suitable for attenuating the effects of high velocity pulses that may occur at near-fault locations. The selection of an appropriate α exponent is based on experience and typically design firms conduct trial-and-error design iterations.

It is noted however, the use of highly nonlinear viscous damping devices (particularly those with a very low velocity exponent) can negatively impact the performance of nonstructural components (Wolff and Constantinou, 2004; Pavlou and Constantinou, 2006). Furthermore, with nonlinear dampers you lose the benefit of the maximum velocity (dampers force) and maximum displacement (maximum elastic story shear) being nominally out of phase by 90 degrees.

Fabrication and detailing. Further practical design considerations which are all interrelated include:

1. Deciding whether to have a large number of small dampers or lesser number of large dampers

2. Deciding how many different types of dampers will be used.

3. Deciding on the damping configuration.

Experience on previous projects helps guide the engineer to arrive at a cost-effective design solution. Based on such experience (see Taylor 1999), quantities of dampers smaller than 32 pieces tend to become costly. Also, the least expensive damper sizes tend to be in the range of 300-600 kip force capacity, that is, one piece of a 300 kip capacity damper costs less than 10 pieces of a 30 kip capacity damper. A trade-off is that larger devices give large concentrations of load in the structure which requires special design considerations for the connected structure. Based on the statement above, the following iterative process is recommended:

- Start out with multiple dampers of the same size and distribute them uniformly throughout the structure.
- Use the next larger size of damper to reduce the number of dampers until:
  - The quantity of dampers goes below 32 pieces
  - The force rating of the dampers goes above 600 kips
  - The structure begins to behave less efficiently because the dampers are not distributed advantageously.
- Alternatively, if the structure is to be optimized for irregularities or other design objectives, it may be advantageous to start out with two or more types/sizes of damper.

In terms of damping configuration, there are three basic ways to incorporate dampers into a building: a) diagonal bracing, b) chevron bracing and c) toggle or geometric amplification configurations. The damper increases in effectiveness from configuration a) to c). For example, the relative movement across the damper, arising from story drifts, is greater if the damper is configured horizontally compared to at an angle.

This example adopts a diagonal configuration. Chevron and toggle configurations may require special out-of-plane detailing. For example out-of-plane bracing at the apex of the chevron apex may be necessary to restrain bucking of the braces. Furthermore, the *Standard* specifically states in *§18.2.4.2* that the connection points of the damping system shall provide sufficient articulation. This is usually achieved by using a spherical bearing connection at each end of the damper, so to accommodate the motion from the relatively small drifts encountered in the out-of-plane /orthogonal direction.

16.3.3 Preliminary Sizing of Damping Devices

 Linear viscous dampers. The preliminary design is based on a practical method presented in Christopoulos and Filiatrault, 2006. The procedure calculates the linear viscous damping coefficients required of dampers at each story in order to achieve a certain damping ratio in a particular mode. This provides a rough initial estimate of order-of-magnitude of damping coefficients, which can later be refined by using nonlinear response history analysis to optimize the parameters of interest.

The steps of this method are as follows:

Step 1: Create a mathematical model of the building without the dampers and conduct a modal analysis to calculate the period of the primary mode of vibration T_m in each principal direction.

Step 2: Select an amount of added damping for each primary mode. For the example building the first and second modes of vibration are translation in the north-south and east-west directions, respectively. An added damping of 20% of critical is targeted in each of these modes, giving a damping ratio in the first and second modes, ξ_1 and ξ_2, of 0.20. For simplicity, the inherent damping of the building without dampers is neglected.

Step 3: Calculate the pseudo braced building primary periods of vibration T_{ps} for each principal direction. For the each mode of interest, this is calculated as:

$$T_{ps,m} = \frac{T_m}{\sqrt{2\xi_m + 1}} \qquad (16.3\text{-}2)$$

Step 4: Calculate the area of pseudo braces to be introduced into the building's mathematical model in order to achieve the pseudo braced period calculated in Step 3, for each principal direction. These pseudo braces are located at the same locations as the proposed FVD. Since the procedure is based on stiffness proportional damping, the pseudo braces (or linear viscous dampers) are distributed according to the lateral stiffness of the structure so as to achieve an identical mode shape to the "un-braced" building.

The calculation of the stiffness of the pseudo braces requires one iteration, and can be further broken down into the following steps:

a) Calculate the lateral stiffness of each story in each principal direction. This can be estimated by applying a unit lateral force at the roof of the building, to give a uniform shear at each story and evaluating the resulting story drifts.

b) Select a trial value of the pseudo horizontal stiffness, for the first level $K_{trial,1}$, and proportion the horizontal stiffness on the upper stories according to their relative story stiffness. The horizontal story stiffness at each story, i, can be simulated in the mathematical (ETABS) model by placing diagonally orientated braces in each bay, each with a pseudo brace area A_{brace}, calculated from:

$$A_{brace,i} = \frac{K_{trial,i} L_{wp-wp}}{N_i E \cos^2 \theta} \qquad (16.3\text{-}3)$$

where L_{wp-wp} is the length of the brace between work points, N is the number of braced bays in the direction of interest, E is the elastic modulus of the brace material and θ is the angle of the brace measured from the horizontal.

c) Using the trial horizontal stiffness, conduct a modal analysis of the pseudo braced building to calculate the trial period, T_{trial}.

d) Re-calculate the pseudo horizontal stiffnesses at each story based on the trial period, as follows:

$$K_{hor,i} = \frac{K_{trial,i}}{\left(\dfrac{T_m^2 - T_{trial}^2}{T_m^2 - T_{ps,m}^2}\right)\left(\dfrac{T_{ps,m}^2}{T_{trial}^2}\right)} \qquad (16.3\text{-}4)$$

Step 5: Calculate the required horizontal linear viscous damping constant $C_{L,hor}$ for each story, i , based on the pseudo stiffness and primary mode period:

$$C_{L,hor,i} = \frac{K_{hor,i} T_m}{2\pi} \qquad (16.4\text{-}5)$$

The equivalent damping constant for a diagonally orientated FVD in each bay is then determined using:

$$C_{L,diag,i} = \frac{C_{L,hor,i}}{N_i \cos^2 \theta} \qquad\qquad (16.4\text{-}6)$$

The calculated damping coefficients for diagonally oriented FVD's in 2 bays at each story in each principal direction are given in Table 16.3-1. The coefficients are based on the method explained above which seeks 20% added damping in the first and second modes using linear viscous dampers with coefficients proportioned according to the mode shapes.

Table 16.3-1 Stiffness-Proportional Linear Viscous Damping Constants for Example Building

Story	North-South Direction $C_{L,diag}$ kip-sec/inch	East-West Direction $C_{L,diag}$ kip-sec/inch
7	41	56
6	37	60
5	37	63
4	41	65
3	51	72
2	94	125
1	96	116

Since it is not practical to use different damping coefficients at every level, engineering judgment can be used to reduce the number of dampers to 1 or 2 types. For this example it is decided to use only one type of damper which is used at every story in both principal directions. That is, a linear FVD with a damping coefficient of 50 kip-sec/inch with an added two bays of dampers in the lower two stories in each principal direction is adopted. This gives a total of 36 dampers in the building.

The plan view of the bays with damping devices for stories 3 to 7 and 1 to 2 are shown in Figures 16.3-1 and 16.3-2, respectively. An elevation view of the frames with dampers is shown in Figures 16.3-3 and 16.3-4 for Gridlines 2, 5 and B, G, respectively.
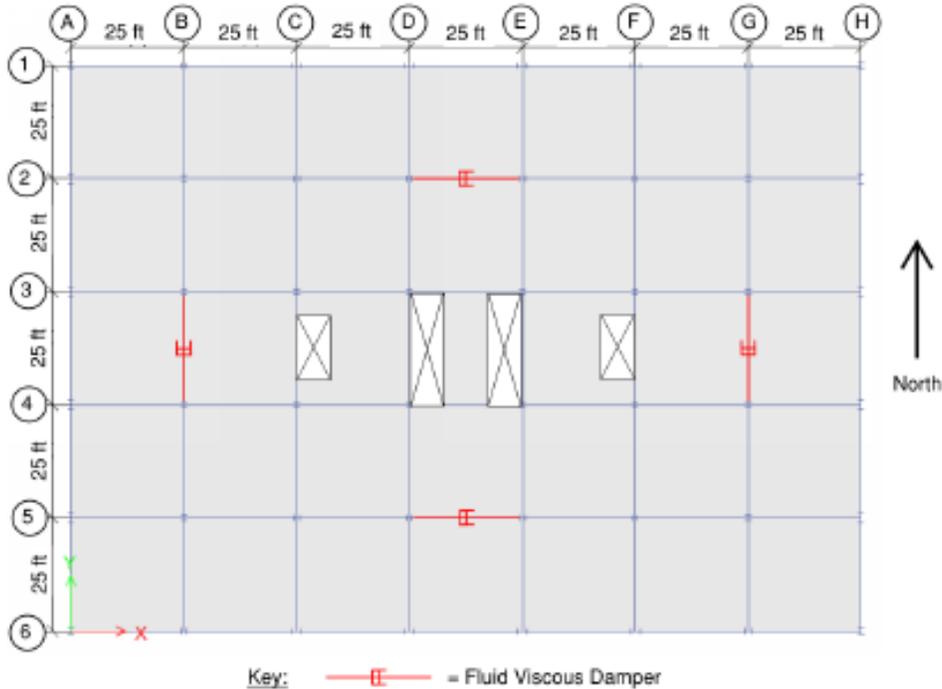
Figure 16.3-1 Floor Framing Plan with Damper Locations in Stories 3-7
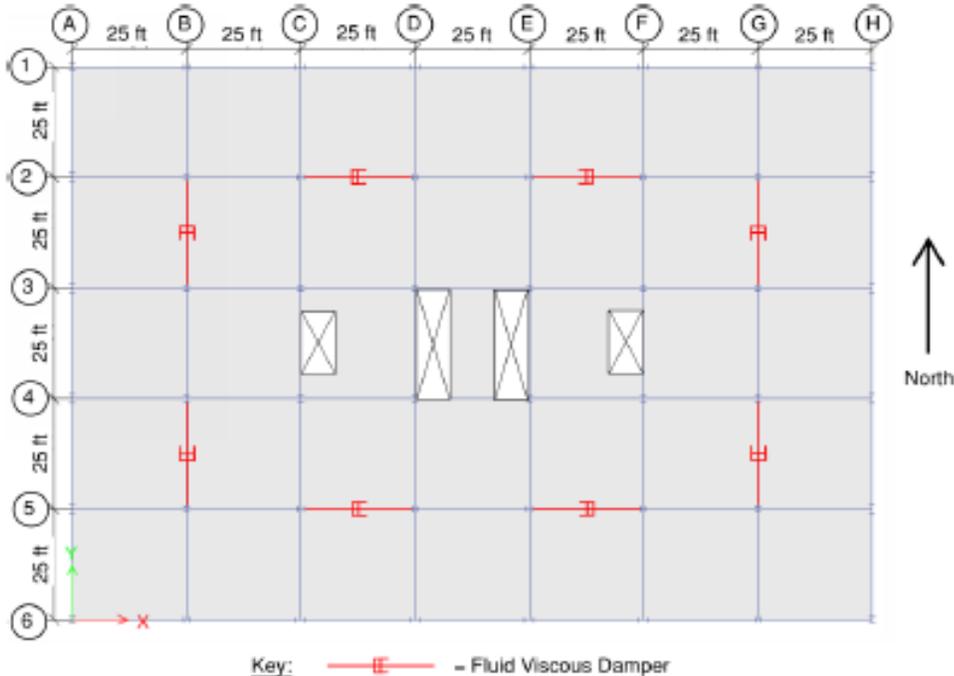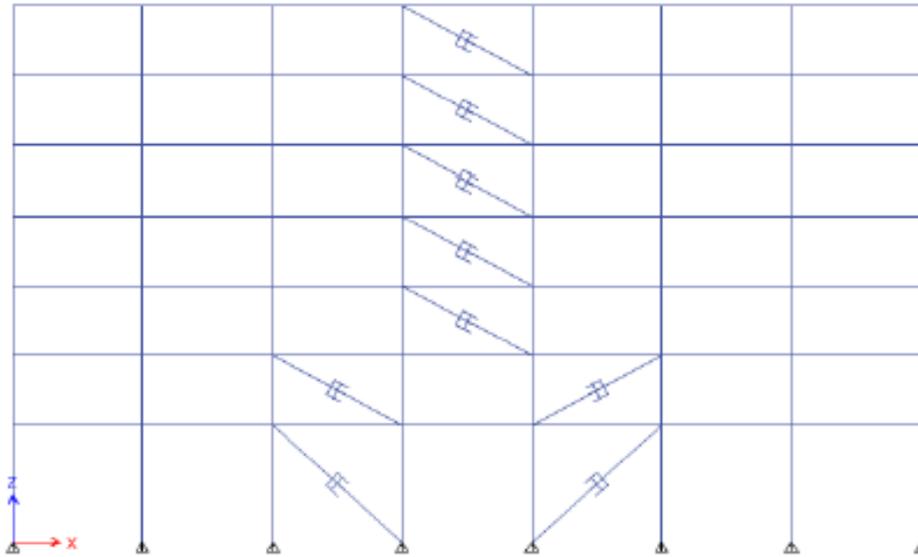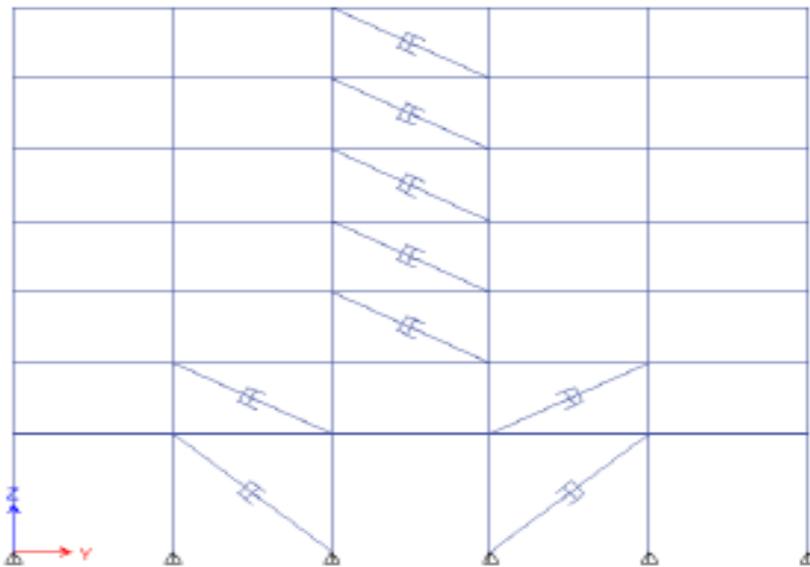

Figure 16.3-2 Floor Framing Plan with Damper Locations in Stories 1-2

Figure 16.3-3 Elevation of Gridlines 2 and 5 with Damper Locations

Figure 16.3-4 Elevation of Gridlines B and G with Damper Locations

 Nonlinear viscous dampers. Due to the advantages of using nonlinear FVD over linear FVD, as discussed in Section 16.3.2.5, it is decided to progress design with a nonlinear FVD with an exponent/alpha value of 0.4.

A procedure to size the nonlinear damper based on energy considerations is provided in Christopoulos and Filiatrault, 2006. The required damping constant of a nonlinear FVD, C_{NL}, to dissipate a similar amount of energy per cycle as a linear FVD, for damping exponent, α, values 0.2-1.0, can be obtained approximately by:

$$C_{NL} \approx C_L \frac{\sqrt{\pi}}{2} (\omega X_0)^{1-\alpha} \qquad\qquad (16.3\text{-}7)$$

where C_L in the linear FVD coefficient , ω is the circular frequency which can be taken as the fundamental frequency of the structure in the direction of interest and X_0 is the displacement in the dampers corresponding to the desired performance drift level.

Using the C_L of 50 kip-sec/inch and assuming a circular frequency of 2.1 rad/sec and displacement amplitude in the dampers of 2.5 inches, gives a nonlinear damping coefficient C_{NL} of 120kip-sec/inch using Equation 16.3-7.

A comparison of the force-velocity and force-displacement behavior of the linear and nonlinear dampers with damping coefficients of 50 kip-sec/inch and 120 kip-sec/inch, respectively, is shown in Figures 16.3-5 and 16.3-6. The peak velocity, based on a sinusoidal displacement, is 5.25 inch/sec. The peak force in the linear and nonlinear dampers is similar at the desired drift/velocity level. However the design of the damper components itself (conducted by the manufacturer) typically is for 1.5 times this peak velocity. As can be seen in the Figure 16.3-5, there is a larger increase in forces for linear dampers than nonlinear dampers at velocities in excess of the design velocity.
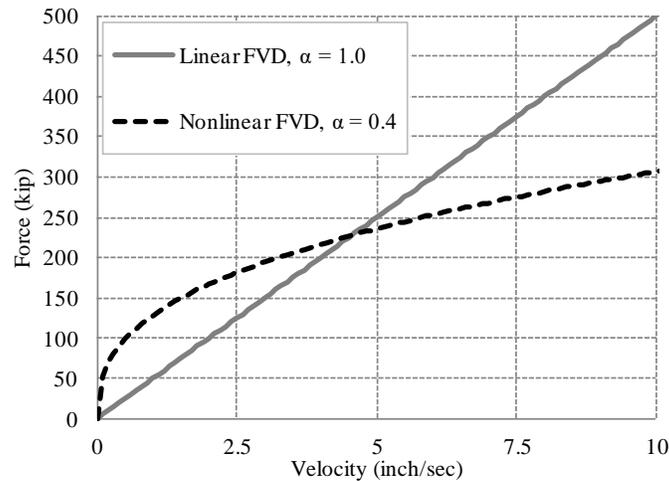
Figure 16.3-5: Force-Velocity Relationships for Linear and Nonlinear Fluid Viscous Dampers

Figure 16.3-6 gives the force-displacement relationships for linear and nonlinear FVD. For nonlinear dampers, there are larger forces induced near the maximum displacements. For linear dampers the force is zero at the maximum displacement and theoretically 90 degrees out of phase with the frame peak forces.
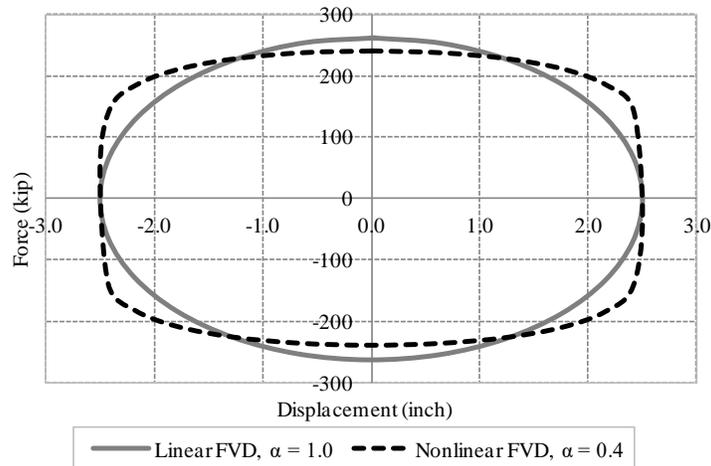
Figure 16.3-6: Force-Displacement Relationships for Linear and Nonlinear Fluid Viscous Dampers

16.4 STRUCTURAL ANALYSIS

16.4.1 Introduction

The *Standard* requires two parallel analyses be performed, one for the design level earthquake and one for the MCE$_R$. For each of these hazard levels, one analysis is conducted using the maximum design properties of the damping device and one using its minimum properties.

As discussed in Section 16.3.2.4, a NLRHA will be used in this example since it is commonly used by consulting engineers. It gives the most realistic prediction of the response and is not overly complex compared to elastic methods. Furthermore the *Standard* is formatted to imply that NLRHA is the preferred procedure. For example, *Standard §18.2.3* states that the damping system shall be analyzed using response history analysis and it is an exception to perform response spectrum or the equivalent lateral force procedure. The response history analysis procedure of *Standard §18.3* is permitted for all project types (i.e. all building types and seismic hazards)

16.4.2 Ground Motions Histories

The *Standard* incorporates new criteria for the determination of design spectral accelerations and of the selection and scaling procedures for the ground motions used in NLRHA. These procedures are explained in Chapter 3.4 of these NEHRP design examples.

Since the 1-second spectral acceleration, S_1, is greater than 0.2 and the soil type is a Site Class D, a site-specific hazard analysis is conducted in accordance *Standard §11.4.7* requirements. For convenience, it is assumed that the resulting design earthquake spectrum and MCE$_R$ response spectrum (the target spectra) are identical to the response spectra developed in accordance with *Standard §11.4.5* with spectral values as in Section 16.2.2.

The example building's site is more than 3 miles away from an active fault, and amplitude scaling is the chosen scaling method. In this case, the *Standard* requires that the earthquake records are scaled to match a target spectrum over the period range of interest, defined as $0.2T_{1D}$ determined using maximum properties to $1.25T_{1M}$ using minimum properties. The fundamental period of the building is not significantly affected by the insertion of the FVDs; therefore the maximum and minimum properties of the dampers and the hazard level do not affect the calculation of the period range. The period range of

interest is calculated as the product of 0.2 and the shorter period in the east-west direction (2.9 sec) and the product of 1.25 and the longer period in the north-south direction (3.1 sec), giving a scaling range of 0.58 to 3.9 seconds.

The selection and scaling of appropriate ground motions should be performed by a ground motion expert experienced with earthquake hazards of the region. Scaling should be carried out with consideration of site conditions, earthquake magnitudes, fault distances and source mechanisms that influence ground motion hazards at the building site. It is assumed that the ground motion expert recommends the suite of ground motions and scaling factors listed in Table 16.4-1 for the MCE$_R$ hazard.

Table 16.4-1 Selected and Scaled Ground Motions for MCE$_R$ Hazard at the Building Site[1]

GM No.	Year	Earthquake name	M	Source type	Recording station	Distance (km)	Scale factor
1	2003	Tokachi-oki, Japan	8.3	Subduction zone	HKD 094	67	3.30
2	2003	Tokachi-oki, Japan	8.3	Subduction zone	HKD 092	46	1.32
3	1968	Tokachi-oki, Japan	8.2	Subduction zone	Hachinohe (S-252)	71	1.82
4	1949	Western Washington	7.1	Deep intraplate	Olympia	75	3.25
5	1989	Loma Prieta	6.9	Shallow crustal	Saratoga -- Aloha Ave	9	1.82
6	1999	Duzce, Turkey	7.1	Shallow crustal	Duzce	7	1.21
7	1995	Kobe, Japan	6.9	Shallow crustal	Nishi-Akashi	7	1.93

3. Motions obtained from K-NET (http://www.kyoshin.bosai.go.jp/kyoshin/quake/index_en.html), PEER Ground Motion Database (http://ngawest2.berkeley.edu/) and with assistance from Doug Lindquist, GE of Hart Crowser, Seattle.

The scaling of ground motions for the design earthquake hazard level are taken as 0.65 times the scale factors in Table 16.4-1 for this example.

The response spectrum for each of the horizontal ground motion components is calculated and the combined square root sum of the square (SRSS) of the two components for each ground motion is shown in Figure 16.4-1. The average SRSS spectrum of the seven ground motions must be above the corresponding spectral acceleration ordinate of the target MCE$_R$ spectrum over the period range of 0.58 to 3.9 seconds. As shown in Figure 16.4- 1, using the scale factors in Table 16.4-1, the scaling of the ground motions meets this requirement of the *Standard*.
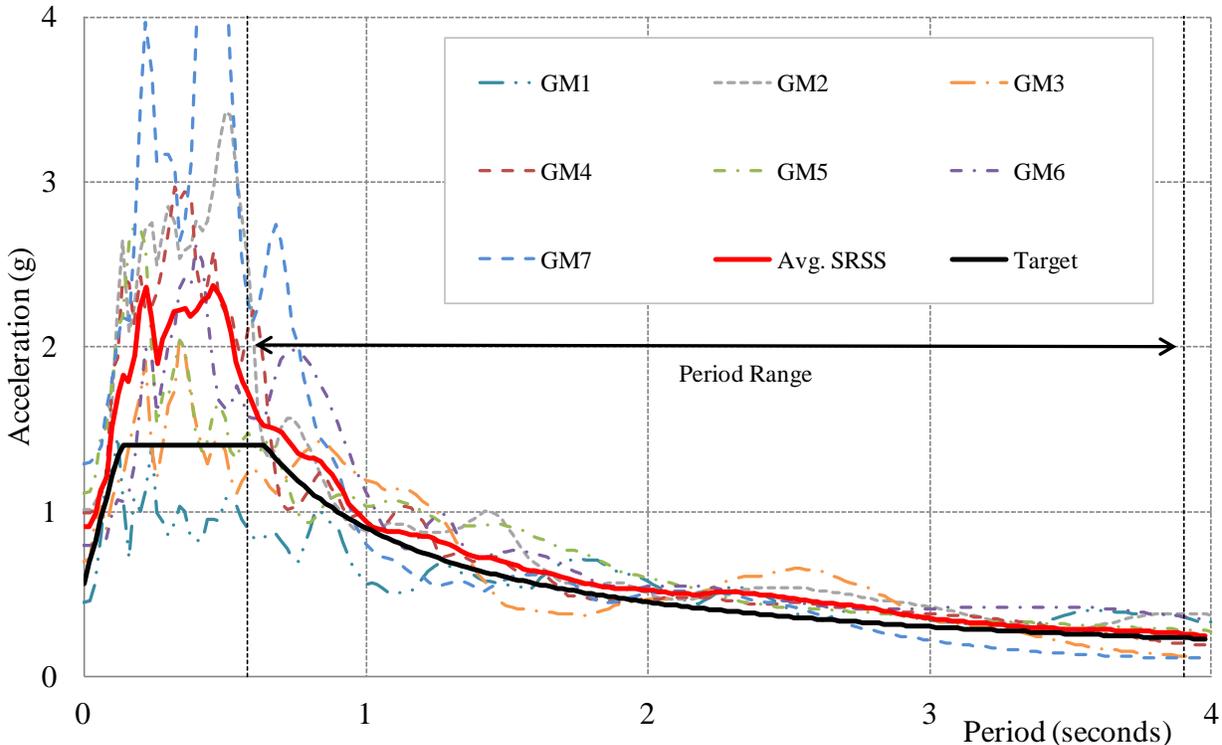
Figure 16.4-1 SRSS Response Spectra of Ground Motions and Comparison of Average to Target MCE$_R$ Spectrum

16.4.3 Maximum and Minimum Damping Device Properties

Overview. The nominal properties of damping devices can vary over their design life due to aging and environmental effects, can vary during seismic excitation due to speed of motion, first cycle and heating effects, and can vary between individual devices due to manufacturing tolerances.

There are no standards which govern how a damping device must be produced and assembled. These details vary by manufacturer and are usually proprietary. Furthermore, in the United States there is no official certification required of manufactures before they start supplying dampers for construction. Consequently, there can be a considerable difference in the performance of damping devices, even for identical types of devices produced by different manufactures.

Given the large variety of damping device types as well as the uncertainty in the quality of different manufacturers, the *Standard* has taken the approach of requiring the registered design professional (RDP) to determine (in consultation with the manufacturer) the nominal design properties and to account for the likely variation in those properties on a project- and product-specific basis. The variation in properties is accounted for by using property modification or λ (lambda) factors, which modify the nominal properties to an appropriate upper- or lower-bound. Maximum and minimum λ factors are determined according to the new *§18.2.4.5* provisions.

The concept of property modification factors is used to account for changes in nominal properties which are not explicitly accounted for in the mathematical analysis model of the damping devices. The approach is to assess the impact of a particular effect on the damper properties (e.g. heating, aging, ambient temperature, etc), and if the effect is appreciable then assigning it a λ-factor and accounting for the effect in analysis and design. Therefore the λ-factors encompass many different effects and describe the deviation

in properties from unity. For example, if an effect causes a 10% increase in a nominal property than it is assigned a λ value of 1.10 and contributes to the overall λ_{max} factor. The λ-factors are determined through testing, rational analysis and engineering judgment and are categorized in the *Standard* into three groups:

- $\lambda_{ae,max}$ and $\lambda_{ae,min}$ which account for aging and environmental effects.
- $\lambda_{test,max}$ and $\lambda_{test,min}$ which account for variations observed during prototype testing.
- $\lambda_{spec,max}$ and $\lambda_{spec,min}$ which account for manufacturing variations.

The *Standard* then combines the λ-factors using *Equations 18.2-3a* and *18.2-3b* as follows:

$$\lambda_{max} = (1 + f_a(\lambda_{ae,max} - 1)) \times \lambda_{test,max} \times \lambda_{spec,max} \geq 1.2$$

$$\lambda_{min} = (1 - f_a(1 - \lambda_{ae,min})) \times \lambda_{test,min} \times \lambda_{spec,min} \leq 0.85$$

The *Standard* specifies a system property adjustment factor f_a of 0.75 based on the assumption that the device will not have full aging and environmental effects occurring simultaneously at the time of the design earthquake. The λ_{max} and λ_{min} factors are applied to each nominal mechanical property of interest and therefore set the maximum and minimum damper properties, respectively.

Nominal properties and λ-factors. The nominal properties are typically determined based on advice from the manufacturer, which can be confirmed later by prototype and/or production testing. For the nonlinear FVD, the parameters of interest are the damping coefficient, C_{NL}, and the nonlinear exponent α. Instead of optimizing for different values of C_{NL} and α it may be more cost effective, and with less uncertainty, to directly adopt a device which the manufacturer has already produced and tested. It so happens that the manufacturer has previous prototype test data for a nonlinear FVD with a C_{NL}=128 kip-sec/inch and α=0.38, which is similar to that calculated from preliminary design.

Results from previous prototype testing are shown in Figure 16.4-2. The solid line in Figure 16.4-2 depicts the nominal force-velocity relationship of the nonlinear damper with the dotted lines representing a ±10% and ±20% change in the damping constant value C_{NL}. The data from prototype tests for each cycle (maximum in each direction) are shown as data points.
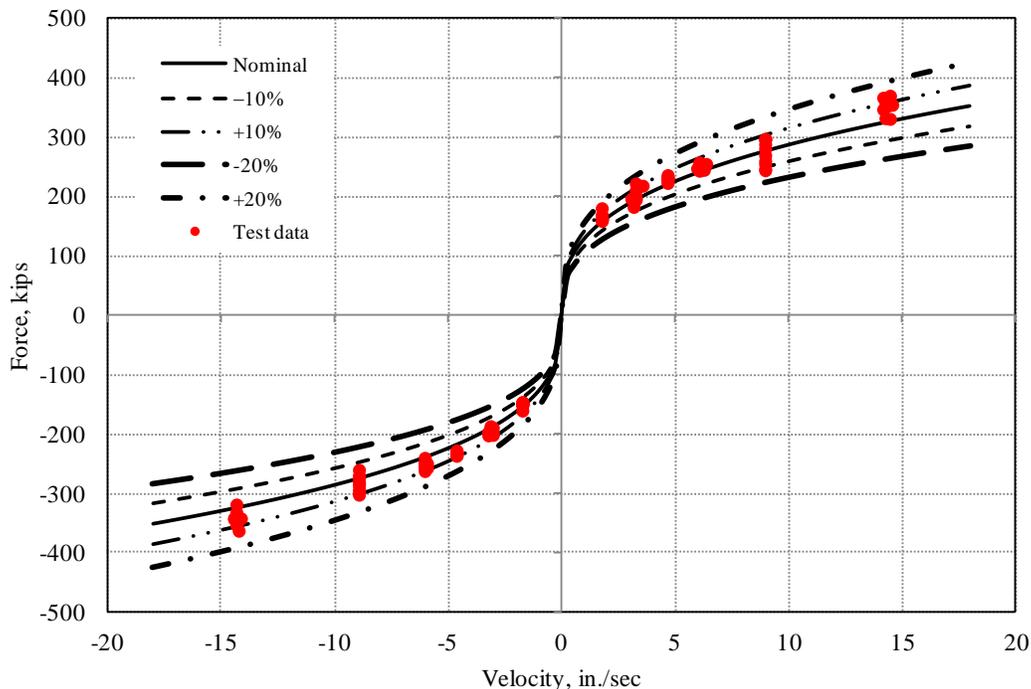
Figure 16.4-2 Force-Velocity Test Data of a Nonlinear Viscous Damper

The previous prototype testing of the dampers were conducted under the following conditions:
- Force-velocity characteristic tests, all conducted at ambient temperature of 70° F. 10 full cycles performed at various amplitudes.
- Temperature tests, three fully reversible cycles conducted at various velocities at the following temperatures 40, 70 and 100° F

This test data are assumed to be consistent with the sequence and cycles of *Standard §18.6.1*. The previously tested device meets the similarity requirements of *Standard §18.6.1.3* since the device is identical to that being proposed for analysis and design and since the strokes and forces are similar to those required for design.

The determination of the three categories of λ-factors should be developed in conjunction with the device manufacturer based on their history of production damper test data and experience with aging and other environmental effects. For this example:
- There are no aging effects to consider for this type of device. Although the previous prototype testing was performed at various ambient temperatures, the FVDs in this example are assumed to be in an enclosed and conditioned environment such that there are small variations in ambient temperature. Hence the aging and environmental factors are taken as unity ($\lambda_{ae,max} = 1.0$, $\lambda_{ae,min} = 1.0$)
- The test data points, which include heating effects, are essentially bounded by the $\pm 10\%$ change in the damping coefficient. This small range is due to the device being specifically designed to alleviate heating effects. This is achieved by using accumulators or by utilizing materials with thermal expansion properties such that the dampers properties are automatically adjusted. Hence the test lambda factors are taken as $\lambda_{test,max} = 1.1$, $\lambda_{test,min} = 0.9$.
- The FVD are highly engineered and precision made, such that there is typically little variation due to manufacturing tolerance. Hence specification lambda factors are taken as $\pm 5\%$ ($\lambda_{spec,max} = 1.05$, $\lambda_{spec,min} = 0.95$).

Using these values in *Standard Equations 18.2-3a* and *18.2-3b* results in:
- $\lambda_{max} = 1.15$
- $\lambda_{min} = 0.85$

These values are allowed to be less than the maximum and minimum limits of *Standard §18.2.4.5* since they are based on similar prototype test data. These maximum and minimum λ factors are applied to the damping coefficient only. There is no independent variation considered for the nonlinear exponent α, since varying the damping coefficient in effect also captures the variation (if any) of the α value.

The analysis with maximum damper properties will typically produce larger damper forces for use in the design of members and connections, whereas the analysis with minimum damper properties will typically produce less total energy dissipation and hence larger building drifts.

### 16.4.4 Nonlinear Response History Analysis

Modeling. A three-dimensional mathematical model of the building is created in ETABS (CSI 2013) to assess the effectiveness of the added damping system and to determine design actions. Structural elements part of the damping systems load path and the SFRS are included in the analysis model so that the deformations that occur in these members are accounted for. For example the in-plane stiffness of the diaphragm and stiffness of elements connected to the dampers (i.e. braces) is explicitly modeled. Failure to account for such deformations along with the load path between all dampers and the main structural system can reduce the effectiveness of the damping system to the point that the damping system simply rides along with the seismic movements and provides virtually no response reduction in an actual earthquake (see Charney and McNamara 2008).

In this example, the in-plane stiffness of the 3.25inch thick concrete diaphragm is modeled and the damper-brace assembly which is installed diagonally across a bay is estimated to have an axial stiffness of 2000 kip/inch. The mathematical model of the building does not specifically include the penthouse roof level as there are no dampers installed at this level and because the weight is only a small fraction of the weight of all other floors. Hence for simplicity the weight of the penthouse roof level is added to the roof level weight. The three-dimensional ETABS mathematical model of the building is shown in Figure 16.4-3.

The perimeter moment frames (see Figure 16.2-1), which provide the primary lateral-force resistance, are modeled with moment resisting connections. The gravity framing, which is all the other beams and columns including those where the FVD are located, are also included in the model. The beams in the gravity framing are modeled with end moment releases (pinned connections) whereas the columns are only pinned at their base. This is considered realistic as the gravity framing beams have end connections which provide limited moment resistance under seismic induced displacements whereas the columns are continuous with moment resisting splice connections.

The performance objective for this example is that the SFRS structural elements remain "essentially" elastic during the MCE$_R$ event. Essentially elastic is defined in the *Standard* as an elastic/linear force that does not exceed 1.5 times the expected strength of the element with a strength reduction factor of ϕ=1.0. This has been increased from previous versions of the *Standard* which used the nominal (lower bound) strength. On the other hand the damping system, which includes the damping devices and all other components required to connect the dampers to the structure, must remain elastic (i.e. linear force does not exceed 1.0 times the nominal strength of the structure with ϕ=1.0) for MCE$_R$ loads per *Standard §18.2.1.2*. If the linear-elastic demands in the beams and columns of the SFRS exceed the essentially elastic definition above then the engineer is faced with two options: a) increase the size of the structural element such that it remains essentially elastic or b) accept damage in the SFRS and explicitly model the nonlinear force-displacement behavior of the yielding elements. The former option of increasing the member sizes has been selected as an option for this example since a higher performance level is desired and it avoids nonlinear response modeling of the structural elements. Hence the only nonlinear behavior occurring in the ETBAS model is in the nonlinear dampers.

The nonlinear FVD are velocity-dependent devices and can be modeled in ETABS as a link element. The damping coefficient, exponent alpha and stiffness of the damper-brace assembly are the required parameters for this link element. The change in properties with temperature is accounted for indirectly by conducting bounding analyses. That is, the maximum and minimum damping properties, as determined in Section 16.4.3, bound the change in properties due to heating effects. This modeling is in compliance with *Standard §18.3.1.*
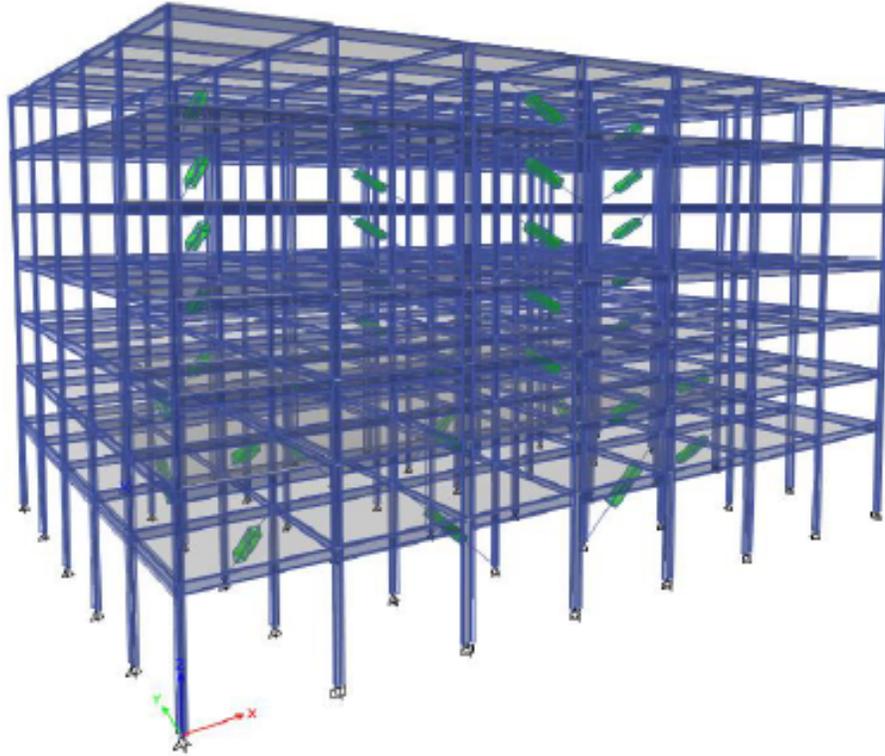
Figure 16.4-3 Three-Dimensional Extruded View of ETABS Model

Inherent damping of the structure is specified as constant damping of 3 percent of critical for all modes of vibration. A higher level of damping is only allowed by the *Standard §18.3* if test data consistent with levels of deformation just below yield is available.

Since the building site is greater than 3 miles away from an active fault the ground motions need not be rotated and applied in the fault-normal and fault-parallel orientations. Instead, the two horizontal components of each ground motion were applied randomly to the building model. Some engineers and jurisdictions may require multiple orientations of the ground motion be considered. It is the experience of the authors that this further analysis has diminishing returns, and it has little effect on the final design specifications (since the design is typically not optimized for certain directions). Furthermore, new language in *Standard §18.3* states that the ground motion components need not be applied in multiple orientations.

 Analysis results. A NLRHA is conducted using the software ETABS with two models: one using the maximum damper properties and one using the minimum damper properties. The analysis is conducted at both the MCE_R and design earthquake hazard levels. The maximum value of story drift, damper force and damper displacement/stroke is calculated for each ground motion. The average of the maximum values from the seven ground motions is permitted to be used for design (*Standard §18.3.3)* and these values are summarized for each principal direction in the tables below. Table 16.4-2 is for the analysis model that uses the maximum dampers properties and Table 16.4-3 is for the minimum damper properties.

The building is symmetrical in both directions with no actual eccentricities (i.e. the center of mass and center of stiffness coincide at every story) and therefore the damper forces on each story are the same on Gridlines B and G, and 2 and 5, respectively. The same principle is true for the SFRS demands on Gridlines 1 and 6, and A and H, respectively. In the lower stories, where there are two dampers on the

same gridline, each damper has the same demand therefore only the demands for one damper is reported in Tables 16.4-2 and 16.4-3. These values do not include an increase due to accidental eccentricity. This is later incorporated in design using amplification factors per Section 16.4.4.3.

Table 16.4-2 MCE$_R$ NLRHA Average Story Drift, Damper Force and Stroke for Maximum Damper Properties, Load Case 0.62D + Q$_E$ (similar for 1.48D + 0.5L + Q$_E$)

Story	Story Drift (%)		Peak Damper Force (kip)		Peak Damper Stroke (inch)	
	UX East	UY North	FX East	FY North	DX East	DY North
7	0.6%	0.6%	227	222	0.6	0.7
6	1.0%	1.1%	288	268	1.2	1.3
5	1.4%	1.6%	321	302	1.7	2.0
4	1.7%	1.8%	329	319	2.1	2.3
3	1.6%	1.6%	321	307	2.1	2.1
2	1.1%	1.1%	295	272	1.5	1.5
1	1.1%	1.0%	375	329	2.1	2.0
Envelope	**1.7%**	**1.8%**	**375**	**329**	**2.1**	**2.3**

Table 16.4-3 MCE$_R$ NLRHA Average Story Drift, Damper Force and Stroke for Minimum Damper Properties, Load Case 0.62D + Q$_E$ (similar for 1.48D + 0.5L + Q$_E$)

Story	Story Drift (%)		Peak Damper Force (kip)		Peak Damper Stroke (inch)	
	UX East	UY North	FX East	FY North	DX East	DY North
7	0.8%	0.8%	204	195	1.0	1.0
6	1.2%	1.3%	226	218	1.6	1.7
5	1.7%	1.8%	251	238	2.1	2.4
4	1.9%	2.0%	255	246	2.5	2.7
3	1.9%	1.9%	248	236	2.5	2.5
2	1.2%	1.2%	230	211	1.8	1.8
1	1.2%	1.2%	286	257	2.4	2.3
Envelope	**1.9%**	**2.0%**	**286**	**257**	**2.5**	**2.7**

The maximum velocity for each damper can be determined from the maximum force through the relationship of Equation 16.3-1. For example, the damper force of 375 kips for the maximum damper properties correspond to a peak velocity of:

$$v = {}_{0.38}\sqrt{\frac{F}{\lambda C_{NL}}} = {}_{0.38}\sqrt{\frac{375}{1.15 \times 128}} = 11.7 \text{ inch/sec}$$

Similarly the maximum velocity from the minimum damper properties from a damper force of 286 kips corresponds to a peak velocity of 12.7 inch/sec. So the maximum velocity is from the minimum dampers properties but the maximum force is from the maximum dampers properties.

The base shear for the SFRS to remain essentially elastic is shown in Table 16.4-4. These values are the average of the maximum values from the seven ground motions for each principal direction. Again, these values do not include the effects due to torsion.

**Table 16.4-4 NLRHA Average Base Shear for SFRS**

Analysis	Base Shear, V (kip)			
	FX East (kip)	V/W	FY North	V/W
Design Earthquake Level				
Maximum Properties	856	0.07	837	0.06
Minimum Properties	1007	0.08	961	0.07
MCE$_R$ Level				
Maximum Properties	1522	0.12	1458	0.11
Minimum Properties	1769	0.13	1659	0.13

These analysis results show that:
- Maximum story drifts, damper stroke and peak velocity, and base shear of the SFRS are experienced with minimum damper properties.
- Maximum damper force is experienced with maximum damper properties.

The critical design actions, whether from the maximum or minimum damper properties will be used for design. Since there is only one type of damper in the building, the critical demands at any story and any gridline will be used to design the damper.

Figure 16.4-4 illustrates of the force-displacement behavior of a nonlinear damper located on the first story on gridline 2, in the bay between gridlines C and D. The response is shown arbitrarily for only one ground motion: record 5 Loma Prieta. The figure shows a comparison of the response for analyses conducted using the maximum damper properties (C_{NL}=147.2kip-sec/inch) and the minimum damper properties (C_{NL}=108.8kip-sec/inch). The maximum force occurs at the peak velocity, and gives a force of 391 kip for ground motion 5 using maximum properties. This peak velocity does not occur at zero displacement, as one would expect for a linear damper, but at around 1.2 inches stroke. The area within the loops represents the energy dissipated by the dampers and large/fat loops indicate that the dampers are working efficiently to dissipate seismic energy.
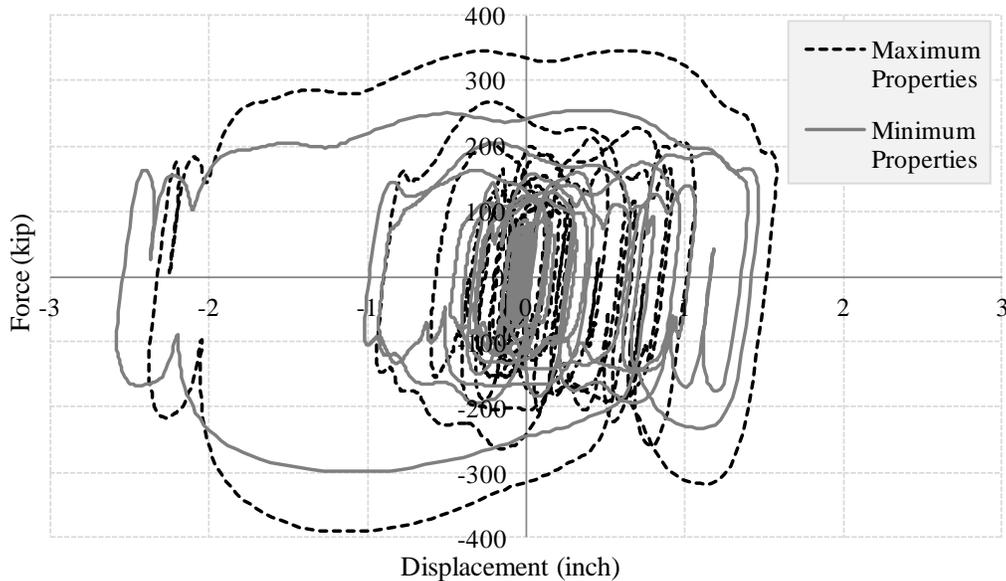
Figure 16.4-4 Force-Displacement Behavior for Maximum and Minimum Analyses, GM5 Record for Damper on 1ˢᵗ Story in East-West Direction.

Since the purpose of adding supplemental damping is to dissipate energy, it is natural to consider the migration of energy quantities in a structure during the earthquake. Christopoulos and Filiatrault 2006 present a "rain-flow" analogy to help understand this flow of energies. Briefly, the earthquake gives energy to the structure, termed the input energy E_{Input}, where its magnitude depends on the characteristics of the structure and the ground motion. This energy excites the building which oscillates back and forth as energy is transferred from maximum strain (or potential) energy, when it is at maximum displacement, to maximum kinetic energy when the building is near its equilibrium position with maximum velocity. For an elastically responding building this fluctuation from maximum strain energy to maximum kinetic energy decays (is dissipated) due to inherent damping ($E_{inherent}$) and, if they are incorporated, also due to supplemental damping systems (E_{damper}). If the strain energy is large enough then energy will also be dissipated by hysteretic behavior ($E_{hysteretic}$) which comes in the form of plastic hinging and damage to the structure. Therefore for energy equilibrium, the follow relationship shall hold:

$$E_{Input} = E_{inherent} + E_{damper} + E_{hysteretic} \qquad (16.4-1)$$

The energy balance for this example is illustrated in Figure 16.4-6 for ground motion 5 using the maximum damper properties. The inherent damping $E_{inherent}$ is modeled using modal damping specified as 3 percent for all modes and makes up only a small proportion of the overall energy dissipated. There is no significant yielding of the SFRS (and it is not modeled anyway) therefore $E_{hysteretic}$ is zero. A majority of the input energy is dissipated by the nonlinear viscous dampers (E_{damper}), which shows good effectiveness. It is noted that energy plots such as Figure 16.4-6 are particularly useful for retrofits to see the reduction in hysteretic energy, and hence damage to the existing structure, and how this energy is transferred to the supplemental damping systems.
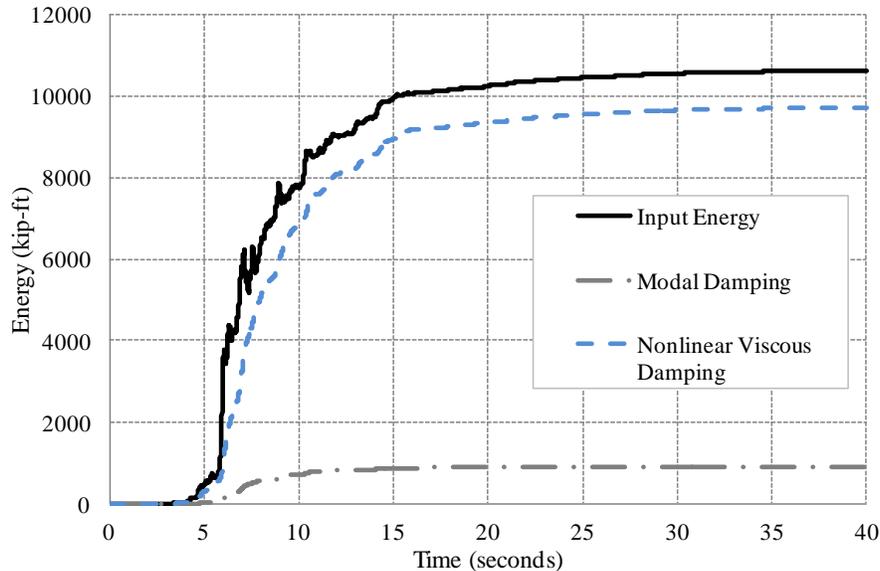
Figure 16.4-5 Energy Equilibrium for Ground Motion 5

Accidental mass eccentricity. The *Standard* has incorporated new provisions which permit the use of amplification factors to account for accidental mass eccentricity. The rationale behind this is to avoid doing (unnecessarily) large amounts of analysis to calculate the worst case of accidental eccentricity.

The requirement to account for accidental mass eccentricity, *Standard §18.3.2*, is intend to increase the design actions. It accounts for effects such as: a) plan distributions of mass being different from that assumed in design, b) non-uniform properties of the SFRS (i.e. strength, stiffness) and/or damping devices, and c) rotational and torsional ground motions.

Artificially altering the center of mass in the mathematical model may lead to the paradox of a reduced response (Basu et al. 2014), which is not the intent of the provision. In this example amplification factors are conservatively developed to account for accidental eccentricity. The procedure explained in this section aligns with that recommended in the commentary of the *Standard*.

Three NLRHA cases will be used to establish the amplification factors. All cases use the minimum dampers properties and include inherent eccentricities (none for the example building). When there are inherent eccentricities, the accidental eccentricities should be applied in the most critical direction such that it adds to this inherent eccentricity. The three cases are:
- Case I: No accidental eccentricity (Baseline case)
- Case II: 5% accidental eccentricity in the X-direction
- Case III: 5% accidental eccentricity in the Y-direction

To simulate the 5% accidental eccentricity in the X (east-west) or Y (north-south) directions, the applied mass on the floor plate at every level is augmented such that the center of mass is offset from the center of rigidity by 8.75ft in the X direction, or 6.25ft in the Y-direction. The mass source in the ETABS model is from specified load patterns (instead of the self-weight calculation), therefore the accidental eccentricity is achieved by artificially altering the floor plate uniformly distributed pressure such that it gives the desired eccentricity.

A NLRHA is conducted for each of the three models/cases and the results from Cases II and III are compared to Case I. The following amplification factors (ratio of Case II or III response to Case I response) are computed.

- **Drift amplification factor**: The amplification for story drift in the structure at the plan location with the highest drift, enveloped over all stories;
- **Force amplification factor**: The amplification for frame-line base shear forces at each story for the frame subjected to the maximum drift.

For this example, Case II gives greater drift and force amplification factors than Case III. The ratio of the Case II results divided by the baseline Case I results (see Table 16.4-2) are provided in Table 16.4-3. The ratios of base shear for the east-west and north-south directions, for Case II divide by Case I is, 1.01 and 1.08, respectively.

Table 16.4-3 NLRHA Average Results- Ratio of Case II to Case I

Story	Story Drift (%)			Peak Damper Force (kip)		Peak Damper Stroke (inch)	
	UX East	UY North	SRSS	FX East	FY North	DX East	DY North
7	0.99	1.14	1.04	1.00	1.03	1.01	1.10
6	0.99	1.11	1.04	1.01	1.03	1.01	1.08
5	0.99	1.09	1.04	1.00	1.03	1.01	1.06
4	0.99	1.09	1.03	1.00	1.02	1.01	1.06
3	0.99	1.08	1.03	1.00	1.02	1.00	1.05
2	0.99	1.08	1.03	1.00	1.02	1.00	1.05
1	0.98	1.07	1.03	1.00	1.02	1.01	1.05
Envelope	**0.99**	**1.14**	**1.04**	**1.01**	**1.03**	**1.01**	**1.10**

Therefore the amplification factors are chosen to be:

- **Drift amplification factor** = 1.14
- **Force amplification factor** = 1.08

The effects of accidental eccentricity are considered as follows. The NLRHA procedure is run for the inherent mass eccentricity case only, considering both maximum and minimum damper properties (see Section16.4.4.3). All resulting deformation response quantities (i.e. story drifts and damper stroke) should be increased by the deformation amplifier of 1.14 and all resulting force quantities (i.e. base shear and damper force) should be increased by the force amplifier of 1.08 before being used for design.

16.5 DESIGN OF LATERAL AND DAMPING STRUCTURAL SYSTEMS

16.5.1 Seismic Force Resisting System

 Configuration and detailing. Structures that have damping system must have an independent SFRS in each lateral direction which provides a complete lateral load path and conforms with a type listed in Table 12.2-1 of the *Standard*. Steel special moment resisting frames (SMRF) are located on the perimeter of the example building to meet this requirement. The SMRF is designed and detailed as if the damping system was disconnected and this process is illustrated in Chapter 9 of these design examples. This is the first step in design as the *Standard* does not have any relaxation on the height, seismic design category, redundancy limitations or detailing requirements (i.e. RBS connections, strong-beam weak-column) for a SFRS in a structure with damping devices.

The benefit of the damping system may be taken into account when assessing the minimum base shear and drift requirements.

Minimum base shear. The minimum base shear V_{min} used for design depends on the number of FVD at each floor level and if any horizontal or vertical irregularities exist. V_{min} is calculated using the design earthquake which is two-thirds of the MCE$_R$.

The building has no vertical irregularities despite the relatively tall height of the first story. The exception of *Standard §12.3.2.2* is taken, in which the drift ratio of adjacent stories are compared rather than the stiffness of the stories. In the three-dimensional analysis, the first story drift ratio is less than 130 percent of that for the story above. Because the building is symmetrical in plan, plan irregularities would not be expected. This assessment of irregularities is conducted on a building model that excludes the FVD's and the inclusion of these damping devices does not exacerbate any irregularity.

At least two FVD's are located at each floor level, in each principal direction and are configured to resist torsion. Using Equations 18.2-1 and 18.2-2 and 20% added damping plus 3% inherent damping, the minimum base shear is:

$$V_{min} = \max\left\{ V/1.59, 0.75V \right\} = 0.75V$$

where V is the seismic base shear in the direction of interest determined in *Standard §12.8* using the following steps:
Determine the building period (T) per *Standard* Equation 12.8-7:

$$T_a = C_t h_n^x = 0.028 \times 102.3^{0.8} = 1.14 \sec$$

where h_n is the height to the main roof taken as 102.3 feet. $C_u T_a$, the upper limit on the building period, is determined per *Standard* Table 12.8-1:

$$T = C_u T_a = 1.4 \times 1.14 = 1.6 \sec$$

The calculated period from the mathematical building model exceeds $C_u T_a$ therefore the period used to calculate C_S is limited to this maximum value. The seismic response coefficient C_s is 0.047 from *Standard* Equation 12.8-2 using:

$$C_s = \min\left(\frac{S_{DS}}{R/I_e}, \frac{S_{D1}}{T(R/I_e)} \right) = \left(\frac{0.93}{8/1}, \frac{0.6}{1.6(8/1)} \right) = 0.047$$

this satisfies the minimum value for Cs per Standard Equation 12.8-1.
Therefore the seismic base shear is computed per *Standard* Equation 12.8-1 as:

$$V = C_s W = 0.047 \times 13151 = 618 \, kip$$

where W is the seismic weight of the building as determined in Section 16.2.2.3. The minimum base shear that may be used for the design of the SFRS in the example building is therefore:

$$V_{min} = 0.75V = 0.75 \times 618 = 464 \, kip$$

 Strength design of SFRS. There are three design checks to ensure that the SFRS is of adequate strength. Foremost the factored nominal capacity of the SMRF shall satisfy:

- The minimum base shear of 464 kip, as given by *Standard §18.2.1.1*
- The demands from the design earthquake NLRHA.

Furthermore if the mathematical model assumes that the SFRS behavior is essentially elastic, then the demands from the NLRHA shall be no more than 1.5 times the expected capacity of the frame.

To check the minimum base shear requirement a modal response spectrum analysis is conducted on a mathematical model of the building which excludes the FVDs, in accordance with *Standard §12.9*. In many cases for SMRFs, analysis will show a much longer period than that determined by approximate methods (*Standard* Equation 12.8-7) and as a result a substantial reduction in base shear forces. For the example building the modal response spectrum analysis calculates a reduced base shear of:

$$V_{\text{modal,reduced}} = \frac{V_{\text{modal,elastic}}}{(R/I_e)} = 297\ kip$$

in the north-south direction and 315 kip in the east-west direction. Therefore the modal base shear and all corresponding element forces are scaled up by a factor of 464/297 = 1.56 in the north-south direction and 464/315 = 1.47 in the east-west direction.

The sizing and detailing of beams and columns is illustrated in Chapter 9 of these design examples and were directly adopted as a starting point for this example. The primary factors affecting SMRF member size selection are the need to control drifts below permissible levels, the need to avoid P-delta instabilities, and the need to proportion the frame to comply with the strong-column/weak-beam criteria of AISC 341 (Hamburger et al. 2009). Consequently from a strength standpoint, the sizing of the RBS typically governs the sizing of other members in the SFRS, since the frame is capacity-designed so that inelastic action occurs primarily in the beam's Reduced Beam Section (RBS). The flexural demand over capacity (D/C) ratios at the center of the beam's RBS on Gridline 1 (or 6) is shown in Figure 16.5-1. The D/C ratio in Figure 16.5-1 is calculated using the following definitions:

- **Reduced Elastic Demand:** Load combinations per Section 16.2.3.4, design earthquake response spectrum, elastic earthquake forces multiplied by $I_e/R = 0.125$ and scaled up to the minimum base shear (i.e. $0.75V/V_{\text{modal,reduced}}$). Accidental eccentricity need not be included.
- **Factored Nominal Capacity:** Located at the RBS center, nominal yield strength with strength reduction factor, ϕ, of 0.9. The selected RBS dimensions per AISC 358 are $a=0.625b_{bf}$, $b=0.75d$ and $c = 0.18b_{bf}$. The W21x73 beam between Gridlines D and E at Story 3 has a factored nominal capacity of:

$$\phi M_n = \phi F_y Z_{RBS} = \phi F_y (Z_x - 2ct_{bf}(d - t_{bf})) = 0.9 \times 50 \times (172 - 2 \times (0.18 \times 8.3) \times 0.74 \times (21.2 - 0.74))$$

$$\phi M_n = 475\ \text{kip-ft}$$
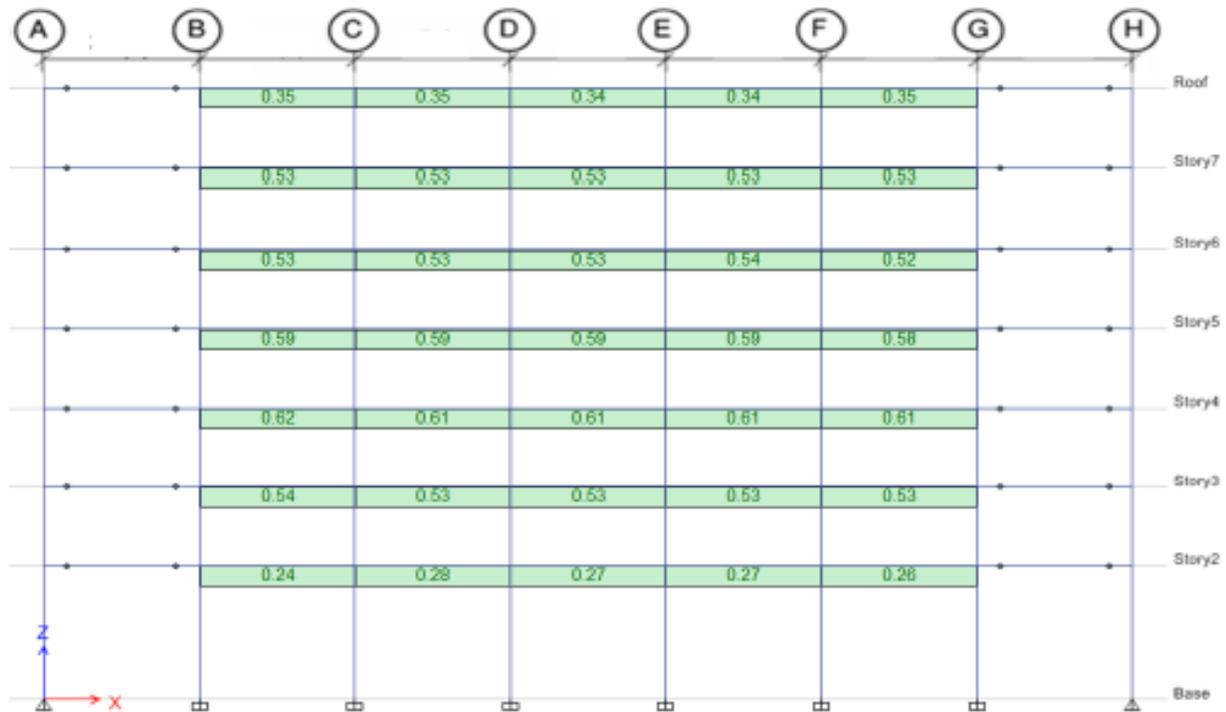
Figure 16.5-1 Modal Response Spectrum Reduced Demands divided by Factored Nominal Capacity Ratios for Gridline 1 SMRF, No Dampers

Figure 16.5-1 shows that the sizing of the frame is of adequate strength to meet the minimum base shear requirement of the *Standard* as no D/C ratio is greater than 1.0. Even for the conventional design of the SMRF (i.e. per Chapter 9) the minimum base shear using modal response spectrum is allowed to be taken as 0.85V . This along with an increase in forces to account for accidental eccentricity would give D/C ratios for the frame of about 15-20% larger than that in Figure 16.5-1. This is still well below a D/C close to 1.0, which one may seek to optimize design. The reason for this is that the sizing of beams, and hence columns (due to strong-column, weak-beam requirements), are typically controlled by considerations for drift (Hamburg et al. 2009).

The strength of the SFRS must also satisfy the demands from the design earthquake NLRHA where the damping devices are included in the analysis model. The critical demands are taken from either the analysis model using the maximum FVD properties or the model using minimum properties. Here the minimum FVD properties give the larger forces on the SFRS. The flexural D/C ratios at the center of the RBS from the NLRHA are shown in Figure 16.5-2. The capacity is taken as the factored nominal capacity as defined above, however the demands from the NLRHA are calculated differently as follows:

- **Unreduced Elastic Demand:** Load combinations per Section 16.2.3.4, where the average from the seven ground motions is used as explained in Section 16.2.3.3. The demands are elastic, unreduced forces on the frame as the only nonlinear element in the model is the FVDs.

Although Figure 16.5-2 shows that the D/C exceeds 1.0, this is acceptable. SMRF are highly ductile systems and have an allowable R-factor of 8; although the *Standard* implies that high levels of ductility would require explicit nonlinear modeling. In this case the SMRF is close to performing purely elastically, with limited damage at the design earthquake and has a much better performance than that shown in Figure 16.5-1. To better compare Figure 16.5-1, the modal response spectrum analysis with no dampers, to Figure 16.5-2, the design earthquake NLRHA with dampers included, the D/C ratios in Figure 16.5-1 should be treated as unreduced forces. The story 3, D-E beam, for example, has elastic

demands which exceed the factored nominal capacity by a factor of $0.53 \times (8/1) = 4.24$ (or 2.88 if not scaled to minimum base shear) in Figure 16.5-1 versus a factor of 0.94 in Figure 16.5-2.
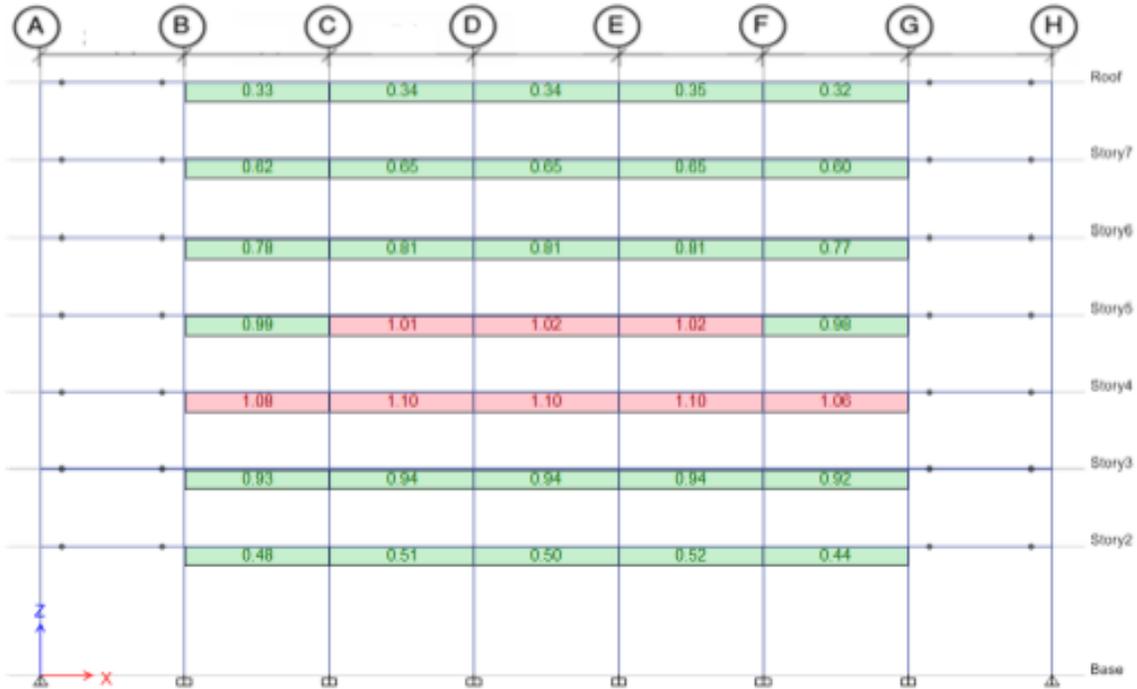

Figure 16.5-2 Design Earthquake NLRHA Unreduced Demand divided by Factored Nominal Capacity Ratios for Gridline 1 SMRF, Dampers Included
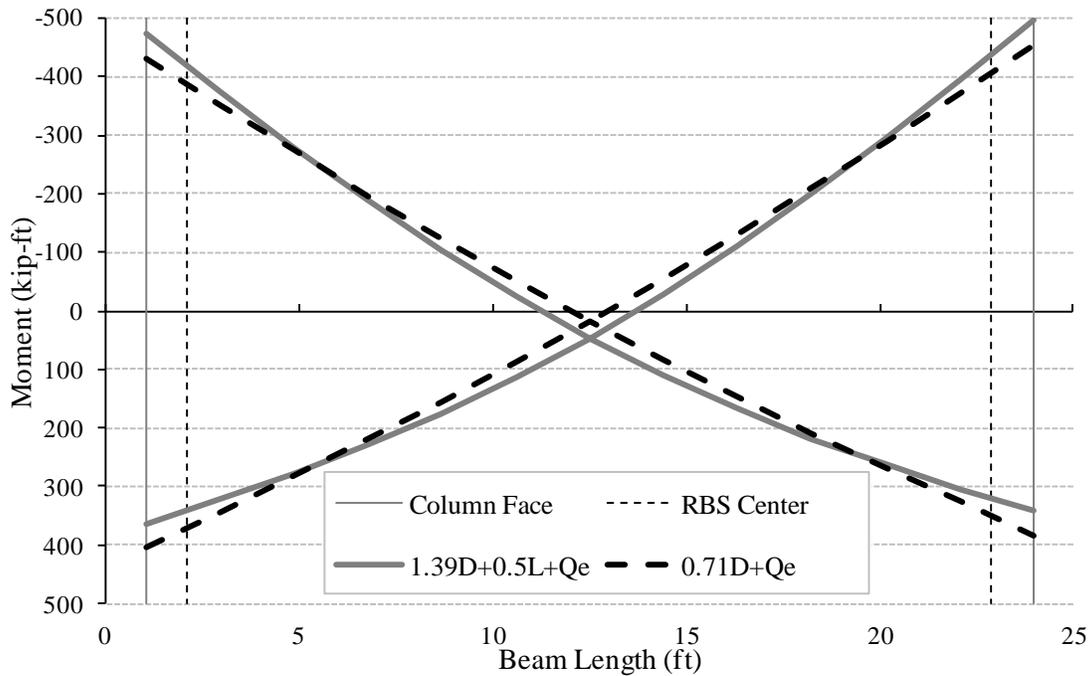

Figure 16.5-3 Design Earthquake NLRHA Moment Demands Envelope, Average of Seven Ground Motions, Beam D-E, Story 3, Gridline 1

The processing of NLRHA results in explained in Section 16.2.3.3 and is further illustrated in Figure 16.5-3 which shows the design earthquake NLRHA average flexural demands on beam D-E at story 3. The maximum flexure in the RBS occurs in negative bending for load combination $1.39D+0.5L+Q_E$ at the right end of the beam. The demand is about -445 kip-ft which gives the 0.94 D/C ratio in Figure 16.5-2.

The mathematical model of the building does not include any nonlinear behavior of the RBS. The SMRF is modeled as linear-elastic with only the nonlinear behavior of the FVDs being modeled. *Standard §18.3* requires that all members and connections undergoing inelastic behavior be directly accounted for in the mathematical model. An exception to this is if the members perform "essentially" elastic, defined as follows:

- **"Essentially" Elastic:** The force in an element of the SFRS or the damping system does not exceed 1.5 times the expected strength using a strength reduction factor, ϕ, of 1.0.

Figure 16.5-4 illustrates the D/C ratios for the flexure in the RBS subject to the MCE_R event on Gridline 1. Since the unreduced elastic demands /capacity ratios do not exceed 1.5, the SFRS is permitted to be modeled as linear. The D/C ratio in Figure 16.5-4 uses a capacity defined as:

- **Expected Capacity:** Located at the RBS center, expected yield strength with strength reduction factor, ϕ, of 1.0. The W21x73 beam between Gridlines D and E at Story 3 has an expected capacity:

$$M_e = \phi R_y F_y Z_{RBS} = 1.0 \times 1.1 \times 50 \times 126.8$$
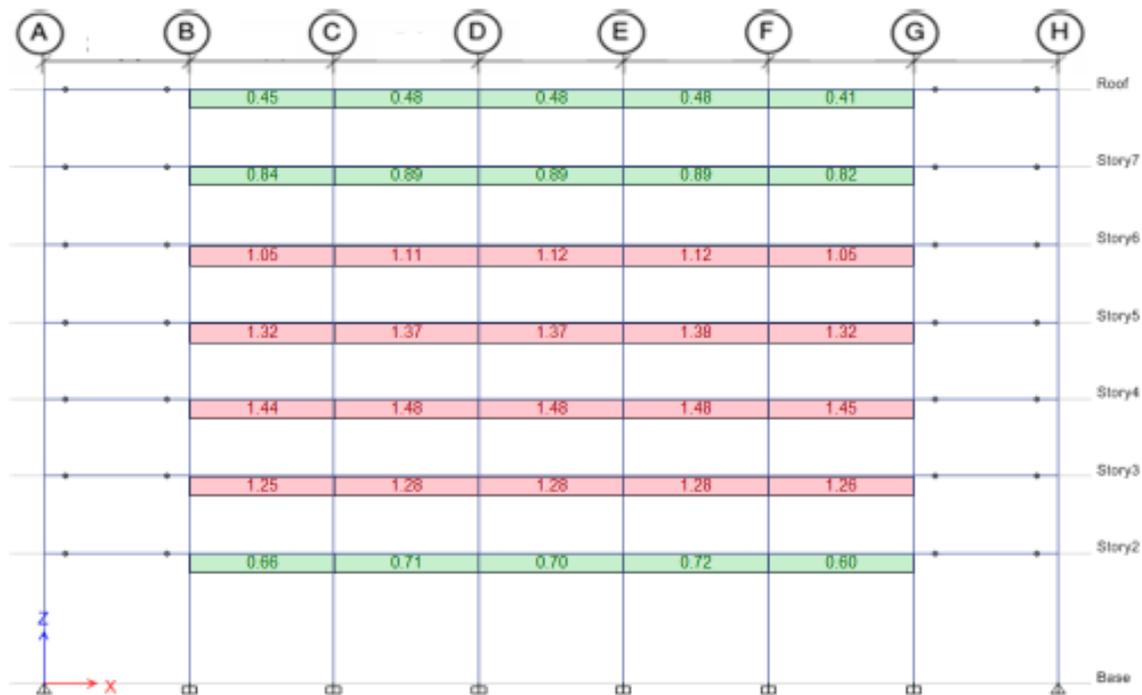
$$M_e = 581 \text{ kip-ft}$$

Figure 16.5-4 MCE$_R$ NLRHA Demand divided by Expected Moment Capacity Ratios for Gridline 1.

The inclusion of the dampers reduces the forces in the SMRF and therefore leads to less damage and better seismic performance. As a side note, a linear RHA of the code-design structure in Chapter 9 (i.e. with no dampers) of these examples gives D/C ratios 2 to 3 times larger than that shown in Figure 16.5-4.

 Permissible drift. The story drifts are only checked using the MCE$_R$ ground motions using a model which includes the damping system. The maximum permitted drift by the *Standard §18.4.1* is the smaller of:

- 3%
- 1.5^X (8/5.5)^{X}2% (*Table 12.12-1* limit) = 4.4%
- 1.9^X 2% (*Table 12.12-1* limit) = 3.8%

Therefore the story drift at any floor and in any principal direction shall not exceed 3%.

The story drift history (i.e. drift vs. time) is calculated for each ground motion by subtracting the node displacement at the floor below from a vertically aligned node from the floor above. The maximum drift, at any instant in time, from each of the ground motions is then averaged to give the MCE$_R$ drifts in Tables 16.4-2 and Table 16.4-3 for maximum and minimum damper properties, respectively. The maximum drift at any story, in either principal direction, is 2.0%. This value needs to be increased to account for accidental eccentricity. As per Section 16.4.4.3 a drift amplifier of 1.14 is applicable, giving a drift demand of 2.3% which is less than the 3% limit.

As a side note, the original design of the SMRF (per Chapter 9) was governed by limiting the drift at the design earthquake level to the 2.0% permissible limit of *Standard Table 12.12-1*. A linear RHA analysis of the building without dampers gave a design earthquake maximum story drift of 2.8% ^{X}(C$_d$/R)=1.9%, which compares well with the modal response spectrum calculated drifts in Chapter 9. The NLRHA with dampers at the design earthquake level gave a maximum drift of 1.2%.

The strength design of the SFRS and the drift demand show that there is scope to reduce the size of members in the SFRS. However since the performance goal of this building is to maintain an "essentially" elastic behavior of the structure during the MCE$_R$, the original SMRF sizes are maintained. A reduction in member sizes may prompt the need to explicitly model their nonlinear behavior since the D/C ratios in 16.5-4 are close to exceeding 1.5.

16.5.2 Damping System

 Damping devices. The damping devices shall be sized to elastically resist the forces, displacements and velocities from the MCE$_R$ ground motions. Furthermore since the redundancy criteria of *§18.2.4.6* are not satisfied for stories 3-7, the devices at these stories must be capable of sustaining the force and displacement associated with a velocity equal to 1.3 times the maximum calculated velocity. For ease of construction and to control damper and detailing costs, all dampers will be designed for this penalty to maintain one type of damper.

Based on the peak velocity that corresponds to the maximum force calculated in Section 16.4.4.3, and increasing for redundancy and accidental eccentricity, the maximum damper design force at the MCE$_R$ level is:

$$\text{Damper Force} = \text{Force amplifier} \times \lambda_{max} C_{NL} (1.3v)^{\alpha}$$
$$= 1.08 \times 1.15 \times 128 \times (1.3 \times 11.7)^{0.38} = 447 \text{ kip}$$

The required stroke of the device is calculated as follows:

$$\text{Damper Stroke} = \text{Displacement amplifier} \times 1.3 \times \text{Max Stroke}$$
$$= 1.14 \times 1.3 \times 2.7 = 4.0 \text{ inch}$$

Usually it is the responsibility of the manufacturer to design the components of the damping device itself and the design engineer provides performance details, as shown in Table 16.5-1.

Table 16.5-1 Nonlinear Viscous Damper Device Details[1]

Parameter	Symbol	Value	Units
Damping Coefficient	C_{NL}	128	kip-sec/in
Velocity Exponent	α	0.38	-
Maximum Force, Max Properties	F_{max}	447	kip
Required Stroke, Min Properties	u_{str}	± 4.0	inch
Peak Velocity, Max Properties[2]	v_{max}	15.2	inch/sec
Peak Velocity, Min Properties[2]	v_{max}	16.5	inch/sec
Allowable Variations on C_{NL}			
Max. Testing Variations	$\lambda_{test,max,C}$	1.10	
Min. Testing Variations	$\lambda_{test,min,C}$	0.90	
Max. Specification Tolerance	$\lambda_{spec,max,C}$	1.05	
Min. Specification Tolerance	$\lambda_{spec,min,C}$	0.95	
Max. and Min Aging and Environmental	$\lambda_{ae,max,C}$ and $\lambda_{ae,min,C}$	1.0	
Max. System Property Mod. Factor	$\lambda_{max,C}$	1.15	
Max. System Property Mod. Factor	$\lambda_{min,C}$	0.85	

1. All values for MCE_R ground motions.
2. Includes a 1.3 factor increase per redundancy clause *§18.2.4.6*.

Framing, braces and connections. Other elements classified as part of the damping system include the braces in-line with the dampers, their connections, the framing (beams and columns) which encompass the damping devices and the collectors and diaphragm which bridge between the gridline where the dampers are located to the gridline where the SFRS's are. The sizing of these elements must be such that they remain elastic for the unreduced linear-elastic MCE_R demands. The capacity of element is defined in this example as follows:

- **Nominal Capacity:** Nominal yield strength with strength reduction factor, ϕ, of 1.0.

The *Standard* makes the distinction that "force-controlled" elements shall be designed for seismic forces that are increased by 20%. Force-controlled actions are defined as element actions for which reliable inelastic deformation capacity is not achievable without critical strength decay. Therefore this is interpreted as meaning actions such as axial loads on the braces and axial and shear loads on columns will be increased by 20% and then designed using nominal material strengths and a strength reduction factor equal to unity.

The NLRHA allows for the determination of the average peak demands in beams and columns over the building height. Conversely, designing a column at story 1 for the maximum damper force occurring at every story would be overly conservative. This is because the peak force in the dampers does not occur simultaneous over the full height of the building, but at different times. In ground motion 5 the maximum damper force of 391kip in story 1 occurs at a time of 6.0 seconds into the record. At this instant in time the damper forces on the upper levels are not at their peak response, for example the damper at story 5 only has a 12 kip force as shown in 16.5-5. Furthermore the NLRHA allows for determination of the peak

demands which may result from the peak drift, peak velocity or a combination of drift and velocity below their peak values.

For this example, the average of the maximum positive and negative demands from the NLRHA is used for the design of the damping system. Figure 16.5-6 shows the axial tension and compression forces in the dampers on gridline 2, using maximum damper properties (which gave the larger damper forces). It is noted that the maximum damper forces shown in the figure (i.e. 359 kip for story 1) are slightly less than that calculated in Section 16.4.4.2 (i.e. 375 kip for story 1). This is because Figure 16.5-6 forces are calculated in ETABS by taking the envelope of the demands from each ground motion, and then averaging the maximum positive and negative demands of the seven ground motions. On the other hand, in Section 16.4.4.2 the absolute maximum of the positive and negative forces is taken for each ground motions and then the absolute maximum is averaged for the seven ground motions (so gives a larger demand). Nevertheless the damper forces compare very well in the upper stories and the difference is small at less than 5%.
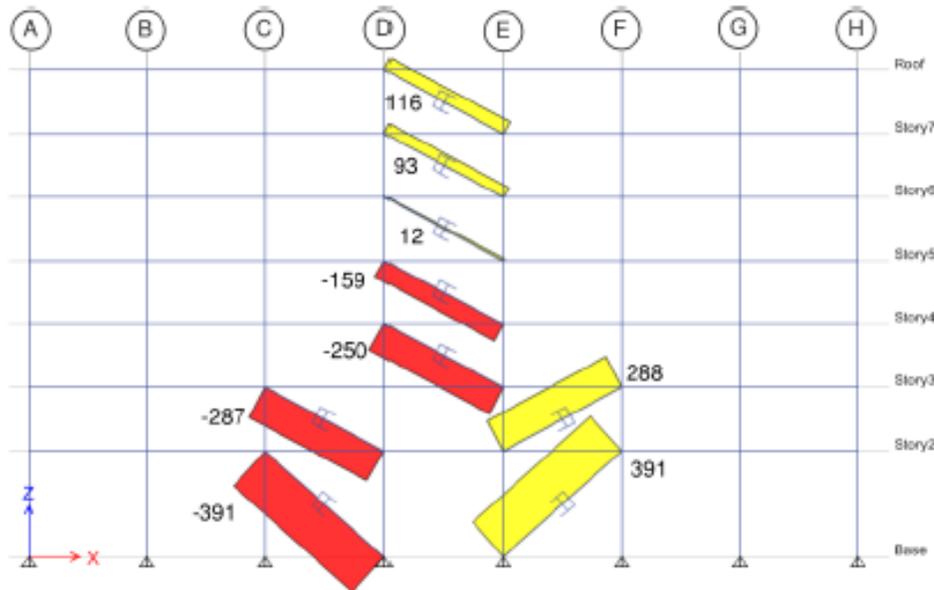

Figure 16.5-5 MCE$_R$ NLRHA Ground Motion 5 Damper Axial Forces on Gridline 2 at 6.0 seconds, Maximum Damper Properties (Units: kip, negative sign = compression force, positive = tension force)
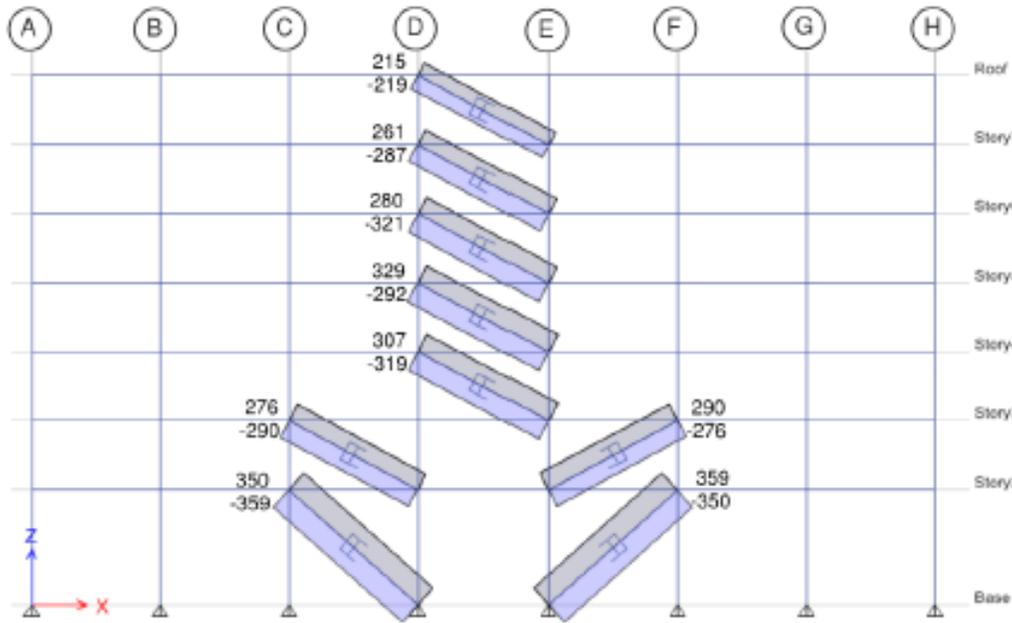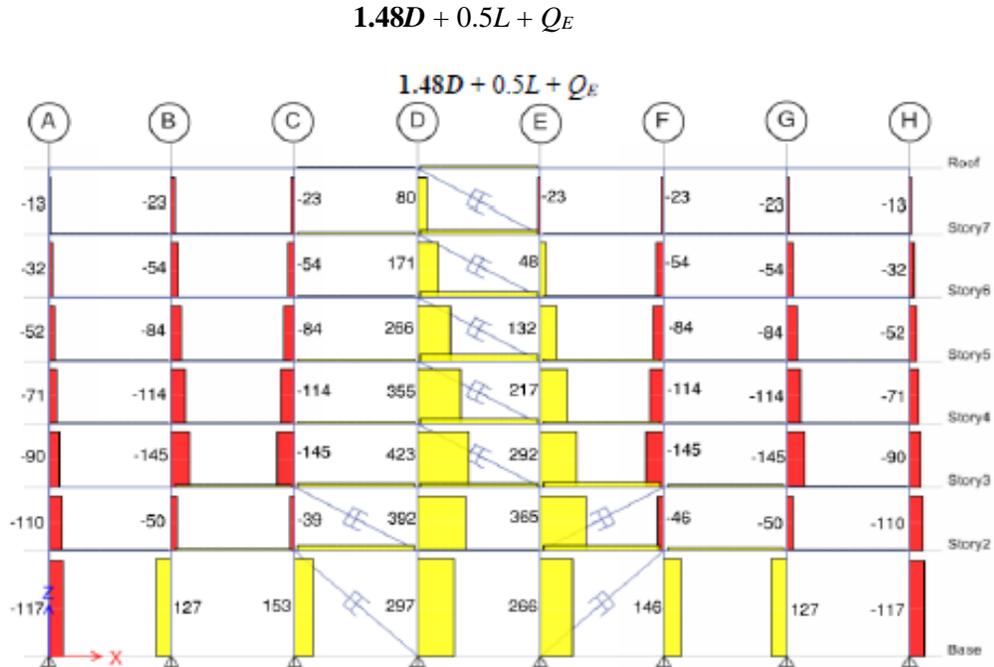
Figure 16.5-6 MCE$_R$ NLRHA Average Results of the Tension and Compression Damper Axial Forces on Gridline 2, excluding accidental eccentricity, Maximum Damper Properties (kip)

Using the post-processing explained previously it is possible to capture the peak compression and tension demands occurring in the columns, averaged for the seven ground motions. Figure 16.5-7 shows the peak compression force in the columns from load combination $1.48D + 0.5L + Q_E$ and Figure 16.5-8 shows the peak tension force for load combination $0.62D + Q_E$.
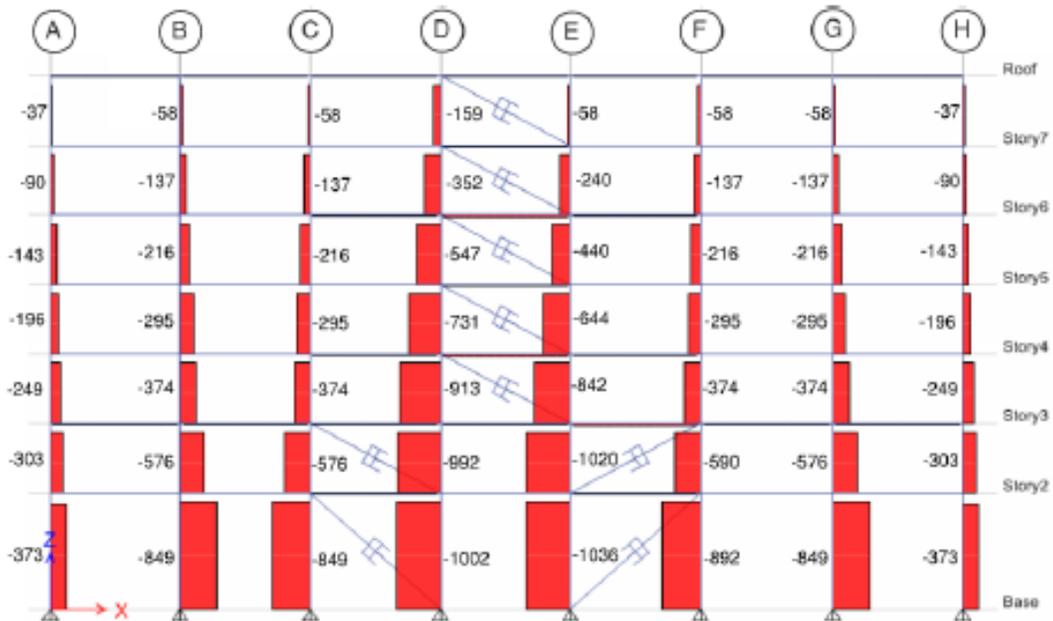
Figure 16.5-7 MCE$_R$ NLRHA Average Results of the Minimum (Peak Compression) Column Axial Forces on Gridline 2, excluding accidental eccentricity, Maximum Damper Properties, Load Case

$$\mathbf{1.48D} + 0.5L + Q_E$$

Figure 16.5-8 MCE_R NLRHA Average Results of the Maximum (Peak Tension) Column Axial Forces on Gridline 2, excluding accidental eccentricity, Maximum Damper Properties, Load Case $0.62D + Q_E$

The design of the damping system components can proceed by taking the forces from the MCE$_R$ NLRHA, increasing the actions for accidental eccentricity by using amplification factors and further increasing the action if it is force-controlled. These amplified actions should be no greater than the nominal member capacity, as defined above.

For example, the design of the brace in-line with the damper at story 1 is based on:
- Required brace axial stiffness of 2000 kip/inch
- Force-controlled design axial force of $1.08 \times 1.2 \times 375 = 486$kip.

The FVD will be pinned and connected directly to the gusset plate at one end, with the other end being a thick plate which is rigidly bolted to the end of the driver brace. The net length of the brace and damper is calculated to be about:

$$L = \sqrt{(L_{bay} - d_{column})^2 + (h - d_{beam})^2} - 2L_{gusset}$$
$$= \sqrt{(25-2)^2 + (22.3-1)^2} - 2 \times 1 = 29.3 \text{ ft}$$

The axial stiffness of 2000 kip/in is the stiffness combination of the brace and damper in series. Simply assuming the brace is the full length gives a required area of the brace of:

$$A \geq KL/E = 2000 \times 29.3 \times 12/29000 = 24.2 \text{ in}^2$$

Adopting HSS of $14 \times 5/8$ gives an area of 25.5in² to satisfy the stiffness requirement.

The buckling capacity of the brace is calculated as follows. Checking the limit on inelastic buckling:

$$\frac{KL}{r} = \frac{1.0 \times 29.3 \times 12}{4.75} = 74 \leq 4.71\sqrt{\frac{E}{F_y}} = 124$$

$$F_e = \frac{\pi^2 E}{\left(\dfrac{kL}{r}\right)^2} = \frac{\pi^2 \times 29000}{\left(\dfrac{1.0 \times 29.3 \times 12}{4.75}\right)^2} = 52.3 \text{ ksi}$$

$$P_n = F_{cr}A_g = 0.658^{\frac{42}{52.3}} \times 42 \times 24.5 = 735 \text{ kip}$$

Therefore the nominal buckling capacity exceeds the maximum force delivered to the brace and the ASTM A500 Grade B HSS $14 \times 5/8$ is adequate.

The design of the other structural members follows conventional design practices and is not addressed in this example. The columns, connections and the foundation must be designed for the large compression and tension axial forces as shown in Figures 16.5-7 and 16.5-8. These tension forces arise as the forces in the dampers overcome the gravity loading in the columns. Other elements not addressed in this example include:
- Connection design, for example gusset plates, splices, collector beams, foundations.
- Diaphragm and beam/collector design.
- Comparison of wind and seismic forces.

17

Nonbuilding Structure Design

By J. G. (Greg) Soules, P.E., S.E., SECB
Originally developed by Harold O. Sprague, Jr., P.E.

Contents

Chapter 15 of the *Standard* is devoted to nonbuilding structures. Nonbuilding structures comprise a myriad of structures constructed of all types of materials with markedly different dynamic characteristics and a wide range of performance requirements.

Nonbuilding structures are a general category of structure distinct from buildings. Key features that differentiate nonbuilding structures from buildings include human occupancy, function, dynamic response and risk to society. Human occupancy, which is incidental in most nonbuilding structures, is the primary purpose of most buildings. The primary purpose and function of nonbuilding structures can be incidental to society, or the purpose and function can be critical for society.

In the past, many nonbuilding structures were designed for seismic resistance using building code provisions developed specifically for buildings. These code provisions were inadequate to address the performance requirements and expectations that are unique to nonbuilding structures. For example, consider secondary containment for a vertical vessel containing hazardous materials. Nonlinear performance and collapse prevention, which are performance expectations for buildings, are insufficient for a secondary containment structure, which must not leak.

Seismic design requirements specific to nonbuilding structures were first introduced in the 2000 *Provisions*. Before the introduction of the 2000 *Provisions*, the seismic design of nonbuilding structures depended on the various trade organizations and standards development organizations that were not connected with the building codes.

This chapter develops examples specifically to help clarify Chapter 15 of the *Standard*. The solutions developed are not intended to be comprehensive but instead focus on correct interpretation of the requirements. Complete solutions to the examples cited are beyond the scope of this chapter.

In addition to the *Provisions* and *Commentary*, the following publications are referenced in this chapter:

API 650	American Petroleum Institute, *Welded Steel Tanks for Oil Storage*, 12th edition, Addendum 1, 2014.
ASCE	American Society of Civil Engineers, *Guidelines for Seismic Evaluation and Design of Petrochemical Facilities,* 2nd Edition, 2011.
ASME BPVC	American Society of Mechanical Engineers, *Section VIII, Division 2, Alternate Rules, Rules for Construction of Pressure Vessels*, 2015 Edition.
AWWA D100	American Water Works Association, *Welded Steel Tanks for Water Storage,* 2011.
Bachman and Dowty	Bachman, Robert and Dowty, Susan, "Nonstructural Component or Nonbuilding Structure?", Building Safety Journal, International Code Council, April-May 2008.
Jacobsen	Jacobsen, L.S., "Impulsive Hydrodynamics of Fluid Inside a Cylindrical Tank and of Fluid Surrounding a Cylindrical Pier," Bulletin of the Seismological Society of America, 39(3), 189-204, 1949.
Morison	Morison, J.R., O'Brien, J.W. and Sohaaf, S.A., "The Forces Exerted by Surface Waves on Piles," Petroleum Transactions, AIME, Vol. 189; 1950.

RMI   Rack Manufacturers Institute, *Specification for the Design, Testing and Utilization of Industrial Steel Storage Racks*, MH16.1, 2012

Soules   Soules, J. G., "The Seismic Provisions of the 2006 IBC – Nonbuilding Structure Criteria," Proceedings of 8th National Conference on Earthquake Engineering, San Francisco, CA, April 18, 2006.

17.1   NONBUILDING STRUCTURES VERSUS NONSTRUCTURAL COMPONENTS

Many industrial structures are classified as either nonbuilding structures or nonstructural components. This distinction is necessary to determine how the practicing engineer designs the structure. The intent of the *Standard* is to provide a clear and consistent design methodology for engineers to follow regardless of whether the structure is a nonbuilding structure or a nonstructural component. Central to the methodology is how to determine which classification is appropriate. Table 17-1 provides a simple method to determine the appropriate classification. Additional discussion on this topic can be found in Bachman and Dowty (2008).

The design methodology contained in Chapter 13 of the *Standard* focuses on nonstructural component design. As such, the amplification by the supporting structure of the earthquake-induced accelerations is critical to the design of the component and its supports and attachments. The design methodology contained in Chapter 15 of the *Standard* focuses on the direct effects of earthquake ground motion on the nonbuilding structure.

**Table 17-1 Applicability of the Chapters of the *Standard***

Supporting Structure	Supported Item	
	Nonstructural Component	Nonbuilding Structure
Building	Chapter 12 for supporting structure; Chapter 13 for supported item	Chapter 12 for supporting structure; Chapter 15 for supported item
Nonbuilding	Chapter 15 for supporting structure; Chapter 13 for supported item	Chapter 15 for both supporting structure and supported item

The example shown in Figure 17.1-1 is a combustion turbine, electric-power-generating facility with four bays. Each bay contains a combustion turbine and supports an inlet filter on the roof. The uniform seismic dead load of the supporting roof structure is 30 psf. Each filter weighs 34 kips.

The following two examples illustrate the difference between nonbuilding structures that are treated as nonstructural components, using *Standard* Chapter 13 and those which are designed in accordance with *Standard* Chapter 15. In many instances, the weight of the supported nonbuilding structure is relatively small compared to the weight of the supporting structure (less than 25 percent of the combined weight) such that the supported nonbuilding structure will have a relatively small effect on the overall nonlinear earthquake response of the primary structure during design-level ground motions. It is permitted to treat such structures as nonstructural components and use the requirements of *Standard* Chapter 13 for their design. Where the weight of the supported structure is relatively large (greater than or equal to 25 percent of the combined weight) compared to the weight of the supporting structure, the overall response can be affected significantly. In such cases it is intended that seismic design loads and detailing requirements be

determined following the procedures of *Standard* Chapter 15. Where there are multiple large nonbuilding structures, such as vessels supported on a primary nonbuilding structure and the weight of an individual supported nonbuilding structure does not exceed the 25 percent limit but the combined weight of the supported nonbuilding structures does, it is recommended that the combined analysis and design approach of *Standard* Chapter 15 be used.

This difference in design approach is explored in the following example.
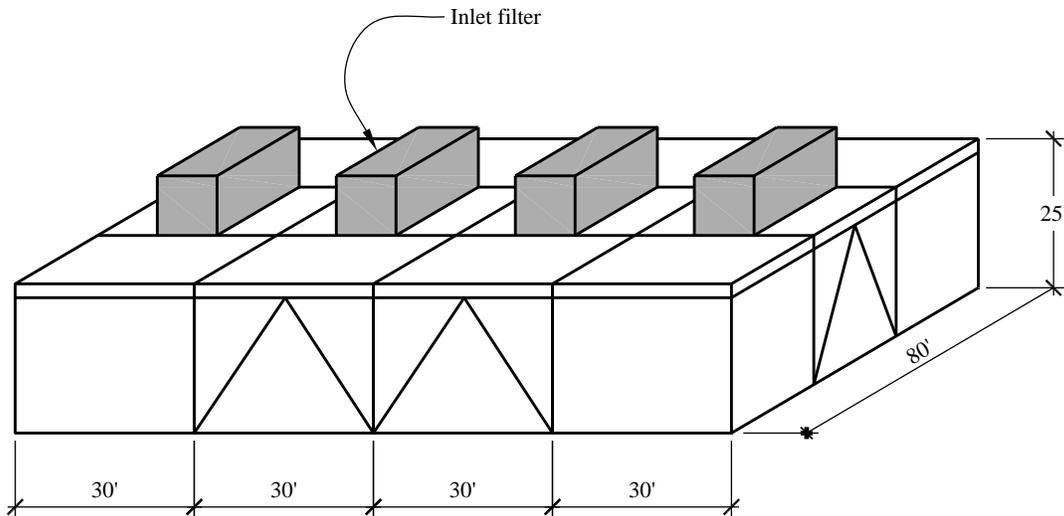
Figure 17.1-1 Combustion turbine building (1.0 ft = 0.3048 m)

17.1.1 Nonbuilding Structure

For the purpose of illustration, assume that the four filter units are connected in a fashion that couples their dynamic response through a rigid diaphragm. Therefore, it is appropriate to combine the masses of the four filter units for both the transverse and longitudinal direction responses.

17.1.1.1 Calculation of seismic weights.

All four inlet filters = W_{IF} = 4(34 kips) = 136 kips

Support structure = W_{SS} = 4(30 ft)(80 ft)(30 psf) = 288 kips

The combined weight of the nonbuilding structure (inlet filters) and the supporting structural system is:

$W_{combined}$ = 136 kips + 288 kips = 424 kips

17.1.1.2 Selection of design method. The ratio of the supported weight to the total weight is:

$$\frac{W_{IF}}{W_{Combined}} = \frac{136}{424} = 0.321 > 25\%$$

Because the weight of the inlet filters is 25 percent or more of the combined weight of the nonbuilding structure and the supporting structure (*Standard* Sec. 15.3.2), the inlet filters are classified as "nonbuilding structures" and the seismic design forces must be determined from analysis of the combined seismic-resistant structural systems. This would require modeling the filters, the structural components of the filters and the structural components of the combustion turbine supporting structure to determine accurately the seismic forces on the structural elements as opposed to modeling the filters as lumped masses.

17.1.2 Nonstructural Component

For the purpose of illustration, assume that the inlet filters are independent structures, although each is supported on the same basic structure. Unlike the previous example where the filter units were connected to each other through a rigid diaphragm, the four filter units are not connected in a fashion that couples their dynamic response. In other words, the four independent structures do not significantly affect the response of the support structure. In this instance, one filter is the nonbuilding structure. The question is whether it is heavy enough to significantly change the response of the combined system.

17.1.2.1 Calculation of seismic weights.

One inlet filter = W_{IF} = 34 kips

Support structure = W_{SS} = 4(30 ft)(80 ft)(30 psf) = 288 kips

The combined weight of the nonbuilding structures (all four inlet filters) and the supporting structural system is:

$W_{combined}$ = 4(34 kips) + 288 kips = 424 kips

17.1.2.2 Selection of design method. The ratio of the supported weight to the total weight is:

$$\frac{W_{IF}}{W_{Combined}} = \frac{34}{424} = 0.08 < 25\%$$

Because the weight of an inlet filter is less than 25 percent of the combined weight of the nonbuilding structures and the supporting structure (*Standard* Sec. 15.3.1), the inlet filters are classified as "nonstructural components" and the seismic design forces must be determined in accordance with *Standard* Chapter 13. In this example, the filters could be modeled as lumped masses. The filters and the filter supports could then be designed as nonstructural components.

17.2   PIPE RACK, SEISMIC DESIGN CATEGORY D

This example illustrates the calculation of design base shears and maximum inelastic displacements for a pipe rack using the equivalent lateral force (ELF) procedure. The pipe rack in this example is supported at grade and is considered a nonbuilding structure.

17.2.1 Description

A two-tier, 12-bay pipe rack in a petrochemical facility has concentrically braced frames in the longitudinal direction and ordinary moment frames in the transverse direction. The pipe rack supports four runs of 12-inch-diameter pipe carrying naphtha on the top tier and four runs of 8-inch-diameter pipe carrying water for fire suppression on the bottom tier. The minimum seismic dead load for piping is

35 psf on each tier to allow for future piping loads. The seismic dead load for the steel support structure is 10 psf on each tier.

Pipe supports connect the pipe to the structural steel frame and are designed to support the gravity load and resist the seismic and wind forces perpendicular to the pipe. The typical pipe support allows the pipe to move in the longitudinal direction of the pipe to avoid restraining thermal movement. The pipe support near the center of the run is designed to resist longitudinal and transverse pipe movement as well as provide gravity support; such supports are generally referred to as fixed supports.

Pipes themselves must be designed to resist gravity, wind, seismic and thermally induced forces, spanning from support to support.

If the pipe run is continuous for hundreds of feet, thermal/seismic loops are provided to avoid a cumulative thermal growth effect. The longitudinal runs of pipe in this example are broken up into sections by providing thermal/seismic loops at spaced intervals as shown in Figure 17.2-1. In Figure 17.2-1, it is assumed thermal/seismic loops are provided at each end of the pipe run.
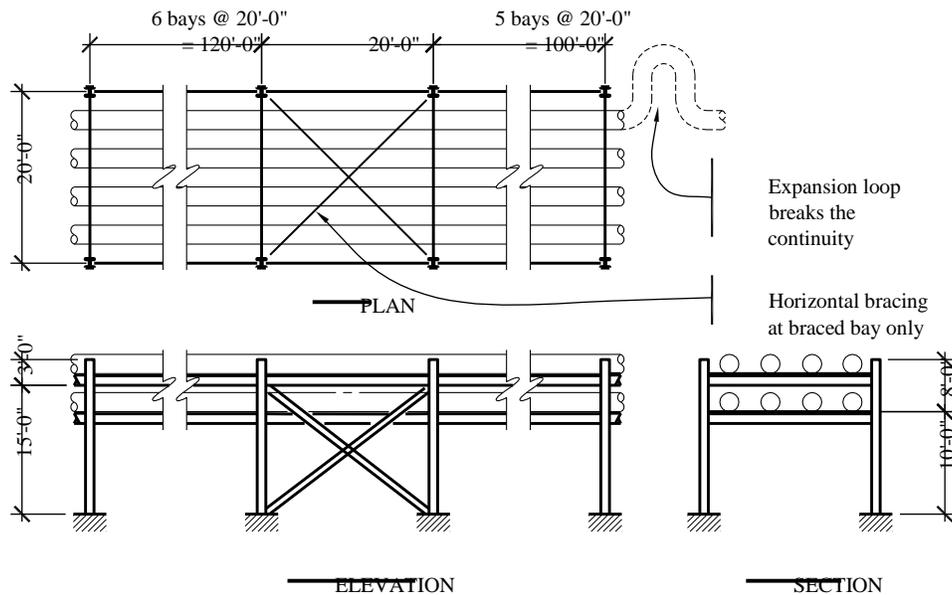

Figure 17.2-1 Pipe rack (1.0 ft = 0.3048 m)

17.2.2 *Provisions* Parameters

17.2.2.1 Ground motion. See Section 3.2 for an example illustrating the determination of design ground motion parameters. For this example, the parameters are as follows:

$S_{DS} = 0.40$
$S_{D1} = 0.18$

17.2.2.2 Risk category and importance factor. The upper piping carries naphtha. A review of a typical material safety datasheet (MSDS) for naphtha indicates that naphtha has a medium lethal concentration [LC(50)] of 5.2 mg per liter. *Standard* Section C1.5.3 defines a toxic material as a chemical with a LC(50) between 2 mg per liter and 20 mg per liter. Therefore, based on a LC(50) of 5.2 mg per liter, naphtha is considered a toxic material and therefore is assigned to Risk Category III per *Standard* Table 1.5-1. The lower piping is required for fire suppression and therefore is assigned to Risk Category IV per *Standard* Table 1,5-1. The naphtha piping and the fire water piping are included in *Standard* Section 1.5.1; therefore, the pipe rack is assigned to Risk Category IV based on the more severe category.

Standard Section 15.4.1.1 directs the user to use the largest value of I_e based on the applicable reference document listed in *Standard* Chapter 23, the largest value selected from *Standard* Table 1.5-2, or as specified elsewhere in *Standard* Chapter 15. It is important to be aware of the requirements of *Standard* Section 15.4.1.1. While the importance factor for most structures will be determined based on *Standard* Table 1.5-2, there are reference documents that define importance factors greater than those found in *Standard* Table 1.5-2. Additionally, *Standard* Section 15.5.3.5 requires that steel storage racks in structures open to the public be assigned an importance factor of 1.5. This additional requirement for steel storage racks addresses a risk to the public that is not addressed by *Standard* Table 1.5-2 and *Standard* Table1.5-1. For this example, *Standard* Table 1.5-2 governs the choice of importance factor. According to *Standard* Table 1.5-2, the importance factor, I_e, is 1.5 based on Risk Category IV.

17.2.2.3 Seismic design category. For this structure assigned to Risk Category IV with $S_{DS} = 0.40$ and $S_{D1} = 0.18$, the Seismic Design Category is D according to *Standard* Section 11.6.

17.2.3 Design in the Transverse Direction
17.2.3.1 Design coefficients. According to *Standard* Section 15.4-1, either *Standard* Table 12.2-1 or *Standard* Table 15.4-1 may be used to determine the seismic parameters, although mixing and matching of values and requirements from the tables is not allowed. In *Standard* Chapter 15, selected nonbuilding structures similar to buildings are provided an option where both lower R values and less restrictive height limits are specified. This option permits selected types of nonbuilding structures which have performed well in past earthquakes to be constructed with fewer restrictions in Seismic Design Categories D, E and F provided seismic detailing is used and design force levels are considerably higher. The R value-height limit trade-off recognizes that the size of some nonbuilding structures is determined by factors other than traditional loadings and result in structures that are much stronger than required for seismic loadings (Soules, 2006). Therefore, the structure's ductility demand is generally much lower than a corresponding building. The R value-height trade-off also attempts to obtain the same structural performance at the increased heights. The user will find that the option of reduced R value with less restricted height will prove to be the economical choice in most situations due to the relative cost of materials and construction labor. It must be emphasized that the R value-height limit trade-off of *Standard* Table 15.4-1 applies only to nonbuilding structures similar to buildings and cannot be applied to building structures.

In *Standard* Table 12.2-1, ordinary steel moment frames are not permitted in Seismic Design Category D (with some exceptions) and cannot be used in this example. There are several options for ordinary steel moment frames found in *Standard* Table 15.4-1. These options are as follows:

1. *Standard* Table 15.4-1, Ordinary moment frames of steel, $R = 3.5$, $\Omega_o = 3$, $C_d = 3$. According to Note c in *Standard* Table 15.4-1, this system is allowed for pipe racks up to 65 feet high using bolted end plate moment connections and per Note (d) this system is allowed for pipe racks up to 35 feet without limitations on the connection type. This option requires the use of the AISC 341.

2. *Standard* Table 15.4-1, Ordinary moment frames of steel with permitted height increase, $R = 2.5$, $\Omega_0 = 2$, $C_d = 2.5$. This option is intended for pipe racks with height greater than 65 feet and limited to 100 feet. This option is not applicable for this example.

3. *Standard* Table 15.4-1, Ordinary moment frames of steel with unlimited height, $R=1$, $\Omega_0 = 1$, $C_d = 1$. This option does not require the use of the AISC 341.

For this example, Option 1 above is chosen. Using *Standard* Table 15.4-1, the parameters for this ordinary steel moment frame are:

$R = 3.5$
$\Omega_0 = 3$
$C_d = 3$

Ordinary steel moment frames are retained for use in nonbuilding structures such as pipe racks because they allow greater flexibility for accommodating process piping and are easier to design and construct than special steel moment frames.

17.2.3.2 Seismic response coefficient. Using *Standard* Equation 12.8-2:

$$C_s = \frac{S_{DS}}{R/I_e} = \frac{0.4}{3.5/1.5} = 0.171$$

From analysis, $T = 0.42$ second. For nonbuilding structures, the fundamental period is generally approximated for the first iteration and must be verified with final calculations. *Standard* Section 15.4.4 makes clear that the approximate period equations of *Standard* Section 12.8.2 do not apply to nonbuilding structures.

Using *Standard* Equation 12.8-3 for $T \leq T_L$, C_s does not need to exceed

$$C_s = \frac{S_{D1}}{T(R/I_e)} = \frac{0.18}{0.42(3.5/1.5)} = 0.184$$

Using *Standard* Equation 12.8-5, C_s must not be less than

$$C_s = 0.044 I_e S_{DS} \geq 0.01 = 0.044(1.5)(0.4) = 0.0264$$

Standard Equation 12.8-2 controls; $C_s = 0.171$.

17.2.3.3 Seismic weight.

The seismic weight resisted by the moment frame in the transverse direction is shown below based on two levels of piping, a 20 ft bent spacing, a bent width (perpendicular with the piping) of 20 ft, piping dead weight of 35 psf and structure dead weight of 10 psf.

$$W = 2(20 \text{ ft})(20 \text{ ft})(35 \text{ psf} + 10 \text{ psf}) = 36 \text{ kips}$$

17.2.3.4 Base shear. Using *Standard* Equation 12.8-1:

$$V = C_s W = 0.171(36 \text{ kips}) = 6.2 \text{ kips}$$

17.2.3.5 Drift. Although not shown here, drift of the pipe rack in the transverse direction was calculated by elastic analysis using the design forces calculated above. The calculated lateral drift, $\delta_{xe} = 0.328$ inch. Using *Standard* Equation 12.8-15:

$$\delta_x = \frac{C_d \delta_{xe}}{I_e} = \frac{3(0.328)}{1.5} = 0.656 \text{ in.}$$

The lateral drift must be checked with regard to acceptable limits. The acceptable limits for nonbuilding structures are not found in codes. Rather, the limits are what is acceptable for the performance of the piping. In general, piping can safely accommodate the amount of lateral drift calculated in this example. P-delta effects must also be considered and checked as required in *Standard* Section 15.4.5.

17.2.3.6 Redundancy factor. Some nonbuilding structures are designed with parameters from *Standard* Table 12.2-1 or 15.4-1 if they are termed "nonbuilding structures similar to buildings". For such structures (assigned to Seismic Design Category D, E, or F) the redundancy factor applies. Pipe racks, being fairly simple moment frames or braced frames, are in the category similar to buildings. Because this structure is assigned to Seismic Design Category D, *Standard* Section 12.3.4.2 applies.

Considering the transverse direction, the seismic force-resisting system is an ordinary moment resisting frame with only two columns in a single frame. The frames repeat in an identical pattern. Loss of moment resistance at the beam-to-column connections at both ends results in a loss of more than 33 percent in story strength. Therefore, *Standard* Section 12.3.4.2, Condition (a) is not met. The moment frame as described above consists only of a single bay. Therefore, *Standard* Section 12.3.4.2, Condition b is not met. The value of ρ in the transverse direction is therefore 1.3.

17.2.3.7 Determining E. In *Standard* Section 12.4.2, *E* is defined to include the effects of horizontal and vertical ground motions and can be summarized as follows:

$$E = \rho Q_E \pm E_v = \rho Q_E \pm 0.2\, S_{DS}\, D$$

where Q_E is the effect of the horizontal earthquake ground motions, which is determined primarily by the base shear just computed and Ev is the effect of the vertical earthquake ground motions, *D* is the effect of dead load. By putting a simple multiplier on the effect of dead load, the last term is an approximation of the effect of vertical ground motion. For the moment frame, the joint moment is influenced by both terms. *E* with the "+" on the second term where combined with dead and live loads will generally produce the largest negative moment at the joints, while *E* with the "-" on the second term where combined with the minimum dead load (0.9*D*) will produce the largest positive joint moments.

The *Standard* also requires the consideration of an overstrength factor, Ω_0, on the effect of horizontal motions in defining E_m for components susceptible to brittle failure. *Standard* Section 12.4.3 defines E_m and this definition can be summarized as follows:

$$E_m = \Omega_0\, Q_E \pm E_v = \Omega_0\, Q_E \pm 0.2\, S_{DS}\, D$$

The moment frame portion of the pipe rack does not have components that require such consideration.

17.2.4 Design in the Longitudinal Direction
17.2.4.1 Design coefficients. In *Standard* Section 15.4-1, either *Standard* Table 12.2-1 or *Standard* Table 15.4-1 may be used to determine the seismic parameters. In *Standard* Table

12.2-1, ordinary steel concentrically braced frames are not permitted for Seismic Design Category D (with some exceptions) and cannot be used for this example. There are several options for ordinary steel concentrically braced frames found in *Standard* Table 15.4-1. These options are as follows:

1. *Standard* Table 15.4-1, Ordinary steel concentrically braced frame, $R = 3.25$, $\Omega_0 = 2$, $C_d = 3.25$. According to Note b in *Standard* Table 15.4-1, this system is allowed for pipe racks up to 65 feet high. This option requires the use of AISC 341.

2. *Standard* Table 15.4-1, Ordinary steel concentrically braced frames with permitted height increase, $R = 2.5$, $\Omega_0 = 2$, $C_d = 2.5$. This option is intended for pipe racks with height greater than 65 feet and limited to 160 feet. This option is not applicable for this example.

3. *Standard* Table 15.4-1, Ordinary steel concentrically braced frames with unlimited height, $R = 1.5$, $\Omega_0 = 1$, $C_d = 1.5$. This option does not require the use of AISC 341.

For this example, Option 1 above is chosen. Using *Standard* Table 15.4-1, the parameters for this ordinary steel concentrically braced frame are:

$R = 3.25$
$\Omega_0 = 2$
$C_d = 3.25$

17.2.4.2 Seismic response coefficient. Using *Standard* Equation 12.8-2:

$$C_s = \frac{S_{DS}}{R/I_e} = \frac{0.4}{3.25/1.5} = 0.185$$

From analysis, $T = 0.24$ second. The fundamental period for nonbuilding structures is generally approximated for the first iteration and must be verified with final calculations.

Using *Standard* Equation 12.8-3, C_s does not need to exceed:

$$C_s = \frac{S_{D1}}{T(R/I_e)} = \frac{0.18}{0.24(3.25/1.5)} = 0.346$$

Using *Standard* Equation 12.8-5, C_s must not be less than:

$$C_s = 0.044I_eS_{DS} \geq 0.01 = 0.044(1.5)(0.4) = 0.0264$$

Standard Equation 12.8-2 controls; $C_s = 0.185$.

17.2.4.3 Seismic weight.

$W = 2(240 \text{ ft})(20 \text{ ft})(35 \text{ psf} + 10 \text{ psf}) = 432 \text{ kips}$

17.2.4.4 Base shear. Using *Standard* Equation 12.8-1:

$V = C_sW = 0.185(432 \text{ kips}) = 79.9 \text{ kips}$

17.2.4.5 Redundancy factor. The pipe rack in this example does not meet either of the two redundancy conditions specified in *Standard* Section 12.3.4.2. Condition a is not met because only one set of bracing is provided on each side, so removal of one brace would result in a reduction of greater than 33 percent in story strength. Condition b is not met because two bays of seismic force-resisting perimeter framing are not provided in each orthogonal direction. Therefore, the redundancy factor, ρ, is 1.3. If two bays of bracing were provided on each side of the pipe rack in the longitudinal direction, the pipe rack would meet Condition (a) and qualify for a redundancy factor, ρ, of 1.0 in that direction.

17.2.4.6 Determine *E*. In *Standard* Section 12.4.2, *E* is defined to include the effects of horizontal and vertical ground motions and can be summarized as follows:

$$E = \rho Q_E \pm E_v = \rho Q_E \pm 0.2\, S_{DS}\, D$$

where Q_E is the effect of the horizontal earthquake ground motions, which is determined primarily by the base shear just computed and Ev is the effect of the vertical earthquake ground motions. *D* is the effect of dead load. By putting a simple multiplier on the effect of dead load, the last term is an approximation of the effect of vertical ground motion.

The *Standard* also requires the consideration of an overstrength factor, Ω_0, on the effect of horizontal motions in defining E_m for components susceptible to brittle failure. *Standard* Section 12.4.3 defines E_m and this definition can be summarized as follows:

$$E_m = \Omega_0\, Q_E \pm E_v = \Omega_0\, Q_E \pm 0.2\, S_{DS}\, D$$

The ordinary steel concentrically braced frame portion of the pipe rack does have components that require such consideration. The beams connecting each moment frame in the longitudinal direction act as collectors and, as required by *Standard* Section 12.10.2.1, must be designed for the seismic load effect including overstrength factor.

17.2.4.7 Orthogonal loads. Because the pipe rack in this example is assigned to Seismic Design Category D, *Standard* Section 12.5.4 requires that the braced sections of the pipe rack be evaluated using the orthogonal combination rule of *Standard* Section 12.5.3a. Two cases must be checked: 100 percent transverse seismic force plus 30 percent longitudinal seismic force and 100 percent longitudinal seismic force plus 30 percent transverse seismic force. The vertical seismic force represented by $0.2S_{DS}D$ is only applied once in each load case. Do not include the vertical seismic force in with both horizontal seismic load combinations. In this pipe rack example, due to the bracing configuration, the foundation and column anchorage would be the only components impacted by the orthogonal load combinations.

17.3 STEEL STORAGE RACK, SEISMIC DESIGN CATEGORY C

This example uses the ELF procedure to calculate the seismic base shear in the east-west direction for a steel storage rack.

17.3.1 Description
A four-tier, five-bay steel storage rack is located in a retail discount warehouse. There are concentrically braced frames in the north-south and east-west directions. The general public has direct access to the aisles and merchandise is stored on the upper racks. The rack is supported on a slab on grade. The design

operating load for the rack contents is 125 psf on each tier. The weight of the steel support structure is assumed to be 5 psf on each tier.
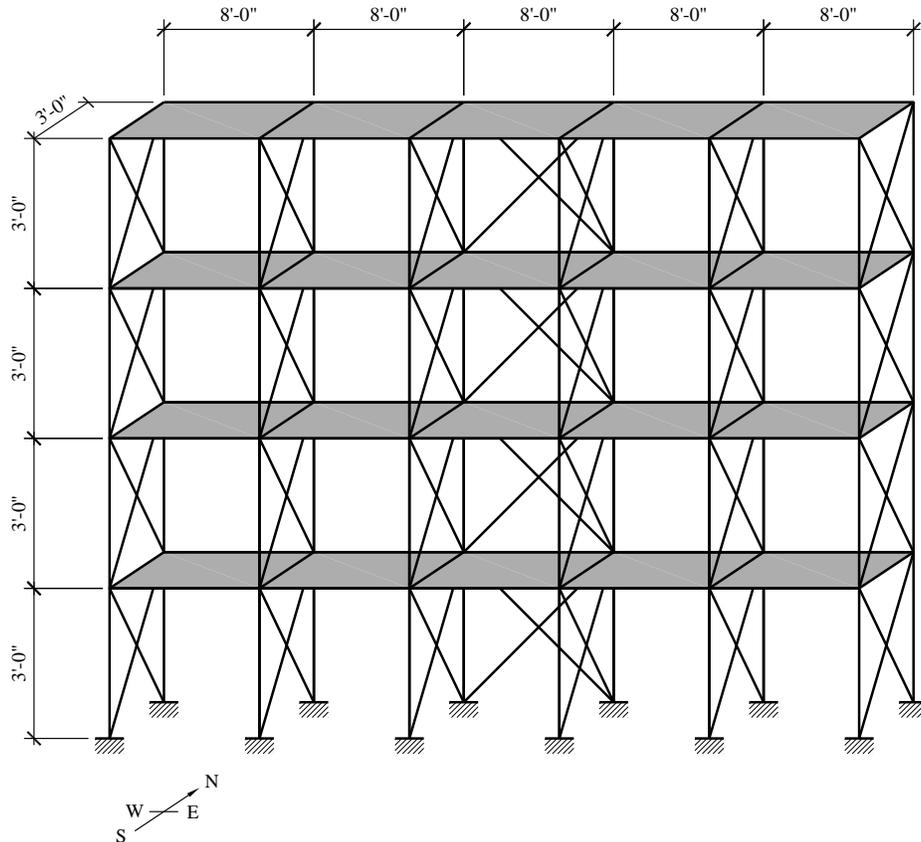
Figure 17.3-1 Steel storage rack (1.0 ft = 0.3048 m)

17.3.2 *Provisions* Parameters

17.3.2.1 Ground motion. The spectral response acceleration coefficients at the site are as follows:

$S_{DS} = 0.40$
$S_{D1} = 0.18$

17.3.2.2 Risk category and importance factor. Use *Standard* Section 1.5.1. The storage rack is in a retail facility. Therefore, the storage rack is assigned to Risk Category II. According to the exception listed in *Standard* Section 15.5.3.5, $I_e = I_p = 1.5$ because the rack is in an area open to the general public.

17.3.2.3 Seismic design category. Use *Standard* Tables 11.6-1 and 11.6-2. Given Risk Category II, $S_{DS} = 0.40$ and $S_{D1} = 0.18$, the Seismic Design Category is C.

17.3.2.4 Design coefficients. According to *Standard* Table 15.4-1, the design coefficients for this steel storage rack are as follows:

$R = 4$

$\Omega_0 = 2$
$C_d = 3.5$

17.3.3 Design of the System

17.3.3.1 Seismic response coefficient. *Standard* Section 15.5.3 allows designers some latitude in selecting the seismic design methodology. Designers may use the Rack Manufacturer's Institute specification (MH16.1-2012) to design steel storage racks as modified by Sections 15.5.3.1 and 15.5.3.2. In other words, racks designed using the RMI method of Section 15.5.3 are deemed to comply as long as the anchorage of the rack complies with Sections 15.5.3.1 and 15.5.3.2. RMI reproduces the seismic ground motion maps from ASCE 7-10. The intent of the *Standard* is to always use the ground motions defined in *Standard* Section 11.4 and not the ground motions defined in a reference standard, such as RMI. ASCE 7-16 Section 15.5.3 has been revised to make this point clear. As an alternate, designers may use the requirements of *Standard* Sections 15.5.3.4 through 15.5.3.8. The RMI approach will be used in this example.

Using RMI Section 2.6.3, from analysis, $T = 0.24$ seconds. For this particular example, the short period spectral value controls the design. The period for taller racks, however, may be significant and will be a function of the operating weight. As shown in the calculations that follow, in the RMI method the importance factor appears in the equation for V rather than in the equation for C_s. The seismic response coefficient from RMI is:

$$C_s = \frac{S_{D1}}{T(R)} = \frac{0.18}{0.24(4)} = 0.188$$

But need not be greater than:

$$C_s = \frac{S_{DS}}{R} = \frac{0.4}{4} = 0.10$$

Nor less than:

$$C_s = 0.044 S_{DS} = 0.044(0.4) = 0.0176$$

The governing value of $C_s = 0.10$. From RMI Section 2.6.2, the seismic base shear is calculated as follows:

$$V = C_s I_p W_s = 0.1(1.5)W_s = 0.15 W_s$$

17.3.3.2 Condition 1 (each rack loaded).

17.3.3.2.1 Seismic weight. In accordance with RMI Section 2.6.9, Item 1:

$W_s = 4(5)(8\ \text{ft})(3\ \text{ft})[0.67(125\ \text{psf})+5\ \text{psf}] = 42.6\ \text{kips}$

17.3.3.2.2 Design forces and moments. Using RMI Section 2.6.2, the design base shear for Condition 1 is calculated as follows:

$V = C_s I_p W_s = 0.15(42.6\ \text{kips}) = 6.39\ \text{kips}$

17-14

In order to calculate the design forces, shears and overturning moments at each level, seismic forces must be distributed vertically in accordance with RMI Section 2.6.7. The calculations are shown in Table 17.3-1.

Table 17.3-1 Seismic Forces, Shears and Overturning Moment

Level X	W_x (kips)	h_x (ft)	$w_x h_x^k$ (k = 1)	$\dfrac{w_x h_x^k}{\sum_{i=1}^{n} w_i h_i}$	F_x (kips)	V_x (kips)	M_x (ft-kips)
5	10.65	12	127.80	0.40	2.56		
						2.56	7.68
4	10.65	9	95.85	0.30	1.92		
						4.48	21.1
3	10.65	6	63.90	0.20	1.28		
						5.76	38.4
2	10.65	3	31.95	0.10	0.63		
						6.39	57.6
Σ	42.6		319.5				

1.0 ft = 0.3048 m, 1.0 kip = 4.45 kN, 1.0 ft-kip = 1.36 kN-m.

17.3.3.2.3 Resisting moment at the base.

$M_{OT, resisting} = W_s (1.5 \text{ ft}) = 42.6(1.5 \text{ ft}) = 63.9$ ft-kips

17.3.3.3 Condition 2 (only top rack loaded).

17.3.3.3.1 Seismic weight. In accordance with RMI Section 2.6.9, Item 2:

$W_s = 1(5)(8 \text{ ft})(3 \text{ ft})(125 \text{ psf}) + 4(5)(8 \text{ ft})(3 \text{ ft})(5 \text{ psf}) = 17.4$ kips

17.3.3.3.2 Base shear. Using RMI Section 2.6.2, the design base shear for Condition 2 is calculated as follows:

$V = C_s I_p W_s = 0.15(17.4 \text{ kips}) = 2.61$ kips

17.3.3.3.3 Overturning moment at the base. Although the forces could be distributed as shown above for Condition 1, a simpler, conservative approach for Condition 2 is to assume that a seismic force equal to the entire base shear is applied at the top level. Using that simplifying assumption,

$M_{OT} = V_b (12 \text{ ft}) = 2.61 \text{ kip } (12 \text{ ft}) = 31.3$ ft-kips

17.3.3.3.4 Resisting moment at the base.

$M_{OT, resisting} = W_s (1.5 \text{ ft}) = 17.4(1.5 \text{ ft}) = 26.1$ ft-kips

17.3.3.4 Controlling conditions. Condition 1 controls shear demands at all but the top level. Although the overturning moment is larger under Condition 1, the resisting moment is larger than the overturning moment. Under Condition 2 the resistance to overturning is less than the applied overturning moment. Therefore, the rack anchors must be designed to resist the uplift induced by the base shear for Condition 2.

17.3.3.5 Torsion. It should be noted that the distribution of east-west seismic shear will induce torsion in the rack system because the east-west brace is only on the back of the storage rack. The torsion should be resisted by the north-south braces at each end of the bay where the east-west braces are placed. If the torsion were to be distributed to each end of the storage rack, the engineer would be required to calculate the transfer of torsional forces in diaphragm action in the shelving, which may be impractical. Therefore, north-south braces are provided in each bay.

17.3.3.6 Anchorage. While RMI is generally viewed as deeming to comply with the *Standard*, *Standard* Sections 15.5.3.1 and 15.5.3.2 were added to address deficiencies in RMI with regards to anchorage. *Standard* Section 15.5.3.1 was added to modify RMI Section 7.1.2 to require that the rack's anchorage to concrete or masonry be based on using design forces determined using load combinations with overstrength provided in *Standard* Section 12.4.3.2 and to require that the anchorage of the rack to concrete comply with *Standard* Section 15.4.9. *Standard* Section 15.5.3.2 was added to modify RMI Section 7.1.4 to require that shim stacks be interlocked or welded together in order to transfer shear forces to the foundation and that bending in the anchors associated with the shims or grout be taken into account in the design of the anchors.

17.4   ELECTRIC GENERATING POWER PLANT, SEISMIC DESIGN CATEGORY D

This example highlights some of the differences between the design of nonbuilding structures and the design of building structures. The boiler building in this example illustrates a solution using the ELF procedure. Due to mass irregularities, the boiler building would probably also require a modal analysis. For brevity, the modal analysis is not illustrated.

17.4.1 Description

Large boilers in coal-fired electric power plants generally are suspended from the supporting steel near the roof level. Additional lateral supports (called buck stays) are provided near the bottom of the boiler. The buck stays resist lateral forces but allow the boiler to move vertically. Lateral seismic forces are resisted at the roof and at the buck stay level. Close coordination with the boiler manufacturer is required in order to determine the proper distribution of seismic forces.

In this example, a boiler building for a 950 MW coal-fired electric power generating plant is braced laterally with ordinary concentrically braced frames in both the north-south and east-west directions. The facility is part of a grid and is not for emergency backup of an Risk Category IV facility.

The dead load of the structure, equipment and piping, W_{DL}, is 16,700 kips.

The weight of the boiler in service, W_{Boiler}, is 31,600 kips.

The natural period of the structure (determined from analysis) is as follows:

North-South, $T_{NS} = 1.90$ seconds
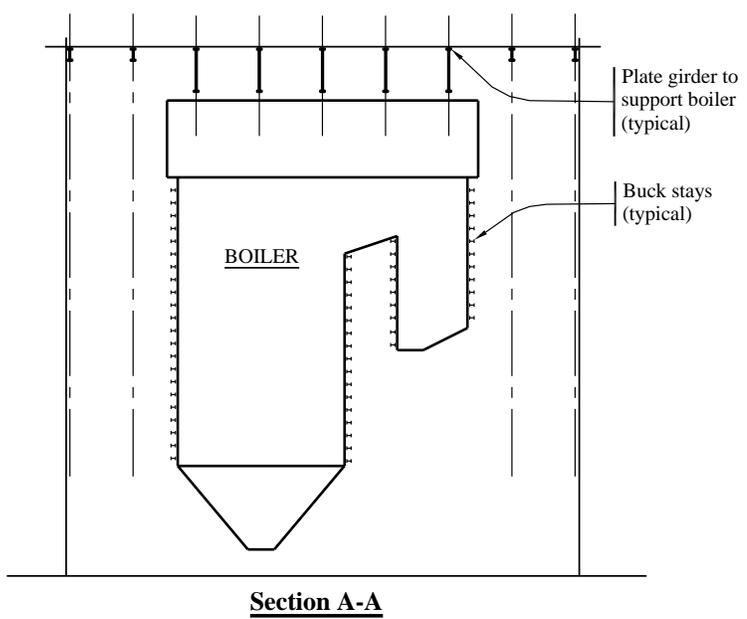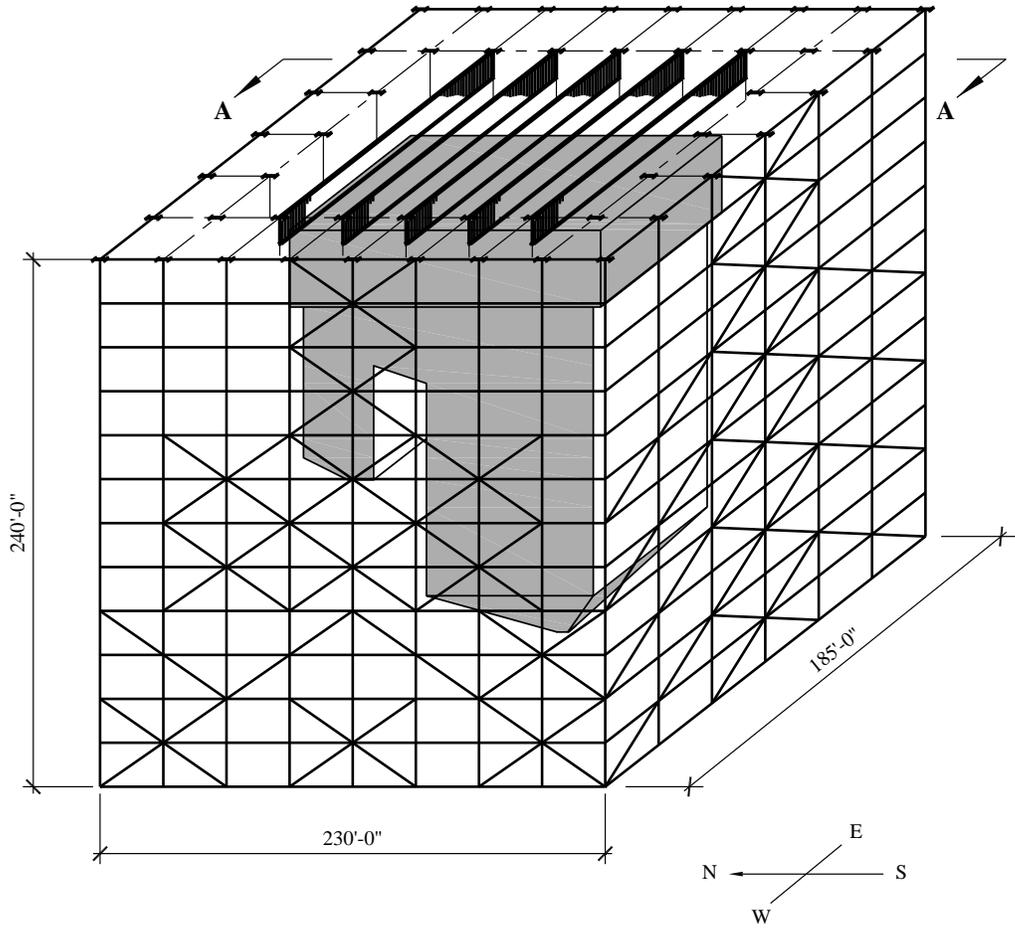East-West, $T_{EW} = 2.60$ seconds

Figure 17.4-1 Boiler building (1.0 ft = 0.3048 m)

17.4.2 *Provisions* Parameters

Risk Category (*Standard* Sec. 1.5.1)	=	III

(for continuous operation, but not for emergency backup of an Risk Category IV facility)

Importance Factor, I_e (*Standard Table* 1.5-2)	=	1.25
Short-period Response, S_S	=	0.864
One-second Period Response, S_1	=	0.261
Site Class (*Standard* Sec. 11.4.2)	=	D

Design Spectral Acceleration Response Parameters

S_{DS}	=	0.665
S_{D1}	=	0.327
Seismic Design Category (*Standard* Sec. 11.6)	=	D
Seismic Force-resisting System (*Standard* Table 15.4-1)	=	Ordinary steel concentrically braced frame with unlimited height
Response Modification Coefficient, R	=	1.5
System Overstrength Factor, Ω_0	=	1
Deflection Amplification Factor, C_d	=	1.5
Height Limit (*Standard* Table 15.4-1)	=	Unlimited

According to *Standard* Section 15.4.1(1), either *Standard* Table 12.2-1 or *Standard* Table 15.4-1 may be used to determine the seismic parameters, although mixing and matching of values and requirements from the tables is not allowed. If the structure were classified as a "building," its height would be limited to 35 feet for a Seismic Design Category D ordinary steel concentrically braced frame, according to *Standard* Table 12.2-1. A review of *Standard* Table 12.2-1 shows that three steel high ductility braced frame systems (two eccentrically braced systems and the special concentrically braced system) and two special moment frame systems can be used at a height of 240 feet. In most of these cases, the additional requirements of *Standard* Section 12.2.5.4 must be met to qualify the system at a height of 240 feet. Boiler buildings normally are constructed using ordinary concentrically braced frames.

As discussed in Section 17.2.3.1 above, Chapter 15 of the *Standard* presents options to increase height limits for design of some nonbuilding structures similar to buildings where *R* factors are reduced. For this example, an ordinary steel concentrically braced frame with unlimited height is chosen from *Standard* Table 15.4-1. By using a significantly reduced *R* value, the seismic design and detailing requirements of AISC 341 need not be applied.

17.4.3 Design in the North-South Direction

17.4.3.1 Seismic response coefficient. Using *Standard* Equation 12.8-2:

$$C_s = \frac{S_{DS}}{R/I_e} = \frac{0.665}{1.5/1.25} = 0.554$$

From analysis, $T = 1.90$ seconds. Using *Standard* Equation 12.8-3, C_S does not need to exceed:

$$C_s = \frac{S_{D1}}{T(R/I_e)} = \frac{0.327}{1.90(1.5/1.25)} = 0.143$$

but using *Standard* Equation 12.8-5, C_s must not be less than:

$$C_s = 0.044 I_e S_{DS} \geq 0.01 = 0.044(1.25)(0.665) = 0.0366$$

Standard Equation 12.8-3 controls; $C_s = 0.143$.

17.4.3.2 Seismic weight. Calculate the total seismic weight, W, as follows:

$$W = W_{DL} + W_{Boiler} = 16{,}700 \text{ kips} + 31{,}600 \text{ kips} = 48{,}300 \text{ kips}$$

17.4.3.3 Base shear. Using *Standard* Equation 12.8-1:

$$V = C_s W = 0.143(48{,}300 \text{ kips}) = 6{,}907 \text{ kips}$$

17.4.3.4 Redundancy factor. The structure in this example meets the requirements of Condition b specified in *Standard* Section 12.3.4.2, because two bays of seismic force-resisting perimeter framing are provided in each orthogonal direction. Therefore, the redundancy factor, ρ, is 1.0.

It is important to note that each story resists more than 35 percent of the base shear because the boiler is hung from the top of the structure. Therefore, each story must comply with the requirements of Condition b. If a story resisted less than 35 percent of the base shear, the requirements of *Standard* Section 12.3.4.2 would not apply and that story would not be considered in establishing the redundancy factor.

17.4.3.5 Determining E. E is defined to include the effects of horizontal and vertical ground motions as follows:

$$E = \rho Q_E \pm E_v$$

where Q_E is the effect of the horizontal earthquake ground motions, which is determined primarily by the base shear just computed and Ev is the effect of the vertical earthquake ground motions.

The *Standard* also requires the consideration of an overstrength factor, Ω_0, on the effect of horizontal motions in defining E for components susceptible to brittle failure.

$$E = \Omega_0 Q_E \pm E_v$$

The ordinary steel concentrically braced frames have components that require such consideration. The beams transferring shear from one set of braces to another act as collectors and, as required by *Standard* Section 12.10.2.1, must be designed for the seismic load effect including overstrength factor.

17.4.3.6 Determining E$_v$. *Standard* Chapter 23A provides an alternate method of determining vertical seismic ground motions that could be used to determine a value of E$_v$ different from the value of $0.2S_{DS}D$ specified in *Standard* Section 12.4.2.2. The *Standard* does not provide any charging language to require the use of *Standard* Chapter 23A. ASCE 7-16 has adopted *Standard* Chapter 23A as a new Section 11.9. ASCE 7-16 Section 11.9 is identical to *Standard* Chapter 23A except that the response spectrum is defined at the MCE$_R$ level. Only ASCE 7-16 Chapter 15 invokes the provisions of Section 11.9. Specifically, ASCE 7-16 Section 15.1.4 requires the use of the provisions of Section 11.9 for tanks, vessels, hanging structures, and nonbuilding structures incorporating horizontal cantilevers.

Because the boiler building of this example contains a hanging boiler, the provisions of ASCE 7-16 Sections 11.9 and 15.1.4 will be applied to determine the vertical seismic load effect, E$_v$.

ASCE 7-16 Section 15.1.4 requires that the design vertical response spectral acceleration, S$_{av}$, be taken as the peak value from the response spectrum of ASCE 7-16 Section 11.9 for hanging structures and nonbuilding structures incorporating horizontal cantilevers. Using ASCE 7-16 Equation 11.9.2-3, the peak vertical response spectral acceleration at the MCE$_R$ is:

$$S_{aMv} = 0.8C_vS_{MS}$$

The coefficient C$_v$ is determined from ASCE 7-16 Table 11.9.2-1 and is based on the value of S$_S$ and the site class. For this example, the value of C$_v$ is 1.23. According to ASCE 7-16 Section 11.9.3, the peak design vertical response spectral acceleration, S$_{av}$, is taken as two-thirds of S$_{aMv}$ and is determined as follows:

$$S_{av} = (2/3)S_{MS}(0.8)(1.23) = 0.665(0.8)(1.23) = 0.654$$

According to ASCE 7-16 Section 12.4.2.2 Exception 1, the value of E$_v$ is determined as follows using ASCE 7-16 Equation 12.4-4b:

$$E_v = 0.3S_{av}D = 0.3(.654)D = 0.197D$$

17.4.4 Design in the East-West Direction
17.4.4.1 Seismic response coefficient. Using *Standard* Equation 12.8-2:

$$C_s = \frac{S_{DS}}{R/I_e} = \frac{0.665}{1.5/1.25} = 0.554$$

From analysis, $T = 2.60$ seconds. Using *Standard* Equation 12.8-3, C_s does not need to exceed:

$$C_s = \frac{S_{D1}}{T(R/I_e)} = \frac{0.327}{2.60(1.5/1.25)} = 0.105$$

Using *Standard* Equation 12.8-5, C_s must not be less than:

$$C_s = 0.044I_eS_{DS} \geq 0.01 = 0.044(1.25)(0.665) = 0.0366$$

Standard Equation 12.8-3 controls; $C_s = 0.105$.

17.4.4.2 Seismic weight. Calculate the total seismic weight, *W,* as follows:

$W = W_{DL} + W_{Boiler} = 16{,}700 \text{ kips} + 31{,}600 \text{ kips} = 48{,}300 \text{ kips}$

17.4.4.3 Base shear. Using *Standard* Equation 12.8-1:

$V = C_sW = 0.105(48{,}300 \text{ kips}) = 5072 \text{ kips}$

17.5   PIER/WHARF DESIGN, SEISMIC DESIGN CATEGORY D

This example illustrates the calculation of the seismic base shear in the east-west direction for the pier using the ELF procedure. Piers and wharves are covered in *Standard* Section 15.5.6.

17.5.1 Description
A cruise ship company is developing a pier in Long Beach, California, to service ocean liners. The pier will be accessible by the general public. The pier contains a large warehouse owned by the cruise ship company. In the north-south direction, the pier is tied directly to an abutment structure supported on grade. In the east-west direction, the pier resists seismic forces using moment frames. Calculations for the abutment are not included in this example, but it is assumed to be much stiffer than the moment frames.

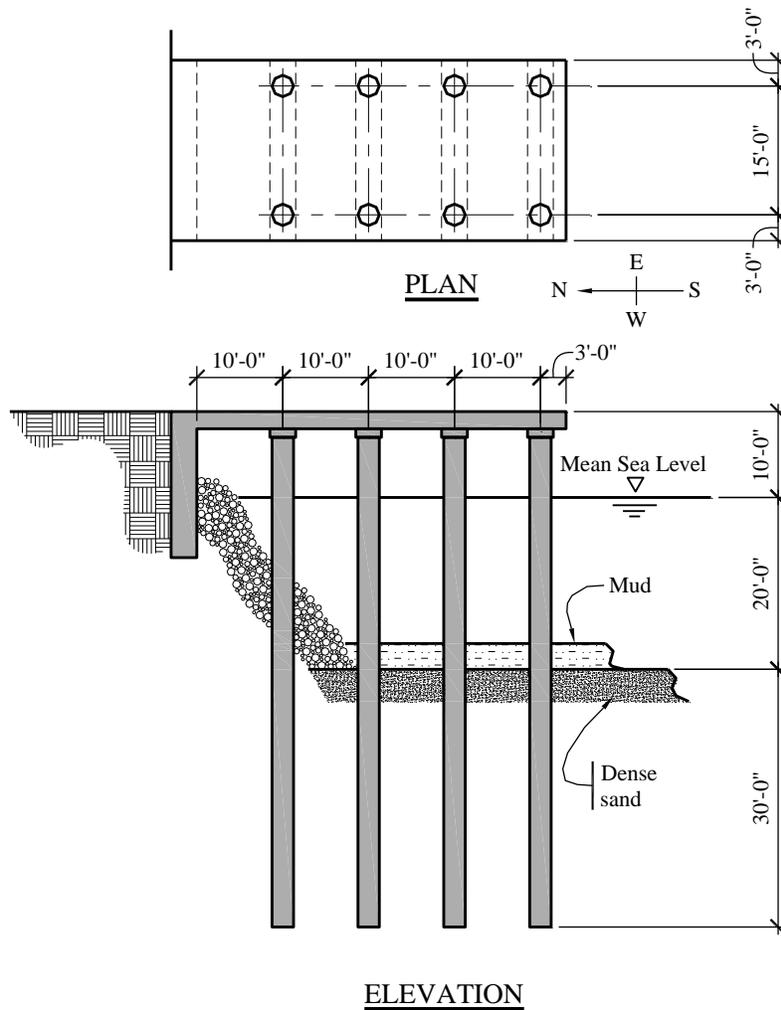The design live load for warehouse storage is 1,000 psf.

Figure 17.5-1 Pier plan and elevation (1.0 ft = 0.3048 m)

17.5.2 *Provisions* Parameters

Risk Category (*Standard* Sec. 1.5.1)	=	II
(The pier serves cruise ships that carry no hazardous materials.)		
Importance Factor, I_e (*Standard Table* 1.5-2)	=	1.0
Site Class (*Standard* Chapter 20)	=	D (dense sand)

Design Spectral Acceleration Response Parameters

S_{DS}	=	1.167
S_{D1}	=	0.60
Seismic Design Category (*Standard* Sec. 11.6)	=	D

Seismic Force-resisting System (*Standard* Table 15.4-1)	=	Intermediate concrete moment frame with permitted height increase
Response Modification Coefficient, R	=	3
System Overstrength Factor, Ω_0	=	2
Deflection Amplification Factor, C_d	=	2.5
Height Limit (*Standard* Table 15.4-1)	=	50 ft

If the structure was classified as a building, an intermediate reinforced concrete moment frame would not be permitted in Seismic Design Category D.

17.5.3 Design of the System

17.5.3.1 Seismic response coefficient. Using *Standard* Equation 12.8-2:

$$C_s = \frac{S_{DS}}{R/I_e} = \frac{1.167}{3.0/1.0} = 0.389$$

From analysis, $T = 0.596$ seconds. Using *Standard* Equation 12.8-3, C_s does not need to exceed:

$$C_s = \frac{S_{D1}}{T(R/I_e)} = \frac{0.60}{0.596(3/1.0)} = 0.336$$

Using *Standard* Equation 12.8-5, C_s must not be less than:

$$C_s = 0.044 I_e S_{DS} \geq 0.01 = 0.044(1.0)(1.167) = 0.0513$$

Standard Equation 12.8-3 controls; $C_s = 0.336$.

17.5.3.2 Seismic weight. In accordance with *Standard* Section 12.7.2, calculate the dead load due to the deck, beams and support piers, as follows:

$$W_{Deck} = 1.0(43 \text{ ft})(21 \text{ ft})(0.150 \text{ kip/ft}^3) = 135.5 \text{ kips}$$

$$W_{Beam} = 4(2 \text{ ft})(2 \text{ ft})(21 \text{ ft})(0.150 \text{ kip/ft}^3) = 50.4 \text{ kips}$$

$$W_{Pier} = 8[\pi(1.25 \text{ ft})^2][(10 \text{ ft - 3 ft}) + (20 \text{ ft})/2](0.150 \text{ kip/ft}^3) = 100.1 \text{ kips}$$

$$W_{DL} = W_{Deck} + W_{Beams} + W_{Piers} = 135.5 + 50.4 + 100.1 = 286.0 \text{ kips}$$

Calculate 25 percent of the storage live load, as follows:

$$W_{1/4 \, LL} = 0.25(1,000 \text{ psf})(43 \text{ ft})(21 \text{ ft}) = 225.8 \text{ kips}$$

Standard Section 15.5.6.2 requires that all applicable marine loading combinations be considered (such as those for mooring, berthing, wave and current on piers and wharves). For this example, additional seismic loads from water flowing around the piles will be considered. A "virtual" mass (Jacobsen, 1959)

of water equal to a column of water of identical dimensions of the circular pile is to be considered in the effective seismic mass. This additional weight is calculated as follows:

$W_{Virtual\ Mass} = 8[\pi(1.25\ \text{ft})^2][(20\ \text{ft})/2](64\ \text{pcf}) = 25.1\ \text{kips}$

Therefore, the total seismic weight is

$W = W_{DL} + W_{1/4LL} + W_{Virtual\ Mass} = 286.0 + 225.8 + 25.1 = 536.9\ \text{kips}$

Additional seismic forces from the water due to wave action may also act on the piles. These additional forces are highly dependent on the acceleration and velocity of the waves and are heavily dependent on the geometry of the body of water. These forces can be calculated using the Morison Equation (Morison, 1950). The determination of these forces is beyond the scope of this example.

17.5.3.3 Base shear. Using *Standard* Equation 12.8-1:

$V = C_sW = 0.336(536.9\ \text{kips}) = 180.4\ \text{kips}$

17.5.3.4 Redundancy factor. The pier in this example has a sufficient number of moment frames that loss of moment resistance at both ends of a single beam would not result in more than a 33 percent reduction in story strength. However, the direct tie to a much stiffer abutment at the north end likely would cause an extreme torsional irregularity for east-west motion, so that Condition (a) would not be met. Condition (b) is not met because two bays of seismic force-resisting perimeter framing are not provided in each orthogonal direction. Therefore, the redundancy factor, ρ, is taken to be 1.3.

17.6   TANKS AND VESSELS, SEISMIC DESIGN CATEGORY D

The seismic response of tanks and vessels can be significantly different from that of buildings. For a structure composed of interconnected solid elements, it is not difficult to recognize how ground motions accelerate the structure and cause inertial forces within the structure. Tanks and vessels, where empty, respond in a similar manner.

Where there is liquid in the tank, the response is much more complicated. As earthquake ground motions accelerate the tank shell, the shell applies lateral forces to the liquid. The response of the liquid to those lateral forces may be amplified significantly if the period content of the earthquake ground motion is similar to the natural sloshing period of the liquid.

Earthquake-induced impulsive fluid forces are those calculated assuming that the liquid is a solid mass. Convective fluid forces are those that result from sloshing in the tank. It is important to account for convective forces on columns and appurtenances inside the tank, because they are affected by sloshing in the same way that waves affect a pier in the ocean.

Freeboard considerations are critical. Oftentimes, the roof acts as a structural diaphragm. If a tank does not have sufficient freeboard, the sloshing wave can rip the roof from the wall of the tank. This could result in failure of the wall and loss of the liquid within.

Seismic design for liquid-containing tanks and vessels is complicated. The fluid mass that is effective for impulsive and convective seismic forces is discussed in AWWA D100 and API 650.

17.6.1 Flat-Bottom Water Storage Tank

17.6.1.1 Description. This example illustrates the calculation of the design base shear and the required freeboard using the procedure outlined in AWWA D100 for a steel water storage tank used to store potable water for fire protection within a chemical plant (Figure 17.6-1). According to *Standard* Section 15.7.7.1, the governing reference document for this tank is AWWA D100. *Standard* Chapter 15 makes no modifications to this document for the seismic design of flat-bottom water storage tanks. ASCE 7-16 has added two exceptions to the use of AWWA D100. The exceptions require that the seismic ground motion values be determined according to ASCE 7-16 Section 11.4 and that the seismic freeboard meet the requirements of ASCE 7-16. AWWA D100 is written in terms of allowable stress design (ASD) while the seismic requirements of the *Standard* are written in terms of strength design. AWWA D100 translates the force equations from the *Standard* by substituting $1.4R$ for R. For the purposes of this example, all loads are calculated in terms of strength design. Where appropriate, AWWA D100 equations are referenced for the determination of impulsive and convective (sloshing) masses.
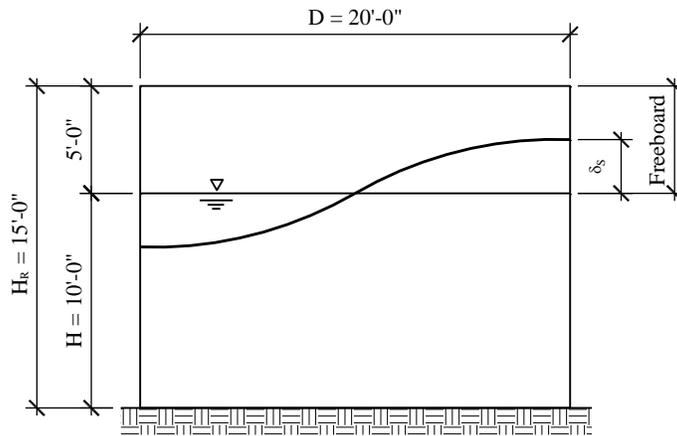
Figure 17.6-1 Storage tank section (1.0 ft = 0.3048 m)

The weight of the tank shell, roof, bottom and equipment is 15,400 pounds.

17.6.1.2 Seismic design parameters.

Risk Category (*Standard* Sec. 1.5.1)	=	IV
Importance Factor, I_e (*Standard Table* 1.5-2)	=	1.5
Long-period Transition Period, T_L	=	6 seconds
Site Class (*Standard* Chapter 20)	=	C (per geotech)

Design Spectral Acceleration Response Parameters

S_{DS}	=	0.824
S_{D1}	=	0.376

Seismic Force-resisting System (*Standard* Table 15.4-2)	=	Flat-bottom, ground-supported, mechanically anchored steel tank
Response Modification Coefficient, R	=	3
System Overstrength Factor, Ω_0	=	2
Deflection Amplification Factor, C_d	=	2.5

17.6.1.3 Calculations for impulsive response.

17.6.1.3.1 Natural period for the first mode of vibration. AWWA D100 Section 13.5.1 does not require the computation of the natural period for the first mode of vibration. The impulsive acceleration is assumed to be equal to S_{DS}.

17.6.1.3.2 Spectral acceleration. Based on AWWA D100 Section 13.5.1, the impulsive acceleration is set equal to S_{DS}.

$$S_{ai} = S_{DS} = 0.824$$

17.6.1.3.3 Seismic (impulsive) weight.

$$W_{tank} = 15.4 \text{ kips}$$

$$W_{iwater} = \pi(10 \text{ ft})^2(10 \text{ ft})(0.0624 \text{ kip/ft}^3) \ (W_i/W_T) = 196.0 \ (0.542) \text{ kips} = 106.2 \text{ kips}$$

The ratio W_i/W_T (= 0.542) was determined from Equation 13-24 (only valid for $D/H \geq 1.333$) of AWWA D100 for a diameter-to-liquid height ratio of 2.0 as shown below:

$$\frac{W_i}{W_T} = \frac{\tanh\left(0.866\dfrac{D}{H}\right)}{0.866\dfrac{D}{H}} = \frac{\tanh\left(0.866\dfrac{20}{10}\right)}{0.866\dfrac{20}{10}} = 0.542$$

$$W_i = W_{tank} + W_{iwater} = 15.4 + 106.2 = 121.6 \text{ kips}$$

17.6.1.3.4 Base Shear.

According to *Standard* Equation 15.7-5:

$$V_i = \frac{S_{ai}W_i}{R/I_e} = \frac{0.824(121.6)}{3/1.5} = 50.1 \text{ kips}$$

17.6.1.4 Calculations for convective response natural period for the first mode of sloshing.

17.6.1.4.1 Natural period for the first mode of sloshing. Using *Standard* Equation 15.7-12:

$$T_c = 2\pi \sqrt{\frac{D}{3.68g \tanh\left(\frac{3.68H}{D}\right)}} = 2\pi \sqrt{\frac{20 \text{ ft}}{3.68\left(32.174 \frac{\text{ft}}{s^2}\right) \tanh\left(\frac{3.68(10 \text{ ft})}{20 \text{ ft}}\right)}} = 2.65 \text{ s}$$

17.6.1.4.2 Spectral acceleration. Using *Standard* Equation 15.7-10 with $T_c < T_L = 6$ seconds:

$$S_{ac} = \frac{1.5S_{D1}}{T_c} = \frac{1.5(0.376)}{2.65} = 0.212$$

17.6.1.4.3 Seismic (convective) weight.

$$W_c = W_{water} (W_c/W_T) = 196 (0.437) = 85.7 \text{ kips}$$

The ratio W_c/W_T ($= 0.437$) was determined from Equation 13-26 (valid for all D/H) of AWWA D100 for a diameter-to-liquid height ratio of 2.0 as shown below:

$$\frac{W_c}{W_T} = 0.230\left(\frac{D}{H}\right)\tanh\left(3.67\frac{H}{D}\right) = 0.230\left(\frac{20}{10}\right)\tanh\left(3.67\frac{10}{20}\right) = 0.437$$

17.6.1.4.4 Base shear. According to *Standard* Equation 15.7-6:

$$V_c = \frac{S_{ac}I_e}{1.5} W_c = \frac{0.212(1.5)}{1.5}(85.7) = 18.2 \text{ kips}$$

17.6.1.5 Design base shear. Item b of *Standard* Section 15.7.2 indicates that impulsive and convective components may, in general, be combined using the SRSS method. *Standard* Equation 15.7-4 requires that the direct sum be used for ground-supported storage tanks for liquids. Note b under *Standard* Section 15.7.6.1 allows the use of the SRSS method in lieu of using *Standard* Equation 15.7-4. Therefore, the base shear is computed as follows:

$$V = \sqrt{V_i^2 + V_c^2} = \sqrt{50.1^2 + 18.2^2} = 53.3 \text{ kips}$$

17.6.1.6 Minimum freeboard. Because the tank is assigned to Risk Category IV, the full value of the theoretical wave height must be provided for freeboard. For the case of Risk Category IV tanks, the wave height is calculated based on the convective acceleration using the actual value of T_L and an importance factor of 1.0. *Standard* Table 15.7-3 indicates that a minimum freeboard equal to δ_s is required for this tank. Using *Standard* Equation 15.7-13 and Note (c) (sets $I_e = 1.0$ for Risk Category IV for wave height determination) from *Standard* Section 15.7.6.1:

$$\delta_s = 0.42D_iI_eS_{ac} = 0.42(20 \text{ ft})(1.0)(0.212) = 1.78 \text{ ft}$$

The 5 feet of freeboard provided is adequate. Please note that AWWA D100 has not been updated to reflect Standard Equation 15.7-13. Under the AWWA D100 rules, the required freeboard is determined as follows:

$$\delta_s = 0.5D_iI_eS_{ac} = 0.5(20 \text{ ft})(1.0)(0.212) = 2.12 \text{ ft}$$

ASCE 7-16 Table 15.7-3, Section 15.7.6.1, and Section 15.7.6.1.2 have been reorganized for increased clarity. No technical changes have occurred relative to the discussions above. Note (c) referenced above has become subsection (b) and placed in Section 15.7.6.1.2.

17.6.2 Flat-Bottom Gasoline Tank

17.6.2.1 Description. This example illustrates the calculation of the base shear and the required freeboard using the procedure outlined in API 650 for a petrochemical storage tank in a refinery tank farm (Figure 17.6-2). The vertical design response spectral acceleration, S_{av}, for use in the determination of shell hoop stress will also be calculated according to the provisions of ASCE 7-16 Sections 11.9 and 15.1.4. An impoundment dike is not provided to control liquid spills. According to Standard Section 15.7.8.1, the governing reference document for this tank is API 650. API 650 is written in terms of allowable stress design (ASD) while the seismic requirements of the *Standard* are written in terms of strength design. API 650 translates the force equations from the *Standard* by substituting R_w for R, where R_w is equal to $1.4R$. For the purposes of this example, all loads are calculated in terms of strength design. Where appropriate, API 650 equations are referenced for the determination of impulsive and convective (sloshing) masses.

The tank is a flat-bottom, ground-supported, self-anchored, welded steel tank constructed in accordance with API 650. The weight of the tank shell, roof, bottom and equipment is 490,000 pounds.
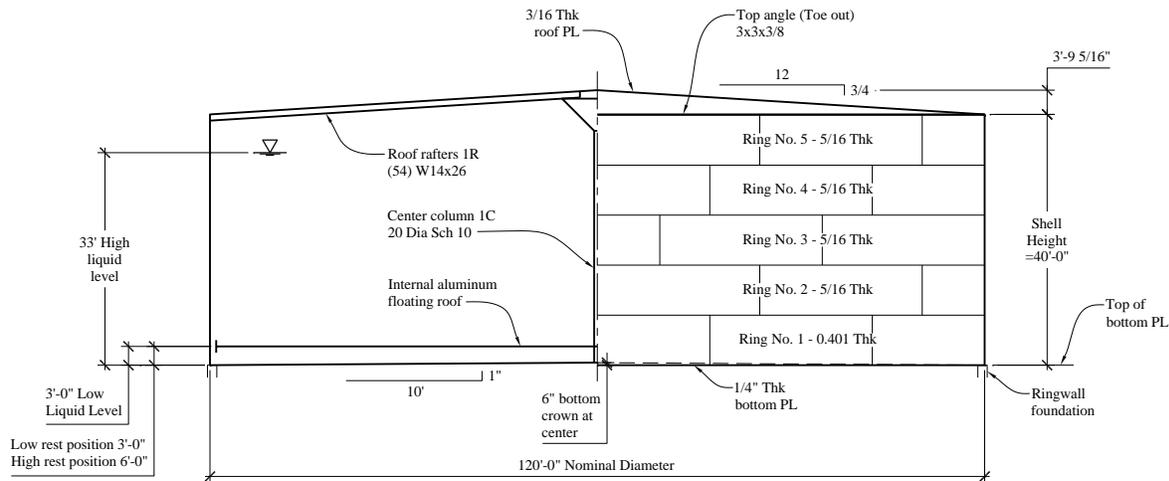
Figure 17.6-2 Storage tank section (1.0 ft = 0.3048 m)

17.6.2.2 Seismic design parameters.

Risk Category (*Standard* Sec. 1.5.1)   =   III
    (The tank is used for storage of toxic or explosive
    material based on an LC(50) value of 5.2 mg per liter
    taken from a typical MSDS for gasoline.)

Importance Factor, I_e (*Standard Table* 1.5-2)   =   1.25

Short-period Response, S_S	=	1.236
One-second Period Response, S_1	=	0.406
Long-period Transition Period, T_L	=	6 seconds
Site Class (*Standard* Chapter 20)	=	C (per geotech)

Design Spectral Acceleration Response Parameters
(Using the same site as in Section 17.6.1)

S_{DS}	=	0.824
S_{D1}	=	0.376
Seismic Force-Resisting System (*Standard* Table 15.4-2)	=	Flat-bottom, ground-supported, self-anchored steel tank
Response Modification Coefficient, R	=	2.5
System Overstrength Factor, Ω_0	=	2
Deflection Amplification Factor, C_d	=	2

17.6.2.3 Calculations for impulsive response.

17.6.2.3.1 Natural period for the first mode of vibration. API 650 Section E.4.5.1 does not require the computation of the natural period for the first mode of vibration. The impulsive acceleration is assumed to be equal to S_{DS}.

17.6.2.3.2 Spectral acceleration. Based on *Standard* Section 15.7.6 Note a, the impulsive acceleration is set equal to S_{DS}.

$S_{ai} = S_{DS} = 0.824$

17.6.2.3.3 Seismic (impulsive) weight.

$W_{tank} = 490.0$ kips

$W_{Gas} = \pi(60 \text{ ft})^2(33 \text{ ft})(0.0474 \text{ kip/ft}^3)(W_i/W_p) = 17{,}691 \text{ kips } (0.316) = 5{,}590 \text{ kips}$

The ratio W_i/W_p (= 0.316) was determined from Equation E.6.1.1-1 (only valid for $D/H \geq 1.333$) of API 650 for a diameter-to-liquid height ratio of 3.636 as shown below:

$$\frac{W_i}{W_p} = \frac{\tanh\left(0.866\dfrac{D}{H}\right)}{0.866\dfrac{D}{H}} = \frac{\tanh\left(0.866\dfrac{120}{33}\right)}{0.866\dfrac{120}{33}} = 0.316$$

$W_i = W_{tank} + W_{Gas} = 490 + 5590 = 6{,}080$ kips

17.6.2.3.4 Base shear. According to *Standard* Equation 15.7-5:

$$V_i = \frac{S_{ai}W_i}{R/I_e} = \frac{0.824(6{,}080)}{2.5/1.25} = 2{,}505 \text{ kips}$$

17.6.2.4 Calculations for convective response.

17.6.2.4.1 Natural period for the first mode of sloshing. Using *Standard* Equation 15.7-12:

$$T_c = 2\pi \sqrt{\frac{D}{3.68g \tanh\left(\frac{3.68H}{D}\right)}} = 2\pi \sqrt{\frac{120 \text{ ft}}{3.68\left(32.174 \frac{\text{ft}}{s^2}\right) \tanh\left(\frac{3.68(33 \text{ ft})}{120 \text{ ft}}\right)}} = 7.22 \text{ s}$$

17.6.2.4.2 Spectral acceleration. Using *Standard* Equation 15.7-11 with $T_c > T_L = 6$ seconds:

$$S_{ac} = \frac{1.5 S_{D1} T_L}{T_c^2} = \frac{1.5(0.376)(6)}{7.22^2} = 0.0649$$

17.6.2.4.3 Seismic (convective) weight.

$$W_c = W_{GAS} (W_c/W_p) = 17{,}691 (0.640) = 11{,}322 \text{ kips}$$

The ratio W_c/W_p (= 0.640) was determined from Equation E.6.1.1-3 (valid for all D/H) of API 650 for a diameter-to-liquid height ratio of 3.636 as shown below:

$$\frac{W_c}{W_T} = 0.230\left(\frac{D}{H}\right)\tanh\left(3.67\frac{H}{D}\right) = 0.230\left(\frac{120}{33}\right)\tanh\left(3.67\frac{33}{120}\right) = 0.640$$

17.6.2.4.4 Base shear. According to *Standard* Equation 15.7-6:

$$V_c = \frac{S_{ac}I_e}{1.5} W_c = \frac{0.0649(1.5)}{1.5}(11{,}322) = 735 \text{ kips}$$

17.6.2.5 Design base shear. Item (b) of *Standard* Section 15.7.2 indicates that impulsive and convective components may, in general, be combined using the SRSS method. *Standard* Equation 15.7-4 requires that the direct sum be used for ground-supported storage tanks for liquids. Note b under *Standard* Section 15.7.6.1 allows the use of the SRSS method in lieu of using *Standard* Equation 15.7-4. Therefore, the base shear is computed as follows:

$$V = \sqrt{V_i^2 + V_c^2} = \sqrt{2505^2 + 735^2} = 2{,}611 \text{ kips}$$

17.6.2.6 Minimum freeboard. Because the tank is assigned to Risk Category III and S_{DS} is greater than 0.50, the freeboard provided must be at least 70 percent of the full value of the theoretical wave height (based on $T_L = 4$ s). For the case of Risk Category III tanks, the wave height is calculated based on the convective acceleration using a value of T_L equal to 4 seconds and an importance factor of 1.25 according

to *Standard* Section 15.7.6.1, Note (d). *Standard* Table 15.7-3 indicates that a minimum freeboard equal to $0.7\delta_s$ is required for this tank. Using *Standard* Equation 15.7-13 and Note (d) (sets $I_e = 1.25$ and T_L to 4 seconds for Risk Category III for wave height determination) from *Standard* Section 15.7.6.1:

$$\delta_s = 0.42 D_i I S_{ac} = 0.42(120 \text{ ft})(1.25)(0.0433) = 2.73 \text{ ft}$$

$$S_{ac} = \frac{1.5 S_{D1} T_L}{T_c^2} = \frac{1.5(0.376)4}{7.22^2} = 0.0433$$

$$0.7\,\delta_s = 1.91 \text{ ft}$$

The 7 feet of freeboard provided also includes a 3-foot allowance for an aluminum internal floating roof and the roof framing. The seismic freeboard must be sufficient to avoid forcing the floating roof into the fixed roof framing. The freeboard provided is adequate. The reduced freeboard requirement recognizes that providing seismic freeboard for Risk Category I, II, or III tanks is an economic decision (reducing damage) and not a life-safety issue. Because of this, a reduced freeboard is allowed. If secondary containment were provided, no freeboard would be required based on *Standard* Table 15.7-3, Footnote (b).

ASCE 7-16 Table 15.7-3, Section 15.7.6.1, and Section 15.7.6.1.2 have been reorganized for increased clarity. No technical changes have occurred relative to the discussions above. Note (d) referenced above has become subsection (c) and placed in Section 15.7.6.1.2. Footnote (b) of *Standard* Table 15.7.3 has been moved to ASCE 7-16 Section 15.7.6.1.2 (d)(3).

17.6.2.7 Determining E_v. *Standard* Chapter 23A provides an alternate method of determining vertical seismic ground motions that could be used to determine a value of E_v different from the value of $0.2S_{DS}D$ specified in *Standard* Section 12.4.2.2. The *Standard* does not provide any charging language to require the use of *Standard* Chapter 23A. ASCE 7-16 has adopted *Standard* Chapter 23A as a new Section 11.9. ASCE 7-16 Section 11.9 is identical to *Standard* Chapter 23A except that the response spectrum is defined at the MCE$_R$ level. Only ASCE 7-16 Chapter 15 invokes the provisions of Section 11.9. Specifically, ASCE 7-16 Section 15.1.4 requires the use of the provisions of Section 11.9 for tanks, vessels, hanging structures, and nonbuilding structures incorporating horizontal cantilevers.

17.6.2.7.1 Natural vertical period. Using ASCE 7-16 Equation C15.7-2:

$$T_v = 2\pi \sqrt{\frac{\gamma_L R H_L^2}{gtE}} = 2\pi \sqrt{\frac{(47.4 \text{ pcf})(60 \text{ ft})(33 \text{ ft})^2}{\left(386 \frac{\text{in}}{s^2}\right)(0.330 \text{ in})(29,000,000 \text{ psi})}} = 0.182 \text{ s}$$

17.6.2.7.2 Design vertical response spectral acceleration. ASCE 7-16 Section 15.1.4 requires that the design vertical response spectral acceleration, S_{av}, used to determine hydrodynamic hoop forces in cylindrical tanks be determined using the requirements of ASCE 7-16 Section 15.7.2c(2).

Using ASCE 7-16 Equation 11.9.2-4 for the natural vertical period $T_v = 0.182$ s, the vertical response spectral acceleration at the MCE$_R$ is:

$$S_{aMv} = 0.8 C_v S_{MS} \left(\frac{0.15}{T_v}\right)^{0.75}$$

The coefficient C_v is determined from ASCE 7-16 Table 11.9.2-1 and is based on the value of S_S and the site class. For this example, the value of C_v is 1.15. According to ASCE 7-16 Section 11.9.3, the design vertical response spectral acceleration, S_{av}, is taken as two-thirds of S_{aMv} and is determined as follows:

$$S_{av} = 0.8C_v \left(\frac{2}{3}\right) S_{MS} \left(\frac{0.15}{T_v}\right)^{0.75} = 0.8(1.15)(0.824)\left(\frac{0.15}{0.182}\right)^{0.75} = 0.656$$

17.7 VERTICAL VESSEL, SEISMIC DESIGN CATEGORY D

17.7.1 Description

This example illustrates the calculation of the base shear using the ELF procedure for a flexible vertical vessel (Figure 17.7-1). The vertical vessel contains highly toxic material (Risk Category IV).

H=100'

D=10'

T=3/8"
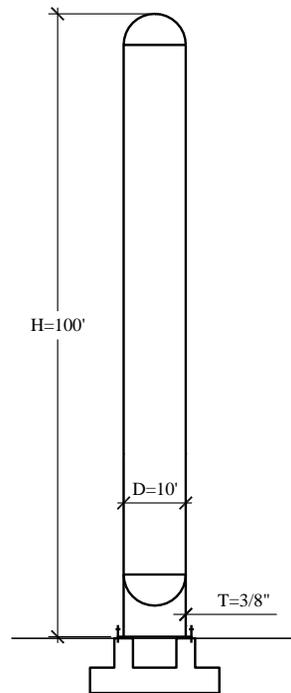
Figure 17.7-1 Vertical vessel (1.0 ft = 0.3048 m)

The weight of the vertical vessel plus contents is 300,000 pounds.

Standard Section 15.4.4 allows the fundamental period of a nonbuilding structure to be determined using a properly substantiated analysis. The period of the vertical vessel is calculated using the equation for a uniform vertical cylindrical steel vessel as found in Appendix 4.A of ASCE (2011). The period of the vessel is calculated as follows:

$$T = \frac{7.78}{10^6}\left(\frac{H}{D}\right)^2 \sqrt{\frac{12WD}{t}} = \frac{7.78}{10^6}\left(\frac{100}{10}\right)^2 \sqrt{\frac{12(300000/100)10}{0.375}} = 0.762\,\text{s}$$

where: T = period (s)
W = weight (lb/ft)
H = height (ft)
D = diameter (ft)
T = shell thickness (in.)

17.7.2 *Provisions* Parameters

17.7.2.1 Ground motion. The design response spectral accelerations are defined as follows:

S_{DS} = 1.86
S_{D1} = 0.79

17.7.2.2 Importance factor. The vertical vessel contains highly toxic material. Therefore, it is assigned to Risk Category IV, as required by *Standard* Section 1.5.1. Using *Standard* Table 11.5.1, the importance factor, I_e, is equal to 1.5.

17.7.2.3 Seismic coefficients. The vertical vessel used in this example is a skirt-supported distributed mass cantilevered structure. There are three possible entries in *Standard* Table 15.4-2 that describe the vessel in question:

1. Elevated tanks, vessels, bins, or hoppers: Single pedestal or skirt supported – welded steel.

2. Elevated tanks, vessels, bins, or hoppers: Single pedestal or skirt supported – welded steel with special detailing.

3. All other steel and reinforced concrete distributed mass cantilever structures not covered herein including stacks, chimneys, silos and skirt-supported vertical vessels that are not similar to buildings.

All three options are keyed to the detailing requirements of *Standard* Section 15.7.10. Two of the options specifically require that Items (a) and (b) of *Standard* Section 15.7.10 be met. The intent of *Standard* Section 15.7.10 and *Standard* Table 15.4-2 is that skirt-supported vessels be checked for seismic loads based on R/I_e = 1.0 if the structure is assigned to Risk Category IV or if an *R* factor of 3.0 is used in the design of the vessel. Skirt-supported vessels fail in buckling, which is not a ductile failure mode, so a more conservative design approach is required. The R/I_e = 1.0 check typically will govern the design of the skirt over using loads determined with an *R* factor of 3 in a moderate to high area of seismic activity. The only benefit of using an *R* factor of 3 in this case is in the design of the foundation. The foundation is not required to be designed for the R/I_e = 1.0 load. For the R/I_e = 1.0 load, the skirt can be designed based on critical buckling (factor of safety of 1.0). The critical buckling strength of a skirt can be determined using a number of published sources. The two most common methods for determining the critical buckling strength of a skirt are ASME BVPC Section VIII, Division 2, Paragraph 4.4 using a factor of safety of 1.0 and AWWA D100 Section 13.4.3.4. An example of calculating the critical buckling strength of the skirt using ASME BVPC Section VIII, Division 2, Paragraph 4.4 is provided.

For this example, the skirt-supported vertical vessel will be treated as "all other steel and reinforced concrete distributed mass cantilever structures not covered herein including stacks, chimneys, silos and skirt-supported vertical vessels that are not similar to buildings" from *Standard* Table 15.4-2. The seismic design parameters for this structure are as follows:

Response Modification Coefficient, R	=	3
System Overstrength Factor, Ω_0	=	2
Deflection Amplification Factor, C_d	=	2.5

17.7.3 Design of the System

17.7.3.1 Seismic response coefficient. Using *Standard* Equation 12.8-2:

$$C_s = \frac{S_{DS}}{R/I_e} = \frac{1.86}{3/1.5} = 0.930$$

Using *Standard* Equation 12.8-3, C_s does not need to exceed:

$$C_s = \frac{S_{D1}}{T(R/I_e)} = \frac{0.79}{0.762(3/1.5)} = 0.518$$

Using *Standard* Equation 15.4-1, C_s must not be less than:

$$C_s = 0.044I_e S_{DS} \geq 0.03 = 0.044(1.5)(1.86) = 0.123$$

Standard Equation 12.8-3 controls; $C_s = 0.518$.

17.7.3.2 Base shear. Using *Standard* Equation 12.8-1:

$$V = C_s W = 0.518(300 \text{ kips}) = 155.4 \text{ kips}$$

17.7.3.3 Vertical distribution of seismic forces. *Standard* Section 12.8.3 defines the vertical distribution of seismic forces in terms of an exponent, k, related to structural period. If the structural period is less than or equal to 0.5 second, $k = 1$ and results in an inverted triangular distribution of forces. If the structural period is greater than or equal to 2.5 seconds, $k = 2$ and results in a parabolic distribution of forces. For periods between 0.5 second and 2.5 seconds, the value of k is determined by linear interpolation between 1 and 2. The significance of the distribution requirements of *Standard* Section 12.8.3 is that the height of the centroid to the horizontal seismic force increases (thus increasing the overturning moment) as the period increases above 0.5 second (Figure 17.7-2).

k = 1 (triangle)	k = value between 1 & 2	k = 2 (parabola)
T = 0.5 s	0.5 s < T < 2.5 s	T = 2.5 s
$\bar{h} = 2/3 \text{ H}$	$\bar{h} = \frac{(k+1)}{(k+2)} \text{ H}$	$\bar{h} = 3/4 \text{ H}$
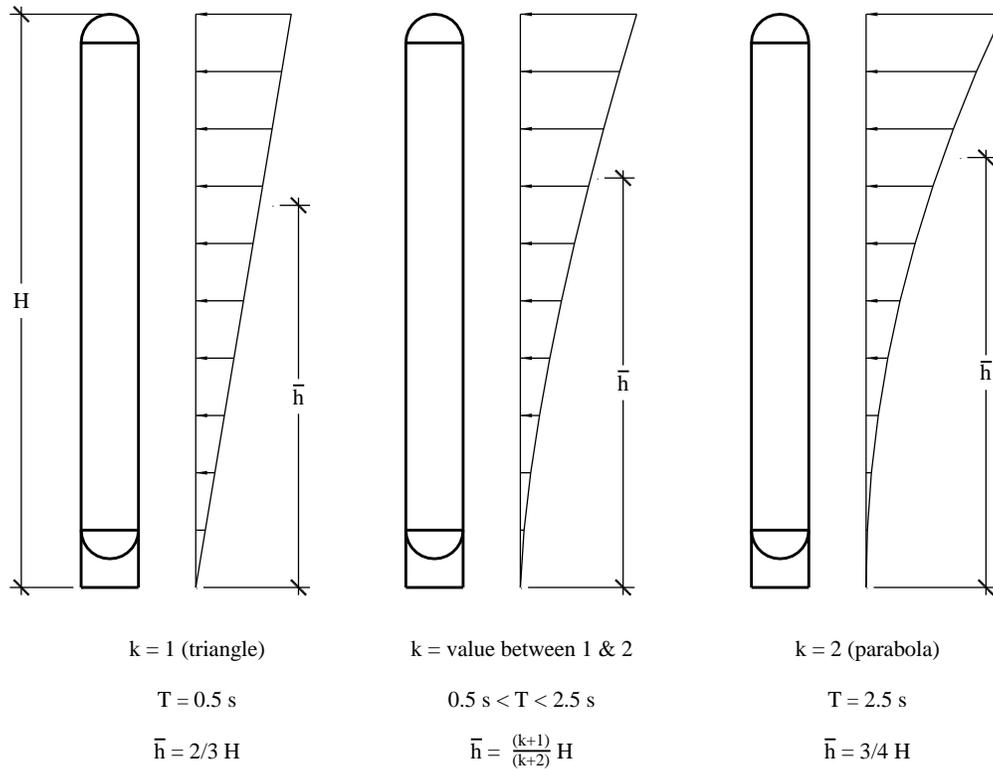
Figure 17.7-2 Vertical distribution of seismic forces

Once k is determined, the height to the centroid, $\bar{h}$, of the horizontal seismic force is equal to:

$$\bar{h} = \frac{(k+1)}{(k+2)}H$$

where H is the vertical height of the vertical vessel.

For the vessel period of $T = 0.762$ second,

$$k = 1 + \frac{0.762 - 0.5}{2.5 - 0.5} = 1.131$$

The value of $\bar{h}$ is then calculated as:

$$\bar{h} = \frac{(1.131 + 1)}{(1.131 + 2)}(100) = 0.681(100) = 68.1 \text{ft}$$

The overturning moment is then calculated as $M = V\bar{h} = 155.4(68.1) = 10,583$ ft-kips.

17.7.3.4 Critical buckling check. The intent of *Standard* Section 15.7.10 and *Standard* Table 15.4-2 is that skirt-supported vessels be checked for seismic loads based on R/I_e = 1.0 (critical buckling check) if the structure is assigned to Risk Category IV or if an *R* factor of 3.0 is used in the design of the vessel. For the R/I_e = 1.0 load, the skirt can be designed based on critical buckling (factor of safety of 1.0). The critical buckling strength of a skirt can be determined using a number of published sources. In this example, the method described in ASME BVPC Section VIII, Division 2, Paragraph 4.4 using a factor of safety of 1.0 will be used.

17.7.3.4.1 Seismic response coefficient with R/I_e = 1.0. Using *Standard* Equation 12.8-2:

$$C_s = \frac{S_{DS}}{R/I_e} = \frac{1.86}{1.0} = 1.86$$

Using *Standard* Equation 12.8-3, C_s does not need to exceed:

$$C_s = \frac{S_{D1}}{T(R/I_e)} = \frac{0.79}{0.762(1.0)} = 1.037$$

Standard Equation 12.8-3 controls; C_s = 1.037.

17.7.3.4.2 Base shear. Using *Standard* Equation 12.8-1:

$V = C_sW = 1.037(300 \text{ kips}) = 311.0 \text{ kips}$

17.7.3.4.3 Vertical distribution of seismic forces. Moment arm from Section 17.7.3.3 above is:

$$\bar{h} = 68.1 \text{ ft}$$

The overturning moment is then calculated as $M = V\bar{h} = 311.0(68.1) = 21{,}181$ ft-kips.

17.7.3.4.4 Stresses at base of skirt.

Axial stress (f_a) = P/A = 300,000/(π(10)12(0.375)) = 2,122 psi

Bending stress (f_b) = M/S = 21,181(1,000)12/[(0.375)π(10(12))^2/4] = 59,930 psi

Shear stress (f_v) = $2V/A$ = 2(311.0)(1,000) /(π(10)12(0.375)) = 4,400 psi

17.7.3.4.5 Evaluation of combined axial stress, bending stress, and shear stress. The procedures outlined in ASME BVPC Section VIII, Division 2, Paragraph 4.4 using a factor of safety of 1.0 will be used below to determine the adequacy of the vessel support skirt under seismic loads based on R/I_e = 1.0. The ASME procedures check many different limit states to arrive at the allowable stress for a particular loading. The example below only identifies the governing conditions for this particular vessel. Please note that all "allowable" stresses shown below are based on a factor of safety of 1.0. Nomenclature is defined in ASME BVPC Section VIII, Division 2.

Uniform Axial Compression (governed by column buckling):

$$F_{xa} = \frac{466F_y}{\left(331 + \frac{D_0}{t}\right)} = 25{,}770 \text{ psi}$$

Allowable longitudinal stress $= F_{ca} = 23{,}081$ psi

Axial compression due to bending moment:

Allowable bending stress $= F_{ba} = F_{xc} = 25{,}770$ psi

In-plane shear:

$a_v = 0.8 \quad C_v = 0.2967 \quad D_o/t = 320$

$$F_{ve} = \frac{a_v C_v E t}{D_0} = 21{,}509 \text{ psi}$$

$n_v = 0.8197$

Allowable shear stress $= F_{va} = n_v F_{ve} = 17{,}631$ psi

Combination of uniform axial compression, axial compression due to bending moment, and shear in the absence of hoop compression:

$$K_s = 1 - \left(\frac{f_v}{F_{va}}\right)^2 = 0.9377$$

$$F_e = \frac{\pi^2 E}{\left(\frac{KL_u}{r}\right)} = 80{,}622 \text{ psi}$$

$C_m = 1.0 \quad K = 2.1 \quad L_u = 1{,}200 \text{ in.}$

$$\delta = \frac{C_m}{\left(1 - \frac{f_a}{F_e}\right)} = 1.027$$

$$\text{Unity} = \frac{f_a}{(2K_s F_{ca})} + \frac{\delta f_b}{(K_s)(F_{ba})} = 2.60 > 1.0 \text{ NG!}$$

The support skirt in this example is inadequate for the seismic loads based on $R/I_e = 1.0$. The thickness of the support skirt must be increased and the critical buckling check repeated.

Design for Nonstructural Components

Robert Bachman, S.E., John Gillengerten, S.E. and Susan Dowty, S.E.

Contents

The 2015 edition of the NEHRP *Recommended Seismic Provisions for New Buildings and Other Structures* adopts by reference the American Society of Civil Engineers, Structural Engineering Institute standard, *ASCE/SEI 7*-10: *Minimum Design Loads for New Buildings and Other Structures*. Since the completion of the 2015 NEHRP *Provisions,* the ASCE *Standard* has been updated. This chapter focuses on illustration and application of the 2015 NEHRP *Provisions*, and changes being made to ASCE/SEI 7 for the 2016 edition. Where the 2015 NEHRP *Provisions* differ from ASCE/SEI 7-16, the differences are indicated, and the focus is on the provisions of ASCE/SEI 7-16.

Chapter 13 of the *Standard* addresses seismic design of the architectural, mechanical and electrical components in buildings. The examples presented here illustrate many of the requirements and procedures. Design and anchorage are illustrated for exterior precast concrete cladding and for a roof-mounted HVAC unit. The rooftop unit is examined in two common installations: directly attached to the structure and a vibration-isolated component installed with snubbers. This chapter also contains an explanation of the fundamental aspects of the *Standard.* Examples are also provided that illustrate how to treat non-ASME piping located within a healthcare facility and a platform-supported vessel located on an upper floor within a building.

The variety of materials and industries involved with nonstructural components is large and numerous documents define and describe methods of design, construction, manufacture, installation, attachment, etc. Some of the documents address seismic issues, but many do not. *Standard* Chapter 23 contains a listing of approved standards for various nonstructural components.

In addition to the *Standard*, the following are referenced in this chapter:

ACI 318	American Concrete Institute. 2014. *Building Code Requirements for Structural Concrete and Commentary.*
ACI 355.2	American Concrete Institute. 2007. *Qualification of Post-Installed Mechanical Anchors in Concrete.*
TMS 402	The Masonry Society. 2011. *Building Code Requirements for Masonry Structures.*
ASHRAE APP IP	American Society of Heating, Refrigeration and Air-Conditioning Engineers (ASHRAE). 1999. *Seismic and Wind Restraint Design*, Chapter 53.
ASME B31.1	American Society of Mechanical Engineers. 2001. *Power Piping*. 2002.
ASME B31.3	American Society of Mechanical Engineers. *Process Piping*. 2002
ASME B31.4	American Society of Mechanical Engineers. *Transportation Systems for Liquid Hydrocarbons and Other Liquids, Pipeline*. 2010.
ASME B31.5	American Society of Mechanical Engineers. *Refrigeration Piping and Heat Transfer Components*.

The symbols used in this chapter are drawn from Chapter 11 of the *Standard* or reflect common engineering usage. The examples are presented in U.S. customary units.

18.1 DEVELOPMENT AND BACKGROUND OF THE REQUIREMENTS FOR NONSTRUCTURAL COMPONENTS

18.1.1 Approach to Nonstructural Components

Nonstructural components include the equipment, distribution systems such as piping, ducts, and electrical raceways, and architectural components. These items make up the majority of the replacement value of most buildings. The *Standard* requires that nonstructural components be checked for two fundamentally different demands placed upon them by the response of the structure to earthquake ground motion: resistance to inertial forces, referred to as seismic forces, and accommodation of imposed displacements. Building codes have long had requirements for resistance to seismic forces and requirements for imposed displacements, due to story of the structure or differential displacements for components spanning between structures, have been added over time. For seismic design, nonstructural components are grouped in broad categories based on their function and behavior under seismic loading. Requirements vary with the ground motion intensity. Components serving essential functions are subject to more stringent requirements.

Specific performance goals for nonstructural components are not explicitly defined, although the commentary of the *Standard* provides expectations of the anticipated behavior of non-critical components in three levels of earthquake shaking intensity:

1. Minor earthquake ground motions—minimal damage not likely to affect functionality;
2. Moderate earthquake ground motions—some damage that may affect functionality; and
3. Design Earthquake ground motions—major damage but significant falling hazards are avoided; likely loss of functionality.

While the nonstructural design provisions focus on reducing the risk to life safety, in some cases the provisions protect functionality and limit economic losses. For example, non-critical equipment in mechanical rooms that are unlikely to topple in an earthquake still requires anchorage, although they pose minimal risk to life safety. The flexible connections between unbraced piping and non-critical equipment are required, but serve mainly to reduce the likelihood of leakage.

Seismic forces for design are computed, considering variation of acceleration with relative height within the structure, and reduction in design force based upon estimated ductility of the component or its attachment. The *Standard* also includes procedures for the evaluating nonstructural components subject to imposed deformations, such as story drift. The seismic force demands tend to control the design for vibration-isolated or heavy components, while the imposed deformations are important for the seismic design of elements that are continuous through multiple levels of a structure or across expansion joints between adjacent structures, such as cladding or piping.

Chapter 13 of the *Standard* is organized into six major sections. Section 13.1 provides information on the applicability of the nonstructural design provisions. Section 13.2 includes general information, with guidance on determining the importance of the component or system, methods for establishing the adequacy of the component for seismic forces, and certification requirements for items identified as critical to life safety or, in essential facilities, items critical to continued function following an earthquake. Section 13.3 contains the procedures for determining the acceleration and displacement demands on nonstructural components. Section 13.4 covers design considerations for attachment of nonstructural components to the structure. Sections 13.5 and 13.6 provide detailed design considerations for architectural components, and mechanical and electrical components, respectively.

The remaining portions of this section describe some of the most important processes described in the *Standard*.

18.1.2 Force Equations

The following seismic force equations are prescribed for nonstructural components (*Standard* Eq. 13.3-1 through 13.3-3):

$$F_p = \frac{0.4a_p S_{DS} W_p}{R_p / I_p}\left(1+2\frac{z}{h}\right)$$

$$F_{p_{max}} = 1.6 S_{DS} I_p W_p$$

$$F_{p_{min}} = 0.3 S_{DS} I_p W_p$$

where:

F_p = horizontal equivalent static seismic design force centered at the component's center of gravity and distributed relative to the component's mass distribution

a_p = component amplification factor (between 1.0 and 2.5) as tabulated in *Standard* Table 13.5-1 for architectural components and *Standard* Table 13.6-1 for mechanical and electrical components

S_{DS} = five percent damped spectral response acceleration parameter at short period as defined in *Standard* Section 11.4.4

W_p = component operating weight

R_p = component response modification factor (between 1.0 to 12.0) as tabulated in *Standard* Table 13.5-1 for architectural components and *Standard* Table 13.6-1 for mechanical and electrical components

I_p = component importance factor (either 1.0 or 1.5) as indicated in *Standard* Section 13.1.3

z = elevation in structure of component point of attachment relative to the base

h = roof elevation of the structure or elevation of highest point of the seismic force-resisting system of the structure relative to the base

The seismic design force, F_p, is to be applied independently in the longitudinal and transverse directions. F_p should be applied in both the positive and negative directions if higher demands will result. The effects of these loads on the component are combined with the effects of static loads. *Standard* Equations 13.3-2 and 13.3-3 provide maximum and minimum limits for the seismic design force.

In addition to force equation Eq. 13.3-1, there are dynamic analysis methods available for determining the seismic design force, F_p. A force equation that utilizes either the linear dynamic analysis procedures of *Standard* Section 12.9, or the nonlinear response history procedures of *Standard* Chapters 16, 17, and 18 is available:

$$F_p = \frac{a_i a_p W_p}{\left(\frac{R_p}{I_p}\right)} A_x$$

(*Standard* Eq. 13.3-4)

where a_i is the acceleration at level i obtained from the modal analysis and A_x is the torsional amplification factor determined by *Standard* Eq.12.8-14. The value of the Response Modification Coefficient of the structure, *R,* is taken as 1.0 when these procedures are used to determined nonstructural forces. Where seismic response history analysis is used with at least seven ground motions, a_i is taken as the average of the maximum accelerations. When less than seven ground motions are used, the maximum acceleration value for each floor is the maximum value obtained from the ground motions analyzed. When using dynamic analysis procedures, the upper and lower limits of F_p determined by *Standard* Eqs. 13.3-2 and 13.3-3 apply.

In the 2016 edition of the *Standard*, additional dynamic analysis options have been introduced. The use of floor response spectra for determination of the seismic design force is now explicitly permitted (*Standard* Sec. 13.3.1.4.1). Application of this approach requires that a floor response spectrum be calculated for the design earthquake at each level of the structure, based on a seismic response history analysis performed in accordance with *Standard* Section 12.9 or in accordance with the procedures in *Standard* Chapters 16, 17 or 18. The floor response spectrum is calculated for each ground motion record analyzed. The floor acceleration, a_i, is the maximum acceleration value from the floor response spectra for the component period, and the value of a_p shall be taken as 1.0.

An alternate floor response spectra method based on a modal analysis is also available (*Standard* Sec. 13.3.1.4.2). The periods of vibration and mode shapes of the structure must be calculated for at least the first three modes in each orthogonal direction using the modal analysis procedure in *Standard* Section 12.9. The modal participation factors for each of the first three modes are calculated in each direction. The component dynamic amplification factor, D_{AF}, determined by the ratio of the component period, T_p, to the building modal period, T_x, is determined based on *Standard* Figure 13.3-1, reproduced in Figure 18.1-1.
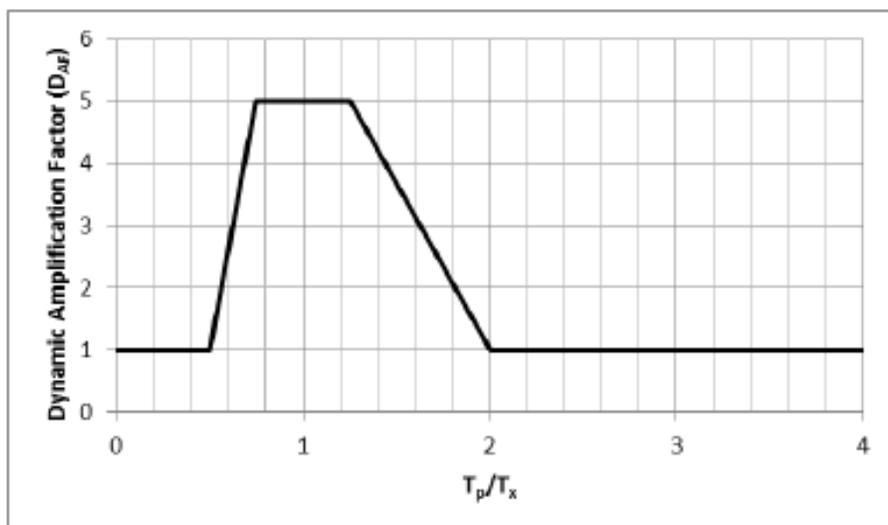
Figure 18.1-1 Component dynamic amplification factor

For each of the first three modes in each direction, the modal acceleration for components at each floor is calculated as a function of the nonstructural component period based on *Standard* Eq. 13.3-5:

$$A_{ix} = p_{ix}S_{ai}D_{AF} \qquad (Standard \text{ Eq. 13.3-5})$$

where A_{ix} is the floor acceleration for mode x at Level i, p_{ix} is the modal participation factor for mode x at Level i obtained from the modal analysis, S_{ai} is the spectral acceleration for mode x, and D_{AF} is the dynamic amplification factor as a function of the ratio of component period to building period for mode x using Figure 18.1-1. The floor response spectrum is taken as the maximum floor acceleration at each building modal period for at least the first three modes, but not less than the spectral acceleration at the base of the building. The design seismic horizontal force in each direction for a nonstructural component shall be determined by *Standard* Eq. 13.3-4 with the product of a_ia_p replaced by A_{ix}, the acceleration from the floor response spectrum for the period of vibration of the nonstructural component at the Level i on which the nonstructural component is anchored.

Many nonstructural components are attached to the structure at different heights in the structure, for example pipe risers and many curtain wall systems. When this condition occurs, a force, F_p, should be determined based on *Standard* Equation 13.3-1 for each point of attachment. The minima and maxima determined from *Standard* Equations 13.3-2 and 13.3-3 must be considered in determining each F_p. The weight, W_p, used to determine each F_p should be based on the tributary weight of the component associated with the point of attachment. When designing the component, the attachment force, F_p, should be distributed relative to the component's mass distribution over the area used to establish the tributary weight. With the exception of structural walls and anchorage of concrete or masonry structural walls, which are covered by *Standard* Chapter 12, each anchorage force should be based on simple statics determined by using all the distributed loads applied to the complete component. Cantilever parapets that are part of a continuous element should be checked separately for parapet forces.

18.1.3 Load Combinations and Acceptance Criteria

Earthquakes cause loads on structures and nonstructural components in both the horizontal and vertical directions. When these loads are applied to structural and nonstructural systems, the results (forces, stresses, displacements, etc.) are called "effects". In *Standard* Section 12.4.2, seismic load effects are defined. The effects resulting from horizontally applied seismic loads are termed horizontal load effects, E_h and the effects resulting from vertically applied seismic loads are termed vertical load effects, E_v. The E_v term is simply a constant $0.2S_{DS}$ multiplied by the dead load.

Load combinations for use in determining the overall demand on an item are defined in *Standard* Section 2.3. Because the load combinations defined in *Standard* Section 2.3 provide a single term, E, to define the earthquake, *Standard* Section 12.4.2 separates the horizontal and vertical components of the seismic load. Unless otherwise noted in the *Standard*, the load combinations provided in *Standard* Section 12.4 are used for the seismic design of all structures and nonstructural components.

18.1.3.1 Seismic load effects. The horizontal seismic load effect E_h and vertical seismic load effect E_v are determined by applying the horizontal component load F_p and the vertical dead load D, respectively, in the structural analysis as indicated below.

$E_h = \rho Q_E$
(*Standard* Eq. 12.4-3)

$E_v = 0.2S_{DS}D$
(*Standard* Eq. 12.4-4a)

where:

Q_E = effect of horizontal seismic forces   (*Standard* Sec. 12.4.2.1)

   (due to application of F_p for nonstructural components)

ρ = redundancy factor = 1.0 for nonstructural components   (*Standard* Sec 13.3.1)

   D = dead load effect (due to vertical load application)

Where the effects of vertical gravity loads and horizontal earthquake loads are additive,

$E = \rho Q_E + 0.2 S_{DS} D$

And where the effects of vertical gravity load counteract those of horizontal earthquake loads,

$E = \rho Q_E - 0.2 S_{DS} D$

where:

E = effect of horizontal and vertical earthquake-induced forces

18.1.3.2 Strength load combinations *Standard* Sections 2.3 and 2.4 provide load combinations to determine design member forces, stresses and displacements. In *Standard* Section 2.3, load combinations are provided for Strength Design and in *Standard* Section 2.4, load combinations are provided for Allowable Stress Design. For purposes of the Chapter 18 examples, only the Strength Load Combinations are used.

The terms defined above in Section 18.1.3.1 are substituted for E in the Basic Load Combinations for Strength Design of *Standard* Section 2.3.6 to determine the design seismic loads. Once the substitutions have been made, the strength load combinations are presented in *Standard* Section 2.3.6:

$1.2D + E_v + E_h + L + 0.2S$ (*Standard* Basic Load Combination 6)

$0.9D - E_v + E_h$ (*Standard* Basic Load Combination 7)

For nonstructural components, the terms L and S are typically zero. For nonstructural components, load combinations with the overstrength factor are applicable only to the design of attachments to concrete and masonry and are discussed in Section 18.1.10.

18.1.4 Component Amplification Factor

The component amplification factor, a_p, found in *Standard* Equations 13.3-1 and 13.3-4 represents the dynamic amplification of the component relative to the maximum acceleration of the component support point(s). Typically, this amplification is a function of the fundamental period of the component, T_p and the fundamental period of the supporting structure, T. An analytical method for determining the fundamental period nonstructural components is provided in *Standard* Section 13.3.3. When this approach is used, the effects of the mass and stiffness of the supports and attachments of the component must be included in the period determination. Use of this approach should limited to nonstructural components that can be reasonably idealized as single-degree of freedom oscillators. The period of nonstructural components with complex mass or stiffness configurations should be obtained using shake-table or pullback tests.

When components are designed or selected, the effective fundamental period of the structure, T, is not always available. Also, for most nonstructural components, the component fundamental period, T_p, can be obtained accurately only by expensive shake-table or pullback tests. As a result, the determination of a component's fundamental period by dynamic analysis, considering T/T_p ratios, is not always practicable. For this reason, acceptable values of a_p are provided in the *Standard* tables. Component amplification factors from either these tables or a dynamic analysis may be used. Values for a_p are tabulated for each component based on the expectation that the component will behave in either a rigid or a flexible manner. For simplicity, a step function increase based on input motion amplifications is provided to help distinguish between rigid and flexible behavior. If the fundamental period of the component is less than 0.06 second, no dynamic amplification is expected and a_p may be taken to equal 1.0. If the fundamental period of the component is greater than 0.06 second, dynamic amplification is expected and a_p is taken to equal 2.5. Acceptable procedures for determining a_p are provided in *Standard Commentary* Chapter 13.

18.1.5 Seismic Coefficient at Grade

The short-period design spectral acceleration, S_{DS}, considers the site seismicity and local soil conditions. The site seismicity is obtained from the design value maps (or software) and S_{DS} is determined in accordance with *Standard* Section 11.4.4. The coefficient S_{DS} is the used to design the structure. The *Standard* approximates the effective peak ground acceleration as $0.4S_{DS}$, which is why 0.4 appears in *Standard* Equation 13.3-1.

18.1.6 Relative Location of the Component in the Structure

The relative location term in *Standard* Eq. 13.3-1, $\left(1 + 2\dfrac{z}{h}\right)$, scales the seismic coefficient at grade, resulting in values varying linearly from 1.0 at grade to 3.0 at roof level. This factor approximates the dynamic amplification of ground acceleration by the supporting structure. As noted in Section 18.1.2 dynamic analysis procedures are provided that permit alternate methods for considering the effects of dynamic amplification of ground accelerations.

18.1.7 Component Response Modification Factor

The component response modification factor, R_p, represents the energy absorption capability of the component's construction and attachments. In the absence of applicable research, these factors are based on judgment based on the following benchmark values:

R_p = 1.0 or 1.5: brittle or buckling failure mode is expected

R_p = 2.5: some minimal level of energy dissipation capacity

R_p = 3.5: ductile materials and detailing

R_p = 4.5: non-ASME B31 conforming piping and tubing with threaded joints and/or mechanical couplings

R_p = 6.0: ASME 31 conforming piping and tubing with threaded joints and/mechanical couplings, or highly ductile equipment.

R_p = 9.0 or 12.0: highly ductile piping and tubing joined with brazing or butt welding. Note that for the purposes of attachment design, *Standard* Section 13.4.1 limits the value of R_p to 6.0.

18.1.8 Component Importance Factor

The component importance factor, I_p, which has a value of either 1.0 or 1.5, is applied to the force and displacement demands on the component. An importance factor of 1.5 is applied to components with greater life safety or hazard exposure importance. The importance factor of 1.5 is intended to improve the functionality of the component or structure by requiring design for a lesser amount of inelastic behavior and providing larger capacity to accommodate seismically induced displacements. It is assumed that reducing the amount of inelastic behavior will result in a component that will have a higher likelihood of functioning after a major earthquake.

18.1.9 Accommodation of Seismic Relative Displacements

In addition to the seismic design force, nonstructural components must be capable of accommodating the effects of seismic relative displacements, both within the structure in the form of interstory drifts, and between structures when nonstructural components are supported on separate adjacent structures. The seismic relative displacement demands, D_{pI}, are determined using equation 13.3-6 of the Standard:

$$D_{pI} = D_p I_e$$

where:

$D_p =$ $\qquad$ displacements within or between structures

I_e = the importance factor for the structure $\hfill$ (*Standard* Sec 11.5.1)

The *Standard* requires that displacements, D_p, be determined in accordance with several equations. For two connection points on Structure A (or on the same structural system), one at Level x and the other at Level y, D_p is determined from *Standard* Equation 13.3-7:

$$D_p = \Delta_{xA} - \Delta_{yA}$$

Because the computed displacements frequently are not available to the designer of nonstructural components, one may use the maximum permissible structural displacements per *Standard* Equation 13.3-8:

$$D_p = \frac{\left(h_x - h_y\right)}{h_{sx}} \Delta_{aA}$$

For two connection points on Structures A and B (or on two separate structural systems), one at Level x *and* the other at Level y, D_P is determined from *Standard* Equations 13.3-9 and 13.3-10:

$$D_p = \left|\delta_{xA}\right| + \left|\delta_{yB}\right|$$

$$D_p = \frac{h_x \Delta_{aA}}{h_{sx}} + \frac{h_y \Delta_{aB}}{h_{sx}}$$

where:

D_p = seismic displacement that the component must be designed to accommodate.

δ_{xA} = deflection of building Level x of Structure A, determined by an elastic analysis as defined in *Standard* Section 12.8.6 including being multiplied by the C_d factor.

δ_{yA} = deflection of building Level y of Structure A, determined in the same fashion as δ_{xA}.

h_x = height of upper support attachment at Level x as measured from the base.

h_y = height of lower support attachment at Level y as measured from the base.

Δ_{aA} = allowable story drift for Structure A as defined in *Standard* Table 12.2-1.

h_{sx} = story height used in the definition of the allowable drift, Δ_a, in *Standard* Table 12.2-1.

δ_{yB} = deflection of building Level y of Structure B, determined in the same fashion as δ_{xA}.

Δ_{aB} = allowable story drift for Structure B as defined in *Standard* Table 12.2-1. Note that Δ_{aA}/h_{sx} = the drift index.

The effects of seismic relative displacements must be considered in combination with displacements caused by other loads as appropriate. Specific methods for evaluating seismic relative displacement effects on components and associated acceptance criteria are not specified in the *Standard*. However, the intention is to satisfy the purpose of the *Standard*. Therefore, for nonessential facilities, nonstructural components can experience serious damage during the design-level earthquake provided they do not constitute a serious life-safety hazard. For essential facilities, nonstructural components can experience some damage or inelastic deformation during the design-level earthquake provided they do not significantly impair the function of the facility.

18.1.10 Component Anchorage Factors and Acceptance Criteria

Design seismic forces in the connected parts, F_p, are prescribed in *Standard* Section 13.4. The requirements for anchorage to concrete and masonry were revised in the 2010 and 2016 editions of the *Standard*.

Design capacity for anchors in concrete is determined in accordance with ACI 318 Appendix D. Design capacity for anchors in masonry is determined in accordance with ACI 530. Anchors are designed to either have ductile behavior or they must have a specified degree of excess strength. In earlier editions of the *Standard*, anchors embedded in concrete or masonry were proportioned to carry the least of 1.3 times the prescribed seismic design force, or the maximum force that can be transferred to the anchor by the component or its support. There was also a limit on the value of the component response modification factor, R_p used in Section 13.3.1 to determine the forces in the connected part (i.e., the anchor).

The provisions for anchorage in ASCE/SEI 7-10 were substantially simplified, both to improve ease of use and to harmonize the provisions for anchor design in concrete and masonry with the reference standards. Adjustments on the R_p value used for the anchorage calculation were eliminated, with the exception of an upper limit on R_p of 6, which is intended primarily to address the anchorage of ductile piping systems that are assigned higher R_p values. Higher values of R_p reflect the inherent ductility and overstrength of ductile piping but resulted in an under prediction of the forces on the anchorage.

For anchors in concrete and masonry, at least one of the following conditions must be satisfied:

Either the component or a support in the load path leading to the structure undergoes ductile yielding at a load level less than the design strength of the corresponding anchor, or

The anchors are designed to resist the load combinations considering Ω_0 in accordance with *Standard* Section 2.3.6.

In the 2016 edition of the *Standard*, the maximum value of Ω_0 for nonstructural components has been reduced from 2½ to 2.

Post-installed anchors in concrete must be prequalified for seismic applications in accordance with the procedures of ACI 355.2 or other approved standards. Post-installed anchors in masonry must be prequalified for seismic applications in accordance with approved qualification procedures. Use of power actuated fasteners in concrete, masonry, or steel is not permitted for sustained tension or bracing applications in Seismic Design Categories D, E and F unless approved for such loading. Exceptions in *Standard* Section 13.4.5 permit the use of power actuated fasteners in certain conditions when the applied loads are low.

Friction clips may be used to resist seismic loads, but are not permitted to resist sustained gravity loads in Seismic Design Categories D, E and F.

Determination of design seismic forces in anchors must consider installation eccentricities, prying effects, multiple anchor effects and the stiffness of the connected system. When there are multiple attachments in one location such as a base plate with multiple anchors, the stiffness and ductility of the all parts of the seismic load path, including the component itself, component supports, attachments, and the supporting structure must be evaluated for their ability to redistribute loads to the attachments in the group.

18.1.11 Construction Documents

Construction documents must be prepared by a registered design professional and must include sufficient detail for use by the owner, building officials, contractors and special inspectors; *Standard* Section 13.2.7 includes specific requirements.

18.1.12 Exempt Items

The requirements in Chapter 13 of the *Standard* are intended to apply only to permanently attached components, not to furniture, temporary items, or mobile units. Permanently attached nonstructural components may be exempt, provided that due to their inherent strength and stability, they can meet the nonstructural performance objectives without explicitly meeting all the requirements of Chapter 13. Examples of nonstructural components that are exempt include:

1) Furniture, (except storage cabinets as noted in *Standard* Table 13.5-1).
2) Temporary or movable equipment.
3) Architectural components in Seismic Design Category B other than parapets supported by bearing walls or shear walls provided that the component importance factor, I_p, is equal to 1.0.
4) Mechanical and electrical components in Seismic Design Category B.
5) Mechanical and electrical components in Seismic Design Category C provided that either:
   a) The component importance factor, I_p, is equal to 1.0 and the component is positively attached to the structure; or

b) The component weighs 20 lb (89 N) or less or, in the case of a distributed system, 5 lb/ft (73 N/m) or less.

6) Discrete mechanical and electrical components in Seismic Design Categories D, E or F that are positively attached to the structure, provided that either

    a) The component weighs 400 lb (1780 N) or less, the center of mass is located 4 ft (1.22 m) or less above the adjacent floor level, flexible connections are provided between the component and associated ductwork, piping and conduit, and the component importance factor, I_p, is equal to 1.0; or

    b) The component weighs 20 lb (89 N) or less or, in the case of a distributed system, 5 lb/ft (73 N/m) or less.

7) Distribution systems in Seismic Design Categories D, E or F included in the exceptions for conduit, cable tray and raceways in *Standard* Section 13.6.6, duct systems in *Standard* Section 13.6.7 and distribution, piping and tubing systems in *Standard* Section 13.6.8, may be exempt provided they meet all the specified conditions listed in the *Standard*. Where in-line components such as valves, in-line suspended pumps, and mixing boxes require independent support, they must be designed as discrete components and must be braced considering the tributary contribution of the attached distribution system.

18.1.13 Pre-Manufactured Modular Mechanical and Electrical Systems

The *Standard* now includes guidance on the design of pre-manufactured modular mechanical and electrical systems. These factory-built units are transported to the site and assembled together. Section 13.1.5 of the *Standard* directs the user to *Standard* Chapter 15, Nonbuilding Structures, for the design of the modular unit itself. Nonstructural components installed or supported by the modular unit are designed in accordance with *Standard* Chapter 13.

18.2 ARCHITECTURAL CONCRETE WALL PANEL

18.2.1 Example Description

In this example, the architectural components are a 4.5-inch-thick precast normal-weight concrete spandrel panel and a column cover supported by the structural steel frame of a five-story building, as shown in Figures 18.2-1 and 18.2-2.
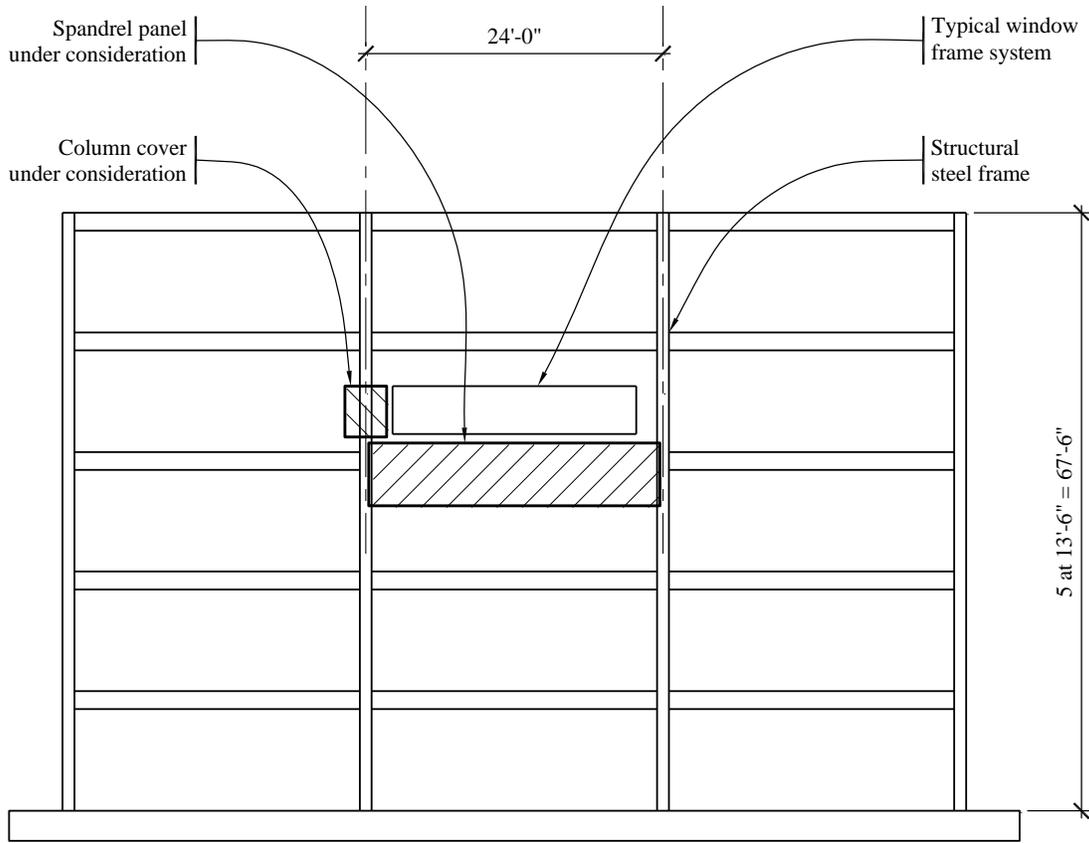
Figure 18.2-1 Five-story building elevation showing panel location
(1.0 ft = 0.3048 m)
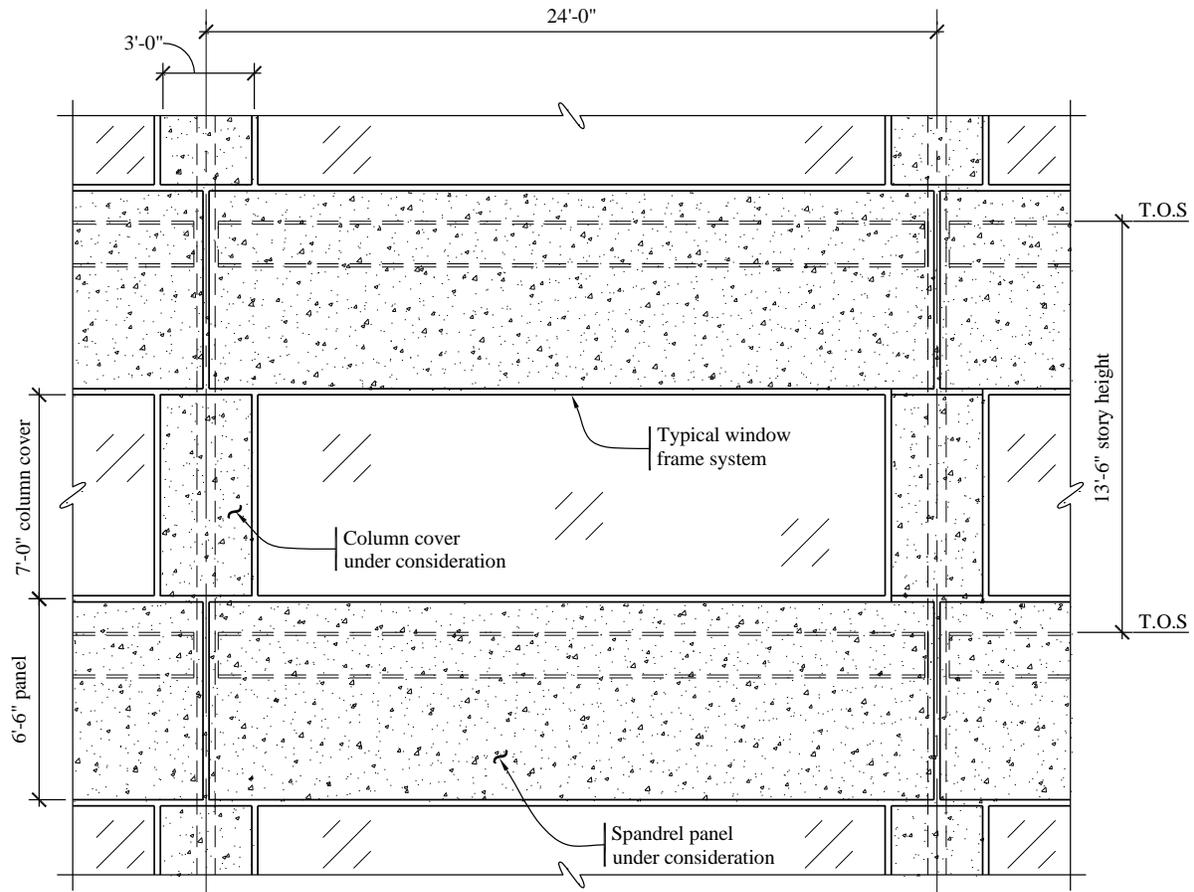
Figure 18.2-2 Detailed building elevation
(1.0 ft = 0.3048 m)

The columns at the third level of the five-story office building support the spandrel panel under consideration. The columns between the third and fourth levels of the building support the column cover under consideration. The building, located near a significant active fault, is assigned to Seismic Risk Category II. Wind pressures normal to the building are 17 psf, determined in accordance with the *Standard*. The spandrel panel supports glass windows weighing 10 psf.

This example develops prescribed seismic forces for the selected spandrel panel and prescribed seismic displacements for the selected column cover, including revisions to the provisions for exterior wall element connections made in the 2016 edition of the *Standard*.

Details of precast connections vary according to the preferences and local practices of the precast panel supplier. In addition, some connections may involve patented designs. This example will concentrate on quantifying the prescribed seismic forces and displacements. After the prescribed seismic forces and displacements are determined, the connections can be detailed and designed according to the appropriate AISC and ACI codes and the recommendations of the Precast/Prestressed Concrete Institute (PCI). New requirements for connections that accommodate story drift through sliding or bending of steel rods are discussed.

18.2.2   Design Requirements

18.2.2.1 *Provisions* Parameters and Coefficients

$a_p = 1.0$ for wall panels and the body of the panel connections (*Standard* Table 13.5-1)

$a_p = 1.25$ for fasteners of the connecting system (*Standard* Table 13.5-1)

$S_{DS} = 1.487$ (for the selected location and site class) (given)

Seismic Design Category = D (*Standard* Table 11.6-1)

Spandrel panel $W_p = (150 \text{ lb/ft}^3)(24 \text{ ft})(6.5 \text{ ft})(0.375 \text{ ft}) = 8{,}775 \text{ lb}$

Glass $W_p = (10 \text{ lb/ft}^2)(21 \text{ ft})(7 \text{ ft}) = 1{,}470 \text{ lb}$ (supported by spandrel panel)

Column cover $W_p = (150 \text{ lb/ft}^3)(3 \text{ ft})(7 \text{ ft})(0.375 \text{ ft}) = 1{,}181 \text{ lb}$

$R_p = 2.5$ for wall panels and the body of the panel connections (*Standard* Table 13.5-1)

$R_p = 1.0$ for fasteners of the connecting system (*Standard* Table 13.5-1)

$I_p = 1.0$ (*Standard* Sec. 13.1.3)

$\Omega_0 = 1.0$ for fasteners of the connecting system (*Standard* Table 13.5-1)

$$\frac{z}{h} = \frac{40.5 \text{ ft}}{67.5 \text{ ft}} = 0.6$$ (at third floor)

According to *Standard* Sections 13.3.1 and 12.3.4.1 Item 3, the redundancy factor, ρ, for nonstructural components is taken as 1.0 in load combinations where it appears.

18.2.2.2 Performance Criteria. Component failure must not cause failure of an essential architectural, mechanical, or electrical component (*Standard* Sec. 13.2.3).

Component seismic attachments must be bolted, welded, or otherwise positively fastened without considering the frictional resistance produced by the effects of gravity (*Standard* Sec. 13.4).

The effects of seismic relative displacements must be considered in combination with displacements caused by other loads as appropriate (*Standard* Sec. 13.3.2).

Exterior nonstructural wall panels that are attached to or enclose the structure must be designed to resist the forces in accordance with *Standard* Section 13.3.1 and must be able to accommodate movements of the structure resulting from response to the design basis ground motion, D_{pl}, or temperature changes (*Standard* Sec. 13.5.3).

18.2.3   Spandrel Panel

18.2.3.1 Connection Details. Figure 18.2-3 shows the types and locations of connections that support one spandrel panel.
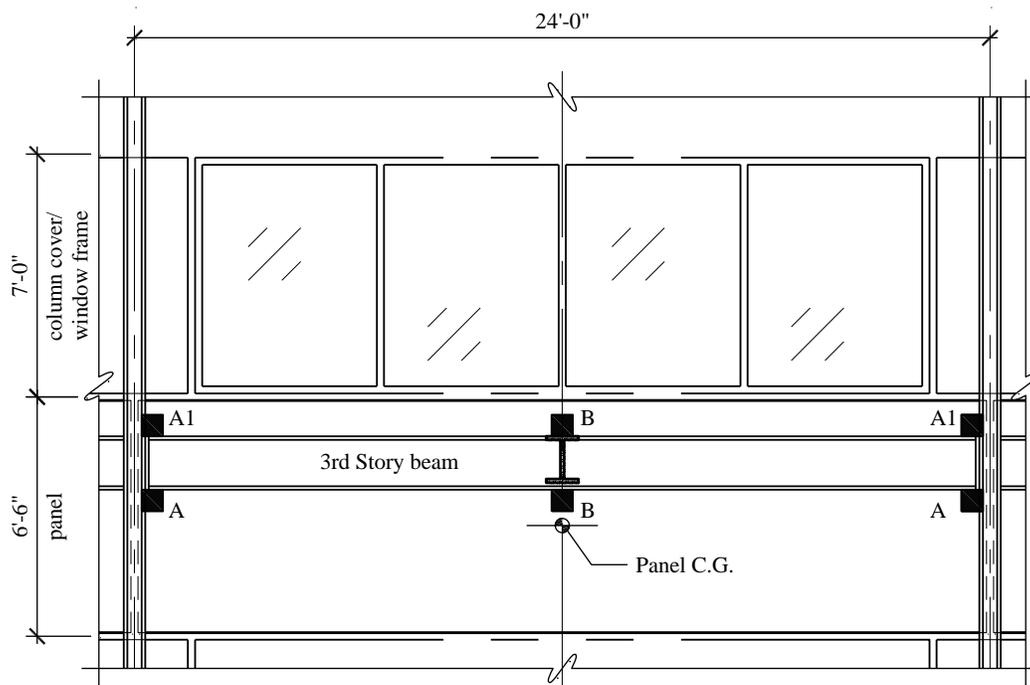
Figure 18.2-3 Spandrel panel connection layout from interior
(1.0 ft = 0.3048 m)

The connection system must resist the weight of the panel and supported construction including the eccentricity between that load and the supports as well as forces generated by response to the seismic motions in all three dimensions. Furthermore, the connection system must not create undue interaction between the structural frame and the panel, such as restraint of thermal movements of the panel or the transfer of floor live load from the floor beam to the panel. The panels are usually very stiff compared to the frame and this requires careful release of potential constraints at connections. PCI's *Architectural Precast Concrete* (Third Edition, 2007) provides an extended discussion of important design concepts for such panels.

For this example, the panel dead load and vertical seismic accelerations are resisted at the two connections identified as A, which provide the recommended simple and statically determinant system for supporting the gravity load of the panel. These connections are often referred to as bearing connections. As shown in Figure 18.2-5, there is an eccentricity between center of mass of the panel and the reaction at the vertical support, which generates a moment that is resisted by a force couple at the pairs of A1 and A connections. Horizontal loads parallel to the panel are resisted by the A connections. Horizontal loads perpendicular to the panel are resisted by the A and A1 connections at the ends of the panel and the pair of B connections mid-span. The bearing connections (A), resist forces in vertical, longitudinal (in-plane), and transverse (out-of-plane) directions while the A1 and B connections resist forces in only the out-of-plane direction.

The practice of resisting the horizontal in-plane force at two points varies with seismic demand and local industry practice. An alternative option is to resist all of the in-plane horizontal force at one connection in order to avoid restraint of panel shrinkage and thermal movements. The decision to use one or several in-

plane horizontal connections is made based on seismic demands, and local experience with restraint issues in precast panels of similar length.

The A and A1 connections are often designed to take the loads directly to the columns, particularly on steel moment frames where attachments to the flexural hinging regions of beams are difficult to accomplish. To provide sufficient stiffness and strength to resist the out-of-plane loads, the lower B connection often requires bracing the bottom flange of the exterior beam to the floor or roof deck in order to control torsional behavior of the exterior beam, unless the connection can be placed near an intersecting beam that will prevent twisting of the exterior beam.

The column cover is supported both vertically and horizontally by the column, transfers no loads to the spandrel panel and provides no support for the window frame.

The window frame is supported both vertically and horizontally along the length of the spandrel panel and transfers no loads to the column covers.

18.2.3.2 Prescribed Seismic Forces. Lateral forces on the wall panels and connection fasteners include seismic loads and wind loads. Design for wind forces is not illustrated here.

18.2.3.2.1 Panels.

$D = W_p = 8,775 \text{ lb} + 1,470 \text{ lb} = 10,245 \text{ lb}$ 　　　　　　　　　　　(vertical gravity effect)

$$F_p = \frac{0.4(1.0)(1.487)(10,245 \text{ lb})}{\left(2.5\big/1.0\right)}\left(1+2(0.6)\right) = 5,362 \text{ lb}$$ 　　　(*Standard* Eq. 13.3-1)

$F_{p_{max}} = 1.6(1.487)(1.0)(10,245 \text{ lb}) = 24,375 \text{ lb}$ 　　　　　　　(*Standard* Eq. 13.3-2)

$F_{p_{min}} = 0.3(1.487)(1.0)(10,245 \text{ lb}) = 4,570 \text{ lb}$ 　　　　　　　(*Standard* Eq. 13.3-3)

Standard Eq. 13.3-1 governs, and $F_p = 5,362$ lb

$E_h = \rho Q_E$ 　　　　　　　　　　　　　　　　　　　　　(*Standard* Eq. 12.4-3)

$E_v = 0.2S_{DS}D$ 　　　　　　　　　　　　　　　　　　　(*Standard* Eq. 12.4-4a)

where:

Q_E (due to horizontal application of F_p) = 5,362 lb 　　　　　(*Standard* Sec. 12.4.2-1)

$\rho = 1.0$ (because panels are nonstructural components) 　　　　　(*Standard* Sec 13.3.1)

D = dead load effect (due to vertical load application)

Substituting, the following is obtained:

$E_h = \rho Q_E = (1.0)(5,362 \text{ lb}) = 5,362 \text{ lb}$ 　　　　　　　(horizontal earthquake effect)

$E_v = 0.2S_{DS}D = 0.2S_{DS}D = (0.2)(1.487)(10,245 \text{ lb}) = 3,047 \text{ lb}$ 　　(vertical earthquake effect)

18-18

The above terms are then substituted into the following Basic Load Combinations for Strength Design from Section 12.4.2.3 to determine the design member and connection forces to be used in conjunction with seismic loads.

$1.2D + E_v + E_h + L + 0.2S$ (*Standard* Basic Load Combination 6)

$0.9D - E_v + E_h$ (*Standard* Basic Load Combination 7)

For nonstructural components, the terms L and S typically are zero.

18.2.3.2.2 Connection fasteners. The *Standard* specifies a reduced R_p and an increased a_p for "fasteners" with the intention of preventing premature failure in those elements of connections that are inherently brittle, such as embedded items that depend on concrete breakout strength, or connection elements that are simply too small to adequately dissipate energy inelastically, such as welds or individual bolts. The net effect more than triples the design seismic force. The higher value of R_p used for the design of the body of the connections limits together with the reduced R_p for fasteners allows the value of Ω_0 to be taken as 1.0.

$$F_p = \frac{0.4(1.25)(1.487)(10,245 \text{ lb})}{\left(1.0 / 1.0\right)}\left(1 + 2(0.6)\right) = 16,757 \text{ lb}$$ (*Standard* Eq. 13.3-1)

$$F_{p_{max}} = 1.6(1.487)(1.0)(10,245 \text{ lb}) = 24,375 \text{ lb}$$ (*Standard* Eq. 13.3-2)

$$F_{p_{min}} = 0.3(1.487)(1.0)(10,245 \text{ lb}) = 4,570 \text{ lb}$$ (*Standard* Eq. 13.3-3)

$$E_h = \rho Q_E$$ (*Standard* Eq. 12.4-3)

$$E_v = 0.2S_{DS}D$$ (*Standard* Eq. 12.4-4a)

where:

Q_E (due to horizontal application of F_p) = 16,757 lb (*Standard* Sec. 12.4.2-1)

$\rho = 1.0$ (because panels are nonstructural components) (*Standard* Sec 13.3.1)

D = dead load effect (due to vertical load application)

Substituting, the following is obtained:

$E_h = \rho Q_E = (1.0)(16,757 \text{ lb}) = 16,757 \text{ lb}$ (horizontal earthquake effect)

$E_v = 0.2S_{DS}D = 0.2S_{DS}D = (0.2)(1.487)(10,245 \text{ lb}) = 3,047 \text{ lb}$ (vertical earthquake effect)

The above terms are then substituted into the following Basic Load Combinations for Strength Design from Section 12.4.2.3 to determine the design member and connection forces to be used in conjunction with seismic loads.

$1.2D + E_v + E_h + L + 0.2S$ (*Standard* Basic Load Combination 6)

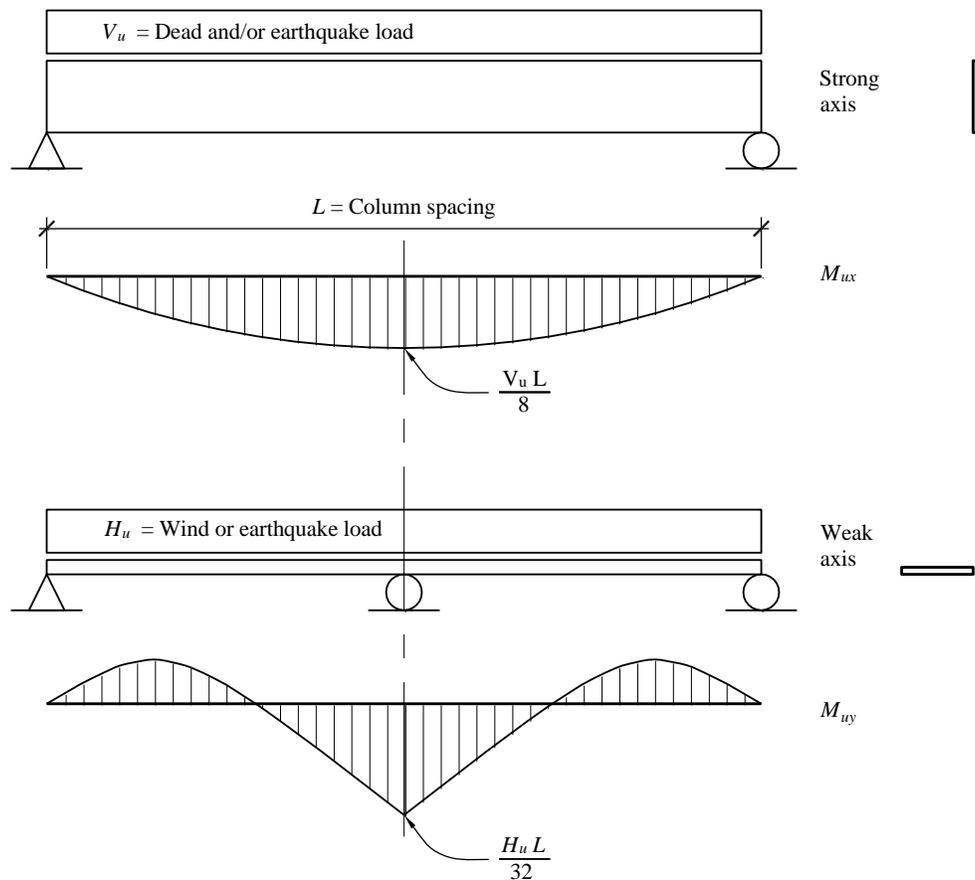$0.9D - E_v + E_h$ (*Standard* Basic Load Combination 7)

For precast panels, the terms L and S typically are zero. Load combinations with overstrength generally are not applicable to nonstructural components.

18.2.3.3 Proportioning and Design.

18.2.3.3.1 Panels. The wall panels should be designed for the following loads in accordance with ACI 318. The design of the reinforced concrete panel is standard and is not illustrated in this example. Spandrel panel moments are shown in Figure 18.2-4. Reaction shears (V_u), forces (H_u) and moments (M_u) are calculated for applicable strength load combinations.

For this example, the values of L and S are assumed to be zero.

Figure 18.2-4 Spandrel panel moments

Standard Basic Load Combination 1: $1.4D$ (from *Standard* Sec. 2.3.1)

$V_u = 1.4(10,245 \text{ lb}) = 14,343 \text{ lb}$ (vertical load downward)

$$M_{ux} = \frac{(14{,}343 \text{ lb})(24 \text{ ft})}{8} = 43{,}029 \text{ ft-lb}$$
(strong axis moment)

Standard Basic Load Combination 6: $1.2D + 0.2S_{DS}D + \rho Q_E + L + 0.2S$

$V_{umax} = [1.2 + 0.2(1.487)]\,(10{,}245 \text{ lb}) = 15{,}341 \text{ lb}$
(vertical load downward)

$\Leftrightarrow H_u = 1.0(5{,}362 \text{ lbs}) = 5{,}362 \text{ lb}$
(horizontal load parallel to panel)

$\perp H_u = 1.0(5{,}362 \text{ lbs}) = 5{,}362 \text{ lb}$
(horizontal load perpendicular to panel)

$$M_{ux_{max}} = \frac{(15{,}341 \text{ lb})(24 \text{ ft})}{8} = 46{,}023 \text{ ft-lb}$$
(strong axis moment)

$$M_{uy} = \frac{(5{,}362 \text{ lb})(24 \text{ ft})}{32} = 4{,}022 \text{ ft-lb}$$
(weak axis moment)

Standard Basic Load Combination 7: $0.9D - 0.2S_{DS}D + \rho Q_E$

$V_{umin} = [1.2 - 0.2(1.487)]\,(10{,}245 \text{ lb}) = 6{,}174 \text{ lb}$
(vertical load downward)

$\Leftrightarrow H_u = 1.0(5{,}362 \text{ lb}) = 5{,}362 \text{ lb}$
(horizontal load parallel to panel)

$\perp H_u = 1.0(5{,}362 \text{ lb}) = 5{,}362 \text{ lb}$
(horizontal load perpendicular to panel)

$$M_{ux_{min}} = \frac{(6{,}174 \text{ lb})(24 \text{ ft})}{8} = 18{,}522 \text{ ft-lb}$$
(strong axis moment)

$$M_{uy} = \frac{(5{,}362 \text{ lb})(24 \text{ ft})}{32} = 4{,}022 \text{ ft-lb}$$
(weak axis moment)

18.2.3.3.2 Connection fasteners. The design of the connection fasteners is not illustrated in this example. They should be designed for the loads calculated below, in accordance with ACI 318 (Appendix D) and the AISC specification. There are special reduction factors for anchorage in high seismic demand locations, such as factors for anchors in cracked concrete, and those reduction factors would apply to this example. Spandrel panel connection forces are shown in Figure 18.2-5. Reaction shears (V_u), forces (H_u) and moments (M_u) are calculated for applicable strength load combinations.
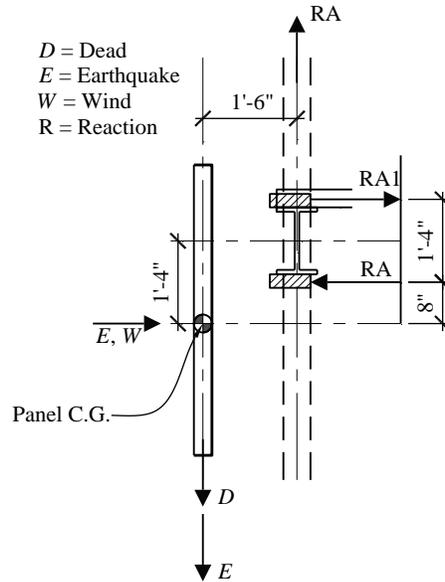
Figure 18.2-5 Spandrel panel connection forces

Standard Basic Load Combination 1: 1.4*D*   (from *Standard* Section 2.3.2)

$$V_{uA} = \frac{1.4(10,245 \text{ lb})}{2} = 7,172 \text{ lb}$$ (vertical load downward at Points A and A1)

M_{uA} = (7,172 lb)(1.5 ft) = 10,758 ft-lb   (moment resisted by paired Points A and A1)

Horizontal couple from moment at A and A1 = 10758 / 1.33 = 8071 lb

Standard Basic Load Combination 6: $1.2D + 0.2S_{DS}D + \rho Q_E + L + 0.2S$

$$V_{uA\max} = \frac{\lfloor 1.2 + 0.2(1.487) \rfloor (10,245 \text{ lb})}{2} = 7,671 \text{ lb}$$ (vertical load downward at Point A)

$$\perp H_{uA} = 1.0(16,757 \text{ lb}) \frac{3}{16} = 3,142 \text{ lb}$$ (horizontal load perpendicular to panel at Points A and A1)

H_{Ain} = (7,671 lb)(1.5 ft) / (1.33 ft) + (3142 lb)(2.0 ft) / (1.33 ft) = 13366 lb   (inward force at Point A)

H_{A1out} = (7671 lb)(1.5 ft) / (1.33 ft) + (3,142 lb)(0.67) / (1.33 ft) = 10222 lb   (outward force at Point A1)

$$\Leftrightarrow H_{uA} = \frac{1.0(16,757 \text{ lb})}{2} = 8,378 \text{ lb}$$ (horizontal load parallel to panel at Point A)

M_{u2A} = (8,378 lb)(1.5 ft) = 12,568 ft-lb   (flexural moment at Point A)

$$\perp H_{uB} = 1.0(16{,}757 \text{ lb})\frac{5}{8} = 10{,}473 \text{ lb}$$ (horizontal load perpendicular to panel at Points B and B1)

$H_B = (10{,}743 \text{ lb})(2.0 \text{ ft}) / (1.33 \text{ ft}) = 15{,}714 \text{ lb}$ (inward or outward force at Point B)

$H_{B1} = (10{,}473 \text{ lb})(0.67 \text{ ft}) / (1.33 \text{ ft}) = 5{,}237 \text{ lb}$ (inward or outward force at Point B1)

Standard Basic Load Combination 7: $0.9D - 0.2S_{DS}D + \rho Q_E$

$$V_{uA\min} = \frac{\left\lfloor 1.2 - 0.2(1.487)\right\rfloor (10{,}245 \text{ lb})}{2} = 3{,}086 \text{ lb}$$ (vertical load downward at Point A)

Horizontal forces are the same as combination $1.2D + 1.0E$. No uplift occurs; the net reaction at Point A is downward. Maximum forces are controlled by prior combination. It is important to realize that inward and outward acting horizontal forces generate different demands where the connections are eccentric to the center of mass, as in this example. Only the maximum reactions are computed above.

18.2.3.4 Prescribed Seismic Displacements. Prescribed seismic displacements are not applicable to the spandrel panel because all connections are at essentially the same elevation.

18.2.4 Column Cover

18.2.4.1 Connection Details. Figure 18.2-6 shows the key to the types of forces resisted at each column cover connection.
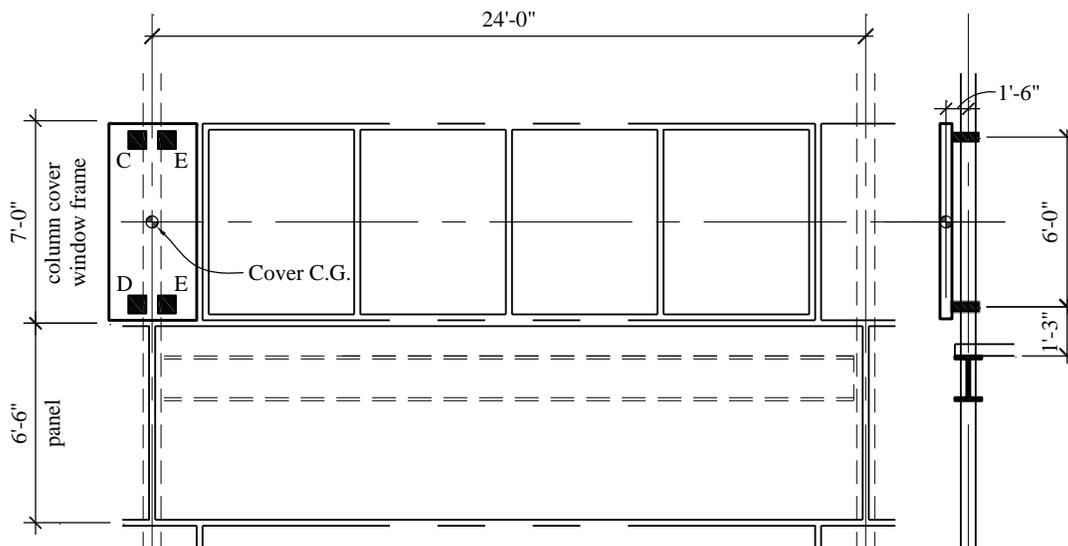
Figure 18.2-6 Column cover connection layout
(1.0 ft = 0.3048 m)

Vertical loads, horizontal loads parallel to the panel and horizontal loads perpendicular to the panel are resisted at Point C. The eccentricity of vertical loads is resisted by a force couple at Points C and D. The horizontal load parallel to the panel eccentricity between the panel and the support is resisted in flexure of the connection at Point C. This connection is designed to take the loads directly to the column.

In-plane horizontal loads parallel to the panel are resisted at Point D. The eccentricity between center of mass of the panel and the reaction at the vertical support generates a moment that is resisted by a force couple of Points C and D. The eccentricity of horizontal loads parallel to the panel is resisted by flexure at the connection at Point D. The connection is designed so as not to restrict vertical movement of the panel due to thermal effects or seismic input. The connection is designed to take the loads directly to the columns.

Out-of-plane horizontal loads perpendicular to the panel are resisted equally at Points C and D and the two points identified as E. The connections are designed to take the loads directly to the columns.

There is no load eccentricity associated with the horizontal loads perpendicular to the panel.

In this example, all connections are made to the sides of the column because usually there is not enough room between the outside face of the column and the inside face of the cover to allow a feasible load-carrying connection.

18.2.4.2 Prescribed Seismic Forces. Calculation of prescribed seismic forces for the column cover is not shown in this example. They should be determined in the same manner as illustrated for the spandrel panels.

18.2.4.3 Prescribed Seismic Displacements. The results of an elastic analysis of the building structure usually are not available in time for use in the design of the precast cladding system. As a result, prescribed seismic displacements usually are calculated based on allowable story drift requirements:

h_{sx} = story height = 13'-6"

h_x = height of upper support attachment = 47'-9"

h_y = height of lower support attachment = 41'-9"

$$\Delta_{aA} = 0.020 h_{sx} \tag{*Standard* Table 12.12-1}$$

$$D_p = \frac{\left(h_x - h_y\right)\Delta_{aA}}{h_{sx}} = \frac{(72 \text{ in.})0.020 h_{sx}}{h_{sx}} = 1.44 \text{ in.} \tag{*Standard* Eq. 13.3-8}$$

$$D_{pI} = D_p I_e = 1.44 \text{ in } (1.0) = 1.44 \text{ in.} \tag{*Standard* Eq. 13.3-6}$$

The joints at the top and bottom of the column cover must be designed to accommodate an in-plane relative displacement of 1.44 inches. The column cover will rotate somewhat as these displacements occur, depending on the nature of the connections to the column. If the supports at one level are "fixed" to the columns while the other level is designed to "float", that is, free to allow vertical movement, then the rotation will be that of the column at the point of attachment.

In the 2016 edition of the *Standard*, requirements were added for exterior wall panel connections which accommodate story drift through sliding mechanisms or bending of threaded steel rods. *Standard* Section 13.5.3 requires that threaded rods in these applications be fabricated of low-carbon or stainless steel.

When cold-worked carbon steel threaded rod is used, the rods as fabricated must meet or exceed the reduction of area, elongation, and tensile strength requirements specified in the *Standard*. For sliding connections utilizing slotted or oversized holes, the rods must have length to diameter ratios of 4 or less, where the length is the clear distance between the nuts or threaded plates. The slots or oversized holes must be proportioned to accommodate the full in-plane design story drift in each direction. In connections where story drift is accommodating d by bending of the threaded rod, it must satisfy *Standard* Eq. 13.5-1:

$(L/d)/D_{pI} \geq 6.0$ [1/in.]

where:

L = clear length of rod between nuts or threaded plates [in.]

d = rod diameter [in.]

Assuming in this example that a ½ inch diameter rod with a clear length of the rod of 10 inches is selected,

$[(10 \text{ in.})/(0.5 \text{ in.})])/(1.44 \text{ in.}) = 13.9 \geq 6.0$, O.K.

18.2.5 Additional Design Considerations

18.2.5.1 Window Frame System. The window frame system is supported by the spandrel panels above and below. Assuming that the spandrel panels move in-plane with each floor level and are rigid when subject to in-plane forces, the window frame system must accommodate the entire prescribed seismic displacement based on the full story height.

$$D_p = \frac{\left(h_x - h_y\right)\Delta_{aA}}{h_{sx}} = \frac{(162 \text{ in.})0.020h_{sx}}{h_{sx}} = 3.24 \text{ in.}$$ (*Standard* Eq. 13.3-8)

$D_{pI} = D_p I_e = 3.24 \text{ in } (1.0) = 3.24 \text{ in.}$ (*Standard* Eq. 13.3-6)

The window frame system must be designed to accommodate an in-plane relative displacement of 3.24 inches between the top and bottom spandrels. Normally this is accommodated by a clearance between the glass and the frame. *Standard* Section 13.5.9.1 prescribes a method of checking such a clearance. It requires that the clearance be large enough so that the glass panel will not fall out of the frame unless the relative seismic displacement at the top and bottom of the panel exceeds 125 percent of the predicted value amplified by the building importance factor. If h_p and b_p are the respective height and width of individual panes and if the horizontal and vertical clearances are designated c_1 and c_2, respectively, then the following expression applies:

$$D_{clear} = 2c_1 \left(1 + \frac{h_p c_2}{b_p c_1}\right) \geq 1.25 D_{pI}$$ (*Standard* Sec. 13.5.9.1, Exception 1)

For h_p = 7 feet, b_p = 5 feet and D_{pI} = 3.24 inches and setting $c_1 = c_2$, the minimum required clearance is:

$$D_{clear} = 1.25 D_{pI} = 1.25(3.24 \text{ in.}) = 4.05 \text{ in.}$$ (*Standard* Eq. 13.3-6)

Solving for c_1:

$$4.05 \; in. = 2(c_1)\left(1 + \frac{(7\,ft.)c_1}{(5\,ft.)c_1}\right) = 4.80 c_1$$

Required clearance = $c_1 = c_2 = 0.84$ inch.

18.2.5.2 Building Corners. Some thought needs to be given to seismic behavior at external building corners. The preferred approach is to detail the corners with two separate panel pieces, mitered at a 45 degree angle, with high grade sealant between the sections. An alternative choice of detailing L-shaped corner pieces introduces more seismic mass and load eccentricity into connections on both sides of the corner column, and may also trigger the need for wider joints between the column cover and adjacent glazing and curtain wall units to prevent interaction under story drift. This is often the case if panels that accommodate story drift by rocking or rotation are adjacent to panels that do not rock or rotate, such as the spandrel in this example.

18.2.5.3 Dimensional Coordination. It is important to coordinate dimensions with the architect and structural engineer. Precast concrete panels must be located a sufficient distance from the building structural frame to allow room for the design of efficient load transfer connection pieces. However, distances must not be so large as to increase unnecessarily the load eccentricities between the panels and the frame.

18.3   SEISMIC ANALYSIS OF EGRESS STAIRS

18.3.1 Example Description

Egress stairs are an essential part of the system used to evacuate building occupants following an earthquake. Failure of the stairs may trap building occupants on the upper levels of the structure. Ladders on emergency vehicles can usually only reach the lower floors in mid- and high-rise structures. This was especially prevalent in the 2011 Christchurch Earthquake. In recognition of their importance, egress stairs are assigned a component importance factor, $I_p =1.5$. In the 2016 edition of the *Standard*, a new section was added to Chapter 13 with specific requirements intended to limit damage and improve functionality of egress stairs following an earthquake. The new requirements do not apply to egress stair systems and ramps that are integral with the building structure since it is assumed that the seismic resistance of these systems is addressed in the overall building design. Examples include stairs and ramps integral with monolithic concrete construction, light-frame wood and cold-formed metal stair systems in multiunit residential construction, and integrally constructed masonry stairs.

In this example, egress stairs of prefabricated steel construction are installed in a five-story reinforced concrete moment frame building. The example focuses on the flight of stairs running between the 3rd and 4th Levels of the building. Elevation, plan, and isometric views of the stairs are shown in Figures 18.3-1, 18.3-2, and 18.3-3. The prescribed seismic forces and displacements for the flight of stairs between Levels 3 and 4 in the buildings are determined. The treads and landings are fabricated from 1/8 inch thick steel checkered plate. The stringers are fabricated from ¼ inch thick steel plate, and other members and supports are fabricated from steel channels, angles, and tube. The effective dead load is estimated at 20 psf, and the design live load is 100 psf. This example focuses on quantifying the prescribed seismic forces and displacements. The design of the stairs themselves and their connections for dead, live, and seismic loads is not covered.

While this example focuses on stairs required for egress, the principles can applied to all types of stairs.
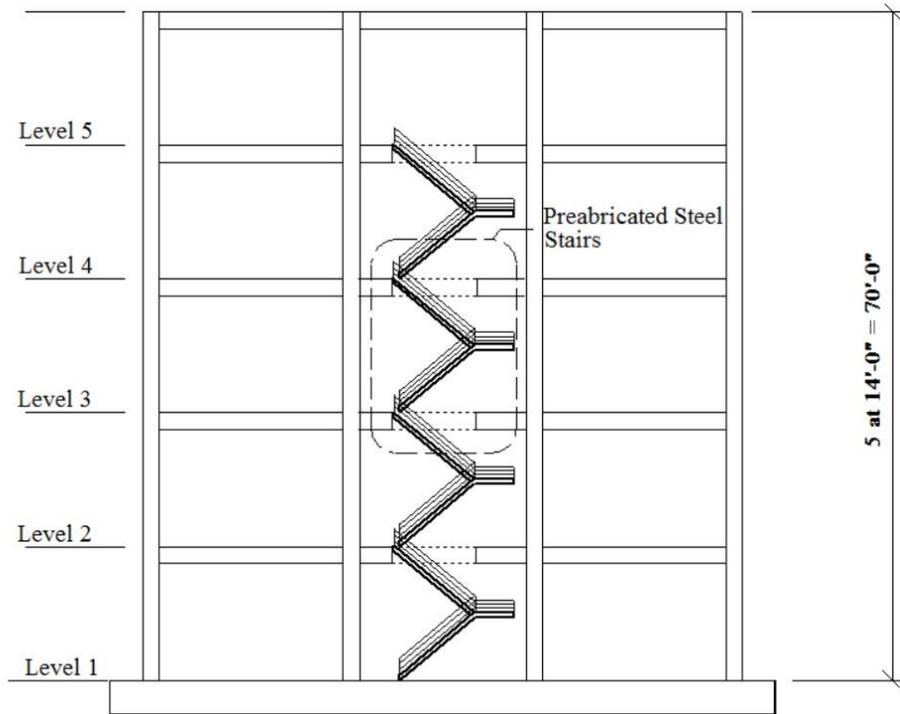
Figure 18.3-1 Elevation of egress stairs
(1.0 ft = 0.3048 m)
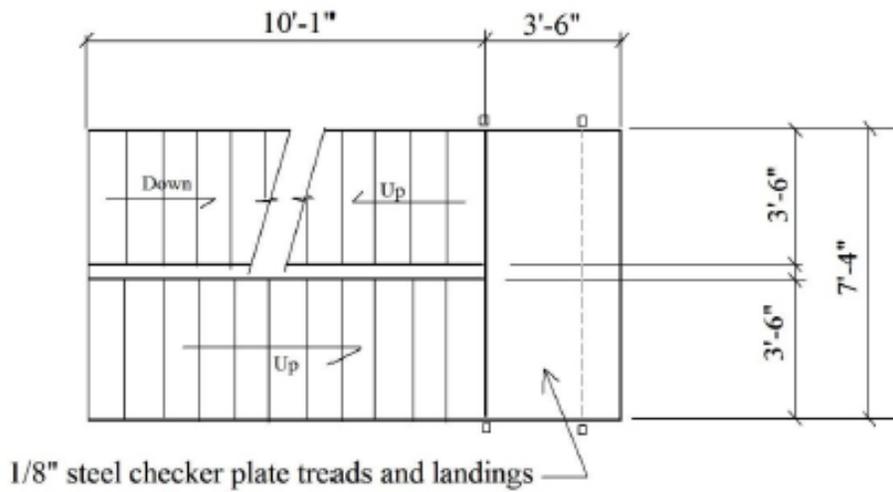
Figure 18.3-2 Plan of egress stairs
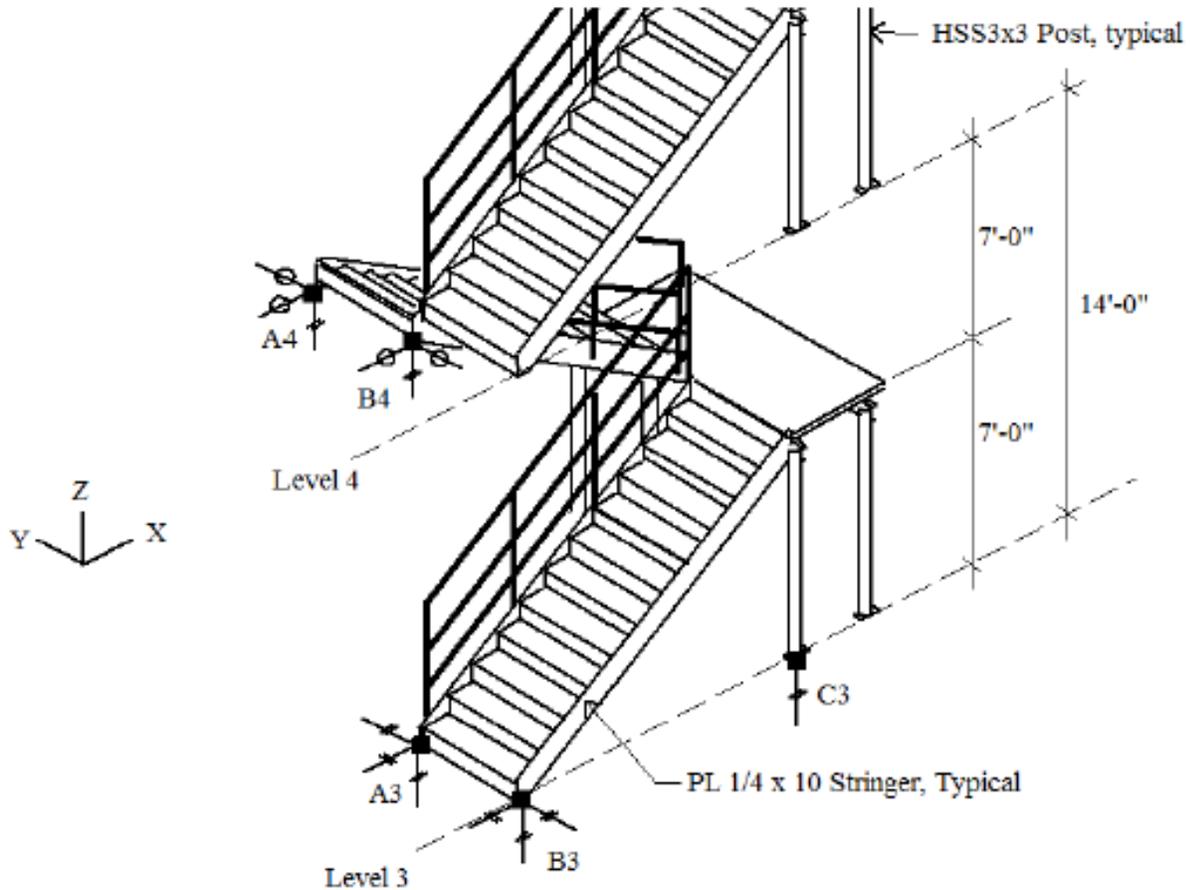(1.0 ft = 0.3048 m)

Figure 18.3-3 Isometric view of egress stairs
(1.0 ft = 0.3048 m)

18.3.2 Design Requirements

18.3.2.1 *Provisions* **parameters and coefficients**

$a_p = 1.0$ Egress stairways not part of the seismic force-resisting system   (*Standard* Table 13.5-1)

$a_p = 2.5$ Egress stairs and ramp fasteners and attachments   (*Standard* Table 13.5-1)

$S_{DS} = 1.00$ (for the selected location and site class)   (given)

Seismic Design Category = D   (*Standard* Table 11.6-1)

$R_p = 2.5$ Egress stairways not part of the seismic force-resisting system   (*Standard* Table 13.5-1)

$R_p = 2.5$ Egress stairs and ramp fasteners and attachments   (*Standard* Table 13.5-1)

$I_p = 1.5$ (*Standard* Sec. 13.1.3)

$\Omega_0 = 2.0$ for fasteners of the connecting system   (*Standard* Table 13.5-1)

Landing $W_p = (20 \text{ lb/ft}^3)(7.33 \text{ ft})(3.5 \text{ ft}) = 513$ lb

Flight $W_p = (20 \text{ lb/ft}^2)(10.08 \text{ ft})(3.5 \text{ ft}) = 706$ lb   (Single flight from landing to floor)

$$\frac{z}{h} = \frac{28 \text{ ft}}{70 \text{ ft}} = 0.4$$ (at Level 3)

$$\frac{z}{h} = \frac{42 \text{ ft}}{70 \text{ ft}} = 0.6$$ (at Level 4)

According to *Standard* Sections 13.3.1 and 12.3.4.1 Item 3), the redundancy factor, ρ, for nonstructural components is taken as 1.0 in load combinations where it appears.

18.3.2.2 Performance Criteria.

Supports, attachments, and the egress stairs themselves must be designed to meet the seismic requirements of the *Standard*, Chapter 13 (*Standard* Sec. 13.2.1).

Component failure must not cause failure of an essential architectural, mechanical, or electrical component (*Standard* Sec. 13.2.3).

Component seismic attachments must be bolted, welded, or otherwise positively fastened without considering the frictional resistance produced by the effects of gravity (*Standard* Sec. 13.4).

The effects of seismic relative displacements must be considered in combination with displacements caused by other loads as appropriate (*Standard* Sec. 13.3.2).

The net relative displacement shall be assumed to occur in any horizontal direction, and shall be accommodated through slotted or sliding connections, or metal supports designed with rotation capacity to accommodate seismic relative displacements (*Standard* Sec. 13.5.10).

Sliding connections with slotted or oversize holes, sliding bearing supports with restraints that engage after the displacement D_{pI}, is exceeded (e.g. keeper assemblies or end stops), and connections that permit movement by deformation of metal attachments, shall accommodate a displacement D_{pI}, but not less than 0.5 in. (13 mm), without loss of vertical support or inducement of displacement-related compression forces in the stair (*Standard* Sec. 13.5.10).

Sliding bearing supports without keeper assemblies or end stops shall be designed to accommodate a displacement $1.5D_{pI}$, but not less than 1.0 in. (25 mm) without loss of vertical support. Break-away restraints are permitted if their failure does not lead to loss of vertical support (*Standard* Sec. 13.5.10).

The strength of the supports shall not be limited by bolt shear, weld fracture or other limit states with lesser ductility (*Standard* Sec. 13.5.10).

If sliding or ductile connections are not provided to accommodate seismic relative displacements, the stiffness and strength of the stair or ramp structure shall be included in the building structural model of *Standard* Section 12.7.3 and the stair shall be designed with Ω_0 corresponding to the seismic force-resisting system but not less than 2½ (*Standard* Sec. 13.5.10).

18.3.3 Force and Displacement Demands

Stairs are generally displacement-controlled. Unless the stairs are included in the design of the structure's lateral force-resisting system, they must be either isolated from the lateral displacement of the building or provided with ductile connections, capable of accepting the lateral displacements without loss of vertical load-carrying capacity. Sufficient ductility must be provided in these connections to accommodate multiple cycles at anticipated maximum drift levels.

There are many different approaches for dealing with seismic displacement demand on egress stairs. In this example, for displacements parallel to the flights of stairs, the X-direction in Figure 18.3-3, the stair assembly is fixed at Level 3 of the structure by connections A3 and B3. Connections A4 and B4 on Level 4 are detailed to accommodate story drift by sliding in the X-direction. For displacements perpendicular to the flights of stairs, the Y-direction in Figure 18.3-3, the stair is fixed in the Y-direction by connections A3 and B3 and connections A4 and B4 are a detailed to accommodate story drift by sliding in the Y-direction. This connection configuration induces twisting of the stairs about the Z axis, due to the eccentricity between the center of gravity of the stairs and the center of resistance of the connections. This eccentricity must be accounted for in the design. When designing the stairs themselves, the seismic forces should be distributed relative to the components mass distribution. For simplicity in the connection calculations in this example, the mass of the stairs is lumped at the landing and at the center of gravity of each flight of stairs. Although the mass of the stairs is distributed between Levels 3 and 4, the lateral force is calculated assuming it is concentrated at Level 3, since the connections at Level 4 are free to slide in the X- and Y- directions.

18.3.3.1 Flights of Stairs.

$D = W_p = 706$ lb   (vertical gravity effect)

$L = (10.08)(3.5)(100 \text{ psf}) = 3{,}528$ lb   (vertical gravity effect)

$F_p = \dfrac{0.4(1.0)(1.0)(706 \text{ lb})}{2.5/1.5}(1 + 2(0.4)) = 306$ lb   (*Standard* Eq. 13.3-1)

$F_{pmax} = 1.6(1.0)(1.5)(706 \text{ lb}) = 1{,}694$ lb   (*Standard* Eq. 13.3-2)

$F_{pmin} = 0.3(1.0)(1.5)(706 \text{ lb}) = 318$ lb   (*Standard* Eq. 13.3-3)

Standard Eq. 13.3-3 governs, and $F_p = 318$ lb

$E_h = \rho Q_E$ (*Standard* Eq. 12.4-3)

$E_v = 0.2 S_{DS} D$ (*Standard* Eq. 12.4-4a)

where:

Q_E (due to horizontal application of F_p) = 318 lb   (*Standard* Sec. 12.4.2.1)

$\rho = 1.0$ (because egress stairs are nonstructural components)   (*Standard* Sec 13.3.1)

D = dead load effect (due to vertical load application)

Substituting, the following is obtained:

$E_h = \rho Q_E = (1.0)(\ 318\ \text{lb}) = 318\ \text{lb}$ (horizontal earthquake effect)

$E_v = 0.2 S_{DS} D = (0.2)(1.0)(706\ \text{lb}) = 141\ \text{lb}$ (vertical earthquake effect)

The above terms are then substituted into the following Basic Load Combinations for Strength Design from *Standard* Section 12.4.2.3 to determine the design member forces to be used in conjunction with seismic and gravity loads.

$1.2D + E_v + E_h + L + 0.2S$ (*Standard* Basic Load Combination 6)

$0.9D - E_v + E_h$ (*Standard* Basic Load Combination 7)

18.3.3.2 Landing.

$D = W_p = 513\ \text{lb}$ (vertical gravity effect)

$L = (7.33)(3.5)(100\ \text{psf}) = 2{,}566\ \text{lb}$ (vertical gravity effect)

$F_p = \frac{0.4(1.0)(1.0)(513\ \text{lb})}{2.5/1.5}(1 + 2(0.4)) = 222\ \text{lb}$ (*Standard* Eq. 13.3-1)

$F_{pmax} = 1.6(1.0)(1.5)(513\ \text{lb}) = 1{,}231\ \text{lb}$ (*Standard* Eq. 13.3-2)

$F_{pmin} = 0.3(1.0)(1.5)(513\ \text{lb}) = 231\ \text{lb}$ (*Standard* Eq. 13.3-3)

Standard Eq. 13.3-3 governs, and $F_p = 231\ \text{lb}$

$E_h = \rho Q_E$ (*Standard* Eq. 12.4-3)

$E_v = 0.2 S_{DS} D$ (*Standard* Eq. 12.4-4a)

where:

Q_E (due to horizontal application of F_p) = 231 lb (*Standard* Sec. 12.4.2-1)

$\rho = 1.0$ (because egress stairs are nonstructural components) (*Standard* Sec 13.3.1)

D = dead load effect (due to vertical load application)

Substituting, the following is obtained:

$E_h = \rho Q_E = (1.0)(\ 231\ \text{lb}) = 231\ \text{lb}$ (horizontal earthquake effect)

$E_v = 0.2 S_{DS} D = 0.2 S_{DS} D = (0.2)(1.0)(513\ \text{lb}) = 103\ \text{lb}$ (vertical earthquake effect)

The above terms are also substituted into the Basic Load Combinations for Strength Design from *Standard* Section 12.4.2.3 to determine the design member forces to be used in conjunction with seismic and gravity loads. After the prescribed seismic forces and displacements are determined, the stairs

members are designed to carry the dead, live, and seismic loads, and the connections can be detailed and designed according to the appropriate standards.

If the connections at Level 4 also provided lateral restraint, then it is recommended that design be based on the average of values of F_p determined individually at each point of attachment, but with the entire component weight, W_p. In this example, F_p would be calculated first assuming the stairs were completely supported at Level 3, then repeating the calculation assuming the stairs were completely supported at Level 4. The results would then be averaged. Alternatively, for each point of attachment, a force F_p may be determined with the portion of the component weight, W_p, tributary to the point of attachment.

18.3.3.3 Egress Stairs and Ramp Fasteners and Attachments. The *Standard* specifies an increased a_p for egress stair and ramp fasteners and attachments with the intention of preventing premature failure in those elements, which could cause loss of vertical support. The change in a_p only effects the force calculated using *Standard* Eq. 13.3-1. For a flight of stairs,

$$F_p = \frac{0.4(1.0)(2.5)(706\ \text{lb})}{2.5/1.5}(1 + 2(0.4)) = 765\ \text{lb} \qquad \text{(\textit{Standard} Eq. 13.3-1)}$$

Standard Eq. 13.3-1 governs, and $F_p = 765$ lb.

For the landing,

$$F_p = \frac{0.4(1.0)(2.5)(513\ \text{lb})}{2.5/1.5}(1 + 2(0.4)) = 555\ \text{lb} \qquad \text{(\textit{Standard} Eq. 13.3-1)}$$

Again, *Standard* Eq. 13.3-1 governs, and $F_p = 555$ lb.

18.3.3.4 Prescribed Seismic Displacements. Assuming the results of an elastic analysis of the building structure is not available for use in the design of the egress stairs, prescribed seismic displacements are calculated based on allowable story drift requirements:

h_{sx} = story height = 14'-0"

h_x = height of upper support attachment, Level 4 = 42'-0"

h_y = height of lower support attachment, Level 3 = 28'-0"

$\Delta_{aA} = 0.020 h_{sx}$ $\qquad\qquad$ (*Standard* Table 12.12-1)

$$D_p = \frac{\left(h_x - h_y\right)\Delta_{aA}}{h_{sx}} = \frac{14(12)(0.020 h_{sx})}{h_{sx}} = 3.36\ \text{in.} \qquad \text{(\textit{Standard} Eq. 13.3-8)}$$

$D_{pI} = D_p I_e = 3.36\ \text{in}\ (1.5) = 5.14\ \text{in.}$ $\qquad\qquad$ (*Standard* Eq. 13.3-6)

Assuming that the connections of the egress stairs to the structure at Level 4 are sliding connections with slotted or oversize holes, sliding bearing supports must be provided with restraints that engage after the displacement D_{pI}, is exceeded (e.g. keeper assemblies or end stops), The connections must be designed to accommodate D_{pI}, without loss of vertical support or inducement of displacement-related compression forces in the stair. The displacement can act in any direction, so the connection must be able to accommodate a total range of movement of two times D_{pI}, or 10.28 inches in all directions, If a keeper

assemblies or end stops are not provided, the connection must be designed accommodate 1.5 $D_p I_e$, or 7.56 inches, or a total range of movememt of 15.12 inches.

Accomodating displacements of these magnitudes may be problamatic from a practical destgn perspective, and connection options that rely on yielding of ductile steel elements may produce a more efficient design.

18.4 HVAC FAN UNIT SUPPORT

18.4.1 Example Description

In this example, the mechanical component is a 4-foot-high, 5-foot-wide, 8-foot-long, 3,000-pound HVAC fan unit that is supported on the two long sides near each corner (Figure 18.4-1). The component is located at the roof level of a five-story office building, near a significant active fault. The building is assigned to Seismic Risk Category II. Two methods of attaching the component to the 4,000 psi, normal-weight roof slab are considered, as follows:

Direct attachment to the structure with 36 ksi, carbon steel, cast-in-place anchors.

Support on vibration isolation springs that are attached to the slab with 36 ksi, carbon steel, post-installed expansion anchors. The nominal gap between the vibration spring seismic restraints and the base frame of the fan unit is presumed to be greater than 0.25 in.
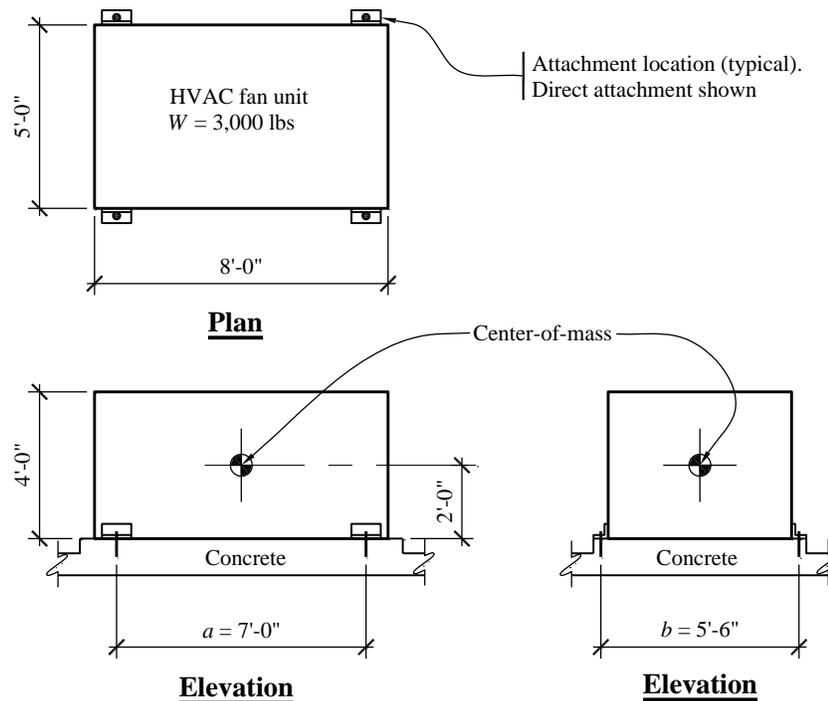
Figure 18.4-1 HVAC fan unit
(1.0 ft = 0.3048 m, 1.0 lb = 4.45 N)

18.4.2 Design Requirements

18.4.2.1 Seismic design parameters and coefficients.

$a_p = 2.5$ for both direct attachment and spring isolated   (*Standard* Table 13.6-1)

$\Omega_0 = 2.0$ for anchorage to concrete with nonductile behavior   (*Standard* Table 13.6-1, footnote c)

$S_{DS} = 1.487$ (for the selected location and site class)   (given)

Seismic Design Category = D   (*Standard* Table 11.6-1)

$W_p = 3,000$ lb   (given)

$R_p = 6.0$ for HVAC fans, directly attached (not vibration isolated)   (*Standard* Table 13.6-1)

$R_p =$ 2.0 for spring isolated components with restraints   (*Standard* Table 13.6-1)

$I_p = 1.0$ (*Standard* Sec. 13.1.3)

$z/h = 1.0$ (for roof-mounted equipment)

18.4.2.2 Performance Criteria. Component failure should not cause failure of an essential architectural, mechanical, or electrical component (*Standard* Sec. 13.2.3).

Component seismic attachments must be bolted, welded, or otherwise positively fastened without consideration of frictional resistance produced by the effects of gravity (*Standard* Sec. 13.4).

Attachments to concrete or masonry must be designed to resist the load combinations considering Ω_0 in accordance with *Standard* Section 2.3.6 unless the component or a support in the load path leading to the structure undergoes ductile yielding at a load level less than the design strength of the corresponding anchor. (*Standard* Sec. 13.4.2).

Attachments and supports transferring seismic loads must be constructed of materials suitable for the application and must be designed and constructed in accordance with a nationally recognized structural standard (*Standard* Sec. 13.6.5).

Components mounted on vibration isolation systems must have a bumper restraint or snubber in each horizontal direction. Vertical restraints must be provided where required to resist overturning. Isolator housings and restraints must also be constructed of ductile materials. A viscoelastic pad, or similar material of appropriate thickness, must be used between the bumper and equipment item to limit the impact load (*Standard* Table 13.6-1, footnote b). Such components also must resist doubled seismic design forces if the nominal clearance (air gap) between the equipment support frame and restraints is greater than 0.25 in. (*Standard* Table 13.6-1, footnote b).

18.4.3 Direct Attachment to Structure

This section illustrates determination of forces for cast-in-place concrete anchors, where the design anchor strength is greater than the strength capacity of the ductile steel anchorage element. Therefore, the load combinations considering Ω_0 are not used for the component anchorage design.

Figure 18.4-2 shows a free-body diagram for seismic force analysis.
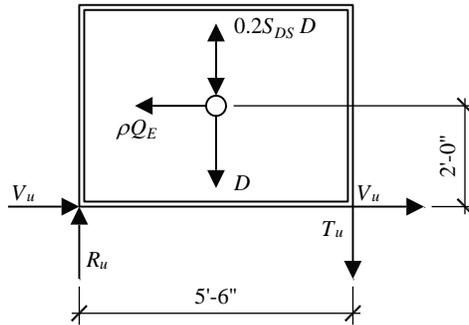
Figure 18.4-2 Free-body diagram for seismic force analysis
(1.0 ft = 0.348 m)

$$F_p = \frac{0.4(2.5)(1.487)(3,000 \text{ lb})}{(6.0/1.0)}\left[1 + 2(1)\right] = 2,231 \text{ lb} \qquad \text{(\textit{Standard} Eq. 13.3-1)}$$

$$F_{p_{max}} = 1.6(1.487)(1.0)(3,000 \text{ lb}) = 7,138 \text{ lb} \qquad \text{(\textit{Standard} Eq. 13.3-2)}$$

$$F_{p_{min}} = 0.3(1.487)(1.0)(3,000 \text{ lb}) = 1,338 \text{ lb} \qquad \text{(\textit{Standard} Eq. 13.3-3)}$$

Since F_p is greater the F_{pmin} and less than F_{pmax}, the value determined from Equation 13.3-1 applies.

$$E_h = \rho Q_E \qquad \text{(\textit{Standard} Eq. 12.4-3)}$$

$$E_v = 0.2S_{DS}D \qquad \text{(\textit{Standard} Eq. 12.4-4a)}$$

where:

Q_E (due to horizontal application of F_p) = 2,231 lb $\qquad$ (*Standard* Sec. 12.4.2-1)

$\rho = 1.0$ (HVAC units are nonstructural components) $\qquad$ (*Standard* Sec. 13.3.1)

D = dead load effect (due to vertical load application)

Substituting, one obtains:

$E_h = \rho Q_E = (1.0)(2,231 \text{ lb}) = 2,231 \text{ lb}$ $\qquad$ (horizontal earthquake effect)

$E_v = 0.2S_{DS}D = 0.2S_{DS}D = (0.2)(1.487)(3,000 \text{ lb}) = 892 \text{ lb}$ $\qquad$ (vertical earthquake effect)

The above terms are then substituted into the following Basic Load Combinations for Strength Design of Section 12.4.2.3 to determine the design member and connection forces to be used in conjunction with seismic loads.

$1.2D + E_v + E_h + L + 0.2S$ $\qquad$ (*Standard* Basic Load Combination 6)

$0.9D - E_v + E_h$ (*Standard* Basic Load Combination 7)

Based on the free-body diagram, the seismic load effects can be used to determine bolt shear, V_u and tension, T_u (where a negative value indicates tension). In the calculations below, the signs of S_{DS} and F_p have been selected to result in the largest value of T_u.

$$U = 1.2D + 0.2S_{DS}D + \rho Q_E$$

$$V_u = \frac{1.0\ (2{,}231\ \text{lb})}{4\ \text{bolts}} = 558\ \text{lb/bolt}$$

$$T_u = \frac{\lfloor 1.2 - 0.2(1.487) \rfloor\ (3{,}000\ \text{lb})(2.75\ \text{ft}) - 1.0\ (2{,}231)\ (2\ \text{ft})}{(5.5\ \text{ft})(2\ \text{bolts})} = 299\ \text{lb/bolt (no tension)}$$

$$U = 0.9D - 0.2S_{DS}D + \rho Q_E$$

$$V_u = \frac{1.0\ (2{,}231\ \text{lb})}{4\ \text{bolts}} = 558\ \text{lb/bolt}$$

$$T_u = \frac{\lfloor 0.9 - 0.2(1.487) \rfloor\ (3{,}000\ \text{lb})(2.75\ \text{ft}) - 1.0\ (2{,}231\ \text{lb})\ (2\ \text{ft})}{(5.5\ \text{ft})(2\ \text{bolts})} = 46\ \text{lb/bolt (no tension)}$$

Anchors with design capacities exceeding the calculated demands would be selected using the procedures in ACI 318 Appendix D.

18.4.4 Support on Vibration Isolation Springs

This portion of the example illustrates the design of the same HVAC unit when the component is supported on vibration isolators and determination of anchor design forces when the attachment to the structure is made with anchors controlled by concrete breakout. The nominal clearance (air gap) between the equipment support frame and the seismic restraint is presumed to be greater than 1/4 in, so the design value of F_p is doubled, per *Standard* Table 13.6-1, footnote c. If a limit of gap clearance to ¼ inch (which would require special inspection during construction to be sure it happened) was specified, it would reduce design seismic forces on seismic restraints and associated anchorage. For anchors to concrete, the load combinations considering Ω_0 are used for the component anchorage design.

Equipment that contains rotating or reciprocating components may be internally isolated. Externally the equipment is directly attached to the structure, but vibration isolators are installed on some of the internal components. Internally isolated components are subject to higher seismic design forces, and the appropriate design coefficients from *Standard* Table 13.6-1 should be used. Any mechanical component that normally would contain rotating or reciprocating items and is directly attached to the structure should be investigated to determine if it is internally isolated. Any component which contains one or more internal items that are mounted on vibration isolators, such as fans or motors inside air handler units, is considered an internally isolated component and should be design for higher loads as specified in the Standard.

Design forces applied to the top of the vibration isolators are determined by an analysis of earthquake forces applied in a diagonal horizontal direction as shown in Figure 18.4-3. Terminology and concept are taken from ASHRAE APP IP. In the equations below, $F_{pv} = E_v = 0.2S_{DS}W_p$:

Angle of diagonal loading:

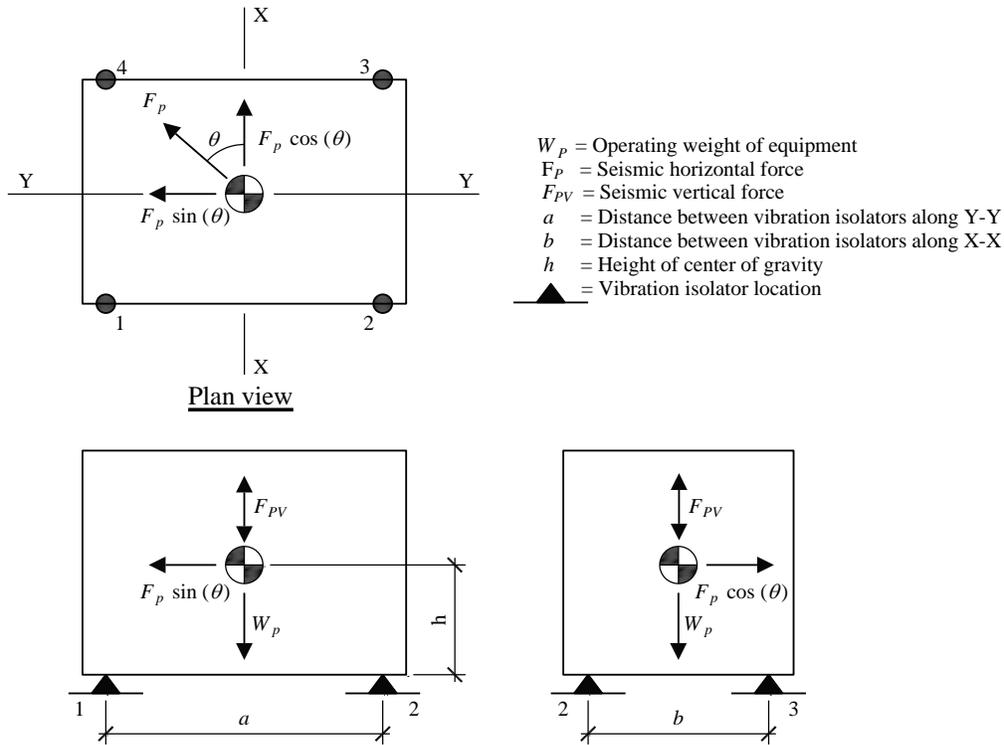$$\theta = \tan^{-1}\left(\frac{b}{a}\right)$$ (ASHRAE APP IP Eq. 17)

Tension per isolator:

$$T_u = \frac{W_p - F_{pv}}{4} - \frac{F_p h}{2}\left(\frac{\cos\theta}{b} + \frac{\sin\theta}{a}\right)$$ (ASHRAE APP IP Eq. 18)

Compression per isolator:

$$C_u = \frac{W_p + F_{pv}}{4} + \frac{F_p h}{2}\left(\frac{\cos\theta}{b} + \frac{\sin\theta}{a}\right)$$ (ASHRAE APP IP Eq. 19)

Shear per isolator:

$$V_u = \frac{F_p}{4}$$ (ASHRAE APP IP Eq. 20)

Figure 18.4-3 ASHRAE diagonal seismic force analysis for vibration isolation springs

Select the worst-case assumption.

$$F_p = \frac{0.4(2.5)(1.487)(3{,}000 \text{ lb})}{(2.0/1.0)}(1 + 2(1)) = 6{,}692 \text{ lb} \qquad \text{(\textit{Standard} Eq. 13.3-1)}$$

$$F_{p_{max}} = 1.6(1.487)(1.0)(3{,}000 \text{ lb}) = 7{,}138 \text{ lb} \qquad \text{(\textit{Standard} Eq.13.3-2)}$$

$$F_{p_{min}} = 0.3(1.487)(1.0)(3{,}000 \text{ lb}) = 1{,}338 \text{ lb} \qquad \text{(\textit{Standard} Eq. 13.3-3)}$$

Components mounted on vibration isolation systems must have a bumper restraint or snubber in each horizontal direction. Per *Standard* Table 13.6-1, footnote b, the design force must be taken as $2F_p$ if nominal clearance (air gap) between equipment and seismic restraint is greater than 0.25 inch.

$$Q_E = 2F_p = 2(6{,}692 \text{ lb}) = 13{,}384 \text{ lb} \qquad \text{(\textit{Standard} Sec. 6.1.3)}$$

$$\rho = 1.0 \text{ (HVAC units are nonstructural components)} \qquad \text{(\textit{Standard} Sec. 13.3.1)}$$

$$\rho Q_E = (1.0)(13{,}384 \text{ lb}) = 13{,}384 \text{ lb} \qquad \text{(horizontal earthquake effect)}$$

$$F_{pv(\text{ASHRAE})} = 0.2 S_{DS}D = (0.2)(1.487)(3{,}000 \text{ lb}) = 892 \text{ lb} \qquad \text{(vertical earthquake effect)}$$

$$D = W_p = 3{,}000 \text{ lb} \qquad \text{(vertical gravity effect)}$$

The above terms are then substituted into the Basic Load Combinations for Strength Design of Section 2.3.6 to determine the design member and connection forces to be used in conjunction with seismic loads.

$1.2D + E_v + E_h + L + 0.2S$ (*Standard* Basic Load Combination 6)

$0.9D - E_v + E_h$ (*Standard* Basic Load Combination 7)

These seismic load effects can be used to determine bolt shear, V_u and tension, T_u (where a negative value indicates tension). In the calculations below, the signs of S_{DS} and F_p have been selected to result in the largest value of T_u. Similar calculations would be performed to determine the maximum compressive force C_u.

$U = 1.2D + 0.2S_{DS}D + \rho Q_E$

$$T_u = \frac{1.2(3,000\text{ lb})-(892\text{ lb})}{4} - \frac{(13,384\text{ lb})(2\text{ ft})}{2}\left[\frac{\cos(51.8\text{ deg})}{7\text{ ft}}+\frac{\sin(51.8\text{ deg})}{5.5\text{ ft}}\right] = -2,405\text{ lb}$$

$$C_u = \frac{1.2(3,000\text{ lb})+(892\text{ lb})}{4} + \frac{(13,384\text{ lb})(2\text{ ft})}{2}\left[\frac{\cos(51.8\text{ deg})}{7\text{ ft}}+\frac{\sin(51.8\text{ deg})}{5.5\text{ ft}}\right] = 4,204\text{ lb}$$

$$V_u = \frac{13,384\text{ lb}}{4} = 3,346\text{ lb}$$

$U = 0.9D - 0.2S_{DS}D + \rho Q_E$

$$\theta = \tan^{-1}\left(\frac{7\text{ ft}}{5.5\text{ ft}}\right) = 51.8°$$

$$T_u = \frac{0.9(3,000\text{ lb})-(892\text{ lb})}{4} - \frac{(13,384\text{ lb})(2\text{ ft})}{2}\left[\frac{\cos(51.8\text{ deg})}{7\text{ ft}}+\frac{\sin(51.8\text{ deg})}{5.5\text{ ft}}\right] = 2,630\text{ lb}$$

$$C_u = \frac{0.9(3,000\text{ lb})+(892\text{ lb})}{4} + \frac{(13,384\text{ lb})(2\text{ ft})}{2}\left[\frac{\cos(51.8\text{ deg})}{7\text{ ft}}+\frac{\sin(51.8\text{ deg})}{5.5\text{ ft}}\right] = -3,980\text{ lb}$$

$$V_u = \frac{13,384\text{ lb}}{4} = 3,346\text{ lb}$$

The vibration isolator would be designed to resist these forces.

18.4.4.2 Proportioning and Details. In this example, there is no component or a support in the load path leading to the structure that undergoes ductile yielding at a load level less than the design strength of the corresponding anchor, so the anchors are designed to resist the load combinations considering Ω_0 in accordance with *Standard* Section 2.3.6. In the calculations below, the signs of S_{DS} and F_p have been selected to result in the largest value of T_u. The geometry of the vibration isolators are shown in Figure 18.4-4. By inspection, the load combination that results in net tension on the anchors governs. Applying

the load combinations of *Standard* Section 2.3.6, Load Combination 7, the vertical design tension force is:

$$U = \underline{0.9D - E_v} + E_{mh}$$ (*Standard* Basic Load Combination 7)

$$\underline{E_{mh}} = \Omega_0 Q_E$$ (*Standard* Eq. 12.4-7)

$$\theta = \tan^{-1}\left(\frac{7 \text{ ft}}{5.5 \text{ ft}}\right) = 51.8°$$

Tension per isolator:

$$T_u = \frac{W_p - F_{pv}}{4} - \Omega_0 \frac{F_p h}{2}\left(\frac{\cos\theta}{b} + \frac{\sin\theta}{a}\right)$$

$$T_u = \frac{0.9(3,000 \text{ lb}) - (892 \text{ lb})}{4} - (2.0)\frac{(13,384 \text{ lb})(2 \text{ ft})}{2}\left(\frac{\cos(51.8 \text{ deg})}{7 \text{ ft}} + \frac{\sin(51.8 \text{ deg})}{5.5 \text{ ft}}\right) = \text{-5,737 lb}$$

Acting concurrently with tension, the horizontal design shear force is:

$$V_u = \frac{\Omega_0 F_p}{4}$$

$$V_u = 2.0\left(\frac{13,384 \text{ } lb}{4}\right) = 6,692 \text{ lb}$$

Since the horizontal shear force is applied at the top of the isolator, it generates a moment that induces prying action, which will increase the tension on the anchor. Other local prying effects are assumed to be negligible, although in some cases these effects will be significant and would further increase the design anchor force. Assuming that each isolator is attached to the concrete slab with two anchors, the design tension force per anchor including the effects of prying, T_b is:

$$T_b = \frac{T_u}{2 \text{ } anchors} - \frac{5 \text{ } in.}{2 \text{ } in.}\left(\frac{V_u}{2 \text{ } anchors}\right) = \frac{-5,737 \text{ } lb}{2} - \left(\frac{5 \text{ } in.}{2 \text{ } in.}\right)\left(\frac{6,692 \text{ } lb}{2}\right) = -8,365 \text{ } lb \text{ } (tension)$$

The design shear force per bolt, V_b is:

$$V_b = \frac{6,692 \text{ } lb}{2 \text{ } anchors} = 3,346 \text{ lb.}$$
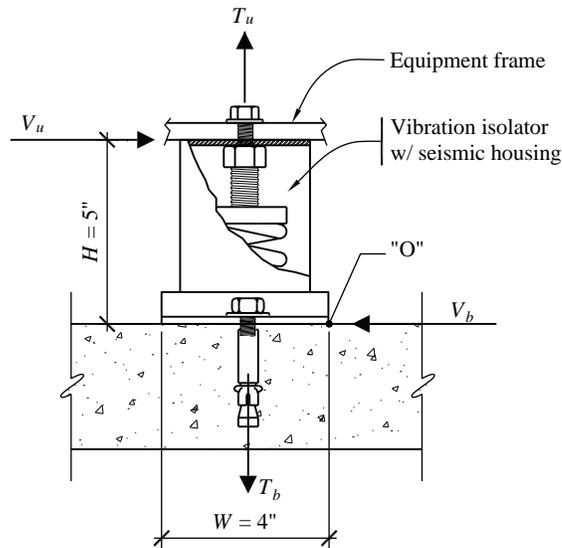
Figure 18.4-4 Anchor and snubber loads for support on vibration isolation springs
(1.0 in. = 25.4 mm)

18.4.5   Additional Considerations for Support on Vibration Isolators

Vibration isolation springs are provided for equipment to prevent vibration from being transmitted to the building structure. However, they provide virtually no resistance to horizontal seismic forces. In such cases, some type of restraint is required to resist the seismic forces. Figure 18.4-5 illustrates one concept where a bolt attached to the equipment base is allowed to displace a controlled distance (gap) in either direction along its longitudinal axis before it contacts resilient impact material.
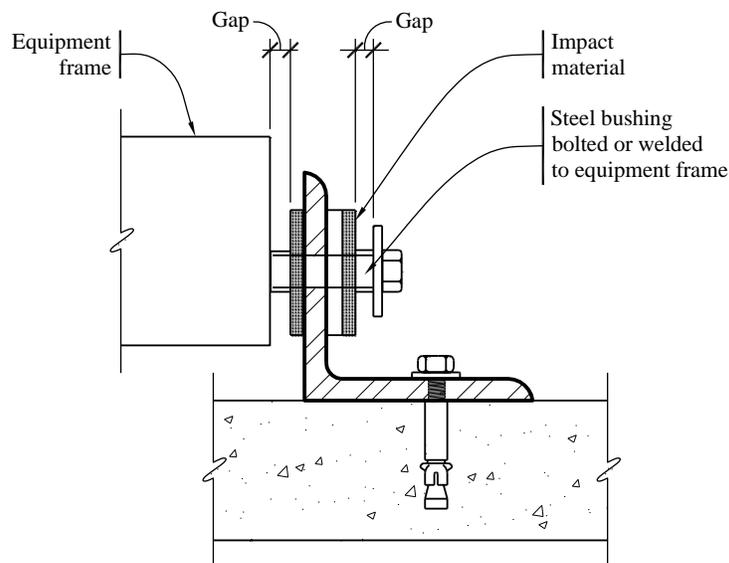
Figure 18.4-5 Lateral restraint required to resist seismic forces

Design of restraints for vibration-isolated equipment varies for different applications and for different manufacturers. In most cases, restraint design incorporates all directional capability with an air gap, a soft impact material and a ductile restraint or housing.

Restraints should have all-directional restraint capability to resist both horizontal and vertical motion. Vibration isolators have little or no resistance to overturning forces. Therefore, if there is a difference in height between the equipment's center of gravity and the support points of the springs, rocking is inevitable and vertical restraint is required.

An air gap between the restraint device and the equipment prevents vibration from transmitting to the structure during normal operation of the equipment. Air gaps generally are no greater than 1/4 inch. Dynamic tests indicate a significant increase in acceleration for air gaps larger than 1/4 inch, and this is reflected in the requirement in *Standard* Table 13.6-1, footnote b. that F_p be doubled if the air gap exceeds ¼ inch.

A soft impact material, often an elastomer such as bridge bearing neoprene, reduces accelerations and impact loads by preventing steel-to-steel contact. The thickness of the elastomer can significantly reduce accelerations to both the equipment and the restraint device and should be addressed specifically for life-safety applications.

In Section 18.4.4, the example was for a housed isolator, where the vibration isolator and seismic restraints are combined into a single unit. A ductile restraint or housing is critical to prevent catastrophic failure. Unfortunately, housed isolators made of brittle materials such as cast iron often are assumed to be capable of resisting seismic loads and continue to be installed in seismic zones.

Overturning calculations for vibration-isolated equipment must consider a worst-case scenario as illustrated in Section 18.4.4.1. However, important variations in calculation procedures merit further discussion. For equipment that is usually directly attached to the structure or mounted on housed vibration isolators, the weight can be used as a restoring force since the equipment will not transfer a tension load to the anchors until the entire equipment weight is overcome at any corner. For equipment installed on any other vibration-isolated system (such as the separate spring and snubber arrangement shown in Figure 18.4-5), the weight of the unit cannot be used to provide a restoring force in the overturning calculations.

As the foregoing illustrates, design of restraints for resiliently mounted equipment is a specialized topic. The *Standard* sets out only a few of the governing criteria. Some suppliers of vibration isolators in the highest seismic zones are familiar with the appropriate criteria and procedures. Consultation with these suppliers may be beneficial.

18.5   PIPING SYSTEM SEISMIC DESIGN

In the 2016 edition of the *Standard*, the design requirements for piping, electrical raceways and ducts were updated and consolidated. Piping and tubing systems requirements are contained in *Standard* Section 13.6.8. Suspended components that are installed in-line and rigidly connected to and supported by the piping system such as valves, strainers, traps, pumps, air separators and tanks are permitted to be considered part of the piping system for the purposes of determining the need for and sizing of lateral bracing. Where components are braced independently due to their weight but the associated piping is not braced, flexibility must be provided to accommodate relative movement between the components.

Piping systems may be exempt from the seismic design requirements if they meet the requirements in *Standard* Section 13.6.8.3. Piping systems with I_p=1.0, may be exempt if flexible connections, expansion

loops or other assemblies are provided to accommodate the relative displacement between component and piping, the piping system is positively attached to the structure, and where one of the following apply:

Trapeze assemblies with 3/8-in. diameter rod hangers not exceeding 12 in. in length from the pipe support point to the connection at the supporting structure are used to support piping and no single pipe exceeds the specified size limits, and the total weight of the piping supported by the any single trapeze assembly is 100 lb or less, or

Trapeze assemblies with 1/2-in. diameter rod hangers not exceeding 12 in. in length from the pipe support point to the connection at the supporting structure are used to support piping and no single pipe exceeds the specified size limits, and the total weight of the piping supported by the any single trapeze assembly is 200 lb or less, or

Trapeze assemblies with 1/2-in. diameter rod hangers not exceeding 24 in. in length from the pipe support point to the connection at the supporting structure are used to support piping and no single pipe exceeds the specified size limits, and the total weight of the piping supported by the any single trapeze assembly is 100 lb or less.

Piping supported by individual rod hangers may be exempt if it is supported by rods of 3/8- or 1/2-in.in diameter, each hanger is 12 in. in length or less, the total weight supported by any hanger is less than 50 lb., and the piping meets specified limitation on diameter and seismic design category.

18.5.1 Example Description

This example illustrates seismic design for a portion of a piping system in an acute care hospital. It illustrates determination of the seismic demands on the system, consideration of anchorage and bracing of the system and design for system displacements within the structure and between structures. The example focuses on the determination of force and displacement demands on the different components of the system. The sizing of the various elements (braces, anchor bolts, etc.) are not covered in detail.

The *Standard* provides requirements for three types of piping systems: ASME B31 pressure piping systems (Sec. 13.6.8.1), fire protection piping systems in accordance with NFPA 13 (Sec. 13.6.8.2) and other piping systems (Sec. 13.6.8). This example considers three piping runs of a chilled water piping system supported from the roof of a two-story structure. The system is not intended to meet the ASME 31 requirements and, therefore, is designed to the "other piping system" requirements of the *Standard*. The piping system is illustrated in Figures 18.5-1 and 18.5-2 and a typical trapeze-type support assembly is shown in Figures 18.5-3 and 18.5-4. One run of the piping system crosses a seismic separation joint to enter an adjacent structure. The building, a hospital, is located in an area of high ground shaking potential and assigned to Seismic Risk Category IV.
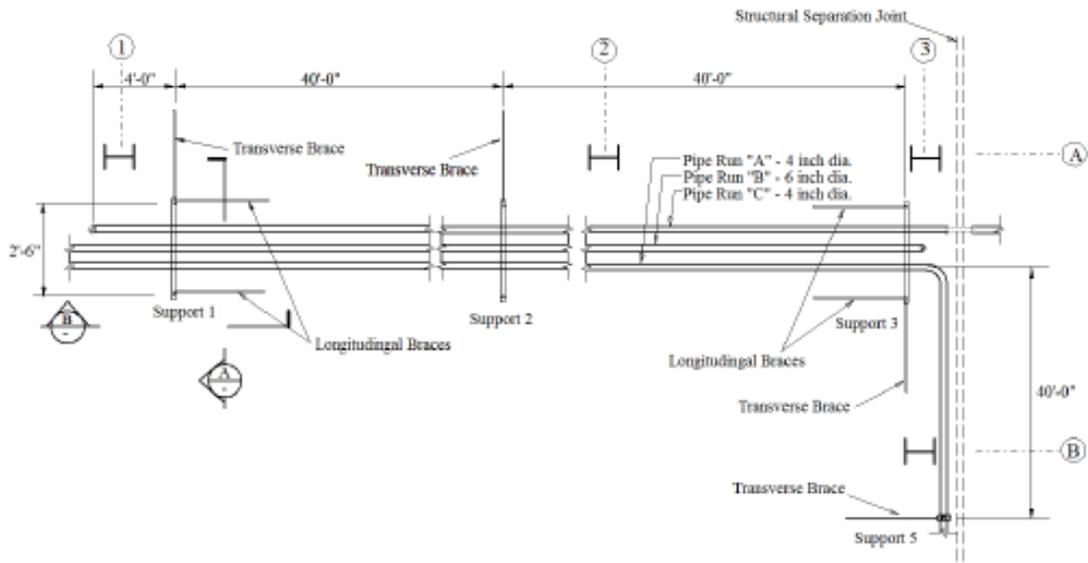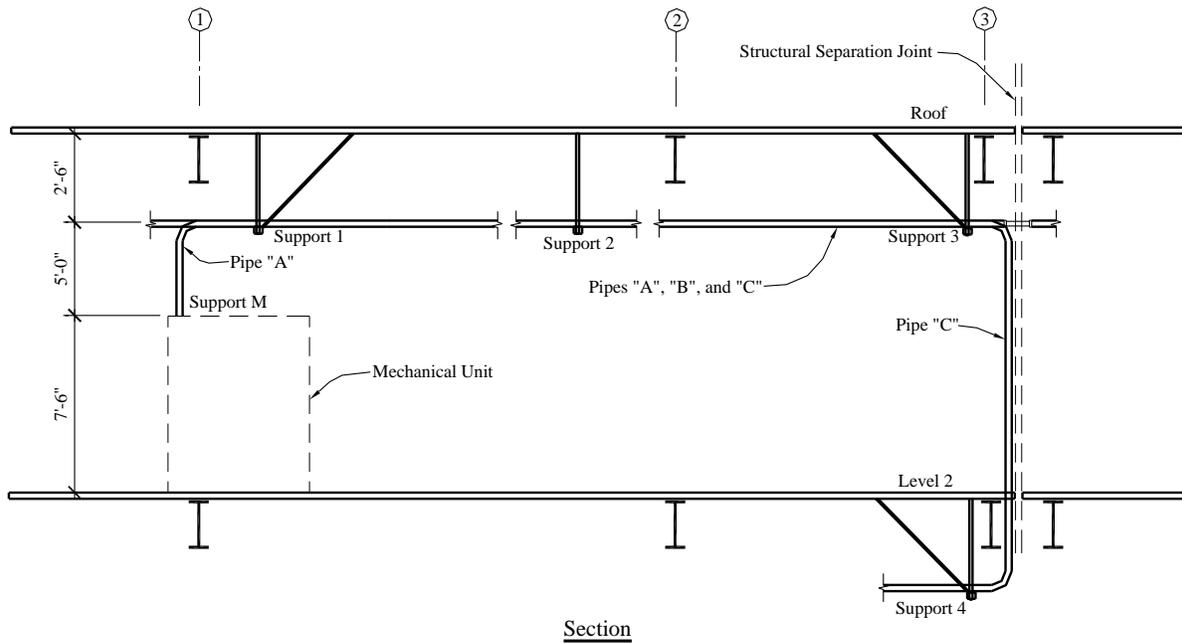
Figure 18.5-1 Plan of Piping system

Figure 18.5-2 Piping system near Column Line A

2'-6"

2'-6"

"A"   "B"   "C"

1
1

A Section
- Support 1
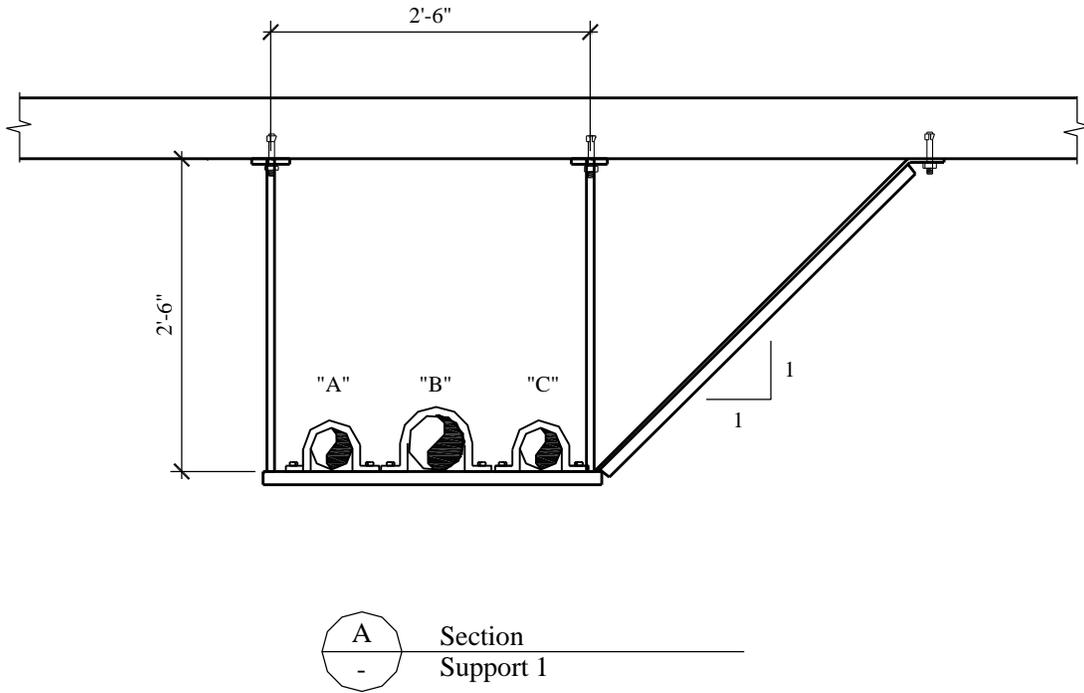
Figure 18.5-3 Typical trapeze-type support assembly with transverse bracing

2'-6"

1
1

B Section
- Support 1
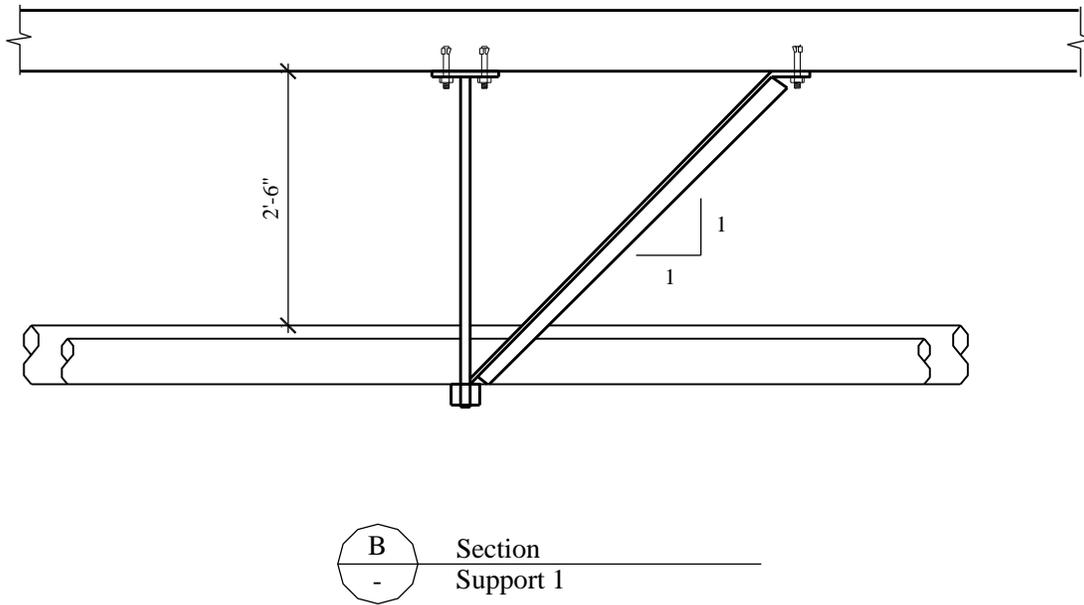
Figure 18.5-4 Typical trapeze-type support assembly with longitudinal bracing

18.5.1.1 Earthquake Design Requirements. Earthquake design requirements for piping systems in the *Standard* depends on the system importance factor (I_p), the pipe diameter and the installation geometry.

The importance factor is determined in *Standard* Section 13.1.3. Given that the structure is assigned to Seismic Risk Category IV, the components are assigned $I_p = 1.5$, unless it can be shown that the component is not needed for continued operation of the facility and failure of the component would not impair operations. Since failure of the piping system will result in flooding of the hospital, $I_p = 1.5$.

Some piping is exempt from some or all of the seismic requirements, provided it meets the criteria in *Standard* Section 13.6.8.3. The exemptions in Section 13.1.4 apply only to components with $I_p = 1.0$ and therefore are not applicable to this example. In Seismic Design Categories D, E, and F, Section 13.6.8.3 Item 4 waives seismic support requirements for piping with I_p greater than 1.0 if the pipe is 1 in. or less in diameter, has an R_p of 4.5 or greater, is supported by rods less than 12 inches long from the pipe support point to the connection to the supporting structure. The total weight supported by any single hanger must be less than 50 lb. Our example piping system does not meet these requirements, so seismic design and lateral supports will be required.

"Other" piping systems must meet the following requirements of the *Standard*:

    Section 13.3: Seismic Demands on Nonstructural Components

    Section 13.4: Nonstructural Component Anchorage

    Section 13.6.3: Mechanical Components

    Section 13.6.5: Component Supports

It is important to note that per *Standard* Section 13.6.3, where I_p is greater than 1.0, the component anchorage, bracing and the component itself (in this example, the pipe) must be designed to resist seismic forces.

18.5.1.2 System Configuration. The portion of the piping system under consideration consists of three piping runs:

    Piping Run "A", a 4-inch-diameter pipe, which connects to a large mechanical unit at Line 1 supported at the second level. It crosses a seismic separation between adjacent structures at Line 3.

    Piping Run "B", a 6-inch-diameter pipe, which has a vertical riser to the second level at Line 3.

    Piping Run "C", a 4-inch-diameter pipe, which turns 90 degrees to parallel Line 3 at Column Line 3-A.

Pipe Run "A" - 4-inch dia.
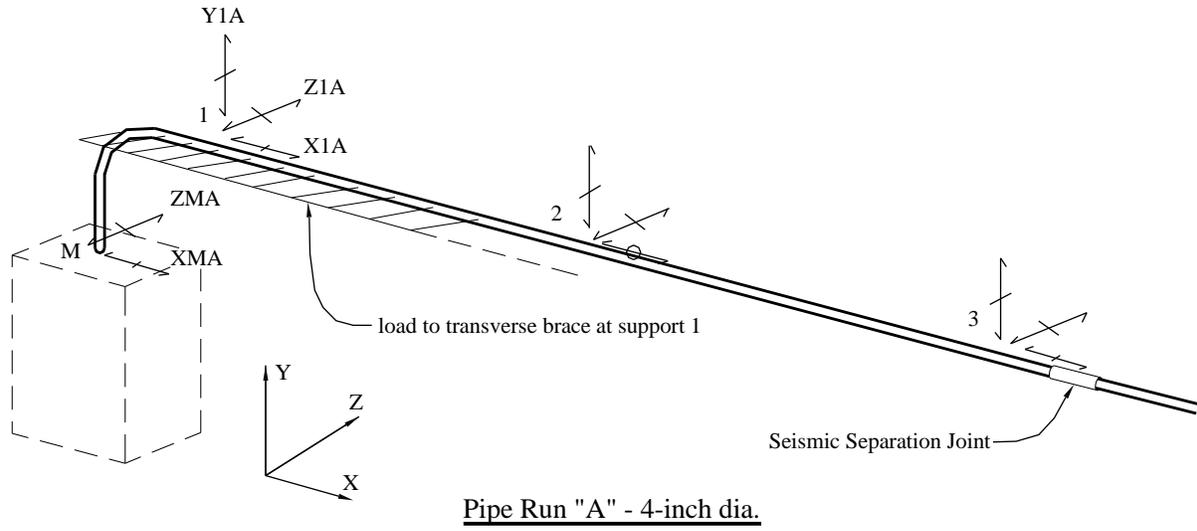
Figure 18.5-5 Piping Run "A"

Pipe Run "B" - 6-inch dia.
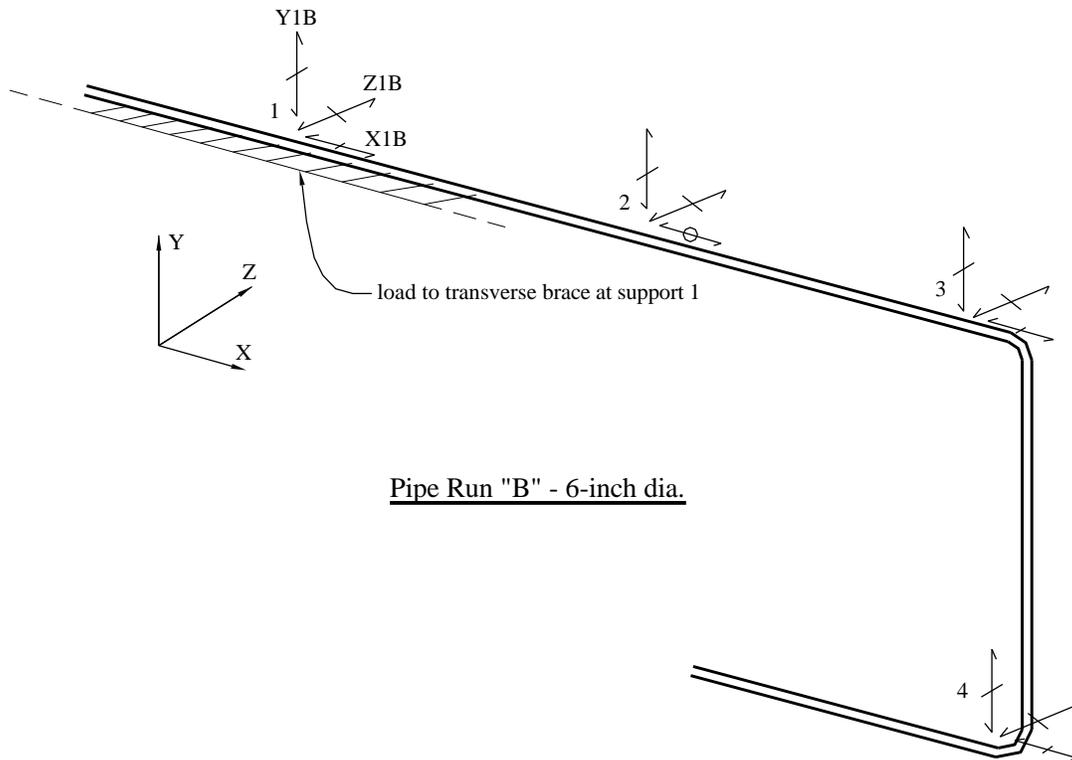
Figure 18.5-6 Piping Run "B"

Figure 18.5-7 Piping Run "C"

The system consists of non-ASME B31 piping fabricated from steel Schedule 40 pipe with threaded connections. This example covers determination of the seismic forces acting on the system, a check of the seismically induced stresses in the pipes using simplifying assumptions, determination of bracing and anchorage forces and a check of the system for seismic relative displacements.
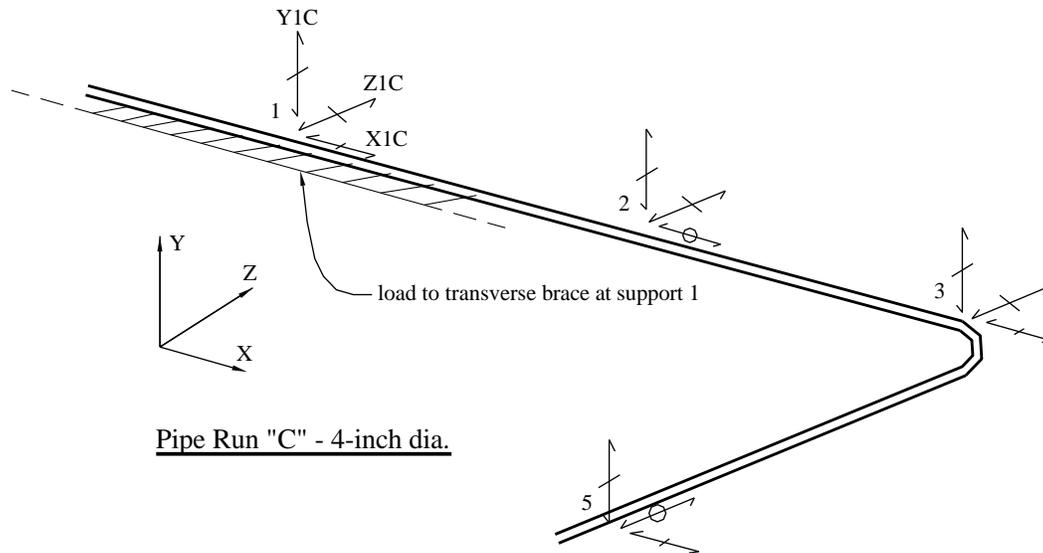
It should be noted that details of pipe bracing systems vary according to the local preferences and practices of mechanical and plumbing contractors. In addition, the use of proprietary pipe hanging and bracing systems is relatively common. As a result, this example concentrates on quantifying the prescribed seismic forces and displacements and on simplified stress checks of the piping system itself. After the seismic forces and displacements are determined, the bracing and anchorage connections can be designed and detailed according to the appropriate AISC and ACI codes.

18.5.2 Design Requirements.

18.5.2.1 Seismic Design Parameters and Coefficients.

$a_p = 2.5$ for piping systems   (*Standard* Table 13.6-1)

$R_p = 4.5$ for piping not in accordance with ASME B31, constructed   (*Standard* Table 13.6-1)
     of high or limited deformability materials, with joints made
     by threading

$\Omega_0 = 2.0$ for anchorage to concrete with nonductile behavior   (*Standard* Table 13.6-1, footnote c)

$S_{DS} = 1.0$ (for the selected location and site class)   (given)

Seismic Design Category = D   (*Standard* Table 11.6-1)

$h = 30$ feet (roof height)   (given)

h_{sx} = 15 feet (story height)   (given)

z = 30 feet (system is braced at the roof level)   (given)

$$\frac{z}{h} = \frac{30.0\ \text{ft}}{30.0\ \text{ft}} = 1.0$$ (at roof)

I_p = 1.5   (*Standard* Sec. 13.1.3)

Gravity (non-seismic) supports provided every 10'-0"   (given)

System working pressure *(P)* = 200 psi   (given)

ASTM A53 Pipe F_y = 35 ksi, threaded connections   (given)

D = Dead Load = W_p = 16.4 plf (4-inch-diameter water-filled pipe)   (given)

                       = 31.7 plf (6-inch-diameter water-filled pipe)

Longitudinal brace spacing = 80 feet   (given)

According to *Standard* Section 13.3.1 (and repeated in Sec. 12.3.4.1), the redundancy factor does not apply to the design of nonstructural components.

18.5.2.2 Seismic Design Forces.

$$F_p = \frac{0.4(2.5)(1.0)W_p}{4.5\big/1.5}(1+2(1)) = 1.00W_p$$ (*Standard* Eq. 13.3-1)

$$F_p = 1.6(1.0)(1.5)W_p = 2.40W_p$$ (*Standard* Eq. 13.3-2)

$$F_p = 0.3(1.0)(1.5)Wp = 0.45W_p$$ (*Standard* Eq. 13.3-3)

$$E_v = 0.2(1.0)D = 0.2D = 0.2W_p$$ (*Standard* Sec. 12.4.2)

Standard Eq. 13.3-1 governs the horizontal seismic force on the piping system.

18.5.2.3 Performance Criteria.

System failure must not cause failure of an essential architectural, mechanical, or electrical component (*Standard* Sec. 13.2.3).

Component seismic attachments must be bolted, welded, or otherwise positively fastened without considering the frictional resistance produced by the effects of gravity (*Standard* Sec. 13.4).

The effects of seismic relative displacements must be considered in combination with displacements caused by other loads as appropriate (*Standard* Sec. 13.3.2).

The piping system must be designed to resist the forces in accordance with *Standard* Section 13.3.1 and must be able to accommodate movements of the structure resulting from response to the design basis ground motion, D_p.

18.5.3 Piping System Design

The requirements for the design of the piping system are summarized in Table 13.2-1 of the *Standard*. The supports and attachments of all mechanical and electrical components must meet the requirements listed in Table 13.2-1. Where $I_p > 1.0$, the component itself, in this case the pipe, must also meet the seismic loading and stress limit requirements.

18.5.3.1 Check of Pipe Stresses.
The spacing of seismic supports is often determined by the need to limit stresses in the pipe. Therefore, the piping stress check is often performed first in order confirm the assumptions on brace spacing. For non-ASME B31 piping that is not subject to high operating temperatures or pressures, the stress check assumptions may be simplified. The pipes can be idealized as continuous beams spanning between lateral braces, while longitudinal forces can be determined using the length of pipe tributary to the longitudinal brace.

The permissible stresses in the pipe are given in *Standard* Section 13.6.11, Item 2. For piping with threaded connections, the permissible stresses are limited to 70 percent of the minimum specified yield strength.

The section properties of the Schedule 40 pipes are as follows:

> 4-inch diameter:
>
> > Inner diameter, $d_1 = 4.026$ in.
> >
> > Outer diameter, $d = 4.5$ in.
> >
> > Wall thickness, $t = 0.237$ in.
> >
> > Plastic modulus, $Z = \dfrac{d^3}{6} - \dfrac{d_1^{\ 3}}{6} = \dfrac{(4.5)^3}{6} - \dfrac{(4.026)^3}{6} = 4.31 \text{ in}^3$
> >
> > Moment of inertia, $I = 0.049807(d^4 - d_1^{\ 4}) = 0.049087((4.5)^4 - (4.026)^4) = 7.23 \text{ in}^4$
>
> 6-inch diameter:
>
> > Inner diameter, $d_1 = 6.065$ in.
> >
> > Outer diameter, $d = 6.625$ in.
> >
> > Wall thickness, $t = 0.28$ in.
> >
> > Plastic modulus, $Z = \dfrac{(6.625)^3}{6} - \dfrac{(6.065)^3}{6} = 11.28 \text{ in}^3$

$$\text{Moment of inertia, } I = 0.049087((6.625)^4 - (6.065)^4) = 28.14 \text{ in}^4$$

18.5.3.1.1 Gravity and Pressure Loads. The longitudinal stresses in piping due to pressure and weight may be estimated using the following equation:

$$S_L = \frac{Pd}{4t} + \frac{M_g}{Z}$$

where:

S_L = sum of the longitudinal stresses due to pressure and weight

P = internal design pressure, psig

d = outside diameter of pipe, in.

t = pipe wall thickness, in.

M_g = resultant moment loading on cross section due to weight and other sustained loads, in-lb

Z = section modulus, in^3

Vertical supports are spaced at 10-foot centers, so the moment due to gravity, M_g, may be conservatively estimated as follows:

$$M_g = \frac{Dl^2}{8} = \frac{D(10)^2}{8} = 12.5D$$

For a 4-inch-diameter pipe, where D = 16.4 plf:

$$M_g = 12.5D = 12.5(16.4) = 205 \text{ ft-lb} = 2,460 \text{ in-lb}$$

$$S_{L\text{-}DeadLoad} = \frac{2,460}{4.31} = 571 \text{ psi}$$

$$S_{L-Pressure} = \frac{200(4.5)}{4(0.237)} = 949 \text{ psi}$$

For a 6-inch-diameter pipe, where D = 31.7 plf:

$$M_g = 12.5(31.7) = 396 \text{ ft-lb} = 4,752 \text{ in-lb}$$

$$S_{L-DeadLoad} = \frac{4,752}{11.28} = 421 \text{ psi}$$

$$S_{L\text{-}Pressure} = 1,183 \text{ psi}$$

18.5.3.1.2 Seismic Loads on Piping Runs A and C. By idealizing the piping runs as continuous beams, the maximum bending moments and reactions can be readily estimated.

Piping Runs A and C are 4-inch-diameter pipes, shown schematically in Figures 18.5-5 and 18.5-7. They are idealized as a two-span continuous beam. The design lateral load, F_p, is taken as:

$$F_p = 1.00W_p = 1.00(16.4) = 16.4 \text{ plf} = w$$

The maximum moment due to horizontal seismic load may be approximated as:

$$M_E = \frac{wl^2}{8} = \frac{16.4(40)^2}{8} = 3,280 \text{ ft-lb} = 39,360 \text{ in-lb}$$

The flexural stress associated with this moment is:

$$f_{bh} = \frac{M_E}{Z} = \frac{39,360}{4.31} = 9,132 \text{ psi}$$

The moment due to vertical seismic load, $E_v = 0.2\ W_p$, may be approximated as:

$$M_v = \frac{E_v l^2}{8} = \frac{0.2(16.4)(10)^2}{8} = 41 \text{ ft-lb} = 492 \text{ in-lb}$$

The flexural stress associated with this moment is:

$$f_{bv} = \frac{M_v}{Z} = \frac{492}{4.31} = 114 \text{ psi}$$

Note that for vertical seismic effects, the span of the pipe is taken as the distance between vertical supports, not the distance between lateral bracing.

The basic strength load combination including earthquake effects from *Standard* Sec. 2.3.6 that will govern is Load Combination 6:

$$1.2D + E_v + E_h + L + 0.2S$$

For nonstructural components, $\rho = 1.0$ and $Q_E =$ the forces (or stresses) resulting from applying F_p.

In this example, live load, L and snow load, S, are equal to zero. The dead load, D, includes bending stress due to dead load. The load factor for internal pressure is the same as that for dead load. The design stress in the pipe is therefore:

$$U = 1.2(421 \text{ psi}) + 0.2(1.0)(421 \text{ psi}) + 1.2(1,183 \text{ psi}) + 1.0(1.0)(9,132 \text{ psi}) = 11,141 \text{ psi}$$

The permissible stress from Section 13.6.11, Item 2, of the *Standard* is $0.7F_y = 0.7(35,000) = 24,500$ psi. Comparing the demand to capacity:

$$U = 11,141 \text{ psi} < 0.7(35,000 \text{ psi}) = 24,500 \text{ psi OK}$$

Note that a number of conservative assumptions were made for the sake of simplicity. A more precise analysis can be performed, where the piping is modeled to achieve more accurate bending moments and the effects of biaxial bending in the pipe are considered separately. Also note that at any point in the pipe wall, the stresses caused by dead (and vertical seismic) load and by horizontal seismic load occur in different physical locations in the pipe. The peak stresses due to vertically applied load occurs at the top and bottom of the pipe, while the peak stress for horizontally applied load occurs at mid-height of the pipe. Assuming that they are both occurring in the same location and are summed algebraically is quite conservative.

18.5.3.1.3 Seismic Loads on Piping Run B. Piping Run B, a 6-inch-diameter pipe, is shown schematically in Figure 18.5-6. It is idealized as a two-span continuous beam. Note that the effects of the 15-foot-high riser between Level 2 and the roof are considered separately. The design lateral load, F_p, is taken as follows:

$$F_p = 1.00 W_p = 1.00(31.7) = 31.7 \ \text{plf} = w$$

The maximum moment due to horizontal seismic load is approximated as:

$$M_E = \frac{wl^2}{8} = \frac{31.7(40)^2}{8} = 6{,}340 \ \text{ft-lb} = 76{,}080 \ \text{in-lb}$$

The flexural stress associated with this moment is:

$$f_{bh} = \frac{M_E}{Z} = \frac{76{,}080}{11.28} = 6{,}745 \ \text{psi}$$

The moment due to the vertical seismic load, $E_v = 0.2 \ W_p$, may be approximated as follows:

$$M_v = \frac{E_v l^2}{8} = \frac{0.2(31.7)(10)^2}{8} = 79.25 \ \text{ft-lb} = 951 \ \text{in-lb}$$

The flexural stress associated with this moment is:

$$f_{bv} = \frac{M_v}{Z} = \frac{951}{11.28} = 84 \ \text{psi}$$

The design stress in the pipe is:

$$U = 1.2(571 \ \text{psi}) + 0.2(1.0)(571 \ \text{psi}) + 1.2(941 \ \text{psi}) + 1.0(1.0)(6{,}745 \ \text{psi}) = 8{,}674 \ \text{psi} < 24{,}500 \ \text{psi} \qquad \text{OK}$$

18.5.4 Pipe Supports and Bracing

As with the design of the pipe itself, design of the vertical and lateral supports of piping systems can be simplified by making conservative assumptions. In this example, design demands on the support assembly at Support 1 (Figure 18.5-8) are determined.
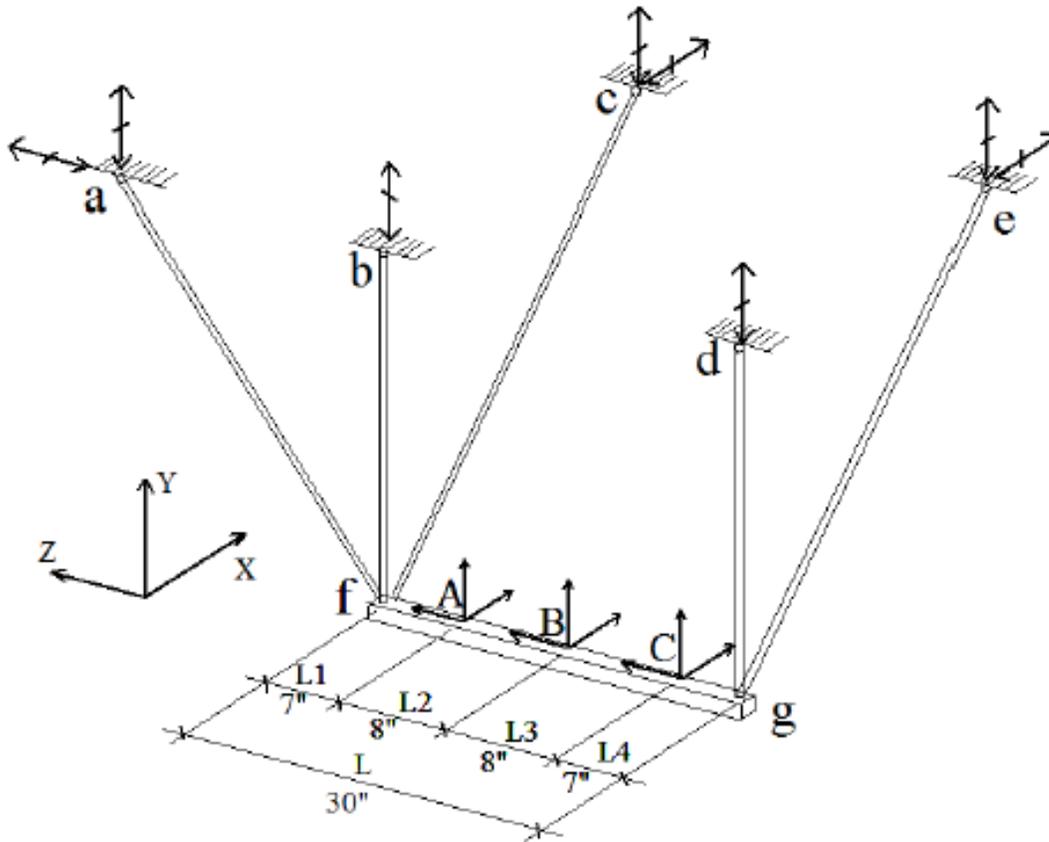
Figure 18.5-8 Design demands on piping support assembly

18.5.4.1 Vertical Loads. Vertical pipe supports are often considered separately from lateral bracing. Configuration and spacing of vertical supports may be governed by plumbing codes or other standards and guidelines. Given that the vertical component of seismic force, E_v, is often low relative to other vertical loads, vertical supports proportioned for gravity and operational loads generally are adequate to resist the vertical seismic forces. However, where a support resists the vertical component of a lateral or longitudinal brace force, it should be designed explicitly to resist all applied forces. This example focuses on vertical supports associated with the lateral bracing system.

Due to the repetitious nature of the pipe gravity support system, the vertical load at the brace assembly due to gravity or vertical seismic load can be estimated based on the tributary length of pipe. Given a 10-foot spacing of vertical supports, the vertical loads due to a 4-inch-diameter pipe are as follows:

Dead load, $P_{v4} = (10 \text{ ft})(16.4 \text{ plf}) = 164 \text{ lb}$

Vertical seismic load, $P_{Ev4} = 0.2(10 \text{ ft})(16.4 \text{ plf}) = 33 \text{ lb}$

For a 6-inch diameter pipe:

Dead load, $P_{v6} = (10 \text{ ft})(31.7 \text{ plf}) = 317 \text{ lb}$

Vertical seismic load, $P_{Ev6} = 0.2(10 \text{ ft})(31.7 \text{ plf}) = 63 \text{ lb}$

18.5.4.2 Longitudinal Lateral Loads. Spacing of longitudinal bracing may be dictated by system geometry, thermal demands on the pipe, anchorage and brace capacities, or prescriptive limitations in standards and guidelines. In this example, we assume longitudinal braces are provided every 80 feet, which is twice the transverse brace spacing.

For Piping Run A, the total length of pipe tributary to Support 1 is approximately 40 feet (half the distance between longitudinal braces at Supports 1 and 3) plus 9 feet (length of pipe from Support 1 to Support M, the mechanical unit), or 49 feet.

The longitudinal seismic load, P_{X1A}, for the 4-inch-diameter Piping Run A is:

$P_{X1A} = (49 \text{ ft})(F_p) = (49 \text{ ft})(16.4 \text{ plf}) = 804 \text{ lb}$

For Piping Runs B and C, the total length of pipe tributary to Support 1 is approximately 80 feet.

The longitudinal seismic load, P_{X1B}, for the 6-inch-diameter Piping Run B is:

$P_{X1B} = (80 \text{ ft})(F_p) = (80 \text{ ft})(31.7 \text{ plf}) = 2,536 \text{ lb}$

The longitudinal seismic load, P_{X1C}, for the 4-inch-diameter Piping Run C is:

$P_{X1C} = (80 \text{ ft})(F_p) = (80 \text{ ft})(16.4 \text{ plf}) = 1,312 \text{ lb}$

18.5.4.3 Transverse Lateral Loads. To determine the transverse loads at support points, the pipes are idealized as continuous beams spanning between transverse braces. Assuming continuity over a minimum of two spans, the maximum reaction can be approximated conservatively as:

$$(2)\frac{5}{8}wl$$

where w is the distributed lateral load and l is the spacing between transverse braces.

For Piping Run A, we assume that 5/8 of the total length of pipe between the mechanical unit and the transverse brace at Support 2 is laterally supported at Support 1 (see Figure 18.5-3). The maximum transverse reaction due to Piping Run A at Support 1 may be approximated as:

$$P_{Z1A} = \frac{5}{8}wl = \frac{5}{8}(16.4 \text{ plf})(40 \text{ ft} + 9 \text{ ft}) = 502 \text{ lb}$$

For Piping Runs B and C, we assume that 5/8 of the total length of pipe on each side of Support 1 is laterally braced at Support 1 (see Figures 18.5-4 and 18.5-5). The maximum transverse reaction due to Piping Run B at Support 1 is then approximated as:

$$P_{Z1B} = (2)\frac{5}{8}wl = (2)\frac{5}{8}(31.7 \text{ plf})(40 \text{ ft}) = 1,585 \text{ lb}$$

The maximum transverse reaction due to Piping Run C at Support 1 is approximated as:

$$P_{Z1C} = (2)\frac{5}{8}wl = (2)\frac{5}{8}(16.4 \text{ plf})(40 \text{ ft}) = 820 \text{ lb}$$

18.5.4.4 Support Design. The bracing system at Support 1 is shown in Figure 18.5-8. The analysis must consider design of the following bracing elements: Beam f-g, Hangers f-b and g-d, Transverse Brace a-f and Longitudinal Braces f-c and g-e. The connections at a, b, c, d and e must also be designed and are subject to special requirements.

18.5.4.4.1 Beam f-g. Beam f-g is subject to biaxial bending under vertical (Y-direction) and longitudinal (X-direction) forces. The maximum moment, which occurs at the center, is equal to:

$$M = \frac{P_A L_1}{2} + \frac{P_B L}{4} + \frac{P_C L_4}{2}$$

The factored vertical loads for the piping runs are:

Piping Run A: $P_A = 1.2(164 \text{ lb}) + 1.0(33 \text{ lb}) = 230 \text{ lb}$

Piping Run B: $P_A = 1.2(317 \text{ lb}) + 1.0(63 \text{ lb}) = 443 \text{ lb}$

Piping Run C: $P_A = 1.2(164 \text{ lb}) + 1.0(33 \text{ lb}) = 230 \text{ lb}$

The maximum moment about the x-axis of the beam due to vertical loads is:

$$M_x = \frac{230(7)}{2} + \frac{443(30)}{4} + \frac{230(7)}{2} = 4,933 \text{ in-lb}$$

The vertical reactions at f and g are equal to $(230 + 443 + 230)/2 = 452$ pounds.

The factored lateral loads in the longitudinal direction determined in Section 18.5.4.2 are:

Piping Run A: $P_A = 804 \text{ lb}$

Piping Run B: $P_A = 2,356 \text{ lb}$

Piping Run C: $P_A = 1,312 \text{ lb}$

The maximum moment about the y-axis of the beam due to lateral loads is approximately:

$$M_y = \frac{804(7)}{2} + \frac{2,356(30)}{4} + \frac{1,312(7)}{2} = 25,076 \text{ in-lb}$$

The horizontal reactions at f and g are:

$$R_f = \frac{P_A(L_2 + L_3 + L_4)}{L} + \frac{P_B}{2} + \frac{P_C L_4}{L} = \frac{804(8+8+7)}{30} + \frac{2,356}{2} + \frac{1,312(7)}{30} = 2,101 \text{ lb}$$

$$R_g = \frac{P_A L_1}{L} + \frac{P_B}{2} + \frac{P_C(L_1 + L_2 + L_3)}{L} = \frac{804(7)}{30} + \frac{2,356}{2} + \frac{1,312(7+8+8)}{30} = 2,371 \text{ lb}$$

Beam f-g must be designed for moments M_x and M_y acting simultaneously.

18.5.4.4.2 Brace Design. By inspection, Brace g-e will govern the longitudinal brace design, since the horizontal reaction at g (2,371 lb) is larger than that at f (2,101 lb).

The horizontal load that must be resisted by the Transverse Brace a-f is the sum of the loads from the three pipes determined in Section 18.5.4.3:

$R_z = 502 \text{ lb} + 1,585 \text{ lb} + 820 \text{ lb} = 2,907 \text{ lb}$

Assuming the same member will be used for all braces, Brace a-f governs the design. Since the brace is installed at a 1:1 slope (45 degrees), the maximum tension or compression in the brace would be:

$$T_{max} = C_{max} = R_z\sqrt{2} = (2,907)(1.414) = 4,110 \text{ lb}$$

The brace selected must be capable of carrying C_{max} with an unbraced length of $(30 \text{ in.})\sqrt{2} = 42$ inches. Bracing elements subject to compression should meet the slenderness ratio requirements of the appropriate material design standards.

18.5.4.4.3 Hangers. By inspection, Hanger f-b will govern the vertical element design, since the brace force in brace f-a governs the brace design. Since the brace is installed at a 1:1 slope (45 degrees), the maximum tension or compression due to seismic forces in the hanger is the same as the horizontal force resisted by the brace: 2,907 pounds. The vertical component of the brace force must be combined with gravity loads and the vertical seismic component.

The maximum tension force in the hanger is determined using the basic strength Load Combination 6 from *Standard* Section 2.3.6 :

$U = 1.2D + E_v + E_h + L + 0.2S$

For nonstructural components, $\rho = 1.0$ and Q_E = the forces (or stresses) resulting from applying F_p.

In this example, live load, L and snow load, $S,$ are equal to zero. The unfactored reaction at f due to the weight of the water-filled pipes is 323 pounds.

$U = 1.2(323 \text{ lb}) + 0.2(1.0)(323 \text{ lb}) + 1.0(1.0)(2,907 \text{ lb}) = 3,359 \text{ lb (tension)}$

The maximum compression force in the hanger is determined using the basic strength Load Combination 7 from *Standard* Section 2.3.6:

$U = 0.9D - E_v + E_h$

Substituting the values from above:

$U = 0.9(323 \text{ lb}) - 0.2(1.0)(323 \text{ lb}) - 1.0(1.0)(2,907 \text{ lb}) = -2,681 \text{ lb (compression)}$

F_p should be applied in the direction which creates the largest value for the item being checked. A negative sign indicates compression. The hanger selected must be capable of carrying the maximum compression with an unbraced length of 30 inches. Again, bracing elements subject to compression should meet the slenderness ratio requirements of the appropriate material design standards. It is also important to note that the length of pipe that contributes dead load to counteract the vertical component of brace force is based on the spacing of the vertical hangers, not the spacing between lateral braces.

18.5.4.5 Anchorage Design. *Standard* Section 13.4 covers the attachment of the hangers and braces to the structure. Component forces and displacements are those determined in *Standard* Sections 13.3.1 and 13.3.2, with important exceptions. When designing the attachments for the piping system, the response modification factor R_p may not exceed a value of 6 (*Standard* Sec. 13.4.1). Anchors in concrete and masonry are proportioned so that either the component or support that the anchor is connecting to the structure undergoes ductile yielding at a load level corresponding to anchor forces not greater than their design strength, or the anchors shall be designed to resist the load combinations considering Ω_0 in accordance with *Standard* Section 2.3.6.

To illustrate the effects of these provisions, consider the design of the attachment to the structure at Point "a" in Figure 18.5-8.

The horizontal and vertical components of the seismic brace force at Point "a" are 2,907 pounds each. Assuming the brace capacity limits the force to the anchor and that the brace does not resist vertical loads due to gravity or the vertical seismic component, the minimum design forces for the anchor are 2,907 pounds in tension acting currently with 2,907 pounds in shear.

The maximum design force for the anchor, assuming that a ductile element does not govern the anchorage capacity is determined using the load combinations considering Ω_0 in accordance with *Standard* Section 2.3.6.

By inspection, the load combination that results in net tension on the anchor will govern the design of the anchor. Applying the load combinations of *Standard* Section 2.3.6, Load Combination 7, the vertical design tension force is:

$$U = 0.9D - E_v + \underline{E}_{mh}$$

$$\underline{E}_{mh} = \Omega_0 Q_E \qquad\qquad\qquad\qquad\qquad\qquad\qquad (\textit{Standard Eq. 12.4-7})$$

$$U = (0) + (0) + 2.0(2,907 \text{ lb}) = 5,814 \text{ lb} = T_U$$

Similarly, the horizontal shear load on the anchors is:

$$V_U = \underline{E}_{mh} = \Omega_0 Q_E = 2.0(2,907 \text{ lb}) = 5,814 \text{ lb}$$

18.5.5 Design for Displacements

In addition to design for seismic forces, the piping system must accommodate seismic relative displacements. For the purposes of this example, we assume that the building has a 15-foot story height and has been designed for a maximum allowable story drift of 1.5% per floor:

$$\Delta_a = 0.015 h_{sx} = 0.015(15)(12) = 2.7 \text{ in. per floor}$$

18.5.5.1 Design for Displacements Within Structures. Piping Run A, a 4-inch-diameter pipe, connects to a large mechanical unit at Line 1 supported at the second level. For a nonstructural component subject to displacements within a structure, the relative displacement, D_p is given in *Standard* Eq. 13.3-6 as the difference between lateral story drifts at the points of attachment. Because the mechanical unit can be assumed to behave as a rigid body and the piping system is rigidly braced to the roof structure, the entire story drift must be accommodated in the 5'-0" piping drop (see Figure 18.5-2).

The seismic relative displacement demands, D_{pI}, are determined using equation 13.3-5 of the *Standard*:

$$D_{pI} = D_p I_e$$

where:

$D_p = $ displacements within or between structures

$I_e = $ the importance factor for the structure　　　　　　　　　　　　　　　　　　(*Standard* Sec 11.5.1)

$D_{pI} = D_p I_e = 2.7$ in $(1.5) = 4.05$ in.

There are several approaches to accommodate the drift. The first is to provide a flexible coupling (articulated connections or braided couplings, for example). A second approach is to accommodate the drift through bending in the pipe. Loops are often used to make the pipe more flexible for thermal expansion and contraction and this approach also works for seismic loads. In this example, a straight length of a pipe is assumed. For a 4-inch-diameter Schedule 40 pipe, the moment of inertia, I, is equal to 7.23 in^4. Assuming the pipe is fixed against rotation at both ends, the shear and moments required to deflect the pipe 4.05 inches are:

$$V = \left. 12EID_{pI} \middle/ l^3 \right. = \frac{12(29,000,000)(7.23)(4.05)}{((5.0)(12))^3} = 47,176 \; lb$$

The stress in the pipe displaced D_{pI} is:

M = (47,176 lb)(60 in.) = 2,830,590 in-lb

$$f_b = \frac{M}{Z} = \frac{2,830,590}{4.31} = 656,749 \; psi$$

These demands far exceed the capacity of the pipe and would overload the nozzle on the mechanical unit as well. Therefore, either a flexible coupling or a loop piping layout is required to accommodate the story drift.

Piping Run B, a 6-inch-diameter pipe, drops from the roof level to the second level at Line 3. Again, the drift demand is 2.7 inches, but in this case, it may be accommodated over the full story height of 15 feet. A simplified analysis assumes that the pipe is fixed at the roof and second level. This assumption is conservative, since in reality the horizontal runs of the pipe at the roof and Level 2 provide restraint but not fixity. For a 6-inch-diameter Schedule 40 pipe, the moment of inertia, I, is equal to 28.14 in^4 and the plastic modulus Z is equal to 11.28 in^3. The shear and moments required to deflect the pipe 4.05 inches are approximately:

$$V = \frac{12EID_{pI}}{l^3} = \frac{12(29,000,000)(28.14)(4.05)}{((15.0)(12))^3} = 6,800 \; lb$$

M = (6,800)((15)(12))/2 = 612,045 in-lb

The stress in the pipe displaced D_{pI} would be:

$$f_b = \frac{M}{Z} = \frac{612,045}{11.28} = 54,259 \; psi$$

This exceeds the permissible stress in the pipe, but not by a wide margin. Refining the analysis to more accurately consider the effects of the rotational restraint provided by the horizontal piping runs (which will tend to reduce the rigidity of the pipe and therefore reduce the bending stress), providing loops in the piping layout, or providing flexible couplings will produce more favorable results. It is critical that the capacity of the nozzle on the equipment where the pipe is attached has the capacity to resist the shears and moments applied by the pipe.

18.5.5.2 Design for Displacements Between Structures. At the roof level, Piping Run A crosses a seismic separation between adjacent two-story structures at Line 3. Assuming story heights of 15 feet and design for a maximum allowable story drift for both buildings, the deflections of the buildings are:

$$\delta_{xA} = \delta_{xB} = (2)0.015h_{sx} = (2)0.015(15)(12) = 5.4 \text{ in.}$$

The displacement demand, D_P is determined from *Standard* Equation 13.3-7 as follows:

$$D_{p_{max}} = \left|\delta_{xA}\right| + \left|\delta_{yB}\right| = \left|5.4\right| + \left|5.4\right| = 10.8 \text{ in.}$$

The seismic relative displacement demands, D_{pI}, determined using equation 13.3-5 of the *Standard* are:

$$D_{pI} = D_p I_e = 10.8 \text{ in } (1.5) = 16.2 \text{ in.}$$

In addition to motions perpendicular to the pipe, the seismic isolation joint must accommodate movement parallel to the pipe. Assuming an 18-inch seismic separation joint is provided, during an earthquake the joint could vary from 1.8 inches (if the structures move towards each other) to 32.4 inches (if the structures move away from each other). The flexible coupling, which could include articulated connections, braided couplings, or pipe loops, must be capable of accommodating this range of movements.

18.6   ELEVATED VESSEL SEISMIC DESIGN

18.6.1   Example Description

This example illustrates seismic design for a small platform-supported vessel in the upper floor of a structure. It includes determination of the seismic design forces, anchorage of the vessel to the supporting platform, design and anchorage of the platform and demands on the floor slab of the supporting structure. The example focuses on the determination of force and displacement demands on the different components of the support system. The sizing of the various elements (beams, columns, braces, connections, anchor bolts, etc.) are not covered in detail.

This example considers a vessel supported by a platform on the second floor of a three-story structure. The contents of the vessel, a compressed non-flammable gas, are not hazardous. The structure is assigned to Seismic Risk Category II.

The design approach for nonstructural components depends on the type, size and location of the component. The *Standard* provides requirements for nonstructural components in Chapter 13 and nonbuilding structures in Chapter 15. Vessels are classified as nonbuilding structures, but in this example the provisions of *Standard* Chapter 13 apply, due to the size and location of the vessel.

18.6.1.1 Earthquake Design Requirements. Earthquake design requirements for vessels in the *Standard* depend on the system importance factor (I_p), the mass of the vessel relative to that of the supporting structure and the installation geometry. There are special analytical requirements triggered by Section 13.1.5 where the weight of the nonstructural component exceeds 25 percent of the effective seismic weight of the structure. This condition is not present in the example but if it were the case, the component would be classified as a nonbuilding structure and the requirements of Section 15.3.2 would apply.

The importance factor is determined in accordance with *Standard* Section 13.1.3. Given that the structure is assigned to Seismic Risk Category II, components are assigned $I_p = 1.0$, unless they must function for life-safety protection or contain hazardous materials. Neither of these conditions apply, so $I_p = 1.0$.

18.6.1.2 System Configuration. The vessel is of steel construction and supported on four legs, which are bolted to a steel frame. A plan of the second level showing the location of the vessel is shown in Figure 18.6-1. A section through the structure showing the location of the vessel is presented in Figure 18.6-2. The supporting frame system consists of ordinary braced frames (tension-only bracing). An elevation of the vessel and supporting frame is shown in Figure 18.6-3.
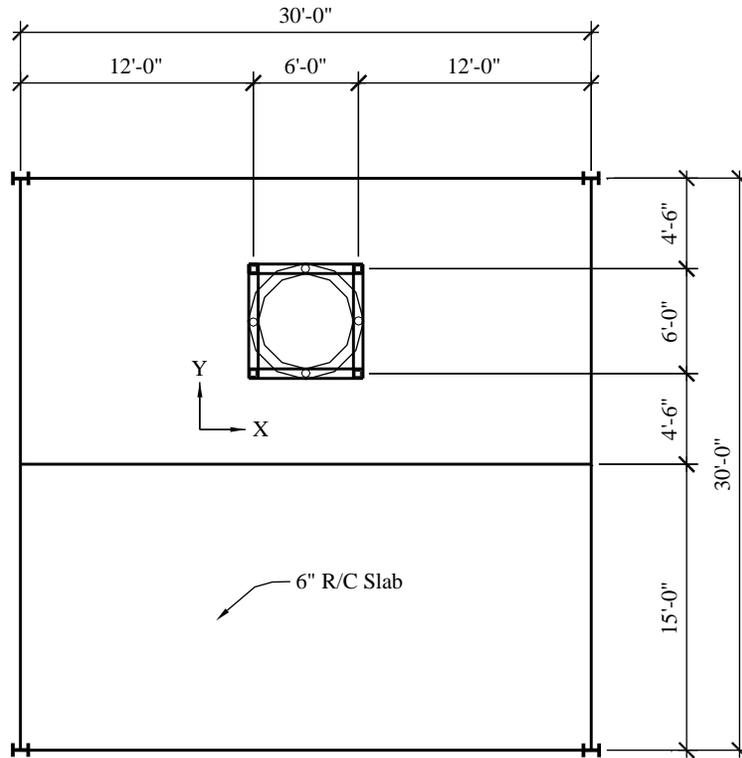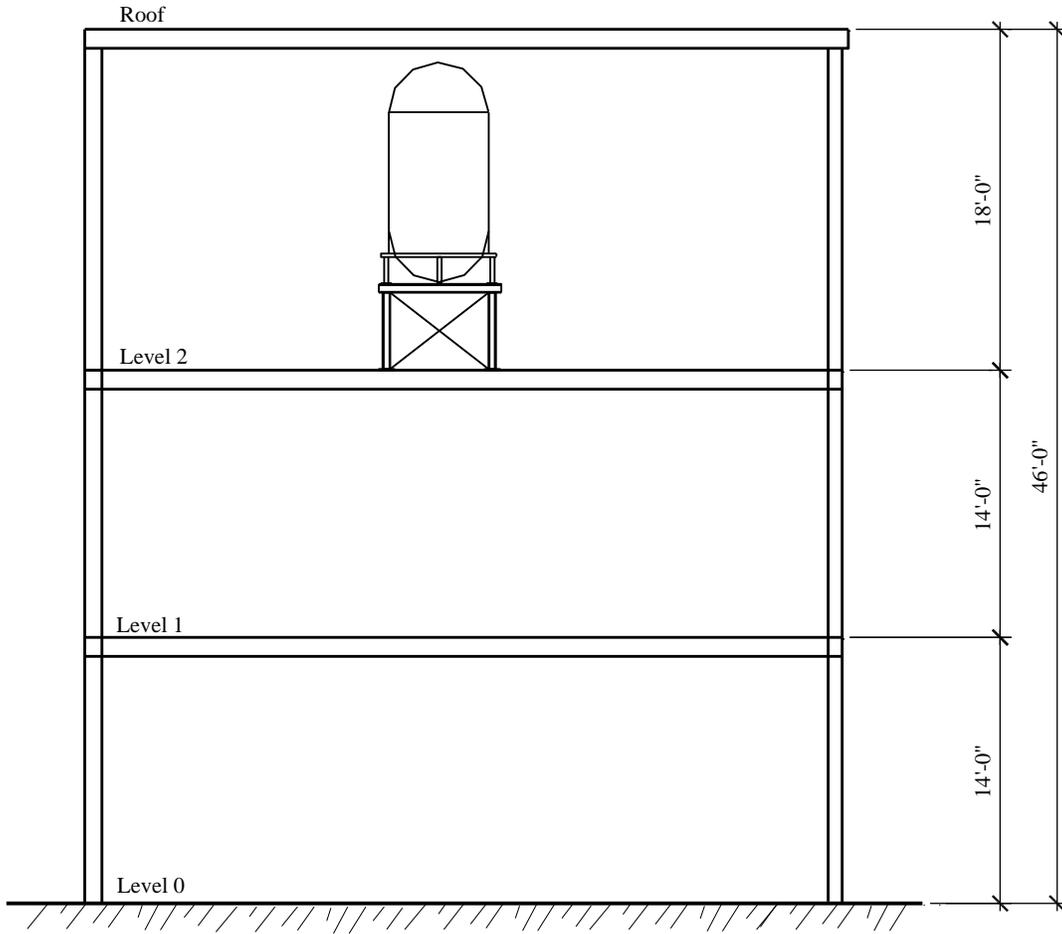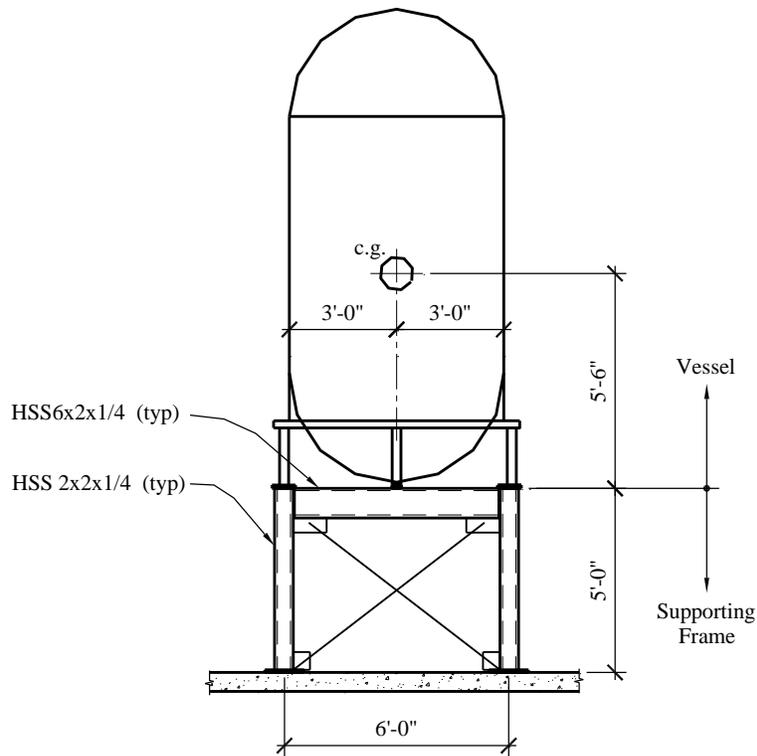
Figure 18.6-1 Elevated vessel - second-level plan

Roof

Level 2

Level 1

Level 0

18'-0"

14'-0"

14'-0"

46'-0"

Figure 18.6-2 Elevated vessel - section

Figure 18.6-3 Elevated vessel - supporting frame system

The example covers the determination of the seismic forces in the supporting steel frame and its connection to the concrete slab at the second level and concentrates on quantifying the prescribed seismic forces for the different elements in the vessel support system. After the seismic demands are determined, the bracing and anchorage connections can be designed and detailed according to the appropriate AISC and ACI codes. Finally, methods of considering the seismic demands on the floor system due to the vessel are discussed.

18.6.2 Design Requirements

18.6.2.1 Seismic Design Parameters and Coefficients.

a_p = 1.0 for vessels not supported on skirts and not subject to Chapter 15   (*Standard* Table 13.6-1)

R_p = 2.5 for vessels not supported on skirts and not subject to Chapter 15   (*Standard* Table 13.6-1)

Ω_0 = 2.0 overstrength factor for nonductile anchorage to concrete   (*Standard* Table 13.6-1)

S_{DS} = 1.2 (for the selected location and site class)   (given)

Seismic Design Category = D   (*Standard* Table 11.6-1)

h = 46 feet (roof height)   (given)

z = 28 feet (system is supported at the second level)   (given)

$$\frac{z}{h} = \frac{28.0 \text{ ft}}{46.0 \text{ ft}} = 0.609$$

$I_p = 1.0$ (*Standard* Sec. 13.1.3)

ASTM A500 Grade B steel HSS sections, $F_y = 46$ ksi, $F_u = 58$ ksi   (given)

ASTM A36 steel bars and plates, $F_y = 36$ ksi, $F_u = 58$ ksi   (given)

ASTM A53 Grade B pipe, $F_y = 35$ ksi, $F_u = 60$ ksi   (given)

ASTM A 307 bolts and threaded rods   (given)

D = Dead Load = W_p = 5,000 lb (vessel and legs)   (given)

     = 1,000 lb (allowance, supporting frame)   (given)

According to *Standard* Section 13.3.1 (and repeated in Sec. 12.3.4.1), the redundancy factor does not apply to the design of nonstructural components.

18.6.2.2 Seismic Design Forces.

$$F_p = \frac{0.4(1.0)(1.2)W_p}{2.5/1.0}(1 + 2(0.609)) = 0.426W_p$$ (*Standard* Eq. 13.3-1)

Maximum $F_p = 1.6(1.2)(1.0)W_p = 1.92W_p$ (*Standard* Eq. 13.3-2)

Minimum $F_p = 0.3(1.2)(1.0)Wp = 0.36W_p$ (*Standard* Eq. 13.3-3)

$E_v = 0.2(1.2)D = 0.24D = 0.24W_p$ (*Standard* Eq. 12.4-4a)

18.6.2.2.1 Vessel. The seismic forces acting on the vessel are as follows:

$F_p = 0.426W_p = 0.426(5,000) = 2,129$ lb

$E_v = 0.24W_p = 0.24(5,000) = 1,200$ lb

18.6.2.2.2 Supporting Frame. The seismic loads due to the supporting frame self-weight are:

$F_p = 0.426W_p = 0.426(1,000) = 426$ lb

$E_v = 0.24W_p = 0.24(1,000) = 240$ lb

18.6.2.3 Performance Criteria. Component failure must not cause failure of an essential architectural, mechanical, or electrical component (*Standard* Sec. 13.2.3).

Component seismic attachments must be bolted, welded, or otherwise positively fastened without considering the frictional resistance produced by the effects of gravity (*Standard* Sec. 13.4).

The effects of seismic relative displacements must be considered in combination with displacements caused by other loads as appropriate (*Standard* Sec. 13.3.2).

The component must be designed to resist the forces in accordance with *Standard* Section 13.3.1 and must be able to accommodate movements of the structure resulting from response to the design basis ground motion, D_p.

Local elements of the structure, including connections, must be designed and constructed for the component forces where they control the design (*Standard* Section 13.4).

Anchors to concrete shall be designed so that either the support or component that the anchor is connecting to the structure undergoes ductile yielding at a load level corresponding to anchor forces not greater than their design strength, or the anchors shall be designed to resist the load combinations considering Ω_0 in accordance with *Standard* Section 2.3.6.

18.6.3 Load Combinations

The basic strength load combinations including earthquake effects from *Standard* Section 2.3.6 that will govern design of the vessel legs, attachments and the supporting frame are the following:

Load Combination 6: $U = 1.2D + E_v + E_h + L + 0.2S$

Load Combination 7: $U = 0.9D - E_v + E_h$

For nonstructural components, $\rho = 1.0$ and $Q_E = $ the forces resulting from applying F_p. In this example, live load (*L*) and snow load (*S)* are equal to zero.

18.6.4 Forces in Vessel Supports

Supports and attachments for the vessel must meet the requirements listed in *Standard* Table 13.2-1. Seismic design of the vessel itself is not required, since $I_p = 1.0$. While the vessel itself need not be checked for seismic loading, the component supports listed in *Standard* Section 13.6.4 must be designed to resist the prescribed seismic forces. The affected components include the following:

The legs supporting the vessel

Connection between the legs and the vessel shell

Base plates and the welds attaching them to the legs

Bolts connecting the base plates to the supporting frame

Standard Section 13.4.1 states that the lateral force, F_p, must be applied independently in at least two orthogonal directions. For vertically cantilevered systems, the lateral force also must be assumed to act in any horizontal direction. In this example, layout of the vessel legs is symmetric and there are two horizontal directions of interest, separated by 45 degrees. These two load cases are illustrated in Figure 18.6-4.
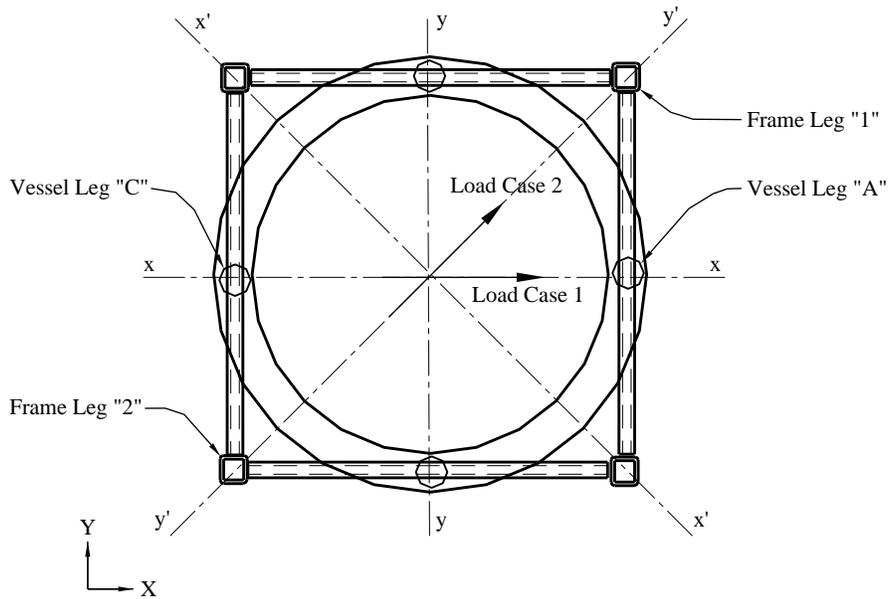
Figure 18.6-4 Elevated vessel support load cases

18.6.4.1 Case 1 - moments about the y-y axis. The height of the vessel's center-of-gravity above the bottom of the leg base plates is 5.5 feet. The moments about the bottom of these base plates are :

$$M = (5.5)F_p = (5.5)(2,129) = 11,710 \text{ ft-lb}$$

Assuming the vessel acts as a rigid body, in Case 1 the overturning moments is resisted by the two legs along the x-x axis. The vessel is assumed to rotate about the legs on the y-y axis. The maximum tension and compression loads in the legs may be estimated as:

$$T = C = M \: / \: d$$

where the distance between legs A and C, *d,* is 6.0 feet. Therefore:

$$T = C = 11,710 \: / \: 6.0 = 1,952 \text{ lb}$$

The vertical load in each leg due to gravity is $W_p/4 = 5,000/4 = 1,250$ pounds.

The shear in each leg due to F_p is $V = F_p/4 = 2,129/4 = 532$ pounds.

18.6.4.2 Case 2 - moments about the x'-x' axis. In Case 2 the overturning moments are resisted by all four legs, two in compression and two in tension. The loads in the legs due to gravity are the same as in Case 1, as is the shear in the legs due to F_p. Under seismic load, the vessel is assumed to rotate about the x'-x' axis. The maximum tension and compression loads in the legs may be estimated as:

$$T = C = \frac{M}{2(0.707d)}$$

where the distance between legs A and C, 0.707d , is 4.24 feet. Therefore:

$$T = C = 11,710 / 2(4.24) = 1,380 \text{ lb}$$

18.6.5   Vessel Support and Attachment

The axial loads in the vessel legs due to seismic overturning about the y-y axis (Case 1, in Section 18.6.4.1) are substantially larger than those obtained for overturning about the x'-x' axis (Case 2, in Section 18.6.4.2) . Therefore, by inspection Case 1 governs the design of the legs.

The design compression loads on the vessel legs is governed by Load Combination 5:

$$U = [1.2 + 0.2(1.2)](1,250 \text{ lb}) + 1.0(1,952 \text{ lb}) = 3,752 \text{ lb} = C_U$$

The design tension load on the vessel legs is governed by Load Combination 7:

$$U = [0.9 - 0.2(1.2)](1,250 \text{ lb}) - 1.0(1,952 \text{ lb}) = -1,127 \text{ lb} = T_U$$

(A negative sign denotes tension.)

The design shear in each leg is $U = 1.0(532 \text{ lb}) = 532 \text{ lb} = V_U$.

18.6.5.1 Vessel Leg Design. The check of the leg involves a check of the connection between the vessel and the leg and a stress check of the leg itself. The length of the leg, L, is 18 inches and the legs are fabricated from 2-inch-diameter standard pipe. The section properties of the leg are:

$A = 1.00 \text{ in}^2$

$Z = 0.713 \text{ in}^3$

Assuming the leg is pinned at the connection to the supporting frame and fixed at the connection to the vessel, the moment and bending stress in the leg are:

$M = V_U L = 532(18) = 9,576 \text{ in-lb}$

$f_b = M/Z = 9,756/0.713 = 13,683 \text{ psi}$

The maximum axial compressive stress in the leg is:

$C_u/A = 3,752/1.00 = 3,752 \text{ psi}$

The capacities of the leg and the connection to the vessel are determined using the structural steel specifications (AISC 360). The permissible strengths are:

$F_a = 31,500 \text{ psi}$

$F_{bw} = 31,500 \text{ psi}$

For combined loading:

$$\left| \frac{f_a}{F_a} + \frac{f_{bw}}{F_{bw}} \right| \le 1.0$$

$$\left| \frac{3,752}{31,500} + \frac{13,683}{31,500} \right| = 0.553 \le 1.0$$

18.6.5.2 Connections of the Vessel Leg. The connection between the vessel leg and the supporting frame is shown in Figure 18.6-5. The design of this connection involves checks of the weld between the pipe leg and the base plate, design of the base plate and design of the bolts to the supporting frame. Load Combination 7, which results in tension in the pipe leg, will govern the design of the base plates and the bolts to the supporting frame. The design of the base plate and bolts should consider the effects of prying on the tension demand in the bolts.
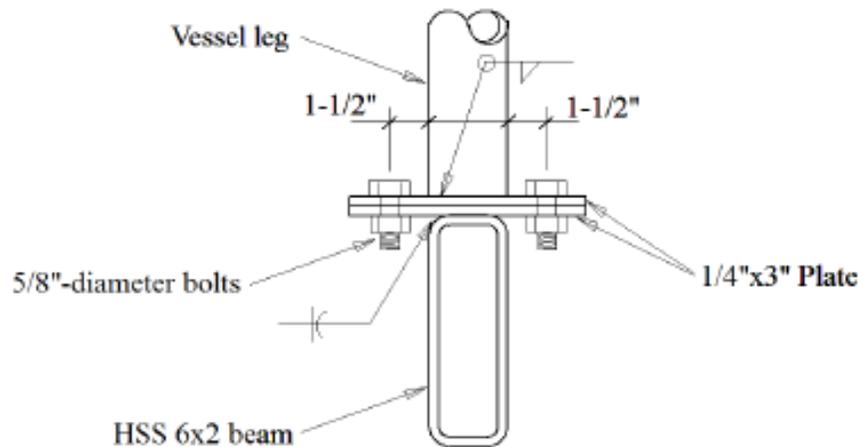
Figure 18.6-5 Elevated vessel leg connection

Each vessel leg is connected to the supporting frame by a pair of 5/8-inch-diameter bolts. The load path for this connection consists of the following elements: the weld of the leg to the connecting plate, the connecting plate acting in bending considering the effects of prying as appropriate, the bolts, the connection plate welded to the supporting frame beam and the welding of the connection plate to the supporting frame beam. Again by inspection, Case 1 (Section 18.6.4.1) governs. The factored loads in the connection are determined using Load Combinations 6 and 7 of *Standard* Section 2.3.6. As previously determined, the maximum compression in the connection (Load Combination 6) is:

$C_U = 3,752$ lb

The maximum tension in the connection (Load Combination 7) is:

$U = 0.9D - E_v + E_h$

$U = 0.9(1,250 \text{ lb}) - 0.2(1.2)(1,250 \text{ lb}) - 1.0(1,952 \text{ lb}) = -1,127 \text{ lb (tension)} = T_U$

The maximum shear per bolt is:

$V_U = 532 \text{ lb}/2 = 266 \text{ lb}$

The designs of the vessel leg base plate and of the connection plate at the supporting frame beams are identical. The maximum tension in each bolt is:

$T_U = -1,127 \text{ lb}/2 = -534 \text{ lb}$

The available shear and tensile strengths of the bolt are as follows:

$\phi_v r_n = 5,520 \text{ lb (shear)}$

$\phi r_n = 10,400 \text{ lb (tension)}$

Therefore, the bolts are adequate.

The connection plates are 1/4 inch thick and 3 inches wide.

$$Z = \frac{bd^2}{4} = \frac{3(0.25)^2}{4} = 0.0469 \text{ in}^3$$

The maximum moment in the plate is:

$M_U = 534 \text{ lb } (1.5 \text{ in.}) = 801 \text{ in-lb}$

The bending stress is:

$f_b = M_U / Z = 801/0.0469 = 17,088 \text{ psi}$ OK

Prying action can have the effect of increasing the tensile forces in the bolts. AISC 360 permits prying action to be neglected if the plate meets minimum thickness requirements, given by:

$$t_{min} = \sqrt{\frac{4.44Tb'}{pF_u}}$$

where $p = 3$ inches is the tributary length per pair of bolts

$b' = (b - d_b/2) = (1.5 - 0.625/2) = 1.1875 \text{ in.}$

$$t_{min} = \sqrt{\frac{4.44(534)(1.1875)}{3(58,000)}} = 0.13 \text{ in.}$$

This is less than the 0.25-inch thickness provided, so prying need not be considered further.

The welds of the vessel leg to the vessel body and of the leg to the upper connection plate are proportioned in a similar manner. The calculation can be simplified by assuming the weld is of unit

thickness. This yields a demand per inch of weld and an appropriate weld thickness can then be selected. The vessel leg has an outer diameter, *d*, of 2.38 inches. The weld properties for a weld of unit thickness are:

$$Z = \frac{d^3}{6} = \frac{2.38^3}{6} = 2.25 \text{ in}^3$$

$A = \pi d = 3.14(2.38) = 7.45 \text{ in.}$

The shear in the weld is:

$v = 532 \text{ lb}/7.45 \text{ in.} = 714 \text{ lb/in.}$

The tension in the weld due to axial load is:

$T = 1{,}127 \text{ lb}/7.45 \text{ in.} = 151 \text{ lb/in.}$

The tension to the weld due to bending (at the connection to the vessel) is:

$T = M/Z = 9{,}756/7.45 = 1{,}310 \text{ lb/in.}$

For E70 electrodes, the capacity of a fillet weld is given by:

$\phi R_n = 1.392 \, Dl$ (kips/in.)

where *D* is the size of the weld in sixteenths of an inch and *l* is the weld length.

For a unit length, a 3/16-inch fillet weld has a capacity of:

$\phi R_n = 1.392(3)(1) = 4.18 \text{ kips/in.}$

This will be adequate.

The same size weld is used for the vessel leg-to-vessel body joint and for the leg-to-upper connection plate joint. A similar design approach is used to proportion the weld of the lower connection plate to the HSS 6x2 beam.

18.6.6 Supporting Frame

The design of the supporting frame can be performed separately from that of the vessel. The reactions from the vessel are applied to the frame and combined with the seismic loads resulting from the supporting frame itself. The configuration of the supporting frame is shown in Figure 18.6-6.
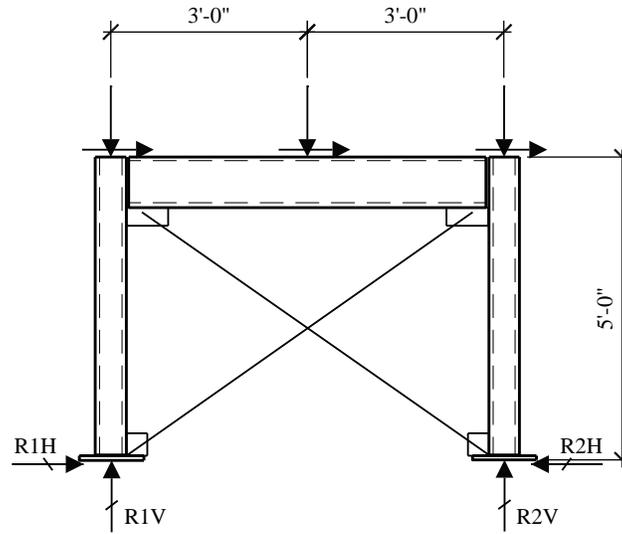
Figure 18.6-6 Elevated vessel supporting frame

The supporting frame uses Steel Ordinary Braced Frames (OBF). While the supporting frame is designed for seismic forces determined in Section 13.3, the design process for the frame itself is similar to that used for building frames or nonbuilding structures similar to buildings. In this example, seismic loads are developed for the following elements:

Beams supporting the vessel legs

Braces

Columns supporting the platform and vessel

Base plates and anchor bolts

To simplify the analysis, the self-weight of the supporting frame is lumped at the vessel leg connection locations.

18.6.6.1 Support Frame Beams. The beams transfer vertical and horizontal loads from the vessel to the brace frames. The beams, fabricated from HSS6x2x1/4 members, are idealized as simply supported with a span of 6 feet. The reactions from the vessel legs are idealized as point loads applied at mid-span. The vertical loads applied to the beam are:

P = [5,000 lb (vessel) + 1,000 lb (frame)]/4 supports = 1,500 lb

The lateral load per beam of the combined vessel and supporting frames is:

V = 0.426[5,000 lb (vessel) + 1,000 lb (frame)]/4 supports = 639 lb

The maximum load on a leg due to overturning of the vessel was computed as P = 1,952 pounds. The maximum factored vertical load, which will generate strong axis bending in the beam, is determined using Load Combination 6:

$P_U = 1.2(1,500 \text{ lb}) + 0.2(1.2)(1,500 \text{ lb}) + 1.0(1,952 \text{ lb}) = 4,112 \text{ lb} = P_v$

Acting with the horizontal load, $V_U = 639$ pounds, the moment in the beams then is:

$M_{x-x} = P_U l/4 = (4,112 \text{ lb})(6.0 \text{ ft})/4 = 6,168 \text{ ft-lb}$

$M_{y-y} = V_U l/4 = (639 \text{ lb})(6.0 \text{ ft})/4 = 959 \text{ ft-lb}$

For an HSS6x2x1/4:

$Z_{x-x} = 5.84 \text{ in}^3$

$Z_{y-y} = 2.61 \text{ in}^3$

$$\left| \frac{f_{bx}}{F_b} + \frac{f_{by}}{F_b} \right| \leq 1.0$$

$F_b = \phi F_y = 0.9(46,000 \text{ psi}) = 41,400 \text{ psi}$

$$\left| \frac{f_{bx}}{F_b} + \frac{f_{by}}{F_b} \right| = \left| \frac{M_{x-x}/Z_{x-x}}{F_b} + \frac{M_{y-y}/Z_{y-y}}{F_b} \right| = \left| \frac{6,168(12)/5.84}{41,400} + \frac{959(12)/2.61}{41,400} \right| = 0.41 \leq 1.0 \qquad \text{OK}$$

18.6.6.2 Support Frame Braces. The maximum brace force occurs where loads are applied in the X- or Y-direction and the loads are resisted by two frames. The horizontal force is:

$V = 0.426[5,000 \text{ lb (vessel)} + 1,000 \text{ lb (frame)}]/2 \text{ braces} = 1,278 \text{ lb}$

The length of the brace is:

$$\sqrt{(5)^2 + (6)^2} = 7.81 \text{ ft}$$

The force in the brace then is:

$$T_u = \frac{7.81}{6} 1,278 = 1,664 \text{ lb (tension)}$$

The braces consist of 5/8-inch-diameter ASTM A307 threaded rod. The nominal tensile capacity is:

$\phi r_n = 10,400 \text{ lb (tension)} > 1,664 \text{ lb}$ \qquad OK

It is good practice to design the supporting frame connections to the same level as a nonbuilding structure subject to Chapter 15. In this example, the supporting frames would be treated as an ordinary braced frame. For this system, AISC 341 requires the strength of the bracing connection to be the lesser of the expected yield strength of the brace in tension, the maximum force that can be developed by the system, or the load effect based on the amplified load.

18.6.6.3 Support Frame Columns. The columns support the vertical loads from the vessel and frame, including the vertical component of the supporting frame brace forces.   The columns are fabricated from HSS2x2x1/4 members and are idealized as pinned top and bottom with a length of 5 feet. The case where the vessel rotates about the x'-x' axis governs the design of the supporting frame columns. The overturning moment is:

$$M = (10.5)F_{p-vessel} + (5.0)F_{p-frame} = (10.5)(2,129) + 5.0(426) = 24,485 \text{ ft-lb}$$

Assuming the vessel acts as a rigid body, in Case 1 the overturning moment is resisted by the two legs along the y'-y' axis. The vessel is assumed to rotate about the legs on the x'-x' axis. The maximum tension and compression loads in the columns due to overturning may be estimated as follows:

$$T = C = M \ / \ d$$

where the distance between Frame Legs 1 and 2, $d = (6.0)\sqrt{2} = 8.48$ feet. Therefore:

$$T = C = 24,485 \ / \ 8.48 = 2,886 \ = 2,886 \text{ lb}$$

The vertical load in each leg due to gravity is $W_p/4 = (5,000+1,000)/4 = 1,500$ pounds.

The design compression load on the supporting frame columns is governed by Load Combination 6:

$$U = 1.2(1, 500 \text{ lb}) + 0.2(1.2)(1, 500 \text{ lb}) + 1.0(2,886 \text{ lb}) = 5,046 \text{ lb} = C_U$$

The design tension load on the supporting frame columns is governed by Load Combination 7:

$$U = 0.9(1,500 \text{ lb}) - 0.2(1.2)(1,500 \text{ lb}) - 1.0(2,886 \text{ lb}) = -1,896 \text{ lb} = T_U$$

The capacity of the HSS2x2x1/4 column is 38,300 pounds and is therefore adequate.

18.6.6.4 Support Frame Connection to the Floor Slab. The connection of the support frame columns to the floor slab includes the following elements:

   Weld of the column and brace connection to the base plate

   Base plate

   Anchor bolts

The design of the connection of the base plate and of the base plate itself follows the typical procedures used for other structures. There are special considerations for the design of the anchor bolts to the concrete slab that are unique to nonstructural components. Anchors in concrete and masonry must be proportioned so that either the component or support that the anchor is connecting to the structure undergoes ductile yielding at a load level corresponding to anchor forces not greater than their design strength, or the anchors shall be designed to resist the load combinations considering Ω_0 in accordance with *Standard* Section 2.3.6. In this example, it is assumed that the anchor design strength is less than the yielding strength of the vessel or supporting frame, and so Ω_0 must be applied to the anchor loads.

The horizontal and vertical reactions of the supporting frame columns calculated in Section 18.6.6.3 are:

Vertical load due to gravity = 1,500 lb

Tension and Compression due to seismic overturning = 2,886 lb

Horizontal seismic force = 1,280 lb

By inspection, the load combination that results in net tension on the anchors will govern. Applying the load combinations of *Standard* Section 2.3.6, Load Combination 7, the vertical design tension force is:

$U = 0.9D - E_v + E_{mh}$

$E_{mh} = \Omega_0 Q_E$ (*Standard* Eq. 12.4-7)

$U = 0.9(1,500 \text{ lb}) - 0.2(1.2)(1,500 \text{ lb}) - 2.0(2,886 \text{ lb}) = -4,782 \text{ lb} = T_U$

Acting concurrently with tension, the horizontal design shear force is:

$U = 2.0(1,280 \text{ lb}) = 2,560 \text{ lb} = V_U$

This is represents a 152 percent increase in the design tension. The design shear forces for the increase 100 percent.

18.6.7   Design Considerations for the Vertical Load-Carrying System

This portion of the example illustrates design considerations for the floor slab supporting the nonstructural component. The floor system at Level 2 consists of a 6-inch-thick reinforced concrete flat-slab spanning between steel beams. To illustrate the effects of the vessel, the contribution of the vessel load to the overall slab demand is examined.

18.6.7.1 Slab Design Assumptions

Dead load = 100 psf

Live load = 100 psf (non-reducible)

18.6.7.2 Effect of Vessel Loading

During design, the slab moments and shear are checked at different points along each span. In order to simply illustrate the potential effects of the vessel, this investigation will be limited to the change in the negative moments about the x-x axis over the center support. In an actual design, a complete analysis of the slab for the loads imposed by the vessel would be required. At the center support, the moments due to dead load and live load are :

Maximum dead load moment, $M_{DL} = wl^2/8 = (100)(15^2)/8 = 2,813$ ft-lb/ft

Maximum live load moment, $M_{LL} = wl^2/8 = (100)(15^2)/8 = 2,813$ ft-lb/ft

The support frame columns are 6 feet apart. Assuming an additional 3 feet of slab on each side of the frame to resist loads generated by the vessel, the design moments for the strip of slab supporting the vessel are:

M_{DL} = 2,813 ft-lb/ft (12 ft) = 33,756 ft-lb

M_{LL} = 2,813 ft-lb/ft (12 ft) = 33,756 ft-lb

The moments at the center support due to a point load, *P,* in one of the spans is:

$$M = \frac{Pab}{4l^2}(l+a)$$

where:

a = distance from the end support to the point load

b = distance from the point load to the center support

l = span between supports = 15 ft

The point loads due to the vessel and support frame self-weight is:

P = 2(1,500 lb) = 3,000 lb

The moment in the slab due to the vessel and support frame is:

$$M_{VD} = \frac{(3,000)(4.5)(10.5)}{4(15)^2}(15+4.5) + \frac{(3,000)(10.5)(4.5)}{4(15)^2}(15+10.5) = 7,088 \text{ ft-lb}$$

The point loads due to the vessel and support frame caused by seismic in the Y-direction are:

$T = C = 24,485 / 6.00 = 4,081$ lb

The moment in the slab due to the overturning of the vessel and support frame for seismic forces in the Y-direction is:

$$M_{VD} = \frac{(4,081)(4.5)(10.5)}{4(15)^2}(15+4.5) + \frac{(-4,081)(10.5)(4.5)}{4(15)^2}(15+10.5) = \text{-1,286 ft-lb}$$

or

$$M_{VD} = \frac{(-4,081)(4.5)(10.5)}{4(15)^2}(15+4.5) + \frac{(4,081)(10.5)(4.5)}{4(15)^2}(15+10.5) = 1,286 \text{ ft-lb}$$

The factored moments for the slab without the vessel not including seismic overturning are:

$D + L$: U = 1.2 D + 1.6 L = 1.2 (33,756 ft-lb) + 1.6(33,756 ft-lb) = 94,517 ft-lb

The factored moments for the slab including the vessel not including seismic overturning are:

$D + L$: U = 1.2 D + 1.6 L = 1.2 (33,756 ft-lb+ 7,088 ft-lb) + 1.6(33,756 ft-lb) = 103,022 ft-lb

The factored moments including seismic are (using 50 percent of the live load per *Standard* Sec. 2.3.6 Exception 1):

Load Combination 6:

$$U = 1.2D + E_v + E_h + L + 0.2S$$

$$= 1.2(33,756+7,088) + 0.2(1.2)(33,756+7,088) + 1.0(1.0)(1,286) + 0.5(33,756) + 0.2(0)$$

$$= 76,979 \text{ ft-lb}$$

Load Combination 7:

$$U = 0.9D - E_v + E_h$$

$$= 0.9(33,756+7,088) - 0.2(1.2)(33,756+7,088) + 1.0(1.0)(-1,286)$$

$$= 25,671 \text{ ft-lb}$$

In this case, the loads from the vessel do not control the design of the slab over the center support.